The Syntheses, Photochromism and Aromaticity of Dimethyldihydropyrene Derivatives Containing Organometallic Fragments and [e]-Fused C7 and C8 Aromatic Systems

by

Pengrong Zhang
B. Sc., East China Normal University, 1999
M. Sc., East China Normal University, 2002

A Dissertation Submitted in Partial Fulfillment
of the Requirements for the Degree of

DOCTOR OF PHILOSOPHY

in the Department of Chemistry

© Pengrong Zhang, 2011
University of Victoria

All rights reserved. This dissertation may not be reproduced in whole or in part, by photocopy or other means, without the permission of the author.

Supervisory Committee

The Syntheses, Photochromism and Aromaticity of Dimethyldihydropyrene Derivatives Containing Organometallic Fragments and [e]-Fused C7 and C8 Aromatic Systems

by

Pengrong Zhang
B. Sc., East China Normal University, 1999
M. Sc., East China Normal University, 2002

Supervisory Committee

Dr. Reginald H. Mitchell, (Department of Chemistry)
Co-Supervisor

Dr. David J. Berg, (Department of Chemistry)
Co-Supervisor

Dr. Peter Wan, (Department of Chemistry)
Departmental Member

Dr. Ross Chapman, (School of Earth and Ocean Sciences)
Outside Member

Abstract

Supervisory Committee

Dr. Reginald H. Mitchell, (Department of Chemistry)
Co-Supervisor

Dr. David J. Berg, (Department of Chemistry)
Co-Supervisor

Dr. Peter Wan, (Department of Chemistry)
Departmental Member

Dr. Ross Chapman, (School of Earth and Ocean Sciences)
Outside Member

A series of *cis*- and *trans*-*bis*(ethynyl)platinum complexes containing dimethyldihydropyrene (DHP) photochromic compounds were synthesized from ^{R}DHPCCH (R = H, CH_3CO, PhCO, 1-naphthoyl and benzo[e]) and platinum chloride with appropriate ancillary ligands (PEt_3, PPh_3, dppe, bipy and phen). The complexes were studied using mass spectrometry, NMR spectroscopy (^{1}H, ^{13}C, ^{31}P and ^{195}Pt) and IR. The X-ray structural information for *bis*(DHP-ethynyl) platinum complexes **44**, **45**, **47**, **49**, and **52** revealed that the Pt complexes possessed a square planar geometry at the metal centers. These platinum complexes are T type photochromic compounds. The BDHP-derived platinum complexes **48**, **49**, and **52** open completely when irradiated by visible light ($\lambda > 590$ nm). The photoopening rates for the platinum complexes are about 4 times slower than the corresponding DHP-alkynes. All the alkynyl platinum complexes close thermally faster than the corresponding free alkynes, and the closing rate is not affected substantially by changing the ancillary phosphine ligands. The BDHP-ethynyl platinum complexes with PEt_3, PPh_3 and dppe ligands have similar thermal closing half lives at 25°C of $\tau_{1/2}$ = 42 h, 38 h and 33 h, respectively, in contrast to the half life $\tau_{1/2}$ = 62 h of the BDHP-ethyne **40**.

The first cyclobutadienyl cobalt substituted dihydropyrenes were prepared by $CpCo(CO)_2$ cyclization of a series of dihydropyrenyl ethynes. When the other alkyne

substituent was small (methyl or carboxyethyl) only *cis* (*head-to-head*) isomers were obtained, but with larger sized groups, mixed *head-to-head* and *head-to-tail* isomers were obtained. The crystal structure of complex **21** indicated some unusually short bond distances were present. By comparison of the NMR and bond length data for complexes **21** or **69** with those for phenyl-DHP **60,** the aromaticity of the cyclobutadienyl cobalt fragment was estimated quantitatively to be at least as large as that of benzene. The organometallic fragment [Cbd-Co-Cp] substantially slowed the DHP photoopening reaction of complex **72** relative to precursors **67** or **35**.

DHP[e]tropone, **17**, DHP[e]tropylium cation, **18** and DHP[e]cyclooctatetraene dianion, **20** were synthesized to study the the relative bond localizing abilities of COT dianion **80** (105 % relative to benzene), tropylium cation **15** (55 % relative to benzene), tropone **79** (13 % relative to benzene) using DHP as the NMR probe. The internal methyl protons of DHP resonated at δ -3.56 for **17**, δ -2.61 for **18** and δ -1.38 for **20**. Cycloheptatrienyl anions **111**, **112** and **19** were made from cyclohepta-2,4,6-triene (CHT) isomers **107** and **108** (for two anions, **112** and **19**). The internal methyl protons of their DHP resonated at δ -2.52, 2.67 for **111**, δ -0.80, -0.84 for **112** and δ +2.10 for **19**. The anion **19** was best taken as a 20π electron paratropic system. The homo-aromaticity of the CHT isomers **107**, **108** and **117** was estimated based on the NMR data and X-ray structural data. Obvious anisotropic effects existed and the bond localization ability of the CHT (24% based on NMR data for **108**) may have a large error. The ring inversion barriers of the COT **82** and CHT **77** were measured using variable temperature NMR spectroscopy as 13.9 and 8.7 kcal/mol, respectively. Five X-ray crystallography structures were obtained for **99B**, **17**, **108**, **117** and **125** and the information was used in estimating the bond localization abilities and in establishing absolute stereochemistry.

Table of Contents

Supervisory Committee ii

Abstract iii

Table of Contents v

List of Tables x

List of Figures xii

List of Numbered Compounds xv

List of Abbreviations and Symbols xxvi

Acknowledgments xxx

Dedication xxxi

Chapter 1. Introduction 1

1.1 Introduction 1

1.1.1 Molecular switches 1

1.1.2 Some remarks associated with photochromism 2

1.1.3 Photochromism and aromaticity 3

1.1.4 Electrochromism 4

1.2 Known photochromic (photoswitchable) systems 5

1.2.1 Azobenzene 5

1.2.2 Spiropyrans and spirooxazines 7

1.2.3 *Cis*-stilbene 8

1.2.4 Fulgides....9

1.2.5 1,2-Dithienylethenes....10

1.2.6 *Trans*-dimethyldihydropyrene....11

1.3 Metal coordination complexes....15

1.3.1 Non-DHP based photoswitchable metal complexes....16

1.3.2 DHP-derived photoswitches containing metals....19

1.4 Aromaticity and anti-aromaticity....22

1.4.1 Background of homo-aromaticity....25

1.4.2 Resonance energy....27

1.4.3 C-C Bond lengths....27

1.4.4 Induced ring current detection by NMR spectroscopy....30

1.4.5 DHP used in measuring aromaticity and anti-aromaticity....32

1.5 Research objectives....34

Chapter 2. Platinum complexes of ethynyl DHPs....36

2.1 Introduction....36

2.2 Syntheses....41

2.2.1 Syntheses of the alkynes....42

2.2.2 Synthesis of platinum complexes with ethynyl DHP ligands....51

2.3 Crystallographic investigations....63

2.3.1 ORTEP3 plots for alkynyl platinum complexes **44**, **45**, **47**, **49** and **52**....63

2.3.2 Summary and discussion....67
2.4 Photoswitch opening and closing rates....71
2.4.1 Photoopening rates....71
2.4.2 Experimental methods....71
2.4.3 Photoopening results....75
2.4.4 UV closing....82
2.4.5 Thermal closing reactions....83
2.5 Conclusions....86
Chapter 3. Cobalt cyclobutadienyl DHP complexes....87
3.1 Introduction....87
3.2 Syntheses....89
3.2.1 Syntheses of alkyne substrates....90
3.2.2 Preparation of cobalt complexes....92
3.3 Results and discussion....95
3.4 Aromaticity....105
3.5 Photochemistry....109
3.6 Conclusions....112
Chapter 4. DHP-fused tropylium cation and cycloheptatrienyl anions and cyclooctatetraene dianion....113
4.1 Introduction....113
4.2 Results and discussion....118

4.2.1 Synthesis of tropone-annelated DHP systems 118

4.2.2 Aromatic 10π electron cyclooctatetraene dianion 149

4.2.3 Cyclization attempt using the Wittig strategy.....173

4.2.4 The ring closing metathesis approach to a COT-fused DHP.....152

4.2.5 Attempted synthesis of **122** from diol via *bis*-(3-butenyl) DHP **131**.....157

4.2.6 Attempt to open the fused furan in oxo-bridged COD **127** or DHP dihydroisofuran **132**.....162

4.2.7 Attempt to synthesize metal complexes.....163

4.3 X-ray crystallographic analysis.....164

4.4 Variable temperature NMR studies 173

4.4.1 Ring flipping studies associated with the cycloheptatriene ring.....176

4.4.2 Ring flipping of the C8 ring in the DHP[e]fused cyclooctatetraene.....179

4.5 Aromaticity 183

4.5.1 Relative aromaticity based on NMR chemical shifts.....183

4.5.2 The influence of charge 188

4.5.3 Cycloheptatrienyl anions **111**, **112** and **19**.....189

4.5.4 The homo-aromaticity of 1,2-DHP[e]fused 4,6-dimethylcycloheptatriene **108**.....191

4.6 Photochemistry 197

4.7 Conclusion 197

4.8 Future work.....198

Chapter 5. Experimental 203

5.1 Experimental for platinum alkynyl-DHP complexes 204

5.2 Experimental for DHP-CBD Cobalt complexes 237

5.3 Experimental for DHP-fused Cycloheptatrienyl systems 249

5.4 Experimental for DHP-fused cyclooctatetraene systems 272

Chapter 6. References 281

List of Tables

Table 1. Selected NMR and IR data for TMS protected DHP-alkynes **23**, **29**, **33** and **38**.....49

Table 2. Selected characterization data for Pt complexes containing acyl substituents.....53

Table 3. Comparisons between Pt complexes **48**, **49** and **52** containing BDHP-ethynyl moities and BDHP-ethyne **40** (L = ancillary ligands) 58

Table 4. The alkynyl platinum complexes having a dppe ligand.....61

Table 5. Comparison of DHP-alkynyl platinum complexes bearing a bipy ligand.....62

Table 6. Selected bond lengths (Å) and angles (°) for *trans*-(^{R}DHP-CC)$_2$Pt(PR'$_3$)$_2$ (**44**: R = $CH_3C(O)$, R' = Et; **45**: R = PhC(O), R' = Et; **47**: R = PhC(O), R' = Ph), *trans*-(BDHP-CC)$_2$Pt(PPh$_3$)$_2$ **49** and *cis*-(BDHP-CC)$_2$Pt(dppe) **52** 67

Table 7. Summary of bond length data for various (ArC≡C)$_2$Pt(L)$_2$ complexes from the Cambridge Structural Database (CSD) 68

Table 8. Photoopening comparison from previous studies.....74

Table 9. Non-complexed compounds comparison relative to BDHP.....76

Table 10. Thermal closing rates of DHP-alkyne ligands, their precursors and metal complexes.....85

Table 11. Selected bond lengths for the major and minor components Y and Y' in **21**. 101

Table 12. The interplane angles in the X-ray structure of **21** 104

Table 13. Selected bond length data (Å) for comparison 108

Table 14. Protons chemical shifts of the internal methyl resonance for **18**$\cdot BF_4^-$ in solutions with different dielectric constants 141

Table 15. Reaction conditions used for the Wittig reaction of aldehyde **116** with phosphonium salts **128**.....174

Table 16. The oxidation reactions tried on diol **123** 159
Table 17. Attempt to react cycloheptatriene **107** or isomer **108** with metal substrates.....163
Table 18. DHP peripheral C-C bond lengths (Å) for **99B** 165
Table 19. DHP peripheral C-C bond lengths for the tropone, **17** 167
Table 20. Bond lengths (Å) for the tropone unit in **17**.....167
Table 21. DHP peripheral C-C bond lengths (Å) for CHT **108**.....169
Table 22. DHP peripheral C-C bond lengths for diphenyl CHT **117** 171
Table 23. Selected chemical shifts (δ) in some DHP-derived aromatic systems.....187
Table 24. The bond localization ability of the aromatics relative to benzene using heptene-fused DHP **110** as the reference. 188
Table 25. The calculated and experimental chemical shifts for H-4,5. 188
Table 26. Selected chemical shifts (δ) for cycloheptatrienyl anions **111**, **112** and **19**.....190
Table 27. The ^{1}H NMR data (δ) for **107**, **108** and **117**. 191
Table 28. Distances in cyclohepta-2,4,6-triene **117** and **108**.....194
Table 29. Distances in cyclohepta-2,4,6-triene **117** and **108**.....194
Table 30. Bond alternation (Å) in **17**, **99B**, **108** and **117**.....196

List of Figures

Figure 1. The typical absorption curves for two forms of photochromic compounds 2

Figure 2. The 2,7-di-*tert*-butyl-*trans*-dimethyldihydropyrene **2**, the benzo[e]-DHP **3** and 4-acyl derivatives 13

Figure 3. The absorption spectra of BDHP **3** in closed (blue line) and open (black line) forms 15

Figure 4. Dinuclear Ru/Os complex containing a dithienylethene derivative as bridging ligand 17

Figure 5. The bond length alternations in some aromatic systems 29

Figure 6. Structural data of 2,7-disubstituted DHP and BDHP 30

Figure 7. The induced ring current and magnetic field of benzene in an external magnetic field B_o 31

Figure 8. Parent DHP **1** and the resonance structures 33

Figure 9. The chemical shifts for the internal methyl protons in **2**, **3**, **12** and **16** 33

Figure 10. Platinum and cobalt metal complex targets 34

Figure 11. Aromatic systems studied and their relevant DHP compounds 35

Figure 12. *Bis*-BDHP butadiyne photochromic compound 40

Figure 13. Two regioisomers of acyl DHP iodides 47

Figure 14. 2D long-range heteronuclear NMR spectrum for (benzoylDHPC≡C)$_2$Pt(PEt$_3$)$_2$ **45B** 56

Figure 15. ORTEP3 drawing of *trans*-(CH$_3$C(O)DHP-CC)$_2$Pt(PEt$_3$)$_2$ **44** 64

Figure 16. ORTEP3 drawing of complex *trans*-(PhC(O)DHP-CC)$_2$Pt(PEt$_3$)$_2$ **45** 64

Figure 17. ORTEP3 drawing of complex *trans*-(PhC(O)DHP-CC)$_2$Pt(PPh$_3$)$_2$ **47** 65

Figure 18. ORTEP3 drawing of complex *trans*-(BDHP-CC)$_2$Pt(PPh$_3$)$_2$ **49** 65

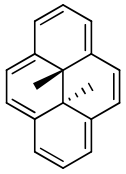
Figure 19. ORTEP3 drawing of *cis*-(BDHP-CC)$_2$Pt(dppe) **52** 66

Figure 20. Examples of known photochromic compounds 74

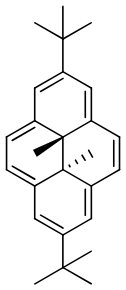
Figure 21. The UV-Vis spectra of BDHP **3** and *trans*-(BDHP-CC)$_2$Pt(PR$_3$)$_2$ (R=Et **48** and Ph **49**) and *cis*-dppe **52** complexes 77
Figure 22. The photoopening of BDHP **3**, BDHP-ethyne **40** and complex **48** 78
Figure 23. The photoopening of BDHP **3** and complex **49** 78
Figure 24. The UV-vis spectra of NpDHP **35** and complex **46** 80
Figure 25. The photoopening rates for NpDHP **35** and *trans*-(NpC(O)DHP-CC)$_2$Pt(PEt$_3$)$_2$ **46** 80
Figure 26. UV closing of 48 monitored by UV-Vis spectroscopy 82
Figure 27. Three possible stereoisomers for **21** 96
Figure 28. The proposed cyclization intermediate 99
Figure 29. The relationship between the two major disorder components Y (black) and Y' (grey) in the crystal strucure of **21** 100
Figure 30. ORTEP3 plot of **21** showing only the major component Y 101
Figure 31. The absorptions of **72** between 580 and 750 nm after irradiation with light of wavelength >590 nm for periods between 0 (top scan) and 40 minutes (bottom scan). 110
Figure 32. Pseudo-first order rate plots for the photoopening of **35**, **67** and **72** 111
Figure 33. The side perspective of the isomers **99A** and **99B** 125
Figure 34. The stereoisomers for **109** and **110** 135
Figure 35. A comparison of the ^{1}H NMR spectra of tropylium cation **18** and alcohol **103** 140
Figure 36. The ^{1}H and ^{13}C NMR spectra of DHP-fused COT **121** 155
Figure 37. The ^{1}H NMR spectrum for the dianion **20** plus unconverted **121** 157
Figure 38. ORTEP3 drawing of **99B** 164
Figure 39. ORTEP3 drawing of 4,5-DHP[e]fused 1,6-dimethyltropone **17** 166
Figure 40. ORTEP3 drawing of the 3,4-DHP [e]fused 1,6-dimethylcycloheptatriene **108** 168
Figure 41. ORTEP3 drawing of **117** 170
Figure 42. ORTEP3 drawing of 1,2-DHP[e]fused 3,8-*bis*(trimethylsilyloxo)-cycloocta-1,5-diene **125** 172

Figure 43. The VT NMR spectra for the symmetrical DHP-fused CHT **107** in $CDCl_3$ and CD_2Cl_2 (1:3) (internal methyl proton region).....177
Figure 44. The full range spectra of DHP-fused CHT **108** in low temperature VT NMR experiments in $CDCl_3$ and CD_2Cl_2 (3:1) 178
Figure 45. The variable temperature NMR spectrum of **117** 179
Figure 46. The ring inversion model for the DHP-fused COT **121** 181
Figure 47. The VT NMR spectrum of **121** (full range).....183
Figure 48. Bridged [12]- and [10]-annulene 184
Figure 51. ORTEP3 plot for 11-H,H-cyclohepta-2,4,6-triene **108** 193

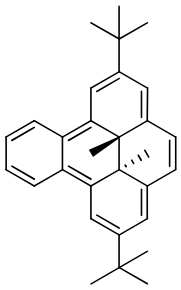
List of Numbered Compounds



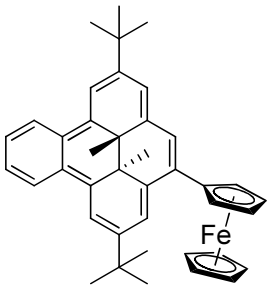
1



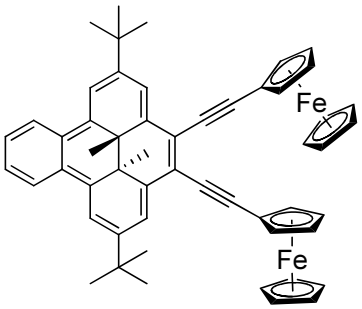
2



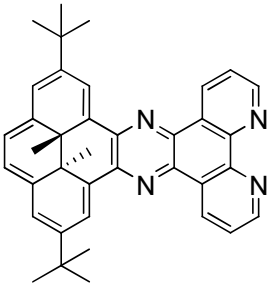
3



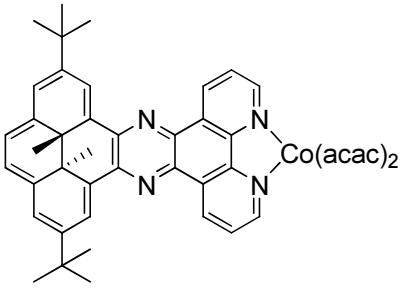
4



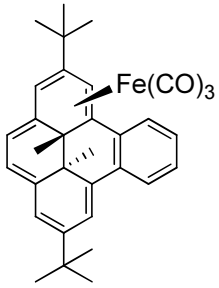
5



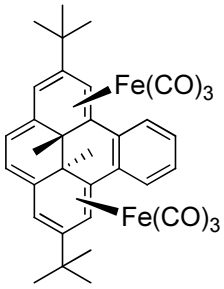
6



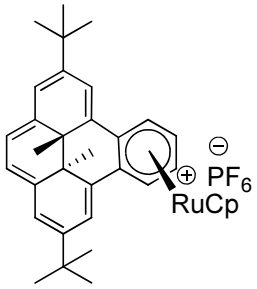
7



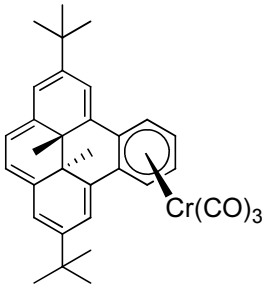
8



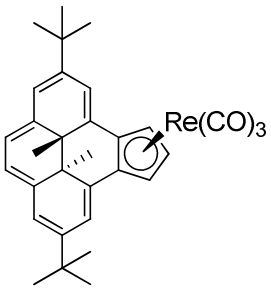
9



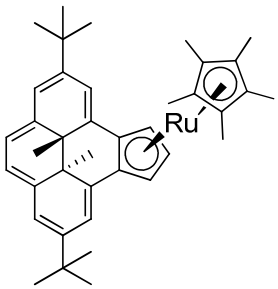
10



11



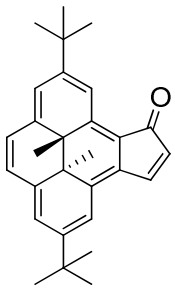
13



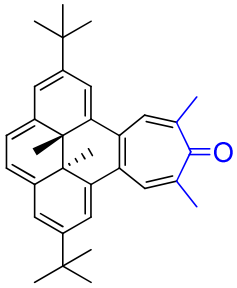
14



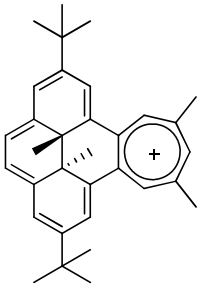
15



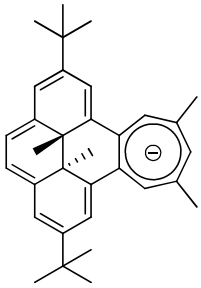
16



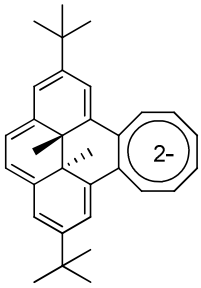
17



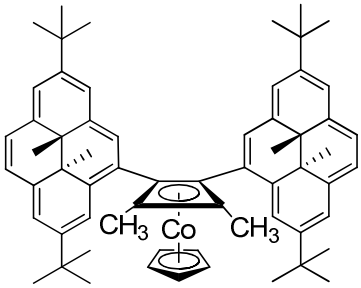
18



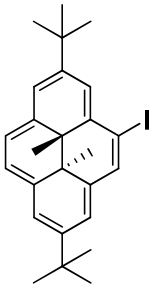
19



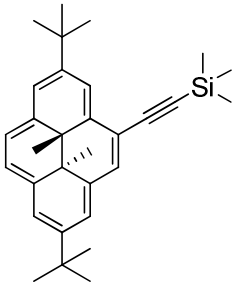
20



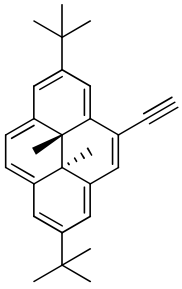
21



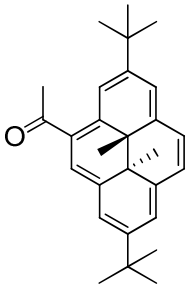
22



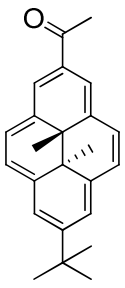
23



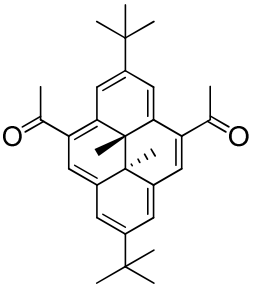
24



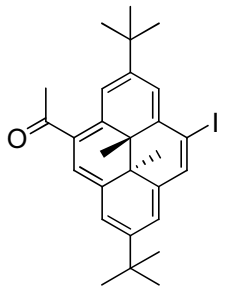
25



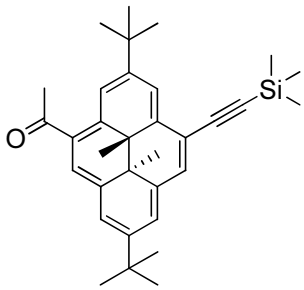
26



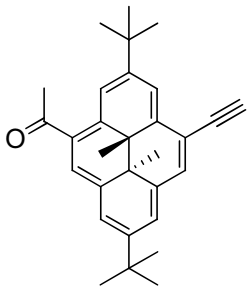
27



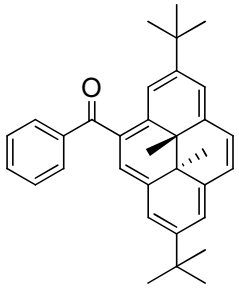
28



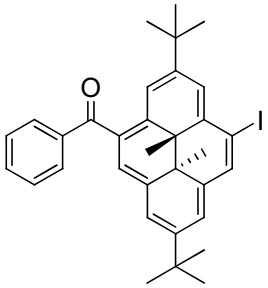
29



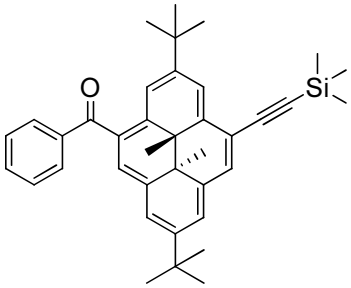
30



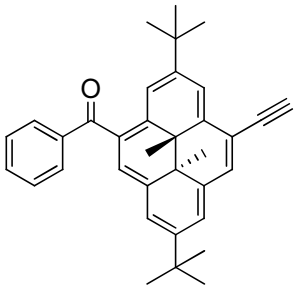
31



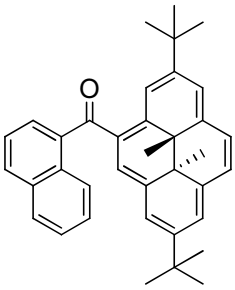
32



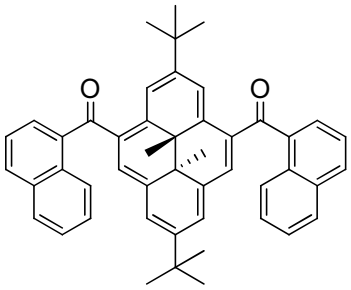
33



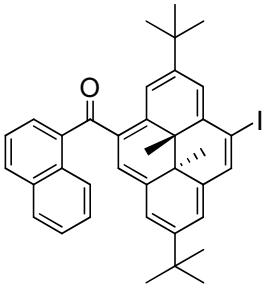
34



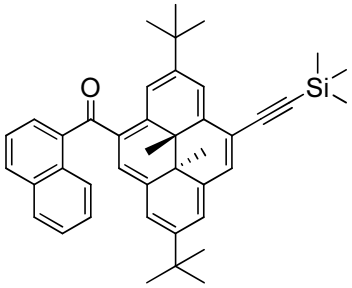
35



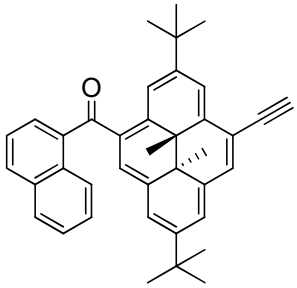
36



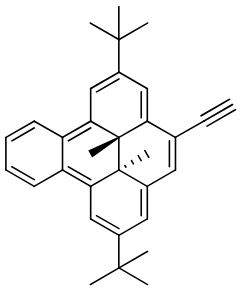
37



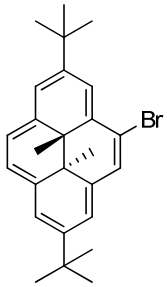
38



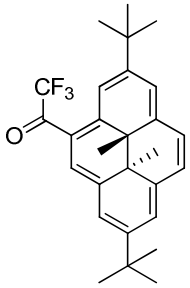
39



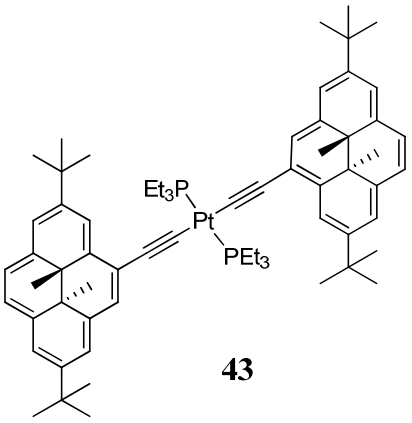
40



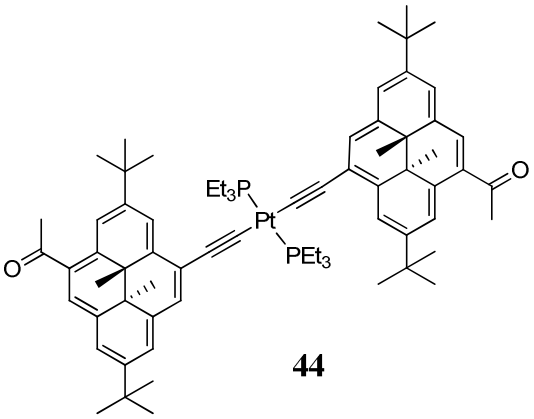
41



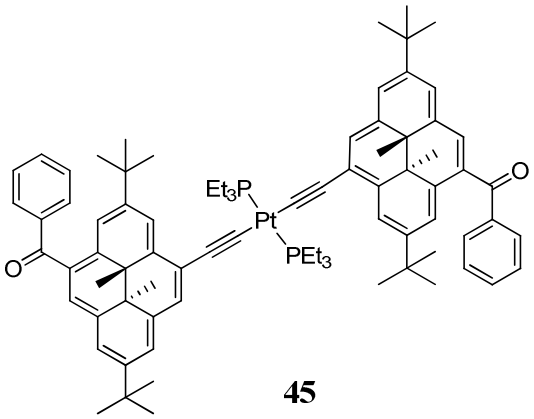
42



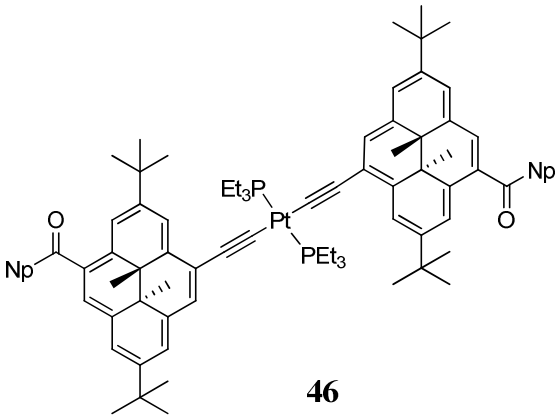
43



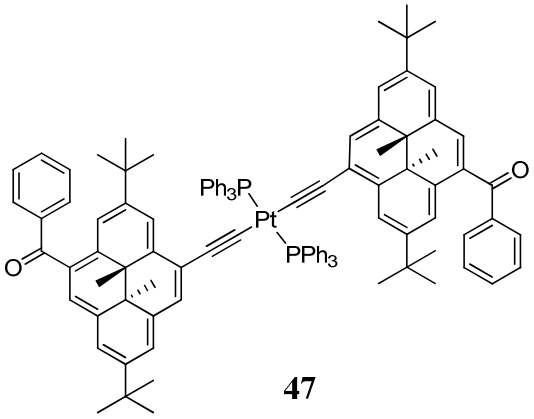
44



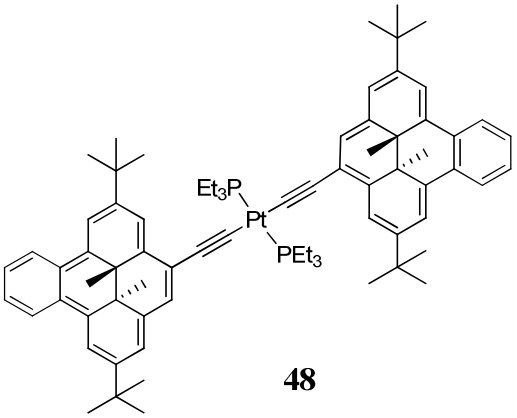
45



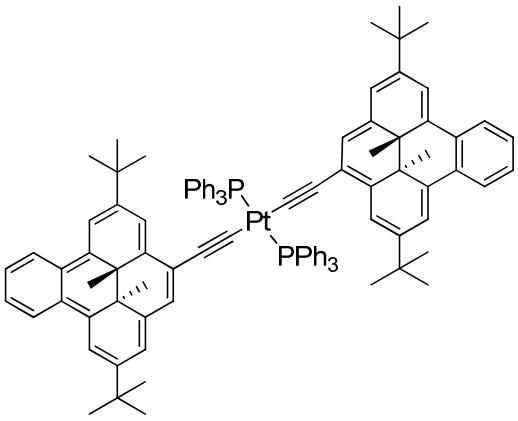
46



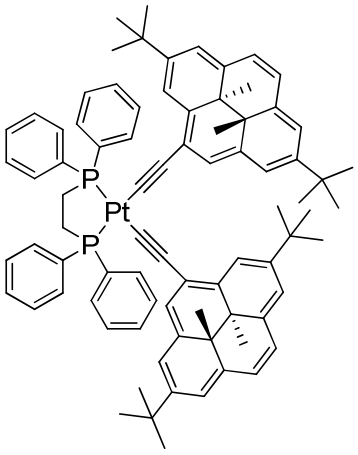
47



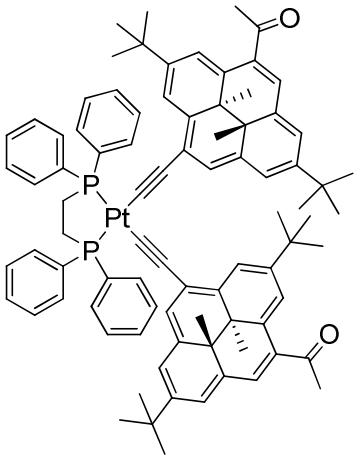
48



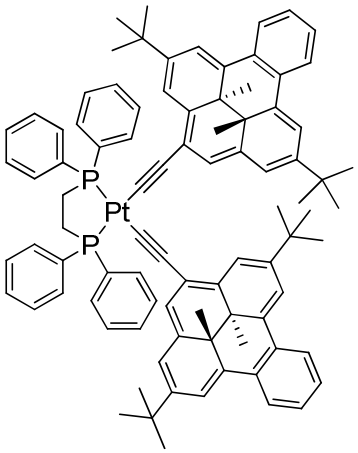
49



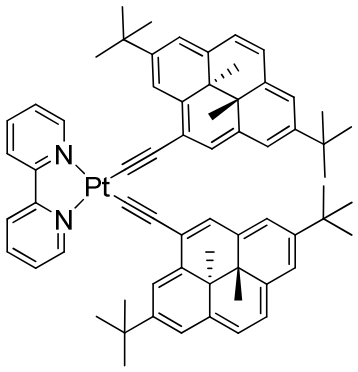
50



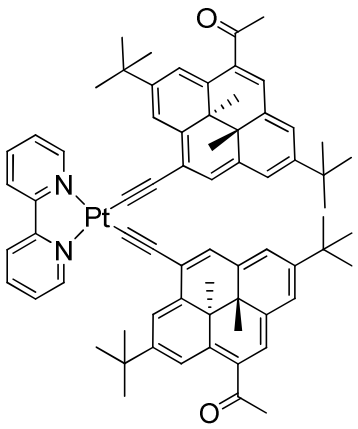
51



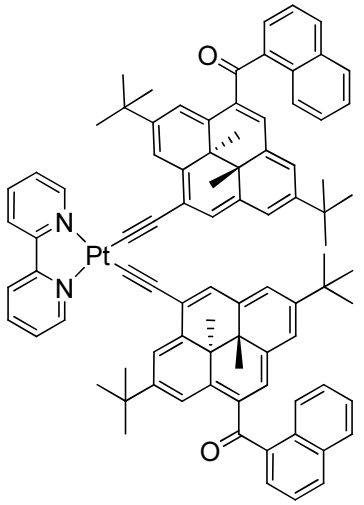
52



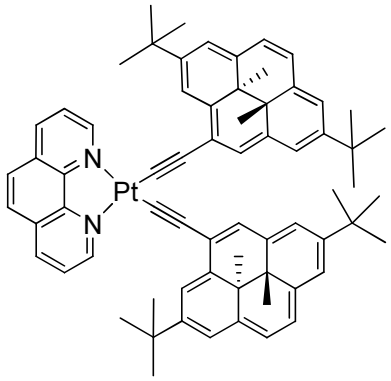
53



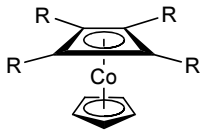
54



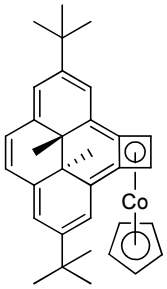
55



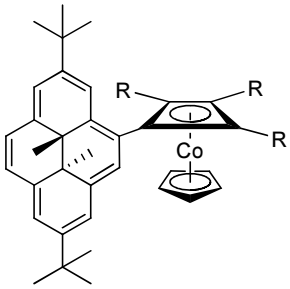
56



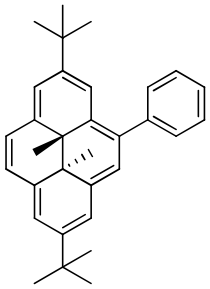
57



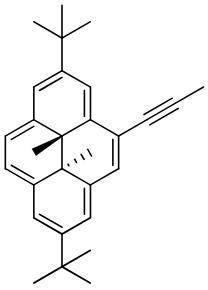
58



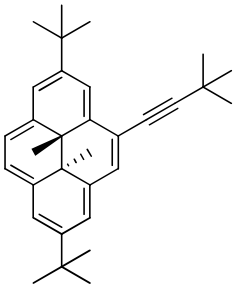
59



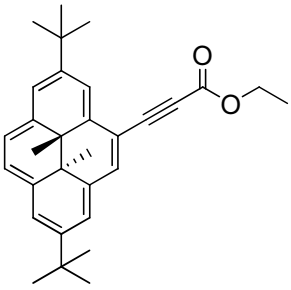
60



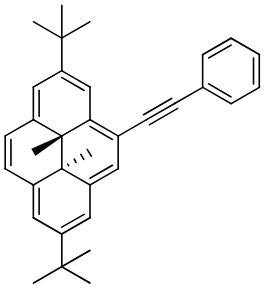
61



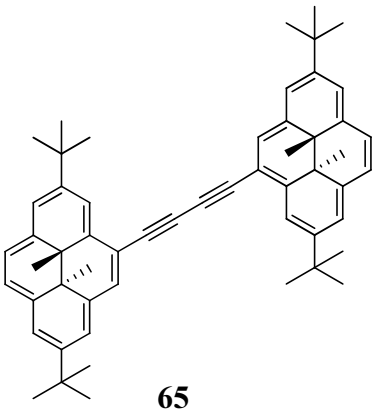
62



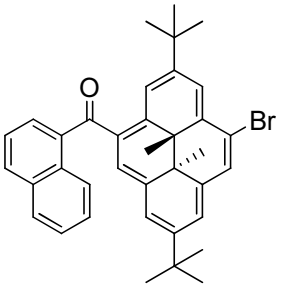
63



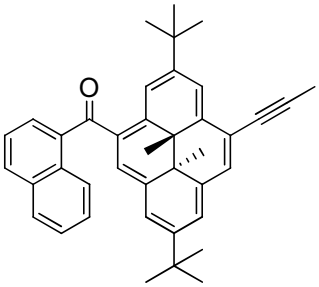
64



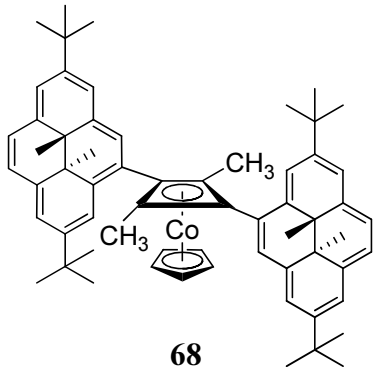
65



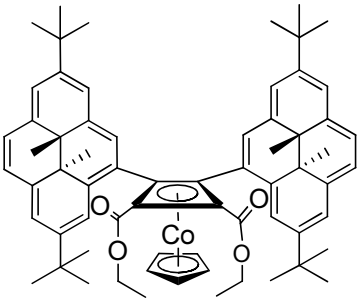
66



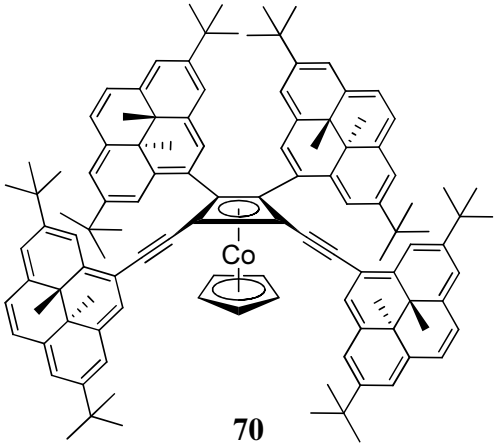
67



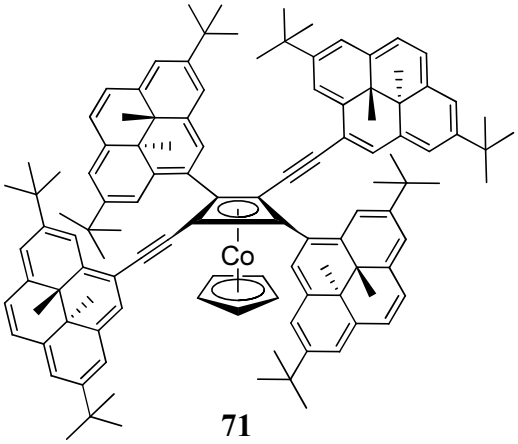
68



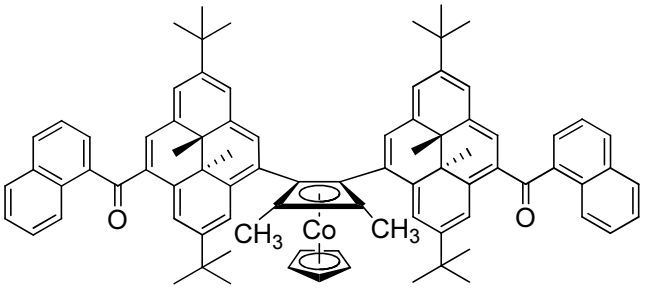
69



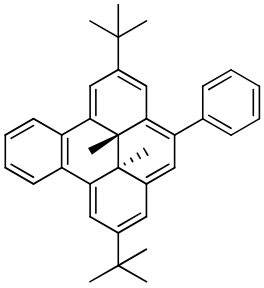
70



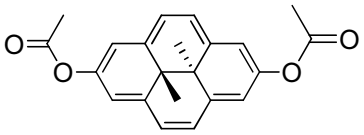
71



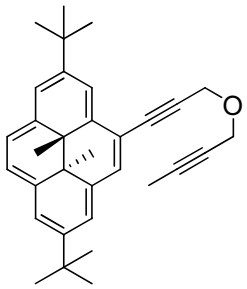
72



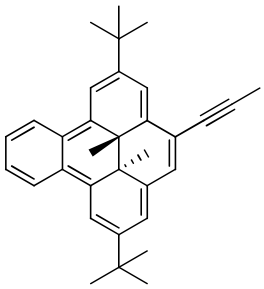
73



74



75



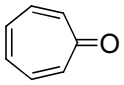
76



77



78



79



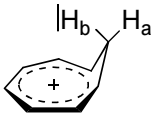
80



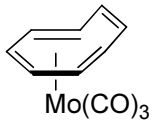
81



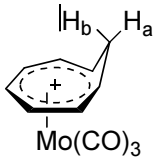
82



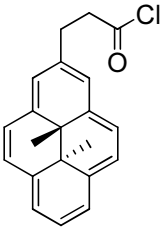
83



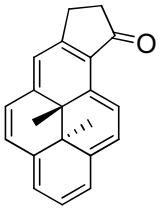
84



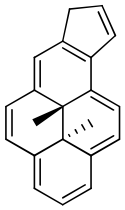
85



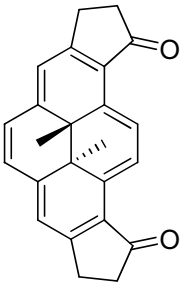
86



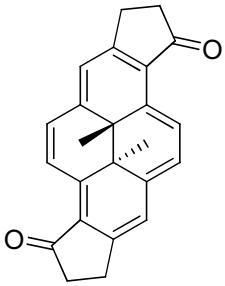
87



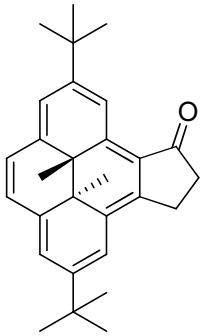
88



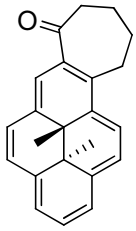
89



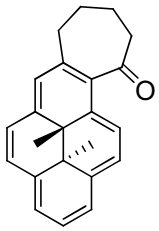
90



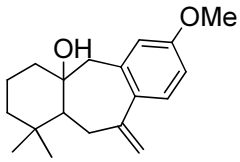
91



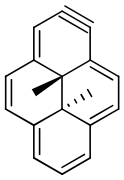
92



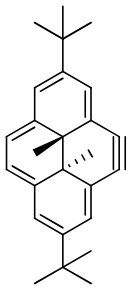
93



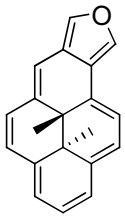
94



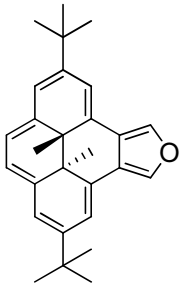
95



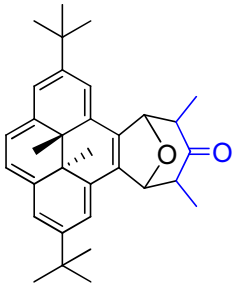
96



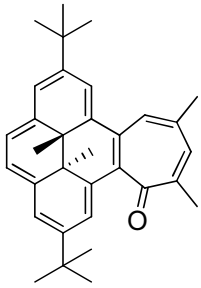
97



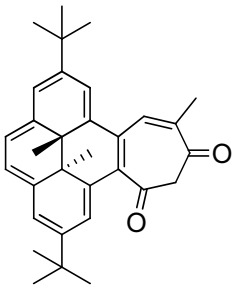
98



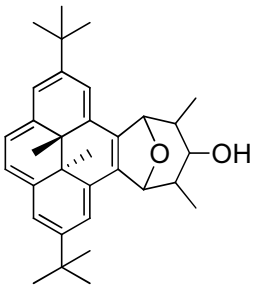
99



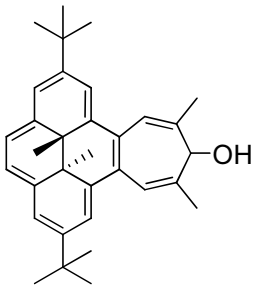
100



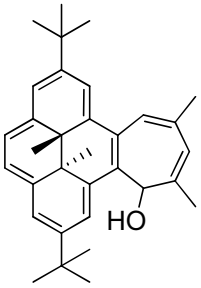
101



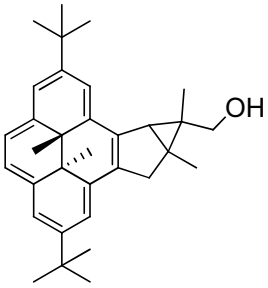
102



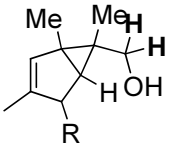
103



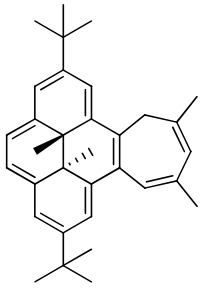
104



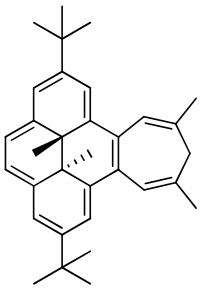
105



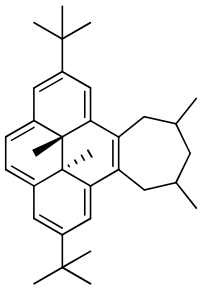
106



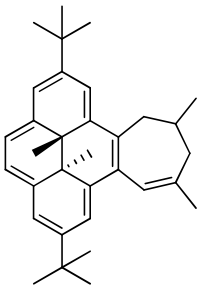
107



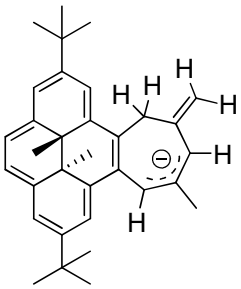
108



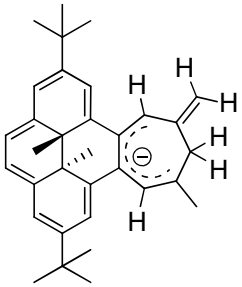
109



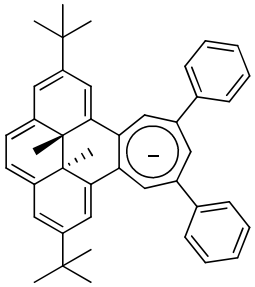
110



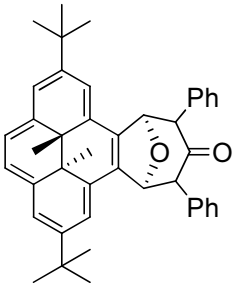
111



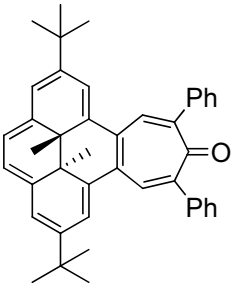
112



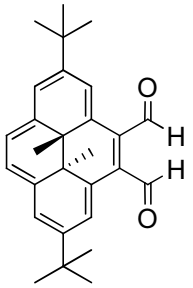
113



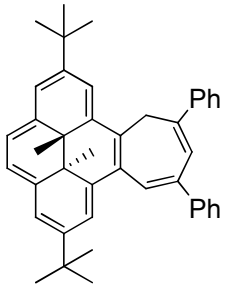
114



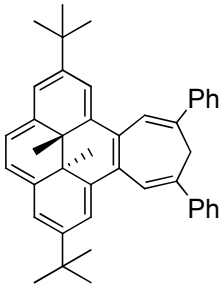
115



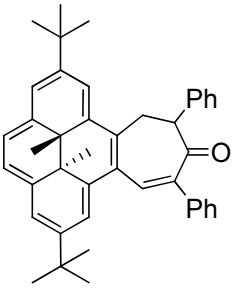
116



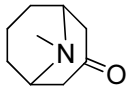
117



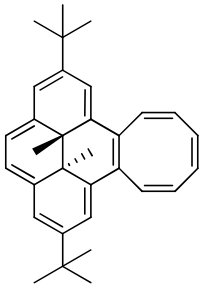
118



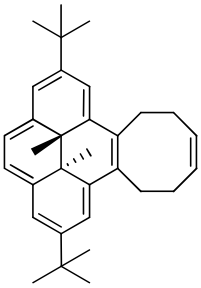
119



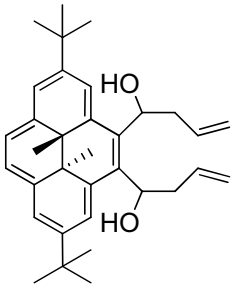
120



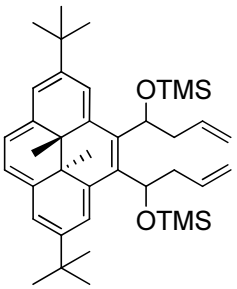
121



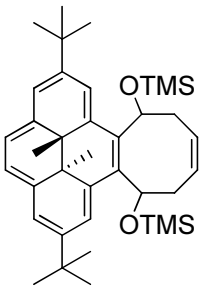
122



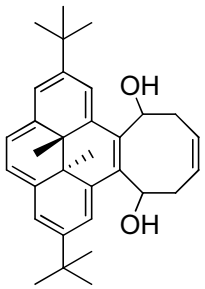
123



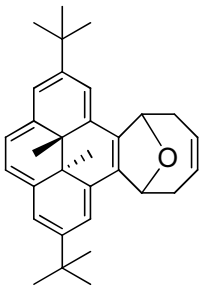
124



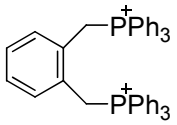
125



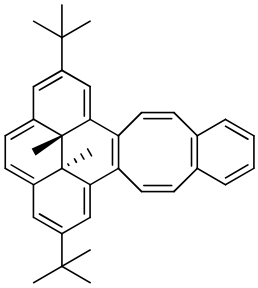
126



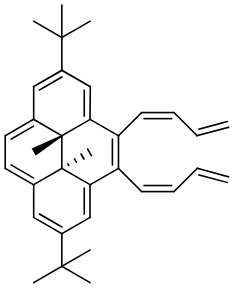
127



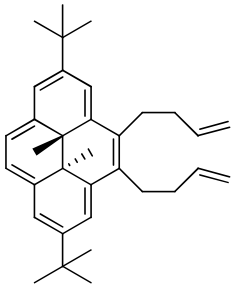
128



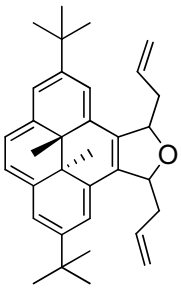
129



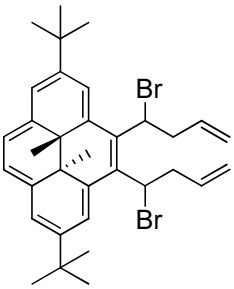
130



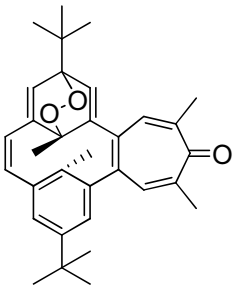
131



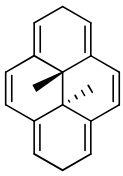
132



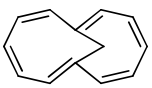
133



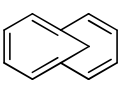
134



135



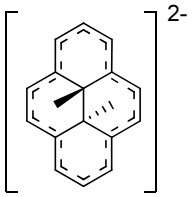
136



137



138



139

List of Abbreviations and Symbols

Symbol	Definition
Å	Angstrom
BDHP	Benzo[e]dimethyldihydropyrene
bp	Boiling point
bs	Broad singlet
c	Closed
Cbd	Cyclobutadiene
CHT	Cycloheptatriene
COD	Cyclooctadiene
COSY	Correlated spectroscopy
COT	Cyclooctatetraene
CPD	Cyclophanediene
d	Deuterium
d	Doublet
DCM	Dichloromethane
dd	Doublet of doublets
de	Diastereomeric excess
dec	Decomposition
DEPT	Distortionless enhancement of polarisation transfer (NMR)
DFT	Density functional theory (calculations)
DHP	Dihydropyrene

DMF	Dimethyformamide
EI	Electron impact
Et	Ethyl
EtOAc	Ethyl acetate
EtOH	Ethanol
E	Entgegen (*trans* orientation of high priority groups on alkene, Cahn-Ingold-Prelog Nomenclature)
eV	Electron volts
E_{act}	Energy of activation
FG	Functional group
GS	Ground state
HMBC	Heteronuclear multiple bond correlation
HOMO	Highest occupied molecular orbital
HRMS	High resolution mass spectrum
HSQC	Heteronuclear single quantum coherence
IR	Infrared
J	Coupling constant
LUMO	Lowest unoccupied molecular orbital
M	Molecular ion
MeLi	Methyl lithium
Me	Methyl
MeI	Methyl iodide
MeO	Methoxy

MeOH	Methanol
mp	Melting point
MS	Mass spectrometry
MV	Methylviologen
NBS	N-bromo succinimide
n-BuLi	*normal* butyl lithium
NMR	Nuclear magnetic resonance
NOESY	Nuclear Overhauser enhancement spectroscopy
Np	1-Naphthyl
n/o	Not observed
o	Open
P	Photochemically reversible
Ph	Phenyl
ppm	Parts per million
Pr	Propyl
pss	Photostationary state
q	Quartet (NMR)
R	Rectus (clockwise orientation of high priority groups, Cahn-Ingold-Prelog Nomenclature)
R	alkyl
R_f	Retention factor
r.t.	Room temperature
s	Singlet (NMR) or seconds

S	Sinister (counter clockwise orientation of high priority groups)
s	Suprafacial (pericyclic reactions)
S/N	Signal to noise ratio
t	Triplet (NMR)
T	Thermally reversible photochrome
TEA	Triethyl amine
THF	Tetrahydrofuran
TIPS	Triisopropylsilyl
TLC	Thin layer chromatography
UV	Ultraviolet
vis	Visible
VT	Variable temperature
ε	Extinction coefficient (L mol^{-1} cm^{-1})
λ_{max}	Maximum wavelength absorption
Δ	Heat
δ	Chemical shift in ppm from standard
Φ	Quantum yield
$\Delta H^{\ddagger}$	Enthalpy of activation
$\Delta S^{\ddagger}$	Entropy of activation

Acknowledgments

I would first like to thank my supervisors Professors Reg Mitchell and David Berg for their guidance, assistance and encouragement during the course of my PhD studies.

I would like to thank Chris Greenwood for her training and assistance in doing NMR spectra. I also would like to thank all the group members of the Mitchell and Berg groups and the department staff. I would like to thank Dr. Brendan Twamley (University of Idaho), Dr. Brian Patrick (University of British Columbia) and Dr. Allen Oliver (University of Notre Dame) for X-ray structure determinations. I would like to thank Yun Ling (University of British Columbia) for mass spectrometric analysis.

Financial support from the Department of Chemistry, the University of Victoria and NSERC is gratefully acknowledged.

Dedication

To Jin Zou and Brandon Yichi Zhang

My parents and parents-in-law

Chapter 1. Introduction

1.1 Introduction

Reversible molecular switching between two isomeric states has potential usage in logic components at the molecule level so as to replace existing silicon materials in building computer chips[1] with a "bottom-up" approach.[2] Electron delocalization energies, particularly ring current energies in cyclic molecules, have very important contributions in switchable systems.[3] Organic based substances are interesting in that they functionalize at the single molecular level and have tunable functions.[3-4] These features are motivating scientists to explore switchable molecules.

1.1.1 Molecular switches

Molecular switches[1b] describe a substance that can be toggled between two isomeric forms, usually accompanied by color changes, with a variety of triggering stimuli. Light (photochromism), heat (thermochromism), electrical current (electrochromism), chemical reagents (chemochromism etc.) and mechanical actions (peizochromism etc.) were successfully used in such reversible transformations.[5] Practically, the superiority of light for data storage is due to its intrinsic physical properties, which include high speed, accuracy and selectivity.[6] Data transfer[7] and data storage[8] are two basic aspects to address in applications based on light. The former involves conversion of electronic signals to photonic information. The latter is about electronic transition processes in the form of photoisomerization. This latter phenomenon is widely interpreted as photochromism and these molecules are frequently referred to as photoswitches. Electrochromism[9] is often a useful additional feature of some photoswitches that provides another trigger for the switching process.[10]

1.1.2 Some remarks associated with photochromism

It wasn't until the 1950s that the term "photochromism" was coined by Hirshberg,[11] even though the phenomenon was first discovered in the late 1880s. Photochromism[12] refers to the reversible transformation of a chemical species between two or more isomeric forms in response to irradiation at different wavelenghs. The process essentially involves chemical reactions that break and re-form bonds intramolecularly. Chemically, it can result in stereochemical rearrangement or changes in electronic conjugation and electron delocalization. Only incident light with the proper wavelength can excite the ground state of a molecule to the excited state and so begin a chemical event. The lowest energy absorption bands are usually more interesting in that each of the isomeric forms absorbs in distinctive visible or near visible regions of the electromagnetic spectrum.

During photoswitching cycles, a single isosbestic point indicates clean interconversion with a single reaction intermediate (Figure 1). For example, irradiation at the absorption maxima (700 nm for **B** in Figure 1) of one isomer allows for complete conversion to the other isomeric form **A**, provided there is no overlap in their absorption spectra. Stimulation at a wavelength (around 400 nm in Figure 1) where both isomers absorb results in an equilibrium between the two isomers, called a photostationary state.

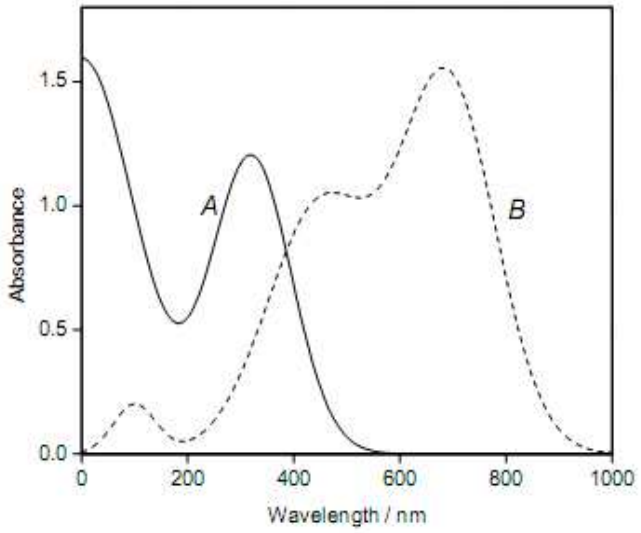


Figure 1. The typical absorption curves for two forms of photochromic compounds

When the absorption maxima of the more thermodynamically stable form **B** in Figure 1 takes place at a longer wavelength than the less stable isomer, this class of photoswitch is called negative photochromism. If the opposite is true, then this is referred to as positive photochromism. This property not only can often cause coloration/decoloration cycles as in dyes, but more importantly it can be used to switch the states of molecular devices. For example, a photoswitch can turn on and off such properties as fluorescence,[13] refractive indices[14] and dielectric constants.[15] Therefore, photochromic compounds are often regarded as photoswitches. In the cases where rupture of a single bond or shift of double bonds is involved in the course of photoirradiation, the state with the ruptured sigma bond is referred to as the open form. The corresponding state with formation of a new sigma bond is referred to as the closed form.

Heat may also trigger a transformation in some molecular switch systems.[16] If the energy barrier for the isomerization is sufficiently low, conversion to the thermodynamically more stable isomer will occur without light. Such dark reactions are a major drawback. For photoswitches in data storage applications, where bistable forms are desired. Practically this may cause information loss in data storage applications. The corresponding photoswitches are classified as T-type, in which the thermally reversible processes are concomitant with the photochemical reaction. In rare cases, when no thermal process is concurrent during the course of photochemical processes, they are referred to as P-type photochromic compounds (photochemically reversible). Theoretically it is possible to adjust the height of the reaction barrier by chemical modifications so it should be possible to suppress the dark reaction.

1.1.3 Photochromism and aromaticity

Aromaticity is often related to photochromism as illustrated by Irie's prediction and successful development of dithienylethane photoswitches.[3] With regard to bistability of the photoisomers of the diarylethene photochromic systems, the five-membered ring heteroaromatic thiophene is the best aromatic moiety among thiophene, furan and benzene based on calculations. Almost all known photochromism processes involve

changes in electron delocalization or aromatic features relevant to electron delocalization. Two important features associated with each photoisomer are the longest wavelengths of absorbed light (often the color) and their stability towards a thermal back reaction. These properties are determined by the energy levels of the system which are often related to the aromatic properties of the heteroaromatic groups in the diarylethene type photoswitches. Therefore, an understanding of aromaticity and electron delocalization is fundamental in finding new photochromic system and in modifying their properties.

1.1.4 Electrochromism

Electrochromism[9] describes the phenomena where reversible conversion takes place between two markedly different colored species upon electron uptake (reduction) and electron loss (oxidation) with the passage of appropriate electrical current.[17] Electrochromic molecules display distinct electronic absorption spectra at different oxidation states because of the feasibility of either internal electronic excitation or inter-valence charge transfer along the molecules. They have already been used in the manufacture of anti-glare rear-view mirrors, sunglasses, and battery state-of-charge indicators.[18] They have potential usage in video displays but so far all the required criteria for their application have not been met. Many electrochromic materials in use today are based on polypyridyl metal complexes and inorganic metal oxides, such as tungsten trioxide. Readily available organic viologens[4] (1,1'-disubstituted-4,4'-bipyridinium salts) represent the organic chromophore compounds. They exhibit excellent electronic absorption features in applications where the colorless dication species and the intensely colored radical cation species are intercoverted by one-electron reduction or oxidation processes. Some nitrogen, oxygen, and sulfur containing compounds also demonstrate interesting electrochromic properties.

1.2 Known photochromic (photoswitchable) systems

Photoexcited species may undergo reactions such as cycloaddition, pericyclic reactions, *trans*/*cis* isomerizations, intramolecular group transfers, dissociation (radicals), electron transfers[19] (oxidation-reduction), and quenching. Chemically, most molecular switches involve one or more of the reactions in the above list. Photochemically induced *trans*/*cis* isomerization and pericyclic reactions are the two main processes in molecular switches to be discussed in this context. Intramolecular group transfer and cycloaddition reactions take place commonly as side reactions in some photoswitchable systems.

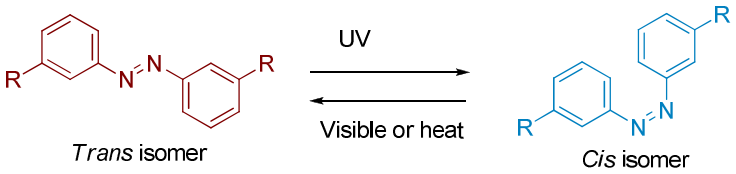
Photochromic switches can be divided into two groups on the basis of the associated photochemical reactions. A large number of analogs of azobenzenes, spiropyrans and spirooxazines involve just photoisomerization and are called type I photochromic compounds. In contrast, derivatives of fulgides, dithienylethenes and dimethyldihydropyrene belong to type II photochromic compounds and these undergo pericyclization reactions.

The mechanism of *trans*/*cis* photoisomerization is debatable.[20] Nevertheless, either lone pair or π electrons are promoted to the π^* orbitals in response to appropriate irradiation. Both n-π^* and π-π^* excitation would weaken the related double bonds and allow a rotation. The excited states adopt thermodynamically favorable low energy geometries, where the substituents are in orthogonal positions. The decay of energy leads to the reformation of the double bonds in both *trans* and *cis* isomers. Upon selective irradiation of one of the two isomers, it converts to the other isomer. Presumably, the π-π^* transition is more efficient in promoting this conversion as the remaining bond is expected to be much weaker than in the n-π^* case although other factors also many play important roles in this regard.

1.2.1 Azobenzene

Azobenzene derivatives belong to T-type photoswitches.[12] Only the *trans* isomer exists in the dark at room temperature. The difference in ground state energy of the two

isomers is caused by a large difference in their molecular shapes. The *trans* isomer forms a planar structure with the π electrons delocalized along the two benzene rings and two nitrogen atoms. In contrast, steric repulsion between the aromatic rings in the *cis* isomer twists the phenyl rings with respect to the N=N double bond and electron delocalization is disturbed, resulting in a higher ground state energy (Scheme 1).

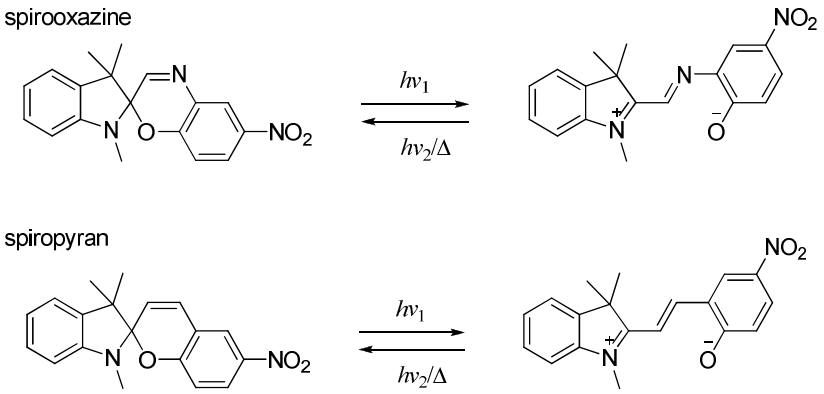


Scheme 1. The photoswitching between azobenzene isomers

Zimmerman[21] has investigated the quantum yield dependence of the reversible isomerization processes on varying the irradiation light wavelength, light intensity and sample concentration. The quantum yields show only a wavelength dependence ranging from 0.10 to 0.50. The UV-Vis spectra for the two isomeric forms are significantly different[22]. *Trans*/*cis* isomerization originates in the promotion of one electron into the π^* orbital, resulting in rotation around the N-N bond due to the lower bond strength in the excited state. In the *trans* isomer, the negligible absorption that occurs in the visible region is ascribed to the orbitally forbidden n-π^* transition and an absorption at 320 nm is due to an allowed π-π^* transition that tailed into the visible region. It is noteworthy that there is no significant absorption from the *cis* form at this wavelength. The conversion sensitivity depends on both the molar absorption coefficients and the quantum yields. Therefore, irradiation by 320 nm UV light leads to a fast increase in intensity of the 440 nm transition associated with the *cis* form. Irradiation with 440 nm wavelength visible light converts the *cis* isomer to the *trans* form. Besides causing color changes, photoisomerization also changes other properties, such as dipole moment, conductance and shape. Recently, studies have mainly focused on its applications in biology,[23] to polymers, and to nanomaterials. In the nanotechnology field, photoisomerization has been used to trigger a mechanical motion of a film or liquid droplet due to large volume change between the two isomers.[24] However, the opening is usually slow or blocked in

the crystalline state, probably because of crystal packing forces. Nevertheless, pulsed laser irradiation with high photon density allowed the isomerization process to be carried out in a solid gel due to cooperative photoisomerization. [25]

1.2.2 Spiropyrans and spirooxazines

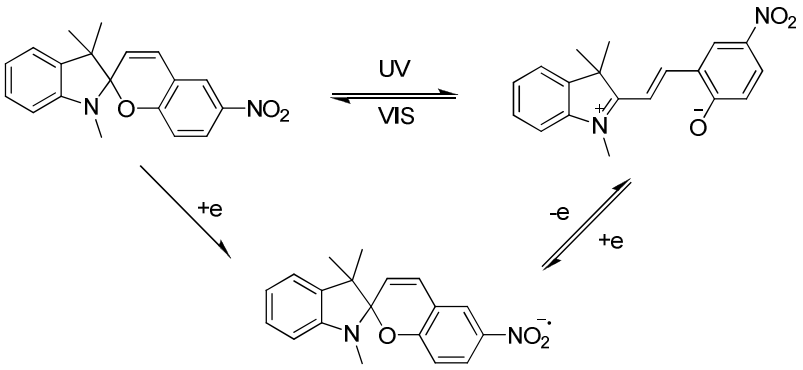


Scheme 2. Spirooxazine and spiropyran photochromic compounds

Spirooxazines and spiropyrans are differentiated in that either a carbon (pyran) or nitrogen (oxazine) is at the methine position of the six-membered ring off of the spiro-carbon atoms (Scheme 2)[26]. Both generally fall in the same family of T-type photochromic switches. In the colorless closed state, the electrons localize, as an orthogonal relationship exists between the two adjacent rings. In this form, spirooxazines and spiropyrans usually absorb in the 200-400 nm range.[27] The open state, generated upon irradiation with UV light, is known as a merocyanine and is a conventional dye known for its intense color. Open forms of both systems revert to the closed form in response to appropriate visible light irradiation or heat. Due to the overlap of the absorption band in the opened and closed forms, photostationary states often exist. The yield and absorption maxima of the open form depends on the solvent polarity because photoswitching results in a dramatic dipole moment change.[28]

The combination of photochromic and electrochromic switching has been realized by incorporating redox-active organic functional groups into photochromic systems. The redox properties are dependent on electronic distribution. Therefore, the functional

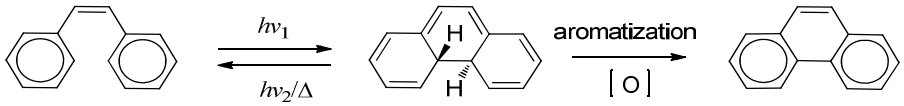
groups in the open and closed species exert different effects on the electronic properties. Fujishima[29] reported that spiropyrans bearing a nitro group are both electrochromic and photochromic (Scheme 3). The colorless ring-closed spiropyran underwent irreversible one-electron reduction to the radical anion. In contrast, a reversible redox process occurred between the radical anion and the ring-opened merocyanine. This is a rare case in which the electrochromism took place involving an organic functional nitro group ($-NO_2$).



Scheme 3. The electrochromism associated with spiropyran photochromic compounds

1.2.3 *Cis*-stilbene

Photochromic stilbenes represent the prototype of modern diarylethene type photochromic compounds. Beside the *trans*/*cis* photoisomerization of stilbene, the *cis* isomers also undergo a photochemical pericyclization giving rise to a closed dihydrophenanthrene.[30] It has to be stressed that the electrons are localized in the closed state, which has a large gap between HOMO and LUMO orbitals. The absorptions of both isomers occur only in the short wavelength UV region, so these are colorless compounds. The interesting aspect of *Z*-stilbene is its reversible electrocyclization conversion in the absence of oxygen (Scheme 4).



Scheme 4. The photochemical pericyclization of Z-stilbene

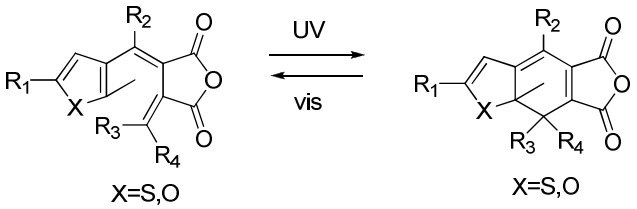
UV light irradiation promotes the ring closing process, while ring opening occurs with visible light. The loss of the aromatic rings in the closed form makes this a higher energy species that thermally reverts back to the open form with a half life $\tau_{1/2}$= 1.5 min at 20ºC.[31] When oxygen is present, aromatization takes place to form a thermodynamically more favorable aromatic phenanthrene with elimination of the hydrogen. The process, however, is an irreversible side reaction.

In order to produce photoswitches with better stability, two approaches to modify stilbene have been taken. The photochemical removal of alkyl groups requires much higher energy than removal of hydrogen, so introduction of substituents such as methyl at the internal positions results in a more stable photoswitch. Fulgides, dithienylethenes and dimethyldihydropyrenes, all have *non*-hydrogen substituents in the internal positions and have useful applications. The second approach is to eliminate unwanted photoisomerization reactions by locking the geometry of the double bonds. This is well-demonstrated in the dithienylethene and dimethyldihydropyrene systems. In the former, a ring prohibits isomersation of the double bond, while in the latter, a tether doubled bond was added to the molecule to lock the double bond in the *cis* geometry. The following three systems: fulgides, dithienylethene and dimethyldihydropyrene, are put in the same group because of the similarity of the arene moieties in the ring system. The driving force to regain aromaticity in the closed form becomes an obvious driving force for thermal back reactions for many of these systems.

1.2.4 Fulgides

Fulgide switches are composed of compounds bearing one aromatic ring on a *bis*(methylene)succinic anhydride core (Scheme 5).[32] It resembles the dithienylethene class of photoswitch discussed in the next section. Stobbe[33] first synthesized and

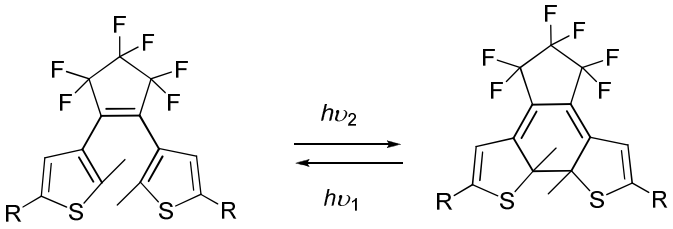
studied the phenyl substituted fulgides in the 1900s. They represent the types of switches that have two processes: *cis/trans* isomerization or 6π-electrocyclization. The substituents have a marked affect on the color and the photocoloration.[34] UV light irradiation drives both the isomerization and the hexatriene ring closing cyclization. Fulgides have been shown to be thermally stable photochromic compounds.



Scheme 5. Fulgide photochromic compounds.

1.2.5 1,2-Dithienylethenes

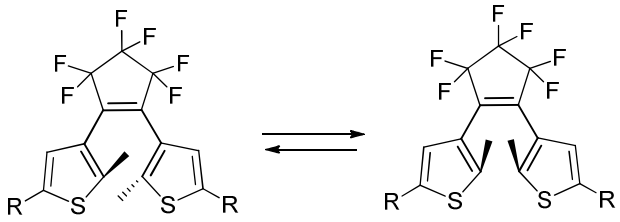
Dithienylethenes[35] are positive P-type electrocyclization photochromic compounds (Scheme 6). The diarylethene analogs where the thiophenes are replaced with other aromatic systems are less explored.[3]



Scheme 6. A dithienylethene photoswitch with a perfluoro-C5 ring.

The generality among them lies in their having a cyclic unit to lock the ethene bridge. Photochromic substances having different side rings exhibit different properties, such as a tunable absorption maximum (i.e., difference in color).[3] It is noteworthy that the absorption maxima and the closing quantum yields are dependent on the size of the ring involving the double bond. The dithienylethene with a C6 ring gave rise to the largest quantum yield and blue shift of the absorption maxima among the perfluoro-C4, C5 and C6 ring structures.[3] The reason was attributed to the planarity and the resulting electron

conjugation. The dithienylethenes bearing a perfluorocyclopentene proved to be one of the best in terms of overall properties. The thermal stability is accounted for by the minor energetic difference between the two states with the carefully chosen thiophene moieties. The extended electron delocalization in the closed form compensates for the destabilization from loss of two aromatic thiophenes in the open form, in contrast to *cis*-stilbene. The aromatic stabilization energy for a thienyl group is only 4.7 kcal/mol, compare to 27.2 kcal/mol for a phenyl group, so the destabilization in the closed dithienylethenes is much less than that of *Z*-stilbene during closing. In addition, the dithienylethenes show excellent fatigue resistance.[3] The best compound has been cycled 10^4 times without loss of photochromic performance.

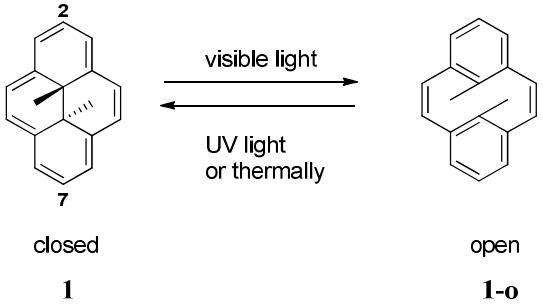


Antiparallel Parallel

Interconversions between the antiparallel (C2 symmetry) and parallel (Cs symmetry) conformations can occur in the open form. This contributes to the photoclosing quantum yields being usually less than 0.5. The visible light opening quantum yields are generally less than 0.1, smaller than the closing quantum yield by an order of magnitude or more. Because of extending electronic conjugation to dangling side chains in the thiophene the quantum yield drops in the closing process with dangling groups on the thiophenes. The electrons in the anti-bonding orbital are spread over a larger molecular surface rather than localized on the central breaking bonds.

1.2.6 *Trans*-dimethyldihydropyrene

Trans-dimethyldihydropyrene 1 (parent DHP) is a photoswitch that undergoes reversible photochemical opening and closing cycles[36] (Scheme 7). Note that the absolute stereochemistry of the internal methyl goups were not established. Both *trans* DHP isomers present unless it is specified.



Scheme 7. Photochemical properties of *trans*-dimethydihydropyrene 1

Upon intense visible irradiation at 436 nm, parent DHP opens to the colorless metacyclophandiene 1-**o** (CPD) with low quantum yields. CPD 1-**o** reverts to *trans*-DHP 1 on irradiation with UV light (254 nm). The UV light closing process is exceptionally fast and efficient with quantum yields of 0.4-0.6 in hexanes. In addition the CPD 1-**o** closes thermally at room temperature to the more stable parent DHP 1 because of the greater stability of the fully delocalized 14π annulene DHP form.[36] The parent DHP 1 exists as thermally stable, green crystalline needles at room temperature. The CPD 1-**o**, comprised of two isolated aromatic benzene rings with two vinyl bridges, only absorbs in the UV region and is therefore the colorless form. Since the more thermally stable closed form 1 absorbs at a longer wavelength than the open form 1-**o**, the DHP systems belong to the rare negative type of photochrome. The 6 π-electron, Woodward-Hoffmann forbidden thermal closing process is common in known DHP systems with a half life for closing spanning from minutes to years. For example, the half life of 1 was found to be 52 hours. Experimental results[37] and calculations[38] suggested that this thermal process involves excited intermediates with obvious radical character. So radical stabilizing groups in place of the internal methyl groups dramatically change the photochemical properties. In many cases, CPD derivatives have a half life for thermal closing that meets the requirements for characterization methods such as NMR and UV-vis spectroscopy. The typical energy difference favors the closed form over the open form by about 3 kcal mol^{-1}. In comparison to other photochromic compounds, the DHP-derived systems show several superior features. For example, DHPs usually open and close completely and no photostationary states take place.

Among the peripheral skeletal carbons, calculations have shown that the 2 and 7 carbons have the highest electron density and so are the most competitive sites for electrophilic reactions. In order to react selectively at other positions, carbons 2 and 7 are blocked by introducing *tert*-butyl groups, i.e. 2,7-di-*tert*-butyl-*trans*-dimethyldihydropyrene 2 (DHP) (Figure 2). More importantly, the synthesis of DHP 2 is more efficient on a large scale than for parent DHP 1. With optimized reaction conditions, one reaction sequence can give more than 10 grams of DHP 2 in contrast to a few hundred mg of the parent DHP 1. The development of DHP 2 was so important that it resulted in a breakthrough in the field of DHP-based photochromic compounds. Molecules bearing much better photochromic properties were synthesized based on this di-*tert*-butylDHP skeleton, including for instance the 2,7-di-*tert*-butyl-*trans*-dimethyldihydrobenzo[e] pyrene (BDHP) 3 and 4-acyl DHP series (Figure 2).

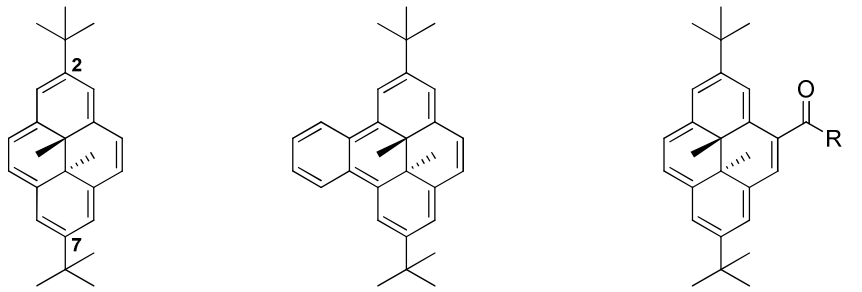


Figure 2. The 2,7-di-*tert*-butyl-*trans*-dimethyldihydropyrene 2, the benzo[e]-DHP 3 and 4-acyl derivatives

However, the photochemical opening rates of DHP 2 are even worse than those of the parent DHP 1. The photoopening efficiencies dropped to Φ_{open} = 0.0015 in the DHP 2 from 0.006 in the parent DHP 1 in hexanes.[39] Note that quantum yields have shown solvent dependence in some rare cases.[37] Using toluene as solvent yielded a dramatically higher ring opening quantum yield (Φ_{open} = 0.66 ± 0.02), the greatest value so far, in a 2-(1'-naphthoyl) DHP molecule and the reason for this is still beyond our understanding.[37] The quantum yields for photoopening of DHP 2 and its derivatives are often low. The photoopening process was found to take place via a singlet excited state

mechanism.[40] Structural modifications have been carried out to improve the photochemical efficiency (quantum yield) and three strategies were identified that achieved this. Modifying the central methyl groups, dangling acyl groups on the periphery and fusing aromatic groups at the [e] (side) positions were all shown to increase the quantum yield for opening substantially.

Benzo[e]DHP (BDHP **3**) is an example of a good photochromic molecule.[41] It quickly opens on visible light irradiation, shows excellent degradation resistance and undergoes a very slow thermal back reaction. As a result, it is usually used as the control molecule in photochemical tests in our group. BDHP 3 has a typical absorption for DHPs at around 400 and 500 nm (Figure 3), arising from the π-π^* transition with a modest extinction coefficient. In the open form 3-**o**, the absorptions occur mostly in the UV (Figure 3) as 3-**o** CPD essentially shows the absorptions due to isolated benzene chromophores. It is worth emphasizing that there are no significant absorptions in the 500 nm region for 3-**o** thus ensuring that complete conversion of 3 to 3-**o** occurs with irradiation at 500 nm with visible light.

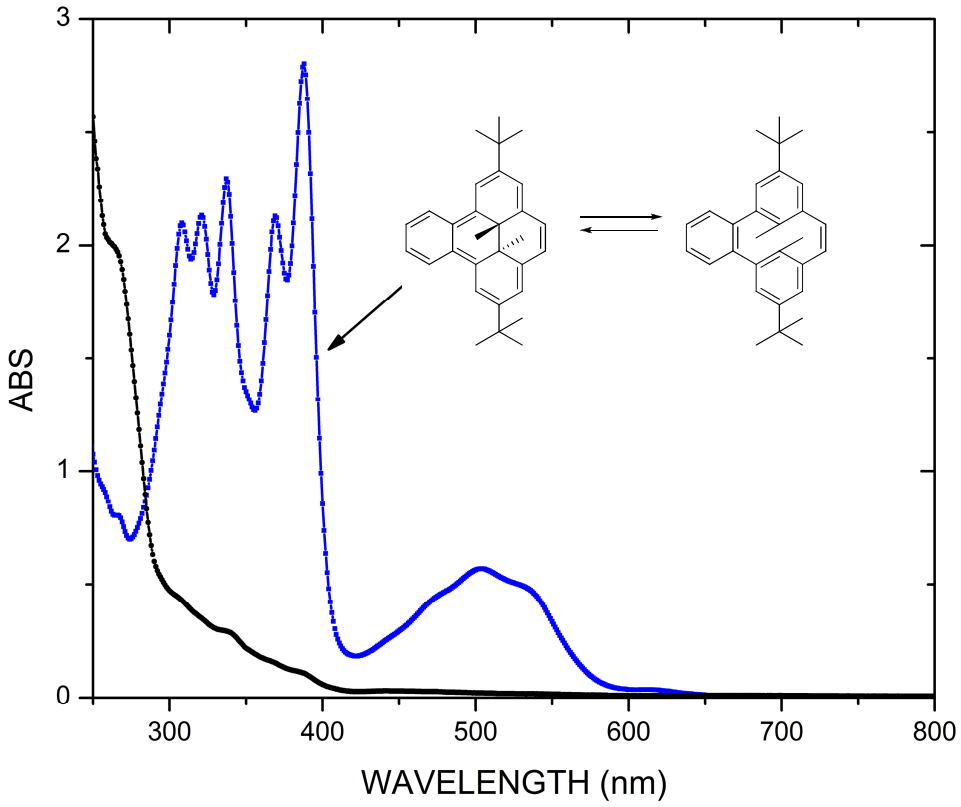


Figure 3. **The absorption spectra of BDHP 3 in closed (blue line) and open (black line) forms**

Benzannelation ensures additional resonance stabilization energy in the open form 3-**o**, diminishing the energy difference between the open form 3-**o** and the lower energy closed form 3. This allows 3-**o** CPD a longer thermal life time with an approximate half life ($\tau_{1/2}$) of one week at room temperature. It is anticipated that modifying the fused aromatic systems should lead to different photochromic features, although how such changes will alter the photochemistry is not yet predictable ahead of time.

1.3 Metal coordination complexes

Photoswitches bonding to transition metals have been explored to investigate the effects of the metal.[42] The complexation of metals on photochromic species alters their electronic properties, which may affect the behavior of the photoswitches in a positive or

negative way.[43] Conversely, it is also interesting to see if switching the photochromic state causes changes in the reactivity of the metal complexes. Metal complexes, prepared by Nishihara,[42c] generally exhibit not only the photochromic characteristics of the organic ligands, but unique properties of the metals. Metals and their complexes contain unique energy transitions between different energy levels corresponding to metal orbitals or metal-ligand orbitals. Absorption energy can be tuned by changing substituents on involved ligands. Unfortunately, metal derivatives often respond poorly on light stimulus. The reason for this is partly because electronic transitions within the ligand field states of the complex may compete with productive transitions of the organic photochrome.

1.3.1 Non-DHP based photoswitchable metal complexes

In metal complexes containing dithienylethene, spiropyran and azobenzene, the metal units usually complex to existing ligands by dangling from the photoswitch molecules.[44] Energy transfer and sensitization of the photochromic molecules have been the main focus. For example, in dithienylethene-derived $[Ru(bpy)_3]^{2+}$ complexes[45] (Figure 4), sensitized, photo-induced cyclization takes place from a triplet state localized on the bridging photochrome upon irradiation into the MLCT band of the $[Ru(bpy)_3]^{2+}$ unit. It was found that efficient energy transfer from the metal-based excited state to the dithienylethene switch caused photo-cyclization of the switch units. High quantum yields and excellent conversion rates were obtained. When the MLCT energy of the metal is lower than that required for switching the photochromic unit, such as in the analogous $[Os(bpy)_3]^{2+}$ complexes (Figure 4), energy transfer occurs from the photochromic unit to the metal center thus reducing the photoreactivity. This exploration was used to fabricate new systems including the heterodinuclear metal units, $[Ru(bpy)_3]^{2+}$ and $[Os(bpy)_3]^{2+}$.[46] Energy transfer occurs from the higher energy $[Ru(bpy)_3]^{2+}$ end to the $[Os(bpy)_3]^{2+}$ end through a dithienylethene (in the open form) bridge. In contrast, energy ends up at the dithienylethene photochromic unit when the dithienylethene was in its closed form.

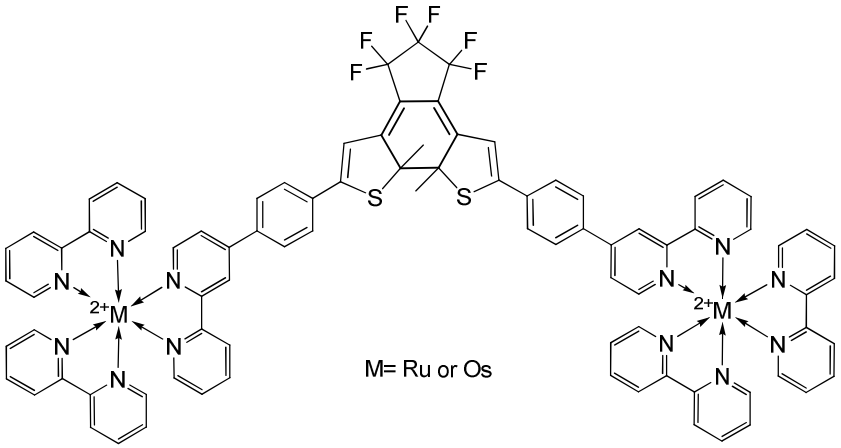
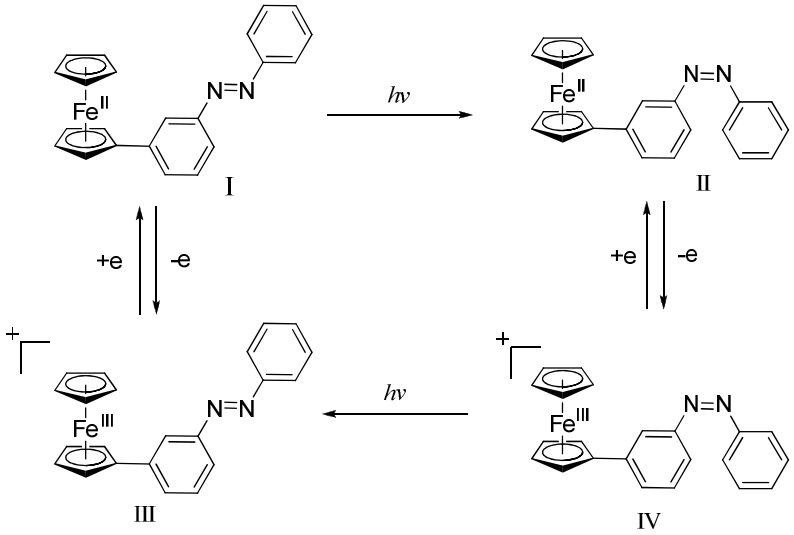


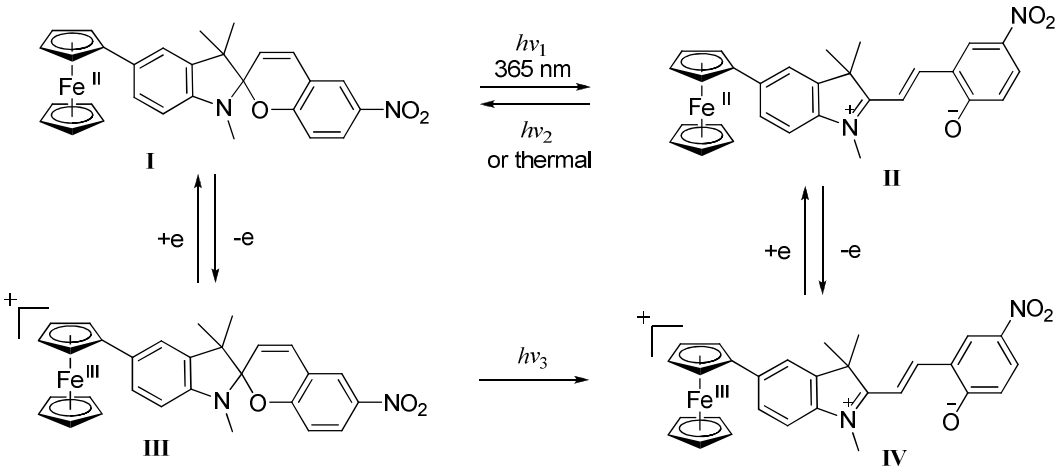
Figure 4. Dinuclear Ru/Os complex containing a dithienylethene derivative as bridging ligand

These results seem sensible in explaining the photoswitching behaviour of many metal complexes. However, photoswitching remains unpredictable as subtle changes can alter the photochromic behaviour. In dinuclear terpyridine complexes containing a dithienylcyclopentene, those with Ru and Fe (II) showed no cyclization in response to UV light irradiation, but they could be cycled electrochemically. In contrast, the Co (II) complex underwent photo-cyclization only, while the Os (II) complex appeared inert both photochemically can electrochemically. Even more confusing, mononuclear complexes containing *one* Fe or Co terpyridine unit are both photochromic and electrochromic.[42d]



Scheme 8. The azobenzene-derived metal complex photoswitches

Attaching a ferrocene unit to different types of photochromic molecules is well established. In ferrocenyl azobenzene (Scheme 8), the UV-Vis spectrum shows two strong absorption bands assigned to a π-π* transition of the azo group and a MLCT (d_{Fe}-π*) transition, respectively.[47] Remarkably, green light (546 nm) promotes *trans/cis* isomerization by irradiation at the edge of the MLCT bands, and also reverts ferrocenium complexes **IV** to **III** (Scheme 8). The different responses to green light let the complexes consisting of $[Fe(C_5H_5)_2]$ (Fc) and $[Fe(C_5H_5)_2]^+$ (Fc^+) reversibly isomerize at a single visible light wavelength by combining with the reversible redox reaction of ferrocene.



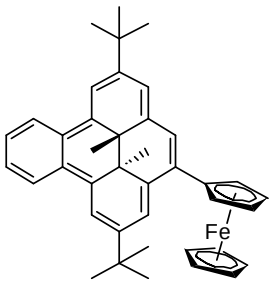
Scheme 9. The spiropyran-derived metal complex photoswitches

The spiropyrans with dangling Fc and Fc^+ moieties act reversibly and irreversibly, respectively, upon irradiation.[48] The spiropyran derivative **I** (Scheme 9) is converted into the colored open form **II** upon irradiation with UV light in 50-80% yield, but reverts to **I** in the dark or upon irradiation with visible light. Combining the reversible photoisomerization **I/II** and Fc/Fc^+ redox cycle completely stabilizes the open form **IV**.[48] Complete conversion to the open form **II** was reached by irradiation. The reason for the stabilization of **IV** by Fc^+ is not fully understood. The authors claimed that π conjugation might contribute to stabilization based on the large blue shift of λ_{max} in **III** relative to **II**. In general, the open form of spiropyran has a larger dipole moment than the closed form, and thus the open form can be largely stabilized by the electronic effects of

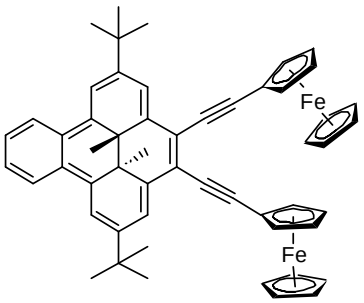
substituents on the indolium and phenyl moieties as well as by increasing the solvent polarity.

1.3.2 DHP-derived photoswitches containing metals

DHP photochromic compounds containing directly appended, or triple bond linked, ferrocene have been synthesized. The ferrocenylBDHP 4 does not open and photochromism is shut down by the pendant ferrocene.[49] However, Nishihara[50] has shown that the BDHP derivative *bis*(2'-ferrocenylethynyl)BDHP 5 having two ferrocenes connected by a conjugated acetylene linker is photochromic and electrochromic, and

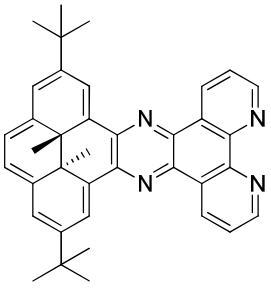


4

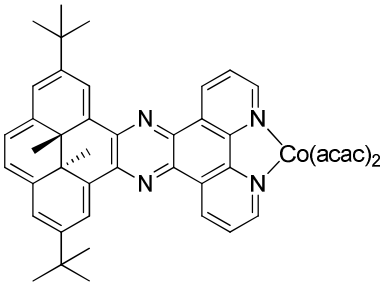


5

exhibits switchable electronic communication between the two ferrocene moieties. However, appending pentamethylferrocene in an analogue of 5 quenches the excited state of the BDHP and the compound no longer opens or closes. The stronger electron donating ability of the pentamethylferrocene compared to Fc probably accounts for the shut-down in photochromism.



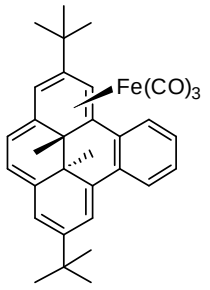
6



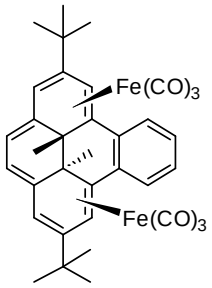
7

Saretcheyva[51] has studied some metal complexes based on phenanthroline-fused conjugated DHP systems and dangling phenanthroline-DHP systems with a alkyne spacer. The phenanthroline-fused to the side of the DHP molecule as in **6** alters the conjugation and therefore the photochromism. The UV-Vis spectrum of **6** shows that the typical absorption peak around 500 nm is less intense than usual and tails to 800 nm. A photostationary state was reached (44% open form) on irradiation of a NMR sample of **6** for 80 h. It was also noted that the opening rate of 6 was only about 30% that of BDHP. The cobalt complex 7 opened about 7 times slower than the ligand 6 itself and also reached a photostationary state with nearly 40% open form.

It was found that the BDHP itself acts as a good olefinic ligand in a series of iron complexes (8, 9). Zhang[52] explored BDHP coordination with $Fe(CO)_3$ to form

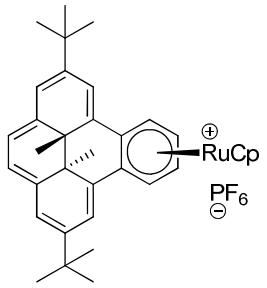


8

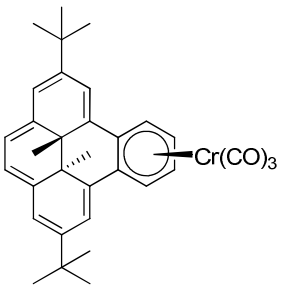


9

complexes 8 and 9, but in this case the complexes did not show any photochromic properties. Some of the iron complexes degraded and slowly lost the $Fe(CO)_3$ fragment in air.



10

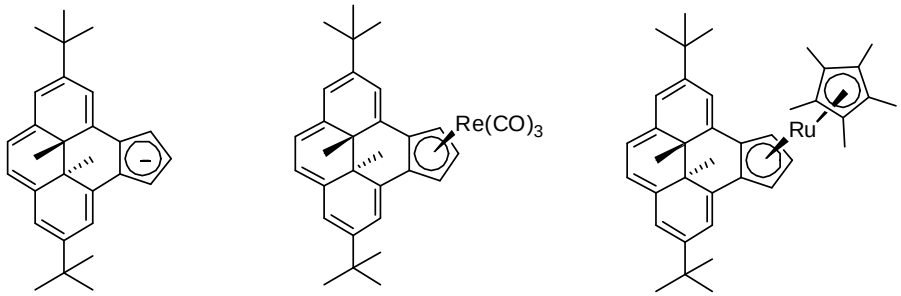


11

Complexation of DHP photoswitches to metals was also shown to occur with the corresponding furan- or benzene-fused DHPs at both the [a]-position and [e]-positions in the Mitchell group.[53] The BDHP and cyclopentadienide-fused DHP metal complexes are

more interesting because they demonstrate different photochemical properties with variation of the metal in the complexes. With incorporation of a metal, interesting redox properties may be introduced and some of these metal complexes are also electrochromic. Complexation on the side benzene moiety of BDHP with ruthenium (III) (RuCp) and chromium (0) ($Cr(CO)_3$) subunits leads to distinctive photochromic behaviors for **10** and **11**. The (η^6-BDHP)Ru(III)Cp$\cdot PF_6^-$ salt **10** is both photochromic and electrochromic.[54] However, the robust complex (η^6-BDHP)$Cr(CO)_3$ **11** neither opens on irradiation nor decomposes.[55]

Fan[56] has synthesized CpDHP anion **12** and a variety of sandwich metal complexes. The Cp anion-fused DHP **12** undergoes reversible opening and closing upon exposure to visible and UV light. A photostationary state was reached with about 85% conversion in



12 **13** **14**

THF-d_8. The opening rate of **12** is about one quarter that of BDHP 3. The anion **12** thermally closes faster than BDHP 3 but not as fast as the DHP 2. The corresponding rhenium and ruthenium complexes **13** and **14** undergo completely reversible photo-bleaching under visible light irradiation. The Re complex **13** photoopens about 2 times faster, and thermally closes about 5 times slower, than the anion **12**. The Ru complex **14** photoopens and thermally closes at a comparable rate to anion **12**.

Mitchell group has also explored the aromaticity of these DHP derivatives. Using DHP as aromaticity probe has been developed and used in measurements of a series of aromatic and antiaromatic systems.

1.4 Aromaticity and anti-aromaticity

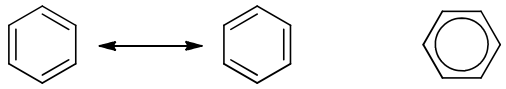
Garratt[57] has defined aromatic molecules as

"*cyclic systems which exhibit a diamagnetic ring current and in which all of the ring atoms are involved in a single conjugation system*".

The origin of the term "aromaticity" is uncertain. The classical definition of aromaticity was tied to the cyclic nature, stability and unique chemical reactivity of certain compounds. The expression "aromatic character" was loosely defined based on the observations: 1) high thermal stability and ease of formation; 2) substitution rather than addition by nitric acid, sulphuric acid and bromine; 3) resistance to oxidation; 4) special physical properties (for instance, acidity and basicity) in contrast to the analogous aliphatic compounds. A conjugated ring system is usually called an aromatic system when there is a measurable degree of cyclic delocalization of the π-electrons in the ground state of the molecule.[58] Its stability is considerably increased compared to that of the equivalent classical localized structure. On the other hand, if electron delocalization causes a decrease in stability of a system, the molecule is considered to be antiaromatic. Antiaromaticity usually leads to reorganization and distortion of the carbons in the system to avoid the destabilizing effects of conjugation. However, electron delocalization cannot be directly measured although it has magnetic effects. The IUPAC definition for delocalization was based on this idea: delocalization is a redistribution of the valence shell electron density throughout a molecular entity as compared with some localized models. In early discussions, the criteria for aromaticity were that the carbon skeleton is reasonably coplanar and contains $(4n+2)$ π-electrons (n is an integer). The $(4n+2)$ π-electron principle established by E. Hückel in 1936 using molecular orbital methods, known now as the Hückel rule, strictly applies only to fully conjugated planar monocyclic polyolefins. Simply stated, a ring system possessing $(4n+2)$ π-electrons would have aromatic character, while one with $4n$ π-electrons antiaromatic character.

A notable feature associated with aromatic systems is equivalence of bond lengths due to the mixing of single and double bonds. The concept of aromatic character is largely based on benzene, which was extensively studied in the early 1800's by Faraday. Its extraordinary stability was established chemically and the empirical formula was

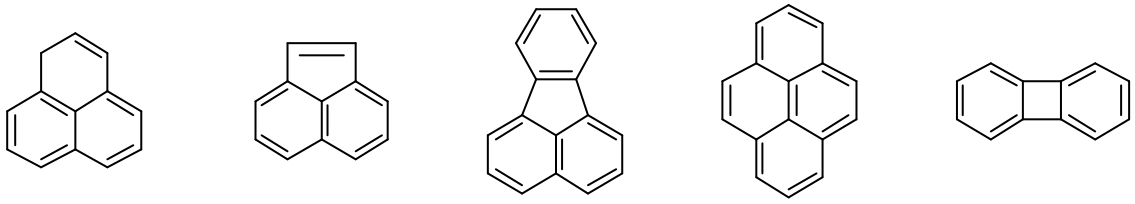
determined as CH. It was not until 1865 that the now well-accepted hexagonal structure of benzene in place of alternating single and double bonds was proposed by Kekulé. This structure was put forward to rationalize the problem of benzene showing only a single *meta* derivative. The form **I** and form **II** (Scheme **10**) are called resonance structures of benzene. The form **III** is used to stand for both form **I** and form **II**. The inscribed circle symbolizes a sextet of the six residual valence electrons, called an "aromatic sextet", and is responsible for the aromatic character of the substance. The circle only helps with visualizing the association of the electrons and provides no view about electron linking.



I **II** **III**

Scheme 10. Benzene and its resonance structures

With respect to polycyclic aromatic hydrocarbons (PAH) such as naphthalene, anthracene and phenanthrene, these PAHs all have $(4n+2)\pi$ electrons and fall in the category as aromatic systems. Difficulties in utilizing Hückel's $(4n+2)\pi$ rule arise when it comes to deal with PAHs with non-peripheral carbons, such as phenalene because of the vagueness about whether the individual subunits or the periphery of the molecule should be counted. However, Randic's[59] circuit theory extended the scope of aromatics to include these systems. Circuit theory says that PAH systems having only $(4n+2)\pi$ electron conjugated circuits are aromatic, while those having only $(4n)\pi$ electron circuits are anti-aromatic regardless of the total π electron count. 1*H*-phenalene, acenaphthylene, fluoranthene and pyrene have only $(4n+2)\pi$ electron circuits and therefore are aromatic systems. However, biphenylene, for example, possesses both $(4n+2)\pi$ and $(4n)\pi$ electron



1*H*-phenalene acenaphthylene fluoranthene pyrene biphenylene

circuits, and can be regarded as either aromatic or anti-aromatic depending on which circuit prevails.

It is worth noting that PAHs systems such as pyrene can be related to their original cyclic polyenes and the 4*n*+2 rule may be applied where only the peripheral carbons are counted, leaving the inner carbons as cross links. The cross links are regarded as small perturbations to the overall aromaticity. In this way, pyrene may be looked on as concentric 14π and 2π system connected by cross links, while fluoranthene has 6π and 10π systems connected together. Unfortunately, the perturbations are not necessarily small and exceptions should be expected. For example, biphenylene has a 12π outer periphery and completely fulfills the (4*n*)π criteria, which, however, may not be aromatic according to the previous method.

Molecules containing one or more heteronuclear atoms (N and O) still show aromatic character if they satisfy the criteria for an aromatic system. Pyridine has the same 6π



benzene pyridine 1*H*-pyrrole furan

electron count as benzene and 1*H*-pyrrole and furan are also analogous aromatic systems to benzene taking the lone pair of electrons on each heteroatom into account.

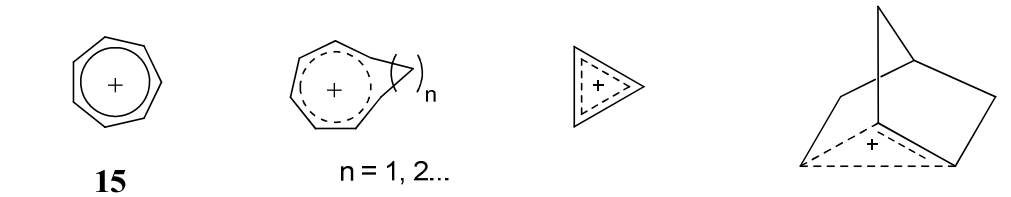
Technically, systems with charges should be treated the same way as neutral ones although electron counts have to be adjusted accordingly. The studies on charged aromatic-type π-electron systems have been extended to three-, four-, five-, seven- and eight-membered rings and representative examples are the cyclopropenium cation isolated by Breslow[60] in 1957, cyclobutadiene dianion (Pettit[61], 1965), cyclopentadiene anion (in the iron complex ferrocene, Pauson[62], 1951; Wilkinson and Woodward[63] 1952) and the tropylium cation (Doering[64], 1954).



Tropylium cation Cyclopentadiene anion Cyclobutadiene dianion Cyclopropenium

1.4.1 Background of homo-aromaticity

The tropylium cation was found to be extremely stable due to its planar structure with six π-electrons, and fulfills the criteria for an aromatic compound. The investigation of some larger ring systems by Pettit[65] and Winstein[66] showed some aromatic character, which was attributed to similarity to the tropylium structure, **15**, i.e. homotropylium

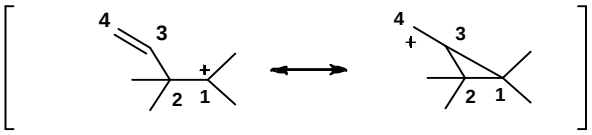


15

Tropylium cation | Homo-tropylium cation | Cyclopropenyl | Norbornyl cation

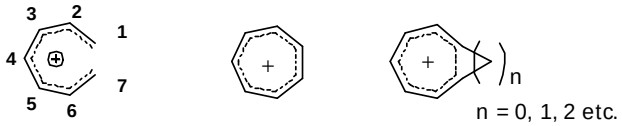
cations.[67] The cyclopropenyl cation is regarded as a common stable cation 2π-3C system. The extra stability of norbornyl cation can be interpreted on the basis of the existence of species containing a cyclopropenyl cation unit.[68] Both tropylium and cyclopropenyl cations involve electron and charge delocalization by employing p-π orbital overlap along existing carbon-carbon bonds. However, the norbornyl cation situation differs in that the electron delocalization occurs by employing orbital overlap on carbon atoms where there is no additional σ-bond. The broken lines represent partial bonds of bond order between 0 and 1. This phenomenon was coined as homo-aromaticity.

The homo-conjugation arises where electron delocalization takes place across adjacent



intervening carbons atoms. For instance, the appreciable atomic *p*-orbital overlap on the olefinic carbon atoms C-3 and C-4 and the cationic carbon C-1 with the *β*-carbonium ion to an olefinic group. In contrast to electron delocalization along three sequential carbons in an allylic cation, homo-conjugation takes place by skipping part of the carbon chain. The carbon atom C-2 interrupts the *σ*- skeleton of an aromatic species.

For the C7 chain sequence of heptatrienyl, tropylium and homo-tropylium species, previous studies have shown that the delocalization energy of the aromatic tropylium cation **15** is considerably greater than the acyclic cation **I**. In the homoaromatic



I **15** **II**

counterpart **II**, the delocalization energy is appreciable but less than that of the tropylium cation **15**. Such a molecule may involve the removal of the entire *σ* bond (n = 0) or interposition of one or more methylene groups (n = 1, 2, etc).

The peculiar properties of the aromatic compounds are dependent on the properties of the ring system. Note that aromaticity is not a function of stability and chemical reactivity. Chemical reactivity is not a property of the molecule in the ground state. Aromaticity is more generally defined on the basis of electronic structure. Therefore, the commonly observed preference for electrophilic substitution over addition reactions is not sufficient to determine aromatic systems. Besides requiring a fully conjugated, planar, cyclic *π* system, unique energetic, geometric and magnetic properties are also characteristics of an aromatic system.[69] The quantitative measure of the energetic criterion is called resonance energy. The geometric criterion related to structural properties include bond lengths and angles. Magnetic properties of aromatic systems

relate to the diatropic ring current, which has been extensively studied by NMR spectroscopy.

1.4.2 Resonance energy

The most basic criterion for an aromatic system is resonance energy, which originated from valence bond theory by Pauling.[70] The resonance energy of an aromatic is the increased stability due to electron delocalization compared to an electron localized structure. The resonance energy influences the reactivity and most physical properties of aromatic systems. The resonance energy is defined within the Hückel rule molecular orbital approach as the energy loss that occurs when a set of hypothetical non-resonating Kekulé type structures for a given molecule is compared to the fully delocalized molecule. Resonance energy therefore directly reflects the energy stabilization an aromatic system gains over a related Kekulé structure. However, one drawback of their approach is that it is difficult to find an appropriate reference structure and the selection is arbitrary. So estimates of resonance energy can vary by as much as 50 kcal/mol. There exist theoretical and experimental approaches to determine resonance energy.[71] The theoretical approach relies on calculations based on physical chemical data, for instance Hess cycles. The experimental methods estimate resonance energy based on calorimetric data, commonly by means of heats of combustion and hydrogenation. Both methods seem to work fairly well in predicting a resonance energy of 36 kcal mol^{-1} for benzene. However, these estimates are perturbed by many structural and configurational factors. For example, unbalanced strains or difference in hybridization and conjugation may cause substantial errors. Therefore in more complicated systems than benzene, the results are less reliable.

1.4.3 C-C Bond lengths

In the classical valence-bond structure, carbon-carbon bond lengths vary in non-conjugated molecules with only minor variations. The typical C-C single bond length has

been determined to be near 1.54 Å in saturated aliphatic compounds. The C=C double bond length is about 1.34 Å in ethylene. While the C≡C triple bond length is about 1.20 Å in acetylene. In conjugated molecules, a shortening of formal single bonds and an elongation of formal double and triple bonds are observed. With conjugated non-aromatic cyclic polyenes, the carbon-carbon bonds alternate between long and short distances. With aromatic compounds, the alternation is insignificant with only small variation in bond lengths. Benzene has equivalent bond lengths of 1.39 Å and shows no bond length alternation.

X-ray diffraction studies on crystalline aromatic compounds determine the bond lengths with aromatic C-C bond lengths near 1.39 Å in benzene and its derivatives. The C-C bond length in benzene itself was found to be 1.392 Å.

With naphthalene and polycyclic benzenoid hydrocarbons, some bond length variation occurs. In naphthalene, the Cα-Cβ bond length of 1.359 Å is significantly shorter than any other bonds in the molecule (bold bond in Figure 5 below). The short bonds were calculated to have the highest bond order. Similar bond length maps were found in anthracene (1.366 Å for Cα-Cβ) and tetracene (1.385 Å for Cα-Cβ). Note that all of these are also shorter than the bond length of 1.39 Å in benzene. Significant bond-length variation was also found in pyrene, where the short bonds are indicated by bold bonds. Note that the short bond lengths alternate around the periphery of the molecule. The bond length variations in polycyclic benzenoid hydrocarbons can be interpreted as a greater contribution of one Kekulé structure to the observed valence bond structure.

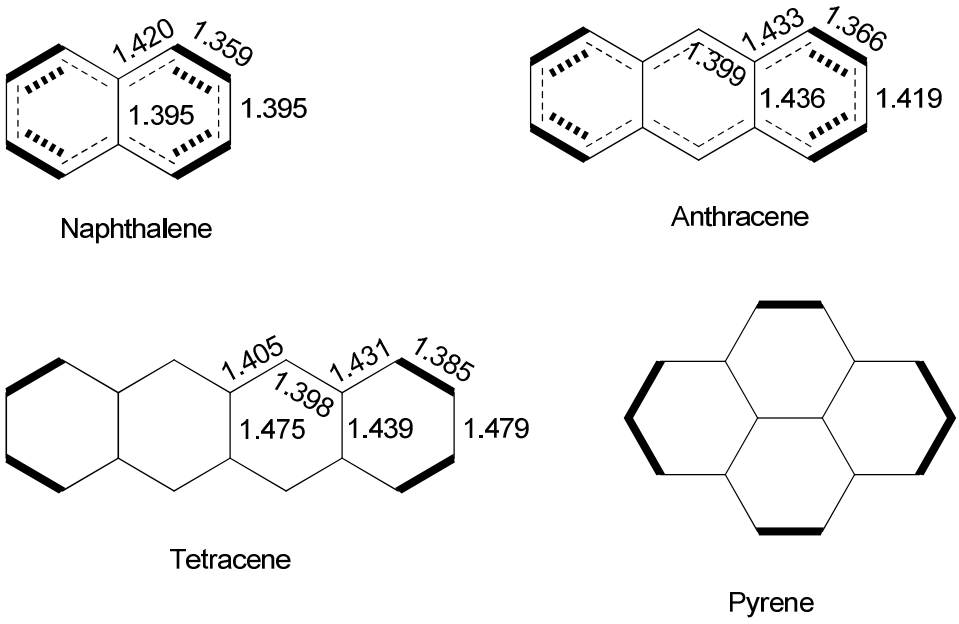
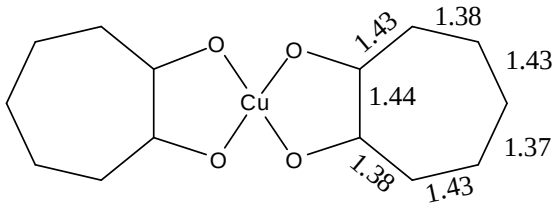


Figure 5. The bond length alternations in some aromatic systems

Investigations on charged aromatic systems demonstrate similar results. The X-ray diffraction on triphenyl cyclopropenium perchlorate indicate equivalent bond lengths of



Cupric tropolone

1.373(5) Å in the three membered ring.[60] The aromatic seven-membered tropylium cation system displays a planar heptagon with average bond lengths of 1.40 Å. The X-ray diffraction data are shown for cupric tropolone[72].

The X-ray crystallographic analysis of the 2,7-disubstituted-*trans*-15,16-dimethyl-15,16-dihydropyrene revealed many similarities (e.g. planarization) in aromatic character (**I** in Figure 6).[49, 73] For example, in the DHP 2 case (**I** in Figure 6) (R = *tert*-Bu-) the peripheral carbons atoms are displaced *ca*. 0.02-0.05 Å from the DHP framework plane. The structure of 2 has a two-fold axes, in which the peripheral bond lengths do not

alternate spanning the range between 1.388 and 1.402 Å (esr 0.002 Å in all lengths).[49] In contrast, the bond lengths in the BDHP structure 3 (Figure 6) showed alternations in the range between 1.351 to 1.463 Å as a result of the partial bond localization due to the annelation of the benzene ring.[49]

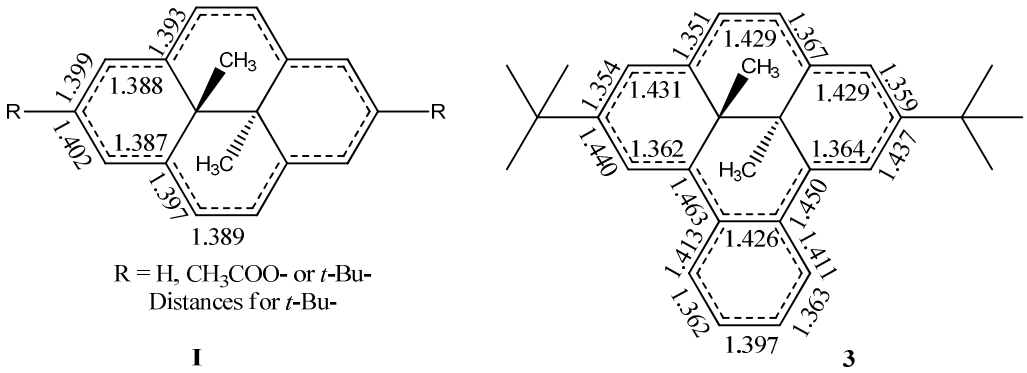


Figure 6. Structural data of 2,7-disubstituted DHP and BDHP

1.4.4 Induced ring current detection by NMR spectroscopy

Diamagnetism arises from circulation of electrons in filled orbitals in isolated atoms in diamagnetic substances. At a molecular level, when a cyclic conjugated molecule is placed in an external magnetic field, electrons in delocalized molecular orbitals make a circuit motion in the plane perpendicular to the external magnetic field direction. The applied external magnetic field on each electron induces a small circuit current that opposes the applied external inducing field. The contribution from each electron in a molecule adds up to the total induced magnetic polarization and the effect becomes significant in poly-atomic molecules. In molecules having only isolated centers of unsaturation or having only saturated centers, the electrons are relatively isolated and the effects occur within a small area. In aromatic molecules, the π-electrons are not confined to individual atoms or bonds. The diamagnetic currents are not limited to specific atoms, but span an extended circuit around the ring. This secondary induced ring current due to the Larmor precession of the whole π-electron cloud is much stronger than the small,

individual circuit currents of each σ-electron in the molecule. The magnetic field generated by the ring current is opposed to the external magnetic field within the ring but reinforces the applied field outside of the ring (Figure 7). Its strength depends on the electron density in the ground state.

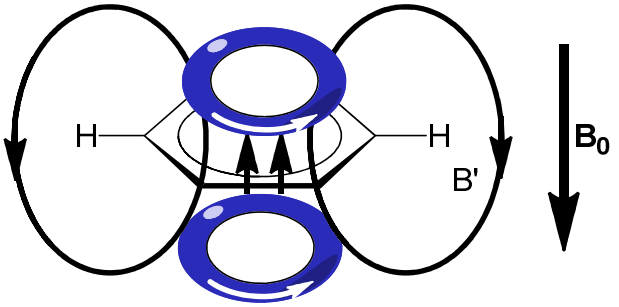


Figure 7. The induced ring current and magnetic field of benzene in an external magnetic field B_o

There exists also a paramagnetic current flowing in the opposite direction to the diamagnetic current. The paramagnetic current depends upon the total contributions from the electronically excited states. For most cyclic aromatic systems, orbital degeneracy exists in respect to the highest occupied and lowest unoccupied molecular orbitals. If the highest occupied pair of orbitals contain only two electrons in the (4n)π electrons system, the degeneracy is removed by a geometric distortion (Jahn-Teller distortion). The resulting lower orbital is filled with the two electrons but the splitting between the two orbitals is small enough to allow the electrons to be excited into the higher energy orbitals. When this excitation is associated with a magnetic moment perpendicular to the ring, a large paramagnetic contribution to the ring current takes place. Molecules containing (4*n*) π-electrons exhibit particularly large paramagnetic ring currents because they possess very low lying exited states, which are accessible through this magnetic dipole transition.

The large diamagnetic anisotropy effects in an aromatic molecule can be detected experimentally by NMR spectroscopy. The observation of diamagnetic ring currents can be used to designate an aromatic system experimentally. It is of considerable interest that different aromatic systems exhibit aromatic character to different extents. However, when

Chapter 1. Introduction

1.1 Introduction

Reversible molecular switching between two isomeric states has potential usage in logic components at the molecule level so as to replace existing silicon materials in building computer chips[1] with a "bottom-up" approach.[2] Electron delocalization energies, particularly ring current energies in cyclic molecules, have very important contributions in switchable systems.[3] Organic based substances are interesting in that they functionalize at the single molecular level and have tunable functions.[3-4] These features are motivating scientists to explore switchable molecules.

1.1.1 Molecular switches

Molecular switches[1b] describe a substance that can be toggled between two isomeric forms, usually accompanied by color changes, with a variety of triggering stimuli. Light (photochromism), heat (thermochromism), electrical current (electrochromism), chemical reagents (chemochromism etc.) and mechanical actions (peizochromism etc.) were successfully used in such reversible transformations.[5] Practically, the superiority of light for data storage is due to its intrinsic physical properties, which include high speed, accuracy and selectivity.[6] Data transfer[7] and data storage[8] are two basic aspects to address in applications based on light. The former involves conversion of electronic signals to photonic information. The latter is about electronic transition processes in the form of photoisomerization. This latter phenomenon is widely interpreted as photochromism and these molecules are frequently referred to as photoswitches. Electrochromism[9] is often a useful additional feature of some photoswitches that provides another trigger for the switching process.[10]

1.1.2 Some remarks associated with photochromism

It wasn't until the 1950s that the term "photochromism" was coined by Hirshberg,[11] even though the phenomenon was first discovered in the late 1880s. Photochromism[12] refers to the reversible transformation of a chemical species between two or more isomeric forms in response to irradiation at different wavelengths. The process essentially involves chemical reactions that break and re-form bonds intramolecularly. Chemically, it can result in stereochemical rearrangement or changes in electronic conjugation and electron delocalization. Only incident light with the proper wavelength can excite the ground state of a molecule to the excited state and so begin a chemical event. The lowest energy absorption bands are usually more interesting in that each of the isomeric forms absorbs in distinctive visible or near visible regions of the electromagnetic spectrum.

During photoswitching cycles, a single isosbestic point indicates clean interconversion with a single reaction intermediate (Figure 1). For example, irradiation at the absorption maxima (700 nm for **B** in Figure 1) of one isomer allows for complete conversion to the other isomeric form **A**, provided there is no overlap in their absorption spectra. Stimulation at a wavelength (around 400 nm in Figure 1) where both isomers absorb results in an equilibrium between the two isomers, called a photostationary state.

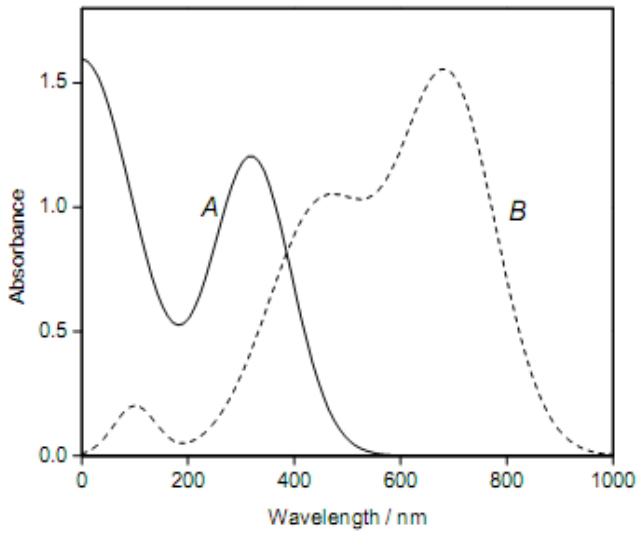


Figure 1. The typical absorption curves for two forms of photochromic compounds

When the absorption maxima of the more thermodynamically stable form **B** in Figure 1 takes place at a longer wavelength than the less stable isomer, this class of photoswitch is called negative photochromism. If the opposite is true, then this is referred to as positive photochromism. This property not only can often cause coloration/decoloration cycles as in dyes, but more importantly it can be used to switch the states of molecular devices. For example, a photoswitch can turn on and off such properties as fluorescence,[13] refractive indices[14] and dielectric constants.[15] Therefore, photochromic compounds are often regarded as photoswitches. In the cases where rupture of a single bond or shift of double bonds is involved in the course of photoirradiation, the state with the ruptured sigma bond is referred to as the open form. The corresponding state with formation of a new sigma bond is referred to as the closed form.

Heat may also trigger a transformation in some molecular switch systems.[16] If the energy barrier for the isomerization is sufficiently low, conversion to the thermodynamically more stable isomer will occur without light. Such dark reactions are a major drawback. For photoswitches in data storage applications, where bistable forms are desired. Practically this may cause information loss in data storage applications. The corresponding photoswitches are classified as T-type, in which the thermally reversible processes are concomitant with the photochemical reaction. In rare cases, when no thermal process is concurrent during the course of photochemical processes, they are referred to as P-type photochromic compounds (photochemically reversible). Theoretically it is possible to adjust the height of the reaction barrier by chemical modifications so it should be possible to suppress the dark reaction.

1.1.3 Photochromism and aromaticity

Aromaticity is often related to photochromism as illustrated by Irie's prediction and successful development of dithienylethane photoswitches.[3] With regard to bistability of the photoisomers of the diarylethene photochromic systems, the five-membered ring heteroaromatic thiophene is the best aromatic moiety among thiophene, furan and benzene based on calculations. Almost all known photochromism processes involve

changes in electron delocalization or aromatic features relevant to electron delocalization. Two important features associated with each photoisomer are the longest wavelengths of absorbed light (often the color) and their stability towards a thermal back reaction. These properties are determined by the energy levels of the system which are often related to the aromatic properties of the heteroaromatic groups in the diarylethene type photoswitches. Therefore, an understanding of aromaticity and electron delocalization is fundamental in finding new photochromic system and in modifying their properties.

1.1.4 Electrochromism

Electrochromism[9] describes the phenomena where reversible conversion takes place between two markedly different colored species upon electron uptake (reduction) and electron loss (oxidation) with the passage of appropriate electrical current.[17] Electrochromic molecules display distinct electronic absorption spectra at different oxidation states because of the feasibility of either internal electronic excitation or inter-valence charge transfer along the molecules. They have already been used in the manufacture of anti-glare rear-view mirrors, sunglasses, and battery state-of-charge indicators.[18] They have potential usage in video displays but so far all the required criteria for their application have not been met. Many electrochromic materials in use today are based on polypyridyl metal complexes and inorganic metal oxides, such as tungsten trioxide. Readily available organic viologens[4] (1,1'-disubstituted-4,4'-bipyridinium salts) represent the organic chromophore compounds. They exhibit excellent electronic absorption features in applications where the colorless dication species and the intensely colored radical cation species are intercoverted by one-electron reduction or oxidation processes. Some nitrogen, oxygen, and sulfur containing compounds also demonstrate interesting electrochromic properties.

1.2 Known photochromic (photoswitchable) systems

Photoexcited species may undergo reactions such as cycloaddition, pericyclic reactions, *trans*/*cis* isomerizations, intramolecular group transfers, dissociation (radicals), electron transfers[19] (oxidation-reduction), and quenching. Chemically, most molecular switches involve one or more of the reactions in the above list. Photochemically induced *trans*/*cis* isomerization and pericyclic reactions are the two main processes in molecular switches to be discussed in this context. Intramolecular group transfer and cycloaddition reactions take place commonly as side reactions in some photoswitchable systems.

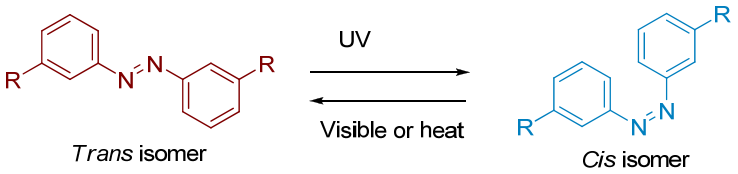
Photochromic switches can be divided into two groups on the basis of the associated photochemical reactions. A large number of analogs of azobenzenes, spiropyrans and spirooxazines involve just photoisomerization and are called type I photochromic compounds. In contrast, derivatives of fulgides, dithienylethenes and dimethyldihydropyrene belong to type II photochromic compounds and these undergo pericyclization reactions.

The mechanism of *trans*/*cis* photoisomerization is debatable.[20] Nevertheless, either lone pair or π electrons are promoted to the π^* orbitals in response to appropriate irradiation. Both n-π^* and π-π^* excitation would weaken the related double bonds and allow a rotation. The excited states adopt thermodynamically favorable low energy geometries, where the substituents are in orthogonal positions. The decay of energy leads to the reformation of the double bonds in both *trans* and *cis* isomers. Upon selective irradiation of one of the two isomers, it converts to the other isomer. Presumably, the π-π^* transition is more efficient in promoting this conversion as the remaining bond is expected to be much weaker than in the n-π^* case although other factors also many play important roles in this regard.

1.2.1 Azobenzene

Azobenzene derivatives belong to T-type photoswitches.[12] Only the *trans* isomer exists in the dark at room temperature. The difference in ground state energy of the two

isomers is caused by a large difference in their molecular shapes. The *trans* isomer forms a planar structure with the π electrons delocalized along the two benzene rings and two nitrogen atoms. In contrast, steric repulsion between the aromatic rings in the *cis* isomer twists the phenyl rings with respect to the N=N double bond and electron delocalization is disturbed, resulting in a higher ground state energy (Scheme 1).

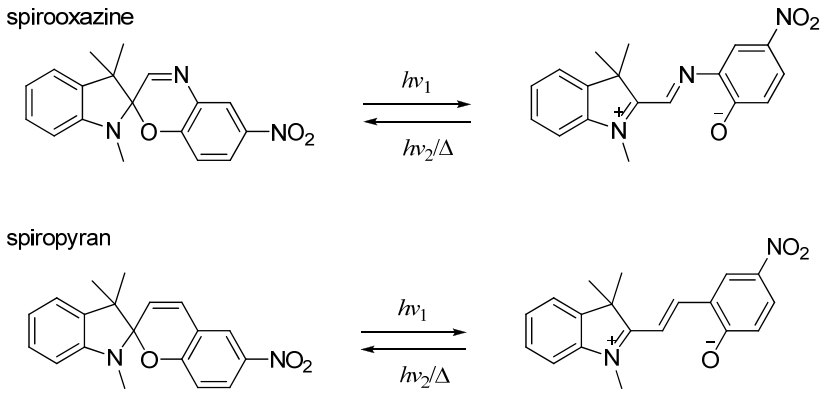


Scheme 1. The photoswitching between azobenzene isomers

Zimmerman[21] has investigated the quantum yield dependence of the reversible isomerization processes on varying the irradiation light wavelength, light intensity and sample concentration. The quantum yields show only a wavelength dependence ranging from 0.10 to 0.50. The UV-Vis spectra for the two isomeric forms are significantly different[22]. *Trans*/*cis* isomerization originates in the promotion of one electron into the π^* orbital, resulting in rotation around the N-N bond due to the lower bond strength in the excited state. In the *trans* isomer, the negligible absorption that occurs in the visible region is ascribed to the orbitally forbidden n-π^* transition and an absorption at 320 nm is due to an allowed π-π^* transition that tailed into the visible region. It is noteworthy that there is no significant absorption from the *cis* form at this wavelength. The conversion sensitivity depends on both the molar absorption coefficients and the quantum yields. Therefore, irradiation by 320 nm UV light leads to a fast increase in intensity of the 440 nm transition associated with the *cis* form. Irradiation with 440 nm wavelength visible light converts the *cis* isomer to the *trans* form. Besides causing color changes, photoisomerization also changes other properties, such as dipole moment, conductance and shape. Recently, studies have mainly focused on its applications in biology,[23] to polymers, and to nanomaterials. In the nanotechnology field, photoisomerization has been used to trigger a mechanical motion of a film or liquid droplet due to large volume change between the two isomers.[24] However, the opening is usually slow or blocked in

the crystalline state, probably because of crystal packing forces. Nevertheless, pulsed laser irradiation with high photon density allowed the isomerization process to be carried out in a solid gel due to cooperative photoisomerization. [25]

1.2.2 Spiropyrans and spirooxazines

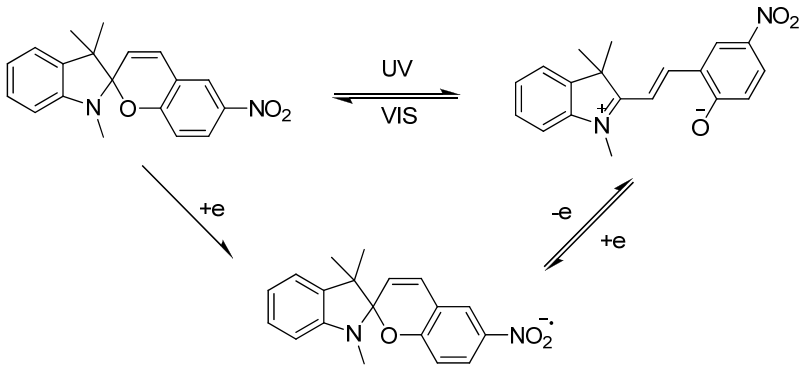


Scheme 2. Spirooxazine and spiropyran photochromic compounds

Spirooxazines and spiropyrans are differentiated in that either a carbon (pyran) or nitrogen (oxazine) is at the methine position of the six-membered ring off of the spiro-carbon atoms (Scheme 2)[26]. Both generally fall in the same family of T-type photochromic switches. In the colorless closed state, the electrons localize, as an orthogonal relationship exists between the two adjacent rings. In this form, spirooxazines and spiropyrans usually absorb in the 200-400 nm range.[27] The open state, generated upon irradiation with UV light, is known as a merocyanine and is a conventional dye known for its intense color. Open forms of both systems revert to the closed form in response to appropriate visible light irradiation or heat. Due to the overlap of the absorption band in the opened and closed forms, photostationary states often exist. The yield and absorption maxima of the open form depends on the solvent polarity because photoswitching results in a dramatic dipole moment change.[28]

The combination of photochromic and electrochromic switching has been realized by incorporating redox-active organic functional groups into photochromic systems. The redox properties are dependent on electronic distribution. Therefore, the functional

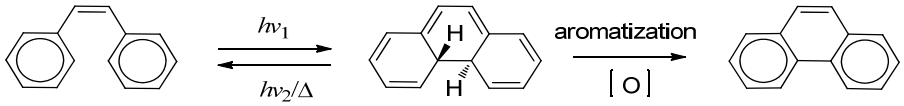
groups in the open and closed species exert different effects on the electronic properties. Fujishima[29] reported that spiropyrans bearing a nitro group are both electrochromic and photochromic (Scheme 3). The colorless ring-closed spiropyran underwent irreversible one-electron reduction to the radical anion. In contrast, a reversible redox process occurred between the radical anion and the ring-opened merocyanine. This is a rare case in which the electrochromism took place involving an organic functional nitro group ($-NO_2$).



Scheme 3. The electrochromism associated with spiropyran photochromic compounds

1.2.3 *Cis*-stilbene

Photochromic stilbenes represent the prototype of modern diarylethene type photochromic compounds. Beside the *trans*/*cis* photoisomerization of stilbene, the *cis* isomers also undergo a photochemical pericyclization giving rise to a closed dihydrophenanthrene.[30] It has to be stressed that the electrons are localized in the closed state, which has a large gap between HOMO and LUMO orbitals. The absorptions of both isomers occur only in the short wavelength UV region, so these are colorless compounds. The interesting aspect of *Z*-stilbene is its reversible electrocyclization conversion in the absence of oxygen (Scheme 4).



Scheme 4. The photochemical pericyclization of Z-stilbene

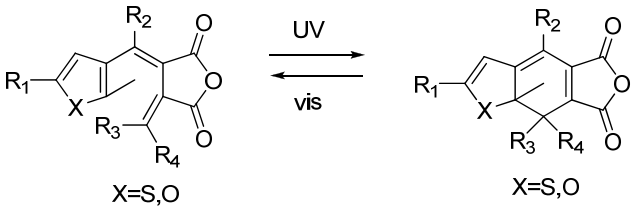
UV light irradiation promotes the ring closing process, while ring opening occurs with visible light. The loss of the aromatic rings in the closed form makes this a higher energy species that thermally reverts back to the open form with a half life $\tau_{1/2}$= 1.5 min at 20ºC.[31] When oxygen is present, aromatization takes place to form a thermodynamically more favorable aromatic phenanthrene with elimination of the hydrogen. The process, however, is an irreversible side reaction.

In order to produce photoswitches with better stability, two approaches to modify stilbene have been taken. The photochemical removal of alkyl groups requires much higher energy than removal of hydrogen, so introduction of substituents such as methyl at the internal positions results in a more stable photoswitch. Fulgides, dithienylethenes and dimethyldihydropyrenes, all have *non*-hydrogen substituents in the internal positions and have useful applications. The second approach is to eliminate unwanted photoisomerization reactions by locking the geometry of the double bonds. This is well-demonstrated in the dithienylethene and dimethyldihydropyrene systems. In the former, a ring prohibits isomersation of the double bond, while in the latter, a tether doubled bond was added to the molecule to lock the double bond in the *cis* geometry. The following three systems: fulgides, dithienylethene and dimethyldihydropyrene, are put in the same group because of the similarity of the arene moieties in the ring system. The driving force to regain aromaticity in the closed form becomes an obvious driving force for thermal back reactions for many of these systems.

1.2.4 Fulgides

Fulgide switches are composed of compounds bearing one aromatic ring on a *bis*(methylene)succinic anhydride core (Scheme 5).[32] It resembles the dithienylethene class of photoswitch discussed in the next section. Stobbe[33] first synthesized and

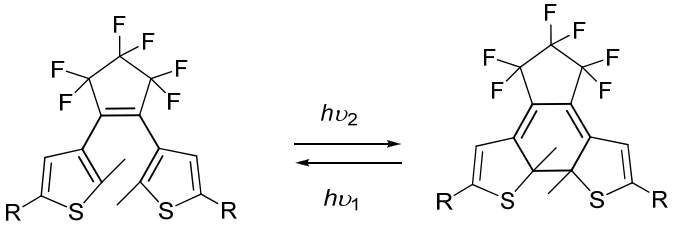
studied the phenyl substituted fulgides in the 1900s. They represent the types of switches that have two processes: *cis/trans* isomerization or 6π-electrocyclization. The substituents have a marked affect on the color and the photocoloration.[34] UV light irradiation drives both the isomerization and the hexatriene ring closing cyclization. Fulgides have been shown to be thermally stable photochromic compounds.



Scheme 5. Fulgide photochromic compounds.

1.2.5 1,2-Dithienylethenes

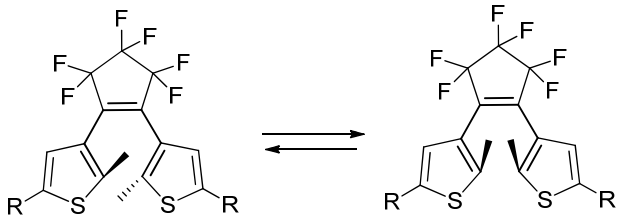
Dithienylethenes[35] are positive P-type electrocyclization photochromic compounds (Scheme 6). The diarylethene analogs where the thiophenes are replaced with other aromatic systems are less explored.[3]



Scheme 6. A dithienylethene photoswitch with a perfluoro-C5 ring.

The generality among them lies in their having a cyclic unit to lock the ethene bridge. Photochromic substances having different side rings exhibit different properties, such as a tunable absorption maximum (i.e., difference in color).[3] It is noteworthy that the absorption maxima and the closing quantum yields are dependent on the size of the ring involving the double bond. The dithienylethene with a C6 ring gave rise to the largest quantum yield and blue shift of the absorption maxima among the perfluoro-C4, C5 and C6 ring structures.[3] The reason was attributed to the planarity and the resulting electron

conjugation. The dithienylethenes bearing a perfluorocyclopentene proved to be one of the best in terms of overall properties. The thermal stability is accounted for by the minor energetic difference between the two states with the carefully chosen thiophene moieties. The extended electron delocalization in the closed form compensates for the destabilization from loss of two aromatic thiophenes in the open form, in contrast to *cis*-stilbene. The aromatic stabilization energy for a thienyl group is only 4.7 kcal/mol, compare to 27.2 kcal/mol for a phenyl group, so the destabilization in the closed dithienylethenes is much less than that of *Z*-stilbene during closing. In addition, the dithienylethenes show excellent fatigue resistance.[3] The best compound has been cycled 10^4 times without loss of photochromic performance.

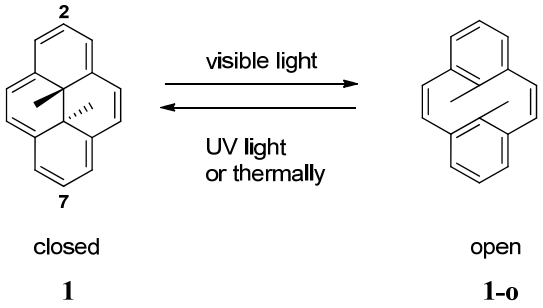


Antiparallel Parallel

Interconversions between the antiparallel (C2 symmetry) and parallel (Cs symmetry) conformations can occur in the open form. This contributes to the photoclosing quantum yields being usually less than 0.5. The visible light opening quantum yields are generally less than 0.1, smaller than the closing quantum yield by an order of magnitude or more. Because of extending electronic conjugation to dangling side chains in the thiophene the quantum yield drops in the closing process with dangling groups on the thiophenes. The electrons in the anti-bonding orbital are spread over a larger molecular surface rather than localized on the central breaking bonds.

1.2.6 *Trans*-dimethyldihydropyrene

Trans-dimethyldihydropyrene 1 (parent DHP) is a photoswitch that undergoes reversible photochemical opening and closing cycles[36] (Scheme 7). Note that the absolute stereochemistry of the internal methyl groups were not established. Both *Trans* DHP isomers present unless it is specified.



Scheme 7. Photochemical properties of *trans*-dimethydihydropyrene 1

Upon intense visible irradiation at 436 nm, parent DHP opens to the colorless metacyclophandiene 1-**o** (CPD) with low quantum yields. CPD 1-**o** reverts to *trans*-DHP 1 on irradiation with UV light (254 nm). The UV light closing process is exceptionally fast and efficient with quantum yields of 0.4-0.6 in hexanes. In addition the CPD 1-**o** closes thermally at room temperature to the more stable parent DHP 1 because of the greater stability of the fully delocalized 14π annulene DHP form.[36] The parent DHP 1 exists as thermally stable, green crystalline needles at room temperature. The CPD 1-**o**, comprised of two isolated aromatic benzene rings with two vinyl bridges, only absorbs in the UV region and is therefore the colorless form. Since the more thermally stable closed form 1 absorbs at a longer wavelength than the open form 1-**o**, the DHP systems belong to the rare negative type of photochrome. The 6 π-electron, Woodward-Hoffmann forbidden thermal closing process is common in known DHP systems with a half life for closing spanning from minutes to years. For example, the half life of 1 was found to be 52 hours. Experimental results[37] and calculations[38] suggested that this thermal process involves excited intermediates with obvious radical character. So radical stabilizing groups in place of the internal methyl groups dramatically change the photochemical properties. In many cases, CPD derivatives have a half life for thermal closing that meets the requirements for characterization methods such as NMR and UV-Vis spectroscopy. The typical energy difference favors the closed form over the open form by about 3 kcal mol^{-1}. In comparison to other photochromic compounds, the DHP-derived systems show several superior features. For example, DHPs usually open and close completely and no photostationary states take place.

Among the peripheral skeletal carbons, calculations have shown that the 2 and 7 carbons have the highest electron density and so are the most competitive sites for electrophilic reactions. In order to react selectively at other positions, carbons 2 and 7 are blocked by introducing *tert*-butyl groups, i.e. 2,7-di-*tert*-butyl-*trans*-dimethyldihydropyrene 2 (DHP) (Figure 2). More importantly, the synthesis of DHP 2 is more efficient on a large scale than for parent DHP 1. With optimized reaction conditions, one reaction sequence can give more than 10 grams of DHP 2 in contrast to a few hundred mg of the parent DHP 1. The development of DHP 2 was so important that it resulted in a breakthrough in the field of DHP-based photochromic compounds. Molecules bearing much better photochromic properties were synthesized based on this di-*tert*-butylDHP skeleton, including for instance the 2,7-di-*tert*-butyl-*trans*-dimethyldihydrobenzo[e] pyrene (BDHP) 3 and 4-acyl DHP series (Figure 2).

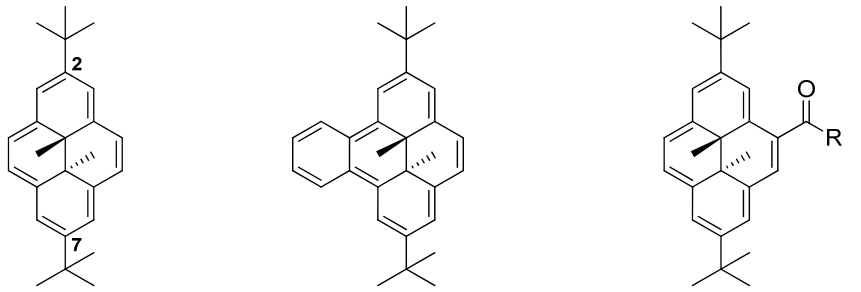


Figure 2. The 2,7-di-*tert*-butyl-*trans*-dimethyldihydropyrene 2, the benzo[e]-DHP 3 and 4-acyl derivatives

However, the photochemical opening rates of DHP 2 are even worse than those of the parent DHP 1. The photoopening efficiencies dropped to Φ_{open} = 0.0015 in the DHP 2 from 0.006 in the parent DHP 1 in hexanes.[39] Note that quantum yields have shown solvent dependence in some rare cases.[37] Using toluene as solvent yielded a dramatically higher ring opening quantum yield (Φ_{open} = 0.66 ± 0.02), the greatest value so far, in a 2-(1'-naphthoyl) DHP molecule and the reason for this is still beyond our understanding.[37] The quantum yields for photoopening of DHP 2 and its derivatives are often low. The photoopening process was found to take place via a singlet excited state

mechanism.[40] Structural modifications have been carried out to improve the photochemical efficiency (quantum yield) and three strategies were identified that achieved this. Modifying the central methyl groups, dangling acyl groups on the periphery and fusing aromatic groups at the [e] (side) positions were all shown to increase the quantum yield for opening substantially.

Benzo[e]DHP (BDHP **3**) is an example of a good photochromic molecule.[41] It quickly opens on visible light irradiation, shows excellent degradation resistance and undergoes a very slow thermal back reaction. As a result, it is usually used as the control molecule in photochemical tests in our group. BDHP 3 has a typical absorption for DHPs at around 400 and 500 nm (Figure 3), arising from the π-π^* transition with a modest extinction coefficient. In the open form 3-**o**, the absorptions occur mostly in the UV (Figure 3) as 3-**o** CPD essentially shows the absorptions due to isolated benzene chromophores. It is worth emphasizing that there are no significant absorptions in the 500 nm region for 3-**o** thus ensuring that complete conversion of 3 to 3-**o** occurs with irradiation at 500 nm with visible light.

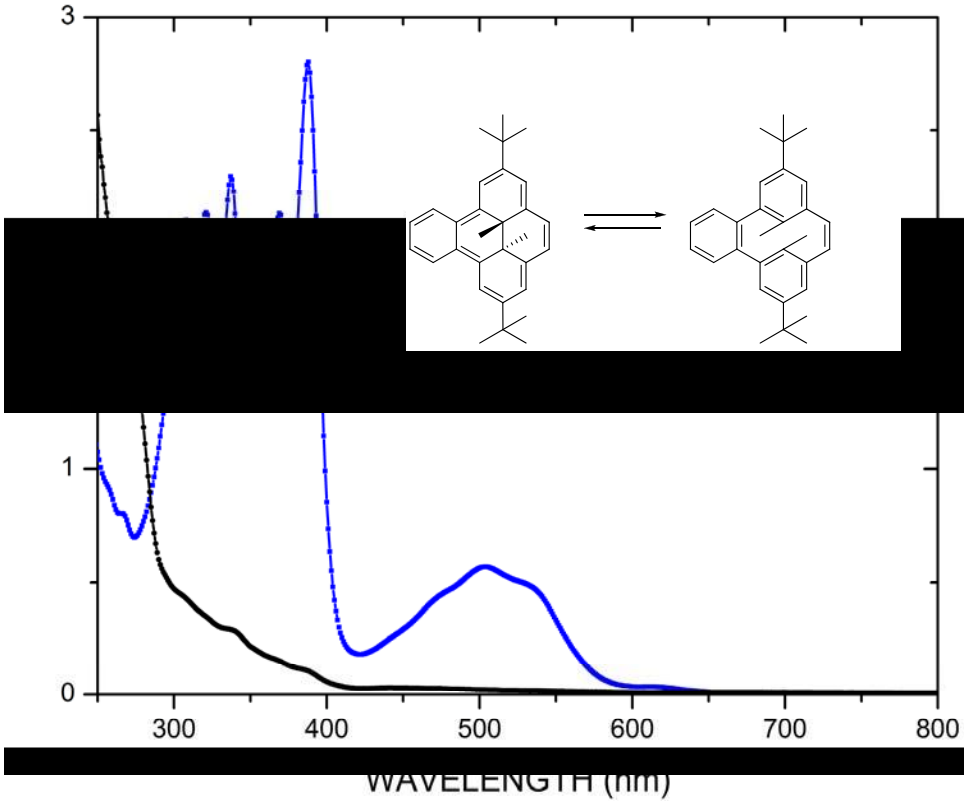


Figure 3. **The absorption spectra of BDHP 3 in closed (blue line) and open (black line) forms**

Benzannelation ensures additional resonance stabilization energy in the open form 3-**o**, diminishing the energy difference between the open form 3-**o** and the lower energy closed form 3. This allows 3-**o** CPD a longer thermal life time with an approximate half life ($\tau_{1/2}$) of one week at room temperature. It is anticipated that modifying the fused aromatic systems should lead to different photochromic features, although how such changes will alter the photochemistry is not yet predictable ahead of time.

1.3 Metal coordination complexes

Photoswitches bonding to transition metals have been explored to investigate the effects of the metal.[42] The complexation of metals on photochromic species alters their electronic properties, which may affect the behavior of the photoswitches in a positive or

negative way.[43] Conversely, it is also interesting to see if switching the photochromic state causes changes in the reactivity of the metal complexes. Metal complexes, prepared by Nishihara,[42c] generally exhibit not only the photochromic characteristics of the organic ligands, but unique properties of the metals. Metals and their complexes contain unique energy transitions between different energy levels corresponding to metal orbitals or metal-ligand orbitals. Absorption energy can be tuned by changing substituents on involved ligands. Unfortunately, metal derivatives often respond poorly on light stimulus. The reason for this is partly because electronic transitions within the ligand field states of the complex may compete with productive transitions of the organic photochrome.

1.3.1 Non-DHP based photoswitchable metal complexes

In metal complexes containing dithienylethene, spiropyran and azobenzene, the metal units usually complex to existing ligands by dangling from the photoswitch molecules.[44] Energy transfer and sensitization of the photochromic molecules have been the main focus. For example, in dithienylethene-derived $[Ru(bpy)_3]^{2+}$ complexes[45] (Figure 4), sensitized, photo-induced cyclization takes place from a triplet state localized on the bridging photochrome upon irradiation into the MLCT band of the $[Ru(bpy)_3]^{2+}$ unit. It was found that efficient energy transfer from the metal-based excited state to the dithienylethene switch caused photo-cyclization of the switch units. High quantum yields and excellent conversion rates were obtained. When the MLCT energy of the metal is lower than that required for switching the photochromic unit, such as in the analogous $[Os(bpy)_3]^{2+}$ complexes (Figure 4), energy transfer occurs from the photochromic unit to the metal center thus reducing the photoreactivity. This exploration was used to fabricate new systems including the heterodinuclear metal units, $[Ru(bpy)_3]^{2+}$ and $[Os(bpy)_3]^{2+}$.[46] Energy transfer occurs from the higher energy $[Ru(bpy)_3]^{2+}$ end to the $[Os(bpy)_3]^{2+}$ end through a dithienylethene (in the open form) bridge. In contrast, energy ends up at the dithienylethene photochromic unit when the dithienylethene was in its closed form.

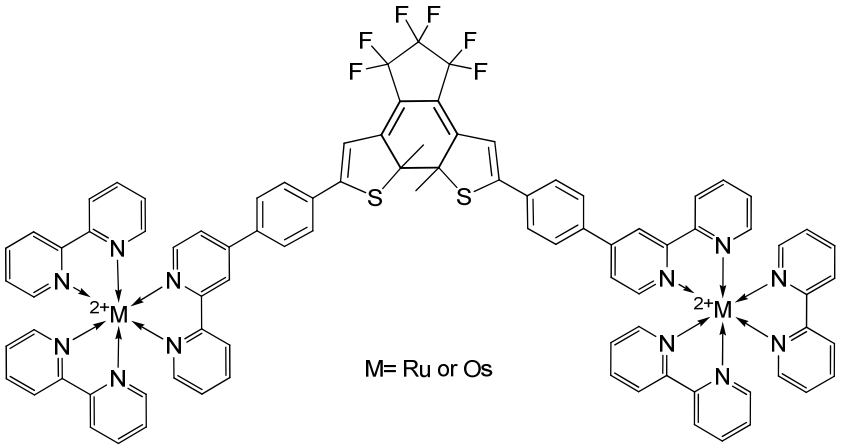
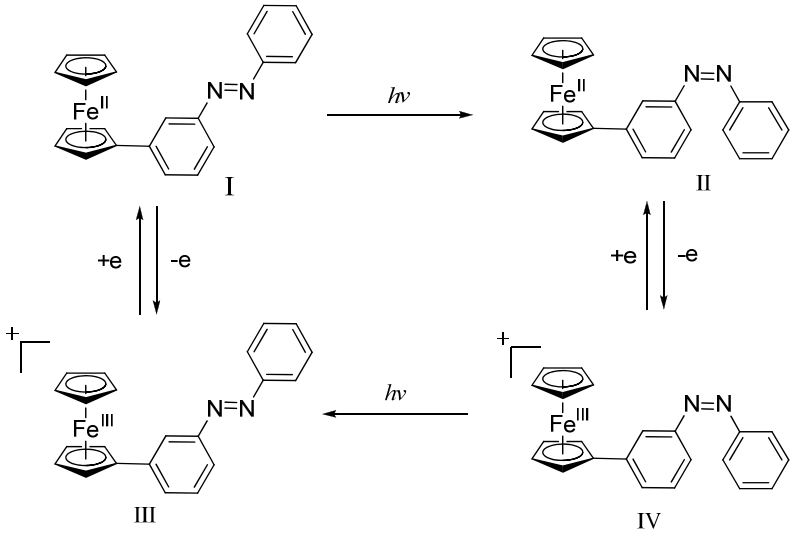


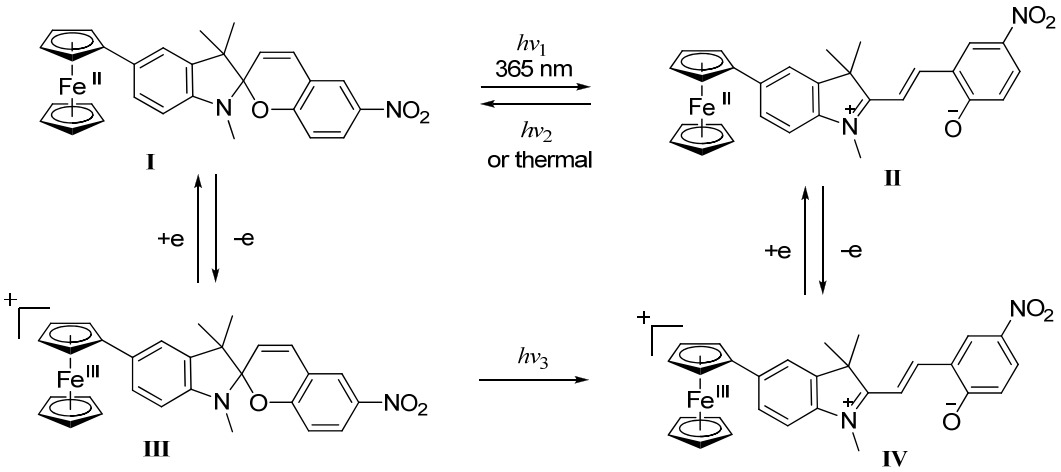
Figure 4. Dinuclear Ru/Os complex containing a dithienylethene derivative as bridging ligand

These results seem sensible in explaining the photoswitching behaviour of many metal complexes. However, photoswitching remains unpredictable as subtle changes can alter the photochromic behaviour. In dinuclear terpyridine complexes containing a dithienylcyclopentene, those with Ru and Fe (II) showed no cyclization in response to UV light irradiation, but they could be cycled electrochemically. In contrast, the Co (II) complex underwent photo-cyclization only, while the Os (II) complex appeared inert both photochemically can electrochemically. Even more confusing, mononuclear complexes containing *one* Fe or Co terpyridine unit are both photochromic and electrochromic.[42d]



Scheme 8. The azobenzene-derived metal complex photoswitches

Attaching a ferrocene unit to different types of photochromic molecules is well established. In ferrocenyl azobenzene (Scheme 8), the UV-Vis spectrum shows two strong absorption bands assigned to a π-π* transition of the azo group and a MLCT (d_{Fe}-π*) transition, respectively.[47] Remarkably, green light (546 nm) promotes *trans/cis* isomerization by irradiation at the edge of the MLCT bands, and also reverts ferrocenium complexes **IV** to **III** (Scheme 8). The different responses to green light let the complexes consisting of $[Fe(C_5H_5)_2]$ (Fc) and $[Fe(C_5H_5)_2]^+$ (Fc^+) reversibly isomerize at a single visible light wavelength by combining with the reversible redox reaction of ferrocene.



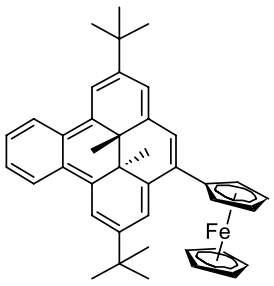
Scheme 9. The spiropyran-derived metal complex photoswitches

The spiropyrans with dangling Fc and Fc^+ moieties act reversibly and irreversibly, respectively, upon irradiation.[48] The spiropyran derivative **I** (Scheme 9) is converted into the colored open form **II** upon irradiation with UV light in 50-80% yield, but reverts to **I** in the dark or upon irradiation with visible light. Combining the reversible photoisomerization **I**/**II** and Fc/Fc^+ redox cycle completely stabilizes the open form **IV**.[48] Complete conversion to the open form **II** was reached by irradiation. The reason for the stabilization of **IV** by Fc^+ is not fully understood. The authors claimed that π conjugation might contribute to stabilization based on the large blue shift of λ_{max} in **III** relative to **II**. In general, the open form of spiropyran has a larger dipole moment than the closed form, and thus the open form can be largely stabilized by the electronic effects of

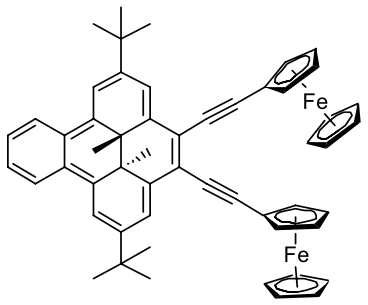
substituents on the indolium and phenyl moieties as well as by increasing the solvent polarity.

1.3.2 DHP-derived photoswitches containing metals

DHP photochromic compounds containing directly appended, or triple bond linked, ferrocene have been synthesized. The ferrocenylBDHP 4 does not open and photochromism is shut down by the pendant ferrocene.[49] However, Nishihara[50] has shown that the BDHP derivative *bis*(2'-ferrocenylethynyl)BDHP 5 having two ferrocenes connected by a conjugated acetylene linker is photochromic and electrochromic, and

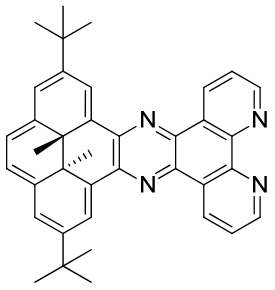


4

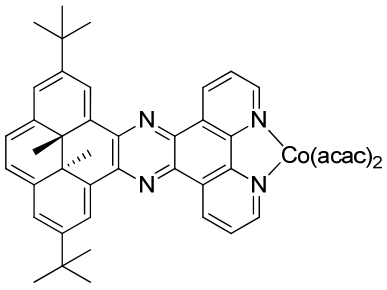


5

exhibits switchable electronic communication between the two ferrocene moieties. However, appending pentamethylferrocene in an analogue of 5 quenches the excited state of the BDHP and the compound no longer opens or closes. The stronger electron donating ability of the pentamethylferrocene compared to Fc probably accounts for the shut-down in photochromism.



6

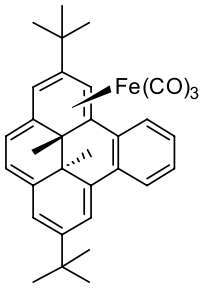


7

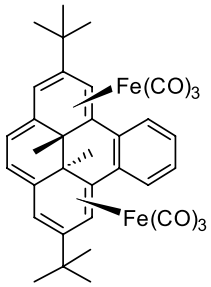
Saretcheyva[51] has studied some metal complexes based on phenanthroline-fused conjugated DHP systems and dangling phenanthroline-DHP systems with a alkyne spacer.

The phenanthroline-fused to the side of the DHP molecule as in **6** alters the conjugation and therefore the photochromism. The UV-Vis spectrum of **6** shows that the typical absorption peak around 500 nm is less intense than usual and tails to 800 nm. A photostationary state was reached (44% open form) on irradiation of a NMR sample of **6** for 80 h. It was also noted that the opening rate of 6 was only about 30% that of BDHP. The cobalt complex 7 opened about 7 times slower than the ligand 6 itself and also reached a photostationary state with nearly 40% open form.

It was found that the BDHP itself acts as a good olefinic ligand in a series of iron complexes (8, 9). Zhang[52] explored BDHP coordination with $Fe(CO)_3$ to form

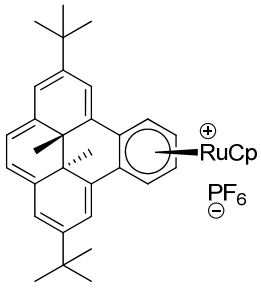


8

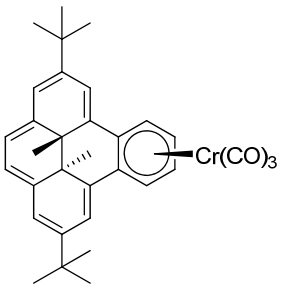


9

complexes 8 and 9, but in this case the complexes did not show any photochromic properties. Some of the iron complexes degraded and slowly lost the $Fe(CO)_3$ fragment in air.



10

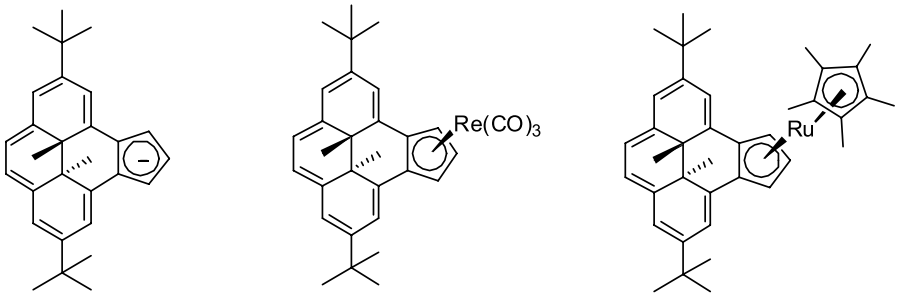


11

Complexation of DHP photoswitches to metals was also shown to occur with the corresponding furan- or benzene-fused DHPs at both the [a]-position and [e]-positions in the Mitchell group.[53] The BDHP and cyclopentadienide-fused DHP metal complexes are more interesting because they demonstrate different photochemical properties with variation of the metal in the complexes. With incorporation of a metal, interesting redox

properties may be introduced and some of these metal complexes are also electrochromic. Complexation on the side benzene moiety of BDHP with ruthenium (III) (RuCp) and chromium (0) ($Cr(CO)_3$) subunits leads to distinctive photochromic behaviors for **10** and **11**. The (η^6-BDHP)Ru(III)Cp·PF_6^- salt **10** is both photochromic and electrochromic.[54] However, the robust complex (η^6-BDHP)$Cr(CO)_3$ **11** neither opens on irradiation nor decomposes.[55]

Fan[56] has synthesized CpDHP anion **12** and a variety of sandwich metal complexes. The Cp anion-fused DHP **12** undergoes reversible opening and closing upon exposure to visible and UV light. A photostationary state was reached with about 85% conversion in



12 **13** **14**

THF-d_8. The opening rate of **12** is about one quarter that of BDHP 3. The anion **12** thermally closes faster than BDHP 3 but not as fast as the DHP 2. The corresponding rhenium and ruthenium complexes **13** and **14** undergo completely reversible photo-bleaching under visible light irradiation. The Re complex **13** photoopens about 2 times faster, and thermally closes about 5 times slower, than the anion **12**. The Ru complex **14** photoopens and thermally closes at a comparable rate to anion **12**.

Mitchell group has also explored the aromaticity of these DHP derivatives. Using DHP as aromaticity probe has been developed and used in measurements of a series of aromatic and antiaromatic systems.

1.4 Aromaticity and anti-aromaticity

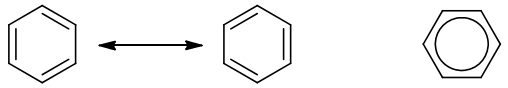
Garratt[57] has defined aromatic molecules as

"*cyclic systems which exhibit a diamagnetic ring current and in which all of the ring atoms are involved in a single conjugation system"*.

The origin of the term "aromaticity" is uncertain. The classical definition of aromaticity was tied to the cyclic nature, stability and unique chemical reactivity of certain compounds. The expression "aromatic character" was loosely defined based on the observations: 1) high thermal stability and ease of formation; 2) substitution rather than addition by nitric acid, sulphuric acid and bromine; 3) resistance to oxidation; 4) special physical properties (for instance, acidity and basicity) in contrast to the analogous aliphatic compounds. A conjugated ring system is usually called an aromatic system when there is a measurable degree of cyclic delocalization of the π-electrons in the ground state of the molecule.[58] Its stability is considerably increased compared to that of the equivalent classical localized structure. On the other hand, if electron delocalization causes a decrease in stability of a system, the molecule is considered to be antiaromatic. Antiaromaticity usually leads to reorganization and distortion of the carbons in the system to avoid the destabilizing effects of conjugation. However, electron delocalization cannot be directly measured although it has magnetic effects. The IUPAC definition for delocalization was based on this idea: delocalization is a redistribution of the valence shell electron density throughout a molecular entity as compared with some localized models. In early discussions, the criteria for aromaticity were that the carbon skeleton is reasonably coplanar and contains $(4n+2)$ π-electrons (n is an integer). The $(4n+2)$ π-electron principle established by E. Hückel in 1936 using molecular orbital methods, known now as the Hückel rule, strictly applies only to fully conjugated planar monocyclic polyolefins. Simply stated, a ring system possessing $(4n+2)$ π-electrons would have aromatic character, while one with $4n$ π-electrons antiaromatic character.

A notable feature associated with aromatic systems is equivalence of bond lengths due to the mixing of single and double bonds. The concept of aromatic character is largely based on benzene, which was extensively studied in the early 1800's by Faraday. Its extraordinary stability was established chemically and the empirical formula was determined as CH. It was not until 1865 that the now well-accepted hexagonal structure of benzene in place of alternating single and double bonds was proposed by Kekulé. This structure was put forward to rationalize the problem of benzene showing only a single

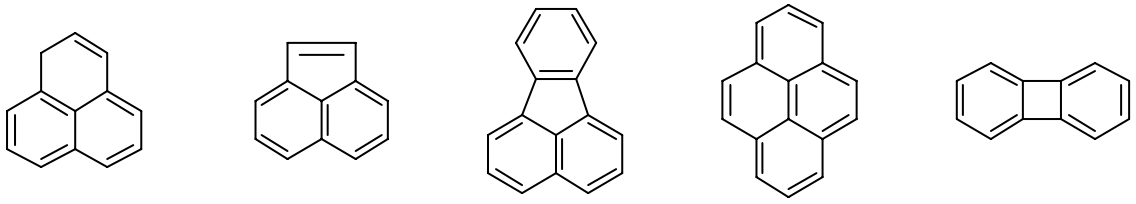
meta derivative. The form **I** and form **II** (Scheme **10**) are called resonance structures of benzene. The form **III** is used to stand for both form **I** and form **II**. The inscribed circle symbolizes a sextet of the six residual valence electrons, called an "aromatic sextet", and is responsible for the aromatic character of the substance. The circle only helps with visualizing the association of the electrons and provides no view about electron linking.



I **II** **III**

Scheme 10. Benzene and its resonance structures

With respect to polycyclic aromatic hydrocarbons (PAH) such as naphthalene, anthracene and phenanthrene, these PAHs all have $(4n+2)\pi$ electrons and fall in the category as aromatic systems. Difficulties in utilizing Hückel's $(4n+2)\pi$ rule arise when it comes to deal with PAHs with non-peripheral carbons, such as phenalene because of the vagueness about whether the individual subunits or the periphery of the molecule should be counted. However, Randic's[59] circuit theory extended the scope of aromatics to include these systems. Circuit theory says that PAH systems having only $(4n+2)\pi$ electron conjugated circuits are aromatic, while those having only $(4n)\pi$ electron circuits are anti-aromatic regardless of the total π electron count. 1*H*-phenalene, acenaphthylene, fluoranthene and pyrene have only $(4n+2)\pi$ electron circuits and therefore are aromatic systems. However, biphenylene, for example, possesses both $(4n+2)\pi$ and $(4n)\pi$ electron



1*H*-phenalene acenaphthylene fluoranthene pyrene biphenylene

circuits, and can be regarded as either aromatic or anti-aromatic depending on which circuit prevails.

It is worth noting that PAHs systems such as pyrene can be related to their original cyclic polyenes and the $4n+2$ rule may be applied where only the peripheral carbons are counted, leaving the inner carbons as cross links. The cross links are regarded as small perturbations to the overall aromaticity. In this way, pyrene may be looked on as concentric 14π and 2π system connected by cross links, while fluoranthene has 6π and 10π systems connected together. Unfortunately, the perturbations are not necessarily small and exceptions should be expected. For example, biphenylene has a 12π outer periphery and completely fulfills the $(4n)\pi$ criteria, which, however, may not be aromatic according to the previous method.

Molecules containing one or more heteronuclear atoms (N and O) still show aromatic character if they satisfy the criteria for an aromatic system. Pyridine has the same 6π



benzene pyridine 1*H*-pyrrole furan

electron count as benzene and 1*H*-pyrrole and furan are also analogous aromatic systems to benzene taking the lone pair of electrons on each heteroatom into account.

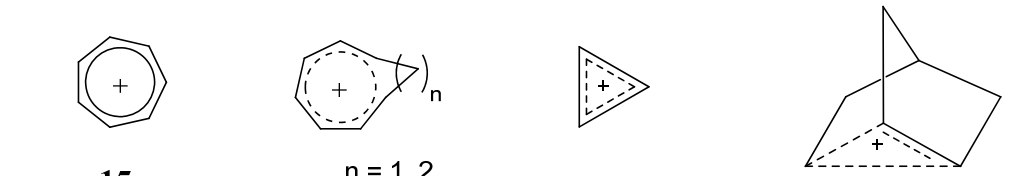
Technically, systems with charges should be treated the same way as neutral ones although electron counts have to be adjusted accordingly. The studies on charged aromatic-type π-electron systems have been extended to three-, four-, five-, seven- and eight-membered rings and representative examples are the cyclopropenium cation isolated by Breslow[60] in 1957, cyclobutadiene dianion (Pettit[61], 1965), cyclopentadiene anion (in the iron complex ferrocene, Pauson[62], 1951; Wilkinson and Woodward[63] 1952) and the tropylium cation (Doering[64], 1954).



Tropylium cation Cyclopentadiene anion Cyclobutadiene dianion Cyclopropenium

1.4.1 Background of homo-aromaticity

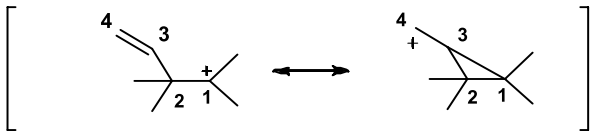
The tropylium cation was found to be extremely stable due to its planar structure with six π-electrons, and fulfills the criteria for an aromatic compound. The investigation of some larger ring systems by Pettit[65] and Winstein[66] showed some aromatic character, which was attributed to similarity to the tropylium structure, **15**, i.e. homotropylium



15
Tropylium cation | Homo-tropylium cation | Cyclopropenyl | Norbornyl cation

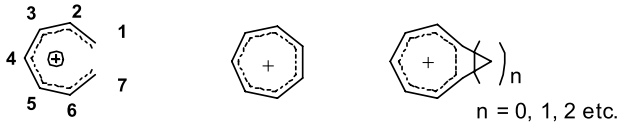
cations.[67] The cyclopropenyl cation is regarded as a common stable cation 2π-3C system. The extra stability of norbornyl cation can be interpreted on the basis of the existence of species containing a cyclopropenyl cation unit.[68] Both tropylium and cyclopropenyl cations involve electron and charge delocalization by employing *p*-π orbital overlap along existing carbon-carbon bonds. However, the norbornyl cation situation differs in that the electron delocalization occurs by employing orbital overlap on carbon atoms where there is no additional σ-bond. The broken lines represent partial bonds of bond order between 0 and 1. This phenomenon was coined as homo-aromaticity.

The homo-conjugation arises where electron delocalization takes place across adjacent intervening carbons atoms. For instance, the appreciable atomic *p*-orbital overlap on the



olefinic carbon atoms C-3 and C-4 and the cationic carbon C-1 with the β-carbonium ion to an olefinic group. In contrast to electron delocalization along three sequential carbons in an allylic cation, homo-conjugation takes place by skipping part of the carbon chain. The carbon atom C-2 interrupts the σ- skeleton of an aromatic species.

For the C7 chain sequence of heptatrienyl, tropylium and homo-tropylium species, previous studies have shown that the delocalization energy of the aromatic tropylium cation **15** is considerably greater than the acyclic cation **I**. In the homoaromatic



I **15** **II**

counterpart **II**, the delocalization energy is appreciable but less than that of the tropylium cation **15**. Such a molecule may involve the removal of the entire σ bond (n = 0) or interposition of one or more methylene groups (n = 1, 2, etc).

The peculiar properties of the aromatic compounds are dependent on the properties of the ring system. Note that aromaticity is not a function of stability and chemical reactivity. Chemical reactivity is not a property of the molecule in the ground state. Aromaticity is more generally defined on the basis of electronic structure. Therefore, the commonly observed preference for electrophilic substitution over addition reactions is not sufficient to determine aromatic systems. Besides requiring a fully conjugated, planar, cyclic π system, unique energetic, geometric and magnetic properties are also characteristics of an aromatic system.[69] The quantitative measure of the energetic criterion is called resonance energy. The geometric criterion related to structural properties include bond lengths and angles. Magnetic properties of aromatic systems relate to the diatropic ring current, which has been extensively studied by NMR spectroscopy.

1.4.2 Resonance energy

The most basic criterion for an aromatic system is resonance energy, which originated from valence bond theory by Pauling.[70] The resonance energy of an aromatic is the increased stability due to electron delocalization compared to an electron localized structure. The resonance energy influences the reactivity and most physical properties of aromatic systems. The resonance energy is defined within the Hückel rule molecular

orbital approach as the energy loss that occurs when a set of hypothetical non-resonating Kekulé type structures for a given molecule is compared to the fully delocalized molecule. Resonance energy therefore directly reflects the energy stabilization an aromatic system gains over a related Kekulé structure. However, one drawback of their approach is that it is difficult to find an appropriate reference structure and the selection is arbitrary. So estimates of resonance energy can vary by as much as 50 kcal/mol. There exist theoretical and experimental approaches to determine resonance energy.[71] The theoretical approach relies on calculations based on physical chemical data, for instance Hess cycles. The experimental methods estimate resonance energy based on calorimetric data, commonly by means of heats of combustion and hydrogenation. Both methods seem to work fairly well in predicting a resonance energy of 36 kcal mol^{-1} for benzene. However, these estimates are perturbed by many structural and configurational factors. For example, unbalanced strains or difference in hybridization and conjugation may cause substantial errors. Therefore in more complicated systems than benzene, the results are less reliable.

1.4.3 C-C Bond lengths

In the classical valence-bond structure, carbon-carbon bond lengths vary in non-conjugated molecules with only minor variations. The typical C-C single bond length has been determined to be near 1.54 Å in saturated aliphatic compounds. The C=C double bond length is about 1.34 Å in ethylene. While the C≡C triple bond length is about 1.20 Å in acetylene. In conjugated molecules, a shortening of formal single bonds and an elongation of formal double and triple bonds are observed. With conjugated non-aromatic cyclic polyenes, the carbon-carbon bonds alternate between long and short distances. With aromatic compounds, the alternation is insignificant with only small variation in bond lengths. Benzene has equivalent bond lengths of 1.39 Å and shows no bond length alternation.

X-ray diffraction studies on crystalline aromatic compounds determine the bond lengths with aromatic C-C bond lengths near 1.39 Å in benzene and its derivatives. The C-C bond length in benzene itself was found to be 1.392 Å.

With naphthalene and polycyclic benzenoid hydrocarbons, some bond length variation occurs. In naphthalene, the Cα-Cβ bond length of 1.359 Å is significantly shorter than any other bonds in the molecule (bold bond in Figure 5 below). The short bonds were calculated to have the highest bond order. Similar bond length maps were found in anthracene (1.366 Å for Cα-Cβ) and tetracene (1.385 Å for Cα-Cβ). Note that all of these are also shorter than the bond length of 1.39 Å in benzene. Significant bond-length variation was also found in pyrene, where the short bonds are indicated by bold bonds. Note that the short bond lengths alternate around the periphery of the molecule. The bond length variations in polycyclic benzenoid hydrocarbons can be interpreted as a greater contribution of one Kekulé structure to the observed valence bond structure.

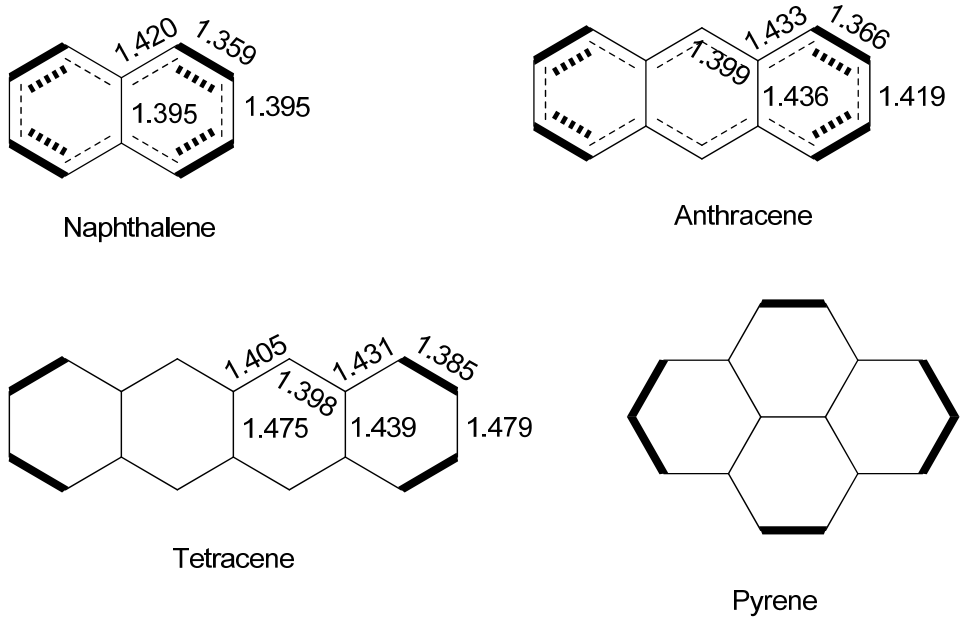
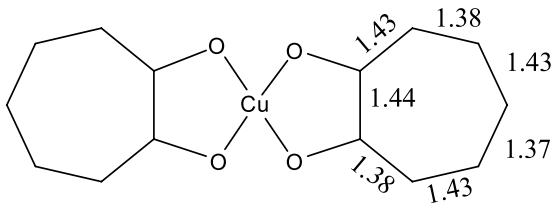


Figure 5. The bond length alternations in some aromatic systems

Investigations on charged aromatic systems demonstrate similar results. The X-ray diffraction on triphenyl cyclopropenium perchlorate indicate equivalent bond lengths of 1.373(5) Å in the three membered ring.[60] The aromatic seven-membered tropylium cation system displays a planar heptagon with average bond lengths of 1.40 Å. The X-ray diffraction data are shown for cupric tropolone[72].



Cupric tropolone

The X-ray crystallographic analysis of the 2,7-disubstituted-*trans*-15,16-dimethyl-15,16-dihydropyrene revealed many similarities (e.g. planarization) in aromatic character (**I** in Figure 6).[49, 73] For example, in the DHP 2 case (**I** in Figure 6) (R = *tert*-Bu-) the peripheral carbons atoms are displaced *ca*. 0.02-0.05 Å from the DHP framework plane. The structure of 2 has a two-fold axes, in which the peripheral bond lengths do not alternate spanning the range between 1.388 and 1.402 Å (esr 0.002 Å in all lengths).[49] In contrast, the bond lengths in the BDHP structure 3 (Figure 6) showed alternations in the range between 1.351 to 1.463 Å as a result of the partial bond localization due to the annelation of the benzene ring.[49]

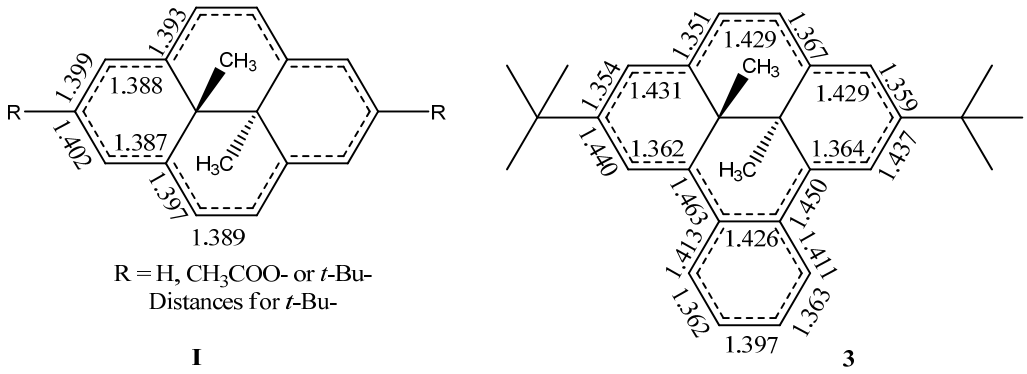


Figure 6. Structural data of 2,7-disubstituted DHP and BDHP

1.4.4 Induced ring current detection by NMR spectroscopy

Diamagnetism arises from circulation of electrons in filled orbitals in isolated atoms in diamagnetic substances. At a molecular level, when a cyclic conjugated molecule is placed in an external magnetic field, electrons in delocalized molecular orbitals make a circuit motion in the plane perpendicular to the external magnetic field direction. The

applied external magnetic field on each electron induces a small circuit current that opposes the applied external inducing field. The contribution from each electron in a molecule adds up to the total induced magnetic polarization and the effect becomes significant in poly-atomic molecules. In molecules having only isolated centers of unsaturation or having only saturated centers, the electrons are relatively isolated and the effects occur within a small area. In aromatic molecules, the π-electrons are not confined to individual atoms or bonds. The diamagnetic currents are not limited to specific atoms, but span an extended circuit around the ring. This secondary induced ring current due to the Larmor precession of the whole π-electron cloud is much stronger than the small, individual circuit currents of each σ-electron in the molecule. The magnetic field generated by the ring current is opposed to the external magnetic field within the ring but reinforces the applied field outside of the ring (Figure 7). Its strength depends on the electron density in the ground state.

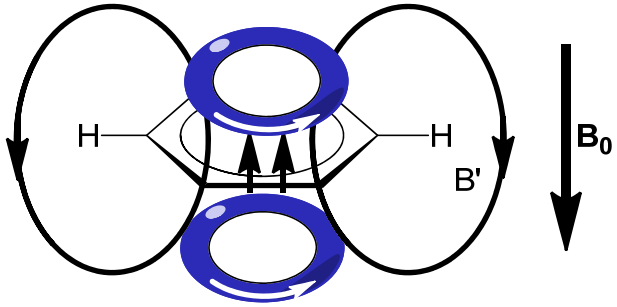


Figure 7. The induced ring current and magnetic field of benzene in an external magnetic field B_o

There exists also a paramagnetic current flowing in the opposite direction to the diamagnetic current. The paramagnetic current depends upon the total contributions from the electronically excited states. For most cyclic aromatic systems, orbital degeneracy exists in respect to the highest occupied and lowest unoccupied molecular orbitals. If the highest occupied pair of orbitals contain only two electrons in the $(4n)\pi$ electrons system, the degeneracy is removed by a geometric distortion (Jahn-Teller distortion). The resulting lower orbital is filled with the two electrons but the splitting between the two orbitals is small enough to allow the electrons to be excited into the higher energy orbitals. When this excitation is associated with a magnetic moment perpendicular to the

ring, a large paramagnetic contribution to the ring current takes place. Molecules containing (4*n*) π-electrons exhibit particularly large paramagnetic ring currents because they possess very low lying exited states, which are accessible through this magnetic dipole transition.

The large diamagnetic anisotropy effects in an aromatic molecule can be detected experimentally by NMR spectroscopy. The observation of diamagnetic ring currents can be used to designate an aromatic system experimentally. It is of considerable interest that different aromatic systems exhibit aromatic character to different extents. However, when it comes to comparison of the degree of aromaticity, more sophisticated arguments must be given.

One consequence of electron delocalization is the ability to sustain a ring current in an applied magnetic field (Figure 7). In the case of aromatic compounds possessing protons inside and outside of a cycle, this induced ring current will shield the inner protons and deshield the outer protons. As a result, protons inside the cycle resonate at a higher magnetic field and those outside resonate at a lower magnetic field relative to those when there is no such influence. For example, the protons on the benzene ring appear at δ 7.2 ppm, which lies outside the hexagon ring and feels the deshielding effects. Larger polyene ring systems with 12, 14 and 16 membered rings are flexible molecules that hardly maintain one conformation.[74] So inversion results in protons switching positions from inside to outside the ring and *vice verse*, resulting in no steady shielding or deshielding effects.

1.4.5 DHP used in measuring aromaticity and anti-aromaticity

Parent DHP 1 is a cyclic conjugated [14]annulene (Figure 8). Due to the presence of bridged saturated carbons in the center, all the peripheral carbons are held in a rigid planar scaffold. The 14π electrons account for its Hückel aromaticity resulting in an aromatic system with all π-electrons delocalizing over the 14 carbon outer ring. Two internal methyl groups are located across the center of the skeleton in the shielding region of the anisotropic magnetic field. Accordingly, these protons show interesting upfield shifts in the NMR spectrum, while the peripheral olefinic protons show the usual

downfield shifts (Figure 8). Ring opening of 2,7-di-*tert*-butyl-dimethyldihydropyrene to the CPD form ruptures the 14π system and its ring current so that the internal methyl protons move from -4.06 ppm to 1.58 ppm.[75]

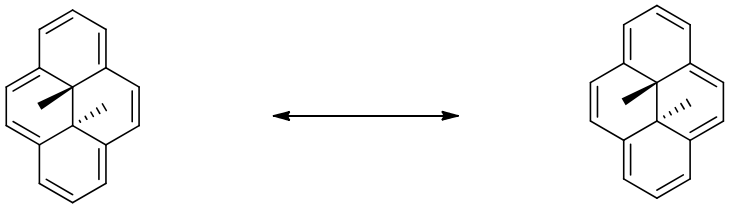


Figure 8. Parent DHP 1 and the resonance structures

DHP has been used as an aromaticity gauge to compare the relative aromaticity of different aromatic systems to benzene by monitoring the changes in chemical shifts for the internal methyl groups or the coupling constants of the peripheral protons.[56b, 76] Fusing a benzene ring to the [e]-position of DHP causes some bond fixation in the DHP ring and a reduction in DHP ring current.[73b, 77] Since the size of the DHP ring current is reflected in the upfield shift of the internal methyls, the reduction in ring current due to benzene fusion is measurable by the downfield shift caused by their fusion (δ -1.58 in BDHP 3 vs. δ -4.06 in DHP 2 in Figure 9).[41]

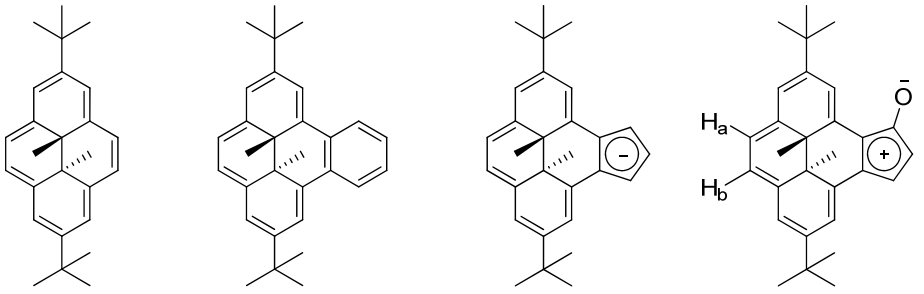


Figure 9. The chemical shifts for the internal methyl protons in 2, 3, 12 and 16

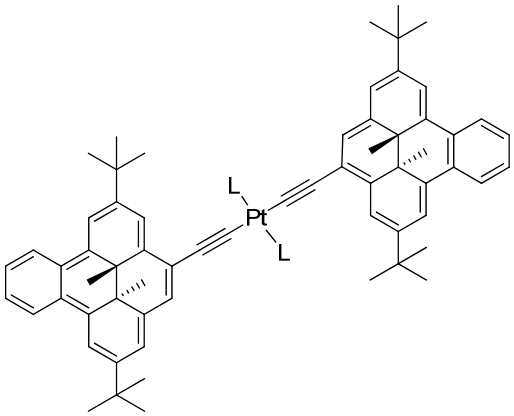
Similarly, fusion of other aromatics (Cp anion in **12** or cyclopentadienone in **16** in Figure 9) at this position will also cause a change in the DHP ring current and hence a

change in internal methyl chemical shifts, which can be compared directly to that of benzene fusion thus providing a direct comparison between the 'aromaticity' of the particular aromatic and benzene.[78] Of course, the assumption that the fused systems do not have significant anisotropic effects on the internal methyl protons through-space has to be made, but so far has proven to be true. Evaluation of the coupling constants of the DHP periphery provides an alternate approach based on the fact that shorter bonds show larger coupling constants in the NMR spectra (J = 8.7 Hz for H_a and H_b of **16** in Figure 9).[78] This method requires unique protons on the DHP and is therefore limited to those systems without mirror symmetry or C2 axes. For the parent DHP systems, for example, annulation at the [a]-position leaves three consecutive proton couplings.[53] The results from the coupling constant evaluation can be compared to that from the internal methyl chemical shifts although the lack of symmetry has the drawback that an average δ value, for example, δ -1.87 and -1.91 in **16**, must be used for the inequivalent internal CH_3.

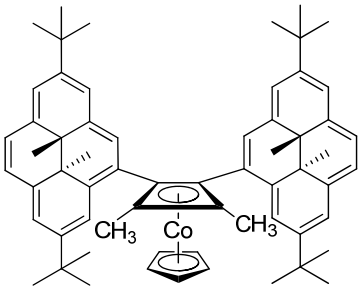
1.5 Research objectives

The goals of this thesis are two-fold: 1) to examine the effects of metal complexation on the photochemistry of the DHP core and 2) to investigate the aromaticity of fused unstaturated C7 and C8 rings as well as dangling organometallic fragments. The thesis includes four topics:

In Chapter 2, two DHP-derived photochromic compounds were joined by a *bis*-ethynyl platinum linker (Figure **10**), to study the photochromism and structural aspects of σ-bond metal ethynyl complexes (*cis* and *trans*).



DHP ethynyl metal complexes



DHP cyclobutadienide cobalt metal complexes

Figure 10. Platinum and cobalt metal complex targets

In Chapter 3, two DHP-derived photochromic compounds were dangled on an aromatic cyclobutadienide cobalt core (Figure **10**). The studies revealed the effects caused by the cyclobutadienide cobalt on the photochemistry of DHP photochromic compounds. Using X-ray crystallographic and NMR spectroscopy means, the aromaticity of the cyclobutadiene dianion was also evaluated.

In Chapter 4, seven- and eight-membered ring systems were fused to the [e]-position of DHP. The investigation focused on aromaticity aspects with regard to tropone, 6π aromatic tropylium cation, cycloheptatriene anions and 10π cyclooctatetraene dianion (Figure **11**).

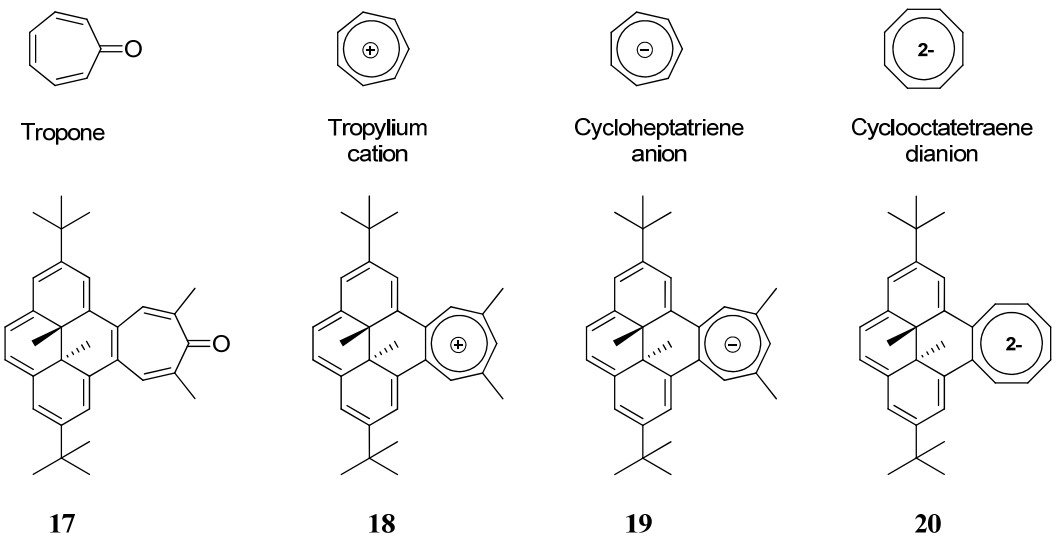


Figure 11. Aromatic systems studied and their relevant DHP compounds

We also tried to understand the homoaromaticity of cycloheptatriene on the basis of the DHP-fused cycloheptatriene. X-ray crystallographic and NMR spectroscopy data were used to reach the above objective.

Chapter 2. Platinum complexes of ethynyl DHPs

2.1 Introduction

Electronic communication between and through molecules is a property that is particularly important in materials chemistry, especially in terms of the electronic coupling and communication through an organic bridge. Marder[79] has commented that the electronic coupling through a -C≡C-Pt-C≡C- linkage is only somewhat smaller than through a -C≡C-Ar-C≡C- bridge. Thus he concluded that electronic delocalization in a π-conjugated –Pt-C≡C- unit was not substantially decreased when compared to a phenyl ethynyl compound. Alkynyl fragments are linear, unsaturated and rigid, and are made up of *sp* hybridized carbon chains. Electrons are able to flow along long conjugated carbon-carbon chains, which can then act as molecular wires.[80] Polyynes themselves have attracted much attention over several decades. There is a growing interest in transition metal connected polyynes because transition metals have extra electrons in their *d* orbitals and have redox properties. Tunable electron configurations are expected by changing ligands and oxidation states, which make it convenient to employ metal polyynes. Metal alkynyl complexes are the fundamental subunits to build up complex macromolecular wires.[81] These complexes provide the basic information to understand the structures and electronic properties of σ-alkynyl complexes in the absence of a highly conjugated electronic system. In the past 30 years, interest has also grown in the optical properties of alkynyl σ-complexes since they have potential applications in optical nonlinearity,[82] light-emitting diodes (LEDs)[83] and luminescent materials.[84]

Alkynes have two pairs of electrons in orthogonal π-orbitals, which can side-on coordinate to metals. Alkynyl ligands on the other hand, originate from the corresponding alkyne precursors by deprotonation and direct σ-bonding between the metal atom and the terminal alkyne carbon. The alkynyl (or alkynide) ligands are therefore regarded as [RC≡C$^-$] (R=H, alkyl or aryl) fragments in such complexes and are isoelectronic with CN$^-$, CO and N_2.[85] However, they have more in common with CN$^-$ because like that

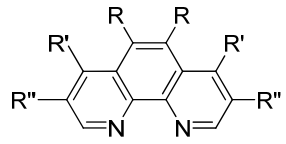
ligand, their negative charge makes them good σ-donors and poor π-acceptors. They also show similar behavior to halides in complex formation and precipitation reactions, which classify them as pseudohalide species.

σ-Alkynyl complexes have been explored for a variety of transition metals in groups 3-12.[86] The complexes of the early and late transition metals differ in aspects of their syntheses, molecular structures, electronic properties and applications. Early transition metal alkynyl complexes have found usage in catalytic or stoichiometric polymerizations and further π-coordination of the C≡C triple bond to other metal centers often results in the formation of cluster compounds.[87] However, since later transition metal σ-bonded alkyne complexes, especially those having octahedral and square planar geometries, are of most interest to material science, platinum alkynyl complexes were chosen as the focus of this study.

Terminal alkynyls form *cis* and *trans* square planar complexes with Pt^{2+}. For group 10 metals, phosphine ligands are the most studied ancillary ligands in building both geometric isomeric alkynyl complexes.[88] Monodentate ligands, for example Ph_3P, Et_3P, $P(tol)_3$, can occupy either the *cis* or *trans* position of a square planar geometry and which forms depends on reaction conditions. Bidentate phosphine ligands with a short chain, such as dppe (1,2-*bis*(diphenylphosphino)ethane) and dppp (1,3-*bis*(diphenylphosphino)propane)), prefer to form monomeric complexes with a *cis*-geometry only.

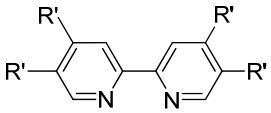
Bidentate chelating diamine-type ligands, such as phenanthroline and 2,2'-bipyridine (Scheme **11**),[89] serve as supporting ligands in σ-alkynyl platinum complexes in the same manner as bidentate phosphine ligands. Their rigid structure and unique low energy excited states make them interesting candidates for optical purposes. Modifications can be applied relatively easily by introducing substituents such as *t*-butyl groups at the 4 and 4'- positions of the 2,2'-bipyridyl group that lead to much greater solubility in organic solvents upon metal complexation while retaining the chelating properties. Eisenberg[90] explored the photochemical application of alkynyl platinum diamine complexes with substituted phenanthroline and 2,2'-bipyridyl ligands. In contrast to phosphine-platinum analogs, the *bis*-alkynyl diamine platinum complexes were brightly luminescent in solution with evidence of self-quenching.[91] The quenching process may be due to the Pt-

Pt interaction. Tridentate terpyridyl (terpy) and isophthalaldimine (Scheme **11**) formed doubly charged platinum metals complexes binding one alkyne moiety with a loose counter anion. X-ray crystallographic data showed close to a square planar geometry as a consequence of the geometric constraints imposed by the terpyridine ligands.[92] Guo[93] observed a metal-to-ligand charge transfer (MLCT) transition occurring at 420-430 nm and an additional solvatochromic charge-transfer band at *ca.* 460−540 nm in the substituted phenylalkynyl terpy platinum complexes. Calculations by Liu[94] revealed that the long wavelength absorptions are dominated by π(C≡C) to π^*(terpy) transitions with some dπ(Pt)-to-terpy transition. Nevertheless, these transitions are tunable by changing electronic features of the substituents on the *para* position of the phenylacetylene.



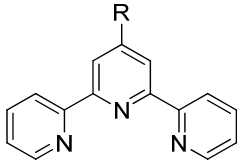
R, R' and R" = Ar or aliphatic group

phenanthroline



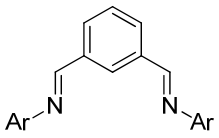
R and R' = Ar or aliphatic group

substituted 2,2'-bipyridine



R = Ar or aliphatic group

Terpyridyl (terpy)



isophthalaldimine

Scheme 11.Heterocylic diamine and diimine ligands

In a rare case, Elsevier[95] has found that isophthalaldimine ligands bond on platinum by *trans* coordinated nitrogen atoms and metallation occurs on the aromatic ring to give C-M σ-bonding. Changing substituted groups on the two N-phenyl rings sterically and electronically affects the bonding to the metal and the lability of the metal complexes. Consequently, both a dimeric μ-η^1:η^2-(σ,π)-alkyne complex with one coordinating nitrogen atom and a monomeric σ-alkynyl (η^1) metal complex with two coordinating

nitrogen atoms were obtained. The rare coordination behavior of the C≡C triple bonds in the former strongly indicates the electron richness of the metal centers. As a result, π-backdonation becomes pronounced allowing formation of the unusual weak side-on interaction with the π orbital of the alkynes.

Spectroscopic data and calculations indicate the presence of strong $d\pi$-$p\pi$ overlap between the metal *d* orbital and the filled *p* orbitals of the alkynes.[96] Therefore, alkynyl ligands can serve as π-electron donors and give electrons to the empty d_{xz} and d_{yz} orbitals of a late transition metal in a higher oxidation state. Alkynyl ligands also have the potential to act as electron acceptors as their π^*-orbitals can interact with filled π-symmetry *d* orbitals on the metal. However, the π^* orbitals of alkynyl ligands lie at much higher energies (~15 eV) than the filled metal *d* orbitals according to molecular orbital calculations,[96] and this makes interaction between the π^* orbitals of the alkynyl group and $d\pi$ orbitals of the metal unimportant.

Experimental data show that *trans* metal complexes, in general, are more thermodynamically and chemically stable than the corresponding *cis* ones. In regard to the alkynyl platinum complexes, the alkynes in the *cis* isomer have the right conformation to undergo reductive elimination reactions.[97] The configuration in the square planar Pt^{2+} metal complexes is usually controllable by the ancillary ligands or reaction conditions. Sonogashira[98] elaborately delivered the selective syntheses of both *trans* and *cis bis*-alkynyl platinum complexes containing two monodentate phosphines, PEt_3 or $P(^{n}Bu)_3$ in good yields (>85%). Keeping the reaction cold (< -20°C) was key to maintaining the initial *cis*-phosphine configuration. In contrast, Vicente[99] obtained exclusively *trans*-dialkynyl platinum(II) complexes starting from the *cis*-*bis*-(PAr_3) (Ar = Ph or tol) platinum(II) chloride under elevated temperature conditions. Tykwinski[100] has also demonstrated the possibility of transforming the *trans* to *cis* conformation by replacement of the monodentate ligand PPh_3 with bidentate *cis* ligands such as 1,2-*bis*(diphenylphosphino)ethane (dppe). Bidentate phosphine ligands with longer chains $Ph_2P(CH_2)_nPPh_2$ (n = 8-14) can form dimers and other large molecule complexes.[101] It is clearly evident that the complexes are labile in solution. The preference for formation of *trans* over *cis* products might be due to steric repulsion.

Several monodentate phosphine ligands show perturbation of the electronic properties of the *trans* alkynyl ligands.[102] For example, the vibrational frequencies associated with the C≡C triple bonds were red shifted when stronger *σ*-donor phosphine ligands were used (PCy_3 versus $P(OPh)_3$). However, an investigation by Schull[102] did not support the use of electronic delocalization in tuning molecular conductance. These controversial results drove us to look for insight into this effect and to seek its possible use in improvement of photoswitch efficiency.

With respect to a DHP-based *bis*-photochrome, the working hypothesis was that energy transfer between chromophores in one molecule through spacers would accelerate photochemical ring-opening and closing processes. Zhang[103] and Wang[104] prepared and studied photochemical properties of DHP photochromic compounds with homo-conjugated (-CO- linker), non-conjugated (-CH_2- linker) and fused conjugation (arene linker) systems. The DHP photochromic compounds opened and closed independently and multiple states were achieved. Disappointingly no significant switching rate enhancement was observed. Bandyopadhyay[105] has synthesized a *bis*-photochrome having two benzo[e]DHP photochromic compounds joined by one butadiyne spacer (Figure **12**).

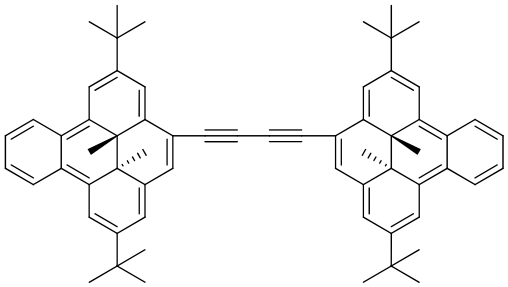


Figure 12. *Bis*-BDHP butadiyne photochromic compound.

During the course of photoopening, the two benzo[e]DHP photochromic compounds probably responded simultaneously to opening upon visible light irradiation. In contrast, during photoclosing UV-Vis spectral evidence indicated an unambiguous stepwise closing process. This system failed to shed any light on the mutual influences of two DHP chromophores through the spacer because of difficulties in distinguishing the open-

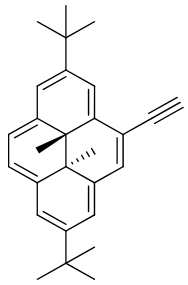
closed and closed-closed forms. Insertion of square planar platinum units into the butadiyne spacer was expected to maintain a rigid geometry and avoid undesired photochemical side reactions. At the same time, metal involvement in the photochemical processes of the photochromic compounds can be tuned by changing the electronic properties of the ancillary ligands and the geometry of the complex.

2.2 Syntheses

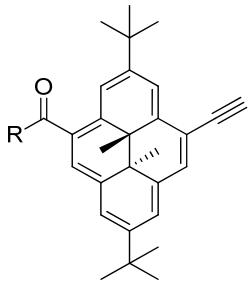
The DHP 2 does not open photochemically using low energy light sources due to its intrinsically low quantum yield (0.0015[39]). To explore the photoopening, enhancement of the photoopening rates was critical. Adding a ketone or aldehyde group to the 2 or 4 position of the DHP molecule increases the photochemical opening rates and slows the thermal return back reaction of CPD. The improvement in opening rate as well as quantum yields of 4-acyl DHPs over DHP 2 has been explored.[106] A benzoyl group on the 4 position of DHP 2 increased the photoopening quantum yield of 4-benzoyl DHP **31** by 2.5 times,[39] while increasing the thermal return rate by 1.5 times. The more electron withdrawing trifluoroacetyl group was introduced onto DHP 2 in order to understand the electronic effects with the added benefit that the opening and closing processes could be monitored by ^{19}F NMR spectroscopy. Either acetyl or ethynyl groups on the 4-position of benzo[e]DHP 3 enhanced the photoopening quantum yields ($\Phi_{opening}$ 0.042) by a factor of *ca*. 2 with $\Phi_{opening}$ = 0.095 and 0.075 for the acetyl and ethynyl group, respectively.[40] Surprisingly, having one alkyne on the side of DHP 2 *diminished* the quantum yields by a factor of 2.7, and having two alkynes in the 4 and 9 positions of DHP 2 resulted in a decrease by a factor of 2.9.[39] The lack of any predictive ability for such alkyne DHP systems prompted us to study the photochemical properties of their platinum complexes systematically in the opening and closing processes.

The DHP-ethyne **24** was prepared and used as a prototype. DHP-ethynes with a variety of acyl groups (acetyl **30**, benzoyl **34**, 1-naphthoyl **39** and trifluoroacetyl **42**) were made in a similar manner from the corresponding acyl DHP precursors. In addition, since benzoDHP systems offer better quantum yields and stability as photochromic compounds, the benzo[e]DHP-ethyne **40** was synthesized following the reported procedure.[40] The

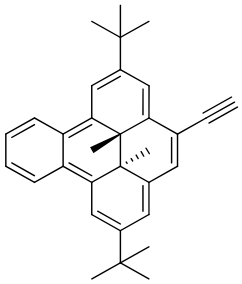
syntheses and characterization of the Pt complexes of these alkynes are reported in this chapter.



24



R	
Me	**30**
Ph	**34**
Np	**39**
CF_3	**42**



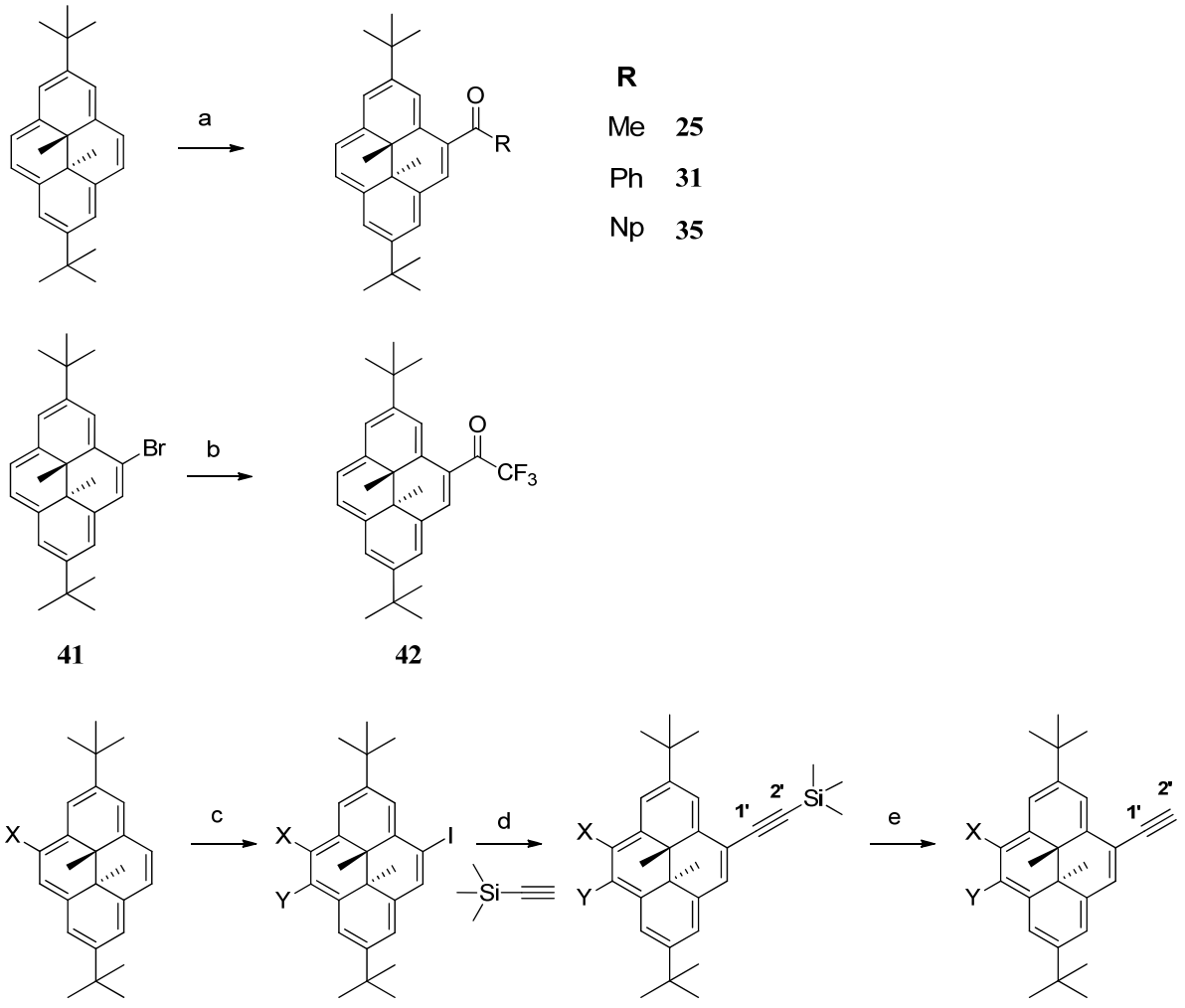
40

2.2.1 Syntheses of the alkynes

The easiest way to establish a series of DHP-alkynes with different substituents is by the method of palladium-catalyzed coupling reactions between DHP halides and alkyne derivatives. Some coupling methods[107] involve harsh reaction conditions, which are not suitable for the moderately thermally unstable DHP derivatives. Both Stille and Sonogashira coupling reactions using $RC{\equiv}CSnR_3$ and $RC{\equiv}CH$, respectively, with bromides and iodides have been successfully used to make DHP-alkyne products in good yields. Nishihara[50] has used the Stille strategy in coupling benzo[e]DHP dibromide with ethynylferrocene to make DHP photoswitches in good yields. Due to the diversity and availability of alkyne precursors, the Sonogashira coupling approach enabled us to quickly access a variety of DHP-alkyne photoswitches.[39, 108] Organic iodides are much more reactive than the corresponding bromides in coupling reactions and therefore involve only mild reaction conditions. Coupling terminal alkynes with DHP bromides often requires elevated temperature, while the DHP iodides react smoothly at room temperature.[39] For reaction with DHP bromide, the usage of tri-*n*-butylsilylethyne or other high boiling point alkyne precursors is necessary to prevent reactant loss from the hot reactions. Trimethylsilylacetylene (b.p. 53 °C) is usually an excellent coupling partner with DHP iodides at room temperature resulting in an easily removed

trimethylsilyl protecting group in the products. DHP bromide had to be used in some cases because the yield from iodination of DHP was unacceptably low. Recently, Fu[109] developed a catalysis system including bulky, electron-rich phosphines (P(*t*-Bu)$_3$) in Sonogashira coupling of aryl bromides with acetylene at room temperature. Olga Saretcheyva of our group adapted similar reaction conditions using a palladium catalyst and tri-*tert*-butylphosphine to couple DHP bromides with alkynes under moderately hot conditions (~80 °C). Finally, the Sonogashira reaction conditions tolerate a wide range of functional groups including ketones and aldehydes. Because the electron richness of DHPs results in sluggish coupling reactions, the use of DHP halides containing electron withdrawing acyl groups was expected to give faster reactions than the parent DHP halides. Sonogashira coupling reactions were adapted to prepare the DHP-ethyne ligands used in this thesis.[110]

The reaction sequence shown in Scheme **12** involves the introduction of the electron withdrawing acyl groups first via a Friedel-Craft acylation with 3 to 10-fold excess of the corresponding acid chlorides relative to DHP, followed by iodination. The resulting DHP iodides were then reacted with excess trimethylsilylethyne, catalyzed by *bis*(triphenylphosphine)palladium(II) dichloride and copper(I) iodide in basic media. The trimethylsilyl protecting group was removed quantitatively from the coupled DHP-alkynes to afford the desired terminal alkyne ligands.



R	
Me	25
Ph	31
Np	35

X	
H	2
CH_3CO	25
PhCO	31
NpCO	35

Y(X)=H, X(Y)	
H	22
CH_3CO	28A (B)
PhCO	32A (B)
NpCO	37A (B)

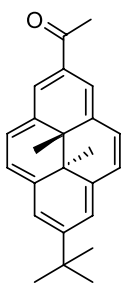
X(Y)	
H	23
CH_3CO	29
PhCO	33
NpCO	38

X(Y)	
H	24
CH_3CO	30
PhCO	34
NpCO	39

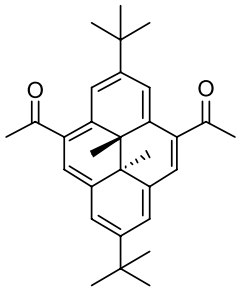
Conditions: a) $AlCl_3$, DCM, Room temperature; b) 1) *n*-BuLi, THF -78 then r.t. 1 hour 2) CF_3COOEt, 12 hours; c) I_2, Ag(collidine)PF_6, DCM, room temperature, 12 hours; d) $Pd(PPh_3)_2Cl_2$, CuI, Triethyl amine, room temperature; e) K_2CO_3, THF/CH_3OH, 100% yield

Scheme 12. The preparation of DHP-derived alkyne precursors.

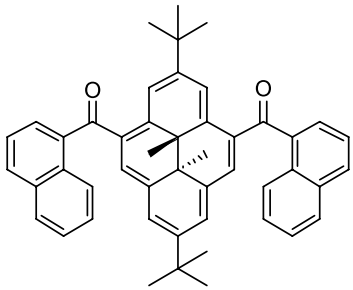
The synthesis of acyl DHPs (DHP-C(O)-R, R = Me **25**, Ph **31** and Np (1-naphthyl) **35**) was accomplished by Yang and other members in our group.[106] The acylation of DHP proceeded by the addition of acid chlorides (CH_3COCl, C_6H_5COCl and NpCOCl) or acid anhydride to a solution of DHP and $AlCl_3$ in dry DCM at room temperature (Scheme **12**). Among the different acid chlorides, 1-naphthoyl chloride gave the best optimised reaction yields. Using excess acid chloride didn't ensure complete conversion of the DHP. The reaction using NpCOCl (10 equivalents) and DHP yielded 1'-naphthoyl DHP **35** in 97% yield in 2 hours. In contrast, if 3 equivalents of 1-naphthoyl chloride to DHP were used, a longer reaction time was required (12 h), resulting in up to 30% of double acylation



26



27



36

product *bis*-1'-naphthoyl DHP **36**. 4,10-DiacetylDHP **27** was also formed for the same reason when DHP reacted with acetyl chloride. The regiochemistry of **27** and **36** was established as having two acyl groups on carbons 4 and 10 on the basis of the 1-D and 2-D NMR spectra. Though double electrophilic acylation is not normally observed on regular arenes, it is more common with very electron rich DHPs. Fast reactions with 1-naphthoyl chloride largely depressed the formation of such products as **36**. However, we did not observe the same results with acetyl chloride. The reason might be attributable to the higher reactivity of acetyl chloride compared to 1-naphthoyl chloride. Additionally, acetylation with CH_3COCl, also happened with replacement of one of the *tert*-butyl groups at the 2-position of DHP resulting in formation of 2-acetyl-7-*tert*-butyl-*trans*-dimethyldihydropyrene **26** in *ca.* 5-10% yields. Similar replacement was not observed in the PhCOCl and NpCOCl cases. Therefore, this is likely due to the higher electrophilicity of the reaction intermediate from acetyl chloride. The desired 4-acetylDHP product **25**, consistent with previous spectroscopic results,[40, 106] was obtained in only 40-60% yield. Prolonged reaction time in the presence of $AlCl_3$ always led to partial decomposition of

DHP that contaminated recovered starting materials. The alternative method on benzo[e]DHP using acetic anhydride and BF_3·EtO gave *ca.* 80% yield,[40, 111] presumably due to the weaker Lewis acidity of BF_3 compared to $AlCl_3$.

2-Acetyl-7-*tert*-butyl-*trans*-dimethyldihydropyrene **26** was confirmed by mass spectrometry and NMR spectroscopy. The molecule of **26** contains C_s (assuming free *t*-Bu rotation) symmetry, as evidenced by the pairing up of protons on the DHP framework in the ^{1}H NMR spectrum. The two protons nearest to the acetyl groups resonated downfield at δ 9.10, consistent with the deshielding effects of a ketone as also observed in 4-acyl DHP. The ^{1}H chemical shifts of the internal methyl groups for **26** were close together at δ -3.89 and δ -3.91, probably mostly affected by the electron withdrawing substituents.

Two different resonances were found at δ -3.77 and -3.79 for the internal methyl protons in 4,10-diacetyl DHP **27**, Similarly, two resonances for the *t*-butyl protons at δ 1.69 and δ 1.68 indicated that this was the 4,10-, rather than 4,9-di-substitution regioisomer. The downfield shift of the internal methyl protons from those of the parent DHP was greater than 4-acetyl DHP **25**, consistent with having two electron-withdrawing groups on the DHP. Similarly the ^{1}H NMR spectrum of *bis*-1'-naphthoyl DHP **36** revealed three signals for the six DHP peripheral protons indicating high symmetry. The internal methyl protons for **36** resonate further downfield than those in naphthoylDHP **35** (δ -3.54, -3.58 for **36** *vs.* δ -3.81, -3.84 for **35**), indicating that the two 1-naphthoyl groups are nearer to the same internal methyl group (4,10-di-1'-naphthoyl regioisomer).

The trifluoroacetyl DHP **42** was prepared in a different manner in 25% yield. Ethyl trifluoroacetate reacted with lithiated DHP (generated *in situ* in dry THF) at -78°C and then at room temperature for 12 h (Scheme **12**). The yield of the reaction is the average of two trials and no optimization has yet been done. The ^{1}H NMR spectrum shows the internal methyl resonances shifted to δ -3.830 and -3.831 in **42** from δ -3.93 and -3.95 in bromo-DHP **41**[41]. The ^{13}C NMR spectrum reveals the carbonyl carbon resonance at δ 182.00, consistent with the electron withdrawing nature of the trifluoromethyl group. The ^{19}F NMR showed a single resonance at δ 68.29. The C=O stretch appeared at 1681 cm^{-1} in the infrared spectrum, indicating the conjugation to DHP.

Iodination of 4-acyl DHP **25** and **35** was accomplished using iodine and Ag(collidine)PF_6 in DCM (Scheme **12**).[39] Apart from the starting material, the resulting reaction mixture was comprised of two regioisomers in about 50-75% total yield based on the NMR analysis. The ratio of the two isomers was determined as a little greater than 5:1 based on the ^{1}H NMR integration. 2-D NMR evidence was used to distinguish the two isomers depicted. The major regioisomer contained an acyl group and an iodine atom at the 4- and 10- positions, while the minor regioisomer was designated as 4,9-regioisomers, (isomer A and B, respectively, Figure 7).

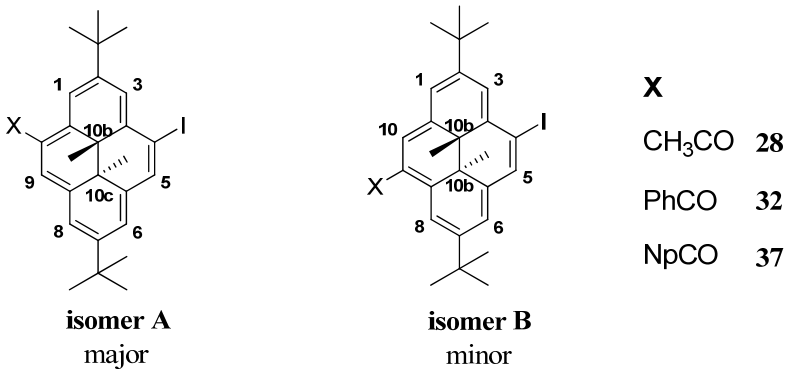
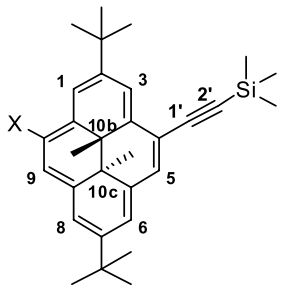


Figure 13. Two regioisomers of acyl DHP iodides

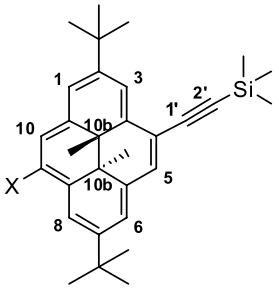
To establish the isomeric structure of the iodination products, 2-D NMR techniques, and crystallographic analysis (discussed in section **2.3**) were utilized. The iodination of acetyl DHP provided a major isomer **28A**, which showed two resonances for the internal methyl protons at δ -3.84 and -3.85 in the ^{1}H NMR spectrum. Its HMBC spectrum revealed explicit correlations between C-10c and both H-5 and H-9, indicating that this regioisomer is 10-acetyl-4-iodo-DHP **28A**. The amount of the minor product **28B** was measured as ~10% from the ^{1}H NMR spectrum. In the phenyl analog **32**, the ^{1}H NMR spectrum for the major isomer **32A** included resonances at δ -3.743 and -3.75 for the internal methyl protons while these were observed at δ 3.736 and 3.77 for the minor isomer **32B**. The distinction between the two isomers, **32A** and **32B,** was based on 2-D NMR spectroscopy in the same manner. The HMBC spectrum revealed that the carbon signal at δ 29.69 (C-10c) is correlated with both H-5 at δ 9.00 and H-9 at δ 8.63 for isomer **32A**. The isomeric structures **37A** and **37B** were determined unambiguously to be

the 4,10 and 4,9 isomers in a similar manner for the 1'-naphthoyl DHP iodide. These isomers are separable by crystallization, but this is usually not necessary as the mixed isomers are not expected to behaviour differently in studies of photoswitching properties. Therefore, the mixture was used in subsequent reactions without further separation. For the sake of simplicity, only the major regioisomers **A** are shown in the following text unless a distinction between the isomers is important to the discussion. Note that the iodo-DHP **22** was prepared following the reported procedure and the characterization properties matched those reported.[39]

For the DHP iodides **22** and both isomers **A** and **B** of the DHP iodides **28**, **32** and **37**, the Sonogashira coupling reactions with trimethylsilylethyne gave the corresponding TMS protected alkynes **23**, **29**, **33** and **38**, respectively, in nearly quantitative yields (Scheme **12**). As expected, their NMR spectra showed the two isomeric molecules **A** and **B** with slightly different chemical shifts. For example, almost all protons between



isomer A
major



isomer B
minor

X	
H	**23**
CH_3CO	**29**
PhCO	**33**
NpCO	**38**

benzoyl DHP derivatives **33A** and **33B** resonated very close to, but distinct from, one another in the ^{1}H NMR spectrum. There exist some obvious steric hinderance contributions to the chemical shifts. The proton chemical shifts for the -Si($C\underline{H}_3$)$_3$ was found at δ 0.426 and 0.431 for **33A** and **33B** respectively. The difference can probably be attributed largely to through-space anisotropy influences. Nevertheless, the differences should not be overstated and indeed their similarities outweigh their differences by NMR.

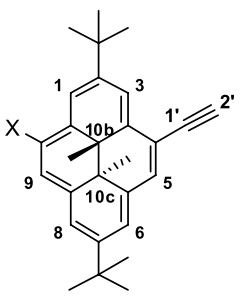
As expected, different substituents **X** cause significant perturbation of the DHP electron density, but insignificant changes to the alkyne moiety in the NMR spectra (Table 1).

Table 1. Selected NMR and IR data for TMS protected DHP-alkynes 23, 29, 33 and 38

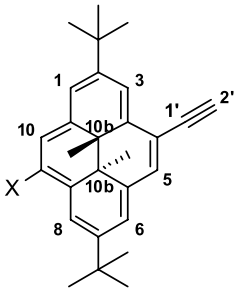
	NMR data			Infrared data (cm^{-1})	
	$\delta_{(10b/10c\text{-}CH_3)}$	$\delta_{(C\text{-}1')}$	$\delta_{(C\text{-}2')}$	$\nu_{(C\equiv C)}$	$\nu_{(C=O)}$
H- **23**	-3.92	106.20	99.27	2140	-
CH_3CO- **29**	-3.80, -3.81	105.54	99.93	2141	1662
Benzoyl **33**	-3.71, -3.72	105.59	99.96	2140	1648
1-Naphthoyl **38**	-3.69, -3.71	105.53	100.01	2139	1640

In the ^{1}H NMR spectra for the major isomers **A**, the internal methyl protons shifted downfield in the order **23** < **29** < **33** < **38**. The C-1' and C-2' were similar at δ 105.5 and 100.0, respectively, in all acyl derivatives in the ^{13}C NMR spectra. The slightly downfield chemical shifts of C-1' at δ 106.20 in the parent DHP-alkyne **23** indicated that the influence of the ketone is small in the ^{13}C NMR spectra. In the same way, DHP substituents **X** had negligible effects on the C≡C triple bond vibrations as all four alkynes showed C≡C stretching vibrations at around 2140 cm^{-1}. The C=O stretches are markedly different between these molecules as might be expected for aliphatic (ν 1662 cm^{-1}) and aromatic (ν 1640 cm^{-1}) substituents due to the existence of conjugation. The quantitative removal of the protecting trimethylsilyl group in alkynes **23**, **29**, **33** and **38** was accomplished by treatment with K_2CO_3 in degassed THF/MeOH (1:1) solvents.

The chemical shift differences between the two regioisomers **A** and **B** in the resulting acyl DHP-derived ethynes **30**, **34** and **39** are very small. For instance, the proton chemical shift for H-2' was found at δ 3.75 for the minor benzoyl DHP-ethyne **34B** in contrast to δ 3.73 for the major alkyne **33A**. As expected, the ^{1}H NMR spectra essentially showed that the internal methyl protons had the same chemical shifts as the TMS-protected alkynes (Table 1). The protons H-2' appeared approximately at δ 3.73 for non-substituted **24** and substituted DHP-ethynes **30**, **34** and **39**. Note that the proton was less deshield at δ 3.50 for the benzo[e]DHP-alkyne **40**, consistent with a lower DHP ring current in the benzo-fused DHP. C-1' and C-2' resonated at δ 84.0 and 82.4 in all DHP-ethynes (**24**, **30**, **34** and **39**) in the ^{13}C NMR spectra. It is worth pointing out that both of

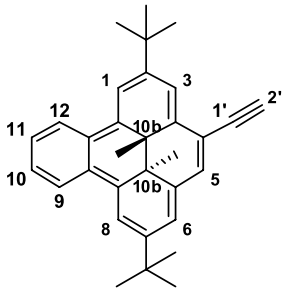


isomer A
major



isomer B
minor

X	
H	**24**
CH_3CO	**30**
PhCO	**34**
NpCO	**39**



40

the corresponding carbon resonances in benzo[e]DHP-ethyne **40** were shifted upfield.[40] The terminal carbon C-2' in **40** resonates at δ 81.4, shifting upfield by 1 ppm from those in the acyl DHP-ethynes **24**, **30**, **34** and **39**. From these observations, it might be implied that the DHP substituents in **33** and **38** cause minimal anisotropy effects on magnetic nuclei on the opposite side of the DHP ring. The IR stretch of the C≡C triple bond was observed at approximately 2090 cm^{-1} in alkynes **5**, **11**, **15**, **20** and benzo[e]DHP-ethyne **40**.

2.2.2 Synthesis of platinum complexes with ethynyl DHP ligands

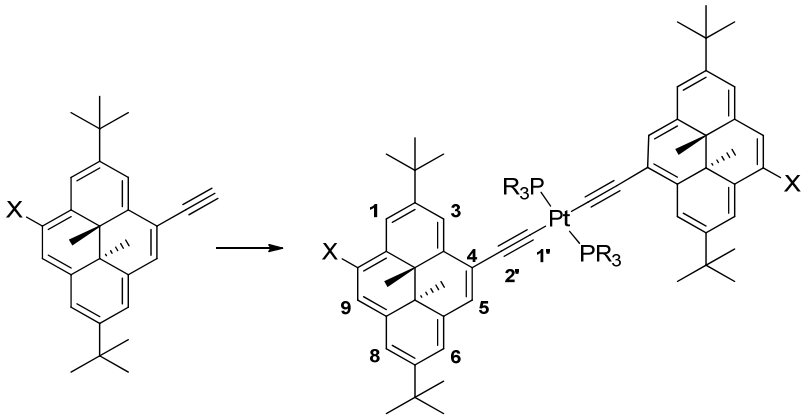
Two strategies have been widely used to make platinum complexes. Both methodologies were tried in this thesis and the second method gave more reproducible results.

a. salt metathesis: MX + M′-C≡CR → M-C≡CR + M′X

b. dehydrohalogenation: MX + H-C≡CR → M-C≡CR + HX (presence of base)

The salt metathesis process is suitable to prepare alkynyl complexes with most transition metals, in that most metal halides will react with an anionic alkali metal alkynide salt.[112] Dehydrohalogenation[113] in basic media was widely used to prepare a variety of alkynyl platinum complexes. The reactions proceeded smoothly with a little heating or cooling. Usually cuprous halide is needed to accelerate the reactions and to activate the alkynes. To synthesize Pt complexes, the dehydrohalogenation methodology was usually adapted from the corresponding metal chloride bearing ancillary ligands, such as phosphines. Using mild reaction conditions, the reaction can often be controlled to introduce only one alkynyl group leaving one chloride in the product.[114]

We decided to employ the commonly used dehydrohalogenation methodology in establishing a series of alkynyl platinum complexes by changing the DHP moiety and the ancillary ligands. In this chapter, all the reactions between terminal DHP-derived ethynes and platinum chloride were carried out using the conditions shown in Scheme **13** unless otherwise specified. The starting chloride $Pt(PEt_3)_2Cl_2$ and 2 equivalents of alkynes in diethylamine at 50°C furnished the desired alkynyl platinum complexes in poor to good yields (10-85%). Diethylamine is a mild base with a pK_b of 11.09 at 20 °C.[115] It can be evaporated easily and any residual amine can be washed away with saturated ammonium chloride. The products were collected by filtration when solid products precipitated from reactions. Otherwise, they were extracted using dichloromethane and then evaporated to afford the desired products. In the latter, the products were purified chromatographically and/or recrystallized in dichloromethane and hexanes to obtain their crystals.



Conditions: $Pt(PEt_3)_2Cl_2$, CuI, diethyl amine, 50°C

Scheme 13. The preparation of the *trans*-(^{X}DHPCC)$_2$(PR_3)$_2$Pt(II) complexes

The identities of the complexes were confirmed using NMR, IR and Mass spectroscopic techniques. ^{31}P NMR spectra were collected in cases where phosphine ligands were present. Crystallographic analyses were carried out to help determine complex geometry in cases where X-ray quality crystals were obtained. *Trans bis*(phosphine) (PEt_3 and PPh_3) complexes **43**, **44**, **45**, **46** and **47** containing either parent or acyl DHP were obtained using the method described in Scheme **13**. The benzene-annelated DHP-alkynyl platinum complexes, **48** and **49**, depicted in Scheme **14**, were prepared in the same manner.

Table 2. Selected characterization data for Pt complexes containing acyl substituents (only the major isomer A series shown)

L =	H PEt_3 **43**	Acetyl PEt_3 **44**	Benzoyl PEt_3 **45**	1-Naphthoyl PEt_3 **46**	Benzoyl *PPh₃* **47**
δ (internal-C$\underline{H}_3$)	-3.83, -3.86 [a]	-3.72, -3.75 [a]	-3.62, -3.64 [b]	-3.62 [b]	-3.87, -3.88 [a]
δ C-α	115.11,	115.13,	n/o,	n/o,	n/o,
δ C-β	110.95	110.46	110.86	110.43	115.29
$^2J_{C\text{-}P}$ (Hz)	29	29	n/o	n/o	n/o
$^1J_{Pt\text{-}P}$ (Hz)	2383	2384	n/o	2383	2655
ν(C≡C) (cm^{-1})	2082	2081	2077	2080	2092

a. CD_2Cl_2; b. $CDCl_3$; c. C_6D_6.

The loss of the acetylenic hydrogen signals in the range of 3-4 ppm provided ^{1}H NMR evidence for formation of Pt DHP-alkynyl complexes. The internal methyl protons also displayed marginal, but evident, shifting (Table 2) from those in the DHP-ethyne precursors (Table 1 on page **49**). For example, complex **47** containing triphenylphosphine ligands showed the internal methyl protons resonances at -3.87 and -3.88 (in CD_2Cl_2) in contrast to -3.71 and -3.72 (in $CDCl_3$) in the precursor benzoyl substituted ethyne **34**. The ^{13}C chemical shifts for the alkyne carbons provided good evidence of complex formation. The C-2' shifted by *ca.* 10 ppm from δ 105.59 in precursor **34** to δ 115.29 in complex **47**. Unfortunately the most interesting C-1' signal was not observed due to the low concentration of the sample in this particular case. ^{31}P NMR was also used as a diagnostic tool to investigate the electronic properties of the metal-ligand bonds. *Trans*-influence effects, a thermodynamic phenomenon, are apparent in the ground state of square planar complexes for d^8 metal ions of groups 9, 10 and 11. A coordinated ligand can influence ground state properties, such as bond lengths, bond vibration frequency and NMR coupling constants of groups *trans* to itself. Phosphine ligands have a relatively strong *trans*-influence as revealed by changes in $^1J_{Pt\text{-}P}$ coupling constants, while the alkynyl is

even stronger. The coupling constants $^{1}J_{Pt\text{-}P}$ decrease in magnitude by *ca.* 300 Hz from 2622 Hz for *trans*-[Pt(PPh_3)$_2$(C≡C-C_6H_4-*p*-OCH_3)$_2$] to 2323 Hz for *cis*-[Pt(PPh_3)$_2$(C≡C-C_6H_4-*p*-OCH_3)$_2$] indicating that the -C≡C-C_6H_4-OCH_3 ligand has a stronger *trans*-influence than PPh_3.[116] The coupling constant of $^{1}J_{Pt\text{-}P}$ = 2651 Hz for **47** is strongly suggestive that this is a *trans* phosphine complex.

Platinum has one medium sensitivity NMR I = ½ nucleus, ^{195}Pt. ^{195}Pt NMR signals span an extremely wide NMR range (*ca*. 15,000 ppm) and ^{195}Pt chemical shifts therefore provide useful structural, conformational and electronic information about the coordinating ligands. The alkynyl phosphine platinum complexes resonate in a window a few hundred ppm wide around 0 with K_2PtCl_4 in D_2O used as standard. Complex **47** shows a chemical shift of -252 ppm, consistent with the literature chemical shifts for complexes with a square planar geometry and a +2 oxidation state at the metal center. Two IR active C≡C stretches were also anticipated for the *cis*-*bis*-acetylenyl complexes of C_{2v} symmetry, while only one stretch was expected for the *trans* isomers with D_{2h} symmetry. In complex **47**, only one stretch was observed at *ca*. 2092 cm^{-1}, consistent with a *trans* geometry. This stretch is shifted *ca.* 50 cm^{-1} to lower frequency in **47** than in the ethyne precursor **34**, indicating that the CC bond is weakened by complexation to Pt.

Similar to the *trans*-triphenylphosphine complex **47**, the *trans*-triethylphosphine platinum complexes **43**, **44**, **45** and **46** all demonstrated a slight downfield shift (< 0.1ppm) for the internal methyl protons upon complexation (Table 2). A significant chemical shift change for the DHP peripheral protons (H-3) next to the alkynylide platinum centers was also observed. For example, the ^{1}H NMR spectrum for platinum complex **44** revealed an H-**3** resonance at δ 9.19 in CD_2Cl_2 in contrast to δ 9.04 in $CDCl_3$ for the free alkyne **30**. The acetylenic carbons appeared at *ca*. δ 115 (α-C, $^{1}J_{Pt\text{-}C}$ *ca*. 30 Hz) and δ 110-111 (β-C), in the ^{13}C NMR spectrum (Table 2). The phosphine resonated around δ 13 ppm with a coupling constant $^{1}J_{Pt\text{-}P}$ of 2384 Hz in the ^{31}P NMR spectrum (Table 2). The coupling constant is in agreement with values of ~2300 Hz in other *trans*-[Pt-(alkynyl)$_2$(PR_3)$_2$] (R = Me, Et and *n*-Bu) complexes.[99, 117] Bear in mind that ^{31}P chemical shifts and Pt-P coupling constants depend on the properties of the R groups in PR_3. These shifts are not easily predictable, thus comparisons only can be made among phosphines containing the same R group. For the PEt_3 ancillary ligand, the Pt-P coupling

constants in **43**, **44** and **45** are 2383 Hz, similar to the 2368 Hz found in *trans*-[Pt(C≡CH)$_2$(PEt$_3$)$_2$].[118] In addition, comparison with the $J_{Pt\text{-}P}$ = 2267 Hz in *cis*-[Pt(C≡CH)$_2$(PEt$_3$)$_2$][118] again suggests that alkynyl ligands have a somewhat stronger *trans* influence than PEt$_3$. The Pt-P coupling constant $^1J_{Pt\text{-}P}$ = 2655Hz for the PPh$_3$ complex **47** is similar to that in *trans*-[Pt(C≡CC$_6$H$_5$)$_2$(PPh$_3$)$_2$] ($^1J_{Pt\text{-}P}$ = 2640Hz).[119] In the ^{195}Pt NMR spectrum for complex **44**, the triplet pattern with respect to 1/3 of the platinum signal appeared at δ -252.22 ($^1J_{P\text{-}Pt}$ = 2655 Hz).

The infrared spectra revealed C≡C stretches at 2077-2082 cm^{-1} in the triethylphosphine complexes **43**-**46**, shifted by *ca*. 60 cm^{-1} from those in the DHP-ethyne precursors (*ca.* 2140 cm^{-1}, Table 1). The triphenylphosphine in **47** increase the C≡C stretching frequency by 10 cm^{-1} to 2092 cm^{-1}. Accordingly the Pt-P bonding should be stronger in **47**, which is evident in the Pt-P coupling constants (2655 Hz in **47** vs 2383 Hz in **43**, **44** and **46**) from NMR spectroscopy. A weaker Pt-C bond was also anticipated in **47**, so the Pt-C coupling constants should also be different from those in **43**-**46**. Unfortunately, we were unable to obtain this data due to the low solubility of the triphenylphosphine complex and the low sensitivity of ^{13}C NMR spectroscopy. Electro-spray mass spectrometry gave the correct molecular mass and showed the expected platinum isotope pattern.

The major regioisomer of (benzoylDHPCC)$_2$Pt(PEt$_3$)$_2$ **45** was determined to be the unusual 4,9-isomer **45B** for both DHP moieties based on the 2D long-range heteronuclear NMR (Figure **14**). There are three correlation lobes to each bridging carbon C-10b and C-10c strongly suggesting three hydrogen atoms are three bonds away from C-10b and 10c. Therefore, in this case, the 4,9-isomer depicted in Figure **14** is the major isolated isomer and the 4,10- isomer is the minor one. The reason for this might be that the mixed alkynes used in that reaction were enriched with the 4,9- isomer through recrystallization prior to reaction with platinum.

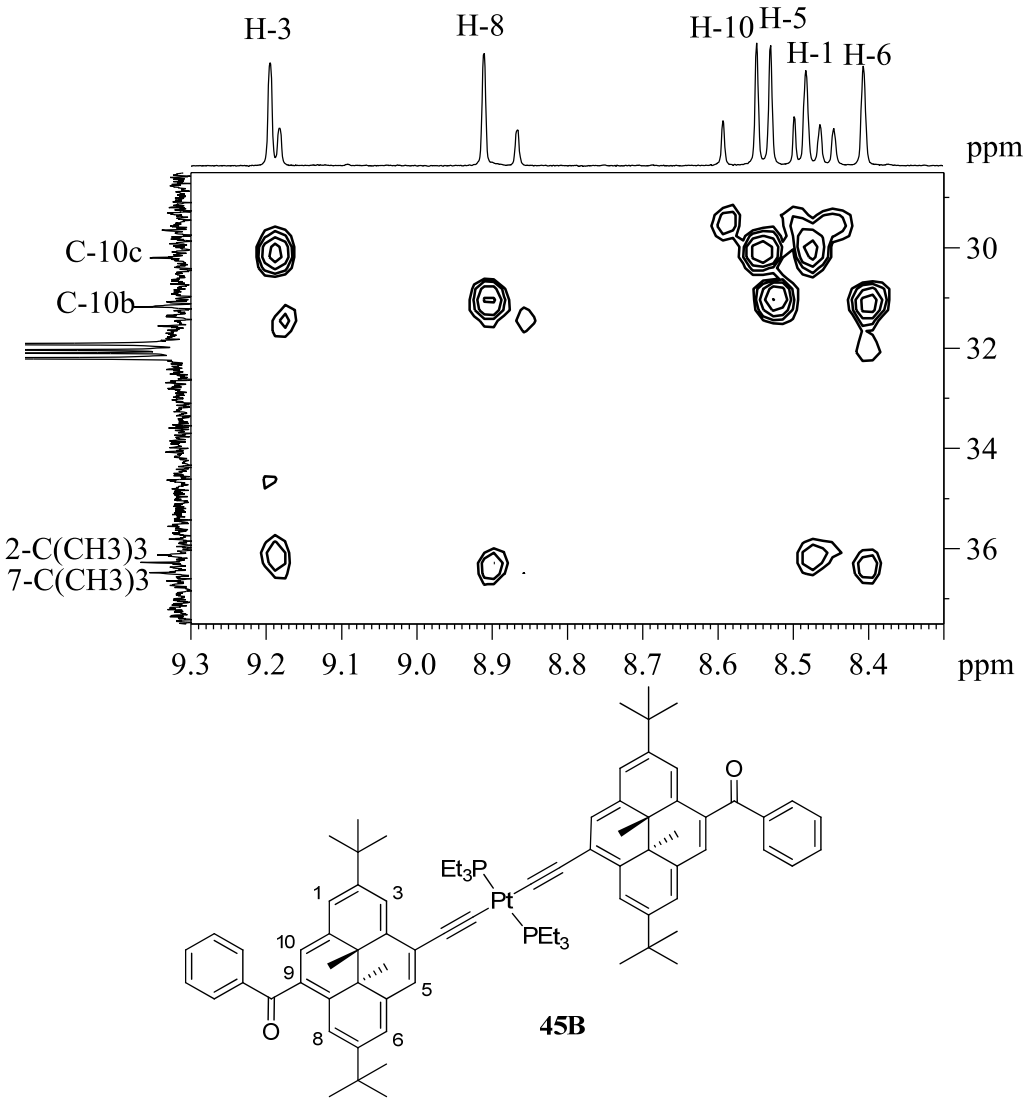
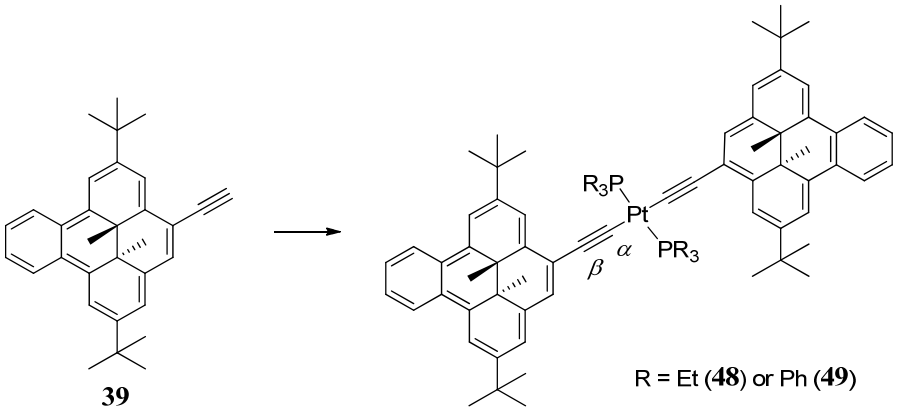


Figure 14. 2D long-range heteronuclear NMR spectrum for (benzoylDHPC≡C)$_2$Pt(PEt$_3$)$_2$ 45B (in CDCl$_3$).

The benzo[e]DHP-alkyne-derived platinum complexes are grouped together because they demonstrate quite different properties from their acyl counterparts. The *trans* platinum complexes **48** and **49** with monodentate triethylphosphine and triphenylphosphine ligands were prepared (Scheme **14**) using the method described in Scheme **13**.



Conditions: $Pt(PR_3)_2Cl_2$, CuI, diethyl amine, 50°C

Scheme 14. The preparation of *trans*-$(BDHPCC)_2Pt(PR_3)_2$ (R = Et, Ph) complexes, 48 and 49

The internal methyl protons of BDHP derivatives normally resonate considerably downfield from those in the parent DHP system (*ca.* δ -1.2 vs. *ca.* -3.5– -4.0) in the ^{1}H NMR spectra due to reduction of the DHP ring current on fusion of a benzene ring (see Chapter **1**). The same effect is seen here as the internal methyl resonances occur at δ -1.02 and -1.04 for **48** and δ -1.22 and -1.27 for **49** in C_6D_6 (Table 3). In the free alkyne **40** these protons resonate at δ -1.18 and -1.20. The fact that the PPh_3 complex **49** shows a greater shift in the opposite direction (upfield vs. downfield) could be due to the shielding ring current effects of the PPh_3 phenyl rings. For the purpose of comparison, ^{1}H NMR spectra were also recorded in $CDCl_3$ and resonances at δ -1.72/-1.73 and -1.54/-1.58 were found for the internal methyl protons of **49** and **48**, respectively (Table 3). In this solvent, the internal methyl protons of both complexes were shifted upfield from those in **40** (δ -1.44 and -1.45). The acetylenic carbons in the ^{13}C NMR spectrum of **49** resonated at δ 118.60 ($^2J_{C\text{-}P}$ = 15.1 Hz) and 115.77 for C-α and C-β, respectively, shifted *ca.* 4 ppm downfield of those in complex **48** and *ca.* 30 ppm downfield of the same resonances in **40**. The shifts in **48** were very similar to those in the acyl DHP complexes (C-α: δ 115.05, $^2J_{C\text{-}P}$ = 14.8 Hz; C-β: δ 111.00). The Pt-C_α coupling constants in **49** and **48** are comparable (**49**: 15.1 Hz; **48**: 14.8 Hz), indicating the same *trans* influence when having

two benzo[e]DHP-alkynyls *trans* to each other in complexes **48** and **49**. However, the $^{2}J_{C\text{-}P}$ values observed here are only half as large as those found in complexes containing acyl DHPs (*ca*. 30 Hz, Table 2). While the larger $^{2}J_{C\text{-}P}$ value for the acyl complexes seems to imply a stronger bond between the alkynyl DHP and Pt than in the alkynyl BDHP (eg. **47** vs. **49**), this is not reflected in either the Pt-C or Pt-P bond distances, discussed in detail in the X-ray section **2.3**. In fact, both bond distances are very similar in the solid state (**47**: Pt-C, 1.995(4); Pt-P, 2.3064(9) and **49**: Pt-C, 1.996(3); Pt-P, 2.2977(8)). However, it is possible that packing effects play a role in the solid state bond lengths and they may differ more in solutions for **47** and **49** than the structures imply. Obviously, coupling constants are extremely sensitive to small changes in distances so they may provide a truer picture of electronic differences between **47** and **49** than do the bond lengths. In the ^{31}P NMR spectrum of **48** and **49**, the phosphine resonances were located at δ 13.5 and 19.0 with coupling constants of $^{1}J_{Pt\text{-}P}$ = 2400 and 2677 Hz, respectively. In the ^{195}Pt NMR spectrum for **48** and **49**, the platinum resonated at δ -219.8 and -253.8, respectively.

Table 3. Comparisons between Pt complexes 48, 49 and 52 containing BDHP-ethynyl moities and BDHP-ethyne 40 (L = ancillary ligands)

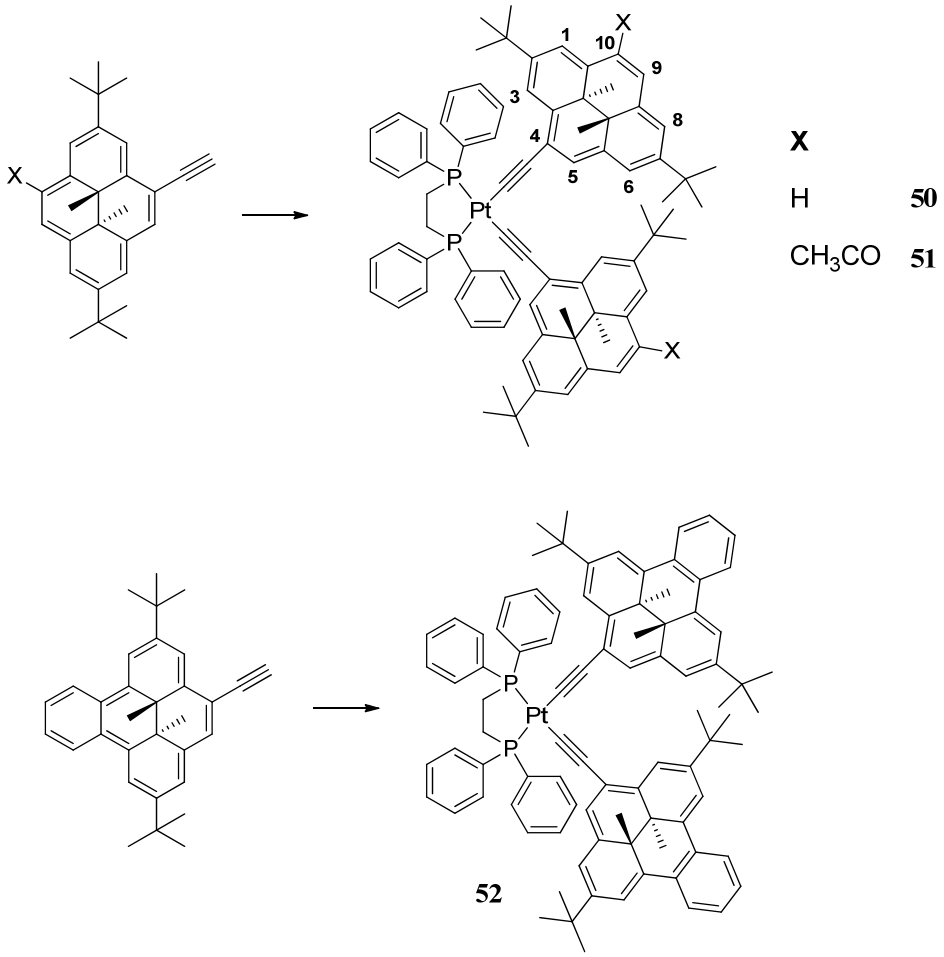
	48 (L = PEt_3) (*trans*)	**49** (L = PPh_3) (*trans*)	**52** (L = dppe) (*cis*)	BDHP-ethyne **40**
δ (internal-C$\underline{H}_3$)	-1.02, -1.04 [a] -1.54, -1.58 [b]	-1.22, -1.27 [a] -1.72, -1.73 [b]	-1.06, -1.07 [a]	-1.18, -1.20 [a] -1.44, -1.45 [b]
δ C-α δ C-β	115.05, 111.00	118.60, 115.77	113.42, 112.5	82.59, 84.33 [a]
$^{2}J_{C\text{-}P}$ (Hz)	15	15	150 (*trans P*), 14 (*cis P*)	--
$^{1}J_{Pt\text{-}P}$ (Hz)	2400	2677	2246 [c]	--
ν(C≡C) (cm^{-1})	2071	2099	2093	2090[40]

a. C_6D_6 solvent; b. $CDCl_3$ solvent; c. CD_2Cl_2 solvent;

In the infrared spectrum (Table 3), in contrast to the 2090 cm^{-1} in alkyne precursor **40**, the vibrational frequency associated with the C≡C bond was found at 2071 and 2099 cm^{-1} for complexes **48** and **49**, respectively. The trend to lower vibrational frequency for the C≡C triple bonds in complex **48** compared with the alkyne precursor **40** is consistent with observations for the acyl complexes but to a smaller extent (19 cm^{-1} for **48** vs. *ca*. 60 cm^{-1} for the acyl complexes in Table 2). Complex **49** shows a higher C≡C bond stretching frequency than **40** which is unique among the complexes investigated here.

In contast to the *trans*-platinum complexes, the *cis* ones were expected to show less mutual influences through the metal center between the two DHP moieties. In the electronic spectra, the absorptions at *ca*. 300 nm, with ε values of 10^4, stem from intramolecular charge transfer transitions between π(-C≡C-) and *p*-orbital mixed π^*(-C≡C-).[120] This absorption band is blue shifted for the *cis* complexes relative to the corresponding *trans* isomers, indicating longer through-metal conjugation in the *trans* isomers. Photophysical properties for a series of phenylacetylene-derived *cis*-platinum complexes bearing dppe as ancillary ligand were investigated by Saha *et al*..[121] The lowest energy absorption bands in the electronic spectra occurred in the range of 318-360 nm in CH_2Cl_2 when the phenylacetylene contains nitro, methyl, ethynyl or phenyl at the *para* position. *Cis*-dialkynyl diimine Pt complexes demonstrated pronounced solvatochromic shifts and electronic properties dependence. The absorption bands blue shifted *ca*. 40 nm from less polar benzene (λ *ca*. 420 nm) to more polar methanol (λ *ca*. 380 nm).

Due to the isomerization from *cis* to *trans* configuration with the monodentate phosphine ligands used in our synthesis, platinum complexes containing the exclusively *cis* binding bidentate phosphine ligand 1,2-*bis*(diphenylphosphino)ethane (dppe) were synthesized using the same method described for their *trans* counterparts (Scheme **15**). As expected, the dppe ligand enforced the *cis* platinum complexes **50**, **51** and **52** in moderate yields containing DHP, 10-acetylDHP and benzo[e]DHP-derived ethynes.



Conditions: $Pt(dppe)Cl_2$, CuI, diethyl amine, 50°C

Scheme 15. Syntheses of the *cis*-dppe platinum complexes

As expected, DHP-ethyne dimerization became significant in the syntheses of the *cis* complexes due to reductive elimination from the platinum centers. The dimer was removed by column chromatography or recrystallization. Steric hinderance disfavors the *cis* complexes so a higher energy barrier is expected when the second alkyne is introduced leading to slower reaction rates and incomplete reactions. In several cases, isolation of an intermediate where only one chlorine was replaced by an alkynyl was observed. Of course, consumption of free alkyne due to the dimerization side reaction also accounted for isolation of the mono alkynyl intermediates since only slightly more

than two equivalents of alkyne were used in the reactions. Therefore it is particularly crucial to suppress dimerization as much as possible.

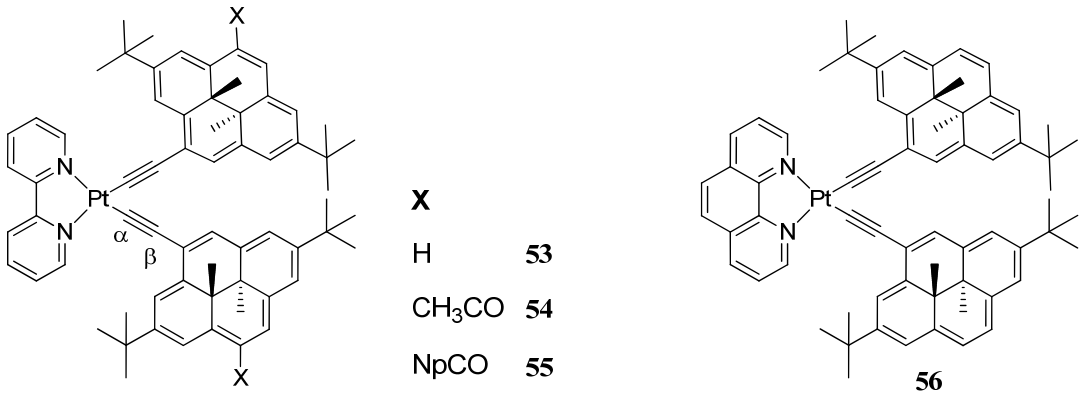
Despite these complications, the *cis*-dppe platinum complex **50** (DHP) and complex **52** (BDHP) were successfully synthesized using the same method as before. Because rotation around the C≡C triple bonds linkers occurred only in a geared manner, low symmetry structures complicated the NMR spectral characteriztion. In the ^{1}H NMR spectrum, the internal methyl protons of complex **52** appeared at δ -1.06 and -1.07, shifted *ca*. 0.1 ppm downfield from those in the alkyne precursor **40** (δ -1.18 and -1.20) (Table 4). The internal methyl protons of **50** resonated at -3.40 and -3.41 (in C_6D_6). The acetylenic carbons in complex **52** resonated close together at δ 113.42 and 112.5 for C-α and C-β, respectively. The C-α of **50** and **52** showed diagnostic $^{2}J_{P\text{-}C}$ coupling constants of 150 and 14 Hz for the *trans* and *cis* phosphorus, respectively, indicating a *cis* geometry product. In the ^{31}P NMR spectrum of **52**, the phosphine resonated at δ 40.24 with a coupling constant of $^{1}J_{Pt\text{-}P}$ = 2246 Hz, which are comparable to the chemical shift range (δ 42-43) and coupling constants (*ca*. 2280 Hz)[121] in analogous dppe complexes bearing phenyl acetylenyl ligands on Pt. In the ^{195}Pt NMR spectrum of **52**, the platinum resonated at δ -378.8 with a coupling constant $^{1}J_{Pt\text{-}P}$ = 2268 Hz. The ^{195}Pt chemical shift in **52** was far upfield of all other DHP analogs.

Table 4. The alkynyl platinum complexes having a dppe ligand

	50 (DHP)	**51** (Acetyl DHP)	**52** (BDHP)
δ (internal-C$\underline{H}_3$)	-3.40, -3.41 [a]		-1.06, -1.07 [a]
δ C-α and C-β	114.16, 113.28		113.42, 112.5
$^{2}J_{C\text{-}P}$ (Hz)	150, (*trans* P) 15 (*cis* P)		150, (*trans* P) 14 (*cis* P)
$^{1}J_{Pt\text{-}P}$ (Hz)	2277 [b]		2246 [c]
ν(C≡C) (cm^{-1})	2093	2097	2093

a. C_6D_6 solvent;b. $CDCl_3$ solvent; c. CD_2Cl_2 solvent;

Alkyne homo-dimerization products were obtained with the *cis* isomers due to reductive elimination reaction. As electron deficient components are reluctant to undergo reductive elimination from metal centers,[122] the electron withdrawing acyl groups should suppress dimerization in acyl DHP-alkynyl complexes. In contrast, π-acceptor ligands such as 1,10-phenanthroline were previously found to promote the reductive elimination process,[123] so it is perhaps not surprising that only 10-20% yields were obtained of the *cis*-(DHP-alkynyl) bipy platinum complexes. Nevertheless, complexes having the N coordinating chelates bipy and 1,10-phenanthroline (phen) were synthesized using methods similar to Scheme **15**.



Scheme 16. Platinum complexes containing bipy or phen ligands

The phenanthroline analog with DHP was made in such low yield and showed such poor solubility in organic solvents that further studies on it were abandoned.

Table 5. Comparison of DHP-alkynyl platinum complexes bearing a bipy ligand

X	**53** (DHP)	**54** (Acetyl DHP)	**55** (Naphthoyl)
δ (internal-C$\underline{H}_3$)	-3.79, -3.81	-3.69, -3.714, -3.715	-3.57, -3.59
δ C-α		92.30	94.13
δ C-β		102.77	102.52
ν(C≡C)	2094	2094	

In the ^{1}H NMR spectra, the internal methyl protons in the bipy platinum complexes (**53**, **54** and **55**) shifted downfield from the corresponding alkynes by about 0.1 ppm, which is analogous to that in complexes with phosphine ancillary ligands. However, the internal methyl for **54** showed three peaks, indicative of C_1 symmetry or the presence of isomers in this molecule. It can be concluded that the rigid bipy structure caused significant steric congestion to the DHP moieties. In general the acetylenic carbons moved upfield (δ 92-94 and *ca*. δ 102.5 for C-α and C-β, respectively) from those of the alkynes (*ca*. δ 100 and 106 for C-α and C-β, respectively) in the ^{13}C NMR spectra. Surprisingly, the infrared spectrum (Table 5) demonstrated essentially the same C≡C stretching frequency (2094 cm^{-1}) as the phosphine ligand complexes (2092 cm^{-1} in **47** in Table 2) suggesting that the ancillary ligand effects on the C≡C stretch are negligible.

2.3 Crystallographic investigations

2.3.1 ORTEP3 plots for alkynyl platinum complexes 44, 45, 47, 49 and 52

Crystal data were obtained for complexes **44**, **45**, **47**, **49** and **52** by slow diffusion of hexanes into dichloromethane or solvents evaporation. ORTEP3[124] ellipsoid plots are shown for each compound in Figure **15** -Figure **19** and selected bond lengths and angles are given in Table 6 (full data are available in Appendix **V**). The structures are compared and discussed collectively following the data. Disorder with respect to the internal methyl and *t*-butyl groups on the DHP moieties was usually observed. Disorder was also observed for acyl groups on DHP moieties in **44**, **45** and **47**. In all ORTEP3 plots, only one orientation of the internal methyl groups of the DHP is shown and all hydrogen atoms and solvent molecules are omitted for clarity.

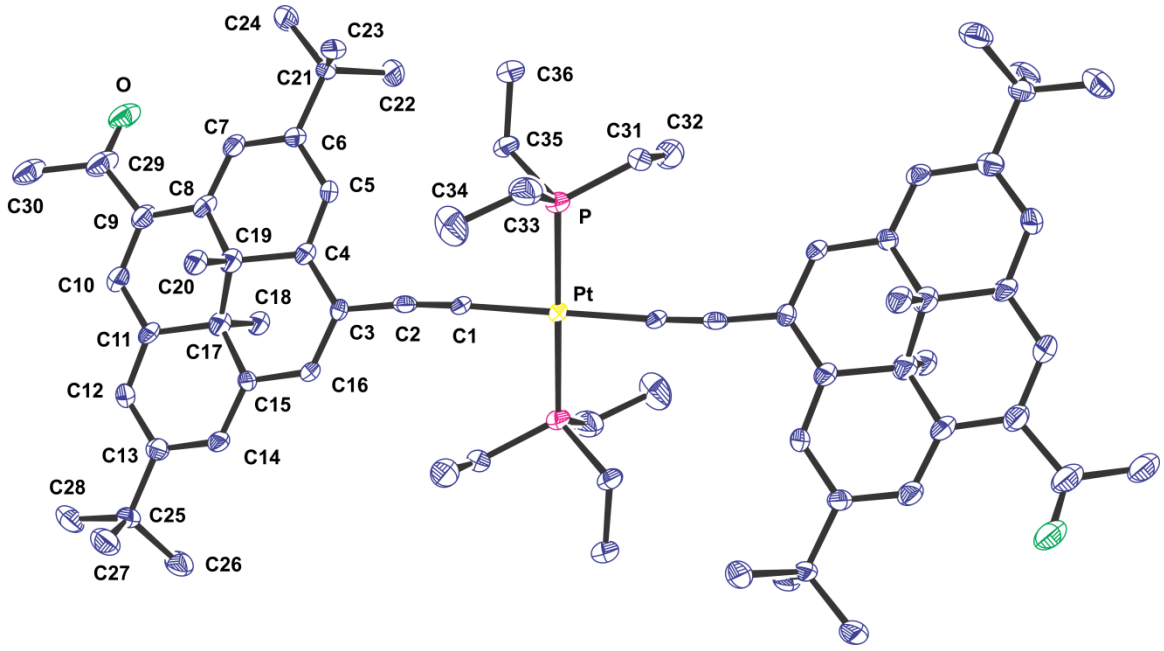


Figure 15. **ORTEP3 drawing of *trans*-$(CH_3C(O)DHP\text{-}CC)_2Pt(PEt_3)_2$ 44 (50% probability level).**

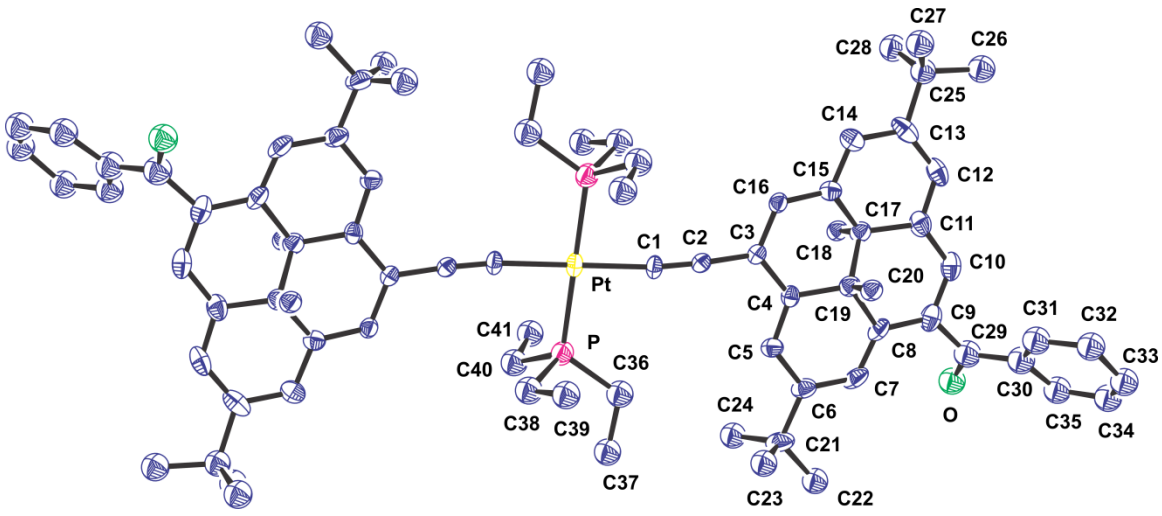


Figure 16. **ORTEP3 drawing of complex *trans*-$(PhC(O)DHP\text{-}CC)_2Pt(PEt_3)_2$ 45 (25% probability level).**

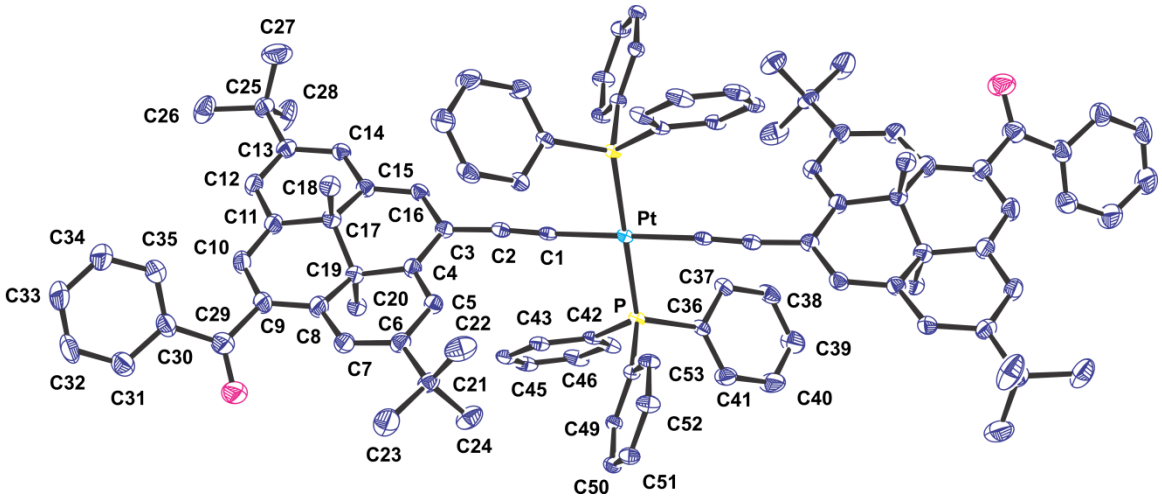


Figure 17. **ORTEP3 drawing of complex *trans*-(PhC(O)DHP-CC)$_2$Pt(PPh$_3$)$_2$ 47 (30% probability level).**

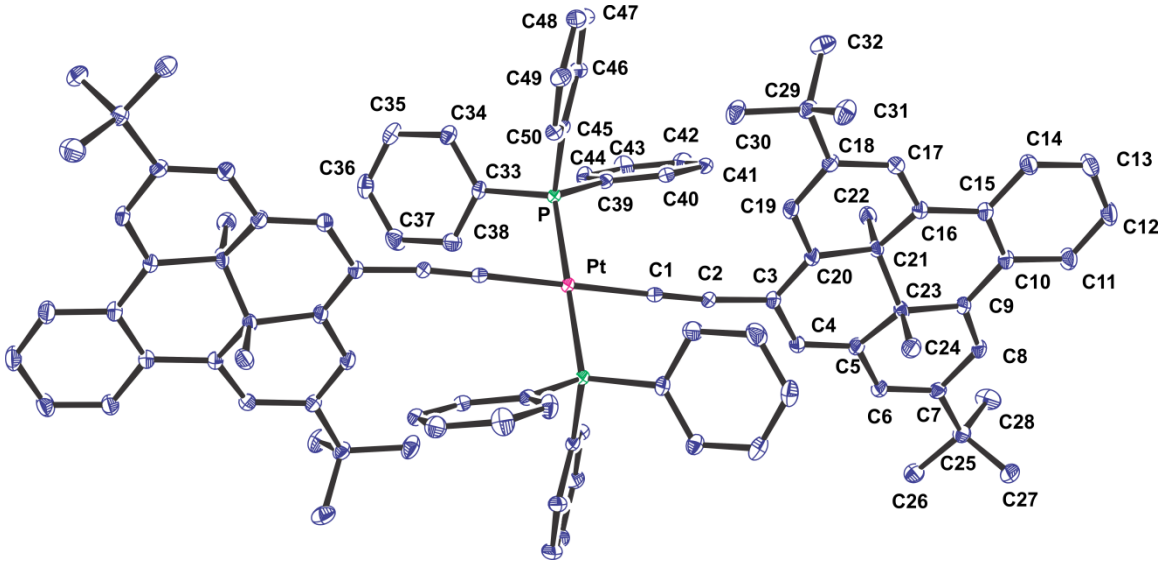


Figure 18. **ORTEP3 drawing of complex *trans*-(BDHP-CC)$_2$Pt(PPh $_3$)$_2$ 49 (25% probability level).**

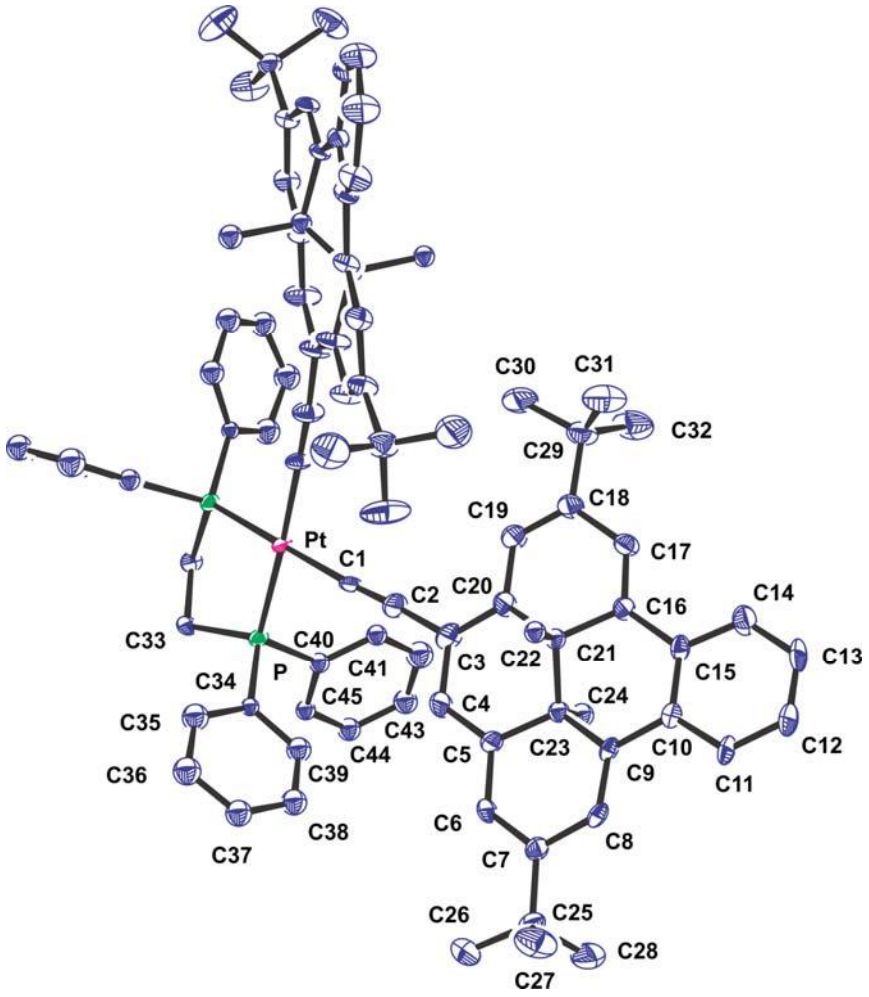


Figure 19. ORTEP3 drawing of *cis*-(BDHP-CC)$_2$Pt(dppe) 52 (30% probability level).

2.3.2 Summary and discussion

Table 6. **Selected bond lengths (Å) and angles (°) for *trans*-(^{R}DHP-CC)$_2$Pt(PR'$_3$)$_2$ (44: R = $CH_3C(O)$, R' = Et; 45: R = PhC(O), R' = Et; 47: R = PhC(O), R' = Ph), *trans*-(BDHP-CC)$_2$Pt(PPh_3)$_2$ 49 and *cis*-(BDHP-CC)$_2$Pt(dppe) 52**

R =	Acetyl	Benzoyl	Benzoyl	BDHP	BDHP
L =	PEt_3	PEt_3	PPh_3	PPh_3	dppe
	44	**45**	**47**	**49**	**52**
Pt(1)-C(1)	2.009(6)	2.009(7)	1.995(4)	1.996(3)	1.995(8)
Pt(1)-P(1)	2.295(2)	2.296(3)	2.3064(9)	2.297(8)	2.261(2)
C(1)-C(2)	1.196(9)	1.191(9)	1.208(6)	1.214(4)	1.191(11)
C(2)-C(3)	1.450(8)	1.430(9)	1.431(6)	1.429(4)	1.450(12)
DHP C-C_{ave}	1.398	1.393	1.400	1.405	1.398
Sum DHP C-C alternation[a]	0.187	0.152	0.190	0.492	0.634
C(1)-Pt(1)-C(1)'	180(2)	180	180	180.0(1)	89.1(4)
P(1)-Pt(1)-P(1)'	180	180	180.00(6)	180	87.01(10)
P(1)-Pt(1)-C(1)	90.7(2)	94.7(2)	93.23(11)	92.93(9)	92.0(2)
P(1)-Pt(1)-C(1)'	89.3(2)	85.3(2)	86.77(11)	87.07(9)	177.1(3)
Pt(1)-C(1)-C(2)	176.3(5)	173.3(7)	174.6(3)	173.6(3)	175.9(8)
C(1)-C(2)-C(3)	173.4(6)	176.2(7)	173.1(4)	173.4(4)	175.9(10)
DHP-SqP dihedral[b]	26.4	6.7	65.6	70.3	32.7
DHP-(PhCO) dihedral[c]			61.1	56.7	

[a] Σ(|bond length - ave bond length|) for the 14 DHP edge bonds [b] dihedral angle between the PtC_2P_2 square plane and the mean DHP plane [c] dihedral angle between the mean C_6 plane of the PhCO substituent and the mean DHP plane.

In order to make comparisons between our complexes and known structures, bond length data for square planar (RCC)$_2$Pt(PR'$_3$)$_2$ complexes have been extracted from the

Cambridge Structure Database (CSD) and are summarized in Table 7 (histogram plots of all data are in Appendix **IV**).

Table 7. Summary of bond length data for various $(ArC{\equiv}C)_2Pt(L)_2$ complexes[a] from the Cambridge Structural Database (CSD)[125]

	Ligands L	Bond length range (Å)	Mean length (Å)	Std. Dev.
Pt-C	PAr_3	1.981-2.027	2.008	0.014
	PR_3	1.981-2.047	2.003	0.015
	dppe (L_2)	1.997-2.031	2.018	0.012
Pt-P	PAr_3	2.286-2.325	2.309	0.013
	PR_3	2.281-2.316	2.299	0.007
	dppe (L_2)	2.258-2.289	2.270	0.003
C1≡C2	PAr_3	1.152-1.217	1.197	0.019
	PR_3	1.128-1.239	1.198	0.026
	dppe (L_2)	1.176-1.211	1.190	0.012
C2–C3	PAr_3	1.434-1.461	1.445	0.007
	PR_3	1.414-1.487	1.443	0.018
	dppe (L_2)	1.411-1.452	1.437	0.012

[a] The number of compounds containing PAr_3, PR_3 and dppe are 13, 29 and 11, respectively.

For the platinum complexes with PAr_3, PR_3 and dppe ligands in the CSD database (Table 7), the Pt-C and Pt-P bonds reveal Gaussian distributions with small standard deviations with the Pt-C bond ranging between 2.003 and 2.018 Å and Pt-P between 2.270-2.309 Å. The C≡C triple bonds are relatively inert to changes in the phosphines or the alkyne substituents, with the average bond lengths in the range of 1.190 to 1.197 Å for PAr_3, PR_3 and dppe ligands. A similar observation can be made for the C2-C3 bonds. In fact the average C2-C3 bond lengths span in a very small range of 1.437-1.445Å with changing ancillary ligands for complexes bearing any of the PAr_3, PR_3 or dppe ligands.

The Pt-C1, Pt-P, C1-C2 and C2-C3 bond lengths for complexes **44**, **45**, **47**, **49** and **52** (Table 6) all fall in the bond length ranges taken from the CSD database in Table 7 within experimental error. The Pt-C1 bond lengths (*ca*. 2.009 Å for **44** and **45** with PEt_3; *ca.* 1.995 Å for **47** and **49** with PPh_3) are very close to the average Pt-C bond lengths of 2.003 Å for PEt_3 and 2.008 Å for PAr_3 complexes in the CSD database. The Pt-C1 bond lengths of 1.995(8) Å in the dppe complex **52** are shorter than the average Pt-C1 bond lengths (2.018 Å) by *ca*. 0.02 Å and are close to the lower end of the bond lengths range (1.997-2.031 Å) of the CSD data. The Pt-P bond lengths of complexes consisting of PEt_3 (2.295 (2) for **44** and 2.296 (3) for **45**) and PPh_3 (2.3064 (9) for **47** and 2.297 (8) for **49**) are very similar to the corresponding average bond lengths for *trans* complexes with PR_3 (2.299 Å) and PAr_3 (2.309 Å) ligands, respectively, in the CSD database (Appendix **IV**). Interestingly, similar to the Pt-C bond length, the Pt-P bond length of 2.261(2) Å for the dppe complex **52** is also shorter than the average Pt-P bond length (2.270 Å) by *ca*. 0.01 Å and is close to the lower end of the Pt-P bond lengths range (2.258 Å) of the CSD data.

Orpen[126] claimed that *trans* influences are dominant in d^8 Pt(II) square planar complexes while *cis* effects are minimal. The *trans* influence refers to the weakening of a bond *trans* to a particular ligand in the ground state, which is also reflected in NMR coupling constants as we have already seen. X-ray crystallography gives a direct measurement of the *trans* influence by comparing bond lengths among complexes with different *trans* groups.[127] More polarisable ligands such as SCN^- and I^- or ligands containing a π acceptor orbital show a stronger *trans* influence. Structural data[128] allows construction of a general *trans* influence series in the order CO ≈ olefin >> H^- ≈ PR_3 > R^- > Cl^- ≈ NH_3 for square planar complexes. Both phosphine and alkynyl ligands have the potential to act as σ-donors and π-acceptors when bonding to transition metals. However, calculations[129] showed that Pt-π* backdonation has minimal effect in alkynyl platinum complexes so they are generally regarded as σ-bonding ligands. A comparison of the Pt-P and Pt-C bond lengths in **47** and **49**, which contain *trans* PPh_3 ligands, with **52**, containing a *cis*-dppe ligand, should allow an estimate of the relative *trans* influence of phosphines and alkynyls. If phosphines exert a stronger *trans* influence then the Pt-P bonds should be shorter and the Pt-C bonds longer in the *cis*-dppe complex **52**. The Pt-C bond lengths in these complexes are essentially the same but the Pt-P distance is

significantly shorter in **52**. A broader comparison of all literature structures seems to reinforce this as the Pt-C bonds are longer and the Pt-P bonds shorter in the *cis*-Pt(C≡CAr)(dppe) complexes (Appendix **IV**). Thus, the evidence from X-ray data suggests that phosphines are somewhat stronger *trans* influence ligands than alkynyl. This contradicts NMR coupling constant evidence presented earlier which suggests alkynyl ligands have a stronger *trans* influence than phosphines. We conclude from this that alkynyls and phosphines probably have a similar *trans* influence.

As expected, the C1-C2 and C2-C3 bonds lengths are in the ranges of the reported complexes in Table 7. Except for 1.214 (4) Å in **49**, the C1-C2 bond lengths for the DHP derived $(RCC)_2Pt(PR'_3)_2$ complexes **44**, **45**, **47** and **52** are in the range of 1.191(9)-1.208(6) Å.

The average DHP peripheral bond alternations range from 0.187 to 0.190 Å for complexes **44**, **45**, and **47** and are identical within experimental error. The bond alternations are larger in complexes **49** (0.492 Å) and **52** (0.634Å) than those in **44**, **45** and **47**, due to the bond localization caused by the fused benzene ring in **49** and **52**. The bond alternations observed here are comparable to that in BDHP 3 (0.539 Å, for more examples refer to Table **13**, Section **3.4**, page **108**).

The dihedral angles (Table 6) between DHP moieties and the PtC_2P_2 plane are very different ranging from 6.7 to 70.3° for complexes **44**, **45**, **47**, **49** and **52**. In contrast to the angles for **44** and **45** bearing PEt_3 (26.4° and 6.7°, respectively), larger angles (65.6° for **47**; 70.3° for **49**) are found for complexes with PPh_3 ancillary ligands, presumably due to steric congestion between the phenyl groups on the phosphines and the DHPs. In addition, due to the steric repulsions between the adjacent protons of DHP and benzoyl benzene ring, the benzene rings twist to 61.1 and 56.7° in **47** and **49** respectively.

2.4 Photoswitch opening and closing rates

As mentioned earlier, features such as photoopening rates and thermal closing rates, associated with photoswitchable molecules are particularly important to their applications. Some of the complexes were selected to investigate the effects caused by changing the ligands and substituents on their photochemical properties.

2.4.1 Photoopening rates

Photochemists have traditionally used quantum yields to compare photoefficiencies. Thus for the reaction DHP 1 → CPD 1-**o**, Φ has been found to be 0.006.[39] Addition of *t*-Bu groups as in 2 → 2-**o** reduces Φ to 0.0015, i.e. reduces the efficiency of opening by about 4-fold. On the other hand, for the BDHP 3, Φ = 0.042, so the efficiency is increased some 7-fold over 1 and 30-fold over that of 2.[39] However, quantum yields are time consuming to measure and we have found that a relatively reliable comparison can be made by measuring the relative rates of opening for two samples side by side under the same conditions of temperature, light source and solvent. The absolute rates measured are not meaningful, but the rate relative to the standard can be used for comparison. We have made much use of BDHP 3 as a standard previously.[130] Providing the two samples measured have absorptions in the region of the light source, good comparative results are consistently observed. By calibrating one standard against another, rates over a wide range can be compared.

2.4.2 Experimental methods

The visible openings were performed using a 500 W tungsten light source and a cut off filter. The processes were followed by either UV-Vis spectroscopy or NMR spectroscopy. For the NMR experiments, the samples were loaded in a glovebox and dry

and oxygen free solvents were used. For the UV-Vis experiments, the UV solutions were prepared after the solvents were bubbled with argon for 15 minutes. During irradiation, the samples were kept cold using an ice bath or circulating cold water system. The opening rates of the complexes were compared with the corresponding precursors where the precursors were available or to compounds with similar opening rates. The UV closing test used a UV light source for thin layer chromatography. Only preliminary tests were performed as the photoclosing is always fast.

The absolute concentrations in UV tests were determined according to Beer's Law where the molar absorption constants had been obtained previously from UV-Vis measurements. The concentrations were then used to calculate the kinetic rates.

Beer's Law: $A = \varepsilon bc$, so $c = A/\varepsilon b$

A, absorption; ε, molar absorptivity; b, the light path length in a solution; c, concentration.

A photochemical reaction rate depends directly on the number of photons and the concentration of the photochrome. When excess photons are provided, the photochemical reaction only depends on the concentration of the photochrome, and is therefore a pseudo-first order reaction. In reality, Robinson[131] found that NMR samples follow a pseudo-zero order rate law expression, while UV-Vis samples follows a pseudo-first order in the photoopening process because of the different concentrations involved and the efficiency of light penetrating through the sample solutions. Only the surface of the NMR sample is irradiated by light and this leads to a constant concentration of photochrome with excess photons. However, this is only true at the beginning of the opening processes so initial rates give more accurate results. Later the concentration is no longer constant and the rate law changes.

For NMR samples, the zero-order rate law describes the relationship between the reactant with time as:

$$Rate = -\frac{d[A]}{dt} = k$$, integration gives rise to

$$[A] = -kt + [A_0].$$

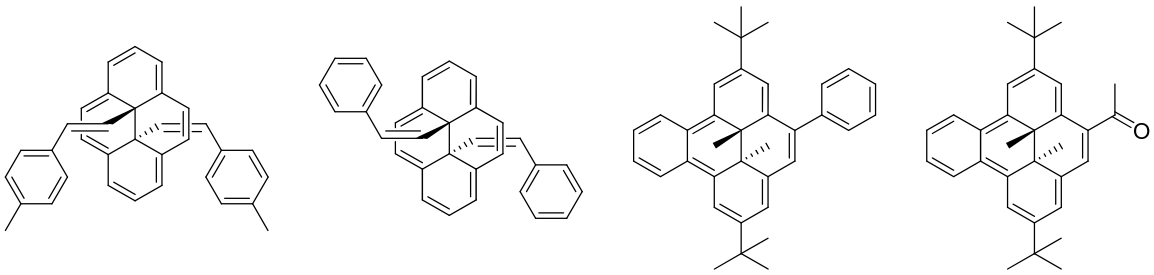
Therefore, the rate contant k will be obtained from a plot of $[A]$ vs time (t).

For a sample irradiated in UV cells at lower UV concentrations, the concentration of the photochrome begins to drop as soon as the irradiation starts. Therefore the photoopening rate depends on the concentration of the photochrome and a pseudo-first order law applies.

$Rate = -\frac{d[A]}{dt} = k[A]$, and integration gives rise to

$\ln[A] = -kt + \ln[A_0]$.

In this case, the apparent rate constant can be obtained from the slope of the plot of *ln[A]* vs time (*t*).



I **II** **III** **IV**

Figure 20. Examples of known photochromic compounds

The photoopening of the four compounds depicted in Figure **20** have shown quite different photoopening rates as shown in Table 8. Substituents at the internal and peripheral positions change the photoopening rates.

Table 8. Photoopening comparison from previous studies

Compounds [a]	Relative rate to BDHP BDHP = 1	
I [132]	0.058	(17 × slower)
II [132]	0.14	(7 × slower)
BDHP 3	1	(standard)
III [104]	4	(faster)
IV [104]	22	(faster)

[a]: I-IV shown in Figure **20**

2.4.3 Photoopening results

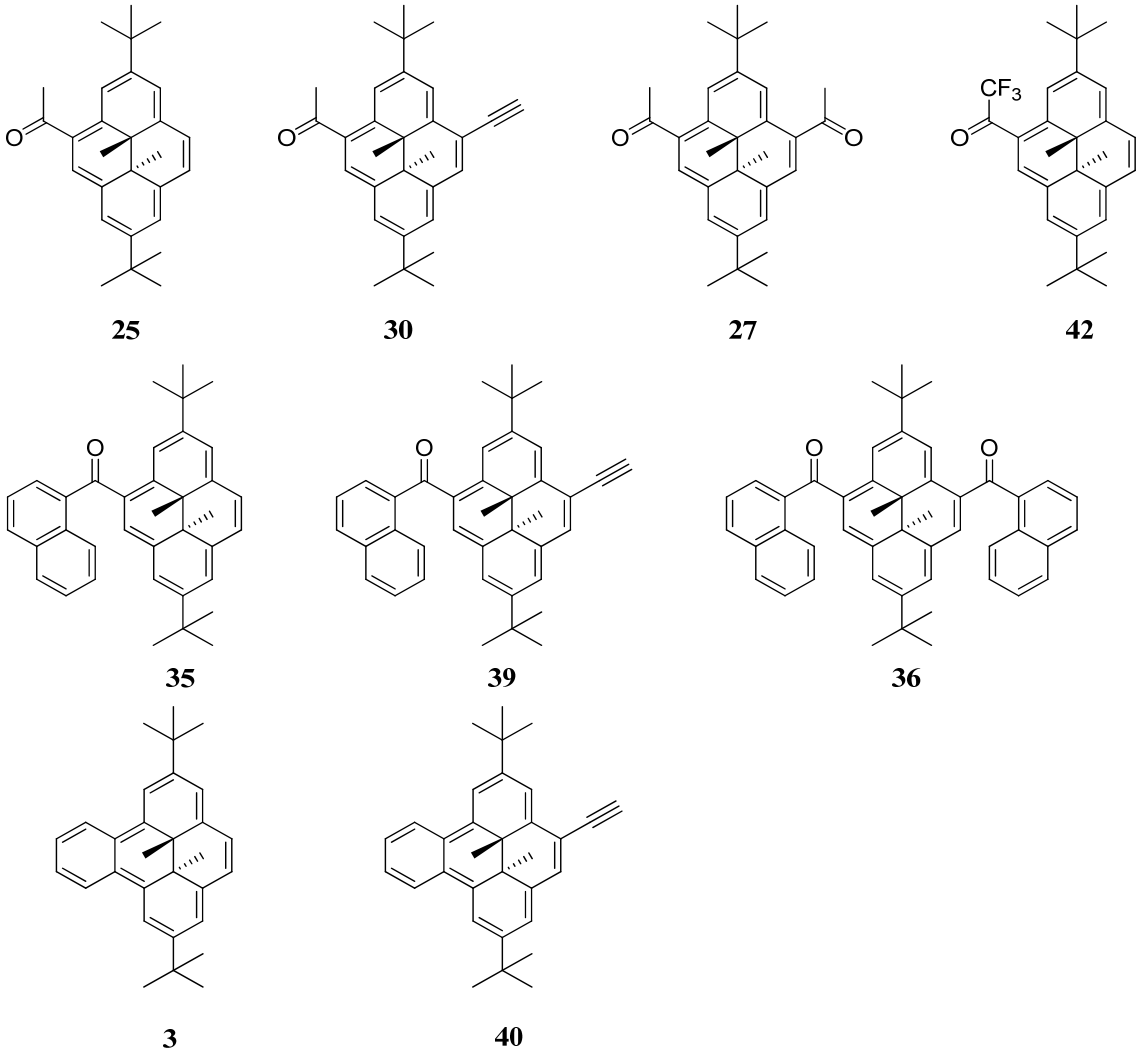
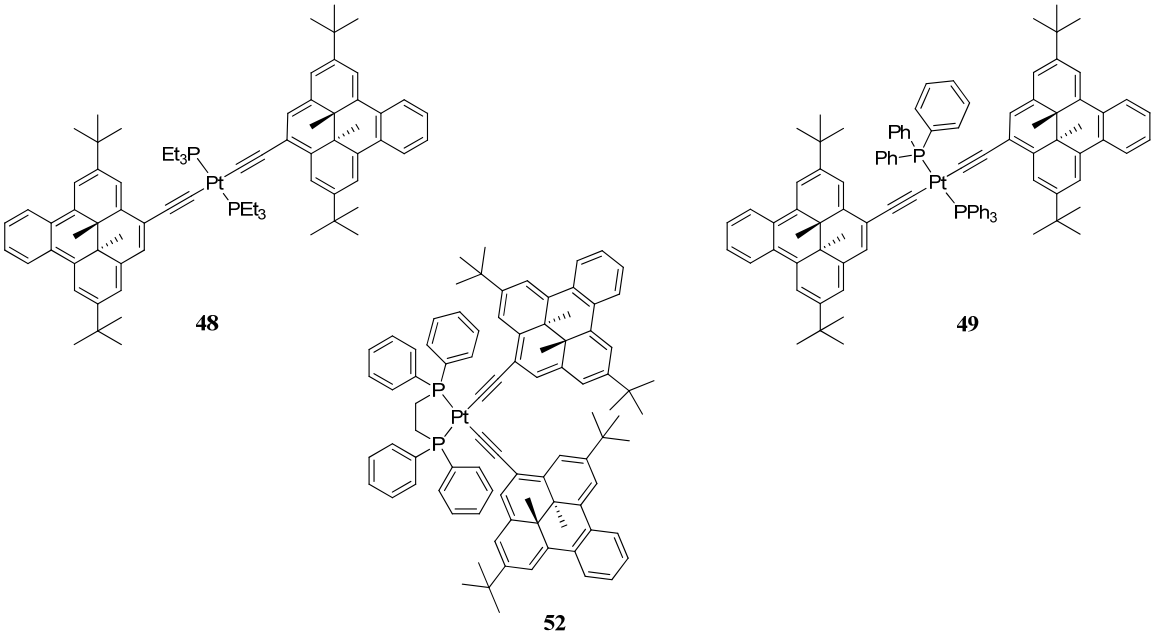


Chart 1. Non-metal DHP systems studied in this section

Table 9. Relative photoopening rates for non-complexed compounds in comparison to BDHP

Compounds	Relative rate to BDHP
CH_3CODHP CCH **30**	0.067 (15 × slower)
CH_3CODHP **25**	0.17 (6 × slower)
BDHP 3	1
$(NpCO)_2DHP$ **36**	3
$(CH_3CO)_2DHP$ **27**	3
DHP-$COCF_3$ **42**	3
BDHP-alkyne **40**	4
NpCODHPCCH **39**	0.25 (4× slower) than **35**
NpCODHP **35**	× slower

The photoopening of the new compound CF_3CODHP **42** is 3 times faster than BDHP, which made it an interesting molecule to explore (Table 9). Having an acetylene substituent slows the photoopening rates in both acetyl DHP acetylene **30** and 1'-naphthoyl DHP acetylene **39** by 2.5 times and 4 times respectively, in comparison with the corresponding acyl DHP precursor. However, the BDHP-alkyne **40** is the fastest photochrome here, so in this case introduction of an alkyne substituent speeds up the opening reaction. We began by investigating the photoopening properties of BDHP-alkynyl complexes **48**, **49** and **52** because of the favourable opening properties of the parent alkyne **40**.



48 **49** **52**

The UV-Vis absorption spectra for BDHP complexes **48**, **49** and **52** are shown in Figure **21**.

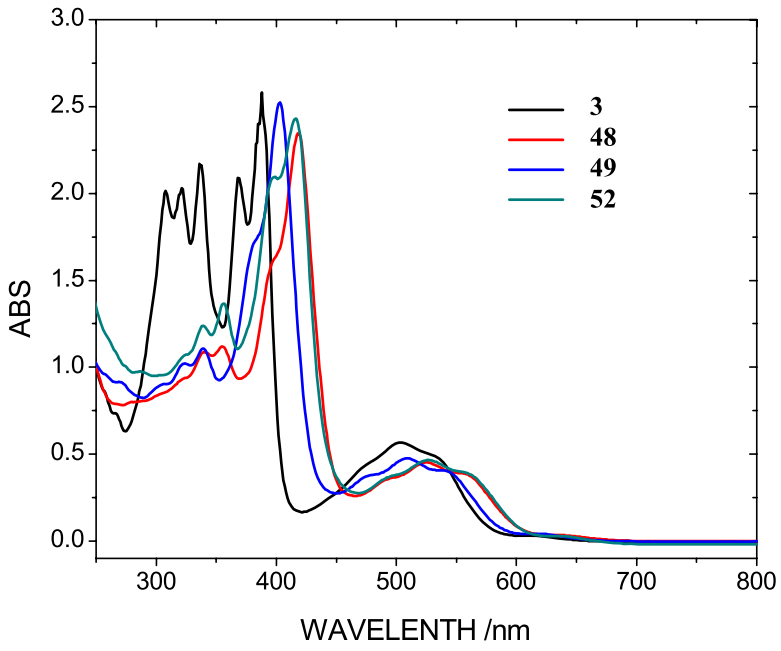


Figure 21. **The UV-Vis spectra of BDHP 3 and *trans*-(BDHP-CC)$_2$Pt(PR$_3$)$_2$ (R=Et 48 and Ph 49) and *cis*-dppe 52 complexes (in hexanes)**

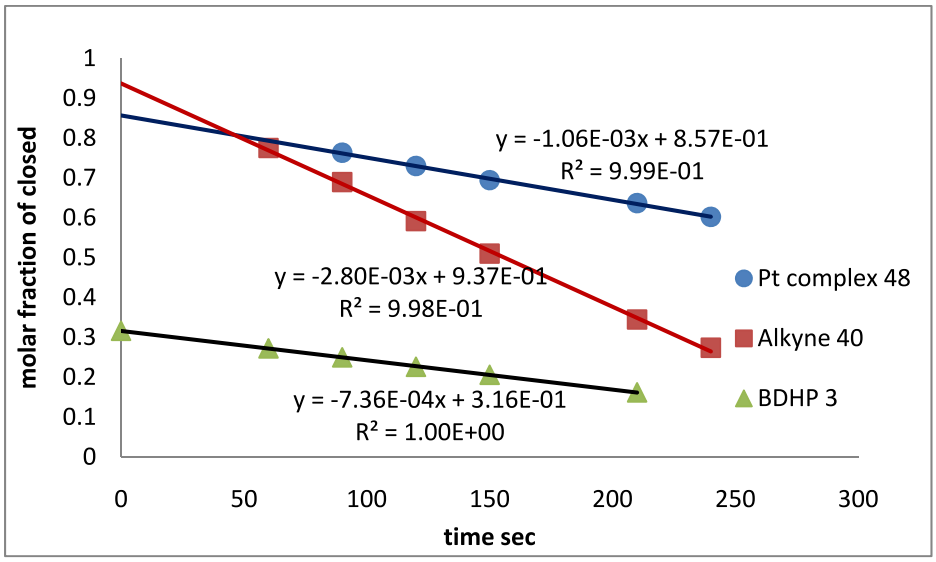


Figure 22. The photoopening of BDHP 3, BDHP-ethyne 40 and complex 48

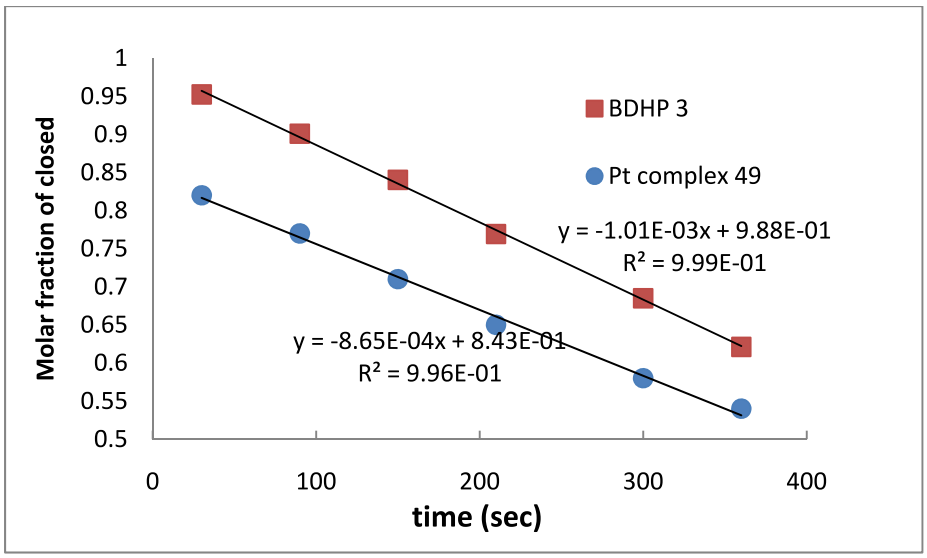
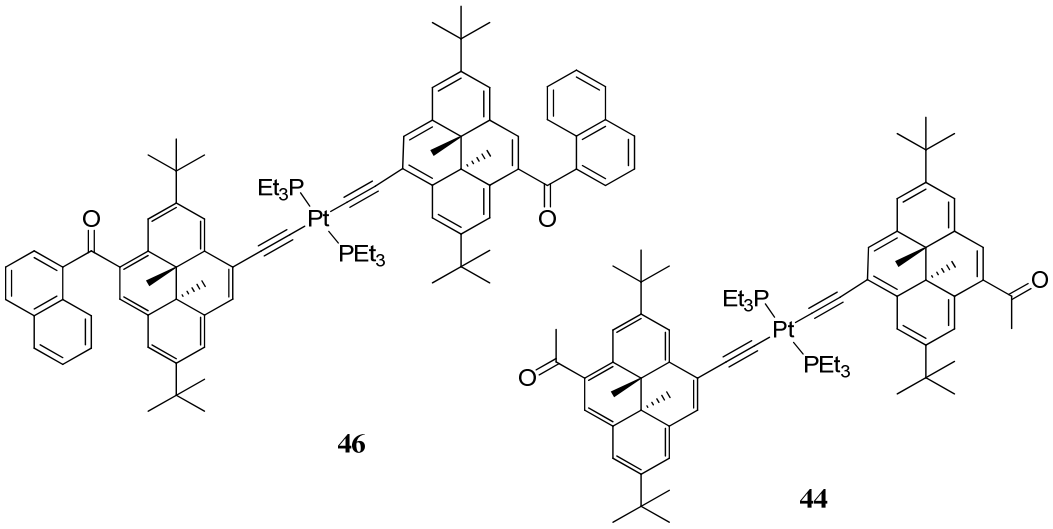


Figure 23. The photoopening of BDHP 3 and complex 49

The photoopening was carried out by irradiating NMR samples. Relative to BDHP 3, the opening of *trans*-(BDHP-CC)$_2$Pt(PR$_3$)$_2$ (R=Et **48** (Figure **22**) and Ph **49** (Figure **23**)) are similar to that of the BDHP. The plot for *cis*-dppe complex **52** is included in the Appendix **I** and similar relative rates were obtained. Thus, since the opening of the BDHP-ethyne is 4 time faster than BDHP 3 (Figure **22**), the BDHP-ethynyl photochromic compounds in complexes **48**, **49** and **52** are slowed by about 4 times compared to the free BDHP-ethyne ligand. We then wanted to explore the complexes *trans*-(CH$_3$C(O)DHP-CC)$_2$Pt(PEt$_3$)$_2$ **44** (graphs in Appendix **I**) and *trans*-(NpC(O)DHP-CC)$_2$Pt(PEt$_3$)$_2$ **46**, whose UV-Vis spectrum revealed the red shift (about 40 nm) of the lowest energy absorption band (Figure **24**).



46 **44**

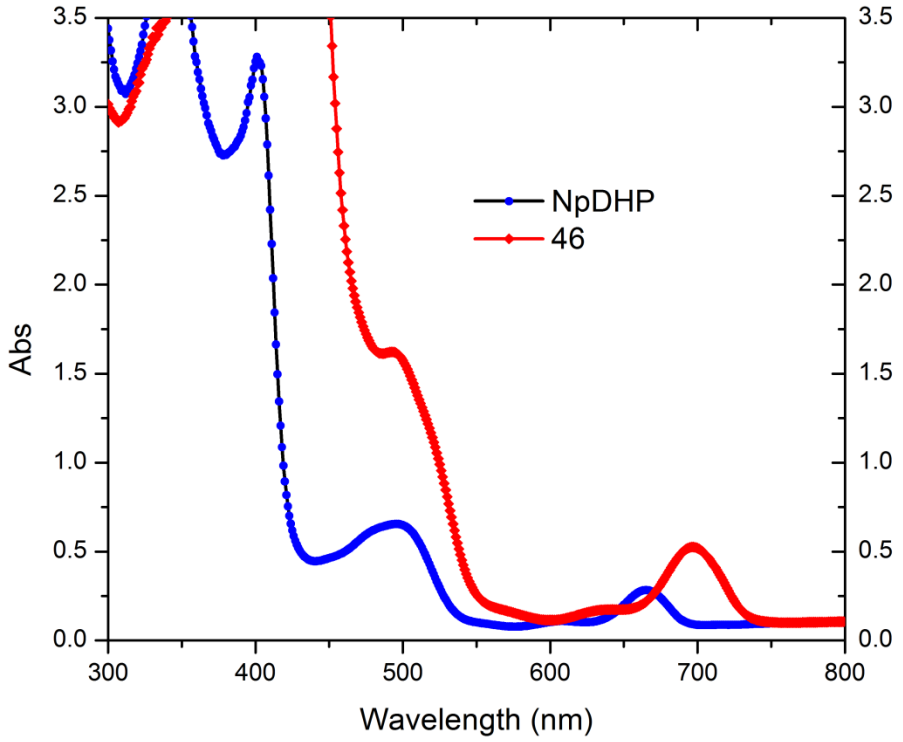


Figure 24. The UV-vis spectra of NpDHP 35 and complex 46

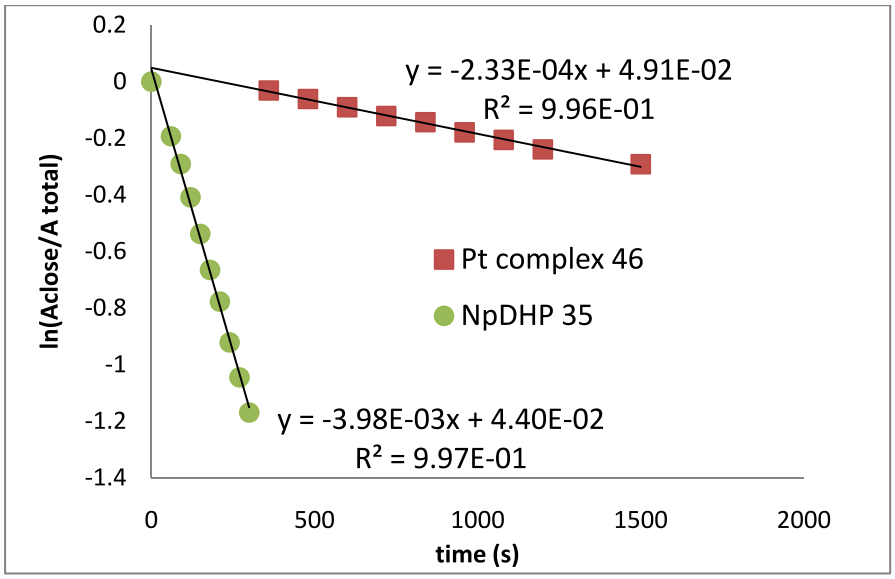


Figure 25. The photoopening rates for NpDHP 35 and *trans*-(NpC(O)DHP-CC)$_2$Pt(PEt$_3$)$_2$ 46

The photoopening was carried out by irradiating a UV-Vis sample of **46** and a *ln[A]* vs time (*t*) plotted based on a pseudo-first order law was used (Figure **25**). The 1'-naphthoyl DHP-derived metal complex *trans*-(NpC(O)DHP-CC)$_2$Pt(PEt$_3$)$_2$ **46** opens 17 times slower than NpDHP **35** (Figure **25**). However, the NpCODHPCCH **39** opens 4 times slower than NpDHP **35,** the complexation slows the opening by about 4 times with respect to the free alkyne ligand NpCODHPCCH **39**. The platinum complex *trans*-(CH$_3$C(O)DHP-CC)$_2$Pt(PEt$_3$)$_2$ **44** also opens about 4 times slower relative rate than the corresponding free alkyne CH$_3$CODHP-CCH **30**, as shown in Appendix **I**.

2.4.4 UV closing

Normally most CPDs close to DHPs with UV (254 nm) light at rates very similar to that of BCPD 3-**o**. We nevertheless decided to test complex **48** see if this was true in our case.

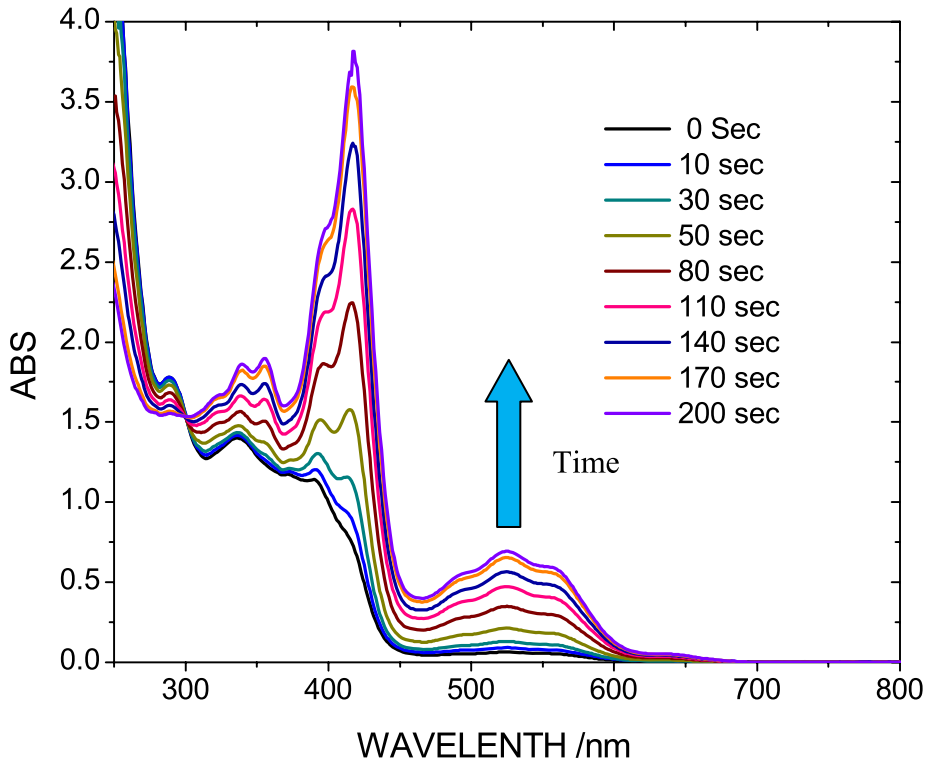


Figure 26. UV closing of 48 monitored by UV-Vis spectroscopy

The exposure of *trans*-(BDHP-CC)$_2$Pt(PEt$_3$)$_2$ **48** to UV light led to the photochrome closing which was monitored by UV-Vis spectroscopy (Figure **26**). Complete closing was achieved with a rate comparable to BCPD 3-**o**. It appears therefore that even for the complexes, the closing rates appear to be comparable to BCPD.

2.4.5 Thermal closing reactions

The thermal closing is first order and so is governed by the Arrhenius equation:

$$k = Ae^{-E_{act}/RT}$$

where k = reaction rate constant, R gas constant, A is a constant for a given reaction, called the pre-exponential factor and T absolute temperature.

$$\ln(k) = -\frac{E_{act}}{RT} + \ln(A) \qquad \text{Arrhenius equation}$$

The slope of the ln(k) vs 1/T plot yields E_{act} as $\boldsymbol{E_{act} = -}$ **slope** × $\boldsymbol{R}$ and the intercept on the ln$k$ axis gives ln(A).

Alternatively the Eyring equation can be used to evaluate $\Delta H^{\ddagger}$ and $\Delta S^{\ddagger}$ in a similar way:

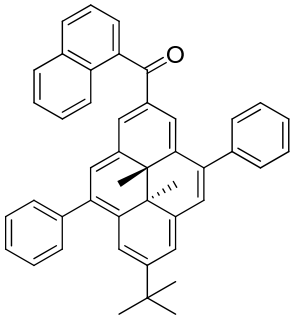
$$k = \frac{k_B T}{h} e^{-\frac{\Delta G^{\ddagger}}{RT}}$$

$$\Delta G^{\ddagger} = \Delta H^{\ddagger} - T\Delta S^{\ddagger}$$

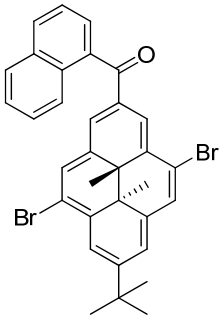
$$\therefore \qquad \ln\frac{k}{T} = \frac{-\Delta H^{\ddagger}}{R} \bullet \frac{1}{T} - \ln\frac{k_B}{h} + \frac{\Delta S^{\ddagger}}{R} \qquad \text{Eyring equation}$$

where $\Delta G^{\ddagger}$ is the Gibbs energy of activation, R ideal gas constant (R = 8.314 J • K^{-1} • mol^{-1}), k_B is Boltzmann's constant (k_B = 1.381×10^{-23} J/K), and h is Planck's constant (h = 6.626×10^{-34} J • S). A plot of $\ln k/T$ vs 1/T yields the enthalpy of activation $\Delta H^{\ddagger}$ as $\Delta \boldsymbol{H^{\ddagger}}$ = **– slope ×*R*** and the entropy of activation $\Delta S^{\ddagger}$ as $\Delta \boldsymbol{S^{\ddagger}}$ **= (intercept + ln(k_b/h)) × R**.

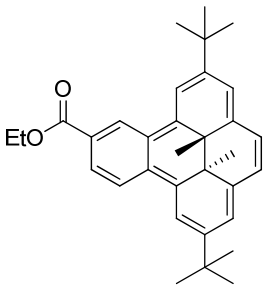
For CPDs → DHPs, quite a variation in the parameters E_{act} and $\Delta H^{\ddagger}$ have been found[131]:



E_{act} = 21.4 kcal/mol
$\Delta H^{\ddagger}$ = 20.7 kcal/mol



E_{act} = 22.5 kcal/mol
$\Delta H^{\ddagger}$ = 21.9 kcal/mol



E_{act} = 25.0 kcal/mol
$\Delta H^{\ddagger}$ = 24.4 kcal/mol

These three DHPs are all fast photochromic compounds. However, the enthalpy of activation $\Delta H^{\ddagger}$ varies by 3.7 kcal/mol and the activation energy E_{act} by 3.6 kcal/mol. Neither $\Delta H^{\ddagger}$ nor E_{act} are good parameters to estimate the relative rates of opening.

Half life: Because there are large variations in the pre-exponential factor ln(A) and entropy of activation ($\Delta S^{\ddagger}$), one cannot easily compare ΔE_{act} and $\Delta H^{\ddagger}$. In fact the half life ($\tau_{1/2}$) is a more useful comparison, since it actually estimates the time for half the molecules of the photochromic compound to close. As the thermal return is first order, when the concentration [A] reaches half the initial concentration [A_0], [A]=1/2[A_0], $\tau_{1/2}$ is calculated as

$$\ln[1/2A_0] = -kt_{1/2} + \ln[A_0].$$

$$\tau_{1/2} = \ln 2 / k .$$

It can be seen that the half life $\tau_{1/2}$ is not concentration dependent. Therefore, it becomes a reliable and convenient parameter to compare the rates of thermal reactions.

Table 10. Thermal closing rates of DHP-alkyne ligands, their precursors and metal complexes

Compounds	$\tau_{1/2}$ (h) 25 °C	ΔE_{act} (kcal·mol^{-1})	$\Delta H^{\ddagger}$ (kcal·mol^{-1})	$\Delta S^{\ddagger}$ (cal·K^{-1}·mol^{-1})	lnA
DHP-$COCH_3$ **25**	67	25.2	24.5	-1.6	29.8
CH_3CODHP CCH **30**	62	23.9	23.21	-3.11	29.0
$(CH_3CO)_2$DHP **27**	79	24.6	23.9	-4.0	28.5
NpCODHP **35**	22	22.4	21.8	-8.6	26.2
$(NpCO)_2$DHP **36**	15	23.6	22.9	-4.0	28.5
BDHP 3[133]	87	24.5	23.9	3.8	N/A
BDHP-alkyne **40**	62	26.6	26.0	3.5	32.3
DHP-$COCF_3$ **42**	18	24.5	23.9	-1.0	30.0
Complex **52**	33	23.7	23.0	-5.2	28.0
Complex **49**	38	24.2	23.6	-3.7	28.7
Complex **48**	42	24.5	23.8	-3.0	29.0

The thermal closing reaction was examined using NMR spectroscopy (Table **10**). For the alkyne ligand complexing with the platinum, the thermal return increases by a factor of about 2 from the free alkyne ligand **40** for complexes **48**, **49**, and **52** ($\tau_{1/2}$, (25°C) = 42 (**48**), 38 (**49**) and 33 (**52**) h), which is also faster than BDHP ($\tau_{1/2}$ = 87 h) itself. The activation energies are comparable among the complexes **48**, **49**, and **52** and are lower than that of the BDHP-alkyne **40** by *ca*. 2 kcal/mol.

The thermal closing rate was not affected significantly by having a triple bond substituent on DHP ($\tau_{1/2}$: 62 h in **30** vs. 67 h in **25**). Although 4,10-diacetylDHP **27** and 4,10-dinaphthoylDHP **36** open about 3 times faster than the mono-acylDHPs **25** and **35**, they show comparable closing rates (compare $\tau_{1/2}$ of **27** (79 h) and **25** (67 h) and **36** (15 h) and **35** (22 h)). Note that the fluoro substitutions in DHP-$COCF_3$ **42** cause the thermal return to be 3 times faster than that of DHP-$COCH_3$ **25**. From Table **10**, there is a trend

that faster thermal return corresponds to lower activation energy. In all the ketone substituted DHP's, the substituents on the DHP peripheral positions increase the thermal return rate which possibly due to stabilization of the radical intermediates caused by electron withdrawing groups. It is known that radical stabilizing functional groups lower the activation barrier leading to a faster thermal return.[134]

$(CH_3CO)_2$DHP **27**, Pt-complex **48** and DHP-$COCF_3$ **42** have similar ΔE_{act} (24.5 kcal/ mol) and enthalpy of activation $\Delta H^{\ddagger}$ (23.9 kcal/ mol) but show quite different half lives of 79, 42 and 18 h, respectively. This suggests that the pre-exponential factor *A* and entropy of activation ($\Delta S^{\ddagger}$) play a significant role in the thermal return.

2.5 Conclusions

Cis- and *trans*-*bis*(ethynyl)platinum complexes containing DHP photochromic compounds were synthesized from ^{R}DHPCCH (R = H, CH_3CO, PhCO, 1-naphthoyl and benzo[e]) and platinum chloride with appropriate ancillary ligands (PEt_3, PPh_3, dppe, bipy and phen). The complexes were studied using mass spectrometry, NMR spectroscopy (^{1}H, ^{13}C, ^{31}P and ^{195}Pt) and IR. The X-ray crystallographic structural information for *bis*(DHP-ethynyl) platinum complexes **44**, **45**, **47**, **49**, and **52** revealed that the Pt complexes processed square planar metal centers. The bond lengths in the complexes are in the normal bond lengths in the CSD database. The platinum complexes are T type of photochromic compounds. The BDHP-derived platinum complexes open completely on irradiation by visible light (cut off 590 nm). The photoopening rates for the platinum complexes are slower by about 4 times than their corresponding alkynes. All the alkynyl platinum complexes close faster than the corresponding alkynes, and are not affected substantially by changing the ancillary phosphine ligands. The BDHP-ethynyl platinum complexes with PEt_3, PPh_3 and dppe ligands have similar half lifes $\tau_{1/2}$ 42 h, 38 h and 33 hour, respectively, in contrast to the half life $\tau_{1/2}$ = 62 h of the BDHP-ethyne **40**.

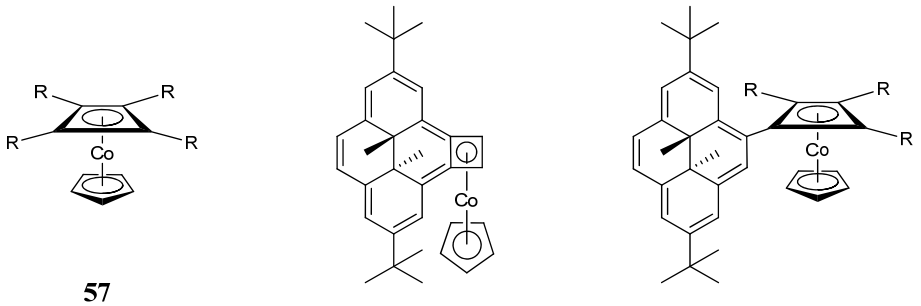
Chapter 3. Cobalt cyclobutadienyl DHP complexes

3.1 Introduction

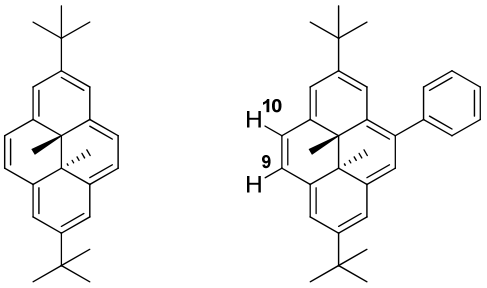
Conjugated cyclic 4-member ring systems have attracted considerable attention since the aromaticity of benzene was visualised more than 100 years ago.[135] Although aromatic compounds, including the cyclopentadienide anion, have been of interest for over 150 years,[136] the synthesis of cyclobutadiene dianion and its metal derivatives is more recent. Many failures in the synthesis of cyclobutadiene preceded the successful preparation of its first metal complexes.[135a, 137] The η^5-cyclopentadienyl tetraphenylcyclobutadiene cobalt complex was accomplished from diphenyl acetylene by Nakamura and Hagihara in 1961.[138] Ever since, largely owing to the interest in the cyclobutadiene unit, many efforts have been made to study these complexes.[135b, 139] More recently, cyclobutadiene cobalt complexes have been incorporated into highly symmetric super-molecular components because of their physical properties and chemical robustness. The remarkable thermal stability of cobalt complexes might attribute to the sterically bulky cyclopentadienyl group. Chiral catalysts were established taking advantage of its planar chirality.[140] Cobalt cyclobutadiene derivatives have found usage in catalytic enantioselective allylic substitutions as planar chiral complexes.[141] Bunz investigated the electronic nature of the incorporated cobalt metals to understand the electronic and energy transfer properties at a molecular level.[142] Typically, electrophilic substitution reactions took place on the cyclopentadienyl ring, while ring additions were denied.[143] Friedel-Crafts acylation took place at the unsubstituted positions of the cyclobutadiene ring but with only very low yield (*ca*. 10%).[144] The metal sandwich structure remained unchanged when the molecules underwent further modifications with strong bases and reductions.[145]

The cyclobutadiene dianion has been demonstrated to be an aromatic structure with D_{4h} symmetry from both NMR data and crystallographic evidence.[146] The corresponding cobalt complexes such as **57** were found to display a diatropic ring current from the 6π-electron cyclobutadiene dianion system. However, little is known about the extent of its aromaticity. Appending cyclobutadiene cobalt linkers to dimethyldihydropyrene drew our

attention for two main reasons. One lies in the growing interest in understanding the aromaticity of cyclobutadienide dianion. Metal complexed aromatic fragments bring up controversy in that they display greater bond averaging, i.e. aromaticity, than might be expected.[53] On the other hand, DHP has been successfully used in measurement the relative aromaticity of many metal complexed aromatic systems.[55, 73b, 76a, 76c, 78] So far we have not been able to fuse a Cbd unit as in **58**, so have attempted here to dangle a cyclobutadiene from a DHP, as in **59**.[147] Previous data have show a marginal fixation of the dimethyldihydropyrene ring current on dangling a benzene ring on a DHP, as in **60**, where $^{3}J_{H}{}^{9}\text{-}_{H}{}^{10}$ = 7.9 ± 0.15 Hz compared to an estimated 7.3 Hz in the parent DHP 2, and internal methyl at δ -3.84 and -3.86 in **60** compared to -4.06 in parent DHP.[148] It would thus be interesting to see if we can evaluate the aromaticity of the cyclobutadiene cobalt segment using DHP as a probe in a similar manner.



57 **58** **59**



2 **60**

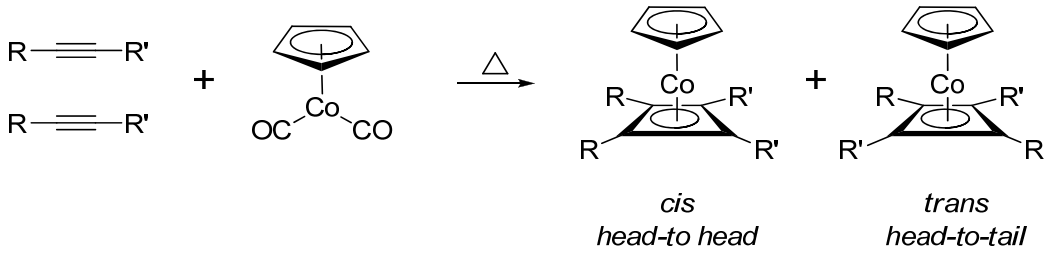
A second area of interest concerns the photochromic behaviour of DHP. Previous work has shown that photochromic ring opening of DHP to the cyclophanediene (CPD) form is affected by specific substituents on the periphery or internal positions of the 14-annulene framework.[149] At this stage, the photochromic properties are not that predictable even though photoopening and thermal return rates for hundreds of substituted DHP

photochromic compounds are in hand. It is certainly interesting to look at the effects that occur upon appending an aromatic cyclobutadiene cobalt linker to the dimethyldihydropyrene core. As the azo counterpart has shown,[150] the multistage photochemical properties of DHP derivatives also possess the potential for use in high data storage capacity molecular devices.[148] Multistage photoswitches based on DHP are even more attractive, by joining two or more photochromic units to benzene or cyclopentadienyl cobalt fragments by either direct fusion or sigma bond linkers or with a single bonding linker.[103, 105]

In this chapter, we describe our studies on the regioselective synthesis of stable cobalt metallacycles bearing two DHP photochromic fragments and our study of their aromaticity and photochromism.

3.2 Syntheses

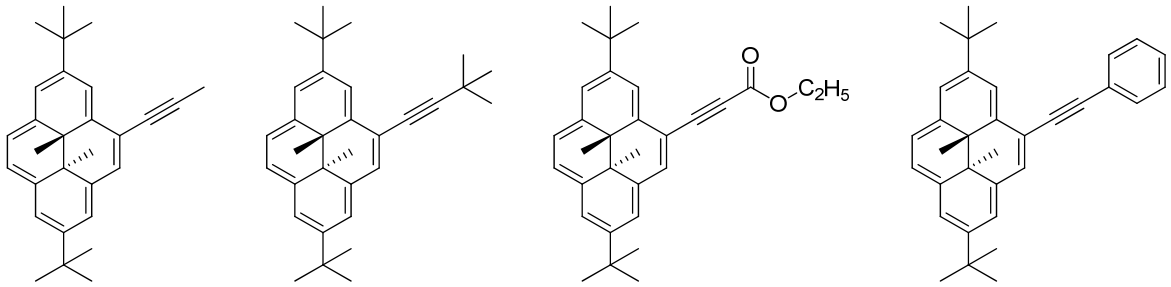
Cobalt cyclobutadiene complexes are best prepared using alkynes and $CpCo(CO)_2$ in a boiling solvent.



Scheme 17. The synthesis of cobalt cyclobutadiene complexes.

In principal, reactions of unsymmetrical alkynes with cobalt sources can produce two isomeric η^4-cyclobutadiene cobalt complexes (Scheme **17**). To eliminate the formation of regioisomers, a symmetrical alkyne could be used but the synthesis of di-DHP substituted alkynes has proven to be very difficult because of sluggish coupling of the very electron rich dimethyldihydropyrene. When alkynes with different end groups are used, formation

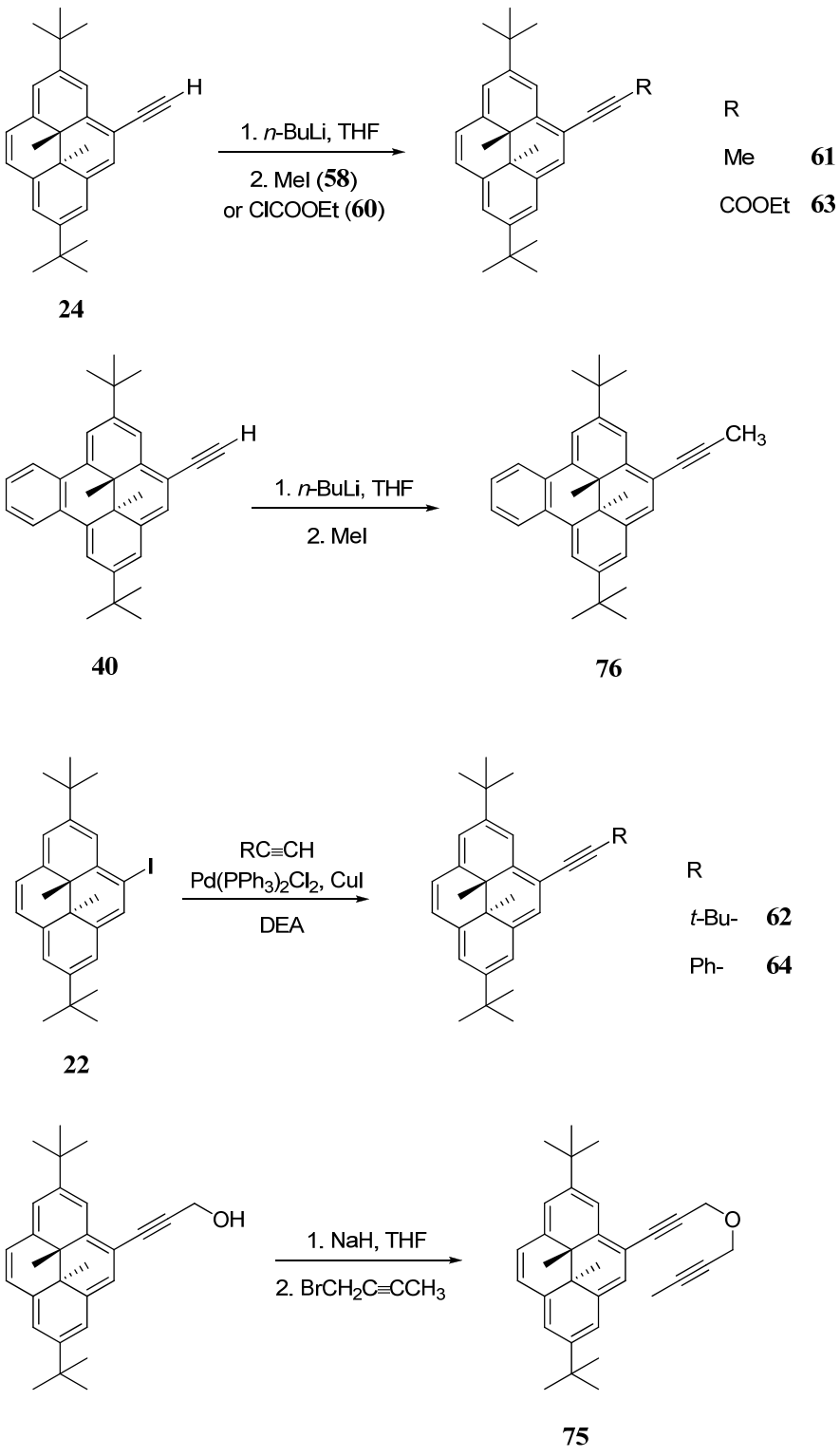
of *head-to-head* (*cis*) and *head-to-tail* (*trans*) regioisomers is probable. As well, the symmetry of the DHP is broken when a single substituent is present leading to additional stereoisomers due to the orientation of the internal methyls. To preferentially enhance chances of one regiocyclization over the other, for instance, *head-to-head* over *head-to-tail*, we thought of alkynes with widely different sized groups might be best. We chose **61** - **64** to start.



61 **62** **63** **64**

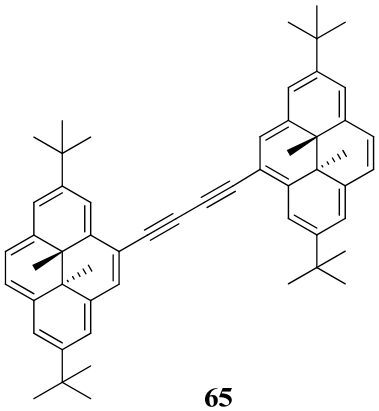
3.2.1 Syntheses of alkyne substrates

The DHP-ethynes **24** and **40** were lithiated with *n*-butyl lithium in dry THF at -78 ^{o}C and methylated with methyl iodide to quantitatively produce the methyl alkynes **61** and **76**, respectively. In the same manner, [151] ethyl chloroformate yielded ester alkyne **63**, and 3,3-dimethyl-1-butyne when coupled with iodide **22** yielded the *t*-butyl alkyne **62**. The phenylethyne analog **64** was obtained by coupling iodide **22** directly with phenyl ethyne; compound **64** was previously made in 64 % yield from the DHP bromide.[152] The alkyne **75** was prepared in 93% yield from the sodium salt of propargyl DHP[153] generated *in situ*.

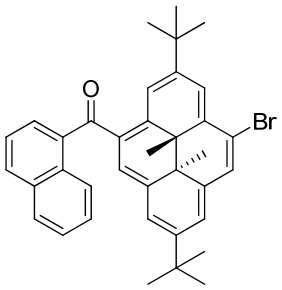


Scheme 18. The syntheses of alkyne precursors.

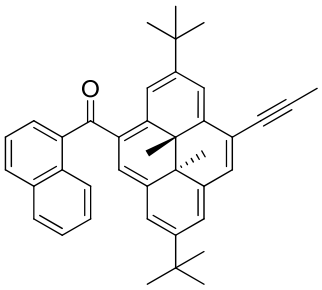
The diyne **65** [152] with only dimethyldihydropyrene termini was prepared by oxidative homo-coupling using Eglinton conditions.[154] Adapted from the reported procedure,[155] the 1'-naphthoyl DHP bromide **66**[130] was coupled with (1-propynyl)tributyltin catalyzed by tetra(triphenylphosphine)palladium in THF to afford the 1-naphthoyl substituted DHP-alkyne **67** in 75% yield.



65



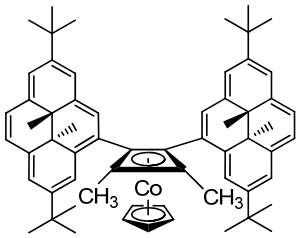
66



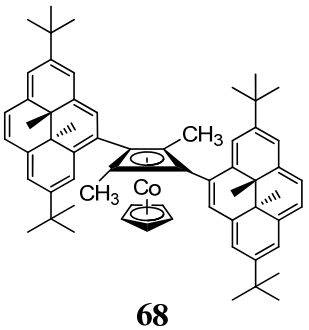
67

3.2.2 Preparation of cobalt complexes

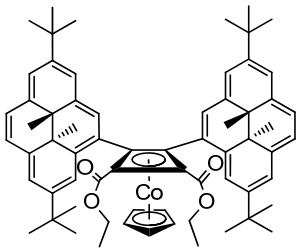
We chose to react η^5-cyclopentadienyl cobalt dicarbonyl $CpCo(CO)_2$ with two equivalents of alkyne to prepare cyclobutadiene cobalt complexes in the absence of oxygen,[156] even though a variety of cyclopentadienyl cobalt(I) complexes coordinated with CO, COD,[157] phosphines[158] or cobaltocene[159] itself have been used to prepare Cp cobalt complexes. A high boiling point solvent is necessary to ensure replacement of the CO ligand.



21



68



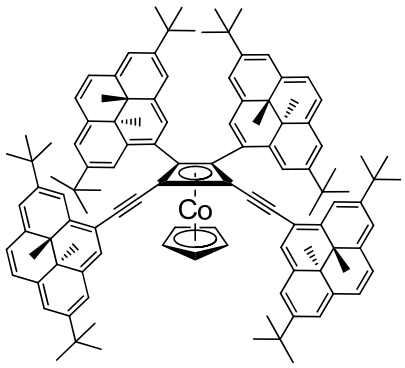
69

Dimethyl complexes 21. A mixture of alkyne **61** and excess $CpCo(CO)_2$ was heated in isooctane at 110°C for 24 hours under argon. After chromatography, dark red **21** was isolated in 30% yield as a mixture of isomers, whose empirical formula was confirmed by HRMS and elemental analysis. Note that the *trans* isomers **68** were not formed based on NMR analysis and X-ray evidence. The ^{1}H NMR spectrum of **21** showed eight peaks for the internal methyl protons (δ -3.74, -3.78, -3.83, -3.89, -3.94, -4.00, -4.01, -4.23) and four peaks for the methyl protons (δ 2.51, 2.27, 2.20, 2.08) on the cyclobutadiene. Three peaks were found for the Cp protons at δ 5.06, 4.99 and 4.95 (double integration). Careful chromatography failed to separate these isomers completely but rather enriched isomers in different fractions. The spectra of the enriched fractions were used to assign the stereochemistry of structure **21** in Figure **27**. There are three different isomers with two, two and four internal methyl resonances. This is also supported by the integration of the Cp protons.

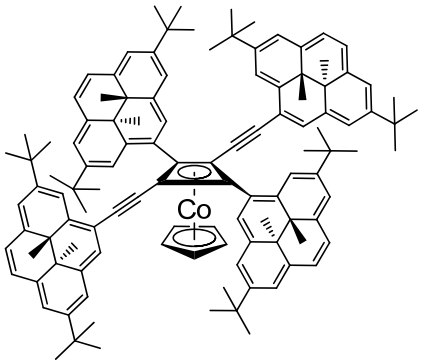
Diester complexes 69. In the same manner, alkyne **63** was used in the cyclization reaction and gave the ester complexes **69**. Again, in the ^{1}H NMR spectra, three groups of two, two and four peaks were obtained for the methyl protons of three isomers (δ -3.81, -3.86, -3.95, -3.96, -4.09, -4.13, -4.29, -4.45). Two peaks at δ 5.35 and δ 5.28 were found for the Cp protons. One isomer was isolated by repeated chromatography on silica gel, for which the Cp protons appeared at δ 5.28 and the internal methyl protons at δ -3.87 and δ -4.10 in the ^{1}H NMR spectrum.

TetraDHP complexes 70 and 71. Our attempt to react the diyne **65** with $CpCo(CO)_2$ gave a 52% yield of cyclobutadiene products **70** (*head-to-head*) and **71** (*head-to-tail*). The empirical formula was indicated by HRMS and elemental analysis. However the ^{1}H

NMR spectrum of the isomeric mixture showed 9 resonances for the cyclopentadienyl groups and 46 resonances for the internal methyl protons indicating a large number of regio and stereoisomers to be present. Crystallization separated the complex mixture into two groups. The less soluble isomers were obtained from hexane-dichloromethane, or from ethanol-acetone-chloroform. This group gave four ^{1}H NMR resonances (δ 5.134, 5.138, 5.150 and 5.162) for the cyclopentadienyl protons and four major resonances for the *t*-butyl protons (δ 1.062, 1.207, 1.723 and 1.730). The second group of isomers remaining in the mother liquor showed cyclopentadienyl protons at δ 5.339, 5.341, 5.360, 5.370 and δ 5.376, and *t*-butyl protons at δ 1.629, 1.635 and 1.638. Further assignment of the isomer structures was not attempted.



70

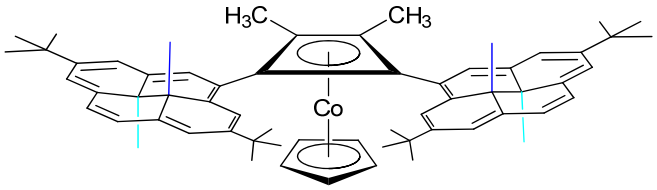


71

Other alkynes. The free alkyne **24** cannot be used in the cyclization reaction because of its well established fast polymerization side reaction. *t*-Butyl alkyne **62** and phenyl compounds **64** did not react with $CpCo(CO)_2$ under these conditions and only starting materials were recovered. Similarly, alkyne **23** failed to give any cobalt product although successful cyclization was reported in the literature for alkynes bearing TMS end groups. The reason for the failure of these alkynes to react is likely to be steric crowding. The alkyne **75** gave no desired products, and complex spectra were obtained, which might be due to intermolecular cyclization reactions. The BDHP-alkyne **76** decomposed during the reaction (perhaps not surprisingly, since BDHP does not tolerate high temperature well).

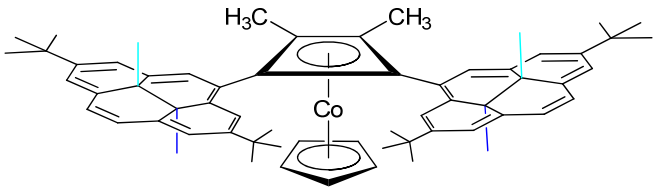
3.3 Results and discussion

Characterization by NMR spectroscopy. Characterization of the cyclization products by NMR is challenging because, in addition to the possibility of *cis* and *trans* regioisomers for the cyclobutadienyl substituents, the *'up'* or *'down'* orientation of the DHP internal methyl group nearest to the point of attachment with the cyclobutadiene ring leads to additional isomers. The enriched three isomers in methyl substituted cyclobutadienyl complex **21** was determined as *cis* (*head-to-head*) regiochemistry rather than the *trans* (*head-to-tail*) regioisomers **68** by 2D ^{1}H NMR studies. It is first necessary to establish which cyclobutadiene ring carbons bear methyl substituent by an HMQC experiment. In all isomers, these carbons are found between δ 80 and 82 ppm, thereby identifying the remaining cyclobutadiene carbons between 79 and 80 ppm as bearing DHP substituents. Once the methyl and DHP-bearing cyclobutadiene carbons have been identified, an HMBC experiment can be used to establish the ring substitution pattern because the cyclobutadiene methyl carbons will only show a cross peak to DHP-bearing cyclobutadiene carbons (79-80 ppm) in the *trans* isomer but to ***both*** methyl (80-82 ppm) and DHP-bearing cyclobutadiene carbons in the *cis* isomer. All three isomers show cross peaks to both types of carbons, clearly establishing all three isomers as *cis* (*head-to-head*) regioisomers. This regiochemistry was confirmed by an X-ray diffraction study (*vide infra*).



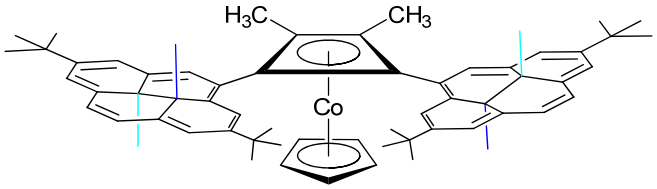
Cis anti , anti

A



Cis syn , syn

B



Cis anti, syn

C

Figure 27. Three possible stereoisomers for 21

As far as the internal methyl groups are concerned, three possible stereoisomers **A** (*cis anti*, *anit*), **B** (*cis syn*, *syn*) and **C** (*cis anti*, *syn*) in **21** are drawn in Figure **27** assuming the DHP groups are free to rotate. Isomers **A** and **B** are *meso* compounds because they possess mirror plane symmetry while isomer **C** has a pair of enantiomers. *meso*-Isomer **A** and **B** with mirror symmetry have two different peaks for the internal methyl groups and one peak for the methyl group on the cyclobutadiene. The early fraction from chromatography consists of the least polar isomer with the cyclobutadiene methyl protons at δ 2.20 and the internal methyl protons at δ -3.75/-3.91. In contrast, the later fraction includes more of the polar isomer with resonances at δ 2.26 and δ -3.86/-4.19, respectively. The Cp protons of **A** and **B** were at δ 5.06 and δ 4.99, respectively. As well, an HMBC NMR spectrum demonstrated that the methyl proton δ 2.20 correlated to two

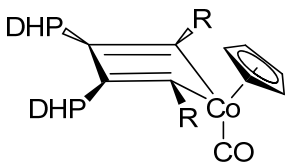
cyclobutadiene carbon signals at δ 80.09 and 79.41 in the former isomer, and the δ 2.26 methyl to two different cyclobutadiene carbons at δ 79.04 and 81.44 respectively in the latter one. This indicates mirror symmetry for the cyclobutadiene ring consistent with isomers **A** and **B**. The middle fractions mainly consist of an isomer showing two cyclobutadiene methyl protons at δ 2.50 and 2.09 four peaks for the internal methyl groups at δ -3.72, -3.77, -3.94, -3.98 and a single resonance for the Cp protons at δ 4.95 in the ^{1}H NMR spectrum. Four cyclobutadiene ^{13}C signals δ 81.70, 80.87, 79.48 and 77.78 are observed for this isomer. This is consistent with the proposed isomer **C** in Figure **27**, which includes a pair of enantiomers.

Since the separation of stereoisomers failed for **21**, difficulties rose in further exploration of its properties. Efforts were therefore made to modify the target molecule so that separation based on polarity would be easier. Compared to the obvious polarity difference between *trans* and *cis* regioisomers, changing the substituent polarity for a group of stereoisomers with *cis* regiochemistry would not be expected to make as much difference to the overall polarity. The complexes **69** with electron withdrawing ester substituents were prepared using the same method. Given the similar polarity of the isomers obtained, the products **69** are likely to belong to the same regioisomers. The internal methyl protons are shielded by the carbonyl on the ester groups and shift upfield by 0.7 to 0.28 ppm in comparison to methyl complexes **21**. The differences between each isomer can be interpreted as due to the location of the methyl groups in the shielding cone of the ester groups. Finally a small sample of a single isomer was obtained by repeated chromatography on an alumina column. The connectivity of this structure was then established based on heteronucleic NMR evidence, and assigned to isomer of **A** or **B** as shown in Figure **27**. Only two internal methyl resonances were found in the proton spectra indicating mirror symmetry of the internal methyl groups. The lack of proton handles on or close to Cbd ring prevents any further assignment from being made using 2D NMR techniques.

The larger number of the isomers observed for cyclization of diyne **65** indicated that both *cis* and *trans* complexes were formed in the cyclization reaction. Presumably this poor regioselectivity occurs because the two end groups (DHP and C≡C-DHP in this case) are both large and there is little steric preference for alkyne orientation. This certainly

makes the characterization extremely difficult and not all isomers could be identified by NMR spectroscopy. In literature examples, reactions of $CpCo(CO)_2$ with 2 equiv of *bis*(trimethylsilyl)butadiyne gave rise to only a small amount of the η^4-cyclobutadiene (1.3 % over all yield of two isomers) while η^5-cyclopentadienone (51 % total yield for two isomers) complexes and the benzene [2+2+2] cyclotrimerization product[160] (10.4% total yield for two isomers) were the major products.[161] Although it has been reported that the preparation of cyclobutadiene complexes is usually accompanied by cyclopentadienone cobalt complexes,[162] these products were not detected (absence of a carbonyl stretch at *ca.* 1580 cm^{-1}[163]) and neither was there any evidence for [2+2+2] cyclotrimerization products.[164]

In contrast to the results with diyne **65**, alkynes **61** and **63** possessing one large (DHP) and one small (Me or CO_2Et) groups gave the *cis* (*head-to-head*) regioisomers exclusively. This is consistent with an intermediate metallacyclopentadiene where the DHP groups are as far as possible from the fairly crowded CpCo group (Figure **28**). This supports the hypothesis that steric effects are more important than electronic properties in the [2+2] cyclodimerization reactions. Therefore, the presence of two DHP substituents on the alkyne (DHP-C≡C-DHP) must disfavour the transition state and hamper the cyclization of this alkyne, since no reactions occurred when the alkyne DHP-C≡C-BDHP was tried in the reaction. In the case of diyne **65**, the relatively large groups (DHP and CCDHP) on the ends of the alkyne presumably lead to little selectivity in the cyclization intermediate and both the *head-to-head* and *heat-to-tail* isomers form. Thus, suitable R groups (Figure **28**) are required in order for the cyclization to occur. Presumably *tert*-butyl, trimethylsilyl and even phenyl end groups on the alkynes are too large to cyclize, since we observed no products in these cases. Our experimental data is consistent with Bunz's, in which the formation of *cis* and *trans* substituted (3.5 to 1 ratio) complexes bearing two TMS and 1,3-dioxanyl substituents was observed.[165]



R= Me or CO_2Et

Figure 28. The proposed cyclization intermediate

Variable temperature NMR experiments. Despite the obvious bulkiness of the DHPs, no restricted rotations were seen in the ^1H NMR spectra. The RT ^1H NMR spectra revealed the number of peaks match the existence of the three isomers, **A**, **B** and **C** (Figure 27). For both complexes **21** and **69** variable temperature NMR[166] was carried out to look for restricted rotation of the DHPs (Appendix **III**). At lower temperatures, some resonances such as those of the internal methyl protons became broad and began to overlap. Several observable peaks broadened and then sharpened again while shifting significantly upfield or downfield, depending on the isomer. One isomer showed markedly stronger temperature dependence. It is noteworthy that no coalescence was observed from room temperature to -95°C. However, the observed shifts might be caused by a restricted range of motion such that the protons sample different magnetic environments at different temperature. The observations lead to the conclusion that there is no change in the symmetry of the molecule caused by slow rotation, since decoalescence was not observed at low temperature.

Crystallographic structure determinations. A dark red crystal of the methyl substituted η^4-cyclobutadiene cobalt complexes **21** was grown from an acetonitrile-dichloromethane solvent mixture. The crystal structure of the methyl complex **21** belongs to the triclinic P-1 space group. Only the *cis* regioisomers are observed in the crystal and all these stereoisomers depicted in Figure **27** are present in the disordered crystal. Two different CpCo units (97 % occupancy) relate with an approximately 180° twist by a vector of the cyclobutadiene edge closest to the DHPs with a 5.6:4 ratio. With the cobalt and Cp sitting in different location of the unit cell, two components (literally being

assigned as Y and Y') are included in the structure with no potential selectivity. The nature of the cobalt disorder is illustrated in Figure **29**.

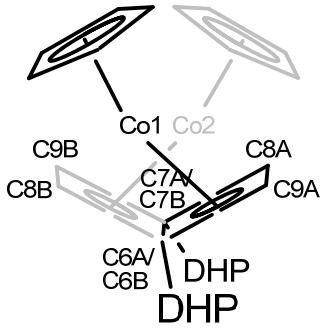


Figure 29. **The relationship between the two major disorder components Y (black) and Y' (grey) in the crystal strucure of 21**

(The DHP and methyl groups are omitted for clarity)

The two components are, however, characterized very differently in their X-ray crystal parameters. The crystal structure shown in Figure **30** depicts **Y**.

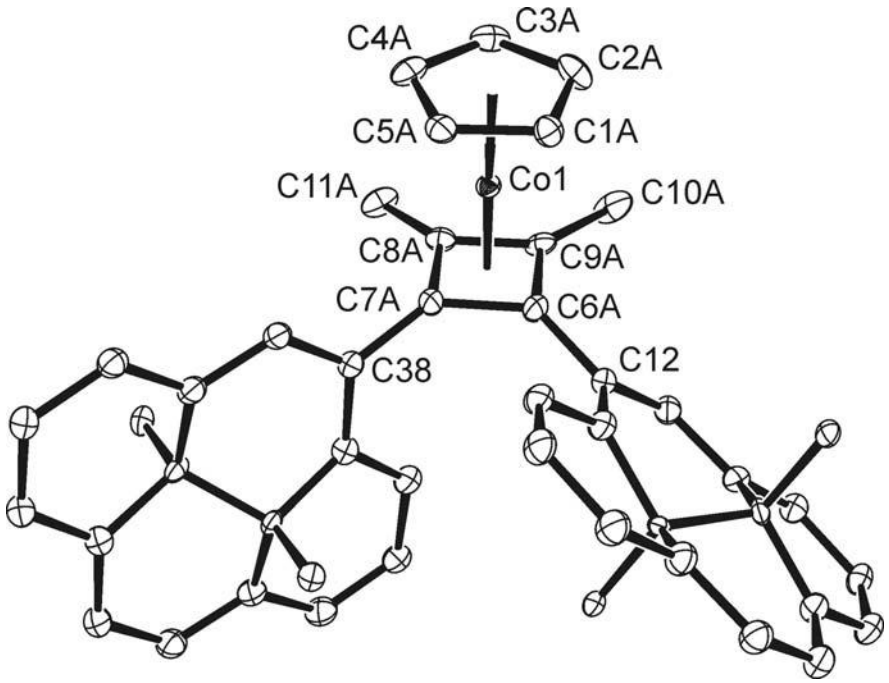


Figure 30. ORTEP3 plot (30% probability level) of 21 showing only the major component Y

(The DHP and methyl groups are omitted for clarity)

Significant bond distances and the interplane angles for the major and minor components **Y** and **Y'** are tabulated in Table **11** and Table **12**, respectively.

Table 11. Selected bond lengths for the major and minor components Y and Y' in 21

Components Y			Components Y'		
Cbd ring Y (Å)			Cbd ring Y' (Å)		
C6Y	C7 Y	1.481(6)	C6 Y	C7 Y'	1.481(6)
C7Y	C8 Y	1.594(9)	C7 Y	C9 Y'	1.585(8)
C8Y	C9 Y	1.47(1)	C9 Y'	C8 Y'	1.55(2)
C9Y	C6 Y	1.591(9)	C8 Y'	C6 Y	1.600(8)

Co1-Cbd_Y Distances (Å)			Co2-$Cbd_{Y'}$ Distances (Å)		
Co1	C6 Y	1.876(3)	Co2	C6 Y	1.768(4)
Co1	C7 Y	1.868(4)	Co2	C7 Y	1.754(5)
Co1	C9 Y	1.976(7)	Co2	C8 Y'	2.009(9)
Co1	C8 Y	1.988(7)	Co2	C9 Y'	1.993(9)
	centroid	1.593		centroid	1.531
Co1-Cp_Y Distances (Å)			Co2-$Cp_{Y'}$ Distances (Å)		
Co1	C1 Y	2.051(5)	Co2	C1 Y'	2.05(1)
Co1	C2 Y	2.067(6)	Co2	C2 Y'	2.06(1)
Co1	C3 Y	2.052(5)	Co2	C3 Y'	2.059(8)
Co1	C4 Y	2.058(6)	Co2	C4 Y'	2.057(7)
Co1	C5 Y	2.060(6)	Co2	C5 Y'	2.067(9)
	centroid	1.673		centroid	1.665

In the literature[167] most cyclobutadiene rings in cobalt complexes demonstrate nearly ideal square planes with equal C-C bond lengths. In contrast, there is a significant bond length alternation in our cyclobutadiene rings of **21**. The C-C bond lengths of the cyclobutadiene ring were found as 1.481(4), 1.594 (8), 1.468 (13) and 1.591 (7) Å in component **Y**, and as 1.481 (4), 1.585 (8), 1.548 (16) and 1.600 (8) Å in component **Y'** (Table **11**). The Cbd ring is indeed rectangular and two side bonds elongate by more than 0.1Å up to 1.600Å, which is significantly out of the reported bond length ranges (1.44-1.47Å) of the four-membered rings in cyclobutadiene CpCo complexes.[167] The bond is even dramatically longer than a typical sp^3 C-C bond length (1.54Å).[168] It is in fact comparable to the long C-C bond (1.587 Å and 1.593Å) in a distorted cyclobutadiene, that shows rectangular distortion so as to avoid the potential antiaromaticity.[169] The 1,2-diacetyl-3,4-*bis*(dimethylamino)cyclobutadiene cobalt complex[170] showed minor deviations in the cyclobutadiene ring, in which C-C bonds of the four-membered ring showed same alternation (1.485, 1.495, 1.459 and 1.468 Å). The data indicated that two

cis electron withdrawing ketones and two electron donating dimethylamino groups do not cause the bond to vary significantly. Therefore, despite the electron richness of the DHP, the large bond alternations are probably caused by the bulkiness of the DHPs.

The cobalt atom is close to the two carbons on the edge bearing the two DHP substituents. As a result, the Co-C to the nearer carbons are 1.868 (4) and 1.876 (3) Å, and 1.768 (4) and 1.754 (5) Å in components **Y** and **Y'**, respectively, compared to the 2.00Å to the carbons on the opposite edge. These bonds are usually slightly less than 2.00Å in structures reported by other groups.[168c] As a consequence, in contrast to an average distance of nearly 1.66 Å in other complexes, the cobalt atoms become very close to the cyclobutadiene centroid with distances of 1.593Å and 1.531Å in the two components **Y** and **Y'**, respectively. This is shorter than the longest Co- Cbd distances of 1.73Å in the literature.[171] It is noteworthy that these distances to the edges are usually identical and lie in a small range of 1.68 to 1.69Å.

The exo C-C bond lengths between the cyclobutadiene ring and DHP are found to average 1.467(4) and 1.476(4) Å, comparable to the 1.487(6) Å distance of the C(sp^2)-C(sp^2) single bond between rings in triphenyl phenol.[172] The bond lengths are similar to the linking C-C distance of 1.469Å between an electron rich ferrocene and a phenyl group in phenylferrocene.[173] Considering the fact that bond lengths 1.47Å are found between the ferrocene and the cyclobutadiene ring in a *cis* ferrocene substituted cyclobutadiene cobalt complex and are longer than 1.44Å in the *trans* one,[174] the shrinkage is presumably due to π conjugation. Therefore, it is indicative of only small π-conjugation between the DHP rings and the cyclobutadiene ring. The studies of the substituents effects on tricarbonyl-(1,2-diphenylcyclobutadiene)iron(III) complexes by NMR spectroscopy showed that change of the electronic character of substituents on the phenyl groups lead to the modification of the molecular geometry of the cyclobutadiene and its bonding to the metal. However, the crystal structure information failed to provide further evidence in terms of the distances of the cyclobutadiene and the phenyl groups. The two *exo* bond lengths (1.467(4) verse 1.454(9)) are indeed very close within the experimental error in the crystal structures of the 1,3-*bis*(4-methoxyphenyl)-2,4-*bis*(trimethylsilyl))-cyclobutadiene and of the 1,3-*bis*(4-trifluorophenyl)-2,4-*bis*(trimethylsilyl))-cyclobutadiene cobalt complexes.[175]

Table 12. The interplane angles in the X-ray structure of 21

Planes		Angle (°)
Cbd Y	DHP1	86.46
Cbd Y	DHP2	40.22
Cbd Y'	DHP1	35.6
Cbd Y'	DHP2	88.03
DHP1	DHP2	75.98
Cp Y	Cbd Y	4.35
Cp2	Cbd2	10.42

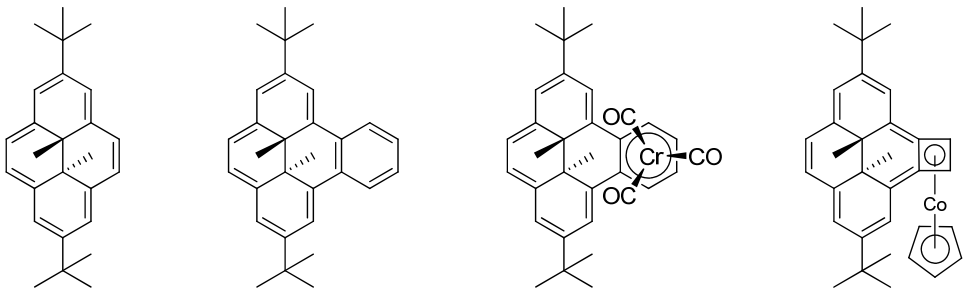
The angles in Table **12** suggest that the cyclobutadiene rings form a square framework with a small deviation ±0.4 (89.8(4)°, 89.7(4)°, 90.1(5)° and 90.4(5)°) in component **Y** and a deviation of ±1.5° (91.44°, 90.97°, 88.47° and 89.13°) in component **Y'**.

In component **Y**, the two methyl groups on the cyclobutadiene are slightly deviated away the CpCo segment from the ring plane by 1.0° and 3.7°, while the two bonds to DHP bend in the same direction but to a much larger extent of 22.5° and 24.0°, respectively. Similarly angles of 2.6° and 4.8° were observed for Me, and 30.7° and 28.8° for bonds with DHP in component **Y'**. The significant distortion of the exo-ring bonds from the planarity must be caused by the steric repulsion between the DHPs and Cp groups. Such a large distortion is very unique. Of the similar cyclobutadiene cobalt complexes, the largest bending angles out of the cyclobutadiene plane were found in the 1,3-dimesityl-2,4-diphenyl-cyclobutadiene cobalt complex (*ca.* 20° and 14°).[167] One of the DHPs is nearly parallel to the cyclobutadiene ring with angles of 3.54° and 1.97° in components **Y** and **Y'**, respectively. More steric hindrance is faced by the other DHP, leading to a larger torsion angles of 40.22° and 35.6° with respect to the cyclobutadiene ring in components **Y** and **Y'**.

The bond lengths and distances related to the cyclopentadiene ring lie in a normal range. The peripheral C-C bond lengths of the DHPs span a narrow range of 1.37-1.42Å in contrast to 1.387-1.402Å in the parent DHP.[176] Because tetramethyl cyclobutadienyl cobalt complexes that have been reported[171, 177] and have no exceptional character in comparison to other substituents, we assume that the unusual distances and angles here can be attributed solely to the DHP groups.

3.4 Aromaticity

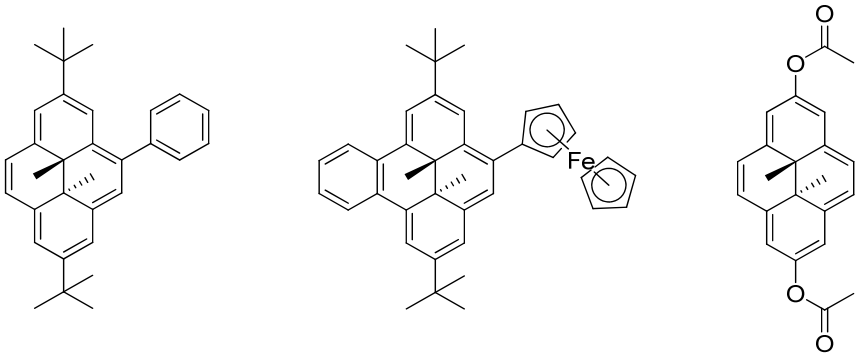
When 4n+2 π-electron aromatic systems are fused to dihydropyrenes as in the benzo derivative **3**, the ring current reduction in the DHP is substantial and the shielding of the internal methyl protons is thus much reduced. The resonances of the internal methyl groups shift from δ -4.06 in the DHP **2** to δ -1.58 in BDHP **3**. The extent of this reduction is directly proportional to the 'aromaticity' (or more strictly bond localization energy) of the fused aromatic, in this case benzene. Comparison of this reduction in shielding for different fused aromatic systems, then directly gives an experimental determination of "resonance energy" of the fused aromatic,[73b] including organometallic derivatives,[53] relative to the archeotype benzene.[76c]



2 **3** **11** **58**

Study of **11** gave an unambiguous experimental estimate of the 'relative aromaticity' of tricarbonylchromium complexed benzene,[55] and so synthesis and study of the fused compound, **58** would undoubtedly have led to a relative aromaticity estimate for the

CpCoCbd fragment in **58**. Unfortunately, our failure to synthesise a fused system **58** made us to examine whether an indirect route was possible or not. Lai[178] has suggested that a substituent aromatic group, as in **60**, also affects the diatropicity of the DHP ring, but to a smaller extent, which can then by comparison to the DHP **2** give an estimate of the relative aromaticity of the dangling ring. Besides the perturbation of ring current of the DHP through the C-C bond, there exist also shielding effects through-space. For fused or substituent groups, the effect on the internal methyl chemical shifts depends upon through-space anisotropic effects and an 'aromaticity derived' effect. With a rigid [a]- or [e]-fused system as in **58** or **11**, the through-space shielding (or deshielding) effect of the organometallic group can be separated from the aromaticity effect because both internal methyl groups feel the same 'aromaticity effect' but because one is on the metal side and the other opposite, different through-space effects.



60 **4** **74**

However, with a dangling group, as in **60** or **4**, rotation about the attaching bond is possible, which means separation of the anisotropic through-space effect is much more difficult. In the case of **60,** free rotation of the phenyl group occurs, and there is only a very small anisotropy difference, so that both internal methyl protons appear at almost the same shift, δ -3.84 and -3.86. However, that is probably less likely for the much larger CbdCoCp groups in **21** or **69**. Having a metal on one side of the ring, as in **11**, produces a substantial through-space anisotropic effect on the internal methyl groups, which was calculated as $\Delta\delta$(Me) = 0.394 ppm.[55] For a rigid system such as **11**, where the molecular structure is known from X-ray analysis, the diamagnetic susceptibility of the complexing group can be determined by, and then used in, the McGlinchey equation[179] to calculate an 'anisotropy free chemical shift' of the internal methyl groups for use in an aromaticity

estimate. In the 'freely rotating system' **4**,[49] the internal methyl groups feel the average and appear surprisingly close together at δ -0.94 and -0.97 but are substantially deshielded from those of BDHP **3** at δ -1.58 and 4-phenyl BDHP **73** at δ -1.453 and -1.456.[49] Without knowing the 'solution geometry' of **4**, calculation of an 'anisotropy free' chemical shift for the internal methyls of **4** is not possible. We were hoping that the much bulkier substituents of **21** and **69** would perhaps have frozen the rotation, which might then permit a similar calculation to that which we used for **11**, where the strucutural data are also available. However, unfortunately, we encountered isomer complexity in the cases of both **21** and **69**. Examination of low temperature VT ^{1}H NMR spectra for **21** suggest that at least partial rotation is permitted. Although for the single isomer of **69**, the internal methyl protons appear at δ -3.86 and -4.09, for the mixed isomers, the range is from δ -3.81 to -4.45 indicating substantial through-space anisotropic effects are occurring depending upon the isomer. The solution geometry must differ from that in the solid state. Moreover, our lack of knowledge as to which geometry of **69** to use in McGlinchey type calculations, prevents us from estimating a suitable chemical shift for comparison, and so also prevents us from estimating the aromaticity of the fragment in this manner.

We have also used the more distant external protons e.g. H-4,5 in **3**, to estimate the bond localization energy of the annelating aromatic, in both [a]- and [e]-annelated derivatives.[41, 73b] The relevant protons for **69** are H-8' (δ 8.34), H-9' (δ 8.26), H-10' (δ 8.17), which are shielded from those in the DHP 2, H-1(δ 8.52) and H-4 (δ 8.44), as would be expected for a small reduction in annulene ring current, *but* since those in the phenyl derivative **60** where H-1,8 (δ 8.51) and H-9,10 (δ 8.42) are not significantly different from the parent, suggests that the observed shielding may be arising from the juxtapositioning of the other dihydropyrene ring.

We thus examined coupling constants next. In a perfectly delocalized annulene, in the absence of steric effects, peripheral $^{3}J_{\text{H-H}}$ coupling constants should be equal. Perturbation of the delocalized structure, e.g. by fusion to an aromatic, causes bond alternation, and hence an alternation of coupling constants.[73b] Thus in DHP **2** (asymmetric derivatives), $^{3}J_{9,10}$ = 7.3 Hz. In the analogous [a]-fused benzannulene of **3**, $^{3}J_{9,10}$ = 8.89 Hz and for $^{3}J_{4,5}$ = 6.64 Hz.[180] Fusion of a benzene ring causes changes of

bond order and therefore pronounced alternation in the coupling constants.[73b] In cobalt complex **69**, $^{3}J_{9',10'}$ = 7.8 Hz, and in phenyl-DHP **60**, $^{3}J_{9,10}$ = 7.9 Hz, which can be compared to 7.3 Hz for 2. We believe this to be a significant change and is experimental evidence that indeed the cobalt Cbd fragment of **69** is behaving in a similar aromatic fashion to the phenyl group in **60**. If the above effect is real, then there should also be significantly more bond order deviation in **21** and **60** than in **2**, and this should be observed as a deviation in the bond lengths of the molecules. Table **13** shows the relevant data that we have.

Table 13. Selected bond length data (Å) for comparison

Molecule	Bond length range	Ave. bond length	Total deviation[a]
DHP 2	1.388-1.402	1.3936	0.069
DHP **74**	1.392-1.408	1.3949	0.071
Phenyl-DHP **60**	1.372-1.414	1.3943	0.142
21 (A)	1.378-1.419	1.3934	0.149
21 (B)	1.375-1.418	1.3923	0.177
BDHP 3	1.351-1.463	1.4044	0.539

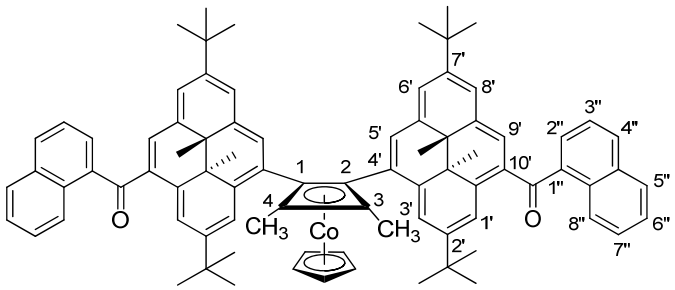
[a] Sum of the modulus of the deviation (14 bonds) from the average

Thus in the di-*t*-butyl DHP **2**, the sum of the modulus of the deviations from the average bond length over all 14 periphary bonds is only 0.069 Å. Even in the relatively electron rich 2,7-diacetoxy derivative **74**,[73a] this sum is still only 0.071 Å. In the cobalt complex **21**, this sum is more than twice these values, 0.163 Å (ave), indicating more substantial bond length alternation, but not of course as much as for the fused benzo-derivative **3**, where this sum is 0.539 Å. While we have not been able to absolutely quantify the aromaticity of the CbdCoCp fragment of **21** or **69**, it seems clear that experimentally it is behaving with a similar aromaticity effect to that of a benzene ring.

3.5 Photochemistry

In the UV spectrum of the unsubstituted cyclobutadiene(cyclopentadienyl) cobalt complex,[181] the lowest energy absorption maximum at 385 nm is weak with (ε = 320). Two more absorptions are observed at 258 nm (ε = 20,000) and 290 nm (ε = 1200). The parent DHP **2** is a rather poor photochrome [Φ=0.0015] and many simple substituted dihydropyrenes open so slowly that they appear not to open at all unless favorable conditions are used.[39] However, substitution with an acyl group enhances the quantum yield [Φ], converting it in to a reasonable one,[106] such that the photoopening reaction referred to those in Section **2.4** can be readily followed by visible spectroscopy.

In fact, when complex **21** was irradiated with visible light, no opening was observed. We thus decided to attach a 1-naphthoyl group to the complex. To do this required us to synthesize first the 1-naphthoyl alkyne **67** from the known[39] bromide **66**, and then cyclize this to give **72** as we did for **21** (full details are given in the experimental section).



72

Opening of the 1-naphthoyl complex **72** on irradiation proceeded much more slowly than for **35**, but it did at least open (Figure **31**).

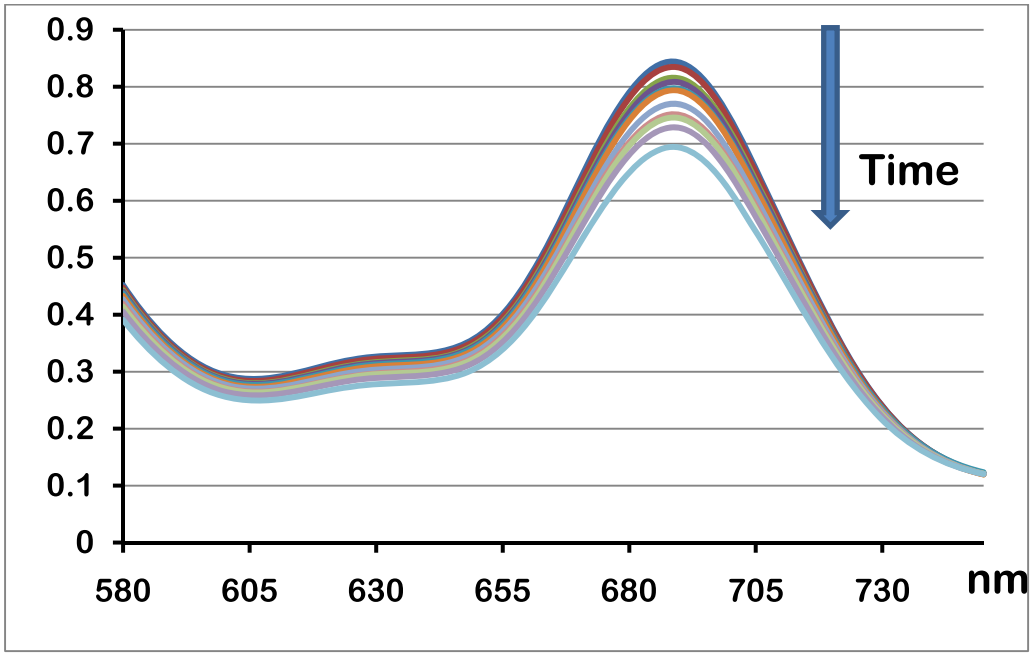
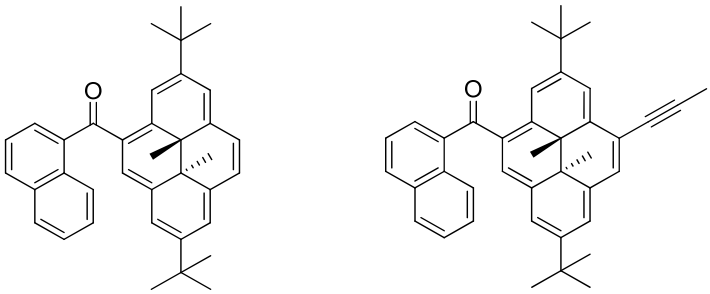


Figure 31. **The absorptions of 72 between 580 and 750 nm after irradiation with light of wavelength >590 nm for periods between 0 (top scan) and 40 minutes (bottom scan).**



35 **67**

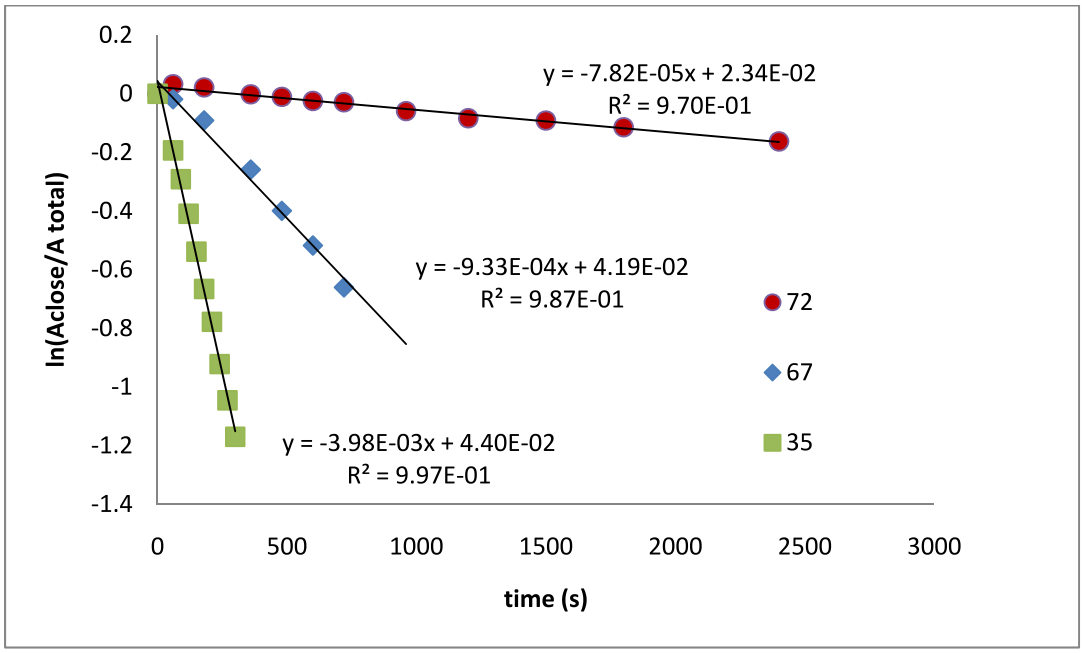


Figure 32. Pseudo-first order rate plots for the photoopening of 35, 67 and 72

We have shown previously[130, 148] that the photoopening reaction follows a pseudo-first order rate equation for a sample in a UV cell. The data is shown graphically in Figure **32** for the naphthoyl-DHP **35**, the propynyl derivative **67** and cobalt complex **72**. Acetylene substitution of DHP's appears to slow the photoopening reaction by about 3 times,[39] and indeed propynyl derivative **67** opens ~4 times slower than **35.** Cobalt complex **72** opens about 12 times slower than **67** and thus approximately 50 times slower than **35**. Although data is limited, it appears that metal complexation generally slows

down photoopening relative to their neutral hydrocarbon precursors; for example, Ru complex **23** opened ~3 times slower than its parent **3**. Both (η^5-CpDHP)Re(CO)$_3$ and (η^5-CpDHP)Ru(C_5Me_5) have been prepared previously by us,[182] and each undergoes visible light ring opening, with the former opening about twice as fast as its parent Cp anion, which itself opens about **5** times slower than **3**, while the latter opens at about the same rate as the anion. We hope to eventually obtain sufficient data to shed more light on these processes.

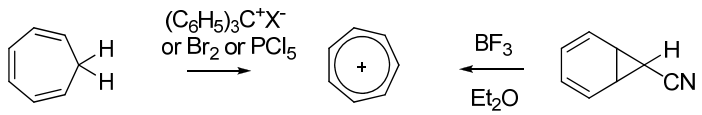
3.6 Conclusions

We have prepared the first cyclobutadienyl cobalt substituted dihydropyrenes by CpCo(CO)$_2$ cyclization of a series of dihydropyrenyl ethynes. When the other alkyne substituent was small, methyl or carboxyethyl, only *cis* (*head-to-head*) isomers were obtained, but with medium or larger sized groups mixed *head-to-head* and *head-to-tail* isomers were obtained. The crystal structure of complex **21** indicated some unusually short bond distances were present. By comparison of NMR and bond length data of complexes **21** or **69** with phenyl-DHP **60,** the aromaticity of the cyclobutadienyl cobalt fragment was estimated quantitatively to be at least as large as that of benzene. The organometallic fragment [Cbd-Co-Cp] substantially slowed the DHP photoopening reaction of complex **72** relative to precursors **67** or **35**.

Chapter 4. DHP-fused tropylium cation and cycloheptatrienyl anions and cyclooctatetraene dianion

4.1 Introduction

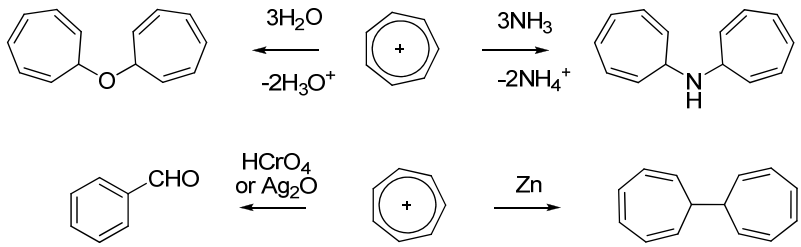
In this chapter, we report the syntheses of several DHP-fused C7 and C8 systems. The aromaticity of the fused C7 and C8 systems is evaluated using DHP as a molecular probe. In addition, the photochromism of these DHP-fused C7 and C8 systems is explored.



77 **15** **78**

Scheme 19. The preparation of the tropylium cation

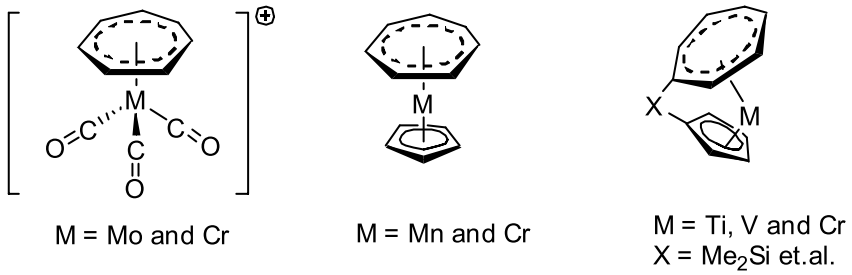
Tropylium cation **15** was readily accessed from cycloheptatriene 77 using a variety of conditions, e.g. DDQ in HBF_4.[183] However, more preferable methods are hydride abstraction by trityl cation (with perchlorate or tetrafluoroborate counter ions) and bromination or chlorination by Br_2 or PCl_5.[64, 184] The cation can also be prepared from other starting materials, such as the benzene-derived cyanide **78**.[185] The cation **15** has a planar structure with D_{7h} symmetry based on its simple infrared and Raman spectra.[186] The protons of **15** resonate at δ 9.28 as a singlet, indicative of both the diamagnetic effects of the induced ring current and deshielding by the positive charge. The absorption maxima of **15** are observed at 217 nm ($\varepsilon = 4.1\times10^4$) and 275 nm ($\varepsilon = 4.3\times10^3$) in the ulatraviolet spectrum.[187] The acidity of the tropylium cation **15** in water ($pK_{R+} = 4.01$) is comparable to that of acetic acid.



Scheme 20. The reactions of tropylium cation

Tropylium cation **15** reacts as an electrophile with a variety of nucleophiles, such as water, and ammonia to form ditropyl ether and ditropyl amine (Scheme **20**). The cation **15** is also readily reduced by zinc to the dimer, bitropyl, and oxidized by $HCrO_4$ or Ag_2O to benzaldehyde.

The cation **15** can form piano stool and sandwich metal complexes with group 4, 5 and 6 metal atoms, reviewed by Green and Ng in 1995.[188] The charged tropylium tricarbonyl



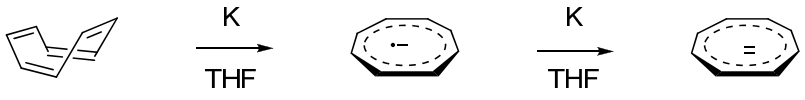
molybdenum (or chromium) complexes were prepared from the corresponding neutral cycloheptatriene complexes $(C_7H_8)M(CO)_3$ (M = Mo and Cr).

The tropylium cyclopentadienyl chromium and manganese complexes (η^7-C_7H_7)M(η^5-C_5H_5) (M = Mn and Cr) were approached from their corresponding benzene complex precursors. Recently, Tamm[189] reviewed the synthesis and activity of a series of sandwich complexes and *ansa*- tropylium cyclopentadienyl metal complexes *ansa*-(η^7:η^7-$(C_7H_6)X(C_5H_4)M$ (M = Ti, V and Cr; X = Me_2Si).



79 **79a**

Formation of the aromatic tropylium cation subunit is considered the main reason for the unusual behaviour of tropone **79**. On the basis of the high dipole moment of tropone, it has been concluded that the ionic form of tropone contributes substantially to the ground state resonance hybrid. Thus the seven-membered tropone is best regarded as a 6π-7*C* aromatic system as a result of the contribution from the dipolar ionic structure **79a**.



82 **80a** **80**

Scheme 21. Reduction of COT 82 to anion radical 80a and dianion 80

The charged 10π-8*C* $C_8H_8^{2-}$ **80** is also a well-studied aromatic system. Before 1945, even the existence of 1,3,5,7-cyclooctatetraene **82** (COT) (Scheme **21**) was debated. It is a pale yellow oil because its electronic spectrum tails into the visible region. The large number of bands in both the Raman and infrared spectra indicated that **82** has a 'tub' conformation of D_{2d} symmetry. The 'tub' structure was confirmed by X-ray diffraction. The carbon-carbon single bonds are 1.54 Å and the double bonds 1.34 Å in cyclooctatetraene, which is thus non-aromatic. The molecule is not planar but rather tub-shaped despite the sp^2 hybridization feature of all the carbons, and as a consequence, the molecule is highly reactive like a polyene.

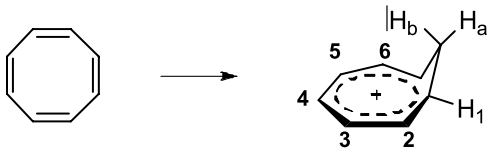
Cyclooctatetraene **82** can undergo single or double electron transfer to form the anion radical **80a** or dianion **80** (Scheme **21**). The anion radical shows paramagnetic features, e.g. a nine-line ESR spectrum with a hyperfine splitting constant of α_H = 3.209 gauss at -84°C.[190] The interpretation of this is that the one electron couples to eight equivalent protons, indicating the planar feature of D_{8h} symmetry. The COT dianion has a planar framework and satisfies the Hückel (4n+2)π rule. It is worth emphasizing that, in the NMR spectra, the protons resonate coincidently at δ 5.7 for both the COT **82** and the corresponding dianion **80**.[191] The interpretation of this surprising observation is that the deshielding effect of the ring current and the shielding effect of the double negative charge cancel each other. A double negative charge distributed over eight carbon atoms

will cause a shielding of the protons by *ca*. 2.5 ppm (in THF). It can then be concluded that deshielding due to the aromatic ring current is quite substantial.

Practically the addition of the first electron to COT is the more difficult because the molecule must flatten. The transformation was achieved by reacting cyclooctatetraene with potassium by Katz[191] in 1960. An important procedure was established by Evans[192] in 1981.

Cyclooctatetraene dianion **80** can react as both a reducing agent and as a nucleophile and is of interest as a planar aromatic ion for use as a ligand in transition, lanthanide and actinide metal complexes. The metal complex, cyclooctatetraeneuranium (IV) $(C_8H_8)_2U$, (uranocene) was prepared from $K_2C_8H_8$ by Streitwieser.[193] X-ray crystallographic analysis for the uranium complex $(C_8H_8)_2U$ demonstrated a D_{8h} symmetric structure with two planar, eclipsed C_8H_8 rings.

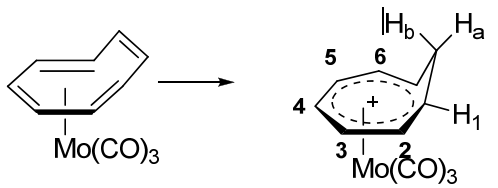
Protonation of cyclooctatetraene **82** with concentrated sulphuric acid give rise to $C_8H_9^+$ **83**,[194] a classic homo-tropylium cation. The $C_8H_9^+SbCl_5^-$ salt can be accessed by



82 **83**

H_a	5.10
H_b	-0.67
H-1	6.42
H-2-6	8.50

replacing the sulphuric acid with HCl and $SbCl_5$. Note that in the ^1H NMR spectrum a single resonance at δ 5.69 was found for the protons in the non-aromatic cyclooctatetraene **82**, while that for the cation **83** revealed a 5:2:1:1 integration pattern. The chemical shift difference for H_a at δ 5.10 and H_b at δ -0.67 indicated the marked anisotropic effect of the resulting ring current excluding a possible flat planar structure. The chemical shift δ 8.50 for the peripheral protons of **83** arises from the deshielding by the ring current but not to the extent of **15**. The long-wavelength absorption maximum λ_{max} was found at 313 nm in the ultraviolet spectrum for **83**, in contrast to the absorption maximum λ_{max} at 470 nm ($\varepsilon = 2.82\times10^5$) in the tropylium cation **15**.[195]



84 **85**

H_a	3.37
H_b	-0.15
H-1	4.27
H-2-6	6.00-6.50

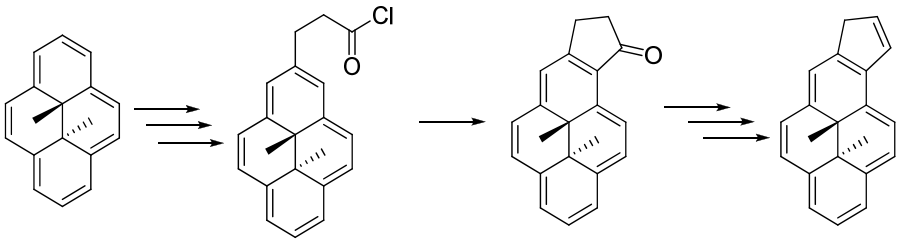
Scheme 22. The $C_8H_9^+$-derived 18e $C_8H_9Mo(CO)_3^+$ complex 85

π-Complexation of neutral C_8H_8 **82** to transition metals requires cooridination of a different number of π-electrons depending on the metal. For example, $Mo(CO)_3$ requires 6 electrons to form stable 18e complex $C_8H_8Mo(CO)_3$, e.g. **84** in Scheme **22**.[196] Such a complex can also be protonated to give rise to the charged 18e complex $C_8H_9Mo(CO)_3^+$ **85**(Scheme **22**). In the ^1H NMR spectrum the splitting pattern of **85** is similar to that of **83**. The two methylenic protons H_a and H_b appeared at δ 3.37 and H_b and δ -0.15 respectively. The marked chemical shifts difference of 3.5 ppm is strongly indicative of the diatropic nature of the C7 unit. Magnetically non-equivalent H_a and H_b are sitting in the shielding and deshielding zone of the C7 ring current. The peripheral protons are shifted to δ 6.0-6.5 due to the complexation to the molybdenum in contrast to δ 5.8 in the non-coordinated cation **83**. The NMR evidence supports the preference of a 6e electron donor feature of the cyclooctatetraene moiety in the cationic $C_8H_9Mo(CO)_3^+$ complex.

In this chapter, we are going to report the synthesis of the DHP[e]tropylium cation **18** and the DHP[e]COT dianion **121** and the investigation of the aromaticity of tropone, tropylium cation and COT dianion, and the homo-aromaticity properties on the cycloheptatriene and COT moieties. Future research would investigate their metal complex properties.

4.2 Results and discussion

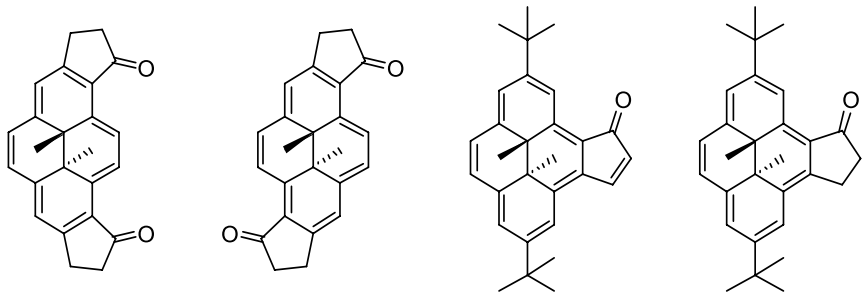
4.2.1 Synthesis of tropone-annelated DHP systems



1 **86** **87** **88**

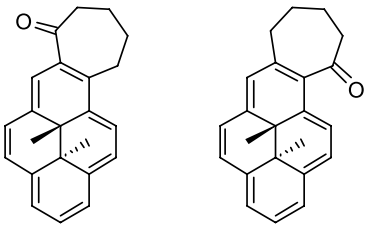
Scheme 23. Fusion of cyclopentanone 87 via Friedel-Crafts cyclization

Several strategies have been used in our group to fuse C5 and C6 membered rings onto the DHP framework 1. The earliest route by Khalifa[197] employed an intramolecular Friedel-Crafts cyclization via an acid chloride intermediate **86** as shown (Scheme **23**). The ketone **87** was then converted to the cyclopentadiene **88**.



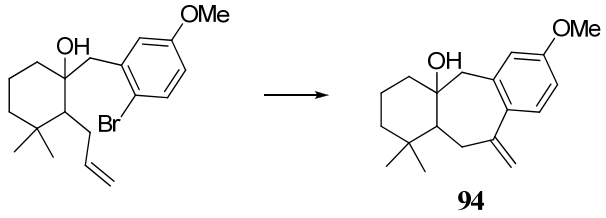
89 **90** **16** **91**

This cyclization was also successful for introducing two five-membered rings in compounds **89** and **90**.[198] A similar approach was used by Fan[56a] and Zhang[78] to synthesize [e]-fused Cp and fulvene derivatives via the ketones **16** and **91**.



92 **93**

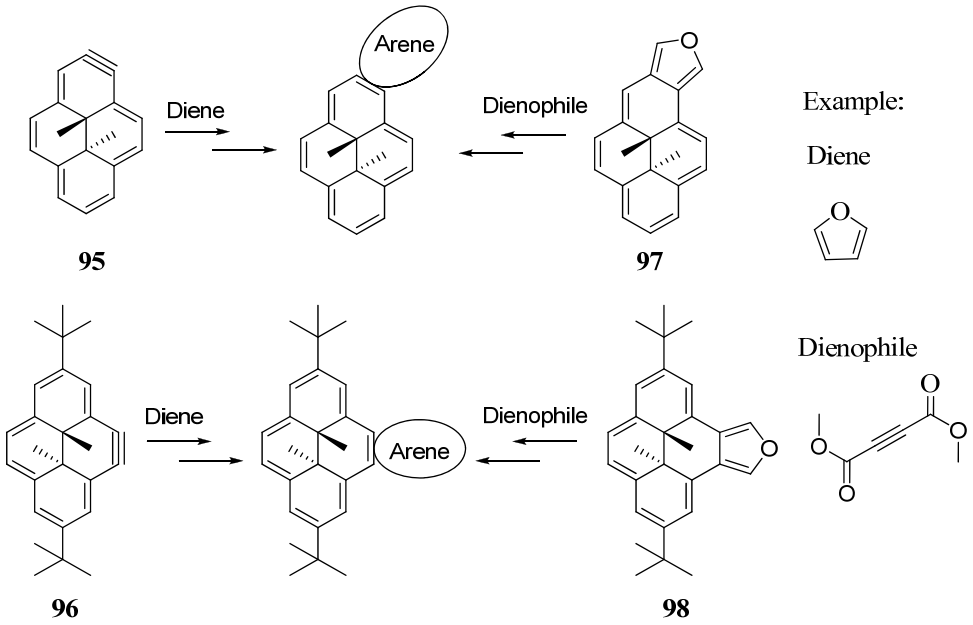
Cyclic C7 ketones **92** and **93**[199] have also been prepared via this route, though further transformations were not successful.



94

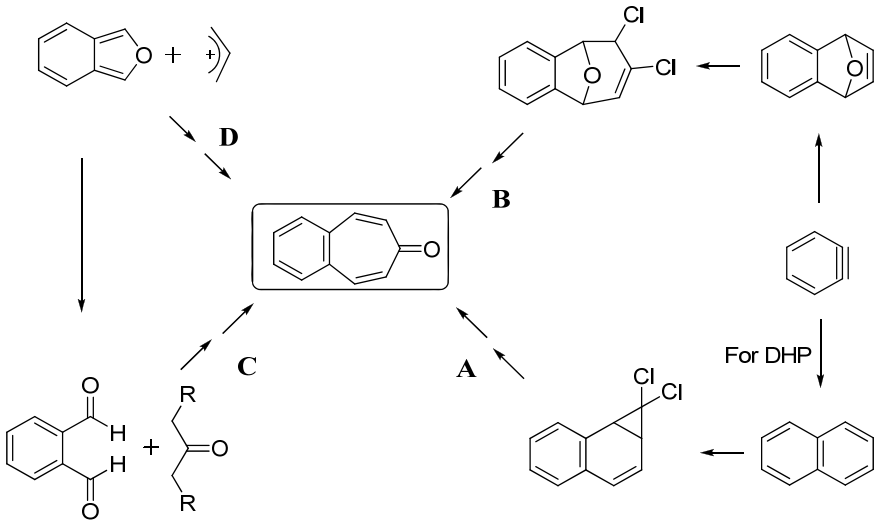
Scheme 24. The synthesis of (±)-faveline methyl ether through Mizoroki-Heck reaction

From the synthetic perspective, DHP behaves much like benzene, and so routes used to yield C7 systems-fused to benzene were considered. DHP halides are both accessible and have successfully been used in a variety of coupling reactions. Use of an intramolecular Heck-type coupling strategy might be possible for establishing a C7 ring system. Banerjee[200] utilized the Mizoroki-Heck reaction to make C7 rings in the synthesis of (±)-faveline methyl ether **94** in good yield (Scheme **24**). An alternate strategy was to attempt a cycloaddition reaction (Scheme **25**). Use of the benzynes **95** and **96** or the isofurans **97** and **98** in Diels-Alder reactions has been extremely successful for synthesis of a number of [a] and [e] arene annelated DHPs.[41, 201] Benzene, naphthalene, and anthracene annelated DHPs were typical examples. However, this protocol has only been used to prepare aromatic C6-fused DHP derivatives in the past. This success was largely due to the extra aromatic stability of the arene systems.



Scheme 25. Syntheses of fused-DHP derivatives by cycloaddition reactions

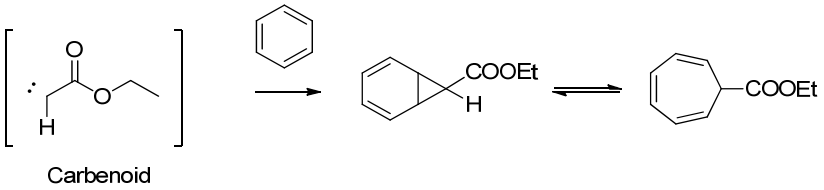
Whereas the Diels-Alder reaction has been widely used in construction of C6 systems starting with an isofuran or a benzyne intermediates, only a few cyclizations have been used to build fused C7 rings. Nevertheless, synthetic pathways towards a C7 ring system do exist, and for benzotropone are summarized below (Scheme **26**).



Scheme 26. Some selected synthetic pathways to benzotropone

They fall in two categories: ring expansion of a C6 ring with carbenes (route A and B) or a [4+3] cyclization of, for instance, benzoisofuran (route C) or benzodialdehyde (route D).

Active carbenes are able to insert into double bonds giving rise to cyclopropane intermediates, which rearrange to yield an expanded ring (Scheme **26**, route **A**). For example, the *Buchner reaction*,[202] reported by Buchner and Curtius in 1885, describes the expansion of benzene to a C7 heptatriene ring (Scheme **27**).



Scheme 27. The *Buchner reaction* in the preparation of a cycloheptatriene

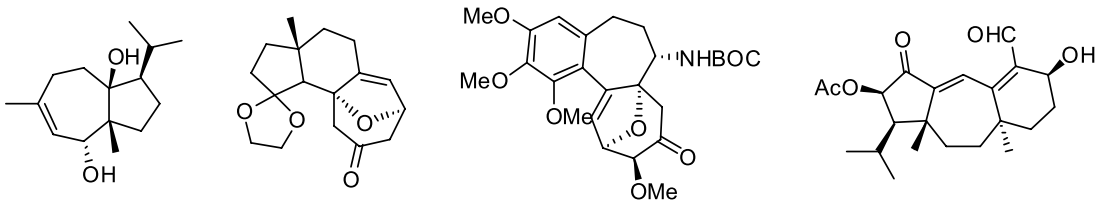
Ring enlargement by this [6+1] method became a convenient way to access tropones since Mosettig and Burger's first success in the smooth conversion of cyclohexanone to cycloheptanone by means of diazomethane in the 1930s.[203] More recently, simple parent cycloheptatrienes were reported to directly form from reactive carbenes and benzene.[204] Using rhodium catalysts has eliminated side reactions and increased yields.[205] Srivastava and Dev investigated the oxidation of benzocycloheptatriene to tropone in moderate yield with selenium dioxide.[206] Balci examined the oxidation of the corresponding heptatriene bromide with different oxidizing agents,[207] but the yields remain low. Use of the ring expansion strategy has been confined largely to symmetrical ketone substrates. For unsymmetrical ones, it leads to regiochemical control difficulties. For example, with DHPs several positions could be attacked.

In 1973, Battiste[208] reported a convenient four-step route to access benzotropone from a benzofuran adduct and a carbene via benzo-8-oxabicyclo[3,2,1]octa-2,5-dienes (Scheme **26**, route **B**) in about 50% overall yield. The drawback of this route might be its generality as it failed on the 8-oxabicyclo[3,2,1]octa-2,5-dienes.

The feasibility of [4+3] cyclization to afford a C7 system is well established. The early approaches utilized the aldol condensation strategy using C3 nucleophilic species (Scheme **26**, route **C**). Thiele and Schneider[209] reported the synthesis of benzotropone

from o-phthalaldehyde and acetonedicarboxylic esters in 1909. In the same manner, the naphthotropones were made from 2,3-diformylnaphthalene by Ried and Schwenecke in 1958.[210] An ortho-dialdehyde is needed to complete the transformation. However, dimethyldihydropyrene 4,5-dialdehyde cannot be accessed in a conventional way. Only recently did it become accessible using an unusual route in our hands. This approach was then used in the preparation of the diphenyl substituted tropone, described later in this thesis.

In contrast, processes involving electron rich diene and electron deficient allylic dienophile equivalents have been more extensively exploited in the last 20 years[211] (Scheme **26**, route **D**). Oxyallyl cations are generated from halo carbonyl derivatives through 1,3-elimination reactions, which are stable enough to engage in both intra- and intermolecular reactions. Cyclopropene can be utilized in place of the oxyallyl cation. The method was used in establishment of natural products and precursors including C7



(+/-)-Lasidiol
Föhlisch

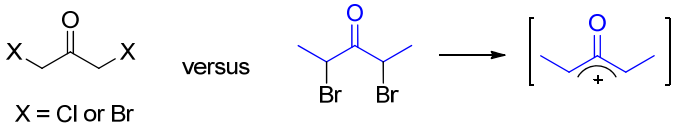
Cyathanes
Wright

Colchicines
Cha

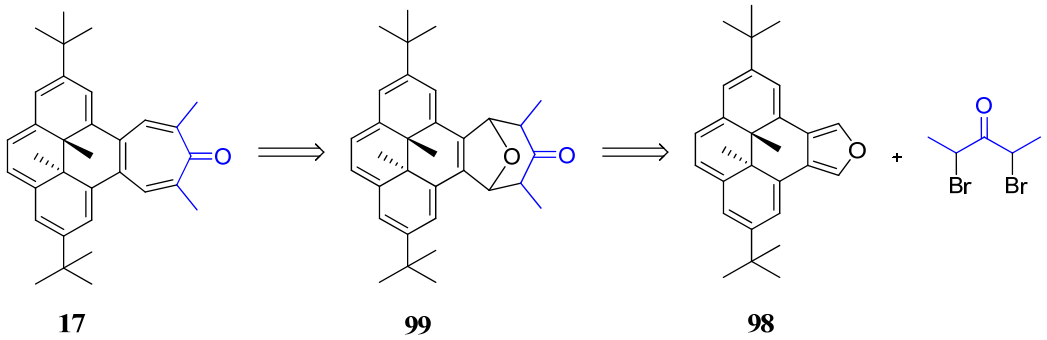
Guanacastepene
Wright/Battiste

rings, such as lasidiol,[212] cyathanes,[213] colchicines[214] and guanacastepene.[215]

Reactions involving the DHP isofuran **98** were extensively studied in our group. Choice of the right substituents in the α,α'-positions of the allylic precursors was crucial in getting good cyclization yields. Having methyl groups in this position enhanced the reactivity and minimized side products. Presumably the presence of methyl groups would not affect the outcomes in our later studies. So instead of 1,3-dibromoacetone, 2,4-dibromo-3-pentanone was used (Scheme **28**).



Scheme 28. The generation of the oxyallylic cation

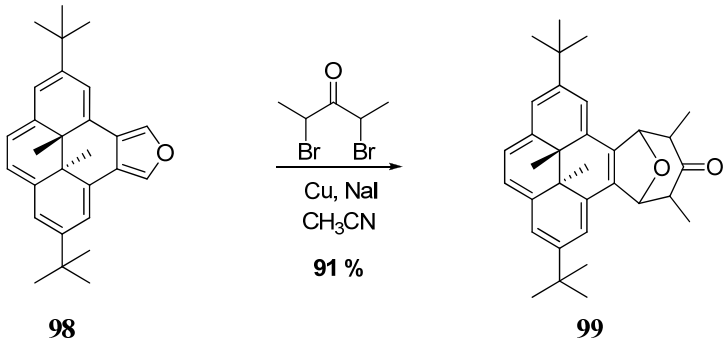


17 **99** **98**

Scheme 29. A retro-synthesis of DHP-fused tropone 17

Thus our plan was to use the DHP isofuran **98** and 2,4-dibromo-3-pentanone, to yield the DHP-fused dimethyl substituted tropone **17** via a [4+3] cycloaddition reaction (Scheme **29**).

The synthesis of tropone 17 via a [4+3] cycloaddition product 99



98 **99**

Scheme 30. The synthesis of a DHP-tropone precursor 99, via a [4+3] cycloaddtion reaction

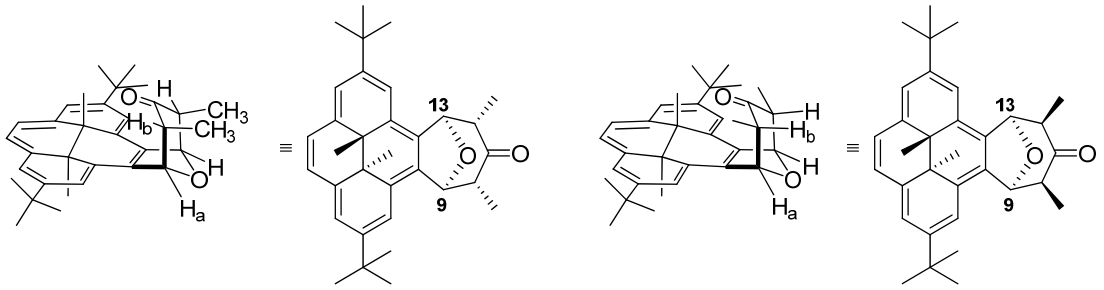
The synthesis of the oxyallylic cation was adapted from Klein's procedure,[216] using 2,4-dibromo-3-pentanone with copper powder and sodium iodide and *in situ* cycloaddition with the DHP isofuran **98** to afford two pairs of enantiomers **99A** and **99B**

in 77% yield. The replacement of the purple color of the isofuran **98** with green indicated the completion of the reaction. However, partial conversion was encountered in several trials even with elongated reaction time. The halide was filtered through a basic alumina plug to remove any accumulated acid from decomposition because the furan is moderately acid sensitive.

Two diastereomers of **99** were obtained in a 2:3 ratio (least polar: more polar). They were separated by chromatography. The isomers in the early fractions were designated as isomer **99A** and the later fraction as isomer **99B**. The skeletons of both were established by NMR spectroscopy, and by X-ray crystallography for **99B**. In the ^{1}H NMR spectra, two peaks in each product were found for the internal methyl protons, shifted upfield by 0.8 ppm from the isofuran **98** to between δ -3.6 and δ -3.8. The identity of isomer **99A** was also confirmed by HRMS (found 468.3019; calculated for $C_{33}H_{40}O_2$: 468.3028). Elemental analysis was obtained for isomer **99B**. Infrared spectra of the isomers showed diagnostic CO stretch frequencies at 1704 cm^{-1} for isomer **99A** and 1705 cm^{-1} for isomer **99B**. The O-C bond stretches were at 1065 cm^{-1} and 1043 cm^{-1} in isomers **99A** and **99B**, respectively.

The stereochemistry of the isomers was elucidated from the NMR spectra, X-ray structure and PC-model calculations. Four chiral carbon centers were generated in this reaction. For a concerted reaction, the relative positions of methyl to the bridge oxygen need to be addressed. For this, the vicinal coupling constants in the ^{1}H NMR spectra were used. The $^{3}J_{H\text{-}H}$ coupling constants for H_a and H_b in Figure **33** were 0 Hz in isomer **99A** and 4.7 Hz in isomer **99B**. According to the Karplus equations, $^{3}J_{ab} = J^{0}\cos^{2}\phi - 0.28$ ($0^{o} < \phi < 90^{o}$) and $^{3}J_{ab} = J^{180}\cos^{2}\phi - 0.28$ ($90^{o} < \phi < 180^{o}$) (where $J^{0} = 8.5$ and $J^{180} = 9.5$ are constants depending on the substituents on the carbon atoms) the coupling constants J are dependent upon the dihedral angle ϕ. Based on the coupling constant data, the dihedral angles are calculated to be 79.5^{o} ($^{3}J_{H\text{-}H}$ = 0 Hz) and 40.0^{o} ($^{3}J_{H\text{-}H}$ = 4.7 Hz) in isomers **99A** and **99B**, respectively. They must be acute here rather than obtuse because of rotation restrictions of the ring. PC model calculations showed the two minimum energy forms, having in isomer **99A** a torsion angle of 57^{o} (J = 3.8 Hz) with the methyls in the equatorial positions, and in isomer **99B** 74-76^{o} (J = 0 Hz) in the axial positions (Figure **33**). Therefore the configurations of isomer **99A** and isomer **99B** are depicted below. The

stereochemistry of isomer **99B** was also established by an X-ray structure to be discussed later. The torsion angles of H_a and H_b were 67.4(2)º and 63.8(2)º for **99B** in solid state (Figure **33**).



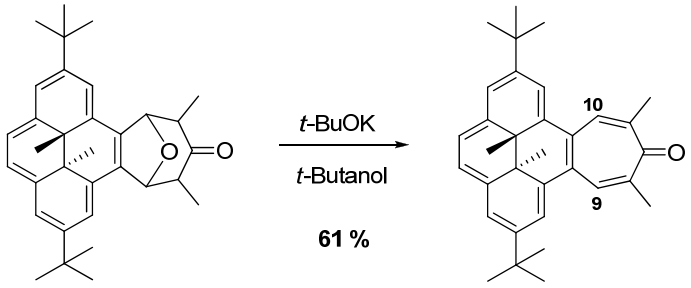
99A **99B**

Figure 33. The side perspective of the isomers 99A and 99B

Each isomer consisted of a pair of enantiomers because attachment could occur on either face of the isofuran **98**. It can be concluded that a concerted cyclization reaction occurred between the highly reactive electron deficient electrophiles and the very electron rich isofurans since only these two isomers were obtained.

The protons of the two internal methyl groups of each isomer show different chemical shifts: δ -3.62/-3.84 for isomer **99A** and δ -3.75/-3.78 for isomer **99B**. The former has the larger chemical shift difference of 0.22 ppm, while that of the latter is only 0.03 ppm. An explanation of this is due to the shielding effects of the carbonyl groups. The strength of the shielding effect is a consequence of the spatial position of the methyl in the carbonyl shielding cone. In isomer **99A**, the carbonyl is forced closer toward the internal methyl group by the two neighbouring methyl groups. The 4,5- protons on the opposite side of the DHP framework resonates as an AB system with coupling constants J = 8.1 and 7.8 Hz for isomers **99A** and **99B**, respectively. The explanation is the deformation of the DHP skeleton. Protons H-9 and H-13 were determined on the basis of their correlations to vicinal protons on DHP in the NOESY spectra.

The synthesis of DHP-fused 2,7-dimethyltropone 17, as well as isomer 100 and unusual dione 101



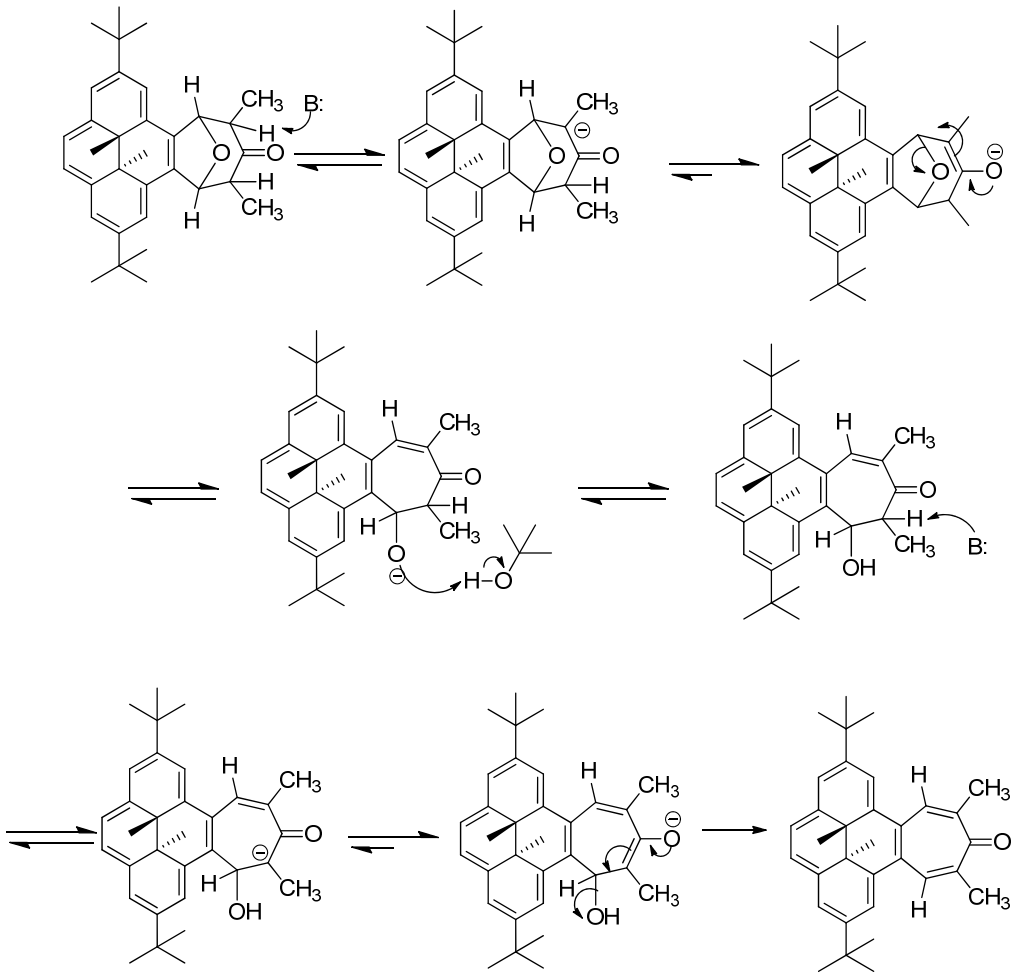
99 **17**

Scheme 31. The preparation of the DHP-fused 2,7-dimethyltropone 17

Elimination of water from **99** to give tropone **17** was achieved in good yields (61 %) using potassium *tert*-butoxide in *t*-butanol at 60 ^{o}C (Scheme **31**). The structural formula of $C_{33}H_{38}O$ for **17** was confirmed by HRMS (found: 450.2913; calculated: 450.2923). The NMR spectrum of DHP-fused 2,7-dimethyltropone **17** was characteristic of a C2 symmetric molecule. The ^{1}H NMR spectra showed a single resonance at δ -3.56 corresponding to the internal methyl protons, shifted from *ca.* δ -3.7 in the starting bicyclic **99A** and **99B**. The protons H-9,13 on the C7 ring at δ 9.27 were shifted from *ca.* δ 6.1 and 6.2 in **99A** and **99B**, respectively. The carbon of the conjugated carbonyl group resonated at δ 189.4, shifted upfield from δ 210 in the starting materials **99**. The diagnostic C=O double bond stretch was found at 1609 cm^{-1} in the infrared spectra and was consistent with that of the parent tropone (1634 cm^{-1}, neat)[217] with a characteristically lower frequency than for a conjugated ketone (*ca*. 1685 cm^{-1}). The lower frequency arose because of a contribution of its charge separated resonance structure. The crystal structural analysis for **17** will be discussed below.

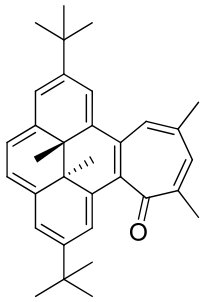
A possible mechanism for the formation of **17** is postulated in Scheme **30**. The mild base-catalyzed elimination of H_2O relies heavily on the acidity of the α-hydrogen. Having protic solvents such as alcohol is very important to force the equilibrium toward the

product side. Deprotonation of the α-protons of the ketone yielded an anion, which sequentially led to opening of the O-bridge and elimination of water.

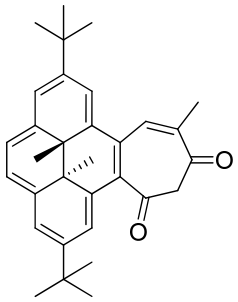


Scheme 32. Proposed mechanism for the formation of 4,5-DHP-tropone 17

Two side products containing DHP were also isolated from the ring-opening reaction, whose identities were assigned as the isomeric DHP[e]tropone **100** and dione **101** by means of NMR spectroscopy and mass spectrometric analysis.

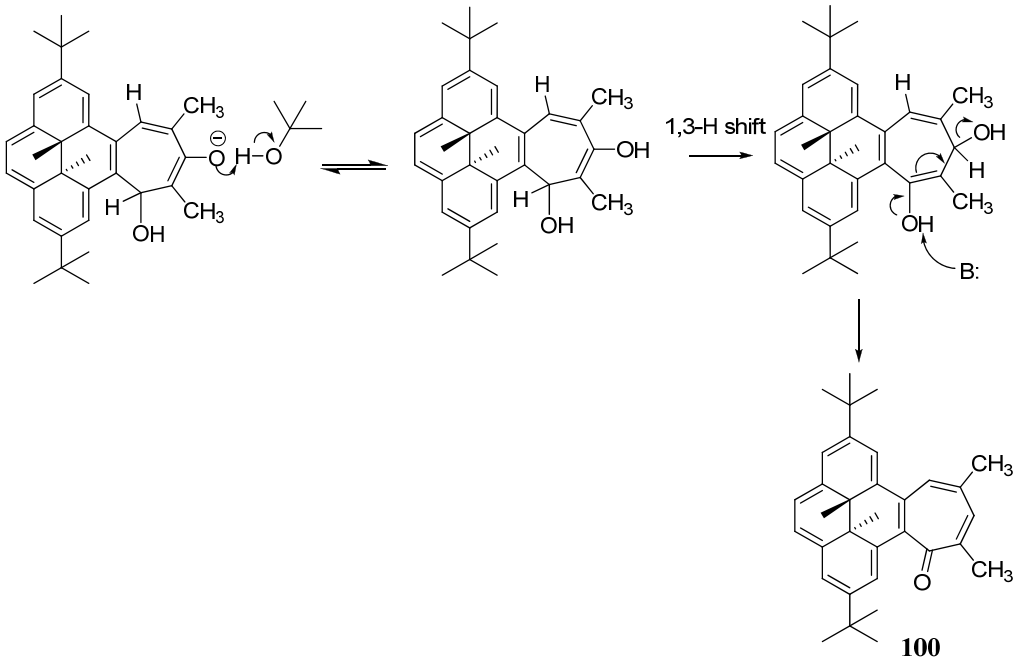


100



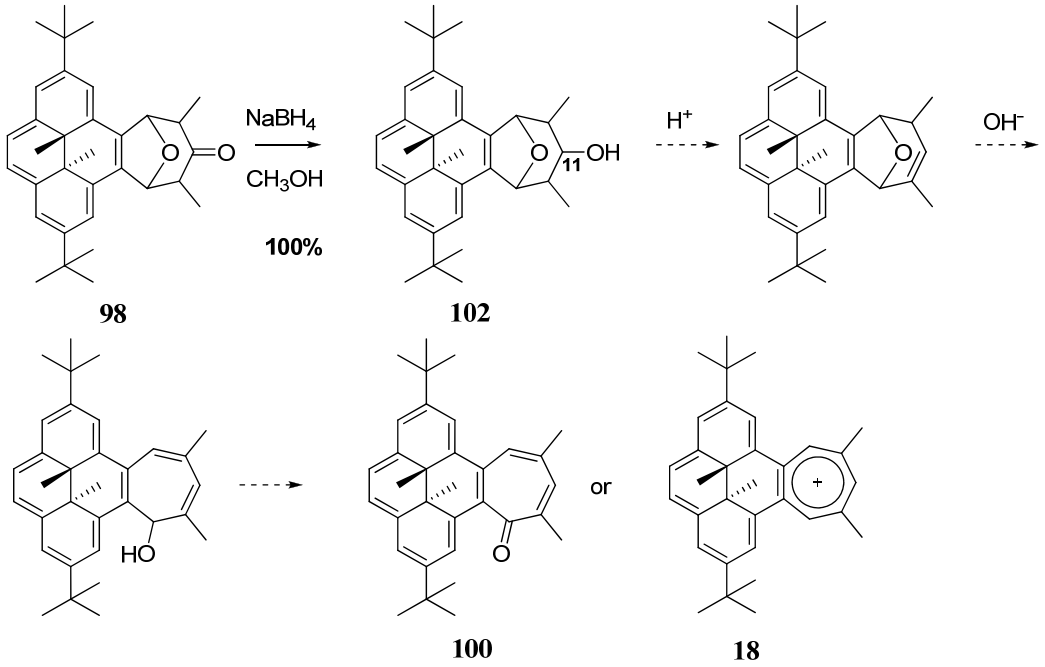
101

The formation of isomeric 5,7-dimethyltropone[e]DHP **100** was suggested by NMR spectroscopy. However the yield of **100** was very small and a pure sample was not separated. The NMR data for **100** was obtained by subtracting the tropone **17** from the ^{1}H NMR spectrum of the mixture. Two resonances for internal methyl protons of **100** at δ -3.74 and -3.76 were found. The 4,5-protons were an AB, with a coupling constant J = 8.2 Hz. Surprisingly, two olefinic protons on the C7 ring resonate closely at δ 5.78 and 5.79 and the corresponding carbons resonate at 82.03 and 81.19, respectively. These carbons were upfield considering their sp^2 hybridized olefinic nature. The carbonyl carbon resonated at δ 183.63, compared to the symmetrical one at δ 189.35. By optimizing the reaction condition, the formation of this isomer was mostly suppressed. No further analyses were carried out on this side product **100**.



Scheme 33. Proposed mechanism for the formation of isomeric 5,7-dimethyltropone[e]DHP 100

The isomeric 5,7-dimethyltropone[e]DHP **100** was probably formed via the route above (Scheme **33**). The elimination of the 11-OH group could possibly proceed through an antarafacial [1,3] hydride shift with base catalyst. Carpenter[218] reported that [1,3]-sigmatropic rearrangements were enhanced by having a potassium alkoxide substituent. It can be confidently concluded that the expulsion of the hydroxide was a slow step in the reaction because it was a poor leaving group.



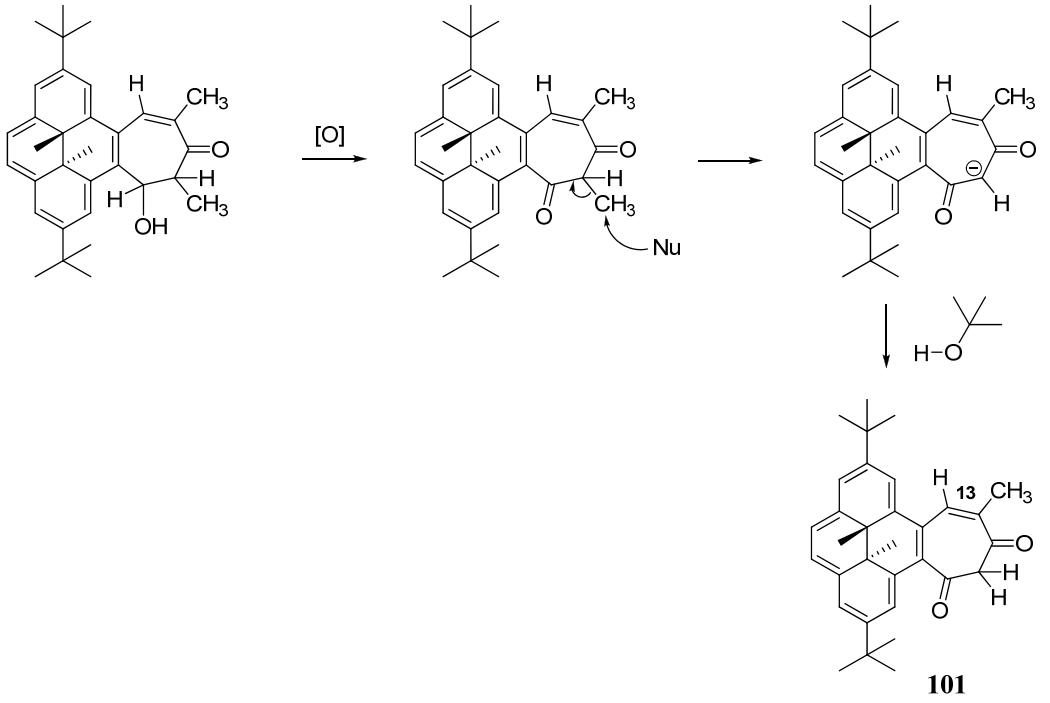
Scheme 34. The proposed route to 5,7-dimethyltropone[e]DHP 100 (as well as the cation 18)

5,7-dimethyltropone[e]DHP **100** is a very interesting compound in terms of photochromism because it resembles the acyl DHPs. In order to access 5,7-dimethyltropone[e]DHP **100** exclusively, an alternate synthetic route was designed (Scheme **34**). The isomers **99** were reduced to the alcohol **102** using $NaBH_4$ in methanol, which was then eliminated to introduce a double bond to the C7 ring. The allylic proton should be easy enough to deprotonate to open the cyclic ether ring. The resulting alcohol should be very useful, upon oxidation to the ketone **100**. Moreover it should lead to formation of the DHP[e]tropylium cation **18**.

The reduction to the alcohol **102** was performed in 100% yield (Scheme **34**). One single isomer was obtained by recrystallization of the products from DCM and hexanes. The H-11 was close to the internal methyl protons at δ -3.76 based on the correlation in the NOESY spectrum. Therefore the -OH group pointed away from the DHP, which left the small hydrogen in the pocket between the DHP and the C7 ring and satisfied the space requirement for the big -OH group (refer to Figure **33** on page **125**). The other

isomer should adopt the same configuration at the newly formed chirality center C-11. Compared with δ -4.06 in DHP 2, the protons on the other internal methyl group resonated at δ -3.96 indicating the negligible disturbance on the chemical shift by the fused C7 ring. Further transformations haven't been carried out due to the success in the elimination and ring opening using potassium *t*-butoxide in *t*-butanol (Scheme **31**).

There was also obtained a small amount of the dione **101**. Its identity was confirmed by both NMR spectroscopy and high resolution mass spectrometry (found 452.2712; calculated 452.2715). The methylene group was confirmed by two resonances at δ 4.69 and δ 4.08 (J = 11.9 Hz) in the ^{1}H NMR spectrum and one resonance at δ 63.02 in ^{13}C NMR spectrum, which showed as a negative peak in DEPT135 spectrum. The olefinic proton H-13 of **101** resonated at δ 8.57 and the corresponding sp^2 carbon resonated at δ 138.37. Only one methyl group on the C7 ring was identified at δ 2.24 in the ^{1}H NMR spectrum. Two carbonyl resonances were found at δ 195.86 and δ 190.06.

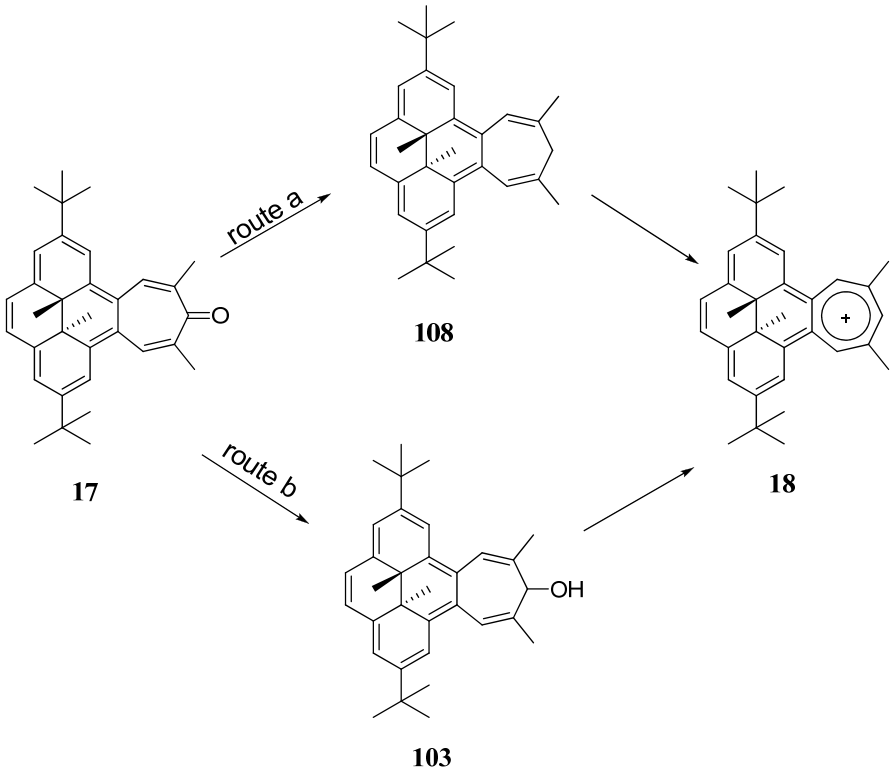


Scheme 35. Proposed mechanism for the formation of 4,5-dihydropyreno hept-6-en-1,3-dione 101

The unusual loss of the methyl group from **101** might happen as shown above (Scheme **35**). The alcohol intermediate was first oxidized to a dione intermediate (Scheme **35**). A nucleophile can remove the methyl group and leave the stable DHP-fused anion. The hypothesis is reasonable given that the anion is stabilized very well by two neighbouring carbonyl groups. The formation of this product was suppressed as the reaction conditions were optimized.

The preparation of DHP-fused tropylium cation 18

Having successfully obtained the tropone **17**, we began to explore conversions of this to the DHP-fused tropylium cation **18** (Scheme **36**).

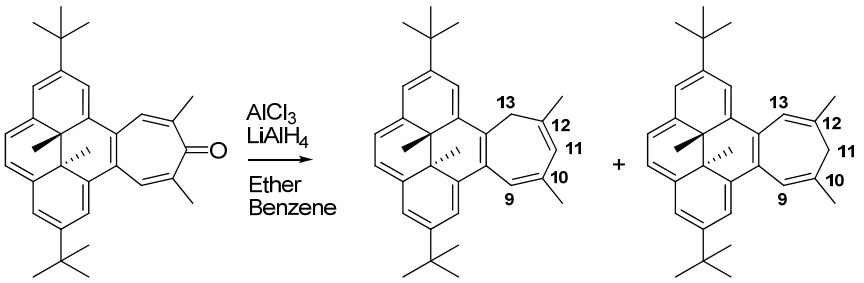


Scheme 36. Proposed reaction pathways towards DHP-annelated tropylium cation 18

The generation of the DHP tropylium cation were carried out using two strategies, namely hydride abstraction by trityl cation from a cycloheptatriene precursor (route **a** in Scheme **36**) or water elimination from a cycloheptatrienyl alcohol by an acid (route **b** in Scheme **36**). The former approach needed the synthesis of a DHP-fused unsaturated cycloheptatriene **108** and the latter could be realized via a DHP-annelated alcohol, such as **103**.

The preparation of DHP-fused cycloheptatrienes from the tropone 17

The strong reducing reagent AlH_3 ($LiAlH_4/AlCl_3$) reduced the carbonyl in **17** directly to a saturated methylene in 85% yield. Two isomeric products **107** and **108** were obtained with a ratio of *ca.* 5:1. They were isolated and the structures were separately verified by NMR spectroscopy. The major isomer **107** was eluted first from a column as a dark orange solid, mp 175-176 °C. The minor isomer **108**, mp 187-188ºC was eluted second. In the ^{1}H NMR spectra of isomer **107**, the internal methyl protons were observed as two peaks at δ -3.65 and δ -3.89, indicative of low symmetry (C1). The methylene protons H-13 resonated at δ 4.38 and δ 3.04 with a coupling constant of J = 12.4 Hz, in the range of typical geminal coupling constants. The olefinic proton H-9 resonated at δ 8.27, while H-11 was at δ 5.91. In its ^{13}C NMR spectra, the sp^2 olefinic C-9 and C11 were found at δ 126.48 and δ 124.44 respectively. The DEPT-135 spectrum of **107** indicated that the carbon C-13 at δ 35.55 was the saturated methylene carbon. An acceptable elemental analysis of **107** for carbon and hydrogen was obtained.



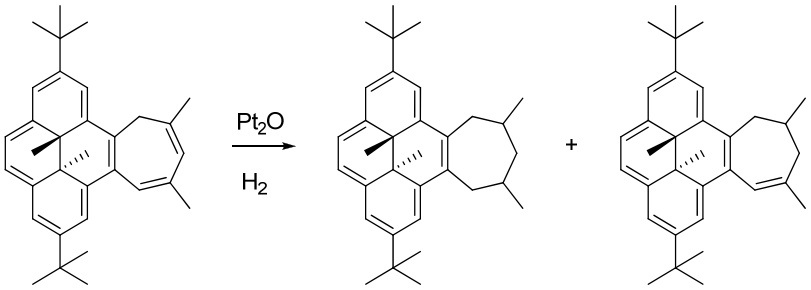
17 **107** **108**

Scheme 37. Reduction of tropone 17 with AlH_3

For isomer **108**, the NMR spectrum showed higher symmetry (C2) as the proton and carbon resonances paired up. In the ^{1}H NMR spectrum, a single resonance at δ -3.32 corresponds to the two identical internal methyl protons. The resonance for the two olefinic protons H-9,13 was shifted downfield to δ 7.46 and the methylene protons H-11 were a singlet at δ 2.53. The DEPT135 spectrum consisted of a negative CH_2 at δ 38.54 for C-11. The HRMS of **108** showed a parent mass at 436.3133 (calc: 436.3130), consistent with $C_{33}H_{40}$.

Reduction of cycloheptatrienes to 109 and 110

Because **110** would be used as a reference compound in the aromaticity caculations, the reduction of **107** was carried out. The cycloheptatriene **107** was reduced to **109** and **110** by hydrogen with a platinum catalyst. PtO_2 was first reduced to the active Pt catalyst by hydrogen in ethyl acetate before the addition of the starting material **107**. Because of the difficulty in controlling the extent of the reaction, products with both double bonds reduced, cycloheptene **109**, and one reduced, cycloheptadiene **110**, were obtained as a mixture with a 100% conversion of **107** (Scheme **38**).



107 **109** **110**

Scheme 38. Hydrogenation of CHT 107 to afford 109 and 110

The saturated **109** and non-saturated **110** formed in a 9:4 ratio were separated first and second on a preparative TLC plate. This ratio should only depend on the stoichiometric

ratio of hydrogen to the substrate **107**. In each, there were two sets of peaks for the internal methyl protons in their ^{1}H NMR spectra as a result of two isomers each (major: -3.97, -4.03 and minor: δ -3.98, -3.99 for **109**; Major: δ -3.83, -3.90 and minor δ -3.85, -3.88 for **110**). Note that in both **109** and **110**, the major isomers showed a larger chemical shifts difference than the minor ones for the internal methyl groups. But the average chemical shifts for both isomers were very close (**109**: δ 4.00 vs. -3.99 for major and minor isomer, respectively; **110**: δ -3.87 for both isomers). The ratio between the major and minor isomers was 5:1 in **109** and 4:1 in **110**. Theoretically there should exist six stereoisomers for **109**, and two for **110** (Scheme **34**). The explanation for the stereo selectivity might be due to the steric requirements of the Pt catalyst. We were unable to assign which isomers of **109** and **110** were the major isomers.

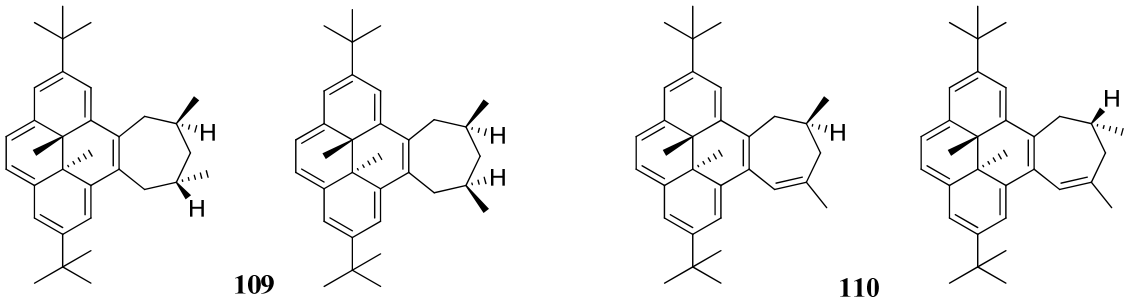
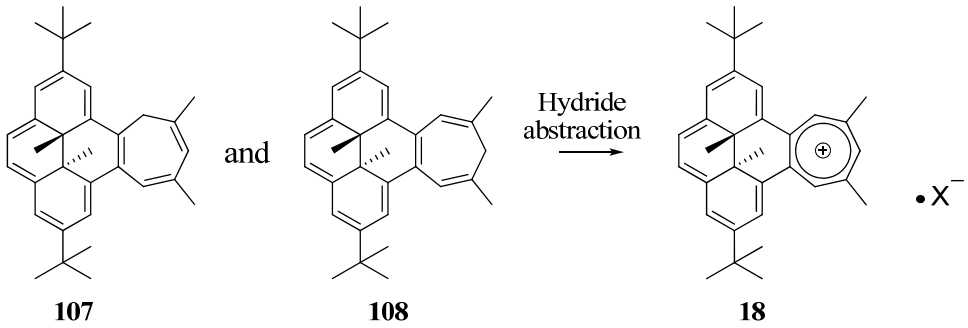


Figure 34. The stereoisomers for 109 and 110

The approach to DHP-annelated tropylium cation 18 from cycloheptatrienes 107 and 108

The hydride abstraction of **107** by trityl cation (Scheme **39**) produced a large amount of triphenylmethane by-product. In the ^{1}H NMR spectrum of the crude products, tiny peaks were found for the correct DHP tropylium compound **18** (X = PF_6) together with a large amount of triphenylmethane products. Literature preparations of trityl cations also reported low yields (approximately 10%). Reaction between 10 to 30 mg of **107** and trityl cation yielded less than 5 mg of product **18**. Other hydride abstraction reagents failed to give decent products.



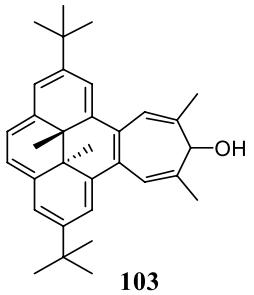
107 **108** **18**

Scheme 39. The attempt to prepare cation 18 via hydride abstraction

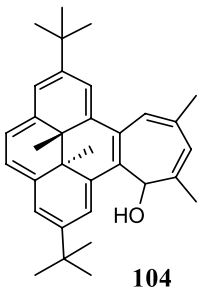
The approach to DHP-annelated tropylium cations 18 via hydride abstraction

(a) Reduction of the tropones 17 and 100 with $NaBH_4$ and $CeCl_3 \cdot 7H_2O$

When $NaBH_4$ and $CeCl_3 \cdot 7H_2O$ (Luche reduction[219]) were used to reduce tropones **17** and **100**, poor reproducibility was encountered. The reaction proceeded giving various products. In one case, the desired alcohol **103** was observed by NMR spectroscopy, together with the isomeric alcohol **104**. Because the starting materials consisted of the two isomeric tropones **17** and **100**, it might be concluded that alcohols **103** and **104** were the products of the corresponding ketone. The alcohols could not be separated from each other chromatographically. No further characterization was carried out on the second

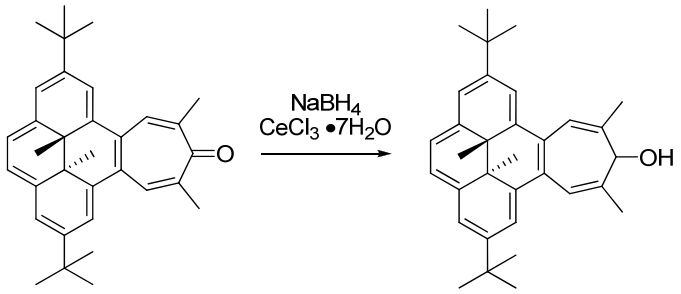


103



104

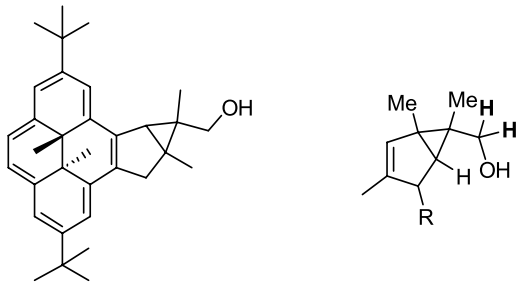
alcohol. The ratio of alcohol **103** to **104** is 3:1. Considering both alcohols should form the same tropylium cation products **18**, the mixture was used directly and no separation was carried out.



17 **103**

Scheme 40. Reduction of tropone 17 with $NaBH_4$ and $CeCl_3 \cdot 7H_2O$

Ring contraction of the C7 ring might also be occurring since there was good evidence that the bicyclo[3.1.0]hexene skeleton (compound **105**) was also obtained. The evidence for **105** was based on ^{1}H NMR spectroscopy. The chemical shifts of the DHP peripheral

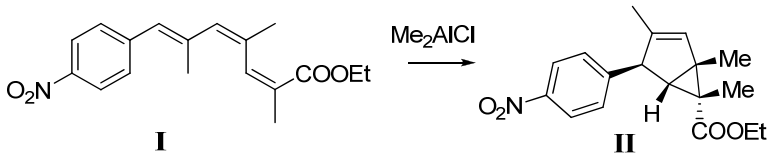


105 **106**

protons of **105** fell in the normal range and the protons of the two internal methyl groups resonated at δ -3.81 and -3.80. The assignment of structure **105** was completed by comparing the NMR data with a known compound **106** reported by Miller.[220] Two sets of methylene protons were found in the ^{1}H NMR spectrum at δ 4.35 and 4.26. Each had a geminal coupling constant of 21.4 Hz. The two protons at δ 3.97-3.93 and 3.89-3.85 were multiplets. The former corresponded to the methylenic carbon at δ 35.20 and the latter to the carbon at δ 67.38, and both appeared negative in the DEPT-135 spectrum. The values

were consistent with the assumption of a benzylic carbon and of a carbon with an OH substituent. The infrared spectrum showed a broad absorption at 3464 cm^{-1}, indicating its alcohol feature.

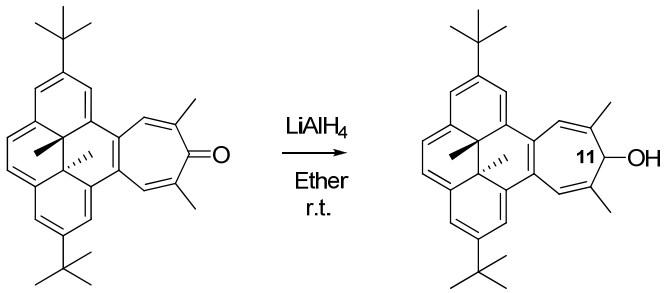
The possibility of formation of **105** was evident by a similar thermal cycloaddition by Miller[220] (Scheme **41**), in which the substituted hexatrienes **I** gave, on Lewis acid catalysis, **II** bearing a bicyclo[3.1.0]hexane core. Miller also obtained the relevant alcohol **106**, which has a structure comparable to our proposed **105**.



I **II**

Scheme 41. The transformation of hexatrienes to a bicyclo[3.1.0]hexane

(b) Reduction of the tropones 17 with $LiAlH_4$



17 **103**

Scheme 42. Reduction of tropone 17 to alcohol 103

Lithium aluminum hydride quantitatively reduced the tropone **17** to its corresponding alcohol **103** in dry ether at room temperature, but some decomposition occurred during work-up. The alcohol **103** was purified by chromatography on deactived alumina with dichloromethane as eluant. The identity of the alcohol was confirmed by NMR

spectroscopy. The product lost the C2 symmetry of the starting tropone **17** so that each proton and carbon signal appeared differently in the NMR spectra. The success of the reduction was evident from the loss of the C=O stretch at 1609 cm^{-1} in **17** and appearance of an OH stretch at 3500 cm^{-1} in the IR spectrum of **103**. In the ^{1}H NMR spectrum, two unique internal methyls resonated differently at δ -3.24 and δ -3.31, shifted downfield from δ -3.56 in tropone **17**. This downfield shift may be because the C-O bond has less covalent character and tends towards an ionic bond which puts partial positive charge on the C7 ring. The proton H-11 of the C7 ring resonates at δ 4.35 and is coupled to the acidic OH proton, J = 5.0 Hz. The ^{13}C NMR spectrum saw the disappearance of the quaternary carbonyl carbon resonance and the appearance of the new methine signal at δ 73.19 for C-11 of the C7 ring. The structural formula of **103** $C_{33}H_{40}O$ was confirmed by HRMS (found, 452.3080; calculated, 452.3079).

When 48% aqueous tetrafluoroboric acid was added into a solution of the alcohol in an appropriate organic solvent (benzene, chloroform, THF etc.), the orange color turned red. The formation of cation **18**$\cdot BF_4^-$ was confirmed by both NMR spectroscopy and electron spray mass spectrometry. In the ^{1}H NMR spectra (Figure 35), the internal methyl protons of **18** resonated at δ -2.61 in C_6D_6 as a singlet, in contrast to two signals at δ -3.24 and -3.21 for the alcohol **103**. The protons of the tropylium cation moiety were found at δ 9.78 (H-9,13) and at δ 8.30 (H-11), deshielded by the delocalized positive charge and the aromatic tropylium moiety. The carbons (C-9,10,11,12 and 13) on the tropylium cation **18** resonated at low field in the range of δ 140-150, again due to the deshielding effects of the positive charge.

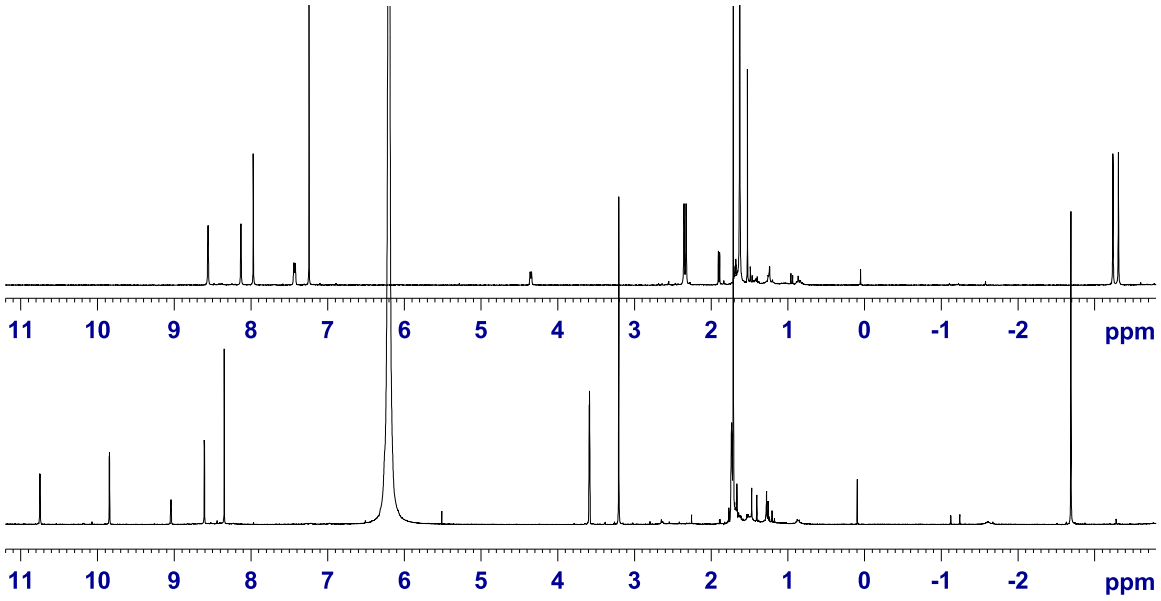
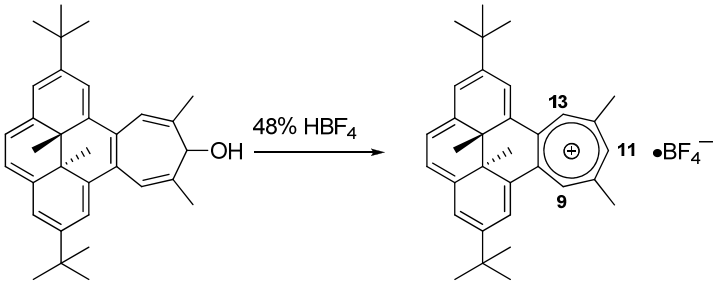


Figure 35. **A comparison of the ^{1}H NMR spectra of tropylium cation 18 (lower) and alcohol 103 (upper)**



103 **18**

Scheme 43. **The generation of cation 18·BF_4^- with aqueous HBF_4 acid**

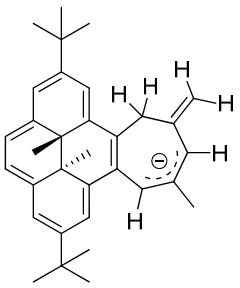
The acid catalyzed elimination towards **18**·Cl^- was first carried out using hydrogen chloride in ether. The quality of the acid solution appeared critical. An ether solution of the alcohol was added to a residual of an old bottle of HCl-ether to afford a nice red crystalline solid. However, a new bottle of this reagent from the same company has never given any products, except for decomposition products of the alcohol **103**.

The ^{1}H NMR for cation **18** was obtained with two different counter anions, namely chloride and BF_4^-. In both cases, decomposition of the cation **18** in deuterated acetone solution occurred during an overnight NMR experiment. The chemical shifts of the internal methyl protons vary somewhat with solvents as illustrated in Table **14**, which also gives the solvent dielectric constants.

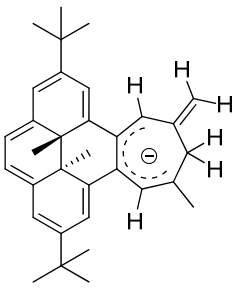
Table 14. Protons chemical shifts of the internal methyl resonance for 18·BF_4^- in solutions with different dielectric constants

Solvents	Benzene	$CDCl_3$	THF	Acetone
Dielectric constants	2.3	4.8	7.6	20.7
δ (PPM)	-2.62	-2.79	-2.69	-2.74

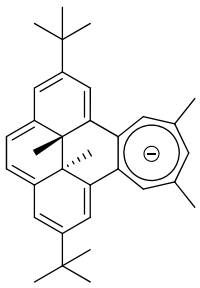
The preparation of the anions 111, 112 and 19



111



112

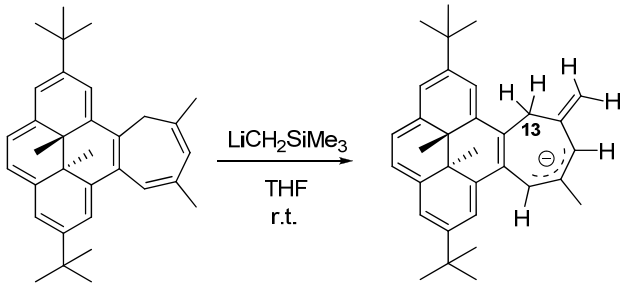


19

(a) Anion 111 from isomeric CHT 107

In a glovebox, asymmetrical CHT **107** was treated with trimethylsilylmethyl lithium at room temperature and gave the dark blue anion **111** (Scheme **44**). The deprotonation

occurred specifically on the methyl group next to the CH_2 in the C7 ring, yielding a single anion **111**. The structure of **111** was verified with NMR spectroscopy. In the ^1H NMR spectra, the methylene protons H-13 in the C7 ring were observed as doublets at δ 3.58 and δ 1.97 with a geminal coupling constant, J = 11.5 Hz. The terminal olefinic protons $=CH_2$ resonated at δ 4.66 and δ 4.28 with a geminal coupling constant, J = 3.0 Hz. All DHP peripheral protons moved upfield by about 1 ppm to 6.9-8.2 ppm from the neutral starting compound **107**. The chemical shifts of the internal methyls in **111** moved downfield compared with the starting compound **107** by more than 1 ppm to δ -2.52 and -2.67. The negative charge appeared to be mainly localized on an allylic skeletal moiety. Clearly the 1 ppm shift of the DHP protons indicated some interaction of the conjugated allylic anion with the DHP ring. The explanation for the limited charge delocalization in the C7 ring was due to its possible geometrical non-planarity with the DHP framework. The DEPT135 spectra revealed two methylene carbons at δ 96.55 ($=CH_2$) and δ 40.30 for C-13.



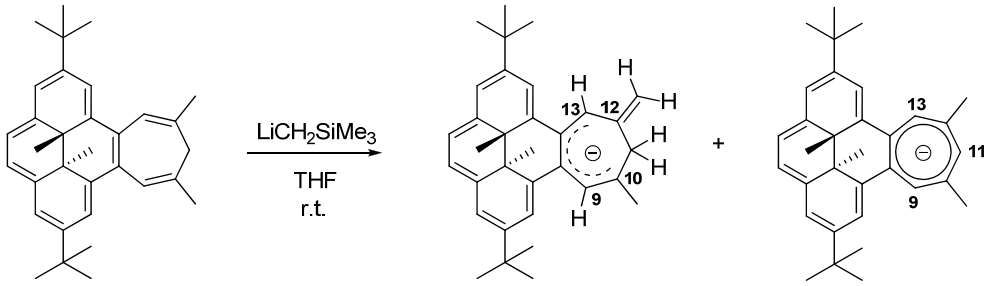
107 **111**

Scheme 44. The generation of the anion 111 from asymmetrical CHT 107

(b) Anions 112 and 19 from 108

For the symmetrical isomer **108**, the competitive deprotonation occurred at both the methyl and methylene groups to give anion **112** and **19** in a 3:2 ratio by ^1H NMR spectroscopy at room temperature (Scheme **45**). These isomers were not separated due to the small amount obtained. However, the data for each could be extracted because of the

unequal amounts of the two anions. As well, the anion **112** had similar spectra to anion **111**, as might be expected given the similarity in their structures.



108 **112** **19**

Scheme 45. The preparation of the anions 112 and 19 from the symmetrical CHT 108

The identification of anion **112** was confirmed by NMR spectroscopy. In the ^{1}H NMR spectrum, the internal methyl protons resonated at δ -0.80 and -0.84 in comparison with δ -3.32 in the neutral symmetrical DHP cycloheptatriene **108**. The peripheral protons of DHP in **112** appeared considerately shielded (from those of **111**) at δ 5.9-7.3. In the anion **112** greater delocalization occurred to include the DHP framework. The H-11 in the C7 ring was identified as resonances at δ 2.65 and 2.27 with a geminal coupling constant of 11.0 Hz. The terminal olefinic protons H-14 were found at δ 4.18 and δ 3.53 with a geminal coupling constant of J = 2.8 Hz. The ^{13}C NMR spectra demonstrated two methylene carbons at δ 91.24 and δ 43.25 from C-14 and C-11, respectively, consistent with their terminal olefinic and saturated secondary carbon character.

The identification of anion **19** was verified by its highly symmetrical character in the NMR spectra. The peripheral protons on the DHP paired up in the chemical shifts range between δ 4.9 and δ 5.5 in the ^{1}H NMR spectra as a result of the two-fold axes symmetry. H-9 and H-13 on the C7 ring showed together as a singlet at δ 3.0, while H-11 at δ 2.9 integrated to one proton, supporting removal of one proton. The internal methyl protons resonances were at δ 2.10 indicating no shielding effects at all. In the ^{13}C NMR spectra,

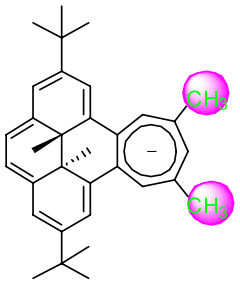
C-9 and C-13 in the C7 ring were found at δ 107.59 and C-11 at δ 111.11. It can thus be concluded that a hydride was removed from the C7 moiety. Clearly anion **19** had very different NMR properties from **112**. In the next section we will discuss the paratropicity of this anion.

Thermodynamic and kinetic products

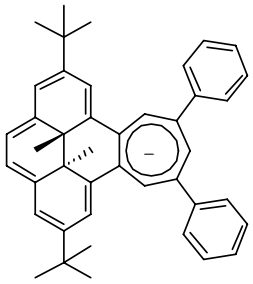
When solutions of both reactants were made and frozen before mixing, the reaction occurred at below room temperature. The deprotonation then took place less on the C7 ring, giving rise to a higher proportion of anion **112**. The ratio of **112**:**19** at -25 ºC was measured as 4:1 by NMR spectroscopy, in contrast to 3:2 at 25 ºC.

Attempts to prepare the diphenyl cycloheptatrienyl anion 113

In order to eliminate the deprotonation of the methyl protons on the C7 ring, the phenyl substituted CHT **117** and **118** were prepared. It was expected that the phenyl substituted analogs of anions **111** and **112** would not form at all. It is worth emphasizing



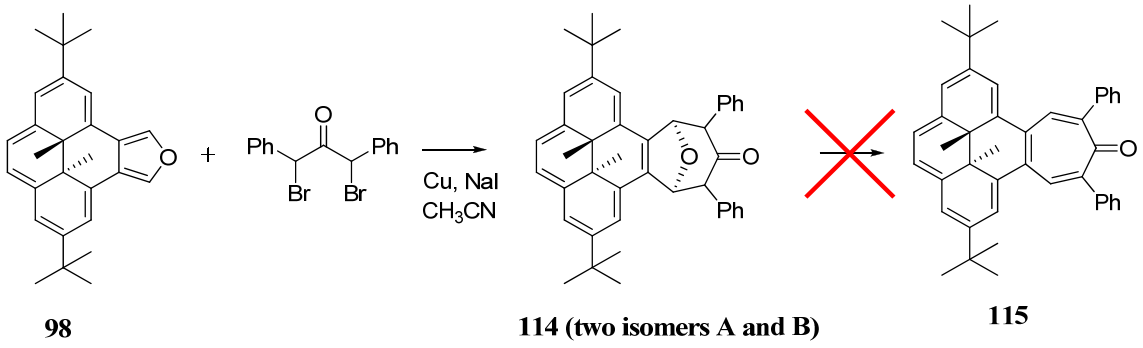
19



113

that both substituted cycloheptatrienes **117** and **118** would presumably give only the anion **113**.

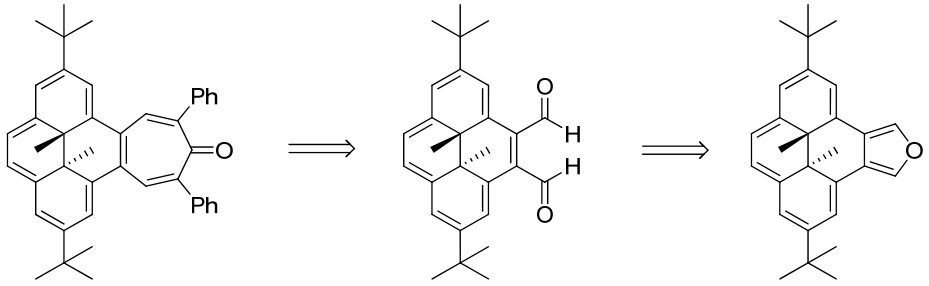
Similarly to the methyl substituted **99**, two isomers of diphenyl substituted oxo-oxa-bicycloocten[e]DHP **114** were obtained via a [4+3] cycloaddtion reaction in good yield (65 % for two isomers) (Scheme **46**).



Scheme 46. The synthesis of the diphenyl tropone direct from isofuran 98

Two groups of green isomers were isolated chromatographically that differed in the stereochemistry of the phenyl groups (*syn* or *anti*). The early fraction was assigned as **114A** and the later isomer **114B** and their identities verified by NMR spectroscopy. In the ^{1}H NMR spectra, the two internal methyl groups resonated differently at δ -3.88 and -4.03 for isomer **114A**, and δ -3.61 and -4.11 for isomer **114B**. In isomer **114A**, the incorporation of a side-fused bicyclic structure was affirmed by having protons on the C7 skeleton at δ 6.87 as a singlet for the DHP vicinal protons H-9,13 and two singlets at δ 4.25 and 4.04 for H-10,12. In the contrast, in isomer **114B**, doublets were found for the corresponding protons at δ 6.45 and 6.38 and δ 4.93 and 4.85 with coupling constants of J = 5.0 Hz. The 0 and 5 Hz coupling constants of adjacent protons matched those observed in the methyl substituted compounds **99A** and **99B** and suggested that **114A** and **114B** are the *anti* and *syn* isomers, respectively. Both isomers showed carbonyl stretching frequencies of 1714 cm^{-1}. The HRMS measurement was in agreement with the formula $C_{43}H_{44}O_2$ (found, 592.3339; calculated, 592.3341). However, all attempts to eliminate water from **114** failed to give tropone **115**.

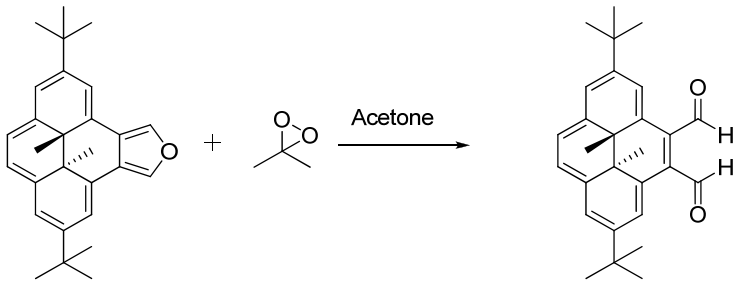
An alternate approach to diphenyl cycloheptatrienyl anion 113



115 **116** **98**

Scheme 47. The approach to the diphenyl tropone 115 via dialdehyde 116

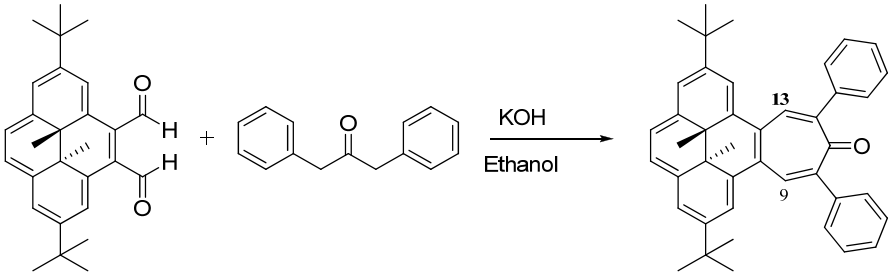
The previous cyclization utilized the electron rich C4 diene **98** and electron deficient C3 oxyallylic cation. It should also be possible to use synthons with electrophilic C4 moieties and nucleophilic C3 fragments, as mentioned previously in Scheme **26**. Since the ortho-DHP dialdehyde **116** is available (see below), a double aldol condensation should give the C7 ring (Scheme **47**). Dialdehyde **116** was synthesized from the DHP isofuran **98** in excellent yield.



98 **116**

Scheme 48. The synthesis of DHP dialdehyde 116

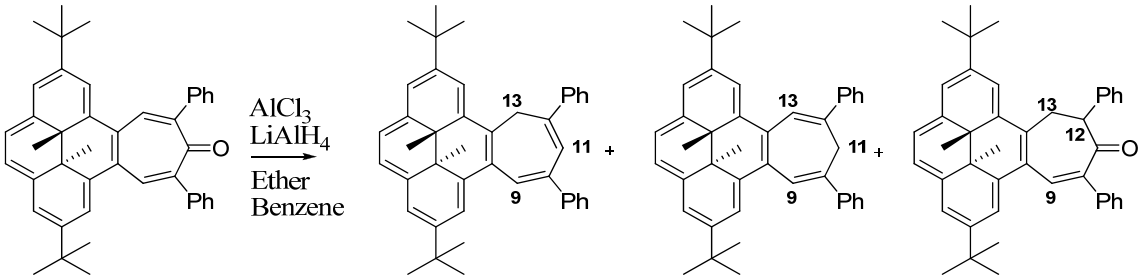
The DHP 4,5-dialdehyde **116** is a very important reaction intermediate, in which two aldehyde functional groups are on the same side of a DHP molecule. It is usually difficult to directly introduce two functional groups on the same side of the DHP molecule. Compound **116** was isolated as a side product by Robinson.[131] Its formation was rationalized as oxidative ring opening of the DHP isofuran in long time reactions by the trace amount of oxygen present. When the isofuran **98** was oxidized in $CHCl_3$ with 30% H_2O_2 solution, no reaction took place and the starting material was recovered. However, we found freshly made dimethyldioxirane[221] oxidatively opened[222] the DHP isofuran **98** to the dialdehyde **116** in 77% yield. The physical data for the dialdehyde **116** were in agreement with those reported by Robinson.[131]



116 **115**

Scheme 49. The synthesis of the DHP-fused diphenyl tropone 115

Aldol condensation of DHP dialdehyde **116** and 1,3-diphenylacetone gave the tropone **115** in 70% yield as a pale solid (Scheme **49**). Its identity was confirmed by NMR spectroscopy. The internal methyl protons for **115** resonated at δ -3.58 as a single peak in the ^{1}H spectrum. The olefinic protons H-9 and H-13 in the C7 moiety were found at δ 9.22, which was comparable with the δ 9.27 resonance in the methyl substituted tropone analog **17**. The carbonyl carbon C-11 of **116** was found at δ 193.55 in the ^{13}C spectrum. The C=O stretch frequency was 1666 cm^{-1} in the infrared spectrum. The HRMS results confirmed the identity of tropone **116** (found: 574.3239; calculated: 574.3236 for $C_{43}H_{42}O$).



115 **117** **118** **119**

Scheme 50. The reduction of the DHP-fused diphenyl tropone 115 with AlH_3

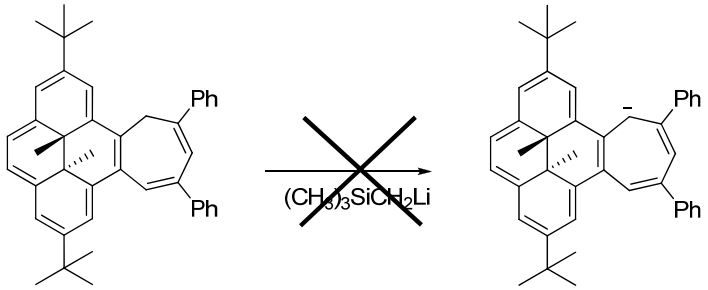
As observed for the methyl substituted tropone **17**, $LiAlH_4$ and $AlCl_3$ efficiently reduced the C=O group in tropone **115** to a CH_2 in 87% yield (Scheme **50**). Two isomeric products **117** and **118** were formed in a ratio of 93:7. In addition, the ketone **119**, in which reduction of one C=C double bond occurred, was obtained in 3% yield. All three isomers **117**, **118** and **119** were separated by chromatography. The unsymmetrical heptatriene **117** eluted first, followed by the symmetrical heptatriene **118** and finally by the ketone **119**. Preparatively, **117** and **118** were not separated and were used in the next step directly.

The identities of the unsymmetrical heptatriene **117** and symmetrical heptatriene **118** were confirmed by the disappearance of the diagnostic carbonyl stretch at 1666 cm^{-1} for tropone **115** in the IR spectrum and by NMR spectroscopy. In the ^1H NMR spectrum, the internal methyl protons resonated at δ -3.62 and δ -3.93 for isomer **117**, in contrast to a single resonance at δ -3.58 for tropone **115**. In isomer **117**, a singlet for the olefinic proton H-11 appeared at δ 6.73. Broadened peaks associated with the methylene protons H-13 were also found at δ 3.58 and 2.48. These resonances sharpened at low *and* high temperatures as illustrated in Figure **45** (see section 4.3.1 below). In the ^{13}C spectrum for **117**, the methylene carbon was found at δ 30.82.

The reduction of one double bond of tropone **115** to give **119** was confirmed by NMR spectroscopy. In the ^1H NMR spectrum for **119**, two peaks at δ -3.81 and δ -3.92 were found for the internal methyl protons resonances, which were shifted upfield from δ -3.58 in tropone **115**. The methylene protons H-13 resonated at δ 4.43 showing both geminal coupling (J = 14.4 Hz) and coupling to the proton H-12 adjacent to the carbonyl group (J = 5.1 Hz). The DEPT-135 spectrum showed the negative methylene signal for C-13 at δ

32.70. The diagnostic C=O stretch frequency for **119** was shifted to 1685 cm^{-1}, in contrast to 1666 cm^{-1} in the tropone **115**, consistent with its lower conjugated pathway. The HRMS for **119** was in agreement with the value for $C_{43}H_{44}O$ (found, 576.3394; calculated, 576.3392).

Attempted formation of the cycloheptatrienide anion 113

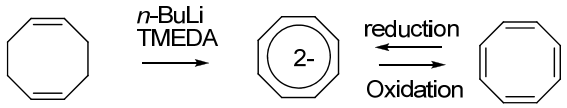


117 (with 7% 118) **113**

The same methods previously used to make the methyl-substituted cycloheptatrienide anions **18** were applied on the mixture of cycloheptatriene isomers **117** and **118** (93:7). However, $(CH_3)_3SiCH_2Li$ in THF failed to afford an anion. Decomposition of the starting materials took place and in the high field of the ^1H NMR spectrum the resonances associated for the DHP internal methyl protons disappeared. The reason could be the bulkiness of the base $(CH_3)_3SiCH_2Li$ in conjunction with the crowded area around H-13. The transformation might require an alternate base to from the anion. However, this has not been tried.

4.2.2 Aromatic 10π electron cyclooctatetraene dianion

Cyclooctatetraenide dianion $[C_8H_8]^{2-}$ **80** is a monocyclic aromatic species, which with 10π electrons, should display aromatic character based on Huckel's (4n+2)π electron rule. The preparation of its lithium salt $[Li(TMEDA)]_2[C_8H_8]$ was initially accomplished by reacting 1,5-cyclooctadiene (COD) **81** with *n*-butyllithium (*n*-BuLi) and tetramethylethylenediamine (TMEDA) (Scheme **51**) by Wilke.[223]

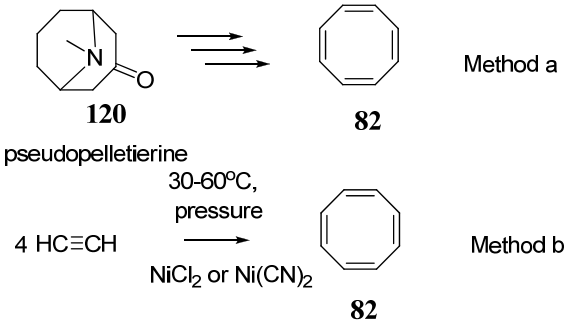


81 **80** **82**

COD **COT**

Scheme 51. The preparation of cyclooctatetraenide dianion 80 and conversion to COT 82

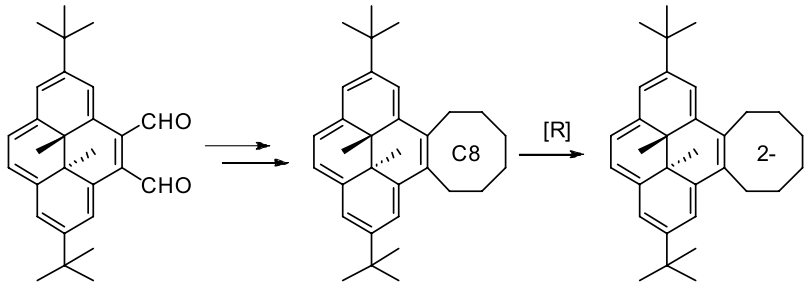
The transformation involved the loss of three protons and one lithium hydride. Hoye[224] investigated the reaction processes by using NMR spectroscopy and found a doubly charged dilithio species accounted for the lithium hydride ejection. The dianion **80** has also been prepared by reduction of 1,3,5,7-cyclooctatetraene (COT) **82** with reducing metallic elements, i.e. potassium (Scheme **51**). The interesting neutral COT **82** has also attracted much attention because of its "tub" shaped geometry, which is consistent with a non-aromatic character of 8π electron species. On coordination COT **82** demonstrates diverse binding modes to Pd(0) and Pd (II).[225] It has been used in asymmetrical catalysis as a bi-dentate ligand with later transition metals by coordinating as an electron rich alkene. For example, the iridium complex of dibenzocyclooctatetraene catalyzed regio and stereo-selective hydroxylation reactions in high yield.[226] Transformation of the dianion **80** to COT **82** can be achieved by oxidizing agents, e.g. cadmium chloride (Wilke[223]), mercuric chloride, a Samarium complex (Roesky[227]) and 1,2-dibromoethane (Odom[228]).



Scheme 52.The synthetic routes towards 1,3,5,7-cyclooctatetraene 82

There are several routes leading specifically to cyclooctatetraene **82**. It was first synthesized in 1905 by Willstätter,[229] from the alkaloid pseudopelletierine **120** (method **a** in Scheme **52**). Later, Reppe[230] discovered a one step method **B** (Scheme **52**) at BASF in Germany by polymerizing acetylene over a nickel catalyst under high pressure. A nickelacyclopentadiene was the key intermediate and a subsequent insertion of the coordinated ethynes directly into the Ni-C bond of the nickel complex led to formation of COT. Isotopic labelling studies by Colborn and Vollhardt[231] and DFT calculations[232] precluded any process involving insertion of ethyne into a benzene or the formation of cyclobutadiene or polyyne intermediates.

Since both COD and COT can be converted to the cyclooctatetraene dianion (Scheme **51**), we need first fuse an eight-membered unit, COT or COD, to DHP in order to study the aromaticity of the COT dianion. However, neither Willstätter's nor Reppe's method

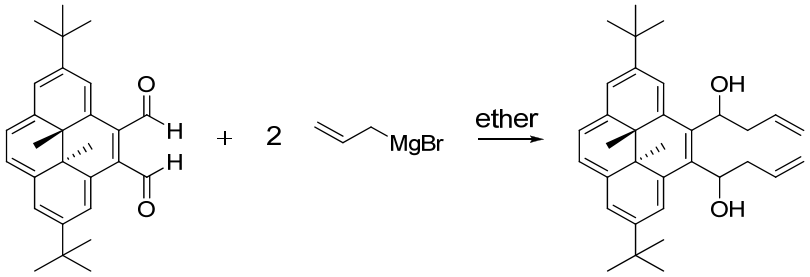


116

was suitable for us (Scheme **52**). We preferred to start from the dialdehyde **116**.

To close an eight-membered ring on a preformed DHP nucleus, requires formation of *cis* double bonds, so both Wittig and McMurry reactions might be useful. As well, ring closing metathesis (RCM) is particularly efficient in construction of medium size rings with as many as 10 carbons.[233] Both the Wittig and metathesis approaches were explored in the construction of DHP-fused C8 ring system.

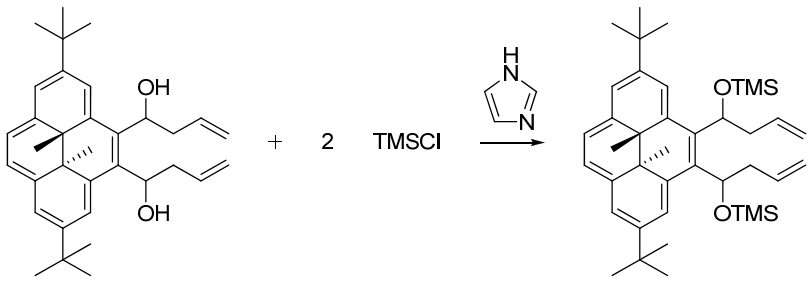
4.2.3 The ring closing metathesis approach to a COT-fused DHP



116 **123**

Scheme 53. Grignard reaction on the dialdehyde

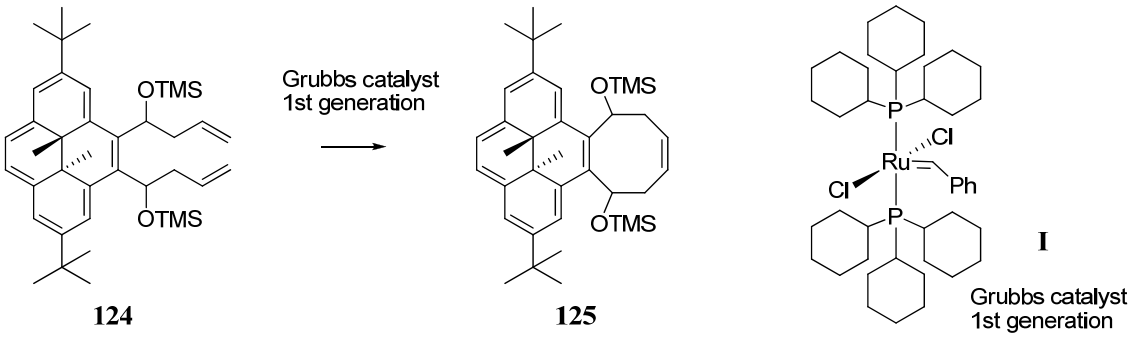
The diol **123** was obtained quantitatively when the dialdehyde **116** reacted with allyl magnesium bromide in ether.[237] The ^{1}H NMR spectrum revealed the disappearance of the aldehyde protons at δ 11.20 and a noticeable upfield chemical shift of the DHP aryl protons. The infrared spectrum demonstrated a broad absorption at 3377 cm^{-1} diagnostic for an alcohol and the absence of the typical C=O stretches of aldehyde **116**. The high resolution mass measurement was in accordance with the calculated value for $C_{34}H_{44}O_2$ (calculated, 484.3341; found, 484.3338). The complexity of the NMR spectra suggested the presence of diastereomers for diol **123**. The isomeric mixture was used in the next step without any attempt at separation.



123 **124**

Scheme 54. The protection of the diol 124

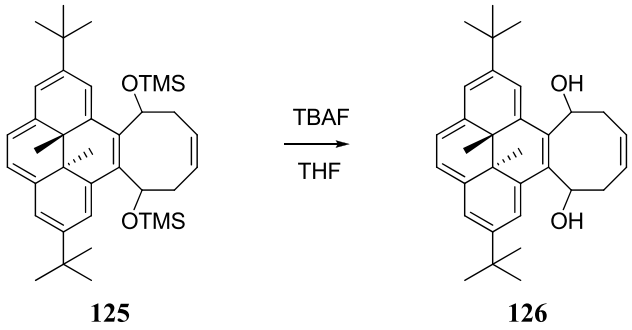
The TMS protected diol **124** was obtained in 88% yield by reacting the diol **123** with TMSCl and imidazole.[238] In contrast, protection of only one alcohol was observed when triethylamine was used as base.[239] The ^{1}H NMR spectrum exhibited several resonances for the TMS protons in the vicinity of δ 0, consistent with diastereoisomers being present. The infrared spectrum showed the disappearance of the diagnostic OH stretch at 3377 cm^{-1}. The crude products, isolated as green DHP-containing fractions after simple chromatography, were used directly in the next step.



124 **125**

Scheme 55. The ring closing metathesis to a C8 system

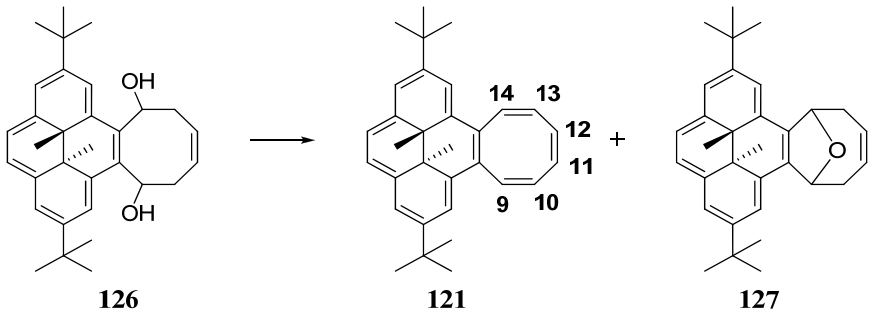
The TMS protected dibutenyl DHP **124** was cyclized using Grubbs first generation catalyst, benzylidene-*bis*(tricyclohexylphosphine)dichlororuthenium (**I** above), in 73% yield, under high dilution conditions to reduce possible intermolecular metathesis.[240] The disappearance of the terminal alkene protons indicated the success of the conversion in the ^{1}H NMR spectrum. The HRMS revealed *m/z* 600.3817 in agreement with the calculated 600.3819 for $C_{38}H_{56}O_2Si_2$. The X-ray analysis also supported the structure of **125** and will be discussed later.



125 **126**

Scheme 56. Deprotection of DHP-fused C8 diol

Treatment of **125** with TBAF in THF at room temperature[241] gave dialcohol **126** qualitatively as mixed isomers having correct molecular weight.



126 **121** **127**

Scheme 57. Elimination toward the DHP-fused COT

Elimination of water from **126** proceeded under acidic or basic conditions. In benzene, *p*-toluenesulfonic acid or hydrochloric acid quickly led to DHP-fused COT **121**, but only in 7% yield with the cyclic ether **127** being the major product in 73% yield. Use of a pyridine and mesyl chloride protocol (Noller[242]) gave the same results. The products **121** and **127** were separated by chromatography. The DHP-fused COT **121** was eluted first as a green solid and the ether **127** second, also as a green solid.

The molecular formula $C_{32}H_{36}$ for DHP-fused COT **121** was confirmed by HRMS (calculated: 420.2817; found: 420.2819). The ^{1}H NMR spectrum of **121** showed a single peak for the internal methyl protons at δ -3.70. Protons of the COT moiety appeared downfield partly due to deshielding by the DHP moiety, having H-9,14 at δ 7.65, H-10,13 at δ 6.48 and H-11,12 at δ 6.05. H-11 and H-12 showed broadening effects from

tub flipping, which is studied by variable temperature NMR (Section 4.3.1). NOE spectra supported the proton assignment of the C8 moiety. The carbons signals of the C8 ring broadened due to conformational effects, similar to that found for COT itself.[231] No complete assignment of the carbons could be made as no correlations were observed in either short or long range heteronuclear NMR experiments except that C-10 and 13 unambiguously were assigned at δ 131.04 in the ^{13}C spectrum. The other four carbons on COT unit appeared as the two broadened signals in the vicinity of δ 133 and δ 132 (Figure **36**). A broad peak at δ 15.3 was associated to the internal methyl carbons.

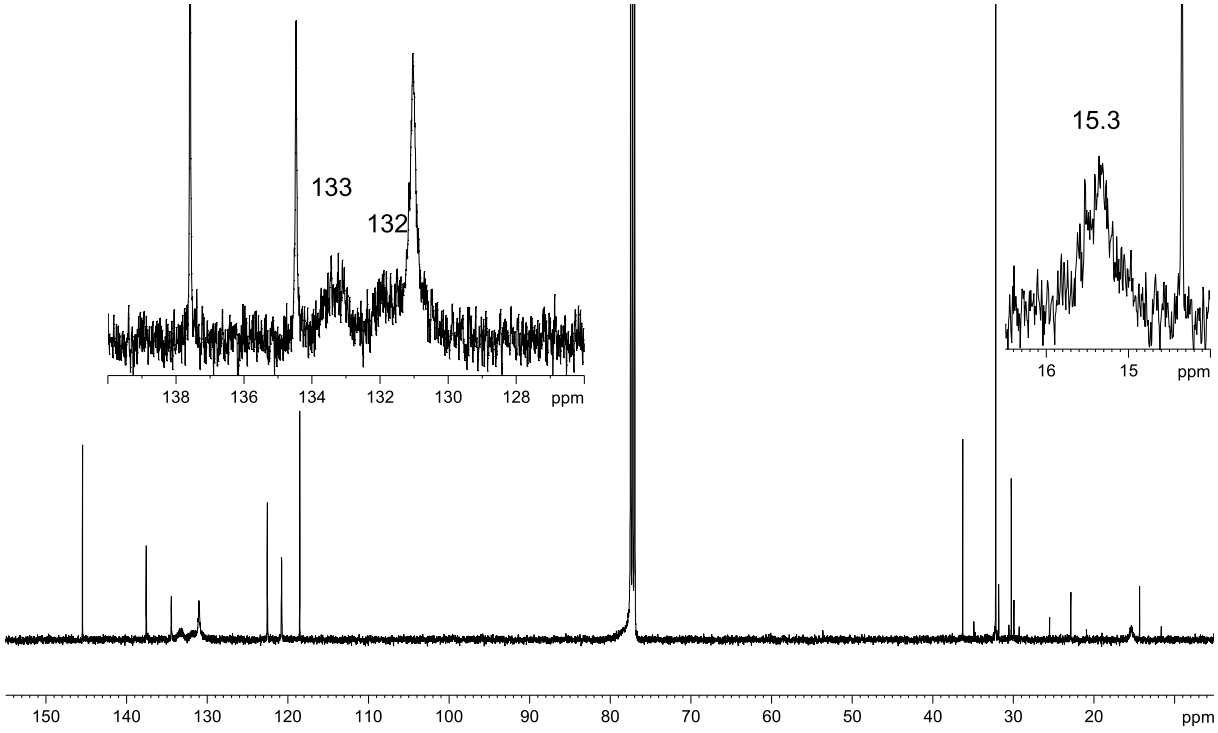
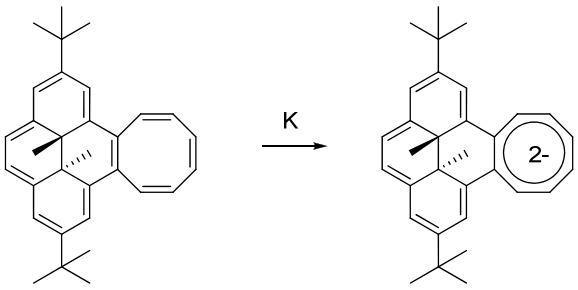


Figure 36. The ^{1}H and ^{13}C NMR spectra of DHP-fused COT 121

The identity of the ether **127** was confirmed by MS (calculated: $C_{32}H_{38}O$: 438.2923; found: 438.2919) and by NMR spectroscopy. In the ^{1}H NMR spectrum, the internal methyl protons resonate at δ -3.96 and δ -3.99. The negligible difference in their chemical shift may be because the double bond in the C8 moiety is oriented away from the internal methyl groups. The protons H-9 and 14 appeared as multiplets at δ 6.45-6.46

probably because of coupling in ring and the possibility of isomers. Protons H-11 and 12 were also found as multiplets at δ 5.21-5.14. An X-ray structure proved the structure of the molecule (Section **0**).

The green COT **121** was dissolved in dry THF-d_8 in a sealed J-Young NMR tube in a glovebox. A piece of potassium was added into the NMR tube, such that it stuck to the upper part glass of the tube. Inversion of the tube allowed the solution to contact the potassium resulting in a colour change to red. The ^{1}H NMR spectrum was recorded immediately to monitor the reaction progress and showed that the dianion **20** was formed in presence of the unreacted DHP-fused COT **121**. This was somewhat different from the results of Katz,[243] who showed that exactly two moles or more of potassium was required to completely reduce cyclooctatetraene to its dianion. The anion radical intermediate would broaden NMR signals during the course of the reaction in the ^{1}H NMR spectrum.



121 **20**

Scheme 58. The reduction to the DHP-fused COT dianion by potassium

The internal methyl protons in the starting DHP-fused COT **121** shifted downfield by 2.1 ppm from δ -3.70 to δ -1.6 in the dianion **20**. The DHP peripheral protons in **20** resonated as singlets at δ 7.18, 6.70 and 6.64, shifting upfield from δ 8.45, 8.34 and 8.22 in DHP-fused COT **121** (Figure **37**). The deshielding effects of the ring current and the shielding effects of the doubly negative charge were the two most important influences on the chemical shifts of the peripheral protons. The doubly negative charge distributed over twenty peripheral carbon atoms, which might cause a shielding of the peripheral

protons by ca. 1 ppm from the COT **121** to the dianion **20**. The ring current applied a *ca*. 2.5 ppm deshielding on the peripheral protons in the cyclooctatetraene dianion. This was reasonably consistent with what appeared in the ^{1}H NMR spectrum (Figure **37**). The NMR spectroscopy showed that the starting COT **121** and the COT dianion **20** co-existed in the solution. The peaks for the DHP-fused COT **121** became broadened in the ^{1}H NMR spectrum of the reaction mixture. Katz[243] ascribed the broadening to the formation of COT anion radical and concluded there was slow electron exchange between the neutral hydrocarbon and the anion radical in the cyclooctatetraene **82**. Thus it might suggest that in the reaction to from **20** the electron exchange between the COT and the dianion is not significant and the radical intermediate is easy to reduce.

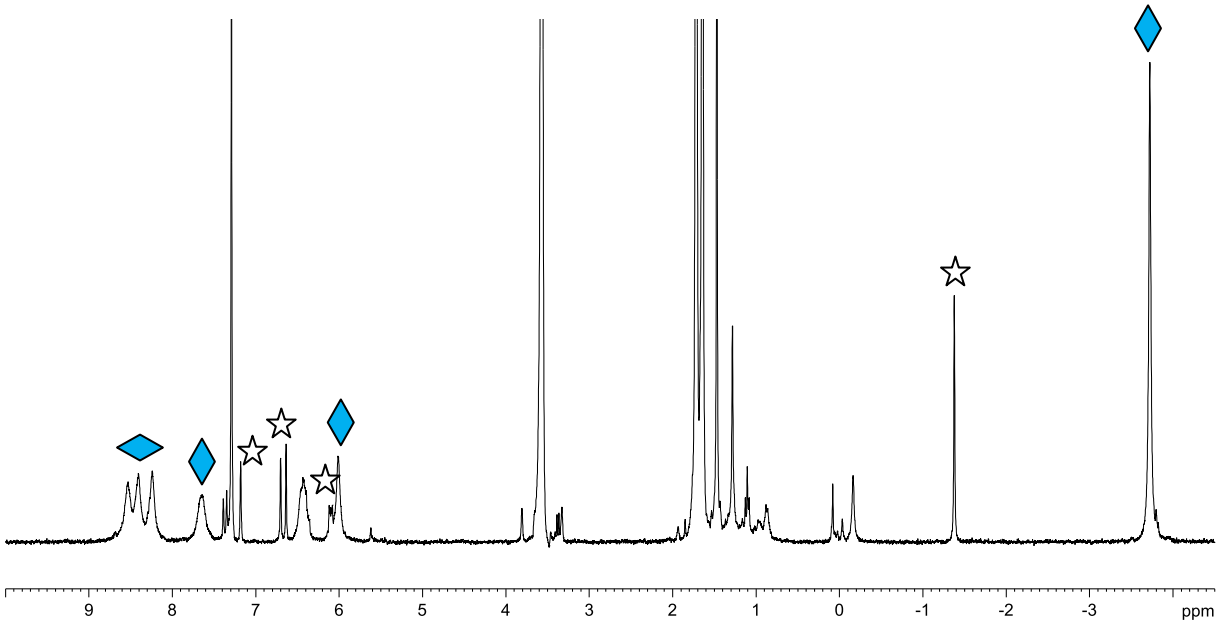
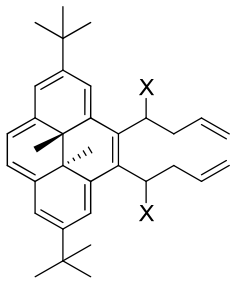


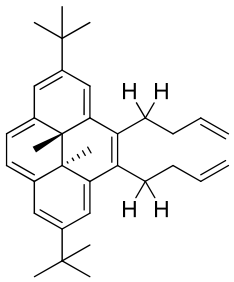
Figure 37. The ^{1}H NMR spectrum for the dianion 20 (☆) plus unconverted 121 (◆)

4.2.4 Attempted synthesis of 122 from diol via *bis*-(3-butenyl) DHP 131

Attempts to reduce the DHP allyl-carbinol **123** directly to *bis*-(3-butenyl) DHP **133** were explored. The optimized protocol explored by Hall[244] utilizing lithium in liquid NH_3 on **123** yielded no DHP products according to the ^{1}H NMR spectrum. 30% Pd/C in methanol gave the product with only reducing the double bonds. Reduction with SmI_2 gave no reaction and the starting materials were recovered.

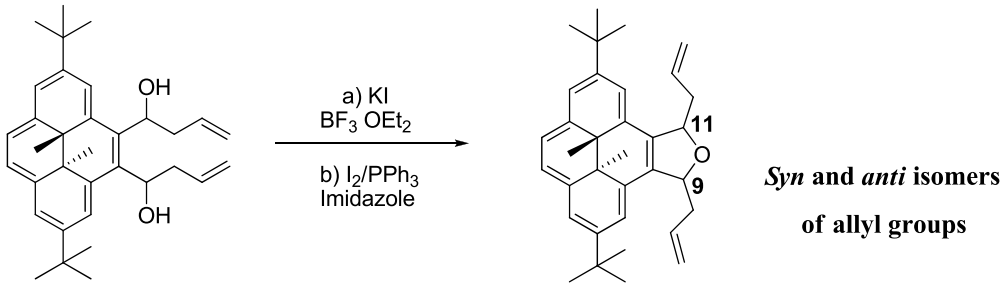


123 X = OH
133 X = Br or I



131

Reductive dehalogenation on alkyl iodides or bromides could also proceed to replace the halides with hydrogens, as reported by Khurana.[245] Mild basic or neutral reaction conditions were desirable in order not to touch the allylic and benzylic hydrogens because acids and bases might trigger elimination or intramolecular cyclization to cyclic ethers (HCl by Brown[246] and *p*-toluenesulfonic acid by Eich[247]). Bandgar[248] described a KI/BF_3 system for converting benzylic and allylic hydroxyls to iodides. But at our hand the protocol transferred the diol **123** to DHP 9,11-dihydroisofuran **132** as the only product in good yield (>75%) (Scheme **59**). The triphenylphosphine–iodine system also led to the exclusive transformation to the DHP dihydroisofuran **132**. It was worth noting that no dehydration of the *β,γ*-unsaturated tertiary alcohol **123** took place.[249] Thus the reactions probably underwent a S_N2 nucleophilic pathway, with cyclization was caused the good leaving nature of the iodide ions. Presumably after one hydroxyl group was replaced by an iodine in the diol **123**, intramolecular cyclizations occurred to afford DHP dihydroisofuran **132**.



123 **132**

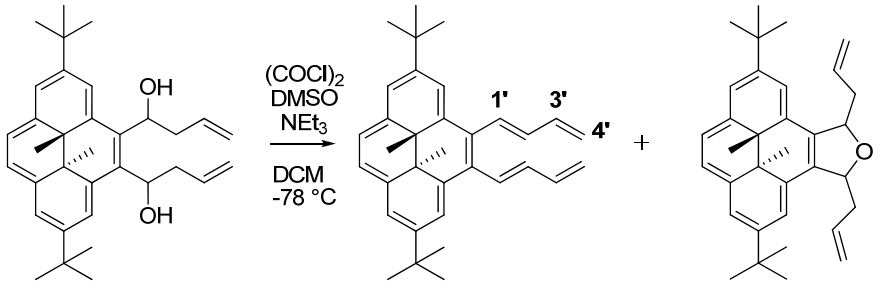
Scheme 59. Iodination attempts on the diol 123

The identity of DHP dihydroisofuran **132** was confirmed by NMR spectroscopy. The protons for two groups of internal methyl protons resonated differently at δ -3.74 and δ -3.97. They belonged to the two diastereomers, in which the allyl groups are *syn* and *anti*.

Table 15. The oxidation reactions tried on diol 123

Entry	Reactions	Conditions	results
1	Dess-Martin reagent		Decomposition
2	PCC		Decomposition
3	Swern oxidation	THF, r.t.	Undesired products

The mixed isomers of diol **123** was subjected to the Dess-Martin reaction conditions [250] employed by Felpin[251] in synthesizing a *β,γ*-unsaturated phenyl allyl ketone (Scheme **60**). The resulting red solution contained no DHPs by both TLC and NMR spectroscopy.

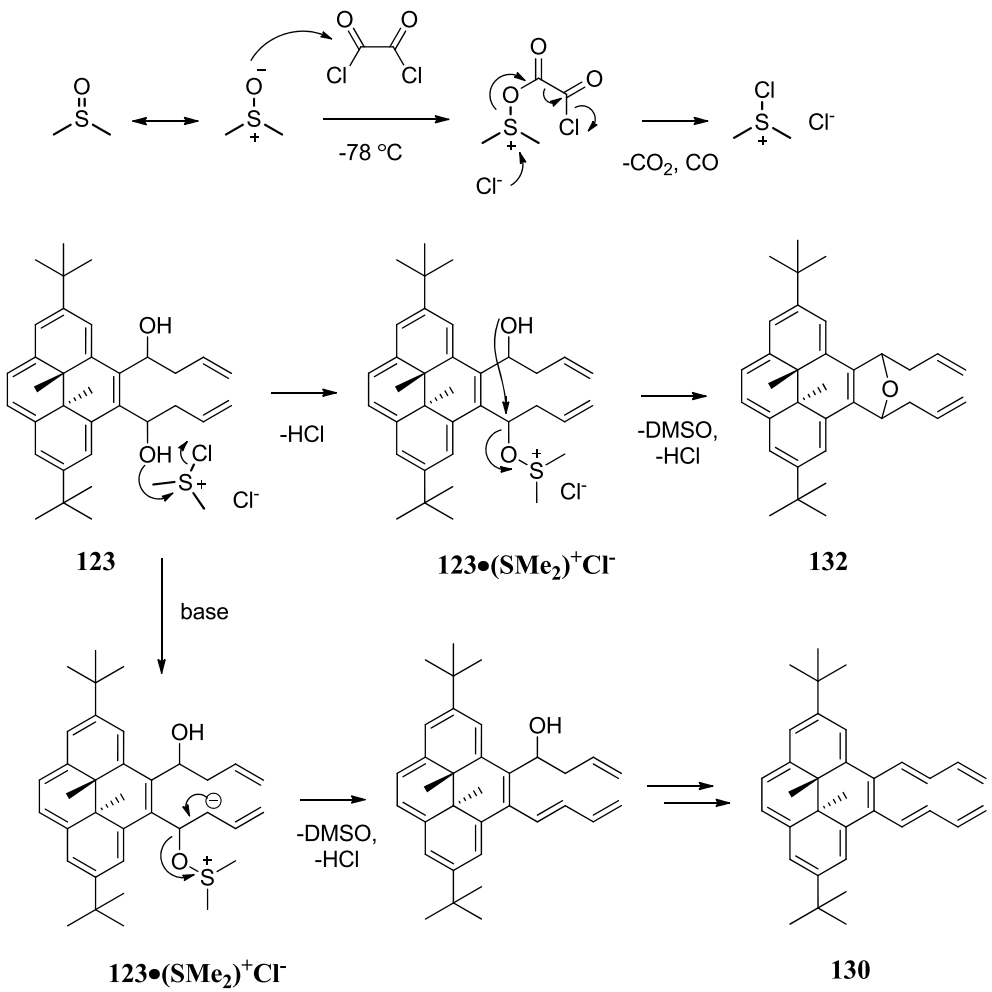


123 **130** **132**

Scheme 60. Oxidation attemps on diol 123

When the diol **123** was subjected to Swern oxidation,[252] there was no oxidation of the alcohol to the corresponding ketone. Instead, the *bis*-diene **130** and a mixture of ether **132** were obtained in 13% and 80% yields respectively. The transformations of a series of diols to the cyclic ethers driven by MnO_2 and compatible with the use of a reductant, triethylsilane, were reported by Panda.[253] However, it is less likely to apply their lactol intermediate explanation in our processes. Rather the reaction could be catalyzed by a trace amount of the HCl acid residual in the oxalyl chloride. The formation of chlorosulfonium salt intermediates would generate HCl because the trimethyl amine was added afterwards to release alkoxysulfonium ylide.

The reaction of DMSO and oxalyl chloride react almost instantaneously to form chlorodimethylslofonium chloride at -60°C, resulting in the evolution of CO_2 and CO. The chlorodimethylslofonium chloride remains stable below -20°C, but decomposes above the temperature to chloromethyl methyl sulphide. It reacts with alcohols very quickly, resulting in the formation of an alkoxydimethylsulfonium chloride. The reaction in Scheme **60** could take place in the mechanism shown as in Scheme **61**.



Scheme 61. The proposed mechanism of formation *bis*-diene 130 and ether 132

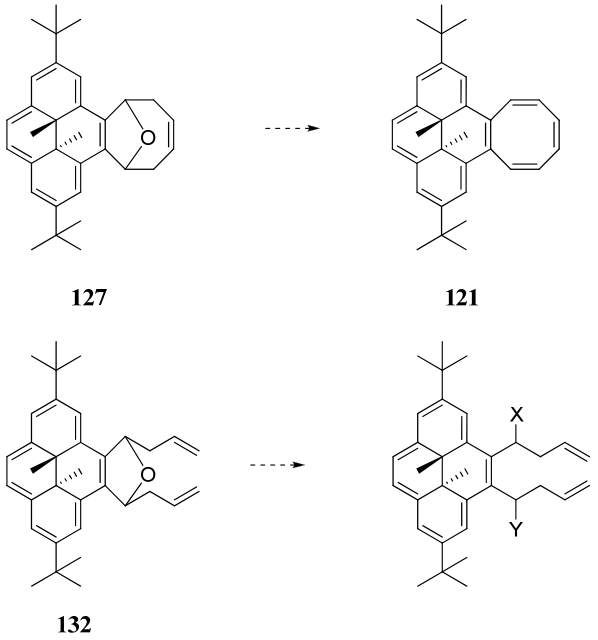
The formation of the *bis*-diene **130** was confirmed by NMR spectroscopy. In the ^{1}H NMR spectrum, the olefinic protons resonated at δ 7.50, 6.87-6.72 and 5.37 for H-1', H-2',3' and H-4', respectively. And the coupling constant J = 15.5 Hz indicated the *trans* configuration of the alkenes. The protons on the internal methyl groups resonated at δ -3.70 in C_6D_6 as a single peak indicative of having substituents on symmetrical sites in DHP. The carbons on the olefinic chains in **130** resonated at δ 132.73, 137.35, 138.08 and 116.97 for C1' through C4' in the ^{13}C NMR spectrum.

When the *bis*-dienyl DHP **130** was subjected to the ring-closing metathesis conditions used for di-3-butenyl DHP **124**, no COT **121** was obtained. The products in elution order consisted of benzoDHP 3, a likely DHP Ruthenium complex and a mixture with high molecular weight. It suggested possible polymerization the substrate **130**. The formation

of a trace amount of benzoDHP might be a side metathesis reaction releasing butadiene species. The ruthenium complex as a major product was indicated by having a chemical shift at around δ 10 in the ^{1}H NMR spectrum, which shifted downfield by over 1 ppm from the most downfield resonance in *bis*-diene **130**. In fact, it has been observed that having large substituents on DHP results in a marked downfield shift of the vicinal DHP protons. Note that α-alkylidene protons resonate at much lower field, at about δ 20, in a series of alkylidene ruthenium complexes.[254] The sample in $CDCl_3$ decomposed before further characterization could be obtained.

4.2.5 Attempt to open the fused furan in oxo-bridged COD 127 or DHP dihydroisofuran 132

Theoretically the major epoxide products, cyclic ethers **127** and **132** can be transformed into the COT **121** (Scheme **62**). Although we tried acid and base catalyzed ring opening and reduction methods, for example, we were unable to open the ether, which was always retrieved.



127 **121**

132

Scheme 62. Proposal of transformation towards the COT 121

4.2.6 Attempt to synthesize metal complexes

Because olefins are good ligands for transition metals, we tried to synthesize some metal complexes. DHP-fused trienes **107** and **108** were tried with several metal complex precursors (Table **16**). But so far all failed and returned starting material.

Table 16. Attempts to react cycloheptatriene 107 or isomer 108 with metal substrates

Entry	Conditions	Conditions	Results
1	$TiCpCl_3$ [a]	$FeCl_3$, Mg for 15 hours, in THF	**107** and **108** recovered
2	$NpCr(CO)_3$ [b]	80°C or 110°C for 15 hours, in dioxane	**108** recovered
3	$Re(CO)_5Br$ [c]	Refluxed for 12 hours, in benzene	**107** recovered
4	$Fe_2(CO)_9$ [c]	Refluxed in benzene	**107** recovered

Started with: [a] mixed substrates **107** and **108**; [b] only substrate **108**; [c] only substrates **107**

4.3 X-ray crystallographic analysis

The crystal structure of 2,7-Di-tert-butyl-11-oxo-trans-10,12-dimethy-13c,13d-dimethy-14-oxabicyclo[3.2.1]oct-13a-eno[13a:13f; e]-trans-13c,13d-dihydropyrene 99B

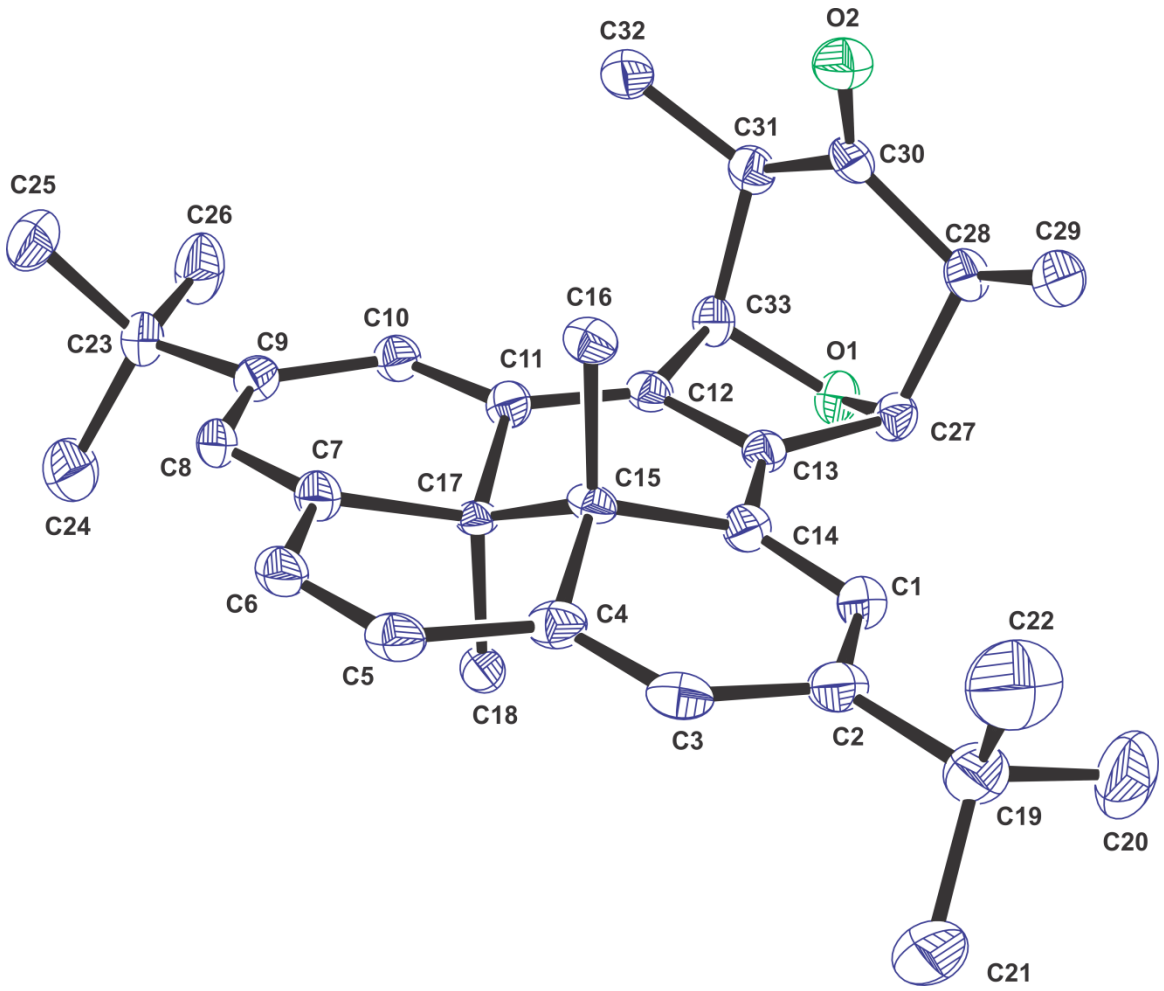


Figure 38. ORTEP3 drawing (50% probability level) of 99B

The structural information of the second fraction **99B** was examined by X-ray crystallography. All DHP carbons are within the range of 0.12 Å from the average DHP plane, with average deviation 0.056 Å. Two furan carbons C-27 and C-33 are out of the DHP plane by 0.071 and 0.174 Å, respectively. The peripheral bond lengths of the DHP skeleton, averaging at 1.395 Å, fall within the normal range (Table **17**). The sum of the modulus of the deviation of 0.271 Å indicates a small 14π electron localisation caused by the fusion of the bicyclic ring on the side as expected.[255] The six-membered ring of the bicyloocteneone adopts a more energetically preferred chair conformation with the methyl groups and the carbonyl in the equatorial positions, with the result that this ring is perpendicular to the DHP framework. The distance between the oxygen atom of the carbonyl group to the closet internal methyl proton is 3.112(1) Å, in contrast to 4.100(1) Å for the bridged oxygen atom to the protons of the other internal methyl group. The adjacent protons (H-9/10 and H-12/13) on the six member ring show torsion angles of 67.41° and 63.81° that are consistent with the NMR data.

Table 17. DHP peripheral C-C bond lengths (Å) for 99B[a]

Bond		Length	Bond		Length
C12	C13	1.417(2)	C5	C6	1.374(2)
C13	C14	1.377(2)	C6	C7	1.418(2)
C14	C1	1.404(2)	C7	C8	1.364(2)
C1	C2	1.385(2)	C8	C9	1.423(2)
C2	C3	1.421(2)	C9	C10	1.385(2)
C3	C4	1.366(2)	C10	C11	1.400(2)
C4	C5	1.418(2)	C11	C12	1.379(2)

[a]: (Σ(|bond length - ave bond length|) the sum of the modulus of the average bond alternation is 0.271 Å.

The crystal structure of 2,7-Di-tert-butyl-11-oxo-10,12,13c,13d-tetramethylcycloheptatrieno[13a:13f; e]-trans-13c,13d-dihydropyrene 17

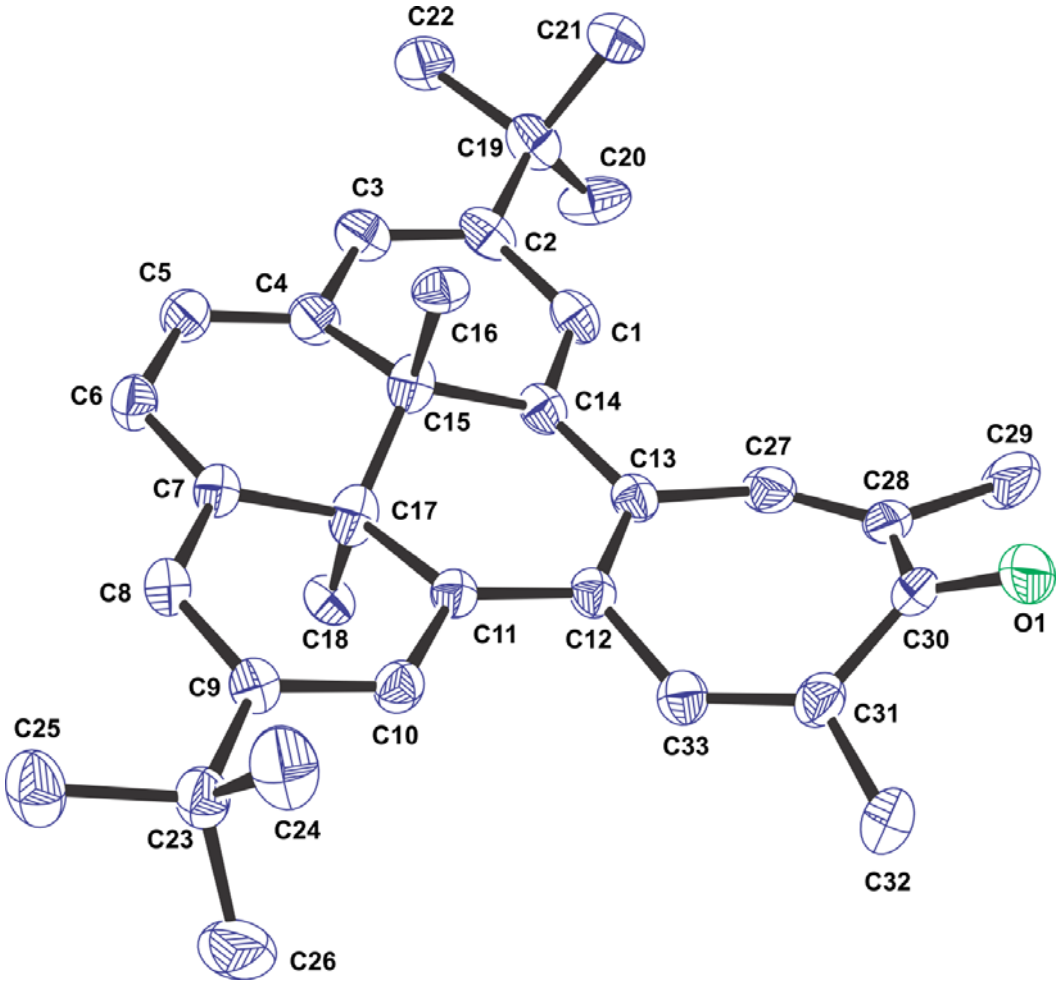


Figure 39. ORTEP3 drawing (50% probability level) of 4,5-DHP[e]fused 1,6-dimethyltropone 17

All the carbons on the DHP framework are close to the mean DHP plane with average deviation 0.028 Å. The average carbon C-C distances for the DHP framework are 1.402 (2) Å with the sum of the modulus of the average bond alternation of 0.307 Å (Table **18**). The fused bond length C12-C13 is 1.414 (2) Å, 0.030 Å shorter than the adjacent ones. The C-O distance is 1.227 (2) Å, which is in the range 1.185 to 1.355 Å and comparable to the average of 1.244 Å for the C=O bond lengths of tropone derivatives in the CSD database. (see the Appendix **IV**)

Table 18. DHP peripheral C-C bond lengths for the tropone 17*

Bond		Length	Bond		Length
C12	C13	1.414(2)	C5	C6	1.409(2)
C13	C14	1.442(2)	C6	C7	1.378(2)
C14	C1	1.373(2)	C7	C8	1.398(2)
C1	C2	1.425(2)	C8	C9	1.379(2)
C2	C3	1.378(2)	C9	C10	1.425(2)
C3	C4	1.402(2)	C10	C11	1.377(2)
C4	C5	1.374(2)	C11	C12	1.447(2)

*: (Σ(|bond length - ave bond length|) the sum of the modulus of the average bond alternation of 0.307 Å.

The tropone moiety is bent up with a dihedral angle of 51.31° between the DHP plane and the plane formed by the middle three carbons (C28, C30 and C31) of the tropone moiety. Two carbons, C27 and C33, are 0.066 and 0.082 Å away from the DHP plane. The distance between the carbonyl carbon and the DHP plane is 1.089 Å. The two carbons C28 and C31 are 0.569 and 0.454 Å out of the DHP plane. Two alkene bonds are slightly elongated to 1.347 (2) and 1.349 (2) Å. All single bonds are in the range for a normal single bond (Table **19**).

Table 19. Bond lengths (Å) for the tropone unit in 17

Bond		Length Å	Bond		Length Å
C12	C13	1.414(2)	C30	C31	1.472(3)
C13	C27	1.453(2)	C31	C33	1.347(2)
C27	C28	1.349(2)	C33	C12	1.456(2)
C28	C30	1.466(2)			

The crystal structure of 2,7-di-tert-butyl-10,12,13c,13d-tetramethyl-11-H,H-cycloheptatrieno[13a:13f; e]-trans-13c,13d-dihydropyrene 108

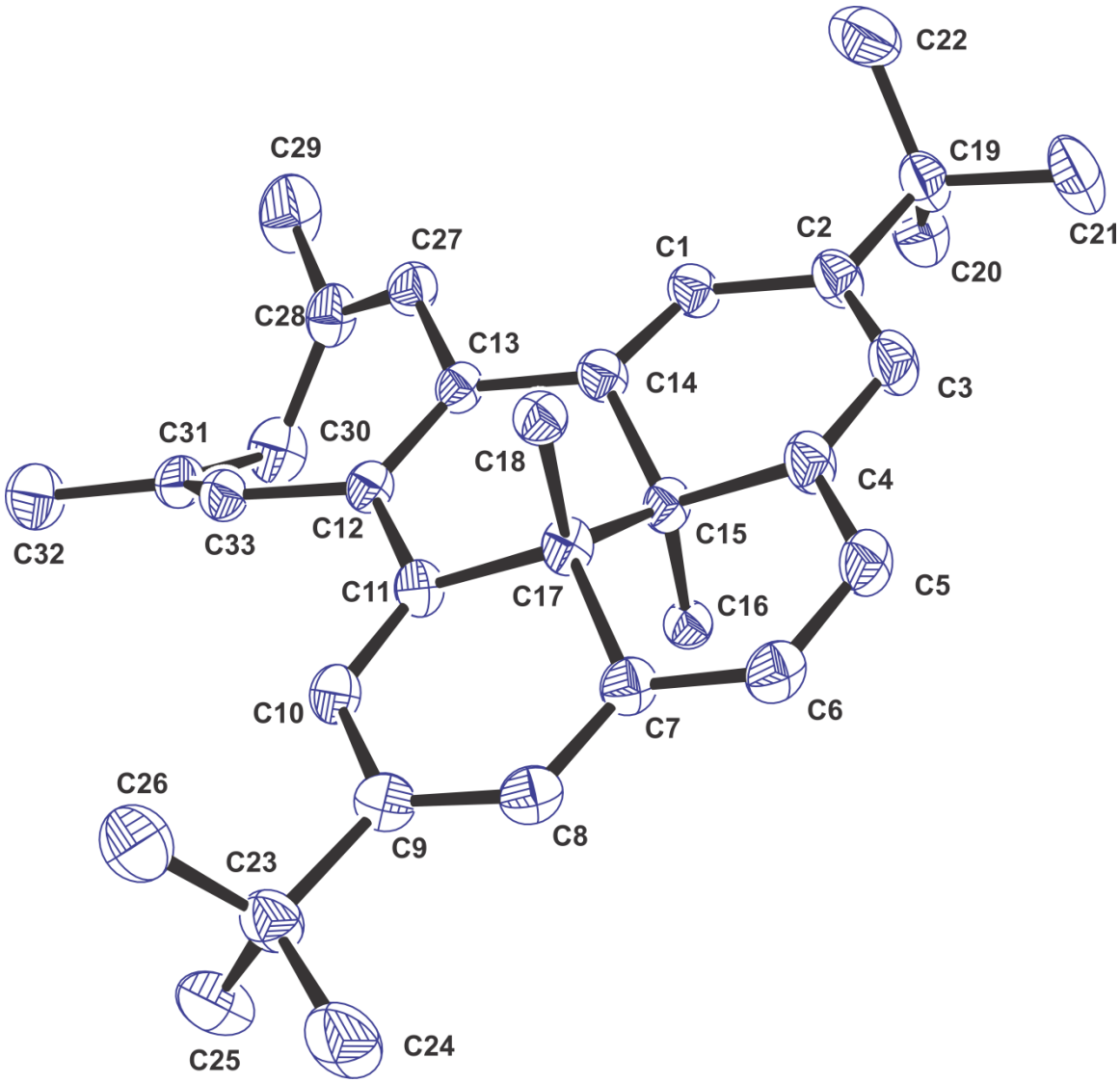


Figure 40. ORTEP3 drawing (50% probability level) of the 3,4-DHP [e]fused 1,6-dimethylcycloheptatriene 108

The bond lengths on the periphery of the planar DHP **108** average at 1.398 (2) Å, and spanned the range 1.357(2) to 1.446(3) Å. The sum of the modulus of the average bond

alternation is 0.361 Å for the DHP peripheral carbons (Table **20**). The carbons of the C7 ring appear displaced 0.11 from the DHP plane for C-27/C-28 and 0.536 and 0.562 Å for C28 and C31. The plane consisting of the three farther ring carbons (C-28, C-30 and C-31) in the C7 ring form a dihedral angle of 84.6° with the DHP plane and 70.7° with the plane consisting of six the sp^2 hybridized carbons in the C7 ring. An angle of 3.35° was formed between the DHP plane and the plane consisting of the other four carbon atoms (C-27, C-28, C-31 and C-33) in the C7 ring.

Table 20. DHP peripheral C-C bond lengths (Å) for CHT 108 [a]

Bond		Lengths (Å)	Bond		Lengths (Å)
C12	C13	1.401(2)	C5	C6	1.403(2)
C13	C14	1.446(3)	C6	C7	1.372(3)
C14	C1	1.357(2)	C7	C8	1.398(2)
C1	C2	1.436(3)	C8	C9	1.374(3)
C2	C3	1.372(3)	C9	C10	1.433(3)
C3	C4	1.406(2)	C10	C11	1.361(2)
C4	C5	1.373(3)	C11	C12	1.443(3)

[a]: (Σ(|bond length - ave bond length|) the sum of the modulus of the average bond alternation is 0.361Å.

The crystal structure of 2,7-di-tert-butyl-13c,13d-dimethyl-10,12-diphenyl-trans-13c,13d-dihydro-13,13-2H- cycloheptatrieno[13a:13f; e]pyrene 117

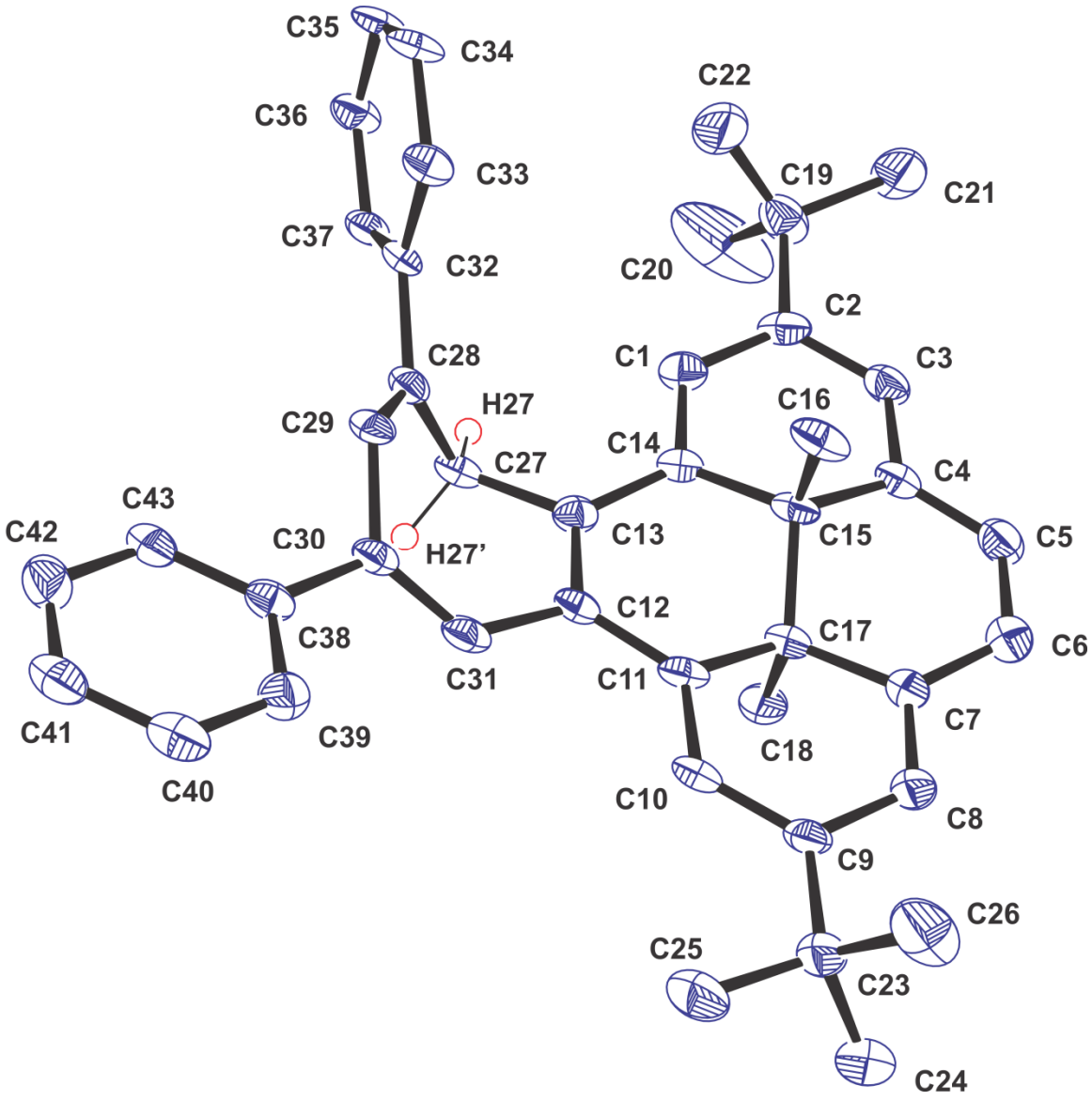


Figure 41. ORTEP3 drawing (50% probability level) of 117

The DHP framework in this molecule is badly distorted. Carbon C-13 shows the largest deviation from the average DHP plane by a distance of 0.111Å, and 0.067 for C-

12. In contrast to the dimethyl symmetric structure **108**, the bond lengths of the DHP periphery fall in a small range, 1.38 to 1.43 Å showing no obvious continuous bond alternations. The average bond length was found to be 1.401 (7) Å. The sum of the modulus of the deviation (14 bonds) from the average is 0.151Å. The C7 ring is strongly distorted and is bent from the DHP plane. The methylene carbon C-27 is bent on the opposite side of the DHP plane with respect to the rest carbon atoms of the C7 ring and the displacement is 0.350 Å for C-27, while the carbon C-31 displaces by 0.327 Å. The C-29 displaces the most with a distance of 1.573 Å from the DHP plane. The inner angles on the sp^2 carbons of the C7 ring are in the range of 117 to 129°. The angle of the sp^3 carbon C13-C27-C28 is 108.7 (4)°. The interplanar angle between the DHP plane and the plane consisting of the six sp^2 hybridized carbons is 29.01°. The plane of the bow of the C7 ring formed by C-27, C-13 and C-28 has an interplanar angle of 74.41° with the plane consisting of the six sp^2 hybridized carbons in the C7 ring.

Table 21. DHP peripheral C-C bond lengths for diphenyl CHT 117*

Bond		Length	Bond		Length
C12	C13	1.428(6)	C5	C6	1.386(8)
C13	C19	1.417(7)	C6	C7	1.416(7)
C19	C1	1.398(6)	C7	C8	1.385(6)
C1	C2	1.400(7)	C8	C9	1.409(7)
C2	C3	1.391(7)	C9	C10	1.387(6)
C3	C4	1.395(8)	C10	C11	1.401(6)
C4	C5	1.389(7)	C11	C12	1.409(6)

*: (Σ(|bond length - ave bond length|) the sum of the modulus of the average bond alternation of 0.151Å.

The crystal structure of 2,7-di-tert-butyl-9,14-*bis*-trimethylsilyloxy-trans-14c,14d-dimethyl-9,10,13,14,14c,14d-hexahydrocycloocta[14a:14f; e]pyrene 125

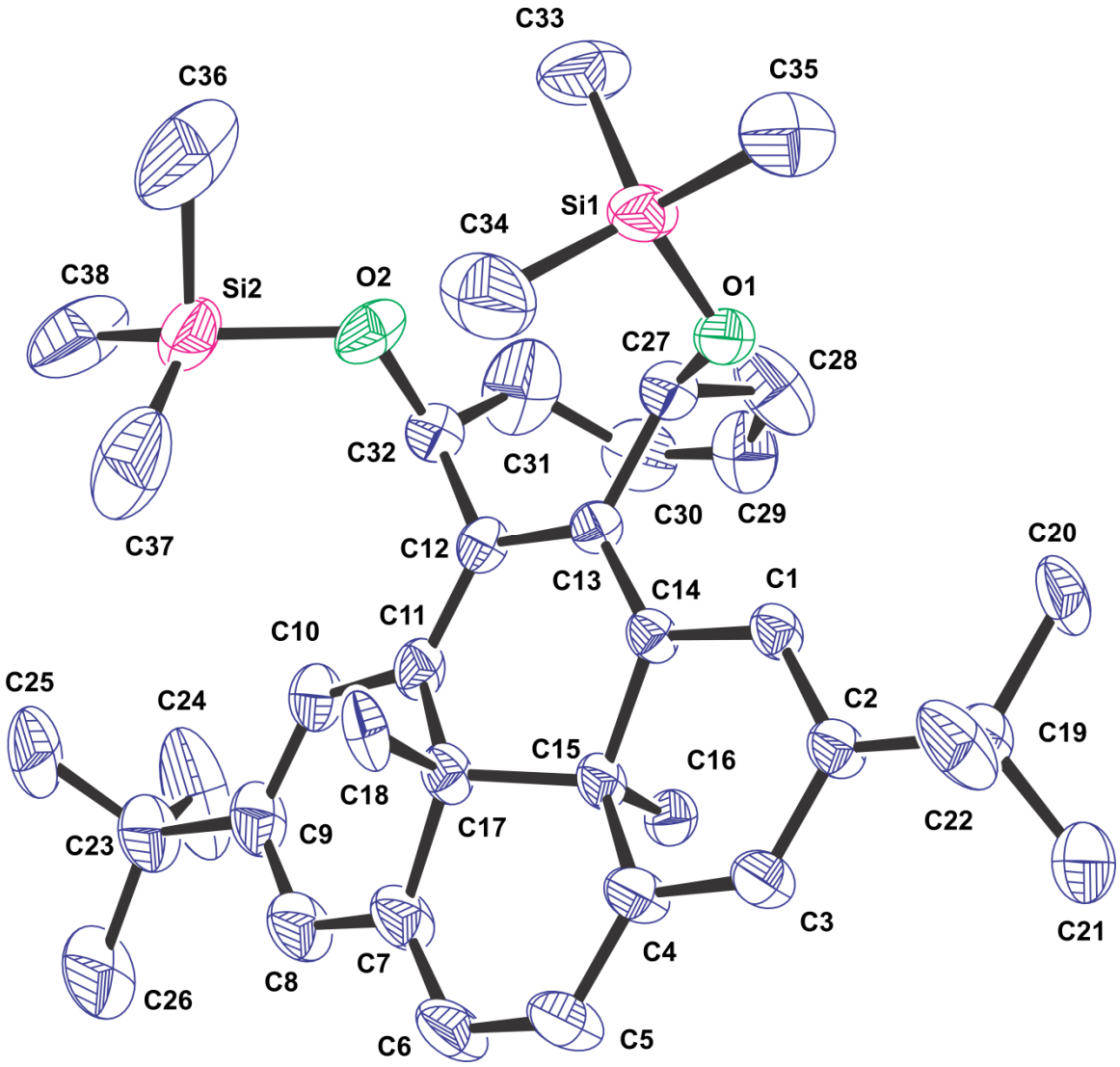
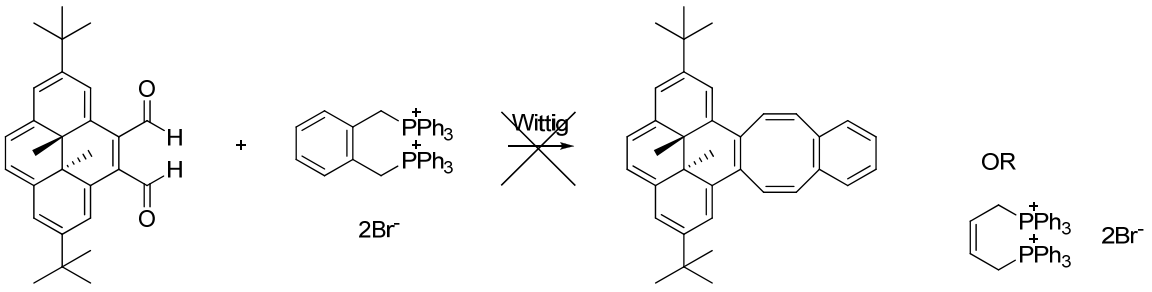


Figure 42. **ORTEP3 drawing (30% probability level) of 1,2-DHP[e]fused 3,8-*bis*(trimethylsilyloxo)-cycloocta-1,5-diene 125**

The structure for **125** clearly shows the the tub shape of the C8 ring. Full bond distances are given in the Appendix **V**. The average DHP peripheral carbon distance is 1.393 Å, and the sum of the modulus of the deviation (14 bonds) from the average is 0.127Å. The double bond between C-29 and C-30 is 1.300(8) Å and the remaining bond lengths of the C8 ring are in the range of 1.466(8) and 1.525(5) Å.

4.3.1 Cyclization attempt using the Wittig strategy

A *cis* geometry of the ylide substituents is crucial for a *bis*-ylide to form an eight-member ring product, and thus the *ortho*-benzene-derived phosphonium salts **128** and the *cis*-1,4-but-2-enyl triphenylphosphonium salt might lead to the desired configurations. Although the benzene backbone might lower the nucleophilicity of the ylide derived from **128** because of charge delocalization, the easy accessibility of **128** prompted us to begin the synthesis of a COT-fused DHP with **129** as the target.



116 **128** **129**

Scheme 63.Wittig strategy for the synthesis of a COT-fused DHP derivative

Unfortunately, the Wittig reaction between aldehyde **116** and *o*-xylene-α,α′-*bis*(triphenylphosphinebromide) salts **128**[234] failed to give any of the desired product, **129**, under a variety of reaction conditions (Table **22**).

Table 22. Reaction conditions used for the Wittig reaction of aldehyde 116 with phosphonium salts 128

Entry	Bases	Solvents	Results
1	Lithium ethoxide in ethanol	DMF, r.t., 12 hours	No product obtained
2	Sodium amide	Liquid ammonia/ THF, r.t., 12 hours	Four fractions, decomposed
3	*n*-BuLi in hexane	THF, r.t. and heated, 3 days	No product obtained

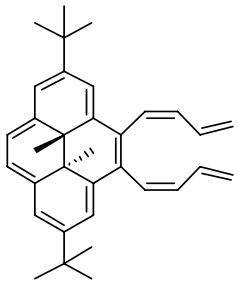
Sodium amide in liquid ammonia (entry **2**) seemed promising since most of the starting aldehyde was consumed. The products had similar polarity to the starting 4,5-DHP dialdehyde **116** on TLC. Presumably reaction on a single aldehyde group occurred. It was worth noting that the ^{1}H NMR spectrum showed the persistence of a DHP moiety in the crude products. Two sets of resonances for the internal methyl groups of the DHP fragments were observed, indicating formation of two DHP-derived products. When a phosphonium salt is hydrolysed in work up, often a methyl group is formed, so the product might be one free aldehyde and a –CH=CH-Ph-o-Me or maybe a longer but similar type of molecule, especially where *trans*-double bonds are formed.

For other bases (entry **1** and **3**), colored ylides were observed, and the aldehyde **116** was consumed when the reactions were followed by TLC, but no products could be obtained. The failure of this reaction might be due to the formation of mostly *trans*-conformation double bonds in the first Wittig reaction so that the second Wittig coupling became very sluggish and did not afford product **129**.

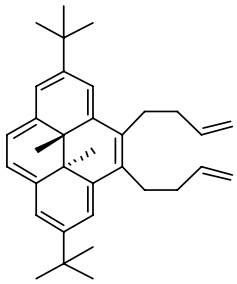
Griffin[235] has used the Wittig reaction in construction of macrocycles from (o-bromomethylbenzyl)triphenylphosphonium bromide in good yields. However, undesired transformations often occurred.

o-Phthalaldehyde was chosen as an *ortho*-diformyl substrate model to mimic the reaction for the 4,5-DHP dialdehyde **116**. Karatholuvhu and Fuchs[236] reported that using sodium hexamethyldisilazane (NaHMDS) with o-phthalaldehyde and 3,3,3-

trichloropropyl-1-triphenylphosphorane afforded alkenes with high *Z*-configuration selectivity in excellent yields. The product from the Wittig reaction of **37** and allyl triphenylphosphorane was expected to be the 4,5-*bis*-1,3-butadienyl-dimethyldihydropyrene **130**. However, the yield was poor in our hands under a variety of

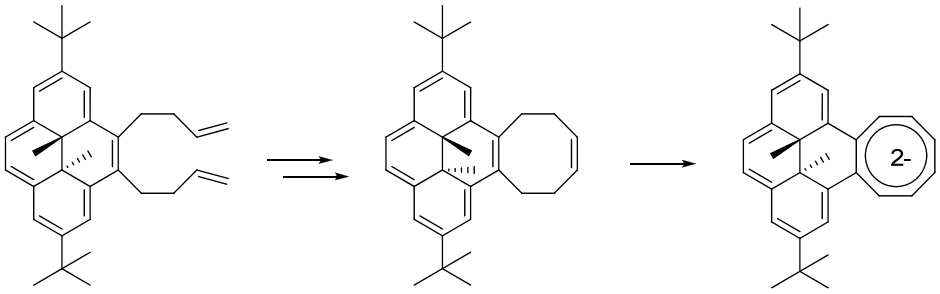


130



131

conditions. Since the yield of **130** was poor, we thought that the partly saturated **131** might be a better choice since ring closure to **122** would have less geometric constraints. Conversion of the COD-fused dimethydihydropyrene **122** to the dianion **20** (Scheme **64**) should be possible using a procedure like that shown in Scheme **51**.



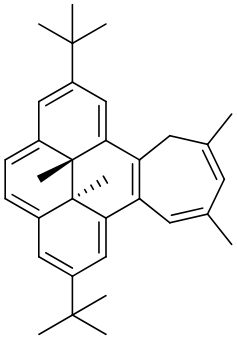
131 **122** **20**

Scheme 64.Proposed synthetic route to DHP-fused COT 122

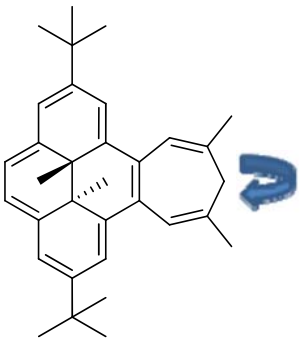
4.4 Variable temperature NMR studies

4.4.1 Ring flipping studies associated with the cycloheptatriene ring

The 3,4-DHP[e]fused 1,6-dimethylcycloheptatriene **108** possesses high symmetry at room temperature in the NMR spectrum, and suggests that the cycloheptatriene undergoes a fast ring inversion process. Anet[256] observed the coalescence of the two methylene protons of cycloheptatriene at -150°C. The activation energy was determined as *ca*. 6.3 kcal/mol.



107



108

As the crystal structure (Figure **40** on page **168**) show for **108**, the CH_2 is puckered by 84.61° with respect to the DHP plane in the solid state. The C-C distance between carbons of the methylene C30 and of the internal methyl is 4.988(3) Å. Therefore no significant NMR impact on the internal methyl protons from the methylene carbons. However the two double bonds are bent towards one face of the DHP. Their shielding zones would likely distinguish the protons of the two internal methyl groups. In solution, at room temperature, only one peak for the internal methyl protons appears, which indicates fast flipping of the methylene unit is taking place. When the NMR sample was cooled, the signal for the internal methyl protons broadened and then split (Figure **43**). From the coalescence temperature of 178K and a separation of 33 Hz, the inversion barrier $\Delta G^{\ddagger}_{c}$ was calculated to be 8.7 kcal/mol. This is slightly greater than Anet's 6.3 kcal/mol for cycloheptatriene itself.

$$\Delta G^{\ddagger}_{c} = 1.912\times10^{-2}\times Tc\times[9.972+\log(Tc/\delta)]\ \text{in kJ/mol} \qquad \text{Equation } \mathbf{1}$$

$$\Delta G^{\ddagger}_{c} = 1.912\times10^{-2}\times178\times[9.972+\log(178/33)] = 36\ \text{kJ/mol} = 8.7\ \text{kcal/mol}$$

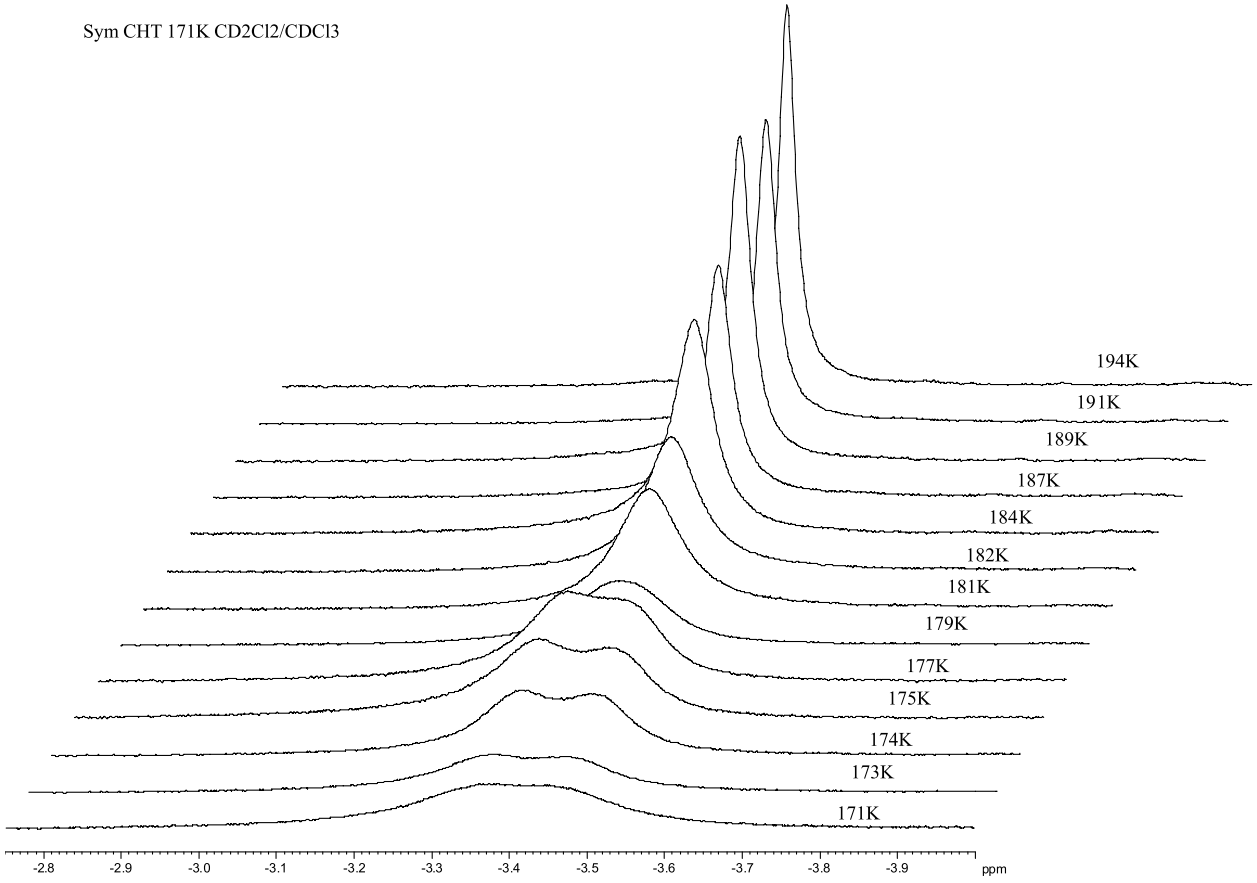


Figure 43. The VT NMR spectra for the symmetrical DHP-fused CHT 107 in $CDCl_3$ and CD_2Cl_2 (1:3) (internal methyl proton region)

It is not obvious whether viscosity effects or a further process induce line broadening below 174°C. In the full VT NMR spectra (Figure **44**), no other protons changed significantly enough to add additional data.

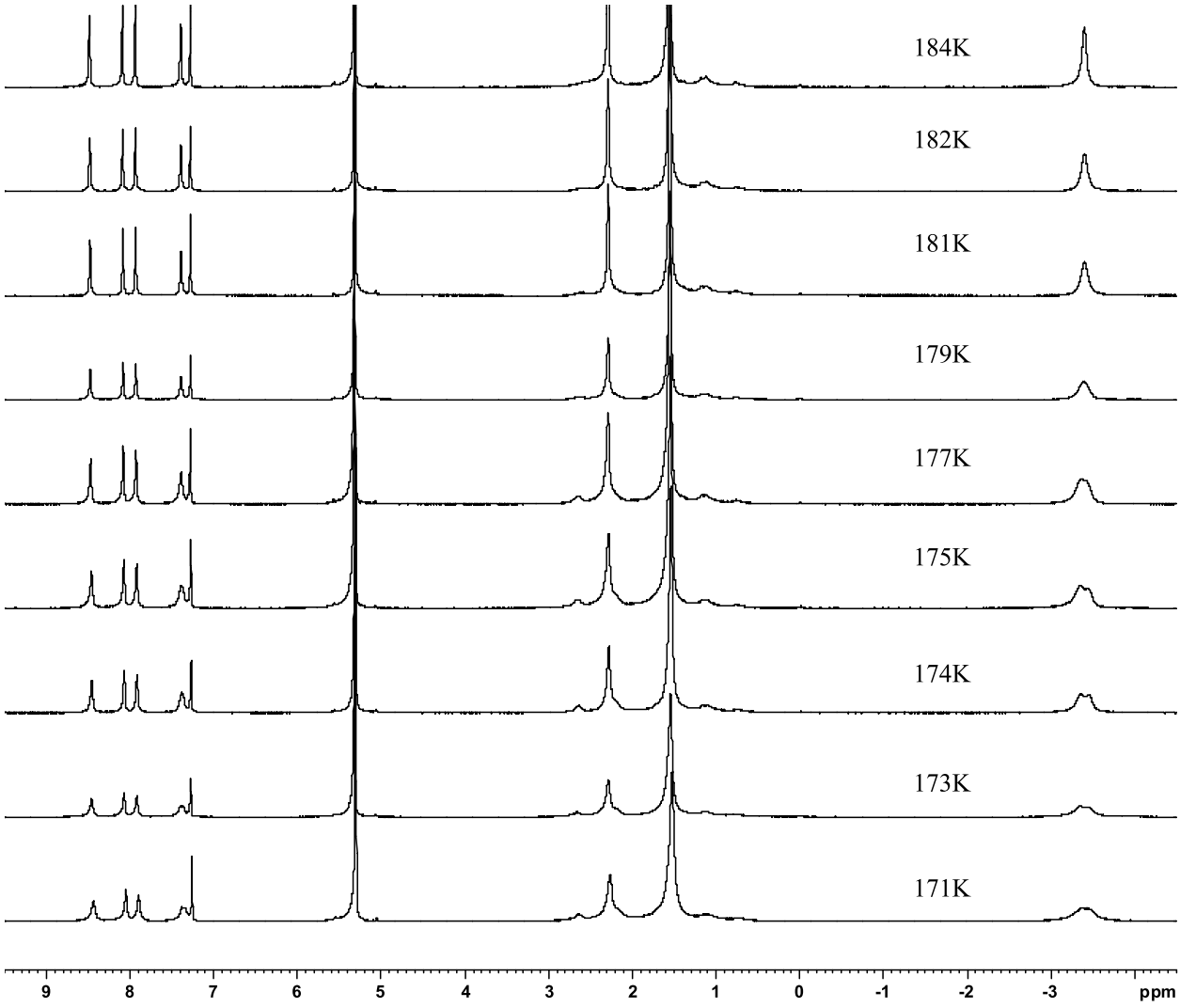


Figure 44. The full range spectra of DHP-fused CHT 108 in low temperature VT NMR experiments in $CDCl_3$ and CD_2Cl_2 (3:1)

Similar low and high temperature VT NMR experiments were also tried on isomer **107** but no such changes for the internal methyl groups were observed. One might anticipate that ring flipping of isomer **107** would require more energy than for isomer **108** because the CH_2 hydrogens would have to pass lose to the H-3 proton on the DHP. Analogously, in the DHP-fused asymmetrical diphenyl CHT **117**, the variable temperature ^1H NMR experiments disclosed two doublets for the protons of the CH_2 that broadened and sharpened with decreasing temperature as shows in Figure **45**. The lower symmetry of

107 and **117** means that two CH_2 resonances are observed at all temperature but the observation of broadening between two regions with sharp doublets indicates a fluxional process is operation here as well.

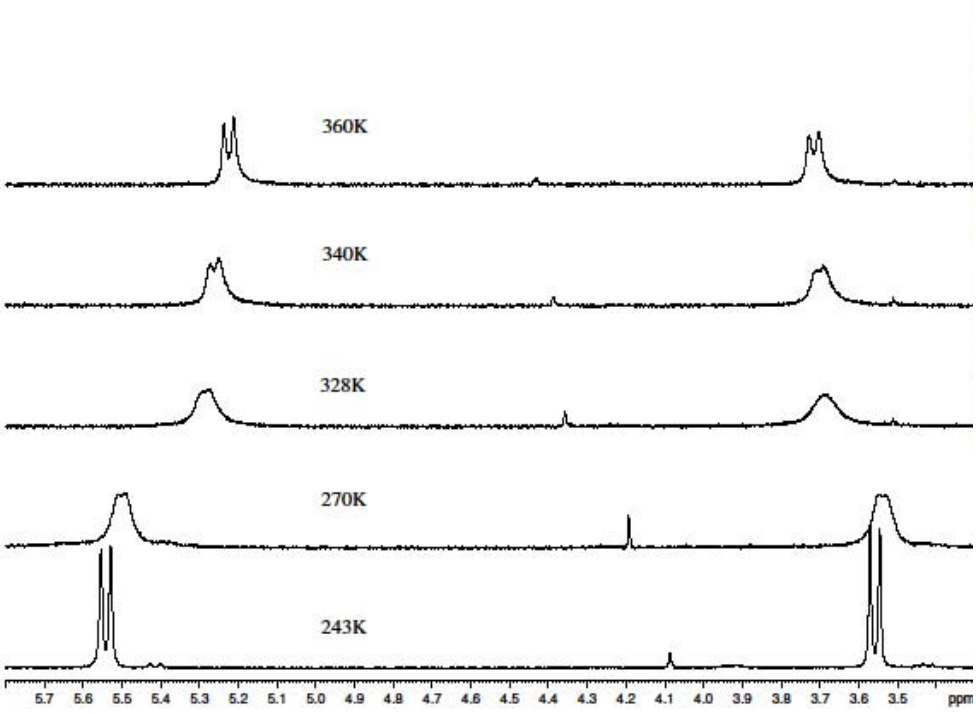
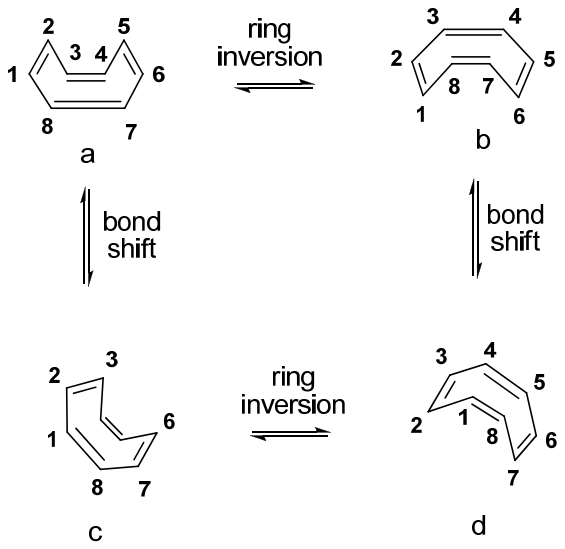


Figure 45. The variable temperature NMR spectrum of 117

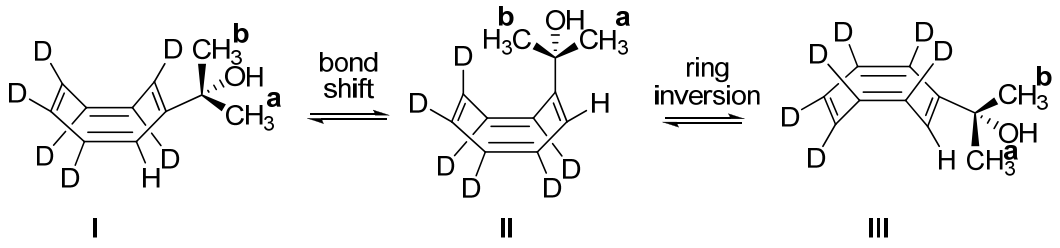
4.4.2 Ring flipping of the C8 ring in the DHP[e]fused cyclooctatetraene 121

The fluxional behaviour of cyclooctatetraene has attracted much attention since the 1950's and because it occurs on the NMR time scale (10^{-2} to 10^{-4} s), NMR spectroscopy has provided insight into the processes. According to the NMR studies by Anet,[257] there are two distinguishable processes associated with inter-conversion: ring inversion and single and double bond shifting[258] (Scheme **65**).



Scheme 65. The fluxional processes of cyclooctatetraene

On cooling, both the coupling constants and the nuclei couplings appear to change because both of these processes slow. Further investigation was carried out by modifying the molecule by the addition of a handle, which was then followed by NMR spectroscopy (Scheme **66**).



Scheme 66. Substitution of cyclooctatetraene

The bond shifting process between **I** and **II** in Scheme **66** was examined by observing the position of the ring substituent $(CH_3)_2(OH)C$-. The chemical shift of the proton H was

different when it was on a di-substituted double bond in I, or on a tri-substituted double bond in **II**. Upon warming the sample, the signals due to the ring protons in **I** and **II** coalesced. On the other hand, the ring inversion was reflected by monitoring the inter-conversion of the two diastereotopic methyl groups ($-CH_3^{\mathbf{a}}$ and $-CH_3^{\mathbf{b}}$) by ^{1}H NMR between **II** and **III**, Scheme **66**. For example, $-CH_3^{\mathbf{b}}$ is in a different magnetic environment when it sits inside the ring (**II** in Scheme **66**) from outside of the ring (**III** in Scheme **66**). Under a fast ring inversion condition, the two states are undistinguishable. Note that the H remained on a di/tri-substituted double bond during the process. It was concluded that, at -2°, the barrier for bond shifting has an activation energy 17.1 kcal/mol, while that for ring inversion is 14.7 kcal/mol. Presumably the activation energy indicated the stability of the corresponding transition states. Therefore the transition state for the inversion process was *ca*. 2 kcal/mol more stable than that for bond shifting.

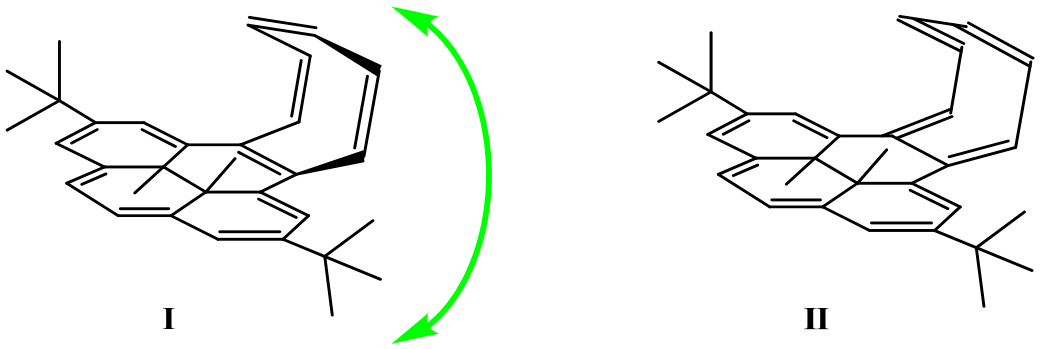


Figure 46. The ring inversion model for the DHP-fused COT 121

It is important to note that DHP is an excellent probe to investigate these two mechanisms. As drawn in Figure **46**, the COT and the DHP in **121** share a double bond, then the 14π electrons of DHP can be fully delocalized in its framework because the alternate single and double bonds can shift freely. In contrast, if bond shifting took place in the COT moiety of the DHP-fused COT molecules, the delocalization of the 14π DHP unit is inhibited, and now the conjugation circuit is along the periphery, a 20 π system. The chemical shifts of the internal methyl protons in compound **II** in Figure **46** would be

expected to be downfield and close to δ 0.16 of isofuran **98**. This loss of aromaticity of the DHP unit would be expected to completely inhibit the bond shift process.

The VT NMR spectra for **121** are shown in Figure **47**. The chemicals shifts of the internal methyl protons remain at -3.8 ppm during the whole process, indicative that only the ring inversion process is occurring. The internal methyl protons change from a singlet at 298K to two singlets at 255K with the coalescence temperature of 278 K and $\Delta\nu$ = 40 Hz, corresponding to an inversion energy of 13.9 kcal/mol.

$$\Delta G^{\ddagger}_{c} = 1.912\times10^{-2}\times280.5\times[9.972+\log(280.5/40)] = 58 \text{ kJ/mol} = 13.9 \text{ kcal/mol}$$

The calculated energy barrier is close to the reported 14.7 kcal/mol for the ring inversion mechanism.

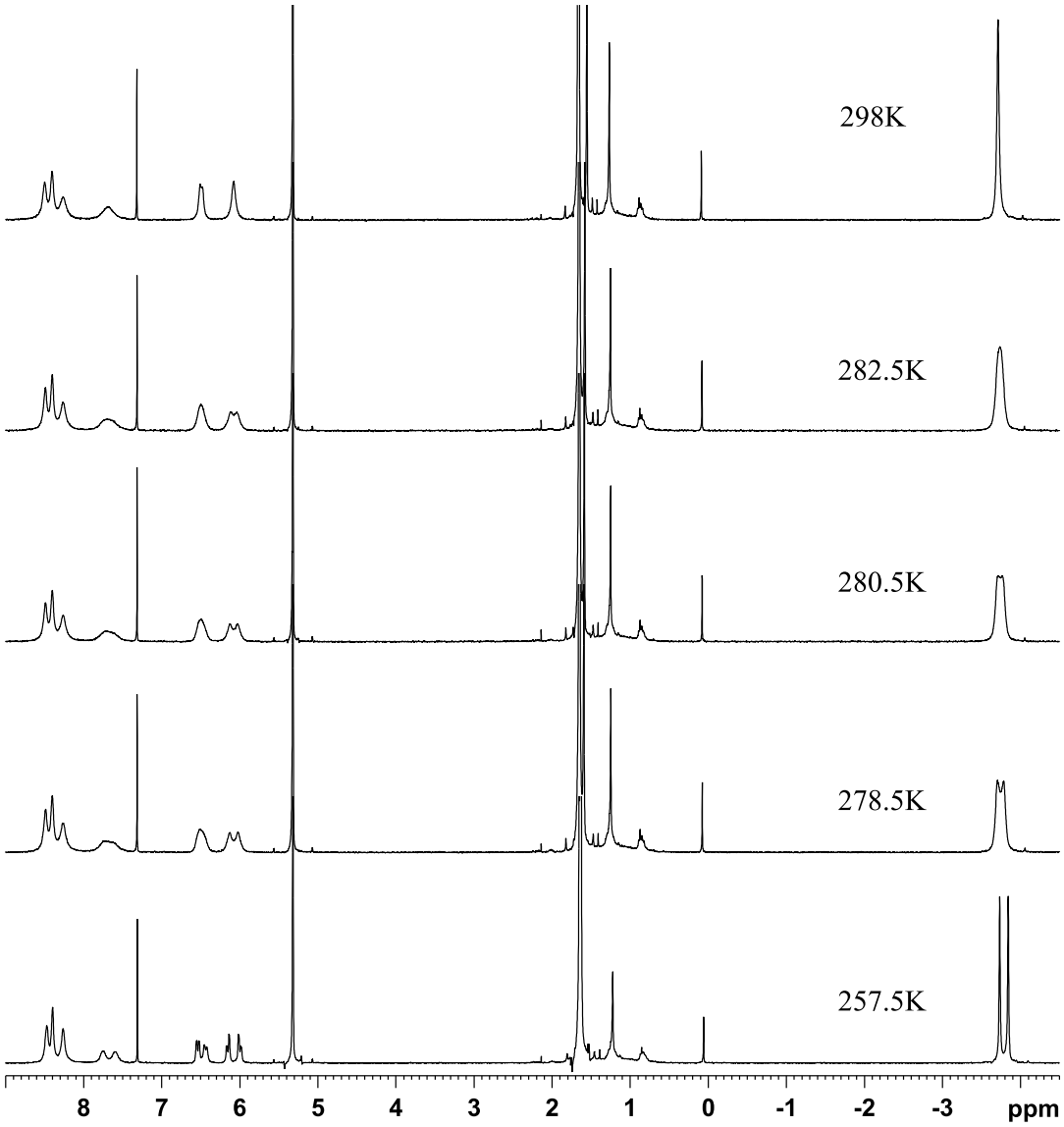


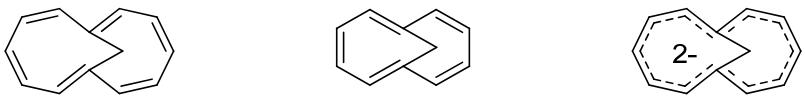
Figure 47. The VT NMR spectrum of 121 (full range)

4.5 Aromaticity

4.5.1 Relative aromaticity based on NMR chemical shifts

As mentioned earlier in the Introduction, resonance energy (RE) is an essential criterion to define the aromaticity of a system. The heat of hydrogenation approach to

determine RE often faces difficulties in finding an appropriate hypothetical reference structure. Haddon[259] has shown that resonance energy is proportional to the ring currents in a given system, which can be measured using the NMR technique. In an applied field, circulation of the π-electrons causes an induced magnetic field, which tends to oppose the applied field inside the cyclic aromatic system and to align with the applied field outside the ring. Thus any internal protons are strongly shielded and any external protons are deshielded. As a result, the internal protons resonate at a higher magnetic field and the external at lower magnetic field than those in non-aromatic systems. The magnitude of the shifts depends on the strength of the ring current. A stronger ring current shifts the given protons more and *vice versa*. The ring current in such a $(4n+2)\pi$ system is called diatropic. In a $(4n)\pi$ system, which has opposite effects the ring current is called paratropic. Two examples illustrating the different effects are the 12π electron 1,7-methano[12]annulene **136**[260] and the 10π electron 1,6-methano[10]annulene **137**[261]. The former has the bridged CH_2 resonance δ 6.06, while the latter is at δ -0.52. when 2e are added to **136** to convert to the 14π electron diatropic dianion **138**, the CH_2 resonance is now at δ -6.44 at (-80°C), shifted by 12.5 ppm upfield by the diamagnetic ring current.[260a]



136 **137** **138**

Figure 48. Bridged [12]- and [10]-annulene

Joining two aromatics by a single bond as in biphenyl, only introduces a small perturbation to the π-system. However, fusing two aromatics, such as benzene to DHP causes dramatic ring current changes of each, proportional to the bond localization energy of each. Thus comparison of the change in chemical shifts of the internal methyl protons on annelations with a variety of aromatics allows an estimation of relative bond

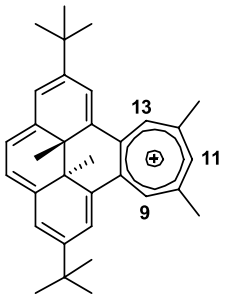
localization energy, and when the change is compared to that caused by benzene leads to aromaticity scale relative to that of benzene.

Local electron density of nuclei also is one of the important factors that usually shows shielding effects in NMR measurements. Having positive charge on a nucleus decreases the local electron density and thus causes deshielding effects, while negative charge cause shielding effects. In 1,7-methano[12]annulene dianion **138** the peripheral protons resonated at δ 7.16, 6.28 and 6.41 (the center proton) upfield from normal aromatic protons. The deshielding effects of positive charges shift the external protons of an aromatic ring in the same direction as the ring current does. Thus charge and ring current effects account for the strong downfield shift of the protons of the tropylium cation to *δ* 9.2. In contrast, the external protons of cyclopentadienide anion resonate at *δ* 5.6, which is upfield due to the shielding effects of the negative charge.

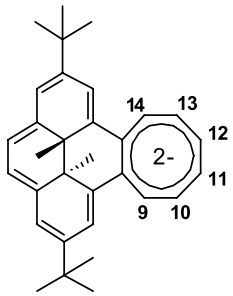
Schneider[262] has established a relationship between chemicals shifts and electron density. Having one charge in a conjugated system would account for a total chemical shift of about 10.6 ppm for the proton and about 200 ppm for the carbon nuclei. The proton chemical shifts of *δ* 9.2 for the tropylium cation and of *δ* 5.6 for cyclopentadienide anion can be explained as being shifted by 1.5 ppm and 2.1 ppm respectively from the calculated *δ* 7.7 of benzene because the charge are to be evenly distributed in the two systems (i.e. 10.6/7 = 1.5 ppm per proton in the tropylium cation). The assumption is that the ring current deshielding effects are equal in tropylium cation, Cp anion and benzene. A similar phenomenon was observed for the carbon-13 chemical shifts. The ^{13}C NMR signals were at δ 156.1 and 102.8 for tropylium cation and cyclopentadienide anion, respectively.[262] In a more complicated, large system, uneven distributions of charge might take place and caution is necessary.

Some additional points need to be addressed here. Previous studies have shown that fused aromatics deshield the internal methyl protons through-space by less than 0.1 ppm in DHP as the deshielding effects diminish quickly with distance.[263] The chemical shifts of the internal methyl protons are affected little (< 0.3 ppm) by *σ*-bonded substituents.[264] For example, having two *t*-butyl groups on the 2- and 7- positions causes the internal methyl protons to shift from *δ* -4.25 in the parent DHP 1 to *δ* -4.06 in the DHP 2.

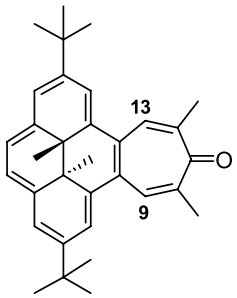
Here our results for aromaticity estimates of tropylium cation, cyclooctatetraene dianion and tropone are included. Selected ^{1}H NMR chemical shift data for DHP[e]cyclooctatetraene dianion, **20**, DHP[e]tropylium cation, **18**, and DHP[e]tropone, **17**, are shown in Table **23**. BDHP 3 and Cp anion **12**[56a] are also included for comparison. The non-conjugated model molecule is the bridged dihydro[14]annulene **135**, whose chemical shift of the internal methyl protons is δ 0.97.[265] The DHP-fused heptene **110** was chosen as the probe DHP molecule for tropylium cation **18** and DHP-tropone **17**, which has a *ca*. +0.2 ppm difference from the DHP 2, presumably due to the substitution effects. Since there is no good reference for DHP[e]COT dianion **20**, DHP-fused heptene **110** is also used in the calculations for **20**.



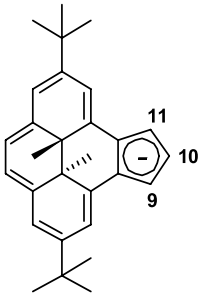
18



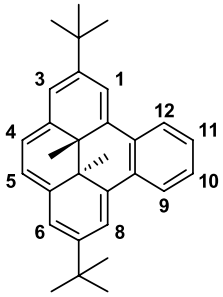
20



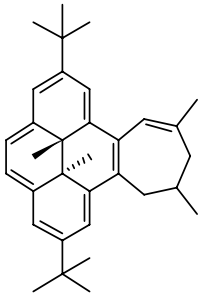
17



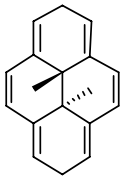
12



3



110



135

Table 23. Selected chemical shifts (δ) in some DHP-derived aromatic systems

	Cp anion **12**[56a]	COT dianion **20**	tropylium cation **18**	DHP tropone **17**	BDHP 3[41]	DHP 2	DHP heptene **110**
H-1,8	7.62	7.18	9.78	9.16	8.28	8.58	N/A
H-3,6	7.02	6.70	8.10	8.41	7.35	8.58	N/A
H-4,5	6.84	6.64	7.62	8.26	7.13	8.46	*ca*.8.34
H-9	6.98	7.37	10.5	9.27	N/A	N/A	N/A
t-Bu	1.48	1.47	1.68	1.70	1.49	1.67	*ca*.1.68
internal Me	-1.82	-1.38	-2.61	-3.56	-1.58	-4.06	-3.87[a]

[a] the average chemical shifts for two isomers (major: δ -3.83, -3.90 and minor: δ -3.85, -3.88).

The annelation of an aromatic system on DHP causes partial bond fixation and reduces the ring current. The extent of ring current deduction is calculated:

$$\text{Ring currents changes (\%)} = \frac{\delta(compound) - \delta(control)}{\delta(standard) - \delta(control)} \times 100\%;$$

For tropylium cation, the percentage of ring currents changes in **18** is

$$= \frac{\delta\,(18) - \delta\,(110)}{\delta\,(135) - \delta\,(110)} \times 100\% = \frac{-2.61 - (-3.87)}{0.97 - (-3.87)} \times 100\% = 26\ \%;$$

Compare to DHP, annelation of benzene in 3 reduces ring current of DHP by

$$= \frac{\delta\,(3) - \delta\,(2)}{\delta\,(135) - \delta\,(2)} \times 100\% = \frac{-1.58 - (-4.06)}{0.97 - (-4.06)} \times 100\% = 49\ \%;$$

Thus the relative bond localizing ab ilities of tropylium cation relative to benzene is

$$\% = {}^{26\ \%}/_{49\ \%} \times 100\% = 53\ \%.$$

Similar calculations are executed to afford the bond localization ability of the aromatics relative to benzene. They are summarised in Table **24**.

Table 24. The bond localization ability of the aromatics relative to benzene using heptene-fused DHP 110 as the reference

COT dianion **80**	Tropylium cation **15**	Tropone **79**
105%	53%	13%

When the DHP (δ -4.06) is used as the probe, the bond localization ability of of tropylium cation **15** relative to benzene is 59%.

4.5.2 The influence of charge

The changes in ring currents should also change the shifts of the external protons. A linear relationship[41] was established between the shift of internal methyl protons and the shift of most distant external protons, H-4,5 for DHP, if there were no other influences as below.

δ (internal Me) = 13.050 – 2.038 δ (H-4,5). Equation **1**

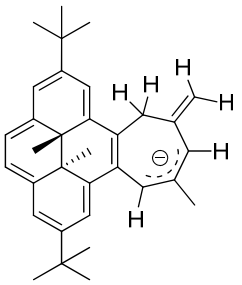
Delocalized charge should affect the peripheral protons more than the internal methyl protons, and so using the above equation, we can calculate the chemical shift for H-4,5 based on that found for the methyl protons, and by comparison to the actual shifts have an idea of the extent of charge delocalization in **20**, **18** and **17**. The calculated and experimental data are showed in Table **25**.

Table 25. The calculated and experimental chemical shifts for H-4,5

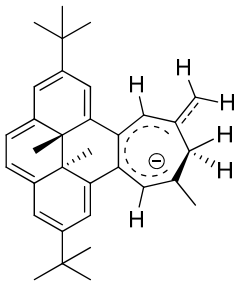
	DHP-COT dianion **20**	Calculated *δ*	tropylium cation **18**	Calculated *δ*	DHP tropone **17**	Calculated *δ*
H-4,5	6.64	*7.08*	7.62	*7.68*	8.26	*8.15*

The actual chemical shifts for H-4,5 in the dianion **20** are 0.44 ppm upfield from the calculated chemical shifts (δ 7.08) indicative that partial delocalization of the dianion's charges do shift the protons upfield. If the two negative charges were evenly distributed over the 20 carbons, the upfield shift should be around 1 ppm (10.6 ppm for each charge based on Schneider's work) and so our value suggests that about 45% is distributed. In COT dianion **20**, H-11, which are somewhat deshielded through-space by the annelated DHP, resonates at δ 6.10, which is close to δ 5.7 in cyclooctatetraene dianion $C_8H_8^{2-}$ **80**. Since the chemical shifts are determined mainly by the shielding effects of charges and paratropic deshielding effects, the comparable values, 6.1 vs 5.7 for **20** and **80**, respectively, could support that the majority of charges stay in the COT moiety in the dianion **20**. The calculated and experimental chemical shifts for H-4,5 for cation **18** and tropone **17** fall within experimental error.

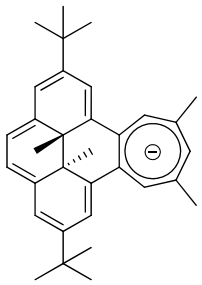
4.5.3 Cycloheptatrienyl anions 111, 112 and 19



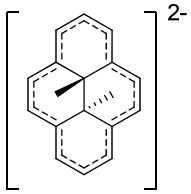
111



112



19



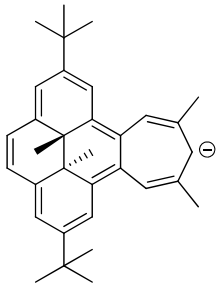
139

A (4n)π DHP-derived paratropic system **139** was investigated [266] and showed a strong paratropic deshielding of the internal methyl protons, which resonated at δ 21, where the external peripheral protons were shielded to δ -3.2 to -4.0. However, when only partial negative charge is delocalised onto the DHP system, the effects to the internal methyl protons are insignificant. The chemical shifts for the internal methyl groups and peripheral protons in anions **111**, **112** and **19** are tabulated in Table **26**.

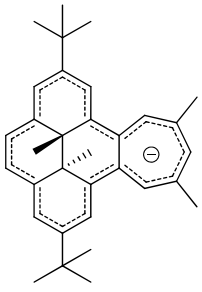
Table 26. Selected chemical shifts (δ) for cycloheptatrienyl anions 111, 112 and 19

	Anion **111**	Anion **112**	Anion **19**
H-1, H-8	8.20, 7.25	7.26, 6.32	5.54
H-3, H-6	7.42, 7.15	6.59, 6.14	5.03
H-4, H-5	7.31, 6.93	6.43, 5.90	4.87
t-Bu	1.58, 1.53	1.32, 1.31	0.92
Internal Me	-2.52, -2.67	-0.80, -0.84	2.10

The anion **112** shows larger shielding effects to the external peripheral protons and deshielding to the internal methyl protons than anion **111**. In anion **111** delocalization of charge into DHP is not required, to stabilise the anion but may happen, in which case delocalization of the DHP is reduced as when any delocalization system is fused, and so reduces the DHP ring current. In **112**, delocalization involving DHP is required to stablise the anion which severely reduces the ring current of the DHP. However, in the anion **19**, the internal methyl protons are deshielded from those of the acylic model **135** (δ 0.97) to 2.10 indicative of a paratropic ring current, which would shield external protons. Anion **19** is thus better represented as **19a**.



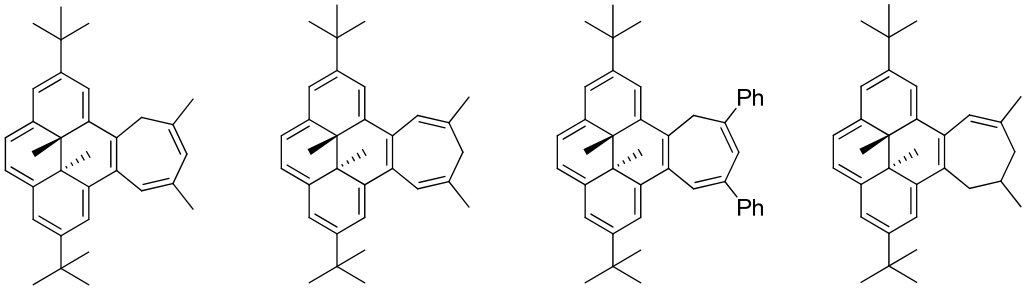
19



19a

4.5.4 The homo-aromaticity of 1,2-DHP[e]fused 4,6-dimethylcycloheptatriene 108

The ^{1}H NMR data for the asymmetrical and symmetrical cyclohepta-2,4,6-triene isomers **107**, **108** and **117** are shown in Table **27**. The chemical shifts for **107** and **117** are very similar, indicating the negligable effect of changing methyl to phenyl groups. For example H-8 appears at δ 8.79 in **107** and at δ 9.04 in **117** suggesting only a small deshielding effect of the phenyl substituents. The major difference between **107** and **117** occurs for the CH_2 group which is more shielded for **117**, possibly because of the orientation of the phenyl group.



107 **108** **117** **110**

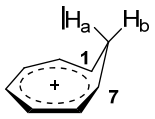
Table 27. The ^{1}H NMR data (δ) for 107, 108 and 117.

	13-H,H-CHT **107**	11-H,H- CHT **108**	Diphenyl CHT **117**	**110**
H-1, H-8	8.80, 8.79	8.59	8.85, 9.04	8.60, 8.74
H-3, H-6	8.36, 8.35	8.16	8.38, 8.45	8.44, 8.43
H-4, H-5	8.24, 8.20	8.00	8.25, 8.24	8.41, 8.31
t-Bu	1.70, 1.69	1.63	1.75, 1.73	N/A
-CH_2-	4.38, 3.04[a]	2.53	3.58, 2.48	N/A
Internal Me	-3.65, -3.89	-3.32	-3.62, -3.93	-3.87[b]

[a] the coupling constant for the bridge CH_2 is J = 12.4 Hz; [b] the average chemical shifts for two isomers (major: δ -3.83, -3.90 and minor: δ -3.85, -3.88)

If calculations for **108** similar to those we made for cation **18** are carried out, then a 24% relative bond fixing ability (compared to benzene) is found, which is larger than the 13% found for tropone. However, when the DHP is fused to the other position of the C7 ring as in **107** and **117**, calculations give only a 4% bond localization ability relative to benzene. This much lower efficiency compare to **108** might be due to the poorer conjugation in **107** and **117** when fusing the double bond next to the bridging CH_2.

One criterion of homoaromaticity is the bond separation of C1 and C7. In **83** for example, it is found to be only 2.28 Å[267]. In **108**, the separation between C28 and C31 is 2.431 Å and in **117** 2.433 Å (Table **28** on page **194**). Both of these are shorter than the sum of the van der Waals radii (3.40 Å), but slightly longer than the separation in **83**. Both of these results suggest that 77 is showing some homoaromaticity effects.



83



77

While it is difficult to estimate the exact chemical shifts of H_a and H_b (Figure **49**), a homoaromaticity component for the C7 ring would be expected to shield H_a relative to H_b. Assuming the through-space effects of the DHP ring are small, one might be able to estimate, using the Johnson-Bovey equation,[268] the degree of shielding of H_a if its position relative to the centroid of the 6π-C7 ring is known.

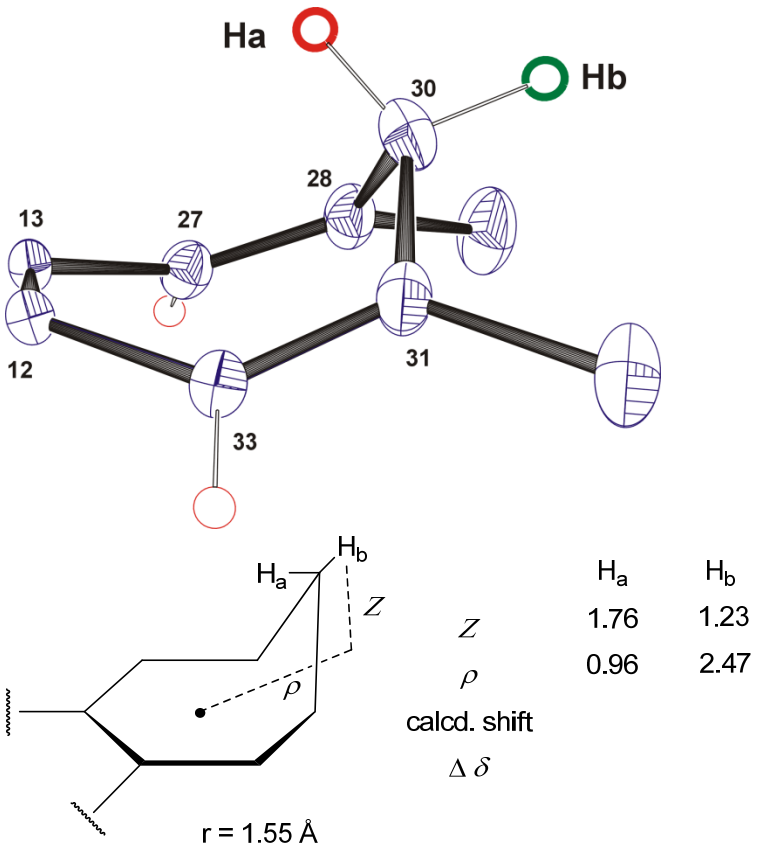


Figure 49. ORTEP3 plot for 11-H,H-cyclohepta-2,4,6-triene 108 (The DHP moiety and hydrogens on the methyl groups were omitted for clarity)

The measurements for **108** were accomplished taking by including C12, C13, C27, C28, C31 and C33 as the basal plane (Table **28**). The radius was calculated by averaging the distances between the centroid to the six above carbons. ρ is calculated from the distances of H to the plane and to the centroid on the basis of Pythagoras theorem as shown in Table **29**. The data for **117** were obtained in the same way and area included Table **29**.

Table 28. Distances in cyclohepta-2,4,6-triene 117 and 108

Number	Object1	Object2	**117**	**108**
1	centroid	C13	1.362	1.407
2	centroid	C27	1.602	1.504
3	centroid	C28	1.731	1.731
4	centroid	C31	1.756	1.740
5	centroid	C12	1.386	1.402
6	centroid	C33	1.533	1.500
7	H_a	plane	1.714	1.760
8	H_a	centroid	1.919	2.004
9	H_b	plane	1.282	1.229
10	H_b	centroid	2.728	2.762
11	C28	C31	2.433(6)	2.431

Table 29. Distances in cyclohepta-2,4,6-triene 117 and 108

	Distances (Å) **117**	Distances (Å) **108**
r	1.562	1.547
ρ (H_a)	0.863	0.958
Z (H_a)	1. 714	1.760
ρ (H_b)	2.408	2.474
Z (H_b)	1. 282	1.229

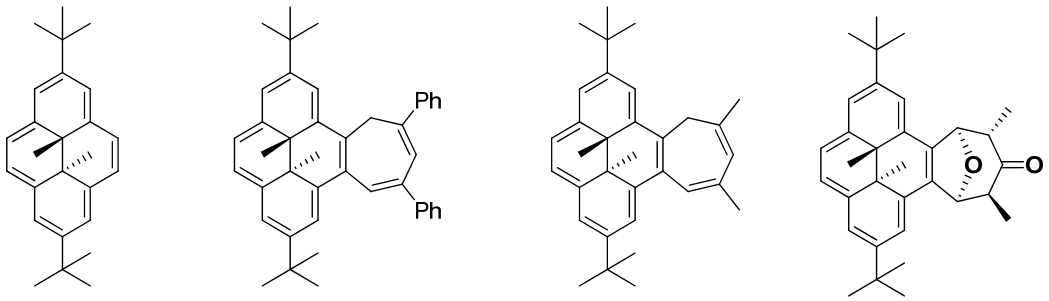
The structural data [268] for **108** were used to estimate the chemical shifts of H_a and H_b with H_a being shielded by *ca*. 2 ppm from H_b. Due to the small inversion energy (8.7 kcal/mol) of the cycloheptatriene **108**, in contrast to that of 93.3 kcal/mol in the

homotropylium cation **83**,[267b] the chemical shifts H_a and H_b coalesced at δ 2.53 even at 170K. However for **107** the protons resonate at δ 4.38 and δ 3.04, a difference of 1.4 ppm, and for **117** at δ 3.58 and δ 2.48, a difference of 1.2 ppm. Considering the assumptions made, these are in quite good agreement with the 2 ppm difference suggested by the Johnson-Bovey calculation, which of course is based on a benzene ring.

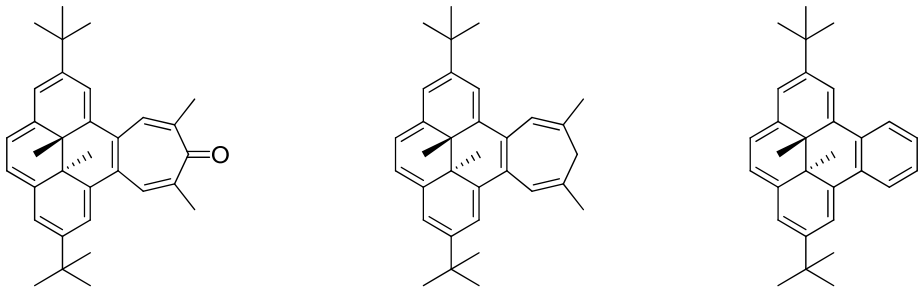
The sum of the moduli for the deviation of bond length from average bond length for the 14π periphery is 0.151 Å in **117** and 0.361 in **108** indicative of the stronger bond localization in the latter, which was consistent with the chemical shifts of the internal methyl protons (δ -3.62 and -3.93 in **117** and -3.32 in **108**).

Calculations in Table **24** have shown that tropone **17** and cycloheptatriene **108** have 13% and 24% relative aromaticity to benzene, respectively, based on the chemical shifts of the internal methyl protons. Similar calculations on the average chemical shifts of δ -3.77 for **107** and δ -3.78 for **117** give *ca*. 4%, which is much less than the 24% ring current reduction in **108**. A large interplanar angle of 29.01° was found between the planes defined by the 14 DHP peripheral carbons and by the six sp^2 hybridized carbons of the C7 moiety in **117**, while this was only 13.9° in **108**. Thus the DHP π-orbitals may not align as efficiently with those of the C7 unit for **117** resulting in poorer conjugation. Therefore, the lower calculated aromaticity of **117** vs. **108** may not be due solely to aromatic effects. However, the lower ring current calculated deduction in **117** vs. **108** is consistent with the X-ray data. The sum of the modulus of the deviations from the average bond length over all 14 periphary bonds is only 0.151 Å in **117** in contrast to 0.361 Å in **108** (Table **30**). The 0.361 Å in **108** is higher than that of the tropone **17** (0.307 Å), which indicates that cycloheptatriene **77** is a stronger aromatic system than the tropone in **17**. The C-O bond distance in **17** 1.227(2) Å is shorter than the average C-O bond distance of 1.244 Å from the CSD database and is comparable with the *ca*. 1.232 Å distance in benzo[e]tropones found by Ibata[269]. These results are consistent with the NMR calculations, thus it can be concluded that both bond alternations and chemical shifts data of the internal methyls realistically reflect the aromaticity of the aromatic systems fused to the DHP core. Caution must be taken when asymmetrical and non-planar systems are involved. The annelation of a bicyclic ring on the side of DHP as in **99B** the ring current substantially alters as is evident from both the sum of the peripheral

bond alternations 0.271 Å (Table **30**) and chemical shifts of the internal groups (δ -3.75 and -3.78) [255].



2 **117** **107** **99B**



17 **108** **3**

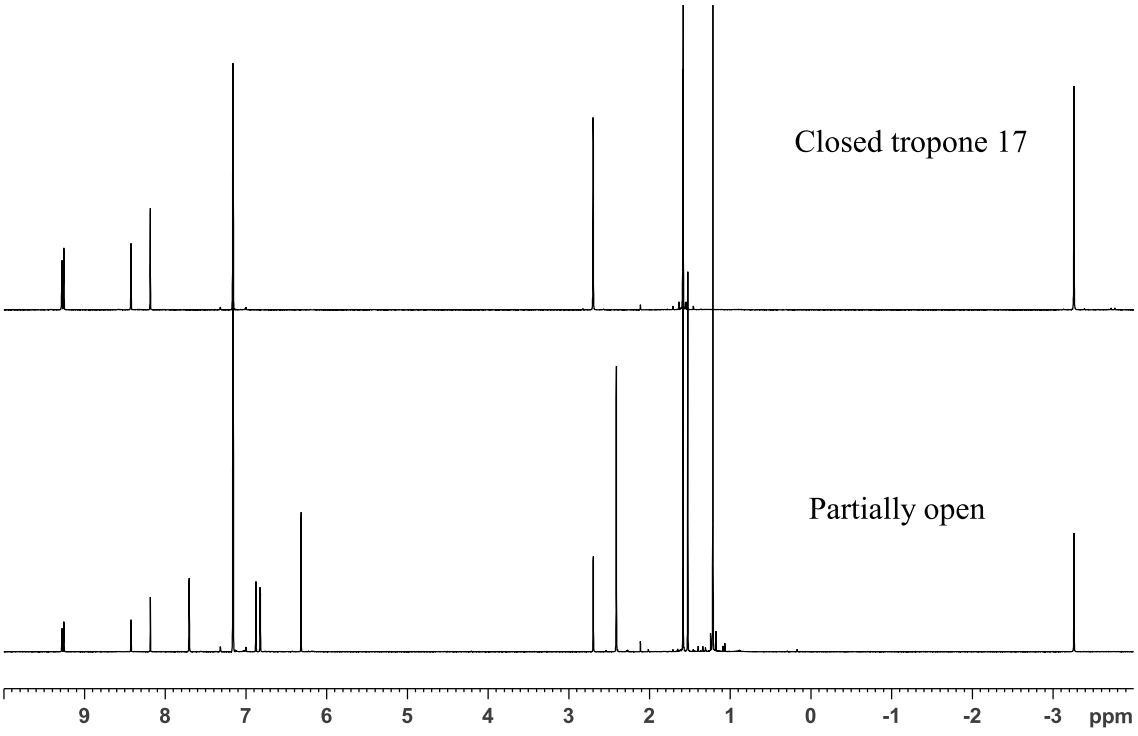
Table 30. Bond alternation (Å) in 17, 99B, 108 and 117

Molecule	Ave. bond length	Total deviation[a]	Chemical shifts internal methyl	Aromaticity relative to benzene
DHP 2	1.3936	0.069	-4.06	0%
Diphenyl CHT **117**	1.401	0.151	-3.62, -3.93	4%
DHP **99B**	1.395	0.271	-3.75, -3.78	N/A
Tropone **17**[b]	1.402	0.307	-3.56	13%
Dimethyl CHT **108**	1.398	0.361	-3.32	24%
BDHP 3	1.4044	0.539	-1.5	100%

4.6 Photochemistry

Only tropone **17** showed photoopening and closing at a slow rate; no photochemical properties have been seen for the other DHP derived compounds in the chapter.

When the NMR sample **17** in $CDCl_3$ was irradiated with visible light, the oxygen adduct **134** formed, which has been observed for other slow photochromic compounds[103]. When a sample in C_6D_6 was irradiated for 15 h at room temperature in the absence of oxygen, the tropone **17** opened to an extent of about 75%, at a rate slower than acetyl DHP. After that point, the thermal back reaction dominated and no further conversion was obtained. The open form closed completely. The thermal closing rate was found to be close to the acetylDHP with a half life 28 h (the plot is in appendix **II**). The switching was repeated five times with no observable decomposition.



4.7 Conclusion

In this chapter, DHP[e]tropone, **17**, DHP[e]tropylium cation, **18** and DHP[e]cyclooctatetraene dianion, **20** were synthesized to study the relative bond

localizing abilities of COT dianion **80** (105 % relative to benzene), tropylium cation **15** (55 % relative to benzene), tropone **79** (13 % relative to benzene) using DHP as the NMR probe. The anion **19** was best looked at as a 20π electron paratropic system. The diphenyl substituted CHT **117** and **118** were synthesized in order to access anion **113**, an analog of **19**, however deprotonation of **117** and **118** with $(CH_3)_3SiCH_2Li$ failed. The homo-aromaticity of the CHT isomers **107**, **108** and **117** was estimated based on the NMR data and X-ray structural data. Obvious anisotropic effects existed and the bond localization ability of the CHT (24% based on NMR data for **108**) may have a large error. The ring inversion barriers of the COT **82** and CHT **77** were measured using variable temperature NMR as 13.9 and 8.7 kcal/mol, respectively. The synthesis of DHP[e]cyclooctatetraene dianion encountered very low yields in the elimination step to DHP-fused COT **121** due to predominant ether cyclization side reactions. Five X-ray crystallography structures were obtained for **99B**, **17**, **108**, **117** and **125** and the information was used in estimating the bond localization abilities and in establishing absolute stereochemistry.

4.8 Future work

Tropylium cation **15**, CHT **77**, COT **82**, COT dianion **80** and cycloheptatrienyl anions are all used as ligands in transition metal complexes. We therefore would like to get insight into the corresponding metal complexes and to study the effects on aromaticity by complexing metals. So far, syntheses of metal complexes with these ligands have not been successful. Scale-up of the syntheses will probably be necessary to allow us to access such metal complexes.

Chapter 5. Conclusions

Mitchell's group, over the last four decades, has been focused on the studies of dimethyldihydropyrene as a photochromic switch and aromaticity probe. The low photoopening quantum yields and dark thermal reactions of CPDs are two issues that need to be addressed in some of their applications as photochromic compounds. To improve the photoopening efficiency, a variety of modifications on the internal and external substituents of DHP have been made. So far the benzene fused on the e-position of DHP, i.e. benzo[e]DHP **3**, has shown the best overall features. The modification with replace of the internal substituents with a 1,1-dimethylvinyl groups increases the photoopening quantum yield of 2-(1□-naphthoyl)-7-*tert*-butylDHP to 0.66 in toluene, which is the highest photoopening quantum yield among DHPs so far synthesized. Coordinating a metal fragment modulates the energy levels of the DHP-derived ligands possibly via metal-to-ligand or inter-ligand pathways. Therefore, this might change the interconversion of the excited states of the DHP chromophores so as to change their photochemical behaviour. This strategy has been demonstrated in the dithionylethene diethynylplatinum systems by Branda and Wolf while the research reported in my thesis was being conducted. Moreover, some metal complexes, such as the $CpRu^+$ fragment complexed to BDHP, **10**, can add electrochromic features to the DHP photochromic compounds due to the fact that different oxidation states of the metals are possible. So our goals were to make photochromic compounds with linkage of metal derivatives to study their impact on the photochromism.

Bis-DHP photochromic compounds containing a dialkynyl platinum linkage were synthesized to study the photochromism with changing electron features and configuration. *Trans* and *cis* square planar alkynyl platinum complexes were prepared with monodentate (PPh_3 and PEt_3) and bidentate (dppe, 2,2-bipyridinyl and 1,10-phenanthroline) ancillary ligands. Acyl DHP (CH_3CO, PhCO and 1-naphthoyl) and benzo[e]DHP ethynes were reacted with platinum chloride bearing the appropriate ancillary ligand giving rise to the desired products, whose identities were confirmed by mass spectrometry, NMR spectroscopy (^1H, ^{13}C, ^{31}P and ^{195}Pt) and IR. The molecular structure data for complexes **44**, **45**, **47**, **49**, and **52** were compared with known

complexes and the bond lengths and angles were found to be in the normal range. The photochemical and thermal closing properties were examined in comparison to the corresponding alkyne precursors. The photoopening rates were found to be about 4-6 times slower than the corresponding alkynes. The photoclosing of the CPDs to DHPs in the complexes occurred in comparable rates to the non-complexed alkynes. The open CPD thermally closed 2 times faster than the alkynes at room temperature. The dialkynyl platinum species absorb close to the UV region of the electromagnetic spectrum (400 nm visible light for the diphenylethynyl platinum complexes). Therefore, the absorptions due to the platinum moiety were not expected to interfere with the DHPs. The photoopening of the DHPs took place in the same way as isolated photochromic compounds indicating that there is negligible communication between DHP units via the diethynyl platinum bridge. However, the energy levels of the DHP photochromic compounds are altered in the complexes due to metal-ligand orbital mixing as revealed by the UV-Vis spectra. The forward photoopening and backward closing conversions reached completion in both directions when oxygen was kept out of solution. The thermal closing took place stepwise and an open-closed intermediate was observed by NMR spectroscopy. The closing rates for the first and second DHP are comparable, which again demonstrates the limited communication between DHPs across the platinum bridge.

Bis-DHP cobalt complexes bearing a Cbd-cobalt linkage were prepared from alkynes and $CpCo(CO)_2$. NMR and X-ray analysis revealed the formation of only the *head-to-head* regioisomers in the cyclization. Due to the internal methyls on the DHPs, three diastereomers were formed. These diastereomers can be partially separated for the Cbd-methyl derived complexes **21** by repeated chromatography and completely separated for the Cbd-ester complex **69**. The photoopening rates of the cobalt complexes were again found to be slower than the corresponding alkyne precursors by a factor of about 6.

C7 and C8 rings were fused to the DHP to study the aromaticity of tropone, tropylium cation and cyclooctatetraene dianion. These species are also known as ligands for transition metals, such as in uranocene, $U(COT)_2$ using the COT dianion. These compounds can be photochromic as aromatic systems e-fused often lead to new DHP derivatives with different photochromic properties based on previous results. The syntheses of the compounds were established by NMR spectroscopy, mass spectrometry

and for important intermediates, by X-ray crystallography. The aromaticity of the tropone, tropylium cation and cyclooctatetraene dianion was found to be 13%, 55% and 105% of benzene, respectively, as calculated from the chemical shifts of the internal methyl protons. When the cycloheptatrienes **107** and **108** were deprotonated by strong bases, three anions were formed from two different DHP cycloheptatriene isomeric precursors. The symmetrical DHP cycloheptatriene **108** gave rise to anions **112** and **19**, in which **19** was assigned as a 20π paratropic system with the internal methyl protons at +2.09 ppm. The anion **111** from the asymmetric DHP cycloheptatriene **107** formed by the deprotonation at the methyl positions on the C7 ring. The negative charges were delocalized mainly on the C7 ring in **111** and also into the DHP peripheral carbons in **112** according to the magnitude of the shift caused by the shielding effects on the internal methyl protons by the DHP ring current. The weak homoaromaticity of cycloheptatriene was also evident in DHP cycloheptatrienes **107** and **108** and was evaluated using the same method for the above aromatic systems. In all these compounds, an index of perturbation for the DHP ring current was established based on the chemical shift of the internal methyl protons when different species (charged or neutral) were fused to the e-position of the DHP. These results validate the 'Mitchell method'— using the internal methyl proton of DHP as aromaticity probe.

The photochromism of the C7/C8-derived DHP compounds were investigated using the same methods described in Chapter 2. The tropone-fused DHP **17** showed photochromic properties. It opened completely, but at a much slower rate than BDHP in sealed NMR tubes. Its thermal back reaction half life was found to be 28 h at room temperature. It is not obvious to us why the DHP-tropylium cation did not show appreciable photoopening upon irradiation with visible light. It could be that the presence of residual acid or other impurities quenched the photoreactions because extensive purification was not carried out. The syntheses of metal complexes of the DHP-cycloheptatriene were attempted with several Fe, Mo and Cr precursors. The failure of these trials might due to the low reactivity of the DHP derivatives with the metal precursors. We have not attempted to make complexes using the tropylium cation and the cyclooctatetraene dianion mainly due to the small quantity of the ligands available from the synthetic methods so far applied.

The work presented in this thesis shows that it is possible to synthesize DHP complexes connected to metals through dangling conjugated groups (alkynyls and cyclobutadienes). But the complexes generally show poor electronic communication and diminished photoopening rates. Nevertheless the internal methyl groups provide a rough estimate of the aromaticity of a dangling cyclobutadiene cobalt cyclopentadienyl fragment. The C7 and C8-fused DHP systems were prepared and give the first measurement of the aromaticity of C7 cation and anion, C8 dianion and the homoaromaticity of tropone and cycloheptatriene using the ‘Mitchell method’.

Chapter 6. Experimental

General information: Both proton (500.1 MHz for ^{1}H) and carbon (125.8 MHz for ^{13}C) NMR spectra were recorded on a Bruker AVANCE 500 NMR spectrometer unless otherwise stated. For air-sensitive compounds, the NMR spectra were measured in J-Young NMR tubes and the samples were loaded in a glovebox.

In NMR assignments, H-1,2 stands for H-1 ***and*** H-2; and H-1/2 stands for H-1 ***or*** H-2.

Infrared spectra were recorded on a Bruker IFS25 FT-IR spectrometer and only the major peaks are reported. All samples were prepared as potassium bromide pellets unless otherwise specified. UV-vis spectra were recorded on a Cary 5 UV-VIS-NIR spectrometer in suitable solvents. Melting points were determined on a Reichert 7905 melting point apparatus with an Omega Engineering Model 199 Chromel alumel thermocouple. Elemental analyses were performed by Canadian Microanalytical Services Ltd., Vancouver, B.C., Canada and University of British Columbia, Vancouver, B.C., Canada. Mass spectrometry was carried out at the University of British Columbia, Vancouver, B.C., Canada.

Both silica gel (Merck silica gel, 60-200 mesh) and alumina (Aldrich aluminum oxide, activated, neutral, Brockmann I, standard grade, ~150 mesh) used for chromatography were deactivated with 5% (w/w) of water.

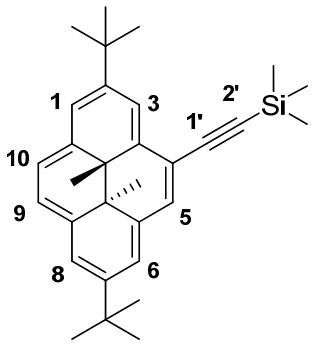
All chemicals were purchased from Sigma-Aldrich Company unless otherwise stated. Acetonitrile was distilled from calcium hydride. Ether, benzene and THF-d_8 were dried over sodium and benzophenone. *tert*-Butanol was used without any purification. Copper powder was made from Zinc and copper (II) sulphate hexahydrate aqueous solution and treated with 1 M hydrochloric acid and acetone. The resulting copper powder was then pumped for 12 hours and kept in a desiccator under argon before being used. Sodium iodide was dried in an oven at 110 ^{o}C for 12 hours.

All evaporations were carried out under vaccum.

6.1 Experimental for platinum alkynyl-DHP complexes

2,7-Di-tert-butyl-10b,10c-dimethyl-4-(2'-trimethylsilylethynyl)-*trans*-10b,10c-dihydropyrene 23

Iodo-DHP **22**[106] (4.24g, 9.02 mmol) was dissolved in Et_3N (150 mL) in an oven-dried Schlenk tube. The triethylamine solution was bubbled with argon for 15 min, and catalysts $Pd(PPh_3)_2Cl_2$ (300 mg, 0.427 mmol) and CuI (85 mg, 0.45 mmol) were added. Then trimethylsilylacetylene (2.0 mL, 14 mmol) was introduced through a syringe. The reaction mixture was stirred for 24 hours at room temperature. Saturated aqueous NaCl solution was added to quench the reaction and the product was extracted three times with dichloromethane. The combined organic extracts were washed, dried over $MgSO_4$ and evaporated under vacuum. The residue was chromatographed on a silica gel column eluting with hexanes and DCM (10:1). Eluted first were un-reacted starting materials 2 and **22** (400 mg, 10% recovery) and eluted second was the product **23** (3.46 g, 87 % yield) as green crystals, M.p. 189-191 °C.



23: ^{1}H NMR (500 MHz, $CDCl_3$) δ 8.99 (d, J = 1.0 Hz, 1H, H-3), 8.54 (s, 1H, H-5), 8.50 (s, 1H, H-1), 8.48 (s, 1H, H-8), 8.46 (s, 1H, H-6), 8.43 (AB, J = 8.0 Hz, 1H, H-9/10), 8.41 (AB, J = 8.0 Hz, 1H, H-9/10), 1.69 (s, 9H, 2-C(C$\underline{H}_3$)$_3$), 1.65 (s, 9H, 7-C(C$\underline{H}_3$)$_3$), 0.42 (s, 9H, -Si(C$\underline{H}_3$)$_3$), -3.92 (s, 6H, 10b/10c-C$\underline{H}_3$); ^{13}C NMR (125 MHz, $CDCl_3$) δ 147.59 (C-2), 146.40 (C-7), 138.63 (C-10a/10d), 138.37 (C-3a), 137.15 (C-10a/10d), 135.85 (C-5a), 125.57 (C-5), 124.15 (C-9/10), 123.52 (C-9/10), 122.05 (C-8), 121.53 (C-

1), 121.29 (C-6), 119.89 (C-3), 114.13 (C-4), 106.20 (C-1'), 99.27 (C-2'), 36.49 (2-$\underline{C}(CH_3)_3$), 36.14 (7-$\underline{C}(CH_3)_3$), 32.10 (2/7-C($\underline{C}H_3)_3$), 32.08 (2/7-C($\underline{C}H_3)_3$), 30.50 (C-10b), 29.68 (C-10c), 15.11 (10b/10c-$\underline{C}H_3$), 14.73 (10b/10c-$\underline{C}H_3$), 0.63 (-Si($\underline{C}H_3)_3$); IR (KBr) ν 2961, 2901, 2866, 2140, 1596, 1476, 1461, 1383, 1360, 1346, 1249, 1233, 1022, 886, 861, 841, 760, 665 cm^{-1}; UV-vis (cyclohexane) λ_{max} (ε_{max}, L Mol^{-1} cm^{-1}) nm, 356 (185,000), 394 (130,100), 472 (8,260), 493 (9,500), 664 (1,960); EI MS *m/z* 424 (M^+); HRMS calcd for $C_{31}H_{40}Si$: 440.2899, found: 440.2904; Anal. Calcd for $C_{31}H_{40}Si$: C, 84.48; H, 9.15; Found: C, 84.53; H, 9.10.

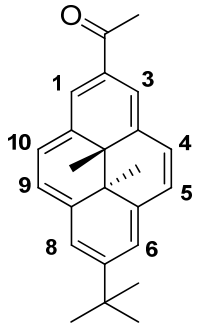
4-Acetyl-2,7-di-*tert*-butyl-10b,10c-dimethyl-*trans*-10b,10c-dihydropyrene 25
and 2-acetyl-7-*tert*-butyl-10b,10c-dimethyl-*trans*-10b,10c-dihydropyrene 26
and 4,10-diacetyl-2,7-di-*tert*-butyl-10b,10c-dimethyl-*trans*-10b,10c-dihydropyrene 27

Method a): DHP 2 (950 mg, 2.76 mmol) was dissolved in dry DCM (200 mL), and acetyl chloride (0.25 mL, 3.5 mmol) and $AlCl_3$ (610 mg, 4.6 mmol) were added under argon. The resulting solution was stirred for 12 hours at room temperature. It was then quenched by adding ice water or pouring to ice water. The organic layer was separated and washed 3 times with water and once with aqueous NaCl solution. The organic extracts were combined and dried over $MgSO_4$ before the solvents were removed. The residue was chromatographed on silica gel eluting first with hexanes to recover unchanged green starting material 2 (~40%) and then secondly with hexanes and DCM (1:1) to give the dark orange product **25** (150 mg, 15% yield). Eluted thirdly was 2-acetyl-7-*tert*-butyl-dimethyldihydropyrene 26 (65 mg, 7% yield) and lastly was 4,10-diacetyl DHP **27** (120 mg, 10% yield). It is worth to point out that the ratio of products varied from batch to batch depending on the quality of reagents and control of the reaction conditions.

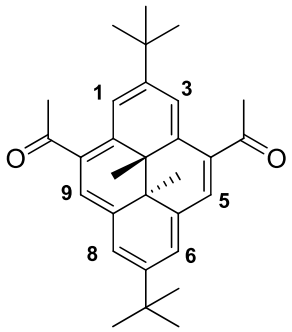
Method b): DHP 2 (500 mg, 1.45 mmol) was dissolved in dry DCM (60 mL) under argon. Acetyl chloride (0.50 mL, 7.0 mmol) and then 48% $BF_3{\cdot}Et_2O$ (1.0 mL, 8.0 mmol) were added through syringes. The reaction mixture was stirred for 15 hours at room

temperature. It was then poured in to ice water and extracted with DCM three times. The organic phase was washed with aqueous NaCl solution and dried over $MgSO_4$. The residue was chromatographed on silica gel eluting with hexanes and DCM (10:1) to elute DHP 2 first (250 mg, 50% recovery) and then hexane-DCM (2:1) to elute 4-acetyl DHP **25** (200 mg, 36% yield).

The NMR analysis on the product 4-acetyl DHP **25** was consisted with the data reported by Tashiro.[111]



26: m.p. 123-124°C. ^{1}H NMR (500MHz, $CDCl_3$) δ 9.10 (s, 2H, H-1,3), 8.73 (d, J = 7.7 Hz, 2H, H-4,10), 8.57 (s, 2H, H-6,8), 8.49 (d, J = 7.7 Hz, 2H, H-5,9), 3.00 (s, 2H, -COC$\underline{H}_3$), 1.68 (s, 9H, 7-C(C$\underline{H}_3$)$_3$), -3.89 (s, 3H, 10b-C$\underline{H}_3$), -3.91 (s, 3H, 10c-C$\underline{H}_3$); ^{13}C NMR (125MHz, $CDCl_3$) δ 199.31 (-$\underline{C}$OCH$_3$), 150.57 (C-7), 141.52 (C-5a,10d), 134.97 (C-3a,10a), 128.82 (C-2), 128.69 (C-4,10), 123.83 (C-1,3), 123.41 (C-5,9), 121.67 (C-6,8), 36.60 (7-$\underline{C}$(CH$_3$)$_3$), 32.00 (7-C($\underline{C}$H$_3$)$_3$), 30.90 (C-10c), 30.29 (C-10b), 27.49 (-CO$\underline{C}$H$_3$), 16.07 (10c-$\underline{C}$H$_3$), 14.56 (10b-$\underline{C}$H$_3$); IR (KBr) ν 2955, 2925, 2865, 1657, 1543, 1466, 1449, 1395, 1352, 1343, 1313, 1284, 1259, 1229, 1199, 1070, 971, 884, 797, 670, 623 cm^{-1}; UV-vis (toluene) λ_{max} (ε_{max}, L Mol^{-1} cm^{-1}) nm, 349 (76,300), 379 (17,900), 401 (31,600), 514 (12,600), 595 (985), 660 (288); EI MS *m/z* 330 (M^+); HRMS calcd for $C_{24}H_{26}O$: 330.1984, found: 330.1981.



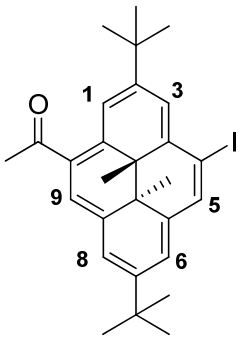
27: m.p. 135-136 °C. ^{1}H NMR (500MHz, $CDCl_3$) δ 9.73 (s, 2H, H-1,3), 8.96 (s, 2H, H-5,9), 8.68 (s, 2H, H-6,8), 3.06 (s, 6H, -COC$\underline{H}_3$), 1.69 (s, 9H, 2/7-C(C$\underline{H}_3$)$_3$), 1.68 (s, 9H, 2/7-C(C$\underline{H}_3$)$_3$), -3.77 (s, 3H, 10c-C$\underline{H}_3$), -3.79 (s, 3H, 10b-C$\underline{H}_3$); ^{13}C NMR (125MHz, $CDCl_3$) δ 202.13 (-$\underline{C}$OCH$_3$), 138.03 (C-3a,10a), 134.75 (C-5a,10d), 126.72 (C-5,9), 126.26 (C-6,8), 121.42 (C-1,3), 37.38 (2-$\underline{C}$(CH$_3$)$_3$), 36.08 (7-$\underline{C}$(CH$_3$)$_3$), 31.99 (2/7-C($\underline{C}$H$_3$)$_3$), 31.96 (2/7-C($\underline{C}$H$_3$)$_3$), 31.14 (-CO$\underline{C}$H$_3$), 31.8 (C-10b), 28.92 (C-10c), 15.66 (10b-$\underline{C}$H$_3$), 14.83 (10c-$\underline{C}$H$_3$); IR (KBr) ν 2959, 2903, 2865, 1663, 1526, 1477, 1450, 1408, 1384, 1349, 1366, 1236, 1204, 1148, 935, 896, 680, 665, 543 cm^{-1}; UV-vis (toluene) λ_{max} (ε_{max}, L Mol^{-1} cm^{-1}) nm, 345 (27,000), 407 (41,200), 504 (5,430), 616 (614), 676 (2,910) EI MS *m/z* 428 (M^+); HRMS calcd for $C_{30}H_{36}O_2$: 428.2715, found: 428.2715; Anal. Calcd for $C_{30}H_{36}O_2$: C, 84.07; H, 8.47; Found: C, 83.69; H, 8.50.

27-o: ^{1}H NMR (300MHz, $CDCl_3$) δ 7.28 (s, 2H), 6.86 (s, 2H), 6.75 (s, 2H), 2.45 (s, 6H, -COC$\underline{H}_3$), 1.35 (s, 3H, internal-C$\underline{H}_3$), 1.25 (s, 9H, 2/7-C(C$\underline{H}_3$)$_3$), 1.24 (s, 9H, 2/7-C(C$\underline{H}_3$)$_3$), 1.21 (s, 3H, internal-C$\underline{H}_3$).

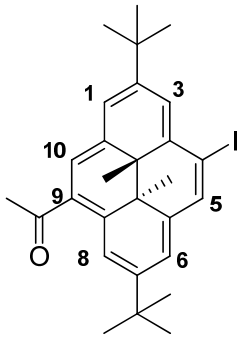
10-Acetyl-2,7-di-*tert*-butyl-10b,10c-dimethyl-4-iodo-*trans*-10b,10c-dihydropyrene 28

The iodination procedure reported by Mitchell[39] was used: I^+(collidine)$_2PF_6^-$ (prepared by reacting I_2 and Ag(collidine)$_2PF_6$ in DCM, 1.58 g, 3.06 mmol) was reacted with 4-acetyl DHP **25** (1.04 g, 2.69 mmol) in dry DCM (50 mL) to afford the iodide **28**. Chromatography of the mixture on silica gel using hexanes and DCM (3:1 to 2:1 ratio) eluted starting material 4-acetyl DHP **25** (0.17 g, 16% recovery) first and mixed isomer

iodide **28A** and **28B** (1.04 g, 75% yield) second. The ratio between isomers **28A** and **28B** was determined as *ca.* 3:1 by NMR spectroscopy. Slowly recrystallization in hexanes afforded mostly isomer **28B**.



28A: ^{1}H NMR (500MHz, $CDCl_3$) δ 9.73 (s, 1H, H-1), 8.97 (s, 1H, H-5), 8.92 (s, 1H, H-9), 8.70 (s, 1H, H-3), 8.66 (s, 1H, H-8), 8.48 (s, 1H, H-6), 3.06 (s, 3H, -COC$\underline{H}_3$), 1.71 (s, 9H, 2-C(C$\underline{H}_3$)$_3$), 1.66 (s, 9H, 7-C(C$\underline{H}_3$)$_3$), -3.83 (s, 3H, 10c-C$\underline{H}_3$), -3.86 (s, 3H, 10b-C$\underline{H}_3$); ^{13}C NMR (125MHz, $CDCl_3$) δ 202.35 (-$\underline{C}$O-), 152.49 (C-2), 147.30 (C-7), 138.07 (C-3a), 137.33 (C-5a/10d), 136.11 (C-10a), 135.46 (C-5a/10d), 135.13 (C-5), 128.95 (C-10), 127.26 (C-3), 125.50 (C-9), 124.64 (C-8), 122.87 (C-6), 121.97 (C-1), 93.38 (C-4), 37.05 (2-$\underline{C}$(CH$_3$)$_3$), 36.21 (7-$\underline{C}$(CH$_3$)$_3$), 33.67 (C-10b), 32.08 (C-2/7), 32.01 (C-7/2), 29.52 (C-10c), 14.91 (C-10b/10c), 14.77 (C-10b/10c);



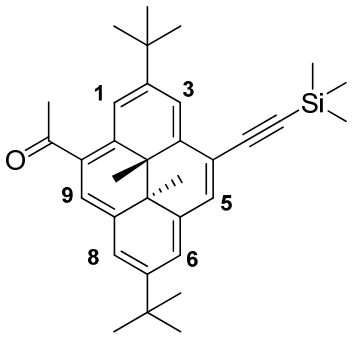
28B: ^{1}H NMR (500MHz, $CDCl_3$) δ 9.76 (s, 1H, H-8), 8.92 (s, 1H, H-10), 8.91 (s, 1H, H-5), 8.70 (d, J = 1.2 Hz, 1H, H-3), 8.66 (s, 1H, H-1), 8.46 (s, 1H, H-6), 3.05 (s, 3H, -CO-CH$_3$), 1.70 (s, 9H, 2-C(C$\underline{H}_3$)$_3$), 1.67 (s, 9H, 7-C(C$\underline{H}_3$)$_3$), -3.84 (s, 3H, 10b/10c-C$\underline{H}_3$), -3.85 (s, 3H, 10b/10c-C$\underline{H}_3$); ^{13}C NMR (125MHz, $CDCl_3$) δ 202.20 (-$\underline{C}$O-), 151.80 (C-7), 148.09 (C-2), 140.28 (C-5a), 136.19 (C-3a/10a), 135.62 (C-3a/10a), 135.48 (C-10d),

133.76 (C-5), 128.95 (C-3), 125.25 (C-10), 125.00 (C-1), 121.78 (C-8), 121.16 (C-6), 95.27 (C-4), 36.85 (7-$\underline{C}(CH_3)_3$), 36.38 (2-$\underline{C}(CH_3)_3$), 32.16 (C-10b), 32.10 (2-C($\underline{C}H_3)_3$), 32.00 (7-C($\underline{C}H_3)_3$), 31.13 (C-10c), 31.01 (-CO-$\underline{C}H_3$), 15.32 (10b/10c-$\underline{C}H_3$), 14.43 (10b/10c-$\underline{C}H_3$);

28A and 28B: IR (KBr) ν 2959, 2923, 2863, 1669, 1476, 1463, 1442, 1415, 1379, 1360, 1345, 1332, 1315, 1253, 1238, 1222, 1205, 1172, 1145, 1118, 948, 935, 889, 773, 669, 543 cm^{-1}; UV-vis (cyclohexane) λ_{max} (ε_{max}, L Mol^{-1} cm^{-1}) nm, 360 (47,800), 401 (51,100), 497 (7,270), 611 (520), 670 (2,660); ESI MS *m/z* 513 (M^++H); HRMS calcd for $C_{28}H_{33}IO$+H: 513.1654; found: 513.1666;.

10-Acetyl-2,7-di-*tert*-butyl-10b,10c-dimethyl-4-(2'-trimethylsilylethynyl)-*trans*-10b,10c-dihydropyrene 29A and 9-acetyl isomer 29B

Using the coupling procedure for compound **23**: iodide **28** (100 mg, 0.195 mmol) was reacted with trimethylsilylacetylene (0.10 mL, 0.70 mmol) in Et_3N (5mL) catalyzed by $Pd(PPh_3)_2Cl_2$ (15 mg, 0.021 mmol) and CuI (3.0 mg, 0.016 mmol) to afford the alkynes **29A,B** (92 mg, 98% yield) as a mixture of the two isomers (~ 85:15 ratio **29A/29B**) as dark orange crystals. Recrystallization from hexanes enriched the major isomer **29A** to ~95%.

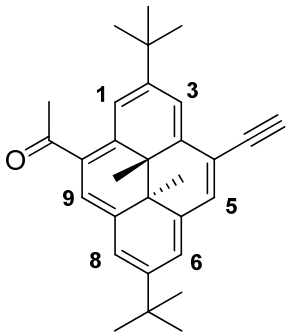


29A: ^{1}H NMR (500MHz, $CDCl_3$) δ 9.73 (d, J = 1.1 Hz, 1H, H-1), 9.05 (d, J = 1.1 Hz, 1H, H-3), 8.91 (s, 1H, H-9), 8.62 (s, 1H, H-5,8), 8.51 (s, 1H, H-6), 3.05 (s, 3H, -COC$\underline{H}_3$),

1.70 (s, 9H, 2-C(C<u>H</u>$_3$)$_3$), 1.65 (s, 9H, 7-C(C<u>H</u>$_3$)$_3$), 0.42 (s, 9H, -Si(C<u>H</u>$_3$)$_3$), -3.80 (s, 3H, 10c-C<u>H</u>$_3$), -3.81 (s, 3H, 10b-C<u>H</u>$_3$); ^{13}C NMR (125MHz, $CDCl_3$) δ 202.24 (-<u>C</u>OCH$_3$), 152.26 (C-2), 146.78 (C-7), 140.78 (C-3a), 136.72 (C-10a), 135.59 (C-5a/10d), 135.22 (C-5a/10d), 128.73 (C-10), 128.02 (C-5), 125.95 (C-9), 125.11 (C-8), 123.89 (C-6), 121.62 (C-1), 120.66 (C-3), 115.12 (C-4), 105.54 (-<u>C</u>≡C-SiMe$_3$), 99.93 (-C≡<u>C</u>-SiMe$_3$), 37.08 (2-<u>C</u>(CH$_3$)$_3$), 36.10 (7-<u>C</u>(CH$_3$)$_3$), 32.01 (2/7-C(<u>C</u>H$_3$)$_3$), 32.00 (2/7-C(<u>C</u>H$_3$)$_3$), 31.50 (C-10b), 31.02 (-CO<u>C</u>H$_3$), 29.20 (C-10c), 15.24 (10b/10c-<u>C</u>H$_3$), 15.20 (10b/10c-<u>C</u>H$_3$), 0.55 (-Si(<u>C</u>H$_3$)$_3$); IR (KBr) ν 2962, 2927, 2903, 2867, 2141, 1662, 1477, 1464, 1445, 1407, 1386, 1372, 1362, 1351, 1247, 1225, 1208, 1154, 1110, 1025, 934, 914, 896, 886, 860, 841, 757, 682, 664, 631, 541 cm^{-1}; UV-vis (toluene) λ_{max} (ε_{max}, L Mol^{-1} cm^{-1}) nm, 375 (47,100), 409 (61,100), 490 (6,740), 558 (545), 621 (615), 683 (3,300); EI MS *m/z* 482 (M^+); HRMS calcd for $C_{33}H_{42}OSi$: 482.3005, found: 482.3007; Anal. Calcd for $C_{33}H_{42}OSi$: C, 82.10; H, 8.77; Found: C, 81.76; H, 8.82.

9-Acetyl and 10-Acetyl-2,7-di-*tert*-butyl-10b,10c-dimethyl-4-ethynyl-*trans*-10b,10c-dihydropyrene 30

Mixed isomers of the TMS alkynes **29** (410 mg, 0.85 mmol) were dissolved in a mixture of THF and methanol (1:1 ratio, 5 mL). The solution was degassed for 15 mins and then anhydrous K_2CO_3 (0.50 g, 3.6 mmol) was added and the suspension mixture was stirred for 2 hours at room temperature. Then the solvents were removed and benzene was added to re-dissolve the products. The catalyst and salt were removed by filtering the solution through a short celite and silica gel pad. The pad was rinsed with benzene until no products presented in the dripping solvent. The organic solution was dried over $MgSO_4$, concentrated to afford desired free alkynes **30** (350 mg, 100% yield). The alkynes were recrystallized from hexanes and methanol to obtain dark orange crystals, enriched in the 10- isomer, **30**A.

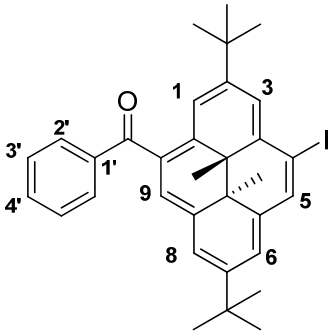


30A: ^{1}H NMR (500MHz, $CDCl_3$) δ 9.73 (d, J = 1.2 Hz, 1H, H-1), 9.04 (d, J = 1.1 Hz, 1H, H-3), 8.92 (s, 1H, H-9), 8.65 (s, 1H, H-5), 8.64 (s, 1H, H-8), 8.53 (s, 1H, H-6), 3.72 (s, 1H, -C≡C-H), 3.06 (s, 3H, -COCH_3), 1.70 (s, 9H, 2-C(CH_3)$_3$), 1.66 (s, 9H, 7-C(CH_3)$_3$), -3.80 (s, 3H, 10c-CH_3), -3.81 (s, 3H, 10b-CH_3); ^{13}C NMR (125MHz, $CDCl_3$) δ 202.27 (-COCH$_3$), 152.38 (C-2), 146.86 (C-7), 140.69 (C-3a), 136.63 (C-10a), 135.53 (C-5a/10d), 135.22 (C-5a/10d), 128.49 (C-5), 125.99 (C-9), 125.21 (C-8), 123.90 (C-6), 121.64 (C-1), 120.44 (C-3), 113.99 (C-4), 84.05 (-C≡C-H), 82.40 (-C≡C-H), 37.10 (2-C(CH$_3$)$_3$), 36.12 (7-C(CH$_3$)$_3$), 32.06 (2/7-C(CH$_3$)$_3$), 32.00 (2/7-C(CH$_3$)$_3$), 31.47 (C-10b), 31.04 (-COCH$_3$), 29.19 (C-10c), 15.21 (10b/10c-CH$_3$), 15.16 (10b/10c-CH$_3$); IR (KBr) ν 3309, 3262, 2963, 2925, 2865, 2091, 1665, 1477, 1444, 1383, 1361, 1348, 1242, 1225, 1207, 1153, 928, 889, 679, 665 cm^{-1}; UV-vis (toluene) λ_{max} (ε_{max}, L Mol^{-1} cm^{-1}) nm, 372 (42,800), 405 (52,200), 493 (6,500), 557 (552), 618 (571), 681 (2,880); EI MS *m/z* 410 (M^+); HRMS calcd for $C_{30}H_{34}O$: 410.2610, found: 410.2613; Anal. Calcd for $C_{30}H_{34}O$: C, 87.76; H, 8.35; Found: C, 86.93; H, 8.48.

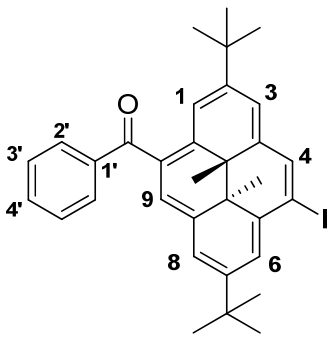
10-Benzoyl-2,7-di-*tert*-butyl-10b,10c-dimethyl-4-iodo-*trans*-10b,10c-dihydropyrene 32A and 5-iodo 32B

Using the procedure for iodide **28**: I^+(collidine)$_2PF_6^-$ (prepared by mixing I_2 and Ag(collidine)$_2PF_6$ in DCM, 0.528 g, 1.02 mmol) was added to a solution of benzoylDHP **31** (0.45 g, 1.0 mmol) in dry DCM (50 mL). The reaction mixture was stirred 18 hours at room temperature and then the reaction solution was washed with water three times and

brine once. The organic layers were dried over $MgSO_4$ and concentrated. The residue was chromatographed on silica gel, using hexanes and ethyl acetate (100:3) to elute firstly the product **32** (0.40 g, 75% yield) and secondly unchanged green benzoylDHP **31** (80 mg, 18% recovery). Recrystallization from hexanes enriched the isomer **32A** (~ 90:10 ratio **32A/32B**).



32A: ^{1}H NMR (500MHz, $CDCl_3$) δ 9.00 (s, 1H, H-5), 8.90 (d, J = 0.7 Hz, 1H, H-1), 8.70 (d, J = 0.7 Hz, 1H, H-3), 8.63 (s, 1H, H-9), 8.59 (s, 1H, H-8[1]), 8.51 (s, 1H, H-6), 7.90-7.87 (m, 2H, H-2'), 7.63-7.60 (m, 1H, H-4'), 7.51-7.47 (m, 2H, H-3'), 1.64 (s, 9H, 7-C(C$\underline{H}_3$)$_3$), 1.57 (s, 9H, 2-C(C$\underline{H}_3$)$_3$), -3.743 (10c- C$\underline{H}_3$)$_3$), -3.75 (10b-C$\underline{H}_3$)$_3$); ^{13}C NMR (125MHz, $CDCl_3$) δ 199.21/199.08 (-$\underline{C}$O-), 150.47 (C-2), 147.58 (C-7), 140.58/140.54 (C-1'), 137.48 (C-5a/10d), 137.21 (C-3a), 136.45 (C-10a), 135.15 (C-5a/10d), 134.75 (C-5), 132.82/132.77 (C-4'), 130.68 (C-10), 130.55 (C-2'), 128.59 (C-3'), 127.19 (C-3), 125.48 (C-9), 124.13 (C-8), 122.43 (C-6), 121.47 (C-1), 93.43 (C-4), 36.76 (2-$\underline{C}$(CH$_3$)$_3$), 36.25 (7-$\underline{C}$(CH$_3$)$_3$), 33.48 (C-10b), 32.01 (7-C($\underline{C}$H$_3$)$_3$), 31.89 (2-C($\underline{C}$H$_3$)$_3$), 29.69 (C-10c), 15.09 (10c-$\underline{C}$H$_3$), 14.65 (10b-$\underline{C}$H$_3$);



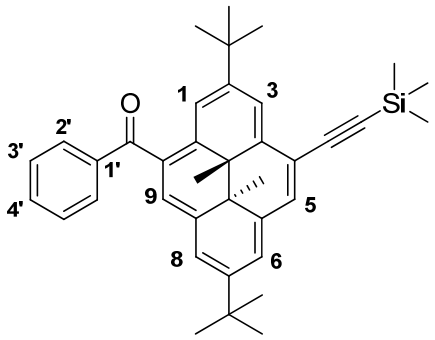
[1] Overlap with the peak of its isomer.

32B: ^{1}H NMR (500MHz, $CDCl_3$) δ 8.96 (s, 1H, H-4), 8.93 (s, 1H, H-5), 8.73 (d, J = 1.0 Hz, 1H, H-1), 8.61 (s, 1H, H-9), 8.59 (s, 1H, H-8), 8.47 (s, 1H, H-3), 7.90-7.87 (m, 2H, H-2'), 7.63-7.60 (m, 1H, H-4'), 7.51-7.47 (m, 2H, H-3'), 1.68 (s, 9H, 2-C(C$\underline{H}_3$)$_3$), 1.54 (s, 9H, 7-C(C$\underline{H}_3$)$_3$), -3.736 (C-10b), -3.77 (C-10c); ^{13}C NMR (125MHz, $CDCl_3$) δ 199.21/199.08 (-$\underline{C}$O-), 149.77 (C-7), 148.38 (C-2), 140.58/140.54 (C-1'), 139.38 (C-3a), 135.97 (C-10a), 135.85 (C-10d), 135.57 (C-5a), 133.76 (C-4), 132.82/132.77 (C-4'), 130.55 (C-2',10), 128.59 (C-3'), 128.54 (C-6), 125.24 (C-9), 124.51 (C-8), 121.21 (C-1), 121.08 (C-3), 94.79 (C-5), 36.57 (7-$\underline{C}$(CH$_3$)$_3$), 36.44 (2-$\underline{C}$(CH$_3$)$_3$), 32.29 (C-10c), 32.10 (2-C($\underline{C}$H$_3$)$_3$), 31.82 (7-C($\underline{C}$H$_3$)$_3$), 31.00 (C-10b), 15.15 (10b-$\underline{C}$H$_3$), 14.60 (10c-$\underline{C}$H$_3$);

32A and **32B:** IR (KBr) ν 2962, 2924, 2865, 1655, 1595, 1579, 1446, 1381, 1258, 1231, 1156, 1018, 906, 889, 771, 725, 692, 674, 555 cm^{-1}; UV-vis (toluene) λ_{max} (ε_{max}, L Mol^{-1} cm^{-1}) nm, 353 (53,100), 402 (48,000), 493 (8,150), 605 (486), 661 (2,300); EI MS *m/z* 574 (M^+); HRMS calcd for $C_{35}H_{35}IO$: 574.1733, found: 574.1738; Anal. Calcd for $C_{35}H_{35}IO$: C, 68.99; H, 6.14; Found: C, 69.24; H, 6.29.

10-Benzoyl-2,7-di-*tert*-butyl-10c,10d-dimethyl-4-(2''-trimethylsilylethynyl)-*trans*-10c,10d-dihydropyrene 33A and 5-silyl isomer 33B

Following the coupling procedure for compound **23**, the compound **32** (0.40 g, 0.70 mmol) and trimethylsilylacetylene (0.15 mL, 1.1 mmol) and $Pd(PPh_3)_2Cl_2$ (45 mg, 0.064 mmol) and CuI (7.8 mg, 0.041 mmol) in degassed Et_3N (50 mL) gave the product **33**. The residue was chromatographed eluting with hexanes and DCM (10:2 to 10:6) and gave the product **33** (350 mg, 95% yield) as a dark orange solid. Recrystallization from DCM/MeOH afforded **33A** and **33B** in a 5:2 ratio.



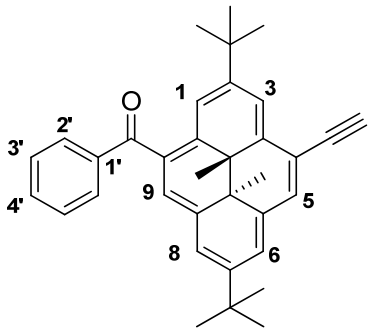
33A: ^{1}H NMR (500MHz, $CDCl_3$) δ 9.05 (s, 1H, H-3), 8.90 (s, 1H, H-1), 8.66 (s, 1H, H-5), 8.60 (s, 1H, H-9), 8.55 (s, 1H, H-8), 8.54 (s, 1H, H-6), 7.89 (d, J = 7.9 Hz, 2H, H-2'), 7.61 (t, J = 7.4 Hz, 1H, H-4'), 7.49 (t, J = 7.7 Hz, 2H, H-3'), 1.64 (s, 9H, 7-C(C$\underline{H}_3$)$_3$), 1.57 (s, 9H, 2-C(C$\underline{H}_3$)$_3$), 0.426 (s, 9H, -Si(C$\underline{H}_3$)$_3$), -3.71 (s, 3H, 10b-$\underline{C}H_3$), -3.72 (s, 3H, 10c-$\underline{C}H_3$); ^{13}C NMR (125MHz, $CDCl_3$) δ 199.22 (-$\underline{C}$O-), 150.27 (C-2), 147.07 (C-7), 140.70 (C-1'), 139.82 (C-3a), 137.09 (C-10a), 135.72 (C-5a/10d), 134.87 (C-5a/10d), 132.70 (C-4'), 130.56 (C-2'), 130.29 (C-10), 128.55 (C-3'), 127.64 (C-5), 125.94 (C-9), 124.62 (C-8), 123.46 (C-6), 121.09 (C-1), 120.60 (C-3), 115.14 (C-4), 105.59 (-$\underline{C}$≡C-Si), 99.96 (≡$\underline{C}$-Si), 36.80 (2-$\underline{C}$(CH$_3$)$_3$), 36.16 (7-$\underline{C}$(CH$_3$)$_3$), 32.00 (7-C(C$\underline{H}_3$)$_3$), 31.83 (2-C(C$\underline{H}_3$)$_3$), 31.37 (10b-$\underline{C}H_3$), 29.35 (10c-$\underline{C}H_3$), 0.56 (-Si(C$\underline{H}_3$)$_3$);

33B: ^{1}H NMR (500MHz, $CDCl_3$) (selected) δ 9.07 (s), 8.87 (s), 8.60 (s, overlap), 8.59 (s), 8.56 (s), 8.50 (s), 7.89 (s), 7.61 (s), 7.49 (s), 1.67 (s), 1.53 (s), 0.431 (s), -3.71 (s), -3.73 (s);

33A and **33B:** IR (KBr) ν 2962, 2925, 2903, 2867, 2140, 1648, 1596, 1477, 1460, 1447, 1385, 1346, 1249, 1231, 1211, 1173, 1024, 895, 861, 842, 803, 759, 695, 679 cm^{-1}; UV-vis (toluene) λ_{max} (ε_{max}, L Mol^{-1} cm^{-1}) nm, 358 (52,900), 408 (50,500), 500 (8,000), 616 (560), 674 (2,820); EI MS *m/z* 544 (M^+); HRMS calcd for $C_{38}H_{44}OSi$: 544.3161, found: 544.3159.

10-Benzoyl-2,7-di-*tert*-butyl-10c,10d-dimethyl-4-ethynyl-*trans*-10c,10d-dihydropyrene 34A and 5-ethynyl 34B

Using the procedure for compound **11**: the mixture of alkynes **33** (110 mg, 0.202 mmol) and K_2CO_3 (40 mg, 0.30 mmol) were reacted in degassed methanol (7 mL) and THF (7 mL) for 2 hours to afford the two isomers of alkyne **34** (90 mg, 94% yield). The dark orange product **34** was recrystallized from DCM and methanol. M.p. 155-157°C



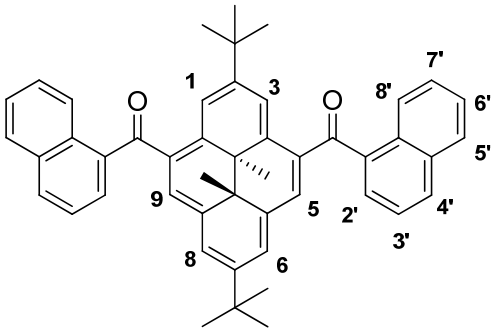
34A: ^{1}H NMR (500MHz, $CDCl_3$) δ 9.04 (d, J = 1.2 Hz, 1H, H-3), 8.91 (d, J = 1.2 Hz, 1H, H-3), 8.68 (s, 1H, H-5), 8.62 (s, 1H, H-9), 8.57 (s, 1H, H-8), 8.56 (s, 1H, H-6), 7.90-7.88 (m, 2H, H-2'), 7.61 (tt, J = 7.4, 1.3 Hz, 1H, H-4'), 7.51-7.47 (m, 2H, H-3'), 3.73 (s, 1H, -C≡C-H), 1.64 (s, 9H, 7-C(CH_3)$_3$), 1.57 (s, 9H, 2-C(CH_3)$_3$), -3.71 (s, 3H, 10b/10c-CH_3), -3.72 (s, 3H, 10b/10c-CH_3); ^{13}C NMR (125MHz, $CDCl_3$) δ 199.19 (-CO-), 150.38 (C-2), 147.13 (C-7), 140.65 (C-1'), 139.72 (C-3a), 136.99 (C-10a), 135.66 (C-5a/10d), 134.88 (C-5a/10d), 132.73 (C-4'), 130.55 (C-2'), 130.40 (C-10), 128.57 (C-3'), 128.13 (C-5), 125.95 (C-9), 124.69 (C-8), 123.46 (C-6), 121.09 (C-1), 120.39 (C-3), 114.01 (C-4), 84.10 (-C≡C-H), 82.41 (-C≡C-H), 36.80 (2-C(CH$_3$)$_3$), 36.17 (7-C(CH$_3$)$_3$), 32.00 (7-C(CH$_3$)$_3$), 31.87 (2-C(CH$_3$)$_3$), 31.33 (C-10b), 29.34 (C-10c), 15.31 (10b/10c-CH$_3$), 15.07 (10b/10c-CH$_3$);

34B: ^{1}H NMR (500MHz, $CDCl_3$)(selected peaks only given) δ 9.07, 8.89, 8.64, 8.60, 8.58, 8.52, 3.75, 1.68, 1.54, -3.71, -3.73.

34A and **34B:** IR (KBr) ν 3293, 3245, 2964, 2924, 2905, 2865, 2091, 1639, 1596, 1476, 1447, 1385, 1362, 1347, 1324, 1267, 1247, 1233, 1210, 1196, 1173, 1023, 941, 901, 872, 804, 729, 697, 681, 669 cm^{-1}; UV-vis (toluene) λ_{max} (ε_{max}, L Mol^{-1} cm^{-1}) nm, 355 (52,700), 406 (26,200), 497 (7,500), 671 (2,400); EI MS *m/z* 472 (M^+); HRMS calcd for $C_{35}H_{36}O$: 472.2766, found: 472.2766.

2,7-Di-*tert*-butyl-10b,10c-dimethyl-4,10-di(1'-naphthoyl)-*trans*-10b,10c-dihydropyrene 36

Using the acylation procedure described for **25**, and DHP 2 (1.21 g, 3.52 mmol), 1-naphthoyl chloride (0.85 g, 4.5 mmol) $AlCl_3$ (0.73 g, 5.5 mmol) and dry DCM (200 mL) followed by chromatography on silica gel eluting with hexanes and then hexane and DCM (1:1) gave firstly starting material (0.58 g, 48% recovery) and then the 4-(1'-naphthoyl) DHP **35** second (0.73 g, 42% yield) and lastly the 4,10-di-1'-naphthoyl DHP **36** third (110 mg, 5% yield). Note that 4-(1'-naphthoyl) DHP **35** can be obtained in higher yield.[106]

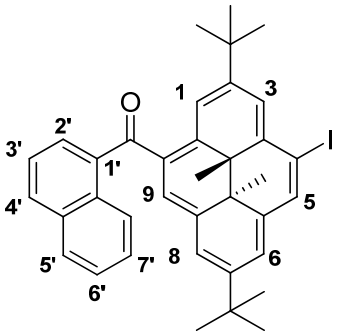


36: m.p. 197-198°C. ^{1}H NMR (500MHz $CDCl_3$) δ 9.34 (s, 2H, H-1,3), 8.71 (s, 2H, H-5,9), 8.54 (s, 2H, H-6,8), 8.48 (d, J = 8.6 Hz, 2H, H-8'), 8.07 (d, J = 8.2 Hz, 2H, H-4'), 7.99 (d, J = 8.0 Hz, 2H, H-5'), 7.63 (dd, J = 7.0, 1.0 Hz, 2H, H-2'), 7.57 (ddd, J = 8.0, 7.0, 1.0 Hz, 2H, H-6'), 7.51 (ddd, J = 8.0, 7.0, 1.0 Hz, 2H, H-7'), 7.50 (dd, J = 8.1, 7.1 Hz, 2H, H-3'), 1.56 (s, 9H, 7-C(C$\underline{H}_3$)$_3$), 1.38 (s, 9H, 2-C(C$\underline{H}_3$)$_3$), -3.54 (s, 3H, 10b/10c-C$\underline{H}_3$), -3.58 (s, 3H, 10b/10c-C$\underline{H}_3$); ^{13}C (500MHz $CDCl_3$) δ 200.67 (-$\underline{C}$O-), 153.88 (C-2), 146.88 (C-7), 139.90 (C-1'), 138.84 (C-3a,10a), 134.42 (C-5a,10d), 134.17 (C-8b), 131.85 (C-4'), 131.47 (C-8a), 130.97 (C-4,10), 129.23 (C-2'), 128.71 (C-5'), 128.34 (C-5,9), 127.75 (C-7'), 126.74 (C-6'), 126.60 (C-6,8), 126.15 (C-8'), 124.83 (C-3'), 121.06 (C-1,3), 37.03 (2-C($\underline{C}$H)$_3$), 36.09 (7-C($\underline{C}$H)$_3$), 32.28 (C-10b), 31.92 (7-C($\underline{C}$H)$_3$), 31.58 (2-C($\underline{C}$H)$_3$), 29.20 (C-10c), 15.47 (10b/10c-$\underline{C}$H$_3$), 15.26 (10b/10c-$\underline{C}$H$_3$); IR (KBr) ν 2962, 2866, 1639, 1507, 1478, 1461, 1273, 1237, 1197, 1120, 934, 903, 887, 784, 770, 675 cm^{-1}; UV-vis (toluene)

λ_{max} (ε_{max}, L Mol^{-1} cm^{-1}) nm, 292 (16,700), 351 (28,100), 426 (46,800), 501 (6,490), 617 (897), 677 (3,540); EI MS *m/z* 652 (M^+); HRMS calcd for $C_{48}H_{44}O_2$: 652.3341, found: 652.3345; Anal. Calcd for $C_{48}H_{44}O_2$: C, 88.31; H, 6.79; Found: C, 87.82; H, 6.88.

2,7-Di-*tert*-butyl-10b,10c-dimethyl-4-iodo-10-(1'-naphthoyl)-*trans*-10b,10c-dihydropyrene 37A and 5-iodo 37B

Using the same procedure for iodide **28**: 4-(1'-naphthoyl) DHP **35** (1.0 g, 2.0 mmol), iodine (0.785 g, 3.09 mmol) and $Ag(collidine)_2PF_6$ in dry DCM (200 mL) gave the isomeric mixture **37** in 90% yield and starting material **35** in 10% recovery based on the ^{1}H NMR spectrum. The mixture of the starting material **35**, **37A** and **37B** (*ca* 4:1 ratio) was used in the next step with no need of separation. The NMR assignments were based on the spectra of the isomeric mixture.



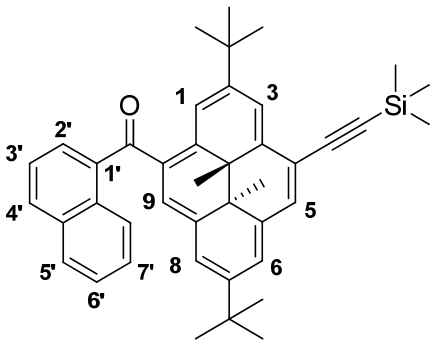
37A: ^{1}H NMR (500MHz, $CDCl_3$) δ 9.32 (s, 1H), 9.00 (s, 1H), 8.71 (s, 1H), 8.63 (s, 1H), 8.52-8.45 (m, 3H), 8.06 (d, J = 8.1 Hz, 1H), 7.98 (d, J = 8.7 Hz, 1H), 7.63-7.44 (m, 4H), 1.60 (s, 9H), 1.55 (s, 9H), -3.730 (s, 3H), -3.733 (s, 3H); ^{13}C NMR (125MHz, $CDCl_3$) δ 151.78, 147.42, 139.83, 137.91, 137.36, 137.19, 135.15, 135.02, 134.13, 131.84, 131.45, 130.95, 129.28, 128.69, 127.73, 127.24, 127.01, 126.71, 126.13, 124.87, 124.80, 122.90, 121.53, 93.36, 36.87, 36.20, 33.82, 32.05, 31.96, 31.88, 31.81, 29.62, 15.08, 14.66.

37B: ^{1}H NMR (500MHz, $CDCl_3$) δ 9.35 (s, 1H, H-), 8.95 (s, 1H, H-), 1.64 (s, 1H, H-), 11.52 (s, 1H, H-), -3.71 (s, 1H, H-), -3.75 (s, 3H, +H);

37A and **37B:** IR (KBr) ν 2958, 2925, 2903, 2865, 1643, 1591, 1508, 1460, 1382, 1362, 1255, 1239, 1228, 1137, 1125, 950, 890, 783, 673 cm^{-1}; UV-vis (toluene) λ_{max} (ε_{max}, L Mol^{-1} cm^{-1}) nm, 355 (45,200), 407 (47,100), 495 (7,000), 668 (2,460); ESI MS *m/z* 626 (M^++H); HRMS calcd for $C_{37}H_{37}IO$+H: 625.1967, found: 625.1970;.

2,7-Di-*tert*-butyl-10b,10c-dimethyl-10-(1'-naphthoyl)-4-trimemthylsilylethynyl-*trans*-10b,10c-dihydropyrene 38A and 5-silyl isomer 38B

Using the coupling procedure for compound **23**: crude isomeric mixture **37** (1.25 g, 2.00 mmol) and trimethylsilylacetylene (0.5 mL, 3.6 mmol), and catalysts $Pd(PPh_3)_2Cl_2$ (67 mg, 0.096 mmol) and CuI (10.8 mg, 0.0526 mmol) in degassed Et_3N (75 mL) gave the isomeric mixture of products **38** (1.15 g, 95% yield). M.p. 134-140 °C. **38A** and **38B** was obtained in a *ca.* 4:1 ratio.



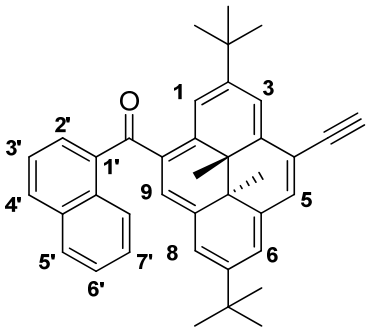
38A: ^{1}H NMR (500MHz, $CDCl_3$) δ 9.34 (d, J = 0.8 Hz, 1H, H-1), 9.06 (s, 1H, H-3), 8.66 (s, 1H, H-5), 8.61 (s, 1H, H-9), 8.52 (s, 1H, H-6), 8.46 (s, 1H, H-8), 8.45 (d, J = 10.5 Hz, 1H, H-8') 8.06 (d, J = 8.2 Hz, 1H, H-4'), 7.98 (d, J = 8.2 Hz, 1H, H-5'), 7.62 (dd, J = 7.0, 1.0 Hz, 1H, H-2'), 7.55 (t, J = 7.1 Hz, 1H, H-6'), 7.50-7.47 (m, 2H, H-3',7'), 1.59 (s, 9H, 7-C(C$\underline{H}_3$)$_3$), 1.55 (s, 9H, 2-C(C$\underline{H}_3$)$_3$), 0.43 (s, 9H, -Si(C$\underline{H}_3$)$_3$), -3.69 (s, 3H, 10b-C$\underline{H}_3$), -3.71 (s, 3H, 10c-C$\underline{H}_3$); ^{13}C NMR (125MHz, $CDCl_3$) δ 200.82 (-$\underline{C}$O-Np), 151.61 (C-2), 146.92 (C-7), 140.59 (C-3a), 134.03 (C-1'), 137.83 (C-10a), 135.64 (C-5a/10d), 134.79 (C-5a/10d), 134.13 (C-8'b), 131.67 (C-4'), 131.50 (C-8'a), 130.64 (C-10), 129.13 (C-2'), 128.66 (C-5'), 128.08 (C-5), 127.64 (C-7'), 127.50 (C-9), 126.67 (C-6'), 126.19 (C-8'),

125.38 (C-8), 124.82 (C-3'), 123.96 (C-6), 121.17 (C-1), 120.68 (C-3), 115.14 (C-4), 105.53 (-C≡CSiMe$_3$), 100.01 (-C≡CSiMe$_3$), 36.92 (2-C(CH$_3$)$_3$), 36.10 (7-C(CH$_3$)$_3$), 31.96 (7-C(CH$_3$)$_3$), 31.83 (2-C(CH$_3$)$_3$), 31.70 (C-10b), 29.31 (C-10c), 15.37 (10c-CH$_3$), 15.15 (10b-CH$_3$), 0.56 (-Si(CH$_3$)$_3$);

38A and **38B:** IR (KBr) ν 2961, 2904, 2866, 2139, 1640, 1508, 1477, 1461, 1386, 1346, 1276, 1247, 1230, 1197, 1098, 896, 860, 842, 782, 758 cm^{-1}; UV-vis (toluene) λ_{max} (ε_{max}, L Mol^{-1} cm^{-1}) nm, 345 (51,900), 402 (46,200), 494 (8,190), 610 (670), 665 (2,690); EI MS *m/z* 594 (M^+); HRMS calcd for $C_{42}H_{46}OSi$: 594.3318, found: 594.3323; Anal. Calcd for $C_{42}H_{46}OSi$: C, 84.80; H, 7.79; Found: C, 83.10; H, 7.80.

2,7-Di-*tert*-butyl-10b,10c-dimethyl-4-ethynyl-10-(1'-naphthoyl)-*trans*-10b,10c-dihydropyrene 39A and 5-ethynyl 39B

Using the procedure for **11**: the protected isomeric mixture of alkynes **38** (190 mg, 0.320 mmol) and K_2CO_3 (130 mg, 0.942 mmol) in 1:1 ratio of THF and methanol (10 mL) gave rise to mixed isomers of **39** (180 mg, 100% yield) The ratio between **39A** and **39B** was found as *ca* 4:1. Recrystallization from hexanes afforded dark orange crystals of **39**. Note that **39** and the starting material **38** behave similarly on a silica gel TLC plate.



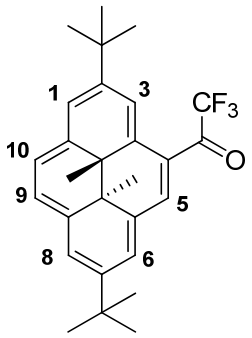
39A: ^{1}H NMR (500MHz, $CDCl_3$) δ 9.34 (d, J = 0.9 Hz, 1H, H-1), 9.05 (d, J = 0.8 Hz, 1H, H-3), 8.68 (s, 1H, H-5), 8.62 (s, 1H, H-9), 8.54 (s, 1H, H-6), 8.47 (s, 1H, H-8), 8.45 (d, J = 7.9 Hz, 1H, H-8'), 8.06 (d, J = 8.3 Hz, 1H, H-4'), 7.98 (d, J = 7.9 Hz, 1H, H-5'), 7.63-7.61 (m, 1H, H-2'), 7.56-7.54 (m, 1H, H-6'), 7.51-7.47 (m, 2H, H-3',7'), 3.73 (s, 1H, -

C≡C-H), 1.60 (s, 9H, 7-C(CH$_3$)$_3$), 1.56 (s, 9H, 2-C(CH$_3$)$_3$), -3.69 (s, 3H, 10b-CH$_3$), -3.70 (s, 3H, 10c-CH$_3$); ^{13}C NMR (125MHz, $CDCl_3$) δ 200.81 (-CO-), 151.71 (C-2), 146.99 (C-7), 140.48 (C-3a), 139.96 (C-1'), 137.72 (C-10a), 135.57 (C-5a/10d), 134.79 (C-5a/10d), 134.12 (C-8'b), 131.71 (C-4'), 131.48 (C-8'), 130.74 (C-10), 129.15 (C-2'), 128.67 (C-5'), 128.55 (C-5), 127.67 (C-9), 127.53 (C-7'), 126.68 (C-6'), 126.16 (C-8'), 125.46 (C-8), 124.81 (C-3'), 123.96 (C-6), 121.18 (C-1), 120.45 (C-3), 114.01 (C-4), 84.04 (-C≡C-H), 82.44 (-C≡C-H), 36.92 (2-C(CH)$_3$), 36.12 (7-C(CH)$_3$), 31.95 (2/7-C(CH)$_3$), 31.87 (2/7-C(CH)$_3$), 31.66 (C-10b), 29.30 (C-10c), 15.28 (10b/10c-CH$_3$), 15.09 (10b/10c-CH$_3$);

39A and 39B: IR (KBr) ν 3304, 3252, 2962, 2923, 2866, 2093, 1631, 1588, 1462, 1383, 1345, 1277, 1258, 1229, 1198, 1121, 1091, 943, 894, 880, 783, 681, 668 cm^{-1}; UV-vis (toluene) λ_{max} (ε_{max}, L Mol^{-1} cm^{-1}) nm, 355 (41,007), 411 (46,473), 493 (6,524), 620 (584), 678 (2,499); EI MS *m/z* 522 (M^+); HRMS calcd for $C_{39}H_{38}O$: 522.2923, found: 522.2921; Anal. Calcd for $C_{39}H_{38}O$: C, 89.61; H, 7.33; Found: C, 86.04; H, 7.39.

2,7-Di-*tert*-butyl-10b,10c-dimethyl-4-trifluoroacetyl-*trans*-10b,10c-dihydropyrene 42

A solution of bromo-DHP **41**[41] (750 mg, 1.77 mmol) in dry THF (20 mL) was cooled with a dry ice bath for 15 mins. A solution of 1.6 M *n*-butyllithium in hexanes (2.4 mL, 3.8 mmol) was added dropwise through a syringe, and then the mixture was warmed to room temperature for 2 hours. Then the reaction mixture was cooled to -78°C again and ethyl trifluoroacetate (0.40 mL, 3.4 mmol) was added quickly by syringe. The reaction was warmed and stirred for 5 hours at room temperature. The green color of the solution turned brown slowly. Finally, ice water was added to quench the reaction. The resulting mixture was extracted with ether three times. The combined organic layers were dried over $MgSO_4$ and then the solvents were removed. The residue was chromatographed on silica gel. Elution with hexane yielded recovered DHP 2 (420 mg, 69%), and then hexane-DCM (9:1) eluted the desired product **42** (200 mg, 25% yield). This was recrystallized from hexanes as a dark red crystals, m.p. 186-188°C.



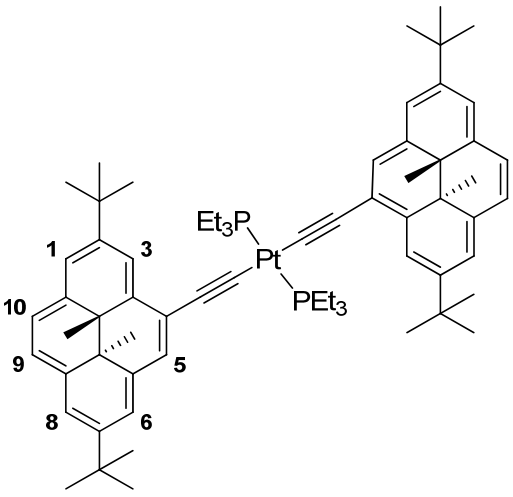
42: ^{1}H NMR (500MHz, CD_2Cl_2) δ 9.96 (d, J = 0.9 Hz, 1H, H-3), 9.01 (q, J = 2.2 Hz, 1H, H-5), 8.70 (s, 1H, H-6), 8.63 (s, 1H, H-8), 8.59 (s, 1H, H-1), 8.58 (d, J = 7.9 Hz, 1H, H-9), 8.48 (d, J = 7.9 Hz, 1H, H-10), 1.70 (s, 9H, 2-C(C<u>H</u>)$_3$), 1.68 (s, 9H, 7-C(C<u>H</u>)$_3$), -3.830 (s, 3H, 10b/10c-C<u>H</u>)$_3$), -3.831 (s, 3H, 10b/10c-C<u>H</u>)$_3$); ^{13}C NMR (125MHz, CD_2Cl_2) δ 182.00 (q, J = 32.5 Hz, -<u>C</u>O-), 154.41 (C-2), 146.92 (C-7), 142.63 (C-10a), 140.26 (C-3a), 136.85 (C-10d), 134.30 (C-5a), 127.27 (C-9), 125.74 (C-6), 125.48 (C-8), 124.30 (q, J = 4.0 Hz, C-5), 124.24 (C-10), 122.07 (C-1), 120.51 (C-3), 118.46 (C-4), 117.95 (q, J = 293.0 Hz, -CO<u>C</u>F$_3$), 37.16 (2-<u>C</u>(CH)$_3$), 36.18 (7-<u>C</u>(CH)$_3$), 32.07 (C-10b), 32.03 (2,7-C(<u>C</u>H)$_3$), 28.93 (C-10c), 15.83 (10b/10c-(<u>C</u>H)$_3$), 14.93 (10b/10c-(<u>C</u>H)$_3$); ^{19}F NMR (282MHz, $CDCl_3$) δ 68.29;); IR (film) ν 2965, 2928, 2869, 1681, 1463, 1464, 1388, 1256, 1235, 1186, 1138, 1105, 1044, 944, 889, 721, 675 cm^{-1}; UV-vis (hexanes) λ_{max} (ε_{max}, L Mol^{-1} cm^{-1}) nm, 245 (1,510), 339 (1,620), 408 (2,430), 493 (360), 520 (380), 687 (286); EI MS *m/z* 440 (M^+); HRMS calcd for $C_{28}H_{31}F_3O$: 440.2327, found: 440.2331; Anal. Calcd for $C_{28}H_{31}F_3O$: C, 76.34; H, 7.09; Found: C, 76.23; H, 7.11.

Open form 42-o: ^{19}F NMR (282MHz, $CDCl_3$) δ 70.47;

***Trans-bis*-2'-[2,7-di-*tert*-butyl-10b,10c-dimethyl-*trans*-10b,10c-dihydropyren-4-yl]ethynyl *bis*(triethylphosphino) platinum (II) 43**

DHP-ethyne **24** (84 mg, 0.23 mmol) and *trans*-Pt$(PEt_3)_2Cl_2$ (50 mg, 0.10 mmol) were mixed in degassed (argon bubbled for 15 minutes) diethylamine (20 mL) in a Schlenk tube at room temperature. Then CuI (1.0 mg, 0.0052 mmol) was added. The reaction

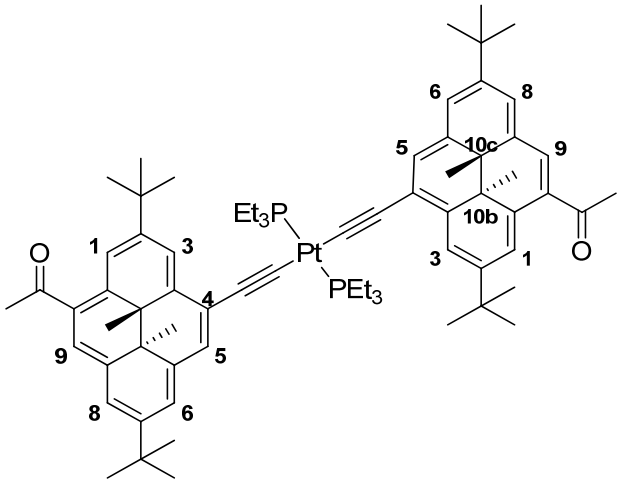
mixture was heated to a mild reflux at 50°C under argon for 12 hours. The amine was evaporated and the crude product was purified on an alumina column (deactivated with 5% water) using hexane and dichloromethane as eluant. The DHP-ethyne **24** (5 mg, 69% recovery) was eluted first (using hexane-DCM 10:1) and complex **43** (100 mg, 95% yield) second (using hexane-DCM 1:1). The isolated Pt complex was then recrystallized from DCM and methanol to afford a dark green crystals of **43**, m.p. 166-168°C.



43: ^{1}H NMR (500MHz, CD_2Cl_2) δ 9.130 (s, 1H, H-3), 9.128 (s, 1H, H-3), 8.52 (s, 2H, H-5), 8.51 (s, 2H, H-1), 8.48 (s, 2H, H-8), 8.45 (s, 2H, H-6), 8.40 (AB, J = 7.8 Hz, 2H, H-9), 8.38 (AB, J = 7.8 Hz, 2H, H-10), 2.56-2.50 (m, 12H, -C$\underline{H}_2$CH$_3$), 1.73 (s, 18H, 2-C(C$\underline{H}_3$)$_3$), 1.70 (s, 18H, 7-C(C$\underline{H}_3$)$_3$), 1.41 (dt, $^{2}J_{P\text{-}H}$ = 16.5 Hz, $^{3}J_{H\text{-}H}$ = 7.7 Hz, 18H, -CH$_2$C$\underline{H}_3$), -3.83 (s, 6H, 10c-C$\underline{H}_3$), -3.86 (s, 6H, 10b-C$\underline{H}_3$); ^{13}C NMR (125MHz, CD_2Cl_2) δ 146.50 (C-7), 145.75 (C-2), 137.61 (C-10a/10d), 137.58 (C-10a/10d), 137.11 (C-5a), 136.46 (C-3a), 127.04 (C-5), 123.43 (C-9/10), 122.82 (C-9/10), 122.17 (C-4), 121.45 (C-1), 121.05 (C-3), 120.77 (C-8), 119.87 (C-6), 115.11 ($^{1}J_{Pt\text{-}C}$ = 29 Hz, -C≡$\underline{C}$-Pt), 110.95 (-$\underline{C}$≡C-Pt), 36.57 (2-$\underline{C}$(CH$_3$)$_3$), 36.38 (7-$\underline{C}$(CH$_3$)$_3$), 32.46 (2-C($\underline{C}$H$_3$)$_3$), 32.26 (7-C($\underline{C}$H$_3$)$_3$), 30.85 (C-10b), 30.30 (C-10c), 17.36 (t, $^{1}J_{P\text{-}C}$ = 17 Hz, -$\underline{C}$H$_2$CH$_3$), 15.60 (C-10c), 14.81 (C-10b), 9.10 (-CH$_2$$\underline{C}H_3$); ^{31}P NMR (202 MHz, CD_2Cl_2) δ 13.24 ($^{1}J_{Pt\text{-}P}$ = 2383 Hz); IR (KBr) ν 3034, 2963, 2904, 2872, 2082, 1457, 1379, 1357, 1343, 1254, 1231, 1034, 882, 768, 733, 664 cm^{-1}; UV-vis (cyclohexane) λ_{max} (ε_{max}, L Mol^{-1} cm^{-1}) nm, 366 (97,300), 408 (136,000), 479 (30,200), 504 (32,700), 670 (5,370); ESI MS *m/z* 1164 (M^{+}); HRMS calcd for $C_{68}H_{92}P_2Pt$: 1164.6301, found: 1164.6389.

***Trans-bis*-2'-[10-acetyl-2,7-*bis*-*t*-butyl-10b,10c-dimethyl-*trans*-10b,10c-dihydropyren-4-yl] ethynyl *bis*(triethylphosphino) platinum(II) 44A and 4-yl,5-yl isomer 44B**

Using the procedure for complex **43**, the ethyne **30** (70 mg, 0.17 mmol) and *trans*-$Pt(PEt_3)_2Cl_2$ (43 mg, 0.086 mmol) with CuI (2.0 mg, 0.011 mmol) in degassed Et_2NH (15 mL) gave complex **44**. Chromatography on silica gel, eluting with hexanes and DCM (1:1), afforded pure **44** (50 mg, 50% yield). The product was recrystallized from DCM and methanol. M.p.180-187°C.



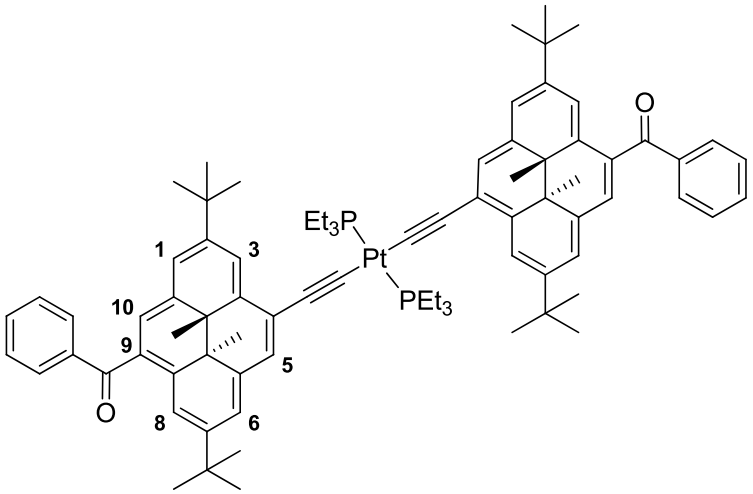
44A: ^{1}H NMR (500 MHz, CD_2Cl_2) δ 9.70 (d, J = 1.0 Hz, 2H, H-1), 9.19 (d, J = 1.1 Hz, 2H, H-3), 8.80 (s, 2H, H-9), 8.57 (s, 2H, H-5), 8.54 (s, 2H, H-8), 8.42 (s, 2H, H-6), 3.05 (s, 6H, -COC$\underline{H}_3$), 2.47-2.45 (m, 12H, -PC$\underline{H}_2$CH$_3$), 1.71 (s, 18H, 7-C(C$\underline{H}_3$)$_3$), 1.67 (s, 18H, 2-C(C$\underline{H}_3$)$_3$), 1.37 (t, J = 7.6 Hz, 18H, -PCH$_2$C$\underline{H}_3$), -3.72 (s, 6H, 10c-C$\underline{H}_3$), -3.75 (s, 6H, 10b-C$\underline{H}_3$); ^{13}C NMR (125MHz, CD_2Cl_2) δ 202.55 (-$\underline{C}$OCH$_3$), 150.43 (C-7), 146.44 (C-2), 139.29 (C-3a), 136.64 (C-5a/10d), 136.24 (C-10a), 135.29 (C-5a/10d), 128.90 (C-5), 128.25 (C-10), 123.88 (C-9), 122.97 (C-8), 122.79 (C-4), 121.76 (C-6), 121.56 (C-3), 120.62 (C-1), 115.13 (d, $^1J_{Pt\text{-}C}$ = 29.4 Hz, -C≡$\underline{C}$Pt-), 110.46 (-$\underline{C}$≡C-Pt-), 36.93 (7-$\underline{C}$(CH$_3$)$_3$), 36.07 (2-$\underline{C}$(CH$_3$)$_3$), 32.21 (7-C(C$\underline{H}_3$)$_3$), 32.10 (2-C(C$\underline{H}_3$)$_3$), 31.67 (C-10b), 31.13 (-CO$\underline{C}$H$_3$), 29.44 (C-10c), 17.04 (t, J = 17.4 Hz, -P$\underline{C}$H$_2$CH$_3$), 15.59 (10c-$\underline{C}$H$_3$),

15.32 (10b-$\underline{C}H_3$), 8.89 (-$PCH_2\underline{C}H_3$); ^{31}P NMR ($CDCl_3$, 202 MHz) δ 13.12 ($^1J_{Pt\text{-}P}$ = 2384 Hz); ^{195}Pt NMR (CD_2Cl_2, 77 MHz) δ -252.22 ($^1J_{P\text{-}Pt}$ = 2655 Hz);

44A and **44B:** IR (KBr) ν 2964, 2784, 2081, 1666, 1459, 1409, 1379, 1348, 1242, 1224, 1207, 1154, 1035, 890, 768, 733 cm^{-1}; UV-vis (cyclohexane) λ_{max} (ε_{max}, L Mol^{-1} cm^{-1}) nm, 279 (7,500), 387 (20,200), 429 (29,600), 494 (8,000), 697 (3,500); ESI MS *m/z* 1249 (M^++H); HRMS calcd for $C_{72}H_{96}O_2P_2Pt$+H: 1249.6591, found: 1249.6556.

***Trans-bis*-2''-[9-benzoyl-2,7-*bis*-*t*-butyl-10b,10c-dimethyl-*trans*-10b,10c-dihydropyren-4-yl]ethynyl -*bis*(triethylphosphino) platinum(II) and 4-yl,5-yl isomer, 45A,B**

Using the described procedure for making complex **43**, the isomeric mixture of benzoyl DHP-ethyne **34** (30 mg, 0.063 mmol), $Pt(PEt_3)_2Cl_2$ (15 mg, 0.030 mmol) and catalyst CuI (1.0 mg, 5.3×10^{-3} mmol) reacted in Et_2NH (6 mL) to afford a solid of **45**. Recrystallization from DCM/hexane/methanol gave a dark red crystal of **45** (14 mg, 35% yield). M.p. 190-198°C.



45B: (the major component in the crystallized mixture) ^{1}H NMR (500MHz, $CDCl_3$) δ 9.19 (s, 1H, H-3), 8.91 (s, 1H, H-8), 8.55 (s, 1H, H-10), 8.53 (s, 1H, H-5), 8.48 (s, 1H, H-1), 8.41 (s, 1H, H-6), 7.93-7.89 (m, 2H, H-2'), 7.60 (t, *J* = 7.5 Hz, 1H, H-4'), 7.52-7.47 (m,

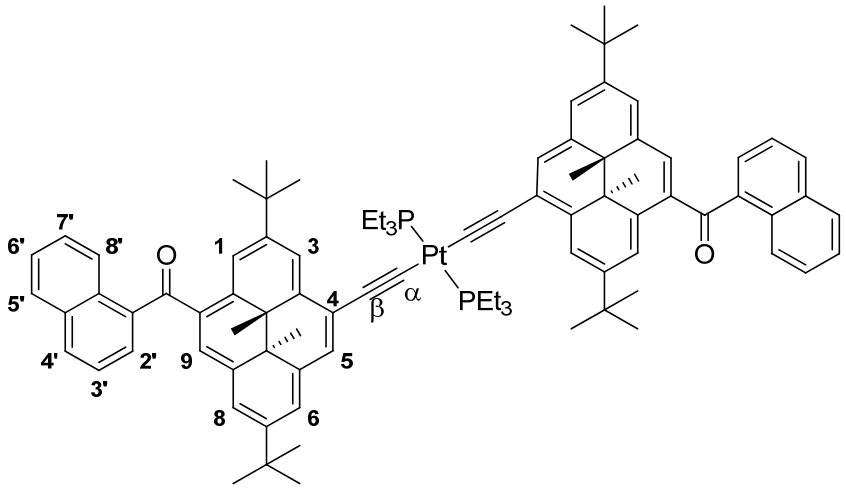
2H, H-3'), 2.54-2.43 (m, 6H, -PC$\underline{H}_2$CH$_3$), 1.68 (s, 9H, 2-C(C$\underline{H}_3$)$_3$), 1.56 (s, 9H, 2-C(C$\underline{H}_3$)$_3$), 1.44-1.35 (m, 9H, -PCH$_2$C$\underline{H}_3$), -3.60 (s, 3H, 10b-C$\underline{H}_3$), -3.65 (s, 3H, 10c-C$\underline{H}_3$); ^{13}C NMR (125MHz, $CDCl_3$) δ 199.36 (-$\underline{C}$OPh), 149.35 (C-2), 145.77 (C-2), 141.24 (C-1'), 139.18 (C-5a), 136.66 (C-10a), 136.29 (C-3a), 134.84 (C-10d), 132.33 (C-4'), 130.57 (C-2'), 128.45 (C-9), 127.39 (C-5), 125.23 (C-10), 124.08 (C-4), 123.44 (C-1), 123.02 (C-3), 119.90 (C-6,8), 110.86 (-$\underline{C}$≡C-Pt-), 36.48 (7-$\underline{C}$(CH$_3$)$_3$), 36.28 (2-$\underline{C}$(CH$_3$)$_3$), 32.20 (2-C(C$\underline{H}_3$)$_3$), 31.92 (2-C(C$\underline{H}_3$)$_3$), 31.17 (C-10c), 30.20 (C-10b), 17.05 (t, J = 14 Hz, -P$\underline{C}$H$_2$CH$_3$), 16.10 (10b-$\underline{C}$H$_3$), 15.10 (10c-$\underline{C}$H$_3$), 8.91 (-PCH$_2\underline{C}$H$_3$); ^{31}P NMR ($CDCl_3$, 145 MHz) δ 12.81 ($^1J_{Pt\text{-}P}$ = 2383 Hz);

45A: ^{1}H NMR (500MHz, $CDCl_3$, clearly observable signals) δ 9.18 (s), 8.87 (s), 8.59 (s), 8.50 (s), 8.46 (s), 8.45 (s), 1.66 (s, -C(C$\underline{H}_3$)$_3$), 1.58 (s, -C(C$\underline{H}_3$)$_3$), -3.62 (s, internal C$\underline{H}_3$), -3.64 (s, internal C$\underline{H}_3$);

45A and 45B: IR (KBr) ν 2963, 2904, 2873, 2077, 1640, 1511, 1446, 1379, 1345, 1258, 1245, 1209, 1174, 1035, 1021, 892, 767, 733, 698 cm^{-1}; UV-vis (toluene) λ_{max} (ε_{max}, L Mol^{-1} cm^{-1}) nm, 370 (sh, 50,200), 427 (96,300), 523 (24,300), 621 (770), 681 (1,990); ESI MS *m/z* 1373 (M^+); HRMS calcd for $C_{82}H_{100}O_2P_2Pt$+H: 1373.6904, found: 1373.6871.

Trans-bis-2''-[10-(1-naphthoyl)-2,7-_bis-t_-butyl-10b,10c-dimethyl-_trans_-10b,10c-dihydropyren-4-yl]ethynyl-_bis_(triethylphosphino) platinum(II) 46A and 4-yl,5-yl isomer 46B

Using the procedure for making complex **43**, the 1'-naphthoyl DHP-ethyne **39** (60 mg, 0.12 mmol) and *trans*-Pt(PEt$_3$)$_2$Cl$_2$ (30 mg, 0.060 mmol) and CuI (1.7 mg, 8.9×10^{-3} mmol) in degassed Et$_2$NH (6 mL) formed complex **46** in 12 hours. Diethyl amine was removed and the solid was dissolved in benzene, dried over MgSO$_4$ and concentrated. Recrystallization on the solid residue from benzene and pentane afforded dark orange complex **46** (40 mg, 70% yield). M.p. 207-212 °C.



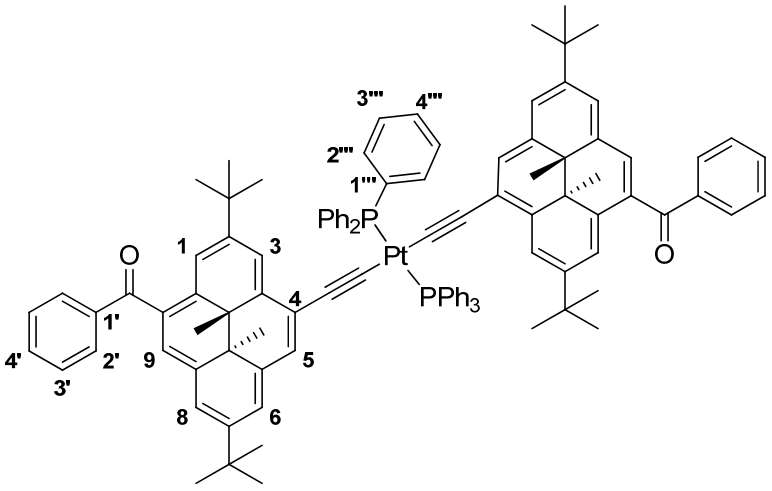
46A: ^{1}H NMR (500 MHz, $CDCl_3$) δ 9.31 (s, 2H, H-1), 9.20 (s, 2H, H-3), 8.60 (s, 2H, H-5), 8.50 (s, 2H, H-9), 8.46 (d, J = 8.4 Hz, 2H, H-8'), 8.43 (s, 2H, H-6), 8.37 (s, 2H, H-8), 8.05 (d, J = 8.3 Hz, 2H, H-4'), 7.98 (d, J = 8.0 Hz, 2H, H-5'), 7.64 (dd, J = 7.0, 1.0 Hz, 2H, H-2'), 7.57-7.52 (m, 2H, H-6'), 7.52-7.44 (m, 4H, H-3',7'), 2.54-2.42 (m, 12H, -PC$\underline{H}_2$CH$_3$), 1.61 (s, 9H, 7-C(C$\underline{H}_3$)$_3$), 1.57 (s, 9H, 2-C(C$\underline{H}_3$)$_3$), 1.43-1.34 (m, 18H, -PCH$_2$C$\underline{H}_3$), -3.62 (s, 6H, 10b,10c-C$\underline{H}_3$); ^{13}C NMR (125 MHz, $CDCl_3$) δ 201.07 (-$\underline{C}$O-), 149.73 (C-2), 146.54 (C-7), 140.39 (C-1'), 139.13 (C-3a), 137.26 (C-10a), 136.62 (C-5a/10d), 134.80 (C-5a/10d), 134.08 (C-8'b), 131.47 (C-8'a), 131.36 (C-4'), 130.05 (C-10), 128.88 (C-5,2'), 128.57 (C-5'), 127.45 (C-7'), 126.54 (C-6'), 126.25 (C-8'), 125.51 (C-9), 124.83 (C-3'), 123.29 (C-8), 121.82 (C-6), 121.48 (C-3), 120.27 (C-1), 119.96 (C-10), 110.43 (C-β), 36.73 (2-$\underline{C}$(CH$_3$)$_3$), 36.03 (7-$\underline{C}$(CH$_3$)$_3$), 31.98 (2/7-C(C$\underline{H}_3$)$_3$), 31.97 (2/7-C(C$\underline{H}_3$)$_3$), 31.86 (C-10b), 29.53 (C-10c), 17.00 (t, J = 17 Hz, -P$\underline{C}$H$_2$CH$_3$), 15.71 (10b-C$\underline{H}_3$), 15.16 (10b-C$\underline{H}_3$), 8.85 (-PCH$_2$C$\underline{H}_3$); ^{31}P NMR ($CDCl_3$, 202 MHz) δ 12.89 ($^{1}J_{Pt\text{-}P}$ = 2383 Hz); ^{195}Pt NMR ($CDCl_3$, 77 MHz) δ -214.77 ($^{1}J_{P\text{-}Pt}$ = 2385 Hz);

46B: ^{1}H NMR (500MHz, $CDCl_3$, clearly observable signals) δ 9.37, 9.18, 8.54, 8.52, 8.42, 8.40 (d, J = 8.6 Hz).

46A and **46B:** IR (KBr) ν 2963, 2905, 2873, 2080, 1641, 1588, 1508, 1477, 1459, 1381, 1345, 1273, 1243, 1196, 1035, 891, 783, 768 cm^{-1}; UV-vis (toluene) λ_{max} (ε_{max}, L Mol^{-1} cm^{-1}) nm, 371 (70,200), 437 (109,000), 495 (25,600), 633 (2,100), 694 (7,500); ESI MS *m/z* 1473 (M^{+}); HRMS calcd for $C_{90}H_{104}O_2P_2Pt$+H: 1473.7217, found: 1473.7190;

***Trans-bis*-2''-[10-benzoyl-2,7-*bis*-*t*-butyl-10b,10c-dimethyl-*trans*-10b,10c-dihydropyren-4-yl]ethynyl *bis*(triphenylphosphino) platinum(II) 47A and 4-yl,5-yl isomer 47B**

Using the procedure for complex **43**, the benzoyl DHP-ethyne **34** (70 mg, 0.15 mmol), *trans*-$Pt(PPh_3)_2Cl_2$ (50 mg, 0.063 mmol) and CuI (1.0 mg, 5.3×10^{-3} mmol) were mixed within Et_2NH (10 mL) to afford solid, which was washed with methanol to give 30 mg (30% yield) of **32** as dark red crystals, m.p. 172-180°C.



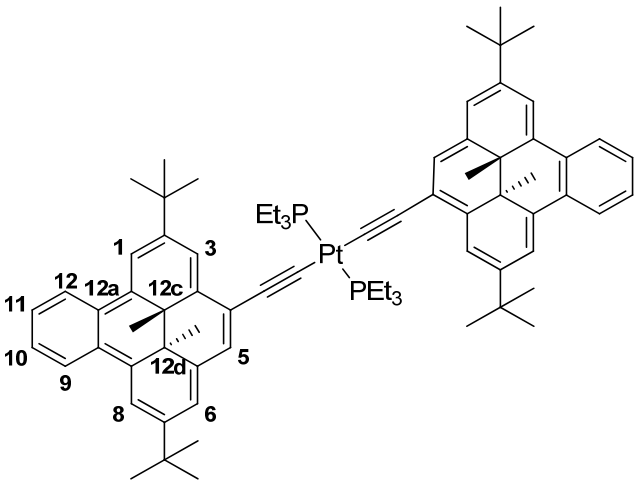
47A: ^{1}H NMR (500 MHz, CD_2Cl_2) δ 8.71 (s, 2H, H-1), 8.61 (s, 2H, H-3), 8.44 (s, 2H, H-8), 8.41 (s, 2H, H-9), 8.26 (s, 2H, H-6), 8.07-8.03 (m, 12H, H-2",6"), 7.86 (d, J = 7.2 Hz, 4H, H-2'), 7.64-7.60 (m, 4H, H-9,4'), 7.49 (t, J = 7.7 Hz, 4H, H-3'), 7.24-7.17 (m, 18H, H-3",4",5"), 1.65 (s, 18H, 7-C($C\underline{H}_3$)$_3$), 1.34 (s, 18H, 2-C($C\underline{H}_3$)$_3$), -3.87 (s, 6H, 10c-$C\underline{H}_3$), -3.88 (s, 6H, 10b-$C\underline{H}_3$); ^{13}C NMR (125MHz, CD_2Cl_2) δ 199.50 (-$\underline{C}$O-Ph), 148.49 (C-7), 146.89 (C-2), 141.49 (C-1'), 137.94 (C-3a), 136.63 (C-5a/10d), 136.34 (C-10a), 135.92 (t, J = 5.6 Hz, C-2",6"), 135.18 (C-5a/10d), 132.78 (C-4'), 132.36 (t, J = 29.2 Hz, C-1"), 130.91 (C-4"), 130.77 (C-2'), 130.18 (C-10), 128.83 (C-3'), 128.49 (C-9/ C-3",5"), 128.44 (C-9/C-3",5"), 128.40 (C-5/C-3",5"), 124.11 (C-9), 123.16 (C-4), 122.72 (C-8), 121.57 (C-3,6), 120.42 (C-1), 115.29 ($\underline{C}$≡C-Pt), 36.70 (7-$\underline{C}(CH_3)_3$), 36.34 (2-$\underline{C}(CH_3)_3$), 32.21 (2-C($\underline{C}H_3$)$_3$), 32.13 (7-C($\underline{C}H_3$)$_3$), 31.55 (C-10b), 29.85 (C-10c), 15.58 (10b-$\underline{C}H_3$), 15.33

(10c-$\underline{C}H_3$); ^{31}P NMR (145 MHz, CD_2Cl_2) δ 18.28 ($^1J_{Pt\text{-}P}$ = 2651 Hz); ^{195}Pt NMR (77 MHz, CD_2Cl_2) δ -252.22 ($J_{P\text{-}Pt}$ = 2655 Hz).

47A and 47B: IR (Film) ν 3056, 2963, 2092, 1650, 1595, 1480, 1435, 1246, 1098, 691 cm^{-1}; UV-vis (toluene) λ_{max} (ε_{max}, L Mol^{-1} cm^{-1}) nm, 373 (47,300), 433 (63,100), 493 (17,800), 684 (4,600); ESI MS *m/z* 1661 (M^+); HRMS calcd for $C_{106}H_{100}O_2P_2Pt$+H: 1661.6904, found: 1661.6877.

***Trans-bis*-2'-[2,7-*bis*-*t*-butyl-12c,12d-dimethyl-*trans*-12c,12d-dihydrobenzo[e]pyren-4-yl]ethynyl *bis*(triethylphosphino) platinum(II) 48**

Using the procedure for complex **43**, the ethyne **40** (40 mg, 0.096 mmol), $Pt(PEt_3)_2Cl_2$ (23 mg, 0.046 mmol) and CuI (1.0 mg, 5.3×10^{-3} mmol) were mixed within Et_2NH (6 mL) to afford product **48** in two hours. The residual was re-dissolved in DCM and filtered through a Celite pad to remove inorganic impurity. The product was then recrystallized from methanol to give a dark red crystals of **48** (50 mg, 84% yield). M.p. 169-170°C.



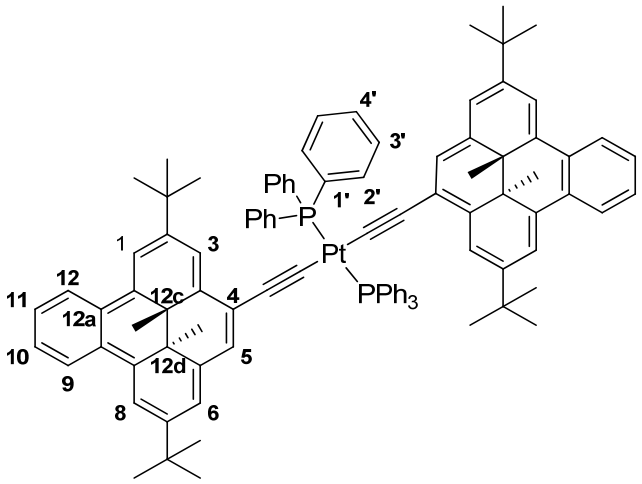
48: ^{1}H NMR (500 MHz, C_6D_6) δ 8.86-8.83 (m, 2H, H-12), 8.80-8.78 (m, 2H, H-9), 8.58 (d, *J* = 1.3 Hz, 2H, H-3), 8.49 (d, *J* = 1.3 Hz, 2H, H-1), 8.381 and 8.379 (s, 2H, H-8), 7.725 and 7.724. (s, 2H, H-5), 7.52 (s, 2H, H-6), 7.53-7.48 (m, 4H, H-10,11), 2.34-2.21 (m, 12H, -PC$\underline{H}_2$CH$_3$), 1.60 (s, 18H, 2-C(C$\underline{H}_3$)$_3$), 1.42 (s, 18H, 7-C(C$\underline{H}_3$)$_3$), 1.28-1.18 (m,

18H, -$PCH_2C\underline{H}_3$), -1.02 (s, 6H, 12d-CH_3), -1.04 (s, 3H, 12c-CH_3); ^{13}C NMR (125 MHz, C_6D_6) δ 144.94 (C-7), 144.02 (C-2), 138.40 (C-5a), 137.32 (C-3a), 136.26 (C-12e), 135.91 (C-12b), 130.65 (C-12a), 130.09 (C-12f), 126.89 (C-5), 126.63 (C-11), 126.37 (C-10), 125.46 (C-12) 125.42 (C-9), 121.32 (C-4), 120.99 (C-3), 120.20 (C-6), 118.18 (C-1), 117.46 (C-8), 115.05 (t, $^2J_{C\text{-}P}$ = 15 Hz, -Pt-$\underline{C}\equiv$C-), 111.00 (-C$\equiv\underline{C}$-C), 37.23 (C-12c), 36.44 (C-12d), 36.18 (2-$\underline{C}(CH_3)_3$), 35.78 (7-$\underline{C}(CH_3)_3$), 31.52 (2-C($\underline{C}H_3)_3$), 31.05 (7-C($\underline{C}H_3)_3$), 19.04 (12d-$\underline{C}H_3$), 18.67 (12c-$\underline{C}H_3$), 17.47 (t, $^1J_{C\text{-}P}$ = 17.8 Hz, $\underline{C}H_2CH_3$), 9.10 ($CH_2\underline{C}H_3$); ^{31}P NMR (145 MHz, C_6D_6) δ 12.18 ($^1J_{Pt\text{-}P}$ = 2398 Hz); ^{195}Pt NMR (77 MHz, C_6D_6) δ -219.79 ($^1J_{Pt\text{-}P}$ = 2400 Hz); IR (KBr) ν 2960, 2924, 2862, 2071, 1460, 1365, 1249, 1035, 870, 772, 749, 632 cm^{-1}; UV-vis (cyclohexane) λ_{max} (ε_{max}, L Mol^{-1} cm^{-1}) nm, 341 (34,610), 355 (35,700), 399 (51,400), 418 (73,700), 502 (11,600), 525 (14,100), 553 (12,200), 641 (1,050); ESI MS *m*/z 1264 (M^+); HRMS calcd for $C_{76}H_{96}P_2Pt$: 1265. 6614, found: 1264.6599.

^{1}H NMR (500 MHz, $CDCl_3$) δ internal methyl protons at -1.46 and -1.49; ^{31}P NMR (145 MHz, $CDCl_3$) δ 12.2 (d, $^1J_{Pt\text{-}P}$ = 2395 Hz); ^{195}Pt NMR (77 MHz, $CDCl_3$) δ -212.20 ($^1J_{Pt\text{-}P}$ = 2400 Hz);

Trans-bis-2''-[2,7-_bis-t_-butyl-12c,12d-dimethyl-_trans_-12c,12d-dihydrobenzo[e]pyren-4-yl]ethynyl _bis_(triphenylphosphino) platinum(II) 49

Using the procedure in making complex **43**, the benzo[e]DHP-ethyne 40 (40 mg, 0.095 mmol), *trans*-$Pt(PPh_3)_2Cl_2$ (35 mg, 0.045 mmol) and CuI (1.0 mg, 5.3×10^{-3} mmol) were mixed within Et_2NH (10 mL) to precipitate a red solid of **49** (45 mg, 65% yield). M.p. decomposed at 180°C. X-ray quality crystals were obtained by slowly evaporating toluene.

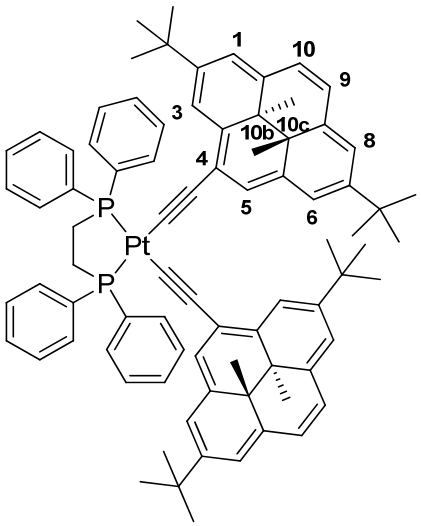


49: ^{1}H NMR (500 MHz, C_6D_6) δ 8.83-8.79 (m, 4H, H-9,12), 8.39 (s, 2H, H-1), 8.37 (d, J = 1.1 Hz, 2H, H-8), 8.19 (m, 12H, H-2'), 7.83 (t, J = 1.1 Hz, 2H, H-3), 7.52-7.47 (m, 4H, H-10,11), 7.26 (d, J = 1.0 Hz, 2H, H-6), 7.04 (t, J = 7.4 Hz, 12H, H-3'), 6.93 (t, J = 7.0 Hz, 6H, H-4'), 6.62 (dd, J = 3.9, 0.8 Hz, 2H, H-5), 1.46 (s, 2H, 7-C(C$\underline{H}_3$)$_3$), 1.35 (s, 2H, 2-C(C$\underline{H}_3$)$_3$), -1.22 (d, J = 3.3 Hz, 2H, 12d-$\underline{C}H_3$), -1.27 (d, J = 4.2 Hz, 2H, 12c-$\underline{C}H_3$); ^{13}C NMR (125 MHz, C_6D_6) δ 143.99 (C-7), 143.23 (C-2), 136.96 (C-5a), 136.86 (C-3a), 136.15 (t, $^{2}J_{C\text{-}P}$ = 6 Hz, C-2'), 135.87 (C-12e), 135.43 (C-12b), 132.63 (t, $^{1}J_{C\text{-}P}$ = 29.2 Hz, C-1'), 130.78 (C-4'), 130.61 (C-12a), 129.99 (C-12f), 128.44 (t, $^{3}J_{C\text{-}P}$ = 5.5 Hz, C-3'), 127.28 (C-5), 126.16 (C-10,11), 125.41 (C-9 or 12), 125.34 (C-9 or 12), 121.24 (C-4), 121.13 (C-3), 120.23 (C-6), 118.60 (t, $^{2}J_{C\text{-}P}$ = 15.1 Hz, Pt-$\underline{C}$≡C-), 118.04 (C-1), 117.29 (C-8), 115.77 (-Pt-C≡$\underline{C}$-), 36.77 (C-12c), 36.05 (C-12d), 35.88 (2-$\underline{C}$(CH$_3$)$_3$), 35.71 (7-$\underline{C}$(CH$_3$)$_3$), 31.38 (2-C($\underline{C}$H$_3$)$_3$), 31.11 (7-C($\underline{C}$H$_3$)$_3$), 18.74 (12c-$\underline{C}H_3$), 18.65 (12d-$\underline{C}H_3$); ^{31}P NMR (202 MHz, C_6D_6) δ 19.02 ($^{1}J_{Pt\text{-}P}$ = 2677 Hz); ^{195}Pt NMR (77MHz, C_6D_6) δ -253.77 (t, $^{1}J_{Pt\text{-}P}$ = 2695 Hz); IR (KBr) ν 3057, 2960, 2922, 2864, 2099, 1476, 1434, 1365, 1254, 1096, 743, 692, 521, 513 cm^{-1}; UV-vis (toluene) λ_{max} (ε_{max}, L Mol^{-1} cm^{-1}) nm, 342 (35,200), 359 (37,000), 423 (78,900), 529 (13,600); ESI MS *m/z* 1553 (M^{+}+H); HRMS calcd for $C_{100}H_{96}P_2Pt$+H: 1553.6692, found: 1553.6676.

Open form 49-o: ^{1}H NMR (500 MHz, C_6D_6) δ 8.17-8.11 (m, 2H), 8.11-8.04 (m, 10H), 7.76-7.69 (m, 4H), 7.22-7.18 (m, 4H), 7.08-6.96 (m, 24H), 6.77-6.74 (m, 2H), 6.00 (s, 1H), 5.97 (s, 1H), 1.43 (s, 3H), 1.42 (s, 3H), 1.39 (s, 6H), 1.278 (s, 9H), 1.276 (s, 9H), 1.137 (s, 9H), 1.134 (s, 9H).

Cis-bis-2''-[2,7-di-_tert_-butyl-10b,10c-dimethyl-_trans_-10b,10c-dihydropyren-4-yl] ethynyl _bis_(diphenylphosphino)ethane-P,P′] platinum (II) 50

Using the procedure for complex **43**, the DHP-ethyne **24** (50 mg, 0.135 mmol), $Pt(dppe)Cl_2$ (44 mg, 0.066 mmol) and CuI (1.6 mg, 8.4×10^{-3} mmol) were mixed within Et_2NH (10 mL) to precipitate a brown solid. This was chromatographed on alumina eluting with hexanes and DCM (3:10). The alkyne dimer[270] was eluted first (6 mg, 12% yield) and then the orange product **50** (22 mg, 25% yield) was eluted second. This was washed with methanol to give orange crystals of **50**. M.p. decomposed at 180°C.

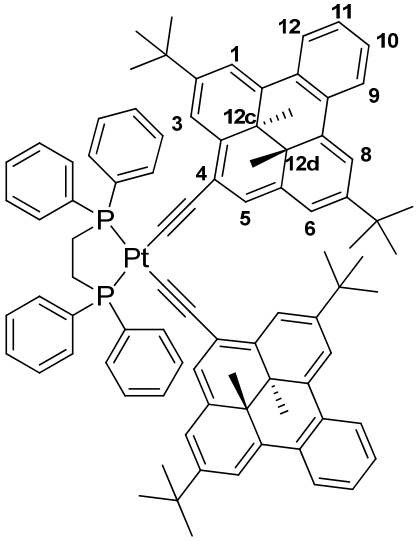


50: ^{1}H NMR (500 MHz, C_6D_6) δ 9.88 and 9.87 (s, 2H, H-3), 8.76 (s, 2H, H-5), 8.57 and 8.56 (s, 2H, H-1), 8.54 (s, 2H, H-8), 8.44 (AB, J = 8.9 Hz, 4H, H-9,10), 8.38 (s, 2H, H-6), 8.26-8.16 (m, 4H, *meta*-H), 7.06-6.92 (m, 6H, *ortho*- and *para*-H), 2.08-1.91 (m, 4H, -PC$\underline{H}_2$C$\underline{H}_2$P-), 1.609 and 1.607 (s, 18H, 7-C(C$\underline{H}_3$)$_3$), 1.435 and 1.424 (s, 18H, 2-C(C$\underline{H}_3$)$_3$), -3.40 (s, 6H, H-10b), -3.41 (s, 6H, H-10c); ^{13}C NMR (125 MHz, C_6D_6) δ 146.31 (C-2), 145.59 (C-7), 138.19 (C-10a/10e), 137.64 (C-3a), 137.04 (C-5a), 134.61-134.50 (*meta*-C), 131.49 (*ortho*-C, *para*-C), 129.35-129.24 (*ortho*-C , *para*-C), 128.5 (underneath the solvent C_6D_6 residual peak, C-5), 123.59 (C-10), 123.18 (C-9), 122.81 (C-4), 122.70 (C-3), 121.80 (C-1), 120.84 (C-8), 120.39 (C-6), 114.16 (dd, $^2J_{P(trans\text{-})\text{-}C}$ = 150 Hz, $^2J_{P(cis\text{-})\text{-}C}$ =

15 Hz, -C≡C-Pt-), 113.28 (d, $^{2}J_{P(trans\text{-})\text{-}C}$ = 35 Hz, -C≡C-Pt-), 36.50 (2-C(CH$_3$)$_3$), 36.26 (7-C(CH$_3$)$_3$), 32.60 (2-C(CH$_3$)$_3$), 32.43 (2-C(CH$_3$)$_3$), 31.34 (C-10b), 30.89 (C-10c), 29.00-28.30 (m, -PCH$_2$CH$_2$P-), 15.98 (C-10b/10c), 15.60 (C-10b/10c); ^{31}P NMR (202 MHz, CDCl$_3$) δ 39.57 ($^{1}J_{Pt\text{-}P}$ = 2277 Hz); ^{195}Pt NMR (77MHz, CDCl$_3$) δ -381.53 (t, $^{1}J_{Pt\text{-}P}$ = 2278 Hz); IR (KBr) ν 2960, 2863, 2093, 1589, 1476, 1459, 1435, 1230, 1103, 881, 704, 690, 531 cm^{-1}; UV-vis (toluene) λ_{max} (ε_{max}, L Mol^{-1} cm^{-1}) nm, 367 (55,200), 405 (54,600), 478 (12,100), 503 (12,100), 669 (2,200); ESI MS *m/z* 1327 (M^{+}); HRMS calcd for $C_{82}H_{86}P_2Pt$+H: 1327.5910, found: 1327.5889.

Cis-_bis_-2''-[2,7-_bis_-_t_-butyl-12c,12d-dimethyl-_trans_-12c,12d-dihydrobenzo[e]pyren-4-yl]ethynyl _bis_((diphenylphosphino)ethane-P,P')platinum(II) 52

Using the procedure for complex **43**, the DHP-ethyne **40** (40 mg, 0.095 mmol), Pt(dppe)Cl$_2$ (30 mg, 0.046 mmol) and CuI (2.6 mg, 13×10^{-3} mmol) in Et$_2$NH (7 mL) gave a red solid. This was chromatographed on alumina eluting with hexanes and DCM (1:2). The ethyne dimer[105] (5 mg, 12% yield) eluted first and red product **52** (16 mg, 25% yield) second. M.p. decomposed at 200°C.



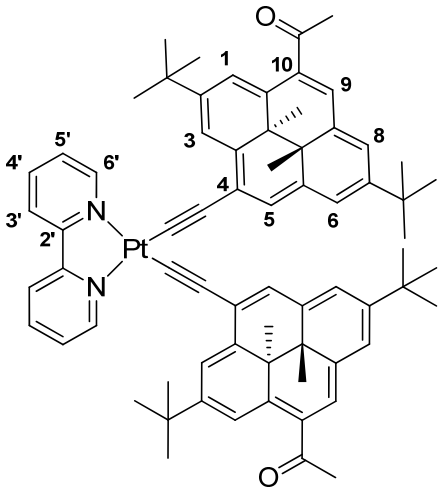
52: ^{1}H NMR (500 MHz, C_6D_6) δ 8.86 and 8.84 (s, 2H, H-3), 8.82-8.77 (m, 4H, H-9,12), 8.43 (s, 2H, H-1), 8.37 (s, 2H, H-8), 8.14-8.07 (m, 8H, *meta*-H), 7.50-7.44 (m, 4H, H-10,11), 7.41 (s, 2H, H-5), 7.29 (s, 2H, H-6), 7.09-6.94 (m, 12H, *ortho*- and *para*-H),1.98-1.81 (m, 4H, -PC$\underline{H}_2$C$\underline{H}_2$P-), 1.42 (s, 18H, 7-C(C$\underline{H}_3$)$_3$), 1.33 (s, 18H, 2-C(C$\underline{H}_3$)$_3$), -1.06, -1.07 and -1.08 (12c,12d-C$\underline{H}_3$); ^{13}C NMR (125 MHz, C_6D_6) δ 144.56 and 144.52 (C-2), 143.93 (C-7), 138.93 (C-3a), 137.45 and 137.43 (C-5a), 135.95 (C-12b/12e), 135.85 (C-12b/12e), 134.56 and 134.46 and 134.38 (*meta*-C), 131.46 (*para*-C), 130.66 (C-12a), 130.09 (C-12f), 129.29 and 129.26 and 129.20 (*ortho*-C), 127.59 and 127.55 (C-5), 126.37 and 126.10 (C-10,11), 125.50 and 125.32 (C-9,12), 122.09 (C-3), 120.80 (C-4), 120.52 (C-6), 118.37 (C-1), 117.33 (C-8), 113.42 (dd, $^{2}J_{P(trans\text{-})\text{-}C}$ = 150 Hz, $^{2}J_{P(cis\text{-})\text{-}C}$ = 14 Hz, -C≡$\underline{C}$Pt-), 112.5 (dd, $^{2}J_{P(trans\text{-})\text{-}C}$ = 36 Hz, $^{2}J_{P(cis\text{-})\text{-}C}$ = 6 Hz, -$\underline{C}$≡CPt-), 37.08 (C-12c), 36.33 (C-12d), 36.09 (2-$\underline{C}$(CH$_3$)$_3$), 35.72 (7-$\underline{C}$(CH$_3$)$_3$), 31.36 (2-C($\underline{C}$H$_3$)$_3$), 31.13 (7-C($\underline{C}$H$_3$)$_3$), 28.76-28.36 (m, -P$\underline{C}$H$_2$$\underline{C}H_2$P-), 18.86 and 18.83 and 18.77 and 18.74 (12c,12d-$\underline{C}$H$_3$); ^{31}P NMR (202 MHz, , C_6D_6) δ 40.24 ($^{1}J_{Pt\text{-}P}$ = 2246 Hz); ^{195}Pt NMR (77 MHz, CD_2Cl_2) δ -378.8 ($^{1}J_{Pt\text{-}P}$ = 2268 Hz); IR (KBr) ν 3054, 2961, 2921, 2865, 2093, 1475, 1435, 1366, 1253, 1104, 873, 753, 712, 703, 690, 530. UV-vis (cyclohexane) λ_{max} (ε_{max}, L Mol^{-1} cm^{-1}) nm, 339 (63,600), 356 (70,700), 416 (130,000), 527 (12,200); ESI MS *m/z* 1427 (M^+), MS calcd for $C_{90}H_{90}P_2Pt$+H: 1427.6223 found: 1427.6248.

^{1}H NMR (360 MHz, CD_2Cl_2) δ 8.75-8.72 (m, 4H), 8.24, 8.23, 8.17-8.09 (m, 4H), 8.07 (t), 7.59-7.55 (m), 7.46-7.41 (m), 7.20, (s), 6.95 (s), 2.57-2.43 (m broad,) 1.47, (s, 18H), 1.269 (s, 9H), 1.266 (s, 9H), -1.539 (12c/12d-$\underline{C}$H$_3$), -1.542 (12c/12d-$\underline{C}$H$_3$); ^{31}P NMR (146 MHz, CD_2Cl_2) δ 41.41 ($^{1}J_{Pt\text{-}P}$ = 2268 Hz).

Open form 52-o: ^{1}H NMR (500 MHz, C_6D_6) δ 8.03-7.85 (m, 8H), 7.75-7.68 (m, 6H), 7.21-7.17 (m, 4H), 7.07-6.92 (m, 16H), 6.91 (s, 1H), 6.89 (s, 1H), 6.80 (d, J = 2.1 Hz , 1H), 6.78 (d, J = 1.9 Hz, 1H), 2.00-1.64 (m, 8H),); ^{13}C NMR (125 MHz, C_6D_6) δ 150.74, 150.04, 145.38, 145.35, 140.77, 140.44, 140.16, 139.91, 139.21, 139.04, 135.25, 135.08, 134.32, 134.14, 131.55, 124.85, 124.80, 123.89, 34.62, 34.48, 31.93, 31.88, 31.43, 31.11, 19.95, 19.42; ^{31}P NMR (202 MHz, C_6D_6) δ 40.34 and 40.31 ($^{1}J_{Pt\text{-}P}$ = 2242 Hz).

***Cis-bis*-2''-[10-acetyl-2,7-*bis*-*t*-butyl-10b,10c-dimethyl-*trans*-10b,10c-dihydropyren-4-yl]-ethynyl (2,2'-bipyridine-N,N') platinum(II) 54A and 4-yl,5-yl isomer 54B**

Using the procedure for complex **43**, the acetyl DHP-ethyne **30** (60 mg, 0.15 mmol), Pt(bipy)Cl_2 (30 mg, 0.067 mmol) and CuI (2.0 mg, 10×10^{-3} mmol) in Et_2NH (6 mL) gave a residue which was recrystallized in DCM/hexanes to afford dark orange crystals of **54A,B** (33 mg, 40% yield). M.p. 182-190°C

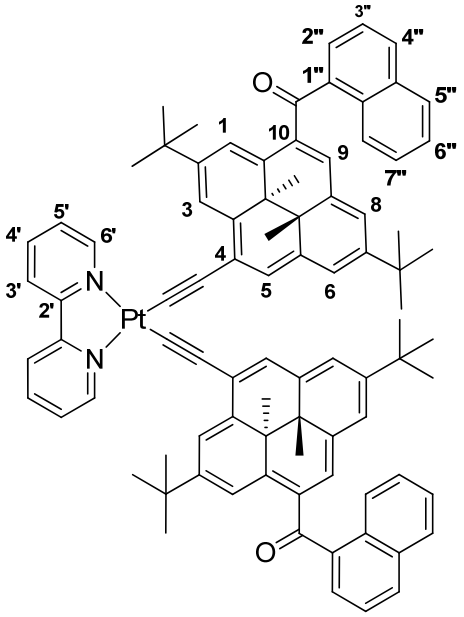


54A: ^{1}H NMR (500 MHz, $CDCl_3$) δ 10.33 (d, J = 5.3 Hz, 2H, H-6'), 9.70 (d×2, J = 1.4 Hz, 2H, H-1), 9.58 (d, J = 1.3 Hz, 2H, H-3), 8.87 (s, 2H, H-5), 8.83 (s, 2H, H-9), 8.55 (s, 2H, H-8), 8.46 (s, 2H, H-6), 8.23 (d, J = 1.4 Hz, 2H, H-3'), 8.22 (td, J = 7.9, 1.4 Hz, 2H, H-4'), 7.68 (td, J = 6.0, 2.3 Hz, 1H, H-5'), 3.05 (s, 6H, -COC$\underline{H}_3$), 1.66 (s, 18H, 7-C(C$\underline{H}_3$)$_3$), 1.60 (s, 9H, 2-C(C$\underline{H}_3$)$_3$), 1.59 (s, 9H, 2-C(C$\underline{H}_3$)$_3$), -3.69 (s, 6H, 10c-C$\underline{H}_3$), -3.714/-3.715 (s, 6H, 10b-C$\underline{H}_3$); ^{13}C NMR (125MHz, $CDCl_3$) δ 202.52 (-$\underline{C}$OCH$_3$), 156.67 (C-2'), 152.08 (C-6'), 151.07 (C-2), 146.27 (C-7), 140.39 (C-3a), 138.91 (C-4'), 136.63 (C-10a), 136.61 (C-10a second), 136.33 (C-5a/10d), 135.17 (C-5a/10d), 130.09 (C-5), 128.09 (C-10), 127.78 (C-5'), 124.29 (C-9), 123.35 (C-8), 122.91 (C-3'), 122.36 (C-6), 122.01 (C-3), 121.72 (C-4), 120.68 (C-1), 120.65 (C-1 second), 102.77 (-$\underline{C}$≡C-Pt), 92.30 (-C≡$\underline{C}$-Pt), 36.96 (2-$\underline{C}$(CH$_3$)$_3$), 36.95 (2-$\underline{C}$(CH$_3$)$_3$) for the other DHP), 36.07 (7-$\underline{C}$(CH$_3$)$_3$), 32.33 (2-C(C$\underline{H}_3$)$_3$), 32.09 (7-C(C$\underline{H}_3$)$_3$), 31.69 (C-10b), 31.11 (-CO$\underline{C}$H$_3$), 29.51 (C-10c), 15.48 (10b/10c-$\underline{C}$H$_3$);

54A and **54B:** IR (KBr) ν 2962, 2923, 2905, 2865, 2094, 1663, 1657, 1606, 1585, 1468, 1449, 1422, 1408, 1378, 1348, 1243, 1225, 1207, 1155, 1123, 934, 891, 764, 747, 681, 665 cm^{-1}; UV-vis (toluene) λ_{max} (ε_{max}, L Mol^{-1} cm^{-1}) nm, 390 (78,400), 424 (87,700), 492 (19,600), 695 (8,500); ESI MS *m/z* 1170 (M^++H); HRMS calcd for $C_{70}H_{74}N_2O_2Pt$: 1169.5455, found: 1169.5481.

Cis-bis-2'''-[10-(1-naphthoyl)-2,7-_bis-t_-butyl-10b,10c-dimethyl-_trans_-10b,10c-dihydropyren-4-yl]-ethynyl (2',2'-bipyridine-N,N') platinum(II) 55A and 4-yl,5-yl isomer 55B

Using the procedure for complex **43**, the 1'-naphthoyl DHP-ethyne **39** (100 mg, 0.192 mmol) and Pt(bipy)Cl_2 (43 mg, 0.096 mmol) and CuI (6.0 mg, 3.2×10^{-2} mmol) in degassed Et_2NH (15 mL) gave complex **55** in 12 hours. The product was recrystallized in DCM and methanol to afford a dark red crystal (10 mg, 7% yield). M.p. 260-267 °C.



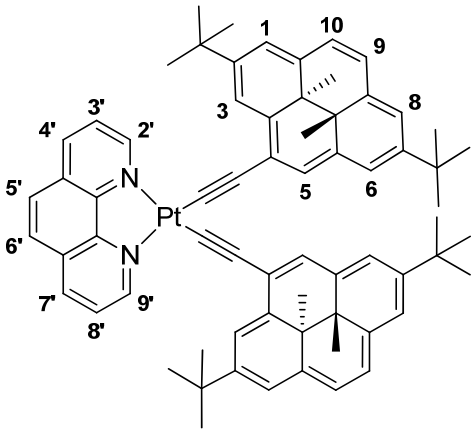
55A: ^1H NMR (500 MHz, CD_2Cl_2) δ 10.34 (d, J = 5.2 Hz, 2H, H-6'), 9.53 (s, 2H, H-3), 9.28 and 9.27 (2s, 2H, H-1), 8.88 (s, 2H, H-5), 8.54 (s, 4H, H-6,9), 8.45 (s, 2H, H-8),

8.40 (d, J = 8.5 Hz, 2H, H-8"), 8.31-8.25 (m, 4H, H-3',4'), 8.08 (d, J = 8.1 Hz, 2H, H-4"), 8.01 (d, J = 8.3 Hz, 2H, H-5"), 7.78 (t, J = 6.7 Hz, 2H, H-5'), 7.64 (d, J = 7.1 Hz, 2H, H-2"), 7.59-7.45 (m, 6H, H-3",6",7"), 1.62 (s, 18H, 7-C(C$\underline{H}_3$)$_3$), 1.46 (s, 9H, 2-C(C$\underline{H}_3$)$_3$), 1.45 (s, 9H, 2-C(C$\underline{H}_3$)$_3$), -3.57 (s, 6H, 10b-C$\underline{H}_3$), -3.59 (s, 6H, 10c-C$\underline{H}_3$); ^{13}C NMR (125MHz, CD_2Cl_2) δ 200.99 (-$\underline{C}$O-), 157.18 (C-2'), 152.28 (C-6'), 150.58 (C-2), 147.01 (C-7), 140.85 (C-1"), 140.36 (C-3a), 139.60 (C-4'), 137.63 (C-10a), 136.80 (C-5a/10d), 135.22 (C-5a/10d), 134.45 (C-8"b), 131.68 (C-8"a), 131.55 (C-4"), 130.49 (C-10), 130.08 (C-5), 129.02 (C-2"), 128.93 (C-5"), 128.35 (C-5'), 127.66 (C-7"), 126.87 (C-6"), 126.56 (C-8"), 126.21 (C-9), 125.28 (C-3"), 124.02 (C-8), 123.31 (C-3'), 122.88 (C-6), 121.92 (C-3,4), 120.88 (C-1), 102.52 (-$\underline{C}$≡C-Pt), 94.13 (-C≡$\underline{C}$-Pt), 37.00 (2-$\underline{C}$(CH$_3$)$_3$), 36.32 (7-$\underline{C}$(CH$_3$)$_3$), 32.22 and 32.21 (2/7-$\underline{C}$(CH$_3$)$_3$), 32.17 (C-10b), 32.09 (2/7-C($\underline{C}$H$_3$)$_3$), 29.97 (C-10c), 15.78 (C-10b/10c), 15.36 (C-10b/10c).

55A and **55B:** UV-vis (toluene) λ_{max} (ε_{max}, L Mol^{-1} cm^{-1}) nm, 370 (70,600), 430 (93,000), 694 (8,600); ESI MS *m/z* 1394 (M^++H); HRMS calcd for $C_{88}H_{82}N_2O_2Pt$: 1393.6081, found: 1393.6063;

Cis-_bis_-2''-[2,7-_bis_-_t_-butyl-10b,10c-dimethyl-_trans_-10b,10c-dihydropyren-4-yl]-ethynyl (1',10'-phenanthroline-N,N')platinum(II) 56A and 4-yl,5-yl isomer 56B

Using the procedure for complex **43**, reacting DHP-ethyne **24** (50 mg, 0.135 mmol), Pt(phen)Cl_2 (29 mg, 0.065 mmol) and CuI (1.5 mg, 7.9×10^{-3} mmol) in Et_2NH (8 mL) precipitated a brown solid of **56** (15 mg, 21% yield).



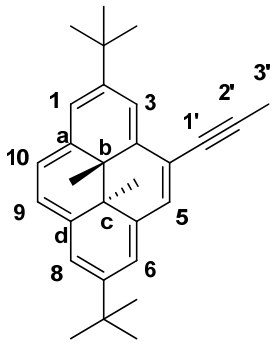
56A: ^{1}H NMR (500MHz, CD_2Cl_2) δ 10.55 (m, 2H, H-2,9), 9.51 (s, 2H), 8.82 (s, 2H), 8.78 (m, 2H), 8.52 (d, J = Hz, 2H), 8.50 (s, 4H), 8.43 (d, J = 1.0 Hz, 2H), 8.40 (d, J = 7.4 Hz, 2H), 8.15 (s, 2H), 8.09 (m, 2H), 1.70, 1.64, 1.62, -3.77, -3.78; ^{13}C NMR (125 MHz, C_6D_6) δ 152.25, 148.69, 146.44, 146.38, 138.57, 138.12, 137.71, 137.54, 136.86, 131.35, 128.15, 127.92, 126.85, 123.33, 123.13 (C-), 121.50, 121.31, 121.06, 120.92, 120.45, 103.18, 54.44, 54.22, 54.00, 53.79, 53.57, 42.63, 36.62, 36.40, 32.54, 32.25, 30.91, 30.42, 15.53, 15.01. **56A** and **56B:** IR (KBr) ν 3035, 2963, 2867, 2096, 1608, 1520, 1460, 1381, 1358, 1343, 1231, 883 cm^{-1}; EI MS *m/z* 1109 (M^+); HRMS calcd for $C_{68}H_{70}N_2Pt$: 1109.5187, (ESI mass spec was tried and failed to give the molecular weight);

6.2 Experimental for DHP-CBD Cobalt complexes

2,7-Di-*tert*-butyl-10b,10c-dimethyl-4-(prop-1'-ynyl)-*trans*-10b,10c-dihydropyrene 61

A solution of *n*-butyl lithium in hexanes (1.6 M, 0.5 mL, 0.8 mmol) was added into a solution of 2,7-di-*tert*-butyl-12c,12d-dimethyl-4-ethynyl-*trans*-12c,12d-dihydropyrene **24** (94 mg, 0.26 mmol) in dry THF (5 mL) under argon at -78^{o}C. The reaction mixture was slowly warmed up to -20 ^{o}C before the addition of methyl iodide (0.050 mL, 0.75 mmol) through a syringe. The reaction was stirred 14 h and then was quenched by addition of aqueous NaCl. The solution was extracted with hexanes and the combined organic

extracts were washed, dried (anhydrous sodium sulphate) and evaporated to afford 107 mg (100%) of the desired green product **61**. M.p. 149-150 ºC.

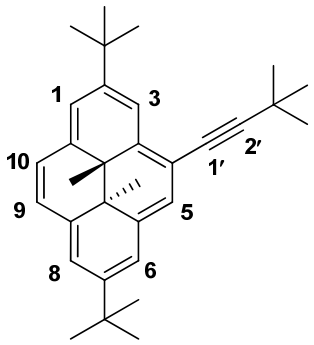


61: ^{1}H NMR (500 MHz, $CDCl_3$) δ 8.95 (d, J = 0.8 Hz, 1H, H-3), 8.50 (s, 1H, H-5), 8.49 (d, J = 1.0 Hz, 1H, H-1), d 8.47 (s, 1H, H-8), 8.44 (s, 1H, H-6), 8.40 (s, 2H, H-9,10), 2.37 (s, 3H, 3'-CH_3), 1.69 (s, 9H, 2-C(C$\underline{H}_3$)$_3$), 1.65 (s, 9H, 7-C(C$\underline{H}_3$)$_3$), -3.927 (s, 3H, 10c-C$\underline{H}_3$), -3.931 (s, 3H, 10b-C$\underline{H}_3$); ^{13}C NMR (125 MHz, $CDCl_3$) δ 146.93 (C-2), 146.30 (C-7), 138.07 (C-10a/10d), 137.34 (C-3a), 137.13 (C-10d/10a), 136.10 (C-5a), 126.02 (C-5), 123.68 (C-9), 123.41 (C-10), 121.60 (C-8), 121.45 (C-1), 120.81 (C-6), 119.76 (C-3), 115.32 (C-4), 90.81 (C-2'), 80.35 (C-1'), 36.39 (2-$\underline{C}$(CH$_3$)$_3$), 36.15 (7-$\underline{C}$(CH$_3$)$_3$), 32.18 (2-C($\underline{C}$H$_3$)$_3$), 32.10 (7-C($\underline{C}$H$_3$)$_3$), 30.38 (C-10b), 29.72 (C-10c), 15.07 (10b/10c-CH_3), 14.69 (10b/10c-CH_3), 5.23 (3'-$\underline{C}$H$_3$); IR (KBr) ν 2961, 2926, 2866, 2223, 1639, 1593, 1476, 1461, 1445, 1381, 1360, 1345, 1260, 1232, 1202, 939, 884, 790, 682, 665 cm^{-1}; UV-vis (cyclohexane) λ_{max} (ε_{max}, L Mol^{-1} cm^{-1}) nm, 232 (13,800), 336 (28,900) 352 (79,100), 363 (33,400), 390 (47,900), 470 (7,390), 488 (8,890), 602 (248), 663 (1,340); EI MS *m/z* 382 (M^+); HRMS calcd for $C_{29}H_{34}$: 382.2661, found: 382.2659;

4-(2'-*tert*-Butylethynyl)-2,7-di-*tert*-butyl-10b,10c-dimethyl-*trans*-10b,10c-dihydropyrene 62

2,7-Di-*tert*-butyl-10b,10c-dimethyl-4-iodo-*trans*-10b,10c-dihydropyrene **22**[106] (690 mg, 1.42 mmol) in triethylamine (30 mL) was degassed with argon for 5 min and then *bis*(triphenylphosphine)palladium dichloride (60 mg, 0.085 mmol) and cuprous iodide

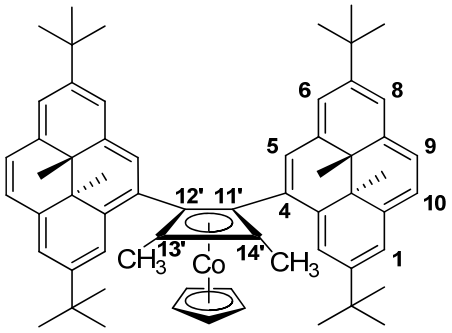
(20 mg, 0.105 mmol) were added, followed by 3,3-dimethylbut-1-yne (0.20 mL, 1.6 mmol) under argon. The reaction mixture was stirred at 20 °C overnight and subsequently quenched by addition of aqueous NaCl. The product was extracted with dichloromethane and the organic extracts were washed with water, dried over anhydrous sodium sulphate, filtered and the filtrate evaporated to give a dark orange solid. This crude product was chromatographed on silica gel using hexanes as eluant. The first fraction consisted of un-reacted starting material followed by a second fraction containing 460 mg (76% yield) of the desired product **62**, isolated as orange crystals after recrystallization from hexane. M.p. 192-193°C.



62: ^{1}H NMR (500 MHz, $CDCl_3$) δ 8.97 (d, 1H, J = 1.1 Hz, H-3), 8.50 (s, 1H, H-5), 8.49 (d, 1H, J = 1.1 Hz, H-1), 8.47 (s, 1H, H-8), 8.44 (s, 1H, H-6), 8.40 (s, 2H, H-9,10), 1.69 (s, 9H, 2-C(C$\underline{H}_3$)$_3$), 1.65 (s, 9H, 7-C(C$\underline{H}_3$)$_3$), 1.55 (s, 9H, 2'-C(C$\underline{H}_3$)$_3$), -3.91 (s, 3H, 10b,10c-C$\underline{H}_3$); ^{13}C NMR (125 MHz, $CDCl_3$) δ 146.72 (C-2), 146.23 (C-7), 138.06 (C-10a or 10d), 137.21 (C-3a), 137.16 (C-10a/10d), 136.11 (C-5a), 125.69 (C-5), 123.56 (C-9), 123.32 (C-10), 121.44 (C-8), 121.35 (C-1), 120.83 (C-6), 119.96 (C-3), 115.58 (C-4), 103.86 (C-2'), 79.65 (C-1'), 36.41 (2-$\underline{C}$(CH$_3$)$_3$), 36.14 (7-$\underline{C}$(CH$_3$)$_3$), 32.16 (2-C($\underline{C}$H$_3$)$_3$), 32.11 (7-C($\underline{C}$H$_3$)$_3$), 31.77 (2'-C($\underline{C}$H$_3$)$_3$), 30.35 (C-10b), 29.76 (C-10c), 28.86 (2'-$\underline{C}$(CH$_3$)$_3$), 15.14 (10b/10c-$\underline{C}$H$_3$), 14.68 (10b/10c-$\underline{C}$H$_3$). IR (KBr) ν 2964, 2927, 2902, 2864, 2209, 1594, 1475, 1460, 1383, 1359, 1346, 1271, 1284, 1233, 1195, 1117, 1069, 976, 939, 884, 796, 682, 665, 510 cm^{-1}; UV-vis (cyclohexane) λ_{max} (ε_{max}, L Mol^{-1} cm^{-1}) nm, 354 (98,300), 292 (62,700), 470 (8,080), 491 (9,610), 662 (1,690); EI MS *m/z* 424 (M^{+}); HRMS calcd for $C_{32}H_{40}$: 424.3130, found: 424.3130; Anal.Calcd for $C_{32}H_{40}$: C, 90.51%; H, 9.49% ; Found: C, 90.37%*; H, 9.63%.

cis-[1',2'-_Bis_-(2,7-di-_tert_-butyl-10b,10c-dimethyl-_trans_-10b,10c-dihydropyren-4-yl)-3',4'-dimethyl-η^4-cyclobutadienyl]-η^5-cyclopetadienylcobalt (II) 21

Cyclopentadienylcobaltdicarbonyl, $CpCo(CO)_2$, (0.20 mL, 1.3 mmol) was added into a solution of **61** (500 mg, 1.31 mmol) in dry iso-octane (20 mL). The reaction mixture was heated to reflux and the reaction was monitored by TLC. After three days, the TLC showed about 65% conversion of the starting material **61**, so more $CpCo(CO)_2$ (0.1 mL, 0.6 mmol) was added to the vessel and reflux was continued for an additional day. The solvent was removed from the reaction mixture under vacuum and the residue was chromatographed on a short alumina column (15 cm) using dichloromethane and hexane (1:4 ratio) as eluant to afford 570 mg (98% yield) of product **21** (R_f=0.85). Attempts to separate the various isomers failed to give single components although individual fractions enriched in different isomers were obtained. M.p. 218-222 °C.

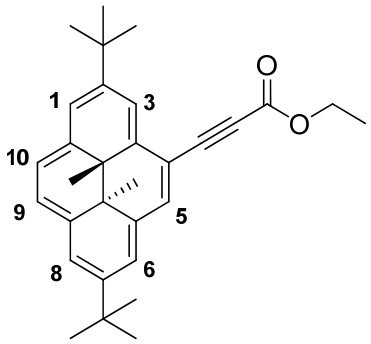


21: ^{1}H NMR (500 MHz, CD_2Cl_2) δ 8.98, 8.94, 8.92, 8.862, 8.857, 8.83, 8.75, 8.64, 8.44, 8.37, 8.35, 8.33, 8.31, 8.30, 8.27, 8.24, 8.22, 8.11, 8.10, 7.80, 5.07(Cp-H), 4.99 (Cp-H), 4.96 (Cp-H), 2.51(Cbd-CH_3), 2.27 (Cbd-CH_3), 2.20 (Cbd-CH_3), 2.08 (Cbd-CH_3), 1.67, 1.66, 1.64, 1.61, 1.60, 1.57, 1.52, 1.51, 1.50, 1.44, 1.38, 1.28, -3.74 (10c/10d-CH_3), -3.78 (10c/10d-CH_3), -3.83 (10c/10d-CH_3), -3.89 (10c/10d-CH_3), -3.94 (10c/10d-CH_3), -4.00 (10c/10d-CH_3), -4.01 (10c/10d-CH_3), -4.23 (10c/10d-CH_3); ^{13}C NMR (125 MHz, $CDCl_3$) δ 146.27, 146.23, 146.13, 146.12, 144.68, 144.60, 137.79, 137.49, 137.34, 137.14, 137.00, 136.27, 136.17, 135.41, 134.49, 133.92, 133.29, 133.20, 131.14, 130.37, 130.09, 129.82, 127.93, 127.38, 127.31, 127.00, 123.82, 123.49, 123.29, 122.91, 122.73, 122.62, 122.26,

121.87, 121.75, 121.56, 121.32, 121.16, 120.89, 120.70, 120.63, 120.53, 120.48, 120.37, 120.29, 120.22, 119.77, 82.35 (Cp-C), 82.22 (Cp-C), 81.98 (Cp-C), 81.70 (Cbd-C), 81.44 (Cbd-C), 80.87 (Cbd-C), 80.09 (Cbd-C), 79.47 (Cbd-C), 79.41 (Cbd-C), 79.04 (Cbd-C), 77.78 (Cbd-C), 36.75, 36.55, 36.51, 36.35, 36.23, 36.13, 35.96, 32.38, 32.19, 32.16, 32.08, 32.06, 32.03, 31.99, 31.37, 31.32, 31.05, 30.69, 30.36, 30.21, 30.09, 16.23, 15.42, 15.30, 15.20, 14.65, 14.49, 13.70, 13.49, 12.43; IR (KBr) ν 3032, 2962, 2921, 2894, 2861, 1592, 1461, 1360, 1270, 1231, 1198, 1106, 1070, 1020, 1001, 971, 938, 883, 801, 666, 462 cm^{-1}; UV-vis (cyclohexane) λ_{max} (ε_{max}, L Mol^{-1} cm^{-1}) nm, 350 (64,500), 388 (68,000), 489 (19,500), 659 (1,600); EI MS *m*/*z* 888.6 (M^+); HRMS calcd for $C_{63}H_{73}Co$: 888.5044, found: 888.5043; Anal. Calcd for $C_{63}H_{73}Co$: C, 85.10; H, 8.27; Found: C, 84.33; H, 8.22.

2,7-Di-*tert*-butyl-10b,10c-dimethyl-4-(2'-ethoxycarbonylethynyl)-*trans*-10b,10c-dihydropyrene 63

A solution of 1.6 M *n*-butyl lithium in hexanes (1.7 mL, 2.7 mmol) was added dropwise into a solution of 2,7-di-*tert*-butyl-10b,10c-dimethyl-4-ethynyl-*trans*-10b,10c-dihydropyrene **24** (0.91 g, 2.5 mmol) in dry THF (20 mL) at -78 °C in an oven dried Schlenk tube under argon. The reaction mixture was stirred for one hour at -78 °C and then allowed to warm to room temperature. After stirring for 1 h at room temperature, the solution was cooled to -78 °C again. Fresh distilled ethyl chloroformate (0.70 mL, 7.3 mmol) was added by syringe to the cold solution before it was allowed to warm slowly to room temperature. Stirring was continued for an additional 3 h after the reaction mixture reached room temperature. The reaction was quenched by the slow addition of water through a syringe and extracted with ether until the extracts no longer showed a green spot on a TLC plate. The combined ether extracts were evaporated to dryness under vacuum and the residue was purified on a deactivated silica gel column eluting with hexanes and DCM (4:1 ratio) to afford first recovered starting material **24** (150 mg, 16% yield) and second pure green product **63** (0.90 g, 83 % yield). M.p. 133-135 °C.

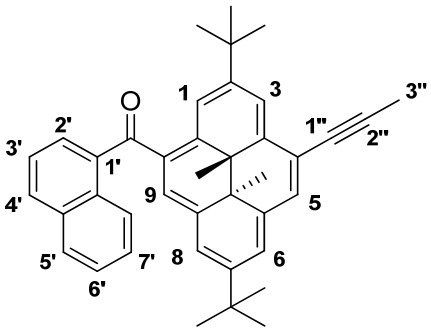


63: ^{1}H NMR (500 MHz, C_6D_6) δ 9.49 (s, 1H, J = 1.0 Hz, H-3), 8.54 (s, 1H, H-1), 8.53 (s, 1H, H-8), 8.51 (s, 1H, H-5), 8.41 (s, 1H, H-6), 8.39 (d, 1H, J = 8.0 Hz, H-9), 8.35 (d, 1H, J = 8.0 Hz, H-10), 4.14 (q, J = 7.0 Hz, 2H, -C$\underline{H}_2$CH$_3$), 1.60 (s, 9H, 2-C(C$\underline{H}_3$)$_3$), 1.56 (s, 9H, 7-C(C$\underline{H}_3$)$_3$), 1.05 (t, J = 7.1 Hz, 3H, -CH$_2$C$\underline{H}_3$), -3.67 (s, 3H, 10c/10d-C$\underline{H}_3$), -3.68 (s, 3H, 10c/10d-C$\underline{H}_3$) ; ^{13}C NMR (125 MHz, C_6D_6) δ 155.19 ($\underline{C}$=O), 149.71 (C-2), 146.93 (C-7), 141.36 (C-3a), 140.17 (C-10a), 137.61 (C-10d), 136.06 (C-5a), 127.01 (C-5), 125.76 (C-9), 124.47 (C-10), 123.52 (C-8), 122.83 (C-6), 122.44 (C-1), 120.22 (C-3), 111.08 (C-4), 88.15 (C≡C), 88.13 (C≡C), 62.05 (-$\underline{C}$H$_2$CH$_3$), 36.78 (2-$\underline{C}$(CH$_3$)$_3$), 36.31 (7-$\underline{C}$(CH$_3$)$_3$), 32.18 (7-C($\underline{C}$H$_3$)$_3$), 32.15 (2-($\underline{C}$H$_3$)$_3$), 31.63 (C-10b), 30.17 (C-10c), 15.42 (10c/10d-$\underline{C}$H$_3$), 15.34 (10c/10d-$\underline{C}$H$_3$), 14.52 (-CH$_2$$\underline{C}H_3$); IR (KBr) ν 2964, 2192, 1697, 1595, 1476, 1459, 1447, 1384, 1363, 1269, 1230, 1186, 1164, 1102, 1043, 885, 745, 680, 665 cm^{-1}; UV-vis (cyclohexane) λ_{max} (ε_{max}, L Mol^{-1} cm^{-1}) nm, 667 (2,510), 604 (482), 495 (9,110), 475 (8,460), 397 (53,700), 356 (52,900), 296 (6,990), 276 (7,230); EI MS m/z 440.6 (M+); HRMS calcd for $C_{31}H_{36}O_2$: 440.2715, found: 440.2699.

2,7-Di-*tert*-butyl-10b,10c-dimethyl-10-(1'-naphthoyl)-4-(prop-1''-ynyl)-*trans*-10b,10c-dihydropyrene 67A and 5-prop-1''-ynyl isomer 67B

n-Propyltributyltin (0.54 mL, 1.8 mmol) was added to a solution of 1'-naphthoyl DHP bromide **66**[130] (390 mg, 0.87 mmol, direct from bromination of 1'-naphthoyl DHP **35**) in dry THF (50 mL). Then tetra(triphenylphosphine)palladium (50 mg, 0.143 mmol) was added. The reaction mixture was refluxed for 15 hours under argon. Then the solvent was

removed and the residue was chromatographed on silica gel. A mixture of un-reacted bromide **66** and 1'-naphthoyl DHP **69** (~20%) was eluted first with hexanes and DCM (1:1) and second was the desired alkyne **67** (350 mg, 90%). M.p. 112-120 ^{o}C.

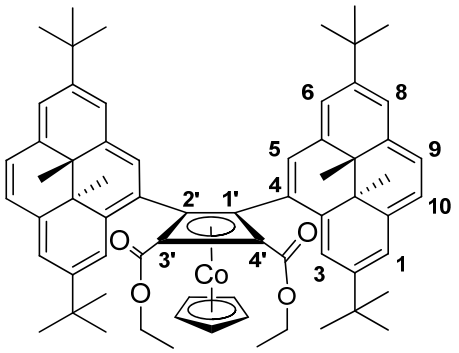


67A: ^{1}H NMR (500 MHz, $CDCl_3$) δ 9.34 (d, J = 0.7 Hz, 1H, H-1), 9.02 (d, J = 0.7 Hz, 1H, H-3), 8.61 (s, 1H, H-5), 8.58 (s, 1H, H-9), 8.50 (s, 1H, H-6), 8.46 (d, J = 8.3 Hz, 1H, H-8'), 8.44 (s, 1H, H-8), 8.05 (d, J = 8.2 Hz, 1H, H-4'), 7.98 (d, J = 8.1 Hz, 1H, H-5'), 7.62 (dd, J = 8.1, 1.0 Hz, 1H, H-2'), 7.55 (dt, J = 7.5, 1.0 Hz, 1H, H-6'), 7.48 (t, J = 7.7 Hz, 2H, H-3',7'), 2.38 (s, 3H, ≡C-C$\underline{H}_3$), 1.59 (s, 9H, 7-C(C$\underline{H}_3$)$_3$), 1.56 (s, 9H, 2-C(C$\underline{H}_3$)$_3$), -3.70 (s, 3H, 10b-C$\underline{H}_3$), -3.72 (s, 3H, 10c-C$\underline{H}_3$). ^{13}C NMR (125 MHz, $CDCl_3$) δ 200.90 ((-$\underline{C}$=O), 151.10 (C-2), 146.83 (C-7), 140.09 (C-1'), 139.77 (C-3a), 137.51 (C-10a), 135.89 (C-5a/10d), 134.76 (C-5a/10d), 134.12 (C-4'a), 131.61 (C-4'), 131.50 (C-4'b), 130.51 (C-10), 129.09 (C-2'), 128.64 (C-5'), 128.47 (C-5), 127.61 (C-7'), 126.96 (C-9), 126.64 (C-6'), 126.21 (C-8'), 124.82 (C-3'), 123.40 (C-6), 121.00 (C-1), 120.56 (C-3), 116.36 (C-4), 91.45 (-C≡$\underline{C}$-CH_3), 79.91 (-$\underline{C}$≡C-CH_3), 36.83 (2-$\underline{C}$(CH_3)$_3$), 36.09 (7-$\underline{C}$(CH_3)$_3$), 31.97 (2/7-C($\underline{C}$H$_3$)$_3$), 31.90 (2/7-C($\underline{C}$H$_3$)$_3$), 31.63 (C-10b), 29.34 (C-10b), 15.35 (C-10b/10c), 15.13 (C-10b/10c), 5.21 (≡C-$\underline{C}$H$_3$). IR (KBr) ν 3047, 2961, 2866, 2221, 1644, 1589, 1508, 1477, 1462, 1446, 1386, 1362, 1346, 1277, 1245, 1232, 1195, 1105, 950, 892, 782 cm^{-1}; UV-vis (cyclohexane) λ_{max} (ε_{max}, L Mol^{-1} cm^{-1}) 357 (42,800), 413 (46,700), 490 (6,700), 622 (570), 681 (2,580) nm; EI MS m/z 536 (M^+); HRMS calcd for $C_{40}H_{40}O$: 536.3081, found: 536.3079;

67B: ^{1}H NMR (500 MHz, $CDCl_3$)(only clearly observable peaks are listed) δ 9.32, 9.01, 8.59, 8.55, 8.48, 1.63, 1.52, -3.69, -3.73.

Cis-[1',2'-_bis_-(2,7-di-_tert_-butyl-10b,10c-dimethyl-_trans_-10b,10c-dihydropyren-4-yl)-3',4'- ethoxycarbonyl-η^4-cyclobutadienyl]-η^5-cyclopetadienylcobalt (II) 69

2,7-Di-*tert*-butyl-10b,10c-dimethyl-4-(2'-ethoxycarbonylethynyl)-*trans*-10b,10c-dihydropyrene, **63**, (0.90 g, 2.0 mmol) was dissolved in dry *iso*-octane (30 mL, previously dried over molecular sieves for several days) in a oven dried Schlenk tube and $CpCo(CO)_2$ (0.50 mL, 40 mmol) was added by syringe under argon. The reaction mixture was heated at between 96 ^oC and 110 ^oC overnight and then raised to a gentle reflux for 6 hours. After 18 hours of total heating, the reaction mixture was cooled to room temperature and purified directly on a silica gel column using dichloromethane as eluant to give product **69** as a mixture of isomers (310 mg, 30% yield). The mixture of isomers was chromatographed again on alumina using ethyl acetate andbenzene (5:95) as eluants. This allowed preferential separation of one isomer from the mixture as the first fraction.



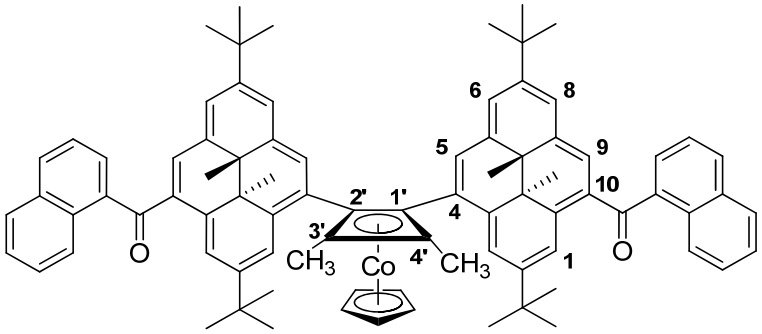
Single isomer in 69: ^1H NMR (500 MHz, $CDCl_3$) δ 8.85 (s, 1H, H-1), 8.64 (s, 1H, H-3), 8.34 (s, 1H, H-8), 8.26 (d, J = 7.8Hz, 1H, H-9), 8.21 (s, 1H, H-6), 8.17 (d, J = 7.8 Hz, 1H, H-10), d 5.28 (s, 5H, Cp), 4.15 (m, 4H, -OC$\underline{H}_2$CH$_3$), 1.57 (s, 9H, 7-C(C$\underline{H}_3$)$_3$), 1.38 (s, 9H, 2-C(C$\underline{H}_3$)$_3$), 0.97 (t, J = 7.1 Hz, 6H, -OCH$_2$C$\underline{H}_3$), -3.87 (s, 3H, 10c-C$\underline{H}_3$), -4.10 (s, H, 10b-C$\underline{H}_3$); ^{13}C NMR (125 MHz, $CDCl_3$) δ 171.03 ($\underline{C}$=O), 145.92 (C-7), 145.19 (C-2), 137.76 (C-10a), 136.84 (C-10d*), 135.30 (C-5a), 133.96 (C-3a), 127.96 (C-5), 124.58 (C-4), 123.48 (C-9/10), 123.42 (C-9 or 10), 121.73 (C-1), 121.20 (C-8), 120.55 (C-6), 119.89 (C-3), 88.51 (C-1'), 83.90 (C-2'), 83.53 (C on Cp), 60.38 (-OC$\underline{H}_2$CH$_3$), 36.18 (2-$\underline{C}$(CH$_3$)$_3$), 35.99 (7-$\underline{C}$(CH$_3$)$_3$), 32.03 (2/7-C($\underline{C}$H$_3$)$_3$), 31.93 (2/7-C($\underline{C}$H$_3$)$_3$), 30.93 (C-10b), 29.84 (C-10c), 14.97 (10b/10c-$\underline{C}$H$_3$), 14.65 (10b/10c-$\underline{C}$H$_3$), 14.44 (-CH$_2\underline{C}$H$_3$);

The isomeric mixture of 69: m.p. 193-198°C. ^{1}H NMR (500 MHz, $CDCl_3$) δ (10 singlets between 9.17 ppm and 8.34 ppm) 9.17, 8.88, 8.85, 8.83, 8.64, 8.59, 8.51, 8.45, 8.41, 8.34, 8.33-8.10 (m, 11 peaks at 8.32, 8.30, 8.28, 8.26, 8.25, 8.23, 8.22, 8.19, 8.16, 8.14, 8.12), 8.06 (s), 7.75 (s), 5.35 (DCM residual), 5.28 (H on Cp), 5.28 (H on Cp), 5.28 (H on Cp), 4.48-3.95 (m, -OC$\underline{H}_2$CH$_3$), 1.69 (-C(C$\underline{H}_3$)$_3$), 1.60 (-C(C$\underline{H}_3$)$_3$), 1.57 (-C(C$\underline{H}_3$)$_3$), 1.51 (-C(C$\underline{H}_3$)$_3$), 1.38 (-C(C$\underline{H}_3$)$_3$), 1.35 (-C(C$\underline{H}_3$)$_3$), 1.30 (-C(C$\underline{H}_3$)$_3$), 1.14 (t, J = 7.2 Hz, -OCH$_2$C$\underline{H}_3$), 1.07, (t, J = 7.0 Hz, -OCH$_2$C$\underline{H}_3$), 0.99 (t, J = 7.0 Hz, -OCH$_2$C$\underline{H}_3$), 0.98 (-C(C$\underline{H}_3$)$_3$), -3.81, -3.86, -3.95, -3.96, -4.09, -4.13, -4.29, -4.45; ^{13}C NMR (125 MHz, $CDCl_3$) δ 171.14, 171.04, 171.01, 145.89, 145.79, 145.39, 145.25, 145.16, 137.89, 137.81, 137.71, 136.79, 136.41, 135.25, 134.97, 134.61, 133.91, 129.06, 128.55, 127.93, 127.54, 124.53, 124.37, 123.62, 123.48, 123.41, 123.24, 123.12, 122.31, 121.73, 121.53, 121.19, 120.84, 120.51, 120.39, 119.95, 119.85, 119.67, 119.53, 89.97, 89.23, 88.86, 88.53, 88.48, 83.89 (C on Cp), 83.86 (C on Cp), 83.79 (C on Cbd), 83.64 (C on Cbd), 83.51 (C on Cp), 60.61, 60.47, 60.38, 60.29, 53.64, 36.36, 36.17, 36.13, 36.07, 35.98, 35.91, 35.75, 32.16, 32.11, 32.01, 31.91, 31.87, 31.77, 30.89, 30.75, 30.59, 30.41, 30.34, 30.24, 29.81, 29.78, 15.92, 14.94, 14.85, 14.64, 14.57, 14.41, 14.21. IR (KBr) ν 2963, 2904, 2867, 1709, 1478, 1461, 1381, 1232, 1181, 1123, 884, 815, 669 cm^{-1}; UV-vis (cyclohexane) λ_{max} (ε_{max}, L Mol^{-1} cm^{-1}) nm, 276 (30,700), 325 (66,800), 366 (64,000), 447 (18,300), 463 (18,010), 636 (2,450); ESI MS m/z 1004 (M^+); HRMS calcd for $C_{67}H_{77}CoO_4$: 1004.5154, found: 1004.5169;.

Cis-[1',2'-_bis_-(2,7-di-_tert_-butyl-10b,10c-dimethyl-10-(1''-naphthoyl)-_trans_-10b,10c-dihydropyren-4-yl)-3',4'-dimethyl-η^4-cyclobutadienyl]-η^5-cyclopetadienylcobalt (II) 72

The alkyne **67** (330 mg, 0.62 mmol) and $CpCo(CO)_2$ (110 mg, 0.56 mmol) were mixed with octane (5mL) in a Schlenk tube under argon. The resulting reaction mixture was heated to 120 ^{o}C for 45 hours. Then the solvent was removed under vacuum and the residue was dissolved in DCM. The solution was filtered through a celite pad to remove

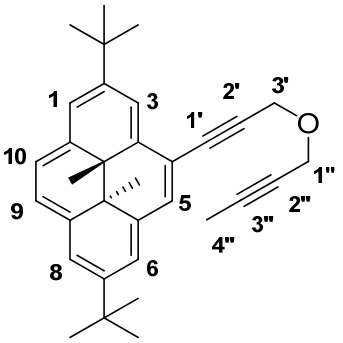
the unknown solid. Then the DCM was removed and the solid was chromatographed on silica gel. The un-reacted alkyne **67** was eluted first with hexanes and DCM (1:1) (110 mg, 33% recovery). The isomeric mixture of **72** was eluted second with DCM. (130 mg, 35% yield). The product was recrystallized from DCM and ethanol to afford red cubic crystals of **72**. M.p. > 300 °C.



Isomeric mixture of 72: ^{1}H NMR (500 MHz, $CDCl_3$) δ (11 singlets for DHP peripheral protons) 9.22, 9.13, 9.08, 9.04, 9.00, 8.98, 8.94, 8.93, 8.89, 8.81, 8.71, 8.51 (s), 8.49 (s), 8.46 (s), 8.45 (s), 8.43-8.28 (m), 8.23 (s), 8.14 (s), 8.12 (s), 8.05-7.90 (m), 7.86 (s), 7.62-7.37 (m), 5.08 (s, H on Cp), 5.02 (s, H on Cp), 4.96 (s, H on Cp), 2.50 (s, C$\underline{H}_3$ on Cbd), 2.25 (s, C$\underline{H}_3$ on Cbd), 2.20 (s, C$\underline{H}_3$ on Cbd), 2.06 (s, C$\underline{H}_3$ on Cbd), (7 singlets for protons on *tert*-butyl group of the DHPs) 1.50, 1.46, 1.45, 1.35, 1.34, 1.29, 1.16, (8 singlets for protons on internal methyl group of the DHPs) -3.53, -3.598, -3.602, -3.65, -3.73, -3.76, -3.81, -4.03; ^{13}C NMR (125 MHz, $CDCl_3$) (selected peaks; the full spectrum can be found in Appendix **VI**) δ 200.90, 200.88, 200.77, 82.13 (C$\underline{H}_3$ on Cp), 81.99 (C$\underline{H}_3$ on Cp), 81.75 (C$\underline{H}_3$ on Cp); IR (KBr) ν 2963, 2904, 2867, 1641, 1591, 1508, 1460, 1387, 1363, 1273, 1255, 1227, 1197, 1111, 893, 802, 781 cm^{-1}; UV-vis (cyclohexane) λ_{max} (ε_{max}, L Mol^{-1} cm^{-1}) 358 (60,400), 412 (68,900), 500 (20,900), 688 (4,880) nm; ESI MS: *m*/*z* 1197 amu (M^+); HRMS calcd for $C_{85}H_{85}CoO_2$+H: 1197.5960, found: 1197.5947.

4-(3'-(But-2''-ynyloxy)prop-1'-ynyl)-2,7-di-*tert*-butyl-10b,10c-dimethyl-*trans*-10b,10c-dihydropyrene 75

60% NaH (140 mg, 3.50 mmol) was added in a solution of DHP-derived propargyl alcohol[153] (200 mg, 0.500 mmol) and 1-bromo-2-butyne (0.10 mL, 1.1 mmol) in dry THF (8 mL) at room temperature. The reaction was stirred overnight. More 1-bromo-2-butyne (0.20 mL) was then added, and the reaction was stirred for a further 5 hours. The mixture was then poured into ice water, extracted with diether ether (50 mL x 3). The organic extracts were combined and washed with water and brine, dried over $MgSO_4$ and evaporated to afford green crystals of **75** (210 mg, 93% yield). M.p. 130-132 ^{o}C.

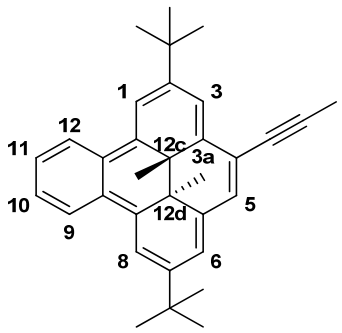


^{1}H NMR (500 MHz, $CDCl_3$) δ 8.95 (s, H, H-3), 8.53 (s, H, H-5), 8.51 (s, H, H-1), 8.49 (s, H, H-8), 8.46 (s, H, H-6), 8.44 and 8.42 (AB, J = 8.0 Hz, 2H, H-9/10), 4.79 (s, 2H, H-'), 4.52 (d, J = 2.3 Hz, 2H, H-1''), 1.91 (t, J = 2.3 Hz, 3H, H-4''), 1.69 (s, 9H, 2-C(C$\underline{H}_3$)$_3$), 1.66 (s, 9H, 7-C(C$\underline{H}_3$)$_3$), -3.92 (s, 3H, 10b/10c-C$\underline{H}_3$), -3.93 (s, 3H, 10b/10c-C$\underline{H}_3$); ^{13}C NMR (125 MHz, $CDCl_3$) δ 147.50 (C-2), 146.45 (C-7), 138.43 (C-10a/10d), 137.90 (C-3a), 137.13 (C-10a/10d), 135.88 (C-5a), 125.84 (C-5), 124.13 (C-9), 123.57 (C-10), 122.05 (C-8), 121.54 (C-1), 121.21 (C-6), 119.65 (C-3), 113.56 (C-4), 89.40 (C-2'), 87.61 (C-1'), 83.35 (C-2''/3''), 74.91 (C-2''/3''), 57.88 (C-3'), 57.31 (C-1''), 36.43 (2-$\underline{C}$(CH$_3$)$_3$), 36.16 (7-$\underline{C}$(CH$_3$)$_3$), 32.13 (2-C($\underline{C}$H$_3$)$_3$), 32.08 (7-C($\underline{C}$H$_3$)$_3$), 30.48 (C-10b), 29.65 (C-10c), 15.04 (10b/10c-$\underline{C}$H$_3$), 14.71 (10b/10c-$\underline{C}$H$_3$), 3.93 (C-4''); IR (KBr) ν 2947, 2902, 2863, 2296, 2210, 1592, 1460, 1445, 1380, 1363, 1345, 1232, 1136, 1064, 974, 940, 911, 881, 794, 684, 667, 647 cm^{-1}; UV-vis (cyclohexane) λ_{max} (ε_{max}, L Mol^{-1} cm^{-1}) nm, 236 (11,900), 267 (5,150), 352 (78,100), 364 (31,500), 391 (48,700), 469 (7,120), 489 (8,410), 545

(223), 606 (237), 663 (1,490); EI MS *m/z* 450 (M^+); HRMS calcd for $C_{33}H_{38}O$: 450.2923, found: 450.2919; Anal. Calcd for $C_{33}H_{38}O$: C, 87.95; H, 8.50; Found: C, 87.78; H, 8.32.

2,7-di-*tert*-butyl-12c,12d-dimethyl-5-(prop-1'-ynyl)-*trans*-12c,12d-dihydrobenzo[e]pyrene 76

The solution of the alkyne **40** (300 mg, 0.72 mmol) in dry THF (20 mL) was cooled to -78°C with a dry ice bath for 15 mins. Then a 1.6 M solution of *n*-BuLi (0.80 mL, 1.3 mmol) was added by syringe. The dry ice bath was removed and the reaction was stirred for 30 mins. Then, the reaction mixture was cooled to -78°C and MeI (0.10 mL, 0.80 mmol) was added by syringe. The dry ice bath was removed. The resulting mixture was warmed to room temperature slowly and stirred for 10 hours. Ice-water was then added to quench the reaction. The product was extracted with hexanes three times. The combined organic phase was dried over $MgSO_4$. The solvents were removed and the residue was chromatographed on silica gel eluting with hexanes and DCM (2:8 ratio). Purple crystals of **76** were crystallized from hexanes (200 mg, 64% yield). M.p. 160-162°C.



76: ^{1}H NMR (500 MHz, $CDCl_3$) δ 8.72-8.70 (m, 2H, H-9,12), 8.25 (s, 1H, H-1), 8.21 (s, 1H, H-8), 7.87 (s, 1H, H-3), 7.61-7.58 (m, 2H, H-10,11), 7.26 (s, 1H, H-6), 7.12 (s, 1H, H-5), 2.23 (s, 3H, ≡CC$\underline{H}_3$), 1.53 (s, 9H, 2-C(C$\underline{H}_3$)$_3$), 1.47 (s, 9H, 7-C(C$\underline{H}_3$)$_3$), -1.46 (s, 3H, 12c-C$\underline{H}_3$), -1.47 (s, 3H, 12d-C$\underline{H}_3$); ^{13}C NMR (125 MHz, $CDCl_3$) δ 146.58 (C-2), 145.24 (C-7), 140.64 (C-3a), 137.90 (C-5a/12e), 136.29 (C-12b), 135.15 (C-5a/12e), 129.56 (C-12a/12f), 129.48 (C-12a/12f), 126.21 (C-10/11), 126.14 (C-10/11), 124.77 (C-9/12),

124.68 (C-9/12), 123.63 (C-5), 119.43 (C-6), 118.31 (C-3), 117.39 (C-1,8), 113.98 (C-4), 90.45 (C≡CMe), 79.58 (C≡CMe), 36.44 (C-12c), 35.92 (2-C(CH$_3$)$_3$), 35.59 (7-C(CH$_3$)$_3$), 35.41 (C-12d), 30.81 (2/7-C(CH$_3$)$_3$), 30.76 (2/7-C(CH$_3$)$_3$), 18.06 (12d-CH$_3$), 17.91 (12c-CH$_3$), 5.06 (≡CCH$_3$); IR (KBr) ν 3060, 2961, 2922, 2864, 2227, 1617, 1475, 1466, 1367, 1343, 1255, 1237, 890, 871, 752, 635 cm^{-1}; UV-vis (cyclohexane) λ_{max} (ε_{max}, L Mol^{-1} cm^{-1}) nm, 225 (30,500), 315 (16,700), 328 (18,700), 344 (21,000), 379 (24,200), 398 (26,300), 481 (4,500), 512 (5,800), 541 (5,100), 620 (400); EI MS *m/z* 432 (M$^+$); HRMS calcd for $C_{33}H_{36}$: 432.2817, found: 432.2820; Anal. Calcd for $C_{33}H_{36}$: C, 91.61; H, 8.39; Found: C, 91.50; H, 8.50.

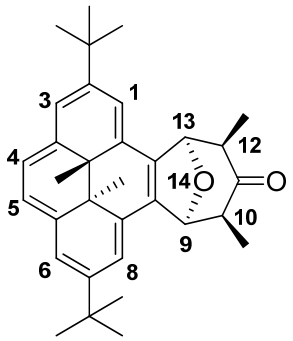
6.3 Experimental for DHP-fused Cycloheptatrienyl systems

2,7-Di-*tert*-butyl-11-oxo-*cis*-10,12-dimethy-13c,13d-dimethy-14-oxabicyclo[3.2.1]oct-13a-eno[13a:13f; e]-*trans*-13c,13d-dihydropyrene 99A
and 2,7-Di-*tert*-butyl-11-oxo-*trans*-10,12-dimethy-13c,13d-dimethy-14-oxabicyclo[3.2.1]oct-13a-eno[13a:13f; e]-*trans*-13c,13d-dihydropyrene 99B

A solution of 0.10 mL of 2,4-dibromopentan-3-one[271] (1.46 g, 5.98 mmol) in dry acetonitrile (50 mL) was added into a solution of isofuran **98**[41] (2.06 g, 5.36 mmol), copper powder (1.27 g, 20.0 mmol) and sodium iodide (5.7 g, 38 mol) in dry acetonitrile (150 mL) under argon. The purple reaction mixture was stirred overnight at 25 ^{o}C under argon. The disappearance of the color indicated the completion of the reaction.

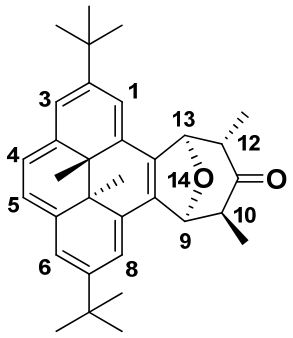
The reaction mixture was filtered through a Celite pad, and the filtrate was evaporated to give a green solid. This residue was re-dissolved in ethyl acetate and washed with 28% ammonia solution, water and aqueous NaCl solution. The organic layer was dried over anhydrous $MgSO_4$ and the solvent removed under vacuum. The resulting green solid was chromatographed over neutral alumina. Eluted first was un-reacted isofuran **98** (0.32 g, 15% recovery). Eluted second and third with benzene: hexanes (1:1) were green products

99A and **99B** (ratio **99A**:**99B** = 2:3 from ^{1}H NMR) (total, 1.94 g, 77.3% yield). Product **99A** was recrystallized from toluene as green crystals, m.p. 211-212 ^{o}C.



99A: ^{1}H NMR (500 MHz, C_6D_6) δ 8.60 (s, 1H, H-3), 8.57 (s, 1H, H-6), 8.45 (d, J = 1.2 Hz, 1H, H-1), 8.43 (d, J = 1.2 Hz, 1H, H-8), 8.41 (AB, J = 8.1 Hz, 1H, H-4), 8.40 (AB, J = 8.1 Hz, 1H, H-5), 6.18 (s, 1H, H-13), 6.16 (s, 1H, H-9), 3.09 (q, J = 7.5 Hz, 1H, H-10), 2.86 (q, J = 7.5 Hz, 1H, H-12), 1.64 (d, 3H, J = 7.4 Hz, 10-C$\underline{H}_3$), 1.61 (s, 9H, 2/7-C(C$\underline{H}_3$)$_3$), 1.60 (d, J = 7.4 Hz, 3H, 12-C$\underline{H}_3$), 1.59 (s, 9H, 2/7-C(C$\underline{H}_3$)$_3$), -3.62 (s, 3H, 13c-C$\underline{H}_3$), -3.84 (s, 3H, 13d-C$\underline{H}_3$); ^{13}C NMR (125 MHz, C_6D_6) δ 212.05 (C-11), 146.55 (C-2/7), 146.37 (C-2/7), 137.59 (C-3a), 137.53 (C-5a), 136.45 (C-13a), 135.88 (C-13f), 128.2* (C-13b,13e), 124.84 (C-4), 124.57 (C-5), 122.27 (C-6), 122.11 (C-3), 118.06 (C-8), 117.12 (C-1), 83.54 (C-13), 83.20 (C-9), 52.10 (C-10,12), 36.46 (2/7-$\underline{C}$(CH$_3$)$_3$), 36.43 (2/7-$\underline{C}$(CH$_3$)$_3$), 32.41 (C-13c/13d), 32.37 (2/7-C($\underline{C}$H$_3$)$_3$), 32.35 (2/7-C($\underline{C}$H$_3$)$_3$), 30.30 (C-13c/13d), 19.03 (10-$\underline{C}$H$_3$), 18.96 (13-$\underline{C}$H$_3$), 15.42 (13c-$\underline{C}$H$_3$), 15.07 (13d-$\underline{C}$H$_3$). IR (KBr) ν 3041, 2951, 2929, 2904, 2869, 1704, 1602, 1458, 1382, 1359, 1346, 1263, 1195, 1082, 1065, 961, 932, 888, 870, 674 cm^{-1}; UV-vis (cyclohexane) λ_{max} (ε_{max}, L Mol^{-1} cm^{-1}) nm, 238 (7,300), 330 (27,900), 347 (98,500), 361 (29,200, sh), 386 (46,800), 438 (4,500, sh), 464 (7,600, sh), 483 (10,200), 595 (200), 645 (900, sh), 615 (1,100); EI MS m/z 468 (M+); HRMS calcd for $C_{33}H_{40}O_2$: 468.3028, found: 468.3019.

* Two indistinguishable peaks are beneath the solvent peak. These could be determined from the HMBC spectrum.

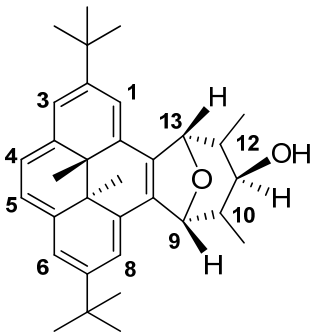


99B

99B: was recrystallized from dichloromethane and methanol as green crystals. M.p. 203-204 °C. ^{1}H NMR (500 MHz, C_6D_6) δ 8.54 (s, 2H, H-3,6), 8.47 (d, 1H, J = 1.0 Hz, H-1), 8.41 (d, J = 1.0 Hz, 1H, H-8), 8.40 (AB, J = 7.8 Hz, 1H, H-5), 8.38 (AB, J = 7.8 Hz, 1H, H-4), 6.25 (d, J = 4.7 Hz, 1H, H-13), 6.22 (d, J = 4.8 Hz, 1H, H-9), 3.32 (dq, J = 6.8, 4.7 Hz, 1H, H-12), 3.20 (dq, J = 6.8, 4.7 Hz, 1H, H-10), 1.60 (s, 9H, 2/7-C(C$\underline{H}_3$)$_3$), 1.59 (s, 9H, 2/7-C(C$\underline{H}_3$)$_3$), 1.26 (d, J = 6.7 Hz, 3H, 12-CH_3), 1.10 (d, J = 6.7 Hz, 3H, 10-CH_3), -3.75 (s, 3H, 13d-C$\underline{H}_3$), -3.78 (s, 3H, 13c-C$\underline{H}_3$); ^{13}C NMR (125 MHz C_6D_6) δ 208.10 (C-11), 146.32 (C-2/7), 145.98 (C-2/7), 137.89 (C-3a), 137.14 (C-5a), 135.22 (C-13f), 134.85 (C-13a), 130.12 (C-13b), 129.58 (C-13e), 124.76 (C-4/5), 124.69 (C-4/5), 122.04 (C-3), 121.64 (C-6), 119.71 (C-1), 118.78 (C-8), 84.57 (C-9), 83.66 (C-13), 54.08 (C-12), 52.81 (C-10), 36.46 (2/7-$\underline{C}$(CH$_3$)$_3$), 36.41 (2/7-$\underline{C}$(CH$_3$)$_3$), 32.32 (2/7-C($\underline{C}$H$_3$)$_3$), 32.28 (2/7-C($\underline{C}$H$_3$)$_3$), 32.24 (C-13c), 30.57 (C-13d), 15.94 (13c-$\underline{C}$H$_3$), 15.22 (13d-$\underline{C}$H$_3$), 11.89 (12-$\underline{C}$H$_3$), 11.70 (10-$\underline{C}$H$_3$); IR (KBr) ν 3026, 2962, 2923, 2902, 2876, 1705, 1601, 1461, 1374, 1359, 1346, 1235, 1199, 1043, 1021, 887, 868, 852, 673 cm^{-1}; UV-vis (cyclohexane) λ_{max} (ε_{max}, L Mol^{-1} cm^{-1}) nm, 205 (23,700), 239 (7,600), 331 (27,800), 349 (99,300), 360 (34,800), 385 (46,100), 438 (5,000), 461 (7,600), 480 (9,900), 537 (200), 600 (200), 644 (900), 651 (1,100); Anal. Calcd for $C_{33}H_{40}O_2$: C, 84.57; H, 8.60; Found: C, 84.64; H, 8.64.

Reduction of the cyclized products 99A,B with $NaBH_4$ to give alcohols 102

A solution of both isomeric oxo-heptanones **99A** and **99B** (115 mg, 0.245 mmol) in MeOH (10 mL) and THF (5 mL) were stirred at room temperature while $NaBH_4$ (28 mg, 0.74 mmol) was added in small portions. After 12 hours, the solvents were removed. The resulting green solid was re-dissolved in benzene. The solution was filtered through Celite to get rid of any salts. Then the benzene was removed and the residue was recrystallized in hexanes and DCM. Crystals of one green isomer of **102A** formed first. Subsequent crystals had needle shapes. M.p. 186-187 ^{o}C.

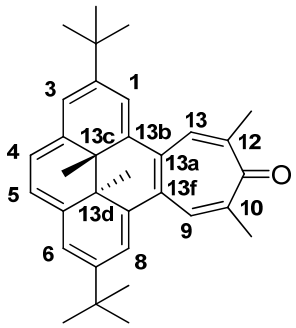


102A

One isomer 102A: ^{1}H NMR (500 MHz, $CDCl_3$) δ 8.46 (s, 2H, H-3,6), 8.42 and 8.40 (AB, J = 7.8 Hz, 2H, H-4/5), 8.39 (s, 1H, H-1), 8.33 (s, 1H, H-8), 5.86 (d, J = 3.7 Hz, 2H, H-13), 5.84 (d, J = 3.7 Hz, 1H, H-9), 3.85-3.80 (m, 1H, H-11), 2.98-2.92 (m, 1H, H-12), 2.88-2.82 (m, 1H, H-10), 1.653 (s, 9H, 2/7-C($\underline{C}H_3)_3$), 1.647 (s, 9H, 7/2-C($\underline{C}H_3)_3$), 1.43 (d, J = 7.4 Hz, 3H, 12-C$\underline{H}_3$), 1.24 (s, J = 7.3 Hz, 1H, 10-C$\underline{H}_3$), -0.01 (d, J = 9.2 Hz, 1H, -O$\underline{H}$), -3.76 (s, 3H, 13d-C$\underline{H}_3$) -3.96 (s, 3H, 13c-C$\underline{H}_3$); ^{13}C NMR (125 MHz, $CDCl_3$) δ 146.32 (C-2/7), 145.92 (C-2/7), 137.09 (C-5a), 136.94 (C-3a), 136.03 (C-13a), 135.53 (C-13f), 129.55 (C-13b), 128.49 (C-13e), 124.19 (C-4/5), 124.15 (C-4/5), 121.44 (C-3), 121.11 (C-6), 118.12 (C-1), 117.71 (C-8), 82.26 (C-9), 81.25 (C-13), 73.11 (C-12), 41.98 (C-12), 40.61 (C-10), 36.27 (2/7-$\underline{C}(CH_3)_3$), 36.22 (2/7-$\underline{C}(CH_3)_3$), 32.10 (2/7-C($\underline{C}H_3)_3$), 32.08 (2/7-C($\underline{C}H_3)_3$), 31.29 (C-10c), 30.46 (C-13d), 15.53 (C-13c), 14.14 (12-$\underline{C}H_3$), 13.90 (10-$\underline{C}H_3$), 13.64 (2/7-C($\underline{C}H_3)_3$); Isomeric mixture of **102**: IR (KBr) ν 3555, 2947, 2926, 2872,

1706, 1608, 1459, 1381, 1359, 1346, 1262, 1232, 1188, 1059, 1010, 966, 930, 888, 867, 674 cm^{-1}; UV-vis (cyclohexane) λ_{max} (ε_{max}, L Mol^{-1} cm^{-1}) nm 349 (80,600), 387 (41,500), 483 (7,500), 651 (835); EI MS *m/z* 452 (M^+); HRMS calcd for $C_{33}H_{42}O_2$: 470.3185, found 452.3187.

2,7-Di-*tert*-butyl-11-oxo-10,12,13c,13d-tetramethylcycloheptatrieno[13a:13f; e]-*trans*-13c,13d-dihydropyrene 17



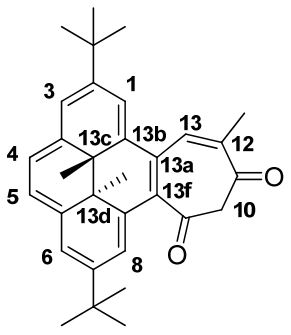
Mixed compounds **99A** and **99B** (2.2 g, 4.7 mmol) were stirred in *tert*-butanol (150 mL) at 60 ºC until completely dissolved. The oil bath was removed and potassium *tert*-butoxide (6.0 g, 53 mmol) was added slowly with stirring under argon. Then the mixture was warmed to 60 ºC and stirred for 40 minutes under argon. TLC indicated that side products were formed on longer reaction times.

The reaction was quenched by pouring it into a mixture of ether and water in a separatory funnel. The aqueous layer was extracted three times with ethyl acetate. The organic layers were combined, washed with aq. NaCl solution and dried over anhydrous $MgSO_4$. The solvent was then removed and the product was chromatographed over neutral aluminum oxide (deactived with 5% water) with hexanes and dichloromethane (ratio 1:4 to 1:1) as eluent. The green starting material was eluted first (0.30 g, 14% recovery). Eluent next was product, which was re-chromatographed over silica gel using dichloromethane as eluant to afford the dark orange product **17** (1.12 g, 61.1 % yield). Recrystallization from benzene gave dark red crystals, mp 191-193 ^oC. Later fractions contained a mixture of **17** and a small (1%) amount of unidentified compound **17-X**.

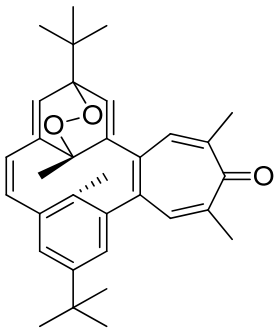
Compound **17-X** is a little more polar than the symmetric product **17**. The NMR data for compound **17-X** were determined by subtraction of the known data for the compound **3** from the spectra. Eluted later was a single isomer of **101** (~1 % yield), obtained in a small amount after repeated chromatography on the polar residue behind isomers **17**.

17: ^{1}H NMR (500 MHz, $CDCl_3$) δ 9.27 (s, 2H, H-9,13), 9.16 (s, 2H, H-1,8), 8.41 (s, 2H, H-3,6), 8.26 (s, 2H, H-4,5), 2.60 (s, 6H, 10,12-C$\underline{H}_3$), 1.70 (s, 18H, 2,7-C(C$\underline{H}_3$)$_3$), -3.56 (s, 6H, 13c,d- C$\underline{H}_3$); ^{13}C NMR (125 MHz, $CDCl_3$) δ 189.35 (C-11), 146.73 (C-2,7), 138.68 (C-3a, 5a), 138.33 (C-10,12), 135.24 (C-13b,13e), 133.78 (C-9,13), 127.67 (C-13a,13f), 123.84 (C-4,5), 122.31 (C-3,6), 119.60 (C-1,8), 36.52 (2,7-$\underline{C}$(CH$_3$)$_3$), 32.00 (2,7-C($\underline{C}$H$_3$)$_3$), 31.03 (C-13c,13d), 24.31 (10, 12-$\underline{C}$H$_3$), 15.01 (internal $\underline{C}$H$_3$); IR (KBr) ν 2962, 2925, 2864, 1609, 1465, 1361, 1345, 1240, 1160, 1035, 895, 869, 674 cm^{-1}; UV-vis (cyclohexane) λ_{max} (ε_{max}, L Mol^{-1} cm^{-1}) nm, 257 (13,900), 268 (16,400), 284 (13,800), 377 (32,900), 401 (39,600), 423 (56,400), 488 (6,200), 513 (7,200), 534 (6,500), 627 (900), 696 (1,700); EI MS *m/z* 450(M+); HRMS calcd for $C_{33}H_{38}O$: 450.2923, found: 450.2913; Anal. Calcd for $C_{33}H_{38}O$: C, 87.95; H, 8.50; Found: C, 87.74; H, 8.45.

Unidentified product 17-X: (only obtained mixed with **17**) ^{1}H NMR (500 MHz, $CDCl_3$) δ 8.39 (s, 1H), 8.37 (s, 1H), 8.36 and 8.34 (AB, J = 8.2 Hz, 2H), 8.14 (s, 1H), 8.11 (s, 1H), 5.79 (d, J = 1.5 Hz, 1H), 5.78 (d, J = 1.5 Hz, 1H), 1.88 (s, 3H, -C$\underline{H}_3$), 1.79 (s, 3H, -C$\underline{H}_3$), 1.63 (s, 9H, -C(C$\underline{H}$)$_3$), 1.62 (s, 9H, -C(C$\underline{H}_3$)$_3$), -3.74(s, 3H), -3.76 (s, 3H); ^{13}C NMR (125 MHz, $CDCl_3$) δ 183.63, 147.26, 147.21, 137.75, 137.67, 134.26, 133.79, 129.09, 127.70, 125.18, 125.05, 122.07, 122.00, 115.89, 115.76, 104.28, 103.85, 82.03, 81.19, 36.22, 36.19, 32.43, 31.89, 30.71, 16.02, 15.81, 15.35, 13.82.



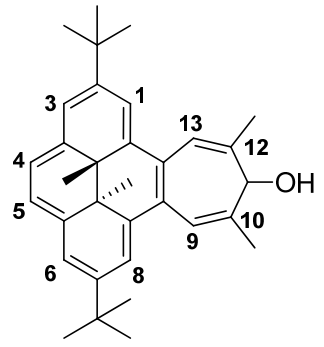
101: ^{1}H NMR (500 MHz, $CDCl_3$) δ 8.99 (s, 1H, H-8), 8.68 (s, 1H, H-1), 8.57 (d, J = 1.4 Hz, 1H, H-13), 8.34 (s, 1H, H-3), 8.32 (s, 1H, H-6), 8.28 (s, 2H, H-4,5), 4.69 (d, J = 11.9 Hz, 1H, -C$\underline{H}_2$-), 4.08 (d, J = 11.9 Hz, 1H, -C$\underline{H}_2$-), 2.24 (d, J = 0.7 Hz, 3H, 12-CH_3), 1.66 (s, 9H, 2-C(CH_3)$_3$), 1.60 (s, 9H, 7-C(CH_3)$_3$), -3.20 (s, 3H, H-13c), -3.23 (s, 3H, H-13d); ^{13}C NMR (125 MHz, $CDCl_3$) δ 195.86 (C-9), 190.06 (C-11), 152.02 (C-7), 149.84 (C-2), 140.55 (C-3a), 139.76 (C-5a), 138.37 (C-13), 138.07 (C-13b), 134.96 (C-13e), 131.97 (C-12), 128.54 (C-13f), 126.45 (C-5), 126.05 (C-4), 123.35 (C-6), 122.82 (C-3), 121.28 (C-13a), 119.29 (C-8), 116.29 (C-1), 63.02 (-$\underline{C}H_2$-), 36.72 (2/7-$\underline{C}$(CH_3)$_3$), 36.65 (2/7-$\underline{C}$(CH_3)$_3$), 32.12 (C-13c), 31.74 (2-C($\underline{C}H_3$)$_3$), 31.60 (7-C($\underline{C}H_3$)$_3$), 31.46 (C-13d), 20.57 (12-CH_3), 17.06 (C-13c), 16.40 (C-13d); EI MS m/z 450(M+); HRMS calcd for $C_{32}H_{36}O_2$: 452.2715, found: 452.2712;



The side product 134 formed during photoopening of 17: ^{1}H NMR (500 MHz $CDCl_3$) δ 7.86 (s, 1H), 7.40 (s, 1H), 7.10 (d, J = 1.9 Hz, 1H), 7.07 (d, J = 2.0 Hz, 1H), 6.82 (d, J = 10.8 Hz, 1H), 6.50 (s, 1H), 6.46 (s, 1H), 6.37 (d, J = 10.7 Hz, 1H), 2.42 (s, 3H), 2.33 (s, 3H), 1.91 (s, 3H), 1.29 (s, 9H), 1.14 (s, 9H), -0.12 (s, 3H); ^{13}C NMR (500 MHz $CDCl_3$) δ 185.40, 155.78, 153.15, 149.99, 147.91, 146.05, 144.31, 144.17, 141.85, 141.61, 141.27, 138.39, 136.89, 133.69, 131.88, 130.74, 129.42, 126.92, 124.20, 84.95, 84.02, 34.54, 33.35, 31.46, 25.17, 24.12, 24.00, 22.69, 12.32.

2,7-Di-*tert*-butyl-10,12,13c,13d-tetramethyl-11H-11-hydroxy-cycloheptatrieno[13a:13f; e]-*trans*-13c,13d-dihydropyrene 103

$LiAlH_4$ (31 mg, 0.82 mmol) was added to the tropone **17** (60 mg, 0.13 mmol) dissolved in dry ether (15 mL) in a dry Schlenk tube under argon and the mixture was stirred at room temperature for one hour. Then the resulting mixture was diluted with ether and poured into a solution of NH_4Cl in ice water. The organic layer was washed with water and aqueous NaCl solution. The ether layer was dried over $MgSO_4$ for one hour and the solvent was removed under vacuum to afford a dark orange solid of **103** (25 mg, yield 45%). This was chromatographed on alumina using dichloromethane and hexane (1:1) and then pure dichloromethane as eluants, which eluted an orange product. This was recrystallized by diffusing hexane into DCM in a freezer to afford dark red crystals of **103**, mp 193-194 ^{o}C.

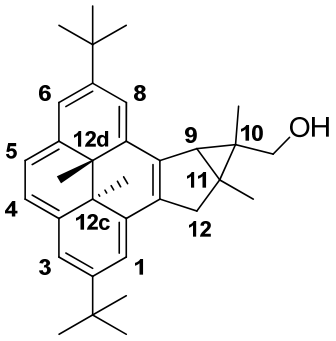


103: ^{1}H NMR (500 MHz C_6D_6) δ 8.56 (m, 2H, H-1,8), 8.14 (m, 2H, H-3,6), 7.97 (s, 2H, H-4,5), 7.44 (s, 1H, H-9), 7.42 (s, 1H, H-13), 4.35 (d, J = 5.0 Hz, 1H, H-11), 2.35 (s, 3H, 10-C$\underline{H}_3$), 2.32 (s, 3H, 12-C$\underline{H}_3$), 1.90 (d, J = 5.3 Hz, 1H, -O$\underline{H}$), 1.63 (s, 18H, 2,7-C(C$\underline{H}_3$)$_3$), -3.24 (s, 3H, 13d-C$\underline{H}_3$), -3.31 (s, 3H, 13c-C$\underline{H}_3$); ^{13}C NMR (125 MHz C_6D_6) δ 145.45 (C-2/7), 145.34 (C-2/7), 143.00 (C-10), 142.15 (C-12), 138.14 (C-5a), 137.41 (C-3a), 135.00 (C-13e), 134.65 (C-13b), 130.37 (C-13a), 129.70 (C-13f), 121.82 (C-4/5), 121.80 (C-4/5), 120.49 (C-3/6), 120.32 (C-9), 120.25 (C-1/3/6/8), 120.23 (C-1/3/6/8), 119.49 (C-1/8), 118.81 (C-13), 73.19 (C-11), 36.21 (C-2,7), 32.00 (2/7-C($\underline{C}$H$_3$)$_3$), 31.97 (2/7-C($\underline{C}$H$_3$)$_3$), 31.05 (C-13c/13d), 30.94 (C-13c/13d), 20.07 (10-$\underline{C}$H$_3$), 19.73 (12-$\underline{C}$H$_3$), 16.28 (13c-$\underline{C}$H$_3$), 15.41 (13d-$\underline{C}$H$_3$). IR (KBr) ν 3579, 2962, 2928, 2904, 2865, 1599, 1461, 1439, 1361,

1343, 1260, 1233, 1174, 1099, 1083, 1021, 884, 845, 669, 598 cm^{-1}; UV-vis (cyclohexane) λ_{max} (ε_{max}, L Mol^{-1} cm^{-1}) nm 362 (65,700), 402 (57,900), 488 (7,490), 508 (7,740), 598 (552), 666 (1,220); EI MS *m/z* 452 (M^+); HRMS calcd for $C_{33}H_{40}O$: 452.3079, found 452.3080; Anal. Calcd for $C_{33}H_{40}O$: C, 87.56; H, 8.91; Found: C, 86.34; H, 8.79.

Reduction of tropone by $NaBH_4$ and $CeCl_3 \cdot 7H_2O$ to give 105

A schlenk tube was loaded with $CeCl_3 \cdot 7H_2O$ (85 mg, 0.20 mmol) and molecular sieves (102 mg). Tropone **17** (60 mg, 0.13 mmol) and anhydrous ethanol (25 mL) were added under argon. A clear solution was obtained and stirred for 5 mins before $NaBH_4$ (77 mg, 2.0 mmol) was added and the reaction mixture was refluxed for 5 hours. The starting tropone was consumed by TLC. Saturated NaCl aqueous solution was added to quench the reaction and white precipitation formed in the aqueous layer. The mixture was extracted with benzene for three times. The combined benzene layers were dried over $MgSO_4$ and dried to afford a dark green solid (quantitatively).



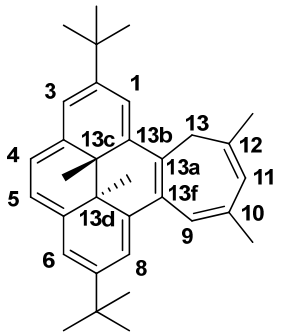
Provisional product **105**: ^{1}H NMR (500 MHz, C_6D_6) δ 8.68 (s, 1H, H-8), 8.58 (s, 1H, H-1), 8.39 (s, 2H, H-3,6), 8.27 and 8.26 (AB, J = 7.5 Hz, 2H, H-4/5), 4.80 (s, 1H, H-9), 4.35 and 4.26 (AB, J = 21.4 Hz, 2H, H-12), 3.97-3.93 (m, 1H, -C$\underline{H}_2$OH), 3.89-3.85 (m, 1H, -C$\underline{H}_2$OH), 2.15 (s, 3H, 10-C$\underline{H}_3$), 2.08 (s, 3H, 11-C$\underline{H}_3$), 1.68 (s, 9H, 2/7-C(C$\underline{H}_3$)$_3$), 1.67 (s, 9H, 2/7-C(C$\underline{H}_3$)$_3$), -3.80 (s, 3H, 12c/12d-C$\underline{H}_3$), -3.81 (s, 3H, 12d/12c-C$\underline{H}_3$); ^{13}C NMR (125 MHz C_6D_6) δ 145.31 (C-2/7), 145.16 (C-2/7), 137.37 (C-5a/3a), 137.24 (C-3a/5a),

133.04 (C-12e/12b), 132.53 (C-12b/12e), 129.10 (C-12f), 128.53 (C-12a), 127.67 (C-10/11), 125.05 (C-10/11), 122.61 (C-4/5), 122.36 (C-4/5), 120.36 (C-3), 120.25 (C-6), 117.00 (C-8), 116.97 (C-1), 67.38 (-$\underline{C}H_2OH$), 47.66 (C-9), 36.35 (2/7-$\underline{C}(CH_3)_3$), 36.33 (2/7-$\underline{C}(CH_3)_3$), 35.20 (C-12), 32.30 (2/7-C($\underline{C}H_3)_3$), 32.19 (2/7-C($\underline{C}H_3)_3$), 30.26 (C-12c/12d), 30.15 (C-12c/12d), 19.53 (11-$\underline{C}H_3$), 18.61 (10-$\underline{C}H_3$), 15.01 (12c/12d-$\underline{C}H_3$), 14.93 (12c/12d-$\underline{C}H_3$); IR (KBr) *v* 3464, 2963, 2867, 1720, 1656, 1601, 1461, 1446, 1362, 1261, 1234, 1208, 1085, 1022, 880, 802, 669 cm^{-1}; ESI mass spec (and EI methods) included the peak at 452 amu with the largest intensity.

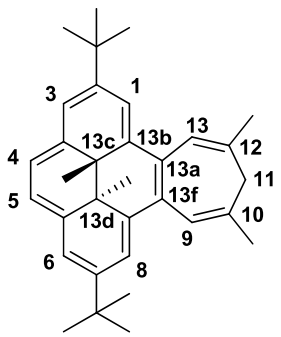
2,7-Di-*tert*-butyl-10,12,13c,13d-tetramethyl-13-H,H-cycloheptatrieno[13a:13f; e]-*trans*-13c,13d-dihydropyrene (107) and 2,7-di-*tert*-butyl-10,12,13c,13d-tetramethyl-11-H,H-cycloheptatrieno[13a:13f; e]-*trans*-13c,13d-dihydropyrene (108)

Aluminum hydride was generated using the procedure adapted from the literature.[265] A three-necked flask was charged with lithium aluminum hydride (3.9 g, 0.10 mol) and dry ether (250 mL). The stirred slurry was warmed to reflux for 2 hours under argon. Then oil bath was replaced with an ice bath. Aluminum chloride (13.65 g, 0.10 mol) was added slowly under argon. Then the resulting slurry was refluxed for another 2 hours. The reaction mixture was then cooled to -78 ^oC in a dry ice/acetone bath. A solution of tropone **17** (0.50 g, 1.1 mmol) in ether (50 mL) and benzene (150 mL) was added dropwise. The resulting mixture was stirred for 12 hours at 25 ^oC under argon.

The reaction was then quenched by addition of ethyl acetate and ice water sequentially with ice bath cooling. The product was extracted with ether three times and the organic layer was then washed with aqueous NaCl solution, dried over anhydrous $MgSO_4$ and evaporated. The products were chromatographed on a silica gel column using hexanes as the eluent. The first fraction contained the asymmetric isomer **107** (0.34 g, 70 % yield) and the second fraction the symmetric isomer **108** (75 mg, 15 % yield). Both were recrystallized from benzene to afford dark orange crystals. An X-ray quality crystal of isomer **108** was obtained from benzene with slow diffusion of diethyl ether.



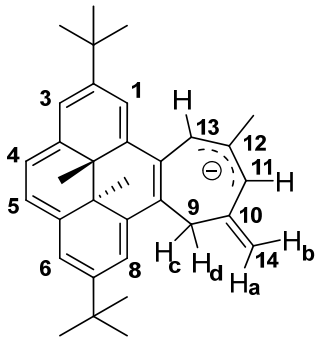
107: M.p. 175-176°C. ^{1}H NMR (500 MHz, $CDCl_3$) δ 8.80 (s, 1H, H-1), 8.79 (s, 1H, H-8), 8.36 (s, 1H, H-3), 8.35 (s, 1H, H-6), 8.27 (s, 1H, H-9), 8.24 (d, J = 7.2 Hz, 1H, H-4), 8.20 (d, J = 7.2 Hz, 1H, H-5), 5.91 (s, 1H, H-11), 4.38 (d, J = 12.4 Hz, 1H, H-13), 3.04 (d, J = 12.3 Hz, 1H, H-13), 2.38 (d, J = 0.9 Hz, 1H, 10-C$\underline{H}_3$), 2.18 (d, J = 1.4 Hz, 1H, 12-C$\underline{H}_3$), 1.70 (s, 9H, 2-C(C$\underline{H}_3$)$_3$), 1.69 (s, 9H, 7-C(C$\underline{H}_3$)$_3$), -3.65 (s, 3H, 13d-C$\underline{H}_3$), -3.89 (s, 3H, 13c-C$\underline{H}_3$); ^{13}C NMR (125 MHz, $CDCl_3$) δ 145.66 (C-7), 144.80 (C-2), 139.39 (C-12), 138.37 (C-10), 137.83 (C-5a), 136.38 (C-3a), 133.94 (C-13e), 132.45 (C-13b), 128.92 (C-13a), 128.83 (C-13f), 126.48 (C-9), 124.44 (C-11), 122.42 (C-4), 121.68 (C-5), 120.25 (C-3), 120.02 (C-6), 118.78 (C-1), 117.41 (C-8), 36.34 (7-$\underline{C}$(CH$_3$)$_3$), 36.22 (2-$\underline{C}$(CH$_3$)$_3$), 35.55 (C-13), 32.19 (7-C($\underline{C}$H$_3$)$_3$), 32.14 (2-C($\underline{C}$H$_3$)$_3$), 30.62 (C-13d), 30.54 (C-13c), 25.48 (10-$\underline{C}$H$_3$), 24.58 (12-$\underline{C}$H$_3$), 14.60 (13d-$\underline{C}$H$_3$), 14.47 (13c-$\underline{C}$H$_3$); IR (KBr) v 3012, 2962, 2922, 2860, 1645, 1590, 1459, 1438, 1345, 1260, 1230, 1193, 886, 856, 831, 795, 672, 647 cm^{-1}; UV-vis (cyclohexane) λ_{max} (ε_{max}, L Mol^{-1} cm^{-1}) nm, 227 (17,500), 287 (9,600), 358 (64,000), 373 (36,600), 399 (57,500), 486 (8,400), 501 (9,400), 600 (300), 666 (1,300); Anal. Calcd for $C_{33}H_{40}$: 90.77 H, 9.23; Found: C, 89.81; H, 9.19.



108: M.p. 187-188°C ^{1}H NMR (500 MHz, $CDCl_3$) δ 8.59 (d, J = 1.0 Hz, 2H, H-1,8), 8.16 (d, J = 1.0 Hz, 2H, H-3,6), 8.00 (s, 2H, H-4,5), 7.46 (q, J = 1.4 Hz, 2H, H-9,13), 2.53 (d, J = 1.0 Hz, 2H, H-11), 2.34 (d, J = 1.4 Hz, 6H, 10,12-C$\underline{H}_3$), 1.63 (s, 18H, 2, 7-C(C$\underline{H}$)$_3$), -3.32 (s, 6H, 13c,d-C$\underline{H}_3$); ^{13}C NMR (125 MHz, $CDCl_3$) δ 145.10 (C-2,7), 140.44 (C-10,12), 137.72 (C-3a,5a), 135.16 (C-13b,13e), 130.75 (C-13a,13f), 121.83 (C-9,13), 121.61 (C-4,5), 120.12 (C-3,6), 119.11 (C-1,8), 38.54 (C-11), 36.19 (2,7-$\underline{C}$(CH)$_3$), 32.04 (2,7-C($\underline{C}$H)$_3$), 31.14 (C-13c,13d), 26.08 (10,12-$\underline{C}$H$_3$), 15.86 (internal-$\underline{C}$H$_3$); UV-vis (cyclohexane) λ_{max} (ε_{max}, L Mol^{-1} cm^{-1}) nm, 256 (13,400), 290 (6,500), 359 (58,100), 374 (39,100), 399 (51,800), 455 (5,600), 484 (7,700), 504 (8,100), 597 (400), 668 (1,200); IR (KBr) v 3052, 2960, 2947, 2926, 2899, 2863, 1601, 1459, 1433, 1372, 1360, 1345, 1239, 1224, 1199, 882, 870, 856, 848, 800, 681, 649 cm^{-1}; EI MS m/z 436 (M^{+}); HRMS calcd for $C_{33}H_{40}$: 436.3130, found 436.3133;

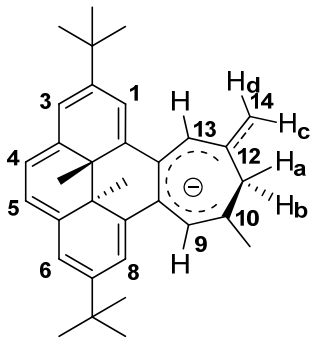
Cycloheptatrienyl anions 111, 112 and 19

Cycloheptatriene **107** or **108** (18 mg, 0.041 mmol) was dissolved in THF-d_8 (about 0.5 mL) in a vial in a dry box. A solution of (trimethylsilyl)methyl lithium[272] (0.041 mmol) in THF-d_8 (about 0.5 mL) was then added. The mixture was transferred into a sealed NMR tube. The ^{1}H NMR spectrum showed that the reaction completed in about 1 hour. The isomeric cycloheptatriene **107** gave rise to the anion **111**. Both anions **112** and **19** were made from isomer **108** in one reaction with a ratio **112**/**19** 3:2 at room temperature. All three products **111**, **112** and **19** were stable when kept in a fridge over a month. However, decomposition occurred when excess lithium salt was present.



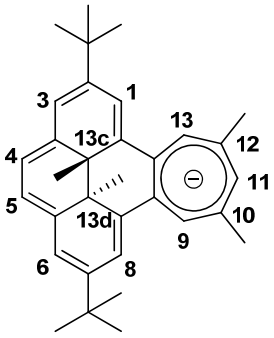
Anion 111: ^{1}H NMR (500 MHz, THF-d_8) δ 8.20 (s, 1H, H-1), 7.42 (s, 1H, H-3), 7.31 (d, J = 7.0 Hz, 1H, H-4), 7.25 (s, 1H, H-8), 7.15 (s, 1H, H-6), 6.93 (d, J=7.0 Hz, 1H, H-5), 6.48 (s, 1H, H-13), 5.58 (s, 1H, H-11), 4.66 (d, J = 3.0 Hz, 1H, H-14a/14b), 4.28 (d, J = 3.1 Hz, 1H, H-14a/14b), 3.58 (d, J = 11.4 Hz, 1H, H-9c/9d), 2.17 (s, 3H, 12-C$\underline{H}_3$), 1.97 (d, J = 11.6 Hz, 1H, H-9c/9d), 1.58 (s, 9H, 7-C(C$\underline{H}_3$)$_3$), 1.53 (s, 9H, 2-C(C$\underline{H}_3$)$_3$), 1.30*, -2.52 (s, 3H, 13c-C$\underline{H}_3$), -2.67 (s, 3H, 13d-C$\underline{H}_3$); ^{13}C NMR (125 MHz $CDCl_3$) δ 150.06 (C-10), 146.63 (C-7), 136.92 (C-2), 134.74 (C-12), 121.77 (C-1), 118.23 (C-3), 113.41 (C-4), 112.97 (C-5), 109.28 (C-6), 109.04 (C-11), 103.06 (C-8), 102.19 (C-13), 96.55 (C-14), 40.30 (C-9), 36.34 (C-13d/7-$\underline{C}$(CH$_3$)$_3$), 36.33 (C-13d/7-$\underline{C}$(CH$_3$)$_3$), 35.80 (2-$\underline{C}$(CH$_3$)$_3$), 33.90 (C-13c), 32.72 (2/7-C($\underline{C}$H$_3$)$_3$), 30.70*, 29.68 (12-$\underline{C}$H$_3$), 18.62 (13d-$\underline{C}$H$_3$), 15.90 (13c-$\underline{C}$H$_3$).

* Solvent (hexanes) residual peak from starting material.



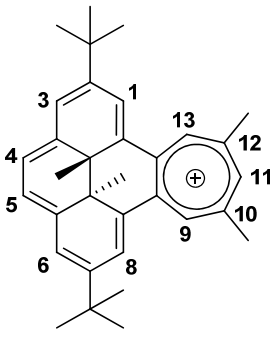
Anion 112: ^{1}H NMR (500 MHz, THF-d_8) δ 7.26 (s, 1H, H-1), 6.71 (s, 1H, H-9), 6.59 (s, 1H, H-3), 6.43 (d, J = 7.0 Hz, 1H, H-4), 6.40 (s, 1H, H-13), 6.32 (s, 1H, H-8), 6.14 (s, 1H, H-6), 5.90 (d, 1H, J = 6.9 Hz, H-5), 4.18 (d, J = 2.8 Hz, 1H, H-14d), 3.53 (d, J = 3.0 Hz, 1H, H-14c), 2.65 (d, J = 11.0 Hz, 1H, H-11b), 2.27 (d, J = 11.0 Hz, 1H, H-11a), 1.83 (s,

3H, 10-C$\underline{H}_3$), 1.32 (s, 9H, 7-C(C$\underline{H}_3$)$_3$), 1.31 (s, 9H, 2-C(C$\underline{H}_3$)$_3$), -0.80 (s, 3H, 13d-C$\underline{H}_3$), -0.84 (s, 3H, 13c-C$\underline{H}_3$); ^{13}C NMR (125 MHz $CDCl_3$) δ 149.40 (C-12), 148.12 (C-7), 144.57 (C-5a), 142.88 (C-13e), 139.73 (C-13b), 136.79 (C-2), 136.27 (C-13a), 131.87 (C-10), 131.33 (C-3a), 125.98 (C-9), 122.49 (C-4), 120.64 (C-13f), 119.82 (C-3), 116.39 (C-1), 109.96 (C-5), 106.34 (C-13), 105.92 (C-6), 102.35 (C-8), 91.24 (=CH_2), 43.25 (C-11), 42.49 (C-13d), 37.50 (C-13c), 35.74 (7-C$\underline{C}$(CH$_3$)$_3$), 35.29 (2-C$\underline{C}$(CH$_3$)$_3$), 32.27 (7-C(C$\underline{H}_3$)$_3$), 32.00 (2-C(C$\underline{H}_3$)$_3$), 23.15 (13d-C$\underline{H}_3$), 17.72 (13c-C$\underline{H}_3$), 0.19 (Si(C$\underline{H}_3$)$_4$).



Anion 19: ^{1}H NMR (500 MHz, THF-d_8) δ 5.54 (s, 2H, H-1,8), 5.03 (d, J = 1.1 Hz, 2H, H-3,6), 4.87 (s, 2H, H-4,5), 3.00 (s, 2H, H-9,13), 2.92 (s, 1H, H-11), 2.10 (s, 6H, 13c,d-C$\underline{H}_3$), 0.92 (s, 18H, 2,7-C(C$\underline{H}_3$)$_3$), 0.81 (s, 6H, 10,12-C$\underline{H}_3$); ^{13}C NMR (125 MHz, $CDCl_3$) δ 143.44 (C-10,12), 141.52 (C-13a,13f), 137.44 (C-3a,5a), 136.98 (C-2,7), 124.57 (C-4,5), 121.04 (C-3,6), 118.92 (C-13b,13e), 116.63 (C-1,8), 111.11 (C-11), 107.59 (C-9,13), 48.54 (C-13c,13d), 34.18 (2,7-C$\underline{C}$(CH$_3$)$_3$), 30.97 (2,7-C(C$\underline{H}_3$)$_3$), 26.66 (10,12-C$\underline{H}_3$), 23.67 (C-13c,13d).

DHP[e]tropylium cation 18:



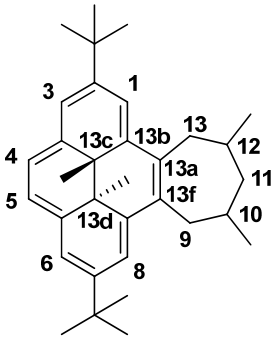
48% Tetrafluoroboric acid (one drop) was added to alcohol **103** (5.0 mg, 0.011 mmol) in deuterated solvents (0.7 mL) (THF-d_8, $CDCl_3$, benzene-d_6 or acetone-d_6) in a NMR tube. The solution turned purple immediately and then the NMR spectrum was recorded. The DHP[e]tropylium salt **18**·BF_4^- was obtained quantitatively by NMR spectroscopy.

18·BF_4^-: ^{1}H NMR (500 MHz, C_6D_6) δ 10.50 (s, 2H, H-9,13), 9.78 (s, 2H, H-1,8), 8.30 (s, 1H, H-11), 8.10 (s, 2H, H-3,6), 7.62 (s, 2H, H-4,5), 2.93 (s, 6H, 10,12-C$\underline{H}_3$), 1.68 (s, 18H, 2,7-C(C$\underline{H}_3$)$_3$), -2.61 (s, 6H, 13c,13d-C$\underline{H}_3$); ^{13}C NMR (125 MHz, C_6D_6) δ 151.79 (C-11), 151.04 (C-2,7), 148.56 (C-10,12), 145.00 (C-9,13), 142.06 (C-3a,5a), 140.76 (C-13a,13f), 135.23 (C-13b,13e), 130.90 (C-1,8), 127.91 (C-3,6), 127.44 (C-4,5), 37.00 (2,7-$\underline{C}$(CH$_3$)$_3$), 33.95 (C-13c,13d), 31.46 (2,7-C($\underline{C}$H$_3$)$_3$), 28.63 (10,12-$\underline{C}$H$_3$), 16.51 (13c,13d-$\underline{C}$H$_3$); IR (KBr) *v* 2963, 2926, 2866, 1599, 1512, 1462, 1437, 1384, 1364, 1345, 1305, 1237, 1198, 1171, 1112, 1081, 1052, 1020, 891, 872, 815, 670 cm^{-1}; UV-vis (Dichloromethane) λ_{max}, nm, 242, 272, 352, 374, 498, 670, 728; ESI *m/z* 435 (M^+); HRMS calcd for $C_{33}H_{39}$: 435.3052, found 435.3054.

2,7-di-*tert*-butyl-10,12,13c,13d-tetramethyl-*trans*-13c,13d-dihydro-9,10,11,12,13-pentahydrocyclohepta[13a:13f; e]pyrene 109
2,7-di-*tert*-butyl-10,12,13c,13d-tetramethyl-*trans*-13c,13d-dihydro-9,10,11-trihydrocyclohepta[13a:13f; e]pyrene 110

Pt_2O (16 mg, 0.070 mmol) were suspended in ethyl acetate (5 mL) in a Schlenk tube sealed with a rubber septa. Hydrogen in a balloon was cannulated to the solution through the septa. The solution was stirred at room temperature until the color turned black. Then a solution of triene **107** (20 mg, 0.046 mmol) in ethyl acetate (2 mL) was added by syringe. The reaction was stirred for an hour. Then the black catalyst was removed by filtration through a Celite pad. The solvent was removed to afford a green solid. Complete conversion to products was proven by NMR spectroscopy and two bands for products were separated on a preparative TLC plate eluting with hexane and DCM (10:2). The first band consisted of the isomeric mixtures of DHP-fused saturated C7 ring **109** (*ca.*

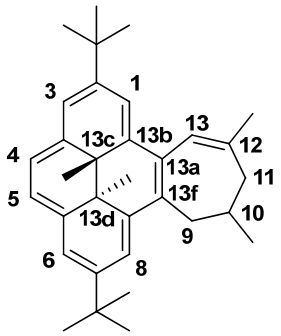
65%) and the second was the partly reduced product **110** (*ca.* 35%), in which one double bond was reduced. In each there were two isomers found with a *ca.* 4:1 ratio. As only the chemical shifts associated with the internal methyl protons were of interest to us, no effort was made to separate the singly reduced products from the doubly reduced ones. So the NMR data was obtained by subtraction of known peaks.



Major isomer 109: ^{1}H NMR (500 MHz $CDCl_3$) δ 8.74 (s, 1H, H-1/8), 8.71 (s, 1H, H-1/8), 8.44 (s, 1H, H-3/6), 8.43 (d, J = 0.7 Hz, 1H, H-3/6), 8.34 (s, 2H, H-4,5), 4.00-3.90 (m, 2H, H-9,13), 3.47-3.35 (m, 1H, H-9/13), 3.34-3.21 (m, 1H, H-9/13), 2.00-1.81 (m, 2H, H-10,12), 1.64-1.47 (m, 2H, H-11), 1.678 and 1.676 (s, 18H, 2,7-C(C$\underline{H}_3$)$_3$), 1.35-1.24 (m, 3H, 10/12-C$\underline{H}_3$), 1.22 (d, J = 6.7 Hz, 3H, 10/12-C$\underline{H}_3$), -3.98 (s, 3H, internal-C$\underline{H}_3$), -4.03 (s, 3H, internal-C$\underline{H}_3$); ^{13}C NMR (125 MHz $CDCl_3$, selected and assigned where it is possible) δ 144.91 and 144.73 (C-2,7), 137.12 (C-3a/5a), 136.98 (C-3a/5a), 132.80 (C-13a/13f), 122.60 and 122.49 (C-4,5), 120.38 (C-3/6), 120.25 (C-3/6), 117.21, 116.94, 116.62 (C-1,8), 36.62, 34.62, 32.25 ;

Minor isomer 109: ^{1}H NMR (500 MHz $CDCl_3$) δ 8.77 (d, J = 1.0 Hz, 1H), 8.74 (d, J = 1.0 Hz, 1H), 8.35 (s, 1H), 3.85 (dd, J = 14.4, 3.4 Hz, 1H), 3.82 (dd, J = 14.8, 3.4 Hz, 1H), 3.70 (dd, J = 14.4, 7.6 Hz, 1H), 3.62 (dd, J = 14.6, 7.4 Hz, 1H), 2.4-2.3 (m), 2.3-2.2 (m), 1.08 (d, J = 7.0 Hz, 3H) 0.96 (d, J = 7.0 Hz, 3H), -3.986 (s, 3H), -3.995 (s, 3H);

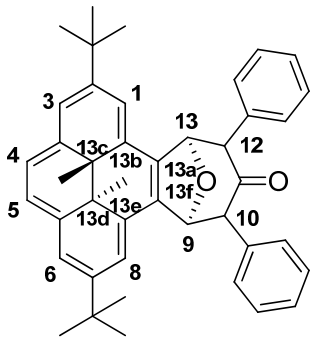
UV-vis (cyclohexane) λ_{max} nm 352, 388, 482, 598, 652; EI MS *m/z* 440 (M^+); HRMS calcd for $C_{33}H_{44}$: 440.3443, found; 440.3443.



Major isomer with singly reducing double bond of CHT 110: ^{1}H NMR (500 MHz $CDCl_3$) δ 8.60 (d, J = 1.0 Hz, 1H), 8.44 (underneath peaks for isomer **109**, 1H), 8.43 (underneath peaks for isomer **109**, 1H), 8.41 (d, J = 1.0 Hz, 1H), 8.31 (s, 2H), 7.57-7.55 (m, 1H, H-13), -3.83 (internal-C$\underline{H}_3$), -3.90 (internal-C$\underline{H}_3$);

Minor isomer with singly reducing double bond of CHT 110: Internal methyl protons at: -3.85 (s) and -3.88 (s). (other peaks overlap with other products)

2,7-Di-*tert*-butyl-*trans*-13c,13d-dimethyl-13c,13d-dihydropyreno]-[e; 13a:13f]-*cis* (or *trans*-)-10,12-diphenyl-14-oxabicyclo[3.2.1]oct-13a-en-11-one 114



The procedure to prepare the methyl substituted bicyclic compounds **99** was used: 2,4-dibromo-2,4-diphenylpentan-3-one (170 mg, 0.46 mmol) isofuran, (170 g, 0.44 mmol), copper powder (110 mg, 1.73 mmol) and sodium iodide (460 mg, 3.07 mol) were reacted in dry acetonitrile (30 mL) under argon for 24 hours. When the reaction finished, the reaction solution was filtered through a Celite pad to remove the solid suspension. The acetonitrile was removed under vacuum. Green isomer **114B** (with the larger separation

of the NMR signals for the internal methyl protons) was obtained from the reaction residue by recrystallization from ethyl acetate. The isomer **114A** with closer NMR signals for the internal methyl protons was separated chromatographically from the mother liquor. The green isomer **114A** was eluted first (80 mg, 30% yield) and isomer **114B** second (85 mg, 35% yield) using DCM and hexanes as eluant (1:1). Isomer **114A** was recrystallized from DCM. M.p. 209-210°C

114A: ^{1}H NMR (500 MHz C_6D_6) δ 8.59 (s, 1H, H-3/6), 8.58 (s, 1H, H-3/6), 8.50 and 8.49 (AB, J = 7.9 Hz, 2H, H-4/5), 8.39 (d, J = 1.1 Hz, 1H, H-1/8), 8.38 (d, J = 1.1 Hz, 1H, H-1/8), 7.65-7.62 (m, 4H, H-2'/2"), 7.29-7.24 (m, 4H, H-3'/3"), 7.23-7.19 (m, 2H, H-4'/4"), 6.87 (s, 2H, H-9/13), 4.25 (s, 1H, H-10/12), 4.04 (s, 1H, H-10/12), 1.66 (s, 9H, 2/7-C(C$\underline{H}_3$)$_3$), 1.66 (s, 9H, 2/7-C(C$\underline{H}_3$)$_3$), -3.88 (s, 1H, 13c/13d-C$\underline{H}_3$), -4.03 (s, 1H, 13c/13d-C$\underline{H}_3$); ^{13}C NMR (125 MHz C_6D_6) δ 206.97 (C-11), 146.60 (C-2/7), 146.46 (C-2/7), 137.67 (C-1'/1"), 137.61 (C-1'/1"), 137.20 (C-3a/5a), 137.02 (C-3a/5a), 135.06 (C-13a/13f), 134.61 (C-13a/13f), 128.76 (C-2'/2"), 128.68 (C-3'/3"), 128.67 (C-3'/3"), 127.82 (C-13b/13e), 127.42 (C-13b/13e), 127.33 (C-4'/4"), 124.31 (C-4/5), 124.03 (C-4/5), 121.89 (C-3/6), 121.85 (C-3/6), 117.88 (C-1/8), 117.02 (C-1/8), 81.53 (C-9/13), 81.21 (C-9/13), 61.55 (C-10/12), 61.32 (C-10/12), 36.37 (2,7-$\underline{C}$(CH$_3$)$_3$), 32.24 (2,7-C($\underline{C}$H$_3$)$_3$), 31.69 (C-13c/13d), 29.64 (C-13c/13d), 14.94 (13c/13d-$\underline{C}$H$_3$), 14.79 (13c/13d-$\underline{C}$H$_3$);

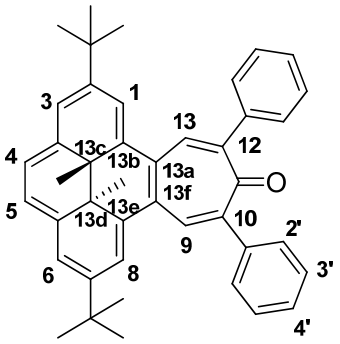
114B[2]**:** ^{1}H NMR (500 MHz C_6D_6) δ 8.38 (s, 3H, H-4,5,6), 8.36 (d, J = 1.0 Hz, 1H, H-3), 7.29 (tt, J = 7.3, 1.2 Hz, 1H, H-4'/4"), 7.24 (tt, J = 7.6, 1.1 Hz, 1H, H-4'/4"), 7.20 (d, J = 1.0 Hz, 1H, H-8), 7.17 (t, J = 7.5 Hz, 2H, H-3'/3"), 7.10 (t, J = 7.6 Hz, 2H, H-3'/3"), 7.10 (s, 1H, H-1), 7.03 (dd, J = 7.6, 1.2 Hz, 2H, H-2'/2"), 6.84 (dd, J = 7.9, 1.0 Hz, 2H, H-2'/2"), 6.45 (d, J = 5.0 Hz, 1H, H-9), 6.38 (d, J = 5.1 Hz, 1H, H-13), 4.93 (d, J = 5.0 Hz, 1H, H-10), 4.85 (d, J = 5.1 Hz, 1H, H-12), 1.33 (s, 9H, 2-C(C$\underline{H}_3$)$_3$), 1.31 (s, 9H, 7-C(C$\underline{H}_3$)$_3$), -3.61 (s, 3H, 13d-C$\underline{H}_3$), -4.11 (s, 3H, 13c-C$\underline{H}_3$); ^{13}C NMR (125 MHz C_6D_6) δ 204.82 (C-11), 146.51 (C-2), 145.83 (C-7), 137.38 (C-5a), 136.60 (C-3a), 134.42 (C-1'/1"), 134.13 (C-1'/1"), 132.84 (C-13f), 132.65 (C-13a), 131.46 (C-2'/2"), 131.00 (C-2'/2"), 129.30 (C-13b), 128.95 (C-13e), 128.54 (C-3'/3"), 128.42 (C-3'/3"), 127.95

[2] The assignments are based on the assumption that the proton with chemical shift 8.36 ppm is H-3.

(C4'/4"), 127.80 (C4'/4"), 124.35 (C-5), 124.00 (C-4), 121.89 (C-3), 121.74 (C-6), 118.69 (C-8), 117.94 (C-1), 84.95 (C-13), 83.77 (C-9), 63.88 (C-10), 63.79 (C-12), 35.95 (2/7-$\underline{C}(CH_3)_3$), 35.90 (2/7-$\underline{C}(CH_3)_3$), 31.74 (2/7-C($\underline{C}H_3)_3$), 31.71 (2/7-C($\underline{C}H_3)_3$), 31.43 (C-13d), 30.41 (C-13c), 16.13 (13d-$\underline{C}H_3$), 14.99 (13c-$\underline{C}H_3$);

114A and **114B:** IR (KBr) *v* 2946, 2934, 2901, 2862, 1714, 1599, 1493, 1451, 1383, 1346, 1259, 1187, 1127, 1079, 1060, 892, 866, 848, 756, 732, 704, 697, 675, 532 cm^{-1}; EI MS *m/z* 592 (M^+); HRMS calcd for $C_{43}H_{44}O_2$: 592.3341, found 592.3339.

2,7-Di-*tert*-butyl-13c,13d-dimethyl-10,12-Diphenyl-11-oxo-cycloheptatrieno[13a:13f; e]-*trans*-13c,13d-dihydropyrene 115

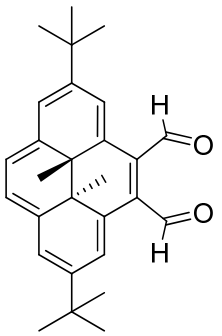


A solution of DHP di-aldehyde **116** (310 mg, 0.775 mmol), 1,3-diphenylacetone (184 mg, 0.876 mmol) in THF (30 mL) and ethanol (50 mL) was heated to reflux (oil bath 80°C). At this temperature a solution of KOH (52.4 mg, 0.934 mmol) in ethanol (10 mL) was added. A red color started to appear. After the addition, the reaction was stirred for 30 min. The oil bath was removed and the reaction was cooled. The solvents were removed under vacuum. The residue was applied to a flash column eluting with DCM/hexanes (1:1 ratio) and then DCM. Dark red flaky crystals of **115** were obtained (313 mg, 70% yield). M.p. 210-211°C.

115: ^{1}H NMR (500 MHz C_6D_6) δ 9.22 (s, 2H, H-9,13), 9.15 (s, 2H, H-1,8), 8.47 (d, J = 0.7 Hz, 2H, H-3,6), 8.33 (s, 2H, H-4,5), 7.86-7.84 (m, 4H, H-2'), 7.51-7.48 (m, 4H, H-3'), 7.42-7.39 (m, 2H, H-4'), 1.69 (s, 18H, 2,7-C(C$\underline{H}_3)_3$), -3.58 (13c/13d-C$\underline{H}_3$); ^{13}C NMR (125 MHz C_6D_6) δ 193.55 (C-11), 147.15 (C-2,7), 142.37 (C-10,12), 140.84 (C-1'), 138.89 (C-3a,5a), 135.65 (C-13b,13e), 133.04 (C-9,13), 129.12 (C-2'), 128.77 (C-3'), 127.99 (C-4'),

127.19 (C-13a,13f), 124.11 (C-4,5), 122.50 (C-3,6), 119.67 (C-1,8), 36.56 (2,7-C($\underline{C}H_3)_3$), 32.07 (2,7-$\underline{C}(CH_3)_3$), 30.97 (C-13c,13d), 15.18 (13c,13d-$\underline{C}H_3$); IR (KBr) *v* 2962, 2924, 2903, 2864, 1666, 1596, 1488, 1462, 1443, 1378, 1364, 1345, 1237, 974, 892, 871, 755, 695, 675, 640, 546 cm^{-1}; UV-vis (toluene) λ_{max} (ε_{max}, L Mol^{-1} cm^{-1}) nm, 381 (41,500), 434 (61,000), 507 (7,510), 633 (1,430), 700 (3,750); EI MS *m/z* 574 (M^+); HRMS calcd for $C_{43}H_{42}O$: 574.3236, found 574.3239.

2,7-Di-*tert*-butyl-4,5-diformyl-*trans*-10b,10c-dimethyl-10b,10c-dihydropyrene 116

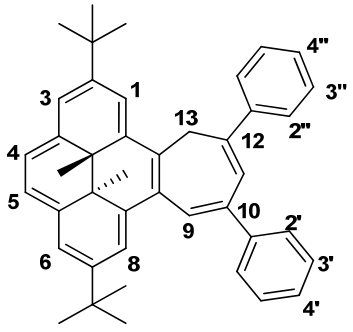


A solution of freshly made[221] dimethyldioxirane in acetone was added to a solution of DHP isofuran **98** (160 mg, 0.416 mmol) in acetone (20 mL) at room temperature until the disappearance of the purple color of **98**. The reaction mixture was then diluted with hexanes and subsequently washed with water three times. The organic layer was dried over $MgSO_4$. And the acetone was evaporated to afford the crude product **116**. The NMR data for **116** are consistent with those previously reported.[131] The yield dropped to 60% when the crude product was chromatographed on a 30 cm long column eluting with DCM. Noted that the concentration of the dimethyldioxirane in acetone varies from batch to batch, which was never close to the concentration (0.04-0.185 M) reported by Murray.[221] The concentration of dimethyldioxirane was unable to be determined with the reported methods due to the very low concentration.

The characterization for dialdehyde **116** can be found in Robinson's PHD thesis. [131]

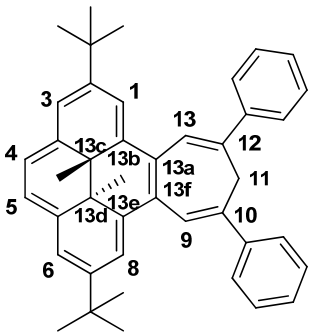
2,7-Di-*tert*-butyl-13c,13d-dimethyl-10,12-diphenyl-*trans*-13c,13d-dihydro-13,13-2*H*-cycloheptatrieno[13a:13f; e]pyrene 117
and 2,7-di-*tert*-butyl-13c,13d-dimethyl-10,12-diphenyl-*trans*-13c,13d-dihydro-11,11-2H-cycloheptatrieno[13a:13f; e]pyrene 118 and 2,7-di-tert-butyl-10,12-diphenyl-13c,13d-tetramethyl-trans-13c,13d-dihydro-13,13-2H-11-cycloheptadieno[13a:13f; e] pyrene 119

$LiAlH_4$ (1.57 g, 0.0413 mmol) was refluxed in dry ether (95 mL) for two hours. The slurry was then cooled to room temperature. Then, $AlCl_3$ (5.6 g, 0.0421 mmol) was added in small portions with the flask being cooled in an ice bath. Gas was generated during the addition. The mixture was then refluxed for two more hours. The reaction was cooled with an ice bath again. A solution of diphenyl tropone **115** (250 mg, 0.435 mmol) in dry ether (50 ml) and THF (150 mL) was added dropwise. The resulting mixture was stirred at room temperature for 12 hours. Then the reaction mixture was carefully quenched with aqueous NH_4Cl solution. The organic phase was washed with water and saturated NaCl solution, dried over $MgSO_4$ and the solvents were removed under vacuum. The residual was chromatographed on a silica gel column eluting with hexanes and DCM (2:1). The unsymmetrical triene **117** was obtained first (130 mg, 53% yield). It was recrystallized from hexanes to afford a dark brown needles. The symmetrical triene **118**, eluted next containing the unsymmetrical triene (*ca* 5%). The dienone **119** was eluted third with hexanes/DCM (1:1) (70 mg, 28% yield).



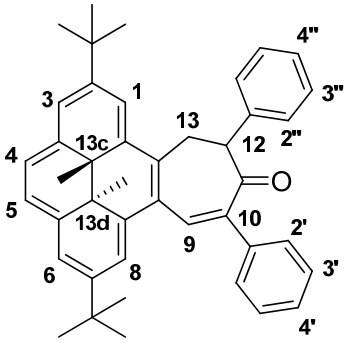
117: ^{1}H NMR (500 MHz, THF-d_6) δ 9.04 (s, 1H, H-8), 9.03 (s, 1H, H-9), 8.85 (s, 1H, H-1), 8.45 (s, 1H, H-6), 8.38 (s, 1H, H-3), 8.25 (AB, J = 7.4 Hz, 1H, H-4), 8.24 (AB, J = 7.4

Hz, 1H, H-5), 7.91 (dd, *J* = 8.3, 1.2 Hz, 2H, H-2'), 7.76 (dd, *J* = 8.2, 1.0 Hz, 2H, H-2"), 7.51 (t, *J* = 7.6 Hz, 2H, H-3'), 7.39-7.36 (m, 3H, H-3",4'), 7.30-7.27 (m, 1H, H-4"), 6.73 (s, 1H, H-11), 3.58* (s, 1H, H-13), 2.48* (s, 1H, H-13), 1.75 (s, 9H, 7-C(C$\underline{H}_3$)$_3$), 1.73 (s, 9H, 2-C(C$\underline{H}_3$)$_3$), -3.62 (s, 3H, 13d-C$\underline{H}_3$), -3.93 (s, 3H, 13c-C$\underline{H}_3$); ^{13}C NMR (125 MHz THF-d_6) δ 146.60 (C-7), 145.79 (C-2), 144.33 (C-1'), 143.59 (C-12), 142.45 (C-1"), 142.18 (C-10), 139.05 (C-5a), 137.47 (C-3a), 135.23 (C-13e), 132.42 (C-13b), 131.33* (C-13a), 129.74 (C-13f), 129.59 (C-3'), 129.53 (C-3"), 128.89 (C-9), 128.52 (C-4"), 128.44 (C-4'), 128.32 (C-2'), 128.21 (C-2"), 124.55 (C-11), 123.81 (C-4), 122.97 (C-5), 121.74 (C-3), 121.27 (C-6), 120.55 (C-1), 118.67 (C-8), 37.01 (7-$\underline{C}$(CH$_3$)$_3$), 36.81 (2-$\underline{C}$(CH$_3$)$_3$), 32.45 (7-C(C$\underline{H}_3$)$_3$), 32.25 (2-C(C$\underline{H}_3$)$_3$), 31.76 (C-13d), 31.44 (C-13c), 30.82 (C-13), 14.85 (C-13c/13d) (notes:* these signals are broad);



118: ^{1}H NMR (500 MHz C_6D_6) δ 8.11 (s), 8.08 (s), 1.64 (s, -C(C$\underline{H}_3$)$_3$), -3.25 (s, internal-C$\underline{H}_3$) (the rest of the protons overlap with those of the other isomer);

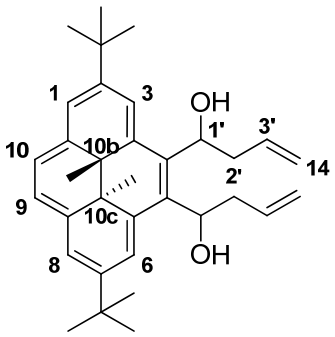
117 and **118:** IR (KBr) *v* 2961, 2923, 2860, 1595, 1492, 1458, 1444, 1361, 1344, 1262, 1235, 885, 870, 763, 693, 675, 659 cm^{-1}; UV-vis (toluene) λ_{max} (ε_{max}, L Mol^{-1} cm^{-1}) nm 362 (30,700), 413 (41,200), 510 (7,850), 673 (1,750); EI MS *m/z* 560 (M$^+$); HRMS calcd for $C_{43}H_{44}$: 560.3443, found 560.3442;



119: M.p. 156-158°C. ^{1}H NMR (500 MHz C_6D_6) δ 8.78 (s, 1H, H-8), 8.73 (s, 1H, H-9), 8.48 (s, 1H, H-6), 8.38 (s, 1H, H-3), 8.35 (s, 2H, H-4,5), 8.14 (s, 1H, H-1), 7.80 (d, J = 8.0 Hz, 2H, H-2'), 7.48 (t, J = 7.7 Hz, 2H, H-3'), 7.40 (t, J = 7.5 Hz, 1H, H-4'), 7.09-7.02 (m, 5H, H-2",3",4"), 4.58 (t, J = 5.1 Hz, 1H, H-12), 4.47-4.37 (m, 2H, H-13), 1.69 (s, 9H, 7-C(C$\underline{H}_3$)$_3$), 1.45 (s, 9H, 2-C(C$\underline{H}_3$)$_3$), -3.81 (s, 3H, 13d-C$\underline{H}_3$), -3.92 (s, 3H, 13c-C$\underline{H}_3$); ^{13}C NMR (125 MHz C_6D_6) δ 206.91 (-$\underline{C}$=O), 147.21 (C-7), 145.94 (C-2), 141.66 (C-10), 139.89 (C-1"), 138.89 (C-1'/5a), 138.86 (C-1'/5a), 137.33 (C-3a), 136.16 (C-13e), 132.87 (C-13b), 132.74 (C-9), 129.50 (C-2"), 128.91 (C-13a), 128.89 (C-3'), 128.51 (C-3"/4"), 128.09 (C-4'), 127.71 (C-2'), 127.25 (C-13f), 127.04 (C-3"/4"), 124.37 (C-4), 123.43 (C-5), 122.13 (C-3), 121.49 (C-6), 119.29 (C-1), 116.80 (C-8), 64.92 (C-12), 36.56 (7-$\underline{C}$(CH$_3$)$_3$), 36.15 (2-$\underline{C}$(CH$_3$)$_3$), 32.70 (C-13), 32.19 (7-C($\underline{C}$H$_3$)$_3$), 31.92 (2-C($\underline{C}$H$_3$)$_3$), 30.62 (C-10d), 30.15 (C-10c), 15.36 (10d-CH$_3$), 15.13 (10c-CH$_3$); IR (KBr) ν 3027, 2953, 2922, 2864, 1685, 1654, 1595, 1560, 1491, 1477, 1458, 1444, 1361, 1345, 1264, 1233, 888, 865, 737, 699, 674, 646 cm^{-1}; UV-vis (toluene) λ_{max} (ε_{max}, L Mol^{-1} cm^{-1}) nm 368 (32,600), 408 (43,800), 498 (10,600), 675 (2,700); EI MS *m/z* 576 (M^+); HRMS calcd for $C_{43}H_{44}O$: 576.3392, found 576.3394; .

6.4 Experimental for DHP-fused cyclooctatetraene systems

4,5-*Bis*-(1'-hydoxy-3'-butenyl)-2,7-di-*tert*-butyl-10b,10c-dimethyl-*trans*-10b,10c-dihydropyrene 123



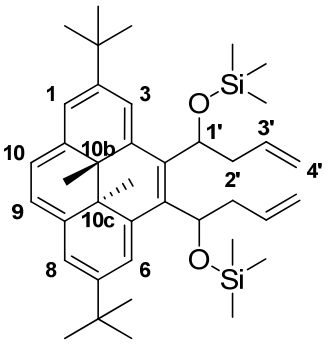
Allyl magnesium bromide was generated from allyl bromide (0.50 mL, 5.8 mmol) and magnesium (0.14 g, 5.8 mmol) in ether (12 mL). The reaction was refluxed for 30 min and then cooled to room temperature. A solution of DHP aldehyde **116** (230 mg, 0.574 mmol) in THF (13 mL) was then added dropwise with stirring. The reaction was then stirred for three hours before it was quenched by addition of ice water. The organic layer was separated and washed with water and brine. Solvents were removed to afford a green oil **123** (320 mg, quantitative). The NMR spectra were consistent with the presence of two diastereomers in a *ca.* 3:2 ratio, which were used directly in the next step to prepare **124**.

123: ^{1}H NMR (500 MHz, $CDCl_3$) δ (four singlets with total integral 2H) 9.32, 9.17, 9.13, 9.06, (five peaks with total integral of 4H between 8.40 and 8.24 ppm) 8.39 (s), 8.36 (d, J = 1.2 Hz), 8.32 (s), 8.32 (s), 8.25 (s), 6.54-6.38 (m, 2H, H-1'), 6.10-5.93 (m, 2H, H-3'), 5.29-4.89 (m, 4H, H-4'), 3.43-2.75 (m, 4H, H-2'), (four singlets with total integral 18H) 1.66, 1.66, 1.65, 1.65, (four singlets with total integral 6H for the internal methyl protons) -3.74, -3.79, -3.81, -3.82; ^{13}C NMR (125 MHz $CDCl_3$) δ 145.62, 145.36, 145.25, 138.23, 137.96, 136.27, 136.23, 136.10, 135.95, 133.47, 132.97, 132.57, 123.91, 123.77, 123.09, 121.12, 121.02, 120.92, 120.09, 118.02, 117.86, 117.80, 117.73, 72.20, 71.80, 71.72, 70.47, 44.34, 44.30, 43.49, 42.96, 36.38, 32.10, 32.07, 32.03, 29.93, 15.28, 14.95, 14.49; IR (KBr) ν 3377, 3074, 3.43, 3005, 2963, 2923, 2865, 1640, 1593, 1479, 1462, 1442,

1391, 1375, 1361, 1343, 1268, 1235, 1198, 1127, 1027, 992, 939, 913, 882, 859, 795, 681, 651 cm^{-1}; EI MS *m/z* 484 (M^+); HRMS calcd for $C_{34}H_{44}O_2$: 484.3341, found 484.3338.

4,5-*Bis*-(1'-trimethylsilyloxy-3'-butenyl)-2,7-di-*tert*-butyl-10b,10c-dimethyl-*trans*-10b,10c-dihydropyrene 124

This procedure was adapted from Corey.[238] Mixed isomers of diol **123** (0.61 g, 1.3 mmol) were dissolved in DMF (40 mL). Imidazole (1.6 g, 32 mmol) and then TMSCl (1.5 mL, 12 mmol) were added. The reaction was stirred for 5 hours at room temperature. Then water was added and the mixture was extracted with ethyl acetate three times. The organic layer was washed with aqueous sodium bicarbonate solution. The solution was then dried and evaporated to affordmixed isomers of **124** as a green solid (quantitative), used directly in the next step.

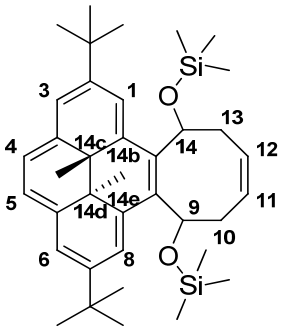


124: ^{1}H NMR (500 MHz, $CDCl_3$) δ (18 singlets with integral of 6H in the aromatic proton region)10.03, 10.02, 9.91, 9.88, 9.76, 9.73 8.80, 8.73, 8.71, 8.42, 8.38, 8.37, 8.35, 8.32, 8.30, 8.28, 8.25, 8.24, 6.74-5.61 (m, 4H, H-1',3'), 5.34-4.89 (m, 4H, H-4'), 3.76-2.30 (m, 4H, H-2'), (3 peaks for the *tert*-butyl protons, integral of 18) 1.661, 1.657, 1.65, (12 peaks for the methyl protons on TMS with integral 18H) 0.19, 0.18, 0.14, 0.13, 0.11, 0.08, 0.03, 0.00, -0.01, -0.06, -0.07, -0.12, (8 peaks for internal methyl protons with integral 6H) -3.77, -3.86, -3.89, -3.90, -3.91, -3.93, -3.95, -4.00; IR (film) *v* 3076, 2962, 2866, 1640, 1594, 1479, 1463, 1444, 1391, 1361, 1344, 1250, 1126, 1077, 994, 951, 913, 882, 841, 748, 737, 684, 648 cm^{-1}; UV-vis (toluene) λ_{max} (ε_{max}, L Mol^{-1} cm^{-1}) nm 353 (87,700), 390

(49,400), 486 (8,390), 655 (1,100); EI MS *m/z* 628 (M^+); HRMS calcd for $C_{40}H_{60}O_2Si_2$: 628.4132, found 628.4122.

2,7-Di-*tert*-butyl-9,14-*bis*-trimethylsilyloxy-*trans*-14c,14d-dimethyl-9,10,13,14,14c,14d-hexahydrocycloocta[14a:14f; e]pyrene 125

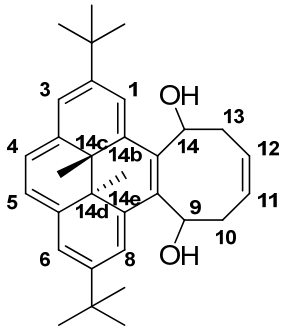
DHP dialkene **124** (100 mg, 0.16 mmol) and Grubbs first generation catalyst (19 mg, 0.023 mmol) were mixed in a schlenk tube. Then benzene (450 mL) was added through a syringe under argon. The mixture was warmed to 55 for 15 hours. The reaction was concentrated to about 50 mL. The resulting solution was filtered through a flash column and rinsed with hexanes and DCM (1:1) to remove the catalyst. The solvents were then removed and the residual was chromatographed on a silica gel column eluting with hexanes and DCM (10:1) to afford a green solid **125** (70 mg, 73% yield).



125: ^{1}H NMR (500 MHz, $CDCl_3$) δ 9.95 (d, J = 1.2 Hz, 1H), 8.82 (s, 1H), 8.42, 8.34 (s, 1H), 8.33 (s, 1H), 7.18-6.55 (m, 2H), 5.33-5.05 (m , 2H), 3.46-2.80 (m, 4H), three singlets 1.69, 1.68, 1.67 (s, 18H), three singlets 0.24, 0.11, 0.00 (s, 18H), four singlets -3.65 (v. small), -3.95 (s, 6H), -4.01 (v. small) -4.11 (s, 6H); ^{13}C NMR (125 MHz $CDCl_3$) δ 144.91, 137.56, 132.96, 132.41, 132.20, 131.12, 127.22, 123.18, 122.93, 122.58, 120.59, 120.30, 115.50, 72.47, 68.31, 40.28, 39.79, 36.48, 36.39, 32.34, 32.27, 32.20, 30.36, 29.74, 14.35, 1.08, 0.64, 0.22; IR (KBr) ν 3027, 2958, 2901, 1591, 1477, 1462, 1441, 1390, 1361, 1261, 1249, 1072, 1039, 1025, 1002, 879, 841, 756, 717, 682, 657, 644 cm^{-1}; EI MS *m/z* 600 (M^+); HRMS calcd for $C_{38}H_{56}O_2Si_2$: 600.3819, found 600.3817.

2,7-di-*tert*-butyl-9,14-dihydoxy-*trans*-14c,14d-dimethyl-9,10,13,14,14c,14d - hexahydrocycloocta[14a:14f; e]pyrene 126

The TMS protected diol **125** (300 mg, 0.500 mmol) was dissolved in THF and methanol (1:1 ratio, 30 mL). Anhydrous potassium carbonate (780 mg, 5.60 mmol) was added. The reaction was stirred at room temperature for 8 hours. The solvents were then removed to afford quantitatively green product **126** (280 mg).



126: ^{1}H NMR (500 MHz, $CDCl_3$)[*3] δ 8.45 (s, 2H, H-3,6), 8.35 (AB, J = 7.6 Hz, 1H, H-4), 8.34 (AB, J = 7.6 Hz, 1H, H-5), 8.30 (d, J = 1.1 Hz, 1H, H-1), 8.29 (d, J = 1.0 Hz, 1H, H-8), 6.47-6.45 (m, 2H, H-9/14), 5.22-5.14 (m, 2H, H-11,12), 3.31-3.25 (m, 2H, H-10,13), 3.20-3.15 (m, 1H, H-13), 2.95-2.90 (m, 1H, H-10), 1.66 (s, 9H, 2/7-C($C\underline{H}_3$)$_3$), 1.66 (s, 9H, 2/7-C($C\underline{H}_3$)$_3$), -3.96 (s, 3H, 14d-$C\underline{H}_3$), -3.99 (s, 3H, 14c-$C\underline{H}_3$); ^{13}C NMR (125 MHz, $CDCl_3$) δ 145.40 (C-2/7), 145.36 (C-2/7), 136.80 (C-3a), 136.70 (C-5a), 134.64 (C-14a/14f), 134.56 (C-14a/14f), 127.87 (C-14e), 127.74 (C-14b), 125.94 (C-11,12), 123.13 (C-4), 123.01 (C-5), 120.76 (C-3/6), 120.48 (C-3/6), 118.09 (C-1), 116.95 (C-8), 81.98 (C-9/14), 81.61 (C-9/14), 40.72 (C-10), 39.32 (C-13), 36.23 (2,7-$\underline{C}$(CH_3)$_3$), 32.21 (2,7-C($\underline{C}H_3$)$_3$), 31.49 (C-14c), 30.10 (C-14d), 14.86 (14c/14d-$\underline{C}H_3$), 14.63 (14c/14d-$\underline{C}H_3$);

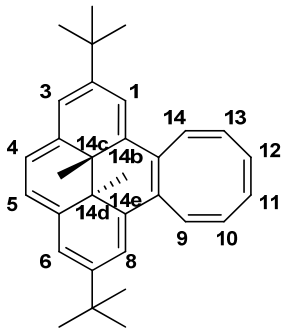
[*3] The assignments are based on the assumption that the proton with chemical shift 8.30 ppm is H-1.

(9Z,11Z,13Z)-2,7-di-*tert*-butyl-*trans*-14c,14d-dimethyl-14c,14d-dihydrocycloocta[e]pyrene 121; Cyclooctatetraene 121

Method a): The cyclized diol **126** (115 mg, 0.252 mmol) was dissolved in benzene (6 mL) and then *p*-toluenesulfonic acid (30 mg, 0.17 mmol) was added in one portion. The resulting mixture was stirring for 1 hour at room temperature under argon. It was washed with water to remove acid. The organic layer was then dried over $MgSO_4$. The solvent was removed and the residue was chromatographed on silica gel. The green COT product **121** was eluted first with hexanes (7.5 mg, 7.1% yield). The green O-bridged alkene product **127** was eluted last with hexanes and DCM (1:1) (81 mg, 73% yield).

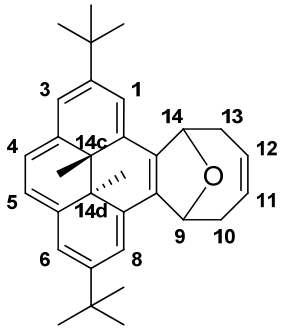
Method b): Freshly distilled 4-toluenesulfonyl chloride (25 mg, 0.13 mmol) (or methylsulfonyl chloride with triethylamine in DCM) was added to a solution of the alcohol **126** (30 mg, 0.066 mmol) in dry pyridine (2 mL). The reaction mixture was heated to 110°C for one and half hours. The solvents and excess reactant were removed and the residue was chromatographed to afford the green cyclic ether **127** (20 mg, 70% yield) with no observed formation of the COT **121**.

Method c): Potassium *tert*-butoxide (95%, 26 mg, 0.23 mmol) was added to a solution of the diol **126** (30 mg, 0.066 mmol) in THF (3mL) at 0°C. Intense color appeared right away. The mixture was kept at 0°C for 2 hours and the NMR showed only the cyclic ether **127**.



121: m.p 155-156°C. ^{1}H NMR (500 MHz, $CDCl_3$) δ 8.45 (s, 2H, H-1,8), 8.34 (s, 2H, H-3,6), 8.22 (s, 2H, H-4,5), 7.65 (s, 2H, H-9,14), 6.48 (s, 2H, H-10,13), 6.05 (s, 2H, H-

11,12), 1.64 (s, 18H, 2,7-C(C<u>H</u>$_3$)$_3$), -3.70 (s, 6H, 14c,14d-C<u>H</u>$_3$); ^{13}C NMR (125 MHz, C_6D_6)[4] δ 145.50 (C-2,7), 137.58 (C-3a,5a), 134.47 (C-14b,14e), 133, 132, 131.04 (C-10,13), 122.56 (C-4,5), 120.79 (C-3,6), 118.54 (C-1,8), 36.28 (2,7-<u>C</u>(CH$_3$)$_3$), 32.19 (2,7-C(<u>C</u>H$_3$)$_3$), 30.25 (C-14c,14d), 15.3 (14c,14d-<u>C</u>H$_3$); IR (film) ν 2963, 1593, 1460, 1361, 1342, 1258, 1236, 909, 877, 826, 792, 734, 659 cm^{-1}; UV-vis (toluene) λ_{max} (ε_{max}, L Mol^{-1} cm^{-1}) nm 309 (10,800), 359 (24,600), 395 (26,700), 495 (8,900), 664 (1,400); EI MS *m/z* 420 (M^+); HRMS calcd for $C_{32}H_{36}$: 420.2817, found: 420.2819;.



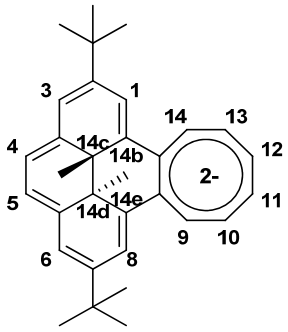
Cyclic ether 127: m.p. 160-161°C. ^{1}H NMR (500 MHz, $CDCl_3$) δ 8.45 (s, 2H, H-3,6), 8.35 and 8.34 (AB, J = 7.6 Hz, 2H, H-4/5), 8.30 (d, J = 0.6 Hz, 1H, H-1/8), 8.29 (s, 1H, H-1/8), 6.46-6.45 (m, 2H, H-9,14), 5.21-5.14 (m, 2H, H-11,12), 3.30-3.26 (m, 2H, H-10/13), 3.20-3.15 (m, 1H, H-10/13), 2.94-2.90 (m, 1H, H-10/13), 1.66 (s, 9H, 2/7-C(C<u>H</u>$_3$)$_3$), 1.65 (s, 9H, 2/7-C(C<u>H</u>$_3$)$_3$), -3.96 (s, 3H, 13c/13d-C<u>H</u>$_3$), -3.99 (s, 3H, 13c/13d-C<u>H</u>$_3$); ^{13}C NMR (125 MHz, $CDCl_3$) δ 145.40 (C-2/7), 145.36 (C-2/7), 136.79 (C-3a/5a), 136.69 (C-3a/5a), 134.62 (C-14a/14f), 134.54 (C-14a/14f), 127.85 (C-14b/14e), 127.73 (C-14b/14e), 125.94 (C-11,12), 123.13 (C-4/5), 123.01 (C-4/5), 120.76 (C-3/6), 120.49 (C-3/6), 118.09 (C-1/8), 116.95 (C-1/8), 81.98 (C-9/14), 81.62 (C-9/14), 40.71 (C-10/13), 39.32 (C-10/13), 36.24 (2-<u>C</u>(CH$_3$)$_3$), 32.21 (2/7-C(<u>C</u>H$_3$)$_3$), 31.48 (C-14c/14d), 30.10 (C-14c/14d), 14.88 (14c/14d-<u>C</u>H$_3$), 14.64 (14c/14d-<u>C</u>H$_3$); IR (KBr) ν 2961, 2921, 2902, 2877, 1600, 1460, 1360, 1346, 1235, 1200, 1098, 1044, 1019, 888, 868, 852, 673, 645 cm^{-1}; UV-vis (toluene) λ_{max} (ε_{max}, L Mol^{-1} cm^{-1}) nm 349 (98,200), 387 (48,000), 485

[4] Peaks at δ133, 132 and 15.3 are broad. Signals for C14a and C14f are missing in the spectrum. No short range correlations were found for the C-H on C9, C11, C12 and C14 in the HSQC spectrum.

(9,280), 651 (939); EI MS *m/z* 438 (M^+); HRMS calcd for $C_{32}H_{38}O$: 438.2923, found: 438.2919.

DHP[e]cyclooctatetraene (COT) dianion 20

COT **121** (~5.0 mg, 0.011 mmol) in THF-d^8 (0.6 mL) was placed in a sealed NMR tube, flushed with argon. A piece of potassium (~100 mg, 2.56 mmol) was adhered to the upper part of the NMR tube. When the potassium was immersed in the THF solution by upending the tube, the green color turned immediately red, indicating the formation of the dianion **20·2K**$^+$. ^{1}H NMR spectrum was examined immediately. Further reaction led to the loss of NMR signals.

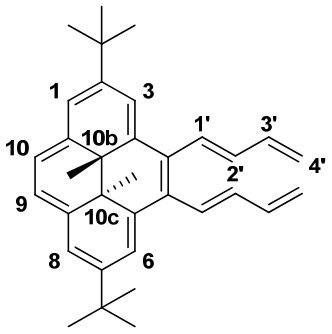


20·2K$^+$: ^{1}H NMR (500 MHz, THF-d_6) δ 7.37 (d, *J* = 11.9 Hz, 2H), 7.35, 7.18 (s, 2H, H-1,8), 6.70 (s, 2H, H-3,6), 6.64 (s, 2H, H-4,5), 6.44-6.40 (m, 2H), 6.11 (dd, *J* = 7.7, 3.1 Hz, 2H), 1.47 (s, 9H, 2,7-C(C$\underline{H}_3$)$_3$), -1.38 (s, 6H, 14c,14d-C$\underline{H}_3$). No other characterization data are available due to decomposition of the sample.

4,5-Di-((E)-buta-1',3'-dienyl)-2,7-di-*tert*-butyl-10b,10c-dimethyl-*trans*-10b,10c-dihydropyrene 130
and 9,11-diallyl-2,7-di-*tert*-butyl- *trans*-11c,11d-dimethyl- 9,11,11b,11c -tetrahydropyren[e]furan 132

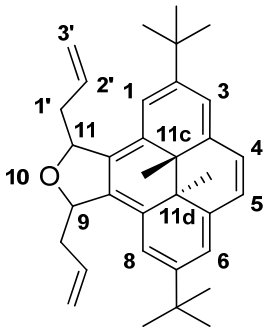
Method a): The procedure was adapted from Panek.[252] Dimethyl sulfoxide (0.17 mL, 2.4 mmol) was added dropwise to a solution of oxalyl chloride (0.10 mL, 1.2 mmol) in DCM (10 mL) at -78 °C. The reaction was stirred for 15 mins before the addition of the diol **123** (100 mg, 0.206 mmol) in DCM (15 mL) by syringe. The reaction was then stirred for 30 mins before triethylamine (0.70 mL, 5.0 mmol) was added dropwise. It was allowed to warm to room temperature for 4 hours. The reaction was then quenched by addition of water (10 mL), and was extracted with DCM three times. The organic layers were combined, washed with water three times and brine. They were dried over $MgSO_4$ and concentrated. The residual was chromatographed on silica gel. The *bis*-dienyl DHP **130** (12 mg, 13% yield) was eluted first with hexanes and DCM (10:1) and then the green cyclic ether **132** (75 mg, 80 % yield) was eluted second.

Method b): The diol **123** (55 mg, 0.11 mmol) was dissolved in DCM (5 mL) at 0 °C. Imidazole (24 mg, 0.35 mmol) and then triphenylphosphine (88 mg, 0.33 mmol) and iodine (90 mg, 0.35 mmol) were added to the cold solution. The reaction was allowed to warm to room temperature for 12 hours. The *bis*-dienyl DHP **130** (15 mg, 30% yield) was eluted first on a silica gel column with hexane and DCM (10:1) as eluants.



130: ^{1}H NMR (500 MHz $CDCl_3$) δ 8.82 (d, J = 0.9 Hz, 2H, H-3,6), 8.40 (s, J = 0.9 Hz, 2H, H-1,8), 8.29 (s, 2H, H-9,10), 7.50 (d, J = 15.5 Hz, 2H, H-1'), 6.87-6.72 (m, 4H, H-2',3'), 5.37 (dd, J = 16.1, 1.5 Hz, 2H, H-4'), 5.25 (dd, J = 9.4, 1.5 Hz, 2H, H-4'), 1.64 (s, 18H, 2,7-C(C$\underline{H}_3$)$_3$), -3.70 (s, 6H, 10b,10c-C$\underline{H}_3$); ^{13}C NMR (125 MHz C_6D_6) δ 145.99 (C-2,7), 138.08 (C-3'), 137.74 (C-3a,5a), 137.35 (C-2'), 133.86 (C-10a,10d), 132.73 (C-1'), 129.78 (C-4,5), 123.01 (C-9,10), 121.20 (C-1,8), 120.03 (C-3,6), 116.97 (C-4'), 36.26

(2,7-C(CH$_3$)$_3$), 32.04 (2,7-C(CH$_3$)$_3$), 30.39 (C-10b,10c), 15.33 (10b,10c-CH$_3$); This was used directly in the RCM reaction and no further characterization was carried out.



The diagram shows the numbering only. Two groups of stereo-isomers were present (from the NMR spectra) due to the *cis* and *trans* allyl groups. They were not separable, but were distinguishable by NMR spectroscopy.

Isomer 132-I: ^{1}H NMR (500 MHz $CDCl_3$) δ 8.47 (s, 2H, H-3,6), 8.44 (s, 2H, H-1,8), 8.38 (s, 2H, H-4,5), 6.42 (t, J = 4.0 Hz, 2H, H-9,11), 5.81-5.70 (m, 2H, H-2'), 4.95 (dd, J = 17.1, 1.7 Hz, 2H, H-3'), 4.77 (dd, J = 10.4, 1.8 Hz, 2H, H-3'), 3.10-2.90 (m, 4H, H-1'), 1.67 (s, 18H, 2,7-C(CH$_3$)$_3$), -3.74 (s, 6H, 11c,11d-CH$_3$); ^{13}C NMR (125 MHz C_6D_6) δ 145.51 (C-2,7), 136.91 (C-3a,5a), 134.70/134.41 (C-2'), 133.51 (C-11a,11f), 128.75 (C-11b,11e), 123.40 (C-4,5), 120.64 (C-3,6), 117.61 (C-1,8), 117.56 (C-3'), 84.11 (C-9,11), 43.10 (C-1'), 36.30 (2/7-C(CH$_3$)$_3$), 36.17 (7/2-C(CH$_3$)$_3$), 32.21 (2,7-C(CH$_3$)$_3$), 30.64 (C-11c,11d), 15.50 (11c,11d-CH$_3$);

Isomer 132-II: ^{1}H NMR (500 MHz $CDCl_3$) δ 8.35 (s, 2H, H-3,6), 8.30 (s, 2H, H-1,8), 8.21 (s, 2H, H-4,5), 6.39 (t, J = 3.3 Hz, 2H, H-9,11), 5.81-5.70 (m, 2H, H-2'), 5.02 (dd, J = 17.1, 1.7 Hz, 2H, H-3'), 4.81 (dd, J = 10.4, 1.9 Hz, 2H, H-3'), 3.20-3.04 (m, 4H, H-1'), 1.64 (s, 18H, 2,7-C(CH$_3$)$_3$), -3.97 (s, 6H, 11c,11d-CH$_3$); ^{13}C NMR (125 MHz C_6D_6) δ 144.95 (C-2,7), 137.06 (C-3a,5a), 134.70/134.41 (C-2'), 133.89 (C-11a,11f), 128.16 (C-11b,11e), 122.57 (C-4,5), 120.71 (C-3,6), 118.63 (C-1,8), 117.43 (C-3'), 83.99 (C-9,11), 32.06 (2,7-C(CH$_3$)$_3$), 41.36 (C-1'), 31.37 (C-11c,11d), 14.60 (11c,11d-CH$_3$);

Chapter 7. References

[1] a) Pardo, R.; Zayat, M. and Levy, D. *Chem. Soc. Rev.* **2011**, *40*, 672-687; b) Feringa, B. L. *Molecular Switches*, Wiley-VCH, Weinheim, **2001**; c) Willner, I. and Willner, B. *J. Mater. Chem.* **1998**, *8*, 2543-2556.

[2] Balzani, V.; Credi, A.; Raymo, F. M. and Stoddart, J. F. *Angew. Chem. Int. Ed.* **2000**, *39*, 3348-3391.

[3] Irie, M. *Chem. Rev.* **2000**, *100*, 1685-1716.

[4] Mortimer, R. J. *Electrochim. Acta* **1999**, *44*, 2971-2981.

[5] Bouas-Laurent, H. and Dürr, H. *Pure Appl. Chem.* **2001**, *73*, 639-665.

[6] Balzani, V.; Credi, A. and Venturi, M. *Chem. Soc. Rev.* **2009**, *38*, 1542-1550.

[7] Delaire, J. A. and Nakatani, K. *Chem. Rev.* **2000**, *100*, 1817-1846.

[8] Kawata, S. and Kawata, Y. *Chem. Rev.* **2000**, *100*, 1777-1788.

[9] Monk, P. M. S.; Mortimer, R. J. and Rosseinsky, D. R. *Electrochromism and electrochromic devices*, Cambridge University Press, Cambridge; New York, **2007**.

[10] Gallardo, I.; Guirado, G.; Prats, G. and Takeshita, M. *PCCP* **2009**, *11*, 1502-1507.

[11] Hirshberg, Y. *Compt. Rend. Acad. Sci.* **1950**, *231*, 903-904.

[12] Dürr, H. and Bouas-Laurent, H. *Photochromism :molecules and systems*, Rev. ed., Elsevier, Amsterdam ;Boston, **2003**.

[13] Yun, C.; You, J.; Kim, J.; Huh, J. and Kim, E. *J. Photochem. Photobiol., C* **2009**, *10*, 111-129.

[14] Bertarelli, C.; Bianco, A.; Castagna, R. and Pariani, G. *J. Photochem. Photobiol., C* **2011**, doi:10.1016/j.jphotochemrev.2011.1005.1003.

[15] Bonhommeau, S.; Guillon, T.; Lawson Daku, L. M.; Demont, P.; Sanchez Costa, J.; Létard, J.-F.; Molnár, G. and Bousseksou, A. *Angew. Chem.* **2006**, *118*, 1655-1659.

[16] Hirshberg, Y. and Fischer, E. *J. Chem. Phys.* **1955**, *23*, 1723.

[17] Mortimer, R. J.; Dyer, A. L. and Reynolds, J. R. *Displays* **2006**, *27*, 2-18.

[18] Rosseinsky, D. R. and Mortimer, R. J. *Adv. Mater.* **2001**, *13*, 783-793.

[19] Raymo, F. M. and Tomasulo, M. *Chem. Soc. Rev.* **2005**, *34*, 327-336.

[20] Momicchioli, F.; Corradini, G. R.; Bruni, M. C. and Baraldi, I. *J. Chem. Soc., Faraday Trans. 2* **1975**, *71*, 215-224.

[21] Zimmerman, G.; Chow, L.-Y. and Paik, U.-J. *J. Am. Chem. Soc.* **1958**, *80*, 3528-3531.

[22] a) Malkin, S. and Fischer, E. *J. Phys. Chem.,* **1962**, *66*, 2482-2486; b) Robin, M. B. and Simpson, W. T. *J. Chem. Phys.* **1962**, *36*, 580.

[23] Renner, C. and Moroder, L. *ChemBioChem* **2006**, *7*, 868-878.

[24] a) Ichimura, K.; Oh, S.-K. and Nakagawa, M. *Science* **2000**, *288*, 1624-1626; b) Yu, Y.; Nakano, M. and Ikeda, T. *Nature* **2003**, *425*, 145-145.

[25] Uchida, K.; Yamaguchi, S.; Yamada, H.; Akazawa, M.; Katayama, T.; Ishibashi, Y. and Miyasaka, H. *Chem. Commun.* **2009**, 4420-4422.

[26] a) Berkovic, G.; Krongauz, V. and Weiss, V. *Chem. Rev.* **2000**, *100*, 1741-1754; b) Lokshin, V. A.; Samat, A. and Metelitsa, A. V. *Russ. Chem. Rev.* **2002**, *71*, 893-916.

[27] Bercovici, T. and Fischer, E. *J. Am. Chem. Soc.* **1964**, *86*, 5687-5688.

[28] Flannery, J. B. *J. Am. Chem. Soc.* **1968**, *90*, 5660-5671.

[29] Zhi, J. F.; Baba, R.; Hashimoto, K. and Fujishima, A. *J. Photochem. Photobiol., A* **1995**, *92*, 91-97.

[30] Waldeck, D. H. *Chem. Rev.* **1991**, *91*, 415-436.

[31] Irie, M. and Mohri, M. *J. Org. Chem.* **1988**, *53*, 803-808.

[32] Yokoyama, Y. *Chem. Rev.* **2000**, *100*, 1717-1740.

[33] Stobbe, H. *Ber. Dtsch. Chem. Ges.* **1905**, *38*, 3673-3682.

[34] Santiago, A. and Becker, R. S. *J. Am. Chem. Soc.* **1968**, *90*, 3654-3658.

[35] Matsuda, K. and Irie, M. *J. Photochem. Photobiol., C* **2004**, *5*, 169-182.

[36] Blattmann, H.-R.; Meuche, D.; Heilbronner, E.; Molyneux, R. J. and Boekelheide, V. *J. Am. Chem. Soc.* **1965**, *87*, 130-131.

[37] Ayub, K.; Li, R.; Bohne, C.; Williams, R. V. and Mitchell, R. H. *J. Am. Chem. Soc.* **2011**, *133*, 4040–4045.

[38] Patel, P. D. and Masunov, A. E. *J. Phys. Chem. C* **2011**, *115*, 10292-10297.

[39] Sheepwash, M. A. L.; Mitchell, R. H. and Bohne, C. *J. Am. Chem. Soc.* **2002**, *124*, 4693-4700.

[40] Sheepwash, M. A. L.; Ward, T. R.; Wang, Y.; Bandyopadhyay, S.; Mitchell, R. H. and Bohne, C. *Photochem. Photobiol. Sci.* **2003**, *2*, 104-112.

[41] Mitchell, R. H. and Ward, T. R. *Tetrahedron* **2001**, *57*, 3689-3695.

[42] a) Adamo, V. and Belser, P. *Chimia* **2003**, *57*, 169-172; b) Tanaka, Y.; Inagaki, A. and Akita, M. *Chem. Commun.* **2007**, 1169-1171; c) Kume, S. and Nishihara, H. *Dalton Trans.* **2008**, 3260-3271; d) Zhong, Y.-W.; Vila, N.; Henderson, J. C. and Abruna, H. D. *Inorg. Chem.* **2009**, *48*, 991-999.

[43] Akita, M. *Organometallics* **2011**, *30*, 43-51.

[44] Guerchais, V. and Le, B. H. *Top. Organomet. Chem.* **2010**, *28*, 171-225.

[45] Jukes, R. T. F.; Adamo, V.; Hartl, F.; Belser, P. and De, C. L. *Inorg. Chem.* **2004**, *43*, 2779-2792.

[46] Jukes, R. T. F.; Adamo, V.; Hartl, F.; Belser, P. and De, C. L. *Coord. Chem. Rev.* **2005**, *249*, 1327-1335.

[47] a) Kurihara, M.; Hirooka, A.; Kume, S.; Sugimoto, M. and Nishihara, H. *J. Am. Chem. Soc.* **2002**, *124*, 8800-8801; b) Sakamoto, A.; Hirooka, A.; Namiki, K.; Kurihara, M.; Murata, M.; Sugimoto, M. and Nishihara, H. *Inorg. Chem.* **2005**, *44*, 7547-7558.

[48] Nagashima, S.; Murata, M. and Nishihara, H. *Angew. Chem., Int. Ed.* **2006**, *45*, 4298-4301.

[49] Bandyopadhyay, S. Ph. D. thesis, Univeristy of Victoria, Victoria, BC, Canada, **2004**.

[50] Muratsugu, S.; Kume, S. and Nishihara, H. *J. Am. Chem. Soc.* **2008**, *130*, 7204-7205.

[51] Sarytcheva, O. V. M. Sc. thesis, Univeristy of Victoria, Victoria, BC, Canada, **2010**.

[52] Zhang, R.; Fan, W.; Twamley, B.; Berg, D. J. and Mitchell, R. H. *Organometallics* **2007**, *26*, 1888-1894.

[53] Mitchell, R. H.; Chen, Y. S.; Khalifa, N. and Zhou, P. Z. *J. Am. Chem. Soc.* **1998**, *120*, 1785-1794.

[54] Mitchell, R. H.; Brkic, Z.; Sauro, V. A. and Berg, D. J. *J. Am. Chem. Soc.* **2003**, *125*, 7581-7585.

[55] Mitchell, R. H.; Brkic, Z.; Berg, D. J. and Barclay, T. M. *J. Am. Chem. Soc.* **2002**, *124*, 11983-11988.

[56] a) Mitchell, R. H.; Fan, W.; Lau, D. Y. K. and Berg, D. J. *J. Org. Chem.* **2004**, *69*, 549-554; b) Fan, W.; Berg, D. J.; Mitchell, R. H. and Barclay, T. M. *Organometallics* **2007**, *26*, 4562-4567.

[57] Garratt, P. J. *Aromaticity*, McGraw-Hill book company (UK) Ltd., Maidenhead, England, **1971**.

[58] Fowler, P. W.; Lillington, M. and Olson, L. P. *Pure Appl. Chem.* **2007**, *79*, 969-979.

[59] Randić, M. *Chem. Rev.* **2003**, *103*, 3449-3605.

[60] Breslow, R. *J. Am. Chem. Soc.* **1957**, *79*, 5318-5318.

[61] Watts, L.; Fitzpatrick, J. D. and Pettit, R. *J. Am. Chem. Soc.* **1965**, *87*, 3253-3254.

[62] Kealy, T. J. and Pauson, P. L. *Nature* **1951**, *168*, 1039-1040.

[63] Wilkinson, G.; Rosenblum, M.; Whiting, M. C. and Woodward, R. B. *J. Am. Chem. Soc.* **1952**, *74*, 2125-2126.

[64] Doering, W. V. E. and Knox, L. *J. Am. Chem. Soc.* **1954**, *76*, 3203-3206.

[65] Keller, C. E. and Pettit, R. *J. Am. Chem. Soc.* **1966**, *88*, 606-607.

[66] Childs, R. F.; Brown, M. A.; Anet, F. A. L. and Winstein, S. *J. Amer. Chem. Soc.* **1972**, *94*, 2175-2183.

[67] Winstein, S. *J. Am. Chem. Soc.* **1959**, *81*, 6524-6525.

[68] a) Yoneda, S.; Yoshida, Z. and Winstein, S. *Tetrahedron* **1972**, *28*, 2395-2401; b) Schleyer, P. v. R.; Watts, W. E.; Fort, R. C.; Comisarow, M. B. and Olah, G. A. *J. Am. Chem. Soc.* **1964**, *86*, 5679-5680.

[69] Cyrański, M. K. *Chem. Rev.* **2005**, *105*, 3773-3811.

[70] Pauling, L. and Wheland, G. W. *J. Chem. Phys.* **1933**, *1*, 362-374.

[71] a) Mo, Y.; Wu, W. and Zhang, Q. *J. Phys. Chem.* **1994**, *98*, 10048-10053; b) Norbeck, J. M. and Gallup, G. A. *J. Am. Chem. Soc.* **1974**, *96*, 3386-3393; c) Tantardini, G. F.; Raimondi, M. and Simonetta, M. *J. Am. Chem. Soc.* **1977**, *99*, 2913-2918.

[72] Macintyre, W. M.; Robertson, J. M. and Zahrobsky, R. F. *Proc. R. Soc. Lond., A* **1966**, *289*, 161-170.

[73] a) Hanson, A. W. *Acta Crystallogr.* **1965**, *18*, 599-604; b) Mitchell, R. H.; Iyer, V. S.; Khalifa, N.; Mahadevan, R.; Venugopalan, S.; Weerawarna, S. A. and Zhou, P. Z. *J. Am. Chem. Soc.* **1995**, *117*, 1514-1532.

[74] a) Spitler, E. L.; Johnson, C. A. and Haley, M. M. *Chem. Rev.* **2006**, *106*, 5344-5386; b) Jug, K. and Fasold, E. *J. Am. Chem. Soc.* **1987**, *109*, 2263-2265.

[75] Cerfontain, H.; KoebergTelder, A.; Bakker, B. H.; Mitchell, R. H. and Tashiro, M. *Liebigs Ann.-Recl.* **1997**, 873-878.

[76] a) Mitchell, R. H.; Zhang, R.; Fan, W. and Berg, D. J. *J. Am. Chem. Soc.* **2005**, *127*, 16251-16254; b) Williams, R. V.; Armantrout, J. R.; Twamley, B.; Mitchell, R. H.; Ward, T. R. and Bandyopadhyay, S. *J. Am. Chem. Soc.* **2002**, *124*, 13495-13505; c) Mitchell, R. H. *Chem. Rev.* **2001**, *101*, 1301-1315.

[77] Mitchell, R. H.; Venugopalan, S.; Zhou, P. Z. and Dingle, T. W. *Tetrahedron Lett.* **1990**, *31*, 5281-5284.

[78] Mitchell, R. H.; Zhang, R.; Berg, D. J.; Twamley, B. and Williams, R. V. *J. Am. Chem. Soc.* **2009**, *131*, 189-199.

[79] Jones, S. C.; Coropceanu, V.; Barlow, S.; Kinnibrugh, T.; Timofeeva, T.; Brédas, J.-L. and Marder, S. R. *J. Am. Chem. Soc.* **2004**, *126*, 11782-11783.

[80] Paul, F. and Lapinte, C. *Coord. Chem. Rev.* **1998**, *178-180*, 431-509.

[81] Zheng, Q.; Hampel, F. and Gladysz, J. A. *Organometallics* **2004**, *23*, 5896-5899.

[82] a) Long, N. J. *Angew. Chem. Int. Ed.* **1995**, *34*, 21-38; b) Powell, C. E. and Humphrey, M. G. *Coord. Chem. Rev.* **2004**, *248*, 725-756; c) Powell, C. E.; Cifuentes, M. P.; Morrall, J. P.; Stranger, R.; Humphrey, M. G.; Samoc, M.; Luther-Davies, B. and Heath, G. a. *J. Am. Chem. Soc.* **2003**, *125*, 602-610.

[83] a) Wilson, J. S.; Dhoot, A. S.; Seeley, A. J. A. B.; Khan, M. S.; Kohler, A. and Friend, R. H. *Nature* **2001**, *413*, 828-831; b) Wong, K. M.-C.; Zhu, X.; Hung, L.-L.; Zhu, N.; Yam, V. W.-W. and Kwok, H.-S. *Chem. Commun.* **2005**, 2906-2908.

[84] Yam, V. *C.R. Chim.* **2005**, *8*, 1194-1203.

[85] Kostic, N. M. and Fenske, R. F. *Organometallics* **1982**, *1*, 974-982.

[86] a) Nast, R. *Coord. Chem. Rev.* **1982**, *47*, 89-124; b) Long, N. J. and Williams, C. K. *Angew. Chem. Int. Ed.* **2003**, *42*, 2586-2617.

[87] Chiang, S.-J.; Chi, Y.; Su, P.-C.; Peng, S.-M. and Lee, G.-H. *J. Am. Chem. Soc.* **1994**, *116*, 11181-11182.

[88] a) Bruce, M. I.; Costuas, K.; Halet, J.-F.; Hall, B. C.; Low, P. J.; Nicholson, B. K.; Skelton, B. W. and White, A. H. *J. Chem. Soc., Dalton Trans.* **2002**, 383-398; b) Khan, M. S.; Al-Mandhary, M. R. A.; Al-Suti, M. K.; Ahrens, B.; Mahon, M. F.; Male, L.; Raithby, P. R.; Boothby, C. E. and Kohler, A. *Dalton Trans.* **2003**, 74-84.

[89] a) Adams, C. J.; James, S. L.; Liu, X.; Raithby, P. R. and Yellowlees, L. J. *J. Chem. Soc., Dalton Trans.* **2000**, 63-67; b) Chan, S.-C.; Chan, M. C. W.; Wang, Y.; Che, C.-M.; Cheung, K.-K. and Zhu, N. *Chem. Eur. J.* **2001**, *7*, 4180-4190.

[90] a) Hissler, M.; Connick, W. B.; Geiger, D. K.; McGarrah, J. E.; Lipa, D.; Lachicotte, R. J. and Eisenberg, R. *Inorg. Chem.* **2000**, *39*, 447-457; b) Chakraborty, S.; Wadas, T. J.; Hester, H.; Schmehl, R. and Eisenberg, R. *Inorg. Chem.* **2005**, *44*, 6865-6878.

[91] Hissler, M.; McGarrah, J. E.; Connick, W. B.; Geiger, D. K.; Cummings, S. D. and Eisenberg, R. *Coord. Chem. Rev.* **2000**, *208*, 115-137.

[92] Yam, V. W.-W.; Tang, R. P.-L.; Wong, K. M.-C. and Cheung, K.-K. *Organometallics* **2001**, *20*, 4476-4482.

[93] Guo, F.; Sun, W.; Liu, Y. and Schanze, K. *Inorg. Chem.* **2005**, *44*, 4055-4065.

[94] Liu, X.-J.; Feng, J.-K.; Meng, J.; Pan, Q.-J.; Ren, A.-M.; Zhou, X. and Zhang, H.-X. *Eur. J. Inorg. Chem.* **2005**, 1856-1866.

[95] Hoogervorst, W. J.; Elsevier, C. J.; Lutz, M. and Spek, A. L. *Organometallics* **2001**, *20*, 4437-4440.

[96] Manna, J.; John, K. D. and Hopkins, M. D. in *Adv. Organomet. Chem., Vol. Volume 38* (Eds.: F. G. A. StoneandW. Robert), Academic Press, **1995**, pp. 79-154.

[97] Siemsen, P.; Livingston, R. C. and Diederich, F. *Angew. Chem. Int. Ed.* **2000**, *39*, 2632-2657.

[98] Sonogashira, K.; Fujikura, Y.; Yatake, T.; Toyoshima, N.; Takahashi, S. and Hagihara, N. *J. Organomet. Chem.* **1978**, *145*, 101-108.

[99] Vicente, J.; Chicote, M.-T.; Alvarez-Falcón, M. M. and Jones, P. G. *Organometallics* **2005**, *24*, 2764-2772.

[100] Campbell, K.; McDonald, R.; Ferguson, M. J. and Tykwinski, R. R. *J. Organomet. Chem.* **2003**, *683*, 379-387.

[101] Owen, G. R.; Gauthier, S.; Weisbach, N.; Hampel, F.; Bhuvanesh, N. and Gladysz, J. A. *Dalton Trans.* **2010**, *39*, 5260-5271.

[102] Schull, T. L.; Kushmerick, J. G.; Patterson, C. H.; George, C.; Moore, M. H.; Pollack, S. K. and Shashidhar, R. *J. Am. Chem. Soc.* **2003**, *125*, 3202-3203.

[103] Zhang, R. Ph. D. thesis, Univ. of Victoria, Victoria, **2007**.

[104] Wang, Y. Ph. D. thesis, Univeristy of Victoria, Victoria, BC, Canada, **2003**.

[105] Mitchell, R. H. and Bandyopadhyay, S. *Org. Lett.* **2004**, *6*, 1729-1732.

[106] Mitchell, R. H.; Bohne, C.; Robinson, S. G. and Yang, Y. H. *J. Org. Chem.* **2007**, *72*, 7939-7946.

[107] Orita, A.; Yoshioka, N.; Struwe, P.; Braier, A.; Beckmann, A. and Otera, J. *Chem.--Eur. J.* **1999**, *5*, 1355-1363.

[108] Kimball, D. B.; Haley, M. M.; Mitchell, R. H.; Ward, T. R.; Bandyopadhyay, S.; Williams, R. V. and Armantrout, J. R. *J. Org. Chem.* **2002**, *67*, 8798-8811.

[109] Hundertmark, T.; Littke, A. F.; Buchwald, S. L. and Fu, G. C. *Org. Lett.* **2000**, *2*, 1729-1731.

[110] Berenguer, J. R.; Forniés, J.; Lalinde, E.; Martín, A. and Serrano, B. *J. Chem. Soc., Dalton Trans.* **2001**, 2926-2936.

[111] Tashiro, M. and Yamato, T. *Org. Prep. Proced. Int.* **1982**, *14*, 216 - 219.

[112] Coat, F.; Guillevic, M.-A.; Toupet, L.; Paul, F. and Lapinte, C. *Organometallics* **1997**, *16*, 5988-5998.

[113] Khan, M. S.; Al-Mandhary, M. R. A.; Al-Suti, M. K.; Al-Battashi, F. R.; Al-Saadi, S.; Ahrens, B.; Bjernemose, J. K.; Mahon, M. F.; Raithby, P. R.; Younus, M.; Chawdhury, N.; Kohler, A.; Marseglia, E. A.; Tedesco, E.; Feeder, N. and Teat, S. J. *Dalton Trans.* **2004**, 2377-2385.

[114] Yam, V. W.-W.; Tao, C.-H.; Zhang, L.; Wong, K. M.-C. and Cheung, K.-K. *Organometallics* **2001**, *20*, 453-459.

[115] http://www.sanderkok.com/techniques/laboratory/pka_pkb.html

[116] Duer, M. J.; Khan, M. S. and Kakkar, A. K. *Solid State Nucl. Magn. Reson.* **1992**, *1*, 13-16.

[117] a) Onitsuka, K.; Fujimoto, M.; Ohshiro, N. and Takahashi, S. *Angew. Chem. Int. Ed.* **1999**, *38*, 689-692; b) Mayor, M.; von Hänisch, C.; Weber, H. B.; Reichert, J. and Beckmann, D. *Angew. Chem. Int. Ed.* **2002**, *41*, 1183-1186.

[118] Janka, M.; Anderson, G. K. and Rath, N. P. *Organometallics* **2004**, *23*, 4382-4390.

[119] Khairul, W. M.; Fox, M. A.; Zaitseva, N. N.; Gaudio, M.; Yufit, D. S.; Skelton, B. W.; White, A. H.; Howard, J. A. K.; Bruce, M. I. and Low, P. J. *Dalton Trans.* **2009**, 610-620.

[120] Masai, H.; Sonogashira, K. and Hagihara, N. *Bull. Chem. Soc. Jpn.* **1971**, *44*, 2226-2230.

[121] Saha, R.; Qaium, M. A.; Debnath, D.; Younus, M.; Chawdhury, N.; Sultana, N.; Kociok-Kohn, G.; Ooi, L.-l.; Raithby, P. R. and Kijima, M. *Dalton Trans.* **2005**, 2760-2765.

[122] Cifuentes, M. P. and Humphrey, M. G. *J. Organomet. Chem.* **2004**, *689*, 3968-3981.

[123] a) Hull, K. L. and Sanford, M. S. *J. Am. Chem. Soc.* **2009**, *131*, 9651-9653; b) Espinet, P. and Echavarren, A. M. *Angew. Chem. Int. Ed.* **2004**, *43*, 4704-4734.

[124] Farrugia, L. J. *J. Appl. Cryst.* **1997**, *30*, 565-565.

[125] CSD Version 5.32`, last updated on November 2010.

[126] Anderson, K. M. and Orpen, A. G. *Chem. Commun.* **2001**, 2682-2683.

[127] Rigamonti, L.; Forni, A.; Manassero, M.; Manassero, C. and Pasini, A. *Inorg. Chem.* **2009**, *49*, 123-135.

[128] Hartley, F. R. *Chem. Soc. Rev.* **1973**, *2*, 163-179.

[129] Ara, I.; Berenguer, J. R.; Eguizábal, E.; Forniés, J.; Gómez, J.; Lalinde, E. and Sáez-Rocher, J. M. *Organometallics* **2000**, *19*, 4385-4397.

[130] Robinson, S. G.; Sauro, V. A. and Mitchell, R. H. *J. Org. Chem.* **2009**, *74*, 6592-6605.

[131] Robinson, S. G. Ph. D. thesis, Univeristy of Victoria, Victoria, BC, Canada, **2008**.

[132] Ayub, K. Ph. D. thesis, Univeristy of Victoria, Victoria, BC, Canada, **2008**.

[133] Mitchell, R. H.; Ward, T. R.; Chen, Y. S.; Wang, Y.; Weerawarna, S. A.; Dibble, P. W.; Marsella, M. J.; Almutairi, A. and Wang, Z. Q. *J. Am. Chem. Soc.* **2003**, *125*, 2974-2988.

[134] Williams, R. V.; Edwards, W. D.; Mitchell, R. H. and Robinson, S. G. *J. Am. Chem. Soc.* **2005**, *127*, 16207-16214.

[135] a) Maitlis, P. M. in *Adv. Organomet. Chem., Vol. 4* (Eds.: F. G. A. StoneandW. Robert), Academic Press, **1966**, pp. 95-143; b) Maitlis, P. M. and Games, M. L. *J. Am. Chem. Soc.* **1963**, *85*, 1887-1888; c) Willstätter, R. and von Schmaedel, W. *Ber. Dtsch. Chem. Ges.* **1905**, *38*, 1992-1999.

[136] a) Kekulé, A. *Bull. Soc. Chim. Fr.* **1865**, *3*, 98-110; b) Erlenmeyer, E. *Justus Liebigs Ann.Chem.* **1866**, *137*, 327-359.

[137] Maier, G. *Angew. Chem. Int. Ed.* **1988**, *27*, 309-332.

[138] Nakamura, A. and Hagihara, N. *Bull. Chem. Soc. Jpn.* **1961**, *34*, 452-453.

[139] Macomber, D. W.; Verma, A. G. and Rogers, R. D. *Organometallics* **1988**, *7*, 1241-1253.

[140] Arrayas, R. G.; Mancheno, O. G. and Carretero, J. C. *Chem. Commun.* **2004**, 1654-1655.

[141] Kang, J.; Hyung Kim, T.; Han Yew, K. and Ki Lee, W. *Tetrahedron: Asymmetry* **2003**, *14*, 415-418.

[142] a) Altmann, M.; Friedrich, J.; Beer, F.; Reuter, R.; Enkelmann, V. and Bunz, U. H. F. *J. Am. Chem. Soc.* **1997**, *119*, 1472-1473; b) Bunz, U. H. F.; Roidl, G.; Altmann, M.; Enkelmann, V. and Shimizu, K. D. *J. Am. Chem. Soc.* **1999**, *121*, 10719-10726.

[143] Rausch, M. D. and Genetti, R. A. *J. Org. Chem.* **1970**, *35*, 3888-3897.

[144] a) Amiet, R. G. and Pettit, R. *J. Am. Chem. Soc.* **1968**, *90*, 1059-1060; b) Rosenblum, M.; North, B.; Wells, D. and Giering, W. P. *J. Am. Chem. Soc.* **1972**, *94*, 1239-1246; c) Adams, C. M.; Crawford, E. S. and Salim, E. *Tetrahedron Lett.* **1992**, *33*, 3963-3966.

[145] O'Donohue, P.; Brusey, S. A.; Seward, C. M.; Ortin, Y.; Molloy, B. C.; Müller-Bunz, H.; Manning, A. R. and McGlinchey, M. J. *J. Organomet. Chem.* **2009**, *694*, 2536-2547.

[146] a) Sekiguchi, A.; Matsuo, T. and Tanaka, M. *Organometallics* **2002**, *21*, 1072-1076; b) Takanashi, K.; Inatomi, A.; Lee, V. Y.; Nakamoto, M.; Ichinohe, M. and Sekiguchi, A. *Eur. J. Inorg. Chem.* **2008**, *2008*, 1752-1755; c) Lee, V.-Y. and Sekiguchi, A. *Angew. Chem. Int. Ed.* **2007**, *46*, 6596-6620; d) Jung, Y.; Heine, T.; Schleyer, P. v. R. and Head-Gordon, M. *J. Am. Chem. Soc.* **2004**, *126*, 3132-3138; e) Matsuo, T. and Sekiguchi, A. *Bull. Chem. Soc. Jpn.* **2004**, *77*, 211-226; f) Sommerfeld, T. *J. Am. Chem. Soc.* **2002**, *124*, 1119-1124.

[147] a) Lai, Y.-H. and Chen, P. *J. Org. Chem.* **1996**, *61*, 935-940; b) Tamm, M.; Bannenberg, T.; Dressel, B.; Fröhlich, R. and Kunz, D. *Organometallics* **2001**, *20*, 900-904.

[148] Mitchell, R. H.; Bohne, C.; Wang, Y. X.; Bandyopadhyay, S. and Wozniak, C. B. *J. Org. Chem.* **2006**, *71*, 327-336.

[149] a) Abel, E. W.; Bennett, M. A.; Burton, R. and Wilkinson, G. *J. Chem. Soc.* **1958**, 4559-4563; b) Ayub, K.; Zhang, R.; Robinson, S. G.; Twamley, B.; Williams, R. V. and Mitchell, R. H. *J. Org. Chem.* **2008**, *73*, 451-456.

[150] Li, H.; Xu, Q.; Li, N.; Sun, R.; Ge, J.; Lu, J.; Gu, H. and Yan, F. *J. Am. Chem. Soc.* **2010**.

[151] Dieter, R. K.; Lu, K. and Velu, S. E. *J. Org. Chem.* **2000**, *65*, 8715-8724.

[152] Fujise, Y.; Saito, H. and Itô, S. *Tetrahedron Lett.* **1976**, *17*, 1117-1120.

[153] Liddell, P. A.; Kodis, G.; Andreasson, J.; de la Garza, L.; Bandyopadhyay, S.; Mitchell, R. H.; Moore, T. A.; Moore, A. L. and Gust, D. *J. Am. Chem. Soc.* **2004**, *126*, 4803-4811.

[154] a) Hayakawa, K.; Hori, N. and Kanematsu, K. *Chem. Pharm. Bull.* **1983**, *31*, 1809-1811; b) Hay, A. S. *J. Org. Chem.* **1962**, *27*, 3320-3321.

[155] Edsall, A. B.; Mohanakrishnan, A. K.; Yang, D.; Fanwick, P. E.; Hamel, E.; Hanson, A. D.; Agoston, G. E. and Cushman, M. *J. Med. Chem.* **2004**, *47*, 5126-5139.

[156] Wakatsuki, Y.; Nomura, O.; Kitaura, K.; Morokuma, K. and Yamazaki, H. *J. Am. Chem. Soc.* **1983**, *105*, 1907-1912.

[157] Nakamura, A. and Hagihara, N. *Bull. Chem. Soc. Jpn.* **1961**, *34*, 452-453.

[158] Stevens, A. M. and Richards, C. J. *Organometallics* **1999**, *18*, 1346-1348.

[159] Boston, J. L.; Sharp, D. W. A. and Wilkinson, G. *J. Chem. Soc.* **1962**, 3488-3494.

[160] a) Hillard, R. L. and Vollhardt, K. P. C. *J. Am. Chem. Soc.* **1977**, *99*, 4058-4069; b) Vollhardt, K. P. C. *Acc. Chem. Res.* **1977**, *10*, 1-8.

[161] Fritch, J. R. and Vollhardt, K. P. C. *Organometallics* **1982**, *1*, 590-602.

[162] Dickson, R. S. and Fraser, P. J. in *Adv. Organomet. Chem., Vol. 12* (Eds.: F. G. A. StoneandW. Robert), Academic Press, **1974**, pp. 323-377.

[163] Johnston, P.; Hutchings, G. J.; Denner, L.; Boeyens, J. C. A. and Coville, N. J. *Organometallics* **1987**, *6*, 1292-1300.

[164] a) Boñaga, L. V. R.; Zhang, H.-C.; Moretto, A. F.; Ye, H.; Gauthier, D. A.; Li, J.; Leo, G. C. and Maryanoff, B. E. *J. Am. Chem. Soc.* **2005**, *127*, 3473-3485; b) Varela, J. A. and Saa, C. *Chem. Rev.* **2003**, *103*, 3787-3802.

[165] a) Laskoski, M.; Morton, J. G. M.; Smith, M. D. and Bunz, U. H. F. *Chem. Commun.* **2001**, 2590-2591; b) Laskoski, M.; Morton, J. G. M.; Smith, M. D. and Bunz, U. H. F. *J. Organomet. Chem.* **2002**, *652*, 21-30.

[166] See the supporting information

[167] Rausch, M. D.; Westover, G. F.; Mintz, E.; Reisner, G. M.; Bernal, I.; Clearfield, A. and Troup, J. M. *Inorg. Chem.* **1979**, *18*, 2605-2615.

[168] a) Werz, D. B.; Schulte, J. H.; Gleiter, R. and Rominger, F. *J. Organomet. Chem.* **2004**, *689*, 3132-3142; b) Riley, P. E. and Davis, R. E. *J. Organomet. Chem.* **1976**, *113*, 157-166; c) Gupta, H. P.; Kumar, M. S.; Upreti, S. and Elias, A. J. *Eur. J. Inorg. Chem.* **2006**, 5022-5032; d) Virtue, G. A.; Coyne, N. E. and Hamilton, D. G. *J. Org. Chem.* **2002**, *67*, 6856-6859.

[169] Irngartinger, H. and Nixdorf, M. *Chem. Ber.* **1988**, *121*, 679-683.

[170] Dreiding, A. S.; Bieri, J. H.; Prewo, R.; Linden, A. and Gesing, E. *Cambridge Structural Database Private Communication Refcode HACKUR* **1993**.

[171] Mutseneck, E. V.; Perekalin, D. S.; Holub, J.; Starikova, Z. A.; Petrovskii, P. V.; Zanello, P.; Corsini, M.; Stibr, B. and Kudinov, A. R. *Organometallics* **2006**, *25*, 2419-2426.

[172] Allmann, R. and Hellner, E. *Chem. Ber.* **1968**, *101*, 2522-2532.

[173] Fan, H.-J.; Carducci, M. D.; Grittini, C.; Mendoza, A. and Lichtenberger, D. L. Ac*ta Crystallogr., Sect. C* **1999**, *55*, IUC9900154.

[174] a) Nakaya, T.; Namiki, K.; Murata, M.; Kanaizuka, K.; Kurashina, M.; Fujita, T. and Nishihara, H. *J. Inorg. Organomet. Polym Mater.* **2008**, *18*, 124-130; b) Murata, M.; Hoshi, T.; Matsuoka, I.; Nankawa, T.; Kurihara, M. and Nishihara, H. *J. Inorg. Organomet. Polym.* **2000**, *10*, 209-219.

[175] Debaerdemaeker, T.; Grafl, D. and Brune, H. A. Ac*ta Crystallogr., Sect. C* **1987**, *43*, 221-224.

[176] Bandyopadhyay, S. Doctor of philosophy thesis, Univeristy of Victoria, Victoria, **2004**.

[177] Mutseneck, E. V.; Loginov, D. A.; Perekalin, D. S.; Starikova, Z. A.; Golovanov, D. G.; Petrovskii, P. V.; Zanello, P.; Corsini, M.; Laschi, F. and Kudinov, A. R. *Organometallics* **2004**, *23*, 5944-5957.

[178] a) Lai, Y.-H. and Jiang, J. *J. Org. Chem.* **1997**, *62*, 4412-4417; b) Lai, Y.-H.; Chen, P. and Dingle, T. W. *J. Org. Chem.* **1997**, *62*, 916-924.

[179] McGlinchey, M. J.; Burns, R. C.; Hofer, R.; Top, S. and Jaouen, G. *Organometallics* **1986**, *5*, 104-109.

[180] Mitchell, R. H.; Carruthers, R. J.; Mazuch, L. and Dingle, T. W. *J. Am. Chem. Soc.* **1982**, *104*, 2544-2551.

[181] Rosenblum, M. and North, B. *J. Am. Chem. Soc.* **1968**, *90*, 1060-1061.

[182] Fan, W. Ph. D. thesis, Univeristy of Victoria, Victoria, BC, Canada, **2005**.

[183] a) Naya, S.-i.; Sakakibara, T. and Nitta, M. *J. Chem. Soc., Perkin Trans. 2* **2001**, 1032-1037; b) Butler, D. N. and Gupta, I. *Can. J. Chem.* **1978**, *56*, 80-84.

[184] Conrow, K. in *Org. Synth., Vol. 43*, John Wiley & Sons, Inc., **1963**, pp. 101-103.

[185] a) Takahashi, K.; Takase, K. and Toda, H. *Chem. Lett.* **1981**, 979-982; b) Klaerner, F. G.; Yaslak, S. and Wette, M. *Chem. Ber.* **1979**, *112*, 1168-1188; c) Klaerner, F. G.; Schmidt, E. K. G.; Abdel, R. M. A. and Kollmar, H. *Angew.*

Chem. **1982**, *94*, 137; d) Klaerner, F. G.; Schmidt, E. K. G. and Abdel, R. M. A. *Angew. Chem.* **1982**, *94*, 136-137.

[186] Sourisseau, C. *Spectrochimica Acta A* **1978**, *34*, 881-887.

[187] Dauben, H. J.; Gadecki, F. A.; Harmon, K. M. and Pearson, D. L. *J. Am. Chem. Soc.* **1957**, *79*, 4557-4558.

[188] Green, M. L. H. and Ng, D. K. P. *Chem. Rev.* **1995**, *95*, 439-473.

[189] Tamm, M. *Chem. Commun.* **2008**, 3089-3100.

[190] Dai, S.; Wang, J. T. and Williams, F. *J. Am. Chem. Soc.* **1990**, *112*, 2837-2839.

[191] Katz, T. J. *J. Am. Chem. Soc.* **1960**, *82*, 3784-3785.

[192] Evans, W. J.; Wink, D. J.; Wayda, A. L. and Little, D. A. *J. Org. Chem.* **1981**, *46*, 3925-3928.

[193] a) Streitwieser, A. and Mueller-Westerhoff, U. *J. Am. Chem. Soc.* **1968**, *90*, 7364-7364; b) Streitwieser, A.; Muller-Westerhoff, U.; Sonnichsen, G.; Mares, F.; Morrell, D. G.; Hodgson, K. O. and Harmon, C. A. *J. Am. Chem. Soc.* **1973**, *95*, 8644-8649.

[194] Keller, C. E. and Pettit, R. *J. Am. Chem. Soc.* **1966**, *88*, 604-606.

[195] Deno, N. C.; Pittman, C. U. and Turner, J. O. *J. Am. Chem. Soc.* **1965**, *87*, 2153-2157.

[196] Winstein, S.; Kaesz, H. D.; Kreiter, C. G. and Friedrich, E. C. *J. Am. Chem. Soc.* **1965**, *87*, 3267-3269.

[197] Mitchell, R. H.; Khalifa, N. A. and Dingle, T. W. *J. Am. Chem. Soc.* **1991**, *113*, 6696-6697.

[198] Mitchell, R. H. and Lau, D. Y. K. *Tetrahedron Lett.* **1995**, *36*, 9281-9284.

[199] Mitchell, R. H.; Lau, D. Y. K. and Miyazawa, A. *Org. Prep. Proced. Int.* **1996**, *28*, 713-716.

[200] Sengupta, S.; Drew, M. G. B.; Mukhopadhyay, R.; Achari, B. and Banerjee, A. K. *J. Org. Chem.* **2005**, *70*, 7694-7700.

[201] a) Mitchell, R. H. and Zhou, P. Z. *Tetrahedron Lett.* **1990**, *31*, 5277-5280; b) Mitchell, R. H. and Zhou, P. Z. *Tetrahedron Lett.* **1991**, *32*, 6319-6322; c) Mitchell, R. H.; Ward, T. R.; Wang, Y. X. and Dibble, P. W. *J. Am. Chem. Soc.* **1999**, *121*, 2601-2602.

[202] Buchner, E. and Curtius, T. *Ber. Dtsch. Chem. Ges.* **1885**, *18*, 2371-2377.

[203] Mosettig, E. and Burger, A. *J. Am. Chem. Soc.* **1930**, *52*, 3456-3463.

[204] Kürti, L. s. and Czakó, B. *Strategic applications of named reactions in organic synthesis :background and detailed mechanisms*, Elsevier Academic Press, Amsterdam; Boston **2005**.

[205] Anciaux, A. J.; Demonceau, A.; Noels, A. F.; Hubert, A. J.; Warin, R. and Teyssie, P. *J. Org. Chem.* **1981**, *46*, 873-876.

[206] Srivastava, K. C. and Dev, S. *Tetrahedron* **1972**, *28*, 1083-1091.

[207] Daştan, A.; Yıldız, Y. K. and Balci, M. *Synth. Commun.* **2001**, *31*, 3807 - 3815.

[208] Ranken, P. F.; Harty, B. J.; Kapicak, L. and Battiste, M. A. *Synth. Commun.* **1973**, *3*, 311 - 315.

[209] Thiele, J. and Schneider, J. *Justus Liebigs Ann.Chem.* **1909**, *369*, 287-299.

[210] Ried, W. and Schwenecke, H. J. *Chem. Ber.* **1958**, *91*, 566-572.

[211] a) Hoffmann, H. M. R. *Angew. Chem. Int. Ed.* **1973**, *12*, 819-835; b) Montana, A. M. and Barcia, J. A. *Tetrahedron Lett.* **2005**, *46*, 8475-8478; c) Rigby, J. H. and Pigge, F. C. in *Org. React., Vol. 51*, John Wiley & Sons, Inc., **1997**, pp. 351-478; d) Ashcroft, M. R. and Hoffmann, H. M. R. in *Org. Synth., Vol. 58*, John Wiley & Sons, Inc., **1978**, pp. 17-22; e) Noyori, R. and Hayakawa, Y. in *Org. React., Vol. 29*, John Wiley & Sons, Inc., **1983**, pp. 163-344.

[212] Kreiselmeier, G. and Föhlisch, B. *Tetrahedron Lett.* **2000**, *41*, 1375-1379.

[213] Wright, D. L.; Whitehead, C. R.; Sessions, E. H.; Ghiviriga, I. and Frey, D. A. *Org. Lett.* **1999**, *1*, 1535-1538.

[214] Lee, J. C.; Jin, S.-j. and Cha, J. K. *J. Org. Chem.* **1998**, *63*, 2804-2805.

[215] Battiste, M. a.; Pelphrey, P. M. and Wright, D. L. *Chem. Eur. J.* **2006**, *12*, 3438-3447.

[216] Klein, S. and Roberts, S. M. *Journal of the Chemical Society, Perkin Transactions 1* **2002**, 2686-2691.

[217] Ikegami, Y. *Bull. Chem. Soc. Jpn.* **1962**, *35*, 972-977.

[218] Zoeckler, M. T. and Carpenter, B. K. *J. Am. Chem. Soc.* **1981**, *103*, 7661-7663.

[219] a) Luche, J. L. *J. Am. Chem. Soc.* **1978**, *100*, 2226-2227; b) Gemal, A. L. and Luche, J. L. *J. Am. Chem. Soc.* **1981**, *103*, 5454-5459.

[220] a) Miller, A. K.; Banghart, M. R.; Beaudry, C. M.; Suh, J. M. and Trauner, D. *Tetrahedron* **2003**, *59*, 8919-8930; b) Miller, A. K. and Trauner, D. *Angew. Chem. Int. Ed.* **2003**, *42*, 549-552.

[221] Murray, R. W. and Jeyaraman, R. *J. Org. Chem.* **1985**, *50*, 2847-2853.

[222] Druckova, A. and Marnett, L. J. *Chem. Res. Toxicol.* **2006**, *19*, 1330-1340.

[223] Gausing, W. and Wilke, G. *Angew. Chem. Int. Ed.* **1978**, *17*, 371-372.

[224] Hoye, T. R.; Kabrhel, J. E. and Hoye, R. C. *Org. Lett.* **2004**, *7*, 275-277.

[225] Murahashi, T.; Kato, N.; Ogoshi, S. and Kurosawa, H. *J. Organomet. Chem.* **2008**, *693*, 894-898.

[226] Gärtner, M.; Mader, S.; Seehafer, K. and Helmchen, G. n. *J. Am. Chem. Soc.* **2011**, *133*, 2072-2075.

[227] Wetzel, T. G.; Dehnen, S. and Roesky, P. W. *Organometallics* **1999**, *18*, 3835-3842.

[228] Majumder, S. and Odom, A. L. *Tetrahedron Lett.* **2008**, *49*, 1771-1772.

[229] Willstätter, R. M. and Waser, E. *Ber* **1911**, *44*, 3422-3445.

[230] Reppe, W.; Schlichting, O.; Klager, K. and Toepel, T. *Justus Liebigs Ann.Chem.* **1948**, *560*, 1-92.

[231] Colborn, R. E. and Vollhardt, K. P. C. *J. Am. Chem. Soc.* **1986**, *108*, 5470-5477.

[232] Straub, B. F. and Gollub, C. *Chem. Eur. J.* **2004**, *10*, 3081-3090.

[233] Nevalainen, M. and Koskinen, A. M. P. *J. Org. Chem.* **2002**, *67*, 1554-1560.

[234] Jones, R. V. H.; Lindsell, W. E.; Paddon-Jones, G. C.; Palmer, D. D.; Preston, P. N.; Rosair, G. M. and Whitton, A. J. *J. Organomet. Chem.* **2006**, *691*, 2378-2385.

[235] Griffin, C. E.; Martin, K. R. and Douglas, B. E. *J. Org. Chem.* **1962**, *27*, 1627-1631.

[236] Karatholuvhu, M. S. and Fuchs, P. L. *J. Am. Chem. Soc.* **2004**, *126*, 14314-14315.

[237] Hathaway, S. J. and Paquette, L. A. *J. Org. Chem.* **1983**, *48*, 3351-3353.

[238] Corey, E. J. and Venkateswarlu, A. *J. Am. Chem. Soc.* **1972**, *94*, 6190-6191.

[239] Corey, E. J. and Snider, B. B. *J. Am. Chem. Soc.* **1972**, *94*, 2549-2550.

[240] Miller, S. J.; Kim, S.-H.; Chen, Z.-R. and Grubbs, R. H. *J. Am. Chem. Soc.* **1995**, *117*, 2108-2109.

[241] Mohapatra, D. K.; Rahaman, H.; Pal, R. and Gurjar, M. K. *Synlett.* **2008**, *12*, 1801-1804.

[242] Noller, C. R.; Luchetti, C. A.; Acton, E. M. and Bernhard, R. A. *J. Am. Chem. Soc.* **1953**, *75*, 3851-3852.

[243] Katz, T. J. *J. Am. Chem. Soc.* **1960**, *82*, 3785-3786.

[244] Small, G. H.; Minnella, A. E. and Hall, S. S. *J. Org. Chem.* **1975**, *40*, 3151-3152.

[245] Khurana, J. M.; Kumar, S. and Nand, B. *Can. J. Chem.* **2008**, *86*, 1052-1054.

[246] Brown, H. C. and Nelson, K. L. *J. Am. Chem. Soc.* **1953**, *75*, 24-28.

[247] Eich, E.; Pertz, H.; Kaloga, M.; Schulz, J.; Fesen, M. R.; Mazumder, A. and Pommier, Y. *J. Med. Chem.* **1996**, *39*, 86-95.

[248] Bandgar, B. P.; Sadavarte, V. S. and Uppalla, L. S. *Tetrahedron Lett.* **2001**, *42*, 951-953.

[249] Alvarez-Manzaneda, E. J.; Chahboun, R.; Cabrera Torres, E.; Alvarez, E.; Alvarez-Manzaneda, R.; Haidour, A. and Ramos, J. *Tetrahedron Lett.* **2004**, *45*, 4453-4455.

[250] Meyer, S. D. and Schreiber, S. L. *J. Org. Chem.* **1994**, *59*, 7549-7552.

[251] Felpin, F.-X. and Lebreton, J. *J. Org. Chem.* **2002**, *67*, 9192-9199.

[252] Wrona, I. E.; Gabarda, A. E.; Evano, G. and Panek, J. S. *J. Am. Chem. Soc.* **2005**, *127*, 15026-15027.

[253] Panda, B. and Sarkar, T. K. *Tetrahedron Lett.* **2008**, *49*, 6701-6703.

[254] Schwab, P.; Grubbs, R. H. and Ziller, J. W. *J. Am. Chem. Soc.* **1996**, *118*, 100-110.

[255] Mitchell, R. H.; Chen, Y. S.; Iyer, V. S.; Lau, D. Y. K.; Baldridge, K. K. and Siegel, J. S. *J. Am. Chem. Soc.* **1996**, *118*, 2907-2911.

[256] Anet, F. A. L. *J. Am. Chem. Soc.* **1964**, *86*, 458-460.

[257] Anet, F. A. L.; Bourn, A. J. R. and Lin, Y. S. *J. Am. Chem. Soc.* **1964**, *86*, 3576-3577.

[258] Stevenson, C. D.; Brown, E. C.; Hrovat, D. A. and Borden, W. T. *J. Am. Chem. Soc.* **1998**, *120*, 8864-8867.

[259] Haddon, R. C. *J. Am. Chem. Soc.* **1979**, *101*, 1722-1728.

[260] a) Oth, J. F. M.; Müllen, K.; Königshofen, H.; Mann, M.; Sakata, Y. and Vogel, E. *Angew. Chem. Int. Ed.* **1974**, *13*, 284-285; b) Vogel, E.; Königshofen, H.;

Müllen, K. and Oth, J. F. M. *Angew. Chem. Int. Ed.* **1974**, *13*, 281-283; c) Vogel, E.; Mann, M.; Sakata, Y.; Müllen, K. and Oth, J. F. M. *Angew. Chem. Int. Ed.* **1974**, *13*, 283-284.

[261] a) Vogel, E. and Roth, H. D. *Angew. Chem. Int. Ed.* **1964**, *3*, 228-229; b) Vogel, E. and Böll, W. A. *Angew. Chem. Int. Ed.* **1964**, *3*, 642-642.

[262] a) Spiesecke, H. and Schneider, W. G. *Tetrahedron Lett.* **1961**, *2*, 468-472; b) Schaefer, T. and Schneider, W. G. *Can. J. Chem.* **1963**, *41*, 966-982.

[263] Memory, J. D. *J. Magn. Reson.* **1977**, *27*, 241-244.

[264] Mitchell, R. H. in *Advances in Theoretically Interesting Molecules, Vol. 1* (Ed.: R. P. Thummel), JAI Press, New York, **1989**, pp. 135-199.

[265] Boekelheide, V. and Phillips, J. B. *J. Am. Chem. Soc.* **1967**, *89*, 1695-1704.

[266] Mitchell, R. H.; Klopfenstein, C. E. and Boekelheide, V. *J. Am. Chem. Soc.* **1969**, *91*, 4931-4932.

[267] a) Childs, R. F. *Acc. Chem. Res.* **1984**, *17*, 347-352; b) Alkorta, I.; Elguero, J.; Eckert-Maksic, M. and Maksic, Z. B. *Tetrahedron* **2004**, *60*, 2259-2265.

[268] Johnson, C. E. J. and Bovey, F. A. *J. Chem. Phys.* **1958**, *29*, 1012-1014.

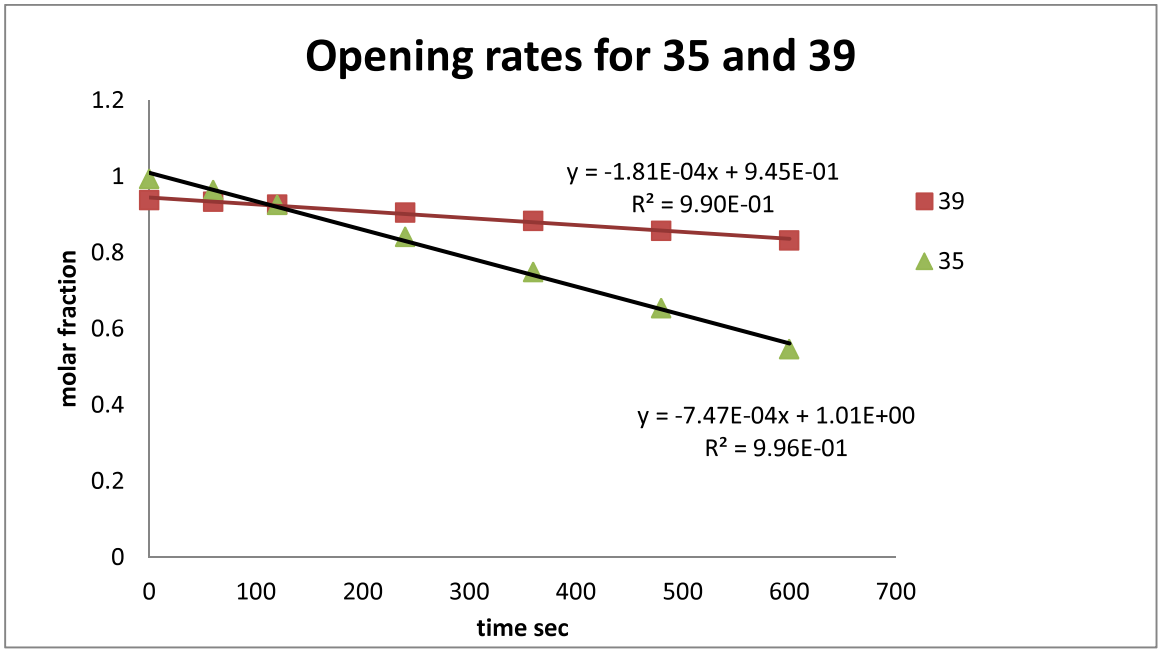
[269] a) Ibata, K.; Shimanouchi, H.; Sasada, Y. and Hata, T. *Acta Crystallogr., B* **1975**, *31*, 2313-2321; b) Ibata, K.; Shimanouchi, H. and Sasada, Y. *Acta Crystallogr., B* **1976**, *32*, 2054-2058; c) Ibata, K.; Shimanouchi, H. and Sasada, Y. *Acta Crystallogr., B* **1977**, *33*, 1129-1138.

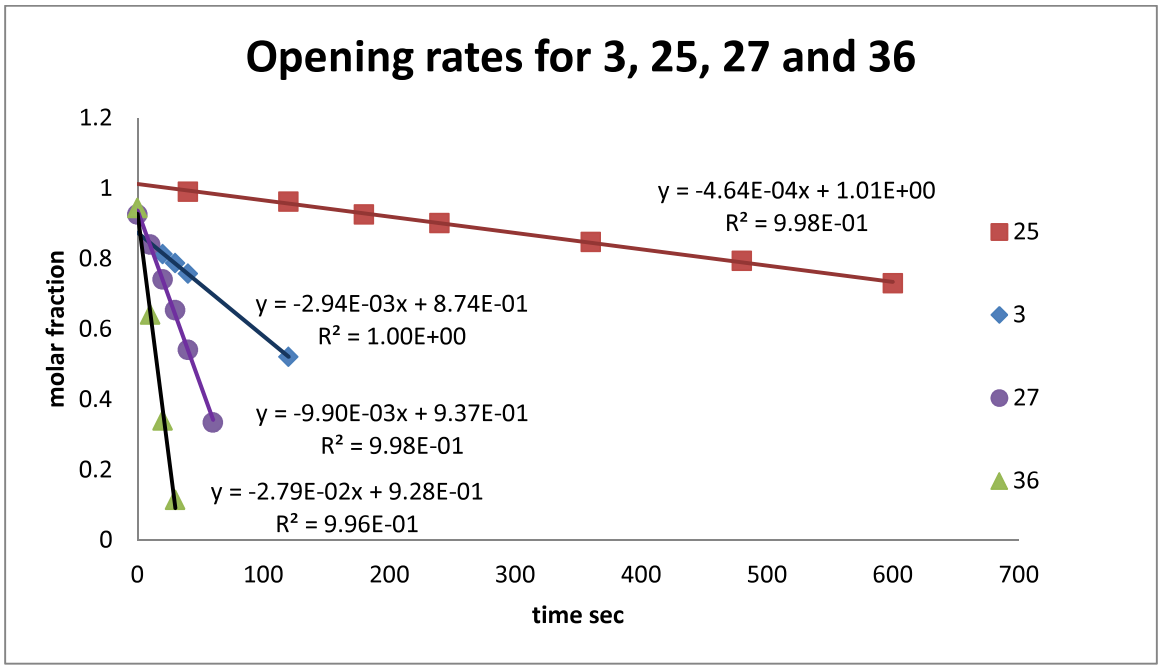
[270] Sheepwash, M. A. L. Ph. D. thesis, Univeristy of Victoria, Victoria, BC, Canada, **2002**.

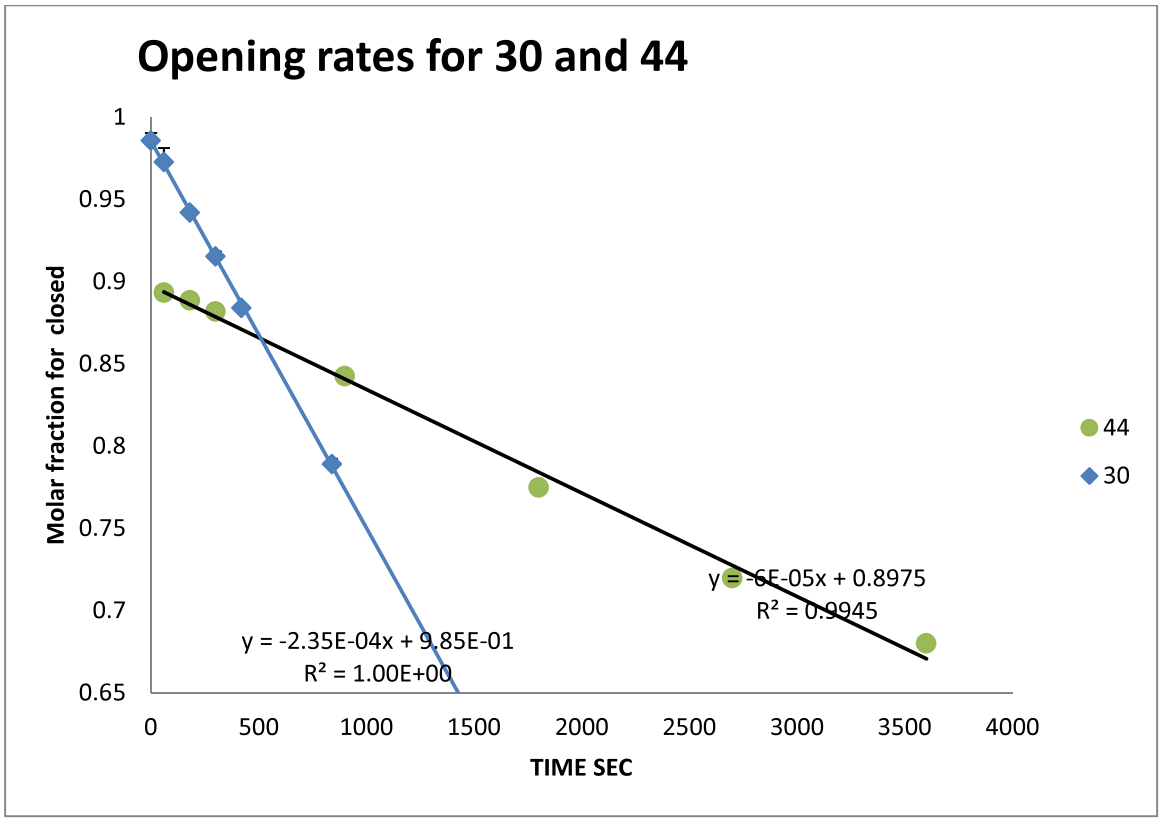
[271] Doerr, R. G. and Skell, P. S. *J. Am. Chem. Soc.* **1967**, *89*, 4684-4687.

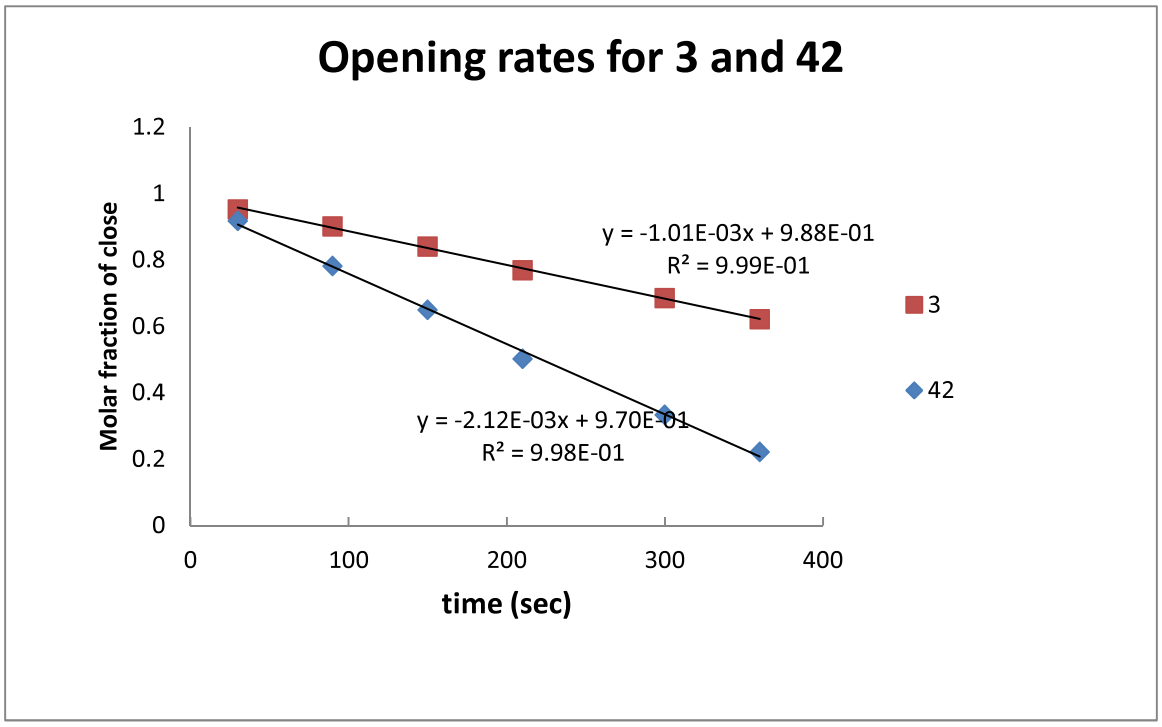
[272] Vaughn, G. D.; Krein, K. A. and Gladysz, J. A. *Organometallics* **1986**, *5*, 936-942.

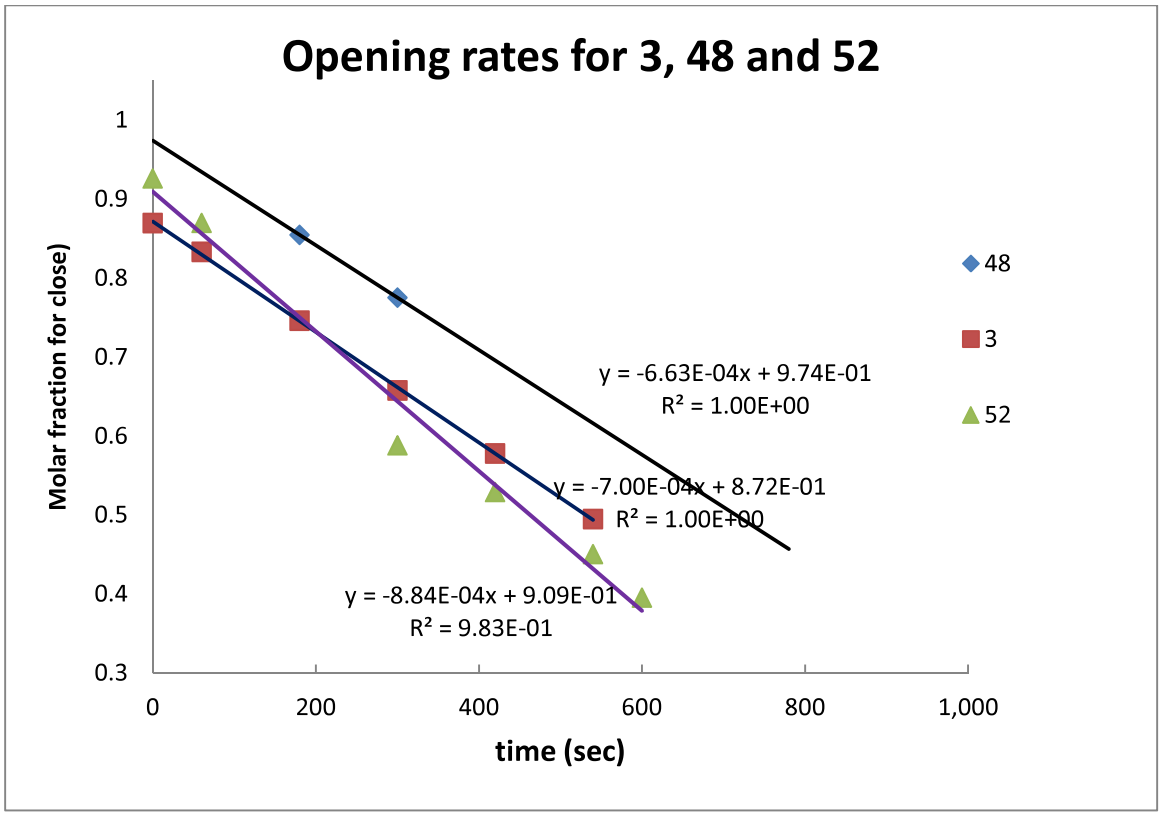
Appendix I. Opening rates comparison plot



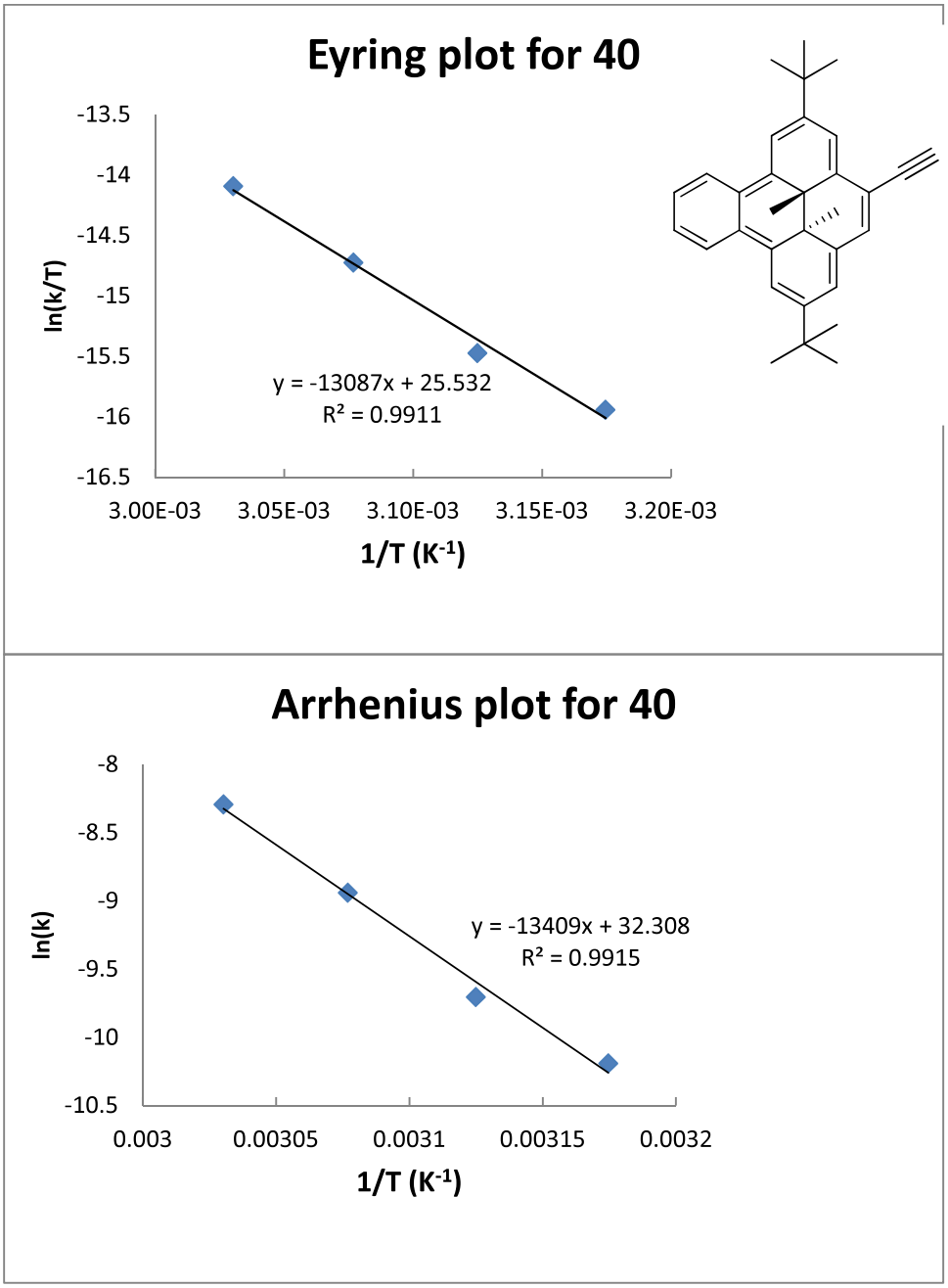


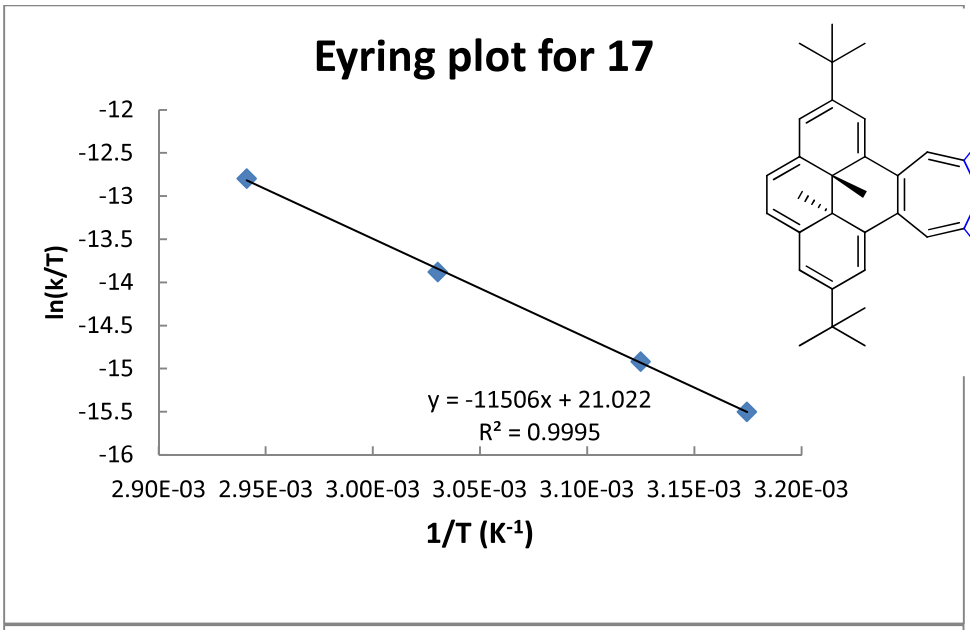

Opening rates for 30 and 44
Molar fraction for closed
1
0.95
0.9
0.85
0.8
0.75
0.7
0.65
0
500
1000
1500
2000
2500
3000
3500
4000
TIME SEC
y = -6E-05x + 0.8975
R² = 0.9945
y = -2.35E-04x + 9.85E-01
R² = 1.00E+00
44
30

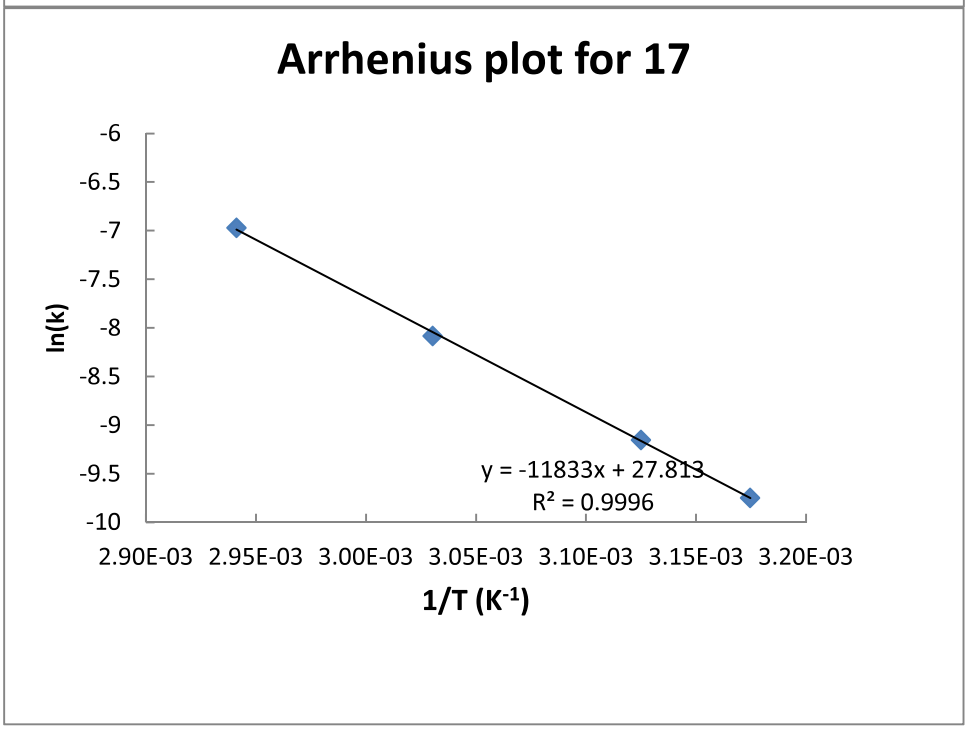

Opening rates for 3 and 42
Molar fraction of close
1.2
1
0.8
0.6
0.4
0.2
0
0
100
200
300
400
time (sec)
y = -1.01E-03x + 9.88E-01
R² = 9.99E-01
y = -2.12E-03x + 9.70E-01
R² = 9.98E-01
3
42

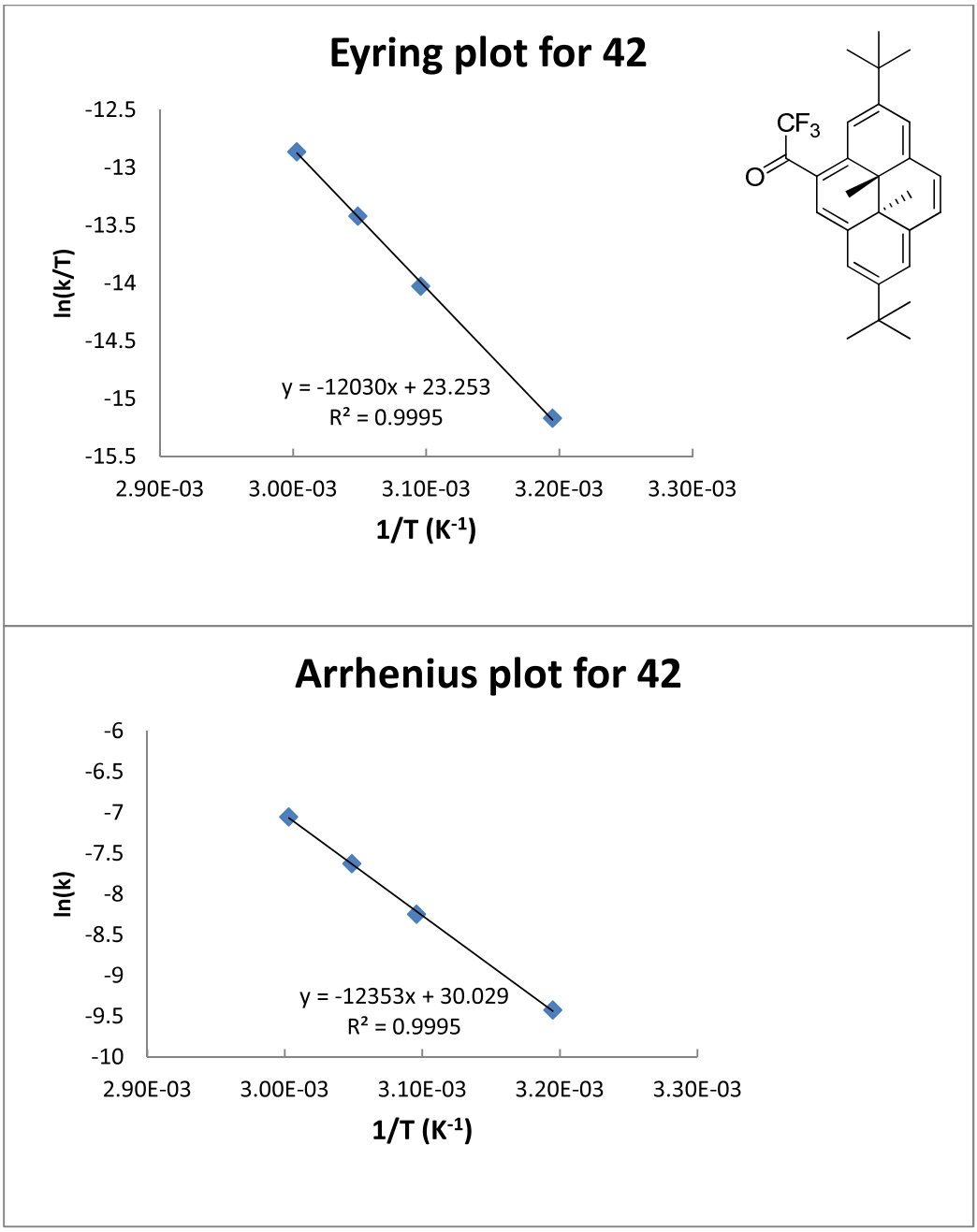

Opening rates for 3, 48 and 52
Molar fraction for close)
1
0.9
0.8
0.7
0.6
0.5
0.4
0.3
0
200
400
600
800
1,000
time (sec)
y = -6.63E-04x + 9.74E-01
R² = 1.00E+00
y = -7.00E-04x + 8.72E-01
R² = 1.00E+00
y = -8.84E-04x + 9.09E-01
R² = 9.83E-01
48
3
52

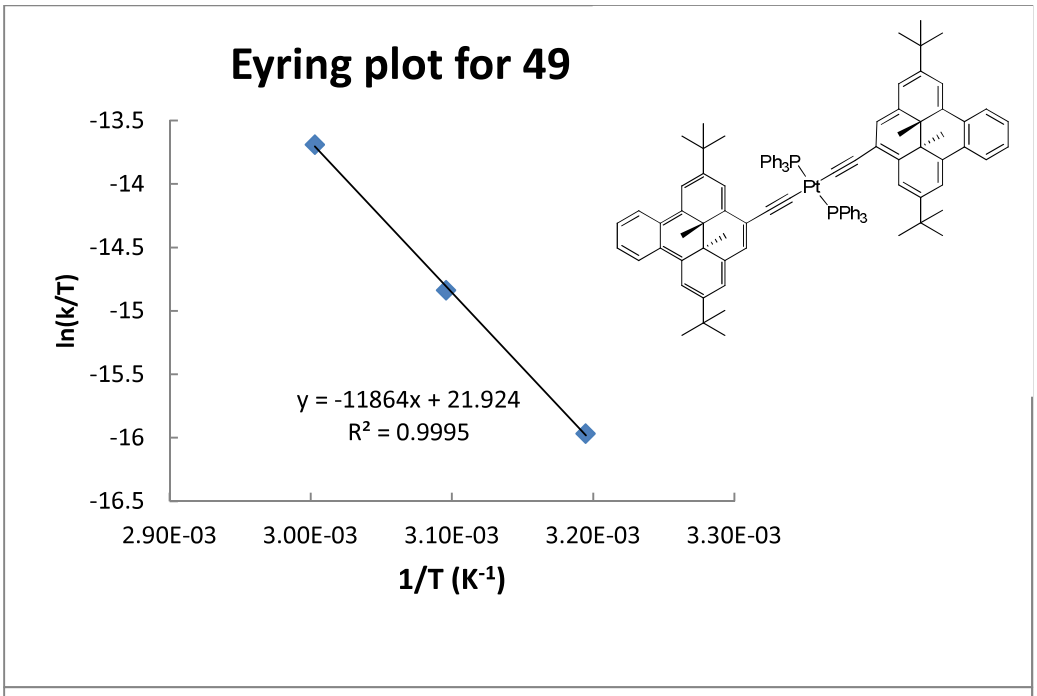
Appendix II. Thermal closing plots (Eyring and Arrhenius plots)

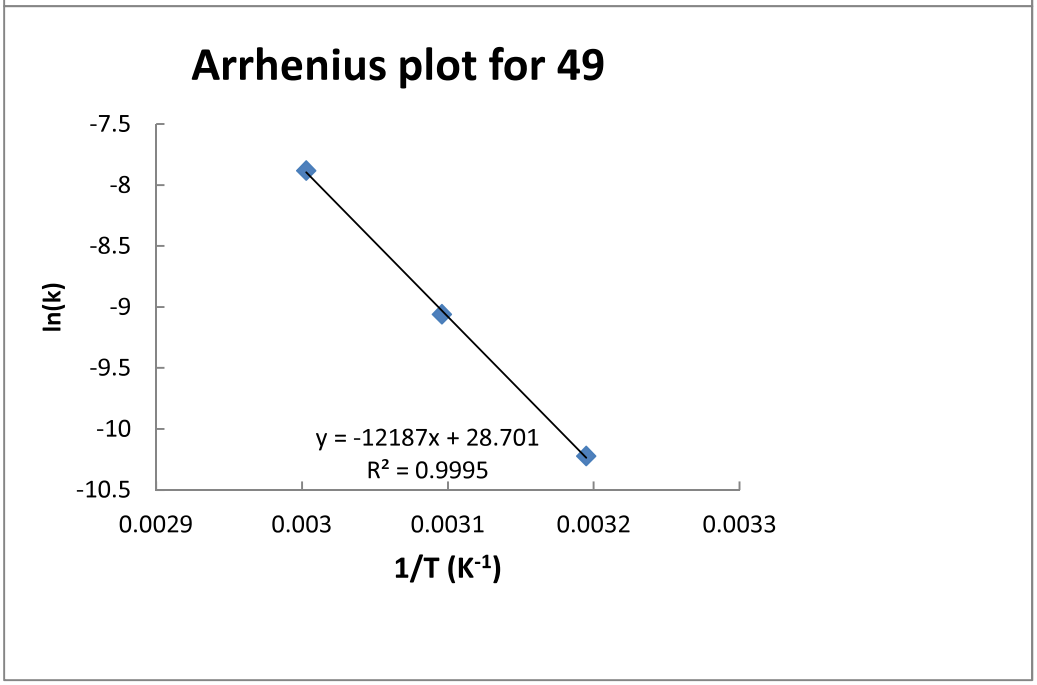


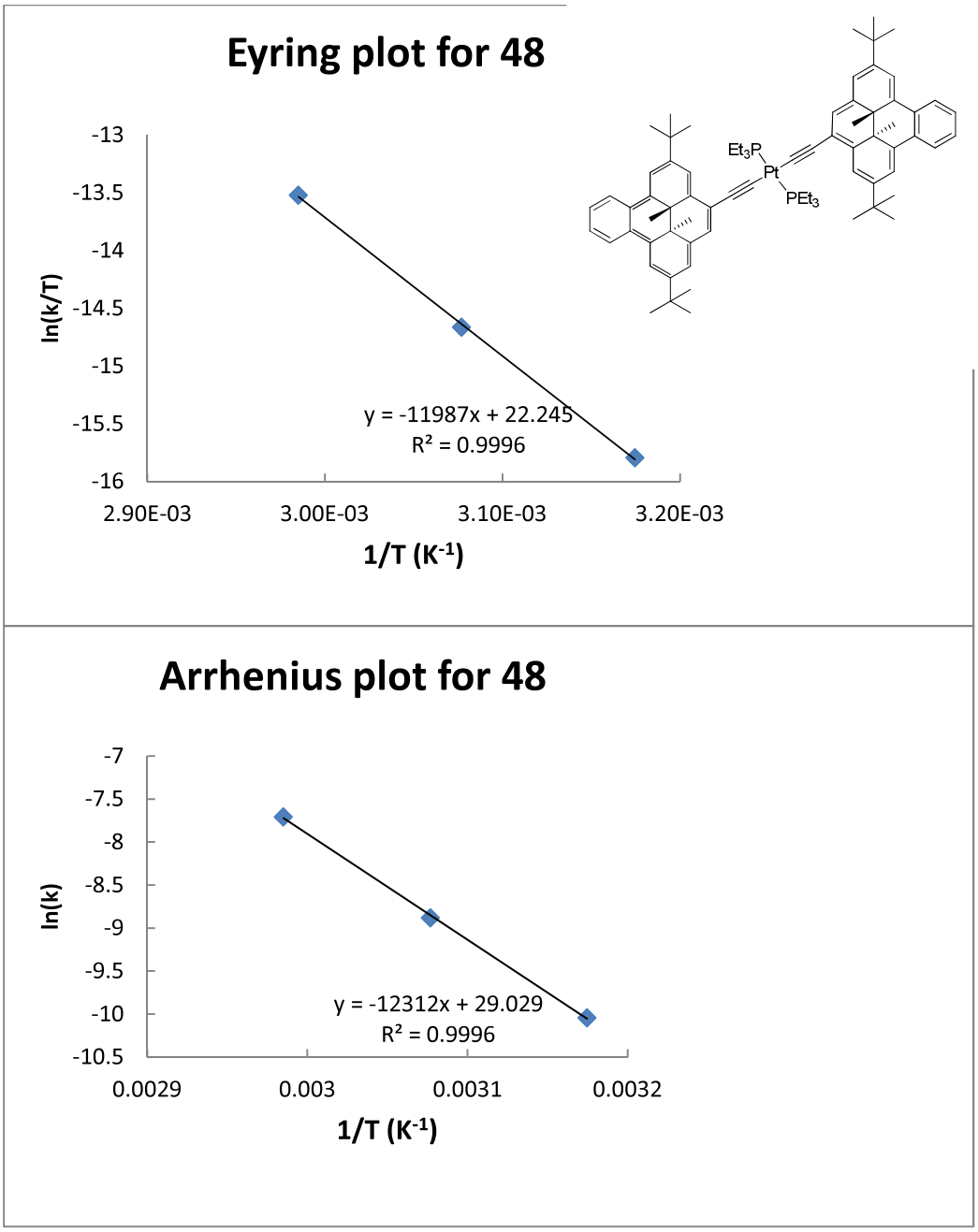

Eyring plot for 17
-12
-12.5
-13
-13.5
-14
-14.5
-15
-15.5
-16
ln(k/T)
y = -11506x + 21.022
R² = 0.9995
2.90E-03 2.95E-03 3.00E-03 3.05E-03 3.10E-03 3.15E-03 3.20E-03
1/T (K-1)
O

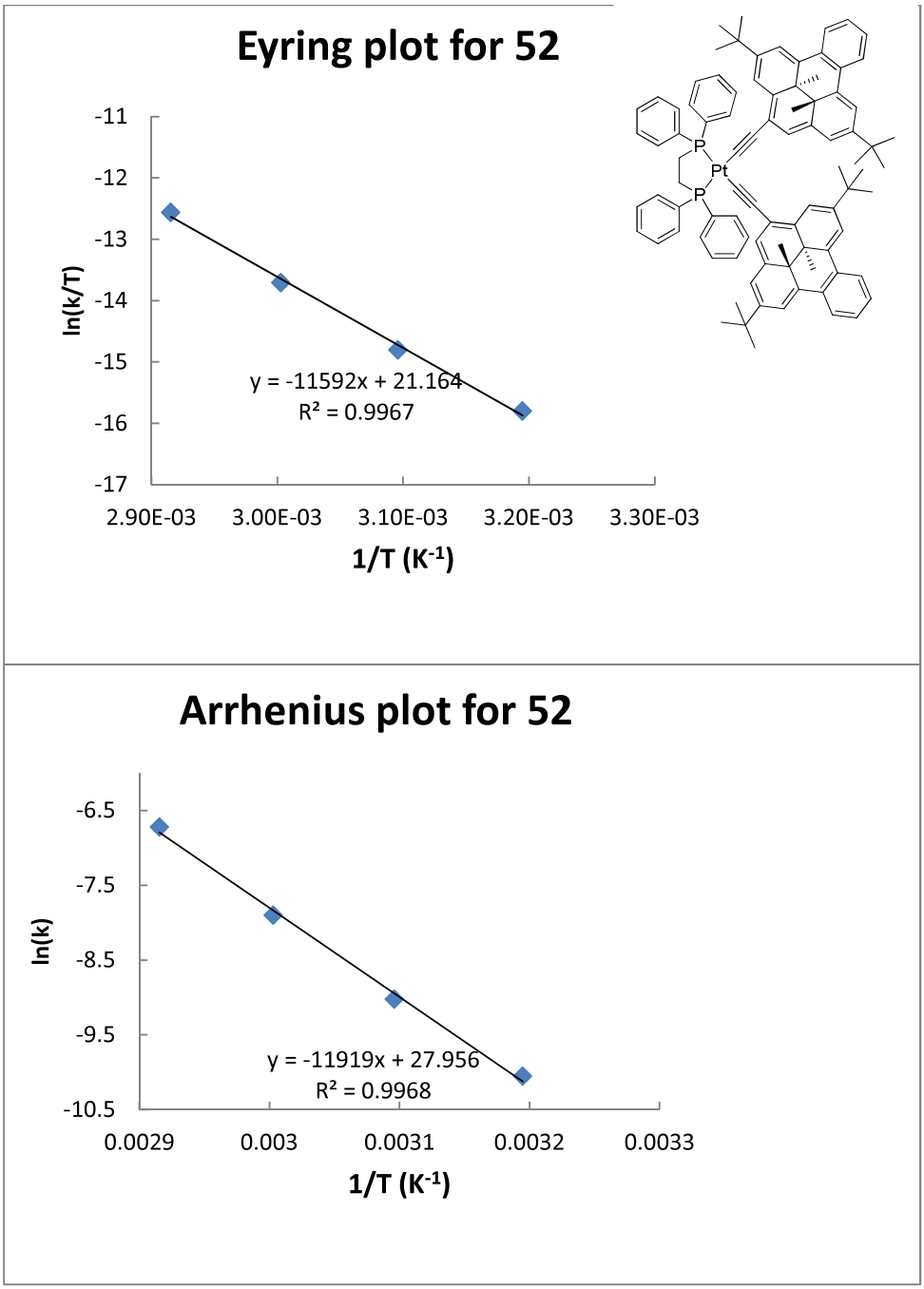

Arrhenius plot for 17
-6
-6.5
-7
-7.5
-8
-8.5
-9
-9.5
-10
ln(k)
y = -11833x + 27.813
R² = 0.9996
2.90E-03 2.95E-03 3.00E-03 3.05E-03 3.10E-03 3.15E-03 3.20E-03
1/T (K-1)

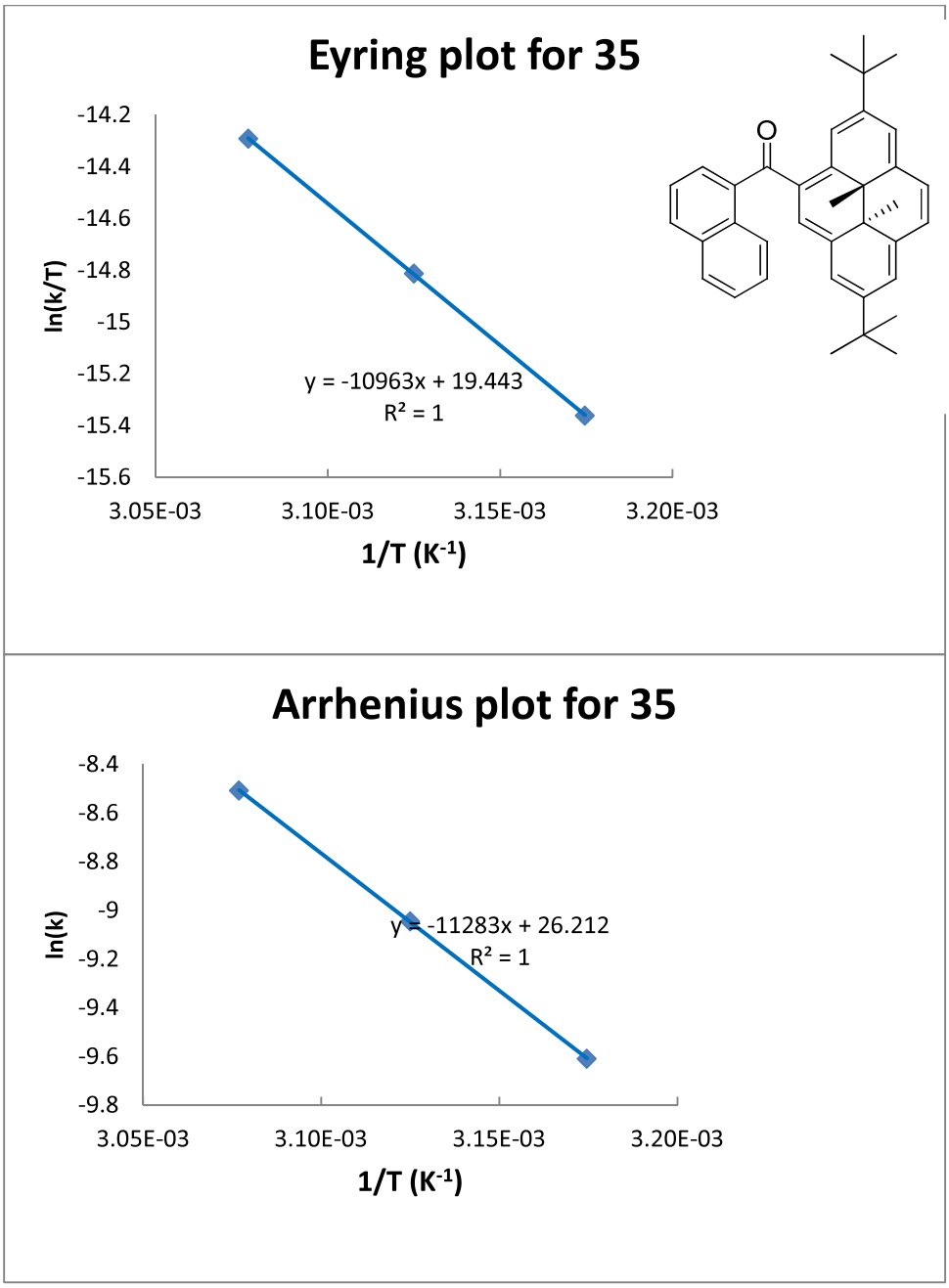

Eyring plot for 42
-12.5
-13
-13.5
-14
-14.5
-15
-15.5
ln(k/T)
y = -12030x + 23.253
R² = 0.9995
2.90E-03
3.00E-03
3.10E-03
3.20E-03
3.30E-03
1/T (K-1)
CF3
O
Arrhenius plot for 42
-6
-6.5
-7
-7.5
-8
-8.5
-9
-9.5
-10
ln(k)
y = -12353x + 30.029
R² = 0.9995
2.90E-03
3.00E-03
3.10E-03
3.20E-03
3.30E-03
1/T (K-1)

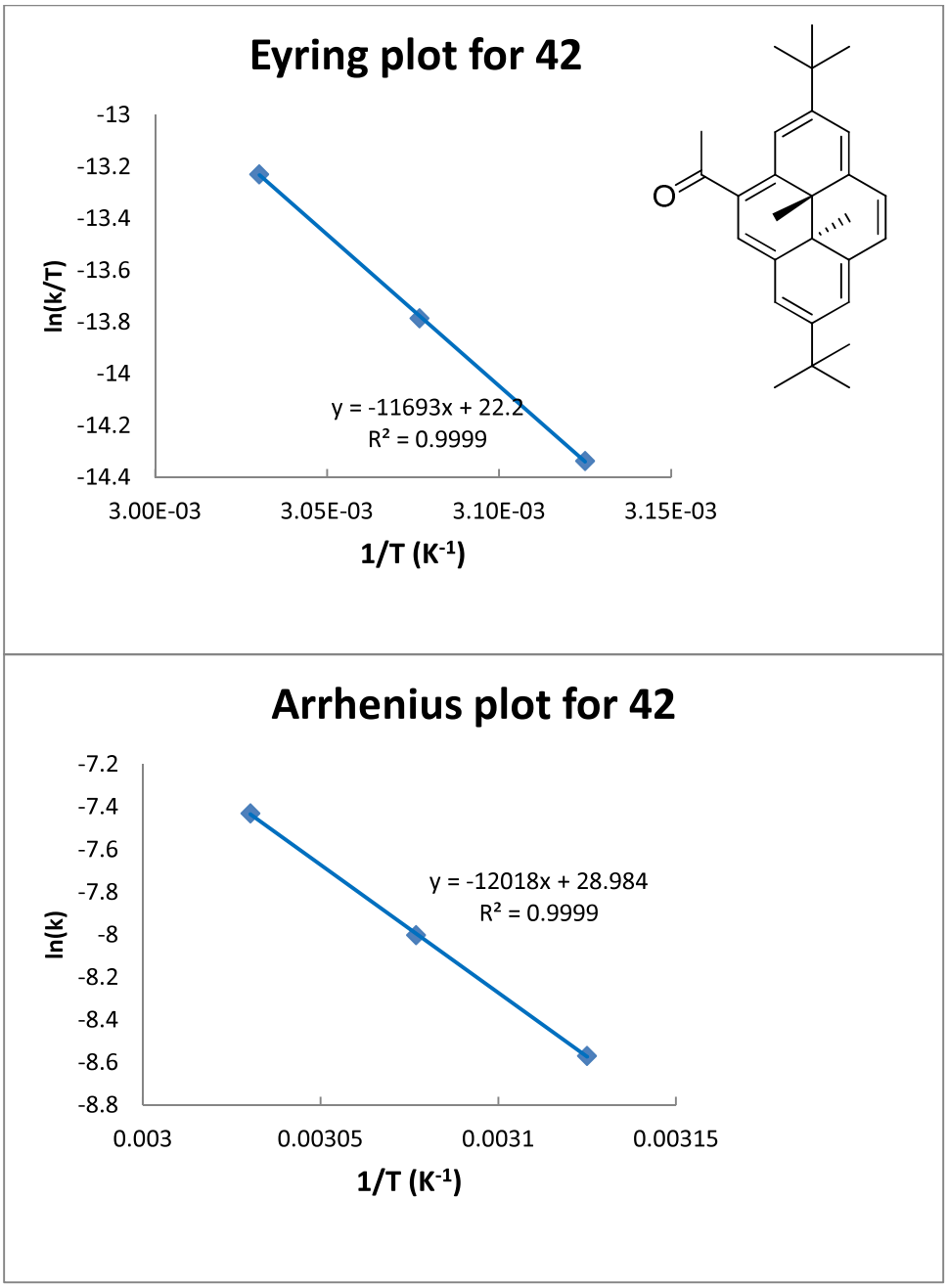

Eyring plot for 49
-13.5
-14
-14.5
-15
-15.5
-16
-16.5
ln(k/T)
y = -11864x + 21.924
R² = 0.9995
2.90E-03
3.00E-03
3.10E-03
3.20E-03
3.30E-03
1/T (K-1)
Ph3P
Pt
PPh3

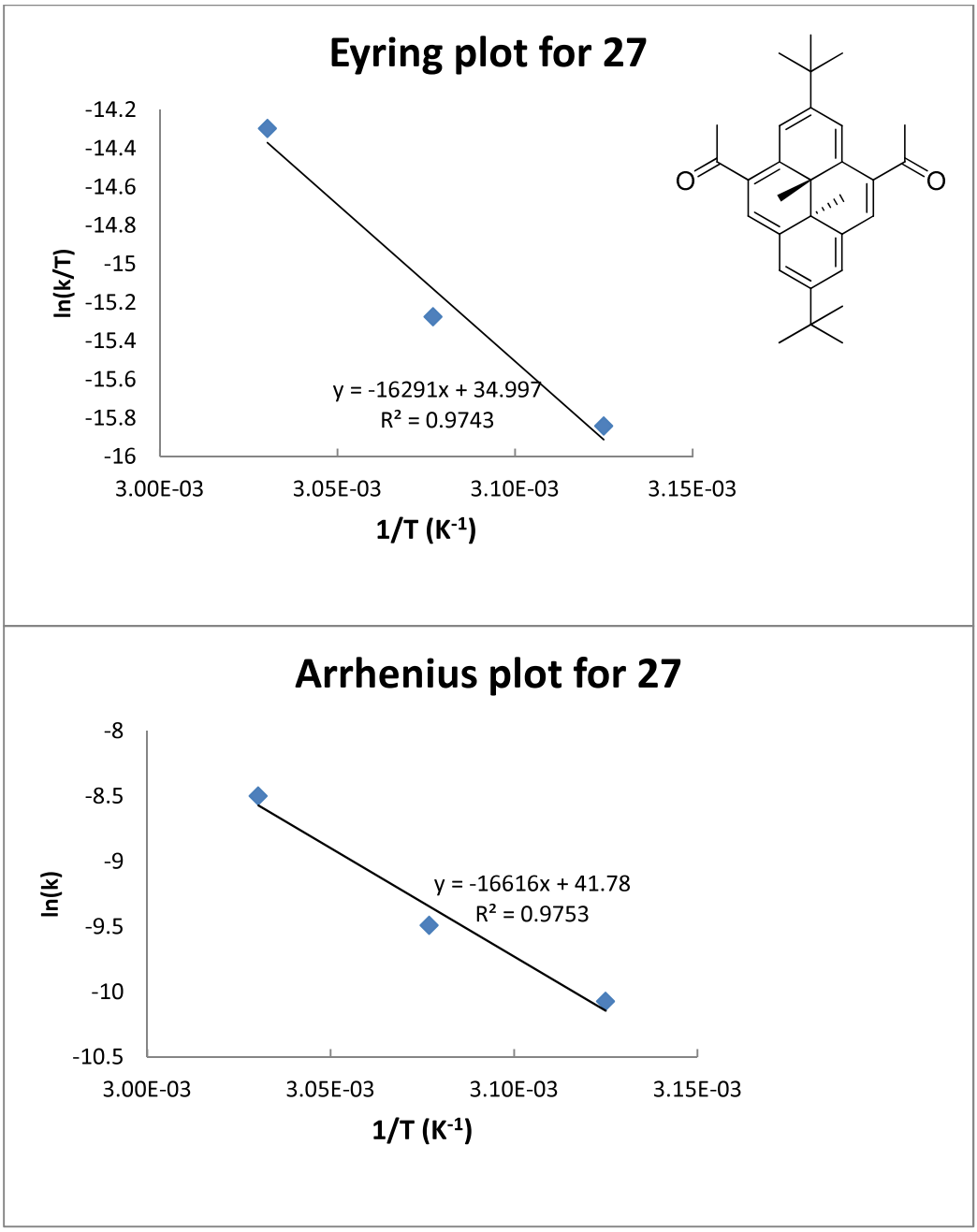

Arrhenius plot for 49
-7.5
-8
-8.5
-9
-9.5
-10
-10.5
ln(k)
y = -12187x + 28.701
R² = 0.9995
0.0029
0.003
0.0031
0.0032
0.0033
1/T (K-1)


Eyring plot for 48
ln(k/T)
-13
-13.5
-14
-14.5
-15
-15.5
-16
2.90E-03
3.00E-03
3.10E-03
3.20E-03
1/T (K-1)
y = -11987x + 22.245
R² = 0.9996
Et3P
Pt
PEt3
Arrhenius plot for 48
ln(k)
-7
-7.5
-8
-8.5
-9
-9.5
-10
-10.5
0.0029
0.003
0.0031
0.0032
1/T (K-1)
y = -12312x + 29.029
R² = 0.9996

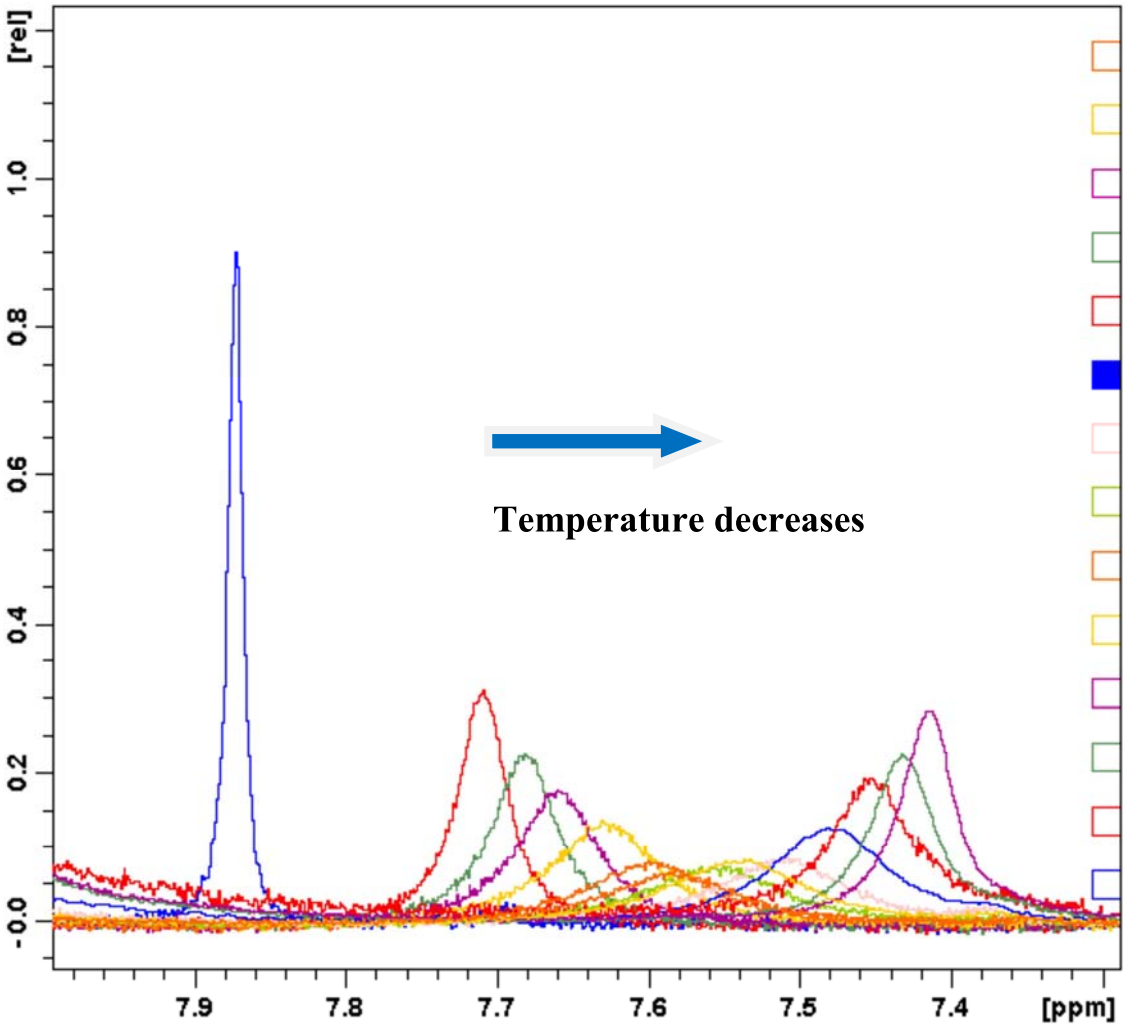

Eyring plot for 52
-11
-12
-13
-14
-15
-16
-17
ln(k/T)
y = -11592x + 21.164
R² = 0.9967
2.90E-03
3.00E-03
3.10E-03
3.20E-03
3.30E-03
1/T (K-1)
P
Pt
P
Arrhenius plot for 52
-6.5
-7.5
-8.5
-9.5
-10.5
ln(k)
y = -11919x + 27.956
R² = 0.9968
0.0029
0.003
0.0031
0.0032
0.0033
1/T (K-1)

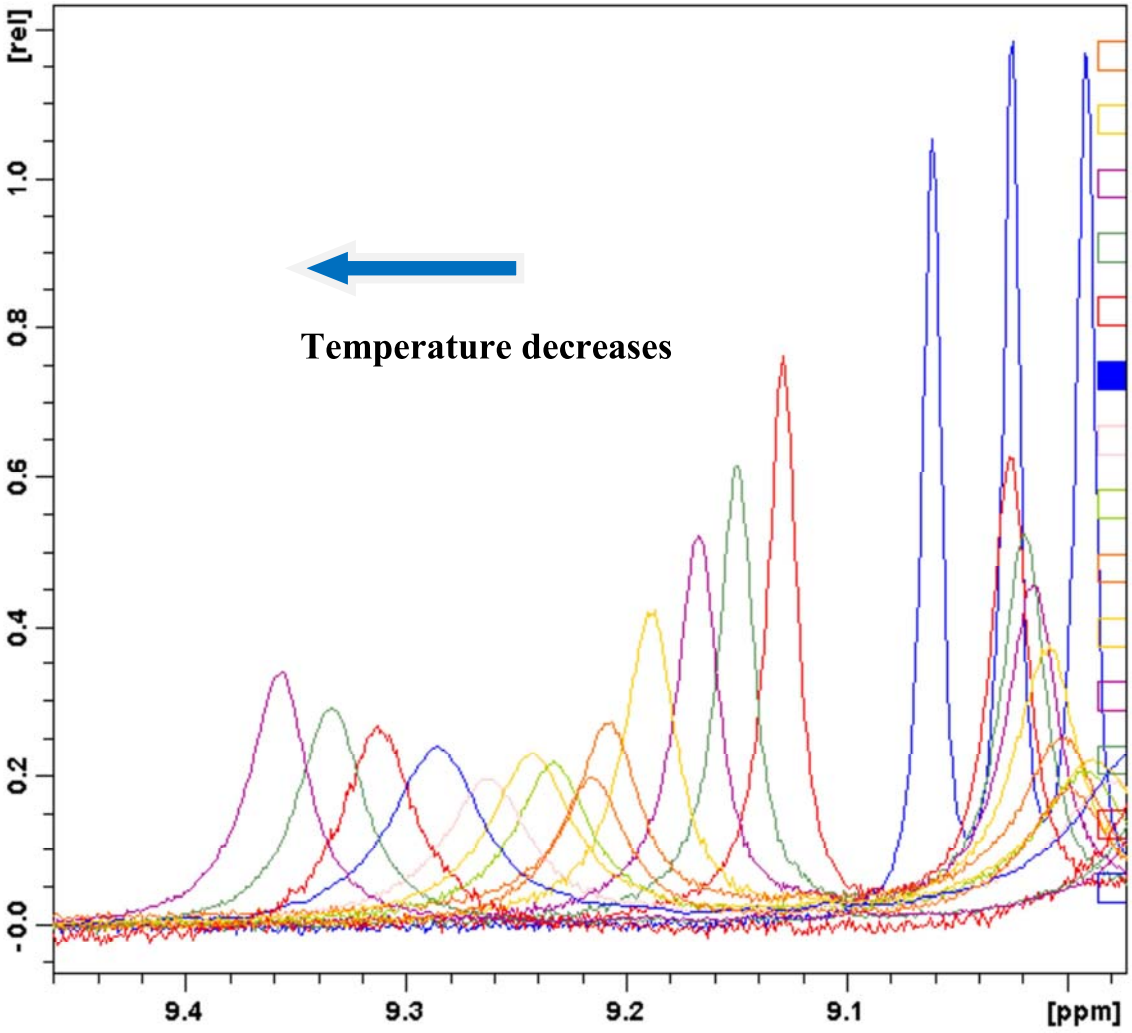

Eyring plot for 35
-14.2
-14.4
-14.6
-14.8
-15
-15.2
-15.4
-15.6
ln(k/T)
y = -10963x + 19.443
R² = 1
3.05E-03
3.10E-03
3.15E-03
3.20E-03
1/T (K-1)
O
Arrhenius plot for 35
-8.4
-8.6
-8.8
-9
-9.2
-9.4
-9.6
-9.8
ln(k)
y = -11283x + 26.212
R² = 1
3.05E-03
3.10E-03
3.15E-03
3.20E-03
1/T (K-1)

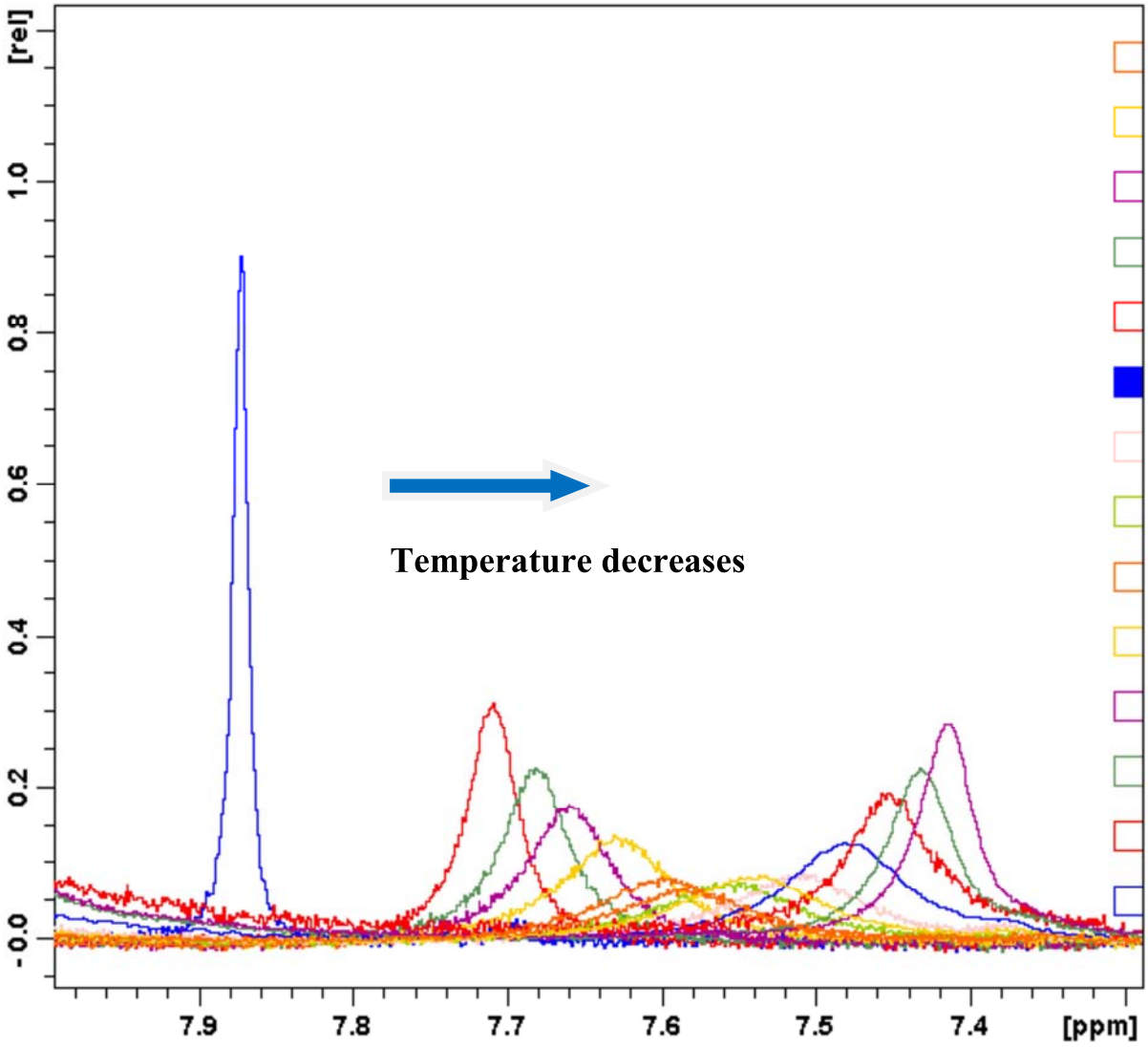

Eyring plot for 42
-13
-13.2
-13.4
-13.6
-13.8
-14
-14.2
-14.4
ln(k/T)
y = -11693x + 22.2
R² = 0.9999
3.00E-03
3.05E-03
3.10E-03
3.15E-03
1/T (K-1)
O
Arrhenius plot for 42
-7.2
-7.4
-7.6
-7.8
-8
-8.2
-8.4
-8.6
-8.8
ln(k)
y = -12018x + 28.984
R² = 0.9999
0.003
0.00305
0.0031
0.00315
1/T (K-1)

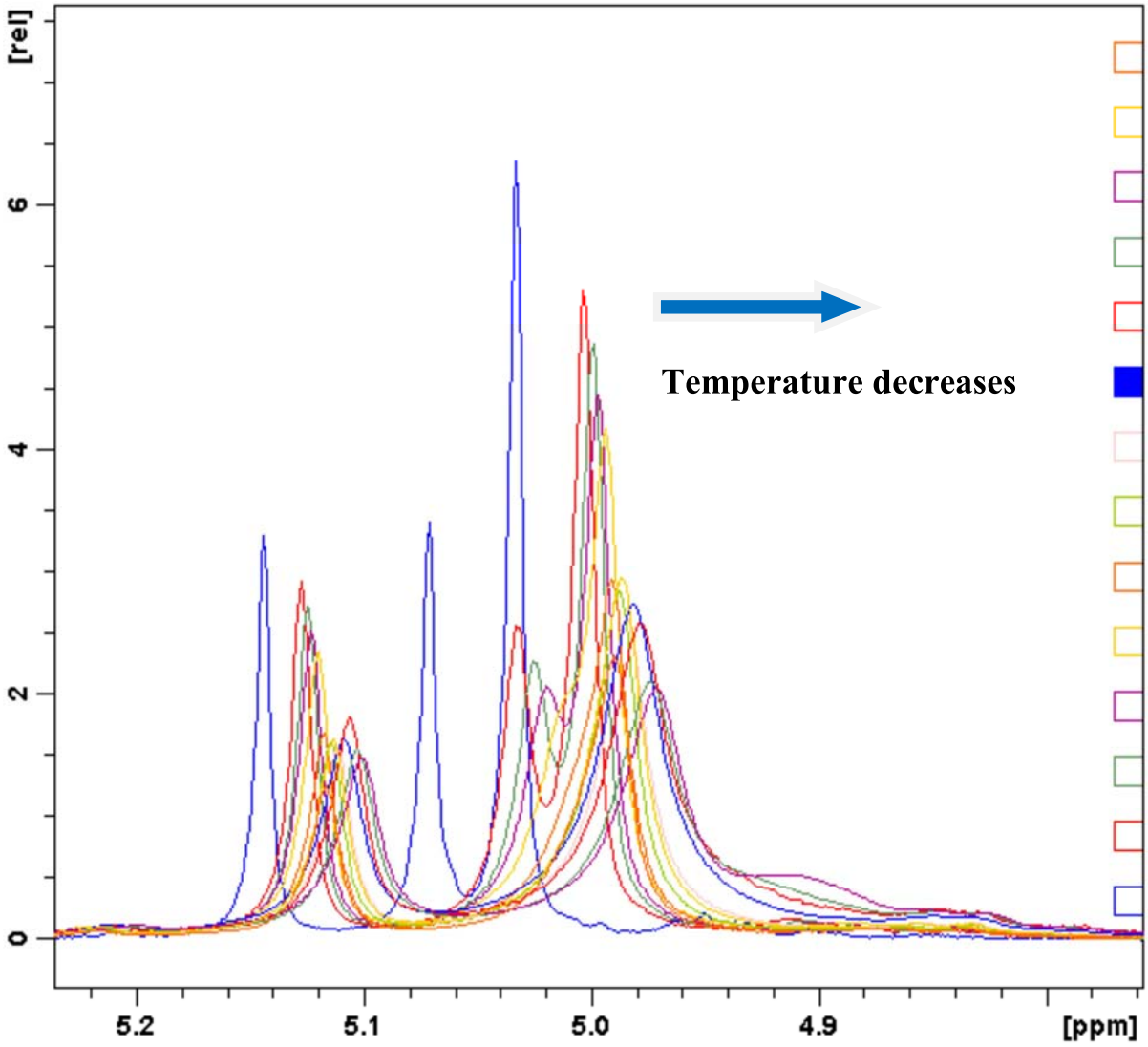

Eyring plot for 27
-14.2
-14.4
-14.6
-14.8
-15
-15.2
-15.4
-15.6
-15.8
-16
ln(k/T)
y = -16291x + 34.997
R² = 0.9743
3.00E-03
3.05E-03
3.10E-03
3.15E-03
1/T (K-1)
O
O
Arrhenius plot for 27
-8
-8.5
-9
-9.5
-10
-10.5
ln(k)
y = -16616x + 41.78
R² = 0.9753
3.00E-03
3.05E-03
3.10E-03
3.15E-03
1/T (K-1)

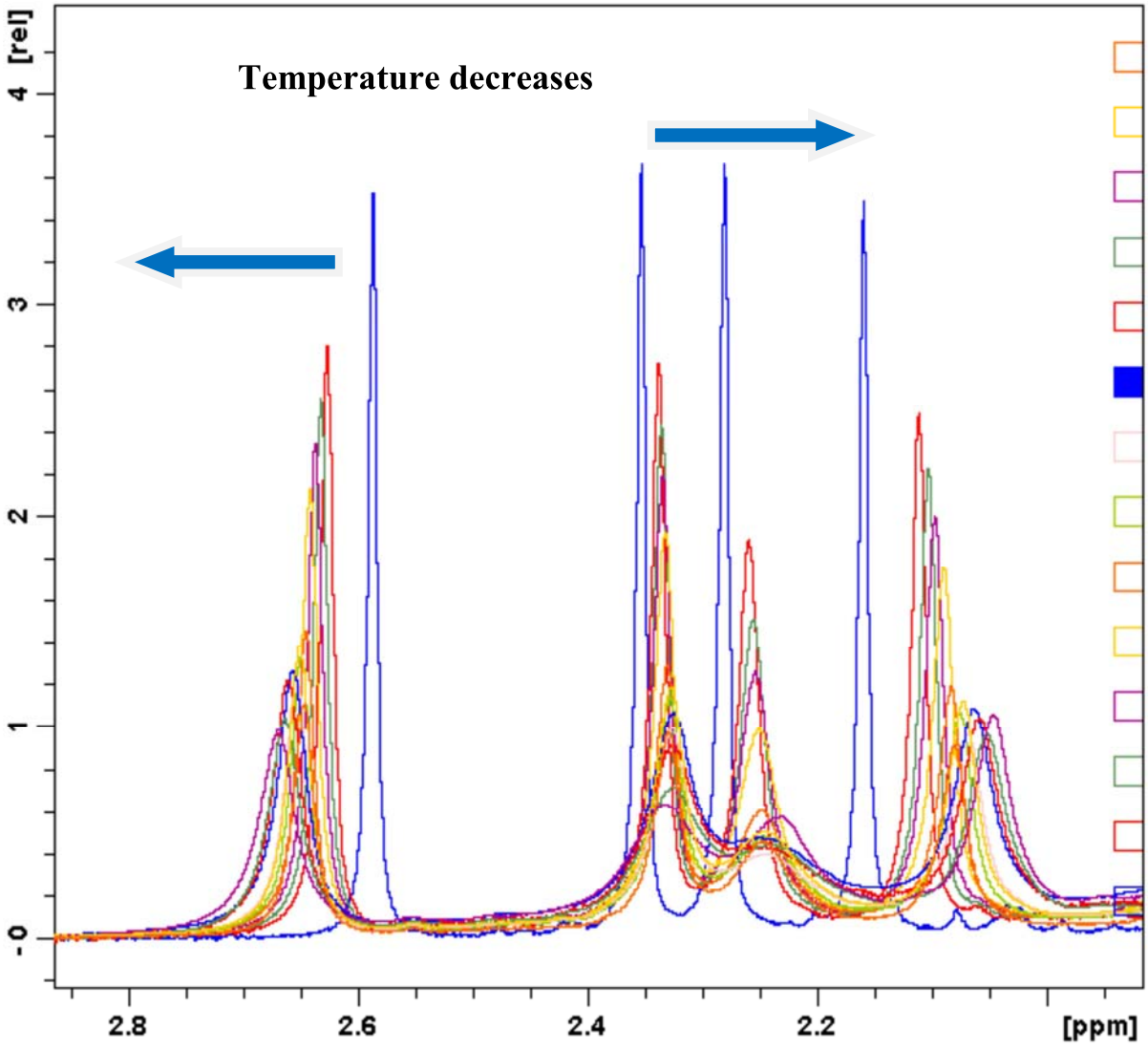
Appendix III. VT NMR plots for 21

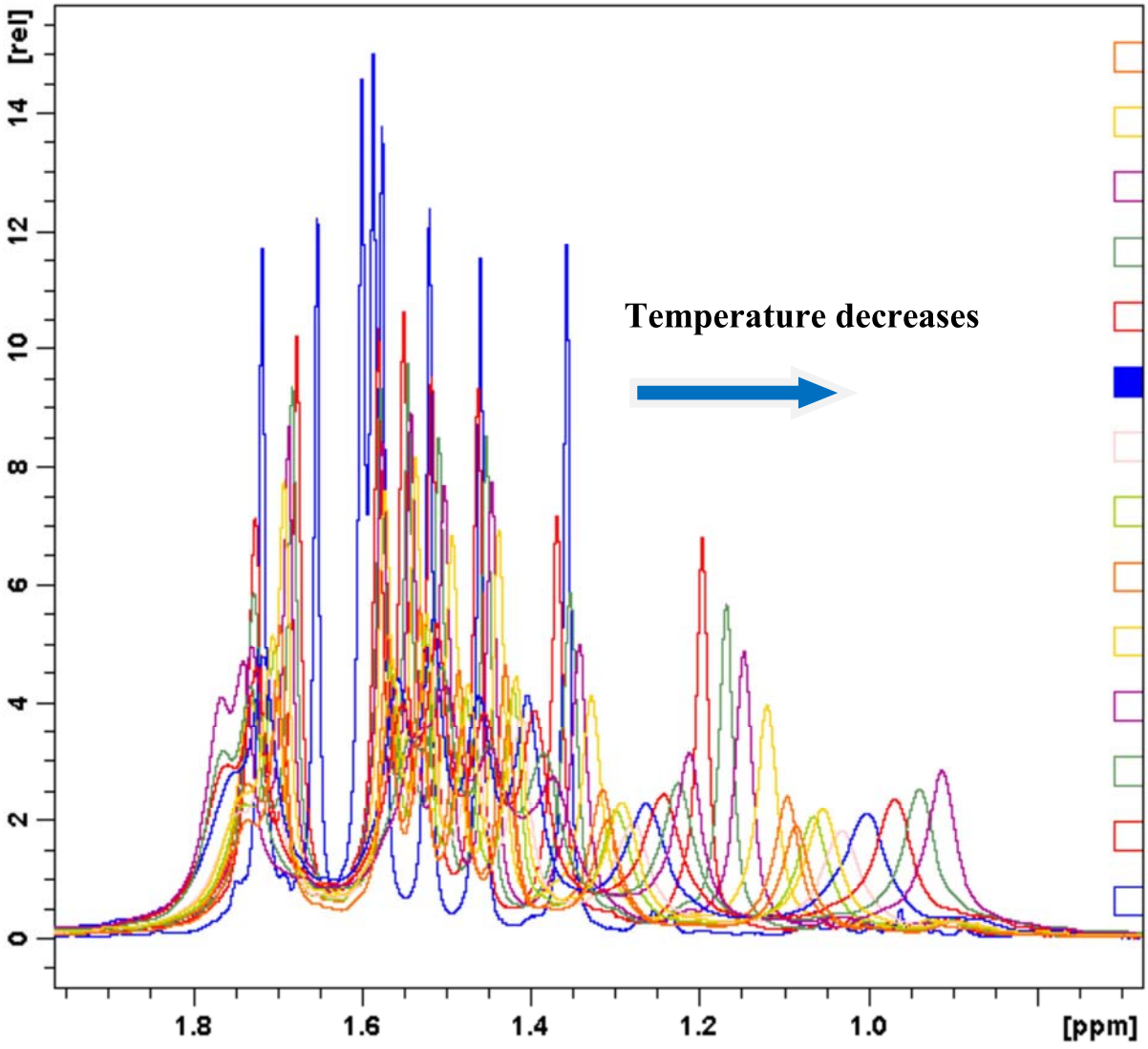


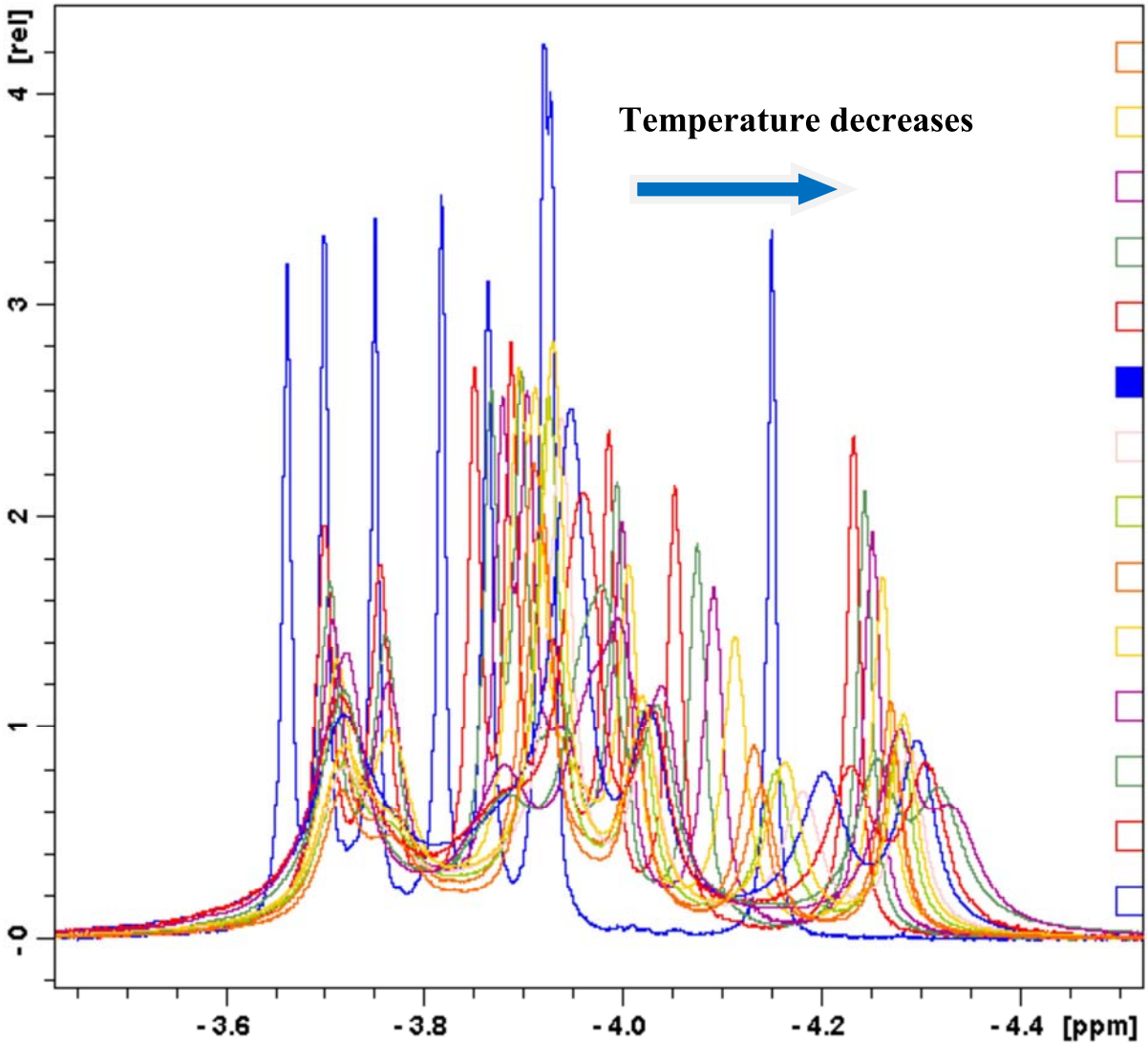

[rel]
1.0
0.8
0.6
0.4
0.2
-0.0
Temperature decreases
9.4
9.3
9.2
9.1
[ppm]


[rel]
1.0
0.8
0.6
0.4
0.2
-0.0
Temperature decreases
7.9
7.8
7.7
7.6
7.5
7.4
[ppm]


[rel]
6
4
2
0
Temperature decreases
5.2
5.1
5.0
4.9
[ppm]


Temperature decreases
4 [rel]
3
2
1
-0
2.8
2.6
2.4
2.2
[ppm]


[rel]
14
12
10
8
6
4
2
0
Temperature decreases
1.8
1.6
1.4
1.2
1.0
[ppm]


Temperature decreases
4 [rel]
3
2
1
-0
-3.6
-3.8
-4.0
-4.2
-4.4 [ppm]

Appendix IV. CSD Histogram Plot

1) Data for $(R_3P)_2Pt(C{\equiv}CDHPs)_2$ (6 pages) 318-324

Distances: Pt-C, Pt-P, C1-C2, C2-C3,

Angle: Ar-Sqp, Ar-Ar

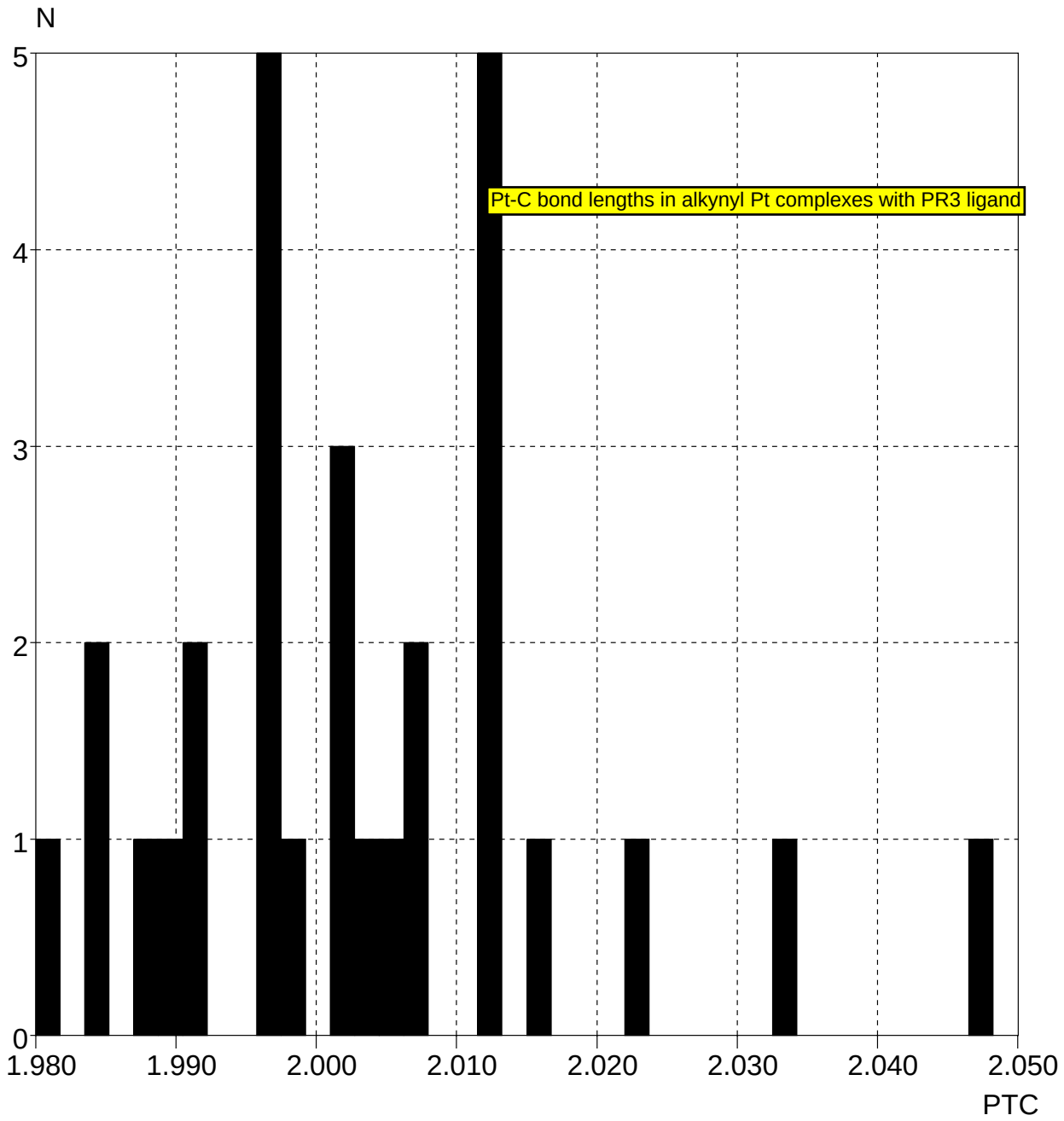
2) Data for $(Ar_3P)_2Pt(C{\equiv}CDHPs)_2$ (6 pages) 325-331

3) Data for (dppe)Pt$(C{\equiv}CDHPs)_2$ (6 pages) 332-338

4) Cobalt C-C bond lengths (2 pages) 339-340

5) Tropone C-O bond lengths (2 pages) 341-342

PTC

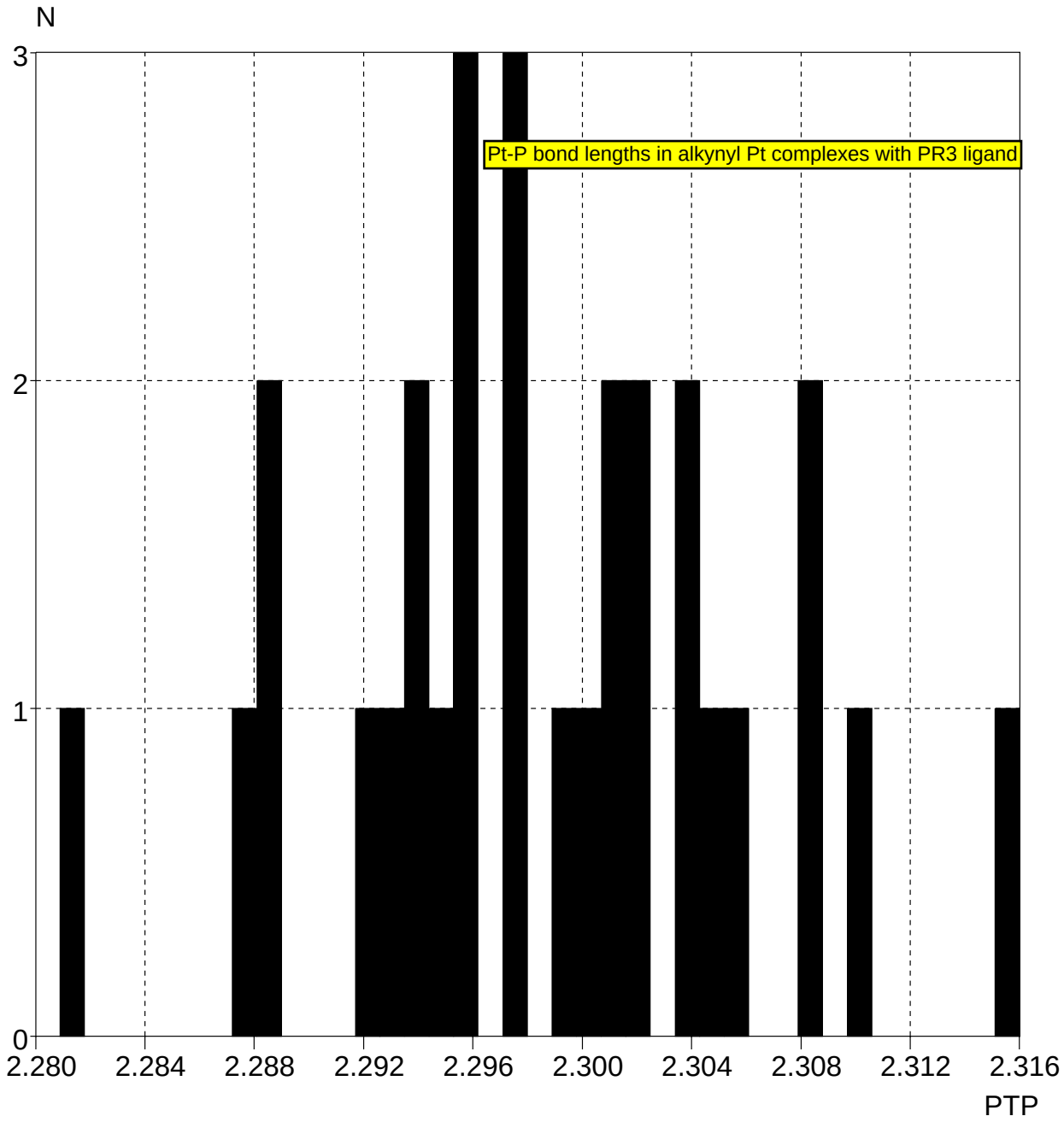


Plot Data
File=cq_temp4
Test=4
Tot.Obs.=29
Obs.=29
Supp.=0

X-axis
Min.=1.981
Max.=2.047
Range=0.066
Mean=2.003
Mean SE=0.003
Sample SD=0.015

Histogram
Median=2.001
Skew=0.969
Quantile=10.000
LQ=1.985
HQ=2.023
Bin Width=0.002
Max. Bin =5.000

PTP

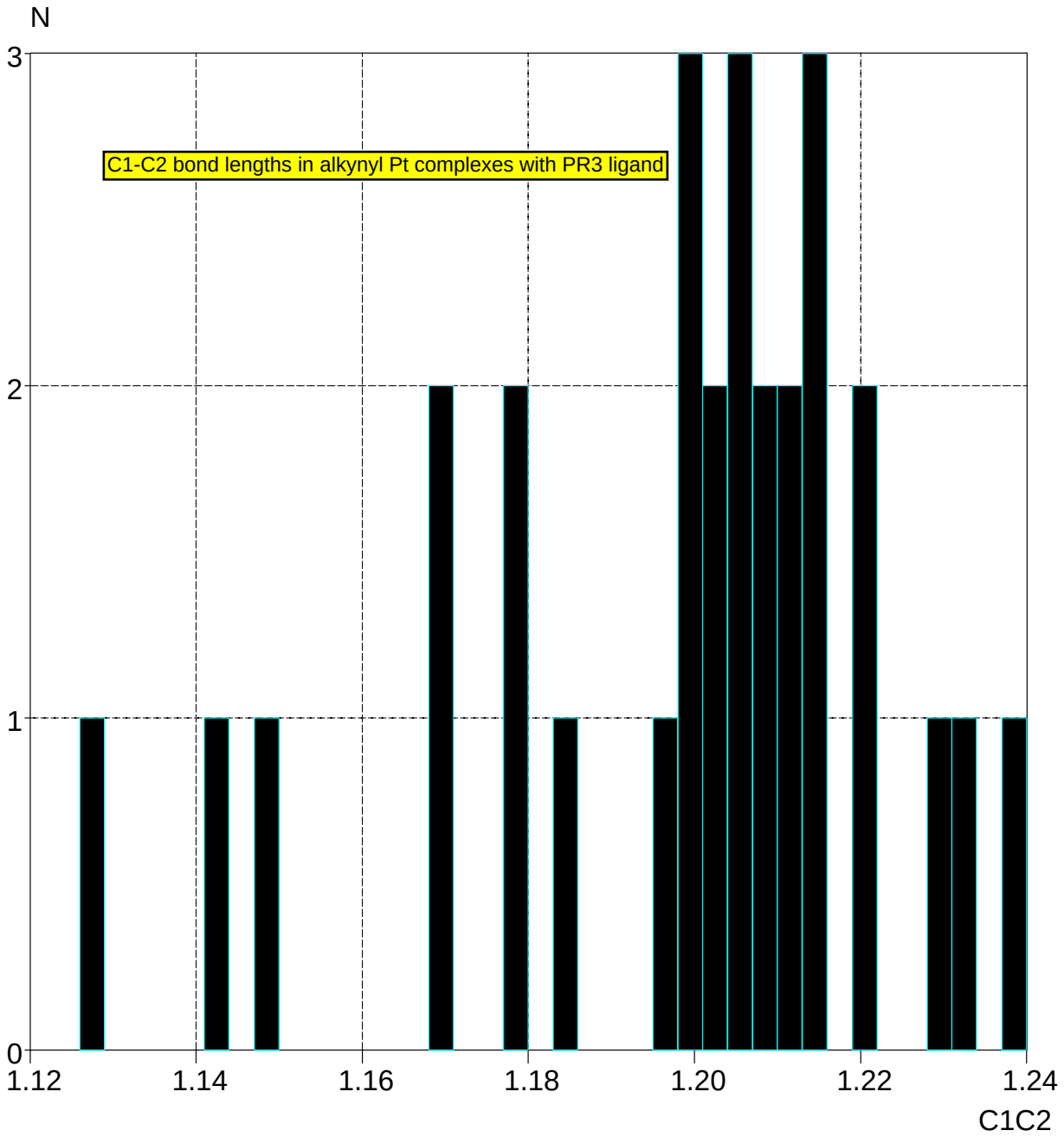


Plot Data
File=cq_temp4
Test=4
Tot.Obs.=29
Obs.=29
Supp.=0

X-axis
Min.=2.281
Max.=2.316
Range=0.035
Mean=2.299
Mean SE=0.001
Sample SD=0.007

Histogram
Median=2.298
Skew=-0.021
Quantile=10.000
LQ=2.288
HQ=2.308
Bin Width=0.001
Max. Bin =3.000

C1C2

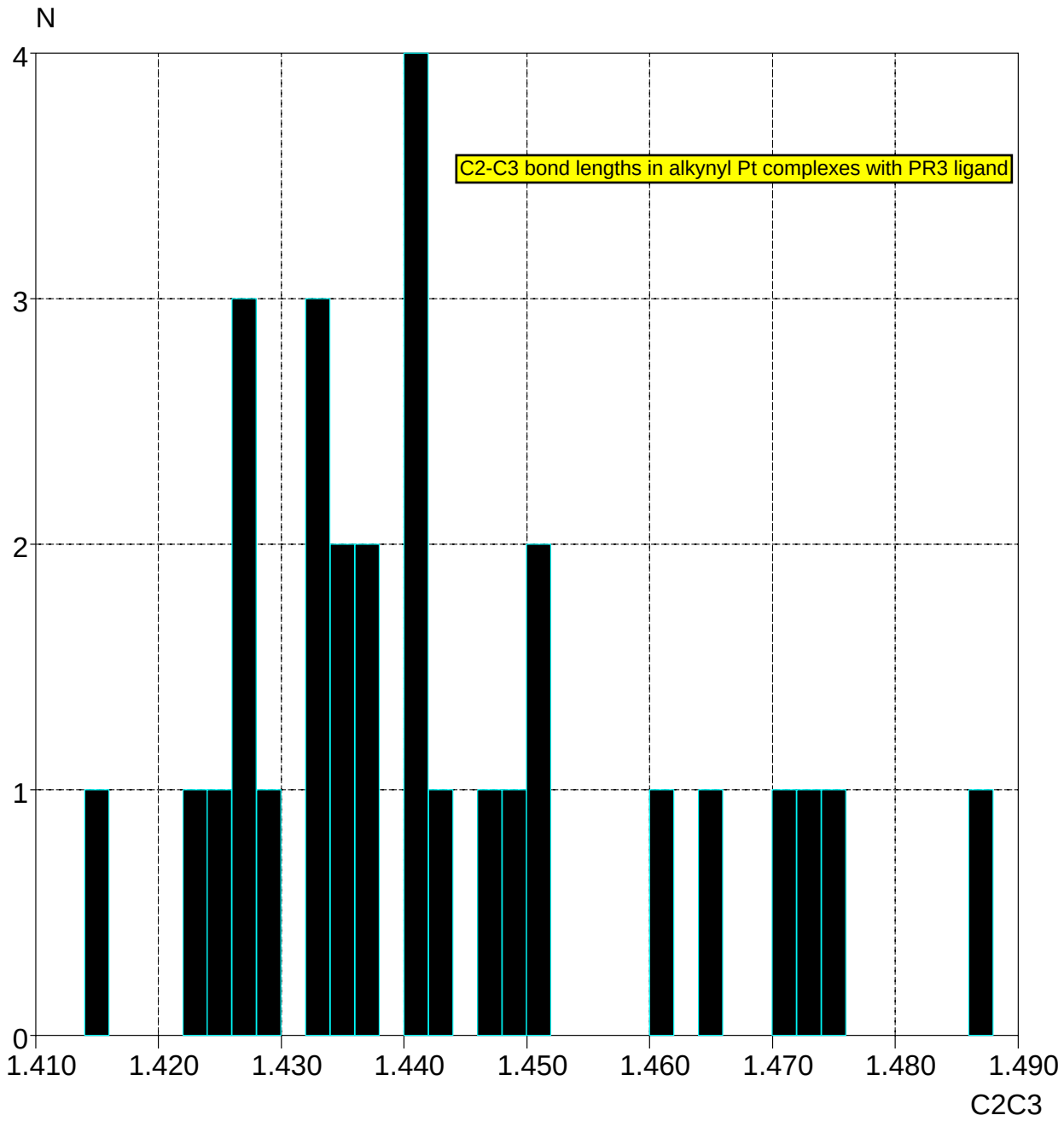


Plot Data
File=cq_temp4
Test=4
Tot.Obs.=29
Obs.=29
Supp.=0

X-axis
Min.=1.128
Max.=1.239
Range=0.111
Mean=1.198
Mean SE=0.005
Sample SD=0.026

Histogram
Median=1.205
Skew=-0.960
Quantile=10.000
LQ=1.143
HQ=1.230
Bin Width=0.003
Max. Bin =3.000

C2C3

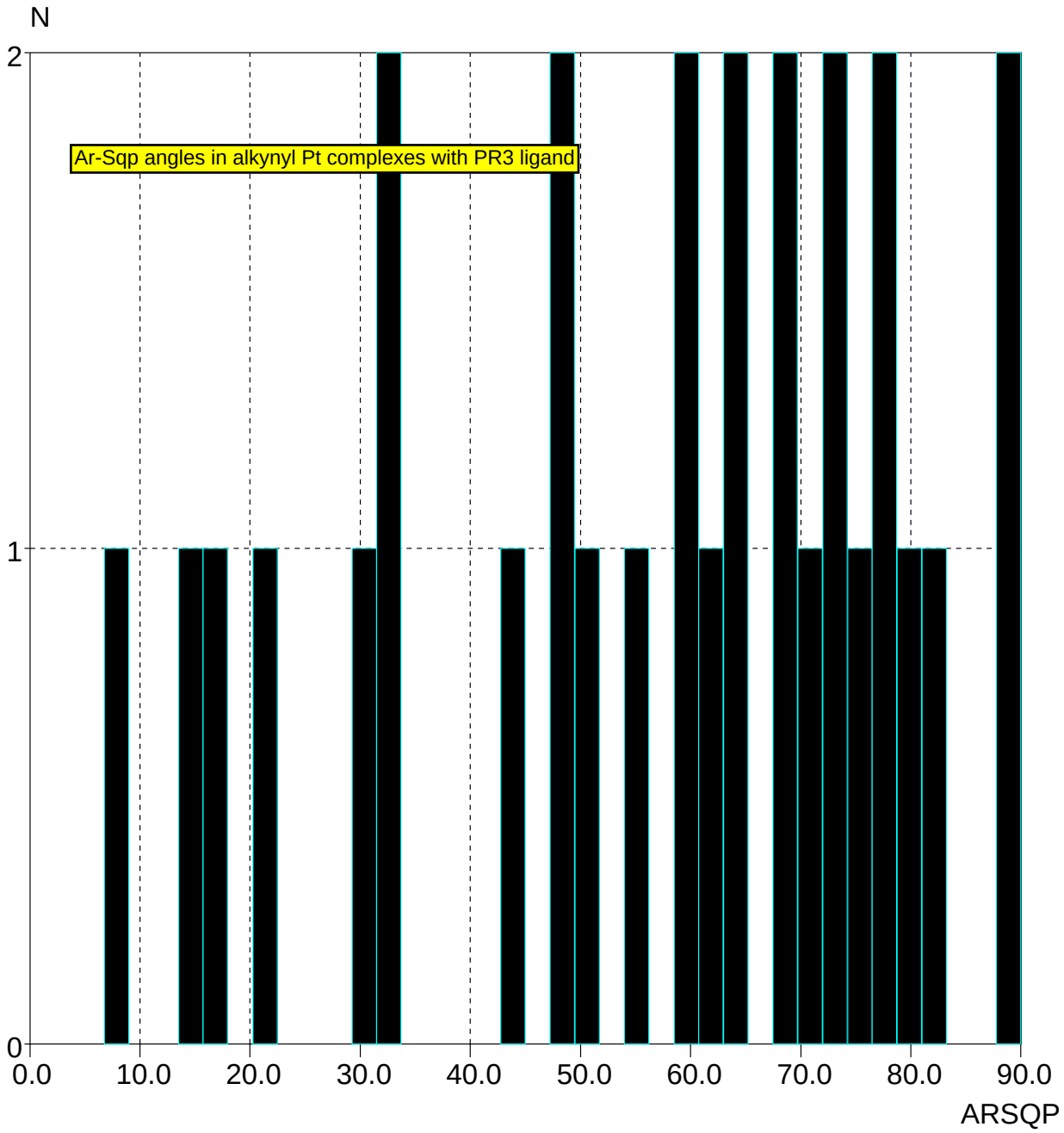


Plot Data
File=cq_temp4
Test=4
Tot.Obs.=29
Obs.=29
Supp.=0

X-axis
Min.=1.414
Max.=1.487
Range=0.073
Mean=1.443
Mean SE=0.003
Sample SD=0.018

Histogram
Median=1.440
Skew=0.797
Quantile=10.000
LQ=1.422
HQ=1.474
Bin Width=0.002
Max. Bin =4.000

ARSQP

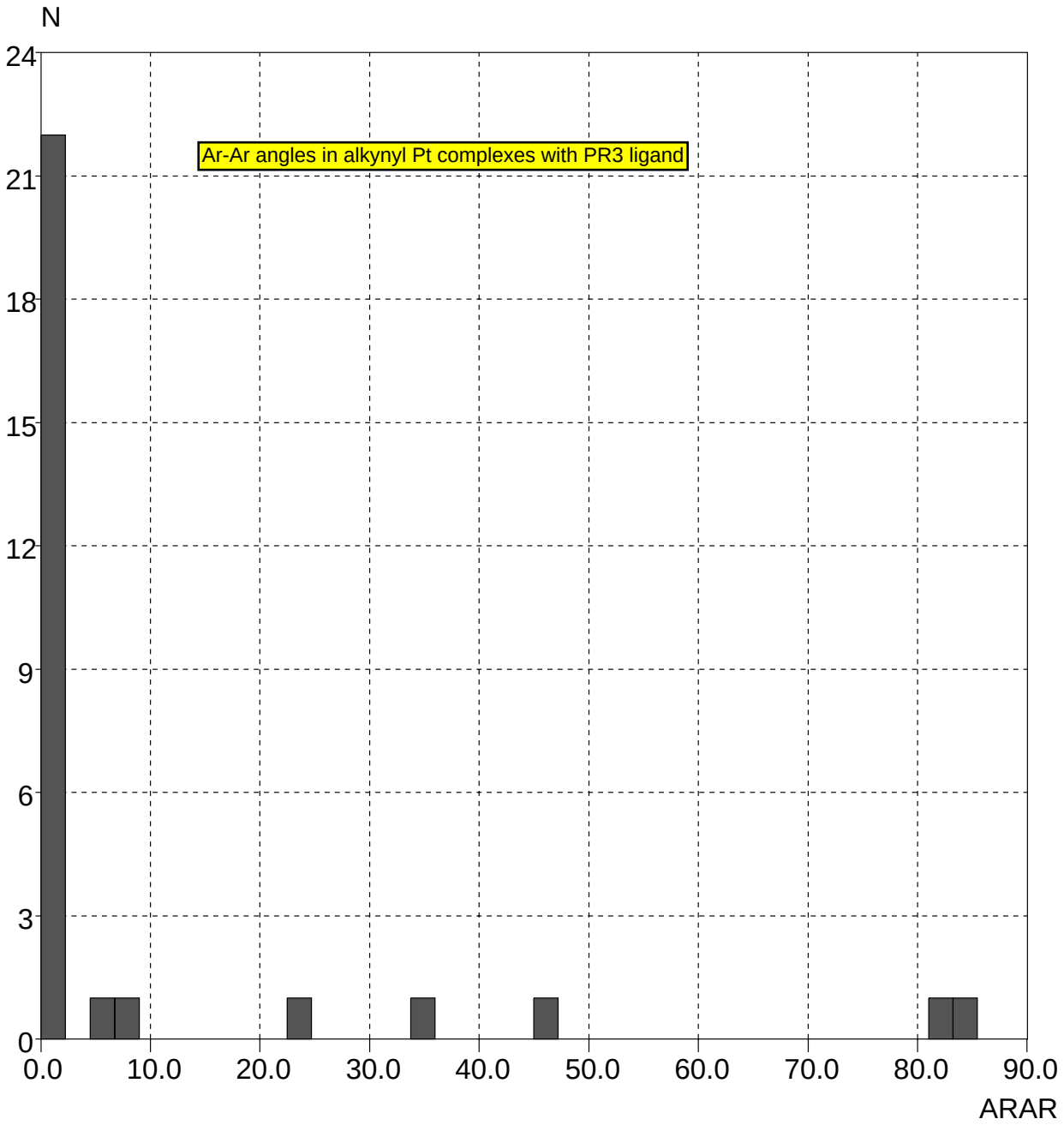


Plot Data
File=cq_temp4
Test=4
Tot.Obs.=29
Obs.=29
Supp.=0

X-axis
Min.=8.836
Max.=89.630
Range=80.794
Mean=56.535
Mean SE=4.289
Sample SD=23.095

Histogram
Median=62.674
Skew=-0.566
Quantile=10.000
LQ=13.702
HQ=82.913
Bin Width=2.250
Max. Bin =2.000

ARAR

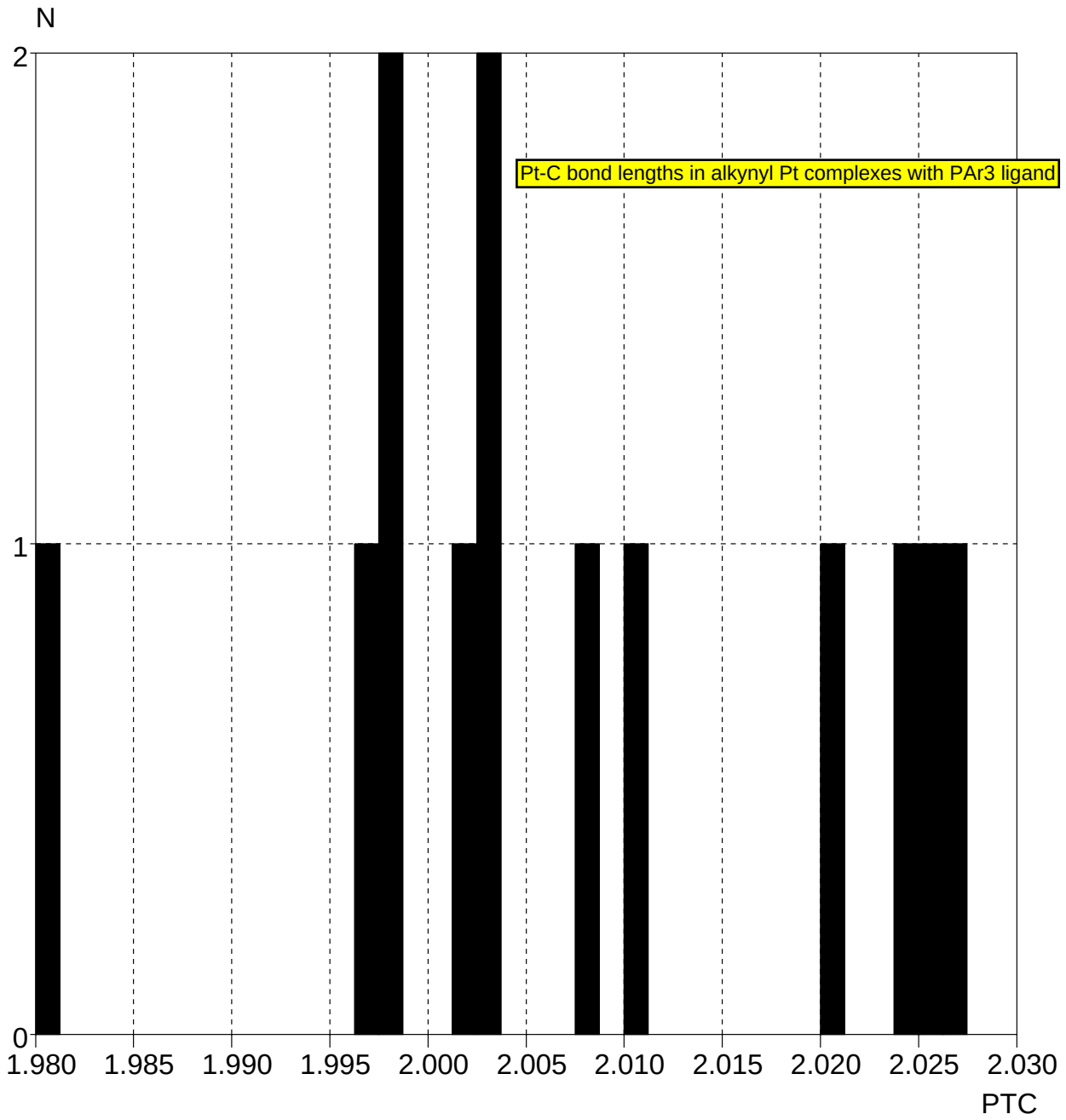


Plot Data
File=cq_temp4
Test=4
Tot.Obs.=29
Obs.=29
Supp.=0

X-axis
Min.=0.000
Max.=85.049
Range=85.049
Mean=9.786
Mean SE=4.296
Sample SD=23.133

Histogram
Median=0.020
Skew=2.323
Quantile=10.000
LQ=0.000
HQ=45.868
Bin Width=2.250
Max. Bin =22.000

PTC

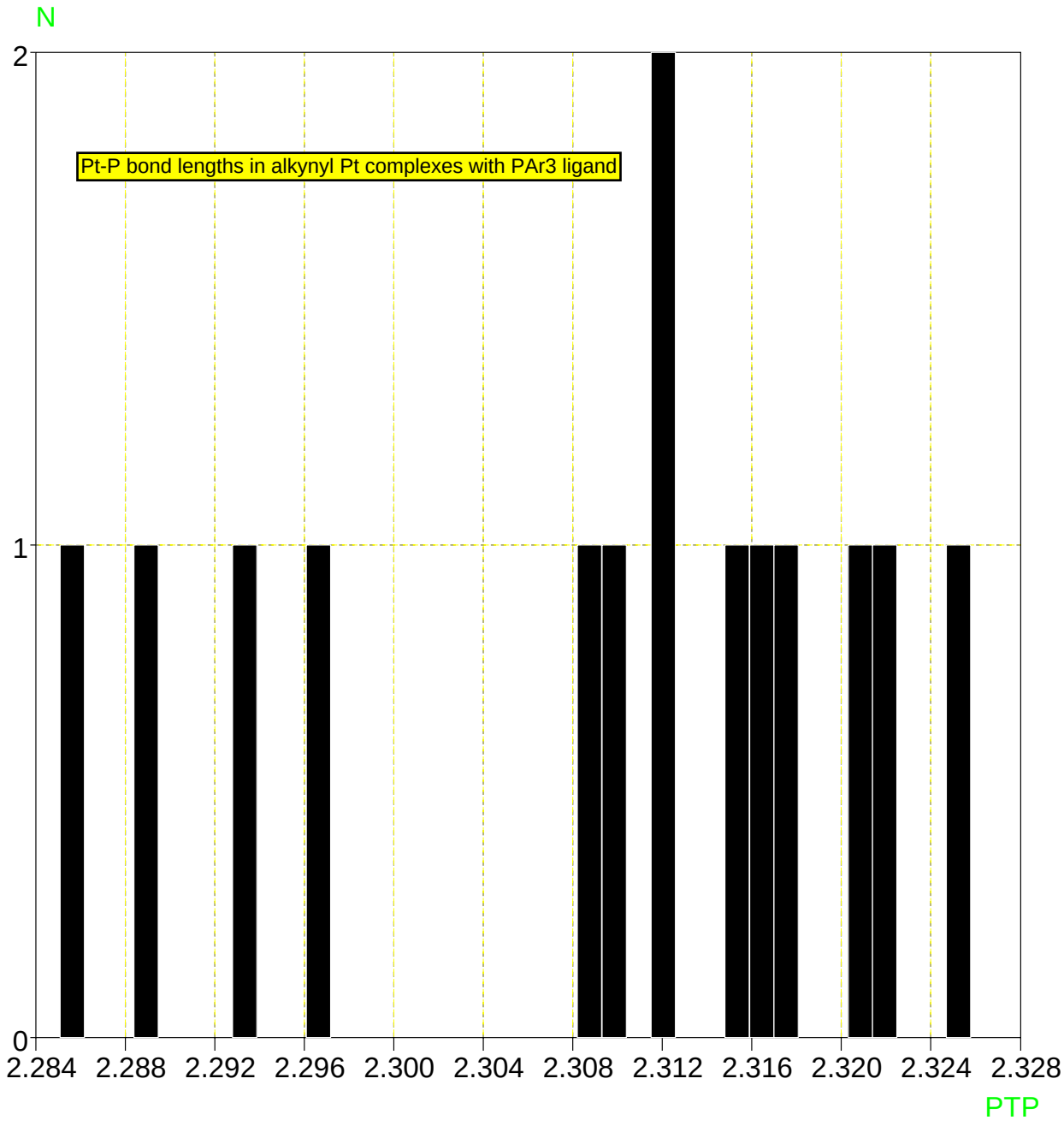


Plot Data
File=cq_temp2
Test=4
Tot.Obs.=14
Obs.=13
Supp.=1

X-axis
Min.=1.981
Max.=2.027
Range=0.046
Mean=2.008
Mean SE=0.004
Sample SD=0.014

Histogram
Median=2.003
Skew=-0.071
Quantile=10.000
LQ=1.981
HQ=2.025
Bin Width=0.001
Max. Bin =2.000

PTP

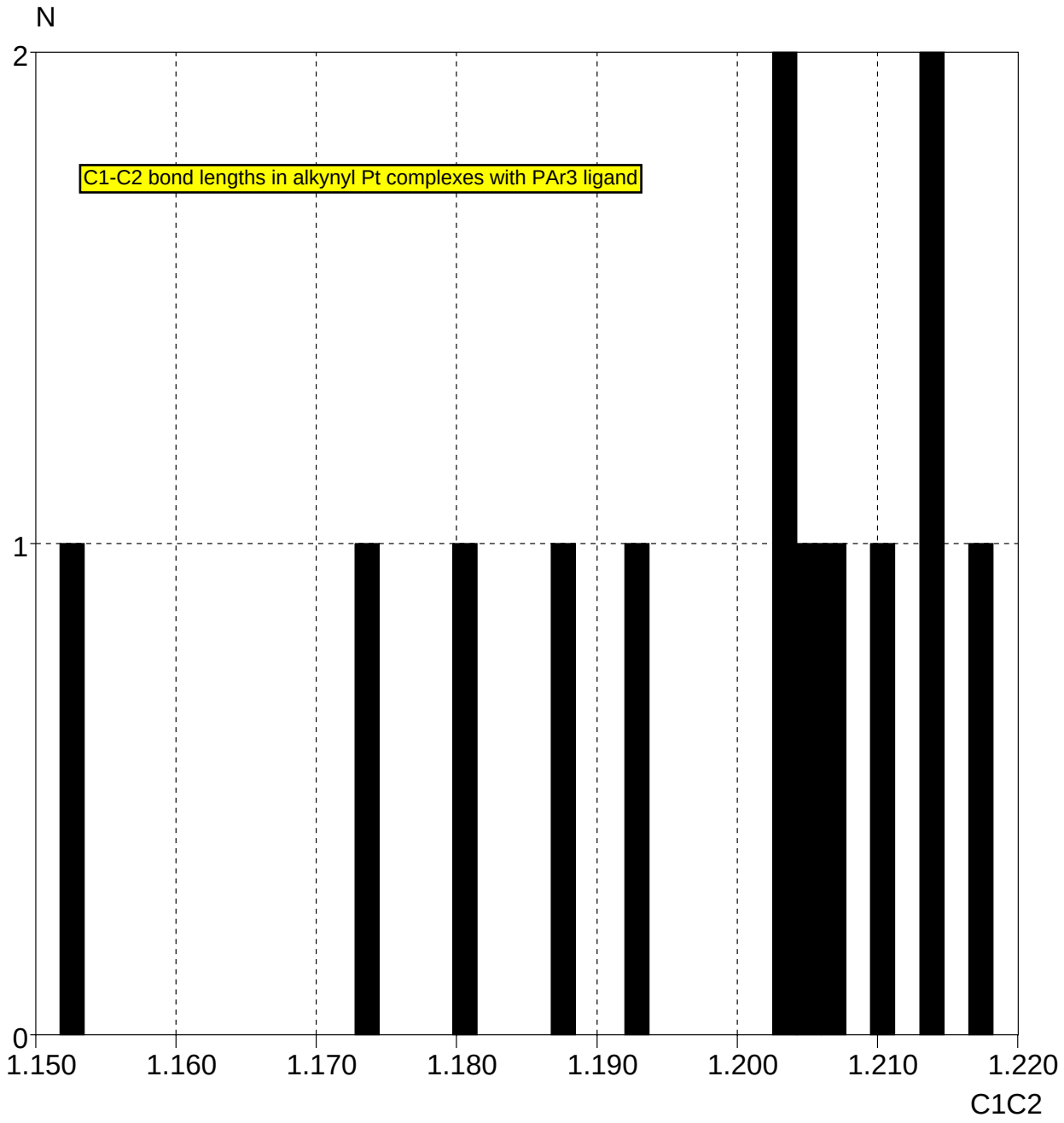


Plot Data
File=cq_temp2
Test=4
Tot.Obs.=14
Obs.=14
Supp.=0

X-axis
Min.=2.286
Max.=2.325
Range=0.039
Mean=2.309
Mean SE=0.003
Sample SD=0.013

Histogram
Median=2.312
Skew=-0.570
Quantile=10.000
LQ=2.286
HQ=2.322
Bin Width=0.001
Max. Bin =2.000

C1C2

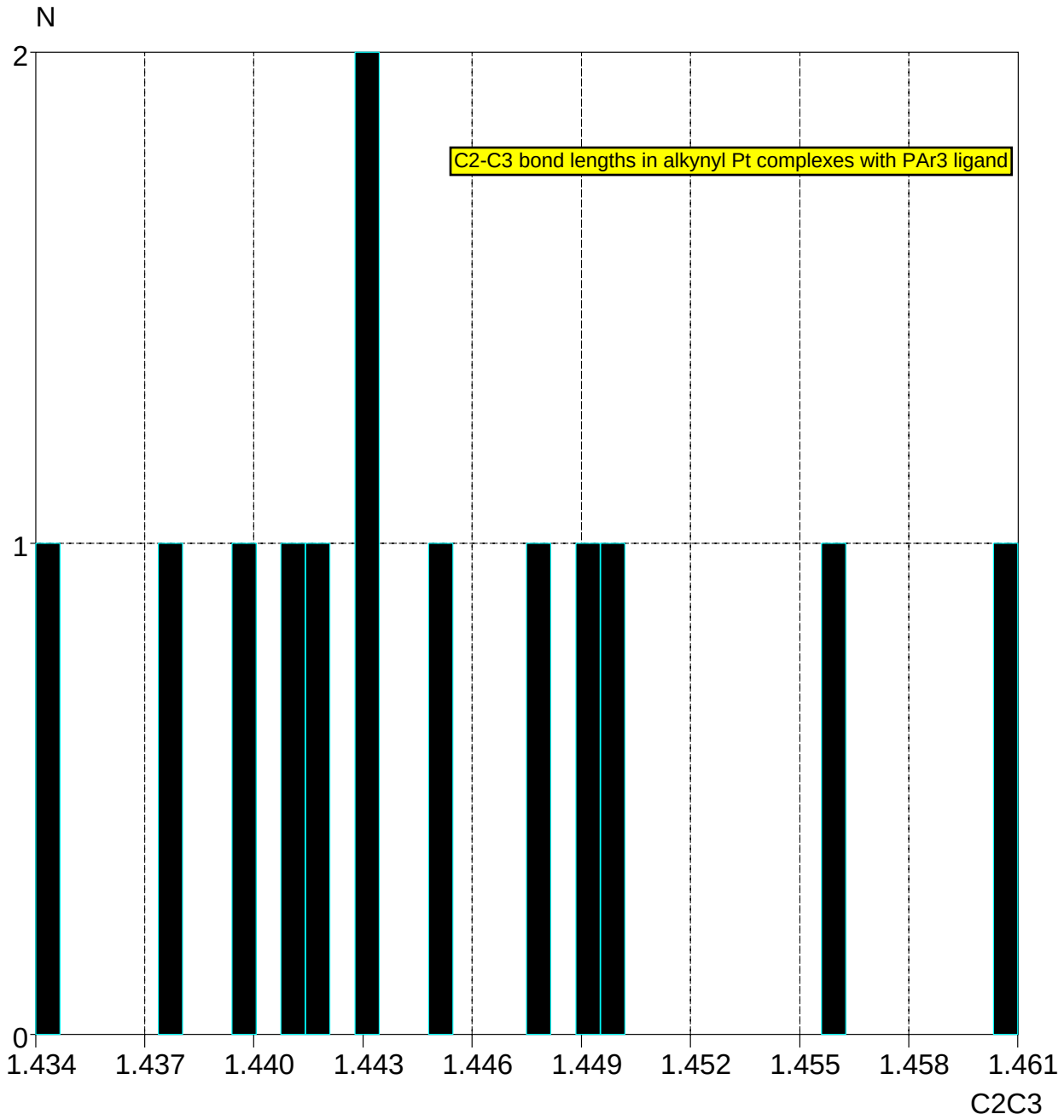


Plot Data
File=cq_temp2
Test=4
Tot.Obs.=14
Obs.=13
Supp.=1

X-axis
Min.=1.152
Max.=1.217
Range=0.065
Mean=1.197
Mean SE=0.005
Sample SD=0.019

Histogram
Median=1.204
Skew=-0.965
Quantile=10.000
LQ=1.152
HQ=1.214
Bin Width=0.002
Max. Bin =2.000

C2C3

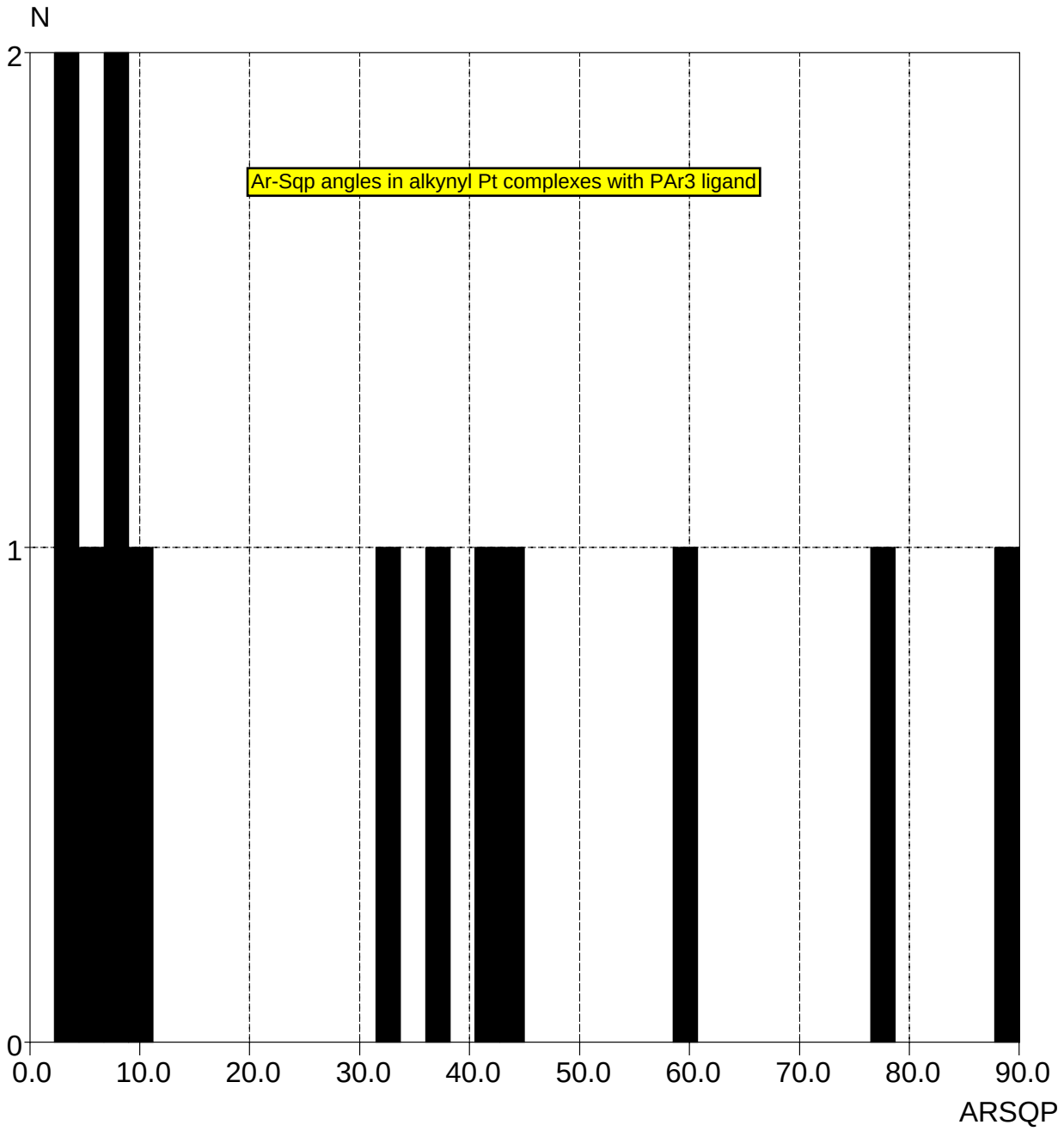


Plot Data
File=cq_temp2
Test=4
Tot.Obs.=14
Obs.=13
Supp.=1

X-axis
Min.=1.434
Max.=1.461
Range=0.027
Mean=1.445
Mean SE=0.002
Sample SD=0.007

Histogram
Median=1.443
Skew=0.572
Quantile=10.000
LQ=1.434
HQ=1.456
Bin Width=0.001
Max. Bin =2.000

ARSQP

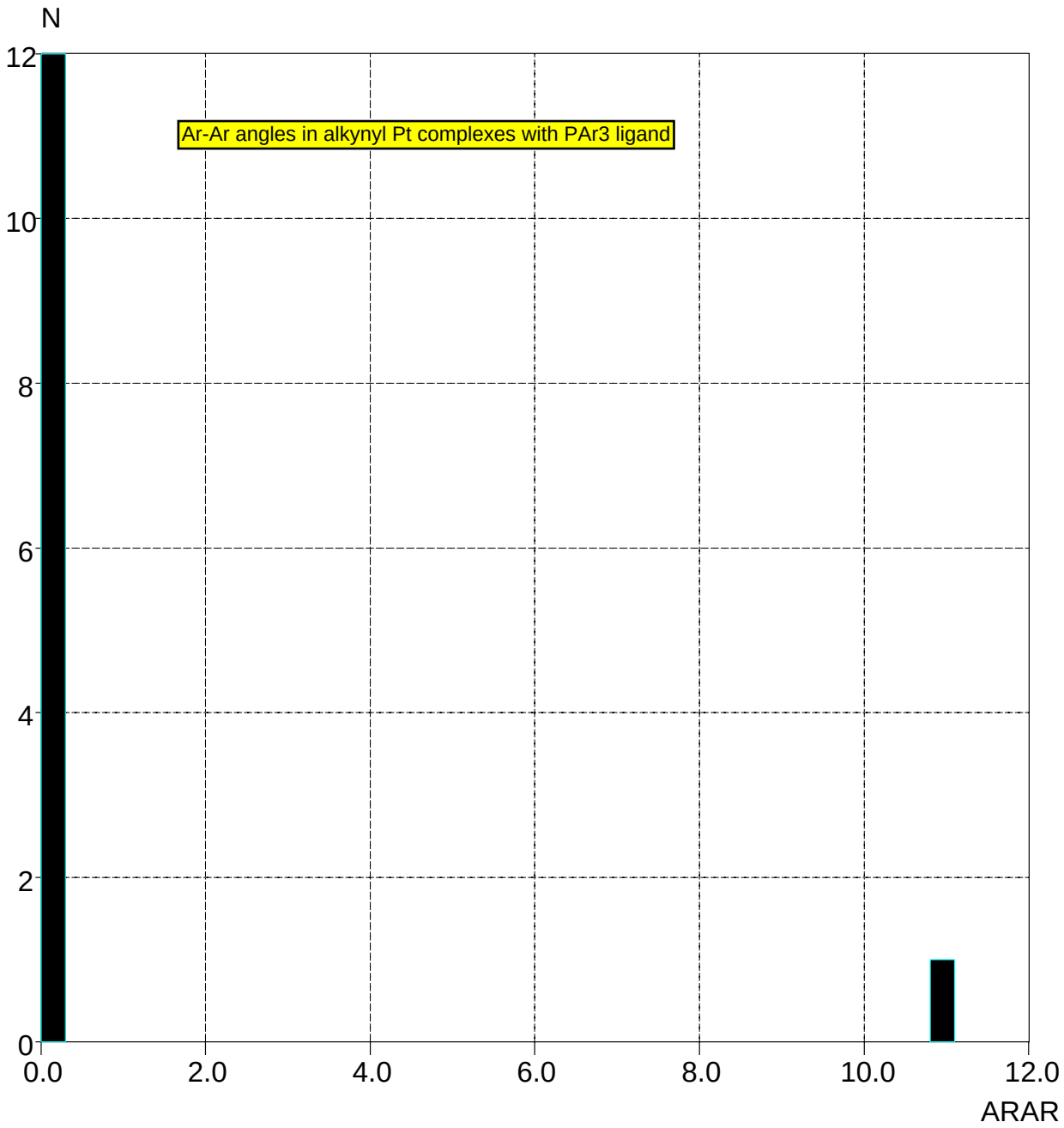


Plot Data
File=cq_temp2
Test=4
Tot.Obs.=14
Obs.=13
Supp.=1

X-axis
Min.=2.906
Max.=89.478
Range=86.572
Mean=32.209
Mean SE=8.148
Sample SD=29.378

Histogram
Median=32.059
Skew=0.586
Quantile=10.000
LQ=2.906
HQ=76.776
Bin Width=2.250
Max. Bin =2.000

ARAR

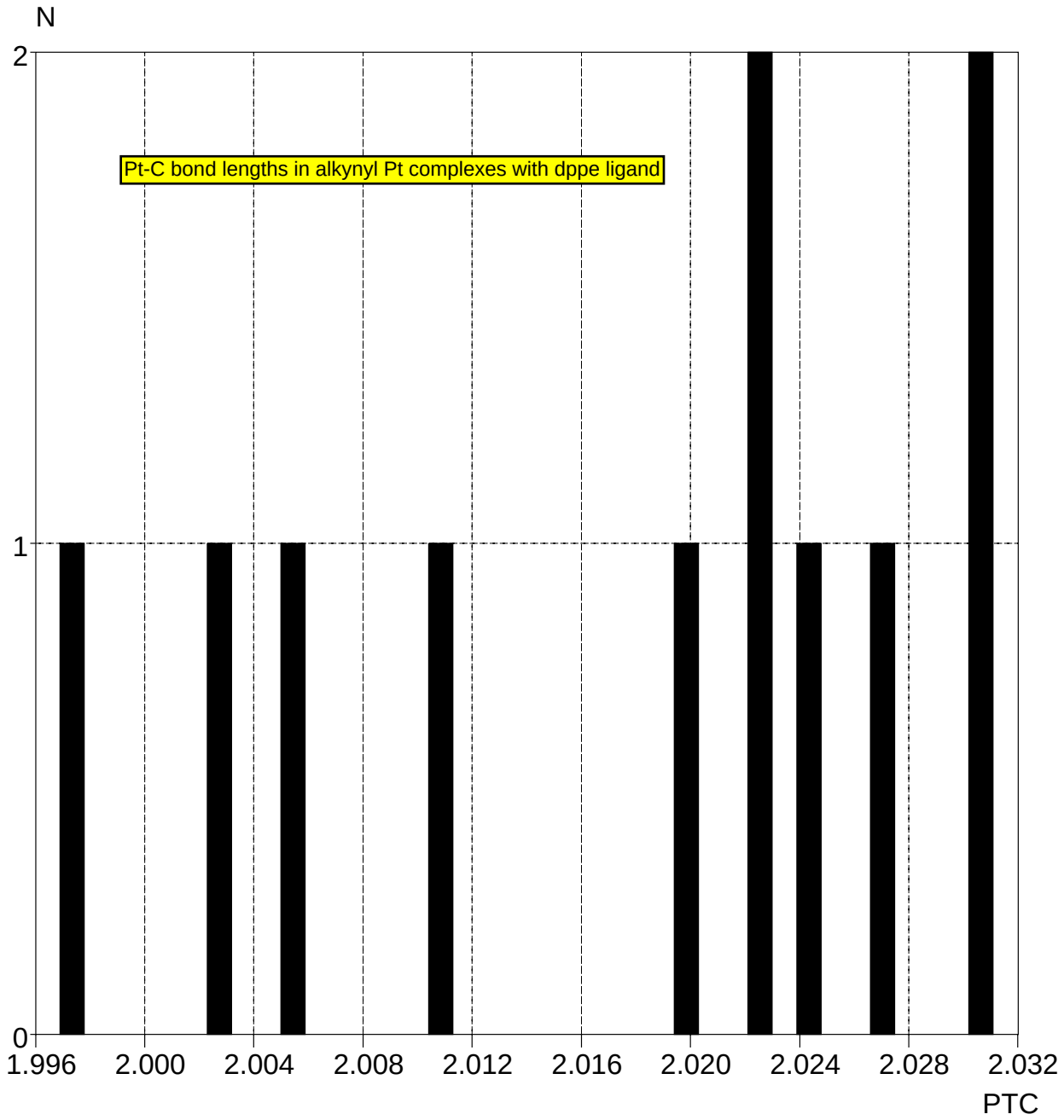


Plot Data
File=cq_temp2
Test=4
Tot.Obs.=14
Obs.=13
Supp.=1

X-axis
Min.=0.000
Max.=10.864
Range=10.864
Mean=0.839
Mean SE=0.835
Sample SD=3.012

Histogram
Median=0.000
Skew=2.816
Quantile=10.000
LQ=0.000
HQ=0.020
Bin Width=0.300
Max. Bin =12.000

PTC

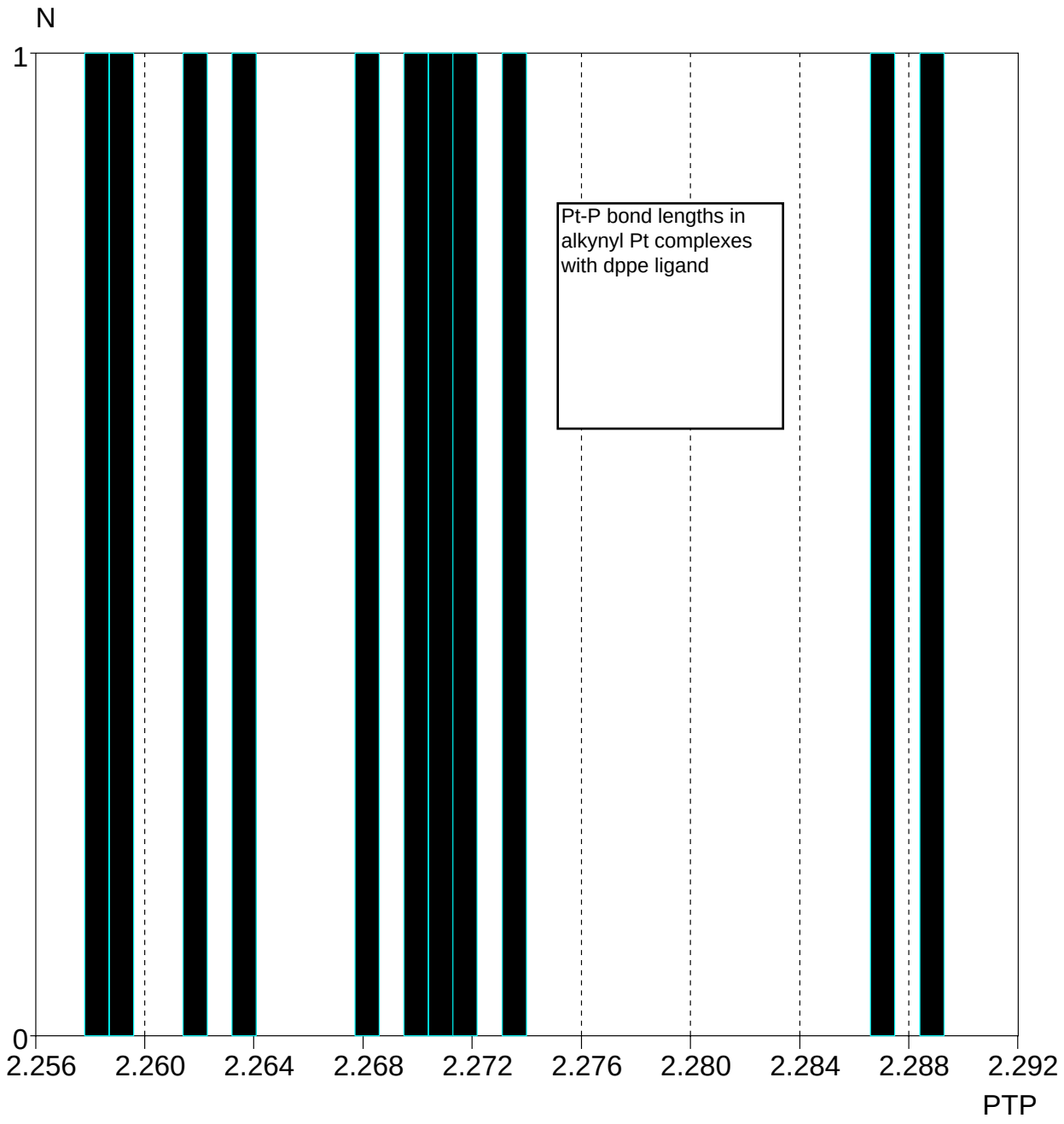


Plot Data
File=cq_temp6
Test=4
Tot.Obs.=11
Obs.=11
Supp.=0

X-axis
Min.=1.997
Max.=2.031
Range=0.034
Mean=2.018
Mean SE=0.004
Sample SD=0.012

Histogram
Median=2.023
Skew=-0.467
Quantile=10.000
LQ=1.997
HQ=2.031
Bin Width=0.001
Max. Bin =2.000

PTP

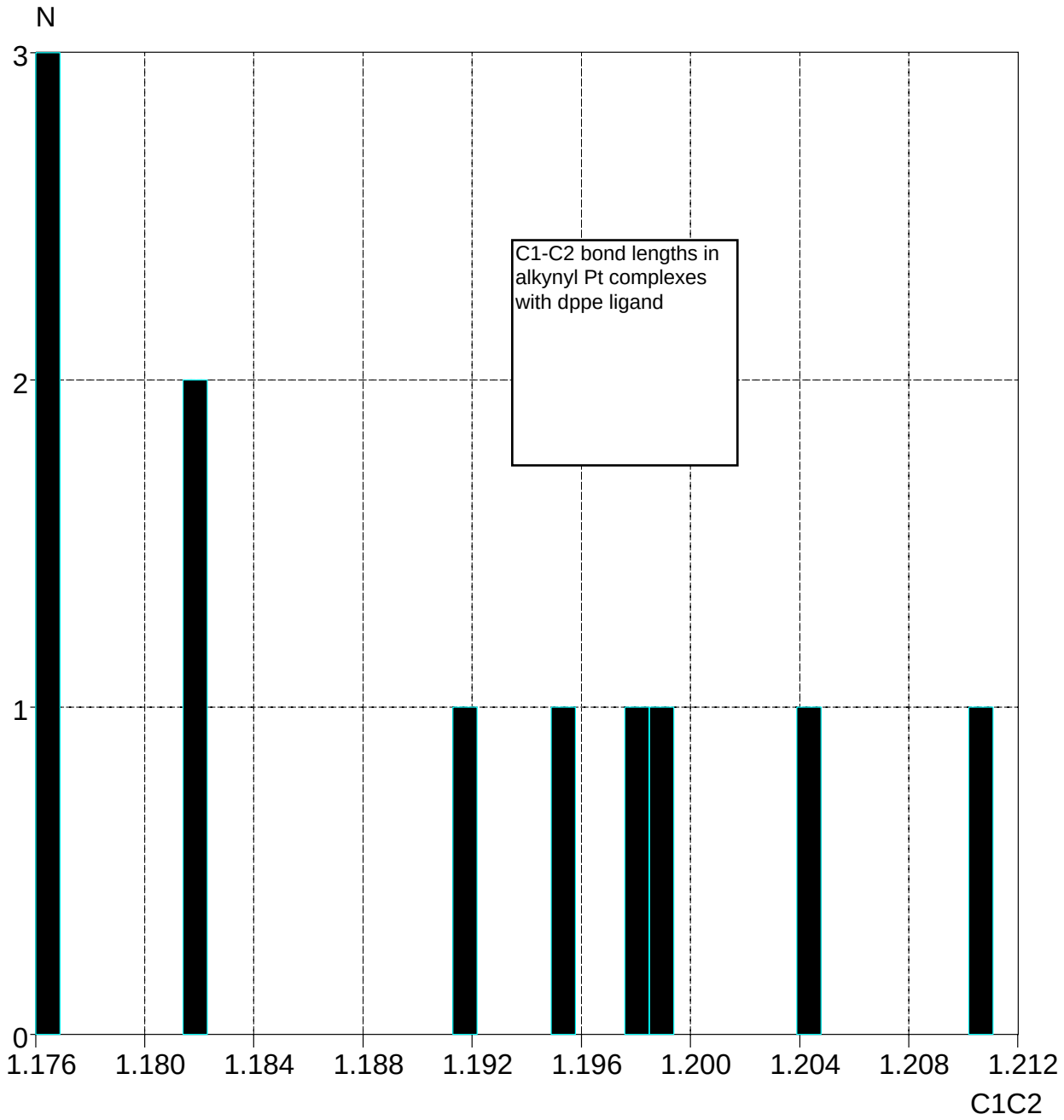


Plot Data
File=cq_temp6
Test=4
Tot.Obs.=11
Obs.=11
Supp.=0

X-axis
Min.=2.258
Max.=2.289
Range=0.031
Mean=2.270
Mean SE=0.003
Sample SD=0.010

Histogram
Median=2.270
Skew=0.594
Quantile=10.000
LQ=2.258
HQ=2.287
Bin Width=0.001
Max. Bin =1.000

C1C2

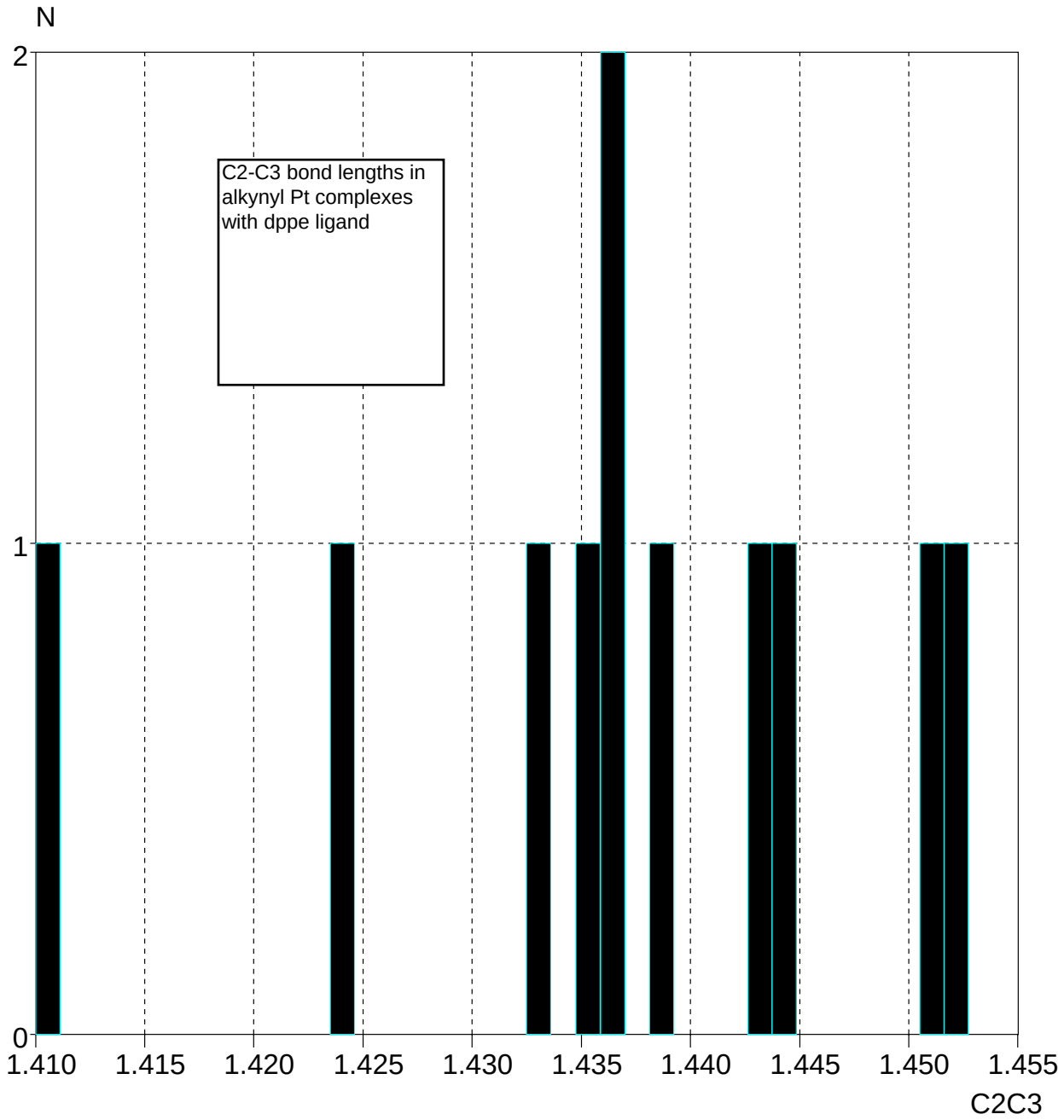


Plot Data
File=cq_temp6
Test=4
Tot.Obs.=11
Obs.=11
Supp.=0

X-axis
Min.=1.176
Max.=1.211
Range=0.035
Mean=1.190
Mean SE=0.004
Sample SD=0.012

Histogram
Median=1.192
Skew=0.179
Quantile=10.000
LQ=1.176
HQ=1.204
Bin Width=0.001
Max. Bin =3.000

C2C3

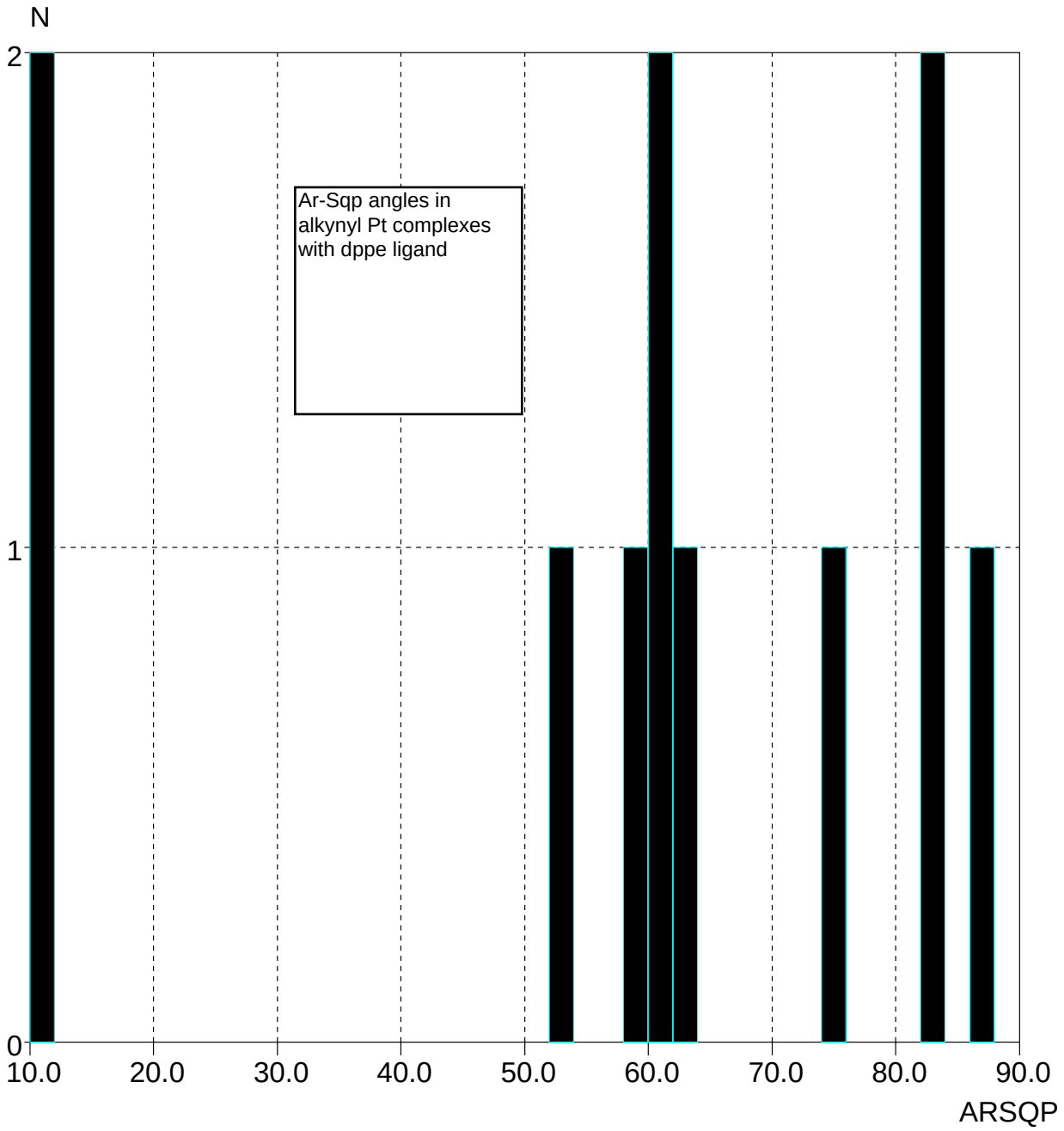


Plot Data
File=cq_temp6
Test=4
Tot.Obs.=11
Obs.=11
Supp.=0

X-axis
Min.=1.411
Max.=1.452
Range=0.041
Mean=1.437
Mean SE=0.004
Sample SD=0.012

Histogram
Median=1.436
Skew=-0.678
Quantile=10.000
LQ=1.411
HQ=1.451
Bin Width=0.001
Max. Bin =2.000

ARSQP

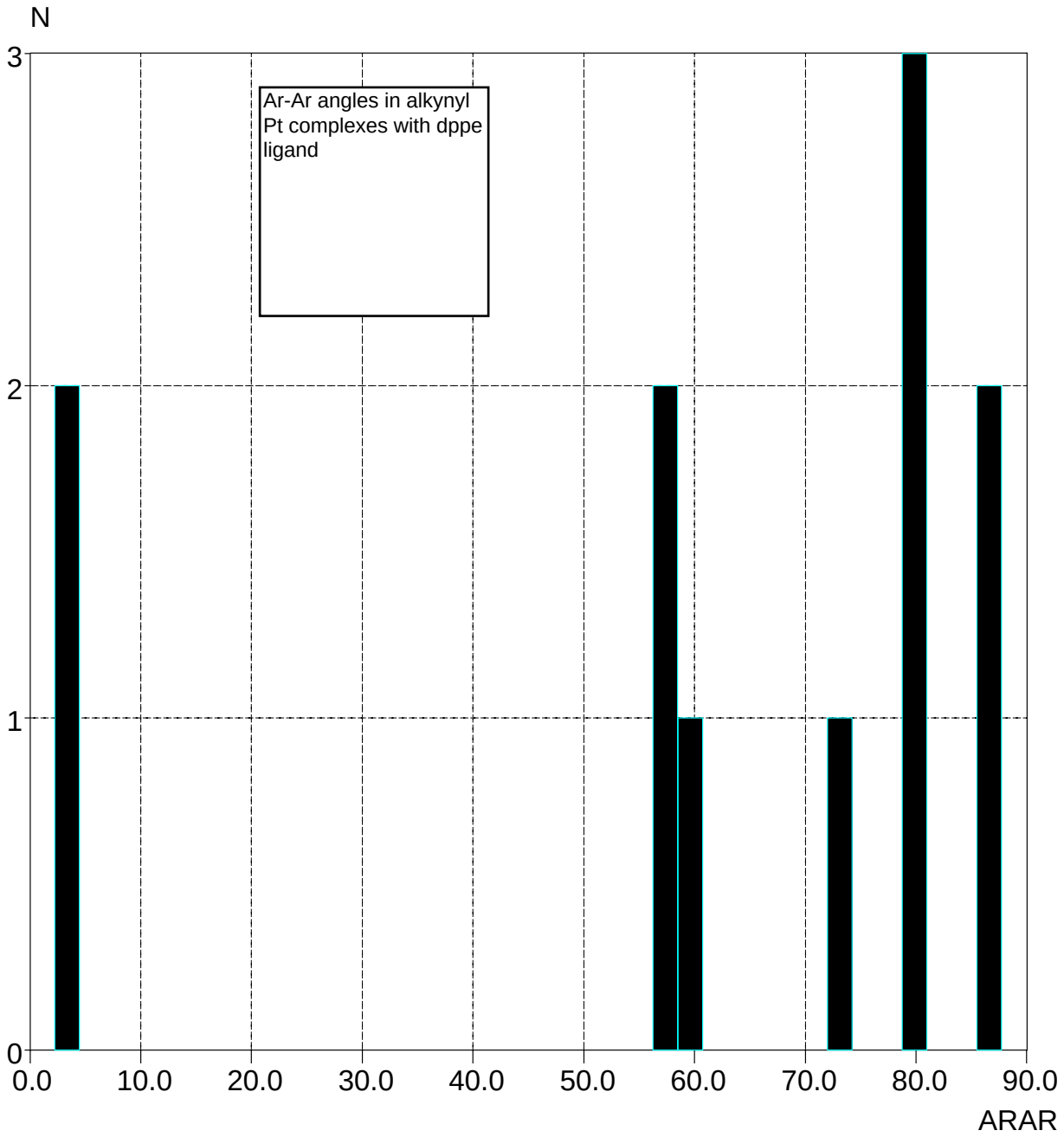


Plot Data
File=cq_temp6
Test=4
Tot.Obs.=11
Obs.=11
Supp.=0

X-axis
Min.=10.229
Max.=86.994
Range=76.765
Mean=58.495
Mean SE=7.949
Sample SD=26.363

Histogram
Median=60.369
Skew=-0.832
Quantile=10.000
LQ=10.229
HQ=82.970
Bin Width=2.000
Max. Bin =2.000

ARAR

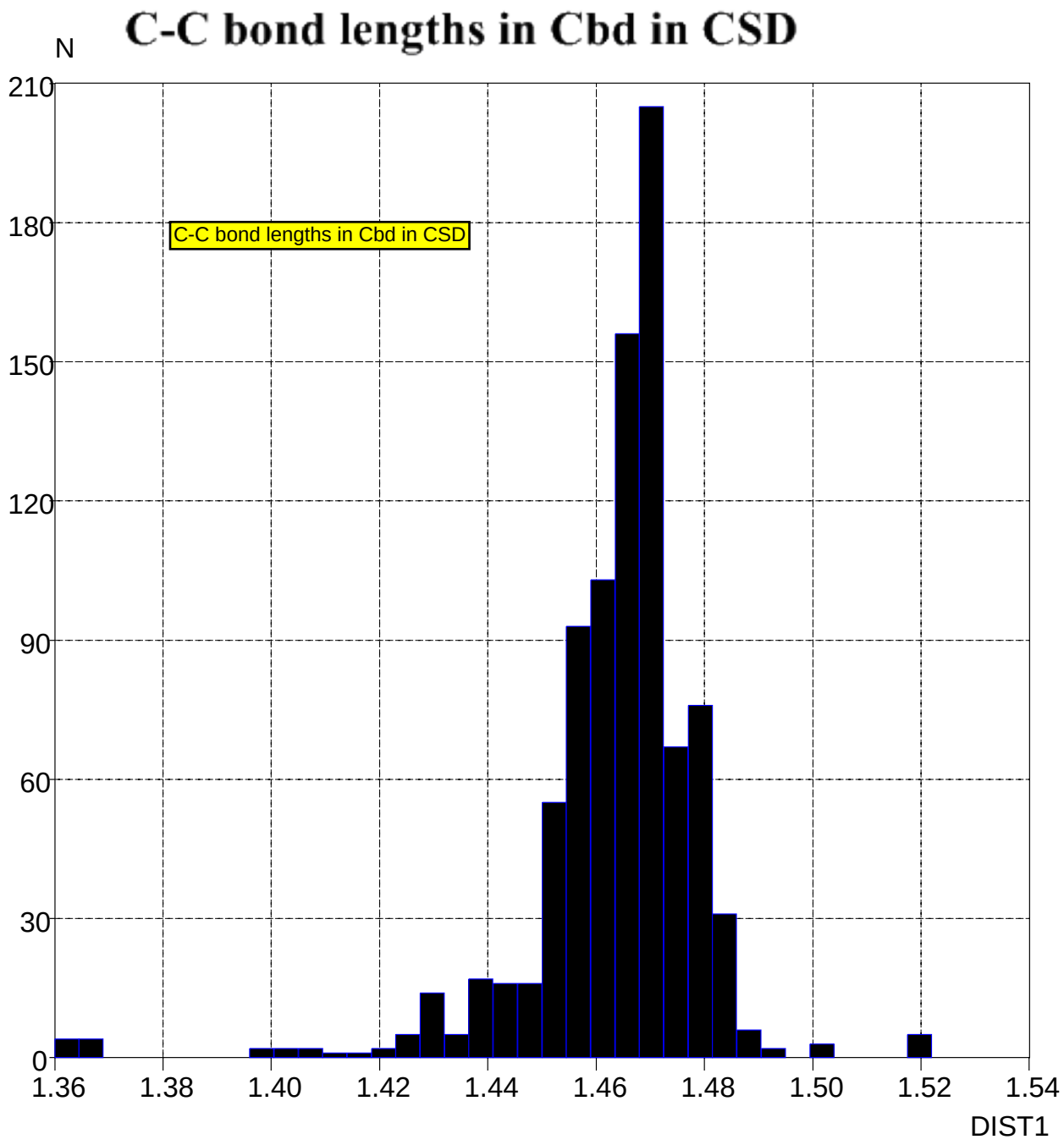


Plot Data
File=cq_temp6
Test=4
Tot.Obs.=11
Obs.=11
Supp.=0

X-axis
Min.=4.223
Max.=87.432
Range=83.209
Mean=61.054
Mean SE=9.057
Sample SD=30.040

Histogram
Median=73.685
Skew=-1.040
Quantile=10.000
LQ=4.223
HQ=86.572
Bin Width=2.250
Max. Bin =3.000

DIST1



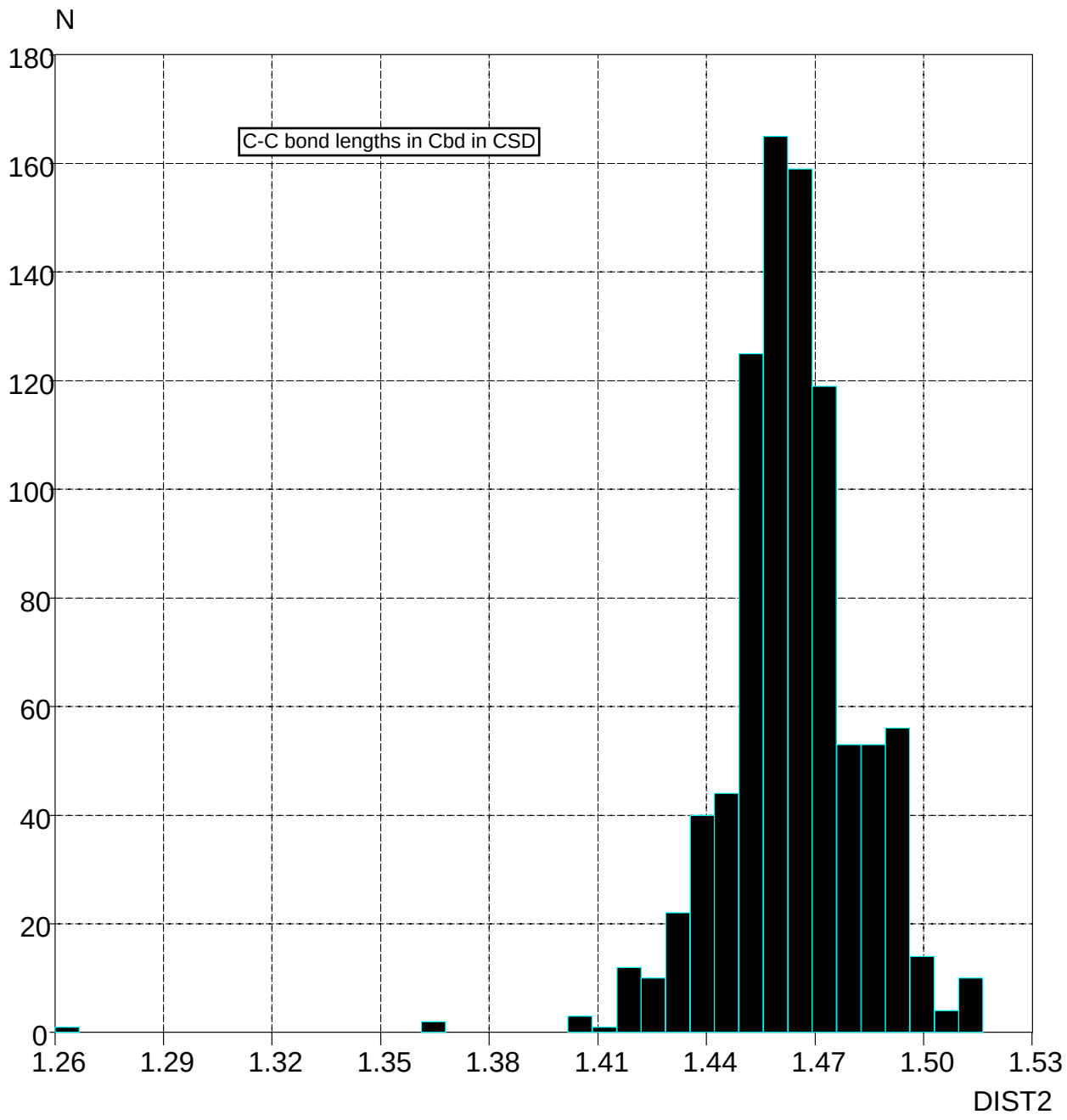
Plot Data
File=cq_temp0
Test=6
Tot.Obs.=893
Obs.=893
Supp.=0

X-axis
Min.=1.360
Max.=1.521
Range=0.161
Mean=1.464
Mean SE=0.001
Sample SD=0.017

Histogram
Median=1.467
Skew=-2.410
Quantile=10.000
LQ=1.449
HQ=1.478
Bin Width=0.005
Max. Bin =205.000

DIST2

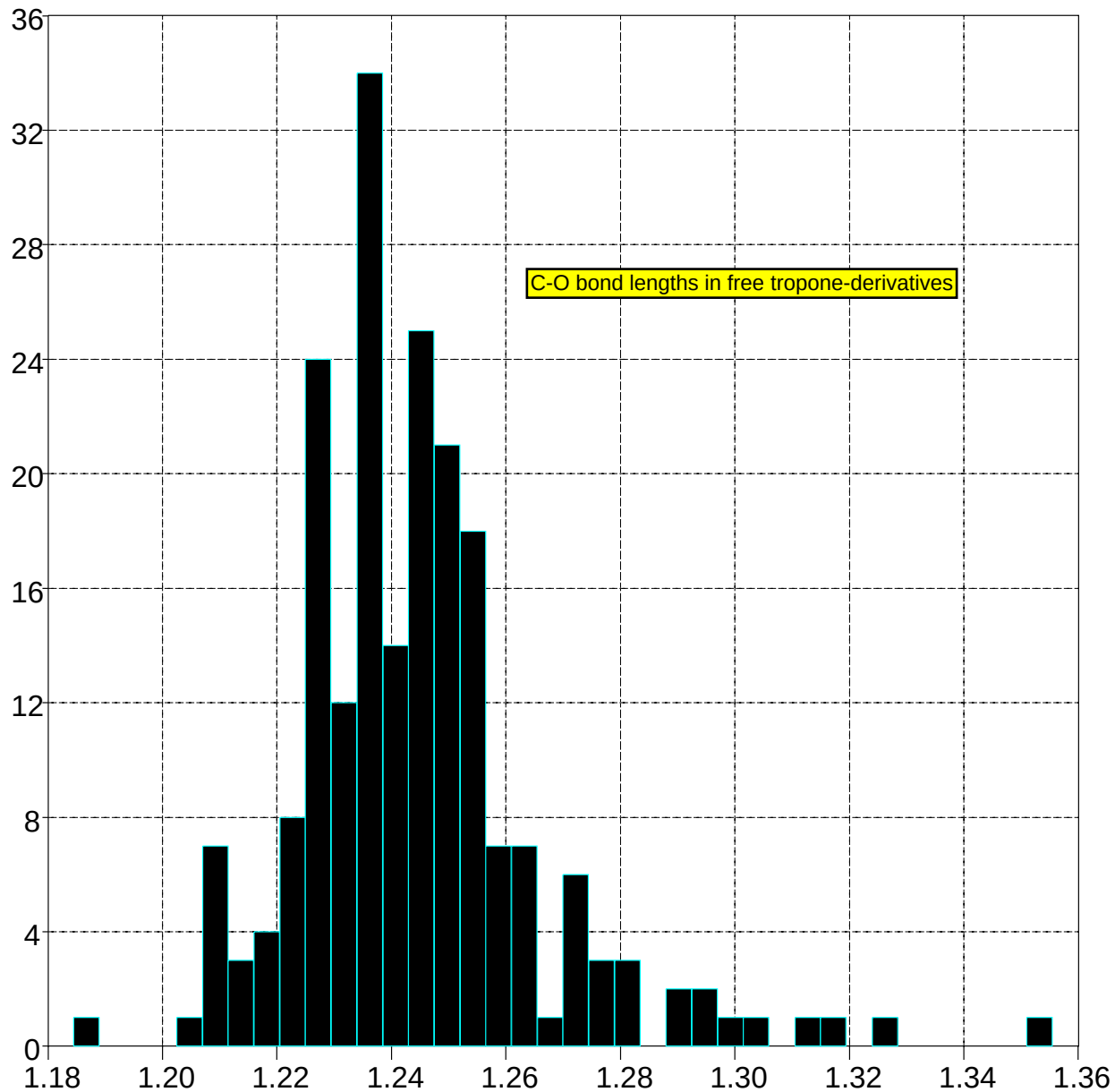
C-C bond lengths in Cbd in CSD



Plot Data
File=cq_temp0
Test=6
Tot.Obs.=893
Obs.=893
Supp.=0

X-axis
Min.=1.265
Max.=1.516
Range=0.251
Mean=1.464
Mean SE=0.001
Sample SD=0.020

Histogram
Median=1.463
Skew=-1.382
Quantile=10.000
LQ=1.442
HQ=1.488
Bin Width=0.007
Max. Bin =165.000

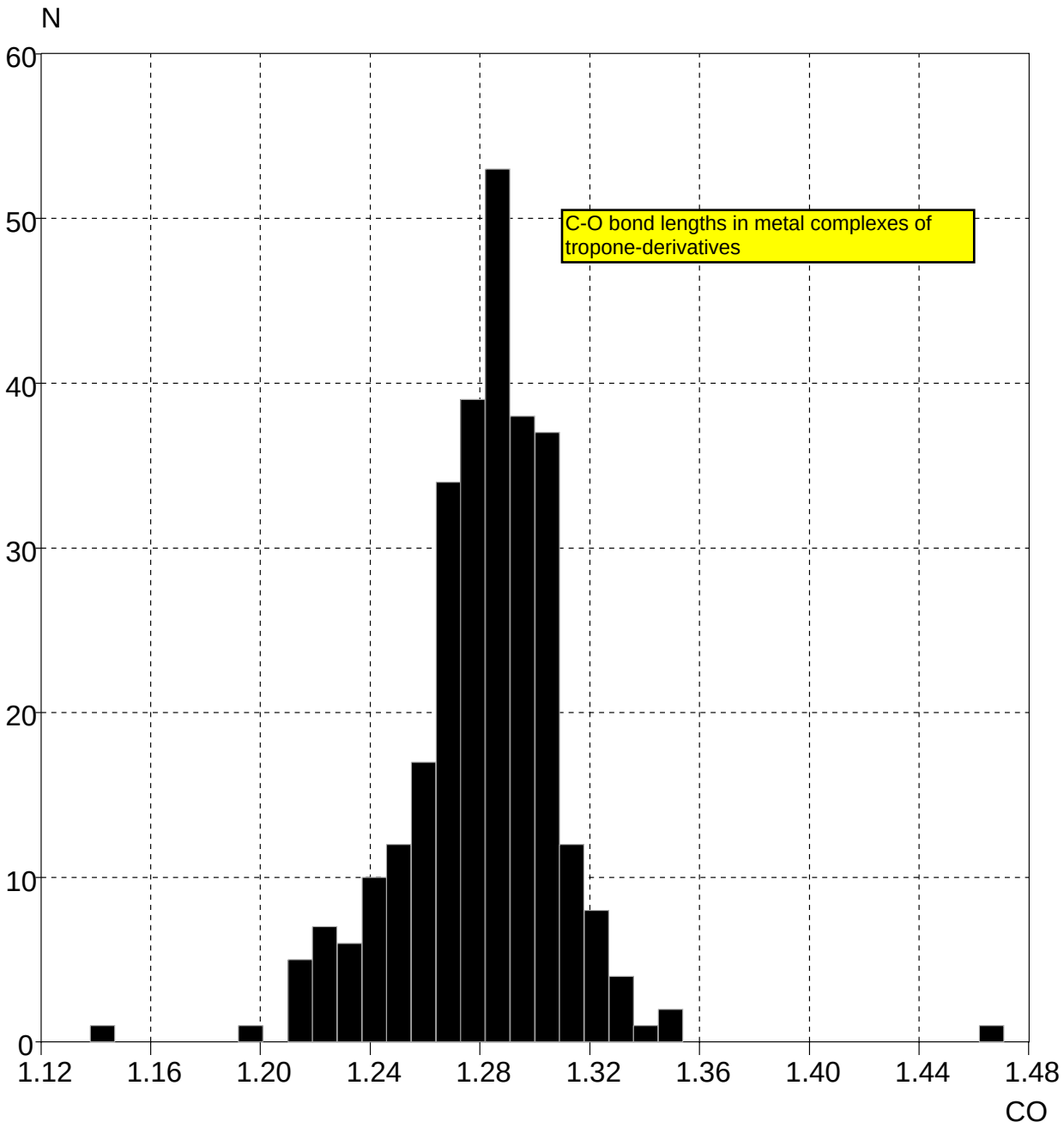


Plot Data
File=cq_temp12
Test=5
Tot.Obs.=213
Obs.=209
Supp.=4

X-axis
Min.=1.185
Max.=1.355
Range=0.170
Mean=1.244
Mean SE=0.002
Sample SD=0.022

Histogram
Median=1.241
Skew=1.406
Quantile=10.000
LQ=1.222
HQ=1.271
Bin Width=0.005
Max. Bin =34.000

CO



Plot Data
File=cq_temp14
Test=5
Tot.Obs.=288
Obs.=288
Supp.=0

X-axis
Min.=1.143
Max.=1.469
Range=0.326
Mean=1.282
Mean SE=0.002
Sample SD=0.029

Histogram
Median=1.285
Skew=0.169
Quantile=10.000
LQ=1.243
HQ=1.309
Bin Width=0.009
Max. Bin =53.000

Appendix V. X-ray Supporting Information.

No.	Compound number	Page
Figure S1.	ORTEP3 plot for **44**	**344**
Figure S2.	ORTEP3 plot **45**	**350**
Figure S3.	ORTEP3 plot for **47**	**358**
Figure S4.	ORTEP3 Plot for **49**	**364**
Figure S5.	ORTEP3 Plot for **52**	**372**
Figure S6	ORTEP plot for **15**	**379**
Figure S7	ORTEP plot for **60**	**391**
Figure S8	ORTEP plot for **5**	**401**
Figure S9	ORTEP plot for **99**	**411**
Figure S10	ORTEP plot for **17**	**421**
Figure S11	ORTEP plot for **108**	**431**
Figure S12	ORTEP plot for **117**	**438**
Figure S12	ORTEP plot for **119**	**448**
Figure S13	ORTEP plot for **125**	**458**

Figure S1. ORTEP3 Plot showing labeling for ***trans*-(MeCODHP)$_2$Pt(PEt$_3$)$_2$ • 0.2 CH$_2$Cl$_2$**

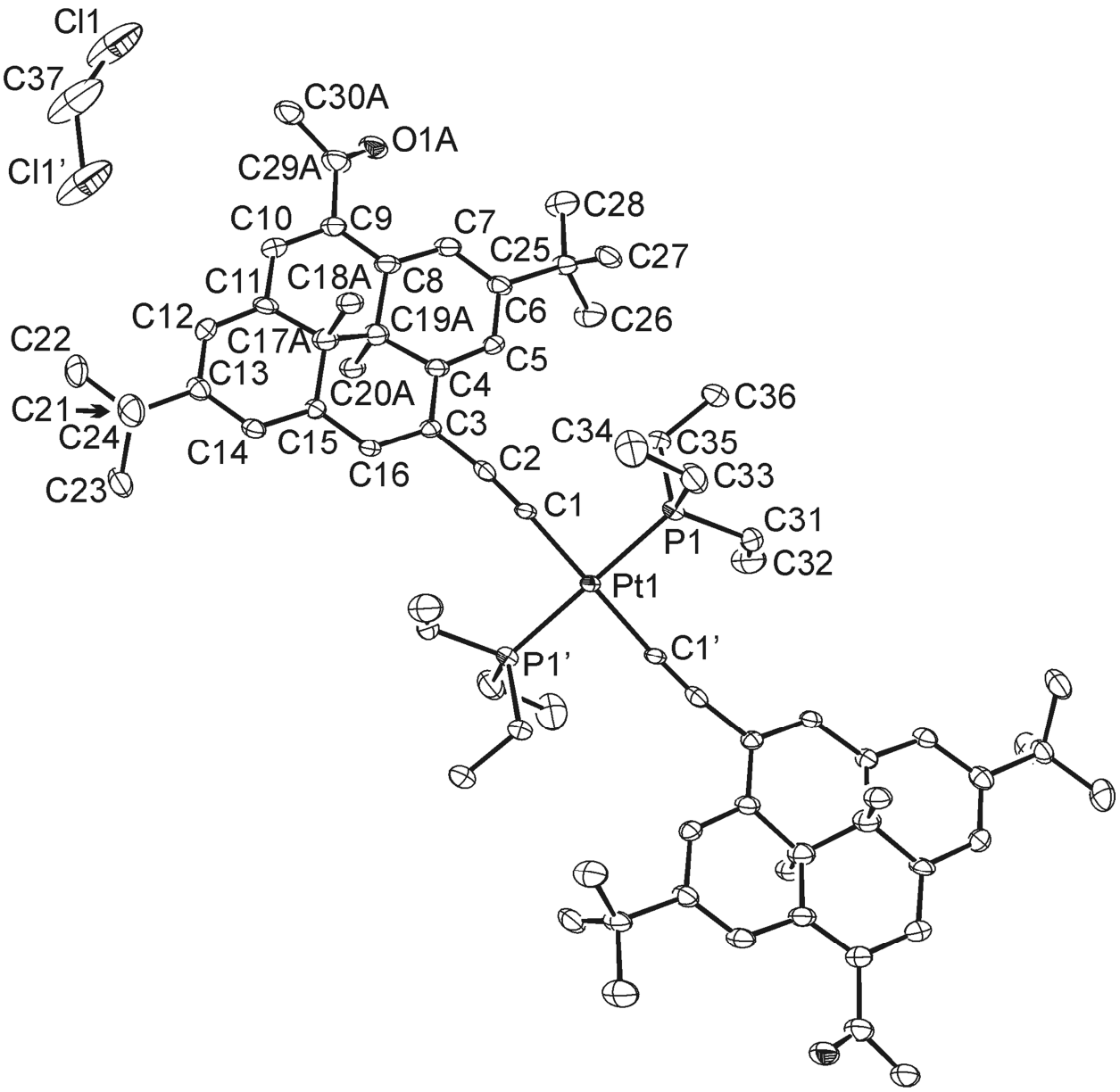


Table S1 Atomic Coordinates [× 10^4] and Equivalent Isotropic Displacement

Parameters [$Å^2 \times 10^3$] for ***trans*-(MeCODHP)$_2$Pt(PEt$_3$)$_2$ • 0.2 CH$_2$Cl$_2$**

	x	y	z	U_{eq}
Pt(1)	5000	5000	0	19(1)
Cl(1)	4433(13)	14948(15)	5417(8)	112(6)
P(1)	3829(1)	4025(2)	-16(1)	25(1)
O(1A)	4012(3)	8910(6)	4582(3)	39(1)
O(1B)	5827(14)	12530(30)	4725(12)	39(1)
C(1)	4929(3)	6338(6)	717(3)	21(1)
C(2)	4932(3)	7143(6)	1155(3)	21(1)
C(3)	5029(3)	8152(5)	1691(3)	20(1)
C(4)	4697(3)	7964(6)	2234(3)	25(1)
C(5)	4243(3)	6876(6)	2275(3)	25(1)
C(6)	3900(4)	6709(6)	2804(3)	28(1)
C(7)	4001(4)	7708(6)	3301(3)	28(1)
C(8)	4454(3)	8867(6)	3318(3)	27(1)
C(9)	4553(3)	9933(7)	3793(3)	29(1)
C(10)	5016(4)	11075(7)	3762(3)	31(1)
C(11)	5359(3)	11253(6)	3250(3)	25(1)
C(12)	5834(3)	12360(6)	3219(3)	25(1)
C(13)	6161(3)	12513(6)	2697(3)	24(1)
C(14)	6034(3)	11499(6)	2184(3)	22(1)
C(15)	5580(3)	10356(5)	2173(3)	20(1)
C(16)	5474(3)	9310(6)	1685(3)	21(1)
C(17A)	5070(4)	10325(7)	2632(4)	29(1)
C(17B)	5392(12)	9997(19)	2837(13)	29(1)
C(18A)	4226(4)	10838(8)	2184(4)	29(1)
C(18B)	6085(19)	9060(40)	3281(18)	29(1)
C(19A)	5005(4)	8891(7)	2870(4)	29(1)
C(19B)	4612(14)	9242(10)	2637(7)	29(1)
C(20A)	5835(4)	8358(8)	3332(4)	29(1)
C(20B)	3936(18)	10130(40)	2141(17)	29(1)
C(21)	2668(4)	5510(7)	2137(4)	43(2)
C(22)	3882(5)	4178(6)	2782(4)	43(2)
C(23)	3387(4)	5458(6)	2784(4)	35(2)

C(24)	3111(5)	5365(7)	3420(5)	53(2)
C(25)	6636(3)	13780(6)	2645(3)	26(1)
C(26)	6840(4)	14671(6)	3291(4)	38(2)
C(27)	7413(4)	13381(7)	2527(4)	38(2)
C(28)	6129(4)	14623(6)	2036(4)	38(2)
C(29A)	4153(5)	9941(10)	4328(4)	39(1)
C(29B)	5169(15)	12090(40)	4447(17)	39(1)
C(30A)	3934(5)	11310(9)	4561(4)	39(1)
C(30B)	4472(19)	12290(50)	4710(20)	39(1)
C(31)	3695(4)	3918(7)	835(3)	30(1)
C(32)	2970(4)	3137(7)	859(4)	35(2)
C(33)	3646(4)	2300(6)	-347(4)	34(2)
C(34)	4240(4)	1310(7)	98(4)	45(2)
C(35)	2957(4)	4920(7)	-570(4)	40(2)
C(36)	2965(4)	6476(7)	-397(5)	51(2)
C(37)	5030(70)	14360(120)	4970(60)	112(6)

U_{eq} is defined as one third of the trace of the orthogonalized U_{ij} tensor.

Table S2. Bond Lengths [Å] for ***trans*-(MeCODHP)$_2$Pt(PEt$_3$)$_2$ • 0.2 CH$_2$Cl$_2$**

Pt(1)-P(1)	2.2945(16)	C(11)-C(12)	1.398(8)
Pt(1)-C(1)’	2.007(5)	C(11)-C(17A)	1.511(9)
Cl(1)-C(37)	1.710(10)	C(11)-C(17B)	1.513(10)
Cl(1)-C(37)’	1.59(10)	C(12)-C(13)	1.382(8)
P(1)-C(31)	1.837(6)	C(13)-C(14)	1.416(8)
P(1)-C(33)	1.822(6)	C(13)-C(25)	1.535(8)
P(1)-C(35)	1.828(7)	C(14)-C(15)	1.385(8)
O(1A)-C(29A)	1.206(10)	C(15)-C(16)	1.405(8)
O(1B)-C(29B)	1.207(11)	C(15)-C(17A)	1.506(9)
C(1)-C(2)	1.197(8)	C(15)-C(17B)	1.54(3)
C(2)-C(3)	1.450(8)	C(17A)-C(18A)	1.573(10)
C(3)-C(4)	1.431(8)	C(17B)-C(18B)	1.573(11)
C(3)-C(16)	1.395(8)	C(17A)-C(19A)	1.514(9)
C(4)-C(5)	1.365(8)	C(17B)-C(19B)	1.516(10)
C(4)-C(19A)	1.538(9)	C(19A)-C(20A)	1.568(10)
C(4)-C(19B)	1.541(10)	C(19B)-C(20B)	1.569(11)
C(5)-C(6)	1.416(8)	C(21)-C(22)	1.518(11)
C(6)-C(7)	1.386(9)	C(21)-C(23)	1.543(9)
C(6)-C(23)	1.530(8)	C(21)-C(24)	1.539(9)
C(7)-C(8)	1.396(8)	C(25)-C(26)	1.530(9)
C(8)-C(9)	1.403(8)	C(25)-C(27)	1.535(8)
C(8)-C(19A)	1.550(8)	C(25)-C(28)	1.526(9)
C(8)-C(19B)	1.554(9)	C(29A)-C(30A)	1.527(12)
C(9)-C(10)	1.412(9)	C(29B)-C(30B)	1.527(13)
C(9)-C(29A)	1.489(9)	C(31)-C(32)	1.521(8)
C(9)-C(29B)	1.68(3)	C(33)-C(34)	1.510(10)
C(10)-C(11)	1.385(8)	C(35)-C(36)	1.575(10)

Table S3. Bond Angles [°] for ***trans*-(MeCODHP)$_2$Pt(PEt$_3$)$_2$ • 0.2 CH$_2$Cl$_2$**

Pt(1)-C(1)-C(2)	176.3(5)	C(7)-C(6)-C(5)	119.5(5)
Pt(1)-P(1)-C(31)	114.2(2)	C(7)-C(6)-C(23)	121.9(5)
Pt(1)-P(1)-C(33)	116.7(2)	C(7)-C(8)-C(9)	125.0(5)
Pt(1)-P(1)-C(35)	113.3(2)	C(7)-C(8)-C(19A)	118.2(5)
P(1)-Pt(1)-P(1)’	180.0	C(7)-C(8)-C(19B)	116.5(8)
P(1)-Pt(1)-C(1)	90.73(15)	C(8)-C(9)-C(10)	120.7(5)
P(1)-Pt(1)-C(1)’	89.27(15)	C(8)-C(9)-C(29A)	122.0(6)
P(1)-C(31)-C(32)	115.7(4)	C(8)-C(9)-C(29B)	124.3(12)
P(1)-C(33)-C(34)	112.0(5)	C(8)-C(19A)-C(17A)	109.5(6)
P(1)-C(35)-C(36)	112.9(5)	C(8)-C(19B)-C(17B)	107.1(17)
O(1A)-C(29A)-C(9)	122.1(8)	C(8)-C(19A)-C(20A)	107.2(6)
O(1B)-C(29B)-C(9)	119(2)	C(8)-C(19B)-C(20B)	112.8(17)
O(1A)-C(29A)-C(30A)	120.0(6)	C(9)-C(8)-C(19A)	115.9(5)
O(1B)-C(29B)-C(30B)	125(3)	C(9)-C(8)-C(19B)	115.1(6)
C(1)-Pt(1)-C(1)’	180.0(2)	C(9)-C(10)-C(11)	123.1(6)
C(1)-C(2)-C(3)	173.4(6)	C(9)-C(29A)-C(30A)	117.9(7)
C(2)-C(3)-C(16)	118.9(5)	C(9)-C(29B)-C(30B)	116(2)
C(2)-C(3)-C(4)	121.4(5)	C(10)-C(11)-C(12)	124.0(6)
C(3)-C(4)-C(5)	123.7(5)	C(10)-C(11)-C(17A)	116.2(6)
C(3)-C(4)-C(19A)	117.0(5)	C(10)-C(11)-C(17B)	115.2(12)
C(3)-C(4)-C(19B)	116.5(6)	C(10)-C(9)-C(29A)	117.2(6)
C(3)-C(16)-C(15)	122.8(5)	C(10)-C(9)-C(29B)	112.3(12)
C(4)-C(19A)-C(8)	111.7(5)	C(11)-C(17A)-C(19A)	109.8(6)
C(4)-C(19B)-C(8)	111.3(6)	C(11)-C(17B)-C(19B)	110.7(11)
C(4)-C(19A)-C(17A)	109.2(6)	C(11)-C(17A)-C(18A)	107.1(5)
C(4)-C(19B)-C(17B)	107.8(9)	C(11)-C(17B)-C(18B)	109.0(19)
C(4)-C(19A)-C(20A)	108.6(6)	C(11)-C(17A)-C(15)	113.5(5)
C(4)-C(19B)-C(20B)	107.5(18)	C(11)-C(17B)-C(15)	111.3(16)
C(4)-C(3)-C(16)	119.6(5)	C(12)-C(11)-C(17A)	118.8(5)
C(4)-C(5)-C(6)	123.5(5)	C(12)-C(11)-C(17B)	118.7(11)
C(5)-C(4)-C(19A)	118.2(5)	C(12)-C(13)-C(14)	119.3(5)
C(5)-C(4)-C(19B)	116.6(7)	C(12)-C(13)-C(25)	121.7(5)
C(5)-C(6)-C(23)	118.6(5)	C(13)-C(12)-C(11)	122.5(5)
C(6)-C(7)-C(8)	122.5(5)	C(13)-C(14)-C(15)	122.7(5)
C(6)-C(23)-C(21)	109.0(6)	C(13)-C(25)-C(28)	107.9(5)
C(6)-C(23)-C(22)	108.8(5)	C(13)-C(25)-C(26)	112.9(5)
C(6)-C(23)-C(24)	112.3(6)	C(13)-C(25)-C(27)	110.5(5)

C(14)-C(13)-C(25)	118.9(5)	C(18A)-C(17A)-C(19A)	109.2(6)
C(14)-C(15)-C(16)	123.6(5)	C(18B)-C(17B)-C(19B)	111(2)
C(14)-C(15)-C(17A)	118.4(5)	C(21)-C(23)-C(22)	110.4(6)
C(14)-C(15)-C(17B)	117.8(7)	C(21)-C(23)-C(24)	109.0(6)
C(15)-C(17A)-C(18A)	106.9(6)	C(22)-C(23)-C(24)	107.2(6)
C(15)-C(17B)-C(18B)	106.7(18)	C(26)-C(25)-C(27)	108.0(5)
C(15)-C(17A)-C(19A)	110.2(5)	C(26)-C(25)-C(28)	107.7(5)
C(15)-C(17B)-C(19B)	108.6(14)	C(27)-C(25)-C(28)	109.8(5)
C(16)-C(15)-C(17A)	117.3(5)	C(33)-P(1)-C(35)	102.0(3)
C(16)-C(15)-C(17B)	116.0(6)	C(31)-P(1)-C(33)	103.6(3)
C(17A)-C(19A)-C(20A)	110.6(6)	C(31)-P(1)-C(35)	105.5(3)
C(17B)-C(19B)-C(20B)	110.3(19)		

Figure S2. ORTEP3 Plot showing labeling for ***trans*-(PhCODHP)$_2$Pt(PEt$_3$)$_2$ • ½ C$_6$H$_{14}$**

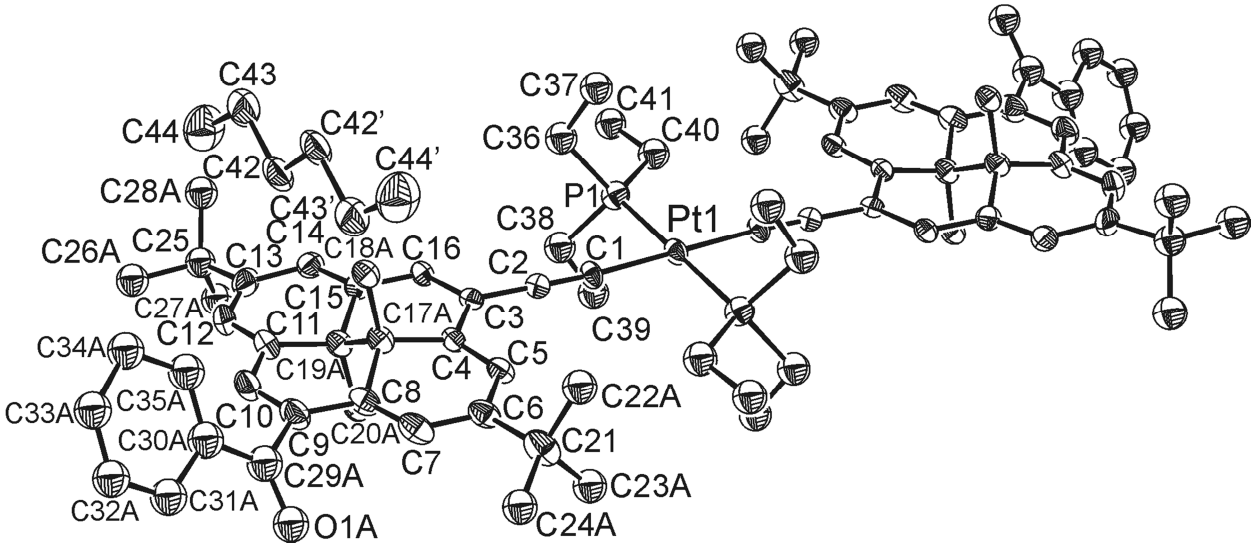


Table S4. Atomic Coordinates [$\times 10^4$] and Equivalent Isotropic Displacement Parameters [$Å^2 \times 10^3$] for ***trans*-(PhCODHP)$_2$Pt(PEt$_3$)$_2$ • ½ C$_6$H$_{14}$**

	x	y	z	U_{eq}
Pt(1)	10000	5000	5000	55(1)
P(1)	8936(3)	5061(1)	5947(1)	70(1)
O(1A)	4570(20)	1271(6)	1732(7)	94(2)
O(1B)	5300(30)	1161(8)	1762(9)	94(2)
C(1)	8879(7)	4240(3)	4711(4)	53(2)
C(2)	8147(7)	3805(3)	4593(4)	49(2)
C(3)	7199(7)	3305(3)	4467(4)	44(2)
C(4)	7118(7)	2891(3)	3876(4)	49(2)
C(5)	7955(7)	2941(4)	3392(4)	56(2)
C(6)	7876(8)	2546(4)	2803(4)	66(2)
C(7)	6916(9)	2081(4)	2682(5)	75(3)
C(8)	6018(9)	1982(3)	3110(5)	65(2)
C(9)	5036(10)	1515(4)	3010(5)	79(3)
C(10)	4135(10)	1456(4)	3472(5)	78(3)
C(11)	4155(9)	1858(4)	4050(5)	72(2)
C(12)	3247(9)	1838(4)	4494(6)	81(3)
C(13)	3292(9)	2253(5)	5059(6)	79(3)
C(14)	4331(8)	2709(4)	5219(5)	64(2)
C(15)	5290(8)	2777(4)	4806(4)	55(2)
C(16)	6289(7)	3230(3)	4917(4)	49(2)
C(17A)	6318(14)	2311(6)	3887(7)	57(1)
C(17B)	5801(16)	2488(8)	3627(10)	57(1)
C(18A)	7272(15)	1885(7)	4488(8)	57(1)
C(18B)	4526(17)	2872(8)	3158(11)	57(1)
C(19A)	4928(14)	2454(6)	4058(7)	57(1)
C(19B)	5488(16)	2218(8)	4300(10)	57(1)
C(20A)	4006(14)	2896(6)	3433(8)	57(1)
C(20B)	6780(18)	1830(8)	4792(11)	57(1)
C(21)	8815(9)	2648(4)	2299(4)	92(3)
C(22A)	8556(18)	3291(6)	1967(9)	86(2)
C(22B)	8000(40)	3095(15)	1708(16)	86(2)
C(23A)	10336(11)	2556(8)	2801(7)	86(2)
C(23B)	10339(18)	2834(18)	2690(20)	86(2)
C(24A)	8507(15)	2249(7)	1598(7)	86(2)
C(24B)	8770(40)	2060(10)	1850(20)	86(2)

C(25)	2160(9)	2259(4)	5494(5)	80(3)
C(26A)	1208(15)	1711(6)	5290(8)	93(2)
C(26B)	2310(40)	1726(11)	6010(17)	93(2)
C(27A)	1215(16)	2797(6)	5247(9)	93(2)
C(27B)	740(20)	2493(17)	5044(18)	93(2)
C(28A)	2913(16)	2198(8)	6308(6)	93(2)
C(28B)	2500(40)	2712(13)	6130(15)	93(2)
C(29A)	4740(20)	1085(8)	2400(10)	94(2)
C(29B)	5090(30)	1020(10)	2371(13)	94(2)
C(30A)	4750(20)	436(8)	2580(11)	94(2)
C(30B)	4960(30)	384(10)	2565(13)	94(2)
C(31A)	4220(20)	43(9)	1939(11)	94(2)
C(31B)	4040(30)	-27(9)	2061(14)	94(2)
C(32A)	4216(19)	-559(9)	2069(11)	94(2)
C(32B)	3910(20)	-606(10)	2250(13)	94(2)
C(33A)	4737(19)	-784(9)	2741(10)	94(2)
C(33B)	4560(20)	-822(10)	2933(14)	94(2)
C(34A)	5180(20)	-410(8)	3430(10)	94(2)
C(34B)	5650(30)	-429(10)	3412(12)	94(2)
C(35A)	5230(20)	216(8)	3283(11)	94(2)
C(35B)	5670(30)	187(10)	3255(13)	94(2)
C(36A)	9148(12)	4378(6)	6533(7)	91(2)
C(36B)	7680(40)	4512(14)	6126(19)	91(2)
C(37A)	10701(12)	4227(7)	6898(7)	91(2)
C(37B)	7520(50)	4720(20)	6878(19)	91(2)
C(38A)	6993(11)	5084(5)	5546(9)	91(2)
C(38B)	8360(40)	5848(7)	5980(20)	91(2)
C(39A)	6526(15)	5663(6)	5105(8)	91(2)
C(39B)	6990(40)	5875(19)	5350(20)	91(2)
C(40A)	9353(14)	5697(6)	6606(7)	91(2)
C(40B)	10400(30)	5206(15)	6805(15)	91(2)
C(41A)	8525(14)	5713(6)	7189(7)	91(2)
C(41B)	11130(40)	4599(15)	7000(20)	91(2)
C(42)	9240(20)	113(9)	5004(11)	86(6)
C(43)	9090(40)	18(11)	5802(15)	130(12)
C(44)	7650(30)	167(13)	5849(19)	132(10)

U_{eq} is defined as one third of the trace of the orthogonalized U_{ij} tensor.

Table S5. Bond Lengths [Å] for ***trans*-(PhCODHP)$_2$Pt(PEt$_3$)$_2$ • ½ C$_6$H$_{14}$**

Pt(1)-P(1)	2.296(3)	C(21)-C(22A)	1.551(9)
Pt(1)-C(1)	2.009(7)	C(21)-C(22B)	1.532(9)
O(1A)-C(29A)	1.274(15)	C(21)-C(23A)	1.540(8)
O(1B)-C(29B)	1.250(17)	C(21)-C(23B)	1.531(10)
C(1)-C(2)	1.191(9)	C(21)-C(24A)	1.535(8)
C(2)-C(3)	1.431(9)	C(21)-C(24B)	1.544(9)
C(3)-C(4)	1.419(9)	C(25)-C(26A)	1.520(9)
C(3)-C(16)	1.400(9)	C(25)-C(26B)	1.506(10)
C(4)-C(5)	1.388(10)	C(25)-C(27A)	1.509(9)
C(4)-C(17A)	1.516(16)	C(25)-C(27B)	1.505(10)
C(4)-C(17B)	1.539(19)	C(25)-C(28A)	1.490(9)
C(5)-C(6)	1.389(10)	C(25)-C(28B)	1.517(10)
C(6)-C(7)	1.377(11)	C(29A)-C(30A)	1.483(17)
C(6)-C(21)	1.510(12)	C(30A)-C(31A)	1.450(18)
C(7)-C(8)	1.367(12)	C(30A)-C(35A)	1.349(17)
C(8)-C(9)	1.397(11)	C(31A)-C(32A)	1.360(16)
C(8)-C(17A)	1.570(16)	C(32A)-C(33A)	1.308(17)
C(8)-C(17B)	1.535(19)	C(33A)-C(34A)	1.486(18)
C(9)-C(10)	1.408(13)	C(34A)-C(35A)	1.423(19)
C(9)-C(29A)	1.45(2)	C(29B)-C(30B)	1.476(19)
C(9)-C(29B)	1.63(3)	C(30B)-C(31B)	1.43(2)
C(10)-C(11)	1.393(12)	C(30B)-C(35B)	1.347(19)
C(11)-C(12)	1.382(12)	C(31B)-C(32B)	1.352(17)
C(11)-C(19A)	1.528(15)	C(32B)-C(33B)	1.336(19)
C(11)-C(19B)	1.498(19)	C(33B)-C(34B)	1.477(19)
C(12)-C(13)	1.389(13)	C(34B)-C(35B)	1.40(2)
C(13)-C(14)	1.414(12)	C(36A)-P(1)	1.847(10)
C(13)-C(25)	1.555(13)	C(36A)-C(37A)	1.528(11)
C(14)-C(15)	1.388(12)	C(36B)-P(1)	1.837(12)
C(15)-C(16)	1.384(10)	C(36B)-C(37B)	1.523(12)
C(15)-C(19A)	1.515(15)	C(38A)-P(1)	1.851(10)
C(15)-C(19B)	1.605(19)	C(38A)-C(39A)	1.527(11)
C(17A)-C(18A)	1.560(14)	C(38B)-P(1)	1.847(12)
C(17B)-C(18B)	1.565(15)	C(38B)-C(39B)	1.524(12)
C(17A)-C(19A)	1.53(2)	C(40A)-P(1)	1.839(10)
C(17B)-C(19B)	1.50(3)	C(40A)-C(41A)	1.533(11)
C(19A)-C(20A)	1.596(14)	C(40B)-P(1)	1.851(12)
C(19B)-C(20B)	1.595(15)	C(40B)-C(41B)	1.526(12)

C(42)-C(43)	1.55(4)	C(43)-C(44)	1.48(4)
C(42)-C(42)’	1.59(4)		

Table S6. Bond Angles [°] for ***trans*-(PhCODHP)$_2$Pt(PEt$_3$)$_2$ • ½ C$_6$H$_{14}$**

P(1)-Pt(1)-P(1)’	180.0	C(8)-C(17B)-C(18B)	106.6(13)
O(1A)-C(29A)-C(9)	119.3(15)	C(9)-C(8)-C(17B)	114.4(10)
O(1A)-C(29A)-C(30A)	121.7(15)	C(9)-C(8)-C(17A)	114.3(9)
O(1B)-C(29B)-C(30B)	120.9(19)	C(9)-C(29A)-C(30A)	118.8(14)
O(1B)-C(29B)-C(9)	122.5(17)	C(10)-C(9)-C(29A)	113.0(11)
C(1)-Pt(1)-P(1)	85.3(2)	C(10)-C(9)-C(29B)	122.5(11)
C(1)-Pt(1)-P(1)’	94.7(2)	C(10)-C(11)-C(19B)	113.7(10)
C(1)-Pt(1)-C(1)’	180.000(1)	C(10)-C(11)-C(19A)	117.5(9)
C(1)-C(2)-C(3)	176.2(7)	C(11)-C(10)-C(9)	122.5(8)
C(2)-C(1)-Pt(1)	173.3(7)	C(11)-C(12)-C(13)	122.9(8)
C(3)-C(4)-C(17A)	117.1(8)	C(11)-C(19A)-C(20A)	110.4(10)
C(3)-C(4)-C(17B)	117.8(9)	C(11)-C(19B)-C(20B)	112.2(14)
C(4)-C(5)-C(6)	123.3(7)	C(11)-C(19B)-C(15)	110.7(11)
C(4)-C(3)-C(2)	121.4(6)	C(12)-C(11)-C(10)	124.8(8)
C(4)-C(17A)-C(8)	110.3(10)	C(12)-C(11)-C(19B)	119.6(10)
C(4)-C(17B)-C(18B)	109.1(13)	C(12)-C(11)-C(19A)	115.4(9)
C(4)-C(17A)-C(19A)	109.2(11)	C(12)-C(13)-C(14)	120.1(8)
C(4)-C(17A)-C(18A)	108.4(10)	C(12)-C(13)-C(25)	121.7(8)
C(5)-C(4)-C(17A)	119.1(8)	C(14)-C(15)-C(19A)	115.9(8)
C(5)-C(4)-C(17B)	117.4(9)	C(14)-C(15)-C(19B)	117.1(9)
C(5)-C(4)-C(3)	122.5(6)	C(14)-C(13)-C(25)	118.1(9)
C(5)-C(6)-C(21)	119.1(7)	C(15)-C(14)-C(13)	122.1(8)
C(6)-C(21)-C(23B)	116.2(16)	C(15)-C(16)-C(3)	123.2(7)
C(6)-C(21)-C(22B)	104.6(14)	C(15)-C(19A)-C(17A)	107.3(10)
C(6)-C(21)-C(24A)	115.5(8)	C(15)-C(19A)-C(11)	114.1(10)
C(6)-C(21)-C(23A)	105.6(8)	C(15)-C(19A)-C(20A)	108.1(10)
C(6)-C(21)-C(22A)	109.0(8)	C(16)-C(15)-C(14)	124.5(7)
C(6)-C(21)-C(24B)	106.1(15)	C(16)-C(15)-C(19A)	117.1(8)
C(7)-C(6)-C(5)	119.0(8)	C(16)-C(15)-C(19B)	116.9(9)
C(7)-C(6)-C(21)	121.9(7)	C(16)-C(3)-C(4)	118.8(6)
C(7)-C(8)-C(9)	125.7(8)	C(16)-C(3)-C(2)	119.8(6)
C(7)-C(8)-C(17B)	118.3(10)	C(17A)-C(19A)-C(11)	107.1(11)
C(7)-C(8)-C(17A)	118.4(8)	C(17A)-C(19A)-C(20A)	109.7(11)
C(8)-C(7)-C(6)	123.9(7)	C(17B)-C(19B)-C(11)	109.1(14)
C(8)-C(9)-C(10)	121.6(8)	C(17B)-C(19B)-C(20B)	112.0(14)
C(8)-C(9)-C(29A)	125.1(12)	C(17B)-C(19B)-C(15)	105.4(13)
C(8)-C(9)-C(29B)	115.7(11)	C(18A)-C(17A)-C(8)	107.0(10)
C(8)-C(17B)-C(4)	111.0(12)	C(19A)-C(17A)-C(18A)	111.9(12)

C(19A)-C(17A)-C(8)	110.0(10)	C(31A)-C(30A)-C(29A)	115.2(14)
C(19B)-C(17B)-C(8)	109.1(14)	C(31B)-C(30B)-C(29B)	122.4(17)
C(19B)-C(17B)-C(4)	109.9(13)	C(32B)-C(31B)-C(30B)	121.8(19)
C(19B)-C(17B)-C(18B)	111.1(14)	C(32A)-C(31A)-C(30A)	117.8(15)
C(20B)-C(19B)-C(15)	107.1(13)	C(32A)-C(33A)-C(34A)	123.2(16)
C(22B)-C(21)-C(24A)	80.2(14)	C(32B)-C(33B)-C(34B)	115.4(17)
C(22B)-C(21)-C(23A)	138.1(16)	C(33A)-C(32A)-C(31A)	121.8(17)
C(22B)-C(21)-C(24B)	103.5(10)	C(33B)-C(32B)-C(31B)	122.4(19)
C(23B)-C(21)-C(22B)	114.2(12)	C(35A)-C(30A)-C(31A)	121.4(14)
C(23B)-C(21)-C(24A)	119.3(18)	C(35A)-C(30A)-C(29A)	123.4(15)
C(23B)-C(21)-C(24B)	111.1(9)	C(35A)-C(34A)-C(33A)	113.6(14)
C(23A)-C(21)-C(24B)	95.1(15)	C(35B)-C(30B)-C(31B)	118.4(16)
C(23B)-C(21)-C(22A)	88.1(16)	C(35B)-C(30B)-C(29B)	119.1(18)
C(23A)-C(21)-C(22A)	112.7(9)	C(35B)-C(34B)-C(33B)	120.1(17)
C(24A)-C(21)-C(23A)	111.1(8)	C(36B)-P(1)-C(40A)	115.2(11)
C(24A)-C(21)-C(22A)	103.1(9)	C(36B)-P(1)-C(36A)	46.7(13)
C(24B)-C(21)-C(22A)	126.2(16)	C(36B)-P(1)-C(38B)	113.3(16)
C(26B)-C(25)-C(26A)	58.1(14)	C(36A)-P(1)-C(38B)	138.0(13)
C(26B)-C(25)-C(27A)	139.6(16)	C(36B)-P(1)-C(40B)	111.2(18)
C(26B)-C(25)-C(28B)	93.8(19)	C(36A)-P(1)-C(40B)	72.8(13)
C(26B)-C(25)-C(13)	111.5(15)	C(36B)-P(1)-C(38A)	54.3(14)
C(26A)-C(25)-C(13)	110.4(9)	C(36A)-P(1)-C(38A)	101.0(6)
C(27A)-C(25)-C(26A)	106.0(10)	C(36B)-P(1)-Pt(1)	125.3(10)
C(27B)-C(25)-C(26B)	122(2)	C(36A)-P(1)-Pt(1)	113.8(4)
C(27B)-C(25)-C(28B)	100(2)	C(37A)-C(36A)-P(1)	112.0(9)
C(27A)-C(25)-C(28B)	72.0(15)	C(37B)-C(36B)-P(1)	103(2)
C(27B)-C(25)-C(26A)	74.2(16)	C(38A)-P(1)-Pt(1)	110.0(5)
C(27B)-C(25)-C(13)	114.1(16)	C(38B)-P(1)-Pt(1)	107.2(13)
C(27A)-C(25)-C(13)	108.8(9)	C(38B)-P(1)-C(40B)	88.6(15)
C(28A)-C(25)-C(27B)	135.3(17)	C(38B)-P(1)-C(38A)	72.3(11)
C(28A)-C(25)-C(26B)	49.5(13)	C(39A)-C(38A)-P(1)	111.1(9)
C(28A)-C(25)-C(27A)	117.9(11)	C(39B)-C(38B)-P(1)	103(2)
C(28A)-C(25)-C(28B)	48.1(14)	C(40A)-P(1)-C(36A)	105.9(7)
C(28A)-C(25)-C(26A)	106.0(10)	C(40A)-P(1)-C(40B)	47.2(11)
C(28B)-C(25)-C(26A)	135.5(16)	C(40A)-P(1)-C(38A)	104.9(6)
C(28A)-C(25)-C(13)	107.6(9)	C(40B)-P(1)-C(38A)	143.9(14)
C(28B)-C(25)-C(13)	112.1(15)	C(40A)-P(1)-Pt(1)	119.5(4)
C(30A)-C(35A)-C(34A)	121.4(15)	C(40B)-P(1)-Pt(1)	104.8(14)
C(30B)-C(29B)-C(9)	116.5(15)	C(41A)-C(40A)-P(1)	115.2(9)
C(30B)-C(35B)-C(34B)	118.9(17)	C(41B)-C(40B)-P(1)	105(2)

C(43)-C(42)-C(42)’	108(2)	C(44)-C(43)-C(42)	112(3)

Figure S3. ORTEP3 Plot showing labeling for ***trans*-(PhCODHP)$_2$Pt(PPh$_3$)$_2$ • 2 CH$_2$Cl$_2$**

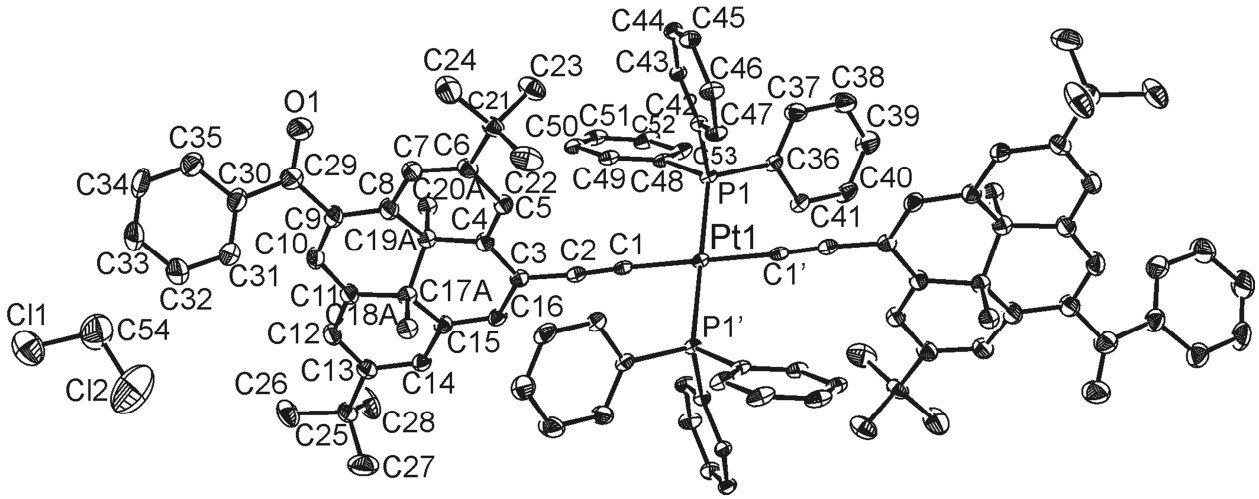


Table S7. Atomic Coordinates [$\times 10^4$] and Equivalent Isotropic Displacement Parameters [$Å^2 \times 10^3$] for ***trans*-(PhCODHP)$_2$Pt(PPh$_3$)$_2$ • 2 CH$_2$Cl$_2$**

	x	y	z	U_{eq}
Pt(1)	0	5000	0	23(1)
Cl(1)	3180(3)	829(3)	7834(1)	113(1)
Cl(2)	1778(5)	2506(4)	6821(3)	205(2)
P(1)	-2255(1)	6153(1)	514(1)	24(1)
O(1)	3955(6)	-1188(4)	3959(2)	79(1)
C(1)	819(4)	4630(3)	836(2)	26(1)
C(2)	1197(5)	4414(4)	1367(2)	31(1)
C(3)	1609(5)	4028(4)	2006(2)	33(1)
C(4)	1865(6)	2827(4)	2292(2)	38(1)
C(5)	1638(5)	2042(4)	2003(2)	36(1)
C(6)	1851(6)	864(4)	2300(2)	43(1)
C(7)	2286(7)	483(4)	2912(2)	46(1)
C(8)	2523(7)	1205(5)	3263(2)	50(1)
C(9)	2859(7)	892(5)	3901(2)	50(1)
C(10)	2947(7)	1725(5)	4230(3)	52(1)
C(11)	2629(6)	2883(4)	3967(2)	45(1)
C(12)	2678(6)	3723(5)	4292(2)	46(1)
C(13)	2395(6)	4887(5)	4007(2)	43(1)
C(14)	2112(6)	5235(4)	3355(2)	39(1)
C(15)	2006(5)	4480(4)	2996(2)	36(1)
C(16)	1737(6)	4797(4)	2353(2)	38(1)
C(21)	1548(6)	67(4)	1935(2)	44(1)
C(22)	-104(8)	618(6)	1776(4)	71(2)
C(23)	2655(8)	-53(6)	1309(3)	62(2)
C(24)	1764(11)	-1170(6)	2327(3)	79(2)
C(25)	2438(7)	5790(5)	4371(3)	48(1)
C(26)	3665(11)	6262(8)	4034(3)	86(2)
C(27)	896(10)	6738(7)	4431(4)	94(3)
C(28)	2769(10)	5252(6)	5071(3)	72(2)
C(29)	3220(7)	-343(5)	4245(3)	56(1)
C(30)	2697(7)	-574(5)	4953(3)	51(1)
C(31)	1418(8)	202(5)	5261(3)	62(2)
C(32)	978(10)	-82(6)	5912(3)	81(2)
C(33)	1714(11)	-1130(7)	6248(3)	83(2)
C(34)	2958(10)	-1906(6)	5959(3)	78(2)

C(35)	3483(8)	-1648(5)	5309(3)	60(2)
C(36)	-2691(5)	5606(4)	1369(2)	30(1)
C(37)	-3399(7)	6368(5)	1811(3)	53(1)
C(38)	-3806(9)	5934(6)	2451(3)	83(3)
C(39)	-3530(8)	4753(5)	2649(3)	69(2)
C(40)	-2799(6)	3985(4)	2213(3)	48(1)
C(41)	-2369(5)	4416(4)	1574(2)	35(1)
C(42)	-2168(4)	7596(3)	496(2)	26(1)
C(43)	-3453(5)	8596(4)	493(2)	28(1)
C(44)	-3342(5)	9673(4)	505(2)	32(1)
C(45)	-1938(5)	9743(4)	521(2)	36(1)
C(46)	-650(5)	8751(4)	525(2)	39(1)
C(47)	-762(5)	7680(4)	512(2)	34(1)
C(48)	-4015(4)	6456(3)	201(2)	28(1)
C(49)	-4202(5)	7061(4)	-422(2)	32(1)
C(50)	-5535(5)	7279(4)	-676(3)	38(1)
C(51)	-6663(5)	6882(4)	-304(3)	43(1)
C(52)	-6491(5)	6278(4)	312(3)	44(1)
C(53)	-5176(5)	6062(4)	567(3)	37(1)
C(54)	3062(12)	1151(11)	6995(5)	128(4)
C(17A)	1900(10)	3313(6)	3341(3)	39(2)
C(18A)	177(8)	3491(7)	3543(4)	45(2)
C(19A)	2669(8)	2383(5)	2899(3)	36(2)
C(20A)	4389(7)	2190(6)	2684(3)	40(2)
C(17B)	2640(30)	3146(16)	3241(9)	30(5)
C(18B)	4310(20)	2740(20)	2888(11)	46(6)
C(19B)	1740(20)	2561(17)	3048(9)	35(5)
C(20B)	-30(30)	3030(20)	3398(11)	47(6)

U_{eq} is defined as one third of the trace of the orthogonalized U_{ij} tensor.

Table S8. Bond Lengths [Å] for ***trans*-(PhCODHP)$_2$Pt(PPh$_3$)$_2$ • 2 CH$_2$Cl$_2$**

Pt(1)-P(1)	2.3064(10)	C(29)-C(30)	1.492(8)
Pt(1)-C(1)	1.994(4)	C(30)-C(31)	1.388(9)
C(1)-C(2)	1.208(6)	C(30)-C(35)	1.402(8)
C(2)-C(3)	1.431(6)	C(31)-C(32)	1.375(9)
C(3)-C(16)	1.392(6)	C(32)-C(33)	1.349(10)
C(3)-C(4)	1.433(6)	C(33)-C(34)	1.354(11)
C(4)-C(5)	1.370(6)	C(34)-C(35)	1.385(9)
C(4)-C(19A)	1.537(8)	C(36)-C(41)	1.383(6)
C(4)-C(19B)	1.566(19)	C(36)-C(37)	1.383(7)
C(5)-C(6)	1.418(7)	C(36)-P(1)	1.824(4)
C(6)-C(7)	1.386(7)	C(37)-C(38)	1.387(8)
C(6)-C(21)	1.530(7)	C(38)-C(39)	1.375(9)
C(7)-C(8)	1.399(7)	C(39)-C(40)	1.381(8)
C(8)-C(9)	1.406(7)	C(40)-C(41)	1.390(7)
C(8)-C(19A)	1.541(8)	C(42)-C(43)	1.383(6)
C(8)-C(19B)	1.57(2)	C(42)-C(47)	1.393(6)
C(9)-C(10)	1.415(8)	C(42)-P(1)	1.823(4)
C(9)-C(29)	1.493(8)	C(43)-C(44)	1.392(6)
C(10)-C(11)	1.368(7)	C(44)-C(45)	1.383(6)
C(11)-C(12)	1.402(7)	C(45)-C(46)	1.379(7)
C(11)-C(17B)	1.514(19)	C(46)-C(47)	1.386(6)
C(11)-C(17A)	1.536(8)	C(48)-C(49)	1.387(6)
C(12)-C(13)	1.388(7)	C(48)-C(53)	1.398(6)
C(13)-C(14)	1.418(7)	C(48)-P(1)	1.817(4)
C(13)-C(25)	1.525(7)	C(49)-C(50)	1.399(6)
C(14)-C(15)	1.386(7)	C(50)-C(51)	1.379(7)
C(15)-C(16)	1.395(7)	C(51)-C(52)	1.373(8)
C(15)-C(17A)	1.505(8)	C(52)-C(53)	1.384(7)
C(15)-C(17B)	1.547(19)	C(54)-Cl(2)	1.690(12)
C(21)-C(23)	1.523(7)	C(54)-Cl(1)	1.769(11)
C(21)-C(24)	1.542(8)	C(17A)-C(19A)	1.532(10)
C(21)-C(22)	1.544(9)	C(17A)-C(18A)	1.554(11)
C(25)-C(26)	1.486(9)	C(19A)-C(20A)	1.551(9)
C(25)-C(27)	1.505(9)	C(17B)-C(19B)	1.48(3)
C(25)-C(28)	1.545(8)	C(17B)-C(18B)	1.56(3)
C(29)-O(1)	1.240(7)	C(19B)-C(20B)	1.64(3)

Table S9. Bond Angles [°] for ***trans*-(PhCODHP)$_2$Pt(PPh$_3$)$_2$ • 2 CH$_2$Cl$_2$**

Pt(1)-C(1)-C(2)	174.6(3)	C(8)-C(9)-C(29)	121.4(5)
Cl(2)-C(54)-Cl(1)	109.2(7)	C(8)-C(19A)-C(20A)	107.8(5)
C(15)-C(17A)-C(19A)	110.5(5)	C(8)-C(19B)-C(20B)	111.4(15)
P(1)-Pt(1)-P(1)’	180.00(6)	C(9)-C(8)-C(19A)	115.4(5)
O(1)-C(29)-C(30)	118.8(5)	C(9)-C(8)-C(19B)	114.1(8)
O(1)-C(29)-C(9)	121.7(5)	C(10)-C(9)-C(29)	117.4(5)
C(1)-Pt(1)-C(1)’	180.0	C(10)-C(11)-C(12)	123.4(5)
C(1)-Pt(1)-P(1)	86.77(11)	C(10)-C(11)-C(17B)	114.7(8)
C(1)-Pt(1)-P(1)#1	93.23(11)	C(10)-C(11)-C(17A)	117.4(5)
C(48)-P(1)-Pt(1)	118.51(14)	C(11)-C(10)-C(9)	122.7(5)
C(42)-P(1)-Pt(1)	109.94(13)	C(11)-C(17A)-C(18A)	106.6(5)
C(36)-P(1)-Pt(1)	114.78(14)	C(11)-C(17B)-C(15)	111.6(12)
C(42)-P(1)-C(36)	104.76(19)	C(11)-C(17B)-C(18B)	110.3(15)
C(48)-P(1)-C(36)	103.0(2)	C(12)-C(11)-C(17B)	120.0(8)
C(48)-P(1)-C(42)	104.47(18)	C(12)-C(11)-C(17A)	118.2(5)
C(1)-C(2)-C(3)	173.1(4)	C(12)-C(13)-C(14)	119.2(4)
C(2)-C(3)-C(4)	118.7(4)	C(12)-C(13)-C(25)	121.5(5)
C(3)-C(4)-C(19A)	116.5(4)	C(13)-C(12)-C(11)	122.3(5)
C(3)-C(4)-C(19B)	115.7(8)	C(13)-C(25)-C(28)	111.9(5)
C(3)-C(16)-C(15)	123.0(4)	C(14)-C(13)-C(25)	119.3(5)
C(4)-C(5)-C(6)	122.8(4)	C(14)-C(15)-C(16)	124.1(4)
C(4)-C(19A)-C(8)	112.0(5)	C(14)-C(15)-C(17A)	118.6(5)
C(4)-C(19A)-C(20A)	108.2(5)	C(14)-C(15)-C(17B)	118.4(8)
C(4)-C(19B)-C(8)	108.8(12)	C(15)-C(14)-C(13)	122.9(4)
C(4)-C(19B)-C(20B)	112.2(14)	C(15)-C(17A)-C(11)	112.7(5)
C(5)-C(6)-C(21)	118.4(4)	C(15)-C(17A)-C(18A)	107.0(6)
C(5)-C(4)-C(3)	123.3(4)	C(15)-C(17B)-C(18B)	104.4(14)
C(5)-C(4)-C(19A)	119.5(4)	C(16)-C(15)-C(17A)	116.4(4)
C(5)-C(4)-C(19B)	116.4(8)	C(16)-C(3)-C(2)	121.4(4)
C(6)-C(21)-C(24)	112.6(5)	C(16)-C(3)-C(4)	120.0(4)
C(6)-C(7)-C(8)	123.4(5)	C(16)-C(15)-C(17B)	115.4(8)
C(6)-C(21)-C(22)	109.4(4)	C(17A)-C(19A)-C(4)	106.9(5)
C(7)-C(8)-C(19B)	115.6(8)	C(17A)-C(19A)-C(8)	109.2(5)
C(7)-C(6)-C(5)	119.2(4)	C(17A)-C(19A)-C(20A)	112.7(6)
C(7)-C(6)-C(21)	122.4(4)	C(17B)-C(19B)-C(4)	107.7(15)
C(7)-C(8)-C(9)	125.8(5)	C(17B)-C(19B)-C(8)	106.8(15)
C(7)-C(8)-C(19A)	118.1(5)	C(17B)-C(19B)-C(20B)	109.8(18)
C(8)-C(9)-C(10)	121.1(5)	C(19A)-C(17A)-C(11)	108.7(6)

C(19A)-C(17A)-C(18A)	111.3(6)	C(36)-C(41)-C(40)	120.5(4)
C(19B)-C(17B)-C(11)	110.7(15)	C(37)-C(36)-P(1)	121.0(3)
C(19B)-C(17B)-C(15)	109.6(15)	C(38)-C(39)-C(40)	120.1(5)
C(19B)-C(17B)-C(18B)	110.1(18)	C(39)-C(38)-C(37)	120.5(6)
C(23)-C(21)-C(6)	108.9(4)	C(39)-C(40)-C(41)	119.6(5)
C(23)-C(21)-C(24)	108.2(5)	C(41)-C(36)-C(37)	119.5(4)
C(23)-C(21)-C(22)	109.4(5)	C(41)-C(36)-P(1)	119.4(3)
C(24)-C(21)-C(22)	108.3(5)	C(42)-C(43)-C(44)	120.4(4)
C(26)-C(25)-C(27)	112.3(6)	C(43)-C(42)-C(47)	119.2(4)
C(26)-C(25)-C(13)	109.5(5)	C(43)-C(42)-P(1)	122.4(3)
C(26)-C(25)-C(28)	107.8(5)	C(45)-C(44)-C(43)	119.8(4)
C(27)-C(25)-C(13)	109.6(5)	C(45)-C(46)-C(47)	119.9(4)
C(27)-C(25)-C(28)	105.7(6)	C(46)-C(47)-C(42)	120.5(4)
C(30)-C(29)-C(9)	119.5(5)	C(46)-C(45)-C(44)	120.2(4)
C(31)-C(30)-C(35)	119.2(5)	C(47)-C(42)-P(1)	118.4(3)
C(31)-C(30)-C(29)	122.5(5)	C(48)-C(49)-C(50)	120.5(4)
C(32)-C(31)-C(30)	119.4(6)	C(49)-C(48)-C(53)	118.9(4)
C(32)-C(33)-C(34)	120.7(7)	C(49)-C(48)-P(1)	119.7(3)
C(33)-C(32)-C(31)	121.1(7)	C(51)-C(50)-C(49)	119.4(5)
C(33)-C(34)-C(35)	120.6(6)	C(51)-C(52)-C(53)	120.1(5)
C(34)-C(35)-C(30)	119.0(6)	C(52)-C(51)-C(50)	120.8(4)
C(35)-C(30)-C(29)	118.2(6)	C(52)-C(53)-C(48)	120.3(5)
C(36)-C(37)-C(38)	119.8(5)	C(53)-C(48)-P(1)	121.4(3)

Figure S4. ORTEP3 Plot showing labeling for ***trans*-(BDHP)$_2$Pt(PPh$_3$)$_2$ • C$_6$H$_{14}$**

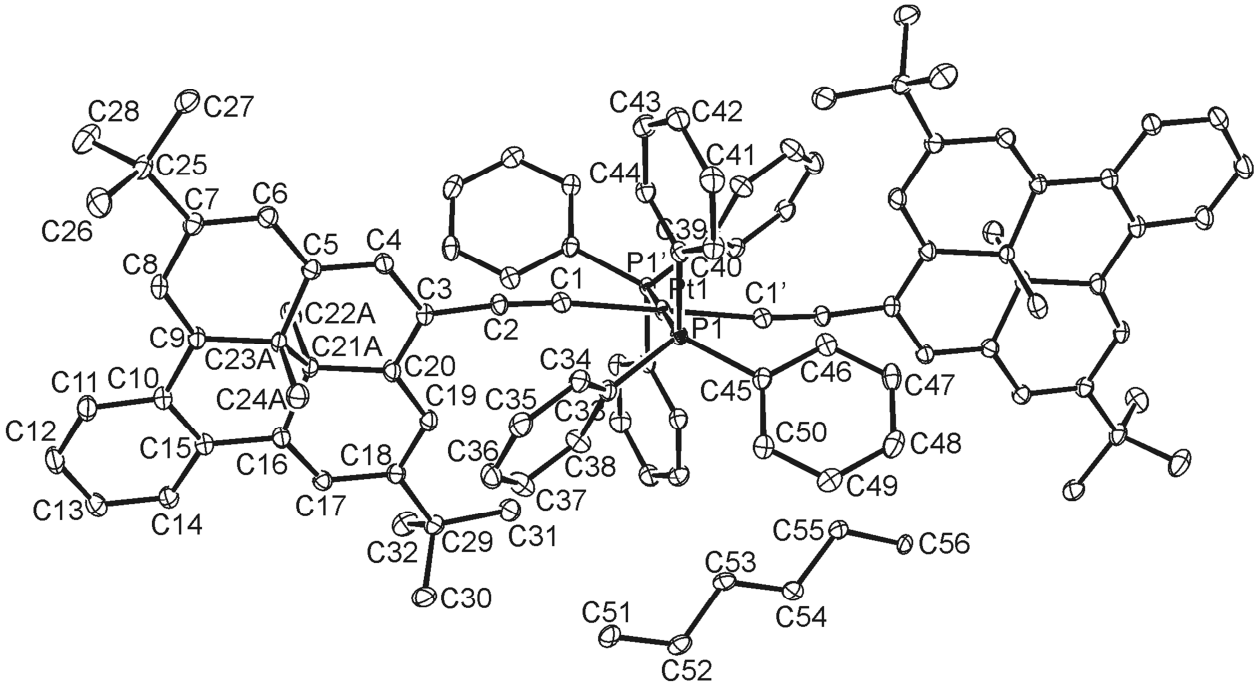


Table S10. Atomic Coordinates [$\times 10^4$] and Equivalent Isotropic Displacement Parameters [$Å^2 \times 10^3$] for ***trans*-(BDHP)$_2$Pt(PPh$_3$)$_2$ • C$_6$H$_{14}$**

	x	y	z	U_{eq}
Pt(1)	5000	0	5000	24(1)
P(1)	6812(1)	-362(1)	4300(1)	23(1)
C(1)	4325(3)	1078(3)	3809(2)	27(1)
C(2)	3955(3)	1647(3)	3046(2)	26(1)
C(3)	3473(3)	2226(3)	2141(2)	28(1)
C(4)	3579(3)	3229(3)	1693(2)	30(1)
C(5)	3133(3)	3825(3)	836(2)	29(1)
C(6)	3225(3)	4833(3)	389(2)	31(1)
C(7)	2789(3)	5411(3)	-473(2)	30(1)
C(8)	2218(3)	4987(3)	-948(2)	31(1)
C(9)	2066(3)	4050(3)	-583(2)	30(1)
C(10)	1443(3)	3636(3)	-1050(2)	32(1)
C(11)	947(4)	4211(3)	-1936(3)	42(1)
C(12)	297(4)	3879(4)	-2357(3)	47(1)
C(13)	109(4)	2951(3)	-1918(3)	44(1)
C(14)	593(3)	2359(3)	-1062(3)	36(1)
C(15)	1265(3)	2679(3)	-601(2)	30(1)
C(16)	1768(3)	2034(3)	313(2)	29(1)
C(17)	1670(3)	1093(3)	770(2)	29(1)
C(18)	2160(3)	461(3)	1670(2)	28(1)
C(19)	2760(3)	838(3)	2101(2)	32(1)
C(20)	2899(3)	1827(3)	1696(2)	32(1)
C(21A)	2107(8)	2645(6)	853(5)	27(2)
C(22A)	957(7)	3498(8)	1194(6)	37(2)
C(23A)	2787(9)	3248(7)	264(6)	32(2)
C(24A)	3965(7)	2416(8)	-98(6)	38(2)
C(21B)	2710(8)	2305(6)	643(5)	24(2)
C(22B)	3888(6)	1840(7)	96(5)	30(2)
C(23B)	2242(8)	3562(7)	465(6)	27(2)
C(24B)	1091(7)	4035(7)	972(6)	31(2)
C(25)	2872(3)	6492(3)	-967(3)	35(1)
C(26)	3569(4)	6381(4)	-1871(3)	47(1)
C(27)	3497(4)	6838(3)	-378(3)	39(1)
C(28)	1622(4)	7385(3)	-1186(4)	54(1)

C(29)	2002(3)	-602(3)	2099(2)	32(1)
C(30)	2582(4)	-1386(3)	1467(3)	44(1)
C(31)	2543(4)	-1161(3)	3062(3)	45(1)
C(32)	689(4)	-363(3)	2180(3)	47(1)
C(33)	6795(3)	-348(3)	3082(2)	27(1)
C(34)	7464(3)	78(3)	2413(2)	33(1)
C(35)	7389(4)	106(3)	1492(3)	39(1)
C(36)	6641(4)	-267(3)	1230(3)	40(1)
C(37)	5990(4)	-699(4)	1891(3)	44(1)
C(38)	6059(3)	-737(3)	2816(3)	37(1)
C(39)	7333(3)	673(3)	4325(2)	26(1)
C(40)	8531(3)	465(3)	4247(2)	33(1)
C(41)	8898(3)	1281(3)	4254(3)	40(1)
C(42)	8093(4)	2283(3)	4350(3)	39(1)
C(43)	6902(3)	2493(3)	4429(3)	37(1)
C(44)	6518(3)	1695(3)	4415(2)	31(1)
C(45)	8029(3)	-1640(3)	4799(2)	28(1)
C(46)	8367(3)	-1834(3)	5705(2)	31(1)
C(47)	9271(3)	-2811(3)	6117(3)	35(1)
C(48)	9851(4)	-3586(3)	5621(3)	42(1)
C(49)	9530(4)	-3398(3)	4719(3)	47(1)
C(50)	8619(4)	-2430(3)	4304(3)	39(1)
C(51)	4127(6)	3512(6)	7309(5)	36(2)
C(52)	3738(6)	4330(6)	6471(5)	36(2)
C(53)	3608(6)	3986(6)	5638(5)	33(2)
C(54)	3296(6)	4820(6)	4766(5)	30(2)
C(55)	3154(8)	4524(6)	3917(5)	46(2)
C(56)	2870(6)	5423(6)	3048(5)	34(2)

U_{eq} is defined as one third of the trace of the orthogonalized U_{ij} tensor.

Table S11. Bond Lengths [Å] for ***trans*-(BDHP)$_2$Pt(PPh$_3$)$_2$ • C$_6$H$_{14}$**

C(1)-C(19)	1.399(6)	C(22)-C(23)	1.565(6)
C(1)-C(2)	1.400(6)	C(23)-H(23A)	0.9800
C(1)-H(1)	0.9500	C(23)-H(23B)	0.9800
C(2)-C(3)	1.390(6)	C(23)-H(23C)	0.9800
C(2)-C(24)	1.516(13)	C(24)-C(26)	1.514(7)
C(2)-C(24B)	1.563(16)	C(24)-C(25)	1.518(7)
C(3)-C(4)	1.395(6)	C(24)-C(27)	1.519(8)
C(3)-H(3)	0.9500	C(25)-H(25A)	0.9800
C(4)-C(5)	1.390(6)	C(25)-H(25B)	0.9800
C(4)-C(20)	1.526(6)	C(25)-H(25C)	0.9800
C(5)-C(6)	1.385(6)	C(26)-H(26A)	0.9800
C(5)-H(5)	0.9500	C(26)-H(26B)	0.9800
C(6)-C(7)	1.416(6)	C(26)-H(26C)	0.9800
C(6)-H(6)	0.9500	C(27)-H(27A)	0.9800
C(7)-C(8)	1.384(6)	C(27)-H(27B)	0.9800
C(7)-C(22)	1.510(6)	C(27)-H(27C)	0.9800
C(8)-C(9)	1.408(6)	C(28)-C(31)	1.526(7)
C(8)-H(8)	0.9500	C(28)-C(30)	1.549(7)
C(9)-C(10)	1.386(6)	C(28)-C(29)	1.555(7)
C(9)-C(28)	1.535(6)	C(29)-H(29A)	0.9800
C(10)-C(11)	1.400(6)	C(29)-H(29B)	0.9800
C(10)-H(10)	0.9500	C(29)-H(29C)	0.9800
C(11)-C(12)	1.410(6)	C(30)-H(30A)	0.9800
C(11)-C(22)	1.522(6)	C(30)-H(30B)	0.9800
C(12)-C(18)	1.428(6)	C(30)-H(30C)	0.9800
C(12)-C(13)	1.459(6)	C(31)-H(31A)	0.9800
C(13)-C(14)	1.364(6)	C(31)-H(31B)	0.9800
C(13)-H(13)	0.9500	C(31)-H(31C)	0.9800
C(14)-C(15)	1.472(6)	C(32)-C(33)	1.395(6)
C(14)-C(32)	1.493(6)	C(32)-C(33')	1.398(6)
C(15)-C(16)	1.341(6)	C(33')-C(34')	1.396(6)
C(15)-H(15)	0.9500	C(33')-H(33')	0.9500
C(16)-C(36)	1.488(6)	C(33)-C(34)	1.393(6)
C(16)-C(17)	1.496(6)	C(33)-H(33)	0.9500
C(17)-C(18)	1.498(6)	C(34')-C(35)	1.380(7)
C(17)-H(17A)	0.9900	C(34')-H(34')	0.9500
C(17)-H(17B)	0.9900	C(34)-C(35)	1.373(7)
C(18)-C(19)	1.417(6)	C(34)-H(34)	0.9500
C(19)-C(20)	1.506(6)	C(35)-H(35)	0.9500
C(20)-C(22)	1.532(6)	C(36)-C(37')	1.393(6)
C(20)-C(21)	1.571(6)	C(36)-C(37)	1.409(6)
C(21)-H(21A)	0.9800	C(37)-C(38)	1.395(6)
C(21)-H(21B)	0.9800	C(37)-H(37)	0.9500
C(21)-H(21C)	0.9800	C(37')-C(38')	1.390(6)

C(37')-H(37')	0.9500
C(38)-C(39)	1.372(6)
C(38)-H(38)	0.9500
C(38')-C(39)	1.394(6)
C(38')-H(38')	0.9500
C(39)-H(39)	0.9500
C(26B)-C(24B)	1.516(8)
C(26B)-H(26D)	0.9800
C(26B)-H(26E)	0.9800
C(26B)-H(26F)	0.9800
C(27B)-C(24B)	1.518(8)
C(27B)-H(27D)	0.9800
C(27B)-H(27E)	0.9800
C(27B)-H(27F)	0.9800
C(25B)-C(24B)	1.515(8)
C(25B)-H(25D)	0.9800
C(25B)-H(25E)	0.9800
C(25B)-H(25F)	0.9800
Pt(1)-P(1)	2.2977(8)
Pt(1)-C(1)	1.996(3)
C(1)-C(2)	1.213(5)
C(2)-C(3)	1.429(5)
C(3)-C(20)	1.385(5)
C(3)-C(4)	1.427(5)
C(4)-C(5)	1.359(5)
C(5)-C(6)	1.426(5)
C(5)-C(23B)	1.511(9)
C(5)-C(23A)	1.525(9)
C(6)-C(7)	1.358(5)
C(7)-C(8)	1.437(5)
C(7)-C(25)	1.526(5)
C(8)-C(9)	1.352(5)
C(9)-C(10)	1.467(5)
C(9)-C(23A)	1.525(9)
C(9)-C(23B)	1.533(9)
C(10)-C(11)	1.410(5)
C(10)-C(15)	1.413(5)
C(11)-C(12)	1.365(6)
C(12)-C(13)	1.382(6)
C(13)-C(14)	1.371(5)
C(14)-C(15)	1.414(5)
C(15)-C(16)	1.462(5)
C(16)-C(17)	1.351(5)
C(16)-C(21A)	1.522(8)
C(16)-C(21B)	1.543(8)
C(17)-C(18)	1.438(5)
C(18)-C(19)	1.371(5)
C(18)-C(29)	1.528(5)
C(19)-C(20)	1.418(5)
C(20)-C(21B)	1.540(8)
C(20)-C(21A)	1.563(8)
C(21A)-C(23A)	1.489(12)
C(21A)-C(22A)	1.577(12)
C(21B)-C(23B)	1.553(11)
C(21B)-C(22B)	1.575(11)
C(23A)-C(24A)	1.598(13)
C(23B)-C(24B)	1.523(12)
C(25)-C(27)	1.526(5)
C(25)-C(26)	1.533(6)
C(25)-C(28)	1.543(5)
C(29)-C(31)	1.524(5)
C(29)-C(32)	1.532(5)
C(29)-C(30)	1.539(5)
C(33)-C(38)	1.385(5)
C(33)-C(34)	1.395(5)
C(33)-P(1)	1.823(3)
C(34)-C(35)	1.383(5)
C(35)-C(36)	1.378(6)
C(36)-C(37)	1.377(6)
C(37)-C(38)	1.386(5)
C(39)-C(44)	1.399(5)
C(39)-C(40)	1.400(5)
C(39)-P(1)	1.822(3)
C(40)-C(41)	1.394(5)
C(41)-C(42)	1.376(6)
C(42)-C(43)	1.391(6)
C(43)-C(44)	1.387(5)
C(45)-C(46)	1.391(5)
C(45)-C(50)	1.398(5)
C(45)-P(1)	1.826(3)
C(46)-C(47)	1.392(5)
C(47)-C(48)	1.381(6)
C(48)-C(49)	1.380(6)

C(49)-C(50)	1.392(6)	C(53)-C(54)	1.456(10)
C(51)-C(52)	1.418(10)	C(54)-C(55)	1.491(10)
C(52)-C(53)	1.502(10)	C(55)-C(56)	1.494(10)

Table S12. Bond Angles [°] for ***trans*-(BDHP)$_2$Pt(PPh$_3$)$_2$ • C$_6$H$_{14}$**

Pt(1)-C(1)-C(2)	173.6(3)	C(8)-C(9)-C(23A)	118.6(4)
Pt(1)-P(1)-C(39)	110.11(11)	C(8)-C(9)-C(23B)	117.4(4)
Pt(1)-P(1)-C(33)	113.13(11)	C(9)-C(23B)-C(21B)	107.7(6)
Pt(1)-P(1)-C(45)	118.35(11)	C(9)-C(8)-C(7)	124.0(3)
P(1)-Pt(1)-P(1)’	180.0	C(9)-C(23A)-C(24A)	107.8(7)
P(1)-Pt(1)-C(1)	87.07(9)	C(10)-C(9)-C(23A)	115.9(4)
P(1)-Pt(1)-C(1)’	92.93(9)	C(10)-C(9)-C(23B)	116.2(4)
P(1)-C(39)-C(44)	119.2(3)	C(10)-C(15)-C(16)	120.9(3)
P(1)-C(39)-C(40)	121.2(3)	C(11)-C(10)-C(15)	117.9(3)
P(1)-C(33)-C(38)	118.4(3)	C(11)-C(10)-C(9)	121.2(3)
P(1)-C(33)-C(34)	121.9(3)	C(11)-C(12)-C(13)	120.2(4)
P(1)-C(45)-C(46)	118.7(3)	C(12)-C(11)-C(10)	122.2(4)
P(1)-C(45)-C(50)	122.1(3)	C(13)-C(14)-C(15)	122.0(4)
C(1)-Pt(1)-C(1)’	180.00(13)	C(14)-C(13)-C(12)	119.4(4)
C(1)-C(2)-C(3)	173.4(4)	C(14)-C(15)-C(10)	118.2(3)
C(3)-C(20)-C(19)	122.6(3)	C(14)-C(15)-C(16)	120.9(3)
C(3)-C(20)-C(21B)	117.3(4)	C(15)-C(16)-C(21A)	114.5(4)
C(3)-C(20)-C(21A)	116.8(4)	C(15)-C(10)-C(9)	120.8(3)
C(4)-C(3)-C(2)	119.7(3)	C(15)-C(16)-C(21B)	115.9(4)
C(4)-C(5)-C(6)	123.0(3)	C(16)-C(17)-C(18)	124.2(3)
C(4)-C(5)-C(23B)	117.2(4)	C(16)-C(21A)-C(20)	110.2(5)
C(4)-C(5)-C(23A)	116.4(4)	C(16)-C(21A)-C(22A)	109.2(6)
C(5)-C(4)-C(3)	122.8(3)	C(16)-C(21B)-C(23B)	108.0(6)
C(5)-C(23A)-C(9)	111.6(6)	C(16)-C(21B)-C(22B)	109.2(6)
C(5)-C(23A)-C(24A)	107.9(7)	C(17)-C(16)-C(15)	124.2(3)
C(5)-C(23B)-C(24B)	107.0(6)	C(17)-C(16)-C(21A)	119.0(4)
C(5)-C(23B)-C(9)	111.9(6)	C(17)-C(16)-C(21B)	118.0(4)
C(5)-C(23B)-C(21B)	108.1(6)	C(17)-C(18)-C(29)	118.7(3)
C(6)-C(5)-C(23B)	117.8(4)	C(18)-C(19)-C(20)	122.5(3)
C(6)-C(5)-C(23A)	119.0(4)	C(18)-C(29)-C(32)	109.3(3)
C(6)-C(7)-C(8)	118.6(3)	C(18)-C(29)-C(30)	109.3(3)
C(6)-C(7)-C(25)	123.4(3)	C(19)-C(18)-C(17)	118.2(3)
C(7)-C(25)-C(28)	109.2(3)	C(19)-C(18)-C(29)	123.0(3)
C(7)-C(6)-C(5)	122.3(3)	C(19)-C(20)-C(21B)	117.9(4)
C(7)-C(25)-C(27)	112.0(3)	C(19)-C(20)-C(21A)	118.5(4)
C(7)-C(25)-C(26)	109.4(3)	C(20)-C(21B)-C(16)	110.3(5)
C(8)-C(7)-C(25)	118.0(3)	C(20)-C(21B)-C(23B)	107.0(6)
C(8)-C(9)-C(10)	124.2(3)	C(20)-C(21A)-C(22A)	110.6(6)

C(20)-C(3)-C(4)	119.6(3)	C(36)-C(35)-C(34)	120.4(4)
C(20)-C(3)-C(2)	120.7(3)	C(36)-C(37)-C(38)	120.5(4)
C(20)-C(21B)-C(22B)	111.0(6)	C(37)-C(36)-C(35)	119.9(3)
C(21A)-C(23A)-C(24A)	109.9(7)	C(38)-C(33)-C(34)	119.6(3)
C(21A)-C(23A)-C(5)	109.7(7)	C(39)-P(1)-C(33)	106.17(15)
C(21A)-C(23A)-C(9)	110.0(7)	C(39)-P(1)-C(45)	103.47(15)
C(23A)-C(21A)-C(16)	111.4(7)	C(41)-C(40)-C(39)	119.7(3)
C(23A)-C(21A)-C(22A)	108.1(7)	C(41)-C(42)-C(43)	120.1(3)
C(23A)-C(21A)-C(20)	107.4(6)	C(42)-C(41)-C(40)	120.4(4)
C(23B)-C(21B)-C(22B)	111.3(7)	C(43)-C(44)-C(39)	119.8(3)
C(24B)-C(23B)-C(9)	109.9(6)	C(44)-C(39)-C(40)	119.6(3)
C(24B)-C(23B)-C(21B)	112.4(7)	C(44)-C(43)-C(42)	120.3(4)
C(26)-C(25)-C(28)	109.7(3)	C(45)-C(46)-C(47)	120.2(3)
C(27)-C(25)-C(26)	107.8(3)	C(46)-C(45)-C(50)	119.2(3)
C(27)-C(25)-C(28)	108.7(3)	C(48)-C(47)-C(46)	120.2(3)
C(31)-C(29)-C(18)	112.4(3)	C(48)-C(49)-C(50)	120.3(4)
C(31)-C(29)-C(32)	108.3(3)	C(49)-C(48)-C(47)	120.1(4)
C(31)-C(29)-C(30)	108.7(3)	C(49)-C(50)-C(45)	120.0(4)
C(32)-C(29)-C(30)	108.7(3)	C(51)-C(52)-C(53)	117.8(6)
C(33)-C(38)-C(37)	119.9(4)	C(53)-C(54)-C(55)	119.3(6)
C(33)-P(1)-C(45)	104.55(15)	C(54)-C(53)-C(52)	117.1(6)
C(35)-C(34)-C(33)	119.8(4)	C(54)-C(55)-C(56)	115.6(7)

Figure S5. ORTEP3 Plot showing labeling for ***cis*-(BDHP)$_2$Pt(dppe)**

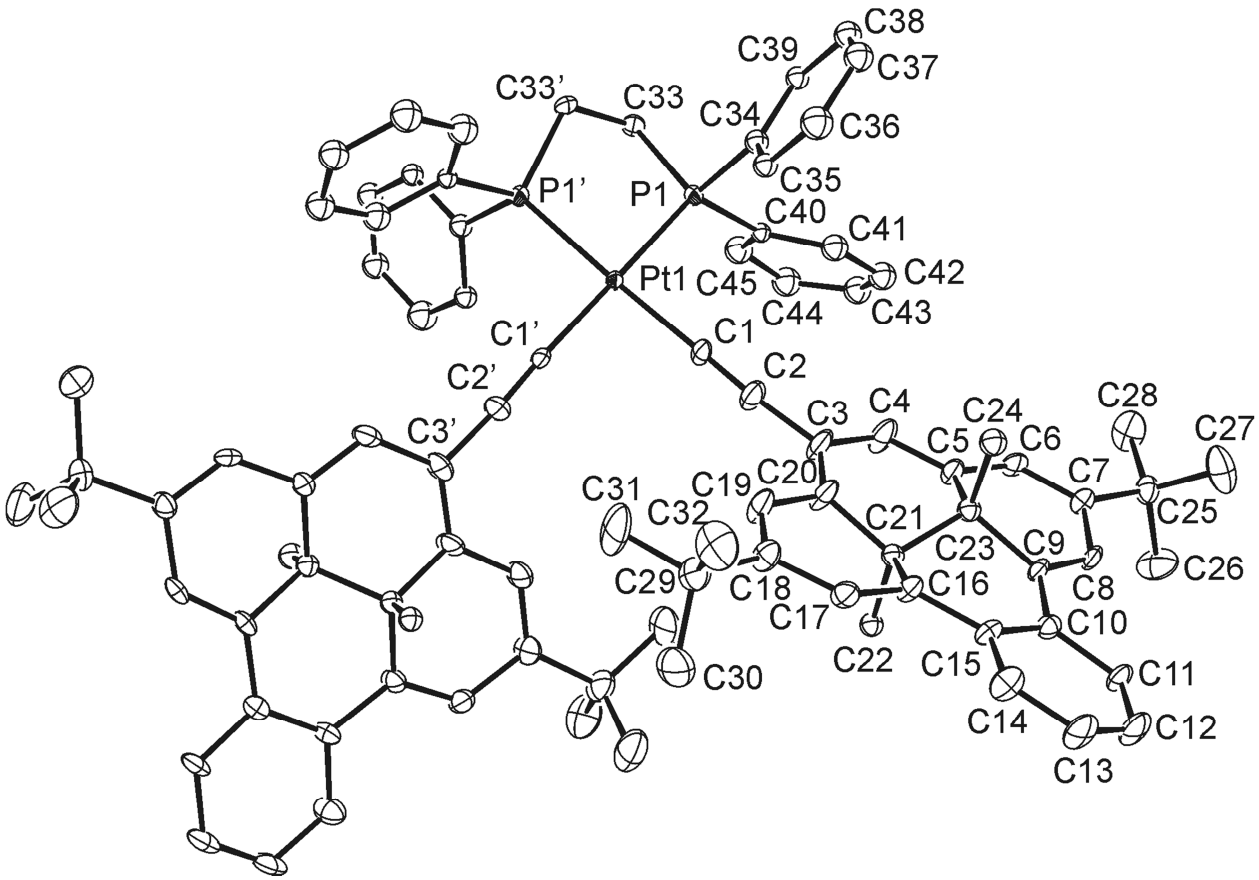


Table S13. Atomic Coordinates [$\times 10^4$] and Equivalent Isotropic Displacement Parameters [$Å^2 \times 10^3$] for ***cis*-(BDHP)$_2$Pt(dppe)**

	x	y	z	U_{eq}	occ
Pt(1)	0	6827(1)	7500	29(1)	
P(1)	-908(1)	6121(1)	7729(1)	28(1)	
C(1)	789(5)	7439(3)	7257(4)	38(2)	
C(2)	1220(6)	7815(4)	7090(4)	53(3)	
C(3)	1786(5)	8242(4)	6872(4)	55(3)	
C(4)	2681(5)	8088(4)	6895(4)	60(3)	
C(5)	3263(5)	8418(3)	6647(4)	38(2)	
C(6)	4144(5)	8285(3)	6650(4)	40(2)	
C(7)	4731(5)	8619(4)	6426(3)	38(2)	
C(8)	4444(5)	9169(3)	6203(3)	37(2)	
C(9)	3620(5)	9341(3)	6157(3)	30(2)	
C(10)	3322(5)	9878(3)	5910(3)	34(2)	
C(11)	3908(6)	10282(3)	5712(3)	43(2)	
C(12)	3625(7)	10763(4)	5433(4)	61(3)	
C(13)	2764(7)	10866(4)	5328(4)	62(3)	
C(14)	2175(6)	10491(4)	5533(4)	53(3)	
C(15)	2430(5)	10003(3)	5843(3)	35(2)	
C(16)	1802(5)	9639(3)	6099(3)	37(2)	
C(17)	964(5)	9744(4)	6096(4)	43(2)	
C(18)	354(5)	9400(4)	6376(4)	47(2)	
C(19)	632(5)	8914(4)	6622(4)	55(3)	
C(20)	1503(5)	8748(4)	6650(4)	51(3)	
C(21)	2168(6)	9206(5)	6527(5)	29(3)	0.73(1)
C(22)	2443(8)	9535(5)	7063(4)	31(3)	0.73(1)
C(23)	2935(8)	8888(6)	6271(6)	31(4)	0.73(1)
C(24)	2648(9)	8597(5)	5723(5)	40(4)	0.73(1)
C(21B)	2120(18)	9014(13)	6174(14)	32(9)	0.27(1)
C(22B)	2150(20)	8720(15)	5593(13)	40(10)	0.27(1)
C(23B)	2961(19)	9016(14)	6460(15)	23(9)	0.27(1)
C(24B)	2930(30)	9335(17)	7059(15)	58(12)	0.27(1)
C(25)	5664(5)	8456(4)	6410(4)	43(2)	
C(26)	6192(6)	8883(5)	6782(5)	84(4)	
C(27)	5931(7)	8488(6)	5831(5)	90(4)	
C(28)	5868(7)	7860(5)	6654(5)	77(3)	

C(29)	-577(6)	9613(4)	6356(5)	59(3)	
C(30)	-620(7)	10198(5)	6621(6)	92(4)	
C(31)	-1143(6)	9211(6)	6675(6)	100(5)	
C(32)	-940(7)	9645(6)	5762(5)	92(4)	
C(33)	-493(5)	5443(3)	7451(3)	34(2)	
C(34)	-936(9)	6038(5)	8501(3)	29(4)	0.61(2)
C(35)	-574(9)	6447(4)	8862(4)	29(4)	0.61(2)
C(36)	-616(9)	6376(5)	9429(4)	53(5)	0.61(2)
C(37)	-1019(8)	5896(5)	9635(3)	39(4)	0.61(2)
C(38)	-1381(8)	5486(5)	9274(4)	34(4)	0.61(2)
C(39)	-1340(8)	5557(4)	8707(4)	24(4)	0.61(2)
C(40)	-2035(9)	6208(7)	7507(8)	25(6)	0.61(2)
C(41)	-2629(9)	6423(8)	7850(6)	47(4)	0.61(2)
C(42)	-3462(9)	6505(7)	7685(7)	51(5)	0.61(2)
C(43)	-3725(10)	6377(7)	7166(8)	52(4)	0.61(2)
C(44)	-3186(11)	6194(7)	6776(7)	60(5)	0.61(2)
C(45)	-2313(11)	6097(7)	6978(7)	55(5)	0.61(2)
C(34B)	-1041(9)	5929(5)	8419(3)	26(5)	0.39(1)
C(35B)	-771(9)	6325(5)	8822(4)	39(5)	0.39(1)
C(36B)	-882(9)	6210(5)	9376(4)	50(5)	0.39(1)
C(37B)	-1264(9)	5698(5)	9527(4)	41(4)	0.39(1)
C(38B)	-1534(9)	5301(5)	9124(5)	42(5)	0.39(1)
C(39B)	-1422(9)	5417(5)	8570(4)	43(5)	0.39(1)
C(40B)	-1971(9)	6172(9)	7401(8)	35(14)	0.39(1)
C(41B)	-2675(13)	6153(12)	7724(8)	53(9)	0.39(1)
C(42B)	-3492(10)	6249(12)	7484(10)	73(11)	0.39(1)
C(43B)	-3604(9)	6362(9)	6922(10)	50(9)	0.39(1)
C(44B)	-2900(12)	6381(9)	6599(7)	57(9)	0.39(1)
C(45B)	-2083(10)	6286(9)	6839(7)	39(7)	0.39(1)

U_{eq} is defined as one third of the trace of the orthogonalized U_{ij} tensor.

Table S14. Bond Lengths [Å] **for *cis*-(BDHP)$_2$Pt(dppe)**

Pt(1)-C(1)	1.994(8)	C(20)-C(21B)	1.67(3)
Pt(1)-P(1)	2.2610(19)	C(21)-C(22)	1.546(16)
P(1)-C(33)	1.848(7)	C(21)-C(23)	1.567(18)
P(1)-C(34)	1.867(7)	C(21B)-C(22B)	1.57(4)
P(1)-C(40)	1.826(13)	C(21B)-C(23B)	1.45(5)
P(1)-C(34B)	1.744(10)	C(23)-C(24)	1.535(19)
P(1)-C(40B)	1.802(13)	C(23B)-C(24B)	1.63(5)
C(1)-C(2)	1.191(11)	C(25)-C(27)	1.490(13)
C(2)-C(3)	1.450(12)	C(25)-C(28)	1.532(13)
C(3)-C(20)	1.356(12)	C(25)-C(26)	1.546(13)
C(3)-C(4)	1.443(12)	C(29)-C(30)	1.506(14)
C(4)-C(5)	1.357(11)	C(29)-C(32)	1.517(14)
C(5)-C(6)	1.414(11)	C(29)-C(31)	1.529(14)
C(5)-C(23)	1.492(14)	C(33)-C(33)’	1.546(14)
C(5)-C(23B)	1.53(3)	C(34)-C(35)	1.3900
C(6)-C(7)	1.341(11)	C(34)-C(39)	1.3900
C(7)-C(8)	1.449(11)	C(34B)-C(35B)	1.3900
C(7)-C(25)	1.510(11)	C(34B)-C(39B)	1.3900
C(8)-C(9)	1.348(11)	C(35)-C(36)	1.3900
C(9)-C(10)	1.448(11)	C(35B)-C(36B)	1.3900
C(9)-C(23B)	1.51(3)	C(36)-C(37)	1.3900
C(9)-C(23)	1.540(14)	C(36B)-C(37B)	1.3900
C(10)-C(11)	1.415(11)	C(37)-C(38)	1.3900
C(10)-C(15)	1.425(11)	C(37B)-C(38B)	1.3900
C(11)-C(12)	1.367(12)	C(38)-C(39)	1.3900
C(12)-C(13)	1.378(13)	C(38B)-C(39B)	1.3900
C(13)-C(14)	1.381(12)	C(40)-C(45)	1.35(2)
C(14)-C(15)	1.406(11)	C(40)-C(41)	1.38(2)
C(15)-C(16)	1.462(10)	C(40B)-C(41B)	1.3900
C(16)-C(17)	1.333(11)	C(40B)-C(45B)	1.3900
C(16)-C(21)	1.533(13)	C(41)-C(42)	1.352(19)
C(16)-C(21B)	1.54(3)	C(41B)-C(42B)	1.3900
C(17)-C(18)	1.446(12)	C(42)-C(43)	1.33(2)
C(18)-C(19)	1.337(12)	C(42B)-C(43B)	1.3900
C(18)-C(29)	1.537(12)	C(43)-C(44)	1.38(2)
C(19)-C(20)	1.415(12)	C(43B)-C(44B)	1.3900
C(20)-C(21)	1.530(13)	C(44)-C(45)	1.44(2)

C(44B)-C(45B)	1.3900

Table S15. Bond Angles [°] for ***cis*-(BDHP)$_2$Pt(dppe)**

Pt(1)-C(1)-C(2)	175.9(8)	C(5)-C(23)-C(24)	106.1(10)
Pt(1)-P(1)-C(33)	106.8(2)	C(5)-C(4)-C(3)	121.2(8)
Pt(1)-P(1)-C(34)	112.7(3)	C(5)-C(23)-C(9)	113.1(9)
Pt(1)-P(1)-C(34B)	123.4(5)	C(5)-C(23)-C(21)	110.3(10)
Pt(1)-P(1)-C(40)	117.3(5)	C(5)-C(23B)-C(24B)	100(2)
Pt(1)-P(1)-C(40B)	114.9(6)	C(6)-C(5)-C(23)	117.6(8)
P(1)-Pt(1)-C(1)	177.1(3)	C(6)-C(5)-C(23B)	119.0(13)
P(1)-Pt(1)-C(1)’	92.0(2)	C(6)-C(7)-C(8)	117.2(7)
P(1)-Pt(1)-P(1)’	87.01(10)	C(6)-C(7)-C(25)	123.4(8)
P(1)-C(33)-C(33)’	108.2(4)	C(7)-C(6)-C(5)	124.2(8)
P(1)-C(34)-C(35)	121.0(5)	C(7)-C(25)-C(28)	113.4(7)
P(1)-C(34B)-C(35B)	116.2(7)	C(7)-C(25)-C(26)	108.0(7)
P(1)-C(34)-C(39)	119.0(5)	C(8)-C(7)-C(25)	119.3(7)
P(1)-C(34B)-C(39B)	123.8(7)	C(8)-C(9)-C(10)	124.9(7)
P(1)-C(40)-C(41)	122.4(13)	C(8)-C(9)-C(23B)	119.3(13)
P(1)-C(40B)-C(41B)	119.4(11)	C(8)-C(9)-C(23)	117.1(8)
P(1)-C(40)-C(45)	120.6(14)	C(9)-C(23B)-C(24B)	105(2)
P(1)-C(40B)-C(45B)	120.3(10)	C(9)-C(8)-C(7)	124.5(7)
C(1)-Pt(1)-C(1)’	89.1(4)	C(9)-C(23)-C(21)	107.9(10)
C(34B)-P(1)-C(40B)	105.1(8)	C(9)-C(23B)-C(5)	113(2)
C(34B)-P(1)-C(40)	97.3(8)	C(10)-C(9)-C(23B)	114.9(13)
C(34B)-P(1)-C(33)	100.5(6)	C(10)-C(9)-C(23)	116.9(8)
C(40B)-P(1)-C(33)	103.6(7)	C(10)-C(15)-C(16)	120.9(7)
C(40)-P(1)-C(33)	110.0(7)	C(11)-C(10)-C(15)	118.4(7)
C(40B)-P(1)-C(34)	110.9(7)	C(11)-C(10)-C(9)	120.8(7)
C(40)-P(1)-C(34)	102.5(7)	C(11)-C(12)-C(13)	121.2(8)
C(33)-P(1)-C(34)	107.1(4)	C(12)-C(11)-C(10)	120.9(8)
C(1)-C(2)-C(3)	175.9(10)	C(12)-C(13)-C(14)	119.4(9)
C(2)-C(3)-C(20)	123.1(8)	C(13)-C(14)-C(15)	121.8(9)
C(3)-C(20)-C(19)	123.1(8)	C(14)-C(15)-C(10)	118.0(7)
C(3)-C(20)-C(21)	118.1(8)	C(14)-C(15)-C(16)	121.1(8)
C(3)-C(20)-C(21B)	114.1(12)	C(15)-C(10)-C(9)	120.7(7)
C(4)-C(3)-C(2)	115.4(8)	C(15)-C(16)-C(21)	115.7(7)
C(4)-C(3)-C(20)	121.5(8)	C(15)-C(16)-C(21B)	112.0(12)
C(4)-C(5)-C(6)	123.6(8)	C(16)-C(17)-C(18)	124.9(8)
C(4)-C(5)-C(23)	117.9(8)	C(16)-C(21)-C(22)	108.5(8)
C(4)-C(5)-C(23B)	116.2(13)	C(16)-C(21)-C(23)	107.8(9)

C(16)-C(21B)-C(20)	103.6(17)
C(16)-C(21B)-C(22B)	109(2)
C(17)-C(16)-C(15)	125.3(8)
C(17)-C(16)-C(21)	116.9(8)
C(17)-C(16)-C(21B)	118.9(13)
C(17)-C(18)-C(29)	117.2(8)
C(18)-C(19)-C(20)	122.5(8)
C(19)-C(18)-C(17)	118.1(8)
C(19)-C(18)-C(29)	124.6(8)
C(19)-C(20)-C(21)	117.8(8)
C(19)-C(20)-C(21B)	117.5(12)
C(20)-C(21)-C(16)	110.9(8)
C(20)-C(21)-C(22)	109.8(9)
C(20)-C(21)-C(23)	107.2(9)
C(21B)-C(23B)-C(9)	113(2)
C(21B)-C(23B)-C(5)	113(3)
C(21B)-C(23B)-C(24B)	111(3)
C(22)-C(21)-C(23)	112.6(10)
C(22B)-C(21B)-C(20)	121(2)
C(23B)-C(21B)-C(20)	102(2)
C(23B)-C(21B)-C(22B)	111(3)
C(23B)-C(21B)-C(16)	109(2)
C(24)-C(23)-C(9)	108.5(9)
C(24)-C(23)-C(21)	111.0(11)
C(27)-C(25)-C(7)	109.8(8)
C(27)-C(25)-C(28)	110.1(9)
C(27)-C(25)-C(26)	110.2(9)
C(28)-C(25)-C(26)	105.3(8)
C(30)-C(29)-C(18)	110.1(8)
C(30)-C(29)-C(32)	109.7(10)
C(30)-C(29)-C(31)	107.0(10)
C(32)-C(29)-C(31)	108.3(9)
C(32)-C(29)-C(18)	110.3(8)
C(31)-C(29)-C(18)	111.3(8)
C(40)-C(45)-C(44)	122.5(15)
C(42)-C(41)-C(40)	122.9(15)
C(42)-C(43)-C(44)	123.5(16)
C(43)-C(44)-C(45)	114.9(16)
C(43)-C(42)-C(41)	119.0(15)
C(45)-C(40)-C(41)	116.9(13)

Figure S6. ORTEP plot (30% probability) for 1,2-*Bis*-4'-[2',7'-di-*tert*-butyl-10b',10c'-dimethyl-*trans*-10b',10c'-dihydropyrenyl]-3,4-dimethyl-η^4-cyclobutadienyl-η^5-cyclopentadienylcobalt, **21**

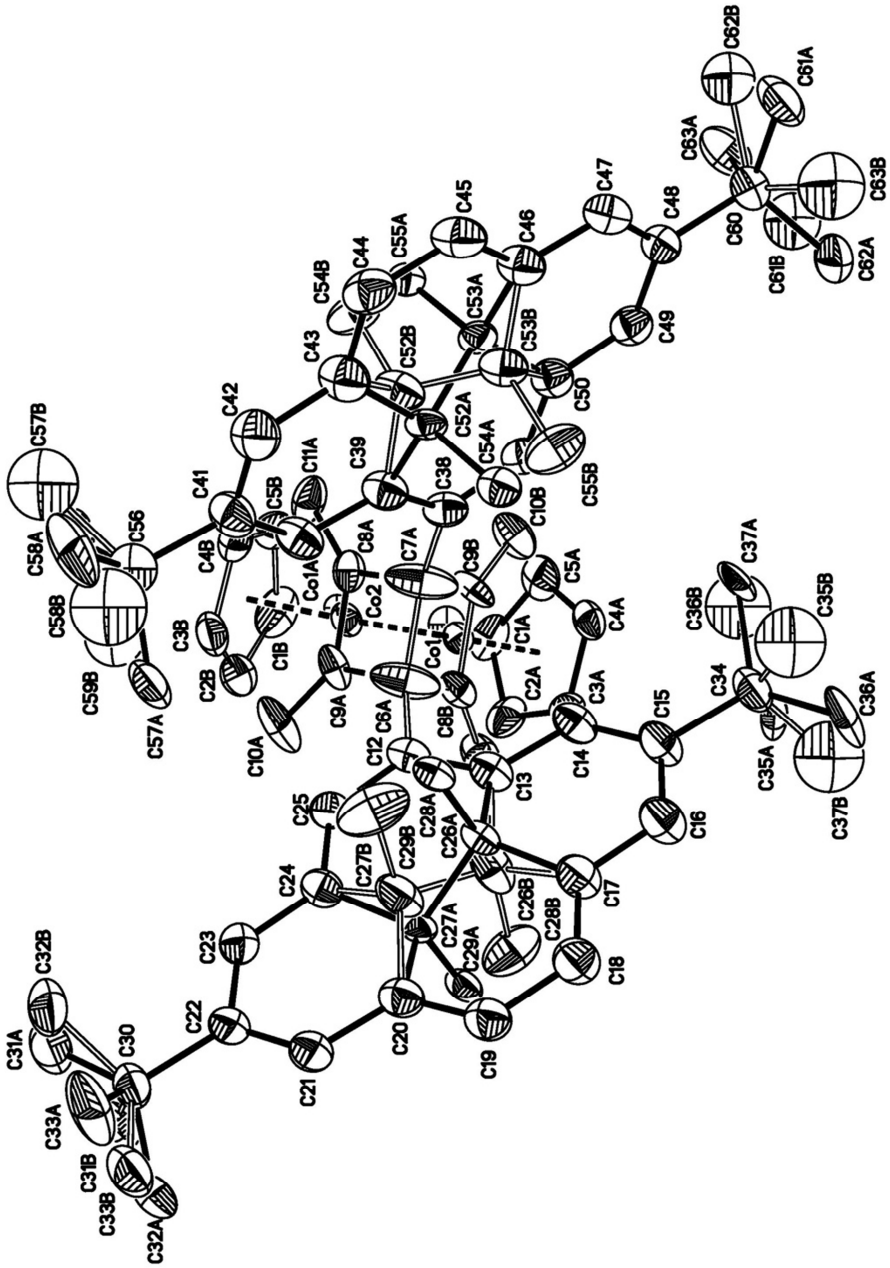


Table S16. Atomic coordinates and equivalent isotropic displacement parameters ($Å^2$) for **21**.

	x	y	z	U(eq)
Co(1)	0.58548(7)	0.21801(8)	0.00852(5)	0.023(1)
Co(1A)	0.4173(7)	0.2747(6)	-0.0068(5)	0.017(5)
Co(2)	0.43397(11)	0.25896(12)	0.05597(7)	0.027(1)
Co(2A)	0.5695(7)	0.2356(5)	-0.0516(5)	0.034(5)
C(1A)	0.6313(5)	0.2121(4)	-0.1211(3)	0.041(1)
C(2A)	0.6540(6)	0.1171(5)	-0.0884(4)	0.044(2)
C(3A)	0.7353(5)	0.1168(4)	-0.0371(3)	0.033(1)
C(4A)	0.7655(5)	0.2139(4)	-0.0413(3)	0.032(1)
C(5A)	0.7019(6)	0.2707(5)	-0.0927(4)	0.042(2)
C(6A)	0.5150(4)	0.1819(3)	0.1192(2)	0.055(1)
C(7A)	0.5363(4)	0.2853(3)	0.1114(2)	0.058(1)
C(8A)	0.4376(6)	0.3109(7)	0.0579(4)	0.030(2)
C(9A)	0.4180(6)	0.2080(7)	0.0646(4)	0.032(1)
C(10A)	0.3388(7)	0.1536(6)	0.0328(4)	0.055(2)
C(11A)	0.3806(6)	0.3997(5)	0.0225(4)	0.042(2)
C(1B)	0.3302(8)	0.2813(7)	-0.0299(6)	0.049(2)
C(2B)	0.2823(8)	0.2165(7)	0.0364(7)	0.047(2)
C(3B)	0.2551(7)	0.2668(6)	0.1125(6)	0.045(2)
C(4B)	0.2853(7)	0.3641(6)	0.0953(5)	0.036(2)
C(5B)	0.3304(9)	0.3731(6)	0.0078(6)	0.038(2)
C(6B)	0.5150(4)	0.1819(3)	0.1192(2)	0.055(1)
C(7B)	0.5363(4)	0.2853(3)	0.1114(2)	0.058(1)
C(8B)	0.5848(7)	0.1609(9)	0.0227(5)	0.031(2)
C(9B)	0.6065(8)	0.2691(8)	0.0155(5)	0.038(2)
C(10B)	0.6636(9)	0.3227(8)	-0.0569(5)	0.043(2)
C(11B)	0.6164(8)	0.0817(6)	-0.0382(6)	0.041(2)
C(12)	0.5212(3)	0.1047(2)	0.18437(18)	0.032(1)
C(13)	0.6256(3)	0.0768(2)	0.21522(19)	0.034(1)
C(14)	0.7314(3)	0.1116(2)	0.18608(19)	0.036(1)
C(15)	0.8340(3)	0.0791(2)	0.2171(2)	0.040(1)
C(16)	0.8295(3)	0.0080(2)	0.2811(2)	0.042(1)
C(17)	0.7272(3)	-0.0319(2)	0.3159(2)	0.038(1)
C(18)	0.7205(3)	-0.1045(2)	0.3786(2)	0.038(1)
C(19)	0.6172(3)	-0.1440(2)	0.4108(2)	0.038(1)
C(20)	0.5161(3)	-0.1176(2)	0.37925(19)	0.034(1)
C(21)	0.4098(3)	-0.1533(2)	0.4096(2)	0.036(1)
C(22)	0.3080(3)	-0.1234(2)	0.3781(2)	0.035(1)
C(23)	0.3133(3)	-0.0522(2)	0.31371(19)	0.034(1)
C(24)	0.4145(3)	-0.0117(2)	0.27863(18)	0.032(1)
C(25)	0.4211(3)	0.0619(2)	0.21644(19)	0.032(1)

C(26A)	0.6106(5)	0.0185(4)	0.3010(4)	0.022(1)
C(27A)	0.5352(6)	-0.0635(4)	0.2961(5)	0.024(1)
C(28A)	0.5547(5)	0.0931(4)	0.3724(3)	0.026(1)
C(29A)	0.5910(5)	-0.1375(4)	0.2259(4)	0.028(1)
C(26B)	0.6256(9)	-0.0163(8)	0.2658(6)	0.042(2)
C(27B)	0.5123(11)	-0.0254(8)	0.3212(8)	0.043(3)
C(28B)	0.6514(11)	-0.1121(7)	0.1999(7)	0.058(3)
C(29B)	0.4829(12)	0.0687(7)	0.3900(6)	0.062(3)
C(30)	0.1933(3)	-0.1641(2)	0.4154(2)	0.044(1)
C(31A)	0.0856(6)	-0.1212(6)	0.3790(5)	0.053(2)
C(32A)	0.2163(7)	-0.2802(5)	0.3890(7)	0.067(3)
C(33A)	0.1602(8)	-0.1630(9)	0.5078(5)	0.067(3)
C(31B)	0.2034(8)	-0.2308(7)	0.4898(7)	0.064(3)
C(32B)	0.0970(6)	-0.0712(6)	0.4483(6)	0.060(2)
C(33B)	0.1607(7)	-0.2115(6)	0.3475(5)	0.058(2)
C(34)	0.9505(3)	0.1178(3)	0.1775(2)	0.046(1)
C(35A)	0.9928(4)	0.0815(4)	0.0815(3)	0.038(1)
C(36A)	1.0532(5)	0.0784(5)	0.2175(4)	0.053(2)
C(37A)	0.9309(5)	0.2301(4)	0.1758(4)	0.042(1)
C(35B)	0.9802(13)	0.1624(11)	0.2646(9)	0.093(4)
C(36B)	0.9400(14)	0.2041(11)	0.1264(10)	0.090(4)
C(37B)	1.0465(14)	0.0364(11)	0.1585(10)	0.099(4)
C(38)	0.5680(3)	0.3551(2)	0.16447(18)	0.032(1)
C(39)	0.4927(3)	0.3807(2)	0.24536(19)	0.036(1)
C(40)	0.3874(3)	0.3456(2)	0.2807(2)	0.040(1)
C(41)	0.3118(3)	0.3763(2)	0.3604(2)	0.040(1)
C(42)	0.3453(3)	0.4455(2)	0.4056(2)	0.044(1)
C(43)	0.4488(3)	0.4862(2)	0.37657(19)	0.040(1)
C(44)	0.4804(3)	0.5582(2)	0.4189(2)	0.041(1)
C(45)	0.5838(3)	0.5978(2)	0.3873(2)	0.041(1)
C(46)	0.6585(3)	0.5716(2)	0.30933(19)	0.036(1)
C(47)	0.7628(3)	0.6104(2)	0.2739(2)	0.037(1)
C(48)	0.8348(3)	0.5824(2)	0.1952(2)	0.033(1)
C(49)	0.8035(3)	0.5115(2)	0.14825(19)	0.034(1)
C(50)	0.7026(3)	0.4694(2)	0.17763(18)	0.033(1)
C(51)	0.6681(3)	0.3982(2)	0.13369(18)	0.033(1)
C(52A)	0.5447(5)	0.4352(4)	0.3044(4)	0.025(1)
C(53A)	0.6077(6)	0.5166(5)	0.2524(4)	0.026(1)
C(54A)	0.6316(5)	0.3585(4)	0.3420(4)	0.032(1)
C(55A)	0.5190(5)	0.5938(4)	0.2157(4)	0.030(1)
C(52B)	0.5122(9)	0.4755(7)	0.2813(6)	0.037(2)
C(53B)	0.6387(9)	0.4802(7)	0.2708(6)	0.034(2)
C(54B)	0.4537(9)	0.5678(6)	0.2292(5)	0.043(2)
C(55B)	0.6983(10)	0.3869(7)	0.3205(6)	0.050(2)
C(56)	0.1933(3)	0.3386(3)	0.3931(2)	0.047(1)
C(57A)	0.2132(4)	0.2238(3)	0.3862(3)	0.045(1)

C(58A)	0.1099(4)	0.3831(4)	0.3409(4)	0.052(1)
C(59A)	0.1391(6)	0.3613(6)	0.4873(3)	0.064(2)
C(57B)	0.0839(17)	0.4364(14)	0.3971(13)	0.095(6)
C(58B)	0.179(2)	0.3028(17)	0.4755(15)	0.103(8)
C(59B)	0.1595(15)	0.2777(12)	0.3283(10)	0.073(4)
C(60)	0.9477(3)	0.6270(2)	0.1576(2)	0.040(1)
C(61A)	0.9741(5)	0.6964(4)	0.2166(4)	0.054(1)
C(62A)	1.0537(4)	0.5429(4)	0.1326(4)	0.054(1)
C(63A)	0.9293(5)	0.6836(4)	0.0768(3)	0.055(1)
C(61B)	1.0147(14)	0.5987(11)	0.0673(9)	0.069(4)
C(62B)	0.9207(12)	0.7420(9)	0.1562(9)	0.057(3)
C(63B)	1.0339(13)	0.6036(6)	0.2166(9)	0.085(5)

U_{eq} is defined as one third of the trace of the orthogonalized U_{ij} tensor.

Table S17. Anisotropic displacement parameters ($Å^2$) for **21**

	U_{11}	U_{22}	U_{33}	U_{23}	U_{13}	U_{12}
Co(1)	0.0223(4)	0.0258(7)	0.0218(4)	0.0006(4)	-0.0035(3)	-0.0061(4)
Co(2)	0.0222(6)	0.0303(10)	0.0320(7)	0.0036(7)	-0.0105(5)	-0.0086(7)
C(1A)	0.039(3)	0.052(3)	0.026(3)	-0.001(2)	-0.008(3)	0.008(3)
C(2A)	0.042(4)	0.039(3)	0.048(4)	-0.019(3)	-0.014(3)	0.006(3)
C(3A)	0.033(3)	0.029(3)	0.036(3)	-0.002(2)	-0.008(2)	-0.001(2)
C(4A)	0.025(3)	0.041(3)	0.030(3)	-0.006(2)	0.001(2)	-0.011(2)
C(5A)	0.036(3)	0.052(4)	0.032(3)	0.009(3)	0.005(3)	-0.009(3)
C(6A)	0.109(3)	0.0374(19)	0.0330(19)	0.0131(14)	-0.032(2)	-0.036(2)
C(7A)	0.121(4)	0.0346(18)	0.0317(19)	0.0095(14)	-0.032(2)	-0.036(2)
C(8A)	0.024(3)	0.040(4)	0.025(3)	-0.002(3)	-0.003(2)	-0.003(3)
C(9A)	0.024(3)	0.052(4)	0.023(3)	0.007(3)	-0.006(2)	-0.017(3)
C(10A)	0.044(4)	0.090(6)	0.047(4)	0.024(4)	-0.021(3)	-0.044(4)
C(11A)	0.030(4)	0.050(4)	0.040(4)	0.015(3)	-0.006(3)	0.007(3)
C(1B)	0.046(5)	0.062(5)	0.045(5)	-0.007(4)	-0.032(4)	0.008(4)
C(2B)	0.030(5)	0.044(5)	0.076(7)	-0.006(5)	-0.028(5)	-0.011(4)
C(3B)	0.023(4)	0.048(5)	0.066(6)	0.020(4)	-0.011(4)	-0.010(3)
C(4B)	0.028(4)	0.039(4)	0.039(4)	0.002(3)	-0.008(3)	0.002(3)
C(5B)	0.043(6)	0.035(4)	0.039(5)	0.008(3)	-0.017(4)	-0.003(4)
C(6B)	0.109(3)	0.0374(19)	0.0330(19)	0.0131(14)	-0.032(2)	-0.036(2)
C(7B)	0.121(4)	0.0346(18)	0.0317(19)	0.0095(14)	-0.032(2)	-0.036(2)
C(8B)	0.032(5)	0.035(5)	0.032(5)	0.005(4)	-0.012(3)	-0.015(4)
C(9B)	0.039(5)	0.037(5)	0.046(5)	0.000(4)	-0.012(4)	-0.027(4)
C(10B)	0.047(6)	0.061(6)	0.027(5)	0.008(4)	-0.005(4)	-0.027(5)
C(11B)	0.039(5)	0.045(5)	0.039(5)	-0.012(4)	-0.003(4)	-0.017(4)
C(12)	0.0415(18)	0.0271(14)	0.0280(15)	0.0009(11)	-0.0062(13)	-0.0119(12)
C(13)	0.0386(18)	0.0342(15)	0.0325(16)	0.0036(12)	-0.0078(14)	-0.0135(13)
C(14)	0.0406(18)	0.0390(16)	0.0320(16)	0.0063(13)	-0.0075(14)	-0.0178(14)
C(15)	0.0379(18)	0.0435(18)	0.0440(19)	0.0067(14)	-0.0121(15)	-0.0201(14)
C(16)	0.0419(19)	0.0465(18)	0.0423(19)	0.0070(14)	-0.0151(15)	-0.0179(15)
C(17)	0.0381(18)	0.0389(17)	0.0392(18)	0.0052(13)	-0.0102(14)	-0.0140(14)
C(18)	0.0398(18)	0.0394(17)	0.0390(18)	0.0063(13)	-0.0140(15)	-0.0100(14)
C(19)	0.0395(18)	0.0339(16)	0.0403(18)	0.0066(13)	-0.0105(15)	-0.0088(13)
C(20)	0.0383(17)	0.0306(15)	0.0323(16)	0.0033(12)	-0.0059(13)	-0.0082(13)
C(21)	0.0361(18)	0.0327(15)	0.0367(17)	0.0080(12)	-0.0029(14)	-0.0073(13)
C(22)	0.0335(17)	0.0286(15)	0.0392(18)	0.0058(12)	-0.0015(14)	-0.0073(12)
C(23)	0.0311(16)	0.0331(15)	0.0362(17)	0.0015(12)	-0.0052(13)	-0.0042(12)
C(24)	0.0362(17)	0.0323(15)	0.0268(15)	0.0016(11)	-0.0062(13)	-0.0097(12)
C(25)	0.0353(17)	0.0292(14)	0.0340(16)	0.0006(12)	-0.0096(13)	-0.0063(12)
C(26A)	0.030(3)	0.025(3)	0.014(3)	-0.001(2)	-0.004(2)	-0.013(2)
C(27A)	0.027(3)	0.016(3)	0.027(3)	-0.006(2)	-0.001(2)	-0.006(2)
C(28A)	0.032(3)	0.024(2)	0.024(3)	0.0052(19)	-0.006(2)	-0.012(2)
C(29A)	0.028(3)	0.025(3)	0.027(3)	0.001(2)	0.003(2)	-0.012(2)

C(26B)	0.040(5)	0.061(7)	0.033(6)	0.013(5)	-0.013(5)	-0.025(5)
C(27B)	0.044(7)	0.045(7)	0.053(8)	0.023(5)	-0.025(6)	-0.023(5)
C(28B)	0.070(8)	0.043(6)	0.057(7)	-0.017(5)	-0.018(6)	0.013(5)
C(29B)	0.095(9)	0.043(5)	0.041(6)	-0.020(4)	-0.018(6)	0.011(6)
C(30)	0.0264(17)	0.0466(19)	0.055(2)	0.0178(16)	-0.0034(15)	-0.0075(14)
C(31A)	0.034(4)	0.064(5)	0.062(5)	0.020(4)	-0.009(4)	-0.014(3)
C(32A)	0.037(4)	0.046(4)	0.118(8)	0.018(5)	-0.009(5)	-0.023(3)
C(33A)	0.041(5)	0.113(8)	0.045(5)	0.028(5)	-0.002(4)	-0.033(5)
C(31B)	0.035(5)	0.064(5)	0.088(7)	0.040(5)	-0.006(4)	-0.016(4)
C(32B)	0.031(4)	0.065(5)	0.071(6)	0.015(4)	0.008(4)	-0.004(3)
C(33B)	0.046(4)	0.057(5)	0.072(5)	0.002(4)	-0.004(4)	-0.028(4)
C(34)	0.0332(18)	0.0450(19)	0.066(2)	0.0148(16)	-0.0162(17)	-0.0198(15)
C(35A)	0.016(2)	0.049(3)	0.047(3)	0.003(2)	-0.007(2)	0.000(2)
C(36A)	0.034(3)	0.084(5)	0.054(4)	0.029(3)	-0.021(3)	-0.042(3)
C(37A)	0.027(3)	0.036(3)	0.063(4)	0.000(3)	0.005(3)	-0.024(2)
C(38)	0.0430(18)	0.0254(14)	0.0287(15)	0.0027(11)	-0.0088(13)	-0.0066(12)
C(39)	0.0431(19)	0.0325(15)	0.0333(17)	0.0018(12)	-0.0069(14)	-0.0113(13)
C(40)	0.046(2)	0.0403(17)	0.0349(17)	0.0048(13)	-0.0072(15)	-0.0174(14)
C(41)	0.0418(19)	0.0425(17)	0.0341(17)	0.0051(13)	-0.0025(14)	-0.0145(14)
C(42)	0.046(2)	0.0479(19)	0.0330(18)	-0.0013(14)	0.0044(15)	-0.0105(15)
C(43)	0.049(2)	0.0404(17)	0.0281(16)	0.0001(13)	0.0011(14)	-0.0146(15)
C(44)	0.050(2)	0.0348(16)	0.0325(17)	-0.0037(13)	-0.0009(15)	-0.0034(14)
C(45)	0.055(2)	0.0318(16)	0.0364(18)	-0.0030(13)	-0.0067(16)	-0.0119(14)
C(46)	0.0436(19)	0.0326(15)	0.0332(17)	-0.0017(12)	-0.0069(14)	-0.0105(13)
C(47)	0.0446(19)	0.0317(15)	0.0386(18)	-0.0001(13)	-0.0119(15)	-0.0108(13)
C(48)	0.0314(16)	0.0301(14)	0.0398(18)	0.0022(12)	-0.0092(14)	-0.0072(12)
C(49)	0.0372(17)	0.0316(15)	0.0319(16)	0.0015(12)	-0.0057(13)	-0.0040(13)
C(50)	0.0370(17)	0.0305(15)	0.0291(16)	0.0042(12)	-0.0051(13)	-0.0067(12)
C(51)	0.0411(18)	0.0281(14)	0.0263(15)	0.0014(11)	-0.0038(13)	-0.0049(12)
C(52A)	0.034(3)	0.017(3)	0.023(3)	0.005(2)	-0.003(2)	-0.007(2)
C(53A)	0.030(3)	0.020(3)	0.026(3)	0.007(2)	-0.003(2)	-0.003(2)
C(54A)	0.036(3)	0.030(3)	0.032(3)	0.000(2)	-0.006(3)	-0.008(2)
C(55A)	0.029(3)	0.022(3)	0.038(3)	0.002(2)	-0.005(3)	-0.005(2)
C(52B)	0.049(6)	0.034(5)	0.030(5)	0.000(4)	-0.004(4)	-0.019(4)
C(53B)	0.047(6)	0.030(5)	0.027(5)	0.002(4)	-0.008(4)	-0.011(4)
C(54B)	0.061(6)	0.030(4)	0.031(4)	0.004(3)	-0.008(4)	0.006(4)
C(55B)	0.066(7)	0.041(5)	0.038(5)	0.000(4)	-0.015(5)	0.009(5)
C(57A)	0.033(3)	0.050(3)	0.057(3)	0.017(2)	-0.008(2)	-0.023(2)
C(58A)	0.034(3)	0.067(3)	0.051(3)	0.010(3)	-0.007(2)	-0.007(2)
C(59A)	0.054(4)	0.107(6)	0.035(3)	-0.001(3)	0.009(3)	-0.049(4)
C(60)	0.0311(17)	0.0398(17)	0.050(2)	-0.0003(14)	-0.0065(15)	-0.0102(13)
C(61A)	0.039(3)	0.062(3)	0.064(4)	-0.020(3)	0.001(3)	-0.027(2)
C(62A)	0.028(3)	0.053(3)	0.077(4)	-0.014(3)	-0.001(3)	-0.008(2)
C(63A)	0.055(3)	0.057(3)	0.054(3)	0.016(2)	-0.002(3)	-0.033(3)

The anisotropic displacement factor exponent takes the form: $-2\pi^2[h^2 a^{*2}U_{11} + ... + 2hka^*b^*U_{12}]$

Table S18. Bond lengths [Å] for **21**.

atom-atom	distance	atom-atom	distance
Co(1)-C(7A)	1.868(4)	C(14)-C(15)	1.412(5)
Co(1)-C(6A)	1.876(4)	C(15)-C(16)	1.397(4)
Co(1)-C(9A)	1.976(6)	C(15)-C(34)	1.532(4)
Co(1)-C(8A)	1.987(7)	C(16)-C(17)	1.387(4)
Co(1)-C(1A)	2.050(6)	C(17)-C(18)	1.396(4)
Co(1)-C(3A)	2.052(5)	C(17)-C(26A)	1.493(7)
Co(1)-C(4A)	2.057(5)	C(17)-C(26B)	1.580(10)
Co(1)-C(5A)	2.060(6)	C(18)-C(19)	1.386(4)
Co(1)-C(2A)	2.067(6)	C(19)-C(20)	1.390(4)
C(1A)-C(2A)	1.399(9)	C(20)-C(21)	1.385(4)
C(1A)-C(5A)	1.411(10)	C(20)-C(27A)	1.504(8)
C(2A)-C(3A)	1.410(8)	C(20)-C(27B)	1.551(11)
C(3A)-C(4A)	1.434(7)	C(21)-C(22)	1.401(4)
C(4A)-C(5A)	1.383(9)	C(22)-C(23)	1.403(4)
C(6A)-C(12)	1.476(4)	C(22)-C(30)	1.520(4)
C(6A)-C(7A)	1.481(4)	C(23)-C(24)	1.380(4)
C(6A)-C(9A)	1.591(7)	C(24)-C(25)	1.400(4)
C(7A)-C(38)	1.467(4)	C(24)-C(27B)	1.459(11)
C(7A)-C(8A)	1.594(8)	C(24)-C(27A)	1.557(8)
C(8A)-C(11A)	1.458(10)	C(26A)-C(28A)	1.531(8)
C(8A)-C(9A)	1.468(13)	C(26A)-C(27A)	1.561(8)
C(9A)-C(10A)	1.479(10)	C(27A)-C(29A)	1.513(8)
Co(2)-C(9B)	1.993(9)	C(26B)-C(27B)	1.433(15)
Co(2)-C(8B)	2.008(10)	C(26B)-C(28B)	1.678(15)
Co(2)-C(1B)	2.045(8)	C(27B)-C(29B)	1.687(15)
Co(2)-C(2B)	2.056(8)	C(30)-C(33A)	1.462(9)
Co(2)-C(4B)	2.057(7)	C(30)-C(33B)	1.464(9)
Co(2)-C(3B)	2.059(8)	C(30)-C(31B)	1.505(9)
Co(2)-C(5B)	2.066(9)	C(30)-C(31A)	1.540(8)
C(1B)-C(5B)	1.430(12)	C(30)-C(32B)	1.574(8)
C(1B)-C(2B)	1.438(14)	C(30)-C(32A)	1.635(9)
C(2B)-C(3B)	1.388(14)	C(34)-C(36B)	1.428(14)
C(3B)-C(4B)	1.441(11)	C(34)-C(37B)	1.433(15)
C(4B)-C(5B)	1.403(12)	C(34)-C(36A)	1.513(6)
C(8B)-C(11B)	1.448(12)	C(34)-C(37A)	1.526(6)
C(8B)-C(9B)	1.548(16)	C(34)-C(35A)	1.597(7)
C(9B)-C(10B)	1.445(12)	C(34)-C(35B)	1.702(14)
C(12)-C(25)	1.378(4)	C(38)-C(51)	1.378(4)
C(12)-C(13)	1.419(4)	C(38)-C(39)	1.418(4)
C(13)-C(14)	1.373(4)	C(39)-C(40)	1.384(4)
C(13)-C(26B)	1.493(10)	C(39)-C(52B)	1.525(9)
C(13)-C(26A)	1.568(6)	C(39)-C(52A)	1.534(7)

C(40)-C(41)	1.419(5)	C(52A)-C(53A)	1.552(8)
C(41)-C(42)	1.388(5)	C(52A)-C(54A)	1.554(8)
C(41)-C(56)	1.529(5)	C(53A)-C(55A)	1.562(8)
C(42)-C(43)	1.390(5)	C(52B)-C(53B)	1.460(14)
C(43)-C(44)	1.378(4)	C(52B)-C(54B)	1.644(13)
C(43)-C(52A)	1.518(6)	C(53B)-C(55B)	1.636(13)
C(43)-C(52B)	1.552(9)	C(56)-C(58B)	1.39(2)
C(44)-C(45)	1.386(5)	C(56)-C(58A)	1.485(6)
C(45)-C(46)	1.380(4)	C(56)-C(59B)	1.536(16)
C(46)-C(47)	1.399(4)	C(56)-C(59A)	1.537(7)
C(46)-C(53A)	1.505(7)	C(56)-C(57A)	1.564(6)
C(46)-C(53B)	1.507(10)	C(56)-C(57B)	1.687(19)
C(47)-C(48)	1.383(4)	C(60)-C(61A)	1.502(6)
C(48)-C(49)	1.412(4)	C(60)-C(61B)	1.523(15)
C(48)-C(60)	1.532(4)	C(60)-C(62A)	1.536(6)
C(49)-C(50)	1.375(4)	C(60)-C(63A)	1.541(6)
C(50)-C(51)	1.402(4)	C(60)-C(63B)	1.542(9)
C(50)-C(53A)	1.520(7)	C(60)-C(62B)	1.563(13)
C(50)-C(53B)	1.523(10)		

Table S19. Bond angles [°] for **21**.

atom-atom-atom	angle	atom-atom-atom	angle
C(7A)-Co(1)-C(6A)	46.62(14)	C(7A)-Co(1)-C(9A)	68.6(3)
C(6A)-Co(1)-C(9A)	48.7(2)	C(7A)-Co(1)-C(8A)	48.7(2)
C(6A)-Co(1)-C(8A)	68.4(2)	C(9A)-Co(1)-C(8A)	43.5(3)
C(7A)-Co(1)-C(1A)	152.9(2)	C(6A)-Co(1)-C(1A)	157.3(2)
C(9A)-Co(1)-C(1A)	116.8(2)	C(8A)-Co(1)-C(1A)	115.0(2)
C(7A)-Co(1)-C(3A)	129.9(2)	C(6A)-Co(1)-C(3A)	108.6(2)
C(9A)-Co(1)-C(3A)	134.0(3)	C(8A)-Co(1)-C(3A)	176.8(3)
C(1A)-Co(1)-C(3A)	67.5(2)	C(7A)-Co(1)-C(4A)	110.8(2)
C(6A)-Co(1)-C(4A)	125.6(2)	C(9A)-Co(1)-C(4A)	173.1(3)
C(8A)-Co(1)-C(4A)	141.5(3)	C(1A)-Co(1)-C(4A)	67.1(2)
C(3A)-Co(1)-C(4A)	40.8(2)	C(7A)-Co(1)-C(5A)	120.7(2)
C(6A)-Co(1)-C(5A)	161.1(2)	C(9A)-Co(1)-C(5A)	147.3(3)
C(8A)-Co(1)-C(5A)	115.8(3)	C(1A)-Co(1)-C(5A)	40.2(3)
C(3A)-Co(1)-C(5A)	67.3(2)	C(4A)-Co(1)-C(5A)	39.3(2)
C(7A)-Co(1)-C(2A)	166.7(2)	C(6A)-Co(1)-C(2A)	122.8(2)
C(9A)-Co(1)-C(2A)	111.6(3)	C(8A)-Co(1)-C(2A)	140.7(3)
C(1A)-Co(1)-C(2A)	39.7(3)	C(3A)-Co(1)-C(2A)	40.0(2)
C(4A)-Co(1)-C(2A)	67.3(2)	C(5A)-Co(1)-C(2A)	66.8(3)
C(2A)-C(1A)-C(5A)	107.9(5)	C(2A)-C(1A)-Co(1)	70.8(3)
C(5A)-C(1A)-Co(1)	70.3(3)	C(1A)-C(2A)-C(3A)	108.4(5)
C(1A)-C(2A)-Co(1)	69.5(3)	C(3A)-C(2A)-Co(1)	69.4(3)
C(2A)-C(3A)-C(4A)	106.9(5)	C(2A)-C(3A)-Co(1)	70.5(3)
C(4A)-C(3A)-Co(1)	69.8(3)	C(5A)-C(4A)-C(3A)	108.0(5)
C(5A)-C(4A)-Co(1)	70.5(3)	C(3A)-C(4A)-Co(1)	69.4(3)
C(4A)-C(5A)-C(1A)	108.7(6)	C(4A)-C(5A)-Co(1)	70.3(3)
C(1A)-C(5A)-Co(1)	69.6(3)	C(12)-C(6A)-C(7A)	134.3(3)
C(12)-C(6A)-C(9A)	128.2(4)	C(7A)-C(6A)-C(9A)	89.7(4)
C(12)-C(6A)-Co(1)	143.9(3)	C(7A)-C(6A)-Co(1)	66.39(19)
C(9A)-C(6A)-Co(1)	68.9(3)	C(38)-C(7A)-C(6A)	136.1(3)
C(38)-C(7A)-C(8A)	125.2(4)	C(6A)-C(7A)-C(8A)	89.8(4)
C(38)-C(7A)-Co(1)	144.3(3)	C(6A)-C(7A)-Co(1)	67.0(2)
C(8A)-C(7A)-Co(1)	69.5(3)	C(11A)-C(8A)-C(9A)	133.7(7)
C(11A)-C(8A)-C(7A)	136.1(7)	C(9A)-C(8A)-C(7A)	90.1(5)
C(11A)-C(8A)-Co(1)	130.5(5)	C(9A)-C(8A)-Co(1)	67.9(4)
C(7A)-C(8A)-Co(1)	61.7(3)	C(8A)-C(9A)-C(10A)	133.7(7)
C(8A)-C(9A)-C(6A)	90.4(5)	C(10A)-C(9A)-C(6A)	135.9(7)
C(8A)-C(9A)-Co(1)	68.7(4)	C(10A)-C(9A)-Co(1)	126.2(5)
C(6A)-C(9A)-Co(1)	62.4(3)	C(9B)-Co(2)-C(8B)	45.5(4)
C(9B)-Co(2)-C(1B)	118.0(4)	C(8B)-Co(2)-C(1B)	115.9(3)
C(9B)-Co(2)-C(2B)	150.0(4)	C(8B)-Co(2)-C(2B)	116.0(4)
C(1B)-Co(2)-C(2B)	41.1(4)	C(9B)-Co(2)-C(4B)	131.7(4)
C(8B)-Co(2)-C(4B)	176.0(3)	C(1B)-Co(2)-C(4B)	67.7(3)

C(2B)-Co(2)-C(4B)	67.8(4)	C(9B)-Co(2)-C(3B)	170.2(4)
C(8B)-Co(2)-C(3B)	141.2(4)	C(1B)-Co(2)-C(3B)	67.7(4)
C(2B)-Co(2)-C(3B)	39.4(4)	C(4B)-Co(2)-C(3B)	41.0(3)
C(9B)-Co(2)-C(5B)	110.5(4)	C(8B)-Co(2)-C(5B)	141.9(4)
C(1B)-Co(2)-C(5B)	40.7(3)	C(2B)-Co(2)-C(5B)	68.5(4)
C(4B)-Co(2)-C(5B)	39.8(3)	C(3B)-Co(2)-C(5B)	68.0(4)
C(5B)-C(1B)-C(2B)	107.9(8)	C(5B)-C(1B)-Co(2)	70.4(5)
C(2B)-C(1B)-Co(2)	69.9(5)	C(3B)-C(2B)-C(1B)	107.9(8)
C(3B)-C(2B)-Co(2)	70.4(4)	C(1B)-C(2B)-Co(2)	69.1(5)
C(2B)-C(3B)-C(4B)	108.4(8)	C(2B)-C(3B)-Co(2)	70.2(5)
C(4B)-C(3B)-Co(2)	69.4(4)	C(5B)-C(4B)-C(3B)	108.3(7)
C(5B)-C(4B)-Co(2)	70.5(5)	C(3B)-C(4B)-Co(2)	69.6(4)
C(4B)-C(5B)-C(1B)	107.5(8)	C(4B)-C(5B)-Co(2)	69.7(4)
C(1B)-C(5B)-Co(2)	68.8(4)	C(11B)-C(8B)-C(9B)	132.0(8)
C(11B)-C(8B)-Co(2)	130.0(6)	C(9B)-C(8B)-Co(2)	66.7(5)
C(10B)-C(9B)-C(8B)	129.9(8)	C(10B)-C(9B)-Co(2)	128.2(7)
C(8B)-C(9B)-Co(2)	67.7(5)	C(25)-C(12)-C(13)	120.6(3)
C(25)-C(12)-C(6A)	118.1(3)	C(13)-C(12)-C(6A)	121.4(3)
C(14)-C(13)-C(12)	125.6(3)	C(14)-C(13)-C(26B)	118.6(5)
C(12)-C(13)-C(26B)	113.6(4)	C(14)-C(13)-C(26A)	116.6(3)
C(12)-C(13)-C(26A)	116.6(3)	C(26B)-C(13)-C(26A)	27.6(4)
C(13)-C(14)-C(15)	123.4(3)	C(16)-C(15)-C(14)	119.3(3)
C(16)-C(15)-C(34)	120.7(3)	C(14)-C(15)-C(34)	119.9(3)
C(17)-C(16)-C(15)	122.3(3)	C(16)-C(17)-C(18)	123.7(3)
C(16)-C(17)-C(26A)	119.1(3)	C(18)-C(17)-C(26A)	115.9(3)
C(16)-C(17)-C(26B)	117.3(4)	C(18)-C(17)-C(26B)	116.8(4)
C(26A)-C(17)-C(26B)	27.4(4)	C(19)-C(18)-C(17)	122.1(3)
C(18)-C(19)-C(20)	121.8(3)	C(21)-C(20)-C(19)	124.5(3)
C(21)-C(20)-C(27A)	119.0(4)	C(19)-C(20)-C(27A)	115.3(4)
C(21)-C(20)-C(27B)	116.9(5)	C(19)-C(20)-C(27B)	117.0(5)
C(27A)-C(20)-C(27B)	24.8(4)	C(20)-C(21)-C(22)	123.4(3)
C(21)-C(22)-C(23)	118.3(3)	C(21)-C(22)-C(30)	120.8(3)
C(23)-C(22)-C(30)	120.9(3)	C(24)-C(23)-C(22)	123.3(3)
C(23)-C(24)-C(25)	124.5(3)	C(23)-C(24)-C(27B)	119.3(5)
C(25)-C(24)-C(27B)	114.3(5)	C(23)-C(24)-C(27A)	118.1(4)
C(25)-C(24)-C(27A)	116.4(4)	C(27B)-C(24)-C(27A)	24.9(4)
C(12)-C(25)-C(24)	124.0(3)	C(17)-C(26A)-C(28A)	107.6(4)
C(17)-C(26A)-C(27A)	107.0(4)	C(28A)-C(26A)-C(27A)	114.7(5)
C(17)-C(26A)-C(13)	112.5(4)	C(28A)-C(26A)-C(13)	107.6(4)
C(27A)-C(26A)-C(13)	107.6(5)	C(20)-C(27A)-C(29A)	108.6(5)
C(20)-C(27A)-C(24)	111.2(5)	C(29A)-C(27A)-C(24)	106.8(5)
C(20)-C(27A)-C(26A)	108.3(5)	C(29A)-C(27A)-C(26A)	114.7(5)
C(24)-C(27A)-C(26A)	107.3(5)	C(27B)-C(26B)-C(13)	114.0(9)
C(27B)-C(26B)-C(17)	110.7(8)	C(13)-C(26B)-C(17)	111.9(6)
C(27B)-C(26B)-C(28B)	103.3(9)	C(13)-C(26B)-C(28B)	109.0(7)
C(17)-C(26B)-C(28B)	107.4(8)	C(26B)-C(27B)-C(24)	113.4(9)

C(26B)-C(27B)-C(20)	113.6(9)	C(24)-C(27B)-C(20)	114.1(7)
C(26B)-C(27B)-C(29B)	105.2(9)	C(24)-C(27B)-C(29B)	106.0(8)
C(20)-C(27B)-C(29B)	103.1(8)	C(33A)-C(30)-C(33B)	137.0(5)
C(33A)-C(30)-C(31B)	39.5(5)	C(33B)-C(30)-C(31B)	113.3(6)
C(33A)-C(30)-C(22)	113.2(4)	C(33B)-C(30)-C(22)	108.4(4)
C(31B)-C(30)-C(22)	112.0(4)	C(33A)-C(30)-C(31A)	110.9(5)
C(33B)-C(30)-C(31A)	56.9(5)	C(31B)-C(30)-C(31A)	131.5(5)
C(22)-C(30)-C(31A)	115.9(4)	C(33A)-C(30)-C(32B)	69.7(6)
C(33B)-C(30)-C(32B)	109.8(5)	C(31B)-C(30)-C(32B)	108.0(6)
C(22)-C(30)-C(32B)	105.0(4)	C(31A)-C(30)-C(32B)	53.0(5)
C(33A)-C(30)-C(32A)	105.5(6)	C(33B)-C(30)-C(32A)	49.8(5)
C(31B)-C(30)-C(32A)	68.3(6)	C(22)-C(30)-C(32A)	107.7(4)
C(31A)-C(30)-C(32A)	102.4(5)	C(32B)-C(30)-C(32A)	145.8(5)
C(36B)-C(34)-C(37B)	124.5(9)	C(36B)-C(34)-C(36A)	126.7(7)
C(37B)-C(34)-C(36A)	46.5(7)	C(36B)-C(34)-C(37A)	34.1(6)
C(37B)-C(34)-C(37A)	139.3(7)	C(36A)-C(34)-C(37A)	110.3(4)
C(36B)-C(34)-C(15)	116.0(7)	C(37B)-C(34)-C(15)	109.3(7)
C(36A)-C(34)-C(15)	114.7(3)	C(37A)-C(34)-C(15)	111.2(3)
C(36B)-C(34)-C(35A)	73.7(7)	C(37B)-C(34)-C(35A)	63.2(7)
C(36A)-C(34)-C(35A)	105.7(4)	C(37A)-C(34)-C(35A)	107.1(4)
C(15)-C(34)-C(35A)	107.4(3)	C(36B)-C(34)-C(35B)	101.8(8)
C(37B)-C(34)-C(35B)	99.5(9)	C(36A)-C(34)-C(35B)	53.0(6)
C(37A)-C(34)-C(35B)	69.4(6)	C(15)-C(34)-C(35B)	100.7(5)
C(35A)-C(34)-C(35B)	150.5(6)	C(51)-C(38)-C(39)	120.6(3)
C(51)-C(38)-C(7A)	119.6(3)	C(39)-C(38)-C(7A)	119.8(3)
C(40)-C(39)-C(38)	125.4(3)	C(40)-C(39)-C(52B)	117.8(4)
C(38)-C(39)-C(52B)	114.1(4)	C(40)-C(39)-C(52A)	117.0(3)
C(38)-C(39)-C(52A)	116.4(3)	C(52B)-C(39)-C(52A)	28.7(3)
C(39)-C(40)-C(41)	123.7(3)	C(42)-C(41)-C(40)	118.2(3)
C(42)-C(41)-C(56)	121.0(3)	C(40)-C(41)-C(56)	120.7(3)
C(41)-C(42)-C(43)	123.3(3)	C(44)-C(43)-C(42)	123.9(3)
C(44)-C(43)-C(52A)	116.7(3)	C(42)-C(43)-C(52A)	118.1(3)
C(44)-C(43)-C(52B)	115.4(4)	C(42)-C(43)-C(52B)	118.0(4)
C(52A)-C(43)-C(52B)	28.6(3)	C(43)-C(44)-C(45)	122.1(3)
C(46)-C(45)-C(44)	122.2(3)	C(45)-C(46)-C(47)	124.5(3)
C(45)-C(46)-C(53A)	115.6(4)	C(47)-C(46)-C(53A)	118.2(3)
C(45)-C(46)-C(53B)	115.5(4)	C(47)-C(46)-C(53B)	118.6(5)
C(53A)-C(46)-C(53B)	25.8(3)	C(48)-C(47)-C(46)	122.6(3)
C(47)-C(48)-C(49)	119.4(3)	C(47)-C(48)-C(60)	121.4(3)
C(49)-C(48)-C(60)	119.1(3)	C(50)-C(49)-C(48)	122.2(3)
C(49)-C(50)-C(51)	124.4(3)	C(49)-C(50)-C(53A)	118.7(4)
C(51)-C(50)-C(53A)	115.6(4)	C(49)-C(50)-C(53B)	118.9(4)
C(51)-C(50)-C(53B)	115.1(4)	C(53A)-C(50)-C(53B)	25.5(3)
C(38)-C(51)-C(50)	123.9(3)	C(43)-C(52A)-C(39)	112.4(4)
C(43)-C(52A)-C(53A)	106.9(4)	C(39)-C(52A)-C(53A)	108.3(5)
C(43)-C(52A)-C(54A)	108.7(4)	C(39)-C(52A)-C(54A)	108.1(4)

C(53A)-C(52A)-C(54A)	112.5(5)	C(46)-C(53A)-C(50)	112.6(5)
C(46)-C(53A)-C(52A)	109.2(5)	C(50)-C(53A)-C(52A)	109.0(5)
C(46)-C(53A)-C(55A)	106.9(4)	C(50)-C(53A)-C(55A)	107.1(5)
C(52A)-C(53A)-C(55A)	112.0(5)	C(53B)-C(52B)-C(39)	112.1(7)
C(53B)-C(52B)-C(43)	108.9(7)	C(39)-C(52B)-C(43)	111.0(5)
C(53B)-C(52B)-C(54B)	108.6(8)	C(39)-C(52B)-C(54B)	107.3(7)
C(43)-C(52B)-C(54B)	108.8(7)	C(52B)-C(53B)-C(46)	112.4(8)
C(52B)-C(53B)-C(50)	109.7(7)	C(46)-C(53B)-C(50)	112.4(6)
C(52B)-C(53B)-C(55B)	108.9(8)	C(46)-C(53B)-C(55B)	106.3(7)
C(50)-C(53B)-C(55B)	106.9(7)	C(58B)-C(56)-C(58A)	134.4(11)
C(58B)-C(56)-C(41)	112.6(10)	C(58A)-C(56)-C(41)	108.4(3)
C(58B)-C(56)-C(59B)	117.7(12)	C(58A)-C(56)-C(59B)	58.3(6)
C(41)-C(56)-C(59B)	114.1(7)	C(58B)-C(56)-C(59A)	33.9(9)
C(58A)-C(56)-C(59A)	110.9(4)	C(41)-C(56)-C(59A)	112.3(3)
C(59B)-C(56)-C(59A)	133.3(7)	C(58B)-C(56)-C(57A)	73.8(10)
C(58A)-C(56)-C(57A)	109.8(4)	C(41)-C(56)-C(57A)	110.0(3)
C(59B)-C(56)-C(57A)	52.9(6)	C(59A)-C(56)-C(57A)	105.4(4)
C(58B)-C(56)-C(57B)	105.7(12)	C(58A)-C(56)-C(57B)	41.8(7)
C(41)-C(56)-C(57B)	106.9(7)	C(59B)-C(56)-C(57B)	97.7(10)
C(59A)-C(56)-C(57B)	73.7(8)	C(57A)-C(56)-C(57B)	139.9(7)
C(61A)-C(60)-C(61B)	129.2(7)	C(61A)-C(60)-C(48)	113.3(3)
C(61B)-C(60)-C(48)	117.5(6)	C(61A)-C(60)-C(62A)	109.9(4)
C(61B)-C(60)-C(62A)	54.8(6)	C(48)-C(60)-C(62A)	108.7(3)
C(61A)-C(60)-C(63A)	108.9(4)	C(61B)-C(60)-C(63A)	54.1(6)
C(48)-C(60)-C(63A)	107.4(3)	C(62A)-C(60)-C(63A)	108.6(4)
C(61A)-C(60)-C(63B)	52.6(5)	C(61B)-C(60)-C(63B)	109.4(9)
C(48)-C(60)-C(63B)	109.0(5)	C(62A)-C(60)-C(63B)	61.9(6)
C(63A)-C(60)-C(63B)	143.5(5)	C(61A)-C(60)-C(62B)	52.9(6)
C(61B)-C(60)-C(62B)	104.5(8)	C(48)-C(60)-C(62B)	111.7(6)
C(62A)-C(60)-C(62B)	139.7(6)	C(63A)-C(60)-C(62B)	58.9(6)
C(63B)-C(60)-C(62B)	103.9(6)		

Figure S7. ORTEP plot (30% probability) for 2,7-di-*tert*-butyl-10b,10c-dimethyl-4-phenyl-*trans*-10b,10c-dihydropyrene, **60**

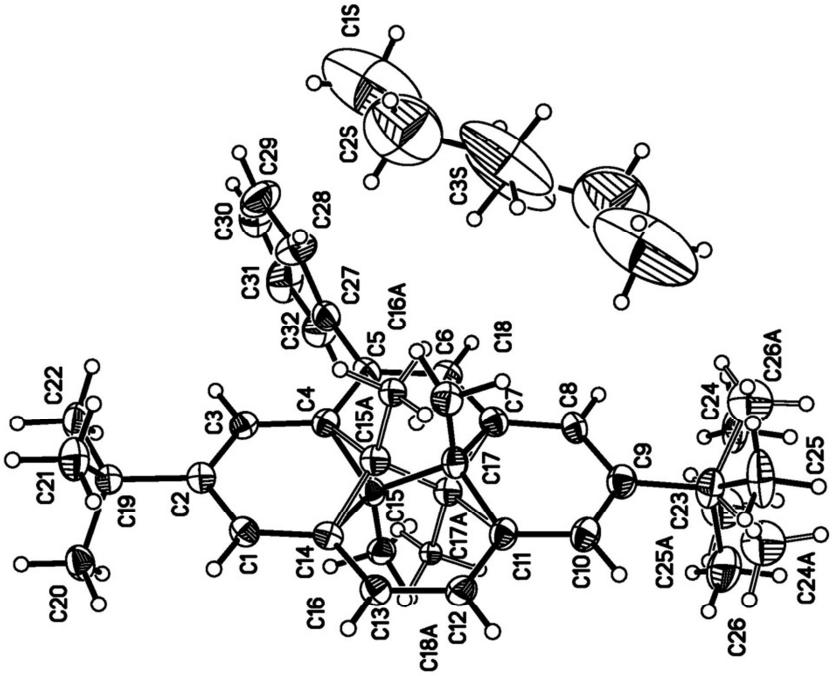


Table S21. Atomic coordinates and equivalent isotropic displacement parameters ($Å^2$) for 2,7-di-*tert*-butyl-10b,10c-dimethyl-4-phenyl-*trans*-10b,10c-dihydropyrene, **60**

	x	y	z	U(eq)
C(1)	0.2928(2)	0.5278(5)	0.31334(10)	0.023(1)
C(2)	0.3602(2)	0.4673(5)	0.34719(11)	0.023(1)
C(3)	0.3324(2)	0.3333(5)	0.37987(10)	0.022(1)
C(4)	0.2417(2)	0.2510(5)	0.38063(10)	0.023(1)
C(5)	0.2109(2)	0.1221(5)	0.41362(10)	0.023(1)
C(6)	0.1182(2)	0.0446(5)	0.41128(10)	0.024(1)
C(7)	0.0505(2)	0.1043(5)	0.37884(11)	0.025(1)
C(8)	-0.0409(2)	0.0256(5)	0.37478(11)	0.025(1)
C(9)	-0.1057(2)	0.0781(5)	0.34024(11)	0.029(1)
C(10)	-0.0774(2)	0.2179(5)	0.30784(11)	0.028(1)
C(11)	0.0104(2)	0.3082(5)	0.30859(10)	0.025(1)
C(12)	0.0422(2)	0.4415(5)	0.27619(11)	0.026(1)
C(13)	0.1331(2)	0.5174(5)	0.27746(10)	0.023(1)
C(14)	0.2018(2)	0.4545(5)	0.31013(10)	0.022(1)
C(15)	0.1770(3)	0.2686(8)	0.33916(14)	0.022(1)
C(16)	0.1905(4)	0.0552(7)	0.31298(13)	0.024(1)
C(17)	0.0744(3)	0.2920(8)	0.35032(15)	0.023(1)
C(18)	0.0614(4)	0.5021(7)	0.37649(14)	0.028(1)
C(15A)	0.1611(15)	0.372(4)	0.3522(7)	0.025(6)
C(16A)	0.1203(17)	0.548(3)	0.3806(6)	0.021(6)
C(17A)	0.0923(16)	0.201(4)	0.3382(7)	0.023(6)
C(18A)	0.1332(16)	0.016(3)	0.3109(6)	0.015(5)
C(19)	0.4605(2)	0.5539(5)	0.34718(10)	0.025(1)
C(20)	0.5025(2)	0.4825(6)	0.30537(11)	0.031(1)
C(21)	0.4587(2)	0.8008(6)	0.34937(12)	0.037(1)
C(22)	0.5244(2)	0.4696(6)	0.38541(11)	0.034(1)
C(23)	-0.2039(2)	-0.0196(6)	0.33613(12)	0.036(1)
C(24)	-0.2216(4)	-0.1704(10)	0.37377(19)	0.051(2)
C(25)	-0.2761(4)	0.1567(10)	0.3327(2)	0.055(2)
C(26)	-0.2119(4)	-0.1605(10)	0.29493(19)	0.053(2)
C(24A)	-0.2747(11)	0.076(3)	0.3003(6)	0.056(5)
C(25A)	-0.2017(11)	-0.256(3)	0.3328(6)	0.055(5)
C(26A)	-0.2544(11)	0.043(3)	0.3797(5)	0.059(5)
C(27)	0.2765(2)	0.0576(6)	0.45176(11)	0.029(1)
C(28)	0.2990(3)	0.2024(7)	0.48475(11)	0.044(1)
C(29)	0.3591(3)	0.1435(8)	0.52047(13)	0.055(1)
C(30)	0.3964(3)	-0.0604(9)	0.52303(14)	0.055(1)
C(31)	0.3745(3)	-0.2057(8)	0.49056(14)	0.054(1)
C(32)	0.3144(3)	-0.1481(6)	0.45530(13)	0.040(1)
C(1S)	0.1555(9)	0.5988(19)	0.5470(3)	0.222(6)
C(2S)	0.1049(7)	0.6822(16)	0.5150(3)	0.144(3)

C(3S)	-0.0088(9)	0.5979(13)	0.4984(3)	0.168(4)
H(1A)	0.3114	0.6239	0.2917	0.027
H(3A)	0.3776	0.2959	0.4029	0.026
H(6A)	0.1011	-0.0531	0.4329	0.029
H(8A)	-0.0602	-0.0684	0.3966	0.030
H(10A)	-0.1215	0.2514	0.2842	0.033
H(12A)	-0.0007	0.4812	0.2524	0.031
H(13A)	0.1498	0.6147	0.2557	0.028
H(16A)	0.1721	-0.0686	0.3300	0.036
H(16B)	0.2565	0.0407	0.3071	0.036
H(16C)	0.1512	0.0603	0.2855	0.036
H(18A)	0.0801	0.6263	0.3597	0.042
H(18B)	0.1005	0.4955	0.4040	0.042
H(18C)	-0.0047	0.5169	0.3823	0.042
H(16D)	0.1703	0.6486	0.3908	0.031
H(16E)	0.0941	0.4809	0.4056	0.031
H(16F)	0.0707	0.6270	0.3635	0.031
H(18D)	0.0840	-0.0903	0.3032	0.023
H(18E)	0.1855	-0.0534	0.3280	0.023
H(18F)	0.1557	0.0767	0.2844	0.023
H(20A)	0.5028	0.3248	0.3038	0.047
H(20B)	0.5669	0.5365	0.3054	0.047
H(20C)	0.4645	0.5407	0.2802	0.047
H(21A)	0.4313	0.8462	0.3759	0.055
H(21B)	0.4208	0.8575	0.3241	0.055
H(21C)	0.5229	0.8564	0.3495	0.055
H(22A)	0.4996	0.5143	0.4126	0.050
H(22B)	0.5877	0.5285	0.3840	0.050
H(22C)	0.5269	0.3120	0.3842	0.050
H(24A)	-0.1748	-0.2864	0.3754	0.076
H(24B)	-0.2846	-0.2325	0.3690	0.076
H(24C)	-0.2165	-0.0890	0.4010	0.076
H(25A)	-0.3389	0.0933	0.3282	0.082
H(25B)	-0.2649	0.2505	0.3082	0.082
H(25C)	-0.2715	0.2414	0.3595	0.082
H(26A)	-0.2013	-0.0713	0.2697	0.080
H(26B)	-0.2748	-0.2243	0.2911	0.080
H(26C)	-0.1647	-0.2753	0.2978	0.080
H(24D)	-0.2566	0.0326	0.2717	0.084
H(24E)	-0.2742	0.2336	0.3024	0.084
H(24F)	-0.3379	0.0223	0.3042	0.084
H(25D)	-0.1829	-0.2977	0.3042	0.083
H(25E)	-0.2643	-0.3143	0.3366	0.083
H(25F)	-0.1566	-0.3144	0.3554	0.083
H(26D)	-0.2156	-0.0078	0.4053	0.089
H(26E)	-0.3163	-0.0255	0.3788	0.089

H(26F)	-0.2616	0.1996	0.3813	0.089
H(28A)	0.2733	0.3436	0.4831	0.053
H(29A)	0.3743	0.2443	0.5431	0.066
H(30A)	0.4375	-0.1006	0.5474	0.066
H(31A)	0.4007	-0.3464	0.4923	0.064
H(32A)	0.2986	-0.2508	0.4331	0.048
H(1SA)	0.2183	0.6633	0.5488	0.333
H(1SB)	0.1606	0.4430	0.5426	0.333
H(1SC)	0.1263	0.6266	0.5740	0.333
H(2SA)	0.1417	0.6691	0.4894	0.173
H(2SB)	0.1007	0.8381	0.5213	0.173
H(3SA)	-0.0555	0.6460	0.5182	0.201
H(3SB)	-0.0288	0.6417	0.4683	0.201

U(eq) is defined as one third of the trace of the orthogonalized U_{ij} tensor.

Table S22. Anisotropic displacement parameters ($Å^2$) for 2,7-di-*tert*-butyl-10b,10c-dimethyl-4-phenyl-*trans*-10b,10c-dihydropyrene, **60**

	U_{11}	U_{22}	U_{33}	U_{23}	U_{13}	U_{12}
C(1)	0.025(2)	0.0188(18)	0.0245(19)	0.0014(15)	0.0047(16)	-0.0006(15)
C(2)	0.0228(19)	0.0202(18)	0.026(2)	0.0003(15)	0.0022(16)	0.0006(15)
C(3)	0.0213(19)	0.0216(19)	0.0226(19)	-0.0004(15)	-0.0009(15)	0.0032(15)
C(4)	0.023(2)	0.0200(18)	0.0246(19)	-0.0010(15)	0.0006(15)	0.0001(15)
C(5)	0.025(2)	0.0206(19)	0.024(2)	0.0004(15)	0.0072(16)	-0.0006(15)
C(6)	0.026(2)	0.0239(19)	0.0224(19)	0.0017(15)	0.0047(16)	0.0002(16)
C(7)	0.025(2)	0.0227(19)	0.028(2)	-0.0015(16)	0.0054(17)	0.0002(16)
C(8)	0.021(2)	0.0238(19)	0.030(2)	0.0012(16)	0.0062(17)	-0.0033(15)
C(9)	0.025(2)	0.028(2)	0.033(2)	-0.0018(17)	0.0022(17)	0.0013(16)
C(10)	0.023(2)	0.028(2)	0.032(2)	0.0002(17)	-0.0022(16)	0.0030(16)
C(11)	0.0194(19)	0.026(2)	0.028(2)	-0.0004(16)	-0.0006(16)	0.0024(16)
C(12)	0.024(2)	0.031(2)	0.023(2)	0.0006(16)	-0.0019(16)	0.0023(16)
C(13)	0.026(2)	0.0209(19)	0.023(2)	0.0041(15)	0.0026(16)	0.0005(15)
C(14)	0.024(2)	0.0223(18)	0.0206(19)	0.0007(15)	0.0030(16)	0.0010(15)
C(15)	0.019(3)	0.024(3)	0.022(3)	0.004(2)	0.0020(19)	0.000(2)
C(16)	0.023(3)	0.027(2)	0.022(2)	-0.0022(19)	0.001(2)	0.002(2)
C(17)	0.019(3)	0.023(3)	0.028(3)	0.002(2)	0.002(2)	0.001(2)
C(18)	0.026(3)	0.023(3)	0.034(3)	-0.004(2)	0.004(2)	0.003(2)
C(19)	0.0217(19)	0.030(2)	0.023(2)	0.0009(16)	0.0018(16)	-0.0035(15)
C(20)	0.0211(19)	0.038(2)	0.034(2)	0.0065(17)	0.0031(16)	0.0006(17)
C(21)	0.030(2)	0.031(2)	0.050(3)	0.0002(19)	0.0046(18)	-0.0076(17)
C(22)	0.0212(19)	0.043(2)	0.035(2)	0.0056(18)	-0.0027(17)	-0.0089(17)
C(23)	0.025(2)	0.038(2)	0.044(2)	0.0044(19)	-0.0021(18)	-0.0060(18)
C(24)	0.026(3)	0.064(4)	0.062(4)	0.014(3)	-0.001(3)	-0.022(3)
C(25)	0.020(3)	0.055(4)	0.090(6)	0.014(4)	0.006(3)	0.000(3)
C(26)	0.042(4)	0.055(4)	0.062(4)	-0.005(3)	-0.001(3)	-0.022(3)
C(27)	0.025(2)	0.037(2)	0.026(2)	0.0047(17)	0.0030(17)	-0.0023(17)
C(28)	0.054(3)	0.045(3)	0.030(2)	-0.002(2)	-0.005(2)	-0.002(2)
C(29)	0.058(3)	0.071(3)	0.034(3)	0.003(2)	-0.013(2)	-0.016(3)
C(30)	0.040(3)	0.084(4)	0.040(3)	0.032(3)	-0.010(2)	-0.011(3)
C(31)	0.040(3)	0.058(3)	0.060(3)	0.021(3)	-0.011(2)	0.005(2)
C(32)	0.037(2)	0.040(2)	0.042(2)	0.0076(19)	-0.0039(19)	0.0061(19)
C(1S)	0.306(17)	0.188(11)	0.192(12)	0.006(9)	0.148(12)	0.012(11)
C(2S)	0.166(9)	0.150(8)	0.117(7)	0.041(6)	0.018(6)	0.014(7)
C(3S)	0.217(10)	0.156(9)	0.149(7)	0.056(8)	0.130(7)	0.068(9)

The anisotropic displacement factor exponent takes the form:
$-2\pi^2[h^2a^{*2}U_{11} + ... + 2hka^*b^*U_{12}]$

Table S23. Bond lengths [Å] for 2,7-di-*tert*-butyl-10b,10c-dimethyl-4-phenyl-*trans*-10b,10c-dihydropyrene, **60**

atom-atom	distance	atom-atom	distance
C(1)-C(14)	1.373(4)	C(1)-C(2)	1.414(4)
C(2)-C(3)	1.392(4)	C(2)-C(19)	1.531(5)
C(3)-C(4)	1.395(4)	C(4)-C(5)	1.396(4)
C(4)-C(15)	1.523(5)	C(4)-C(15A)	1.58(2)
C(5)-C(6)	1.406(4)	C(5)-C(27)	1.500(5)
C(6)-C(7)	1.386(4)	C(7)-C(8)	1.392(4)
C(7)-C(17)	1.517(5)	C(7)-C(17A)	1.56(2)
C(8)-C(9)	1.394(5)	C(9)-C(10)	1.410(5)
C(9)-C(23)	1.524(5)	C(10)-C(11)	1.372(4)
C(11)-C(12)	1.404(5)	C(11)-C(17)	1.523(5)
C(11)-C(17A)	1.57(2)	C(12)-C(13)	1.380(4)
C(13)-C(14)	1.406(4)	C(14)-C(15)	1.522(5)
C(14)-C(15A)	1.55(2)	C(15)-C(17)	1.540(7)
C(15)-C(16)	1.573(7)	C(17)-C(18)	1.554(7)
C(15A)-C(17A)	1.49(3)	C(15A)-C(16A)	1.55(3)
C(17A)-C(18A)	1.57(3)	C(19)-C(22)	1.526(4)
C(19)-C(21)	1.535(5)	C(19)-C(20)	1.536(5)
C(23)-C(25A)	1.473(16)	C(23)-C(25)	1.502(7)
C(23)-C(24)	1.531(6)	C(23)-C(26)	1.543(7)
C(23)-C(24A)	1.557(16)	C(23)-C(26A)	1.628(16)
C(27)-C(28)	1.379(5)	C(27)-C(32)	1.387(5)
C(28)-C(29)	1.392(5)	C(29)-C(30)	1.373(6)
C(30)-C(31)	1.367(6)	C(31)-C(32)	1.380(5)
C(1S)-C(2S)	1.286(11)	C(2S)-C(3S)	1.743(14)
C(3S)-C(3S)#1	1.244(14)	C(1)-H(1A)	0.9500
C(3)-H(3A)	0.9500	C(6)-H(6A)	0.9500
C(8)-H(8A)	0.9500	C(10)-H(10A)	0.9500
C(12)-H(12A)	0.9500	C(13)-H(13A)	0.9500
C(16)-H(16A)	0.9800	C(16)-H(16B)	0.9800
C(16)-H(16C)	0.9800	C(18)-H(18A)	0.9800
C(18)-H(18B)	0.9800	C(18)-H(18C)	0.9800
C(16A)-H(16D)	0.9800	C(16A)-H(16E)	0.9800
C(16A)-H(16F)	0.9800	C(18A)-H(18D)	0.9800
C(18A)-H(18E)	0.9800	C(18A)-H(18F)	0.9800
C(20)-H(20A)	0.9800	C(20)-H(20B)	0.9800
C(20)-H(20C)	0.9800	C(21)-H(21A)	0.9800
C(21)-H(21B)	0.9800	C(21)-H(21C)	0.9800
C(22)-H(22A)	0.9800	C(22)-H(22B)	0.9800
C(22)-H(22C)	0.9800	C(24)-H(24A)	0.9800
C(24)-H(24B)	0.9800	C(24)-H(24C)	0.9800
C(25)-H(25A)	0.9800	C(25)-H(25B)	0.9800

C(25)-H(25C)	0.9800	C(26)-H(26A)	0.9800
C(26)-H(26B)	0.9800	C(26)-H(26C)	0.9800
C(24A)-H(24D)	0.9800	C(24A)-H(24E)	0.9800
C(24A)-H(24F)	0.9800	C(25A)-H(25D)	0.9800
C(25A)-H(25E)	0.9800	C(25A)-H(25F)	0.9800
C(26A)-H(26D)	0.9800	C(26A)-H(26E)	0.9800
C(26A)-H(26F)	0.9800	C(28)-H(28A)	0.9500
C(29)-H(29A)	0.9500	C(30)-H(30A)	0.9500
C(31)-H(31A)	0.9500	C(32)-H(32A)	0.9500
C(1S)-H(1SA)	0.9800	C(1S)-H(1SB)	0.9800
C(1S)-H(1SC)	0.9800	C(2S)-H(2SA)	0.9900
C(2S)-H(2SB)	0.9900	C(3S)-H(3SA)	0.9900
C(3S)-H(3SB)	0.9900		

Symmetry transformations used to generate equivalent atoms:
#1 -x,-y+1,-z+1

Table S24. Bond angles [°] for 2,7-di-*tert*-butyl-10b,10c-dimethyl-4-phenyl-*trans*-10b,10c-dihydropyrene, **60**

atom-atom-atom	angle	atom-atom-atom	angle
C(14)-C(1)-C(2)	123.3(3)	C(3)-C(2)-C(1)	118.7(3)
C(3)-C(2)-C(19)	122.2(3)	C(1)-C(2)-C(19)	119.1(3)
C(2)-C(3)-C(4)	123.5(3)	C(3)-C(4)-C(5)	124.8(3)
C(3)-C(4)-C(15)	117.4(3)	C(5)-C(4)-C(15)	116.8(3)
C(3)-C(4)-C(15A)	116.8(8)	C(5)-C(4)-C(15A)	114.9(8)
C(15)-C(4)-C(15A)	29.8(8)	C(4)-C(5)-C(6)	120.7(3)
C(4)-C(5)-C(27)	121.0(3)	C(6)-C(5)-C(27)	118.3(3)
C(7)-C(6)-C(5)	123.0(3)	C(6)-C(7)-C(8)	124.5(3)
C(6)-C(7)-C(17)	116.7(3)	C(8)-C(7)-C(17)	118.1(3)
C(6)-C(7)-C(17A)	113.4(8)	C(8)-C(7)-C(17A)	118.8(8)
C(17)-C(7)-C(17A)	27.6(8)	C(7)-C(8)-C(9)	123.2(3)
C(8)-C(9)-C(10)	118.5(3)	C(8)-C(9)-C(23)	121.3(3)
C(10)-C(9)-C(23)	120.1(3)	C(11)-C(10)-C(9)	123.7(3)
C(10)-C(11)-C(12)	125.3(3)	C(10)-C(11)-C(17)	118.2(3)
C(12)-C(11)-C(17)	115.9(3)	C(10)-C(11)-C(17A)	118.2(8)
C(12)-C(11)-C(17A)	113.3(8)	C(17)-C(11)-C(17A)	27.4(8)
C(13)-C(12)-C(11)	122.7(3)	C(12)-C(13)-C(14)	121.8(3)
C(1)-C(14)-C(13)	124.1(3)	C(1)-C(14)-C(15)	118.3(3)
C(13)-C(14)-C(15)	116.9(3)	C(1)-C(14)-C(15A)	117.8(8)
C(13)-C(14)-C(15A)	113.9(8)	C(15)-C(14)-C(15A)	30.2(9)
C(14)-C(15)-C(4)	113.4(3)	C(14)-C(15)-C(17)	109.5(4)
C(4)-C(15)-C(17)	110.0(4)	C(14)-C(15)-C(16)	106.9(3)
C(4)-C(15)-C(16)	106.4(3)	C(17)-C(15)-C(16)	110.7(5)
C(7)-C(17)-C(11)	113.3(3)	C(7)-C(17)-C(15)	108.8(4)
C(11)-C(17)-C(15)	109.4(4)	C(7)-C(17)-C(18)	107.4(4)
C(11)-C(17)-C(18)	107.3(4)	C(15)-C(17)-C(18)	110.7(4)
C(17A)-C(15A)-C(16A)	114(2)	C(17A)-C(15A)-C(14)	106.0(18)
C(16A)-C(15A)-C(14)	115.4(16)	C(17A)-C(15A)-C(4)	104.8(18)
C(16A)-C(15A)-C(4)	108.1(15)	C(14)-C(15A)-C(4)	108.5(14)
C(15A)-C(17A)-C(7)	109.2(17)	C(15A)-C(17A)-C(18A)	114(2)
C(7)-C(17A)-C(18A)	109.7(15)	C(15A)-C(17A)-C(11)	108.1(18)
C(7)-C(17A)-C(11)	108.5(14)	C(18A)-C(17A)-C(11)	106.7(14)
C(22)-C(19)-C(2)	112.3(3)	C(22)-C(19)-C(21)	108.6(3)
C(2)-C(19)-C(21)	109.4(3)	C(22)-C(19)-C(20)	107.7(3)
C(2)-C(19)-C(20)	109.2(3)	C(21)-C(19)-C(20)	109.5(3)
C(25A)-C(23)-C(25)	137.7(7)	C(25A)-C(23)-C(9)	112.2(7)
C(25)-C(23)-C(9)	109.8(3)	C(25A)-C(23)-C(24)	56.6(7)
C(25)-C(23)-C(24)	110.1(4)	C(9)-C(23)-C(24)	112.8(3)
C(25A)-C(23)-C(26)	51.5(7)	C(25)-C(23)-C(26)	110.5(4)
C(9)-C(23)-C(26)	107.4(3)	C(24)-C(23)-C(26)	106.0(4)
C(25A)-C(23)-C(24A)	110.3(9)	C(25)-C(23)-C(24A)	43.0(6)

C(9)-C(23)-C(24A)	116.6(7)	C(24)-C(23)-C(24A)	129.6(7)
C(26)-C(23)-C(24A)	68.1(7)	C(25A)-C(23)-C(26A)	108.0(10)
C(25)-C(23)-C(26A)	62.4(7)	C(9)-C(23)-C(26A)	107.7(6)
C(24)-C(23)-C(26A)	53.4(6)	C(26)-C(23)-C(26A)	144.3(7)
C(24A)-C(23)-C(26A)	101.1(9)	C(28)-C(27)-C(32)	118.4(3)
C(28)-C(27)-C(5)	120.1(3)	C(32)-C(27)-C(5)	121.5(3)
C(27)-C(28)-C(29)	120.5(4)	C(30)-C(29)-C(28)	120.0(4)
C(31)-C(30)-C(29)	120.1(4)	C(30)-C(31)-C(32)	120.0(4)
C(31)-C(32)-C(27)	121.0(4)	C(1S)-C(2S)-C(3S)	123.9(10)
C(3S)#1-C(3S)-C(2S)	95.3(13)	C(14)-C(1)-H(1A)	118.4
C(2)-C(1)-H(1A)	118.4	C(2)-C(3)-H(3A)	118.3
C(4)-C(3)-H(3A)	118.3	C(7)-C(6)-H(6A)	118.5
C(5)-C(6)-H(6A)	118.5	C(7)-C(8)-H(8A)	118.4
C(9)-C(8)-H(8A)	118.4	C(11)-C(10)-H(10A)	118.2
C(9)-C(10)-H(10A)	118.2	C(13)-C(12)-H(12A)	118.7
C(11)-C(12)-H(12A)	118.7	C(12)-C(13)-H(13A)	119.1
C(14)-C(13)-H(13A)	119.1	C(15A)-C(16A)-H(16D)	109.5
C(15A)-C(16A)-H(16E)	109.5	H(16D)-C(16A)-H(16E)	109.5
C(15A)-C(16A)-H(16F)	109.5	H(16D)-C(16A)-H(16F)	109.5
H(16E)-C(16A)-H(16F)	109.5	C(17A)-C(18A)-H(18D)	109.5
C(17A)-C(18A)-H(18E)	109.5	H(18D)-C(18A)-H(18E)	109.5
C(17A)-C(18A)-H(18F)	109.5	H(18D)-C(18A)-H(18F)	109.5
H(18E)-C(18A)-H(18F)	109.5	C(19)-C(20)-H(20A)	109.5
C(19)-C(20)-H(20B)	109.5	H(20A)-C(20)-H(20B)	109.5
C(19)-C(20)-H(20C)	109.5	H(20A)-C(20)-H(20C)	109.5
H(20B)-C(20)-H(20C)	109.5	C(19)-C(21)-H(21A)	109.5
C(19)-C(21)-H(21B)	109.5	H(21A)-C(21)-H(21B)	109.5
C(19)-C(21)-H(21C)	109.5	H(21A)-C(21)-H(21C)	109.5
H(21B)-C(21)-H(21C)	109.5	C(19)-C(22)-H(22A)	109.5
C(19)-C(22)-H(22B)	109.5	H(22A)-C(22)-H(22B)	109.5
C(19)-C(22)-H(22C)	109.5	H(22A)-C(22)-H(22C)	109.5
H(22B)-C(22)-H(22C)	109.5	C(23)-C(24)-H(24A)	109.5
C(23)-C(24)-H(24B)	109.5	C(23)-C(24)-H(24C)	109.5
C(23)-C(25)-H(25A)	109.5	C(23)-C(25)-H(25B)	109.5
C(23)-C(25)-H(25C)	109.5	C(23)-C(26)-H(26A)	109.5
C(23)-C(26)-H(26B)	109.5	C(23)-C(26)-H(26C)	109.5
C(23)-C(24A)-H(24D)	109.5	C(23)-C(24A)-H(24E)	109.5
H(24D)-C(24A)-H(24E)	109.5	C(23)-C(24A)-H(24F)	109.5
H(24D)-C(24A)-H(24F)	109.5	H(24E)-C(24A)-H(24F)	109.5
C(23)-C(25A)-H(25D)	109.5	C(23)-C(25A)-H(25E)	109.5
H(25D)-C(25A)-H(25E)	109.5	C(23)-C(25A)-H(25F)	109.5
H(25D)-C(25A)-H(25F)	109.5	H(25E)-C(25A)-H(25F)	109.5
C(23)-C(26A)-H(26D)	109.5	C(23)-C(26A)-H(26E)	109.5
H(26D)-C(26A)-H(26E)	109.5	C(23)-C(26A)-H(26F)	109.5
H(26D)-C(26A)-H(26F)	109.5	H(26E)-C(26A)-H(26F)	109.5
C(27)-C(28)-H(28A)	119.7	C(29)-C(28)-H(28A)	119.7

C(30)-C(29)-H(29A)	120.0	C(28)-C(29)-H(29A)	120.0
C(31)-C(30)-H(30A)	120.0	C(29)-C(30)-H(30A)	120.0
C(30)-C(31)-H(31A)	120.0	C(32)-C(31)-H(31A)	120.0
C(31)-C(32)-H(32A)	119.5	C(27)-C(32)-H(32A)	119.5
C(2S)-C(1S)-H(1SA)	109.5	C(2S)-C(1S)-H(1SB)	109.5
H(1SA)-C(1S)-H(1SB)	109.5	C(2S)-C(1S)-H(1SC)	109.5
H(1SA)-C(1S)-H(1SC)	109.5	H(1SB)-C(1S)-H(1SC)	109.5
C(1S)-C(2S)-H(2SA)	106.3	C(3S)-C(2S)-H(2SA)	106.3
C(1S)-C(2S)-H(2SB)	106.3	C(3S)-C(2S)-H(2SB)	106.3
H(2SA)-C(2S)-H(2SB)	106.4	C(3S)#1-C(3S)-H(3SA)	112.7
C(2S)-C(3S)-H(3SA)	112.7	C(3S)#1-C(3S)-H(3SB)	112.7
C(2S)-C(3S)-H(3SB)	112.7	H(3SA)-C(3S)-H(3SB)	110.2

Symmetry transformations used to generate equivalent atoms:
#1 -x,-y+1,-z+1

Figure S8. ORTEP3 Plot showing labeling for **99**

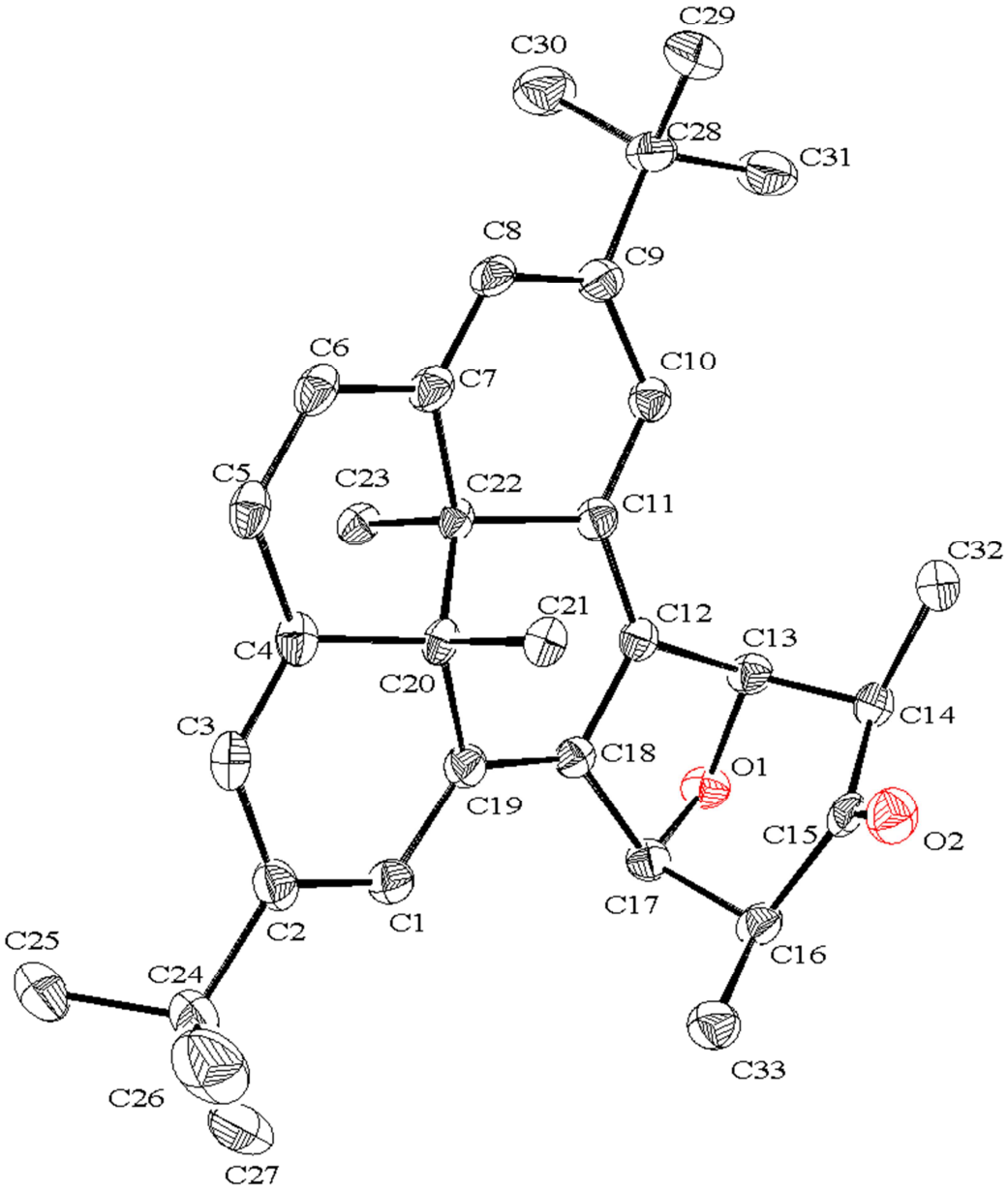


Table 2. Atomic coordinates (x 10^4) and equivalent isotropic displacement parameters (A^2 x 10^3) for **99**.
U(eq) is defined as one third of the trace of the orthogonalized Uij tensor.

	x	y	z	U(eq)	occ
C(1)	7222(3)	-854(1)	6536(1)	24(1)	
C(2)	8500(2)	-1443(1)	6434(1)	25(1)	
C(3)	8914(3)	-1926(1)	6911(1)	23(1)	
C(4)	8083(2)	-1846(1)	7466(1)	22(1)	
C(5)	8419(2)	-2340(1)	7939(1)	23(1)	
C(6)	7482(3)	-2257(1)	8483(1)	24(1)	
C(7)	6082(3)	-1687(1)	8606(1)	22(1)	
C(8)	5026(3)	-1605(1)	9127(1)	23(1)	
C(9)	3605(2)	-1032(1)	9234(1)	23(1)	
C(10)	3354(2)	-505(1)	8802(1)	21(1)	
C(11)	4352(2)	-538(1)	8250(1)	19(1)	
C(12)	4128(2)	-45(1)	7795(1)	18(1)	
C(13)	2938(2)	658(1)	7769(1)	21(1)	
C(14)	4318(3)	1301(1)	7949(1)	23(1)	
C(15)	6237(2)	1309(1)	7554(1)	21(1)	
C(16)	5863(3)	1147(1)	6897(1)	23(1)	
C(17)	4353(2)	504(1)	6858(1)	21(1)	
C(18)	5055(2)	-135(1)	7228(1)	18(1)	
C(19)	6321(2)	-710(1)	7092(1)	21(1)	
C(20)	7143(5)	-1124(2)	7638(1)	17(1)	0.578(5)
C(21)	8867(4)	-661(1)	7936(2)	19(1)	0.578(5)
C(22)	5328(5)	-1267(2)	8056(1)	16(1)	0.578(5)
C(23)	3615(5)	-1727(2)	7751(2)	19(1)	0.578(5)
C(24)	9514(3)	-1580(1)	5828(1)	31(1)	
C(25)	9175(4)	-2368(1)	5640(1)	47(1)	
C(26)	11831(3)	-1441(1)	5886(1)	56(1)	
C(27)	8639(4)	-1097(1)	5339(1)	51(1)	
C(28)	2384(3)	-1026(1)	9818(1)	26(1)	
C(29)	3902(3)	-1061(1)	10345(1)	36(1)	
C(30)	964(3)	-1690(1)	9832(1)	39(1)	
C(31)	1056(3)	-350(1)	9889(1)	39(1)	
C(32)	4859(3)	1317(1)	8608(1)	30(1)	
C(33)	7845(3)	1042(1)	6545(1)	28(1)	
O(1)	2465(2)	718(1)	7145(1)	23(1)	
O(2)	7944(2)	1437(1)	7749(1)	30(1)	
C(20B)	6181(8)	-1346(2)	7550(2)	19(1)	0.422(5)
C(21B)	4167(7)	-1778(2)	7430(2)	22(1)	0.422(5)

C(22B)	6194(8)	-1041(2)	8178(2)	20(1)	0.422(5)
C(23B)	8242(6)	-607(2)	8303(2)	24(1)	0.422(5)

Table 3. Bond lengths [A] for **99**.

atom-atom	distance	atom-atom	distance
C(1)-C(2)	1.385(2)	C(18)-C(19)	1.377(2)
C(1)-C(19)	1.404(2)	C(19)-C(20)	1.542(3)
C(1)-H(1)	0.9500	C(19)-C(20B)	1.567(4)
C(2)-C(3)	1.421(2)	C(20)-C(22)	1.526(4)
C(2)-C(24)	1.533(2)	C(20)-C(21)	1.556(5)
C(3)-C(4)	1.366(2)	C(21)-H(21A)	0.9800
C(3)-H(3)	0.9500	C(21)-H(21B)	0.9800
C(4)-C(5)	1.418(2)	C(21)-H(21C)	0.9800
C(4)-C(20)	1.518(3)	C(22)-C(23)	1.555(5)
C(4)-C(20B)	1.549(4)	C(23)-H(23A)	0.9800
C(5)-C(6)	1.373(2)	C(23)-H(23B)	0.9800
C(5)-H(5)	0.9500	C(23)-H(23C)	0.9800
C(6)-C(7)	1.418(2)	C(24)-C(26)	1.524(3)
C(6)-H(6)	0.9500	C(24)-C(27)	1.526(3)
C(7)-C(8)	1.364(2)	C(24)-C(25)	1.535(2)
C(7)-C(22B)	1.535(4)	C(25)-H(25A)	0.9800
C(7)-C(22)	1.539(3)	C(25)-H(25B)	0.9800
C(8)-C(9)	1.423(2)	C(25)-H(25C)	0.9800
C(8)-H(8)	0.9500	C(26)-H(26A)	0.9800
C(9)-C(10)	1.385(2)	C(26)-H(26B)	0.9800
C(9)-C(28)	1.531(2)	C(26)-H(26C)	0.9800
C(10)-C(11)	1.400(2)	C(27)-H(27A)	0.9800
C(10)-H(10)	0.9500	C(27)-H(27B)	0.9800
C(11)-C(12)	1.379(2)	C(27)-H(27C)	0.9800
C(11)-C(22B)	1.520(4)	C(28)-C(31)	1.526(2)
C(11)-C(22)	1.552(3)	C(28)-C(30)	1.534(2)
C(12)-C(18)	1.417(2)	C(28)-C(29)	1.539(2)
C(12)-C(13)	1.514(2)	C(29)-H(29A)	0.9800
C(13)-O(1)	1.4390(17)	C(29)-H(29B)	0.9800
C(13)-C(14)	1.540(2)	C(29)-H(29C)	0.9800
C(13)-H(13)	1.0000	C(30)-H(30A)	0.9800
C(14)-C(15)	1.524(2)	C(30)-H(30B)	0.9800
C(14)-C(32)	1.524(2)	C(30)-H(30C)	0.9800
C(14)-H(14)	1.0000	C(31)-H(31A)	0.9800
C(15)-O(2)	1.2106(19)	C(31)-H(31B)	0.9800
C(15)-C(16)	1.525(2)	C(31)-H(31C)	0.9800
C(16)-C(33)	1.518(2)	C(32)-H(32A)	0.9800
C(16)-C(17)	1.542(2)	C(32)-H(32B)	0.9800
C(16)-H(16)	1.0000	C(32)-H(32C)	0.9800
C(17)-O(1)	1.4360(19)	C(33)-H(33A)	0.9800
C(17)-C(18)	1.516(2)	C(33)-H(33B)	0.9800
C(17)-H(17)	1.0000	C(33)-H(33C)	0.9800

C(20B)-C(22B)	1.522(6)
C(20B)-C(21B)	1.550(7)
C(21B)-H(21D)	0.9800
C(21B)-H(21E)	0.9800
C(21B)-H(21F)	0.9800
C(22B)-C(23B)	1.573(7)
C(23B)-H(23D)	0.9800
C(23B)-H(23E)	0.9800
C(23B)-H(23F)	0.9800

Table 3. Bond angles [deg] for **99**.

C(2)-C(1)-C(19)	122.93(14)	C(11)-C(12)-C(18)	123.01(14)
C(2)-C(1)-H(1)	118.5	C(11)-C(12)-C(13)	130.64(13)
C(19)-C(1)-H(1)	118.5	C(18)-C(12)-C(13)	106.34(12)
C(1)-C(2)-C(3)	118.87(14)	O(1)-C(13)-C(12)	102.21(11)
C(1)-C(2)-C(24)	122.10(15)	O(1)-C(13)-C(14)	108.58(12)
C(3)-C(2)-C(24)	119.02(14)	C(12)-C(13)-C(14)	111.12(12)
C(4)-C(3)-C(2)	123.11(14)	O(1)-C(13)-H(13)	111.5
C(4)-C(3)-H(3)	118.4	C(12)-C(13)-H(13)	111.5
C(2)-C(3)-H(3)	118.4	C(14)-C(13)-H(13)	111.5
C(3)-C(4)-C(5)	123.61(14)	C(15)-C(14)-C(32)	112.32(14)
C(3)-C(4)-C(20)	118.98(16)	C(15)-C(14)-C(13)	108.97(12)
C(5)-C(4)-C(20)	116.05(16)	C(32)-C(14)-C(13)	113.77(13)
C(3)-C(4)-C(20B)	119.12(19)	C(15)-C(14)-H(14)	107.1
C(5)-C(4)-C(20B)	114.6(2)	C(32)-C(14)-H(14)	107.1
C(20)-C(4)-C(20B)	29.14(15)	C(13)-C(14)-H(14)	107.1
C(6)-C(5)-C(4)	121.85(14)	O(2)-C(15)-C(14)	122.10(14)
C(6)-C(5)-H(5)	119.1	O(2)-C(15)-C(16)	122.26(14)
C(4)-C(5)-H(5)	119.1	C(14)-C(15)-C(16)	115.64(13)
C(5)-C(6)-C(7)	122.49(14)	C(33)-C(16)-C(15)	113.34(13)
C(5)-C(6)-H(6)	118.8	C(33)-C(16)-C(17)	113.92(13)
C(7)-C(6)-H(6)	118.8	C(15)-C(16)-C(17)	107.93(12)
C(8)-C(7)-C(6)	124.62(14)	C(33)-C(16)-H(16)	107.1
C(8)-C(7)-C(22B)	118.38(19)	C(15)-C(16)-H(16)	107.1
C(6)-C(7)-C(22B)	115.37(19)	C(17)-C(16)-H(16)	107.1
C(8)-C(7)-C(22)	118.41(16)	O(1)-C(17)-C(18)	102.88(11)
C(6)-C(7)-C(22)	114.95(16)	O(1)-C(17)-C(16)	107.31(11)
C(22B)-C(7)-C(22)	28.28(15)	C(18)-C(17)-C(16)	112.42(12)
C(7)-C(8)-C(9)	123.34(14)	O(1)-C(17)-H(17)	111.3
C(7)-C(8)-H(8)	118.3	C(18)-C(17)-H(17)	111.3
C(9)-C(8)-H(8)	118.3	C(16)-C(17)-H(17)	111.3
C(10)-C(9)-C(8)	118.85(14)	C(19)-C(18)-C(12)	122.82(13)
C(10)-C(9)-C(28)	122.32(14)	C(19)-C(18)-C(17)	131.20(13)
C(8)-C(9)-C(28)	118.83(14)	C(12)-C(18)-C(17)	105.99(12)
C(9)-C(10)-C(11)	122.43(14)	C(18)-C(19)-C(1)	126.30(14)
C(9)-C(10)-H(10)	118.8	C(18)-C(19)-C(20)	114.31(15)
C(11)-C(10)-H(10)	118.8	C(1)-C(19)-C(20)	118.08(15)
C(12)-C(11)-C(10)	125.53(14)	C(18)-C(19)-C(20B)	113.61(18)
C(12)-C(11)-C(22B)	114.2(2)	C(1)-C(19)-C(20B)	117.70(18)
C(10)-C(11)-C(22B)	118.76(19)	C(20)-C(19)-C(20B)	28.74(14)
C(12)-C(11)-C(22)	114.18(16)	C(4)-C(20)-C(22)	108.1(2)
C(10)-C(11)-C(22)	118.27(16)	C(4)-C(20)-C(19)	111.9(2)
C(22B)-C(11)-C(22)	28.27(15)	C(22)-C(20)-C(19)	108.2(2)

C(4)-C(20)-C(21)	108.0(2)	C(28)-C(30)-H(30B)	109.5
C(22)-C(20)-C(21)	112.4(3)	H(30A)-C(30)-H(30B)	109.5
C(19)-C(20)-C(21)	108.4(2)	C(28)-C(30)-H(30C)	109.5
C(20)-C(22)-C(7)	109.8(2)	H(30A)-C(30)-H(30C)	109.5
C(20)-C(22)-C(11)	109.5(2)	H(30B)-C(30)-H(30C)	109.5
C(7)-C(22)-C(11)	110.0(2)	C(28)-C(31)-H(31A)	109.5
C(20)-C(22)-C(23)	111.8(4)	C(28)-C(31)-H(31B)	109.5
C(7)-C(22)-C(23)	107.6(2)	H(31A)-C(31)-H(31B)	109.5
C(11)-C(22)-C(23)	108.1(2)	C(28)-C(31)-H(31C)	109.5
C(26)-C(24)-C(27)	109.01(17)	H(31A)-C(31)-H(31C)	109.5
C(26)-C(24)-C(2)	108.45(15)	H(31B)-C(31)-H(31C)	109.5
C(27)-C(24)-C(2)	112.62(15)	C(14)-C(32)-H(32A)	109.5
C(26)-C(24)-C(25)	108.90(18)	C(14)-C(32)-H(32B)	109.5
C(27)-C(24)-C(25)	107.78(16)	H(32A)-C(32)-H(32B)	109.5
C(2)-C(24)-C(25)	110.03(14)	C(14)-C(32)-H(32C)	109.5
C(24)-C(25)-H(25A)	109.5	H(32A)-C(32)-H(32C)	109.5
C(24)-C(25)-H(25B)	109.5	H(32B)-C(32)-H(32C)	109.5
H(25A)-C(25)-H(25B)	109.5	C(16)-C(33)-H(33A)	109.5
C(24)-C(25)-H(25C)	109.5	C(16)-C(33)-H(33B)	109.5
H(25A)-C(25)-H(25C)	109.5	H(33A)-C(33)-H(33B)	109.5
H(25B)-C(25)-H(25C)	109.5	C(16)-C(33)-H(33C)	109.5
C(24)-C(26)-H(26A)	109.5	H(33A)-C(33)-H(33C)	109.5
C(24)-C(26)-H(26B)	109.5	H(33B)-C(33)-H(33C)	109.5
H(26A)-C(26)-H(26B)	109.5	C(17)-O(1)-C(13)	103.71(11)
C(24)-C(26)-H(26C)	109.5	C(22B)-C(20B)-C(21B)	110.9(5)
H(26A)-C(26)-H(26C)	109.5	C(22B)-C(20B)-C(4)	109.2(3)
H(26B)-C(26)-H(26C)	109.5	C(21B)-C(20B)-C(4)	109.7(3)
C(24)-C(27)-H(27A)	109.5	C(22B)-C(20B)-C(19)	109.3(3)
C(24)-C(27)-H(27B)	109.5	C(21B)-C(20B)-C(19)	108.8(3)
H(27A)-C(27)-H(27B)	109.5	C(4)-C(20B)-C(19)	108.9(3)
C(24)-C(27)-H(27C)	109.5	C(20B)-C(21B)-H(21D)	109.5
H(27A)-C(27)-H(27C)	109.5	C(20B)-C(21B)-H(21E)	109.5
H(27B)-C(27)-H(27C)	109.5	H(21D)-C(21B)-H(21E)	109.5
C(31)-C(28)-C(9)	112.71(13)	C(20B)-C(21B)-H(21F)	109.5
C(31)-C(28)-C(30)	108.58(14)	H(21D)-C(21B)-H(21F)	109.5
C(9)-C(28)-C(30)	108.68(13)	H(21E)-C(21B)-H(21F)	109.5
C(31)-C(28)-C(29)	108.12(14)	C(11)-C(22B)-C(20B)	108.7(4)
C(9)-C(28)-C(29)	109.38(14)	C(11)-C(22B)-C(7)	112.0(3)
C(30)-C(28)-C(29)	109.32(14)	C(20B)-C(22B)-C(7)	107.0(4)
C(28)-C(29)-H(29A)	109.5	C(11)-C(22B)-C(23B)	109.0(3)
C(28)-C(29)-H(29B)	109.5	C(20B)-C(22B)-C(23B)	111.1(5)
H(29A)-C(29)-H(29B)	109.5	C(7)-C(22B)-C(23B)	109.0(3)
C(28)-C(29)-H(29C)	109.5	C(22B)-C(23B)-H(23D)	109.5
H(29A)-C(29)-H(29C)	109.5	C(22B)-C(23B)-H(23E)	109.5
H(29B)-C(29)-H(29C)	109.5	H(23D)-C(23B)-H(23E)	109.5
C(28)-C(30)-H(30A)	109.5	C(22B)-C(23B)-H(23F)	109.5

H(23D)-C(23B)-H(23F)	109.5	H(23E)-C(23B)-H(23F)	109.5

Symmetry transformations used to generate equivalent atoms:

Table 4. Anisotropic displacement parameters (A^2 x 10^3) for **99.**

The anisotropic displacement factor exponent takes the form:
-2 pi^2 [h^2 a*^2 U11 + ... + 2 h k a* b* U12]

	U11	U22	U33	U23	U13	U12
C(1)	28(1)	22(1)	21(1)	2(1)	-1(1)	-1(1)
C(2)	25(1)	24(1)	25(1)	-6(1)	3(1)	-4(1)
C(3)	20(1)	18(1)	32(1)	-7(1)	-2(1)	1(1)
C(4)	21(1)	20(1)	26(1)	-3(1)	-6(1)	2(1)
C(5)	23(1)	16(1)	29(1)	-2(1)	-9(1)	4(1)
C(6)	28(1)	16(1)	28(1)	3(1)	-11(1)	1(1)
C(7)	26(1)	18(1)	23(1)	3(1)	-6(1)	1(1)
C(8)	31(1)	18(1)	19(1)	5(1)	-7(1)	-1(1)
C(9)	24(1)	23(1)	20(1)	2(1)	-4(1)	-4(1)
C(10)	21(1)	19(1)	22(1)	0(1)	-1(1)	1(1)
C(11)	20(1)	18(1)	20(1)	1(1)	-2(1)	3(1)
C(12)	16(1)	17(1)	21(1)	-1(1)	-2(1)	-2(1)
C(13)	21(1)	21(1)	21(1)	4(1)	-1(1)	4(1)
C(14)	28(1)	16(1)	24(1)	1(1)	1(1)	4(1)
C(15)	28(1)	11(1)	24(1)	3(1)	-2(1)	1(1)
C(16)	25(1)	19(1)	24(1)	5(1)	0(1)	1(1)
C(17)	21(1)	22(1)	19(1)	2(1)	-3(1)	2(1)
C(18)	17(1)	18(1)	19(1)	1(1)	-3(1)	-2(1)
C(19)	24(1)	19(1)	20(1)	0(1)	-2(1)	0(1)
C(20)	14(2)	13(1)	23(2)	-1(1)	-4(1)	-1(1)
C(21)	16(1)	17(1)	25(2)	0(1)	-4(1)	0(1)
C(22)	20(2)	13(1)	17(2)	-1(1)	-7(1)	-2(1)
C(23)	19(2)	19(1)	21(2)	2(1)	-3(1)	-2(1)
C(24)	35(1)	29(1)	30(1)	-6(1)	10(1)	-1(1)
C(25)	70(2)	39(1)	33(1)	-13(1)	15(1)	-7(1)
C(26)	41(1)	69(2)	58(1)	-14(1)	21(1)	-9(1)
C(27)	75(2)	49(1)	29(1)	1(1)	19(1)	12(1)
C(28)	32(1)	27(1)	20(1)	5(1)	1(1)	-2(1)
C(29)	48(1)	40(1)	20(1)	0(1)	-2(1)	1(1)
C(30)	42(1)	43(1)	33(1)	6(1)	6(1)	-12(1)
C(31)	48(1)	43(1)	26(1)	6(1)	10(1)	10(1)
C(32)	41(1)	23(1)	26(1)	-4(1)	3(1)	-3(1)
C(33)	29(1)	30(1)	26(1)	0(1)	3(1)	-5(1)
O(1)	21(1)	26(1)	21(1)	5(1)	-3(1)	5(1)
O(2)	30(1)	29(1)	31(1)	-2(1)	-4(1)	-4(1)
C(20B)	19(2)	14(2)	25(2)	-4(2)	-6(2)	3(2)

C(21B)	24(2)	19(2)	24(3)	-3(2)	-2(2)	-2(2)
C(22B)	28(3)	19(2)	13(2)	-5(2)	-4(2)	2(2)
C(23B)	24(2)	22(2)	26(3)	-7(2)	-5(2)	-3(2)

Figure S9. ORTEP3 Plot showing labeling for tropone **17.**

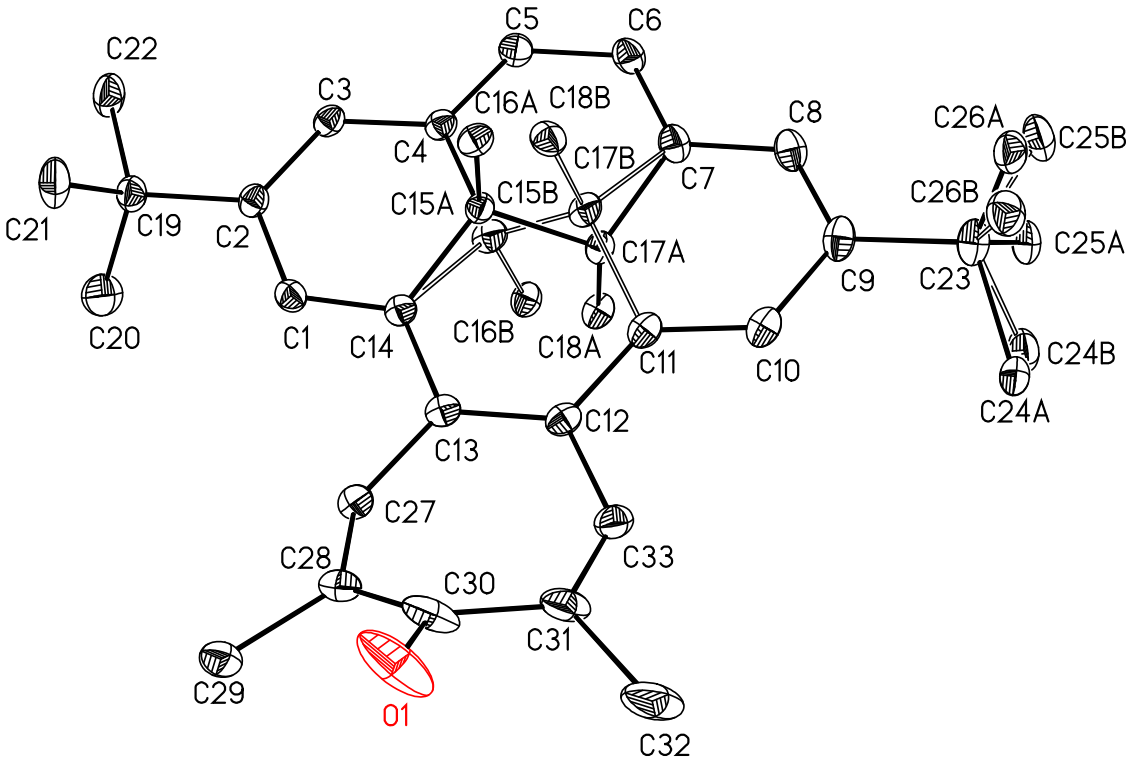


Table 2. Atomic coordinates (x 10^4) and equivalent isotropic displacement parameters ($Å^2$x 10^3)

for **17**. U(eq) is defined as one third of the trace of the orthogonalized U^{ij} tensor.

	x	y	z	U(eq)
O(1)	10517(2)	1200(1)	5051(1)	75(1)
C(1)	2535(2)	1800(1)	2568(1)	26(1)
C(2)	1203(2)	2035(1)	1887(1)	25(1)
C(3)	764(2)	1977(1)	608(1)	25(1)
C(4)	1623(2)	1700(1)	-54(1)	24(1)
C(5)	1125(2)	1629(1)	-1313(1)	28(1)
C(6)	2006(2)	1347(1)	-1952(1)	30(1)
C(7)	3289(2)	1114(1)	-1318(1)	30(1)
C(8)	4253(2)	840(1)	-1937(2)	32(1)
C(9)	5660(2)	624(1)	-1315(2)	31(1)
C(10)	6179(2)	686(1)	0(1)	28(1)
C(11)	5281(2)	939(1)	725(1)	26(1)
C(12)	5822(2)	1010(1)	2052(1)	24(1)
C(13)	4884(2)	1288(1)	2697(1)	24(1)
C(14)	3497(2)	1523(1)	2022(1)	22(1)
C(19)	353(2)	2346(1)	2606(1)	30(1)
C(20)	-828(3)	2227(1)	3775(2)	52(1)
C(21)	2239(3)	2571(1)	3020(2)	44(1)
C(22)	-1110(3)	2569(1)	1772(2)	41(1)
C(23)	6764(2)	336(1)	-2035(2)	34(1)
C(27)	5255(2)	1359(1)	4048(1)	27(1)
C(28)	6940(2)	1314(1)	4836(1)	29(1)
C(29)	7007(3)	1477(1)	6144(1)	36(1)
C(30)	8845(2)	1129(1)	4509(1)	41(1)
C(31)	8683(2)	824(1)	3677(1)	40(1)
C(32)	10321(3)	551(1)	3970(2)	73(1)
C(33)	7332(2)	781(1)	2678(1)	32(1)
C(15A)	3455(4)	1501(1)	575(2)	22(1)

C(16A)	5492(3)	1682(1)	130(2)	26(1)
C(17A)	3395(4)	1125(1)	146(2)	23(1)
C(18A)	1407(3)	940(1)	634(2)	28(1)
C(15B)	2585(17)	1401(2)	721(9)	28(2)
C(16B)	838(11)	1134(2)	988(7)	28(2)
C(17B)	4320(15)	1260(2)	-36(7)	25(2)
C(18B)	6088(13)	1527(2)	-291(8)	27(2)
C(24A)	7981(7)	74(1)	-1005(4)	33(1)
C(25A)	5038(6)	99(1)	-2605(4)	36(1)
C(26A)	8180(8)	476(1)	-2861(5)	38(1)
C(24B)	6539(6)	5(1)	-1441(3)	43(1)
C(25B)	5931(4)	304(1)	-3505(2)	41(1)
C(26B)	9127(5)	438(1)	-2191(3)	36(1)

Table 3. Bond lengths [Å] for **17**.

atom-atom	distance	atom-atom	distance
O(1)-C(30)	1.227(2)	C(14)-C(15A)	1.517(2)
C(1)-C(14)	1.3729(19)	C(14)-C(15B)	1.540(8)
C(1)-C(2)	1.4254(19)	C(19)-C(20)	1.528(2)
C(1)-H(1A)	0.9500	C(19)-C(22)	1.529(2)
C(2)-C(3)	1.3780(19)	C(19)-C(21)	1.541(2)
C(2)-C(19)	1.5301(19)	C(20)-H(20A)	0.9800
C(3)-C(4)	1.4022(19)	C(20)-H(20B)	0.9800
C(3)-H(3A)	0.9500	C(20)-H(20C)	0.9800
C(4)-C(5)	1.3735(19)	C(21)-H(21A)	0.9800
C(4)-C(15B)	1.533(9)	C(21)-H(21B)	0.9800
C(4)-C(15A)	1.535(2)	C(21)-H(21C)	0.9800
C(5)-C(6)	1.409(2)	C(22)-H(22A)	0.9800
C(5)-H(5A)	0.9500	C(22)-H(22B)	0.9800
C(6)-C(7)	1.378(2)	C(22)-H(22C)	0.9800
C(6)-H(6A)	0.9500	C(23)-C(26A)	1.382(4)
C(7)-C(8)	1.398(2)	C(23)-C(24B)	1.437(3)
C(7)-C(17A)	1.532(2)	C(23)-C(25A)	1.543(4)
C(7)-C(17B)	1.582(7)	C(23)-C(26B)	1.577(3)
C(8)-C(9)	1.379(2)	C(23)-C(25B)	1.617(3)
C(8)-H(8A)	0.9500	C(23)-C(24A)	1.658(4)
C(9)-C(10)	1.425(2)	C(27)-C(28)	1.349(2)
C(9)-C(23)	1.535(2)	C(27)-H(27A)	0.9500
C(10)-C(11)	1.377(2)	C(28)-C(30)	1.466(2)
C(10)-H(10A)	0.9500	C(28)-C(29)	1.506(2)
C(11)-C(12)	1.447(2)	C(29)-H(29A)	0.9800
C(11)-C(17A)	1.517(2)	C(29)-H(29B)	0.9800
C(11)-C(17B)	1.594(8)	C(29)-H(29C)	0.9800
C(12)-C(13)	1.4139(19)	C(30)-C(31)	1.472(3)
C(12)-C(33)	1.4560(19)	C(31)-C(33)	1.347(2)
C(13)-C(14)	1.4426(18)	C(31)-C(32)	1.513(2)
C(13)-C(27)	1.4530(19)	C(32)-H(32A)	0.9800

C(32)-H(32B)	0.9800	C(18B)-H(18F)	0.9800
C(32)-H(32C)	0.9800	C(24A)-H(24A)	0.9800
C(33)-H(33A)	0.9500	C(24A)-H(24B)	0.9800
C(15A)-C(17A)	1.529(4)	C(24A)-H(24C)	0.9800
C(15A)-C(16A)	1.564(4)	C(25A)-H(25A)	0.9800
C(16A)-H(16A)	0.9800	C(25A)-H(25B)	0.9800
C(16A)-H(16B)	0.9800	C(25A)-H(25C)	0.9800
C(16A)-H(16C)	0.9800	C(26A)-H(26A)	0.9800
C(17A)-C(18A)	1.560(3)	C(26A)-H(26B)	0.9800
C(18A)-H(18A)	0.9800	C(26A)-H(26C)	0.9800
C(18A)-H(18B)	0.9800	C(24B)-H(24D)	0.9800
C(18A)-H(18C)	0.9800	C(24B)-H(24E)	0.9800
C(15B)-C(17B)	1.487(15)	C(24B)-H(24F)	0.9800
C(15B)-C(16B)	1.556(14)	C(25B)-H(25D)	0.9800
C(16B)-H(16D)	0.9800	C(25B)-H(25E)	0.9800
C(16B)-H(16E)	0.9800	C(25B)-H(25F)	0.9800
C(16B)-H(16F)	0.9800	C(26B)-H(26D)	0.9800
C(17B)-C(18B)	1.562(13)	C(26B)-H(26E)	0.9800
C(18B)-H(18D)	0.9800	C(26B)-H(26F)	0.9800
C(18B)-H(18E)	0.9800		

Table 3. Angles [deg] for **17**.

C(14)-C(1)-C(2)	124.29(13)	C(9)-C(10)-H(10A)	117.9
C(14)-C(1)-H(1A)	117.9	C(10)-C(11)-C(12)	125.03(13)
C(2)-C(1)-H(1A)	117.9	C(10)-C(11)-C(17A)	117.31(13)
C(3)-C(2)-C(1)	118.83(12)	C(12)-C(11)-C(17A)	117.15(13)
C(3)-C(2)-C(19)	122.78(12)	C(10)-C(11)-C(17B)	116.3(3)
C(1)-C(2)-C(19)	118.39(12)	C(12)-C(11)-C(17B)	114.0(3)
C(2)-C(3)-C(4)	122.28(12)	C(13)-C(12)-C(11)	120.74(12)
C(2)-C(3)-H(3A)	118.9	C(13)-C(12)-C(33)	122.49(13)
C(4)-C(3)-H(3A)	118.9	C(11)-C(12)-C(33)	116.76(12)
C(5)-C(4)-C(3)	123.00(13)	C(12)-C(13)-C(14)	120.78(12)
C(5)-C(4)-C(15B)	115.7(3)	C(12)-C(13)-C(27)	123.43(12)
C(3)-C(4)-C(15B)	118.5(4)	C(14)-C(13)-C(27)	115.78(12)
C(5)-C(4)-C(15A)	117.56(14)	C(1)-C(14)-C(13)	124.71(12)
C(3)-C(4)-C(15A)	118.68(13)	C(1)-C(14)-C(15A)	117.65(13)
C(4)-C(5)-C(6)	121.74(13)	C(13)-C(14)-C(15A)	116.48(13)
C(4)-C(5)-H(5A)	119.1	C(1)-C(14)-C(15B)	116.5(3)
C(6)-C(5)-H(5A)	119.1	C(13)-C(14)-C(15B)	116.7(3)
C(7)-C(6)-C(5)	121.46(13)	C(20)-C(19)-C(22)	108.57(13)
C(7)-C(6)-H(6A)	119.3	C(20)-C(19)-C(2)	110.36(13)
C(5)-C(6)-H(6A)	119.3	C(22)-C(19)-C(2)	112.73(12)
C(6)-C(7)-C(8)	122.69(13)	C(20)-C(19)-C(21)	110.38(14)
C(6)-C(7)-C(17A)	118.15(13)	C(22)-C(19)-C(21)	107.48(13)
C(8)-C(7)-C(17A)	118.51(14)	C(2)-C(19)-C(21)	107.28(12)
C(6)-C(7)-C(17B)	113.6(3)	C(19)-C(20)-H(20A)	109.5
C(8)-C(7)-C(17B)	119.2(3)	C(19)-C(20)-H(20B)	109.5
C(9)-C(8)-C(7)	122.27(14)	H(20A)-C(20)-H(20B)	109.5
C(9)-C(8)-H(8A)	118.9	C(19)-C(20)-H(20C)	109.5
C(7)-C(8)-H(8A)	118.9	H(20A)-C(20)-H(20C)	109.5
C(8)-C(9)-C(10)	118.90(13)	H(20B)-C(20)-H(20C)	109.5
C(8)-C(9)-C(23)	121.03(14)	C(19)-C(21)-H(21A)	109.5
C(10)-C(9)-C(23)	119.95(13)	C(19)-C(21)-H(21B)	109.5
C(11)-C(10)-C(9)	124.28(13)	H(21A)-C(21)-H(21B)	109.5
C(11)-C(10)-H(10A)	117.9	C(19)-C(21)-H(21C)	109.5

H(21A)-C(21)-H(21C)	109.5	C(28)-C(29)-H(29C)	109.5
H(21B)-C(21)-H(21C)	109.5	H(29A)-C(29)-H(29C)	109.5
C(19)-C(22)-H(22A)	109.5	H(29B)-C(29)-H(29C)	109.5
C(19)-C(22)-H(22B)	109.5	O(1)-C(30)-C(28)	120.14(16)
H(22A)-C(22)-H(22B)	109.5	O(1)-C(30)-C(31)	119.92(16)
C(19)-C(22)-H(22C)	109.5	C(28)-C(30)-C(31)	119.28(14)
H(22A)-C(22)-H(22C)	109.5	C(33)-C(31)-C(30)	126.21(14)
H(22B)-C(22)-H(22C)	109.5	C(33)-C(31)-C(32)	119.77(17)
C(26A)-C(23)-C(24B)	134.3(2)	C(30)-C(31)-C(32)	113.90(15)
C(26A)-C(23)-C(9)	109.9(2)	C(31)-C(32)-H(32A)	109.5
C(24B)-C(23)-C(9)	112.76(16)	C(31)-C(32)-H(32B)	109.5
C(26A)-C(23)-C(25A)	117.9(3)	H(32A)-C(32)-H(32B)	109.5
C(24B)-C(23)-C(25A)	63.5(2)	C(31)-C(32)-H(32C)	109.5
C(9)-C(23)-C(25A)	106.84(17)	H(32A)-C(32)-H(32C)	109.5
C(24B)-C(23)-C(26B)	112.3(2)	H(32B)-C(32)-H(32C)	109.5
C(9)-C(23)-C(26B)	108.90(15)	C(31)-C(33)-C(12)	132.49(15)
C(25A)-C(23)-C(26B)	142.0(2)	C(31)-C(33)-H(33A)	113.8
C(26A)-C(23)-C(25B)	68.9(3)	C(12)-C(33)-H(33A)	113.8
C(24B)-C(23)-C(25B)	108.0(2)	C(14)-C(15A)-C(17A)	110.18(19)
C(9)-C(23)-C(25B)	112.27(15)	C(14)-C(15A)-C(4)	113.01(15)
C(25A)-C(23)-C(25B)	51.38(19)	C(17A)-C(15A)-C(4)	110.02(19)
C(26B)-C(23)-C(25B)	102.17(18)	C(14)-C(15A)-C(16A)	106.44(17)
C(26A)-C(23)-C(24A)	110.1(3)	C(17A)-C(15A)-C(16A)	110.8(2)
C(9)-C(23)-C(24A)	110.00(17)	C(4)-C(15A)-C(16A)	106.31(16)
C(25A)-C(23)-C(24A)	101.7(2)	C(11)-C(17A)-C(15A)	108.96(19)
C(26B)-C(23)-C(24A)	77.8(2)	C(11)-C(17A)-C(7)	113.41(14)
C(25B)-C(23)-C(24A)	134.97(19)	C(15A)-C(17A)-C(7)	108.59(18)
C(28)-C(27)-C(13)	132.37(14)	C(11)-C(17A)-C(18A)	107.38(16)
C(28)-C(27)-H(27A)	113.8	C(15A)-C(17A)-C(18A)	110.9(2)
C(13)-C(27)-H(27A)	113.8	C(7)-C(17A)-C(18A)	107.63(16)
C(27)-C(28)-C(30)	125.21(14)	C(17B)-C(15B)-C(4)	106.9(8)
C(27)-C(28)-C(29)	120.09(14)	C(17B)-C(15B)-C(14)	108.3(7)
C(30)-C(28)-C(29)	114.62(13)	C(4)-C(15B)-C(14)	111.8(6)
C(28)-C(29)-H(29A)	109.5	C(17B)-C(15B)-C(16B)	113.8(9)
C(28)-C(29)-H(29B)	109.5	C(4)-C(15B)-C(16B)	108.6(6)
H(29A)-C(29)-H(29B)	109.5	C(14)-C(15B)-C(16B)	107.5(7)

C(15B)-C(16B)-H(16D)	109.5
C(15B)-C(16B)-H(16E)	109.5
H(16D)-C(16B)-H(16E)	109.5
C(15B)-C(16B)-H(16F)	109.5
H(16D)-C(16B)-H(16F)	109.5
H(16E)-C(16B)-H(16F)	109.5
C(15B)-C(17B)-C(18B)	113.8(9)
C(15B)-C(17B)-C(7)	106.5(7)
C(18B)-C(17B)-C(7)	112.3(6)
C(15B)-C(17B)-C(11)	107.7(7)
C(18B)-C(17B)-C(11)	109.5(5)
C(7)-C(17B)-C(11)	106.7(5)
C(17B)-C(18B)-H(18D)	109.5
C(17B)-C(18B)-H(18E)	109.5
H(18D)-C(18B)-H(18E)	109.5
C(17B)-C(18B)-H(18F)	109.5
H(18D)-C(18B)-H(18F)	109.5
H(18E)-C(18B)-H(18F)	109.5
C(23)-C(24A)-H(24A)	109.5
C(23)-C(24A)-H(24B)	109.5
C(23)-C(24A)-H(24C)	109.5
C(23)-C(25A)-H(25A)	109.5
C(23)-C(25A)-H(25B)	109.5
C(23)-C(25A)-H(25C)	109.5
C(23)-C(26A)-H(26A)	109.5
C(23)-C(26A)-H(26B)	109.5
C(23)-C(26A)-H(26C)	109.5
C(23)-C(24B)-H(24D)	109.5
C(23)-C(24B)-H(24E)	109.5
H(24D)-C(24B)-H(24E)	109.5
C(23)-C(24B)-H(24F)	109.5
H(24D)-C(24B)-H(24F)	109.5
H(24E)-C(24B)-H(24F)	109.5
C(23)-C(25B)-H(25D)	109.5
C(23)-C(25B)-H(25E)	109.5
H(25D)-C(25B)-H(25E)	109.5
C(23)-C(25B)-H(25F)	109.5
H(25D)-C(25B)-H(25F)	109.5
H(25E)-C(25B)-H(25F)	109.5
C(23)-C(26B)-H(26D)	109.5
C(23)-C(26B)-H(26E)	109.5
H(26D)-C(26B)-H(26E)	109.5
C(23)-C(26B)-H(26F)	109.5
H(26D)-C(26B)-H(26F)	109.5
H(26E)-C(26B)-H(26F)	109.5

Table 4. Anisotropic displacement parameters ($Å^2 x\ 10^3$)for **17**. The anisotropic displacement factor exponent takes the form: $-2\ ^2[\ h^2 a^{*2} U^{11} + ... + 2\ h\ k\ a^*\ b^*\ U^{12}\ ]$

	U^{11}	U^{22}	U^{33}	U^{23}	U^{13}	U^{12}
O(1)	27(1)	165(2)	31(1)	-15(1)	-6(1)	10(1)
C(1)	28(1)	27(1)	22(1)	-2(1)	-2(1)	1(1)
C(2)	24(1)	22(1)	29(1)	-2(1)	-2(1)	-1(1)
C(3)	24(1)	21(1)	29(1)	1(1)	-4(1)	0(1)
C(4)	24(1)	22(1)	26(1)	1(1)	-3(1)	-2(1)
C(5)	28(1)	30(1)	27(1)	0(1)	-5(1)	3(1)
C(6)	30(1)	35(1)	25(1)	-5(1)	-3(1)	0(1)
C(7)	28(1)	33(1)	28(1)	-7(1)	-1(1)	1(1)
C(8)	29(1)	34(1)	33(1)	-10(1)	2(1)	-3(1)
C(9)	23(1)	26(1)	43(1)	-10(1)	4(1)	-4(1)
C(10)	21(1)	22(1)	40(1)	-2(1)	0(1)	-2(1)
C(11)	22(1)	22(1)	33(1)	1(1)	1(1)	-1(1)
C(12)	21(1)	23(1)	30(1)	4(1)	2(1)	-2(1)
C(13)	20(1)	24(1)	27(1)	3(1)	-1(1)	-3(1)
C(14)	21(1)	22(1)	24(1)	1(1)	0(1)	-3(1)
C(19)	34(1)	27(1)	30(1)	-5(1)	-3(1)	7(1)
C(20)	62(1)	48(1)	48(1)	1(1)	20(1)	22(1)
C(21)	48(1)	35(1)	49(1)	-19(1)	-12(1)	8(1)
C(22)	45(1)	33(1)	45(1)	-10(1)	-9(1)	13(1)
C(23)	31(1)	30(1)	42(1)	-12(1)	1(1)	1(1)
C(27)	27(1)	25(1)	29(1)	1(1)	-1(1)	0(1)
C(28)	30(1)	33(1)	25(1)	7(1)	-1(1)	-3(1)
C(29)	40(1)	37(1)	29(1)	3(1)	-8(1)	1(1)
C(30)	27(1)	76(1)	19(1)	10(1)	0(1)	6(1)
C(31)	35(1)	63(1)	23(1)	13(1)	8(1)	22(1)
C(32)	74(1)	116(2)	30(1)	20(1)	10(1)	67(1)
C(33)	35(1)	31(1)	30(1)	8(1)	9(1)	9(1)
C(15A)	24(1)	19(1)	24(1)	-1(1)	-2(1)	0(1)

C(16A)	26(1)	22(1)	30(1)	2(1)	0(1)	-3(1)
C(17A)	23(1)	21(1)	26(1)	-3(1)	-1(1)	0(1)
C(18A)	22(1)	24(1)	37(1)	-1(1)	2(1)	-2(1)
C(15B)	30(5)	22(5)	31(4)	1(3)	-9(4)	-9(4)
C(16B)	24(4)	25(5)	34(4)	-2(3)	3(3)	1(3)
C(17B)	28(4)	18(4)	29(4)	-2(3)	-8(3)	-7(4)
C(18B)	28(4)	28(5)	25(4)	0(3)	5(3)	-6(3)
C(24A)	44(3)	26(2)	30(2)	-6(2)	2(2)	10(2)
C(25A)	44(2)	28(2)	37(2)	-13(2)	3(2)	2(2)
C(26A)	44(3)	29(2)	42(3)	-1(2)	20(2)	7(2)
C(24B)	66(2)	26(1)	37(2)	-7(1)	20(2)	-2(1)
C(25B)	45(2)	46(2)	32(2)	-15(1)	4(1)	7(1)
C(26B)	31(2)	39(2)	39(2)	-3(1)	8(1)	4(1)

Figure S10. ORTEP3 Plot showing labeling for **108**

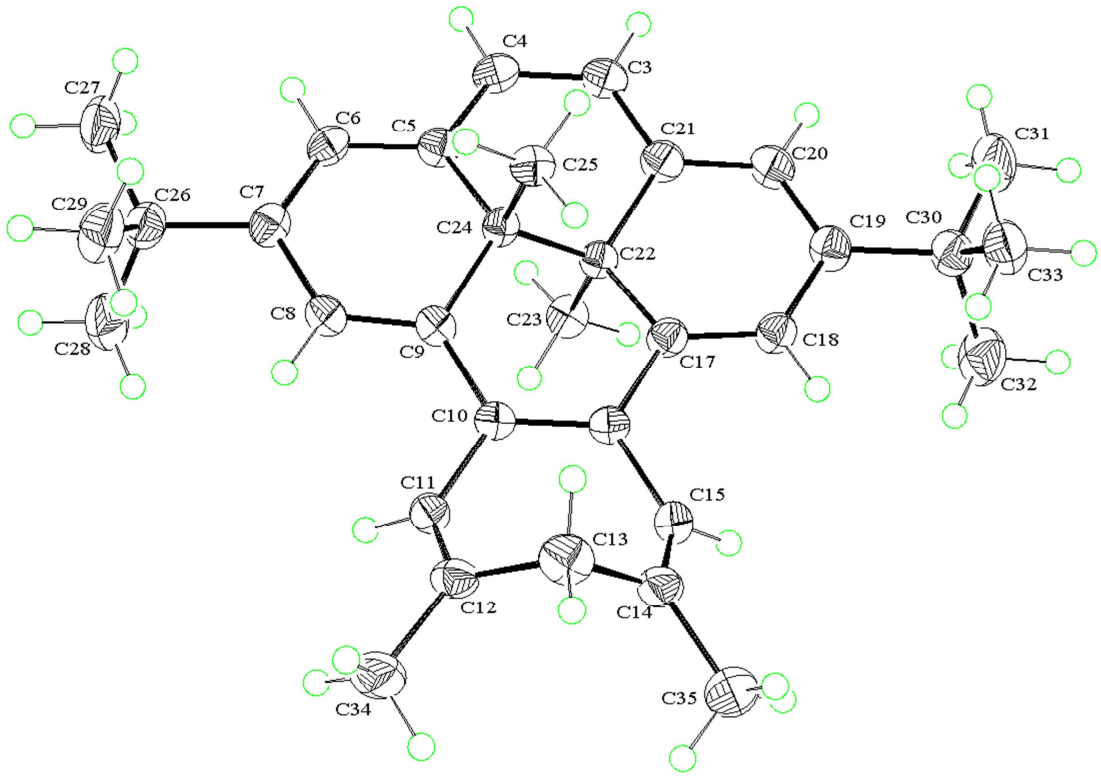


Table 2. Atomic coordinates (x 10^4) and equivalent isotropic displacement parameters (A^2 x 10^3) for **108**.
U(eq) is defined as one third of the trace of the orthogonalized Uij tensor.

	x	y	z	U(eq)	occ
C(3)	5507(1)	1053(1)	9245(2)	31(1)	
C(4)	5476(1)	1952(1)	9280(2)	30(1)	
C(5)	6146(1)	2454(1)	9083(1)	26(1)	
C(6)	6143(1)	3350(1)	9115(2)	28(1)	
C(7)	6843(1)	3838(1)	8963(2)	28(1)	
C(8)	7614(1)	3409(1)	8785(1)	26(1)	
C(9)	7695(1)	2541(1)	8737(1)	24(1)	
C(10)	8481(1)	2109(1)	8584(1)	23(1)	
C(11)	9238(1)	2649(1)	8487(2)	26(1)	
C(12)	9702(1)	2524(1)	7720(2)	29(1)	
C(13)	9483(1)	1751(1)	6898(2)	36(1)	
C(14)	9770(1)	967(1)	7687(2)	32(1)	
C(15)	9312(1)	749(1)	8426(2)	28(1)	
C(16)	8512(1)	1212(1)	8551(1)	23(1)	
C(17)	7780(1)	698(1)	8721(2)	26(1)	
C(18)	7732(1)	-169(1)	8609(2)	27(1)	
C(19)	7001(1)	-680(1)	8765(2)	30(1)	
C(20)	6286(1)	-273(1)	8999(2)	33(1)	
C(21)	6244(1)	623(1)	9096(2)	31(1)	
C(22)	7123(2)	1162(2)	9251(3)	25(1)	0.753(5)
C(23)	7663(2)	1302(2)	10652(2)	29(1)	0.753(5)
C(24)	6834(2)	2010(2)	8588(3)	23(1)	0.753(5)
C(25)	6307(2)	1870(2)	7185(2)	28(1)	0.753(5)
C(26)	6857(1)	4819(1)	9026(2)	34(1)	
C(27)	5981(2)	5179(1)	9203(2)	49(1)	
C(28)	7715(2)	5116(1)	10100(2)	48(1)	
C(29)	6904(2)	5177(1)	7820(2)	46(1)	
C(30)	7032(1)	-1652(1)	8608(2)	33(1)	
C(31)	6230(2)	-2108(1)	8851(2)	50(1)	
C(32)	7960(2)	-2004(1)	9501(2)	49(1)	
C(33)	6952(1)	-1844(1)	7287(2)	41(1)	
C(34)	10446(1)	3125(1)	7646(2)	43(1)	
C(35)	10596(1)	467(1)	7637(2)	52(1)	
C(23B)	6311(5)	1332(6)	7102(6)	24(2)	0.247(5)
C(22B)	6842(5)	1153(5)	8496(9)	24(2)	0.247(5)
C(25B)	7608(5)	1785(6)	10659(6)	25(2)	0.247(5)
C(24B)	7068(6)	1956(5)	9257(9)	23(2)	0.247(5)

Table 3. Bond lengths [A] for **108.**

atom-atom	distance	atom-atom	distance
C(34)-C(12)	1.500(2)	C(13)-H(13B)	0.9900
C(34)-H(34A)	0.9800	C(14)-C(15)	1.332(2)
C(34)-H(34B)	0.9800	C(15)-C(16)	1.471(2)
C(34)-H(34C)	0.9800	C(15)-H(15)	0.9500
C(35)-C(14)	1.502(2)	C(16)-C(17)	1.445(2)
C(35)-H(35A)	0.9800	C(17)-C(18)	1.357(2)
C(35)-H(35B)	0.9800	C(17)-C(22)	1.535(3)
C(35)-H(35C)	0.9800	C(18)-C(19)	1.436(2)
C(23B)-C(22B)	1.563(12)	C(18)-H(18)	0.9500
C(23B)-H(23A)	0.9800	C(19)-C(20)	1.372(2)
C(23B)-H(23B)	0.9800	C(19)-C(30)	1.529(2)
C(23B)-H(23C)	0.9800	C(20)-C(21)	1.406(2)
C(22B)-C(24B)	1.502(13)	C(20)-H(20)	0.9500
C(22B)-C(17)	1.538(7)	C(21)-C(22)	1.541(3)
C(22B)-C(21)	1.568(7)	C(22)-C(24)	1.516(4)
C(25B)-C(24B)	1.571(13)	C(22)-C(23)	1.562(4)
C(25B)-H(25A)	0.9800	C(23)-H(23D)	0.9800
C(25B)-H(25B)	0.9800	C(23)-H(23E)	0.9800
C(25B)-H(25C)	0.9800	C(23)-H(23F)	0.9800
C(24B)-C(5)	1.557(8)	C(24)-C(25)	1.561(4)
C(24B)-C(9)	1.591(8)	C(25)-H(25D)	0.9800
C(3)-C(21)	1.373(2)	C(25)-H(25E)	0.9800
C(3)-C(4)	1.403(2)	C(25)-H(25F)	0.9800
C(3)-H(3)	0.9500	C(26)-C(28)	1.530(3)
C(4)-C(5)	1.372(2)	C(26)-C(27)	1.533(2)
C(4)-H(4)	0.9500	C(26)-C(29)	1.537(3)
C(5)-C(6)	1.398(2)	C(27)-H(27A)	0.9800
C(5)-C(24)	1.532(3)	C(27)-H(27B)	0.9800
C(6)-C(7)	1.374(2)	C(27)-H(27C)	0.9800
C(6)-H(6)	0.9500	C(28)-H(28A)	0.9800
C(7)-C(8)	1.433(2)	C(28)-H(28B)	0.9800
C(7)-C(26)	1.530(2)	C(28)-H(28C)	0.9800
C(8)-C(9)	1.361(2)	C(29)-H(29A)	0.9800
C(8)-H(8)	0.9500	C(29)-H(29B)	0.9800
C(9)-C(10)	1.443(2)	C(29)-H(29C)	0.9800
C(9)-C(24)	1.512(3)	C(30)-C(31)	1.529(2)
C(10)-C(16)	1.401(2)	C(30)-C(33)	1.530(3)
C(10)-C(11)	1.468(2)	C(30)-C(32)	1.534(3)
C(11)-C(12)	1.336(2)	C(31)-H(31A)	0.9800
C(11)-H(11)	0.9500	C(31)-H(31B)	0.9800
C(12)-C(13)	1.501(2)	C(31)-H(31C)	0.9800
C(13)-C(14)	1.499(3)	C(32)-H(32A)	0.9800
C(13)-H(13A)	0.9900	C(32)-H(32B)	0.9800

C(32)-H(32C)	0.9800	C(33)-H(33B)	0.9800
C(33)-H(33A)	0.9800	C(33)-H(33C)	0.9800

Table 3. Bond angles [deg] for **108**.

C(12)-C(34)-H(34A)	109.5	C(5)-C(4)-C(3)	121.98(15)
C(12)-C(34)-H(34B)	109.5	C(5)-C(4)-H(4)	119.0
H(34A)-C(34)-H(34B)	109.5	C(3)-C(4)-H(4)	119.0
C(12)-C(34)-H(34C)	109.5	C(4)-C(5)-C(6)	123.77(15)
H(34A)-C(34)-H(34C)	109.5	C(4)-C(5)-C(24)	117.32(17)
H(34B)-C(34)-H(34C)	109.5	C(6)-C(5)-C(24)	118.05(16)
C(14)-C(35)-H(35A)	109.5	C(4)-C(5)-C(24B)	112.9(3)
C(14)-C(35)-H(35B)	109.5	C(6)-C(5)-C(24B)	120.4(3)
H(35A)-C(35)-H(35B)	109.5	C(24)-C(5)-C(24B)	27.6(3)
C(14)-C(35)-H(35C)	109.5	C(7)-C(6)-C(5)	122.69(15)
H(35A)-C(35)-H(35C)	109.5	C(7)-C(6)-H(6)	118.7
H(35B)-C(35)-H(35C)	109.5	C(5)-C(6)-H(6)	118.7
C(22B)-C(23B)-H(23A)	109.5	C(6)-C(7)-C(8)	118.53(15)
C(22B)-C(23B)-H(23B)	109.5	C(6)-C(7)-C(26)	123.05(15)
H(23A)-C(23B)-H(23B)	109.5	C(8)-C(7)-C(26)	118.38(15)
C(22B)-C(23B)-H(23C)	109.5	C(9)-C(8)-C(7)	124.17(15)
H(23A)-C(23B)-H(23C)	109.5	C(9)-C(8)-H(8)	117.9
H(23B)-C(23B)-H(23C)	109.5	C(7)-C(8)-H(8)	117.9
C(24B)-C(22B)-C(17)	106.2(7)	C(8)-C(9)-C(10)	124.14(15)
C(24B)-C(22B)-C(23B)	113.0(8)	C(8)-C(9)-C(24)	117.43(16)
C(17)-C(22B)-C(23B)	111.7(5)	C(10)-C(9)-C(24)	117.33(15)
C(24B)-C(22B)-C(21)	102.9(6)	C(8)-C(9)-C(24B)	118.6(3)
C(17)-C(22B)-C(21)	109.8(5)	C(10)-C(9)-C(24B)	114.8(3)
C(23B)-C(22B)-C(21)	112.8(5)	C(24)-C(9)-C(24B)	27.4(3)
C(24B)-C(25B)-H(25A)	109.5	C(16)-C(10)-C(9)	120.51(14)
C(24B)-C(25B)-H(25B)	109.5	C(16)-C(10)-C(11)	122.33(14)
H(25A)-C(25B)-H(25B)	109.5	C(9)-C(10)-C(11)	117.15(14)
C(24B)-C(25B)-H(25C)	109.5	C(12)-C(11)-C(10)	125.98(16)
H(25A)-C(25B)-H(25C)	109.5	C(12)-C(11)-H(11)	117.0
H(25B)-C(25B)-H(25C)	109.5	C(10)-C(11)-H(11)	117.0
C(22B)-C(24B)-C(5)	109.3(7)	C(11)-C(12)-C(34)	122.70(17)
C(22B)-C(24B)-C(25B)	113.5(9)	C(11)-C(12)-C(13)	119.48(15)
C(5)-C(24B)-C(25B)	109.8(5)	C(34)-C(12)-C(13)	117.82(15)
C(22B)-C(24B)-C(9)	107.3(6)	C(14)-C(13)-C(12)	108.22(15)
C(5)-C(24B)-C(9)	107.7(5)	C(14)-C(13)-H(13A)	110.1
C(25B)-C(24B)-C(9)	109.1(6)	C(12)-C(13)-H(13A)	110.1
C(21)-C(3)-C(4)	121.89(16)	C(14)-C(13)-H(13B)	110.1
C(21)-C(3)-H(3)	119.1	C(12)-C(13)-H(13B)	110.1
C(4)-C(3)-H(3)	119.1	H(13A)-C(13)-H(13B)	108.4

C(15)-C(14)-C(13)	119.80(16)	C(28)-C(26)-C(29)	109.49(16)
C(15)-C(14)-C(35)	122.34(18)	C(7)-C(26)-C(29)	108.91(14)
C(13)-C(14)-C(35)	117.82(16)	C(27)-C(26)-C(29)	108.40(16)
C(14)-C(15)-C(16)	125.83(16)	C(26)-C(27)-H(27A)	109.5
C(14)-C(15)-H(15)	117.1	C(26)-C(27)-H(27B)	109.5
C(16)-C(15)-H(15)	117.1	H(27A)-C(27)-H(27B)	109.5
C(10)-C(16)-C(17)	120.95(14)	C(26)-C(27)-H(27C)	109.5
C(10)-C(16)-C(15)	121.97(14)	H(27A)-C(27)-H(27C)	109.5
C(17)-C(16)-C(15)	116.95(15)	H(27B)-C(27)-H(27C)	109.5
C(18)-C(17)-C(16)	123.83(15)	C(26)-C(28)-H(28A)	109.5
C(18)-C(17)-C(22)	119.19(16)	C(26)-C(28)-H(28B)	109.5
C(16)-C(17)-C(22)	116.26(15)	H(28A)-C(28)-H(28B)	109.5
C(18)-C(17)-C(22B)	115.3(3)	C(26)-C(28)-H(28C)	109.5
C(16)-C(17)-C(22B)	116.2(3)	H(28A)-C(28)-H(28C)	109.5
C(22)-C(17)-C(22B)	31.4(3)	H(28B)-C(28)-H(28C)	109.5
C(17)-C(18)-C(19)	123.93(15)	C(26)-C(29)-H(29A)	109.5
C(17)-C(18)-H(18)	118.0	C(26)-C(29)-H(29B)	109.5
C(19)-C(18)-H(18)	118.0	H(29A)-C(29)-H(29B)	109.5
C(20)-C(19)-C(18)	118.65(16)	C(26)-C(29)-H(29C)	109.5
C(20)-C(19)-C(30)	122.87(15)	H(29A)-C(29)-H(29C)	109.5
C(18)-C(19)-C(30)	118.42(15)	H(29B)-C(29)-H(29C)	109.5
C(19)-C(20)-C(21)	122.60(16)	C(31)-C(30)-C(19)	112.20(15)
C(19)-C(20)-H(20)	118.7	C(31)-C(30)-C(33)	108.16(16)
C(21)-C(20)-H(20)	118.7	C(19)-C(30)-C(33)	108.60(14)
C(3)-C(21)-C(20)	123.94(16)	C(31)-C(30)-C(32)	108.60(16)
C(3)-C(21)-C(22)	116.13(16)	C(19)-C(30)-C(32)	109.52(15)
C(20)-C(21)-C(22)	119.22(16)	C(33)-C(30)-C(32)	109.74(16)
C(3)-C(21)-C(22B)	115.7(3)	C(30)-C(31)-H(31A)	109.5
C(20)-C(21)-C(22B)	115.8(3)	C(30)-C(31)-H(31B)	109.5
C(22)-C(21)-C(22B)	31.0(3)	H(31A)-C(31)-H(31B)	109.5
C(24)-C(22)-C(17)	108.7(2)	C(30)-C(31)-H(31C)	109.5
C(24)-C(22)-C(21)	109.3(2)	H(31A)-C(31)-H(31C)	109.5
C(17)-C(22)-C(21)	111.36(19)	H(31B)-C(31)-H(31C)	109.5
C(24)-C(22)-C(23)	111.2(3)	C(30)-C(32)-H(32A)	109.5
C(17)-C(22)-C(23)	107.92(19)	C(30)-C(32)-H(32B)	109.5
C(21)-C(22)-C(23)	108.34(19)	H(32A)-C(32)-H(32B)	109.5
C(9)-C(24)-C(22)	109.5(2)	C(30)-C(32)-H(32C)	109.5
C(9)-C(24)-C(5)	113.29(19)	H(32A)-C(32)-H(32C)	109.5
C(22)-C(24)-C(5)	108.5(2)	H(32B)-C(32)-H(32C)	109.5
C(9)-C(24)-C(25)	107.6(2)	C(30)-C(33)-H(33A)	109.5
C(22)-C(24)-C(25)	111.2(3)	C(30)-C(33)-H(33B)	109.5
C(5)-C(24)-C(25)	106.78(19)	H(33A)-C(33)-H(33B)	109.5
C(28)-C(26)-C(7)	109.57(15)	C(30)-C(33)-H(33C)	109.5
C(28)-C(26)-C(27)	108.41(16)	H(33A)-C(33)-H(33C)	109.5
C(7)-C(26)-C(27)	112.02(15)	H(33B)-C(33)-H(33C)	109.5

Symmetry transformations used to generate equivalent atoms:

Table 4. Anisotropic displacement parameters (A^2 x 10^3) for p21c.
The anisotropic displacement factor exponent takes the form:
-2 pi^2 [h^2 a*^2 U11 + ... + 2 h k a* b* U12]

	U11	U22	U33	U23	U13	U12
C(34)	34(1)	48(1)	56(1)	10(1)	26(1)	-3(1)
C(35)	42(1)	48(1)	80(2)	-13(1)	39(1)	0(1)
C(22B)	22(4)	33(4)	21(5)	3(3)	14(4)	-3(3)
C(24B)	26(4)	33(4)	16(4)	0(4)	15(4)	-2(3)
C(3)	28(1)	38(1)	33(1)	2(1)	19(1)	-4(1)
C(4)	26(1)	39(1)	30(1)	1(1)	17(1)	3(1)
C(5)	26(1)	31(1)	27(1)	-1(1)	14(1)	2(1)
C(6)	27(1)	32(1)	29(1)	-2(1)	16(1)	6(1)
C(7)	31(1)	28(1)	27(1)	-3(1)	13(1)	2(1)
C(8)	25(1)	30(1)	26(1)	-2(1)	13(1)	-3(1)
C(9)	26(1)	26(1)	23(1)	-2(1)	13(1)	-3(1)
C(10)	21(1)	27(1)	21(1)	-1(1)	10(1)	-1(1)
C(11)	23(1)	26(1)	30(1)	1(1)	11(1)	-1(1)
C(12)	23(1)	34(1)	34(1)	7(1)	14(1)	0(1)
C(13)	38(1)	47(1)	33(1)	-2(1)	23(1)	-3(1)
C(14)	28(1)	34(1)	41(1)	-9(1)	19(1)	-3(1)
C(15)	25(1)	26(1)	35(1)	-2(1)	12(1)	0(1)
C(16)	21(1)	28(1)	23(1)	1(1)	11(1)	-1(1)
C(17)	26(1)	26(1)	31(1)	3(1)	16(1)	1(1)
C(18)	29(1)	27(1)	31(1)	4(1)	17(1)	1(1)
C(19)	34(1)	27(1)	35(1)	4(1)	19(1)	-3(1)
C(20)	34(1)	32(1)	41(1)	4(1)	23(1)	-5(1)
C(21)	30(1)	31(1)	38(1)	3(1)	21(1)	-3(1)
C(22)	24(1)	28(1)	26(2)	2(1)	15(1)	1(1)
C(23)	33(1)	33(2)	22(1)	1(1)	12(1)	2(1)
C(24)	24(1)	24(1)	26(2)	-1(1)	14(1)	1(1)
C(25)	25(1)	38(2)	21(1)	0(1)	10(1)	-1(1)
C(26)	37(1)	26(1)	42(1)	-2(1)	19(1)	2(1)
C(27)	54(1)	29(1)	77(2)	-4(1)	37(1)	6(1)
C(28)	52(1)	33(1)	56(1)	-12(1)	14(1)	-1(1)
C(29)	56(1)	34(1)	53(1)	10(1)	26(1)	9(1)
C(30)	37(1)	26(1)	42(1)	3(1)	22(1)	-3(1)
C(31)	60(1)	29(1)	74(2)	3(1)	41(1)	-9(1)
C(32)	57(1)	34(1)	55(1)	11(1)	19(1)	6(1)
C(33)	47(1)	34(1)	48(1)	-5(1)	24(1)	-6(1)

Figure S11. ORTEP3 Plot showing labeling for **117**

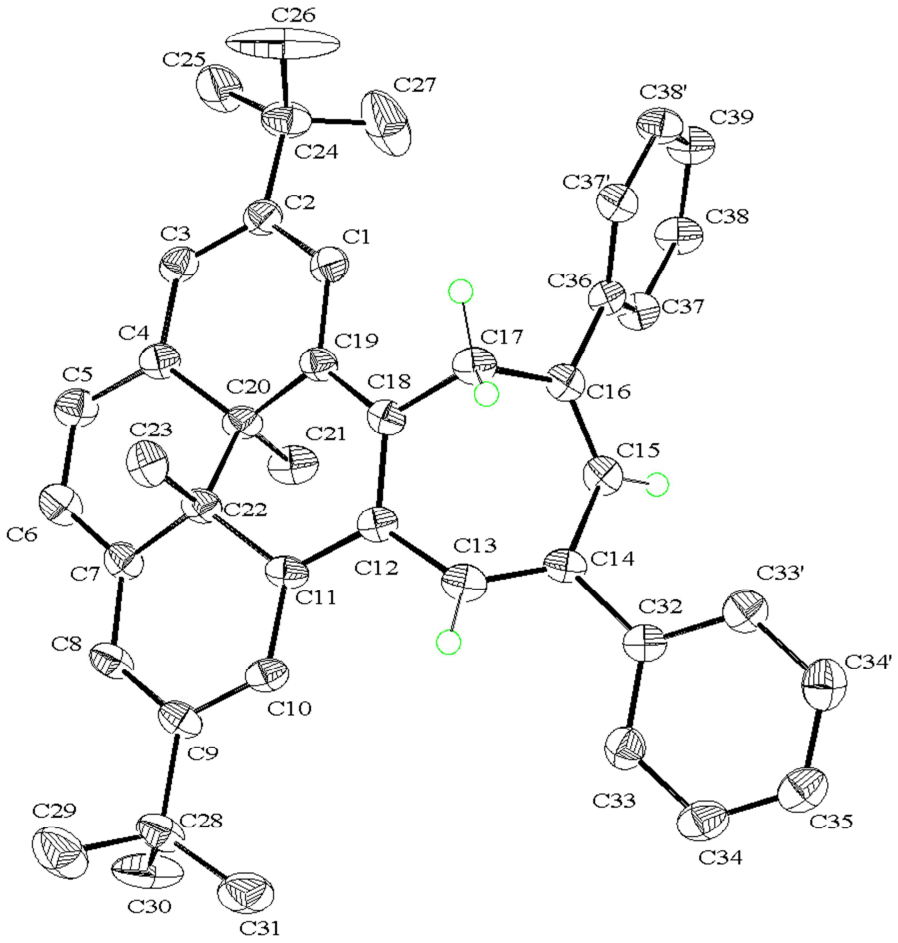


Table 2. Atomic coordinates (x 10^4) and equivalent isotropic displacement parameters (A^2 x 10^3) for **117.**

U(eq) is defined as one third of the trace of the orthogonalized Uij tensor.

	x	y	z	U(eq)	occ
C(1)	7356(3)	-1393(2)	3848(4)	27(1)	
C(2)	6659(3)	-1425(3)	4387(4)	29(1)	
C(3)	5972(3)	-922(3)	4085(4)	28(1)	
C(4)	5987(3)	-337(3)	3353(4)	27(1)	
C(5)	5299(3)	162(3)	3007(4)	32(1)	
C(6)	5353(3)	736(3)	2284(4)	35(1)	
C(7)	6058(3)	802(2)	1744(4)	26(1)	
C(8)	6146(3)	1387(2)	1064(4)	30(1)	
C(9)	6879(3)	1459(2)	588(4)	27(1)	
C(10)	7565(3)	958(2)	879(4)	26(1)	
C(11)	7550(3)	343(2)	1552(4)	24(1)	
C(12)	8256(3)	-156(2)	1914(4)	22(1)	
C(13)	9106(3)	-47(2)	1638(4)	26(1)	
C(14)	9959(3)	-236(2)	2297(4)	23(1)	
C(15)	10163(3)	-663(2)	3407(4)	24(1)	
C(16)	9655(3)	-1203(2)	3590(4)	23(1)	
C(17)	8800(3)	-1376(2)	2623(4)	26(1)	
C(18)	8141(3)	-784(2)	2543(4)	23(1)	
C(19)	7450(3)	-828(2)	3113(4)	24(1)	
C(20)	6868(3)	-181(2)	3065(4)	26(1)	
C(21)	7406(3)	340(3)	4082(4)	34(1)	
C(22)	6671(3)	170(2)	1823(4)	26(1)	
C(23)	6146(3)	-348(3)	799(4)	31(1)	
C(24)	6679(6)	-1976(6)	5346(10)	36(4)	0.59(1)
C(25)	5978(6)	-1867(9)	6009(13)	55(4)	0.59(1)
C(26)	6526(13)	-2692(7)	4725(12)	112(7)	0.59(1)
C(27)	7608(6)	-1969(8)	6268(10)	75(5)	0.59(1)
C(28)	6916(3)	2124(3)	-159(4)	35(1)	
C(29)	6094(4)	2109(3)	-1317(5)	54(2)	
C(30)	6857(4)	2795(3)	587(5)	57(2)	
C(31)	7776(3)	2175(3)	-541(5)	46(2)	
C(32)	10762(3)	9(2)	1943(4)	24(1)	
C(33')	11538(3)	-413(3)	2207(4)	30(1)	
C(33)	10781(3)	663(3)	1386(4)	31(1)	

C(34')	12303(3)	-182(3)	1914(4)	36(1)	
C(34)	11548(3)	886(3)	1095(4)	36(1)	
C(35)	12305(3)	466(3)	1358(4)	35(1)	
C(36)	9900(3)	-1628(2)	4722(4)	20(1)	
C(37)	10281(3)	-1299(3)	5850(4)	27(1)	
C(37')	9787(3)	-2362(2)	4694(4)	25(1)	
C(38)	10545(3)	-1712(3)	6894(4)	30(1)	
C(38')	10053(3)	-2769(3)	5740(4)	30(1)	
C(39)	10440(3)	-2436(3)	6846(4)	30(1)	
C(26B)	7429(8)	-2583(10)	5430(20)	98(9)	0.41(1)
C(27B)	6477(19)	-1838(13)	6316(17)	111(10)	0.41(1)
C(25B)	5789(9)	-2532(9)	4469(16)	63(6)	0.41(1)
C(24B)	6609(8)	-2102(7)	5143(14)	24(5)	0.41(1)

Table 3. Bond lengths [A] for **119.**

atom-atom	distance	atom-atom	distance
C(1)-C(19)	1.399(6)	C(21)-H(21C)	0.9800
C(1)-C(2)	1.400(6)	C(22)-C(23)	1.565(6)
C(1)-H(1)	0.9500	C(23)-H(23A)	0.9800
C(2)-C(3)	1.390(6)	C(23)-H(23B)	0.9800
C(2)-C(24)	1.516(13)	C(23)-H(23C)	0.9800
C(2)-C(24B)	1.563(16)	C(24)-C(26)	1.514(7)
C(3)-C(4)	1.395(6)	C(24)-C(25)	1.518(7)
C(3)-H(3)	0.9500	C(24)-C(27)	1.519(8)
C(4)-C(5)	1.390(6)	C(25)-H(25A)	0.9800
C(4)-C(20)	1.526(6)	C(25)-H(25B)	0.9800
C(5)-C(6)	1.385(6)	C(25)-H(25C)	0.9800
C(5)-H(5)	0.9500	C(26)-H(26A)	0.9800
C(6)-C(7)	1.416(6)	C(26)-H(26B)	0.9800
C(6)-H(6)	0.9500	C(26)-H(26C)	0.9800
C(7)-C(8)	1.384(6)	C(27)-H(27A)	0.9800
C(7)-C(22)	1.510(6)	C(27)-H(27B)	0.9800
C(8)-C(9)	1.408(6)	C(27)-H(27C)	0.9800
C(8)-H(8)	0.9500	C(28)-C(31)	1.526(7)
C(9)-C(10)	1.386(6)	C(28)-C(30)	1.549(7)
C(9)-C(28)	1.535(6)	C(28)-C(29)	1.555(7)
C(10)-C(11)	1.400(6)	C(29)-H(29A)	0.9800
C(10)-H(10)	0.9500	C(29)-H(29B)	0.9800
C(11)-C(12)	1.410(6)	C(29)-H(29C)	0.9800
C(11)-C(22)	1.522(6)	C(30)-H(30A)	0.9800
C(12)-C(18)	1.428(6)	C(30)-H(30B)	0.9800
C(12)-C(13)	1.459(6)	C(30)-H(30C)	0.9800
C(13)-C(14)	1.364(6)	C(31)-H(31A)	0.9800
C(13)-H(13)	0.9500	C(31)-H(31B)	0.9800
C(14)-C(15)	1.472(6)	C(31)-H(31C)	0.9800
C(14)-C(32)	1.493(6)	C(32)-C(33)	1.395(6)
C(15)-C(16)	1.341(6)	C(32)-C(33')	1.398(6)
C(15)-H(15)	0.9500	C(33')-C(34')	1.396(6)
C(16)-C(36)	1.488(6)	C(33')-H(33')	0.9500
C(16)-C(17)	1.496(6)	C(33)-C(34)	1.393(6)
C(17)-C(18)	1.498(6)	C(33)-H(33)	0.9500
C(17)-H(17A)	0.9900	C(34')-C(35)	1.380(7)
C(17)-H(17B)	0.9900	C(34')-H(34')	0.9500
C(18)-C(19)	1.417(6)	C(34)-C(35)	1.373(7)
C(19)-C(20)	1.506(6)	C(34)-H(34)	0.9500
C(20)-C(22)	1.532(6)	C(35)-H(35)	0.9500
C(20)-C(21)	1.571(6)	C(36)-C(37')	1.393(6)
C(21)-H(21A)	0.9800	C(36)-C(37)	1.409(6)
C(21)-H(21B)	0.9800	C(37)-C(38)	1.395(6)

C(37)-H(37)	0.9500	C(26B)-H(26F)	0.9800
C(37')-C(38')	1.390(6)	C(27B)-C(24B)	1.518(8)
C(37')-H(37')	0.9500	C(27B)-H(27D)	0.9800
C(38)-C(39)	1.372(6)	C(27B)-H(27E)	0.9800
C(38)-H(38)	0.9500	C(27B)-H(27F)	0.9800
C(38')-C(39)	1.394(6)	C(25B)-C(24B)	1.515(8)
C(38')-H(38')	0.9500	C(25B)-H(25D)	0.9800
C(39)-H(39)	0.9500	C(25B)-H(25E)	0.9800
C(26B)-C(24B)	1.516(8)	C(25B)-H(25F)	0.9800
C(26B)-H(26D)	0.9800		
C(26B)-H(26E)	0.9800		

Table 3. Bond angles [deg] for **119.**

C(19)-C(1)-C(2)	122.5(4)	C(13)-C(14)-C(32)	121.0(4)
C(19)-C(1)-H(1)	118.8	C(15)-C(14)-C(32)	115.3(4)
C(2)-C(1)-H(1)	118.8	C(16)-C(15)-C(14)	124.7(4)
C(3)-C(2)-C(1)	119.5(4)	C(16)-C(15)-H(15)	117.7
C(3)-C(2)-C(24)	120.0(5)	C(14)-C(15)-H(15)	117.7
C(1)-C(2)-C(24)	120.4(5)	C(15)-C(16)-C(36)	122.5(4)
C(3)-C(2)-C(24B)	122.4(6)	C(15)-C(16)-C(17)	118.6(4)
C(1)-C(2)-C(24B)	117.2(6)	C(36)-C(16)-C(17)	118.9(4)
C(24)-C(2)-C(24B)	12.2(8)	C(16)-C(17)-C(18)	108.7(4)
C(2)-C(3)-C(4)	122.8(4)	C(16)-C(17)-H(17A)	109.9
C(2)-C(3)-H(3)	118.6	C(18)-C(17)-H(17A)	109.9
C(4)-C(3)-H(3)	118.6	C(16)-C(17)-H(17B)	109.9
C(5)-C(4)-C(3)	124.1(4)	C(18)-C(17)-H(17B)	109.9
C(5)-C(4)-C(20)	117.8(4)	H(17A)-C(17)-H(17B)	108.3
C(3)-C(4)-C(20)	117.5(4)	C(19)-C(18)-C(12)	120.9(4)
C(6)-C(5)-C(4)	121.6(4)	C(19)-C(18)-C(17)	121.6(4)
C(6)-C(5)-H(5)	119.2	C(12)-C(18)-C(17)	117.5(4)
C(4)-C(5)-H(5)	119.2	C(1)-C(19)-C(18)	123.9(4)
C(5)-C(6)-C(7)	122.0(4)	C(1)-C(19)-C(20)	118.0(4)
C(5)-C(6)-H(6)	119.0	C(18)-C(19)-C(20)	117.5(4)
C(7)-C(6)-H(6)	119.0	C(19)-C(20)-C(4)	113.6(4)
C(8)-C(7)-C(6)	122.8(4)	C(19)-C(20)-C(22)	109.6(4)
C(8)-C(7)-C(22)	119.7(4)	C(4)-C(20)-C(22)	110.2(3)
C(6)-C(7)-C(22)	117.2(4)	C(19)-C(20)-C(21)	107.4(4)
C(7)-C(8)-C(9)	121.8(4)	C(4)-C(20)-C(21)	105.5(3)
C(7)-C(8)-H(8)	119.1	C(22)-C(20)-C(21)	110.5(4)
C(9)-C(8)-H(8)	119.1	C(20)-C(21)-H(21A)	109.5
C(10)-C(9)-C(8)	119.2(4)	C(20)-C(21)-H(21B)	109.5
C(10)-C(9)-C(28)	122.6(4)	H(21A)-C(21)-H(21B)	109.5
C(8)-C(9)-C(28)	118.0(4)	C(20)-C(21)-H(21C)	109.5
C(9)-C(10)-C(11)	124.1(4)	H(21A)-C(21)-H(21C)	109.5
C(9)-C(10)-H(10)	117.9	H(21B)-C(21)-H(21C)	109.5
C(11)-C(10)-H(10)	117.9	C(7)-C(22)-C(11)	113.8(4)
C(10)-C(11)-C(12)	125.4(4)	C(7)-C(22)-C(20)	110.2(4)
C(10)-C(11)-C(22)	117.1(4)	C(11)-C(22)-C(20)	110.1(3)
C(12)-C(11)-C(22)	117.3(4)	C(7)-C(22)-C(23)	105.6(4)
C(11)-C(12)-C(18)	120.1(4)	C(11)-C(22)-C(23)	105.9(3)
C(11)-C(12)-C(13)	120.8(4)	C(20)-C(22)-C(23)	111.0(4)
C(18)-C(12)-C(13)	119.1(4)	C(22)-C(23)-H(23A)	109.5
C(14)-C(13)-C(12)	129.0(4)	C(22)-C(23)-H(23B)	109.5
C(14)-C(13)-H(13)	115.5	H(23A)-C(23)-H(23B)	109.5
C(12)-C(13)-H(13)	115.5	C(22)-C(23)-H(23C)	109.5
C(13)-C(14)-C(15)	123.7(4)	H(23A)-C(23)-H(23C)	109.5

H(23B)-C(23)-H(23C)	109.5	C(34)-C(35)-C(34')	119.5(5)
C(26)-C(24)-C(2)	107.1(8)	C(34)-C(35)-H(35)	120.2
C(26)-C(24)-C(25)	109.1(6)	C(34')-C(35)-H(35)	120.2
C(2)-C(24)-C(25)	114.6(9)	C(37')-C(36)-C(37)	118.2(4)
C(26)-C(24)-C(27)	109.0(6)	C(37')-C(36)-C(16)	121.0(4)
C(2)-C(24)-C(27)	108.7(8)	C(37)-C(36)-C(16)	120.8(4)
C(25)-C(24)-C(27)	108.3(6)	C(38)-C(37)-C(36)	119.7(4)
C(31)-C(28)-C(9)	113.4(4)	C(38)-C(37)-H(37)	120.1
C(31)-C(28)-C(30)	108.2(4)	C(36)-C(37)-H(37)	120.1
C(9)-C(28)-C(30)	109.4(4)	C(38')-C(37')-C(36)	121.6(4)
C(31)-C(28)-C(29)	108.3(4)	C(38')-C(37')-H(37')	119.2
C(9)-C(28)-C(29)	108.4(4)	C(36)-C(37')-H(37')	119.2
C(30)-C(28)-C(29)	109.2(4)	C(39)-C(38)-C(37)	121.2(4)
C(28)-C(29)-H(29A)	109.5	C(39)-C(38)-H(38)	119.4
C(28)-C(29)-H(29B)	109.5	C(37)-C(38)-H(38)	119.4
H(29A)-C(29)-H(29B)	109.5	C(37')-C(38')-C(39)	119.4(5)
C(28)-C(29)-H(29C)	109.5	C(37')-C(38')-H(38')	120.3
H(29A)-C(29)-H(29C)	109.5	C(39)-C(38')-H(38')	120.3
H(29B)-C(29)-H(29C)	109.5	C(38)-C(39)-C(38')	119.8(4)
C(28)-C(30)-H(30A)	109.5	C(38)-C(39)-H(39)	120.1
C(28)-C(30)-H(30B)	109.5	C(38')-C(39)-H(39)	120.1
H(30A)-C(30)-H(30B)	109.5	C(24B)-C(26B)-H(26D)	109.5
C(28)-C(30)-H(30C)	109.5	C(24B)-C(26B)-H(26E)	109.5
H(30A)-C(30)-H(30C)	109.5	H(26D)-C(26B)-H(26E)	109.5
H(30B)-C(30)-H(30C)	109.5	C(24B)-C(26B)-H(26F)	109.5
C(28)-C(31)-H(31A)	109.5	H(26D)-C(26B)-H(26F)	109.5
C(28)-C(31)-H(31B)	109.5	H(26E)-C(26B)-H(26F)	109.5
H(31A)-C(31)-H(31B)	109.5	C(24B)-C(27B)-H(27D)	109.5
C(28)-C(31)-H(31C)	109.5	C(24B)-C(27B)-H(27E)	109.5
H(31A)-C(31)-H(31C)	109.5	H(27D)-C(27B)-H(27E)	109.5
H(31B)-C(31)-H(31C)	109.5	C(24B)-C(27B)-H(27F)	109.5
C(33)-C(32)-C(33')	117.9(4)	H(27D)-C(27B)-H(27F)	109.5
C(33)-C(32)-C(14)	122.2(4)	H(27E)-C(27B)-H(27F)	109.5
C(33')-C(32)-C(14)	119.9(4)	C(24B)-C(25B)-H(25D)	109.5
C(34')-C(33')-C(32)	120.5(5)	C(24B)-C(25B)-H(25E)	109.5
C(34')-C(33')-H(33')	119.7	H(25D)-C(25B)-H(25E)	109.5
C(32)-C(33')-H(33')	119.7	C(24B)-C(25B)-H(25F)	109.5
C(34)-C(33)-C(32)	121.0(4)	H(25D)-C(25B)-H(25F)	109.5
C(34)-C(33)-H(33)	119.5	H(25E)-C(25B)-H(25F)	109.5
C(32)-C(33)-H(33)	119.5	C(25B)-C(24B)-C(26B)	108.4(7)
C(35)-C(34')-C(33')	120.6(5)	C(25B)-C(24B)-C(27B)	108.9(7)
C(35)-C(34')-H(34')	119.7	C(26B)-C(24B)-C(27B)	108.8(7)
C(33')-C(34')-H(34')	119.7	C(25B)-C(24B)-C(2)	108.7(10)
C(35)-C(34)-C(33)	120.5(5)	C(26B)-C(24B)-C(2)	115.8(11)
C(35)-C(34)-H(34)	119.8	C(27B)-C(24B)-C(2)	106.0(13)
C(33)-C(34)-H(34)	119.8		

Symmetry transformations used to generate equivalent atoms:

Table 4. Anisotropic displacement parameters (A^2 x 10^3) for 117.

The anisotropic displacement factor exponent takes the form:
-2 pi^2 [h^2 a*^2 U11 + ... + 2 h k a* b* U12]

	U11	U22	U33	U23	U13	U12
C(1)	28(3)	29(3)	22(3)	1(2)	4(2)	4(2)
C(2)	30(3)	36(3)	19(3)	8(2)	3(2)	-6(2)
C(3)	29(3)	35(3)	23(3)	3(2)	13(2)	-4(2)
C(4)	33(3)	32(3)	18(2)	2(2)	12(2)	-1(2)
C(5)	38(3)	33(3)	30(3)	1(2)	18(2)	1(2)
C(6)	40(3)	35(3)	31(3)	3(2)	14(2)	8(2)
C(7)	31(3)	29(3)	21(3)	2(2)	10(2)	4(2)
C(8)	40(3)	28(3)	27(3)	8(2)	15(2)	10(2)
C(9)	39(3)	28(3)	15(2)	3(2)	10(2)	5(2)
C(10)	34(3)	31(3)	15(2)	2(2)	12(2)	-4(2)
C(11)	36(3)	23(3)	12(2)	1(2)	6(2)	-3(2)
C(12)	30(3)	25(3)	13(2)	-3(2)	8(2)	-3(2)
C(13)	38(3)	27(3)	14(2)	-2(2)	10(2)	0(2)
C(14)	34(3)	21(3)	16(2)	-1(2)	11(2)	0(2)
C(15)	29(2)	29(3)	12(2)	-2(2)	6(2)	0(2)
C(16)	30(3)	25(3)	17(2)	-1(2)	11(2)	3(2)
C(17)	35(3)	31(3)	14(2)	1(2)	10(2)	-2(2)
C(18)	28(2)	22(3)	17(2)	-2(2)	4(2)	-1(2)
C(19)	28(3)	26(3)	16(2)	3(2)	5(2)	-1(2)
C(20)	32(3)	31(3)	15(2)	6(2)	9(2)	-3(2)
C(21)	51(3)	35(3)	18(3)	-5(2)	14(2)	-8(2)
C(22)	32(3)	31(3)	17(2)	5(2)	10(2)	1(2)
C(23)	34(3)	37(3)	19(3)	-3(2)	4(2)	2(2)
C(24)	51(8)	29(7)	36(8)	3(6)	24(6)	0(6)
C(25)	48(7)	72(9)	56(9)	40(7)	31(6)	15(6)
C(26)	240(20)	32(8)	95(12)	3(8)	104(14)	-33(12)
C(27)	65(7)	114(12)	59(8)	54(8)	38(6)	44(7)
C(28)	46(3)	32(3)	30(3)	9(2)	18(2)	11(2)
C(29)	61(4)	69(4)	40(3)	24(3)	25(3)	22(3)
C(30)	100(5)	25(3)	66(4)	10(3)	54(4)	5(3)
C(31)	58(4)	51(4)	39(3)	14(3)	28(3)	4(3)
C(32)	33(3)	24(3)	17(2)	-4(2)	9(2)	-3(2)
C(33')	36(3)	36(3)	21(3)	0(2)	13(2)	1(2)
C(33)	29(3)	36(3)	26(3)	0(2)	7(2)	0(2)
C(34')	35(3)	45(4)	30(3)	-6(3)	13(2)	4(2)

C(34)	43(3)	41(3)	25(3)	2(2)	13(2)	-8(3)
C(35)	39(3)	45(4)	23(3)	-2(3)	14(2)	-7(3)
C(36)	26(2)	25(3)	13(2)	-2(2)	10(2)	-1(2)
C(37)	35(3)	28(3)	20(3)	-4(2)	9(2)	-4(2)
C(37')	33(3)	29(3)	15(2)	-1(2)	10(2)	1(2)
C(38)	47(3)	34(3)	11(2)	1(2)	10(2)	-4(2)
C(38')	42(3)	29(3)	22(3)	4(2)	15(2)	-1(2)
C(39)	46(3)	36(3)	12(3)	4(2)	13(2)	-2(2)
C(26B)	40(9)	70(14)	190(20)	102(15)	34(11)	15(9)
C(27B)	250(30)	70(14)	28(11)	-4(10)	64(18)	0(20)
C(25B)	65(11)	44(11)	66(11)	25(9)	-1(9)	-25(9)
C(24B)	35(9)	12(10)	27(9)	5(8)	11(7)	-4(7)

Figure S12. ORTEP3 Plot showing labeling for **119**

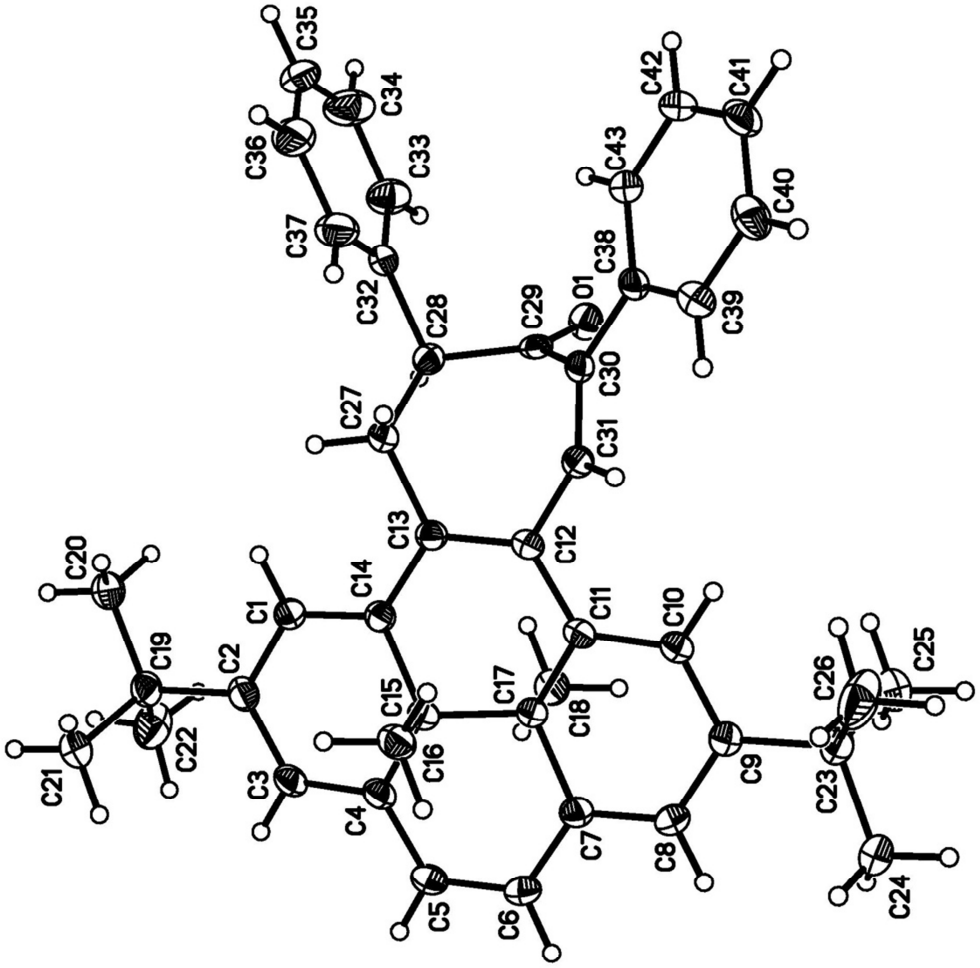


Table 2. Atomic coordinates and equivalent isotropic displacement parameters ($Å^2$) for **uvic020.**

U(eq) is defined as one third of the trace of the orthogonalized U_{ij} tensor.

	x	y	z	U(eq)
O(1)	0.97574(15)	0.67151(5)	0.16276(4)	0.025(1)
C(1)	0.7712(2)	0.48388(7)	0.32871(5)	0.021(1)
C(2)	0.7833(2)	0.45994(7)	0.38120(5)	0.023(1)
C(3)	0.6946(2)	0.49748(7)	0.41968(5)	0.024(1)
C(4)	0.5846(2)	0.55522(7)	0.40758(5)	0.022(1)
C(5)	0.5032(2)	0.59458(7)	0.44570(6)	0.027(1)
C(6)	0.3992(2)	0.65359(7)	0.43232(6)	0.026(1)
C(7)	0.3923(2)	0.68078(7)	0.38125(5)	0.021(1)
C(8)	0.2858(2)	0.73853(7)	0.36572(5)	0.023(1)
C(9)	0.2726(2)	0.76311(7)	0.31369(5)	0.022(1)
C(10)	0.3593(2)	0.72601(7)	0.27461(5)	0.022(1)
C(11)	0.4656(2)	0.66702(6)	0.28537(5)	0.019(1)
C(12)	0.5390(2)	0.62663(7)	0.24583(5)	0.018(1)
C(13)	0.6499(2)	0.56710(6)	0.25926(5)	0.019(1)
C(14)	0.6636(2)	0.54123(6)	0.31143(5)	0.019(1)
C(15)	0.5255(2)	0.57350(7)	0.34928(5)	0.021(1)
C(16)	0.2981(2)	0.54496(7)	0.33399(6)	0.025(1)
C(17)	0.5294(2)	0.64847(7)	0.34322(5)	0.020(1)
C(18)	0.7576(2)	0.67613(7)	0.35833(6)	0.025(1)
C(19)	0.8956(2)	0.39527(7)	0.39892(6)	0.026(1)
C(20)	1.0032(3)	0.36274(7)	0.35462(6)	0.030(1)
C(21)	0.7298(3)	0.34699(8)	0.41566(7)	0.036(1)
C(22)	1.0669(3)	0.40837(8)	0.44618(7)	0.041(1)
C(23)	0.1632(3)	0.82857(7)	0.29737(6)	0.027(1)
C(24)	0.0457(3)	0.85726(8)	0.34144(7)	0.036(1)
C(25)	0.3341(3)	0.87810(8)	0.28553(7)	0.042(1)
C(26)	0.0027(3)	0.81949(9)	0.24777(7)	0.049(1)
C(27)	0.7236(2)	0.52808(7)	0.21394(5)	0.020(1)
C(28)	0.8968(2)	0.56055(6)	0.18562(5)	0.019(1)
C(29)	0.8400(2)	0.63018(7)	0.16622(5)	0.019(1)
C(30)	0.6115(2)	0.64658(6)	0.15055(5)	0.018(1)
C(31)	0.4861(2)	0.64727(6)	0.18972(5)	0.019(1)
C(32)	0.9465(2)	0.52157(7)	0.13662(5)	0.021(1)
C(33)	1.1436(2)	0.52842(8)	0.11901(6)	0.031(1)
C(34)	1.1944(3)	0.49408(10)	0.07504(7)	0.042(1)

C(35)	1.0500(3)	0.45165(8)	0.04810(7)	0.042(1)
C(36)	0.8531(3)	0.44524(8)	0.06437(7)	0.044(1)
C(37)	0.8012(3)	0.48044(8)	0.10804(6)	0.034(1)
C(38)	0.5443(2)	0.66842(6)	0.09485(5)	0.019(1)
C(39)	0.3439(2)	0.69521(7)	0.07954(6)	0.024(1)
C(40)	0.2841(2)	0.71598(7)	0.02763(6)	0.029(1)
C(41)	0.4219(3)	0.71010(7)	-0.01060(6)	0.031(1)
C(42)	0.6192(3)	0.68286(7)	0.00367(6)	0.030(1)
C(43)	0.6804(2)	0.66209(7)	0.05567(6)	0.025(1)
H(1A)	0.8400	0.4597	0.3036	0.025
H(3A)	0.7110	0.4824	0.4556	0.029
H(5A)	0.5194	0.5806	0.4819	0.032
H(6A)	0.3311	0.6760	0.4585	0.031
H(8A)	0.2192	0.7623	0.3915	0.027
H(10A)	0.3441	0.7422	0.2390	0.026
H(16A)	0.3021	0.4969	0.3375	0.038
H(16B)	0.2472	0.5568	0.2970	0.038
H(16C)	0.2024	0.5633	0.3578	0.038
H(18A)	0.7551	0.7243	0.3552	0.038
H(18B)	0.8519	0.6578	0.3341	0.038
H(18C)	0.8091	0.6637	0.3951	0.038
H(20A)	0.8972	0.3530	0.3241	0.045
H(20B)	1.0713	0.3217	0.3680	0.045
H(20C)	1.1102	0.3927	0.3433	0.045
H(21A)	0.6251	0.3373	0.3849	0.053
H(21B)	0.6588	0.3668	0.4441	0.053
H(21C)	0.7997	0.3061	0.4286	0.053
H(22A)	1.1658	0.4417	0.4360	0.061
H(22B)	1.1439	0.3675	0.4559	0.061
H(22C)	1.0002	0.4242	0.4768	0.061
H(24A)	-0.0608	0.8257	0.3505	0.054
H(24B)	-0.0240	0.8984	0.3290	0.054
H(24C)	0.1467	0.8661	0.3731	0.054
H(25A)	0.2671	0.9199	0.2736	0.063
H(25B)	0.4119	0.8605	0.2575	0.063
H(25C)	0.4324	0.8855	0.3180	0.063
H(26A)	-0.1044	0.7872	0.2553	0.074
H(26B)	0.0754	0.8037	0.2182	0.074
H(26C)	-0.0660	0.8617	0.2380	0.074
H(27A)	0.5998	0.5195	0.1871	0.024
H(27B)	0.7767	0.4849	0.2281	0.024
H(28A)	1.0287	0.5630	0.2114	0.023
H(31A)	0.3461	0.6630	0.1801	0.023
H(33A)	1.2452	0.5572	0.1375	0.037
H(34A)	1.3296	0.4998	0.0633	0.050
H(35A)	1.0864	0.4271	0.0185	0.050

H(36A)	0.7519	0.4166	0.0457	0.053
H(37A)	0.6634	0.4762	0.1185	0.041
H(39A)	0.2470	0.6992	0.1052	0.029
H(40A)	0.1475	0.7344	0.0182	0.035
H(41A)	0.3811	0.7246	-0.0461	0.037
H(42A)	0.7142	0.6782	-0.0224	0.036
H(43B)	0.8167	0.6433	0.0647	0.030

Table 3. Anisotropic displacement parameters ($Å^2$) for uvic020.

The anisotropic displacement factor exponent takes the form:
$-2\pi^2[h^2a^{*2}U_{11} + ... + 2hka^*b^*U_{12}]$

	U_{11}	U_{22}	U_{33}	U_{23}	U_{13}	U_{12}
O(1)	0.0220(5)	0.0221(5)	0.0323(6)	-0.0002(4)	0.0059(4)	-0.0025(4)
C(1)	0.0249(7)	0.0194(7)	0.0178(7)	-0.0015(5)	0.0028(5)	-0.0010(5)
C(2)	0.0265(7)	0.0195(7)	0.0210(7)	0.0023(5)	0.0013(6)	-0.0012(6)
C(3)	0.0337(8)	0.0239(7)	0.0154(7)	0.0045(5)	0.0026(6)	-0.0002(6)
C(4)	0.0283(8)	0.0224(7)	0.0167(7)	0.0028(5)	0.0035(5)	-0.0012(6)
C(5)	0.0372(8)	0.0292(8)	0.0147(7)	0.0037(6)	0.0051(6)	0.0031(6)
C(6)	0.0332(8)	0.0273(8)	0.0178(7)	-0.0020(6)	0.0077(6)	0.0033(6)
C(7)	0.0254(7)	0.0216(7)	0.0174(7)	-0.0020(5)	0.0038(5)	-0.0008(6)
C(8)	0.0277(7)	0.0223(7)	0.0193(7)	-0.0039(5)	0.0056(6)	0.0015(6)
C(9)	0.0234(7)	0.0204(7)	0.0219(7)	-0.0001(5)	0.0031(5)	0.0000(6)
C(10)	0.0272(7)	0.0215(7)	0.0167(7)	0.0019(5)	0.0032(5)	0.0008(6)
C(11)	0.0203(7)	0.0201(7)	0.0166(7)	0.0017(5)	0.0035(5)	-0.0019(5)
C(12)	0.0193(7)	0.0200(7)	0.0163(7)	0.0011(5)	0.0029(5)	-0.0015(5)
C(13)	0.0203(7)	0.0190(7)	0.0170(7)	-0.0010(5)	0.0033(5)	-0.0020(5)
C(14)	0.0206(7)	0.0177(6)	0.0175(7)	-0.0009(5)	0.0020(5)	-0.0024(5)
C(15)	0.0250(7)	0.0202(7)	0.0164(7)	0.0013(5)	0.0033(5)	0.0010(6)
C(16)	0.0271(8)	0.0260(7)	0.0236(7)	0.0014(6)	0.0059(6)	-0.0047(6)
C(17)	0.0250(7)	0.0191(7)	0.0167(7)	0.0008(5)	0.0037(5)	0.0015(5)
C(18)	0.0263(8)	0.0240(7)	0.0243(7)	-0.0015(6)	0.0009(6)	-0.0030(6)
C(19)	0.0366(8)	0.0210(7)	0.0202(7)	0.0032(6)	0.0008(6)	0.0043(6)
C(20)	0.0363(9)	0.0251(8)	0.0287(8)	0.0058(6)	0.0051(7)	0.0084(6)
C(21)	0.0538(11)	0.0229(8)	0.0327(9)	0.0068(6)	0.0158(8)	0.0043(7)
C(22)	0.0526(11)	0.0341(9)	0.0323(9)	0.0001(7)	-0.0104(8)	0.0140(8)
C(23)	0.0380(9)	0.0220(7)	0.0227(7)	-0.0001(6)	0.0045(6)	0.0072(6)
C(24)	0.0492(10)	0.0258(8)	0.0361(9)	0.0037(7)	0.0142(8)	0.0133(7)
C(25)	0.0617(12)	0.0241(8)	0.0440(10)	0.0068(7)	0.0215(9)	0.0039(8)
C(26)	0.0627(12)	0.0405(10)	0.0399(10)	-0.0085(8)	-0.0158(9)	0.0272(9)
C(27)	0.0261(7)	0.0182(7)	0.0164(7)	0.0006(5)	0.0034(5)	0.0007(5)
C(28)	0.0192(7)	0.0203(7)	0.0180(7)	-0.0010(5)	0.0011(5)	0.0016(5)
C(29)	0.0220(7)	0.0213(7)	0.0132(6)	-0.0034(5)	0.0055(5)	-0.0009(6)
C(30)	0.0214(7)	0.0150(6)	0.0172(7)	0.0000(5)	0.0018(5)	-0.0006(5)
C(31)	0.0199(7)	0.0188(7)	0.0178(7)	0.0002(5)	0.0018(5)	0.0010(5)
C(32)	0.0271(7)	0.0183(7)	0.0186(7)	0.0031(5)	0.0043(5)	0.0044(5)
C(33)	0.0249(8)	0.0417(9)	0.0271(8)	-0.0016(7)	0.0042(6)	0.0043(7)
C(34)	0.0362(9)	0.0604(12)	0.0312(9)	0.0012(8)	0.0109(7)	0.0195(9)
C(35)	0.0679(13)	0.0332(9)	0.0261(8)	-0.0015(7)	0.0155(8)	0.0190(9)
C(36)	0.0745(13)	0.0301(9)	0.0293(9)	-0.0087(7)	0.0144(9)	-0.0157(9)
C(37)	0.0446(10)	0.0326(9)	0.0271(8)	-0.0060(7)	0.0141(7)	-0.0133(7)
C(38)	0.0254(7)	0.0154(6)	0.0170(7)	0.0003(5)	0.0027(5)	-0.0023(5)

C(39)	0.0256(7)	0.0260(7)	0.0204(7)	0.0026(6)	0.0025(6)	-0.0022(6)
C(40)	0.0312(8)	0.0282(8)	0.0255(8)	0.0054(6)	-0.0040(6)	-0.0016(6)
C(41)	0.0497(10)	0.0252(8)	0.0156(7)	0.0028(6)	-0.0009(6)	-0.0027(7)
C(42)	0.0471(9)	0.0266(8)	0.0180(7)	0.0003(6)	0.0111(6)	0.0041(7)
C(43)	0.0331(8)	0.0219(7)	0.0203(7)	0.0011(6)	0.0070(6)	0.0045(6)

Table 4. Bond lengths [Å] for **uvic020**.

atom-atom	distance	atom-atom	distance
O(1)-C(29)	1.2152(16)	C(30)-C(31)	1.3442(19)
C(1)-C(14)	1.3934(19)	C(30)-C(38)	1.4867(18)
C(1)-C(2)	1.4046(19)	C(32)-C(37)	1.382(2)
C(2)-C(3)	1.406(2)	C(32)-C(33)	1.388(2)
C(2)-C(19)	1.5347(19)	C(33)-C(34)	1.382(2)
C(3)-C(4)	1.380(2)	C(34)-C(35)	1.378(3)
C(4)-C(5)	1.398(2)	C(35)-C(36)	1.372(3)
C(4)-C(15)	1.5198(18)	C(36)-C(37)	1.387(2)
C(5)-C(6)	1.390(2)	C(38)-C(39)	1.398(2)
C(6)-C(7)	1.3981(19)	C(38)-C(43)	1.3977(19)
C(7)-C(8)	1.387(2)	C(39)-C(40)	1.385(2)
C(7)-C(17)	1.5222(19)	C(40)-C(41)	1.386(2)
C(8)-C(9)	1.3978(19)	C(41)-C(42)	1.379(2)
C(9)-C(10)	1.4057(19)	C(42)-C(43)	1.389(2)
C(9)-C(23)	1.5331(19)	C(1)-H(1A)	0.9500
C(10)-C(11)	1.3860(19)	C(3)-H(3A)	0.9500
C(11)-C(12)	1.4143(18)	C(5)-H(5A)	0.9500
C(11)-C(17)	1.5148(18)	C(6)-H(6A)	0.9500
C(12)-C(13)	1.4197(19)	C(8)-H(8A)	0.9500
C(12)-C(31)	1.4761(18)	C(10)-H(10A)	0.9500
C(13)-C(14)	1.4106(18)	C(16)-H(16A)	0.9800
C(13)-C(27)	1.5117(18)	C(16)-H(16B)	0.9800
C(14)-C(15)	1.5227(18)	C(16)-H(16C)	0.9800
C(15)-C(17)	1.5299(18)	C(18)-H(18A)	0.9800
C(15)-C(16)	1.5636(19)	C(18)-H(18B)	0.9800
C(17)-C(18)	1.5612(19)	C(18)-H(18C)	0.9800
C(19)-C(20)	1.531(2)	C(20)-H(20A)	0.9800
C(19)-C(21)	1.537(2)	C(20)-H(20B)	0.9800
C(19)-C(22)	1.539(2)	C(20)-H(20C)	0.9800
C(23)-C(26)	1.528(2)	C(21)-H(21A)	0.9800
C(23)-C(24)	1.529(2)	C(21)-H(21B)	0.9800
C(23)-C(25)	1.537(2)	C(21)-H(21C)	0.9800
C(27)-C(28)	1.5335(18)	C(22)-H(22A)	0.9800
C(28)-C(29)	1.5249(18)	C(22)-H(22B)	0.9800
C(28)-C(32)	1.5332(18)	C(22)-H(22C)	0.9800
C(29)-C(30)	1.4975(18)	C(24)-H(24A)	0.9800

C(24)-H(24B)	0.9800	C(31)-H(31A)	0.9500
C(24)-H(24C)	0.9800	C(33)-H(33A)	0.9500
C(25)-H(25A)	0.9800	C(34)-H(34A)	0.9500
C(25)-H(25B)	0.9800	C(35)-H(35A)	0.9500
C(25)-H(25C)	0.9800	C(36)-H(36A)	0.9500
C(26)-H(26A)	0.9800	C(37)-H(37A)	0.9500
C(26)-H(26B)	0.9800	C(39)-H(39A)	0.9500
C(26)-H(26C)	0.9800	C(40)-H(40A)	0.9500
C(27)-H(27A)	0.9900	C(41)-H(41A)	0.9500
C(27)-H(27B)	0.9900	C(42)-H(42A)	0.9500
C(28)-H(28A)	1.0000	C(43)-H(43B)	0.9500

Symmetry transformations used to generate equivalent atoms:

Table 5. Bond angles [°] for uvic020.

atom-atom-atom	angle	atom-atom-atom	angle
C(14)-C(1)-C(2)	123.57(13)	C(1)-C(2)-C(3)	118.91(12)
C(1)-C(2)-C(19)	122.77(12)	C(3)-C(2)-C(19)	118.30(12)
C(4)-C(3)-C(2)	122.88(12)	C(3)-C(4)-C(5)	123.60(13)
C(3)-C(4)-C(15)	118.74(12)	C(5)-C(4)-C(15)	117.27(12)
C(6)-C(5)-C(4)	122.05(13)	C(5)-C(6)-C(7)	121.65(13)
C(8)-C(7)-C(6)	123.63(13)	C(8)-C(7)-C(17)	118.95(12)
C(6)-C(7)-C(17)	117.08(12)	C(7)-C(8)-C(9)	122.61(13)
C(8)-C(9)-C(10)	118.96(12)	C(8)-C(9)-C(23)	122.37(12)
C(10)-C(9)-C(23)	118.67(12)	C(11)-C(10)-C(9)	123.30(12)
C(10)-C(11)-C(12)	123.91(12)	C(10)-C(11)-C(17)	118.11(12)
C(12)-C(11)-C(17)	117.59(12)	C(11)-C(12)-C(13)	121.48(12)
C(11)-C(12)-C(31)	117.14(12)	C(13)-C(12)-C(31)	121.31(12)
C(14)-C(13)-C(12)	120.82(12)	C(14)-C(13)-C(27)	121.45(12)
C(12)-C(13)-C(27)	117.14(11)	C(1)-C(14)-C(13)	125.13(12)
C(1)-C(14)-C(15)	117.53(12)	C(13)-C(14)-C(15)	116.80(12)
C(4)-C(15)-C(14)	114.12(11)	C(4)-C(15)-C(17)	109.54(11)
C(14)-C(15)-C(17)	110.32(11)	C(4)-C(15)-C(16)	105.17(11)
C(14)-C(15)-C(16)	105.88(11)	C(17)-C(15)-C(16)	111.69(11)
C(11)-C(17)-C(7)	113.17(11)	C(11)-C(17)-C(15)	109.76(11)
C(7)-C(17)-C(15)	110.35(11)	C(11)-C(17)-C(18)	106.20(11)
C(7)-C(17)-C(18)	106.19(11)	C(15)-C(17)-C(18)	111.06(11)
C(20)-C(19)-C(2)	112.95(12)	C(20)-C(19)-C(21)	108.01(12)
C(2)-C(19)-C(21)	108.34(12)	C(20)-C(19)-C(22)	107.62(13)
C(2)-C(19)-C(22)	109.84(12)	C(21)-C(19)-C(22)	110.06(13)
C(26)-C(23)-C(24)	107.71(14)	C(26)-C(23)-C(9)	110.64(12)
C(24)-C(23)-C(9)	112.39(12)	C(26)-C(23)-C(25)	109.78(15)
C(24)-C(23)-C(25)	108.22(13)	C(9)-C(23)-C(25)	108.05(13)
C(13)-C(27)-C(28)	115.73(11)	C(29)-C(28)-C(32)	106.46(10)
C(29)-C(28)-C(27)	113.07(11)	C(32)-C(28)-C(27)	112.63(11)
O(1)-C(29)-C(30)	120.26(12)	O(1)-C(29)-C(28)	121.32(12)
C(30)-C(29)-C(28)	118.41(11)	C(31)-C(30)-C(38)	124.32(12)
C(31)-C(30)-C(29)	116.91(12)	C(38)-C(30)-C(29)	118.36(11)
C(30)-C(31)-C(12)	128.01(12)	C(37)-C(32)-C(33)	117.83(13)
C(37)-C(32)-C(28)	122.83(13)	C(33)-C(32)-C(28)	119.32(13)
C(34)-C(33)-C(32)	121.02(16)	C(35)-C(34)-C(33)	120.30(16)
C(36)-C(35)-C(34)	119.40(15)	C(35)-C(36)-C(37)	120.23(17)
C(32)-C(37)-C(36)	121.15(16)	C(39)-C(38)-C(43)	117.62(12)
C(39)-C(38)-C(30)	121.74(12)	C(43)-C(38)-C(30)	120.64(12)
C(40)-C(39)-C(38)	121.13(14)	C(39)-C(40)-C(41)	120.52(14)
C(42)-C(41)-C(40)	119.08(13)	C(41)-C(42)-C(43)	120.72(14)
C(42)-C(43)-C(38)	120.92(14)	C(14)-C(1)-H(1A)	118.2

C(2)-C(1)-H(1A)	118.2	C(4)-C(3)-H(3A)	118.6
C(2)-C(3)-H(3A)	118.6	C(6)-C(5)-H(5A)	119.0
C(4)-C(5)-H(5A)	119.0	C(5)-C(6)-H(6A)	119.2
C(7)-C(6)-H(6A)	119.2	C(7)-C(8)-H(8A)	118.7
C(9)-C(8)-H(8A)	118.7	C(11)-C(10)-H(10A)	118.3
C(9)-C(10)-H(10A)	118.3	C(15)-C(16)-H(16A)	109.5
C(15)-C(16)-H(16B)	109.5	H(16A)-C(16)-H(16B)	109.5
C(15)-C(16)-H(16C)	109.5	H(16A)-C(16)-H(16C)	109.5
H(16B)-C(16)-H(16C)	109.5	C(17)-C(18)-H(18A)	109.5
C(17)-C(18)-H(18B)	109.5	H(18A)-C(18)-H(18B)	109.5
C(17)-C(18)-H(18C)	109.5	H(18A)-C(18)-H(18C)	109.5
H(18B)-C(18)-H(18C)	109.5	C(19)-C(20)-H(20A)	109.5
C(19)-C(20)-H(20B)	109.5	H(20A)-C(20)-H(20B)	109.5
C(19)-C(20)-H(20C)	109.5	H(20A)-C(20)-H(20C)	109.5
H(20B)-C(20)-H(20C)	109.5	C(19)-C(21)-H(21A)	109.5
C(19)-C(21)-H(21B)	109.5	H(21A)-C(21)-H(21B)	109.5
C(19)-C(21)-H(21C)	109.5	H(21A)-C(21)-H(21C)	109.5
H(21B)-C(21)-H(21C)	109.5	C(19)-C(22)-H(22A)	109.5
C(19)-C(22)-H(22B)	109.5	H(22A)-C(22)-H(22B)	109.5
C(19)-C(22)-H(22C)	109.5	H(22A)-C(22)-H(22C)	109.5
H(22B)-C(22)-H(22C)	109.5	C(23)-C(24)-H(24A)	109.5
C(23)-C(24)-H(24B)	109.5	H(24A)-C(24)-H(24B)	109.5
C(23)-C(24)-H(24C)	109.5	H(24A)-C(24)-H(24C)	109.5
H(24B)-C(24)-H(24C)	109.5	C(23)-C(25)-H(25A)	109.5
C(23)-C(25)-H(25B)	109.5	H(25A)-C(25)-H(25B)	109.5
C(23)-C(25)-H(25C)	109.5	H(25A)-C(25)-H(25C)	109.5
H(25B)-C(25)-H(25C)	109.5	C(23)-C(26)-H(26A)	109.5
C(23)-C(26)-H(26B)	109.5	H(26A)-C(26)-H(26B)	109.5
C(23)-C(26)-H(26C)	109.5	H(26A)-C(26)-H(26C)	109.5
H(26B)-C(26)-H(26C)	109.5	C(13)-C(27)-H(27A)	108.3
C(28)-C(27)-H(27A)	108.3	C(13)-C(27)-H(27B)	108.3
C(28)-C(27)-H(27B)	108.3	H(27A)-C(27)-H(27B)	107.4
C(29)-C(28)-H(28A)	108.2	C(32)-C(28)-H(28A)	108.2
C(27)-C(28)-H(28A)	108.2	C(30)-C(31)-H(31A)	116.0
C(12)-C(31)-H(31A)	116.0	C(34)-C(33)-H(33A)	119.5
C(32)-C(33)-H(33A)	119.5	C(35)-C(34)-H(34A)	119.8
C(33)-C(34)-H(34A)	119.8	C(36)-C(35)-H(35A)	120.3
C(34)-C(35)-H(35A)	120.3	C(35)-C(36)-H(36A)	119.9
C(37)-C(36)-H(36A)	119.9	C(32)-C(37)-H(37A)	119.4
C(36)-C(37)-H(37A)	119.4	C(40)-C(39)-H(39A)	119.4
C(38)-C(39)-H(39A)	119.4	C(39)-C(40)-H(40A)	119.7
C(41)-C(40)-H(40A)	119.7	C(42)-C(41)-H(41A)	120.5
C(40)-C(41)-H(41A)	120.5	C(41)-C(42)-H(42A)	119.6
C(43)-C(42)-H(42A)	119.6	C(42)-C(43)-H(43B)	119.5
C(38)-C(43)-H(43B)	119.5		

Symmetry transformations used to generate equivalent atoms:

Figure S13. ORTEP3 Plot showing labeling for **125**

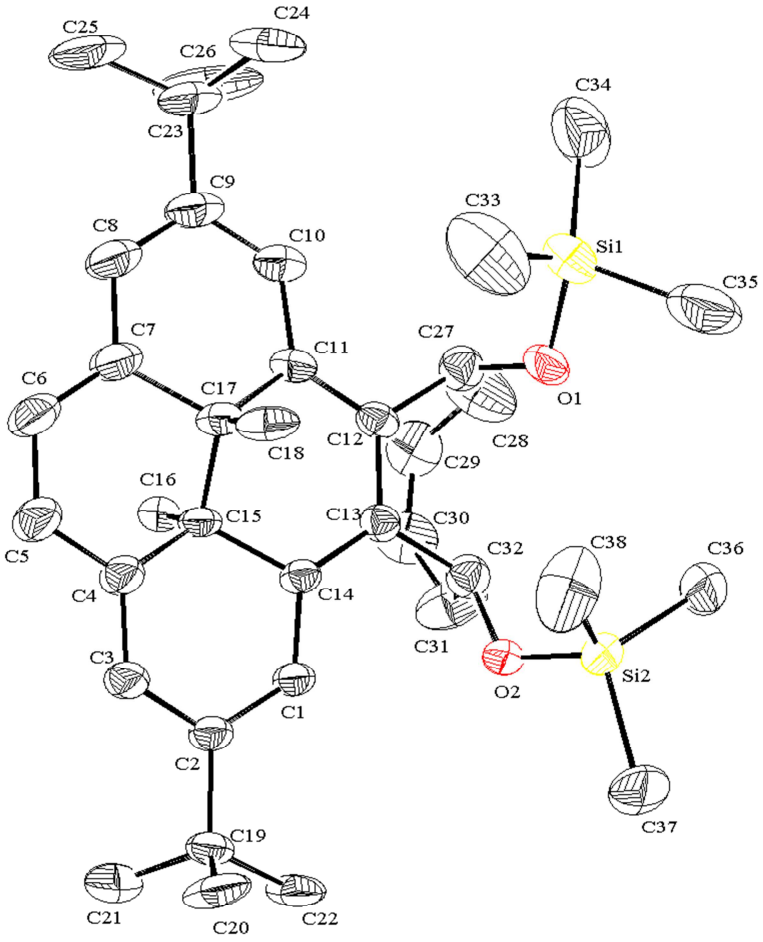


Table 2. Atomic coordinates (x 10^4) and equivalent isotropic displacement parameters (A^2 x 10^3) for db007.
U(eq) is defined as one third of the trace of the orthogonalized Uij tensor.

	x	y	z	U(eq)	occ
C(1)	15066(4)	1298(3)	2571(2)	48(1)	
C(2)	15672(4)	586(4)	2040(2)	53(1)	
C(3)	15476(4)	912(4)	1287(2)	61(1)	
C(4)	14730(4)	1928(4)	1039(2)	60(1)	
C(5)	14543(5)	2282(4)	297(2)	79(2)	
C(6)	13860(5)	3348(5)	83(2)	81(2)	
C(7)	13301(5)	4126(5)	596(3)	74(1)	
C(8)	12651(5)	5228(5)	400(3)	81(2)	
C(9)	12117(5)	6005(5)	931(3)	77(1)	
C(10)	12213(4)	5646(4)	1681(3)	65(1)	
C(11)	12838(4)	4545(4)	1959(2)	56(1)	
C(12)	12963(4)	4160(3)	2715(2)	47(1)	
C(13)	13672(4)	3066(3)	2928(2)	45(1)	
C(14)	14279(4)	2328(3)	2405(2)	44(1)	
C(15)	14411(14)	2904(13)	1621(8)	50(3)	0.53(2)
C(16)	15577(9)	4021(12)	1698(5)	56(3)	0.53(2)
C(17)	13103(13)	3463(11)	1376(5)	52(3)	0.53(2)
C(18)	11911(10)	2348(11)	1314(6)	63(3)	0.53(2)
C(19)	16522(5)	-539(4)	2272(2)	61(1)	
C(20)	15756(9)	-1823(6)	2016(5)	89(3)	0.72(1)
C(21)	17850(10)	-350(11)	1904(6)	104(4)	0.72(1)
C(22)	16857(11)	-584(9)	3110(4)	77(3)	0.72(1)
C(23)	11372(5)	7206(5)	691(3)	96(2)	0.72(1)
C(24)	9923(6)	6925(7)	852(5)	105(3)	0.80(1)
C(25)	11363(9)	7407(8)	-167(4)	130(4)	0.80(1)
C(26)	11992(9)	8395(6)	1103(6)	171(6)	0.80(1)
C(27)	12378(4)	4973(4)	3305(2)	63(1)	0.67(1)
C(28)	13302(7)	5707(6)	3868(4)	126(2)	
C(29)	14752(6)	5804(5)	3802(3)	89(2)	
C(30)	15495(6)	4835(6)	3935(3)	92(2)	
C(31)	15125(7)	3465(5)	4124(3)	110(2)	
C(32)	13879(4)	2790(4)	3764(2)	59(1)	0.80(1)
C(33)	9269(14)	3568(17)	2271(9)	151(6)	0.67(1)
C(34)	8820(13)	5939(12)	3096(9)	144(6)	0.67(1)
C(35)	8811(15)	3343(14)	3937(11)	200(9)	0.67(1)
C(36)	11820(8)	1666(7)	4988(4)	111(3)	0.80(1)

C(37)	13038(9)	-893(6)	4652(4)	98(3)	0.80(1)
C(38)	11227(7)	343(9)	3440(4)	138(4)	0.80(1)
O(1)	11258(5)	4258(4)	3589(3)	79(2)	0.67(1)
O(2)	13810(3)	1464(3)	3953(2)	57(1)	0.80(1)
Si(1)	9586(5)	4399(6)	3169(3)	96(2)	0.67(1)
Si(2)	12462(3)	664(3)	4240(2)	69(1)	0.80(1)
C(15B)	13801(16)	2560(15)	1580(9)	48(3)	0.47(2)
C(16B)	12397(13)	1825(11)	1422(6)	57(3)	0.47(2)
C(17B)	13807(14)	4012(12)	1446(6)	49(3)	0.47(2)
C(18B)	15241(11)	4719(13)	1617(6)	58(3)	0.47(2)
C(27B)	12378(4)	4973(4)	3305(2)	63(1)	0.33(1)
O(1B)	11186(9)	5409(9)	3139(5)	73(4)	0.33(1)
Si(1B)	9853(8)	4660(9)	3546(5)	71(2)	0.33(1)
C(35B)	9380(30)	4240(30)	4356(15)	144(11)	0.33(1)
C(34B)	9570(20)	6377(18)	3514(14)	98(7)	0.33(1)
C(33B)	9230(40)	3740(40)	2696(16)	163(15)	0.33(1)
C(22B)	17570(20)	-50(20)	2909(17)	84(8)	0.28(1)
C(21B)	17180(30)	-1200(30)	1637(11)	93(9)	0.28(1)
C(20B)	15532(18)	-1592(17)	2637(16)	81(8)	0.28(1)
O(2B)	12550(19)	1936(13)	3919(9)	90(6)	0.20(1)
Si(2B)	12160(20)	396(18)	3996(9)	150(10)	0.20(1)
C(32B)	13879(4)	2790(4)	3764(2)	59(1)	0.20(1)
C(38B)	11960(30)	-470(20)	3080(11)	100(10)	0.20(1)
C(37B)	13360(30)	-367(18)	4658(12)	70(9)	0.20(1)
C(36B)	10720(50)	690(50)	4540(30)	193(19)	0.20(1)
C(26B)	11000(30)	7930(20)	1400(8)	130(13)	0.20(1)
C(25B)	12230(20)	8227(17)	277(13)	71(8)	0.20(1)
C(24B)	10103(18)	6840(30)	206(14)	44(15)	0.20(1)

Table 3. Bond lengths [A] for **db007**.

atom-atom	distance	atom-atom	distance
C(1)-C(14)	1.387(5)	C(19)-C(20)	1.513(8)
C(1)-C(2)	1.395(5)	C(19)-C(21B)	1.532(19)
C(1)-H(1)	0.9500	C(19)-C(21)	1.541(10)
C(2)-C(3)	1.392(5)	C(19)-C(22B)	1.54(2)
C(2)-C(19)	1.528(5)	C(19)-C(20B)	1.59(2)
C(3)-C(4)	1.385(5)	C(20)-H(20A)	0.9800
C(3)-H(3)	0.9500	C(20)-H(20B)	0.9800
C(4)-C(5)	1.381(5)	C(20)-H(20C)	0.9800
C(4)-C(15)	1.500(14)	C(21)-H(21A)	0.9800
C(4)-C(15B)	1.567(16)	C(21)-H(21B)	0.9800
C(5)-C(6)	1.376(6)	C(21)-H(21C)	0.9800
C(5)-H(5)	0.9500	C(22)-H(22A)	0.9800
C(6)-C(7)	1.385(6)	C(22)-H(22B)	0.9800
C(6)-H(6)	0.9500	C(22)-H(22C)	0.9800
C(7)-C(8)	1.380(6)	C(23)-C(26)	1.479(6)
C(7)-C(17B)	1.573(11)	C(23)-C(24B)	1.512(8)
C(7)-C(17)	1.577(11)	C(23)-C(24)	1.522(6)
C(8)-C(9)	1.395(7)	C(23)-C(25B)	1.535(8)
C(8)-H(8)	0.9500	C(23)-C(26B)	1.544(8)
C(9)-C(10)	1.393(6)	C(23)-C(25)	1.549(6)
C(9)-C(23)	1.535(6)	C(24)-H(24A)	0.9800
C(10)-C(11)	1.407(5)	C(24)-H(24B)	0.9800
C(10)-H(10)	0.9500	C(24)-H(24C)	0.9800
C(11)-C(12)	1.411(5)	C(25)-H(25A)	0.9800
C(11)-C(17B)	1.519(11)	C(25)-H(25B)	0.9800
C(11)-C(17)	1.559(10)	C(25)-H(25C)	0.9800
C(12)-C(13)	1.411(5)	C(26)-H(26A)	0.9800
C(12)-C(27)	1.516(5)	C(26)-H(26B)	0.9800
C(13)-C(14)	1.399(5)	C(26)-H(26C)	0.9800
C(13)-C(32)	1.526(5)	C(27)-O(1)	1.428(6)
C(14)-C(15)	1.538(15)	C(27)-C(28)	1.473(7)
C(14)-C(15B)	1.542(17)	C(27)-H(27)	1.0000
C(15)-C(17)	1.518(18)	C(27)-H(27B)	0.972(4)
C(15)-C(16)	1.569(19)	C(28)-C(29)	1.477(8)
C(16)-H(16A)	0.9800	C(28)-H(28A)	0.9900
C(16)-H(16B)	0.9800	C(28)-H(28B)	0.9900
C(16)-H(16C)	0.9800	C(29)-C(30)	1.299(7)
C(17)-C(18)	1.586(18)	C(29)-H(29)	0.9500
C(18)-H(18A)	0.9800	C(30)-C(31)	1.466(7)
C(18)-H(18B)	0.9800	C(30)-H(30)	0.9500
C(18)-H(18C)	0.9800	C(31)-C(32)	1.484(7)
C(19)-C(22)	1.513(9)	C(31)-H(31A)	0.9900

C(31)-H(31B)	0.9900	Si(1B)-C(34B)	1.794(19)
C(32)-O(2)	1.394(5)	Si(1B)-C(33B)	1.82(2)
C(32)-H(32)	1.0000	C(35B)-H(35D)	0.9800
C(32)-H(32B)	0.970(4)	C(35B)-H(35E)	0.9800
C(33)-Si(1)	1.800(14)	C(35B)-H(35F)	0.9800
C(33)-H(33A)	0.9800	C(34B)-H(34D)	0.9800
C(33)-H(33B)	0.9800	C(34B)-H(34E)	0.9800
C(33)-H(33C)	0.9800	C(34B)-H(34F)	0.9800
C(34)-Si(1)	1.805(12)	C(33B)-H(33D)	0.9800
C(34)-H(34A)	0.9800	C(33B)-H(33E)	0.9800
C(34)-H(34B)	0.9800	C(33B)-H(33F)	0.9800
C(34)-H(34C)	0.9800	C(22B)-H(22D)	0.9800
C(35)-Si(1)	1.931(14)	C(22B)-H(22E)	0.9800
C(35)-H(35A)	0.9800	C(22B)-H(22F)	0.9800
C(35)-H(35B)	0.9800	C(21B)-H(21D)	0.9800
C(35)-H(35C)	0.9800	C(21B)-H(21E)	0.9800
C(36)-Si(2)	1.859(6)	C(21B)-H(21F)	0.9800
C(36)-H(36A)	0.9800	C(20B)-H(20D)	0.9800
C(36)-H(36B)	0.9800	C(20B)-H(20E)	0.9800
C(36)-H(36C)	0.9800	C(20B)-H(20F)	0.9800
C(37)-Si(2)	1.872(6)	O(2B)-Si(2B)	1.60(2)
C(37)-H(37A)	0.9800	Si(2B)-C(38B)	1.837(9)
C(37)-H(37B)	0.9800	Si(2B)-C(37B)	1.849(9)
C(37)-H(37C)	0.9800	Si(2B)-C(36B)	1.86(4)
C(38)-Si(2)	1.833(6)	C(38B)-H(38D)	0.9800
C(38)-H(38A)	0.9800	C(38B)-H(38E)	0.9800
C(38)-H(38B)	0.9800	C(38B)-H(38F)	0.9800
C(38)-H(38C)	0.9800	C(37B)-H(37D)	0.9800
O(1)-Si(1B)	1.507(9)	C(37B)-H(37E)	0.9800
O(1)-H(27B)	0.804(4)	C(37B)-H(37F)	0.9800
O(2)-Si(2)	1.652(5)	C(36B)-H(36D)	0.9800
O(2)-H(32B)	0.907(3)	C(36B)-H(36E)	0.9800
Si(1)-O(1B)	1.854(11)	C(36B)-H(36F)	0.9800
C(15B)-C(17B)	1.50(2)	C(26B)-H(26D)	0.9800
C(15B)-C(16B)	1.56(2)	C(26B)-H(26E)	0.9800
C(16B)-H(16D)	0.9800	C(26B)-H(26F)	0.9800
C(16B)-H(16E)	0.9800	C(25B)-H(25D)	0.9800
C(16B)-H(16F)	0.9800	C(25B)-H(25E)	0.9800
C(17B)-C(18B)	1.574(19)	C(25B)-H(25F)	0.9800
C(18B)-H(18D)	0.9800	C(24B)-H(24D)	0.9800
C(18B)-H(18E)	0.9800	C(24B)-H(24E)	0.9800
C(18B)-H(18F)	0.9800	C(24B)-H(24F)	0.9800
Si(1B)-C(35B)	1.61(3)		

Table 3. Bond angles [deg] for **db007**.

C(14)-C(1)-C(2)	124.5(3)	C(11)-C(12)-C(13)	120.7(3)
C(14)-C(1)-H(1)	117.7	C(11)-C(12)-C(27)	119.1(3)
C(2)-C(1)-H(1)	117.7	C(13)-C(12)-C(27)	120.2(3)
C(3)-C(2)-C(1)	118.6(3)	C(14)-C(13)-C(12)	121.9(3)
C(3)-C(2)-C(19)	120.3(3)	C(14)-C(13)-C(32)	120.2(3)
C(1)-C(2)-C(19)	121.1(3)	C(12)-C(13)-C(32)	117.6(3)
C(4)-C(3)-C(2)	123.3(4)	C(1)-C(14)-C(13)	125.7(3)
C(4)-C(3)-H(3)	118.3	C(1)-C(14)-C(15)	114.6(6)
C(2)-C(3)-H(3)	118.3	C(13)-C(14)-C(15)	117.7(5)
C(5)-C(4)-C(3)	124.2(4)	C(1)-C(14)-C(15B)	119.2(6)
C(5)-C(4)-C(15)	117.0(6)	C(13)-C(14)-C(15B)	114.2(6)
C(3)-C(4)-C(15)	116.8(6)	C(15)-C(14)-C(15B)	25.7(5)
C(5)-C(4)-C(15B)	115.0(7)	C(4)-C(15)-C(17)	109.2(10)
C(3)-C(4)-C(15B)	119.7(7)	C(4)-C(15)-C(14)	114.3(9)
C(15)-C(4)-C(15B)	25.7(5)	C(17)-C(15)-C(14)	107.4(10)
C(6)-C(5)-C(4)	122.1(4)	C(4)-C(15)-C(16)	107.9(9)
C(6)-C(5)-H(5)	119.0	C(17)-C(15)-C(16)	110.9(13)
C(4)-C(5)-H(5)	119.0	C(14)-C(15)-C(16)	107.2(9)
C(5)-C(6)-C(7)	122.1(4)	C(15)-C(16)-H(16A)	109.5
C(5)-C(6)-H(6)	118.9	C(15)-C(16)-H(16B)	109.5
C(7)-C(6)-H(6)	118.9	H(16A)-C(16)-H(16B)	109.5
C(8)-C(7)-C(6)	123.3(4)	C(15)-C(16)-H(16C)	109.5
C(8)-C(7)-C(17B)	116.9(5)	H(16A)-C(16)-H(16C)	109.5
C(6)-C(7)-C(17B)	117.0(5)	H(16B)-C(16)-H(16C)	109.5
C(8)-C(7)-C(17)	120.0(5)	C(15)-C(17)-C(11)	108.4(9)
C(6)-C(7)-C(17)	114.6(5)	C(15)-C(17)-C(7)	106.2(10)
C(17B)-C(7)-C(17)	32.1(4)	C(11)-C(17)-C(7)	109.0(7)
C(7)-C(8)-C(9)	122.1(4)	C(15)-C(17)-C(18)	111.4(12)
C(7)-C(8)-H(8)	119.0	C(11)-C(17)-C(18)	110.1(7)
C(9)-C(8)-H(8)	119.0	C(7)-C(17)-C(18)	111.5(7)
C(10)-C(9)-C(8)	119.3(4)	C(17)-C(18)-H(18A)	109.5
C(10)-C(9)-C(23)	120.0(5)	C(17)-C(18)-H(18B)	109.5
C(8)-C(9)-C(23)	120.7(4)	H(18A)-C(18)-H(18B)	109.5
C(9)-C(10)-C(11)	124.7(4)	C(17)-C(18)-H(18C)	109.5
C(9)-C(10)-H(10)	117.7	H(18A)-C(18)-H(18C)	109.5
C(11)-C(10)-H(10)	117.7	H(18B)-C(18)-H(18C)	109.5
C(10)-C(11)-C(12)	126.2(4)	C(22)-C(19)-C(20)	108.5(5)
C(10)-C(11)-C(17B)	114.4(5)	C(22)-C(19)-C(2)	113.2(4)
C(12)-C(11)-C(17B)	116.5(5)	C(20)-C(19)-C(2)	108.0(4)
C(10)-C(11)-C(17)	117.1(5)	C(22)-C(19)-C(21B)	128.9(8)
C(12)-C(11)-C(17)	114.9(4)	C(20)-C(19)-C(21B)	68.8(12)
C(17B)-C(11)-C(17)	32.8(4)	C(2)-C(19)-C(21B)	115.8(8)

C(22)-C(19)-C(21)	107.0(6)	C(9)-C(23)-C(26B)	108.8(10)
C(20)-C(19)-C(21)	111.3(6)	C(25B)-C(23)-C(26B)	105.6(6)
C(2)-C(19)-C(21)	108.9(4)	C(26)-C(23)-C(25)	110.5(4)
C(21B)-C(19)-C(21)	43.2(11)	C(24B)-C(23)-C(25)	61.2(10)
C(22)-C(19)-C(22B)	36.7(10)	C(24)-C(23)-C(25)	105.8(4)
C(20)-C(19)-C(22B)	137.6(11)	C(9)-C(23)-C(25)	111.3(5)
C(2)-C(19)-C(22B)	109.3(9)	C(25B)-C(23)-C(25)	52.4(8)
C(21B)-C(19)-C(22B)	110.7(13)	C(26B)-C(23)-C(25)	139.4(10)
C(21)-C(19)-C(22B)	74.4(11)	C(23)-C(24)-H(24A)	109.5
C(22)-C(19)-C(20B)	69.8(9)	C(23)-C(24)-H(24B)	109.5
C(20)-C(19)-C(20B)	44.3(8)	H(24A)-C(24)-H(24B)	109.5
C(2)-C(19)-C(20B)	104.8(7)	C(23)-C(24)-H(24C)	109.5
C(21B)-C(19)-C(20B)	109.6(13)	H(24A)-C(24)-H(24C)	109.5
C(21)-C(19)-C(20B)	144.0(7)	H(24B)-C(24)-H(24C)	109.5
C(22B)-C(19)-C(20B)	106.0(13)	C(23)-C(25)-H(25A)	109.5
C(19)-C(20)-H(20A)	109.5	C(23)-C(25)-H(25B)	109.5
C(19)-C(20)-H(20B)	109.5	H(25A)-C(25)-H(25B)	109.5
H(20A)-C(20)-H(20B)	109.5	C(23)-C(25)-H(25C)	109.5
C(19)-C(20)-H(20C)	109.5	H(25A)-C(25)-H(25C)	109.5
H(20A)-C(20)-H(20C)	109.5	H(25B)-C(25)-H(25C)	109.5
H(20B)-C(20)-H(20C)	109.5	C(23)-C(26)-H(26A)	109.5
C(19)-C(21)-H(21A)	109.5	C(23)-C(26)-H(26B)	109.5
C(19)-C(21)-H(21B)	109.5	H(26A)-C(26)-H(26B)	109.5
H(21A)-C(21)-H(21B)	109.5	C(23)-C(26)-H(26C)	109.5
C(19)-C(21)-H(21C)	109.5	H(26A)-C(26)-H(26C)	109.5
H(21A)-C(21)-H(21C)	109.5	H(26B)-C(26)-H(26C)	109.5
H(21B)-C(21)-H(21C)	109.5	O(1)-C(27)-C(28)	115.8(5)
C(19)-C(22)-H(22A)	109.5	O(1)-C(27)-C(12)	110.6(4)
C(19)-C(22)-H(22B)	109.5	C(28)-C(27)-C(12)	118.0(4)
H(22A)-C(22)-H(22B)	109.5	O(1)-C(27)-H(27)	103.4
C(19)-C(22)-H(22C)	109.5	C(28)-C(27)-H(27)	103.4
H(22A)-C(22)-H(22C)	109.5	C(12)-C(27)-H(27)	103.4
H(22B)-C(22)-H(22C)	109.5	O(1)-C(27)-H(27B)	32.6(2)
C(26)-C(23)-C(24B)	136.7(12)	C(28)-C(27)-H(27B)	99.0(5)
C(26)-C(23)-C(24)	111.7(5)	C(12)-C(27)-H(27B)	98.8(4)
C(24B)-C(23)-C(24)	46.0(11)	H(27)-C(27)-H(27B)	135.9
C(26)-C(23)-C(9)	109.6(4)	C(27)-C(28)-C(29)	121.3(5)
C(24B)-C(23)-C(9)	112.8(11)	C(27)-C(28)-H(28A)	107.0
C(24)-C(23)-C(9)	107.9(4)	C(29)-C(28)-H(28A)	107.0
C(26)-C(23)-C(25B)	60.7(8)	C(27)-C(28)-H(28B)	107.0
C(24B)-C(23)-C(25B)	108.6(7)	C(29)-C(28)-H(28B)	107.0
C(24)-C(23)-C(25B)	138.6(9)	H(28A)-C(28)-H(28B)	106.8
C(9)-C(23)-C(25B)	112.8(9)	C(30)-C(29)-C(28)	123.7(6)
C(26)-C(23)-C(26B)	48.2(9)	C(30)-C(29)-H(29)	118.2
C(24B)-C(23)-C(26B)	107.8(7)	C(28)-C(29)-H(29)	118.2
C(24)-C(23)-C(26B)	66.5(10)	C(29)-C(30)-C(31)	129.9(6)

C(29)-C(30)-H(30)	115.0	H(37A)-C(37)-H(37C)	109.5
C(31)-C(30)-H(30)	115.0	H(37B)-C(37)-H(37C)	109.5
C(30)-C(31)-C(32)	119.2(4)	Si(2)-C(38)-H(38A)	109.5
C(30)-C(31)-H(31A)	107.5	Si(2)-C(38)-H(38B)	109.5
C(32)-C(31)-H(31A)	107.5	H(38A)-C(38)-H(38B)	109.5
C(30)-C(31)-H(31B)	107.5	Si(2)-C(38)-H(38C)	109.5
C(32)-C(31)-H(31B)	107.5	H(38A)-C(38)-H(38C)	109.5
H(31A)-C(31)-H(31B)	107.0	H(38B)-C(38)-H(38C)	109.5
O(2)-C(32)-C(31)	109.2(4)	C(27)-O(1)-Si(1B)	126.4(5)
O(2)-C(32)-C(13)	115.7(3)	C(27)-O(1)-H(27B)	40.7(3)
C(31)-C(32)-C(13)	113.0(4)	Si(1B)-O(1)-H(27B)	164.1(6)
O(2)-C(32)-H(32)	106.1	C(32)-O(2)-Si(2)	123.4(3)
C(31)-C(32)-H(32)	106.1	C(32)-O(2)-H(32B)	43.8(2)
C(13)-C(32)-H(32)	106.1	Si(2)-O(2)-H(32B)	157.9(3)
O(2)-C(32)-H(32B)	40.3(2)	C(33)-Si(1)-C(34)	107.0(8)
C(31)-C(32)-H(32B)	92.5(4)	C(33)-Si(1)-O(1B)	106.5(6)
C(13)-C(32)-H(32B)	91.5(3)	C(34)-Si(1)-O(1B)	85.9(5)
H(32)-C(32)-H(32B)	146.3	C(33)-Si(1)-C(35)	110.1(8)
Si(1)-C(33)-H(33A)	109.5	C(34)-Si(1)-C(35)	109.8(6)
Si(1)-C(33)-H(33B)	109.5	O(1B)-Si(1)-C(35)	133.0(7)
H(33A)-C(33)-H(33B)	109.5	O(2)-Si(2)-C(38)	109.5(3)
Si(1)-C(33)-H(33C)	109.5	O(2)-Si(2)-C(36)	108.7(3)
H(33A)-C(33)-H(33C)	109.5	C(38)-Si(2)-C(36)	111.8(3)
H(33B)-C(33)-H(33C)	109.5	O(2)-Si(2)-C(37)	105.2(3)
Si(1)-C(34)-H(34A)	109.5	C(38)-Si(2)-C(37)	112.1(4)
Si(1)-C(34)-H(34B)	109.5	C(36)-Si(2)-C(37)	109.2(3)
H(34A)-C(34)-H(34B)	109.5	C(17B)-C(15B)-C(14)	109.6(11)
Si(1)-C(34)-H(34C)	109.5	C(17B)-C(15B)-C(16B)	112.8(15)
H(34A)-C(34)-H(34C)	109.5	C(14)-C(15B)-C(16B)	108.0(10)
H(34B)-C(34)-H(34C)	109.5	C(17B)-C(15B)-C(4)	109.5(11)
Si(1)-C(35)-H(35A)	109.5	C(14)-C(15B)-C(4)	110.3(10)
Si(1)-C(35)-H(35B)	109.5	C(16B)-C(15B)-C(4)	106.6(10)
H(35A)-C(35)-H(35B)	109.5	C(15B)-C(16B)-H(16D)	109.5
Si(1)-C(35)-H(35C)	109.5	C(15B)-C(16B)-H(16E)	109.5
H(35A)-C(35)-H(35C)	109.5	H(16D)-C(16B)-H(16E)	109.5
H(35B)-C(35)-H(35C)	109.5	C(15B)-C(16B)-H(16F)	109.5
Si(2)-C(36)-H(36A)	109.5	H(16D)-C(16B)-H(16F)	109.5
Si(2)-C(36)-H(36B)	109.5	H(16E)-C(16B)-H(16F)	109.5
H(36A)-C(36)-H(36B)	109.5	C(15B)-C(17B)-C(11)	106.7(11)
Si(2)-C(36)-H(36C)	109.5	C(15B)-C(17B)-C(7)	105.1(11)
H(36A)-C(36)-H(36C)	109.5	C(11)-C(17B)-C(7)	111.3(7)
H(36B)-C(36)-H(36C)	109.5	C(15B)-C(17B)-C(18B)	111.2(14)
Si(2)-C(37)-H(37A)	109.5	C(11)-C(17B)-C(18B)	110.8(8)
Si(2)-C(37)-H(37B)	109.5	C(7)-C(17B)-C(18B)	111.6(8)
H(37A)-C(37)-H(37B)	109.5	C(17B)-C(18B)-H(18D)	109.5
Si(2)-C(37)-H(37C)	109.5	C(17B)-C(18B)-H(18E)	109.5

H(18D)-C(18B)-H(18E)	109.5	H(20D)-C(20B)-H(20F)	109.5
C(17B)-C(18B)-H(18F)	109.5	H(20E)-C(20B)-H(20F)	109.5
H(18D)-C(18B)-H(18F)	109.5	O(2B)-Si(2B)-C(38B)	112.1(11)
H(18E)-C(18B)-H(18F)	109.5	O(2B)-Si(2B)-C(37B)	111.3(10)
O(1)-Si(1B)-C(35B)	102.2(11)	C(38B)-Si(2B)-C(37B)	111.9(7)
O(1)-Si(1B)-C(34B)	119.3(9)	O(2B)-Si(2B)-C(36B)	92.5(18)
C(35B)-Si(1B)-C(34B)	102.9(13)	C(38B)-Si(2B)-C(36B)	122(2)
O(1)-Si(1B)-C(33B)	98.0(14)	C(37B)-Si(2B)-C(36B)	105(2)
C(35B)-Si(1B)-C(33B)	121.5(18)	Si(2B)-C(38B)-H(38D)	109.5
C(34B)-Si(1B)-C(33B)	113.6(17)	Si(2B)-C(38B)-H(38E)	109.5
Si(1B)-C(35B)-H(35D)	109.5	H(38D)-C(38B)-H(38E)	109.5
Si(1B)-C(35B)-H(35E)	109.5	Si(2B)-C(38B)-H(38F)	109.5
H(35D)-C(35B)-H(35E)	109.5	H(38D)-C(38B)-H(38F)	109.5
Si(1B)-C(35B)-H(35F)	109.5	H(38E)-C(38B)-H(38F)	109.5
H(35D)-C(35B)-H(35F)	109.5	Si(2B)-C(37B)-H(37D)	109.5
H(35E)-C(35B)-H(35F)	109.5	Si(2B)-C(37B)-H(37E)	109.5
Si(1B)-C(34B)-H(34D)	109.5	H(37D)-C(37B)-H(37E)	109.5
Si(1B)-C(34B)-H(34E)	109.5	Si(2B)-C(37B)-H(37F)	109.5
H(34D)-C(34B)-H(34E)	109.5	H(37D)-C(37B)-H(37F)	109.5
Si(1B)-C(34B)-H(34F)	109.5	H(37E)-C(37B)-H(37F)	109.5
H(34D)-C(34B)-H(34F)	109.5	Si(2B)-C(36B)-H(36D)	109.5
H(34E)-C(34B)-H(34F)	109.5	Si(2B)-C(36B)-H(36E)	109.5
Si(1B)-C(33B)-H(33D)	109.5	H(36D)-C(36B)-H(36E)	109.5
Si(1B)-C(33B)-H(33E)	109.5	Si(2B)-C(36B)-H(36F)	109.5
H(33D)-C(33B)-H(33E)	109.5	H(36D)-C(36B)-H(36F)	109.5
Si(1B)-C(33B)-H(33F)	109.5	H(36E)-C(36B)-H(36F)	109.5
H(33D)-C(33B)-H(33F)	109.5	C(23)-C(26B)-H(26D)	109.5
H(33E)-C(33B)-H(33F)	109.5	C(23)-C(26B)-H(26E)	109.5
C(19)-C(22B)-H(22D)	109.5	H(26D)-C(26B)-H(26E)	109.5
C(19)-C(22B)-H(22E)	109.5	C(23)-C(26B)-H(26F)	109.5
H(22D)-C(22B)-H(22E)	109.5	H(26D)-C(26B)-H(26F)	109.5
C(19)-C(22B)-H(22F)	109.5	H(26E)-C(26B)-H(26F)	109.5
H(22D)-C(22B)-H(22F)	109.5	C(23)-C(25B)-H(25D)	109.5
H(22E)-C(22B)-H(22F)	109.5	C(23)-C(25B)-H(25E)	109.5
C(19)-C(21B)-H(21D)	109.5	H(25D)-C(25B)-H(25E)	109.5
C(19)-C(21B)-H(21E)	109.5	C(23)-C(25B)-H(25F)	109.5
H(21D)-C(21B)-H(21E)	109.5	H(25D)-C(25B)-H(25F)	109.5
C(19)-C(21B)-H(21F)	109.5	H(25E)-C(25B)-H(25F)	109.5
H(21D)-C(21B)-H(21F)	109.5	C(23)-C(24B)-H(24D)	109.5
H(21E)-C(21B)-H(21F)	109.5	C(23)-C(24B)-H(24E)	109.5
C(19)-C(20B)-H(20D)	109.5	H(24D)-C(24B)-H(24E)	109.5
C(19)-C(20B)-H(20E)	109.5	C(23)-C(24B)-H(24F)	109.5
H(20D)-C(20B)-H(20E)	109.5	H(24D)-C(24B)-H(24F)	109.5
C(19)-C(20B)-H(20F)	109.5	H(24E)-C(24B)-H(24F)	109.5

Symmetry transformations used to generate equivalent atoms:

Table 4. Anisotropic displacement parameters (A^2 x 10^3) for db007.

The anisotropic displacement factor exponent takes the form:
-2 pi^2 [h^2 a*^2 U11 + ... + 2 h k a* b* U12]

	U11	U22	U33	U23	U13	U12
C(1)	60(2)	41(2)	44(2)	3(2)	0(2)	18(2)
C(2)	72(3)	41(2)	47(2)	1(2)	1(2)	22(2)
C(3)	90(3)	51(2)	44(2)	-3(2)	4(2)	33(2)
C(4)	90(3)	49(2)	42(2)	0(2)	2(2)	24(2)
C(5)	130(4)	69(3)	43(3)	2(2)	3(3)	41(3)
C(6)	123(4)	75(3)	47(3)	12(2)	-6(3)	39(3)
C(7)	101(4)	66(3)	60(3)	12(2)	-5(3)	37(3)
C(8)	102(4)	67(3)	76(3)	24(3)	-3(3)	32(3)
C(9)	78(3)	57(3)	98(4)	24(3)	-6(3)	26(2)
C(10)	64(3)	50(3)	83(3)	6(2)	0(2)	20(2)
C(11)	56(3)	46(2)	68(3)	4(2)	4(2)	21(2)
C(12)	47(2)	35(2)	60(3)	-3(2)	6(2)	7(2)
C(13)	49(2)	39(2)	47(2)	-4(2)	4(2)	6(2)
C(14)	53(2)	34(2)	43(2)	1(2)	-2(2)	9(2)
C(15)	63(8)	43(7)	47(5)	4(5)	-1(6)	27(6)
C(16)	59(6)	53(6)	60(5)	9(5)	10(4)	20(5)
C(17)	61(7)	41(6)	55(5)	2(4)	-6(5)	18(5)
C(18)	62(6)	49(6)	75(6)	-2(5)	-32(5)	17(5)
C(19)	81(3)	50(2)	56(3)	1(2)	2(2)	36(2)
C(20)	157(8)	44(4)	68(6)	2(4)	-28(5)	46(4)
C(21)	114(8)	113(8)	98(8)	27(6)	13(6)	73(6)
C(22)	102(8)	70(6)	61(5)	-6(4)	-24(5)	55(6)
C(23)	108(5)	79(4)	108(4)	30(3)	-4(4)	54(3)
C(24)	95(6)	91(5)	130(7)	-5(5)	-34(5)	59(4)
C(25)	154(9)	99(7)	146(8)	48(6)	-16(6)	76(6)
C(26)	194(11)	31(4)	270(14)	6(6)	-119(10)	36(5)
C(28)	122(5)	104(5)	152(6)	-74(4)	-3(4)	27(4)
C(29)	108(5)	66(3)	90(4)	-21(3)	0(3)	-9(3)
C(30)	86(4)	79(4)	103(4)	-27(3)	-22(3)	2(3)
C(31)	161(6)	74(4)	87(4)	-5(3)	-47(4)	13(4)
C(33)	72(7)	165(12)	209(18)	-56(13)	0(11)	-17(7)
C(34)	145(12)	100(9)	202(16)	31(9)	95(11)	22(8)
C(35)	156(13)	142(12)	340(20)	128(13)	125(15)	100(11)

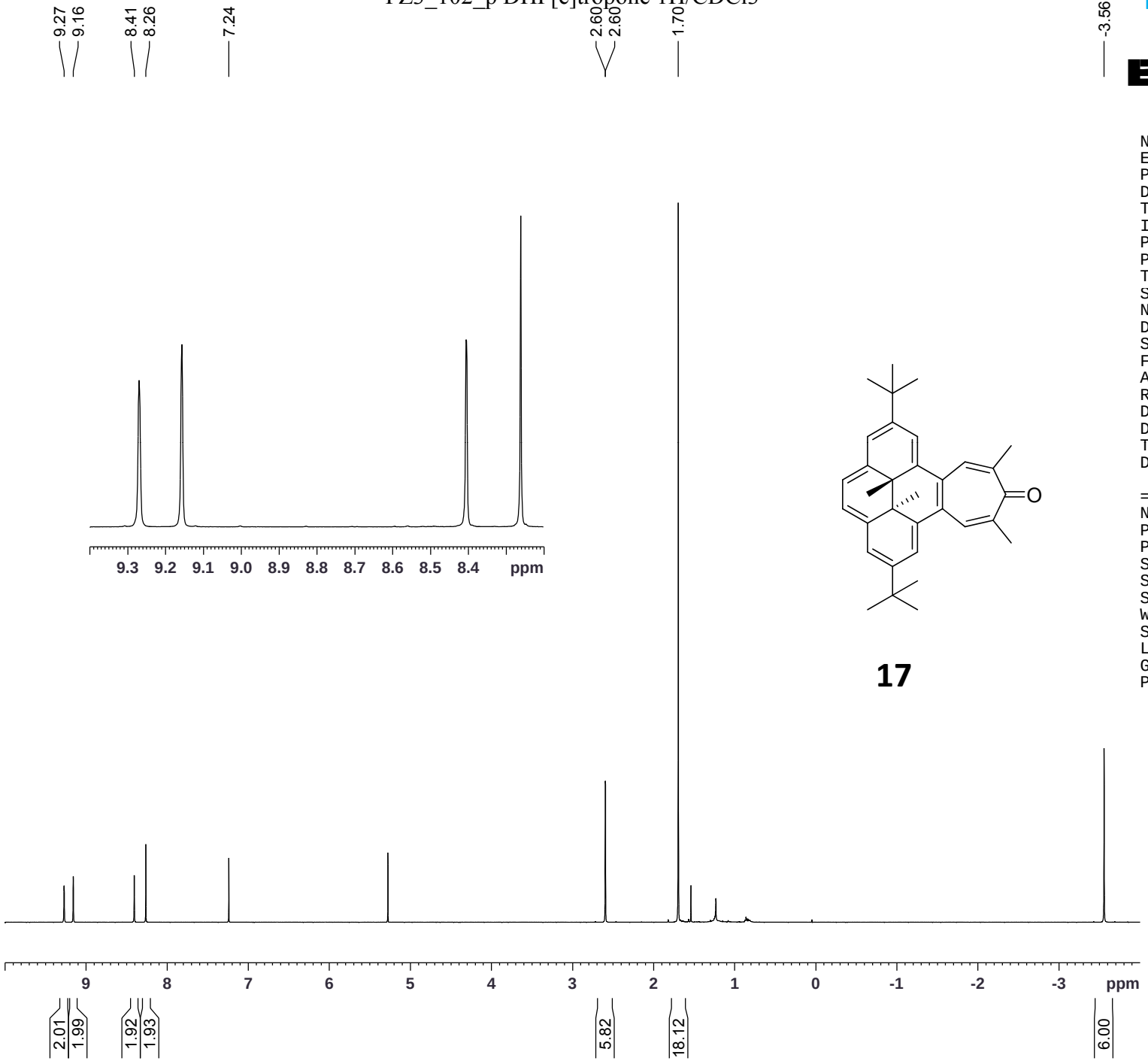
C(36)	153(7)	92(5)	105(6)	28(4)	68(5)	52(5)
C(37)	150(8)	38(5)	113(6)	12(4)	31(6)	21(5)
C(38)	108(7)	194(11)	99(7)	21(7)	-14(5)	-47(7)
O(1)	83(3)	53(3)	112(4)	23(3)	49(3)	34(2)
O(2)	72(3)	50(2)	56(2)	8(2)	17(2)	26(2)
Si(1)	66(3)	117(4)	114(4)	19(3)	25(3)	35(2)
Si(2)	87(2)	64(2)	61(1)	20(1)	24(1)	26(2)
C(15B)	61(9)	41(7)	46(6)	4(5)	3(7)	18(6)
C(16B)	62(8)	46(6)	60(6)	7(5)	-22(5)	15(5)
C(17B)	59(7)	41(6)	46(5)	9(4)	0(5)	7(5)
C(18B)	58(7)	48(7)	71(7)	14(5)	7(5)	12(5)
O(1B)	69(6)	63(6)	91(7)	2(5)	5(5)	38(5)
Si(1B)	43(3)	80(4)	92(6)	-13(4)	5(4)	21(2)
C(35B)	170(30)	150(20)	121(19)	10(17)	-8(16)	90(20)
C(34B)	87(14)	53(11)	170(20)	8(11)	36(13)	48(10)
C(33B)	150(20)	230(30)	90(20)	-90(20)	-20(17)	-70(20)
C(22B)	62(15)	77(16)	110(20)	-22(13)	-23(13)	34(11)
C(21B)	130(20)	94(17)	60(12)	-17(11)	-7(12)	81(16)
C(20B)	89(13)	48(10)	104(19)	8(11)	-6(12)	20(9)
O(2B)	106(13)	86(12)	85(11)	16(9)	34(10)	18(10)
Si(2B)	201(19)	121(12)	120(16)	22(10)	33(13)	-56(11)
C(38B)	120(20)	90(20)	80(20)	-22(16)	-20(18)	-7(18)
C(37B)	140(20)	31(16)	32(12)	-14(11)	17(13)	-26(16)
C(36B)	160(30)	160(40)	270(50)	-30(30)	70(30)	60(30)
C(26B)	100(20)	100(20)	190(30)	120(20)	20(20)	31(18)
C(25B)	120(20)	29(11)	64(16)	7(11)	-10(14)	10(12)
C(24B)	100(20)	130(20)	190(30)	-10(30)	-110(20)	2(19)

Appendix VI. 1H and 13 C NMR spectra

(120 pages)

PZ3_102_p DHP[e]tropone 1H/CDCl3

PZ_III_102 Tropone 1H NMR



17

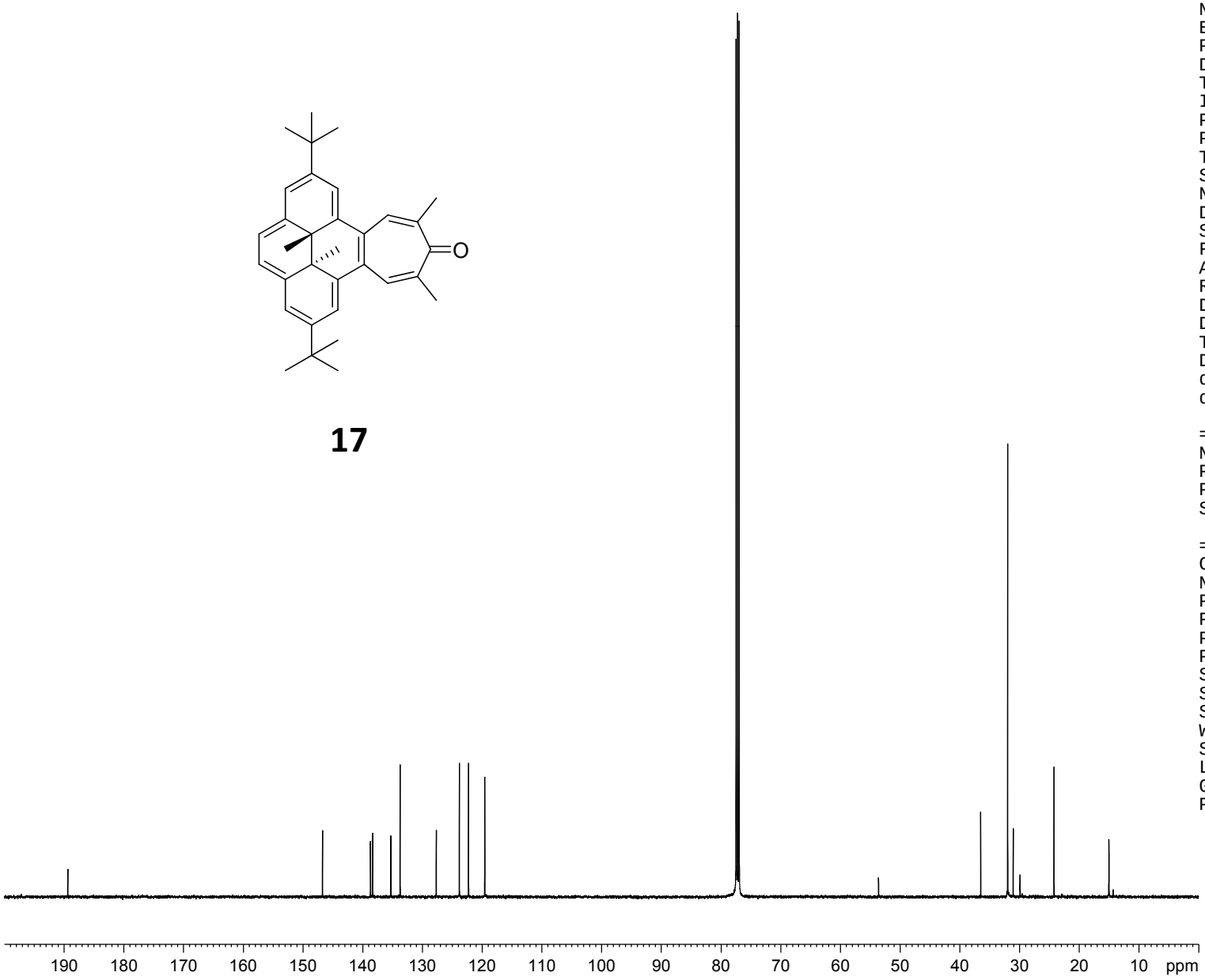
NAME	pz3_102_p 2D
EXPNO	1
PROCNO	1
Date_	20080124
Time	8.11
INSTRUM	AV500
PROBHD	5 mm BBI 1H-BB
PULPROG	zg30
TD	32768
SOLVENT	CDCl3
NS	16
DS	2
SWH	8012.820 Hz
FIDRES	0.244532 Hz
AQ	2.0448356 sec
RG	101.6
DW	62.400 usec
DE	6.00 usec
TE	300.0 K
D1	1.00000000 sec
======== CHANNEL f1 ========	
NUC1	1H
P1	10.00 usec
PL1	-4.00 dB
SFO1	500.1315200 MHz
SI	16384
SF	500.1300236 MHz
WDW	GM
SSB	0
LB	-0.20 Hz
GB	0.5
PC	1.00

PZ3_102 (trans-13c,13d)-10,12,13c,13d-tetramethyl-13c,13d-dihydropyreno[e]tropone 13C/CDCl3

PZ_III_102 Tropone 13C NMR



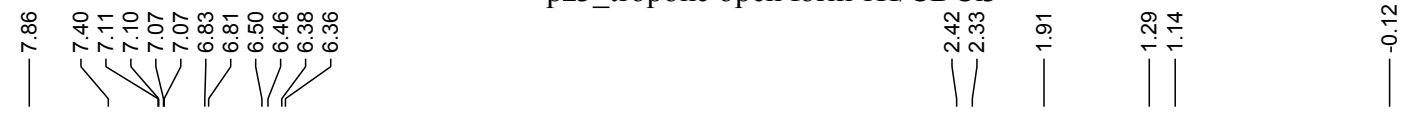
17

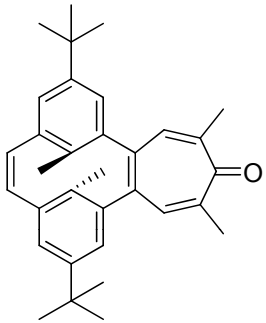


NAME	pz3_102_13C
EXPNO	1
PROCNO	1
Date_	20080128
Time	18.20
INSTRUM	AV500
PROBHD	5 mm BBO BB-1H
PULPROG	zgpg30
TD	65536
SOLVENT	CDCl3
NS	15360
DS	4
SWH	30864.197 Hz
FIDRES	0.470950 Hz
AQ	1.0617495 sec
RG	18390.4
DW	16.200 usec
DE	18.00 usec
TE	300.0 K
D1	1.00000000 sec
d11	0.03000000 sec
d12	0.00002000 sec
======== CHANNEL f1 ========	
NUC1	13C
P1	10.00 usec
PL1	3.00 dB
SFO1	125.7715390 MHz
======== CHANNEL f2 ========	
CPDPRG2	waltz16
NUC2	1H
PCPD2	80.00 usec
PL2	-4.00 dB
PL12	14.24 dB
PL13	14.24 dB
SFO2	500.1325200 MHz
SI	32768
SF	125.7577610 MHz
WDW	EM
SSB	0
LB	0.90 Hz
GB	0
PC	1.40

pz3_tropone open form 1H/CDCl3

PZ_III_102 tropone open 1H nmr

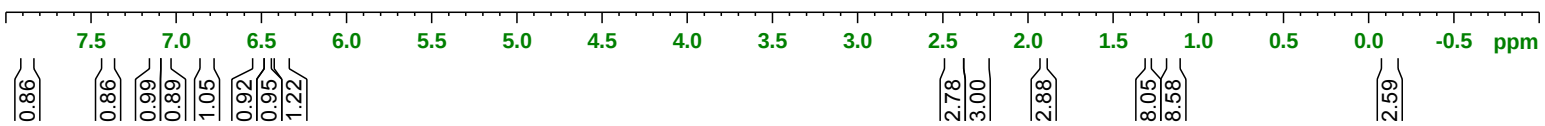




17-o

```
NAME      pz3_tropone open
EXPNO                    1
PROCNO                   1
Date_             20080709
Time                 20.54
INSTRUM              spect
PROBHD   5 mm PABBO BB-
PULPROG              zg30
TD                  32768
SOLVENT             CDCl3
NS                     16
DS                      2
SWH              8012.820 Hz
FIDRES           0.244532 Hz
AQ               2.0448356 sec
RG                   40.3
DW                 62.400 usec
DE                  6.50 usec
TE                 296.4 K
D1              1.00000000 sec
TD0                      1

======== CHANNEL f1 ========
NUC1                    1H
P1                   9.60 usec
PL1                 -4.00 dB
SFO1          500.1315200 MHz
SI                   16384
SF            500.1300237 MHz
WDW                     GM
SSB                      0
LB                   -0.20 Hz
GB                    0.5
PC                   1.00
```

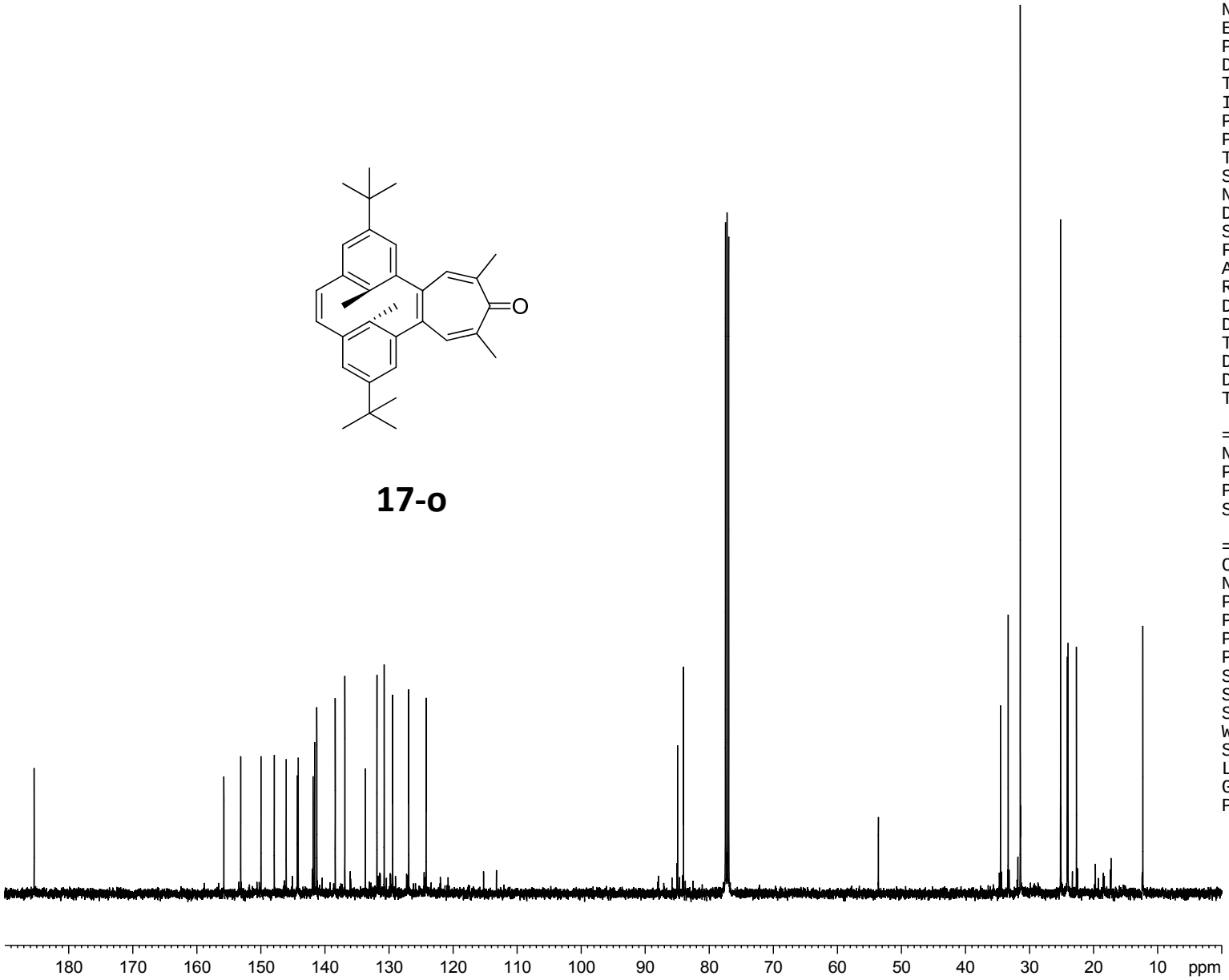


pz3_tropone open form 400 scans 13C/CDCl3

PZ_III_102 TROPONE OPEN 13C NMR



17-o



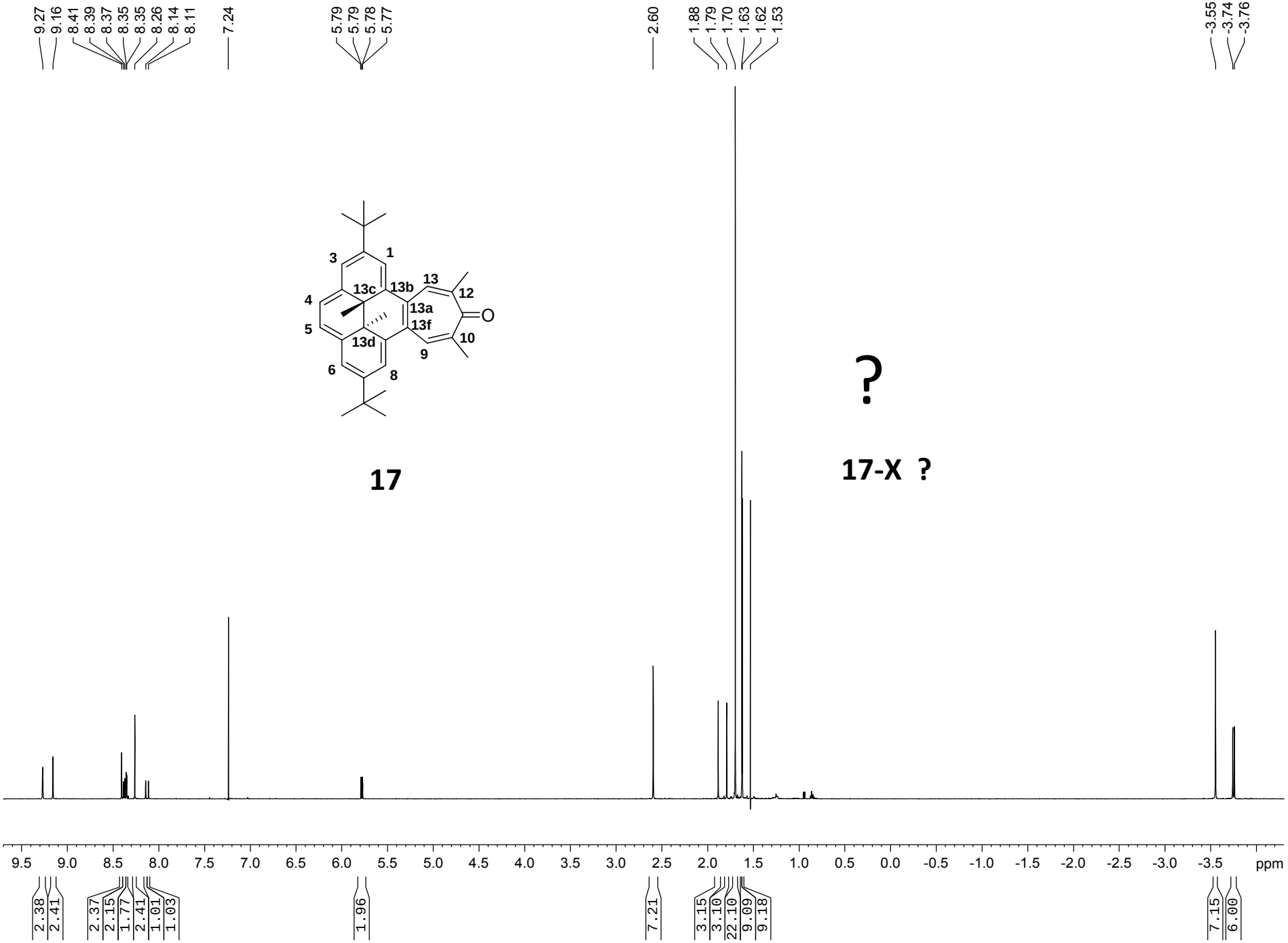

```
NAME        pz3_tropone open
EXPNO                     2
PROCNO                    1
Date_              20080709
Time                 21.02
INSTRUM              spect
PROBHD    5 mm PABBO BB-
PULPROG             zgpg30
TD                   65536
SOLVENT              CDCl3
NS                     400
DS                       4
SWH              30864.197 Hz
FIDRES            0.470950 Hz
AQ                1.0617495 sec
RG                  14596.5
DW                  16.200 usec
DE                   6.50 usec
TE                  298.0 K
D1               1.00000000 sec
D11              0.03000000 sec
TD0                      1

======== CHANNEL f1 ========
NUC1                   13C
P1                  10.00 usec
PL1                  3.00 dB
SFO1          125.7715390 MHz

======== CHANNEL f2 ========
CPDPRG2           waltz16
NUC2                   1H
PCPD2               80.00 usec
PL2                 -4.00 dB
PL12                14.42 dB
PL13                14.24 dB
SFO2          500.1325200 MHz
SI                  32768
SF            125.7577684 MHz
WDW                    EM
SSB                     0
LB                   0.90 Hz
GB                      0
PC                   1.40
```

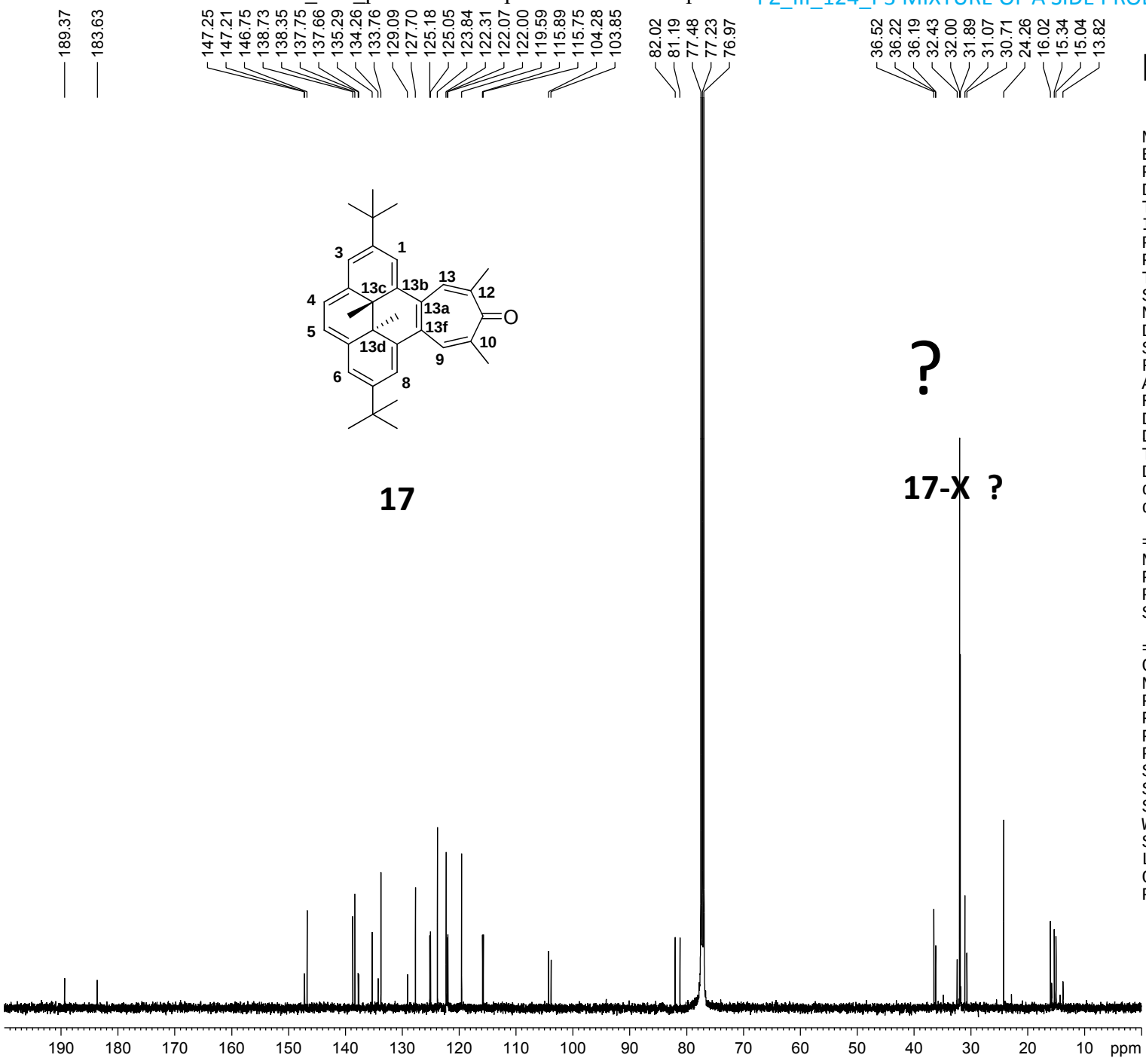
PZ3_124_p3 Mixture of product and a side product 1H/CDCl3

PZ_III_124_P3 MIXTURE OF A SIDE PRODUCT OF TROPONE 1H NMR



PZ3_124_p3 Mixture of product and a side product 13C/CDCl3

PZ_III_124_P3 MIXTURE OF A SIDE PRODUCT OF TROPONE 13C NMR



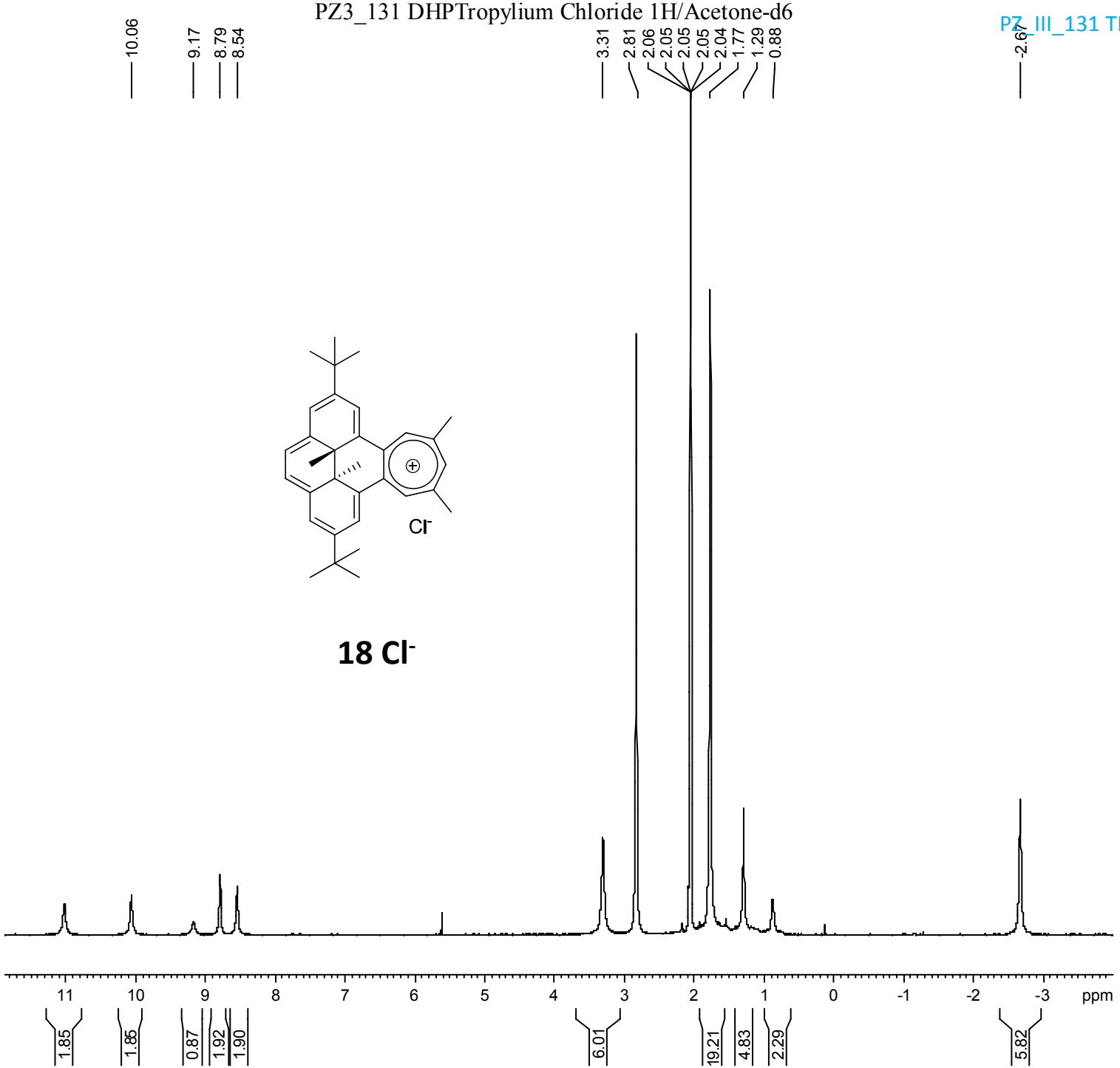

```
NAME          pz3_124_p3 p
EXPNO                   2
PROCNO                  1
Date_            20080222
Time                18.58
INSTRUM             AV500
PROBHD   5 mm BBO BB-1H
PULPROG           zgpg30
TD                 65536
SOLVENT             CDCl3
NS                  18432
DS                      4
SWH           30864.197 Hz
FIDRES         0.470950 Hz
AQ             1.0617495 sec
RG                  16384
DW                16.200 usec
DE                18.00 usec
TE                300.0 K
D1             1.00000000 sec
d11            0.03000000 sec
d12            0.00002000 sec

======== CHANNEL f1 ========
NUC1                  13C
P1                 10.00 usec
PL1                 3.00 dB
SFO1         125.7715390 MHz

======== CHANNEL f2 ========
CPDPRG2           waltz16
NUC2                  1H
PCPD2              80.00 usec
PL2                -4.00 dB
PL12               14.24 dB
PL13               14.24 dB
SFO2         500.1325200 MHz
SI                 32768
SF           125.7577615 MHz
WDW                   EM
SSB                    0
LB                  0.90 Hz
GB                     0
PC                  1.40
```

PZ3_131 DHPTropylium Chloride 1H/Acetone-d6

PZ_III_131 TROPYLIUM CHLORIDE 1H NMR




```
Current Data Parameters
NAME                  pz3_131
EXPNO                       1
PROCNO                      1

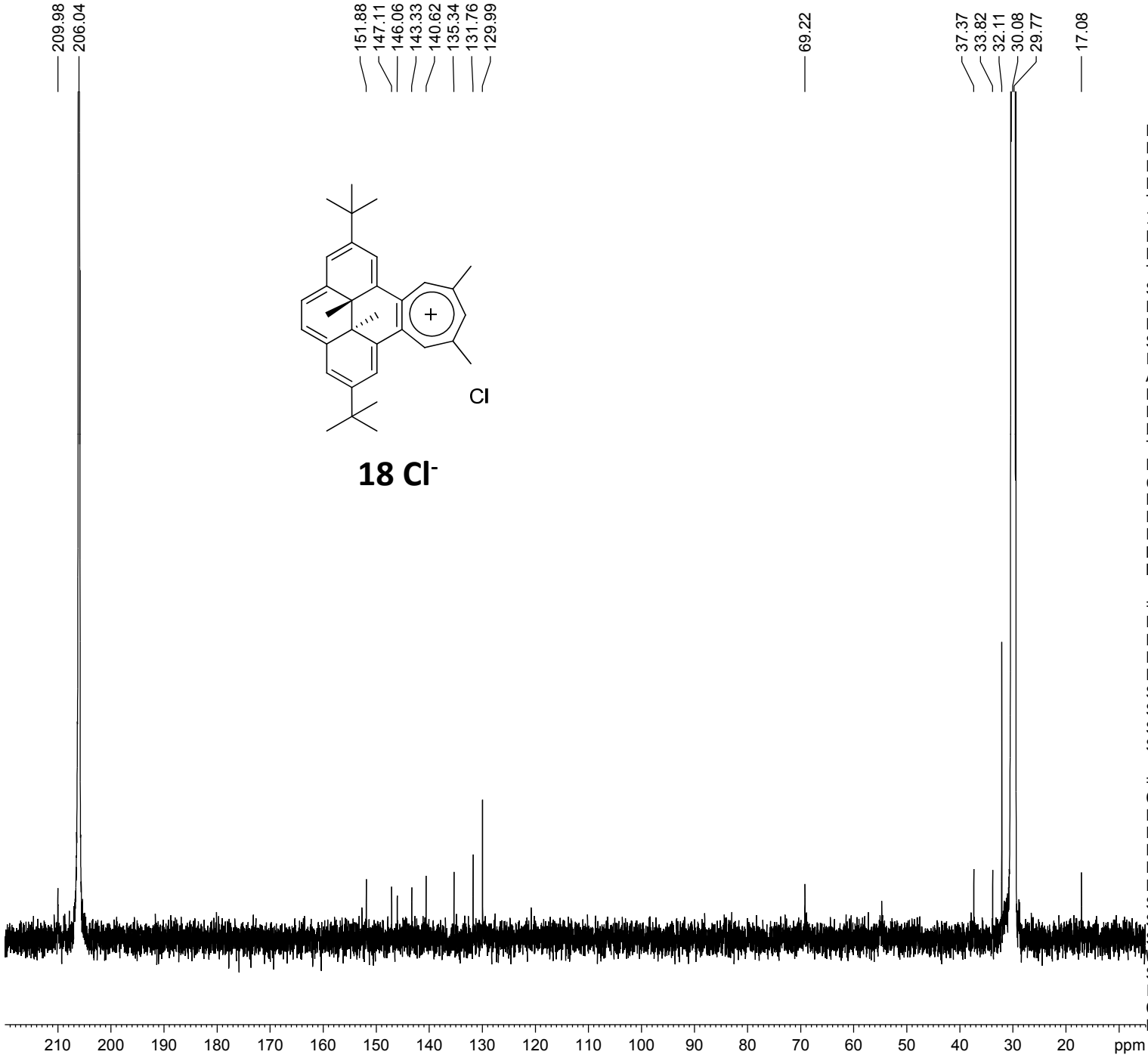
F2 - Acquisition Parameters
Date_                20080313
Time                    19.27
INSTRUM                 AV500
PROBHD    5 mm BBI 1H-BB
PULPROG                  zg30
TD                      32768
SOLVENT               Acetone
NS                         16
DS                          2
SWH                10000.000 Hz
FIDRES             0.305176 Hz
AQ                 1.6385000 sec
RG                        362
DW                     50.000 use
DE                      6.00 use
TE                     300.0 K
D1                 1.00000000 sec

======== CHANNEL f1 ========
NUC1                       1H
P1                      10.20 use
PL1                      1.00 dB
SFO1              500.1315200 MHz

F2 - Processing parameters
SI                      16384
SF                500.1300148 MHz
WDW                        EM
SSB                         0
LB                      0.50 Hz
GB                          0
PC                      1.00
```

PZ3_131 DHPTropylium Chloride 13C/Acetone-d6

PZ_III_131 TROPYLIUM Cl CATION 13C NMR



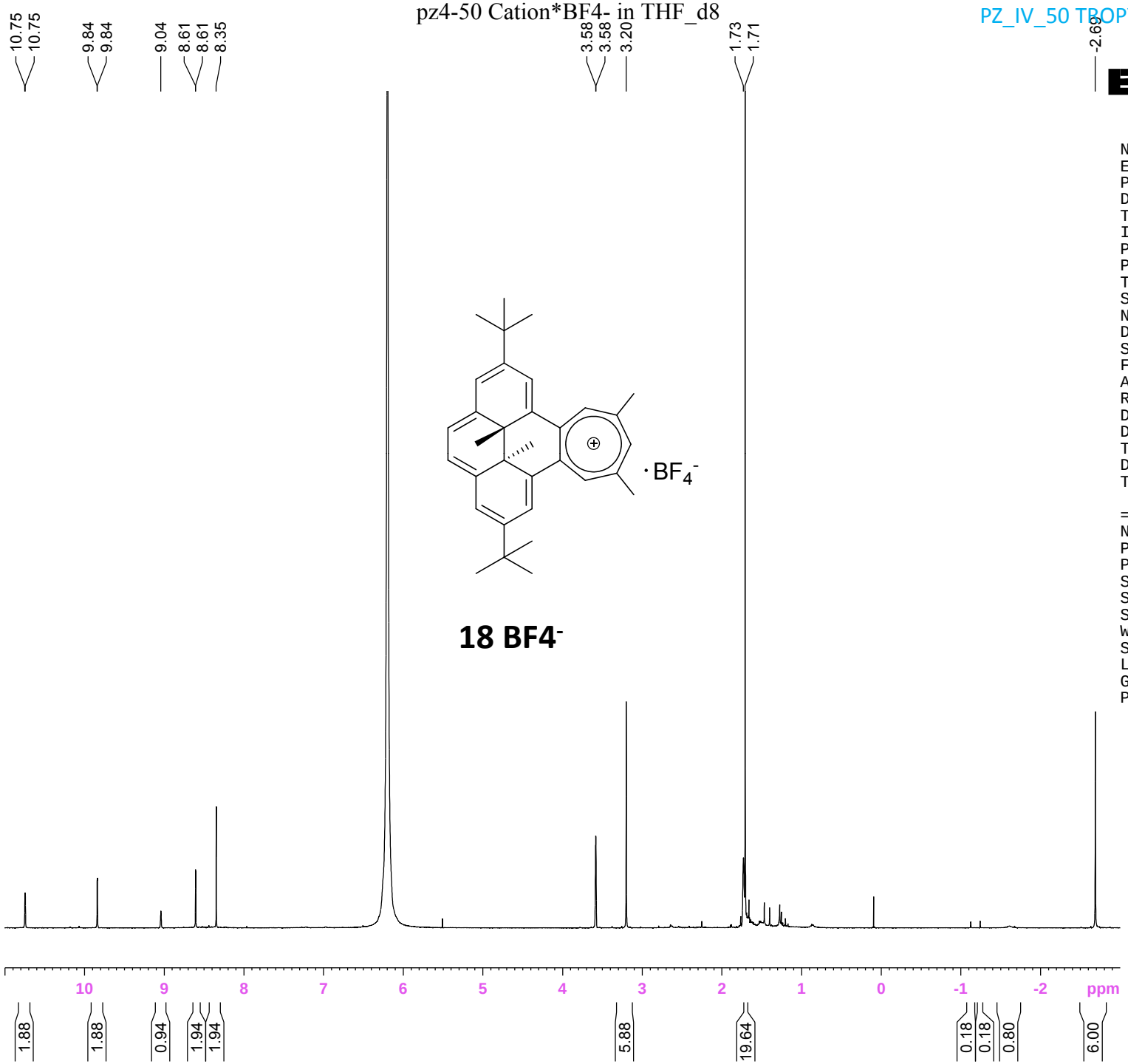

```
NAME            pz3_131 2D
EXPNO                    5
PROCNO                   1
Date_             20080314
Time                 8.35
INSTRUM              AV500
PROBHD    5 mm BBI 1H-BB
PULPROG    zgpg_echo1.mm
TD                   65536
SOLVENT           Acetone
NS                   14864
DS                       4
SWH            30864.197 Hz
FIDRES          0.470950 Hz
AQ              1.0617495 sec
RG                   16384
DW                  16.200 usec
DE                  18.00 usec
TE                  300.0 K
D1              1.00000000 sec
d11             0.03000000 sec
D20             0.00010000 sec
D21             0.00011460 sec
DELTA           0.89999998 sec
MCREST          0.01500000 sec
MCWRK           0.01500000 sec

======== CHANNEL f1 ========
NUC1                   13C
P1                   14.60 usec
P8                 2000.00 usec
PL1                  -1.00 dB
SFO1          125.7715390 MHz
SP13                 3.87 dB
SPNAM13      Crp60comp.4
SPOFF13              0.00 Hz

======== CHANNEL f2 ========
CPDPRG2           waltz16
NUC2                   1H
PCPD2                80.00 usec
PL2                   1.00 dB
PL12                 19.40 dB
PL13                 19.40 dB
SFO2          500.1325200 MHz
SI                   32768
SF            125.7576851 MHz
WDW                    EM
SSB                     0
LB                   1.50 Hz
GB                      0
PC                   1.40
```

pz4-50 Cation*BF4- in THF_d8

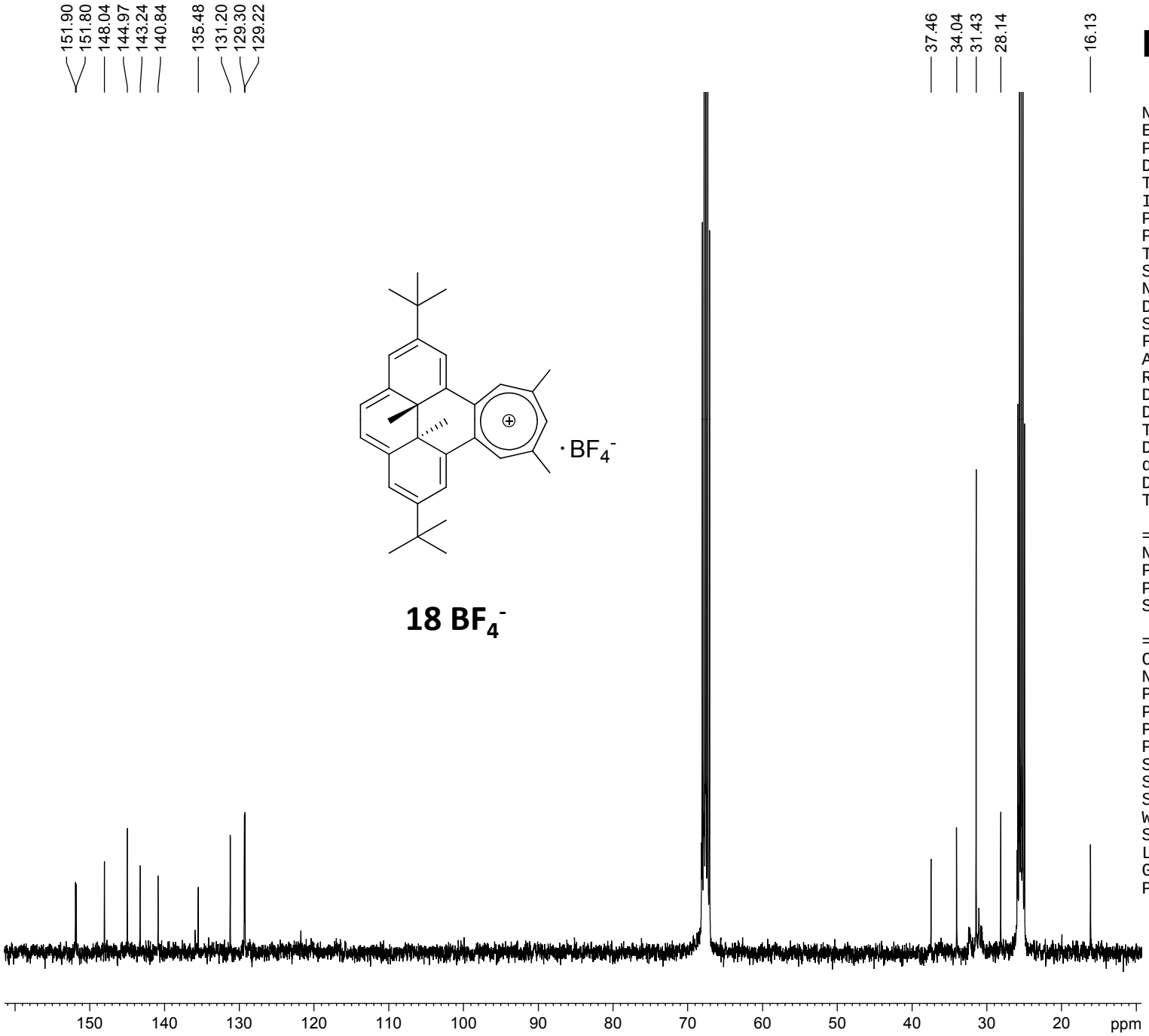
PZ_IV_50 TROPYLIUM BF4 CATION 1H NMR



NAME	PZ4_50 cation
EXPNO	1
PROCNO	1
Date_	20090416
Time	19.46
INSTRUM	av360
PROBHD	5 mm Multinucl
PULPROG	zg30
TD	32768
SOLVENT	THF
NS	16
DS	2
SWH	6493.506 Hz
FIDRES	0.198166 Hz
AQ	2.5231860 sec
RG	144
DW	77.000 usec
DE	6.00 usec
TE	292.6 K
D1	1.00000000 sec
TD0	1
======== CHANNEL f1 ========	
NUC1	1H
P1	8.00 usec
PL1	-2.00 dB
SFO1	360.1310804 MHz
SI	16384
SF	360.1300102 MHz
WDW	GM
SSB	0
LB	-0.20 Hz
GB	0.5
PC	1.00

pz4-50 Cation*BF4- 13C in THF_d8

PZ_IV_50 TROPYLIUM BF4 CATION 13C NMR



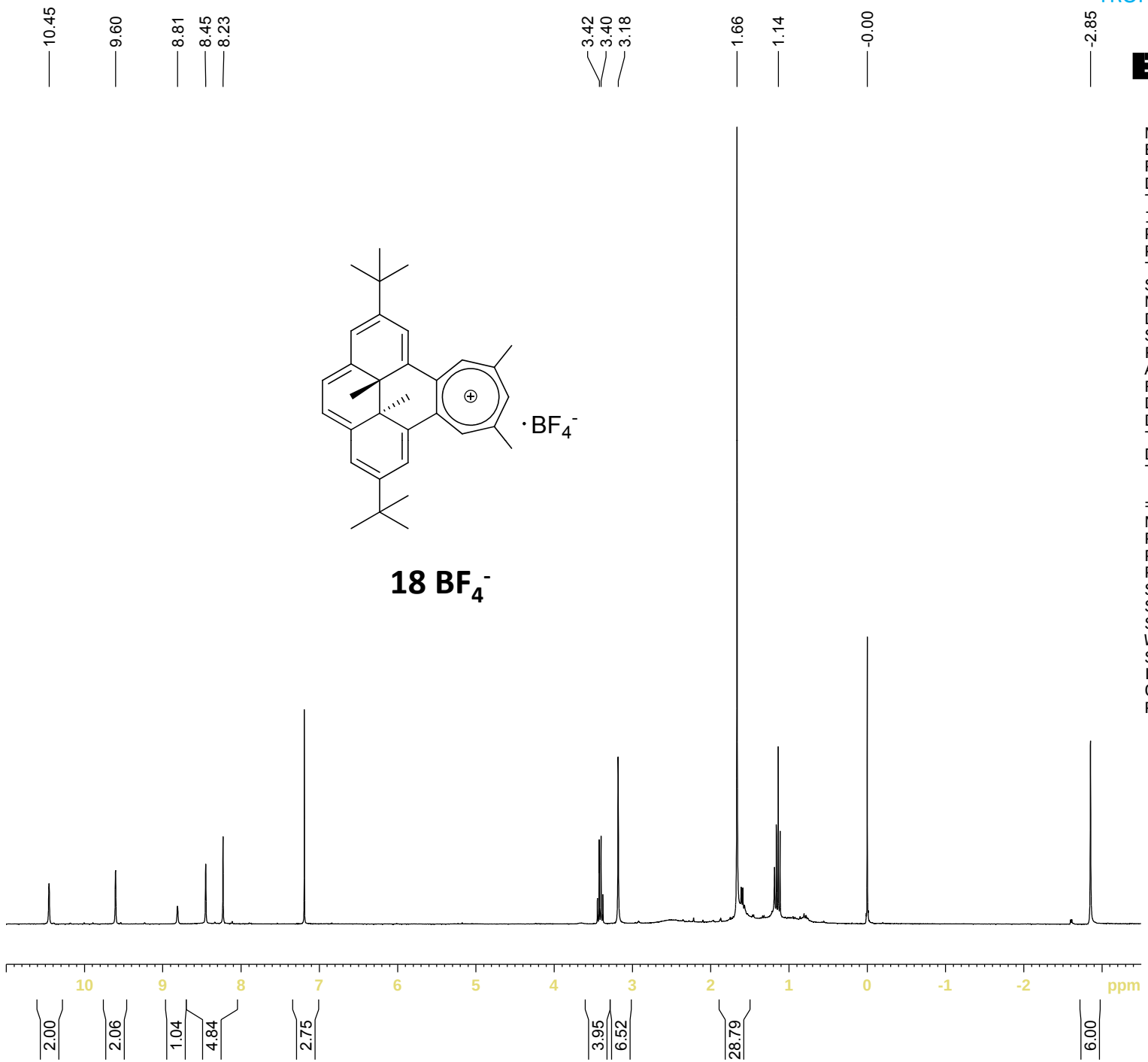

```
NAME          PZ4_50 cation
EXPNO                    4
PROCNO                   1
Date_             20090416
Time                 22.37
INSTRUM              av360
PROBHD    5 mm Multinucl
PULPROG             zgpg30
TD                   32768
SOLVENT                THF
NS                    2048
DS                       2
SWH             20000.000 Hz
FIDRES          0.610352 Hz
AQ              0.8192500 sec
RG                     228
DW                25.000 usec
DE                 6.00 usec
TE                293.4 K
D1            1.00000000 sec
d11           0.03000000 sec
DELTA         0.89999998 sec
TD0                      1

======== CHANNEL f1 ========
NUC1                   13C
P1                  9.10 usec
PL1                -2.00 dB
SFO1          90.5633610 MHz

======== CHANNEL f2 ========
CPDPRG2           waltz16
NUC2                   1H
PCPD2              80.00 usec
PL2                -2.00 dB
PL12               17.47 dB
PL13               17.47 dB
SFO2         360.1317200 MHz
SI                   16384
SF            90.5546612 MHz
WDW                    EM
SSB                     0
LB                 1.20 Hz
GB                      0
PC                 1.40
```

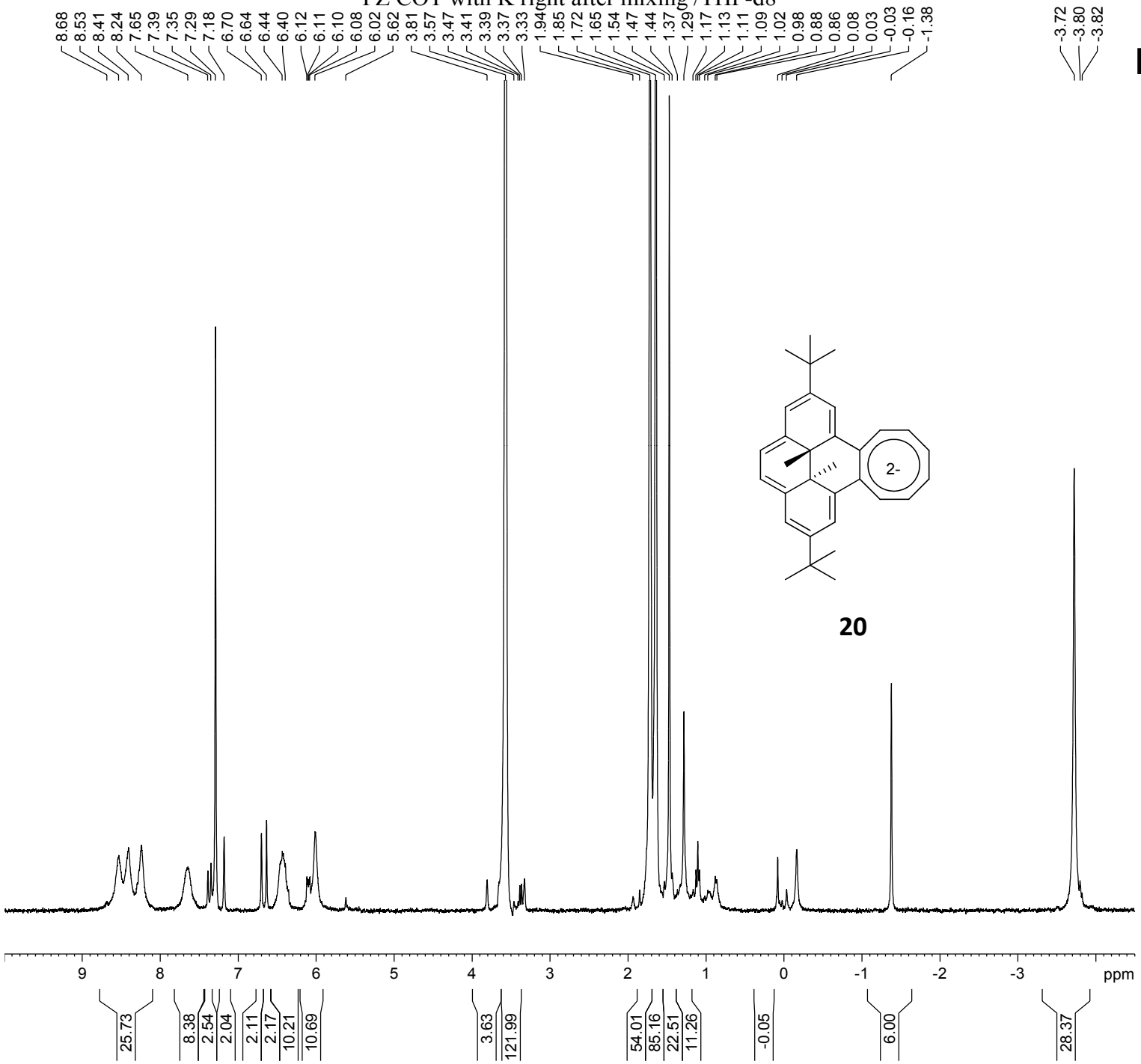
PZ CAtion CDCl3

TROPYLIUM BF4 CATION 1H NMR



NAME	May20-2009
EXPNO	45
PROCNO	1
Date_	20090520
Time	17.03
INSTRUM	spect
PROBHD	5 mm PABBO BB-
PULPROG	zg30
TD	32768
SOLVENT	CDCl3
NS	16
DS	2
SWH	6009.615 Hz
FIDRES	0.183399 Hz
AQ	2.7263477 sec
RG	203
DW	83.200 usec
DE	6.50 usec
TE	300.0 K
D1	1.00000000 sec
TD0	1
======== CHANNEL f1 ========	
NUC1	1H
P1	14.10 usec
PL1	2.00 dB
PL1W	7.33805561 W
SFO1	300.1312000 MHz
SI	16384
SF	300.1300229 MHz
WDW	EM
SSB	0
LB	0.35 Hz
GB	0
PC	1.00

PZ COT with K right after mixing /THF-d8



20

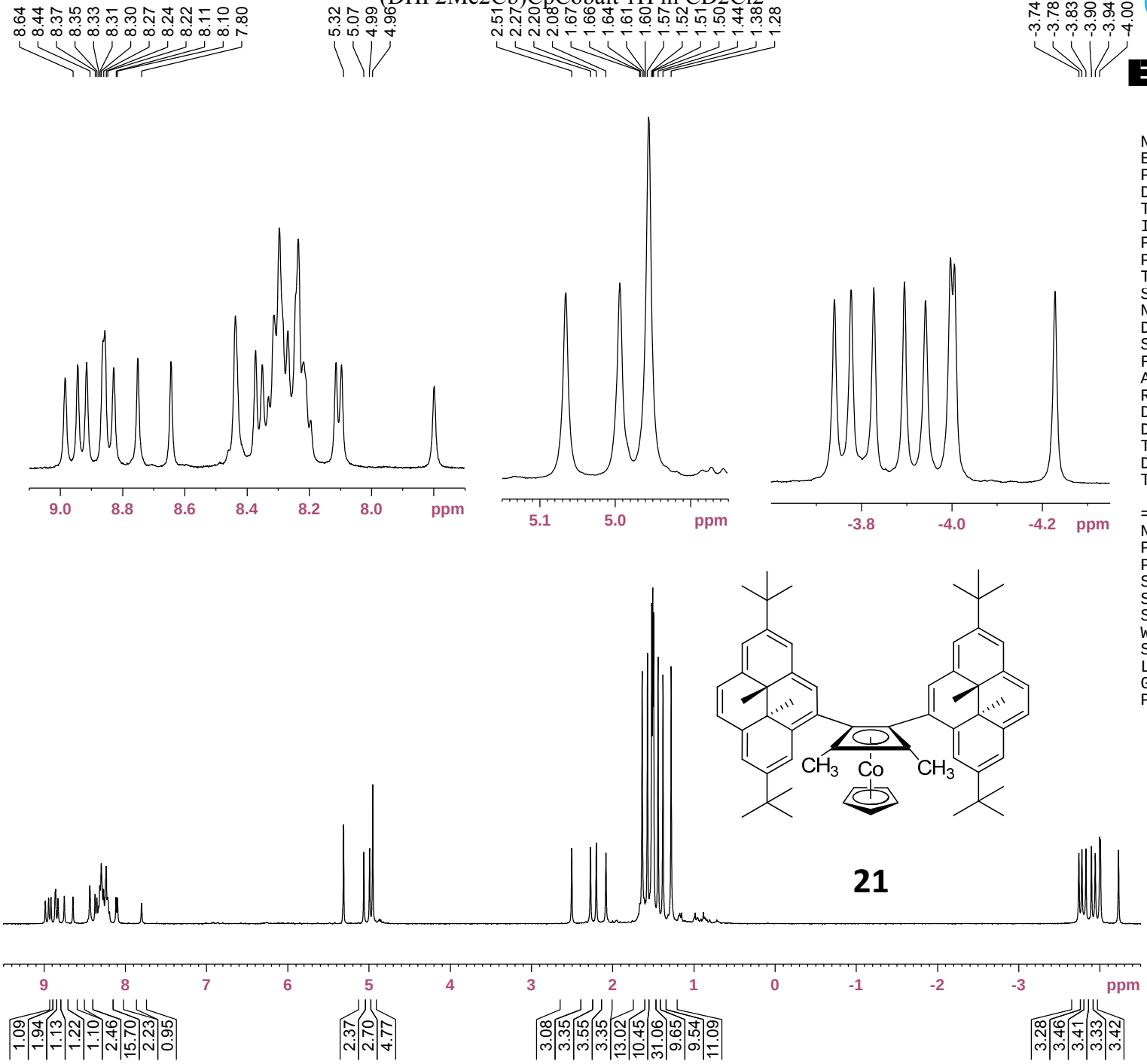
dianion

BRUKER

NAME	Sep18-2009
EXPNO	2
PROCNO	1
Date_	20090918
Time	9.49
INSTRUM	spect
PROBHD	5 mm PABBO BB-
PULPROG	zg30
TD	32768
SOLVENT	THF
NS	16
DS	2
SWH	6009.615 Hz
FIDRES	0.183399 Hz
AQ	2.7263477 sec
RG	203
DW	83.200 usec
DE	6.50 usec
TE	300.0 K
D1	1.00000000 sec
TD0	1
======== CHANNEL f1 ========	
NUC1	1H
P1	14.10 usec
PL1	2.00 dB
PL1W	7.33805561 W
SFO1	300.1312000 MHz
SI	16384
SF	300.1300073 MHz
WDW	EM
SSB	0
LB	0.35 Hz
GB	0
PC	1.00

(DHP2Me2Cb)CpCobalt 1H in CD2Cl2

(DHP2Me2)CbCoCp 1H NMR

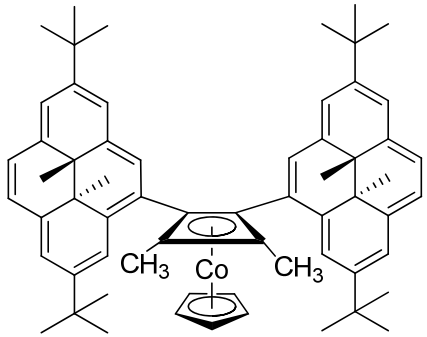



```
NAME          PZ4_Cobalt Me
EXPNO                    1
PROCNO                   1
Date_             20100514
Time                 15.04
INSTRUM              spect
PROBHD    5 mm PABBO BB-
PULPROG               zg30
TD                   32768
SOLVENT            CD2Cl2
NS                       16
DS                        2
SWH               8012.820 Hz
FIDRES               0.244532 Hz
AQ                2.0448356 sec
RG                       90.5
DW                  62.400 usec
DE                   6.50 usec
TE                  296.3 K
D1               1.00000000 sec
TD0                      1

======== CHANNEL f1 ========
NUC1                    1H
P1                   9.60 usec
PL1                 -4.00 dB
SFO1          500.1315200 MHz
SI                   16384
SF            500.1300233 MHz
WDW                     GM
SSB                      0
LB                  -0.20 Hz
GB                     0.5
PC                    1.00
```

CpCyclobutadiene(Me)2Cobalt 1H/CDCl3

(DHP2Me2)CbCoCp 1H NMR



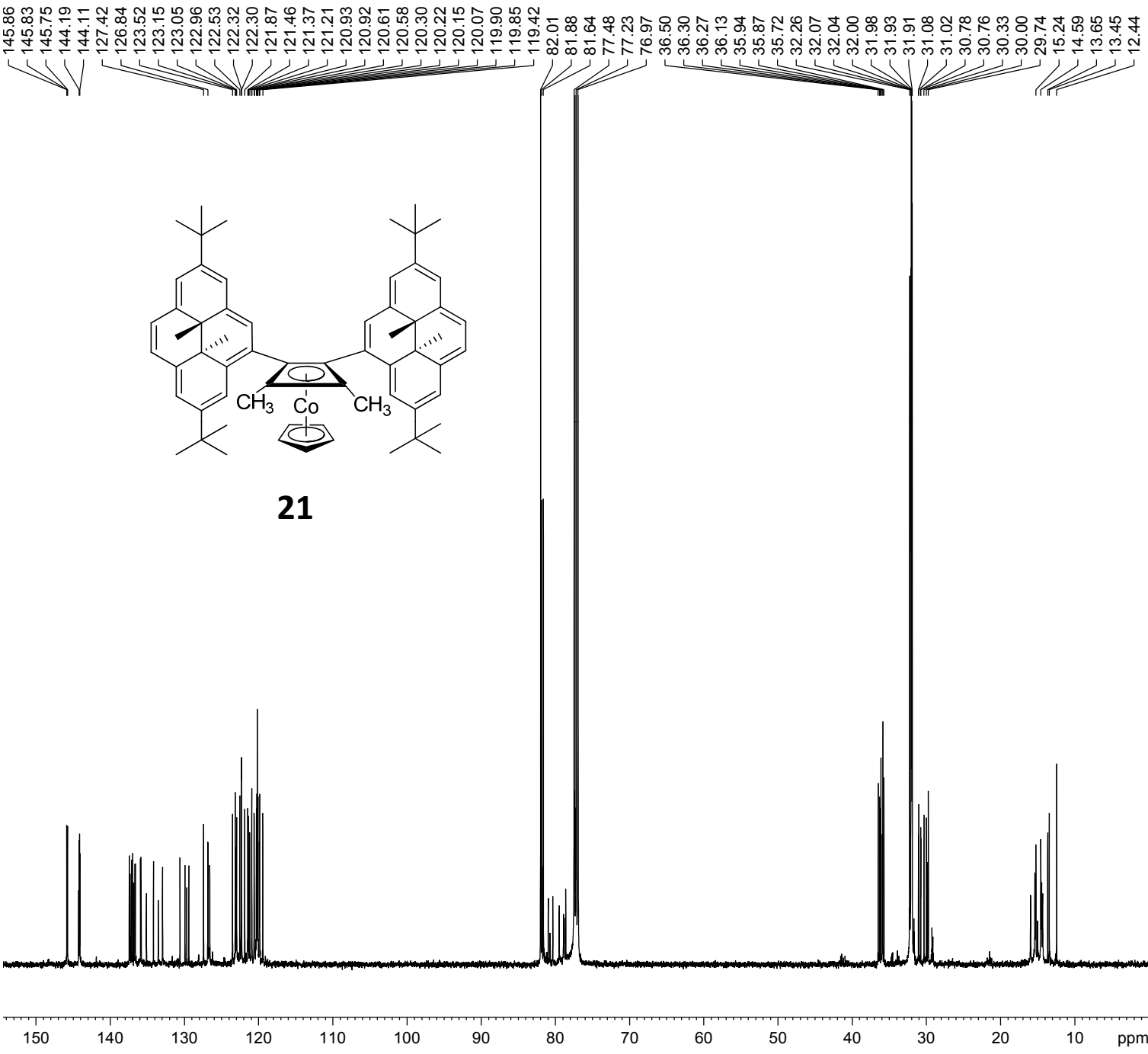
21

```
NAME      Cyclobutadiene Cobalt Me
EXPNO                1
PROCNO               1
Date_         20081119
Time             18.04
INSTRUM          spect
PROBHD   5 mm PABBO BB-
PULPROG           zg30
TD               32768
SOLVENT          CDCl3
NS                  16
DS                   2
SWH           8012.820 Hz
FIDRES        0.244532 Hz
AQ            2.0448356 sec
RG                90.5
DW              62.400 usec
DE               6.50 usec
TE              297.8 K
D1           1.00000000 sec
TD0                  1

======== CHANNEL f1 ========
NUC1                1H
P1                9.60 usec
PL1              -4.00 dB
SFO1       500.1315200 MHz
SI               16384
SF         500.1300232 MHz
WDW                 GM
SSB                  0
LB               -0.20 Hz
GB                 0.5
PC                1.00
```

CpCyclobutadiene(Me)2Cobalt 13C/CDCl3

(DHP2Me2)CbCoCp 13C NMR



21

```
NAME      Cyclobutadiene Cobalt Me
EXPNO                3
PROCNO               1
Date_         20081120
Time              8.53
INSTRUM          spect
PROBHD   5 mm PABBO BB-
PULPROG         zgpg30
TD                65536
SOLVENT           CDCl3
NS                24872
DS                    4
SWH           30864.197 Hz
FIDRES         0.470950 Hz
AQ             1.0617495 sec
RG               14596.5
DW                16.200 usec
DE                 6.50 usec
TE                298.8 K
D1            1.00000000 sec
D11           0.03000000 sec
TD0                   1

======== CHANNEL f1 ========
NUC1                 13C
P1                10.00 usec
PL1                3.00 dB
SFO1        125.7715390 MHz

======== CHANNEL f2 ========
CPDPRG2          waltz16
NUC2                 1H
PCPD2             80.00 usec
PL2               -4.00 dB
PL12              14.42 dB
PL13              14.24 dB
SFO2        500.1325200 MHz
SI                32768
SF          125.7577630 MHz
WDW                  EM
SSB                   0
LB                 0.90 Hz
GB                    0
PC                 1.40
```

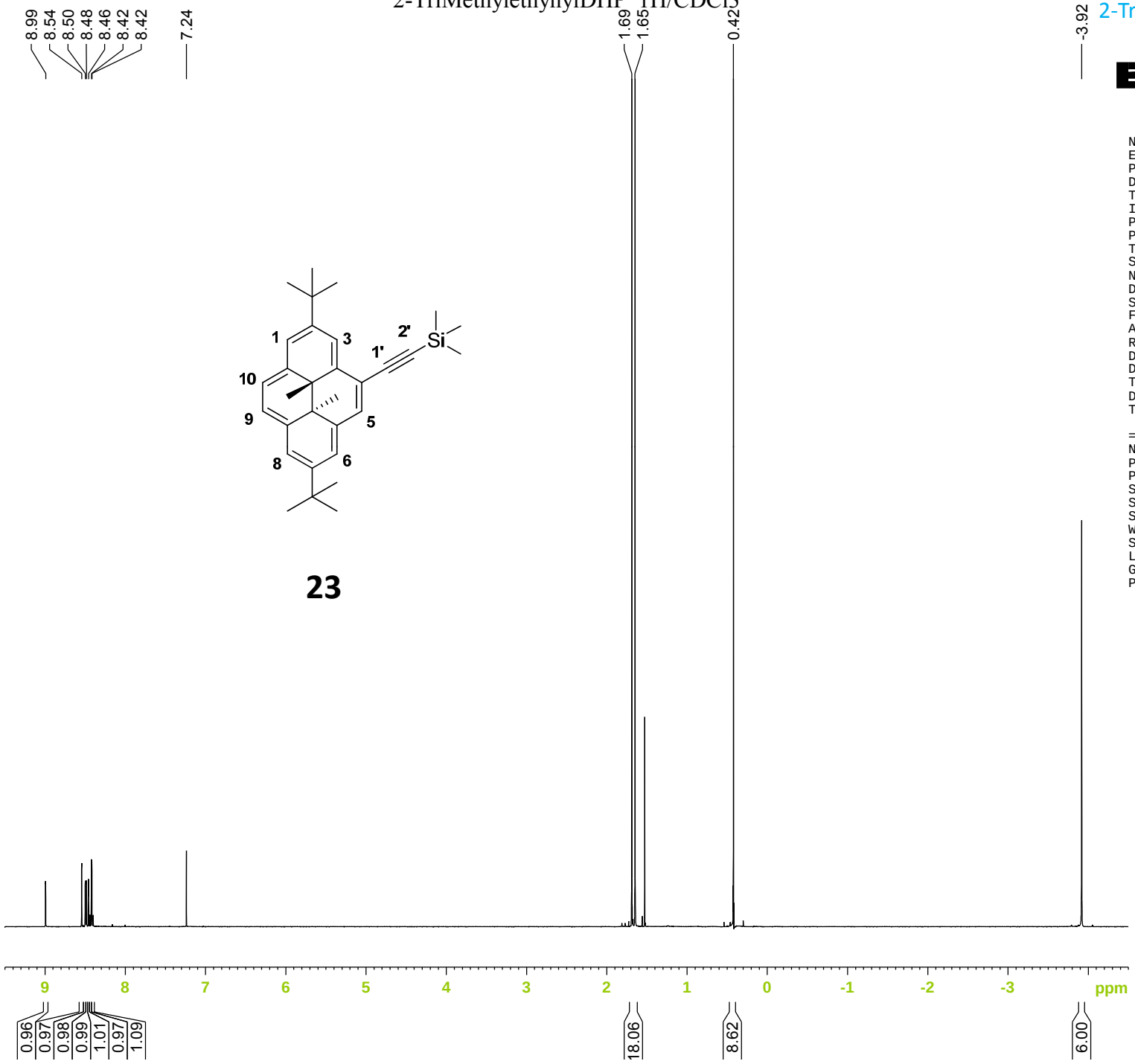
2-TriMethylethynylDHP_1H/CDCl3

2-Trimethylethynyl DHP 1H NMR

23

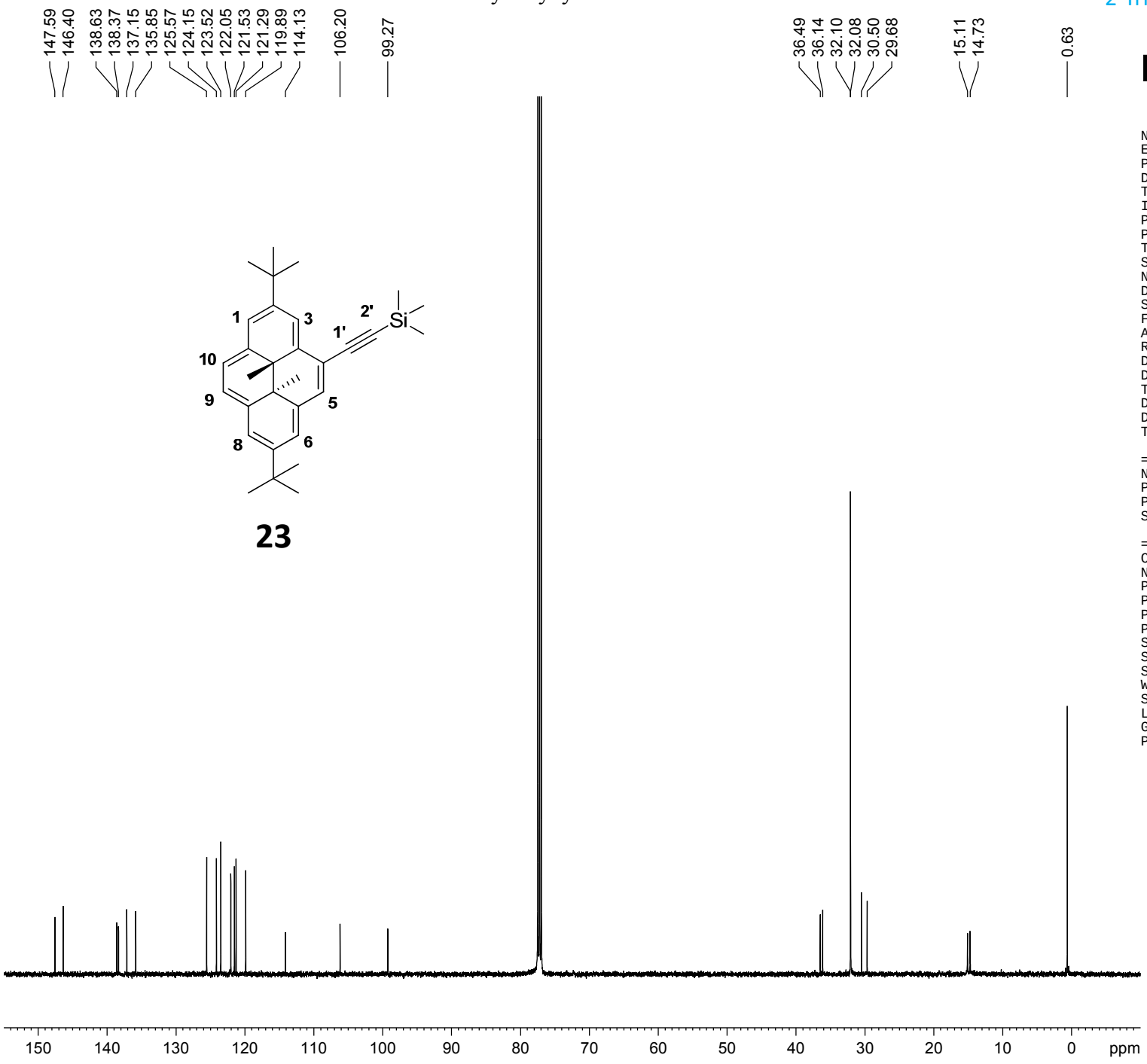
```
NAME        2-TriMethylsilylethynylDHP
EXPNO                   1
PROCNO                  1
Date_            20081123
Time                13.35
INSTRUM             spect
PROBHD    5 mm PABBO BB-
PULPROG              zg30
TD                  32768
SOLVENT             CDCl3
NS                     16
DS                      2
SWH              8012.820 Hz
FIDRES           0.244532 Hz
AQ               2.0448356 sec
RG                    256
DW                 62.400 usec
DE                  6.50 usec
TE                 297.3 K
D1            1.00000000 sec
TD0                     1

======== CHANNEL f1 ========
NUC1                   1H
P1                  9.60 usec
PL1                -4.00 dB
SFO1         500.1315200 MHz
SI                  16384
SF           500.1300238 MHz
WDW                    GM
SSB                     0
LB                 -0.20 Hz
GB                    0.5
PC                   1.00
```



2-TriMethylethynylDHP 13C/CDCl3

2-TrimethylethynylDHP 13C NMR



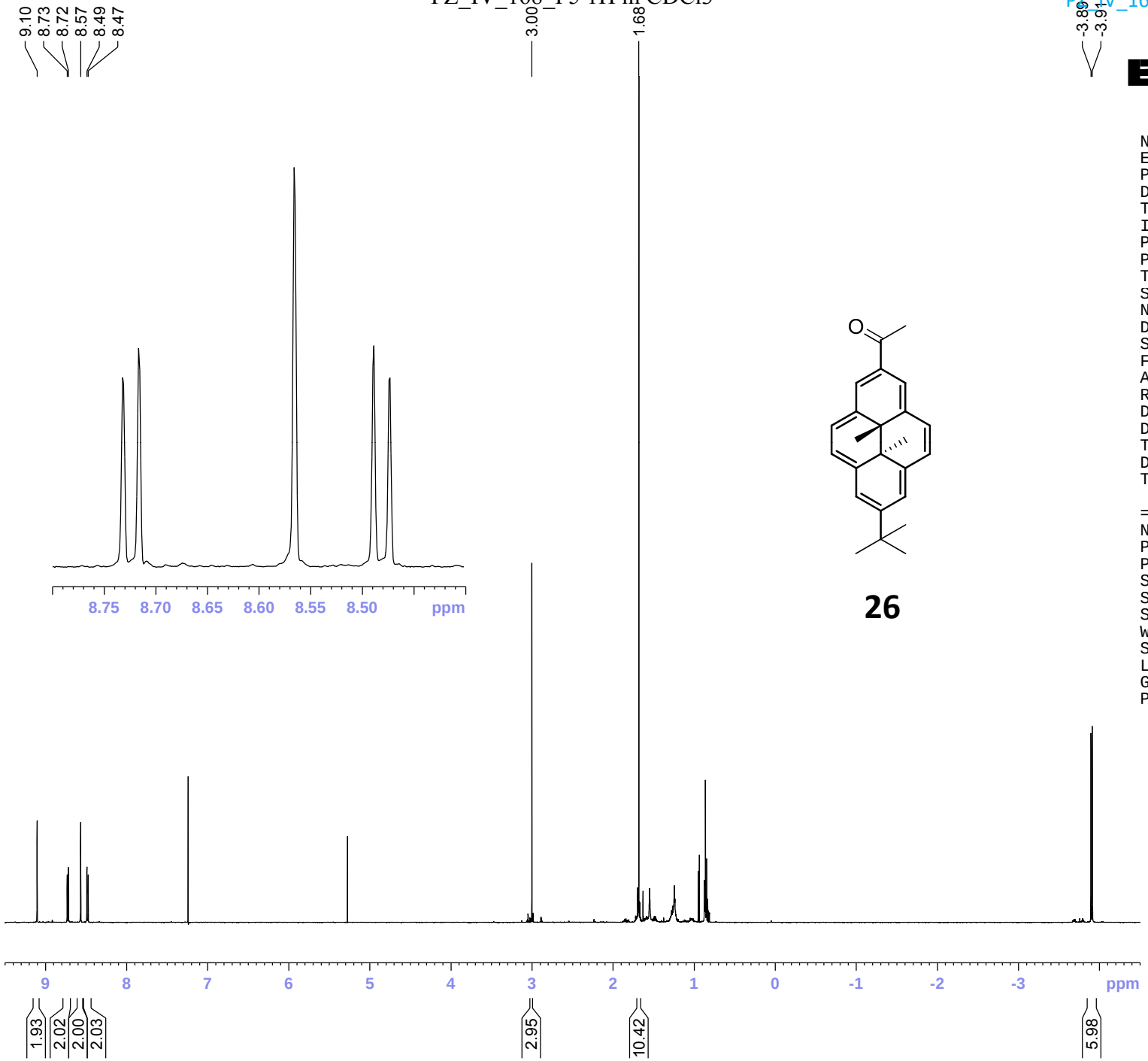

```
NAME      2-TriMethylsilylethynylDHP
EXPNO                  3
PROCNO                 1
Date_           20081123
Time               13.53
INSTRUM            spect
PROBHD   5 mm PABBO BB-
PULPROG          zgpg30
TD                 65536
SOLVENT            CDCl3
NS                  4410
DS                     4
SWH           30864.197 Hz
FIDRES         0.470950 Hz
AQ             1.0617495 sec
RG               14596.5
DW                16.200 usec
DE                 6.50 usec
TE                298.6 K
D1           1.00000000 sec
D11          0.03000000 sec
TD0                    1

======== CHANNEL f1 ========
NUC1                 13C
P1                10.00 usec
PL1                3.00 dB
SFO1        125.7715390 MHz

======== CHANNEL f2 ========
CPDPRG2          waltz16
NUC2                 1H
PCPD2             80.00 usec
PL2               -4.00 dB
PL12              14.42 dB
PL13              14.24 dB
SFO2        500.1325200 MHz
SI                32768
SF          125.7577619 MHz
WDW                  EM
SSB                   0
LB                0.90 Hz
GB                    0
PC                1.40
```

PZ_IV_168_F5 1H in CDCl3

PZ_IV_168_F5 top CH3CODHP 1H NMR

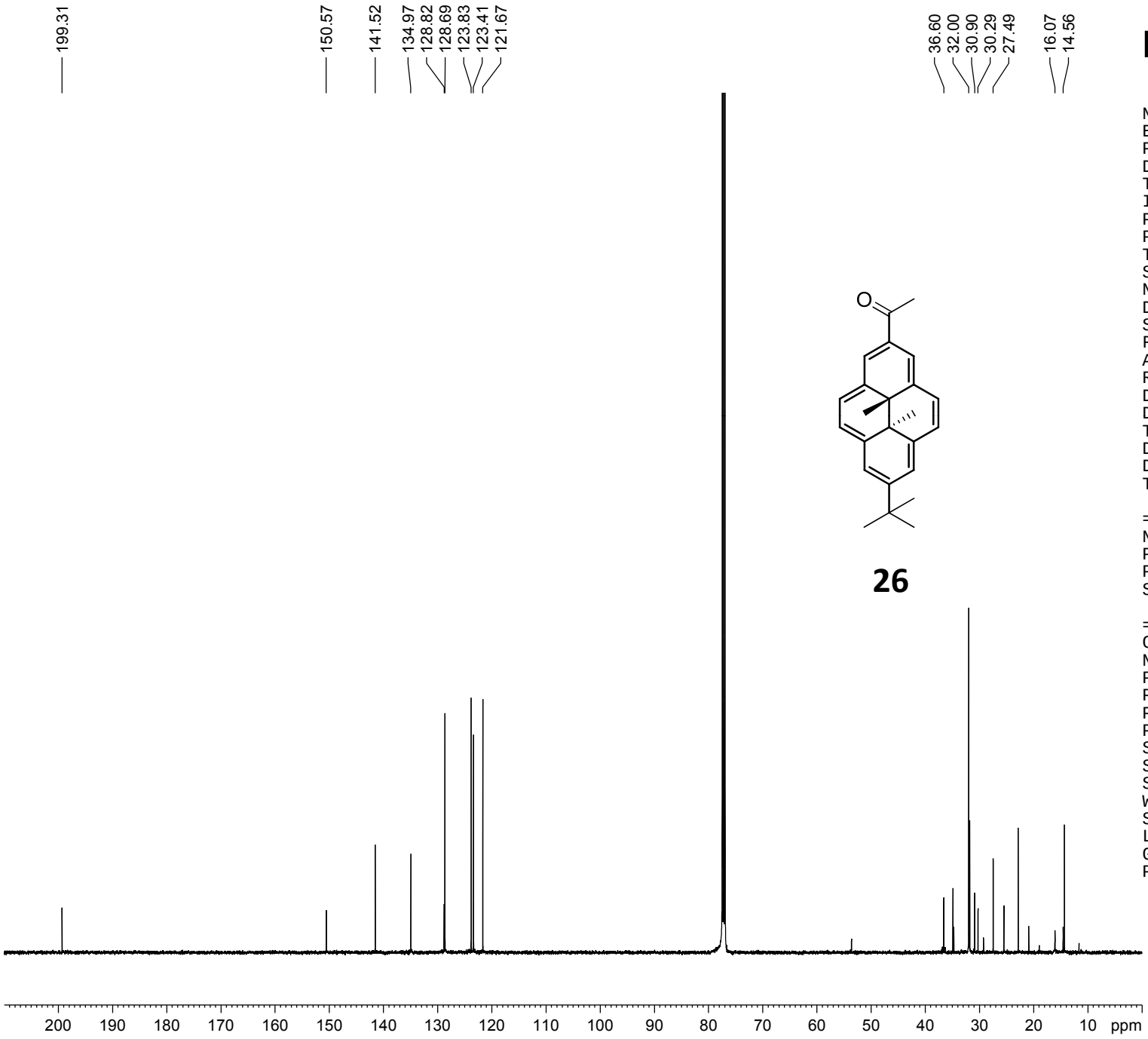


26

NAME	PZ4_168_F5
EXPNO	1
PROCNO	1
Date_	20100731
Time	11.55
INSTRUM	spect
PROBHD	5 mm PABBO BB-
PULPROG	zg30
TD	32768
SOLVENT	CDCl3
NS	16
DS	2
SWH	8012.820 Hz
FIDRES	0.244532 Hz
AQ	2.0448356 sec
RG	362
DW	62.400 usec
DE	6.50 usec
TE	298.4 K
D1	1.00000000 sec
TD0	1
======== CHANNEL f1 ========	
NUC1	1H
P1	9.60 usec
PL1	-4.00 dB
SFO1	500.1315200 MHz
SI	16384
SF	500.1300233 MHz
WDW	GM
SSB	0
LB	-0.20 Hz
GB	0.5
PC	1.00

PZ_IV_168_F5 13C in CDCl3

PZ_IV_168_F5 top CH3CODHP_13C NMR



26

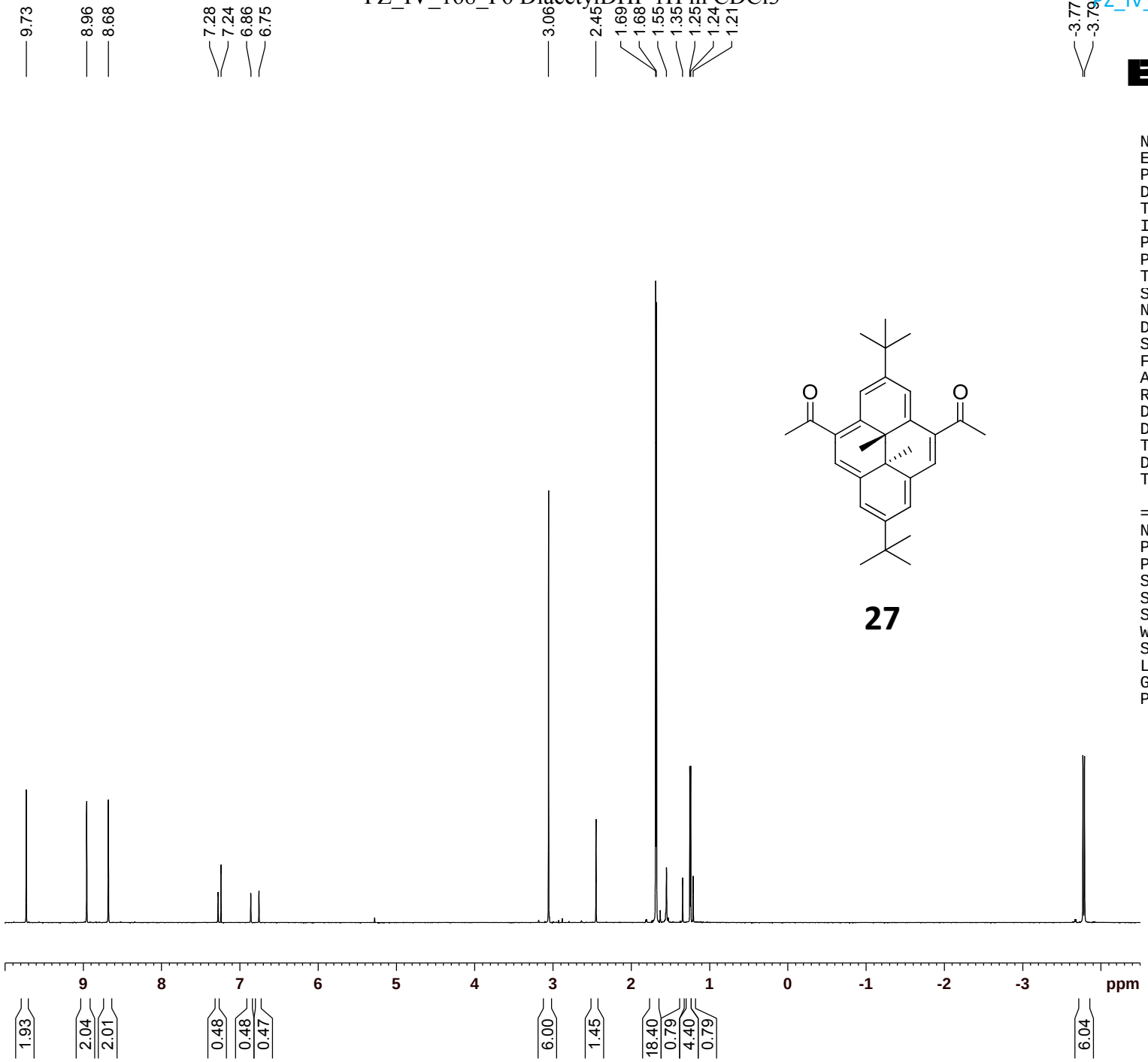
```
NAME            PZ4_168_F5
EXPNO                    3
PROCNO                   1
Date_             20100801
Time                 9.03
INSTRUM             spect
PROBHD    5 mm PABBO BB-
PULPROG             zgpg30
TD                   65536
SOLVENT              CDCl3
NS                   32768
DS                       4
SWH             30864.197 Hz
FIDRES           0.470950 Hz
AQ               1.0617495 sec
RG                 14596.5
DW                 16.200 usec
DE                  6.50 usec
TE                 299.7 K
D1              1.00000000 sec
D11             0.03000000 sec
TD0                      1

======== CHANNEL f1 ========
NUC1                   13C
P1                 10.00 usec
PL1                 3.00 dB
SFO1          125.7715390 MHz

======== CHANNEL f2 ========
CPDPRG2           waltz16
NUC2                   1H
PCPD2              80.00 usec
PL2                -4.00 dB
PL12               14.42 dB
PL13               60.00 dB
SFO2          500.1325200 MHz
SI                   32768
SF            125.7577620 MHz
WDW                    EM
SSB                     0
LB                 0.90 Hz
GB                      0
PC                 1.40
```

PZ_IV_168_F6 DiacetylDHP 1H in CDCl3

PZ_IV_168_F6 DiacetylDHP 1H NMR



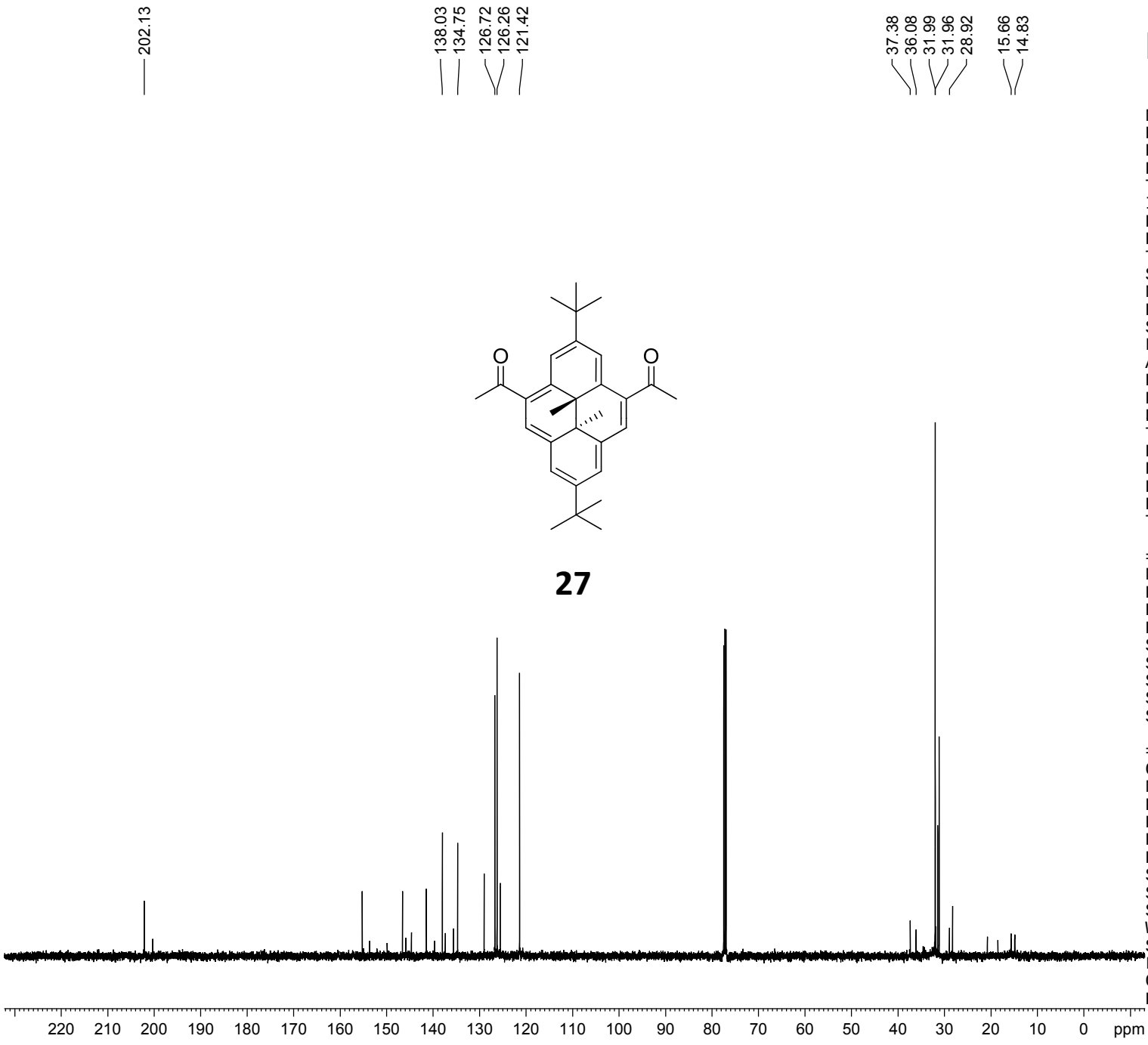
27

```
NAME            PZ4_168_F6
EXPNO                    1
PROCNO                   1
Date_             20100802
Time                 22.42
INSTRUM              spect
PROBHD   5 mm PABBI 1H/
PULPROG               zg30
TD                   32768
SOLVENT              CDCl3
NS                      16
DS                       2
SWH               8012.820 Hz
FIDRES            0.244532 Hz
AQ                2.0448356 sec
RG                     128
DW                  62.400 usec
DE                   6.50 usec
TE                  298.8 K
D1               1.00000000 sec
TD0                      1

======== CHANNEL f1 ========
NUC1                    1H
P1                   10.20 usec
PL1                   1.00 dB
SFO1          500.1315200 MHz
SI                   16384
SF            500.1300224 MHz
WDW                     GM
SSB                      0
LB                   -0.20 Hz
GB                     0.5
PC                    1.00
```

PZ_IV_168_F6 DiacetylDHP 13C in CDCl3

PZ_IV_168_F6 DiacetylDHP_13C NMR



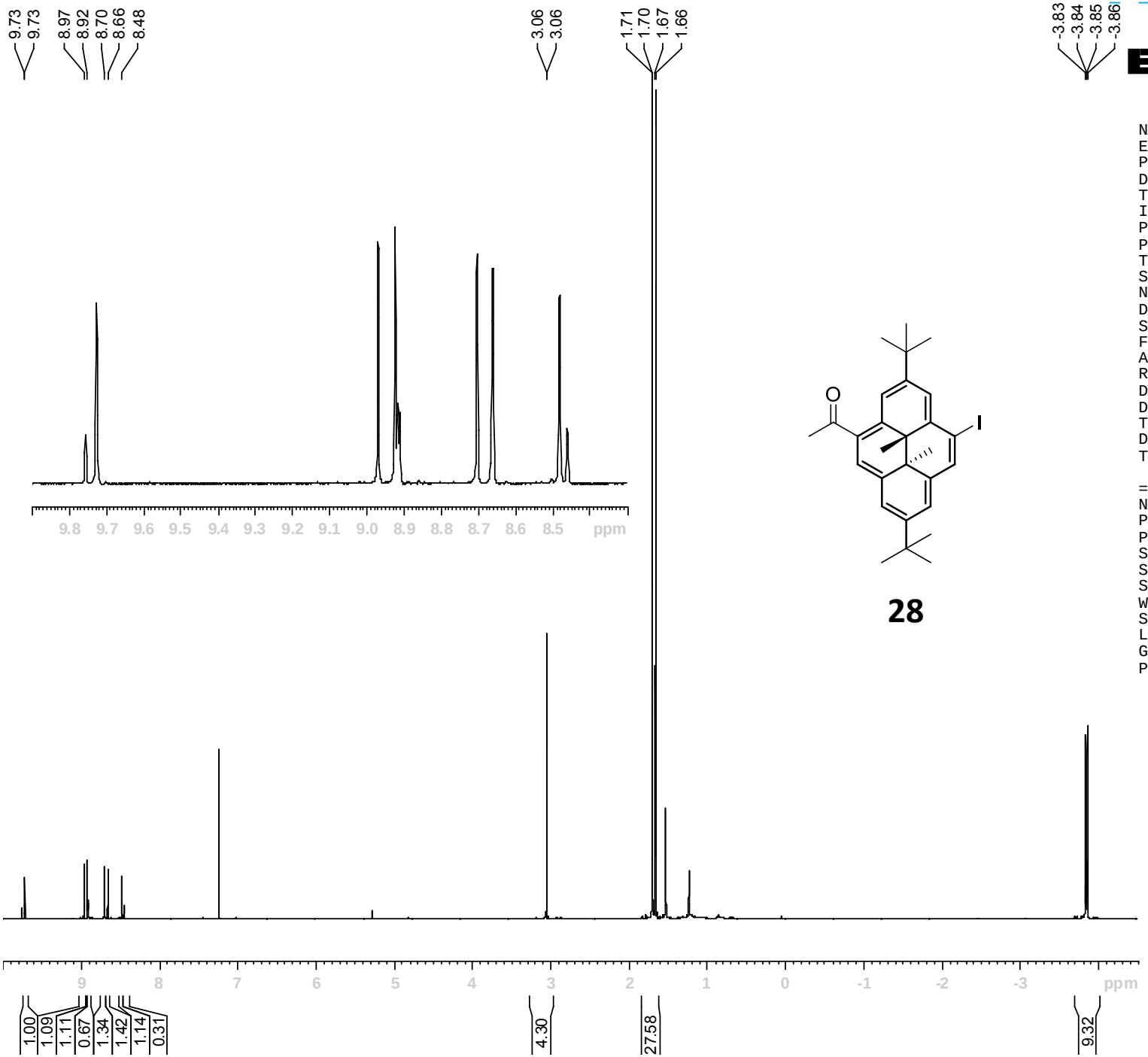

```
NAME            PZ4_168_F6
EXPNO                    8
PROCNO                   1
Date_             20100803
Time                 8.08
INSTRUM             spect
PROBHD    5 mm PABBI 1H/
PULPROG   zgpg_echo1.mmod
TD                   65536
SOLVENT              CDCl3
NS                    9216
DS                       4
SWH             30864.197 Hz
FIDRES           0.470950 Hz
AQ               1.0617495 sec
RG                   16384
DW                  16.200 usec
DE                   6.50 usec
TE                  298.9 K
D1               1.00000000 sec
D11              0.03000000 sec
D20              0.00010000 sec
D21              0.00011460 sec
TD0                      1

======== CHANNEL f1 ========
NUC1                   13C
P1                   14.60 usec
P12                2000.00 usec
PL1                  -1.00 dB
SFO1          125.7715390 MHz
SP2                  3.87 dB
SPNAM2       Crp60comp.4
SPOAL2             0.500
SPOFFS2              0.00 Hz

======== CHANNEL f2 ========
CPDPRG2           waltz16
NUC2                   1H
PCPD2                80.00 usec
PL2                   1.00 dB
PL12                 19.40 dB
PL13                 60.00 dB
SFO2          500.1325200 MHz
SI                   32768
SF            125.7577612 MHz
WDW                    EM
SSB                     0
LB                   0.90 Hz
GB                      0
PC                   1.40
```

PZ_V_ acetylDHP iodide isomer A 1H in CDCl3

PZ_IV_CH3CODHP-I isomer A 1H NMR



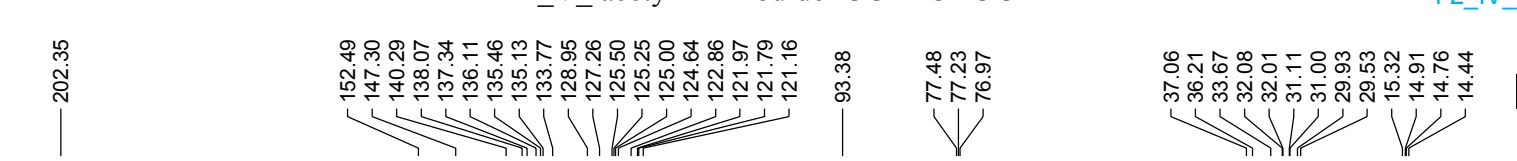
28

```
NAME        PZ5_acetylDHP iodide
EXPNO                     1
PROCNO                    1
Date_              20110531
Time                  15.19
INSTRUM               spect
PROBHD    5 mm PABBI 1H/
PULPROG                zg30
TD                    32768
SOLVENT               CDCl3
NS                       16
DS                        2
SWH                8012.820 Hz
FIDRES            0.244532 Hz
AQ                2.0448356 sec
RG                      128
DW                   62.400 usec
DE                    6.50 usec
TE                   297.4 K
D1              1.00000000 sec
TD0                       1

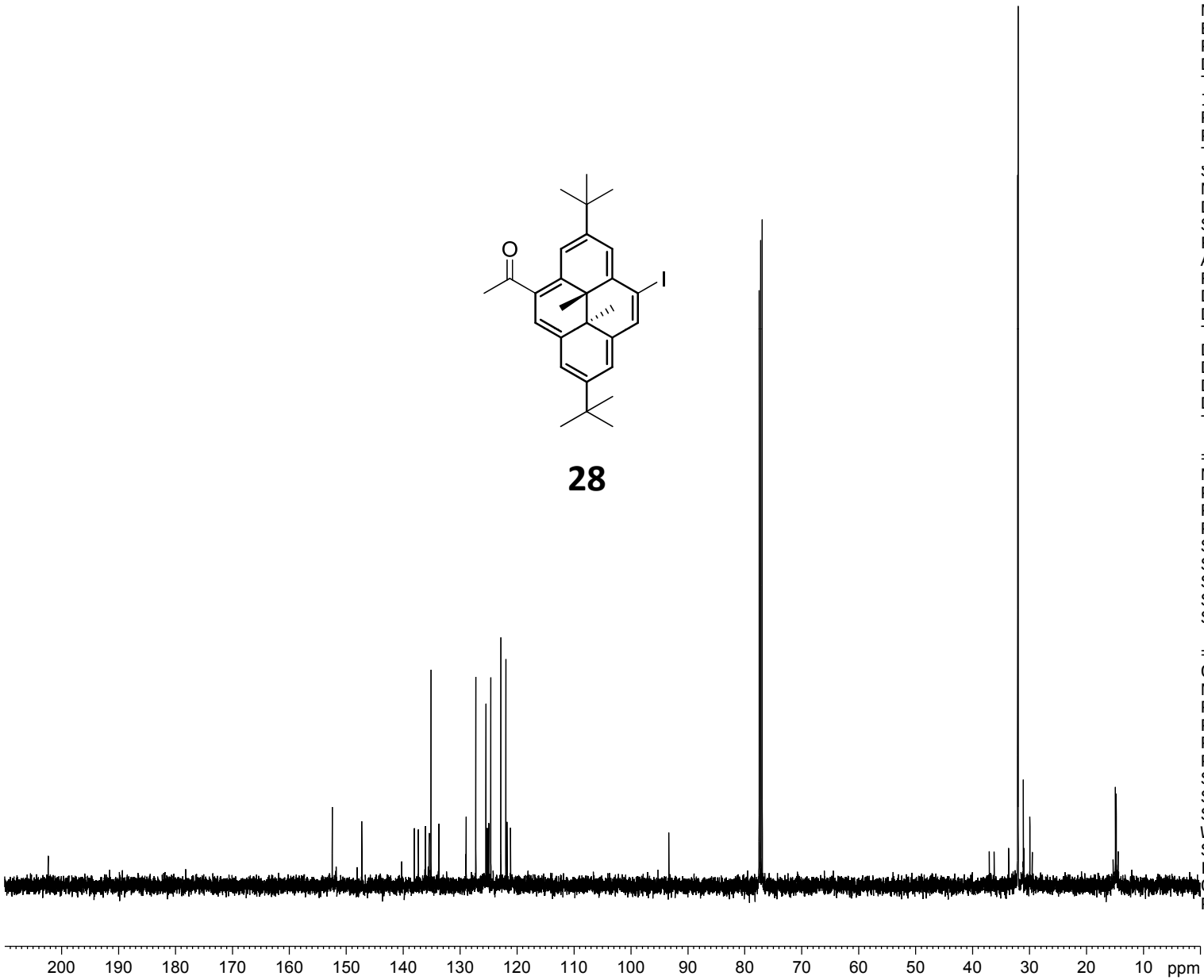
======== CHANNEL f1 ========
NUC1                     1H
P1                    9.60 usec
PL1                  -4.00 dB
SFO1           500.1315200 MHz
SI                    16384
SF             500.1300238 MHz
WDW                      GM
SSB                       0
LB                   -0.20 Hz
GB                      0.5
PC                     1.00
```

PZ_V_ acetylDHP iodide 13C in CDCl3

PZ_IV_CH3CODHP-I isomer A 1H NMR



28



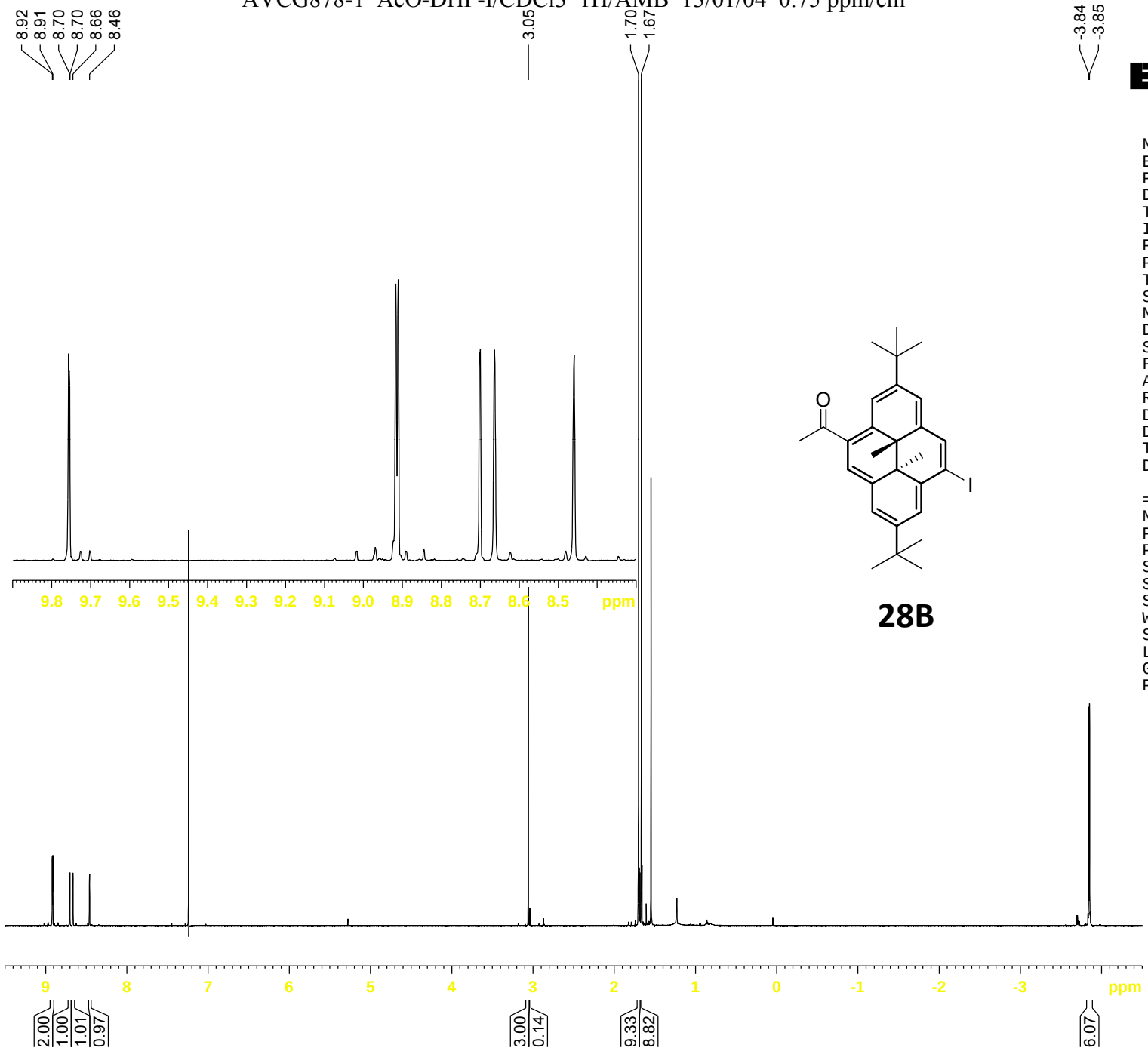

```
NAME      PZ5_acetylDHP iodide
EXPNO                    2
PROCNO                   1
Date_             20110531
Time                 15.25
INSTRUM              spect
PROBHD   5 mm PABBI 1H/
PULPROG  zgpg_echo1.mmod
TD                   65536
SOLVENT              CDCl3
NS                   21312
DS                       4
SWH              30864.197 Hz
FIDRES           0.470950 Hz
AQ               1.0617495 sec
RG                   16384
DW                 16.200 usec
DE                  6.50 usec
TE                  297.6 K
D1              1.00000000 sec
D11             0.03000000 sec
D20             0.00010000 sec
D21             0.00011460 sec
TD0                      1

======== CHANNEL f1 ========
NUC1                   13C
P1                   14.60 usec
P12                2000.00 usec
PL1                  -1.00 dB
SFO1          125.7715390 MHz
SP2                  3.87 dB
SPNAM2       Crp60comp.4
SPOAL2               0.500
SPOFFS2              0.00 Hz

======== CHANNEL f2 ========
CPDPRG2            waltz16
NUC2                   1H
PCPD2                80.00 usec
PL2                   1.00 dB
PL12                 19.40 dB
PL13                 60.00 dB
SFO2          500.1325200 MHz
SI                   32768
SF            125.7577611 MHz
WDW                    EM
SSB                     0
LB                   0.90 Hz
GB                      0
PC                   1.40
```

AVCG878-1 AcO-DHP-I/CDCl3 1H/AMB 13/01/04 0.75 ppm/cm

PZ_IV_CH3CODHP-I 1H NMR

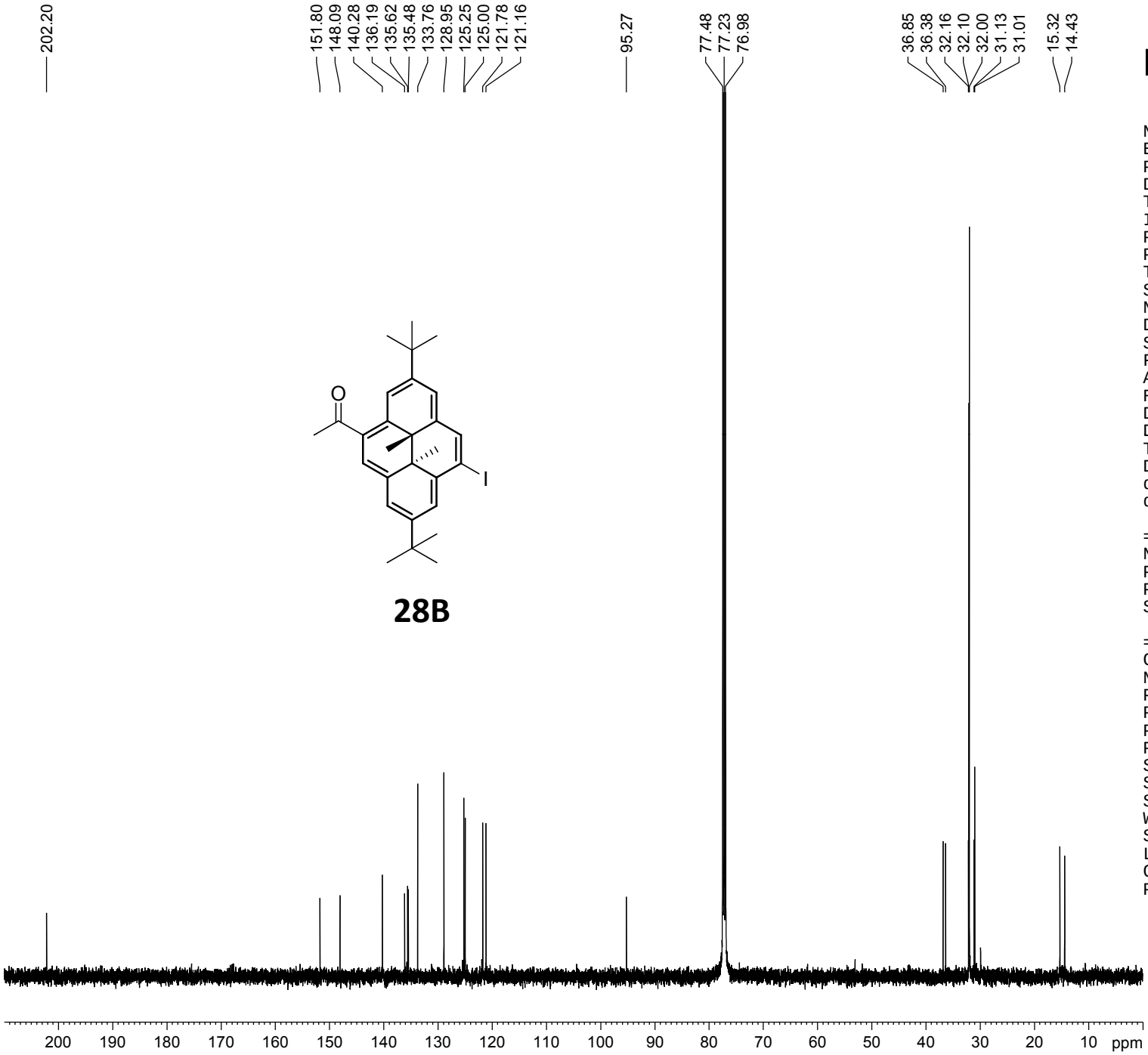


28B

NAME	avcg878
EXPNO	1
PROCNO	1
Date_	20040113
Time	11.08
INSTRUM	AV500
PROBHD	5 mm BBI 1H-BB
PULPROG	zg30
TD	32768
SOLVENT	CDCl3
NS	16
DS	2
SWH	8012.820 Hz
FIDRES	0.244532 Hz
AQ	2.0448356 sec
RG	228.1
DW	62.400 usec
DE	6.00 usec
TE	300.0 K
D1	1.00000000 sec
======== CHANNEL f1 ========	
NUC1	1H
P1	5.60 usec
PL1	-4.00 dB
SFO1	500.1315200 MHz
SI	16384
SF	500.1300236 MHz
WDW	GM
SSB	0
LB	-0.40 Hz
GB	0.5
PC	1.00

AVCG881 ACO-DHP-I/CDCl3 13C/AMB 14/01/04 11 ppm/cm

PZ_IV_CH3CODHP-I 13C NMR

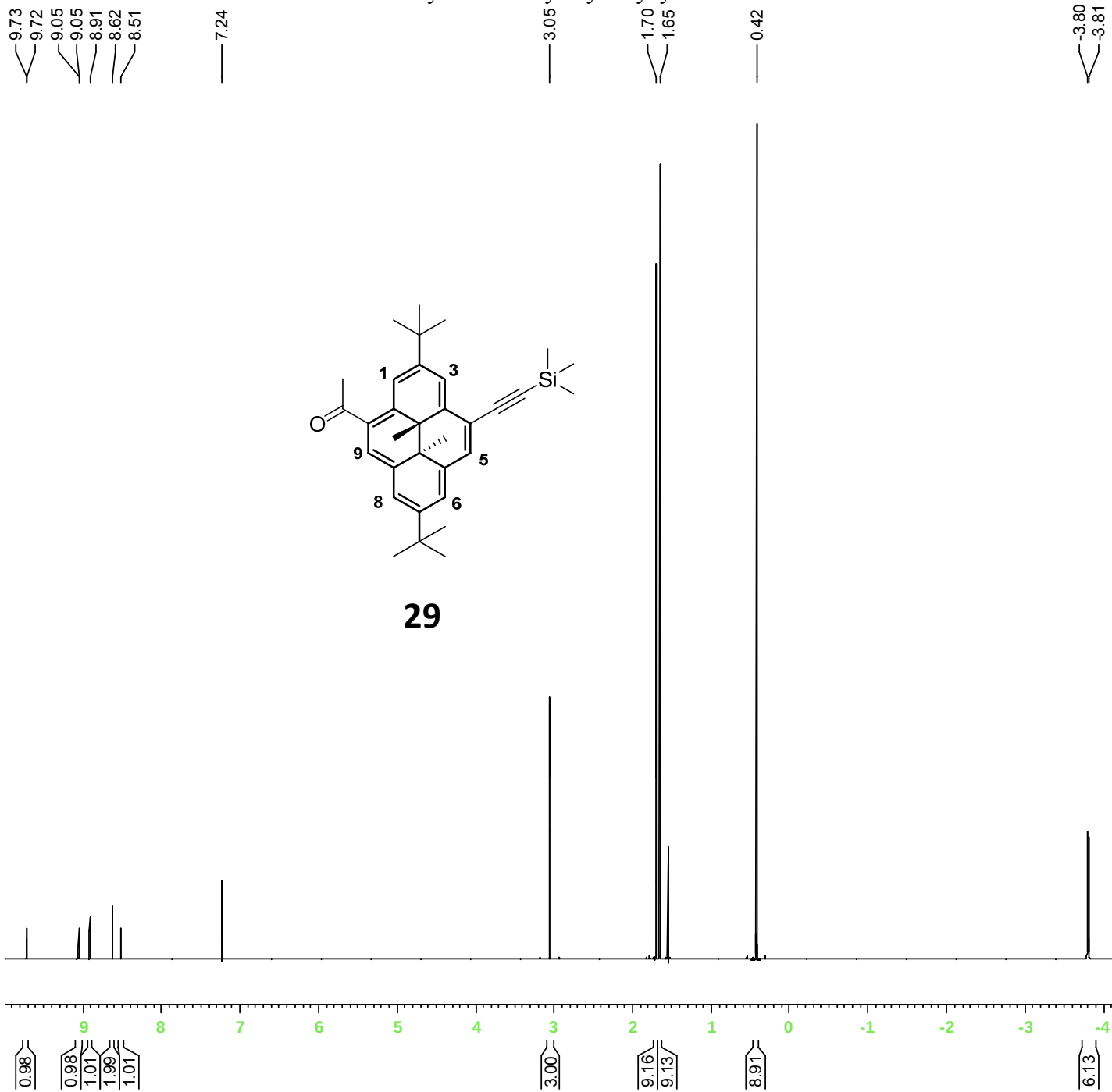


28B

NAME	avcg881
EXPNO	1
PROCNO	1
Date_	20040114
Time	11.58
INSTRUM	AV500
PROBHD	5 mm BBO BB-1H
PULPROG	zgpg30
TD	65536
SOLVENT	CDCl3
NS	7060
DS	4
SWH	30864.197 Hz
FIDRES	0.470950 Hz
AQ	1.0617495 sec
RG	16384
DW	16.200 usec
DE	6.00 usec
TE	300.0 K
D1	1.00000000 sec
d11	0.03000000 sec
d12	0.00002000 sec
======== CHANNEL f1 ========	
NUC1	13C
P1	8.60 usec
PL1	-1.00 dB
SFO1	125.7703640 MHz
======== CHANNEL f2 ========	
CPDPRG2	waltz16
NUC2	1H
PCPD2	80.00 usec
PL2	-4.00 dB
PL12	14.00 dB
PL13	14.00 dB
SFO2	500.1315200 MHz
SI	32768
SF	125.7577620 MHz
WDW	EM
SSB	0
LB	0.90 Hz
GB	0
PC	1.40

10-Acetyl-4-trimethylsilylethynylDHP 1H/CDCl3

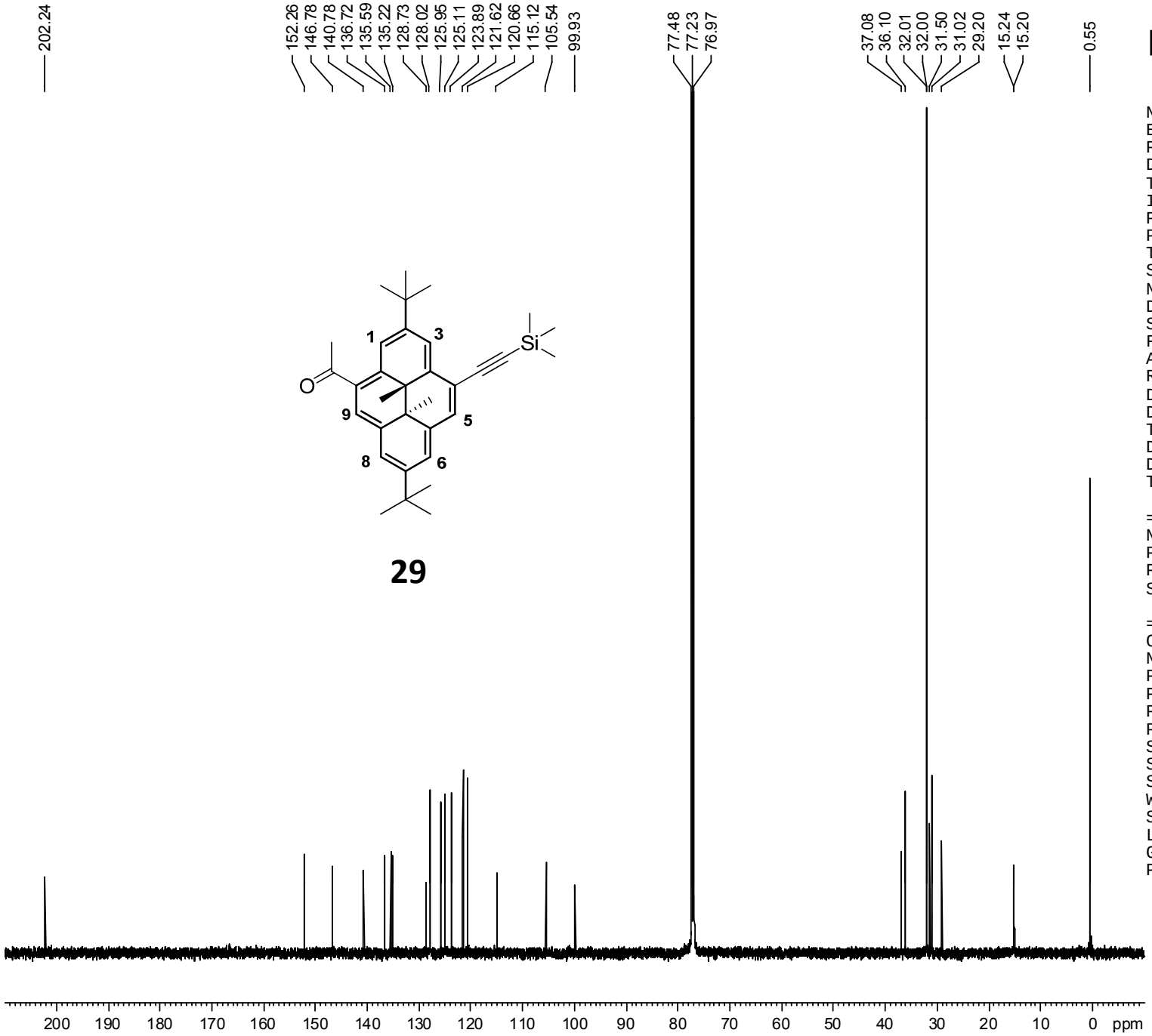
PZ_I_?? CH3CODHPC≡CTMS 1H NMR



NAME	Acetyl-TMSCCDHP
EXPNO	1
PROCNO	1
Date_	20081128
Time	11.49
INSTRUM	spect
PROBHD	5 mm PABBO BB-
PULPROG	zg30
TD	32768
SOLVENT	CDCl3
NS	16
DS	2
SWH	8012.820 Hz
FIDRES	0.244532 Hz
AQ	2.0448356 sec
RG	228.1
DW	62.400 usec
DE	6.50 usec
TE	297.0 K
D1	1.00000000 sec
TD0	1
========	CHANNEL f1 ========
NUC1	1H
P1	9.60 usec
PL1	-4.00 dB
SFO1	500.1315200 MHz
SI	16384
SF	500.1300238 MHz
WDW	GM
SSB	0
LB	-0.20 Hz
GB	0.5
PC	1.00

10-Acetyl-4-trimethylsilylethynylDHP 13C/CDCl3

PZ_I_?? CH3CODHPC≡CTMS 13C NMR

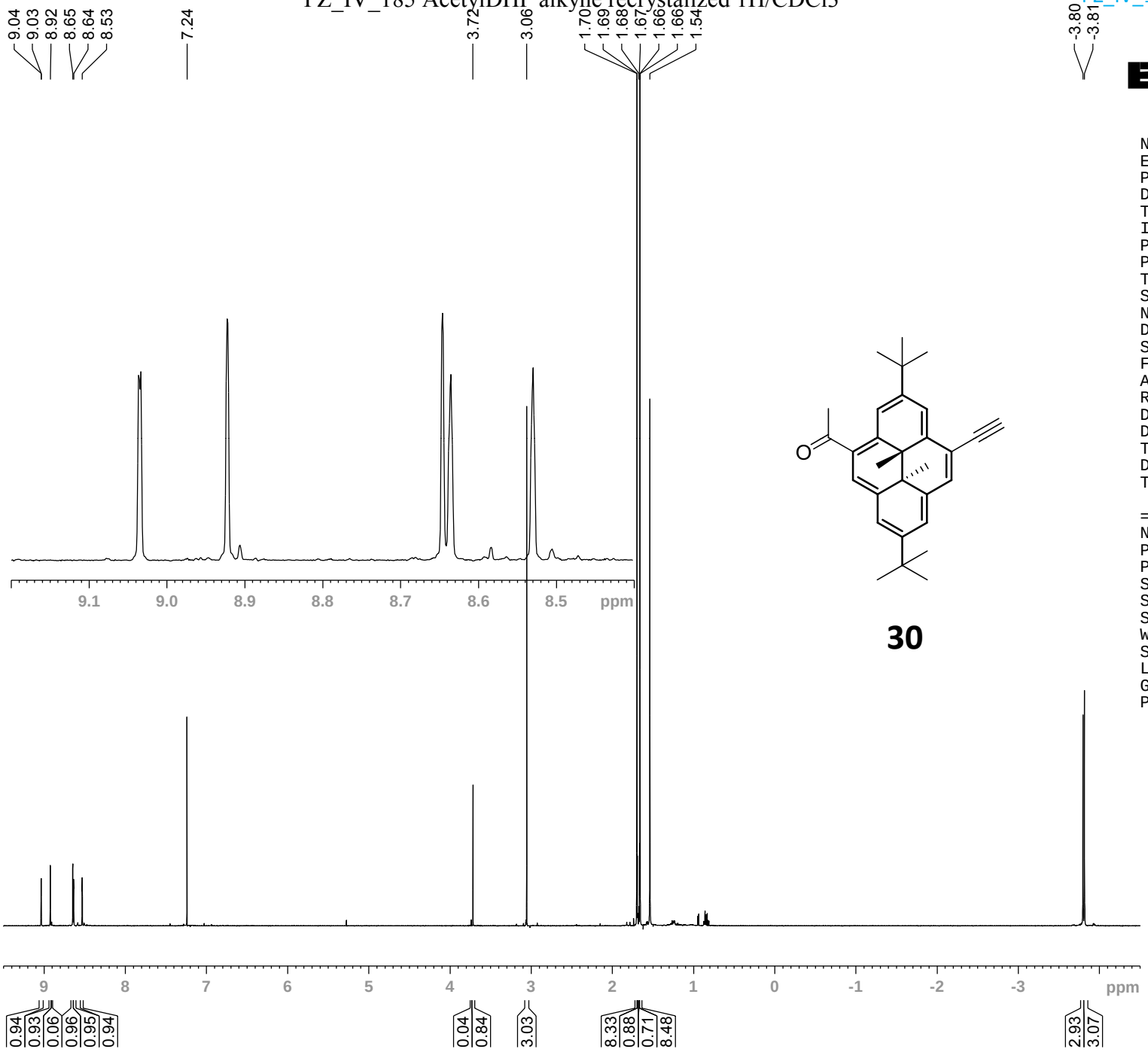


29

NAME	Acetyl-TMSCCDHP
EXPNO	3
PROCNO	1
Date_	20081128
Time	12.03
INSTRUM	spect
PROBHD	5 mm PABBO BB-
PULPROG	zgpg30
TD	65536
SOLVENT	CDCl3
NS	5120
DS	4
SWH	30864.197 Hz
FIDRES	0.470950 Hz
AQ	1.0617495 sec
RG	14596.5
DW	16.200 usec
DE	6.50 usec
TE	298.5 K
D1	1.00000000 sec
D11	0.03000000 sec
TD0	1
======== CHANNEL f1 ========	
NUC1	13C
P1	10.00 usec
PL1	3.00 dB
SFO1	125.7715390 MHz
======== CHANNEL f2 ========	
CPDPRG2	waltz16
NUC2	1H
PCPD2	80.00 usec
PL2	-4.00 dB
PL12	14.42 dB
PL13	14.24 dB
SFO2	500.1325200 MHz
SI	32768
SF	125.7577619 MHz
WDW	EM
SSB	0
LB	0.90 Hz
GB	0
PC	1.40

PZ_IV_185 AcetylDHP alkyne recrystalized 1H/CDCl3

PZ_IV_185CH3CODHPC≡C-H 1H NMR

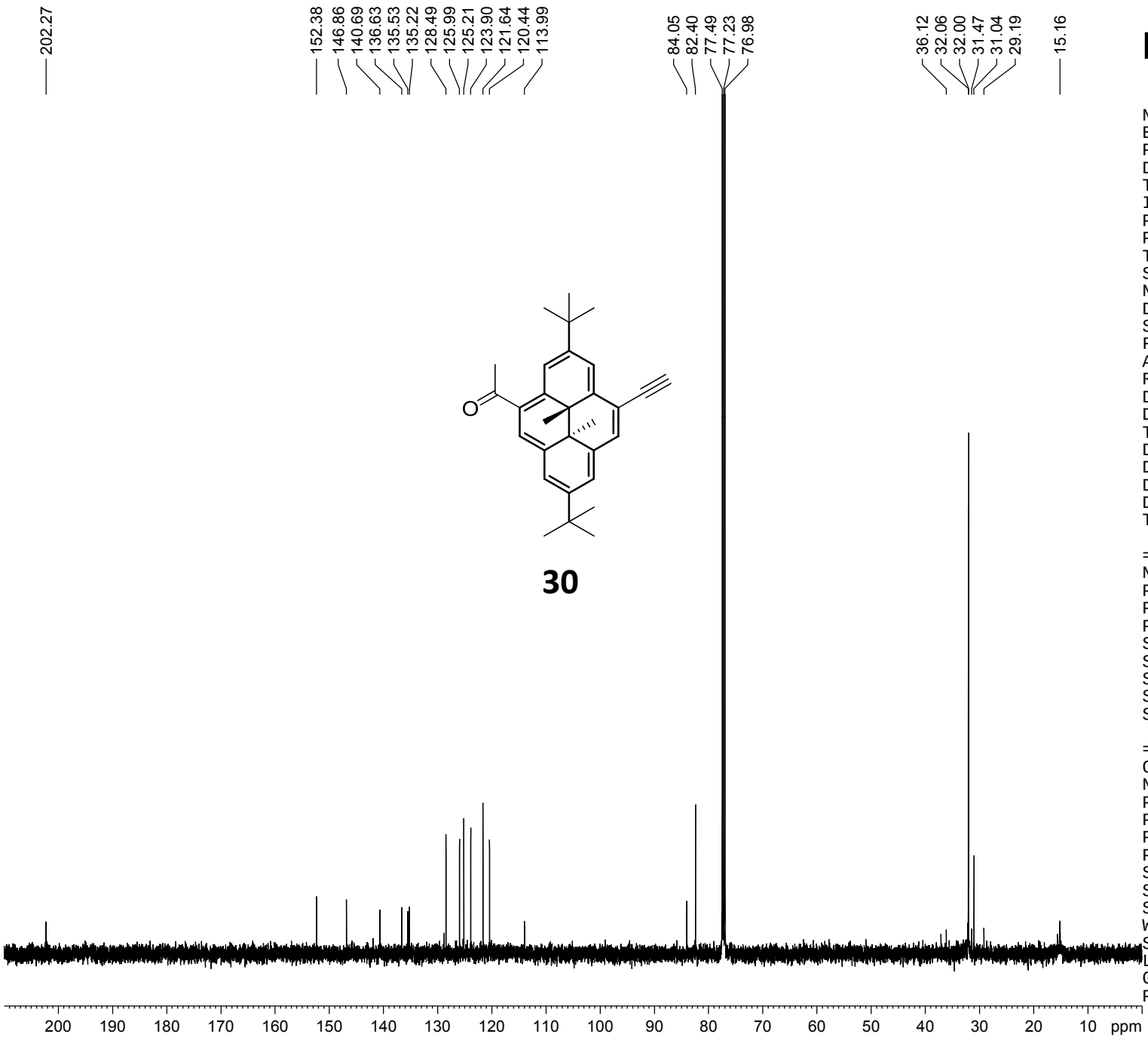


30

NAME	PZ4_185	
EXPNO	1	
PROCNO	1	
Date_	20100908	
Time	16.44	
INSTRUM	spect	
PROBHD	5 mm PABBI 1H/	
PULPROG	zg30	
TD	32768	
SOLVENT	CDCl3	
NS	16	
DS	2	
SWH	8012.820	Hz
FIDRES	0.244532	Hz
AQ	2.0448356	sec
RG	228.1	
DW	62.400	usec
DE	6.50	usec
TE	297.4	K
D1	1.00000000	sec
TD0	1	
======== CHANNEL f1 ========		
NUC1	1H	
P1	10.20	usec
PL1	1.00	dB
SFO1	500.1315200	MHz
SI	16384	
SF	500.1300243	MHz
WDW	GM	
SSB	0	
LB	-0.20	Hz
GB	0.5	
PC	1.00	

PZ_IV_185 AcetylDHP alkyne recrystalized 13C/CDCl3

PZ_IV_185 CH3CODHPC≡C-H_13C NMR



30

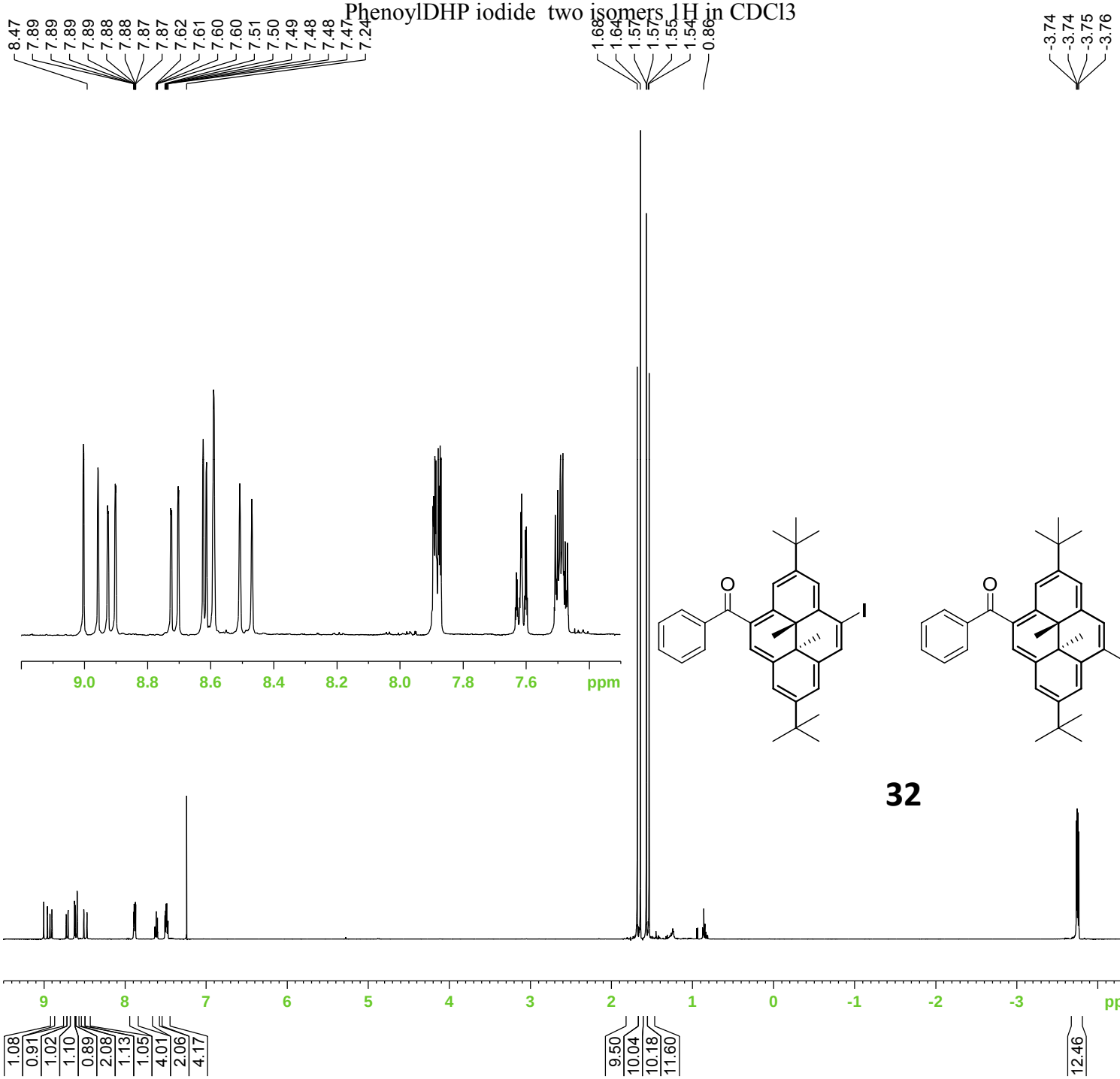
```
NAME                PZ4_185
EXPNO                     3
PROCNO                    1
Date_              20100908
Time                  20.18
INSTRUM                spect
PROBHD    5 mm PABBI 1H/
PULPROG   zgpg_echo1.mmod
TD                    65536
SOLVENT                CDCl3
NS                    11035
DS                        4
SWH               30864.197 Hz
FIDRES             0.470950 Hz
AQ                 1.0617495 sec
RG                    16384
DW                   16.200 usec
DE                    6.50 usec
TE                   298.4 K
D1                1.00000000 sec
D11               0.03000000 sec
D20               0.00010000 sec
D21               0.00011460 sec
TD0                       1

======== CHANNEL f1 ========
NUC1                    13C
P1                    14.60 usec
P12                 2000.00 usec
PL1                   -1.00 dB
SFO1            125.7715390 MHz
SP2                   3.87 dB
SPNAM2          Crp60comp.4
SPOAL2                0.500
SPOFFS2               0.00 Hz

======== CHANNEL f2 ========
CPDPRG2             waltz16
NUC2                    1H
PCPD2                80.00 usec
PL2                   1.00 dB
PL12                 19.40 dB
PL13                 60.00 dB
SFO2            500.1325200 MHz
SI                    32768
SF              125.7577619 MHz
WDW                     EM
SSB                      0
LB                    0.90 Hz
GB                       0
PC                    1.40
```

PhenoylDHP iodide two isomers 1H in CDCl3

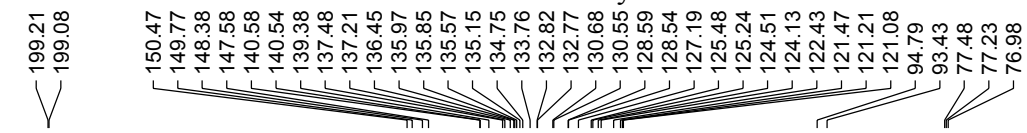
PZ_IV_PhCODHP-I 1H NMR



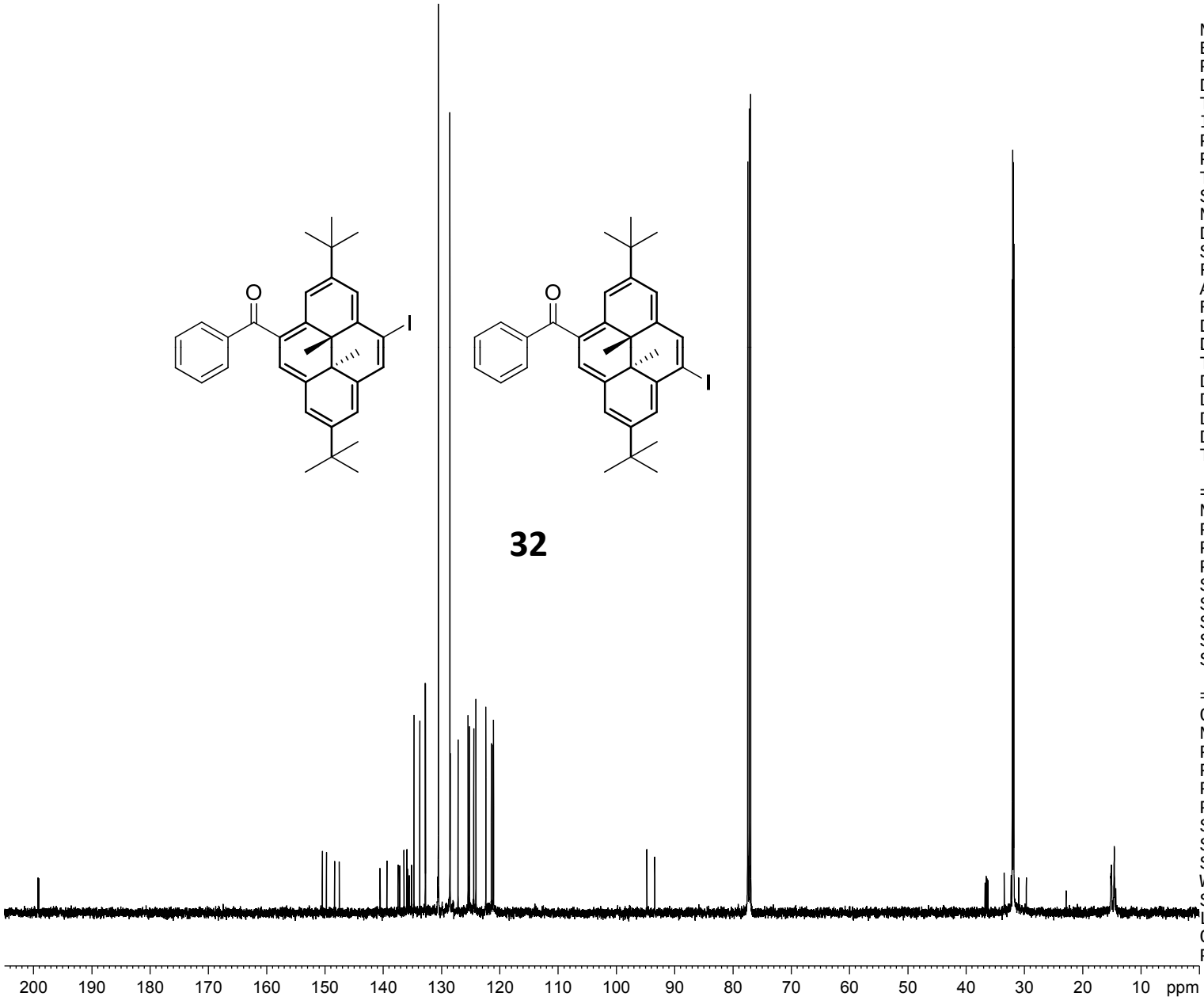
NAME	PZ091010
EXPNO	1
PROCNO	1
Date_	20100911
Time	11.05
INSTRUM	spect
PROBHD	5 mm PABBI 1H/
PULPROG	zg30
TD	32768
SOLVENT	CDCl3
NS	16
DS	2
SWH	8012.820 Hz
FIDRES	0.244532 Hz
AQ	2.0448356 sec
RG	128
DW	62.400 usec
DE	6.50 usec
TE	297.7 K
D1	1.00000000 sec
TD0	1
======== CHANNEL f1 ========	
NUC1	1H
P1	10.20 usec
PL1	1.00 dB
SFO1	500.1315200 MHz
SI	16384
SF	500.1300237 MHz
WDW	GM
SSB	0
LB	-0.20 Hz
GB	0.5
PC	1.00

PhenoylDHP iodide 13C in CDCl3

PZ_IV_PhCODHP-I_13C NMR



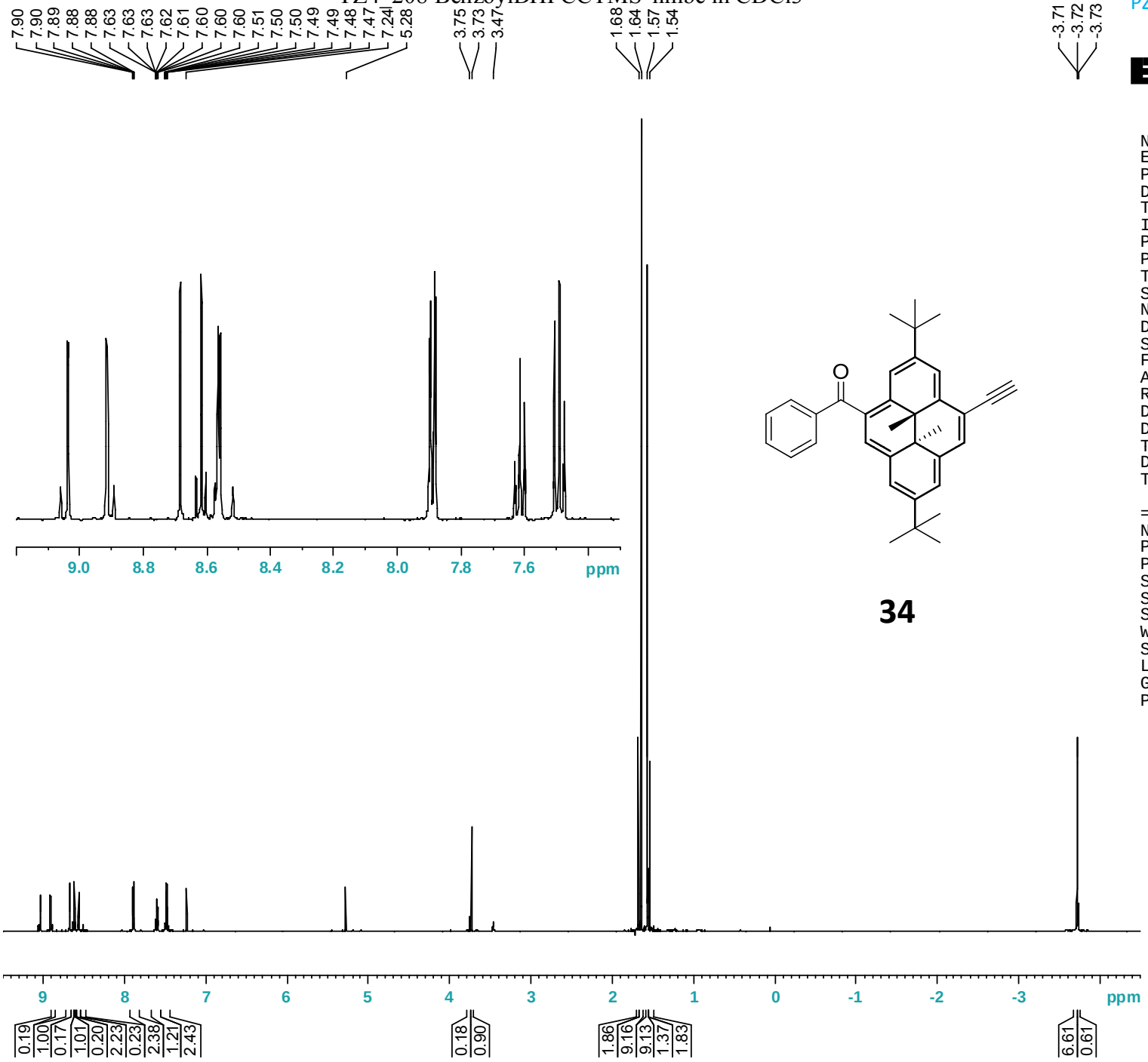
32



NAME	PZ091010	
EXPNO	2	
PROCNO	1	
Date_	20100911	
Time	10.56	
INSTRUM	spect	
PROBHD	5 mm PABBI 1H/	
PULPROG	zgpg_echo1.mmod	
TD	65536	
SOLVENT	CDCl3	
NS	28050	
DS	4	
SWH	30864.197	Hz
FIDRES	0.470950	Hz
AQ	1.0617495	sec
RG	16384	
DW	16.200	usec
DE	6.50	usec
TE	297.9	K
D1	1.00000000	sec
D11	0.03000000	sec
D20	0.00010000	sec
D21	0.00011460	sec
TD0	1	
======== CHANNEL f1 ========		
NUC1	13C	
P1	14.60	usec
P12	2000.00	usec
PL1	-1.00	dB
SFO1	125.7715390	MHz
SP2	3.87	dB
SPNAM2	Crp60comp.4	
SPOAL2	0.500	
SPOFFS2	0.00	Hz
======== CHANNEL f2 ========		
CPDPRG2	waltz16	
NUC2	1H	
PCPD2	80.00	usec
PL2	1.00	dB
PL12	19.40	dB
PL13	19.40	dB
SFO2	500.1325200	MHz
SI	32768	
SF	125.7577620	MHz
WDW	EM	
SSB	0	
LB	0.90	Hz
GB	0	
PC	1.40	

PZ4_208 BenzoylDHPCCTMS hmbc in CDCl3

PZ_IV_208 Benzoyl DHP 1H/CDCl3



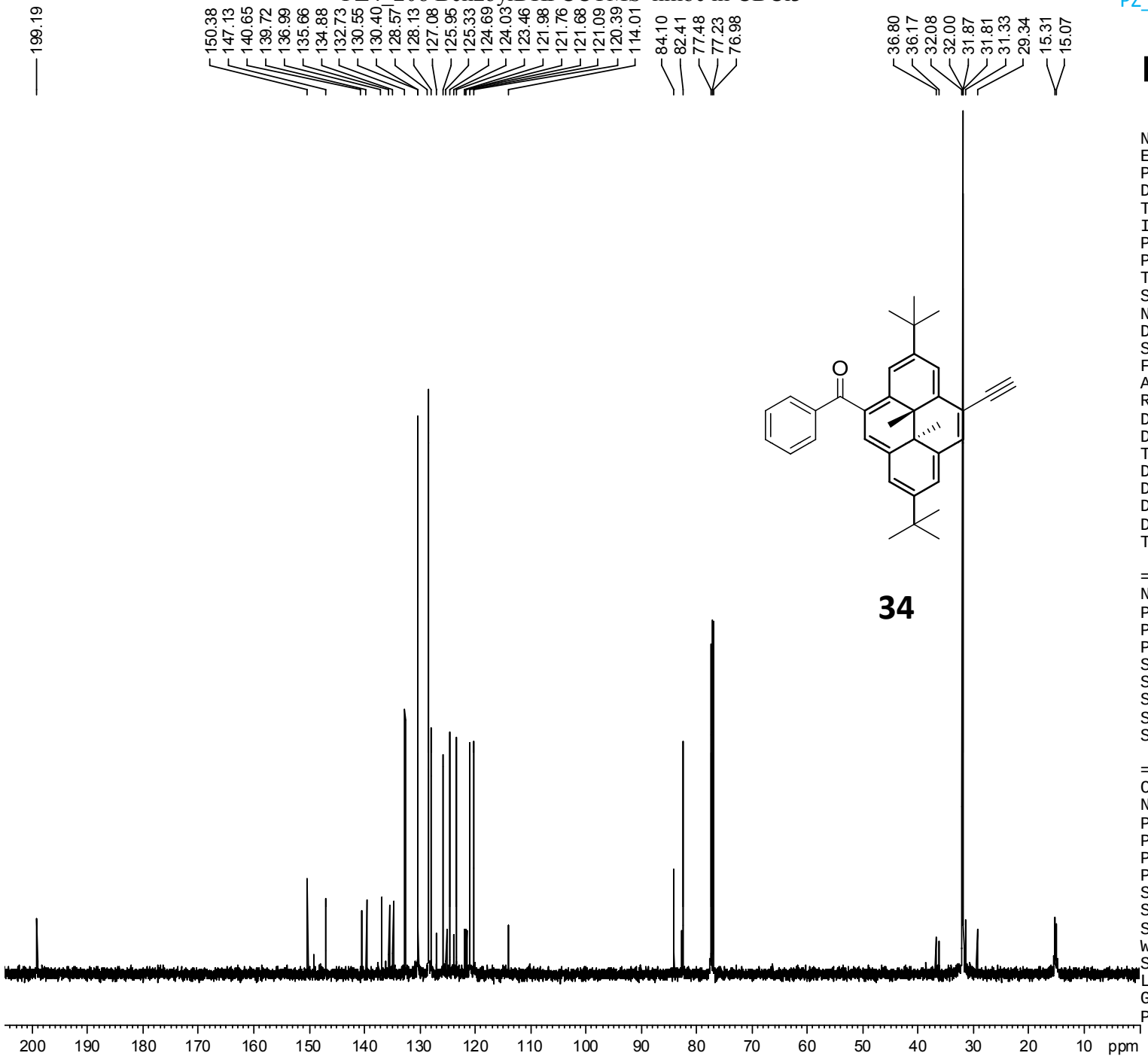
34

```
NAME                 PZ5_100
EXPNO                      1
PROCNO                     1
Date_               20110509
Time                   19.25
INSTRUM                spect
PROBHD   5 mm PABBI 1H/
PULPROG                 zg30
TD                     32768
SOLVENT                CDCl3
NS                        16
DS                         2
SWH                 8012.820 Hz
FIDRES              0.244532 Hz
AQ                  2.0448356 sec
RG                      71.8
DW                     62.400 usec
DE                      6.50 usec
TE                     296.0 K
D1                  1.00000000 sec
TD0                        1

======== CHANNEL f1 ========
NUC1                      1H
P1                     10.20 usec
PL1                     1.00 dB
SFO1             500.1315200 MHz
SI                     16384
SF               500.1300238 MHz
WDW                       GM
SSB                        0
LB                     -0.20 Hz
GB                       0.5
PC                      1.00
```

PZ4_208 BenzoylDHPCCTMS hmbc in CDCl3

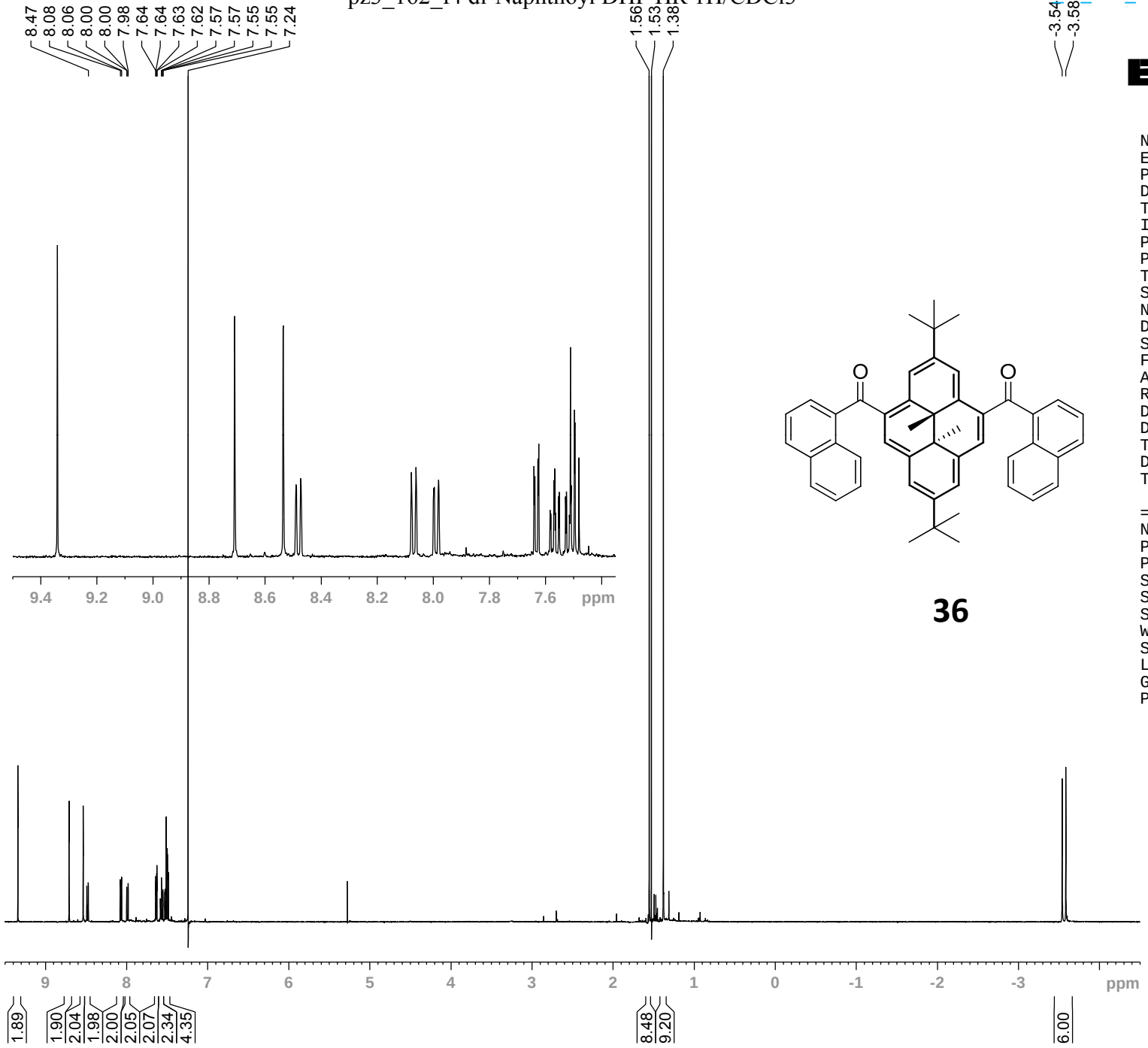
PZ_IV_208 Benzoyl DHP 13C/CDCl3



NAME	PZ5_100
EXPNO	2
PROCNO	1
Date_	20110510
Time	6.32
INSTRUM	spect
PROBHD	5 mm PABBI 1H/
PULPROG	zgpg_echo1.mmod
TD	65536
SOLVENT	CDCl3
NS	10240
DS	4
SWH	30864.197 Hz
FIDRES	0.470950 Hz
AQ	1.0617495 sec
RG	16384
DW	16.200 usec
DE	6.50 usec
TE	298.1 K
D1	1.00000000 sec
D11	0.03000000 sec
D20	0.00010000 sec
D21	0.00011460 sec
TD0	1
======== CHANNEL f1 ========	
NUC1	13C
P1	14.60 usec
P12	2000.00 usec
PL1	-1.00 dB
SFO1	125.7715390 MHz
SP2	3.87 dB
SPNAM2	Crp60comp.4
SPOAL2	0.500
SPOFFS2	0.00 Hz
======== CHANNEL f2 ========	
CPDPRG2	waltz16
NUC2	1H
PCPD2	80.00 usec
PL2	1.00 dB
PL12	19.40 dB
PL13	60.00 dB
SFO2	500.1325200 MHz
SI	32768
SF	125.7577630 MHz
WDW	EM
SSB	0
LB	0.90 Hz
GB	0
PC	1.40

pz3_162_f4 di-Naphthoyl DHP HR 1H/CDCl3

PZ_III_162_f4 di-Naphthoyl DHP 13C/CDCl3

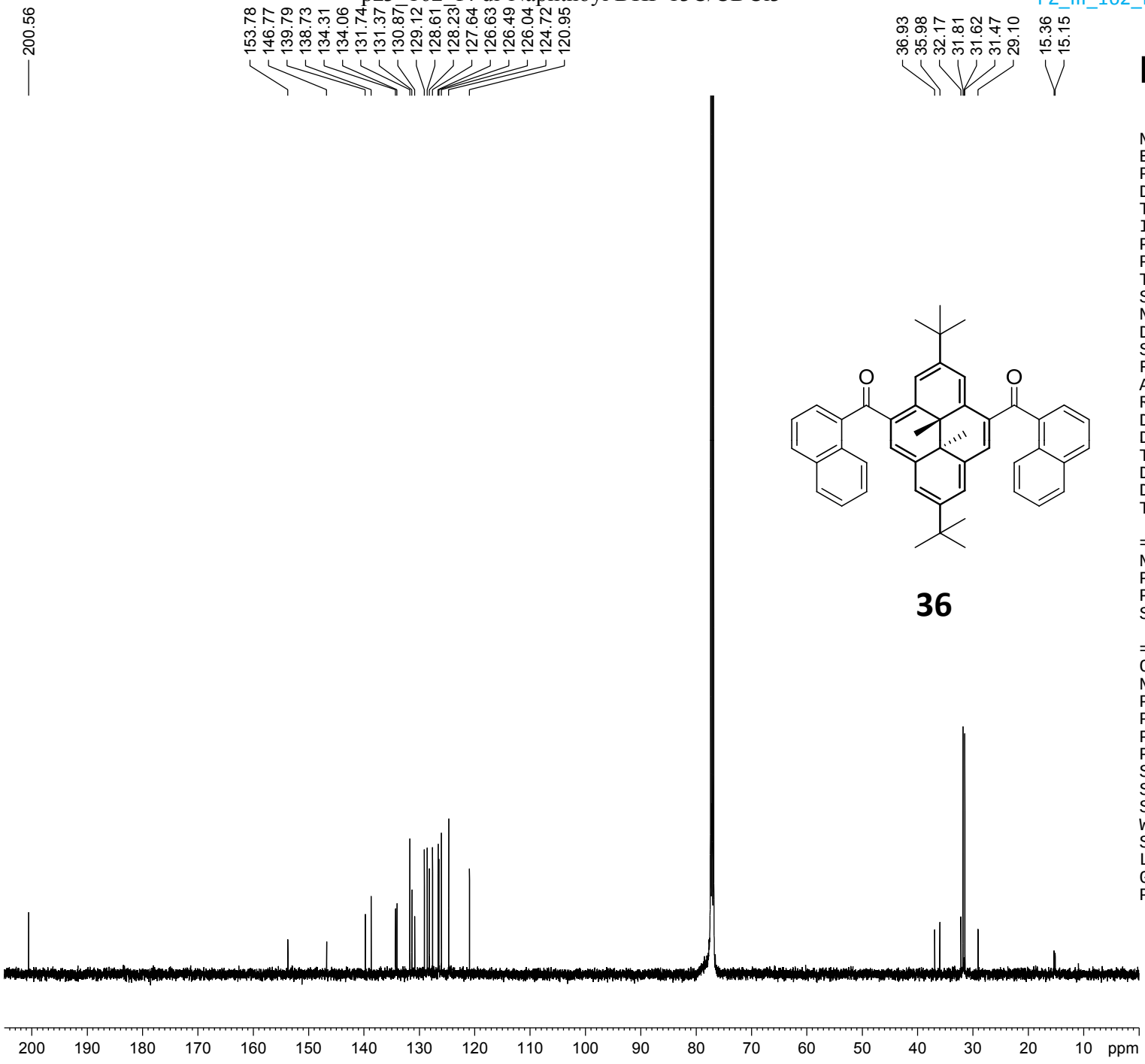


36

NAME	pz3_162_f4
EXPNO	1
PROCNO	1
Date_	20080602
Time	17.22
INSTRUM	spect
PROBHD	5 mm PABBO BB-
PULPROG	zg30
TD	32768
SOLVENT	CDCl3
NS	16
DS	2
SWH	8012.820 Hz
FIDRES	0.244532 Hz
AQ	2.0448356 sec
RG	812.7
DW	62.400 usec
DE	6.50 usec
TE	297.7 K
D1	1.00000000 sec
TD0	1
======== CHANNEL f1 ========	
NUC1	1H
P1	9.60 usec
PL1	-4.00 dB
SFO1	500.1315200 MHz
SI	16384
SF	500.1300233 MHz
WDW	GM
SSB	0
LB	-0.20 Hz
GB	0.5
PC	1.00

pz3_162_f4 di-Naphthoyl DHP 13C/CDCl3

PZ_III_162_f4 di-Naphthoyl DHP 13C/CDCl3

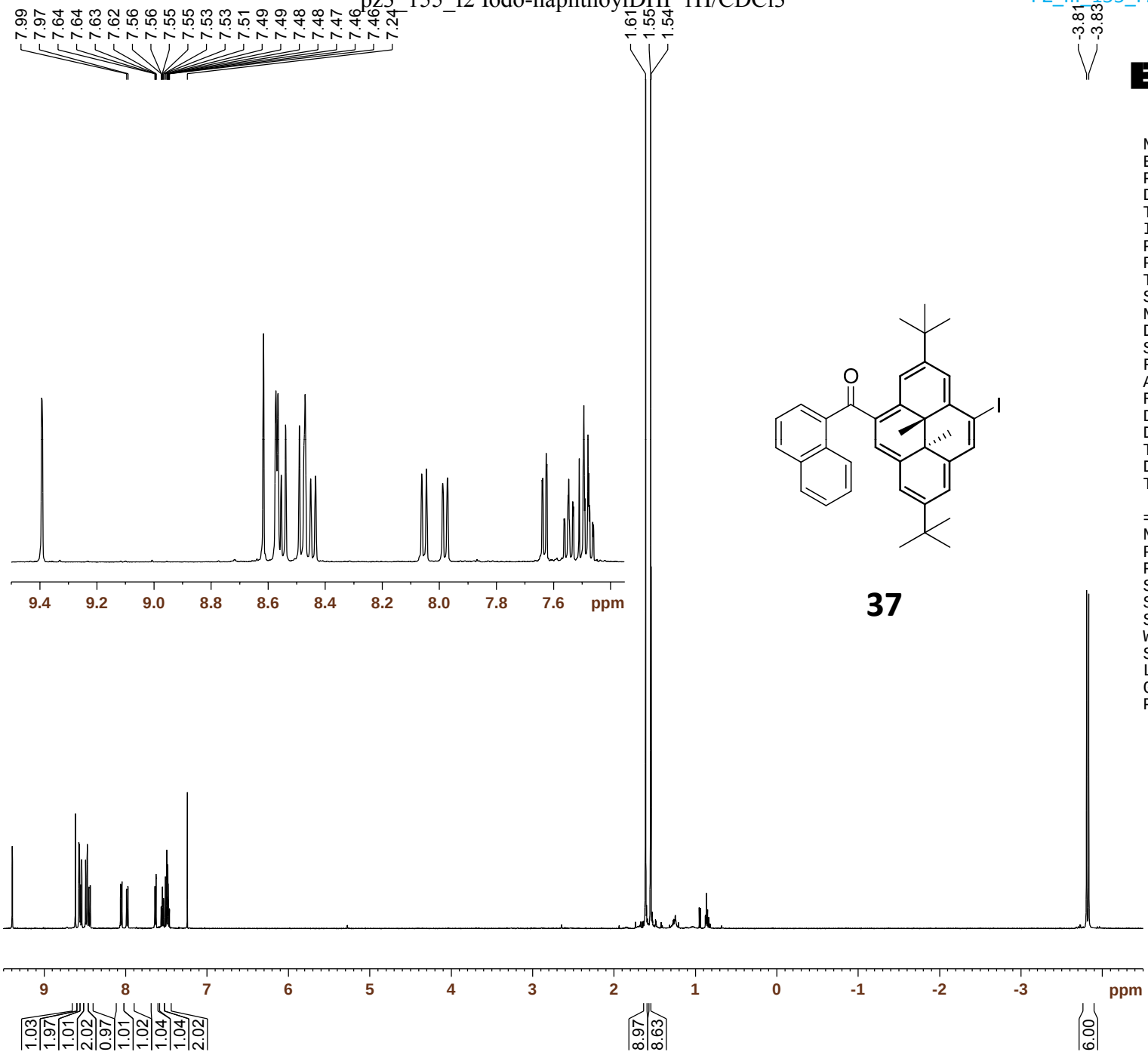


36

NAME	pz3_162_f4
EXPNO	3
PROCNO	1
Date_	20080602
Time	18.33
INSTRUM	spect
PROBHD	5 mm PABBO BB-
PULPROG	zgpg30
TD	65536
SOLVENT	CDCl3
NS	20480
DS	4
SWH	30864.197 Hz
FIDRES	0.470950 Hz
AQ	1.0617495 sec
RG	14596.5
DW	16.200 usec
DE	6.50 usec
TE	299.9 K
D1	1.00000000 sec
D11	0.03000000 sec
TD0	1
======== CHANNEL f1 ========	
NUC1	13C
P1	10.00 usec
PL1	3.00 dB
SFO1	125.7715390 MHz
======== CHANNEL f2 ========	
CPDPRG2	waltz16
NUC2	1H
PCPD2	80.00 usec
PL2	-4.00 dB
PL12	14.42 dB
PL13	14.24 dB
SFO2	500.1325200 MHz
SI	32768
SF	125.7577742 MHz
WDW	EM
SSB	0
LB	0.90 Hz
GB	0
PC	1.40

pz3_155_f2 Iodo-naphthoylDHP 1H/CDCl3

PZ_III_155_F2 Iodo-naphthoylDHP 1H NMR

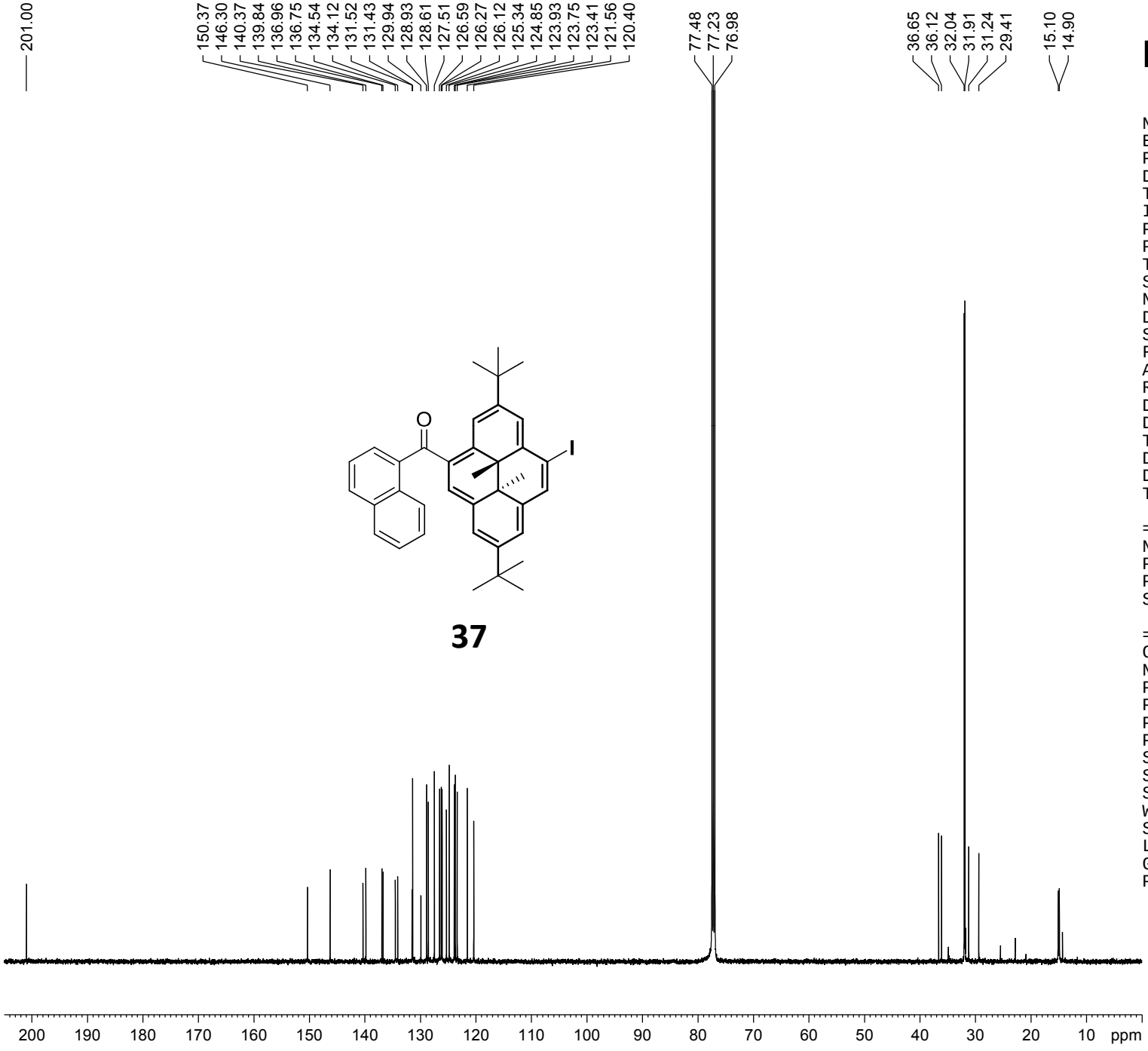


37

NAME	pz3_155_f2
EXPNO	1
PROCNO	1
Date_	20080522
Time	17.50
INSTRUM	spect
PROBHD	5 mm PABBO BB-
PULPROG	zg30
TD	32768
SOLVENT	CDCl3
NS	16
DS	2
SWH	8012.820 Hz
FIDRES	0.244532 Hz
AQ	2.0448356 sec
RG	256
DW	62.400 usec
DE	6.50 usec
TE	297.2 K
D1	1.00000000 sec
TD0	1
======== CHANNEL f1 ========	
NUC1	1H
P1	9.60 usec
PL1	-4.00 dB
SFO1	500.1315200 MHz
SI	16384
SF	500.1300233 MHz
WDW	GM
SSB	0
LB	-0.20 Hz
GB	0.5
PC	1.00

pz3_155_f2 Iodo-naphthoylDHP 13C/CDCl3

PZ_III_155_F2 Iodo-naphthoylDHP_13C NMR



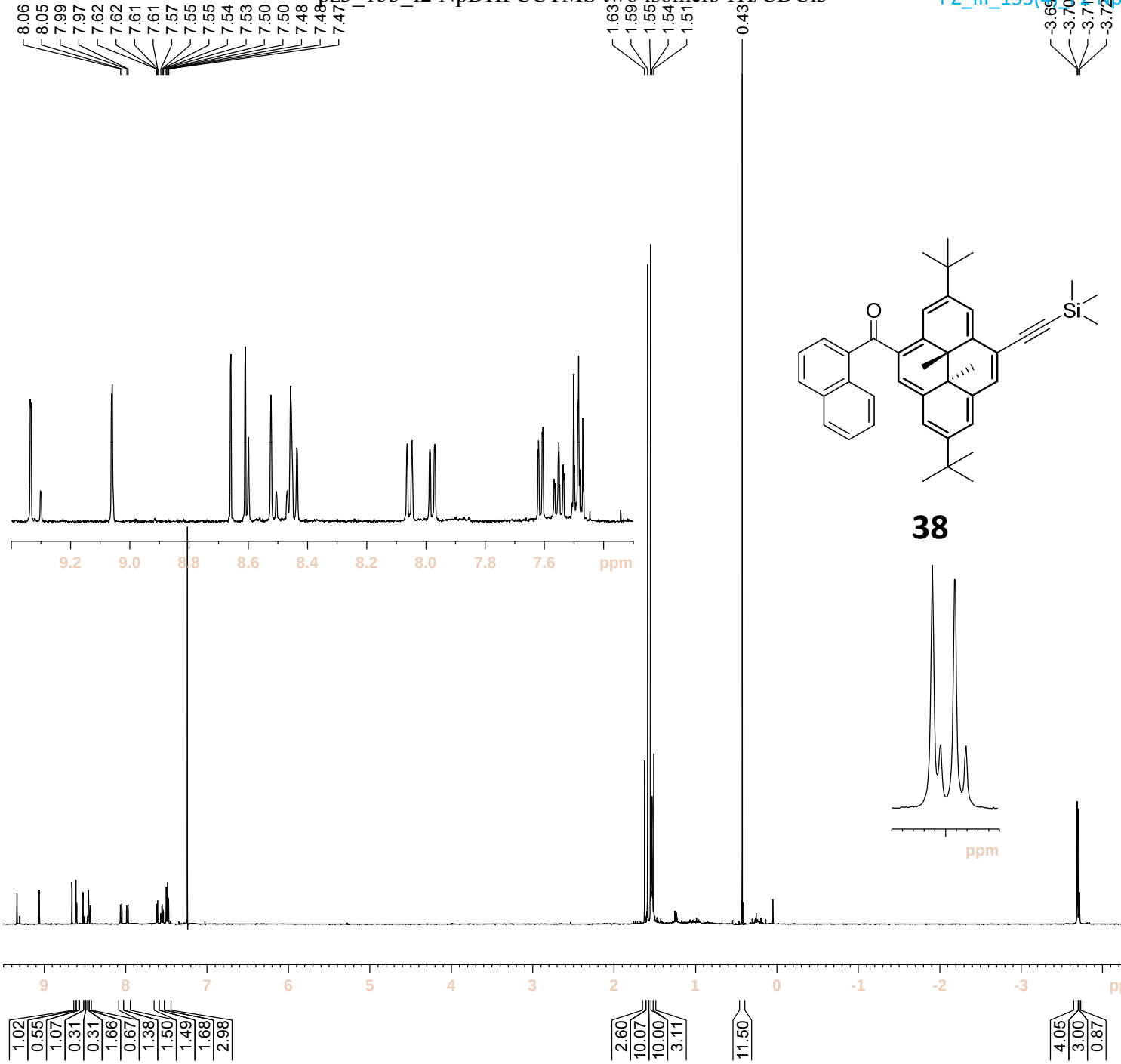

```
NAME            pz3_155_f2
EXPNO                    3
PROCNO                   1
Date_             20080523
Time                 3.04
INSTRUM             spect
PROBHD    5 mm PABBO BB-
PULPROG            zgpg30
TD                  65536
SOLVENT             CDCl3
NS                  15360
DS                      4
SWH            30864.197 Hz
FIDRES          0.470950 Hz
AQ              1.0617495 sec
RG                14596.5
DW                16.200 usec
DE                 6.50 usec
TE                 300.1 K
D1             1.00000000 sec
D11            0.03000000 sec
TD0                     1

======== CHANNEL f1 ========
NUC1                   13C
P1                 10.00 usec
PL1                 3.00 dB
SFO1         125.7715390 MHz

======== CHANNEL f2 ========
CPDPRG2           waltz16
NUC2                   1H
PCPD2              80.00 usec
PL2                -4.00 dB
PL12               14.42 dB
PL13               14.24 dB
SFO2         500.1325200 MHz
SI                  32768
SF           125.7577622 MHz
WDW                    EM
SSB                     0
LB                 0.90 Hz
GB                      0
PC                 1.40
```

pz3_153_f2 NpDHPCCTMS two isomers 1H/CDCl3

PZ_III_153(4)_F2 NpDHPCCTMS two isomers 1H NMR

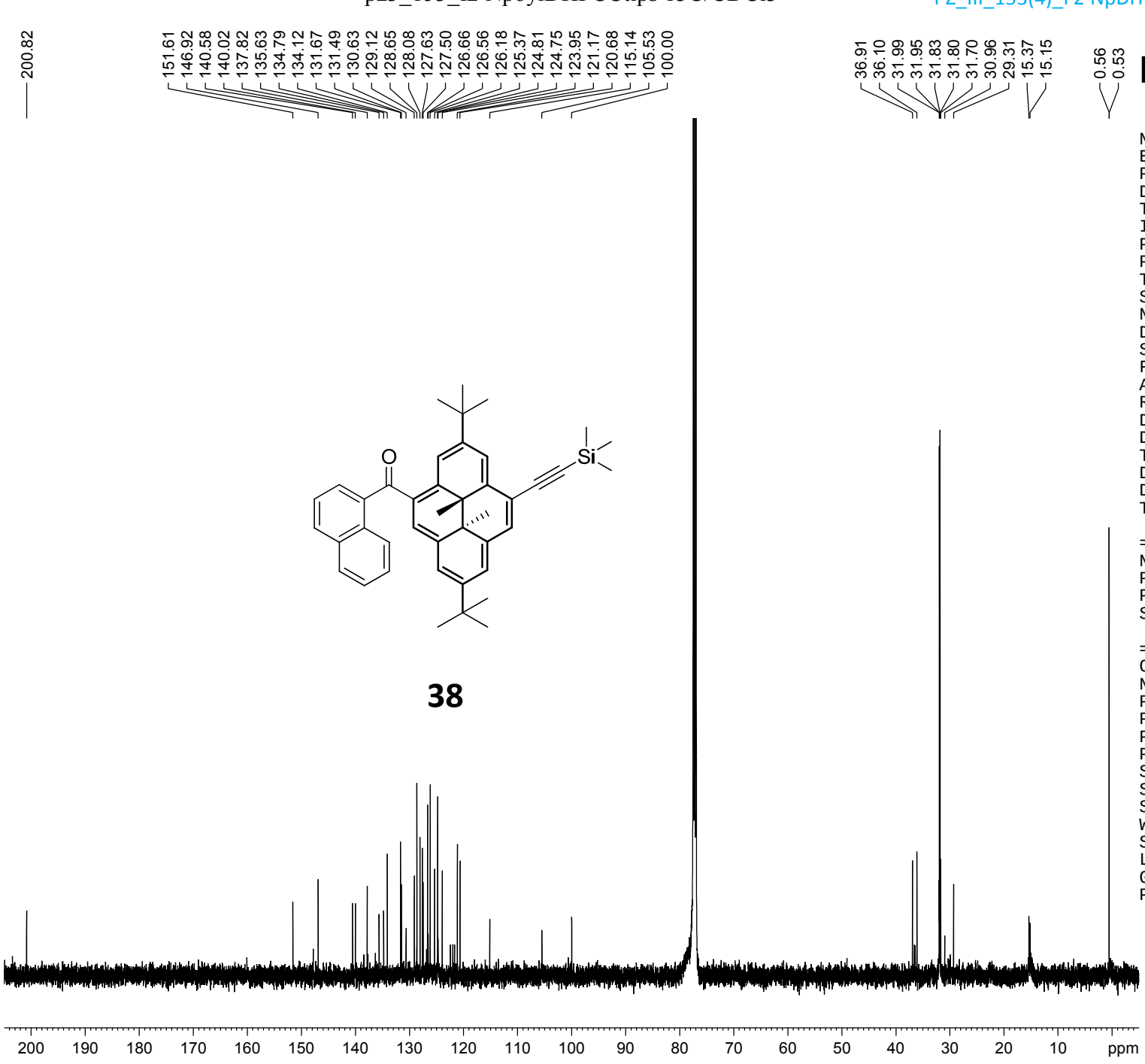


38

NAME	PZ3_153_F2
EXPNO	1
PROCNO	1
Date_	20080524
Time	13.53
INSTRUM	spect
PROBHD	5 mm PABBO BB-
PULPROG	zg30
TD	32768
SOLVENT	CDCl3
NS	16
DS	2
SWH	8012.820 Hz
FIDRES	0.244532 Hz
AQ	2.0448356 sec
RG	574.7
DW	62.400 usec
DE	6.50 usec
TE	297.8 K
D1	1.00000000 sec
TD0	1
======== CHANNEL f1 ========	
NUC1	1H
P1	9.60 usec
PL1	-4.00 dB
SFO1	500.1315200 MHz
SI	16384
SF	500.1300233 MHz
WDW	GM
SSB	0
LB	-0.20 Hz
GB	0.5
PC	1.00

pz3_153_f2 NpoylDHPCCtips 13C/CDCl3

PZ_III_153(4)_F2 NpDHPCCTMS two isomers_13C NMR



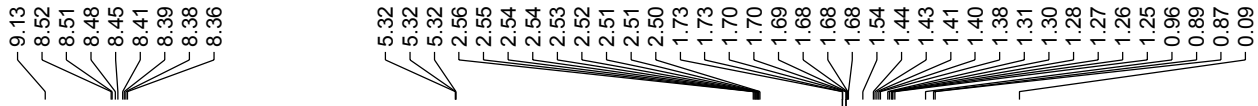

```
NAME            PZ3_153_F2
EXPNO                    3
PROCNO                   1
Date_             20080525
Time                 2.06
INSTRUM             spect
PROBHD    5 mm PABBO BB-
PULPROG            zgpg30
TD                  65536
SOLVENT             CDCl3
NS                  20480
DS                      4
SWH           30864.197 Hz
FIDRES         0.470950 Hz
AQ             1.0617495 sec
RG               14596.5
DW                16.200 usec
DE                 6.50 usec
TE                299.7 K
D1             1.00000000 sec
D11            0.03000000 sec
TD0                     1

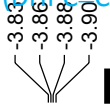
======== CHANNEL f1 ========
NUC1                  13C
P1                 10.00 usec
PL1                 3.00 dB
SFO1         125.7715390 MHz

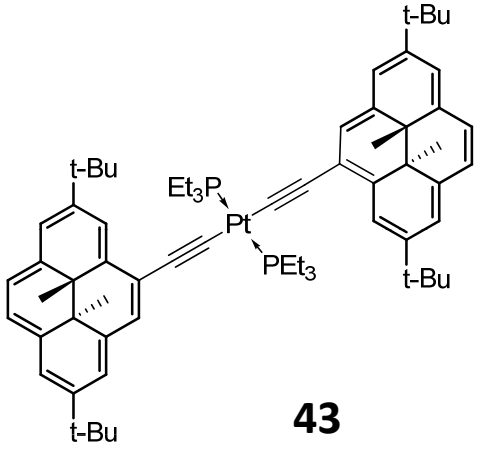
======== CHANNEL f2 ========
CPDPRG2           waltz16
NUC2                  1H
PCPD2              80.00 usec
PL2                -4.00 dB
PL12               14.42 dB
PL13               14.24 dB
SFO2         500.1325200 MHz
SI                 32768
SF           125.7577620 MHz
WDW                   EM
SSB                    0
LB                 0.90 Hz
GB                     0
PC                 1.40
```

AVCG1767-1 PZ-117-P/CD2Cl2 1H/AMB 25/07/05 0.7 ppm/cm

PZ_I_117 (DHPC≡C)2Pt(PEt3)2 1H NMR AVCG1767

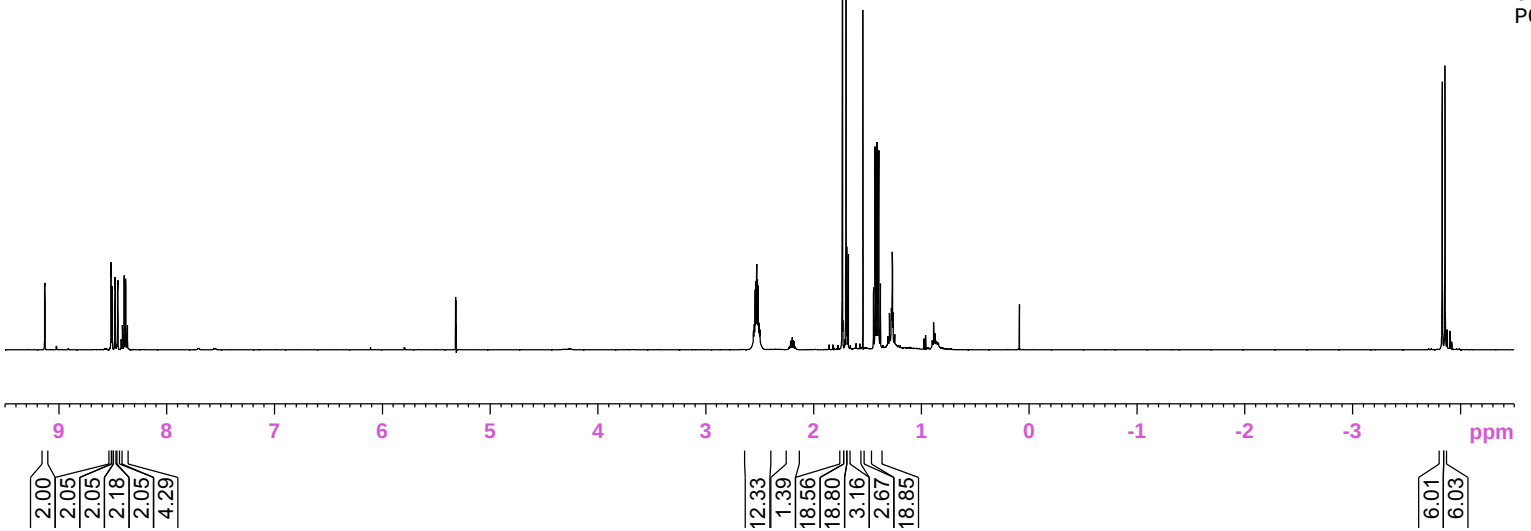






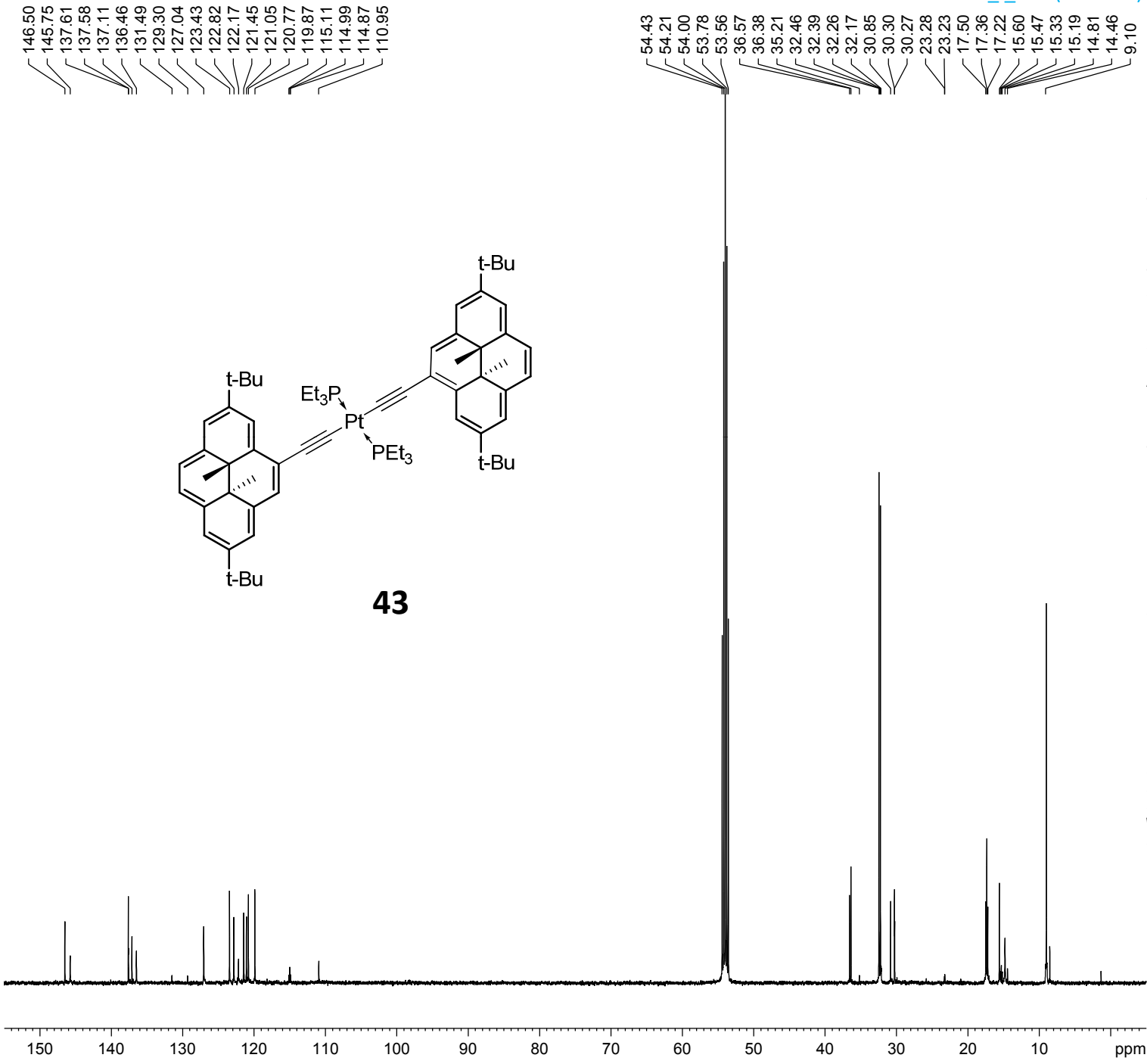
43

NAME	avcg1767
EXPNO	1
PROCNO	1
Date_	20050725
Time	9.46
INSTRUM	AV500
PROBHD	5 mm BBO BB-1H
PULPROG	zg30
TD	32768
SOLVENT	CD2Cl2
NS	16
DS	2
SWH	8012.820 Hz
FIDRES	0.244532 Hz
AQ	2.0448356 sec
RG	114
DW	62.400 usec
DE	6.00 usec
TE	300.0 K
D1	1.00000000 sec
======== CHANNEL f1 ========	
NUC1	1H
P1	11.50 usec
PL1	-4.00 dB
SFO1	500.1315200 MHz
SI	16384
SF	500.1300208 MHz
WDW	GM
SSB	0
LB	-0.40 Hz
GB	0.5
PC	1.00



AVCG1769 PZ-117-P/CD2Cl2 13C/AMB 25/07/05 10 ppm/cm

PZ_I_117 (DHPC≡C)2Pt(PEt3)2 13C NMR AVCG1769



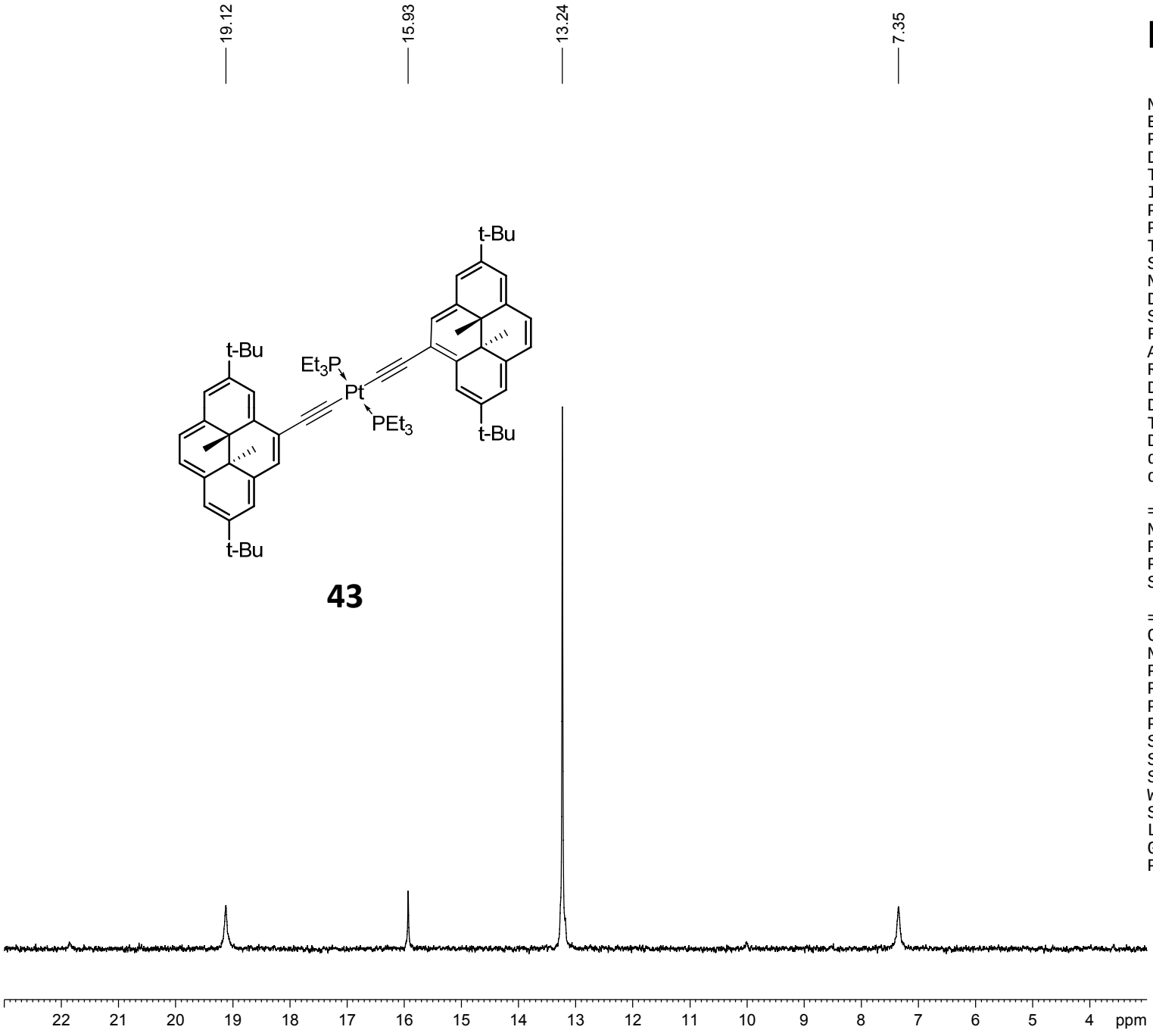

```
NAME              avcg1769
EXPNO                    1
PROCNO                   1
Date_             20050725
Time                 10.20
INSTRUM              AV500
PROBHD    5 mm BBO BB-1H
PULPROG             zgpg30
TD                   65536
SOLVENT             CD2Cl2
NS                     6088
DS                        4
SWH             30864.197 Hz
FIDRES           0.470950 Hz
AQ               1.0617495 sec
RG                   143.7
DW                  16.200 usec
DE                  10.00 usec
TE                  300.0 K
D1              1.00000000 sec
d11             0.03000000 sec
d12             0.00002000 sec

======== CHANNEL f1 ========
NUC1                   13C
P1                    9.00 usec
PL1                   0.00 dB
SFO1          125.7703640 MHz

======== CHANNEL f2 ========
CPDPRG2           waltz16
NUC2                   1H
PCPD2                80.00 usec
PL2                  -4.00 dB
PL12                 14.00 dB
PL13                 14.00 dB
SFO2          500.1315200 MHz
SI                    32768
SF            125.7577145 MHz
WDW                     EM
SSB                      0
LB                    1.00 Hz
GB                       0
PC                    1.40
```

AVCG1768 PZ-117-P/CD2Cl2 31P/AMB 25/07/05 1 ppm/cm

PZ_I_117 (DHPC≡C)2Pt(PEt3)2 31P NMR AVCG1768



43

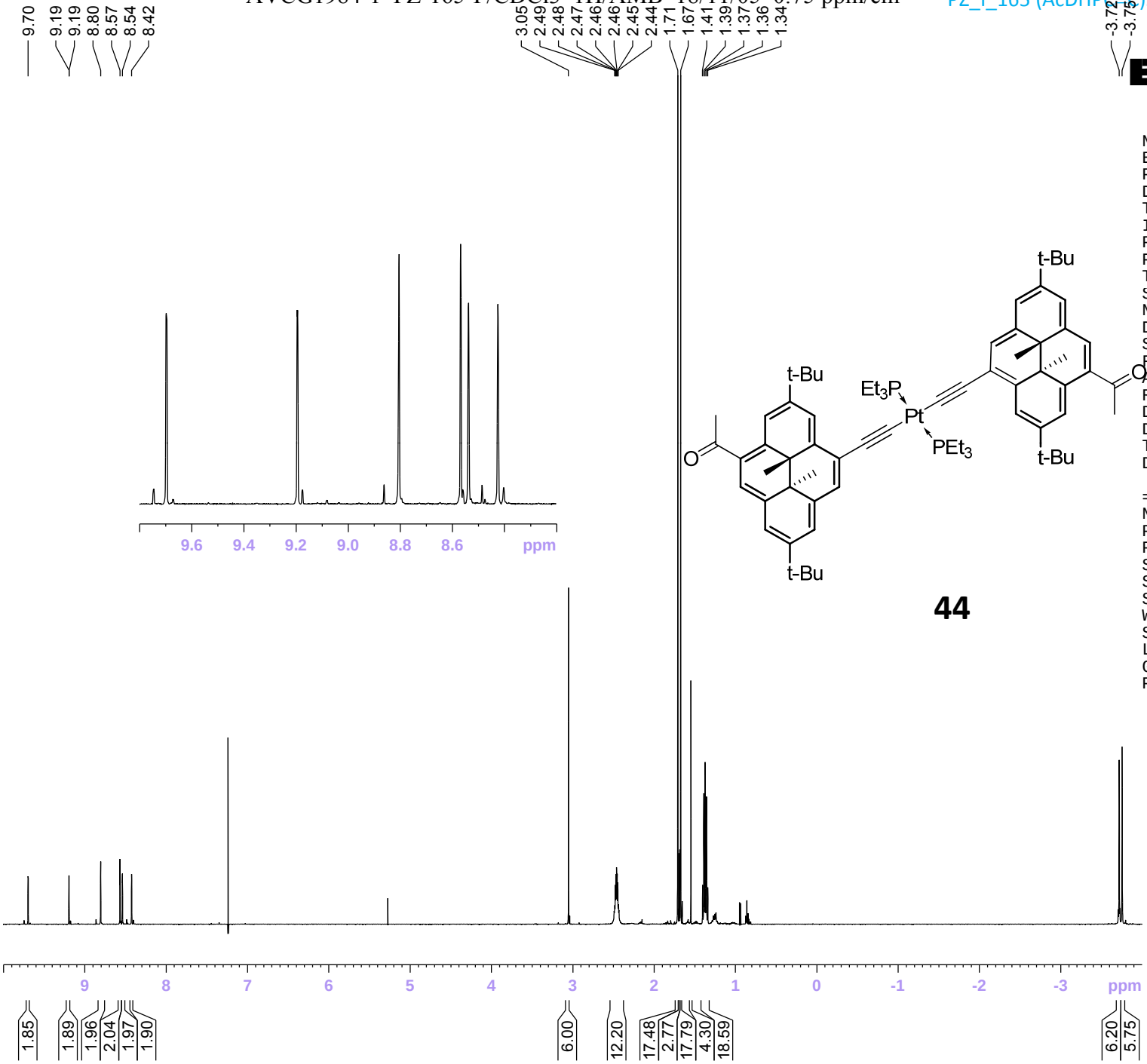
```
NAME              avcg1768
EXPNO                    1
PROCNO                   1
Date_             20050725
Time                 10.03
INSTRUM              AV500
PROBHD   5 mm BBO BB-1H
PULPROG           zgpg30
TD                32768
SOLVENT           CD2Cl2
NS                   32
DS                    2
SWH           14005.603 Hz
FIDRES         0.427417 Hz
AQ             1.1699033 sec
RG                16384
DW                35.700 usec
DE                 6.00 usec
TE                300.0 K
D1             1.00000000 sec
d11            0.03000000 sec
d12            0.00002000 sec

======== CHANNEL f1 ========
NUC1                 31P
P1                10.00 usec
PL1               -1.00 dB
SFO1         202.4586600 MHz

======== CHANNEL f2 ========
CPDPRG2          waltz16
NUC2                 1H
PCPD2             80.00 usec
PL2               -4.00 dB
PL12              14.00 dB
PL13              14.00 dB
SFO2         500.1325200 MHz
SI                16384
SF           202.4562660 MHz
WDW                  EM
SSB                   0
LB                 0.80 Hz
GB                    0
PC                 1.40
```

AVCG1984-1 PZ-165-P/CDCl3 1H/AMB 18/11/05 0.75 ppm/cm

PZ_I_165 (AcDHPC≡C)2Pt(Et3P)2 1H NMR AVCG1984



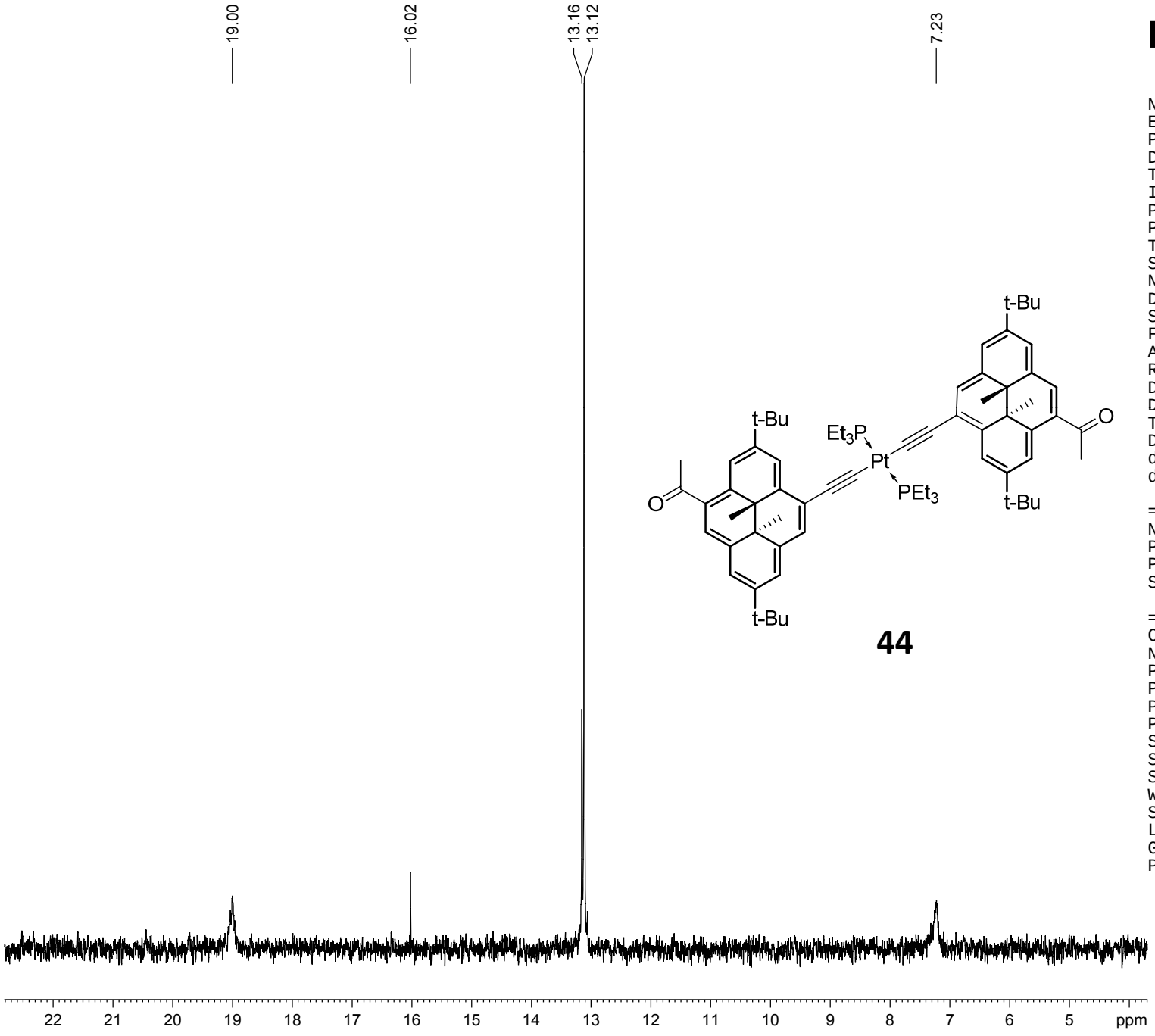
44

```
NAME                avcg1984
EXPNO                      1
PROCNO                     1
Date_               20051118
Time                   10.16
INSTRUM                AV500
PROBHD    5 mm BBO BB-1H
PULPROG                zg30
TD                    32768
SOLVENT               CDCl3
NS                       16
DS                        2
SWH                8012.820 Hz
FIDRES             0.244532 Hz
AQ                 2.0448356 sec
RG                       256
DW                  62.400 usec
DE                   6.00 usec
TE                   300.0 K
D1                1.00000000 sec

======== CHANNEL f1 ========
NUC1                      1H
P1                    9.70 usec
PL1                  -4.00 dB
SFO1           500.1315200 MHz
SI                    16384
SF             500.1300240 MHz
WDW                      GM
SSB                       0
LB                   -0.40 Hz
GB                    0.42
PC                    1.00
```

AVCG1987 PZ-165-P/CDCl3 31P/AMB 18/11/05 1 ppm/cm

PZ_I_165 (AcDHPC≡C)2Pt(Et3P)2 31P NMR AVCG1984



44

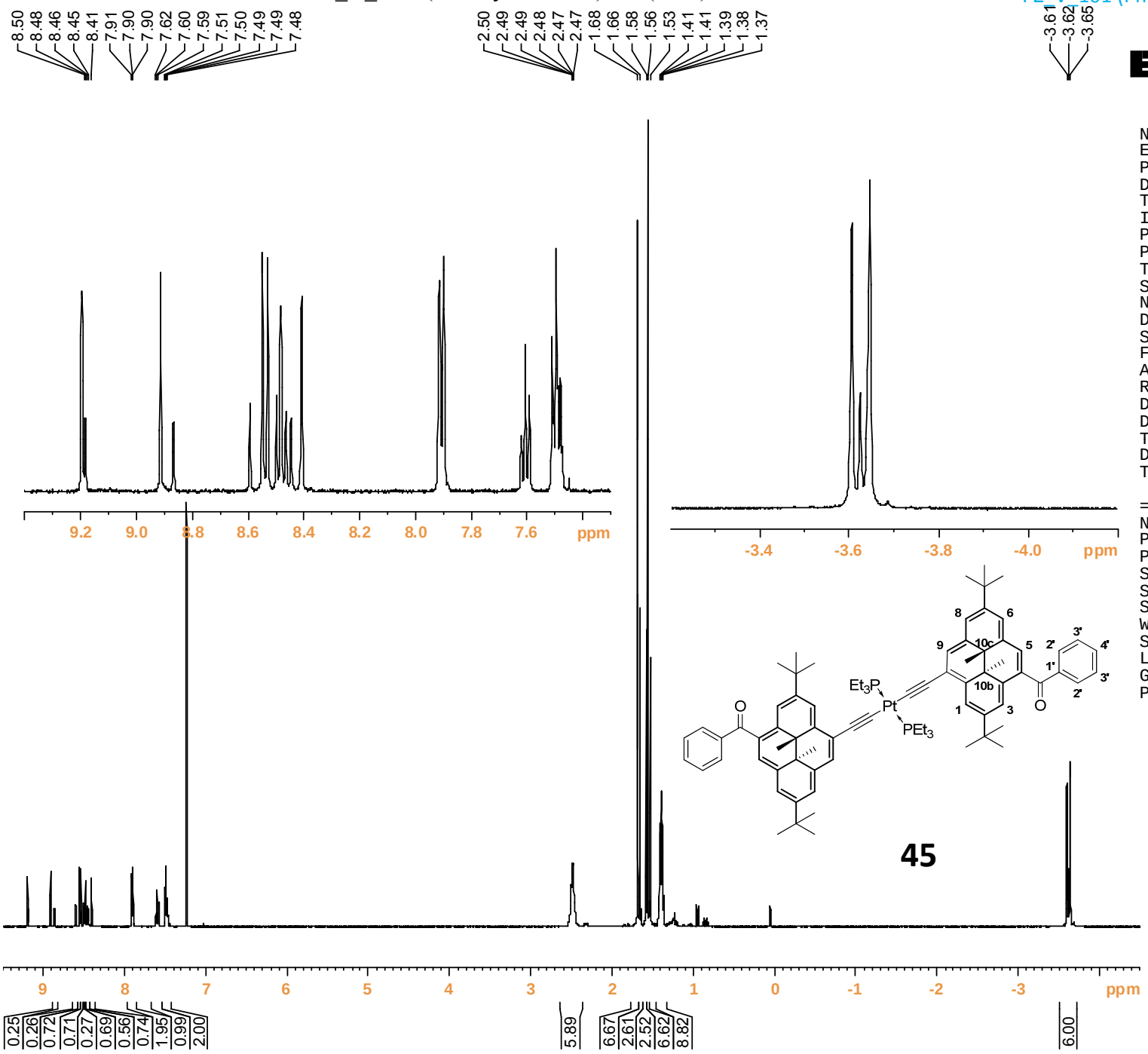
```
NAME              avcg1987
EXPNO                    1
PROCNO                   1
Date_             20051118
Time                14.21
INSTRUM              AV500
PROBHD   5 mm BBO BB-1H
PULPROG             zgpg30
TD                   32768
SOLVENT              CDCl3
NS                      32
DS                       2
SWH             10000.000 Hz
FIDRES          0.305176 Hz
AQ              1.6385000 sec
RG                20642.5
DW                 50.000 usec
DE                  6.00 usec
TE                 300.0 K
D1              1.00000000 sec
d11             0.03000000 sec
d12             0.00002000 sec

======== CHANNEL f1 ========
NUC1                   31P
P1                    8.20 usec
PL1                  -1.00 dB
SFO1          202.4589600 MHz

======== CHANNEL f2 ========
CPDPRG2            waltz16
NUC2                   1H
PCPD2               80.00 usec
PL2                 -4.00 dB
PL12                14.40 dB
PL13                14.40 dB
SFO2          500.1315200 MHz
SI                   16384
SF            202.4562143 MHz
WDW                    EM
SSB                     0
LB                   0.60 Hz
GB                      0
PC                   1.40
```

PZ_V_101 (Benzoyl DHPCC)2 Pt (PEt3)2 1H/CDCl3

PZ_V_101 (PhCODHPC≡C)2Pt(PEt3)2 1H NMR

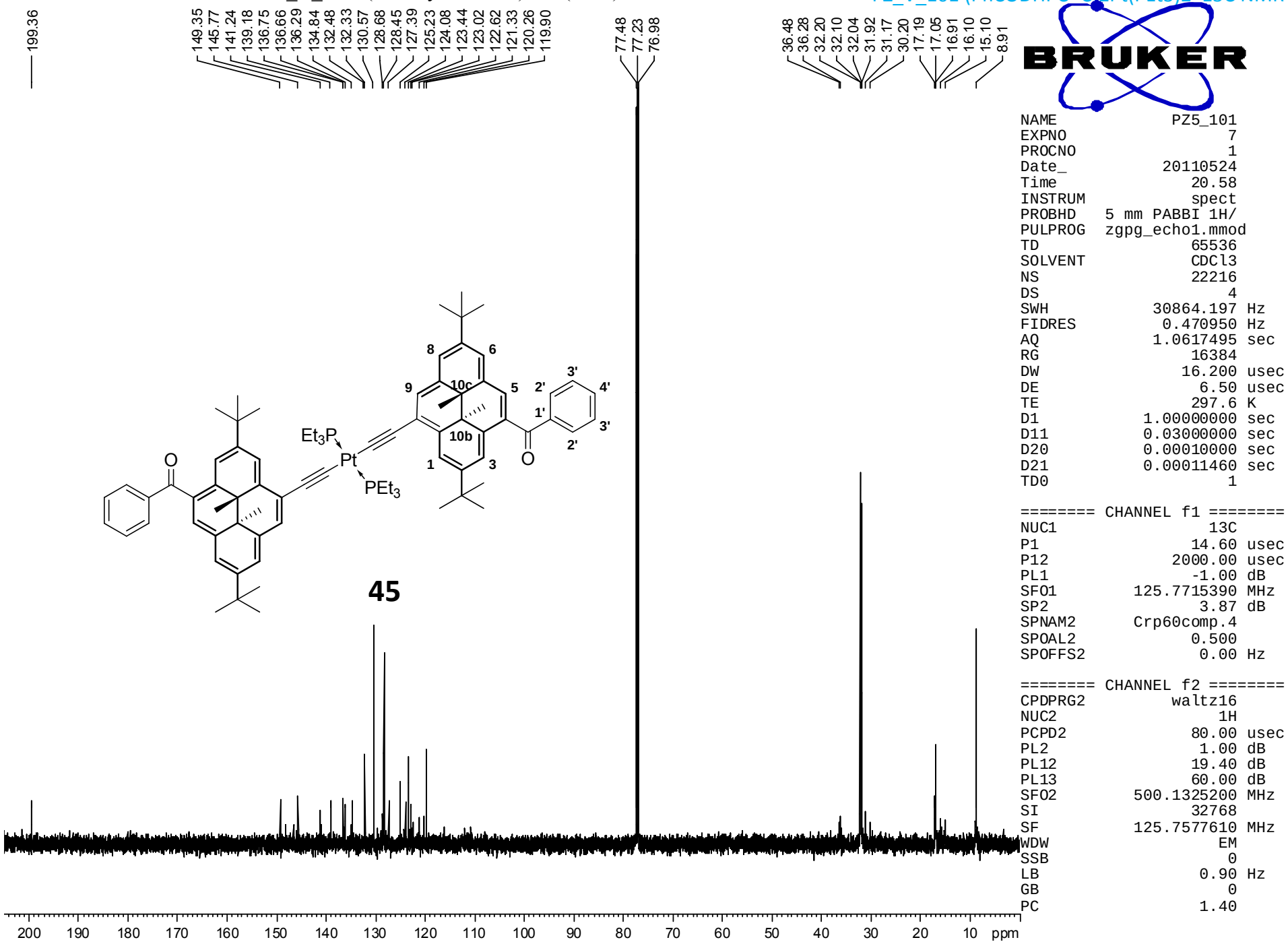


BRUKER

NAME	PZ5_101
EXPNO	6
PROCNO	1
Date_	20110524
Time	16.26
INSTRUM	spect
PROBHD	5 mm PABBI 1H/
PULPROG	zg30
TD	32768
SOLVENT	CDCl3
NS	16
DS	2
SWH	8012.820 Hz
FIDRES	0.244532 Hz
AQ	2.0448356 sec
RG	228.1
DW	62.400 usec
DE	6.50 usec
TE	297.2 K
D1	1.00000000 sec
TD0	1
======== CHANNEL f1 ========	
NUC1	1H
P1	10.20 usec
PL1	1.00 dB
SFO1	500.1315200 MHz
SI	16384
SF	500.1300233 MHz
WDW	GM
SSB	0
LB	-0.20 Hz
GB	0.5
PC	1.00

PZ_V_101 (Benzoyl DHPCC)2 Pt (PEt3)2 13C in CDCl3

PZ_V_101 (PhCODHPC≡C)2Pt(PEt3)2_13C NMR

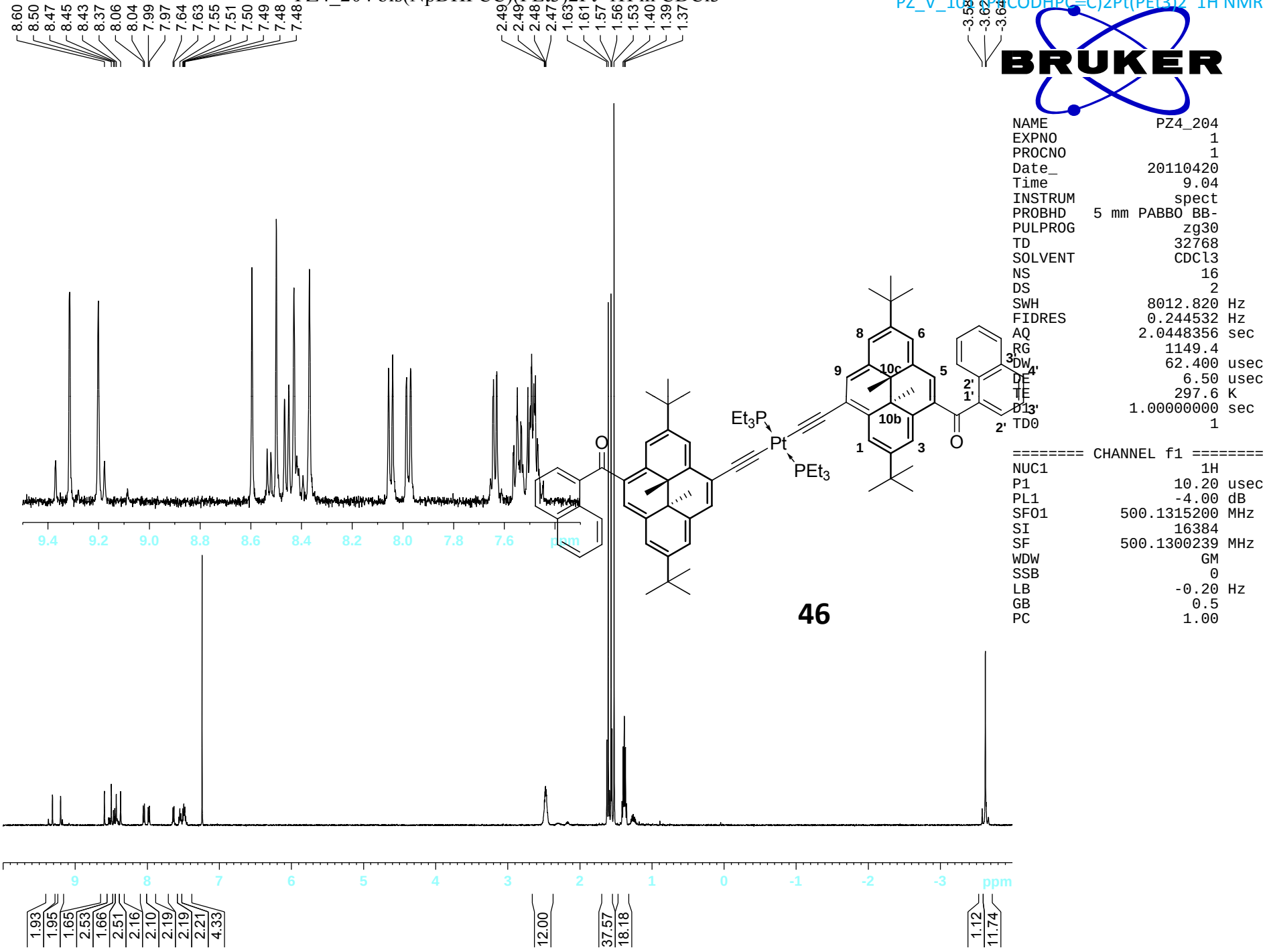


BRUKER

NAME	PZ5_101
EXPNO	7
PROCNO	1
Date_	20110524
Time	20.58
INSTRUM	spect
PROBHD	5 mm PABBI 1H/
PULPROG	zgpg_echo1.mmod
TD	65536
SOLVENT	CDCl3
NS	22216
DS	4
SWH	30864.197 Hz
FIDRES	0.470950 Hz
AQ	1.0617495 sec
RG	16384
DW	16.200 usec
DE	6.50 usec
TE	297.6 K
D1	1.00000000 sec
D11	0.03000000 sec
D20	0.00010000 sec
D21	0.00011460 sec
TD0	1
======== CHANNEL f1 ========	
NUC1	13C
P1	14.60 usec
P12	2000.00 usec
PL1	-1.00 dB
SFO1	125.7715390 MHz
SP2	3.87 dB
SPNAM2	Crp60comp.4
SPOAL2	0.500
SPOFFS2	0.00 Hz
======== CHANNEL f2 ========	
CPDPRG2	waltz16
NUC2	1H
PCPD2	80.00 usec
PL2	1.00 dB
PL12	19.40 dB
PL13	60.00 dB
SFO2	500.1325200 MHz
SI	32768
SF	125.7577610 MHz
WDW	EM
SSB	0
LB	0.90 Hz
GB	0
PC	1.40

PZ4_204 bis(NpDHPCC)(PEt3)2Pt_1H in CDCl3

PZ_V_101 (PhCODHPC≡C)2Pt(PEt3)2_1H NMR

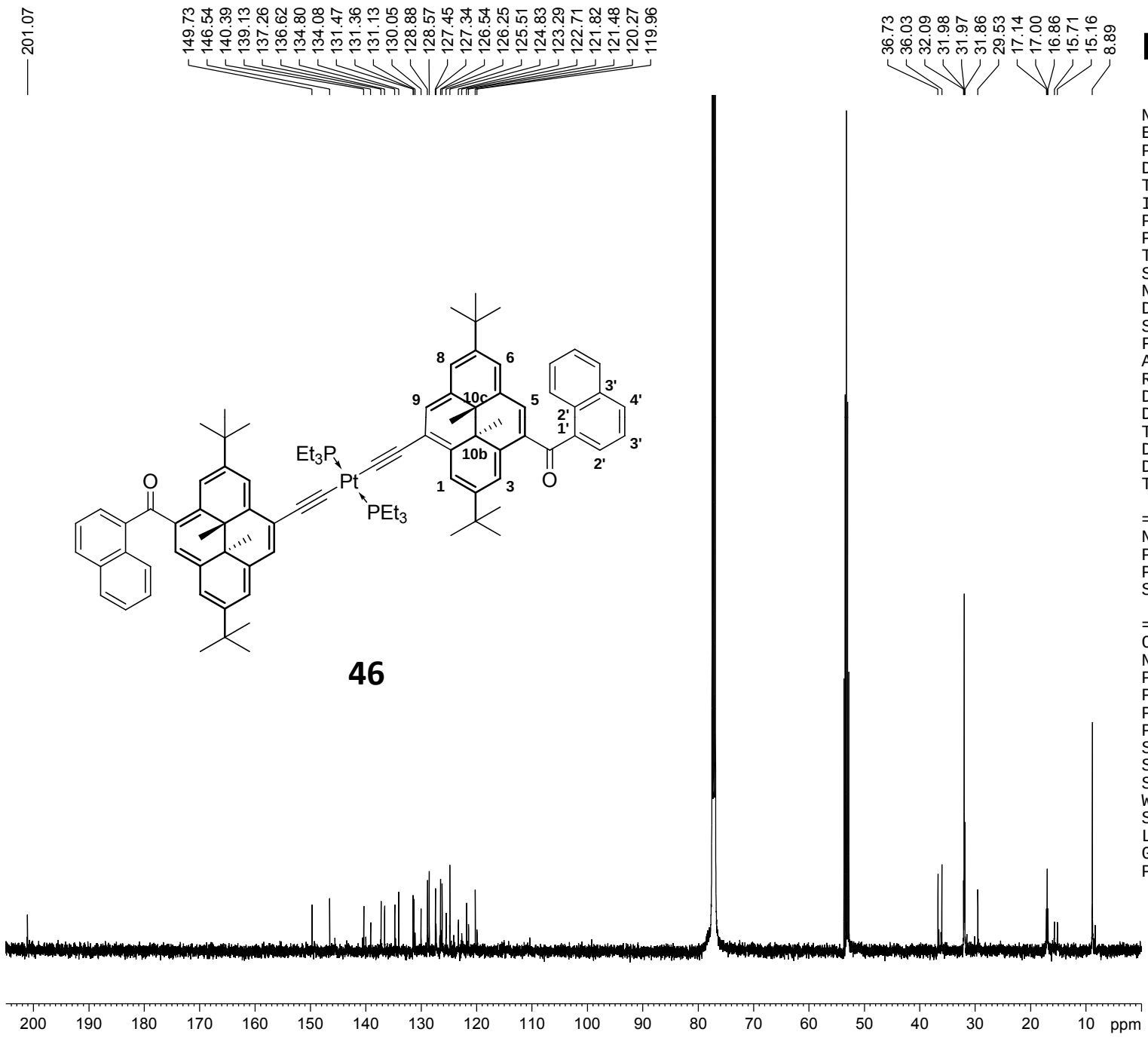


46

```
NAME                 PZ4_204
EXPNO                      1
PROCNO                     1
Date_               20110420
Time                    9.04
INSTRUM                spect
PROBHD    5 mm PABBO BB-
PULPROG                zg30
TD                    32768
SOLVENT               CDCl3
NS                       16
DS                        2
SWH                8012.820 Hz
FIDRES             0.244532 Hz
AQ                 2.0448356 sec
RG                    1149.4
DW                  62.400 usec
DE                   6.50 usec
TE                   297.6 K
D13                1.00000000 sec
TD0                        1

======== CHANNEL f1 ========
NUC1                      1H
P1                    10.20 usec
PL1                   -4.00 dB
SFO1           500.1315200 MHz
SI                     16384
SF             500.1300239 MHz
WDW                       GM
SSB                        0
LB                    -0.20 Hz
GB                       0.5
PC                      1.00
```

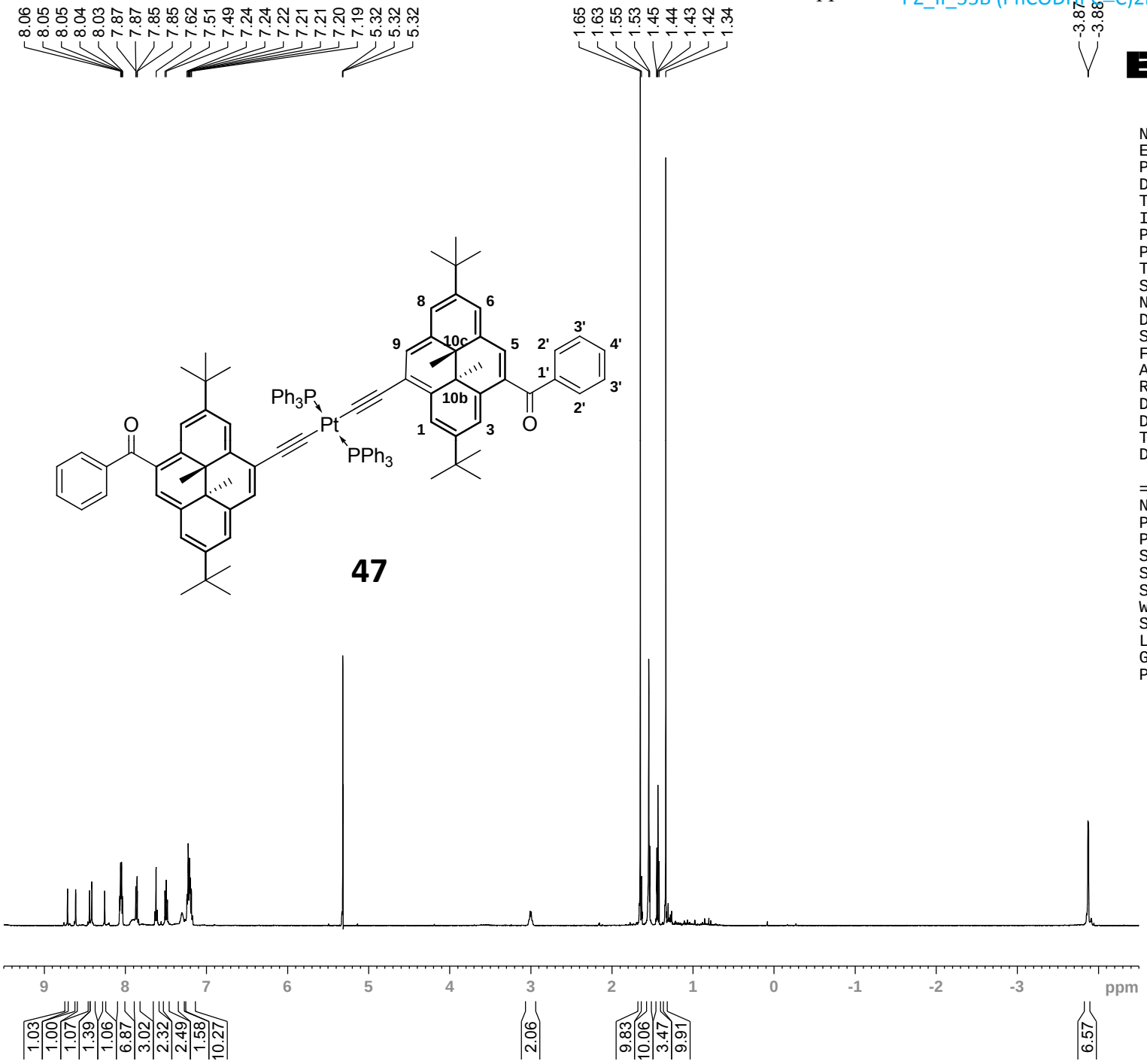
PZ4_204 bis(NpDHPCC)(PEt3)2Pt 13C in CDCl3



NAME	PZ4_204
EXPNO	4
PROCNO	1
Date_	20110422
Time	10.24
INSTRUM	spect
PROBHD	5 mm PABBO BB-
PULPROG	zgpg30
TD	65536
SOLVENT	CDCl3
NS	64778
DS	4
SWH	30864.197 Hz
FIDRES	0.470950 Hz
AQ	1.0617495 sec
RG	2580.3
DW	16.200 usec
DE	6.50 usec
TE	298.6 K
D1	1.00000000 sec
D11	0.03000000 sec
TD0	1
======== CHANNEL f1 ========	
NUC1	13C
P1	10.00 usec
PL1	3.00 dB
SFO1	125.7715390 MHz
======== CHANNEL f2 ========	
CPDPRG2	waltz16
NUC2	1H
PCPD2	80.00 usec
PL2	-4.00 dB
PL12	14.24 dB
PL13	60.00 dB
SFO2	500.1325200 MHz
SI	32768
SF	125.7577647 MHz
WDW	EM
SSB	0
LB	0.90 Hz
GB	0
PC	1.40

AVCG2286-1 PZ2-55B/CD2Cl2 1H/AMB 29/08/06 0.7 ppm/cm

PZ_II_55B (PhCODHPC≡C)2Pt(PPh3)2 1H NMR AVCG2086



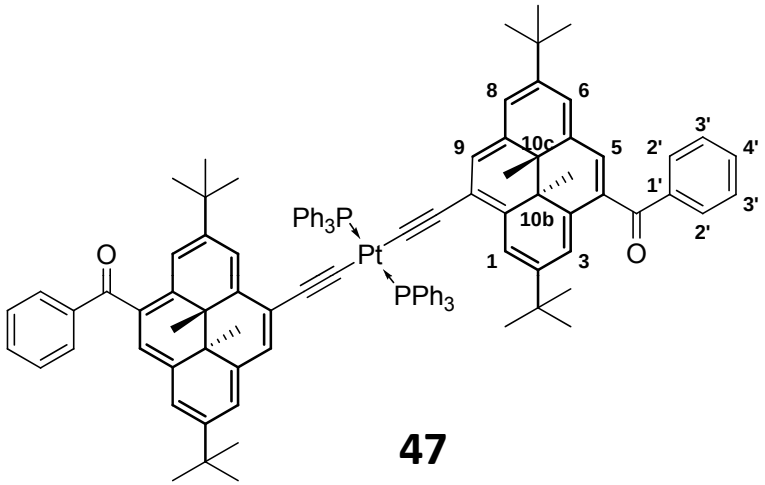
NAME	avcg2286
EXPNO	1
PROCNO	1
Date_	20060829
Time	15.18
INSTRUM	AV500
PROBHD	5 mm BBO BB-1H
PULPROG	zg30
TD	32768
SOLVENT	CD2Cl2
NS	16
DS	2
SWH	8012.820 Hz
FIDRES	0.244532 Hz
AQ	2.0448356 sec
RG	512
DW	62.400 usec
DE	6.00 usec
TE	300.0 K
D1	1.00000000 sec
======== CHANNEL f1 ========	
NUC1	1H
P1	9.80 usec
PL1	-4.00 dB
SFO1	500.1315200 MHz
SI	16384
SF	500.1300208 MHz
WDW	GM
SSB	0
LB	-0.20 Hz
GB	0.5
PC	1.00

AVCG2287 PZ2-55B/CD2Cl2 13C/AMB 30/08/06 11 ppm/cm PZ_II_55B (PhCODHPC≡C)2Pt(PPh3)2 13C NMR AVCG2087

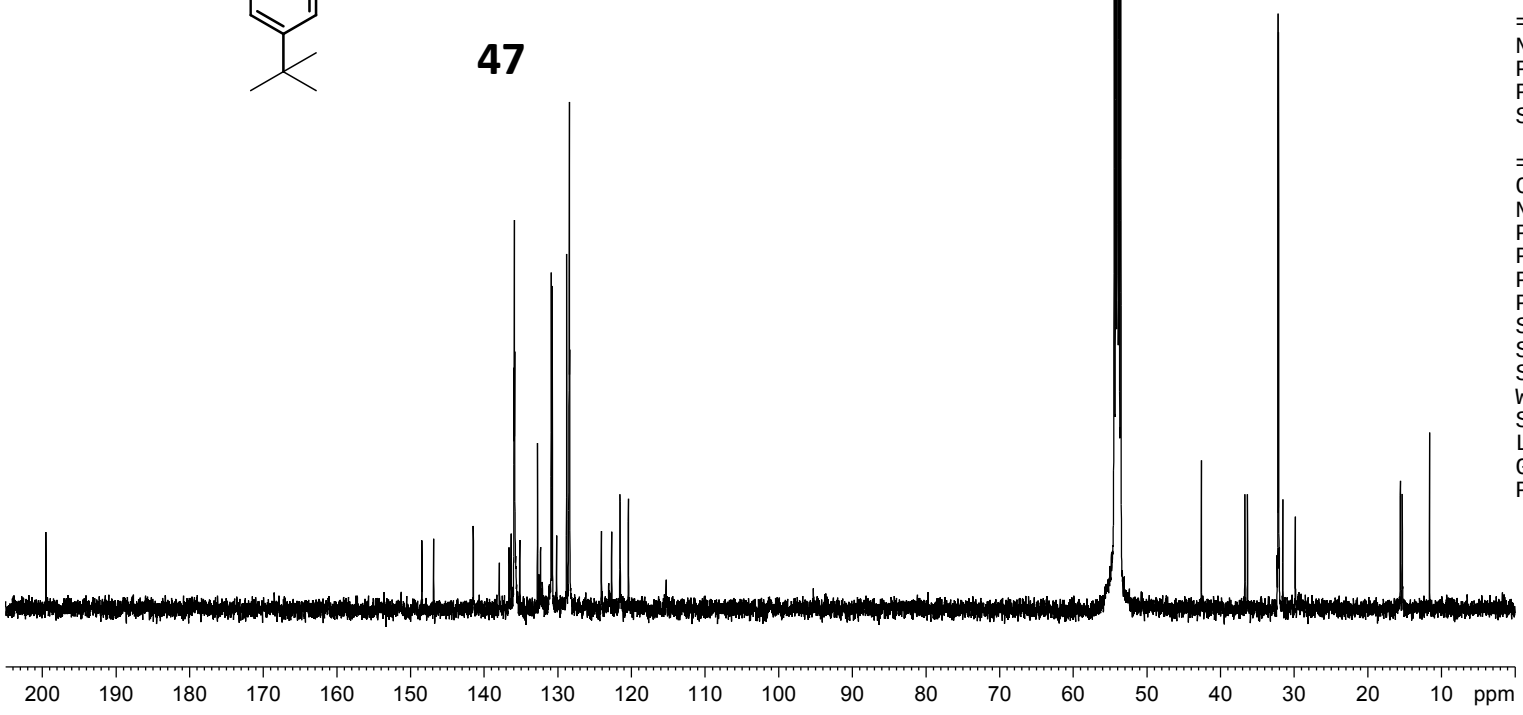
199.50

148.49 146.89 141.49 137.94 136.63 136.34 135.96 135.92 135.87 135.18 132.78 132.59 132.36 130.91 130.77 130.18 128.83 128.49 128.44 128.40 124.11 122.72 121.57 120.42 115.29

54.43 54.21 53.99 53.78 53.56 42.61 36.70 36.34 32.31 32.21 32.13 31.55 29.85 15.58 15.33 11.62



47

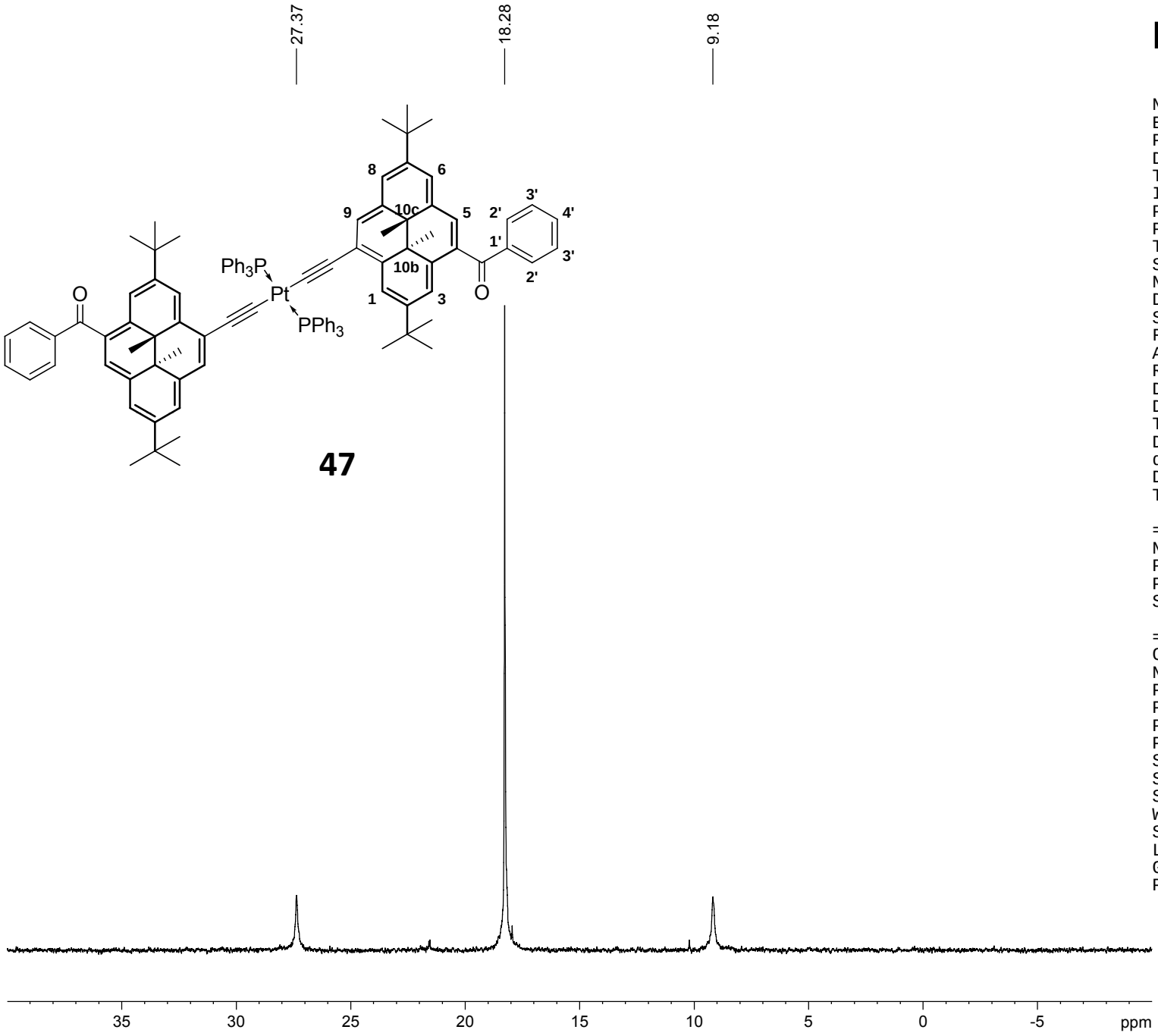


BRUKER

NAME	avcg2287
EXPNO	1
PROCNO	1
Date_	20060829
Time	15.28
INSTRUM	AV500
PROBHD	5 mm BBO BB-1H
PULPROG	zgpg30
TD	65536
SOLVENT	CD2Cl2
NS	28672
DS	4
SWH	30864.197 Hz
FIDRES	0.470950 Hz
AQ	1.0617495 sec
RG	16384
DW	16.200 usec
DE	18.00 usec
TE	300.0 K
D1	1.00000000 sec
d11	0.03000000 sec
d12	0.00002000 sec
======== CHANNEL f1 ========	
NUC1	13C
P1	9.80 usec
PL1	3.00 dB
SFO1	125.7715390 MHz
======== CHANNEL f2 ========	
CPDPRG2	waltz16
NUC2	1H
PCPD2	80.00 usec
PL2	-4.00 dB
PL12	14.69 dB
PL13	14.69 dB
SFO2	500.1315200 MHz
SI	32768
SF	125.7577036 MHz
WDW	EM
SSB	0
LB	1.50 Hz
GB	0
PC	1.40

CGAV70 PZ-55B/CD2Cl2 31P/AMB 15/08/06 2 ppm/cm

PZ_II_55B (PhCODHPC≡C)2Pt(PPh3)2 31P NMR AVCG70

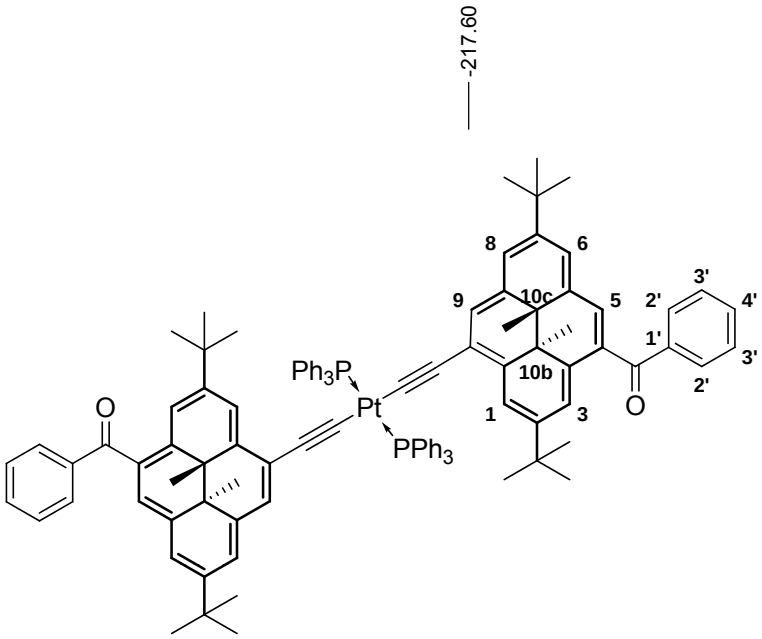


BRUKER

NAME	cgav70
EXPNO	1
PROCNO	1
Date_	20060815
Time	15.40
INSTRUM	av360
PROBHD	5 mm Multinucl
PULPROG	zgpg30
TD	32768
SOLVENT	CD2Cl2
NS	2300
DS	2
SWH	22058.824 Hz
FIDRES	0.673182 Hz
AQ	0.7427914 sec
RG	2050
DW	22.667 usec
DE	12.00 usec
TE	295.4 K
D1	1.00000000 sec
d11	0.03000000 sec
DELTA	0.89999998 sec
TD0	1
======== CHANNEL f1 ========	
NUC1	31P
P1	9.50 usec
PL1	1.00 dB
SFO1	145.7846460 MHz
======== CHANNEL f2 ========	
CPDPRG2	waltz16
NUC2	1H
PCPD2	80.00 usec
PL2	-2.00 dB
PL12	18.00 dB
PL13	18.00 dB
SFO2	360.1317200 MHz
SI	16384
SF	145.7832090 MHz
WDW	EM
SSB	0
LB	1.30 Hz
GB	0
PC	1.40

CGAV72 PZ2-55B/CD2Cl2 195Pt/AMB 31/08/06 10 ppm/cm

PZ_II_55B (PhCODHPC≡C)2Pt(PPh3)2 195Pt NMR AVCG72

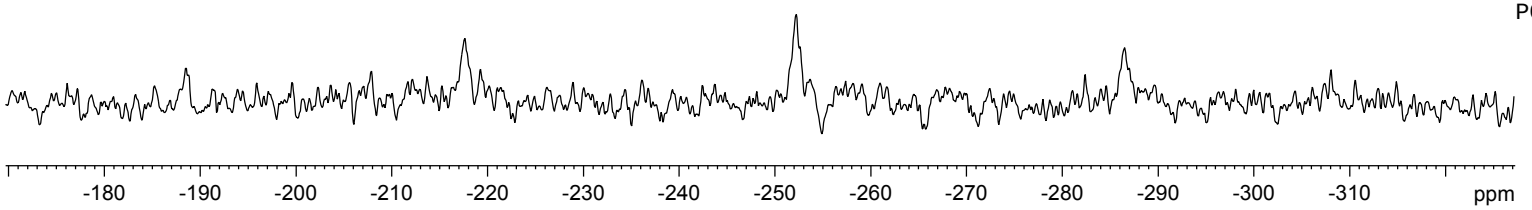


47

```
NAME                 cgav72
EXPNO                     1
PROCNO                    1
Date_              20060831
Time                  10.20
INSTRUM               av360
PROBHD    5 mm Multinucl
PULPROG              zgpg30
TD                    16384
SOLVENT             CD2Cl2
NS                    43008
DS                        0
SWH              50000.000 Hz
FIDRES            3.051758 Hz
AQ               0.1638900 sec
RG                     2050
DW                   10.000 usec
DE                   10.00 usec
TE                   294.2 K
D1              0.20000000 sec
d11             0.03000000 sec
DELTA           0.10000000 sec
TD0                       1

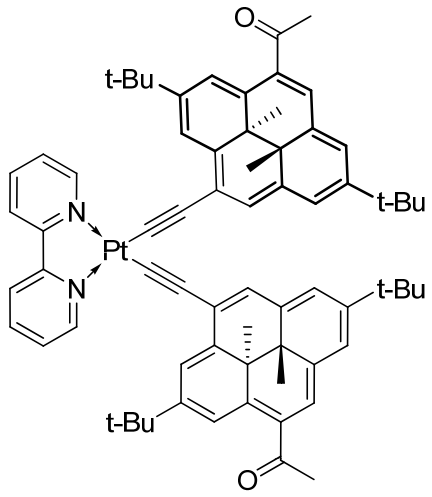
======== CHANNEL f1 ========
NUC1                  195Pt
P1                   10.70 usec
PL1                   2.00 dB
SFO1           77.0602527 MHz

======== CHANNEL f2 ========
CPDPRG2            waltz16
NUC2                   1H
PCPD2                80.00 usec
PL2                  -2.00 dB
PL12                 18.00 dB
PL13                 18.00 dB
SFO2          360.1316210 MHz
SI                    8192
SF             77.0685680 MHz
WDW                     EM
SSB                      0
LB                   20.00 Hz
GB                       0
PC                    1.40
```



AVCG2078-1 PZ-181/CDCl3 1H/AMB 12/01/06 0.75 ppm/cm

PZ_I_181 (AcDHPC≡C)2PtBpy 1H NMR AVCG2078



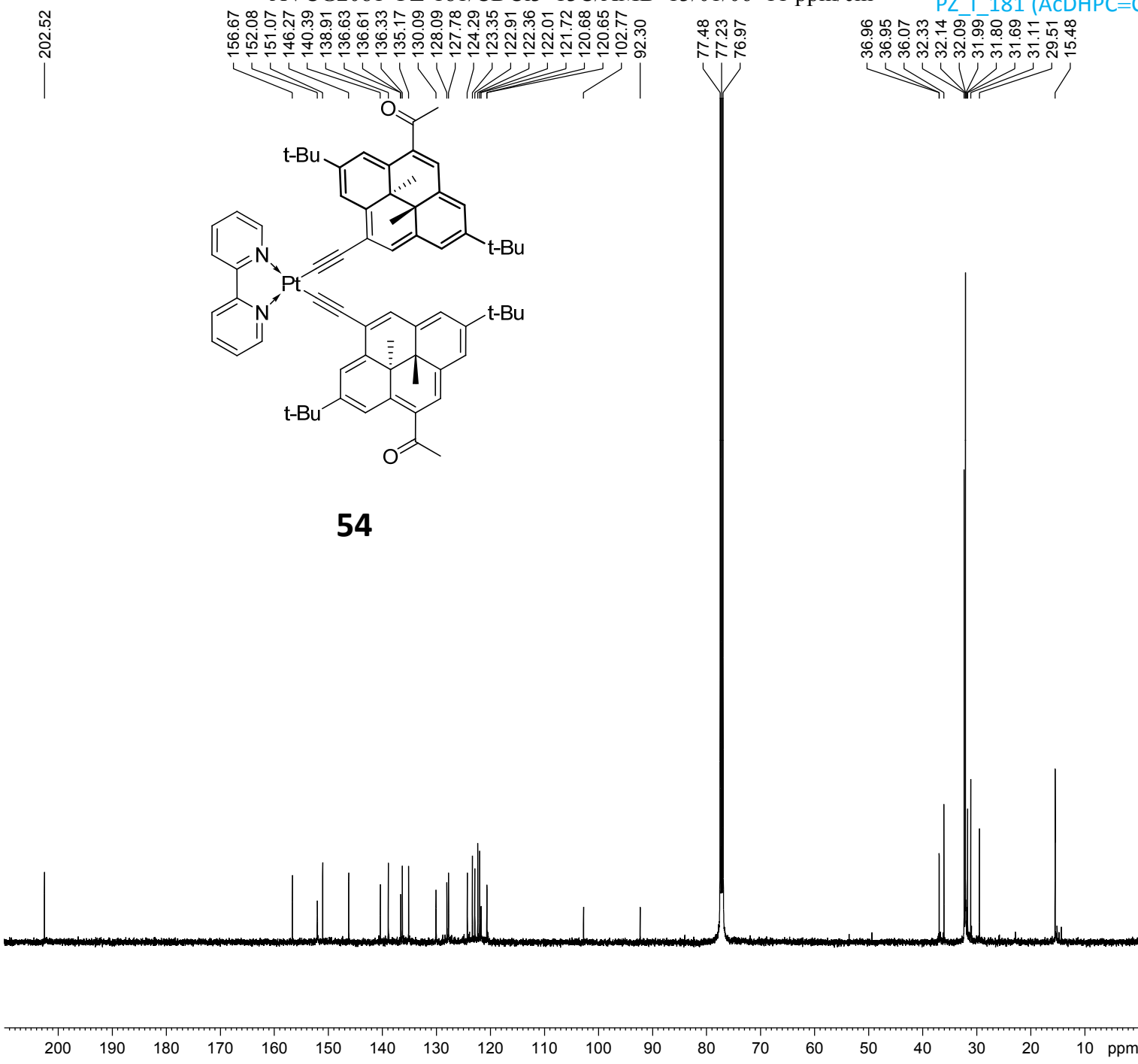
54

```
NAME              avcg2078
EXPNO                    1
PROCNO                   1
Date_             20060112
Time                 13.32
INSTRUM              AV500
PROBHD    5 mm BBI 1H-BB
PULPROG              zg30
TD                  32768
SOLVENT             CDCl3
NS                     16
DS                      2
SWH              8012.820 Hz
FIDRES           0.244532 Hz
AQ               2.0448356 sec
RG                    128
DW                 62.400 usec
DE                  6.00 usec
TE                 300.0 K
D1            1.00000000 sec

======== CHANNEL f1 ========
NUC1                   1H
P1                  9.80 usec
PL1                 1.00 dB
SFO1         500.1315200 MHz
SI                   16384
SF           500.1300240 MHz
WDW                    GM
SSB                     0
LB                 -0.40 Hz
GB                    0.5
PC                   1.00
```

AVCG2081 PZ-181/CDCl3 13C/AMB 13/01/06 11 ppm/cm

PZ_I_181 (AcDHPC≡C)2PtBpy 13C NMR AVCG2078

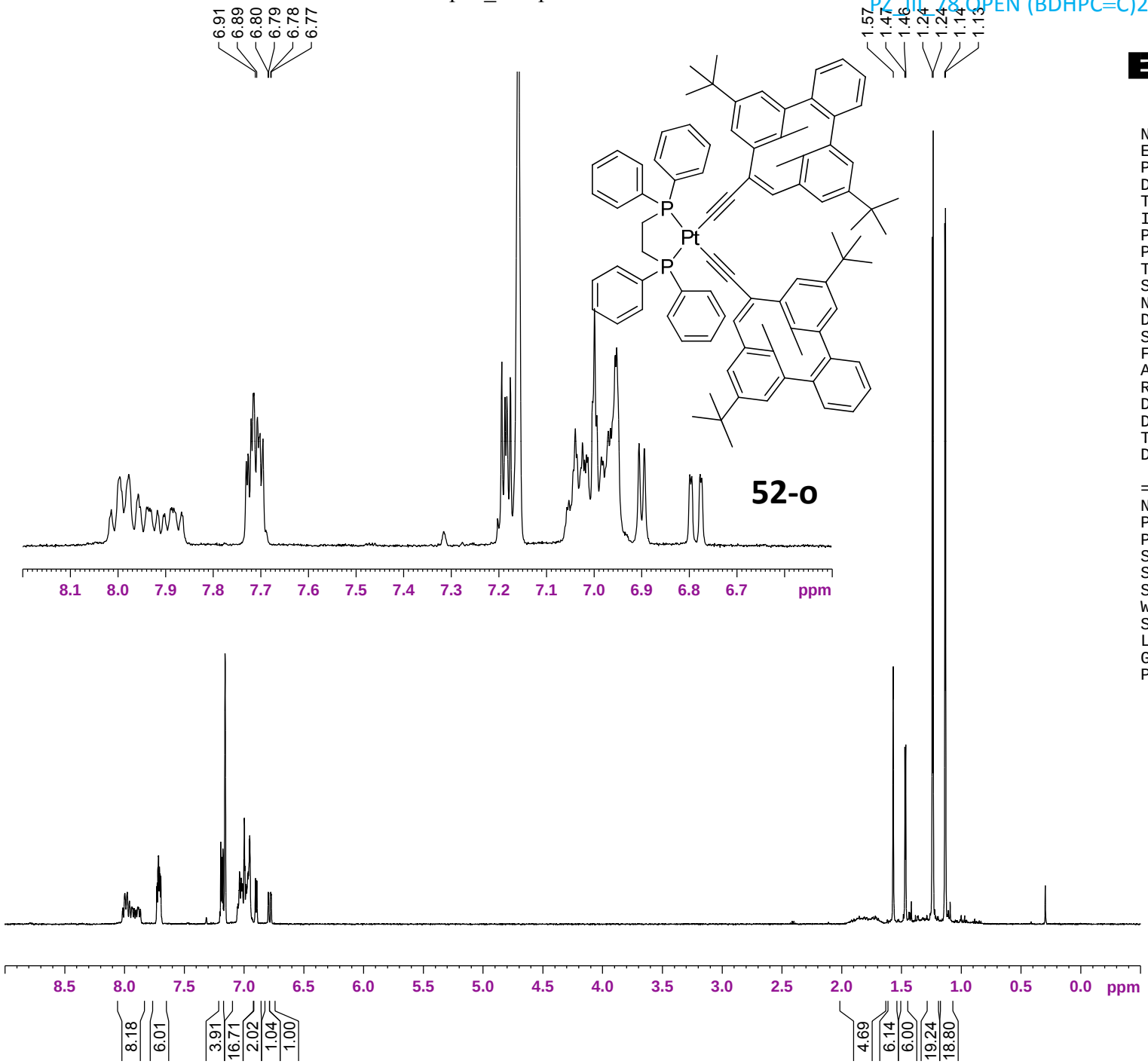


54

NAME	avcg2081
EXPNO	1
PROCNO	1
Date_	20060112
Time	15.58
INSTRUM	AV500
PROBHD	5 mm BBO BB-1H
PULPROG	zgpg30
TD	65536
SOLVENT	CDCl3
NS	24576
DS	4
SWH	30864.197 Hz
FIDRES	0.470950 Hz
AQ	1.0617495 sec
RG	16384
DW	16.200 usec
DE	18.00 usec
TE	300.0 K
D1	1.00000000 sec
d11	0.03000000 sec
d12	0.00002000 sec
======== CHANNEL f1 ========	
NUC1	13C
P1	9.80 usec
PL1	3.00 dB
SFO1	125.7715390 MHz
======== CHANNEL f2 ========	
CPDPRG2	waltz16
NUC2	1H
PCPD2	80.00 usec
PL2	-4.00 dB
PL12	14.40 dB
PL13	14.40 dB
SFO2	500.1315200 MHz
SI	32768
SF	125.7577624 MHz
WDW	EM
SSB	0
LB	0.90 Hz
GB	0
PC	1.40

pz3_78 open 1H in C6D6

PZ_JIL_78 OPEN (BDHPC≡C)2Pt DPPF 1H NMR AVCG2078

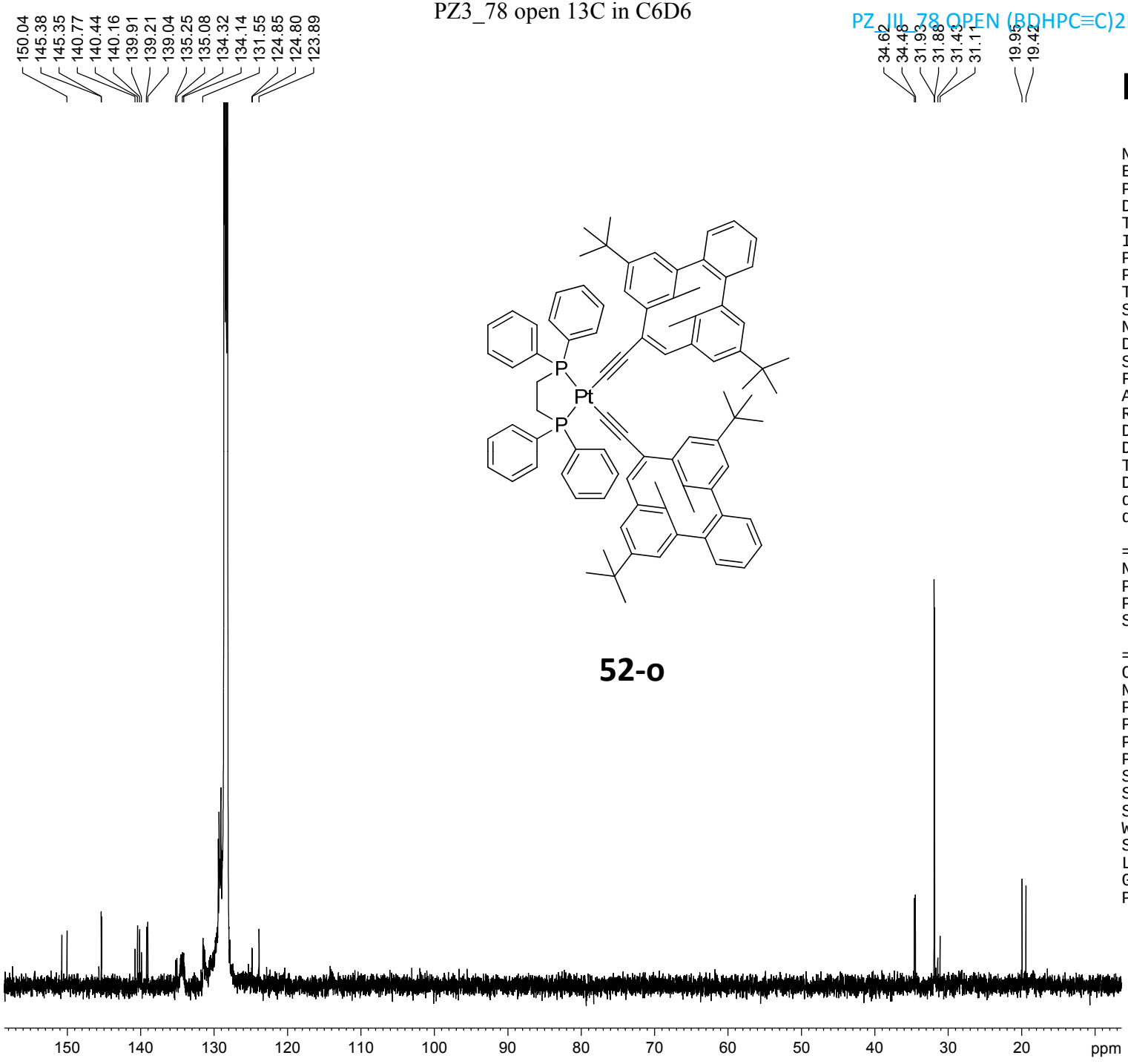


BRUKER

NAME	pz3_78 open
EXPNO	1
PROCNO	1
Date_	20071111
Time	17.24
INSTRUM	AV500
PROBHD	5 mm BBO BB-1H
PULPROG	zg30
TD	32768
SOLVENT	C6D6
NS	16
DS	2
SWH	8012.820 Hz
FIDRES	0.244532 Hz
AQ	2.0448356 sec
RG	406.4
DW	62.400 usec
DE	6.00 usec
TE	300.0 K
D1	1.00000000 sec
======== CHANNEL f1 ========	
NUC1	1H
P1	10.00 usec
PL1	-4.00 dB
SFO1	500.1315200 MHz
SI	16384
SF	500.1299975 MHz
WDW	GM
SSB	0
LB	-0.20 Hz
GB	0.5
PC	1.00

PZ3_78 open 13C in C6D6

PZ_JU_78 OPEN (BDHPC≡C)2Pt DPPE 13C NMR AVCG2078



52-o

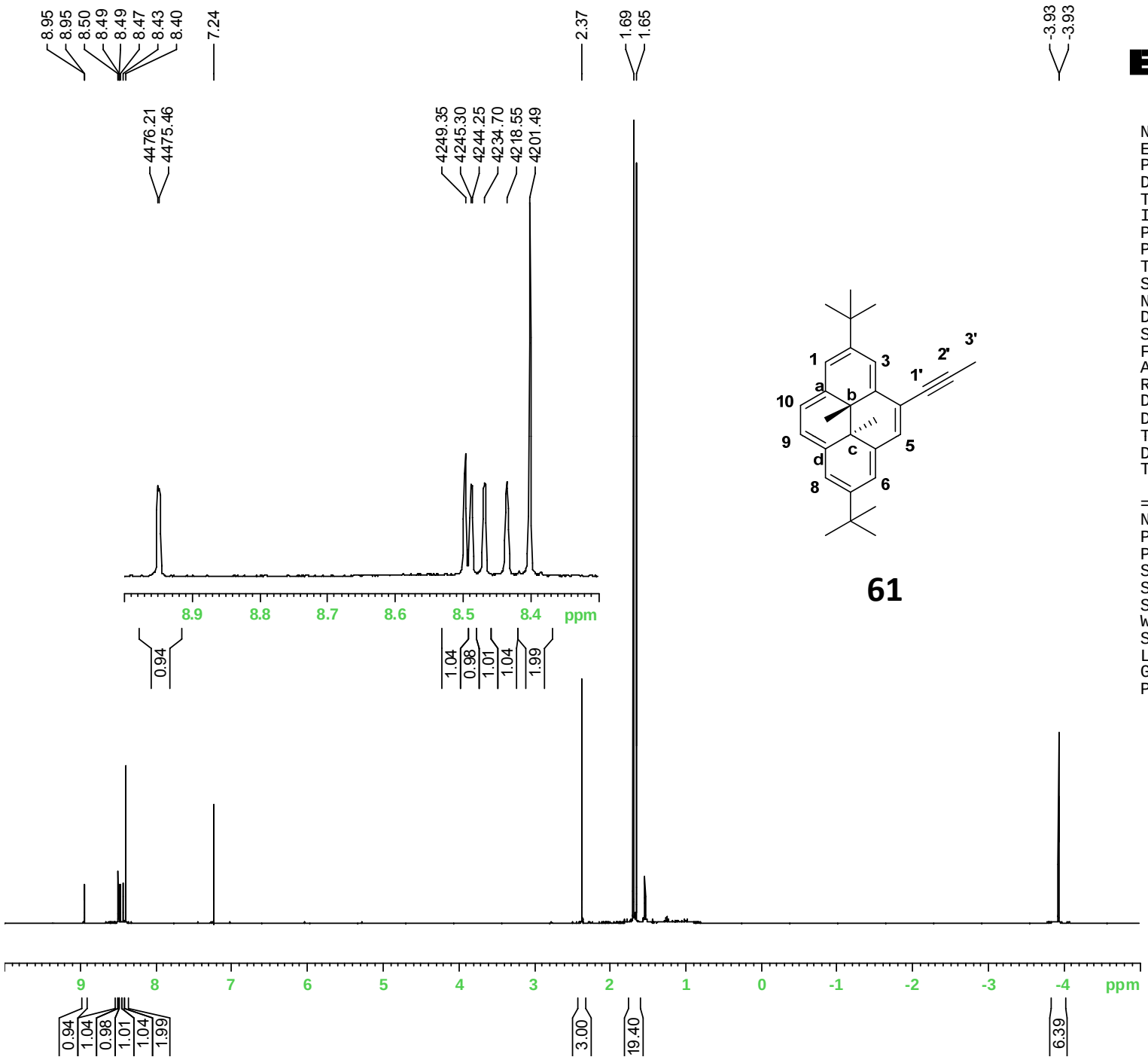
```
NAME          pz3_78 open
EXPNO                  3
PROCNO                 1
Date_           20071111
Time               17.49
INSTRUM            AV500
PROBHD   5 mm BBO BB-1H
PULPROG          zgpg30
TD                65536
SOLVENT             C6D6
NS                  4096
DS                     4
SWH           30864.197 Hz
FIDRES         0.470950 Hz
AQ             1.0617495 sec
RG                5792.6
DW                16.200 usec
DE                18.00 usec
TE                300.0 K
D1           1.00000000 sec
d11          0.03000000 sec
d12          0.00002000 sec

======== CHANNEL f1 ========
NUC1                 13C
P1                  9.00 usec
PL1                 0.00 dB
SFO1        125.7715390 MHz

======== CHANNEL f2 ========
CPDPRG2          waltz16
NUC2                 1H
PCPD2              80.00 usec
PL2                -4.00 dB
PL12               14.00 dB
PL13               14.00 dB
SFO2        500.1325200 MHz
SI                 32768
SF          125.7576993 MHz
WDW                  EM
SSB                   0
LB                 0.90 Hz
GB                    0
PC                 1.40
```

MethylethynylDHP 1H/CDCl3

PZ_I_?? DHPC≡CMe 1H NMR



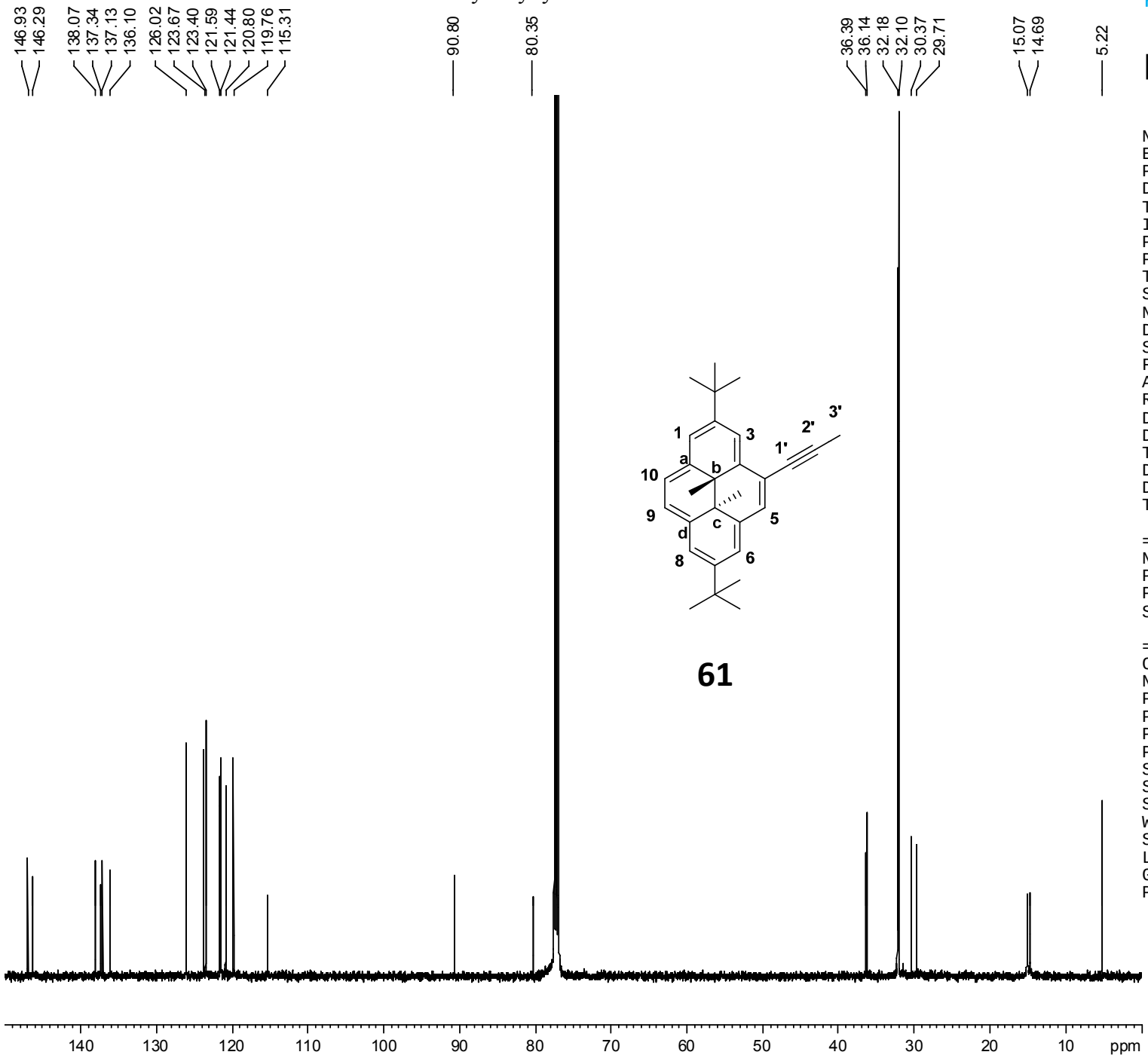
61

```
NAME          MethylethynylDHP
EXPNO                       1
PROCNO                      1
Date_            20081110
Time                16.47
INSTRUM             spect
PROBHD    5 mm PABBO BB-
PULPROG              zg30
TD                  32768
SOLVENT             CDCl3
NS                     16
DS                      2
SWH              8012.820 Hz
FIDRES           0.244532 Hz
AQ               2.0448356 sec
RG                  322.5
DW                 62.400 usec
DE                  6.50 usec
TE                 296.6 K
D1             1.00000000 sec
TD0                     1

======== CHANNEL f1 ========
NUC1                   1H
P1                  9.60 usec
PL1                -4.00 dB
SFO1         500.1315200 MHz
SI                  16384
SF           500.1300238 MHz
WDW                    GM
SSB                     0
LB                 -0.20 Hz
GB                    0.5
PC                   1.00
```

MethylethynylDHP 13C/CDCl3

PZ_I_?? DHPC≡CMe 13C NMR



61

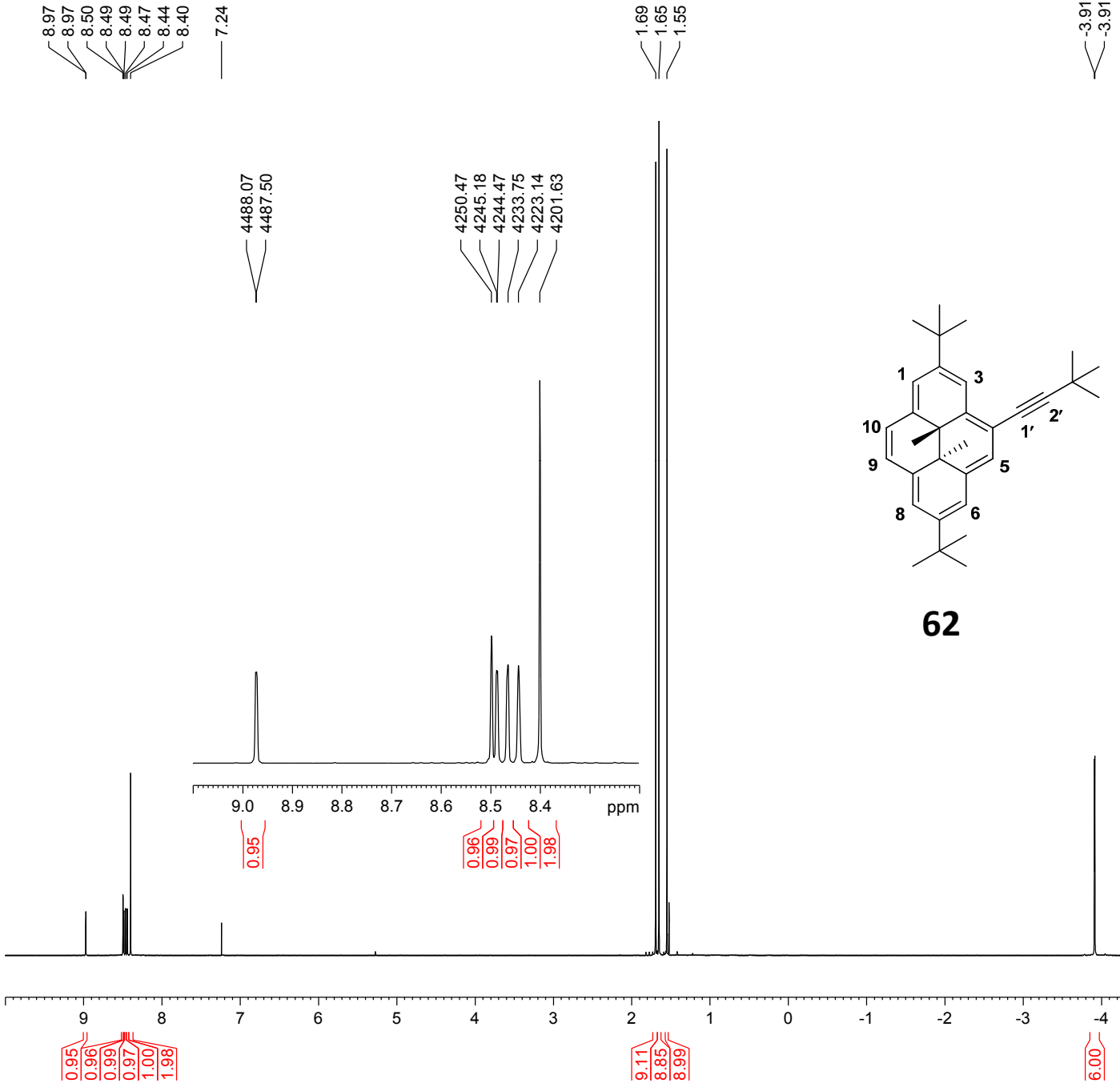
```
NAME          MethylethynylDHP
EXPNO                       3
PROCNO                      1
Date_              20081114
Time                    3.38
INSTRUM                spect
PROBHD   5 mm PABBO BB-
PULPROG               zgpg30
TD                     65536
SOLVENT                CDCl3
NS                     15360
DS                         4
SWH               30864.197 Hz
FIDRES             0.470950 Hz
AQ                 1.0617495 sec
RG                   14596.5
DW                    16.200 usec
DE                     6.50 usec
TE                    298.6 K
D1                1.00000000 sec
D11               0.03000000 sec
TD0                        1

======== CHANNEL f1 ========
NUC1                     13C
P1                     10.00 usec
PL1                     3.00 dB
SFO1             125.7715390 MHz

======== CHANNEL f2 ========
CPDPRG2              waltz16
NUC2                     1H
PCPD2                 80.00 usec
PL2                   -4.00 dB
PL12                  14.42 dB
PL13                  14.24 dB
SFO2             500.1325200 MHz
SI                     32768
SF               125.7577619 MHz
WDW                       EM
SSB                        0
LB                     0.90 Hz
GB                         0
PC                     1.40
```

(2-tert-butylethynyl)DHP 1H/CDCl3

PZ_I_?? DHPC≡CCMe3 1H NMR



62

```
Current Data Parameters
NAME      pz (2-tert-butylethynyl)DHP
EXPNO                 1
PROCNO                1

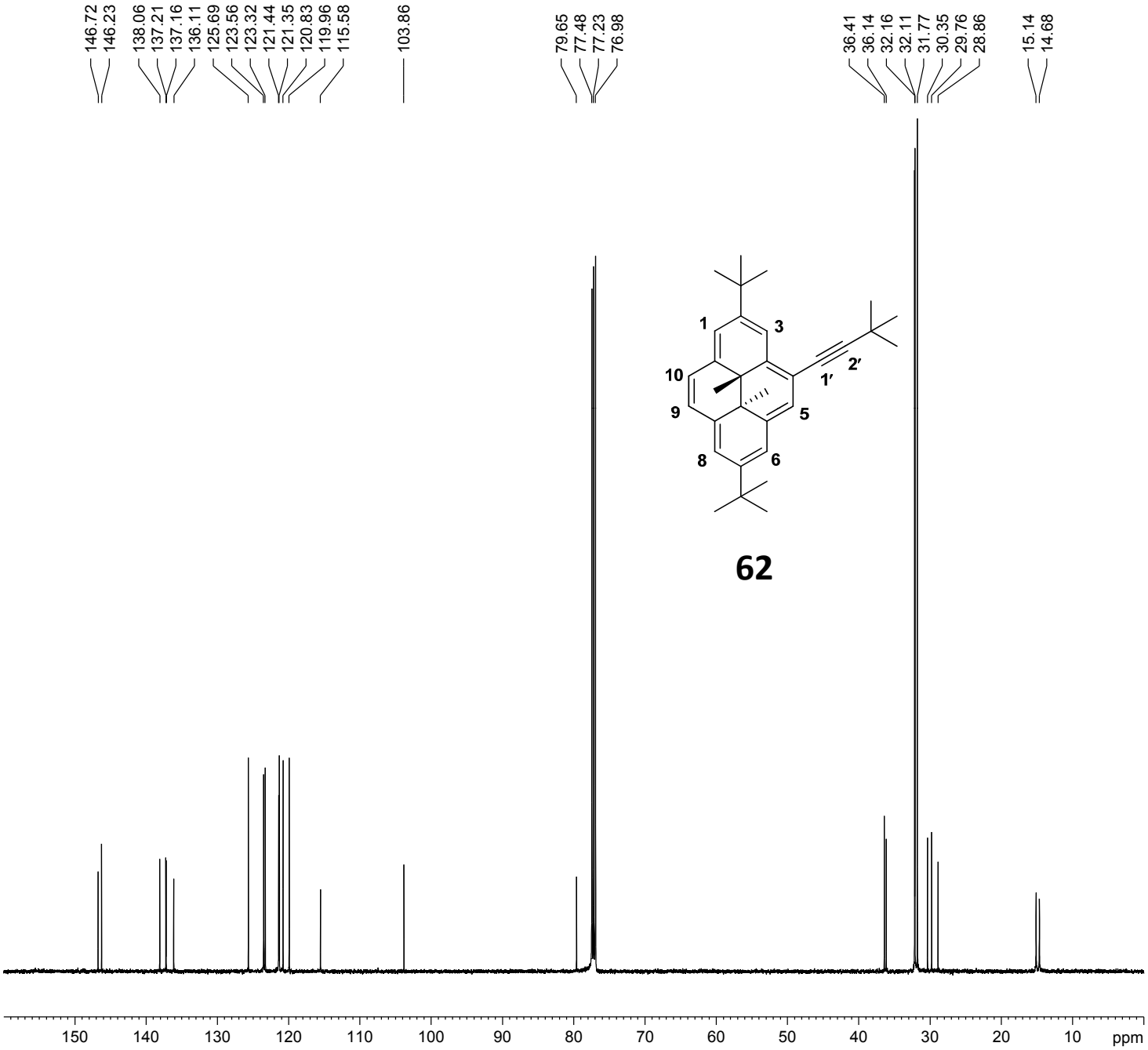
F2 - Acquisition Parameters
Date_           20081105
Time              17.48
INSTRUM           spect
PROBHD   5 mm PABBO BB-
PULPROG           zg30
TD               32768
SOLVENT          CDCl3
NS                  16
DS                   2
SWH            8012.820 Hz
FIDRES         0.244532 Hz
AQ             2.0448356 sec
RG                90.5
DW               62.400 usec
DE                6.50 usec
TE                297.4 K
D1           1.00000000 sec
TD0                  1

======== CHANNEL f1 ========
NUC1                1H
P1                9.60 usec
PL1              -4.00 dB
SFO1        500.1315200 MHz

F2 - Processing parameters
SI                16384
SF          500.1300233 MHz
WDW                 GM
SSB                  0
LB               -0.20 Hz
GB                 0.5
PC                1.00
```

PZ_I_?? DHPC≡CCMe3 13C NMR

(2-tert-butylethynyl)DHP 13C/CDCl3




```
Current Data Parameters
NAME      pz (2-tert-butylethynyl)DHP
EXPNO                 3
PROCNO                1

F2 - Acquisition Parameters
Date_          20081105
Time              18.05
INSTRUM           spect
PROBHD   5 mm PABBO BB-
PULPROG          zgpg30
TD                65536
SOLVENT           CDCl3
NS                 4096
DS                    4
SWH           30864.197 Hz
FIDRES         0.470950 Hz
AQ             1.0617495 sec
RG               14596.5
DW                16.200 usec
DE                 6.50 usec
TE                298.6 K
D1             1.00000000 sec
D11            0.03000000 sec
TD0                   1

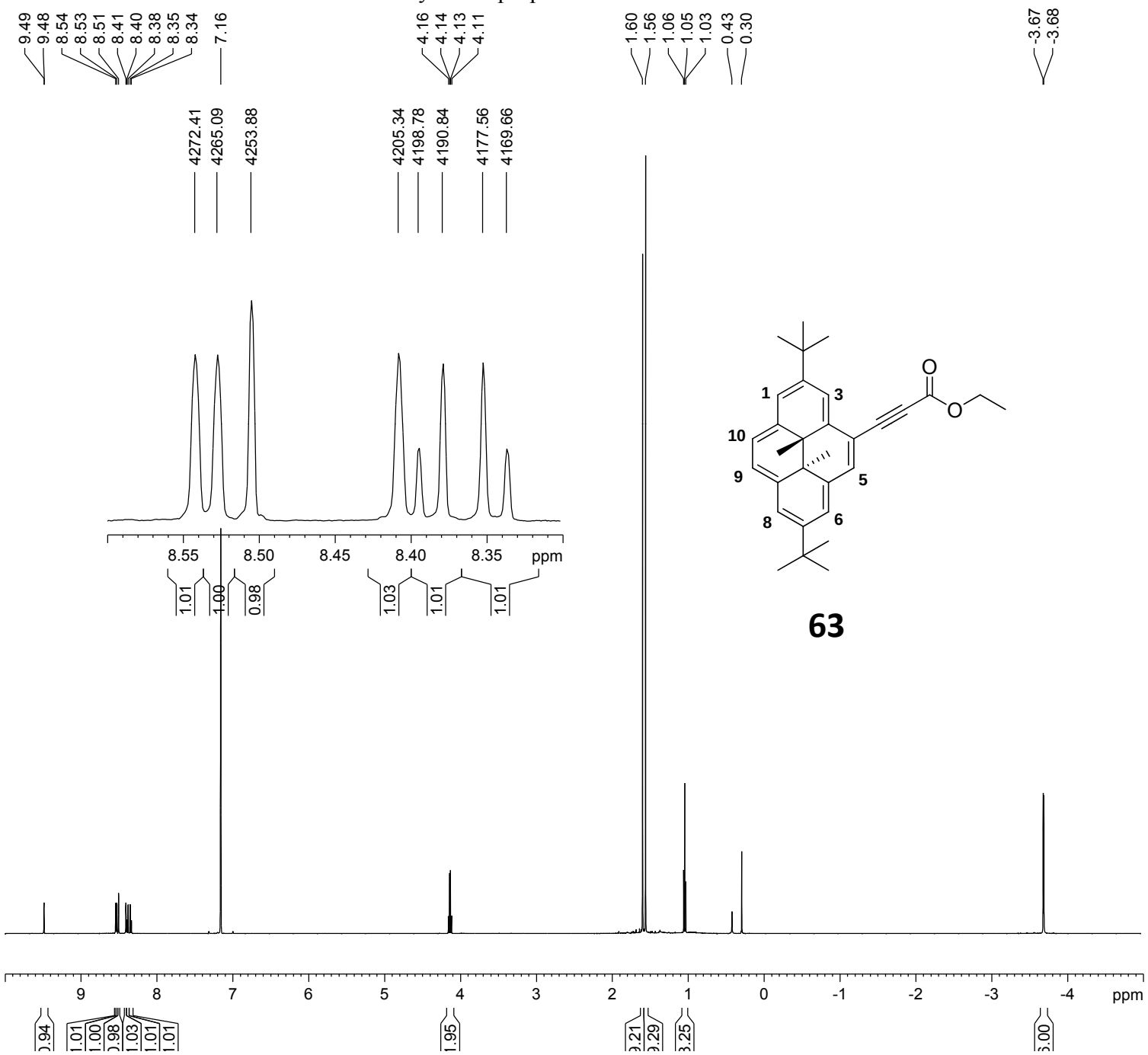
======== CHANNEL f1 ========
NUC1                 13C
P1                 10.00 usec
PL1                 3.00 dB
SFO1        125.7715390 MHz

======== CHANNEL f2 ========
CPDPRG2          waltz16
NUC2                 1H
PCPD2              80.00 usec
PL2                -4.00 dB
PL12               14.42 dB
PL13               14.24 dB
SFO2        500.1325200 MHz

F2 - Processing parameters
SI                32768
SF          125.7577628 MHz
WDW                  EM
SSB                   0
LB                 0.90 Hz
GB                    0
PC                 1.40
```

PZ_I_168 DHPC≡CCOOMe 1H NMR

Ethyl DHP-propioate ester 1H in C6D6



63

Current Data Parameters
NAME Ethyl DHP-propioate ester
EXPNO 1
PROCNO 1

F2 - Acquisition Parameters

Date_	20080105
Time	16.45
INSTRUM	AV500
PROBHD	5 mm BBO BB-1H
PULPROG	zg30
TD	32768
SOLVENT	CDCl3
NS	16
DS	2
SWH	8012.820 Hz
FIDRES	0.244532 Hz
AQ	2.0448356 sec
RG	228.1
DW	62.400 usec
DE	6.00 usec
TE	300.0 K
D1	1.00000000 sec

======== CHANNEL f1 ========

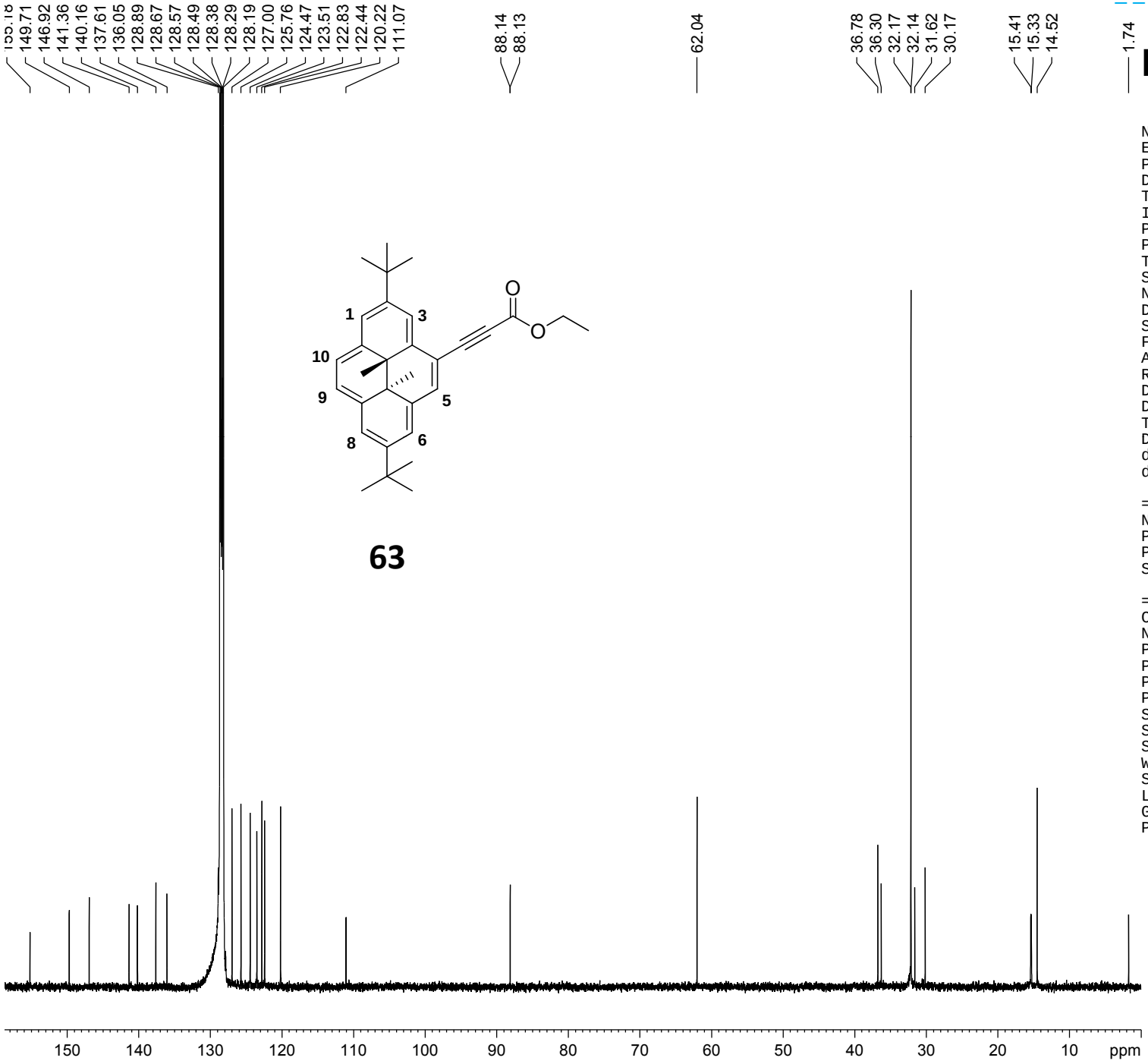
NUC1	1H
P1	10.10 usec
PL1	-4.00 dB
SFO1	500.1315200 MHz

F2 - Processing parameters

SI	16384
SF	500.1299975 MHz
WDW	GM
SSB	0
LB	-0.20 Hz
GB	0.5
PC	1.00

PZ Ethyl ester of DHPacetynyl acid 13C in C6D6

PZ_I_168 DHPC≡CCOOMe 13C NMR



63

```
NAME      Ethyl DHP-propioate este
EXPNO                        3
PROCNO                       1
Date_                 20080105
Time                     17.10
INSTRUM                  AV500
PROBHD   5 mm BBO BB-1H
PULPROG                 zgpg30
TD                        65536
SOLVENT                   C6D6
NS                        8192
DS                           4
SWH                  30864.197 Hz
FIDRES                0.470950 Hz
AQ                    1.0617495 sec
RG                       7298.2
DW                        16.200 usec
DE                        18.00 usec
TE                        300.0 K
D1                 1.00000000 sec
d11                0.03000000 sec
d12                0.00002000 sec

======== CHANNEL f1 ========
NUC1                        13C
P1                        10.00 usec
PL1                        3.00 dB
SFO1               125.7715390 MHz

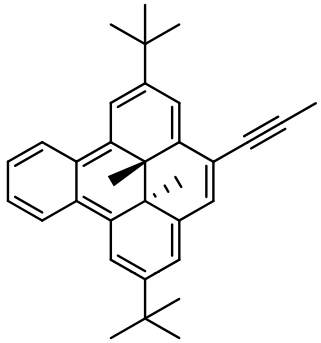
======== CHANNEL f2 ========
CPDPRG2                 waltz16
NUC2                        1H
PCPD2                     80.00 usec
PL2                       -4.00 dB
PL12                      14.24 dB
PL13                      14.24 dB
SFO2               500.1325200 MHz
SI                         32768
SF                 125.7577016 MHz
WDW                          EM
SSB                           0
LB                         0.90 Hz
GB                            0
PC                         1.40
```

BDHP-CC-Me 1H in CDCl3

PZ_IV_165B BDHPC≡CMe 1H NMR



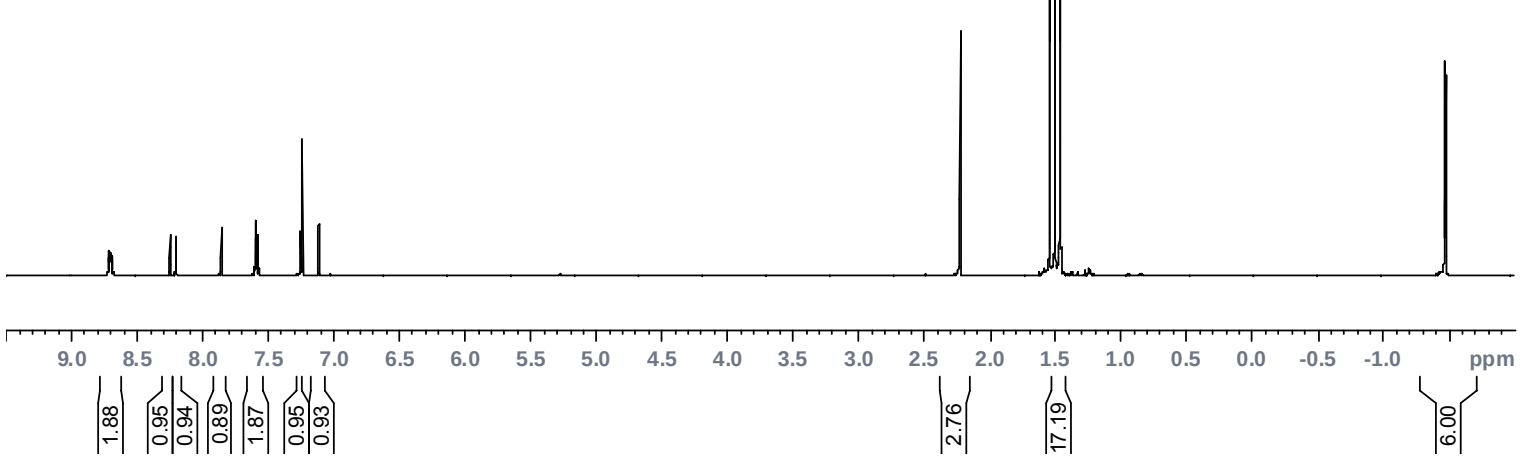




76

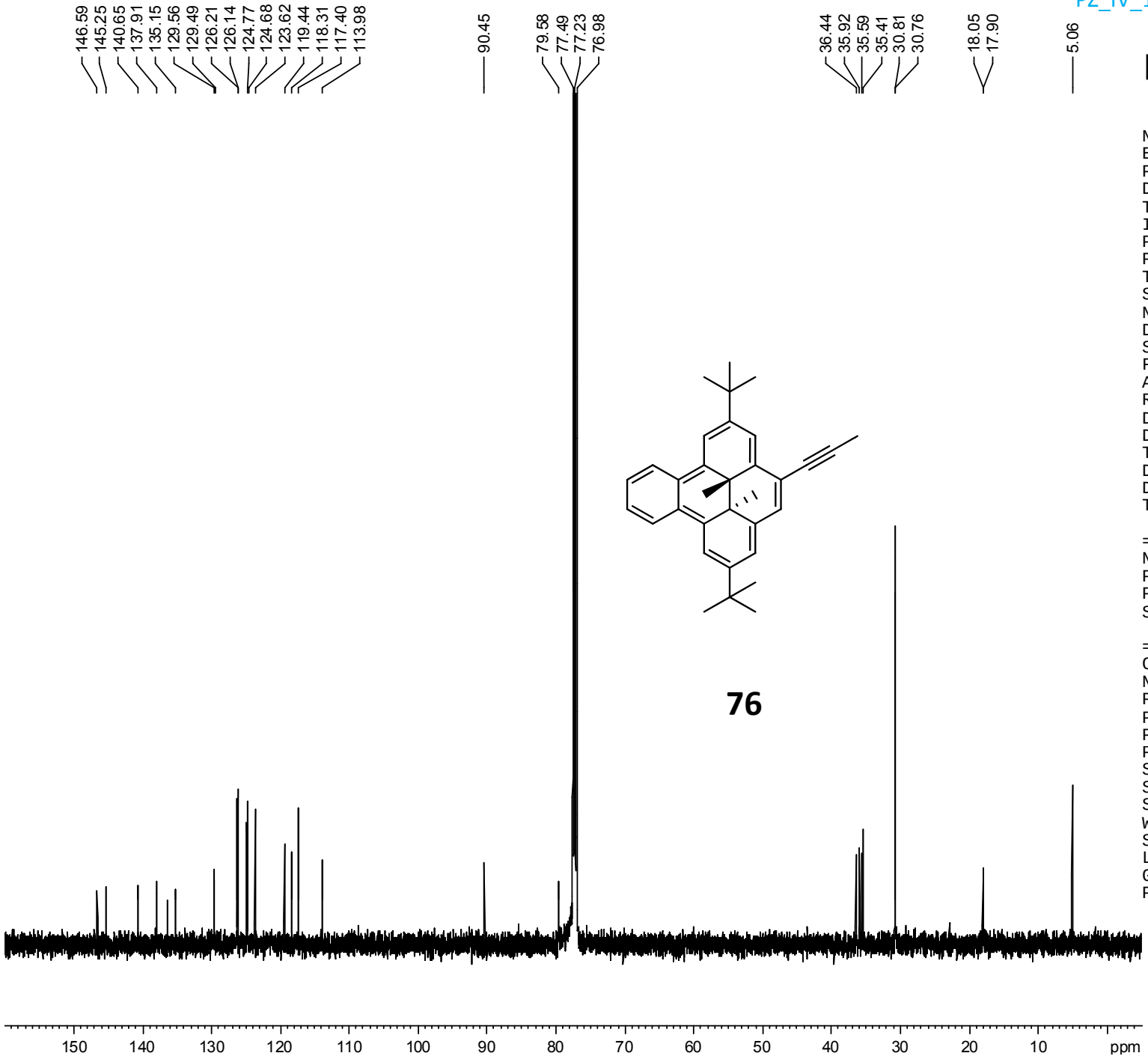
```
NAME          PZ4_BDHPCCMe
EXPNO                    2
PROCNO                   1
Date_             20100709
Time                 12.14
INSTRUM              spect
PROBHD   5 mm PABBO BB-
PULPROG               zg30
TD                   32768
SOLVENT              CDCl3
NS                      16
DS                       2
SWH               8012.820 Hz
FIDRES            0.244532 Hz
AQ                2.0448356 sec
RG                   456.1
DW                  62.400 usec
DE                   6.50 usec
TE                  297.0 K
D1              1.00000000 sec
TD0                      1

======== CHANNEL f1 ========
NUC1                    1H
P1                    9.60 usec
PL1                  -4.00 dB
SFO1          500.1315200 MHz
SI                   16384
SF            500.1300232 MHz
WDW                     GM
SSB                      0
LB                   -0.20 Hz
GB                     0.5
PC                    1.00
```



BDHP-CC-Me 1H in CDCl3

PZ_IV_165B BDHPC≡CMe 13C NMR

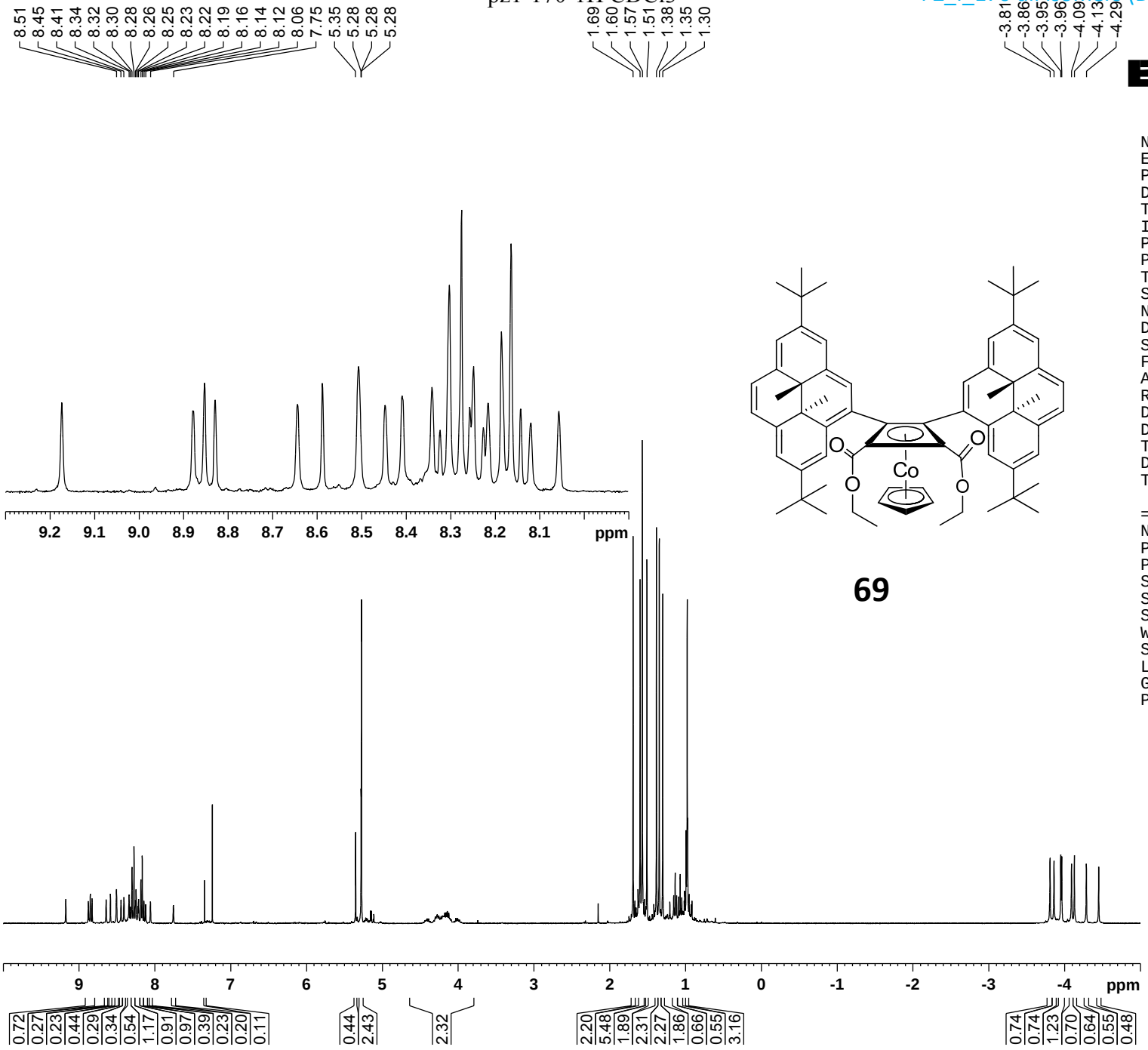


76

NAME	PZ4_BDHPCCMe
EXPNO	12
PROCNO	1
Date_	20100709
Time	14.47
INSTRUM	spect
PROBHD	5 mm PABBO BB-
PULPROG	zgpg30
TD	65536
SOLVENT	CDCl3
NS	4936
DS	4
SWH	30864.197 Hz
FIDRES	0.470950 Hz
AQ	1.0617495 sec
RG	14596.5
DW	16.200 usec
DE	6.50 usec
TE	297.9 K
D1	1.00000000 sec
D11	0.03000000 sec
TD0	1
======== CHANNEL f1 ========	
NUC1	13C
P1	10.00 usec
PL1	3.00 dB
SFO1	125.7715390 MHz
======== CHANNEL f2 ========	
CPDPRG2	waltz16
NUC2	1H
PCPD2	80.00 usec
PL2	-4.00 dB
PL12	14.42 dB
PL13	60.00 dB
SFO2	500.1325200 MHz
SI	32768
SF	125.7577627 MHz
WDW	EM
SSB	0
LB	0.90 Hz
GB	0
PC	1.40

pz1-170-1H CDCl3

PZ_I_170 all isomers (DHP2Ester2)CbCoCp 1H NMR

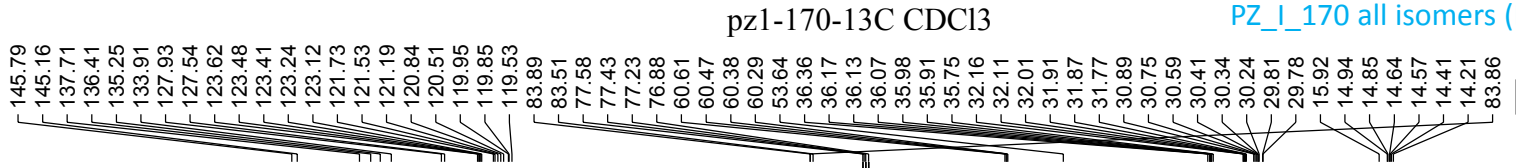


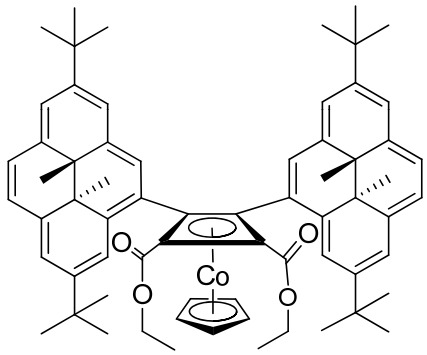
69

NAME	pz1-170-1H	
EXPNO	1	
PROCNO	1	
Date_	20070503	
Time	9.20	
INSTRUM	av360	
PROBHD	5 mm Multinucl	
PULPROG	zg30	
TD	32768	
SOLVENT	CDCl3	
NS	16	
DS	2	
SWH	6009.615	Hz
FIDRES	0.183399	Hz
AQ	2.7263477	sec
RG	256	
DW	83.200	usec
DE	6.00	usec
TE	294.4	K
D1	1.00000000	sec
TD0	1	
======== CHANNEL f1 ========		
NUC1	1H	
P1	8.00	usec
PL1	-2.00	dB
SFO1	360.1308200	MHz
SI	16384	
SF	360.1300139	MHz
WDW	GM	
SSB	0	
LB	-0.20	Hz
GB	0.5	
PC	1.00	

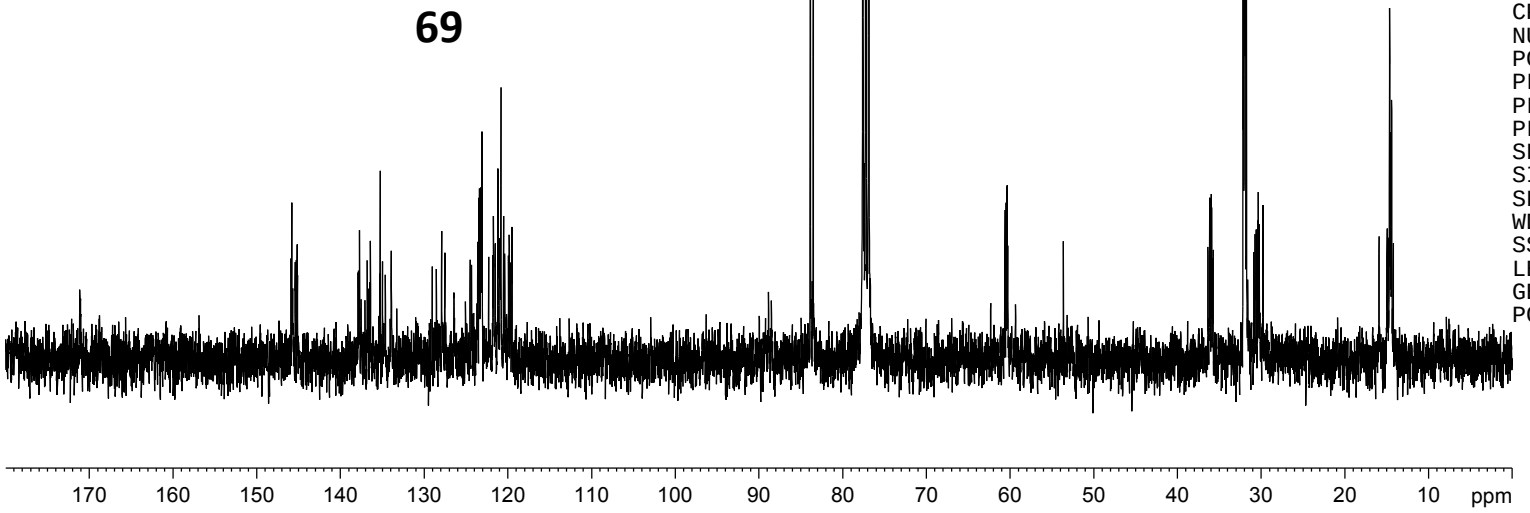
pz1-170-13C CDCl3

PZ_I_170 all isomers (DHP2Ester2)CbCoCp 1H NMR





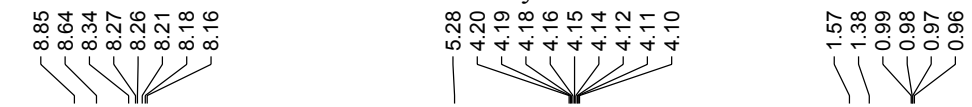
69



NAME	pz1-170-13C	
EXPNO	1	
PROCNO	1	
Date_	20070503	
Time	9.50	
INSTRUM	av360	
PROBHD	5 mm Multinucl	
PULPROG	zgpg30	
TD	32768	
SOLVENT	CDCl3	
NS	1027	
DS	2	
SWH	20000.000	Hz
FIDRES	0.610352	Hz
AQ	0.8192500	sec
RG	912	
DW	25.000	usec
DE	6.00	usec
TE	295.0	K
D1	1.00000000	sec
d11	0.03000000	sec
DELTA	0.89999998	sec
TD0	1	
======== CHANNEL f1 ========		
NUC1	13C	
P1	9.10	usec
PL1	-2.00	dB
SFO1	90.5633610	MHz
======== CHANNEL f2 ========		
CPDPRG2	waltz16	
NUC2	1H	
PCPD2	80.00	usec
PL2	-2.00	dB
PL12	18.00	dB
PL13	18.00	dB
SFO2	360.1317200	MHz
SI	16384	
SF	90.5547422	MHz
WDW	EM	
SSB	0	
LB	1.20	Hz
GB	0	
PC	1.40	

Cyclobutadiene Cobalt ester 1H/CDCl3

PZ_I_170 (DHP2Ester2)CbCoCp 1H NMR

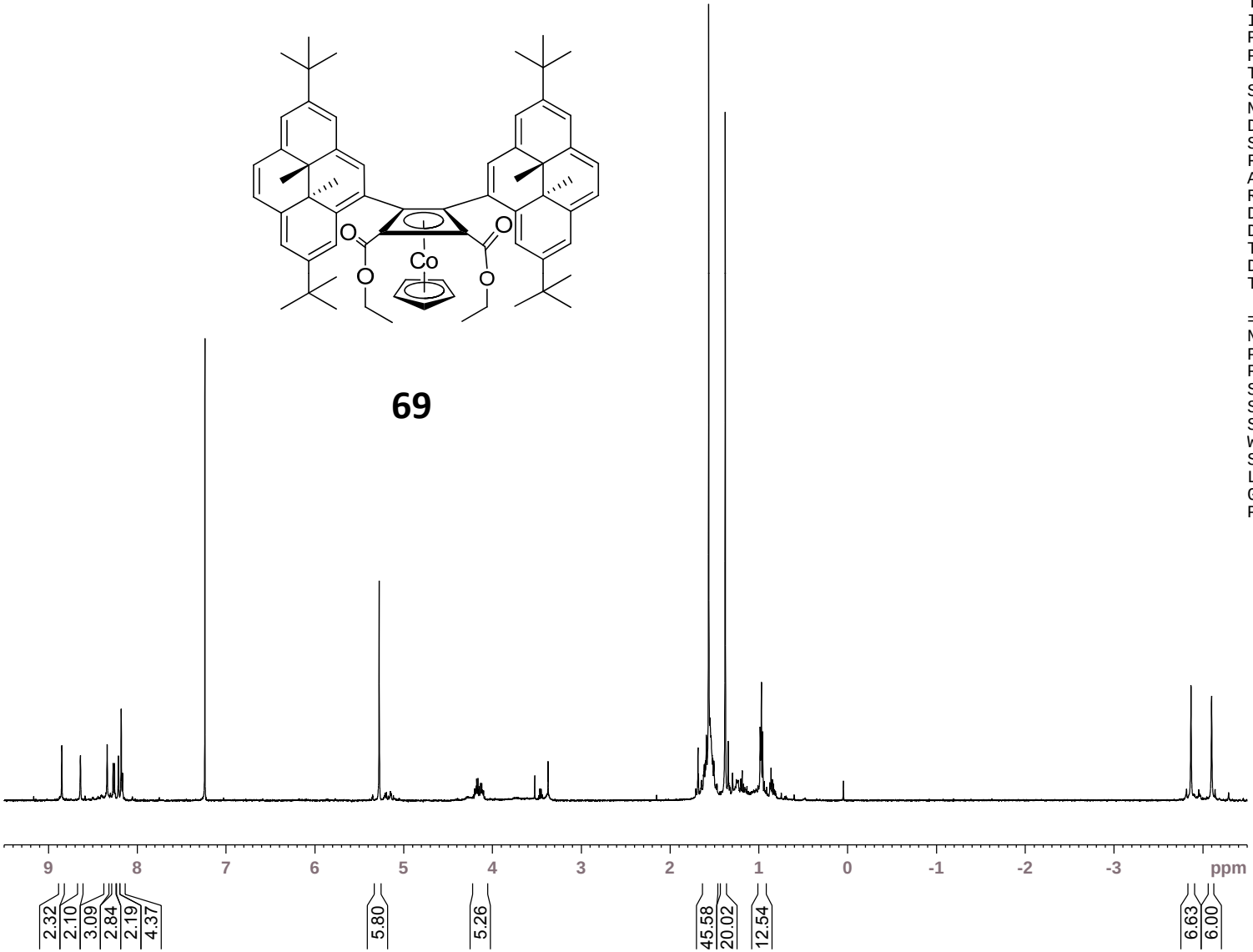


BRUKER

```
NAME        Cyclobutadiene Cobalt est
EXPNO                   1
PROCNO                  1
Date_            20081116
Time                14.23
INSTRUM             spect
PROBHD    5 mm PABBO BB-
PULPROG               zg30
TD                 32768
SOLVENT            CDCl3
NS                    16
DS                     2
SWH              8012.820 Hz
FIDRES           0.244532 Hz
AQ               2.0448356 sec
RG                   512
DW                 62.400 usec
DE                  6.50 usec
TE                 297.2 K
D1             1.00000000 sec
TD0                    1

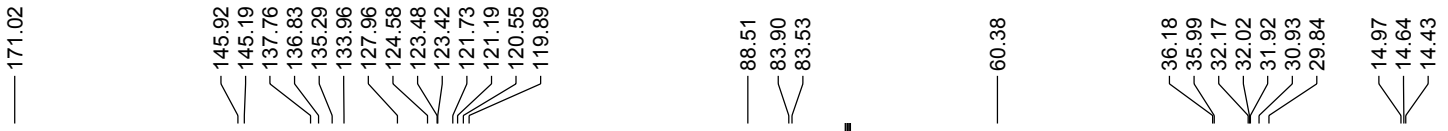
======== CHANNEL f1 ========
NUC1                  1H
P1                  9.60 usec
PL1                -4.00 dB
SFO1         500.1315200 MHz
SI                 16384
SF           500.1300233 MHz
WDW                   GM
SSB                    0
LB                 -0.20 Hz
GB                   0.5
PC                  1.00
```


69

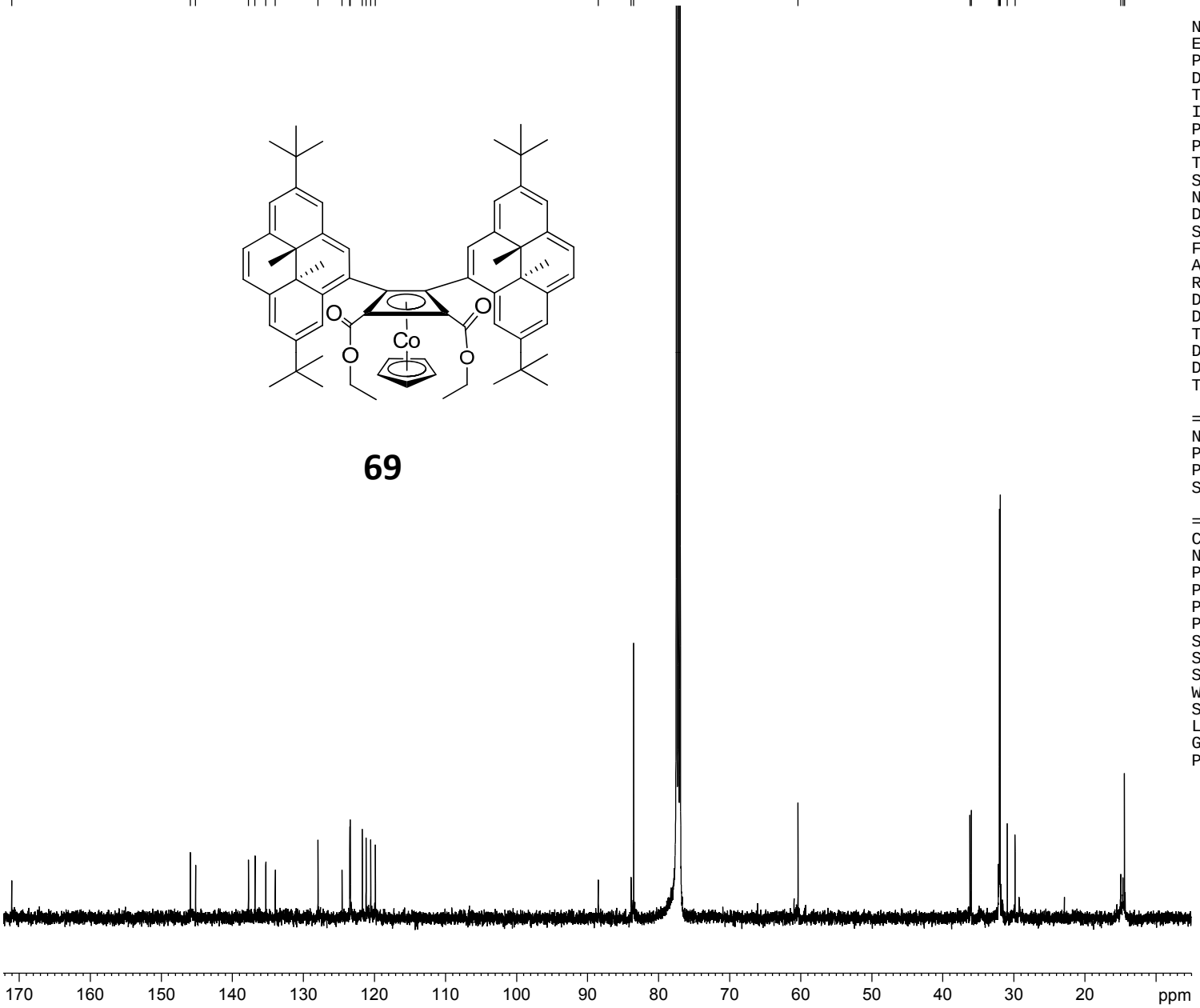


Cyclobutadiene Cobalt ester 13C/CDCl3

PZ_I_170 (DHP2Ester2)CbCoCp 13C NMR



69



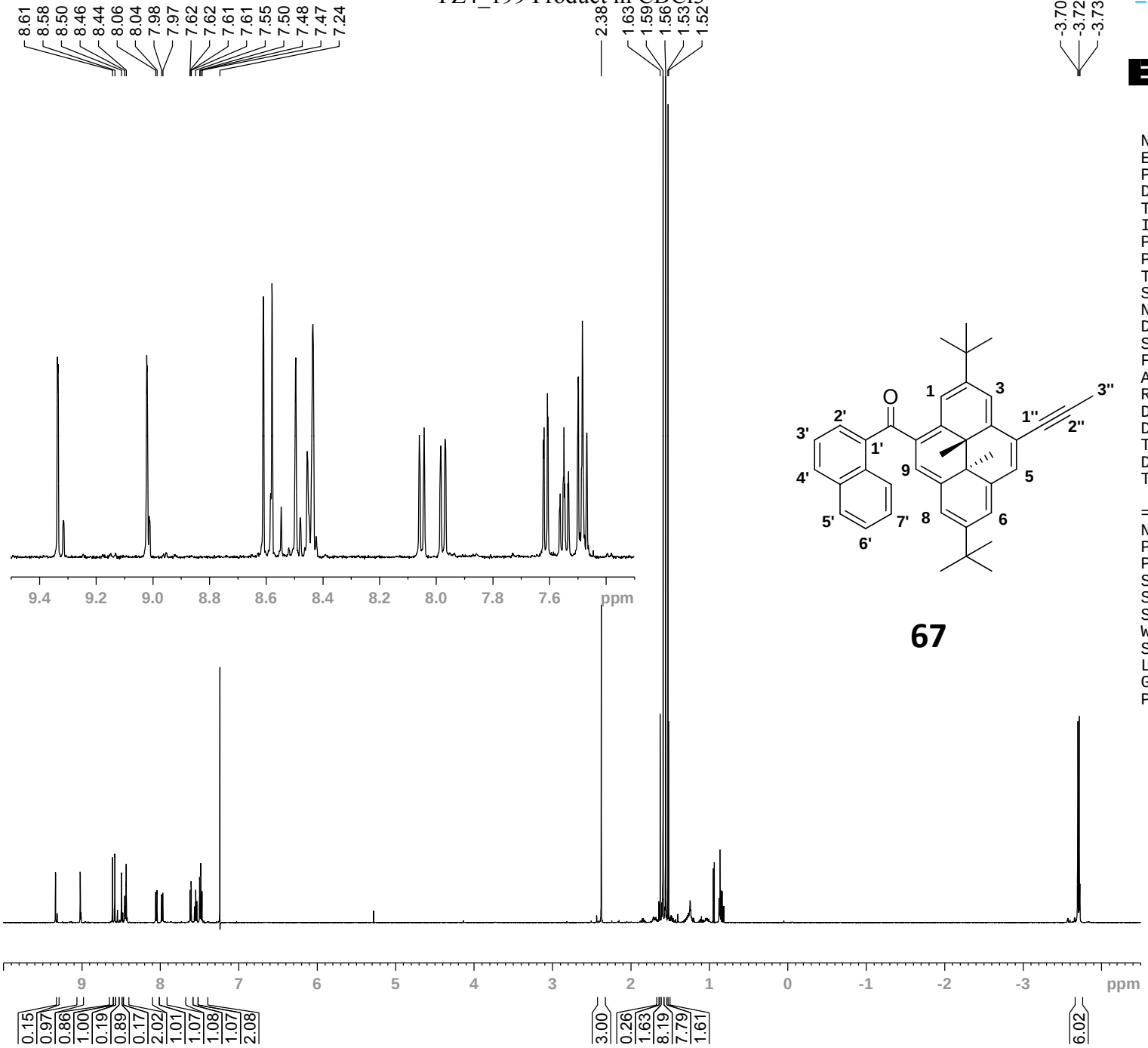

```
NAME      Cyclobutadiene Cobalt est
EXPNO                 3
PROCNO                1
Date_          20081116
Time              14.54
INSTRUM           spect
PROBHD   5 mm PABBO BB-
PULPROG          zgpg30
TD                65536
SOLVENT           CDCl3
NS                30720
DS                    4
SWH           30864.197 Hz
FIDRES         0.470950 Hz
AQ             1.0617495 sec
RG               14596.5
DW                16.200 usec
DE                 6.50 usec
TE                298.6 K
D1             1.00000000 sec
D11            0.03000000 sec
TD0                   1

======== CHANNEL f1 ========
NUC1                 13C
P1                10.00 usec
PL1                3.00 dB
SFO1         125.7715390 MHz

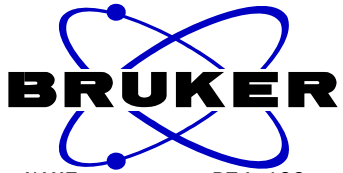
======== CHANNEL f2 ========
CPDPRG2          waltz16
NUC2                 1H
PCPD2             80.00 usec
PL2               -4.00 dB
PL12              14.42 dB
PL13              14.24 dB
SFO2         500.1325200 MHz
SI                32768
SF           125.7577611 MHz
WDW                  EM
SSB                   0
LB                 0.90 Hz
GB                    0
PC                 1.40
```

PZ4_199 Product in CDCl3

PZ_IV_199 NpDHPCCMe 1H NMR



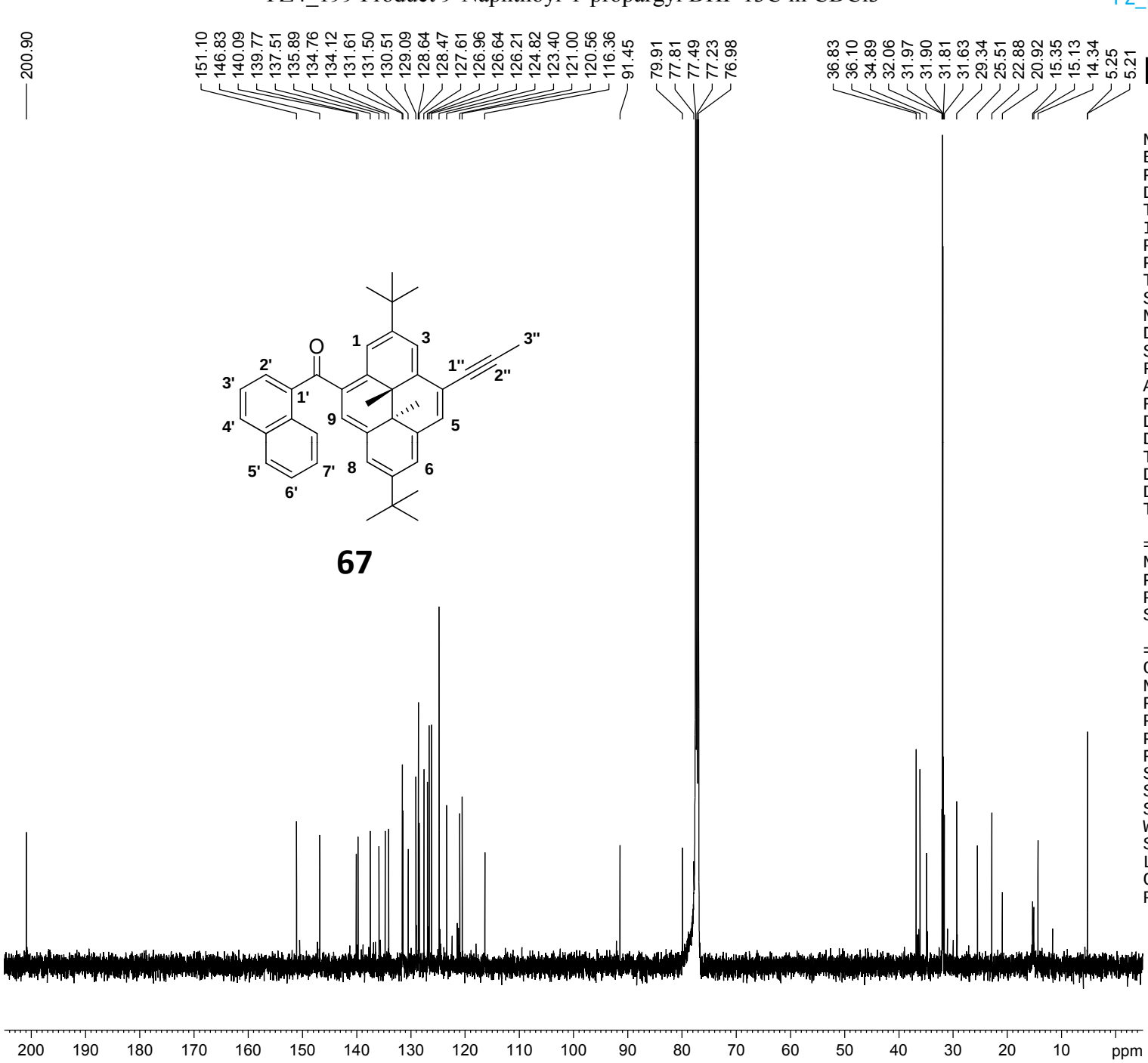
67



NAME	PZ4_199_p
EXPNO	1
PROCNO	1
Date_	20110401
Time	21.03
INSTRUM	spect
PROBHD	5 mm PABBO BB-
PULPROG	zg30
TD	32768
SOLVENT	CDCl3
NS	16
DS	2
SWH	8012.820 Hz
FIDRES	0.244532 Hz
AQ	2.0448356 sec
RG	574.7
DW	62.400 usec
DE	6.50 usec
TE	297.7 K
D1	1.00000000 sec
TD0	1
======== CHANNEL f1 ========	
NUC1	1H
P1	10.20 usec
PL1	-4.00 dB
SFO1	500.1315200 MHz
SI	16384
SF	500.1300233 MHz
WDW	GM
SSB	0
LB	-0.20 Hz
GB	0.5
PC	1.00

PZ4_199 Product 9-Naphthoyl-1-propargyl DHP 13C in CDCl3

PZ_IV_199_NpDHPCCMe_13C NMR



67

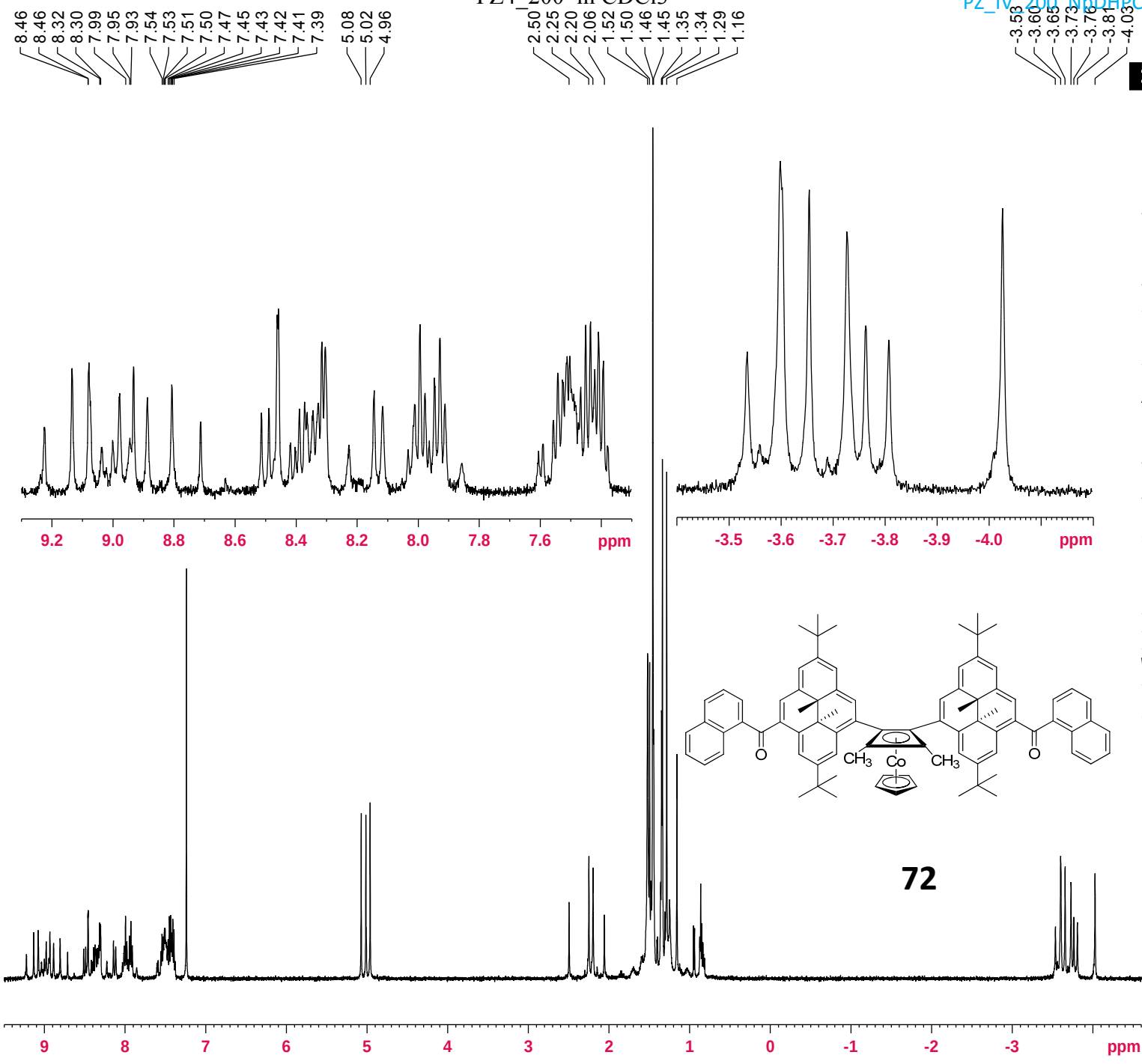
```
NAME              PZ4_199_p
EXPNO                     4
PROCNO                    1
Date_              20110402
Time                 15.18
INSTRUM              spect
PROBHD    5 mm PABBO BB-
PULPROG             zgpg30
TD                   65536
SOLVENT              CDCl3
NS                   29116
DS                       4
SWH             30864.197 Hz
FIDRES           0.470950 Hz
AQ               1.0617495 sec
RG                 14596.5
DW                  16.200 usec
DE                   6.50 usec
TE                  297.8 K
D1              1.00000000 sec
D11             0.03000000 sec
TD0                      1

======== CHANNEL f1 ========
NUC1                   13C
P1                   10.00 usec
PL1                   3.00 dB
SFO1          125.7715390 MHz

======== CHANNEL f2 ========
CPDPRG2           waltz16
NUC2                   1H
PCPD2                80.00 usec
PL2                  -4.00 dB
PL12                 14.24 dB
PL13                 60.00 dB
SFO2          500.1325200 MHz
SI                   32768
SF            125.7577619 MHz
WDW                    EM
SSB                     0
LB                   0.90 Hz
GB                      0
PC                   1.40
```

PZ4_200 in CDCl3

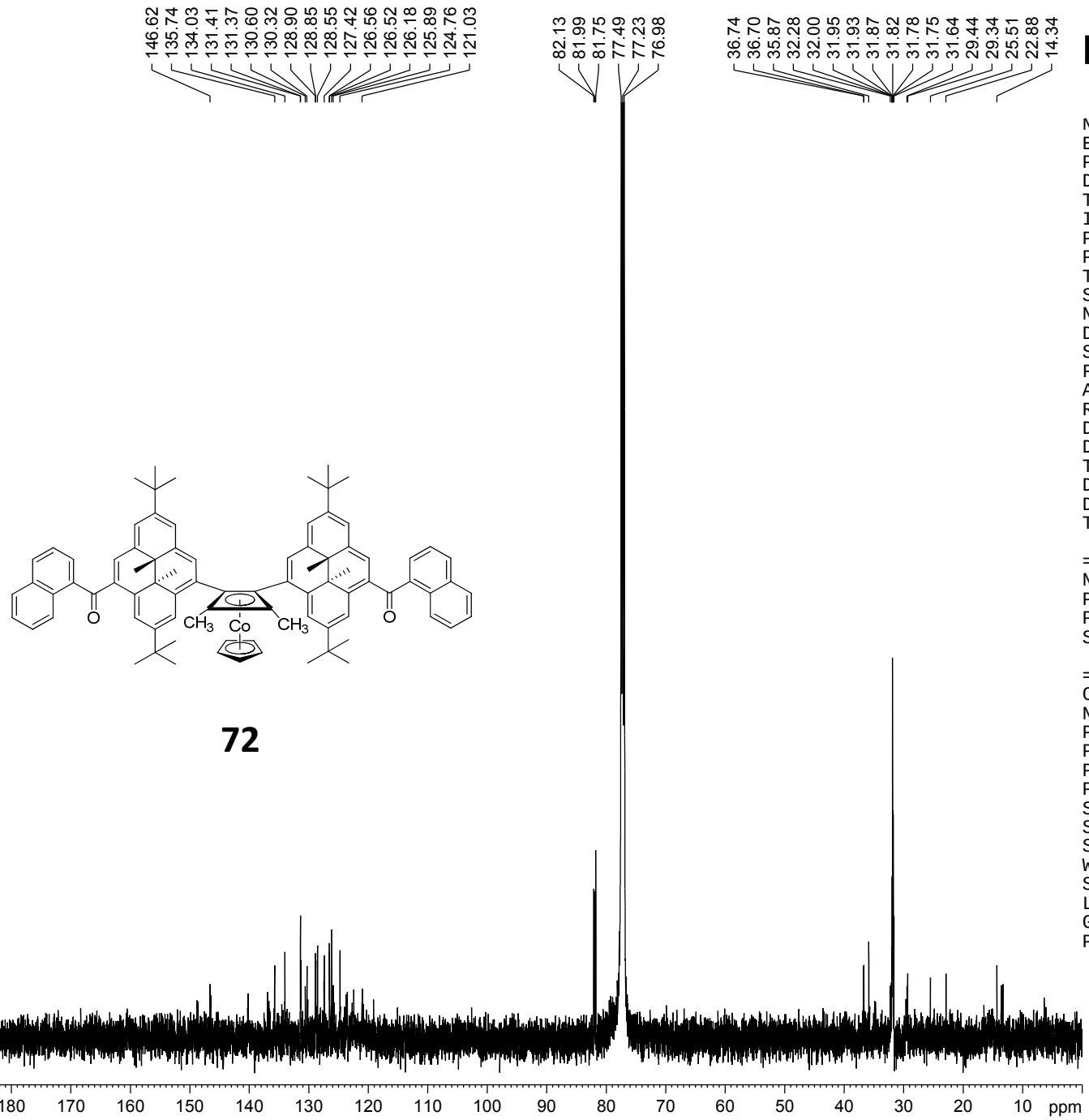
PZ_IV_200_NpDHPCCMe_cobalt complex 1H NMR



NAME	PZ4_200
EXPNO	1
PROCNO	1
Date_	20110419
Time	23.21
INSTRUM	spect
PROBHD	5 mm PABBO BB-
PULPROG	zg30
TD	32768
SOLVENT	CDCl3
NS	16
DS	2
SWH	8012.820 Hz
FIDRES	0.244532 Hz
AQ	2.0448356 sec
RG	574.7
DW	62.400 usec
DE	6.50 usec
TE	297.6 K
D1	1.00000000 sec
TD0	1
======== CHANNEL f1 ========	
NUC1	1H
P1	10.20 usec
PL1	-4.00 dB
SFO1	500.1315200 MHz
SI	16384
SF	500.1300233 MHz
WDW	GM
SSB	0
LB	-0.20 Hz
GB	0.5
PC	1.00

PZ4_200 in CDCl3

PZ_IV_200 NpDHPCCMe cobalt complex 13C NMR



72

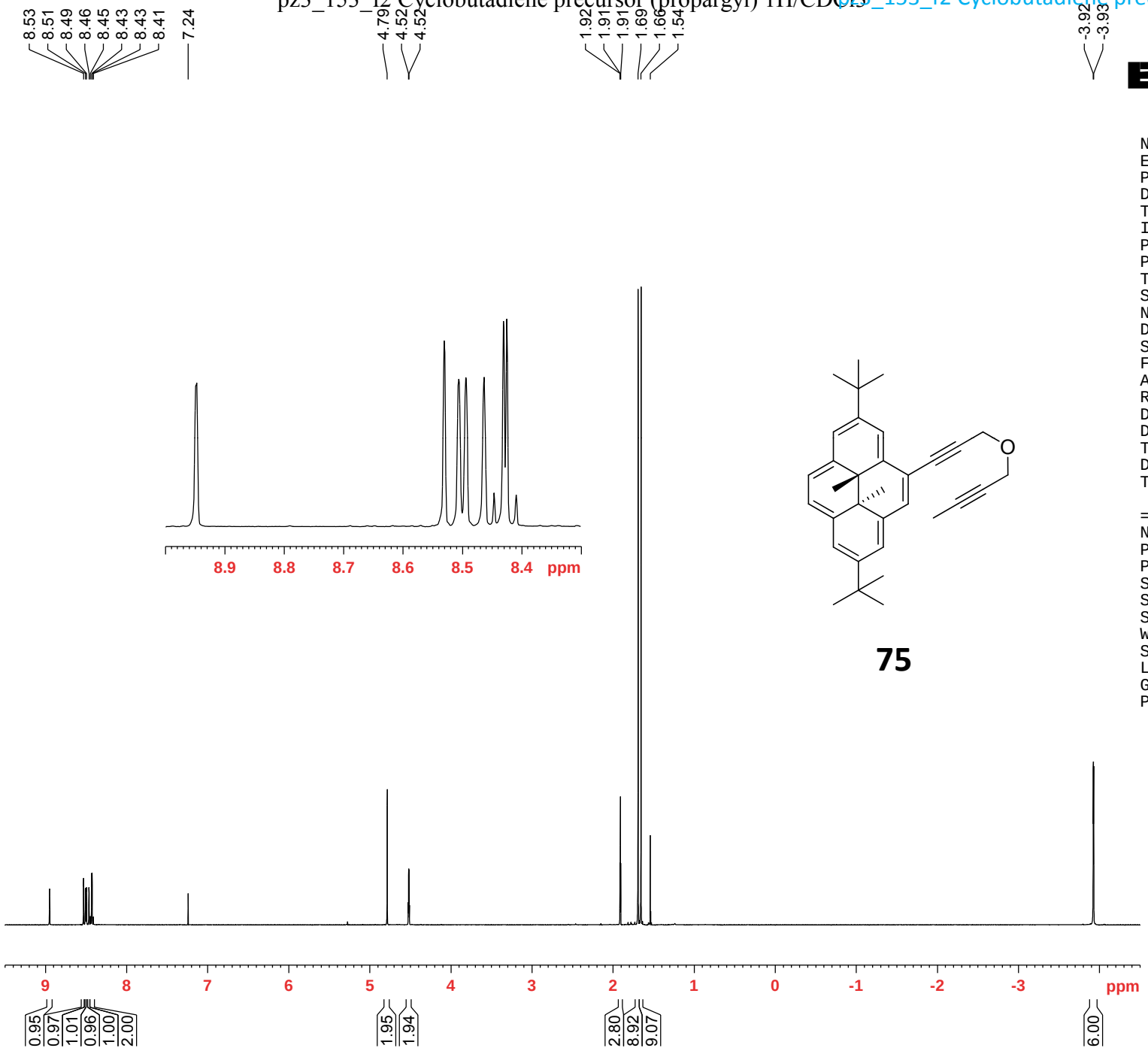
```
NAME                PZ4_200
EXPNO                     2
PROCNO                    1
Date_              20110419
Time                 23.25
INSTRUM              spect
PROBHD   5 mm PABBO BB-
PULPROG              zgpg30
TD                    65536
SOLVENT               CDCl3
NS                    16142
DS                        4
SWH              30864.197 Hz
FIDRES            0.470950 Hz
AQ                1.0617495 sec
RG                  14596.5
DW                  16.200 usec
DE                    6.50 usec
TE                   298.0 K
D1              1.00000000 sec
D11             0.03000000 sec
TD0                       1

======== CHANNEL f1 ========
NUC1                    13C
P1                   10.00 usec
PL1                   3.00 dB
SFO1           125.7715390 MHz

======== CHANNEL f2 ========
CPDPRG2            waltz16
NUC2                    1H
PCPD2                80.00 usec
PL2                  -4.00 dB
PL12                 14.24 dB
PL13                 60.00 dB
SFO2           500.1325200 MHz
SI                    32768
SF             125.7577619 MHz
WDW                     EM
SSB                      0
LB                    0.90 Hz
GB                       0
PC                    1.40
```

pz3_153_f2 Cyclobutadiene precursor (propargyl) 1H/CDCl3

pz3_153_f2 Cyclobutadiene precursor (propargyl) 1H/CDCl3



75

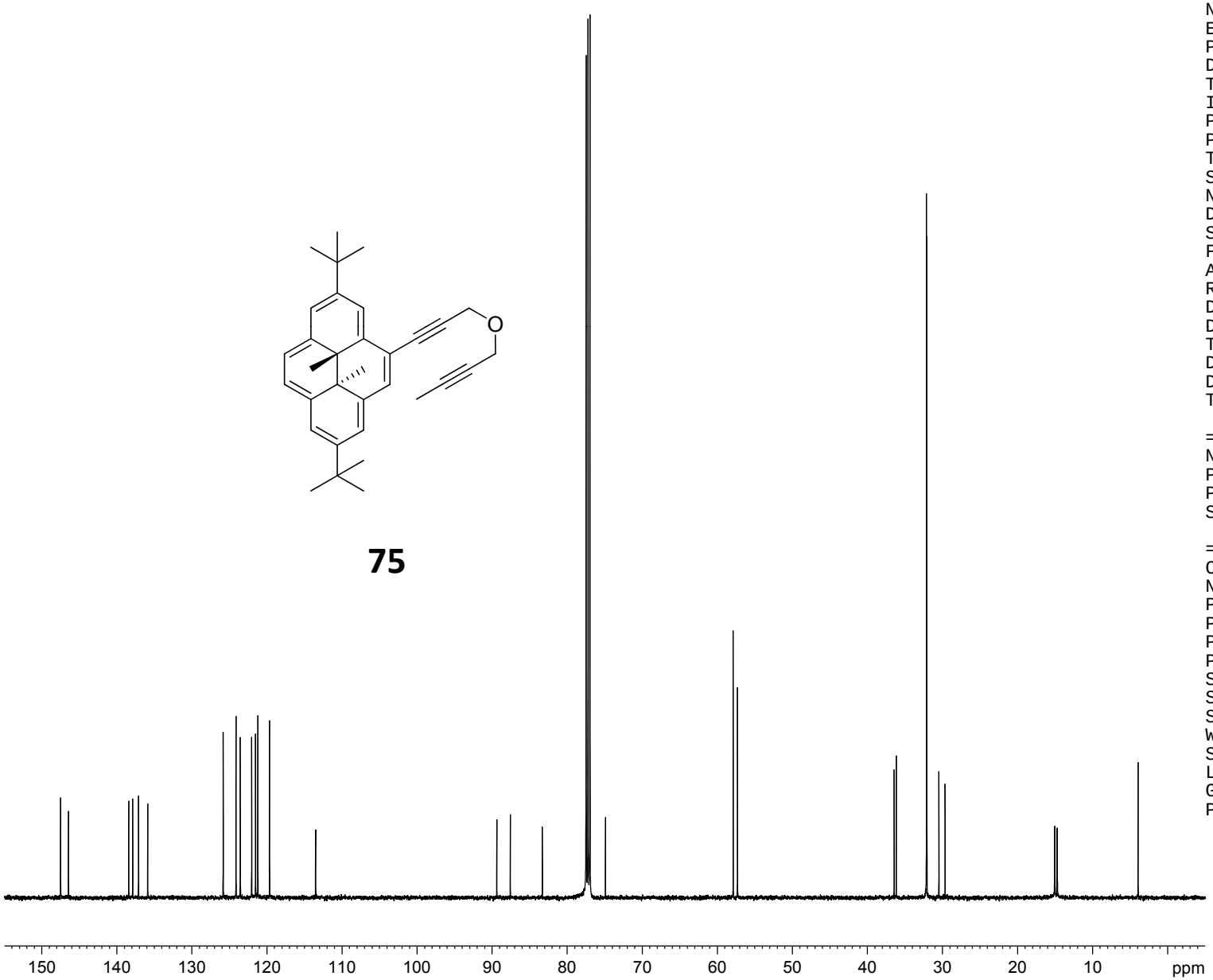
NAME	pz3_153_f2
EXPNO	1
PROCNO	1
Date_	20080523
Time	9.53
INSTRUM	spect
PROBHD	5 mm PABBO BB-
PULPROG	zg30
TD	32768
SOLVENT	CDCl3
NS	16
DS	2
SWH	8012.820 Hz
FIDRES	0.244532 Hz
AQ	2.0448356 sec
RG	128
DW	62.400 usec
DE	6.50 usec
TE	297.8 K
D1	1.00000000 sec
TD0	1
======== CHANNEL f1 ========	
NUC1	1H
P1	9.60 usec
PL1	-4.00 dB
SFO1	500.1315200 MHz
SI	16384
SF	500.1300233 MHz
WDW	GM
SSB	0
LB	-0.20 Hz
GB	0.5
PC	1.00

pz3_153_f2 Cyclobutadiene precursor propargyl 13C/CDCl3

pz3_153_f2 Cyclobutadiene precursor (propargyl) 13C/CDCl3

147.50 146.45 138.43 137.90 137.13 135.88 125.84 124.13 123.57 122.05 121.54 121.21 119.65 113.56 89.40 87.61 83.35 77.48 77.23 76.97 74.91 57.88 57.31 36.43 36.16 32.13 32.08 30.48 29.65 15.04 14.71 3.93

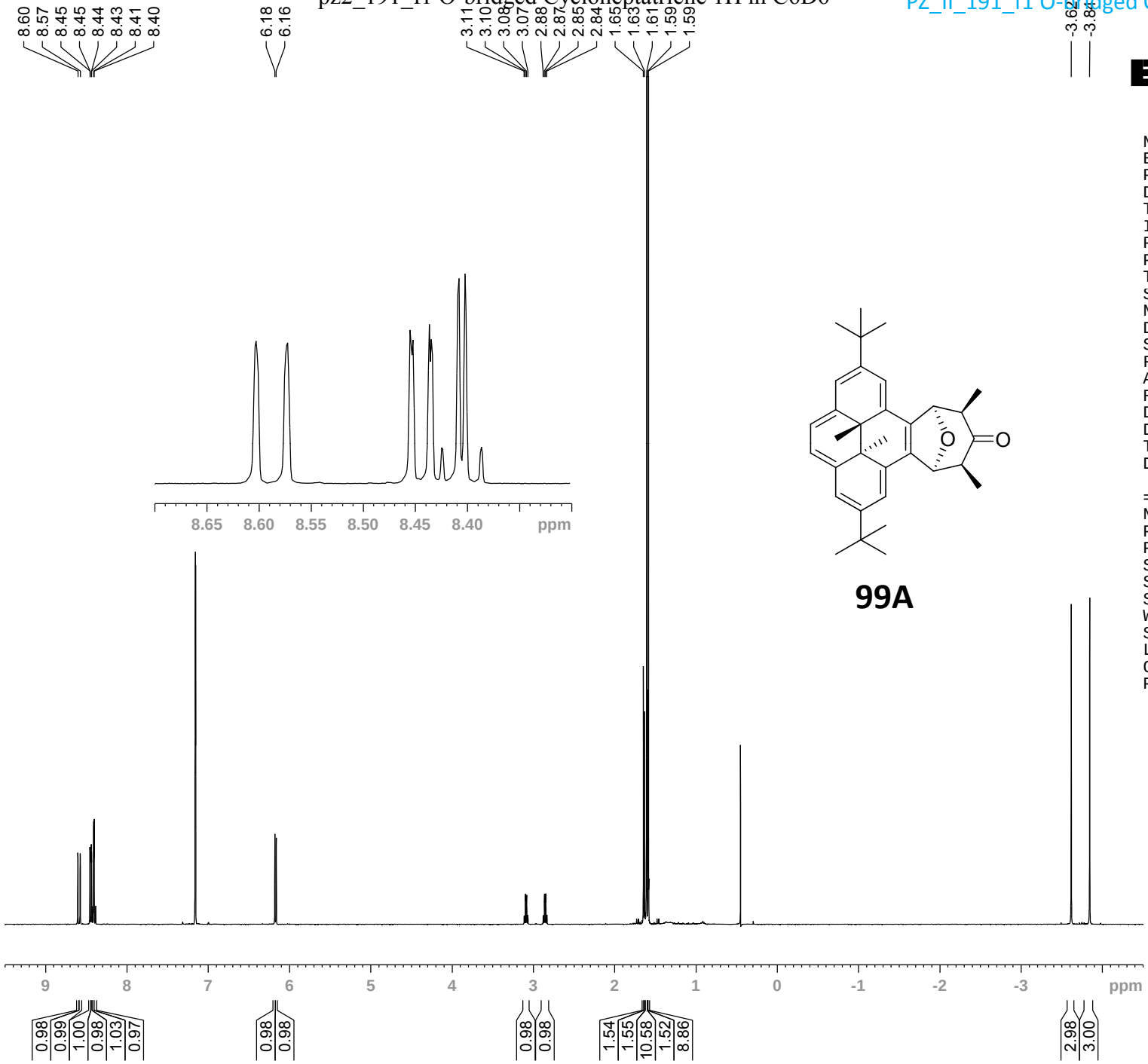
75



NAME	pz3_153_f2
EXPNO	3
PROCNO	1
Date_	20080523
Time	10.15
INSTRUM	spect
PROBHD	5 mm PABBO BB-
PULPROG	zgpg30
TD	65536
SOLVENT	CDCl3
NS	6050
DS	4
SWH	30864.197 Hz
FIDRES	0.470950 Hz
AQ	1.0617495 sec
RG	14596.5
DW	16.200 usec
DE	6.50 usec
TE	299.2 K
D1	1.00000000 sec
D11	0.03000000 sec
TD0	1
======== CHANNEL f1 ========	
NUC1	13C
P1	10.00 usec
PL1	3.00 dB
SFO1	125.7715390 MHz
======== CHANNEL f2 ========	
CPDPRG2	waltz16
NUC2	1H
PCPD2	80.00 usec
PL2	-4.00 dB
PL12	14.42 dB
PL13	14.24 dB
SFO2	500.1325200 MHz
SI	32768
SF	125.7577628 MHz
WDW	EM
SSB	0
LB	0.90 Hz
GB	0
PC	1.40

pz2_191_f1 O-bridged Cycloheptatriene 1H in C6D6

PZ_II_191_f1 O-bridged Cycloheptatriene 1H in C6D6

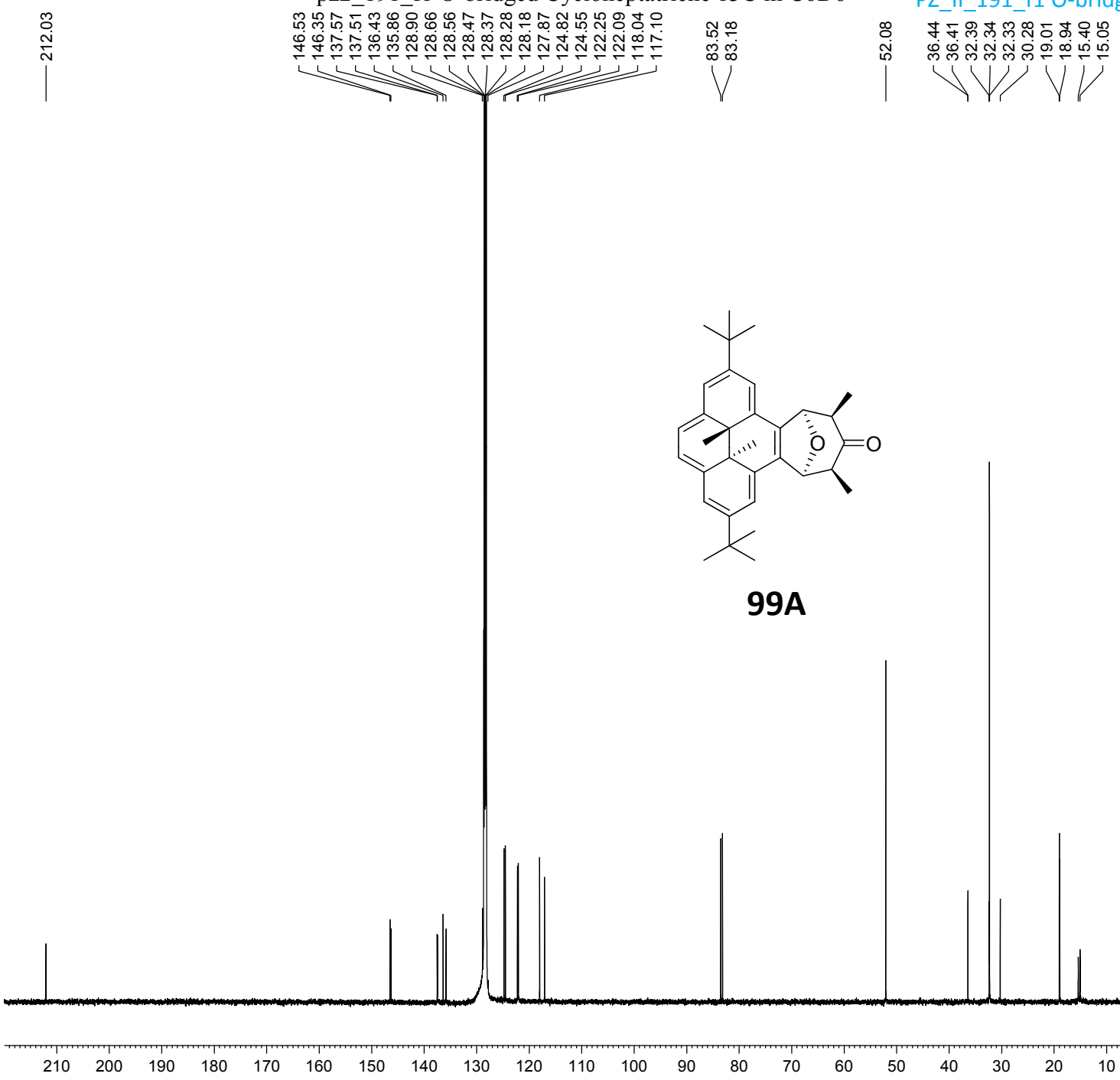



```
NAME          pz2_191_f1a1H
EXPNO                     1
PROCNO                    1
Date_              20070814
Time                  17.39
INSTRUM               AV500
PROBHD    5 mm BBO BB-1H
PULPROG               zg30
TD                   32768
SOLVENT                C6D6
NS                       16
DS                        2
SWH               8012.820 Hz
FIDRES               0.244532 Hz
AQ                2.0448356 sec
RG                      181
DW                   62.400 usec
DE                    6.00 usec
TE                   300.0 K
D1               1.00000000 sec

======== CHANNEL f1 ========
NUC1                      1H
P1                     9.80 usec
PL1                   -4.00 dB
SFO1           500.1315200 MHz
SI                    16384
SF             500.1299971 MHz
WDW                       GM
SSB                        0
LB                    -0.20 Hz
GB                       0.5
PC                      1.00
```

pz2_191_f1 O-bridged Cycloheptatriene 13C in C6D6

PZ_II_191_f1 O-bridged Cycloheptatriene 13C in C6D6

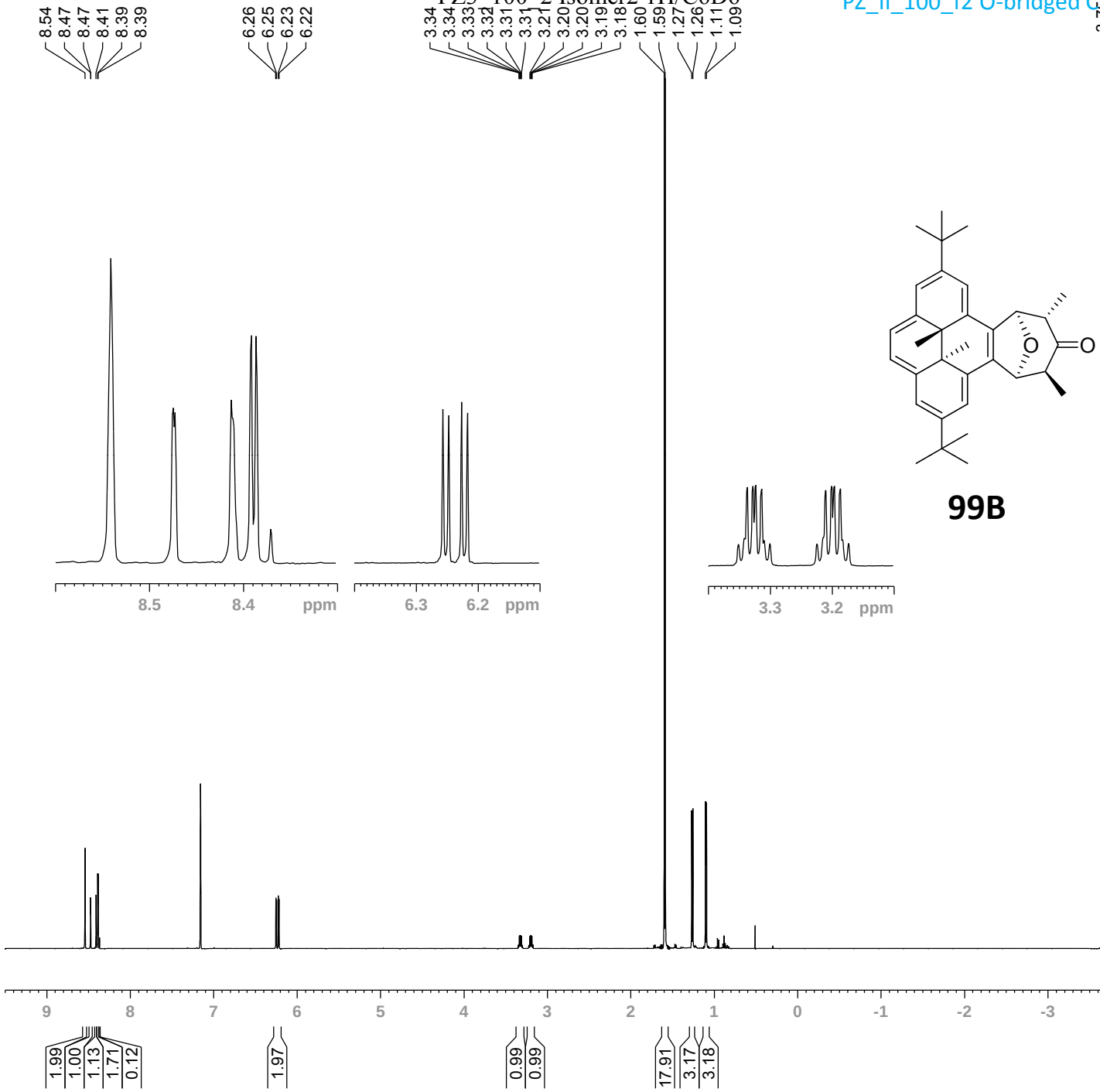


99A

NAME	pz2_191_f1a13C
EXPNO	1
PROCNO	1
Date_	20070814
Time	17.49
INSTRUM	AV500
PROBHD	5 mm BBO BB-1H
PULPROG	zgpg30
TD	65536
SOLVENT	C6D6
NS	4682
DS	4
SWH	30864.197 Hz
FIDRES	0.470950 Hz
AQ	1.0617495 sec
RG	5792.6
DW	16.200 usec
DE	18.00 usec
TE	300.0 K
D1	1.00000000 sec
d11	0.03000000 sec
d12	0.00002000 sec
======== CHANNEL f1 ========	
NUC1	13C
P1	9.80 usec
PL1	3.00 dB
SFO1	125.7715390 MHz
======== CHANNEL f2 ========	
CPDPRG2	waltz16
NUC2	1H
PCPD2	80.00 usec
PL2	-4.00 dB
PL12	14.69 dB
PL13	14.69 dB
SFO2	500.1325200 MHz
SI	32768
SF	125.7577027 MHz
WDW	EM
SSB	0
LB	0.90 Hz
GB	0
PC	1.40

PZ3_100_2 Isomer2 1H/C6D6

PZ_II_100_f2 O-bridged Cycloheptatriene isomer2 1H in C6D6

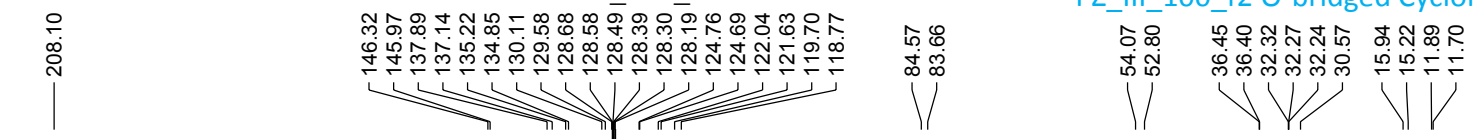


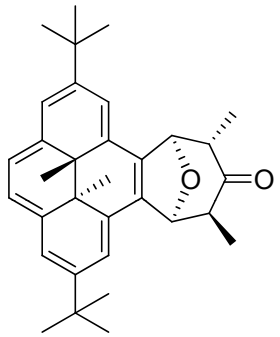
99B

NAME	pz3_100_2
EXPNO	1
PROCNO	1
Date_	20080123
Time	18.31
INSTRUM	AV500
PROBHD	5 mm BBO BB-1H
PULPROG	zg30
TD	32768
SOLVENT	C6D6
NS	16
DS	2
SWH	8012.820 Hz
FIDRES	0.244532 Hz
AQ	2.0448356 sec
RG	71.8
DW	62.400 usec
DE	6.00 usec
TE	300.0 K
D1	1.00000000 sec
======== CHANNEL f1 ========	
NUC1	1H
P1	10.10 usec
PL1	-4.00 dB
SFO1	500.1315200 MHz
SI	16384
SF	500.1299975 MHz
WDW	GM
SSB	0
LB	-0.20 Hz
GB	0.5
PC	1.00

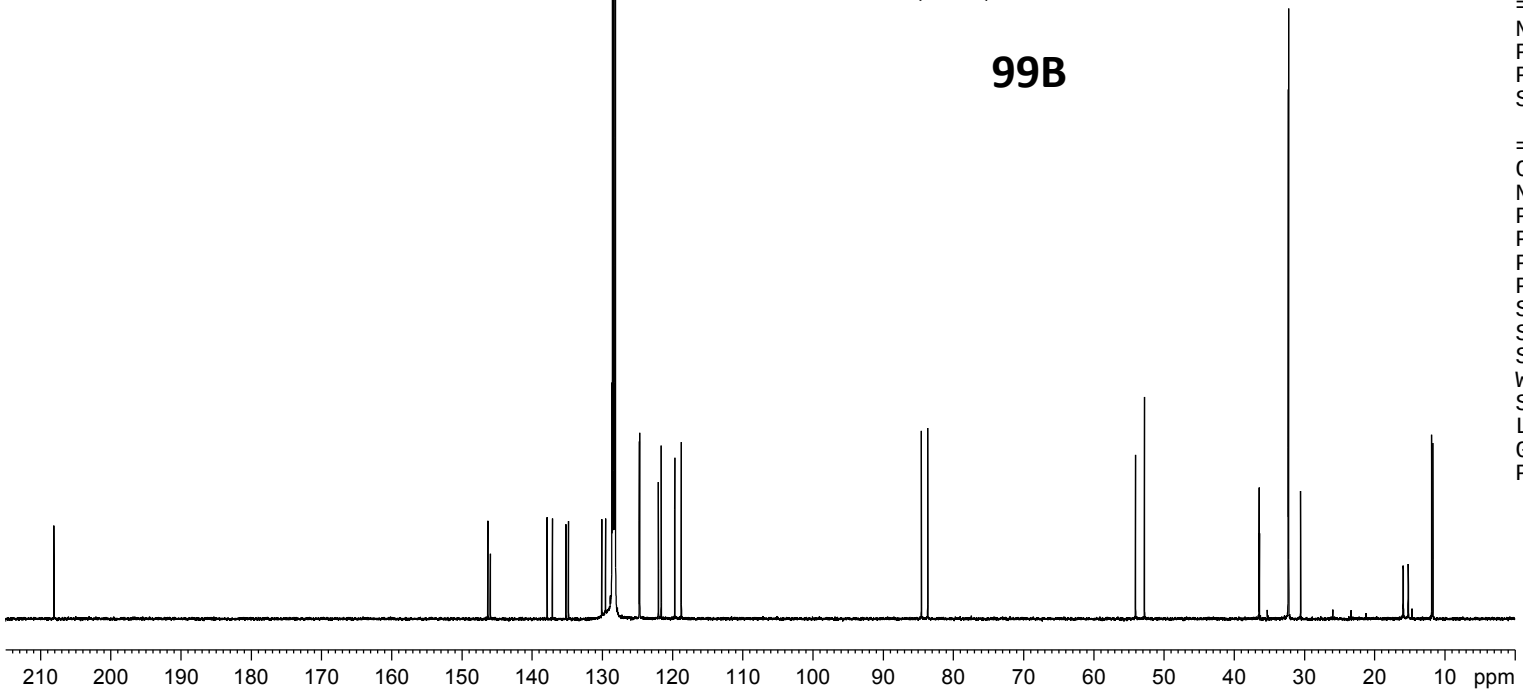
PZ3_100_2 Isomer2 13C/C6D6

PZ_III_100_f2 O-bridged Cycloheptatriene isomer2 13C in C6D6





99B

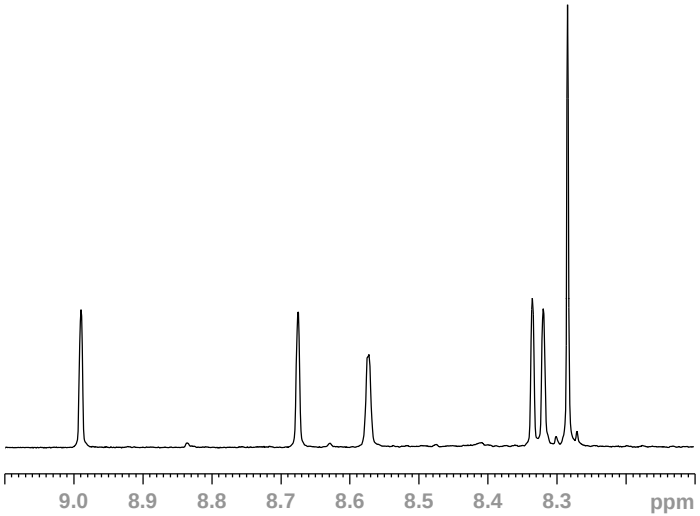


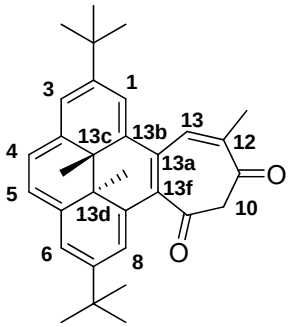
NAME	pz3_100_2
EXPNO	2
PROCNO	1
Date_	20080123
Time	18.38
INSTRUM	AV500
PROBHD	5 mm BBO BB-1H
PULPROG	zgpg30
TD	65536
SOLVENT	C6D6
NS	3072
DS	4
SWH	30864.197 Hz
FIDRES	0.470950 Hz
AQ	1.0617495 sec
RG	5792.6
DW	16.200 usec
DE	18.00 usec
TE	300.0 K
D1	1.00000000 sec
d11	0.03000000 sec
d12	0.00002000 sec
======== CHANNEL f1 ========	
NUC1	13C
P1	10.00 usec
PL1	3.00 dB
SFO1	125.7715390 MHz
======== CHANNEL f2 ========	
CPDPRG2	waltz16
NUC2	1H
PCPD2	80.00 usec
PL2	-4.00 dB
PL12	14.24 dB
PL13	14.24 dB
SFO2	500.1325200 MHz
SI	32768
SF	125.7577011 MHz
WDW	EM
SSB	0
LB	0.90 Hz
GB	0
PC	1.40

pz3_ A tropone side product 1H/CDCl3

PZ A TROPONE SIDE PRODUCT 1H NMR



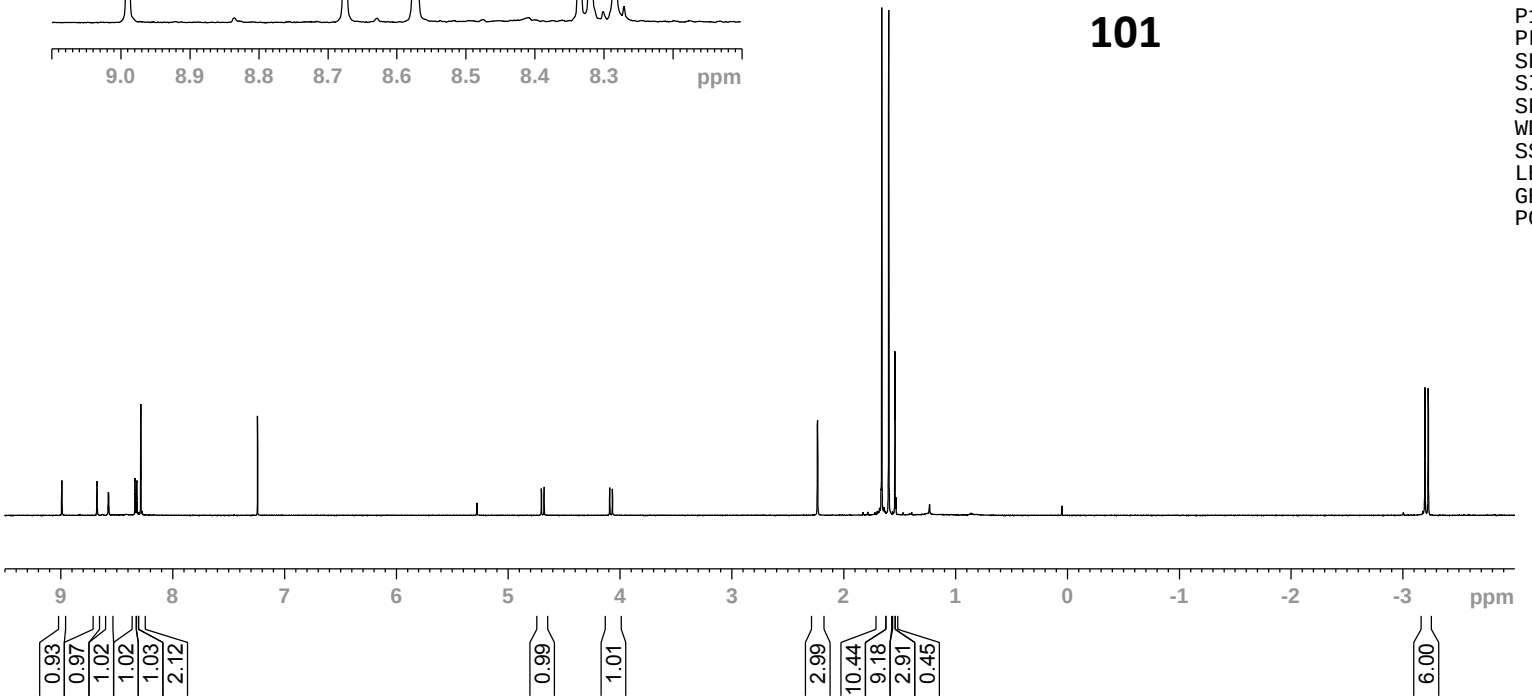




101

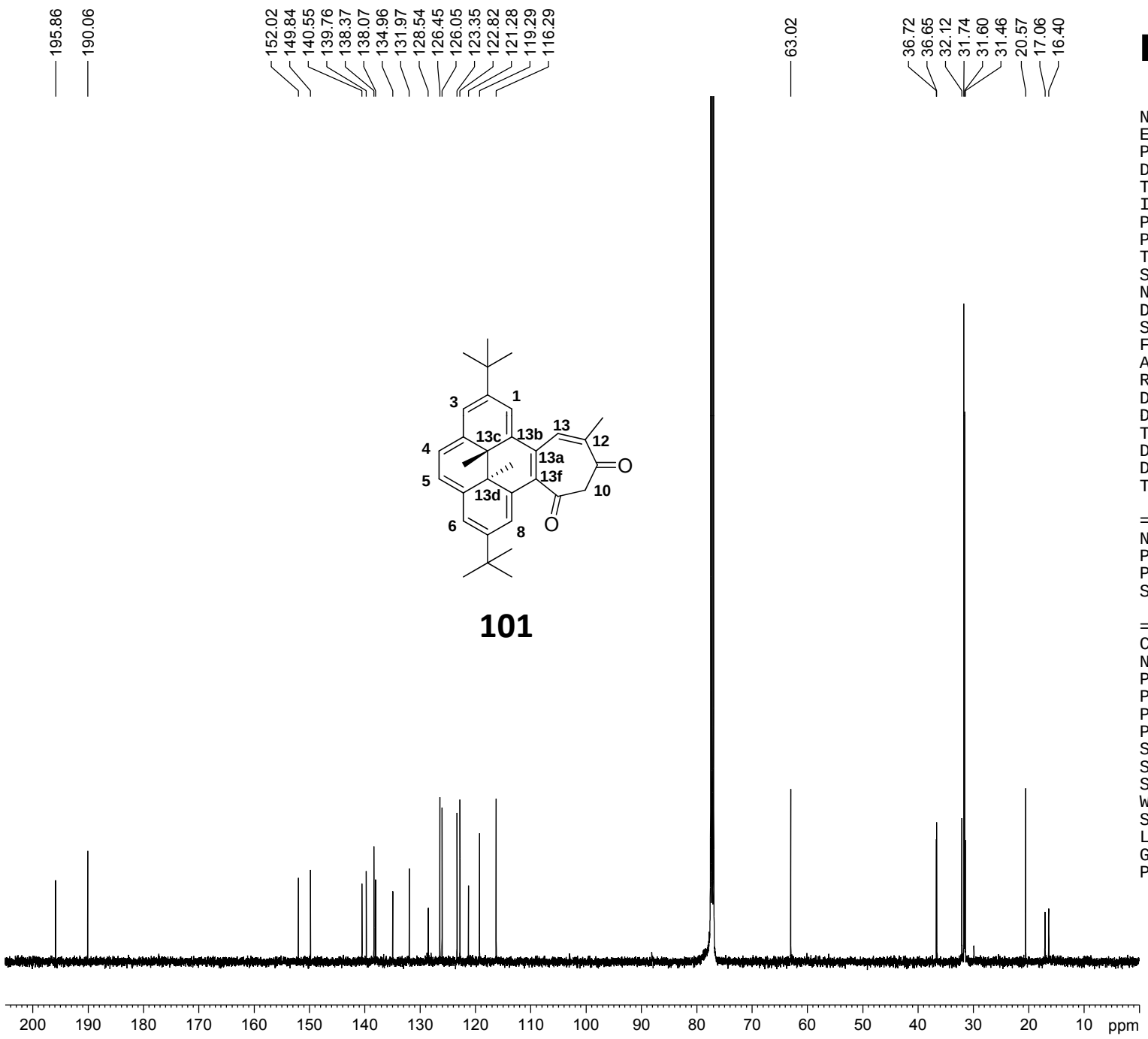
```
NAME          pz3_a tropone
EXPNO                    1
PROCNO                   1
Date_             20080616
Time                 17.42
INSTRUM              spect
PROBHD    5 mm PABBO BB-
PULPROG               zg30
TD                   32768
SOLVENT              CDCl3
NS                      16
DS                       2
SWH               8012.820 Hz
FIDRES            0.244532 Hz
AQ                2.0448356 sec
RG                     362
DW                  62.400 usec
DE                   6.50 usec
TE                  297.5 K
D1              1.00000000 sec
TD0                      1

======== CHANNEL f1 ========
NUC1                    1H
P1                    9.60 usec
PL1                  -4.00 dB
SFO1          500.1315200 MHz
SI                   16384
SF            500.1300233 MHz
WDW                     GM
SSB                      0
LB                   -0.20 Hz
GB                     0.5
PC                    1.00
```



pz3_ A tropone side product 13C/CDCl3

PZ A TROPONE SIDE PROUDCT 13C NMR



101

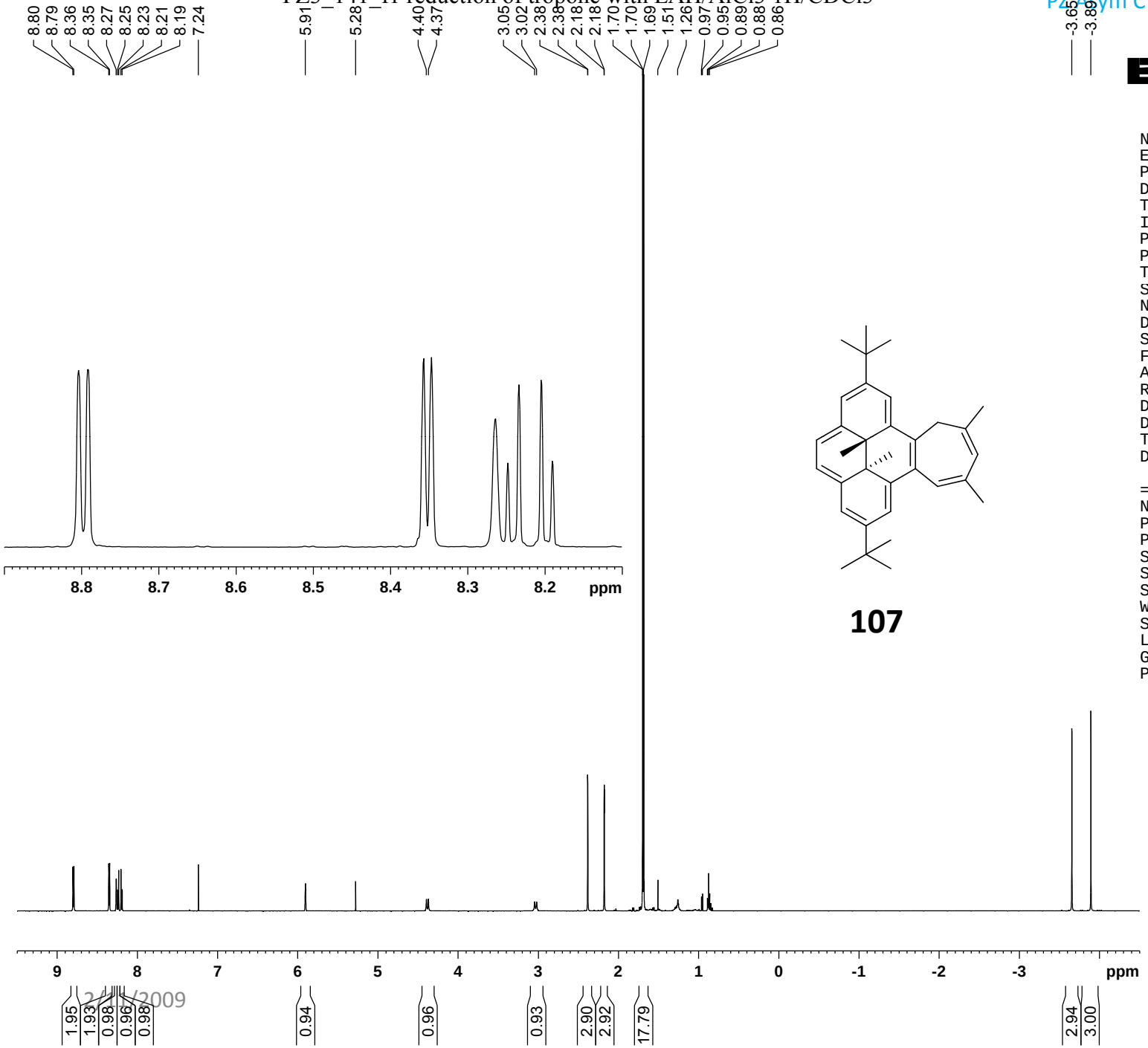
```
NAME          pz3_a tropone
EXPNO                    3
PROCNO                   1
Date_             20080617
Time                 3.00
INSTRUM             spect
PROBHD    5 mm PABBO BB-
PULPROG           zgpg30
TD                 65536
SOLVENT            CDCl3
NS                 15360
DS                     4
SWH            30864.197 Hz
FIDRES          0.470950 Hz
AQ              1.0617495 sec
RG                14596.5
DW                16.200 usec
DE                 6.50 usec
TE                299.6 K
D1             1.00000000 sec
D11            0.03000000 sec
TD0                    1

======== CHANNEL f1 ========
NUC1                  13C
P1                 10.00 usec
PL1                 3.00 dB
SFO1         125.7715390 MHz

======== CHANNEL f2 ========
CPDPRG2          waltz16
NUC2                  1H
PCPD2              80.00 usec
PL2                -4.00 dB
PL12               14.42 dB
PL13               14.24 dB
SFO2         500.1325200 MHz
SI                 32768
SF           125.7577620 MHz
WDW                   EM
SSB                    0
LB                 0.90 Hz
GB                     0
PC                 1.40
```

PZ3_141_f1 reduction of tropone with LAH/AlCl3 1H/CDCl3

PZ Asym CYCLOHEPTATRIENE 1H NMR



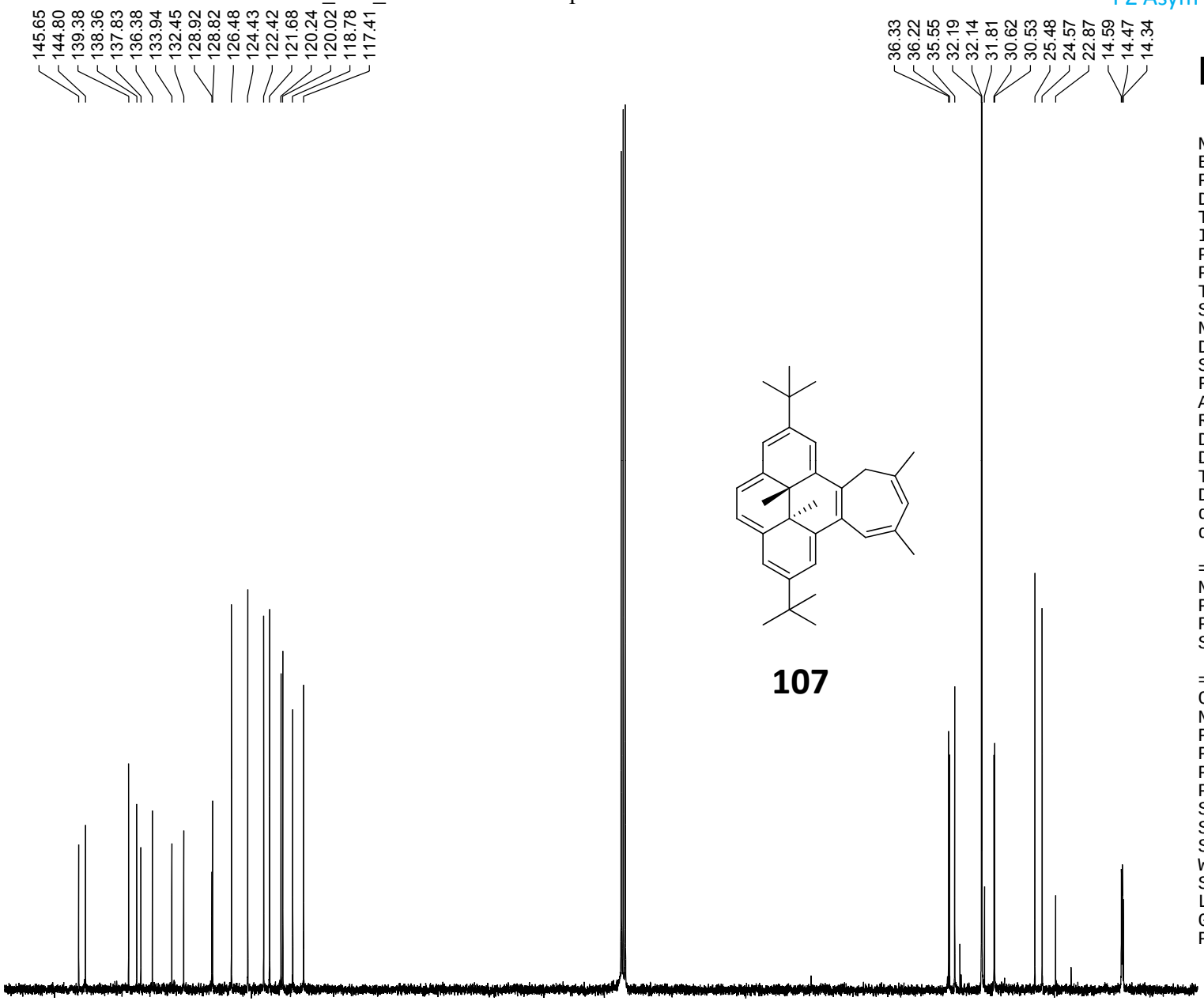
107

NAME	pz3_141_f1
EXPNO	1
PROCNO	1
Date_	20080421
Time	19.48
INSTRUM	AV500
PROBHD	5 mm BBO BB-1H
PULPROG	zg30
TD	32768
SOLVENT	CDCl3
NS	16
DS	2
SWH	8012.820 Hz
FIDRES	0.244532 Hz
AQ	2.0448356 sec
RG	90.5
DW	62.400 usec
DE	6.00 usec
TE	300.0 K
D1	1.00000000 sec
========	CHANNEL f1 ========
NUC1	1H
P1	10.10 usec
PL1	-4.00 dB
SFO1	500.1315200 MHz
SI	16384
SF	500.1300236 MHz
WDW	GM
SSB	0
LB	-0.20 Hz
GB	0.5
PC	1.00

2/11/2009

PZ3_141_f1 reduction of tropone with LAH/AlCl3 13C/CDCl3

PZ Asym CYCLOHEPTATRIENE 1H NMR



107

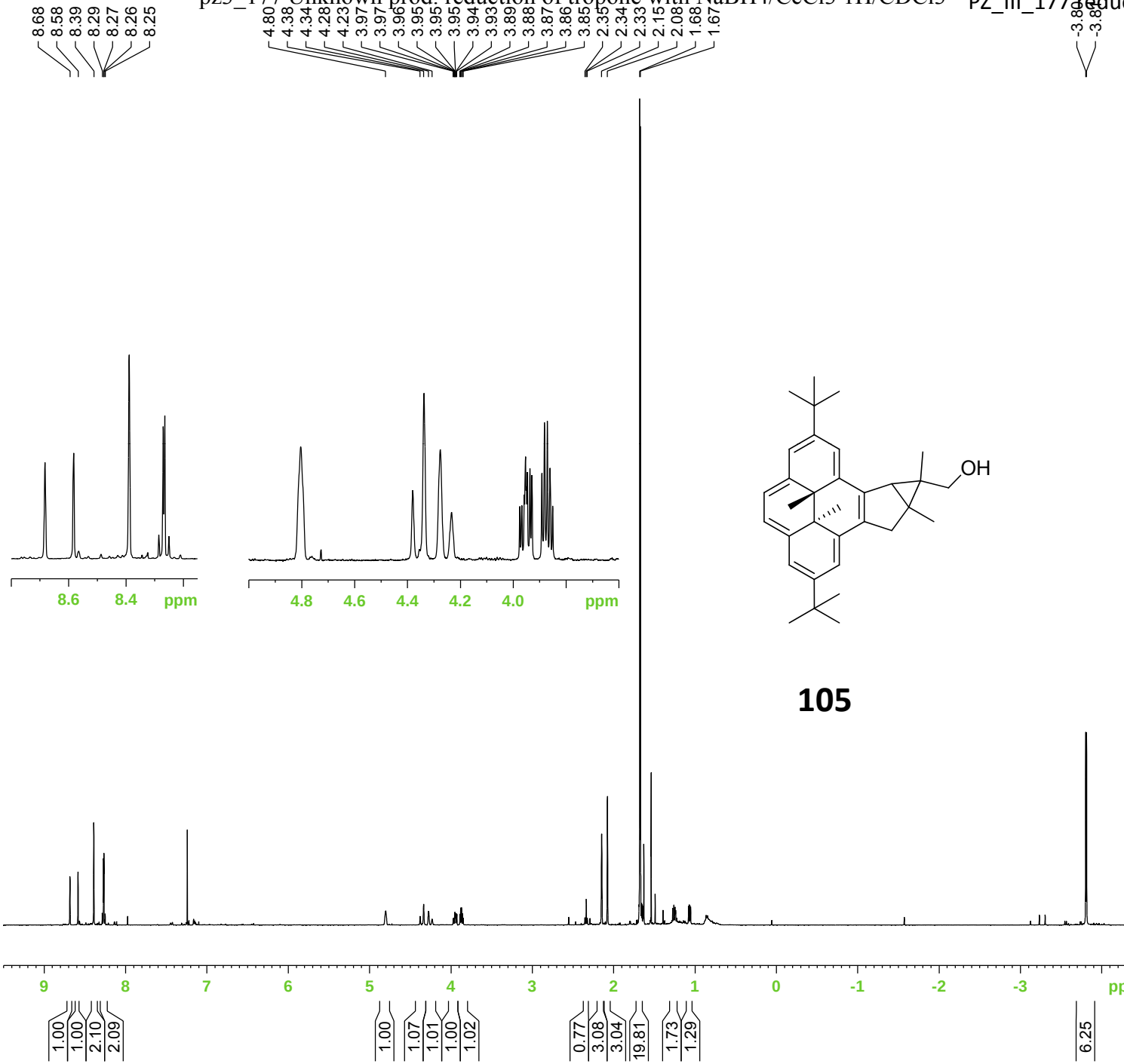
```
NAME            pz3_141_f1
EXPNO                    2
PROCNO                   1
Date_             20080421
Time                 19.57
INSTRUM              AV500
PROBHD    5 mm BBO BB-1H
PULPROG             zgpg30
TD                    65536
SOLVENT               CDCl3
NS                     1024
DS                        4
SWH              30864.197 Hz
FIDRES            0.470950 Hz
AQ                1.0617495 sec
RG                  14596.5
DW                   16.200 usec
DE                   18.00 usec
TE                   300.0 K
D1               1.00000000 sec
d11              0.03000000 sec
d12              0.00002000 sec

======== CHANNEL f1 ========
NUC1                    13C
P1                   10.00 usec
PL1                   3.00 dB
SFO1           125.7715390 MHz

======== CHANNEL f2 ========
CPDPRG2            waltz16
NUC2                    1H
PCPD2                80.00 usec
PL2                  -4.00 dB
PL12                 14.24 dB
PL13                 14.24 dB
SFO2           500.1325200 MHz
SI                    32768
SF             125.7577634 MHz
WDW                     EM
SSB                      0
LB                    0.90 Hz
GB                       0
PC                    1.40
```

pz3_177 Unknown prod. reduction of tropone with NaBH4/CeCl3 1H/CDCl3

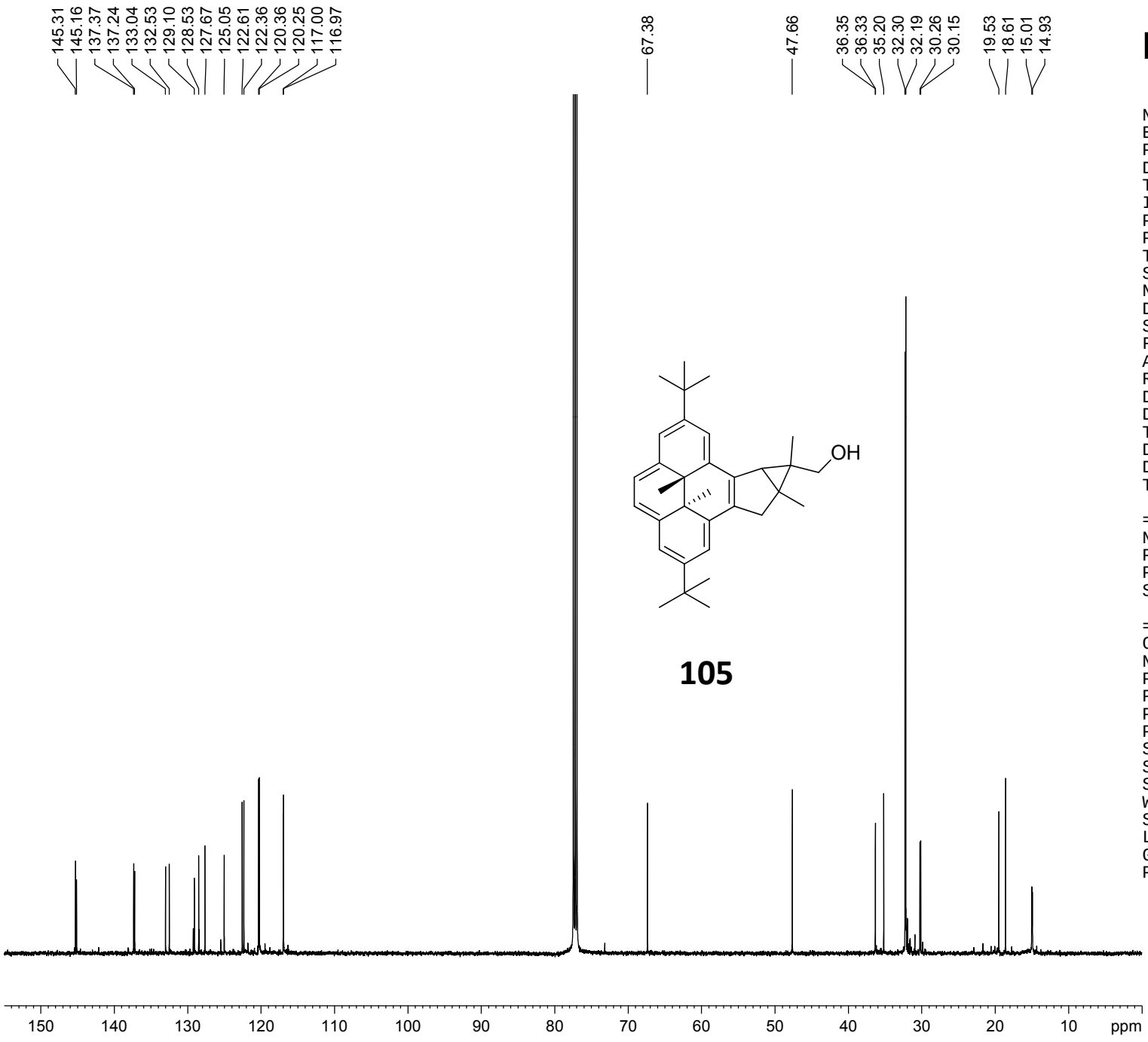
PZ_III_177 reduction of tropone with CeCl3 1H



NAME	pz3_177
EXPNO	1
PROCNO	1
Date_	20080719
Time	9.13
INSTRUM	spect
PROBHD	5 mm PABBO BB-
PULPROG	zg30
TD	32768
SOLVENT	CDCl3
NS	16
DS	2
SWH	8012.820 Hz
FIDRES	0.244532 Hz
AQ	2.0448356 sec
RG	161.3
DW	62.400 usec
DE	6.50 usec
TE	298.8 K
D1	1.00000000 sec
TD0	1
======== CHANNEL f1 ========	
NUC1	1H
P1	9.60 usec
PL1	-4.00 dB
SFO1	500.1315200 MHz
SI	16384
SF	500.1300233 MHz
WDW	GM
SSB	0
LB	-0.20 Hz
GB	0.5
PC	1.00

pz3_177 13C/CDCl3

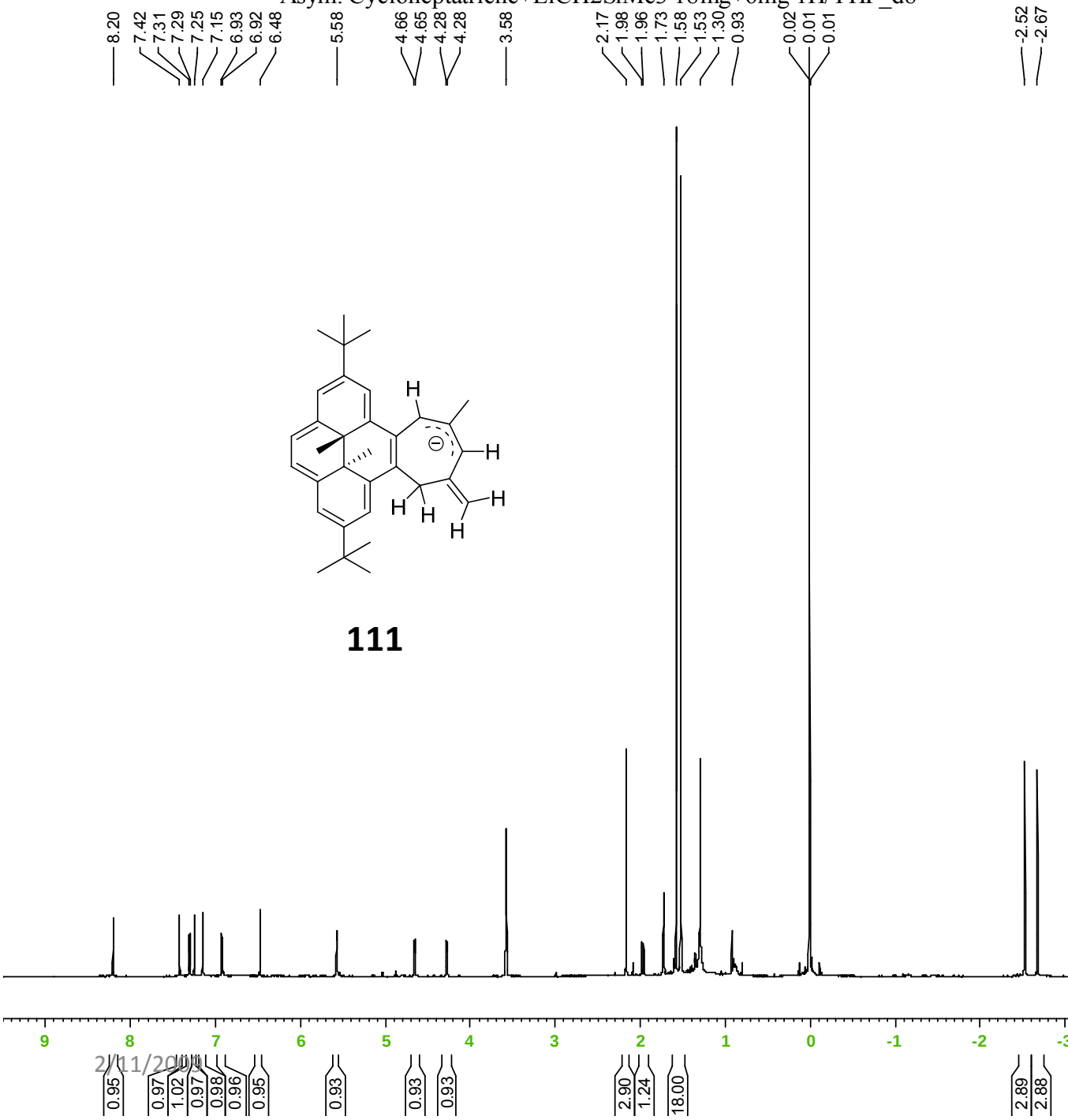
PZ_III_177 reduction of tropone with CeCl3 1H



NAME	pz3_177
EXPNO	2
PROCNO	1
Date_	20080719
Time	16.44
INSTRUM	spect
PROBHD	5 mm PABBO BB-
PULPROG	zgpg30
TD	65536
SOLVENT	CDCl3
NS	12704
DS	4
SWH	30864.197 Hz
FIDRES	0.470950 Hz
AQ	1.0617495 sec
RG	14596.5
DW	16.200 usec
DE	6.50 usec
TE	299.1 K
D1	1.00000000 sec
D11	0.03000000 sec
TD0	1
======== CHANNEL f1 ========	
NUC1	13C
P1	10.00 usec
PL1	3.00 dB
SFO1	125.7715390 MHz
======== CHANNEL f2 ========	
CPDPRG2	waltz16
NUC2	1H
PCPD2	80.00 usec
PL2	-4.00 dB
PL12	14.42 dB
PL13	14.24 dB
SFO2	500.1325200 MHz
SI	32768
SF	125.7577619 MHz
WDW	EM
SSB	0
LB	0.90 Hz
GB	0
PC	1.40

Asym. Cycloheptatriene+LiCH2SiMe3 18mg+6mg 1H/THF_d8

ANION 1H NMR



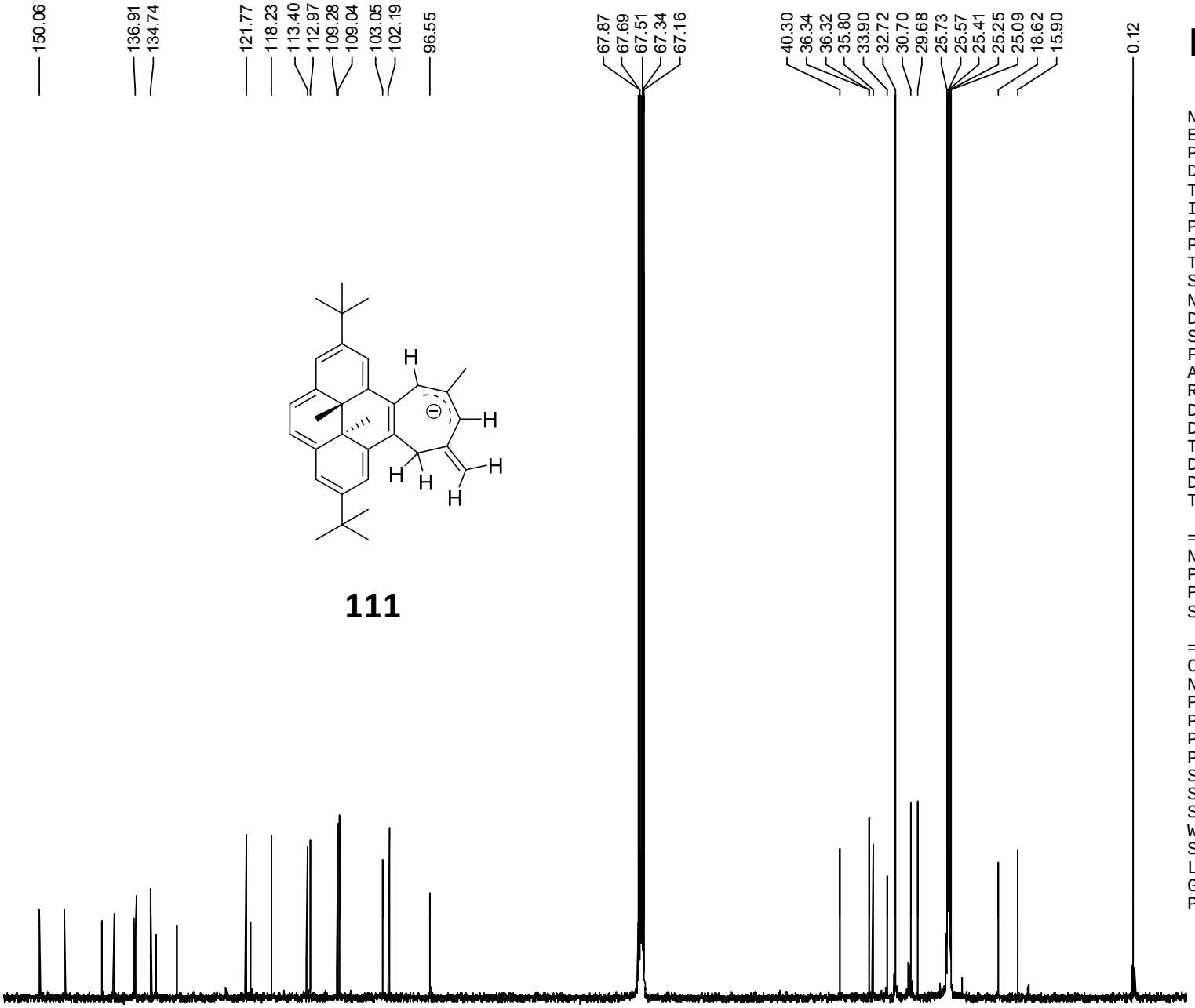
111

```
NAME                PZ4_20
EXPNO                   12
PROCNO                   1
Date_             20090207
Time                 16.35
INSTRUM              spect
PROBHD   5 mm PABBI 1H/
PULPROG              zg30
TD                  32768
SOLVENT               THF
NS                       16
DS                        2
SWH                8012.820 Hz
FIDRES                0.244532 Hz
AQ                 2.0448356 sec
RG                      35.9
DW                    62.400 usec
DE                     6.50 usec
TE                    297.0 K
D1                1.00000000 sec
TD0                      1

======== CHANNEL f1 ========
NUC1                     1H
P1                     9.60 usec
PL1                   -4.00 dB
SFO1           500.1315200 MHz
SI                   16384
SF             500.1300206 MHz
WDW                     GM
SSB                      0
LB                    -0.20 Hz
GB                      0.5
PC                     1.00
```

Asym. Cycloheptatriene+LiCH2SiMe3 18mg+6mg 13C/THF_d8

ANION 13 C NMR

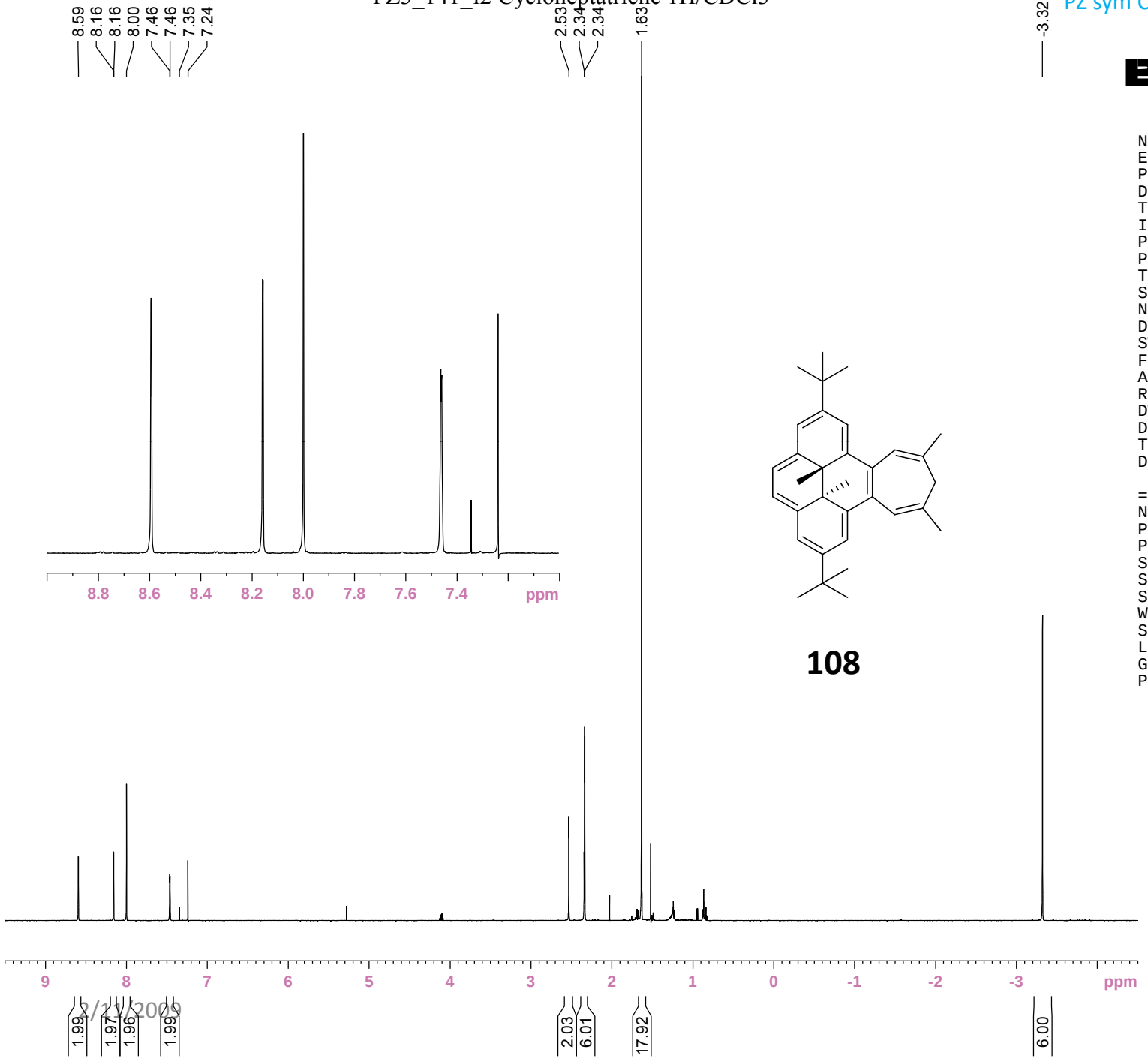


111

NAME	PZ4_20
EXPNO	11
PROCNO	1
Date_	20090208
Time	11.04
INSTRUM	spect
PROBHD	5 mm PABBO BB-
PULPROG	zgpg30
TD	65536
SOLVENT	THF
NS	2364
DS	4
SWH	25000.000 Hz
FIDRES	0.381470 Hz
AQ	1.3107899 sec
RG	14596.5
DW	20.000 usec
DE	6.50 usec
TE	297.4 K
D1	1.00000000 sec
D11	0.03000000 sec
TD0	1
======== CHANNEL f1 ========	
NUC1	13C
P1	10.00 usec
PL1	3.00 dB
SFO1	125.7665890 MHz
======== CHANNEL f2 ========	
CPDPRG2	waltz16
NUC2	1H
PCPD2	80.00 usec
PL2	-4.00 dB
PL12	14.42 dB
PL13	14.24 dB
SFO2	500.1315200 MHz
SI	32768
SF	125.7576583 MHz
WDW	EM
SSB	0
LB	0.90 Hz
GB	0
PC	1.40

PZ3_141_f2 Cycloheptatriene 1H/CDCl3

PZ sym CYCLOHEPTATRIENE 1H NMR



108

```
NAME            pz3_141_f2
EXPNO                    1
PROCNO                   1
Date_             20080422
Time                 17.07
INSTRUM              AV500
PROBHD   5 mm BBO BB-1H
PULPROG               zg30
TD                   32768
SOLVENT              CDCl3
NS                      16
DS                       2
SWH              8012.820 Hz
FIDRES           0.244532 Hz
AQ               2.0448356 sec
RG                   161.3
DW                  62.400 usec
DE                   6.00 usec
TE                  300.0 K
D1              1.00000000 sec

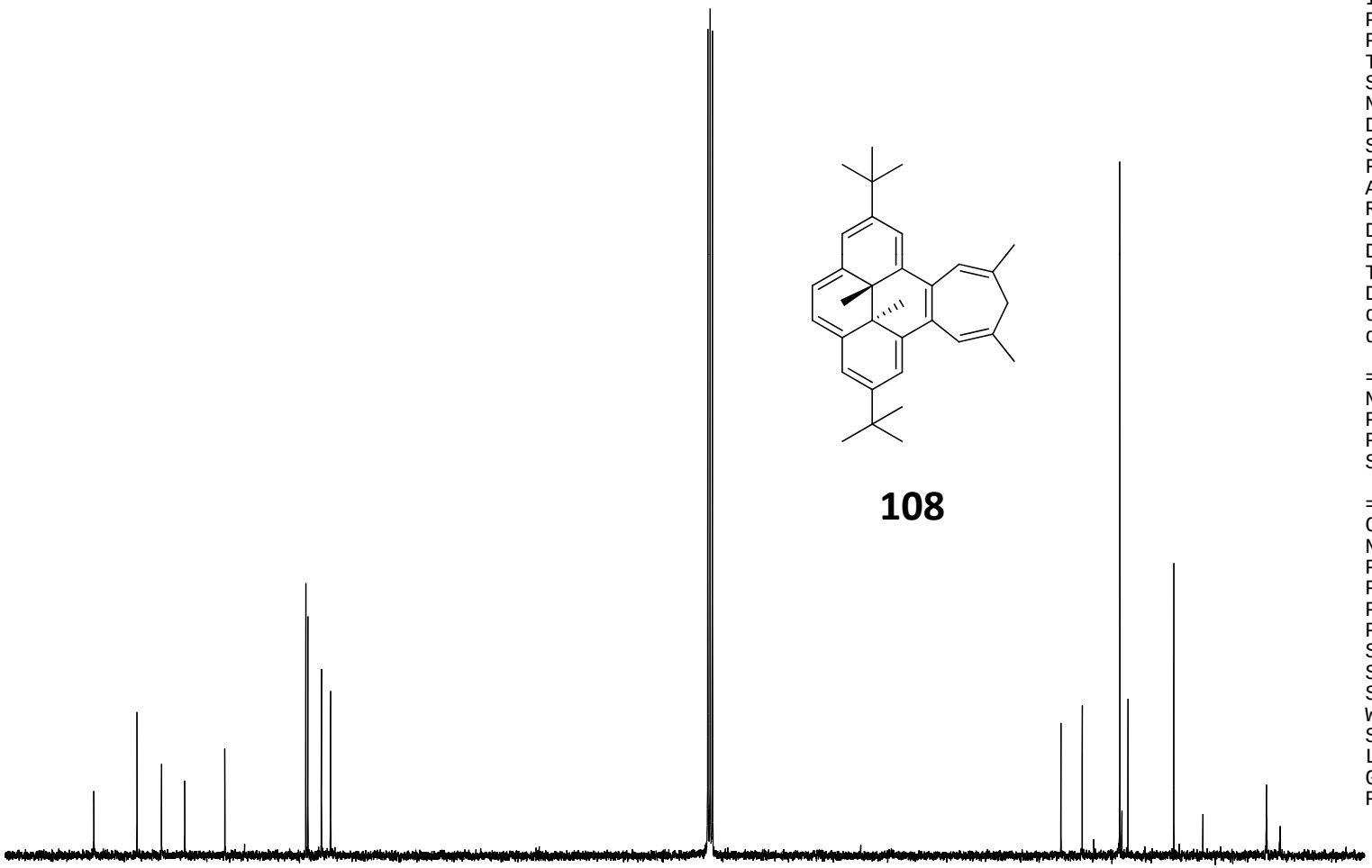
======== CHANNEL f1 ========
NUC1                    1H
P1                   10.10 usec
PL1                  -4.00 dB
SFO1          500.1315200 MHz
SI                   16384
SF            500.1300236 MHz
WDW                     GM
SSB                      0
LB                   -0.20 Hz
GB                     0.5
PC                    1.00
```

PZ3_141_f2 Cycloheptatriene 13C/CDCl3

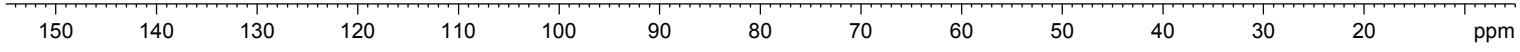
PZ sym CYCLOHEPTATRIENE 13C NMR



108



2/11/2009



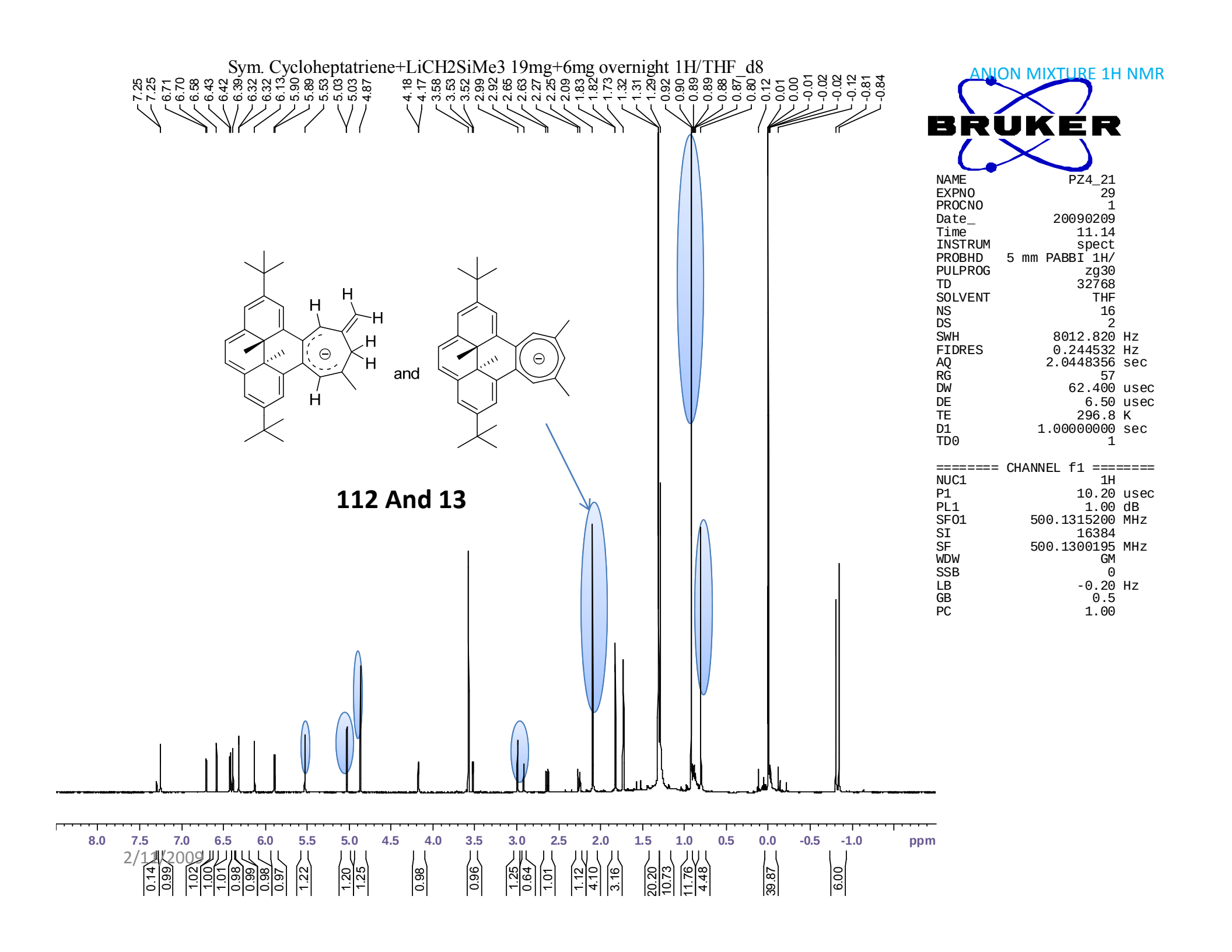

```
NAME           pz3_141_f2
EXPNO                   3
PROCNO                  1
Date_            20080422
Time                17.55
INSTRUM             AV500
PROBHD   5 mm BBO BB-1H
PULPROG           zgpg30
TD                 65536
SOLVENT            CDCl3
NS                  1024
DS                     4
SWH           30864.197 Hz
FIDRES         0.470950 Hz
AQ             1.0617495 sec
RG               11585.2
DW                16.200 usec
DE                18.00 usec
TE                300.0 K
D1            1.00000000 sec
d11           0.03000000 sec
d12           0.00002000 sec

======== CHANNEL f1 ========
NUC1                 13C
P1                10.00 usec
PL1                3.00 dB
SFO1        125.7715390 MHz

======== CHANNEL f2 ========
CPDPRG2          waltz16
NUC2                 1H
PCPD2             80.00 usec
PL2               -4.00 dB
PL12              14.24 dB
PL13              14.24 dB
SFO2        500.1325200 MHz
SI                32768
SF          125.7577624 MHz
WDW                  EM
SSB                   0
LB                 0.90 Hz
GB                    0
PC                 1.40
```

Sym. Cycloheptatriene+LiCH2SiMe3 19mg+6mg overnight 1H/THF_d8

ANION MIXTURE 1H NMR

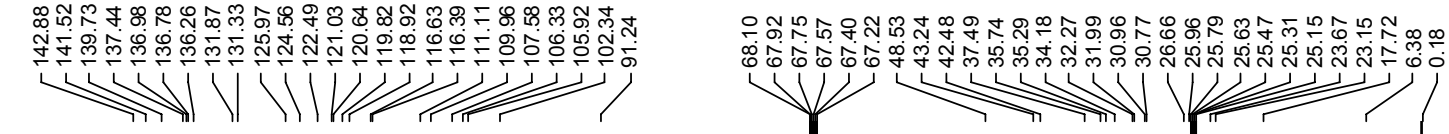


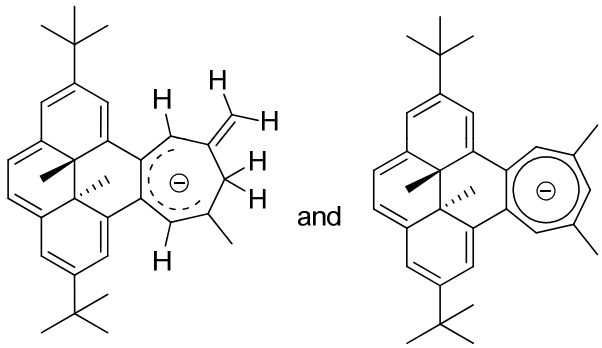
2/11/2009

NAME	PZ4_21
EXPNO	29
PROCNO	1
Date_	20090209
Time	11.14
INSTRUM	spect
PROBHD	5 mm PABBI 1H/
PULPROG	zg30
TD	32768
SOLVENT	THF
NS	16
DS	2
SWH	8012.820 Hz
FIDRES	0.244532 Hz
AQ	2.0448356 sec
RG	57
DW	62.400 usec
DE	6.50 usec
TE	296.8 K
D1	1.00000000 sec
TD0	1
======== CHANNEL f1 ========	
NUC1	1H
P1	10.20 usec
PL1	1.00 dB
SFO1	500.1315200 MHz
SI	16384
SF	500.1300195 MHz
WDW	GM
SSB	0
LB	-0.20 Hz
GB	0.5
PC	1.00

Sym. Cycloheptatriene+LiCH2SiMe3 19mg+6mg 13C/THF_d8

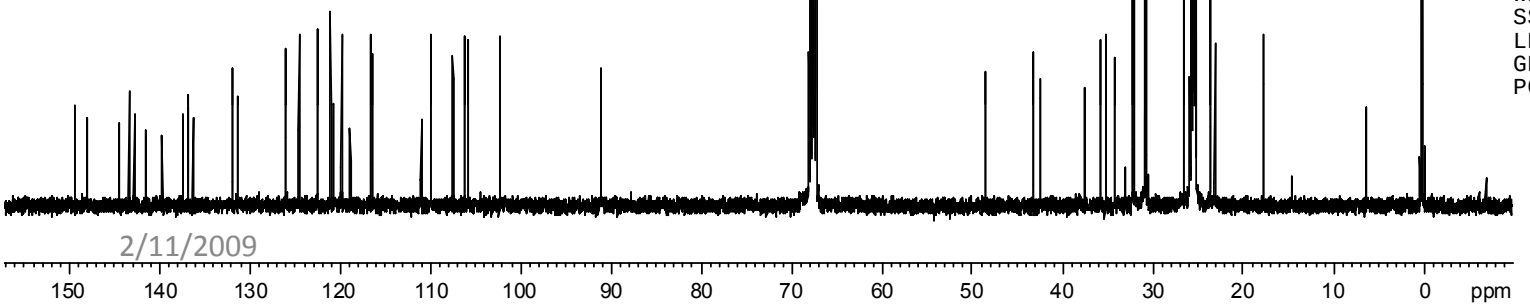
ANION MIXTURE 13C NMR





112 And 13

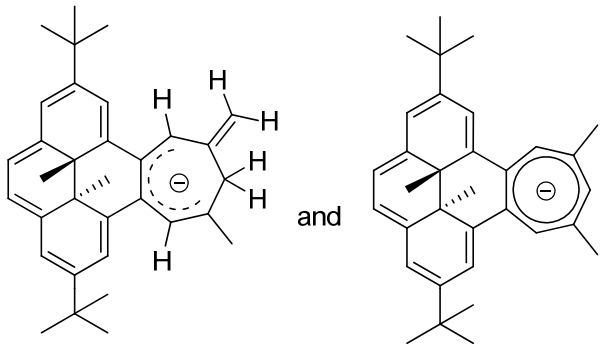
NAME	PZ4_21
EXPNO	5
PROCNO	1
Date_	20090208
Time	20.12
INSTRUM	spect
PROBHD	5 mm PABBO BB-
PULPROG	zgpg30
TD	65536
SOLVENT	THF
NS	2048
DS	4
SWH	30864.197 Hz
FIDRES	0.470950 Hz
AQ	1.0617495 sec
RG	14596.5
DW	16.200 usec
DE	6.50 usec
TE	297.8 K
D1	1.00000000 sec
D11	0.03000000 sec
TD0	1
======== CHANNEL f1 ========	
NUC1	13C
P1	10.00 usec
PL1	3.00 dB
SFO1	125.7697890 MHz
======== CHANNEL f2 ========	
CPDPRG2	waltz16
NUC2	1H
PCPD2	80.00 usec
PL2	-4.00 dB
PL12	14.42 dB
PL13	14.24 dB
SFO2	500.1315200 MHz
SI	32768
SF	125.7576471 MHz
WDW	EM
SSB	0
LB	0.90 Hz
GB	0
PC	1.40



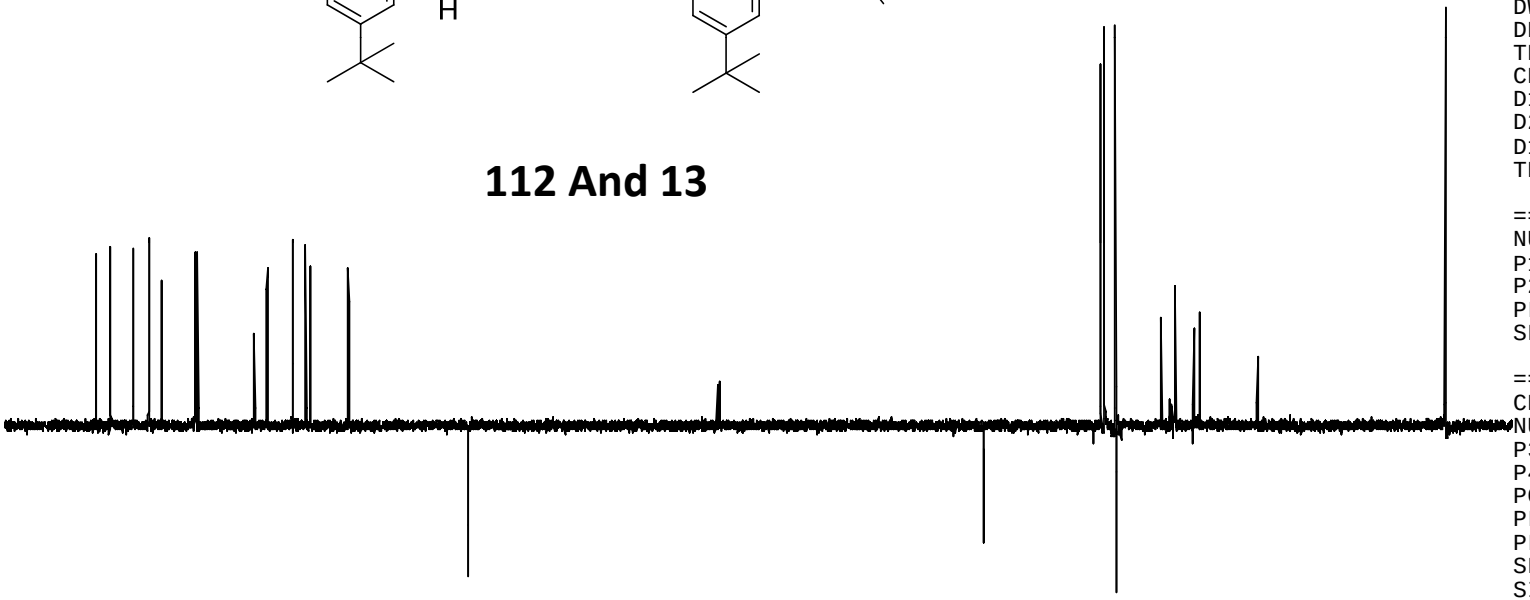
Sym. Cycloheptatriene+LiCH2SiMe3 19mg+n mg Dept/THF_d8

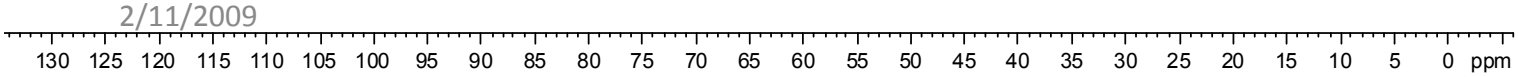
ANION MIXTURE DEPT NMR





112 And 13

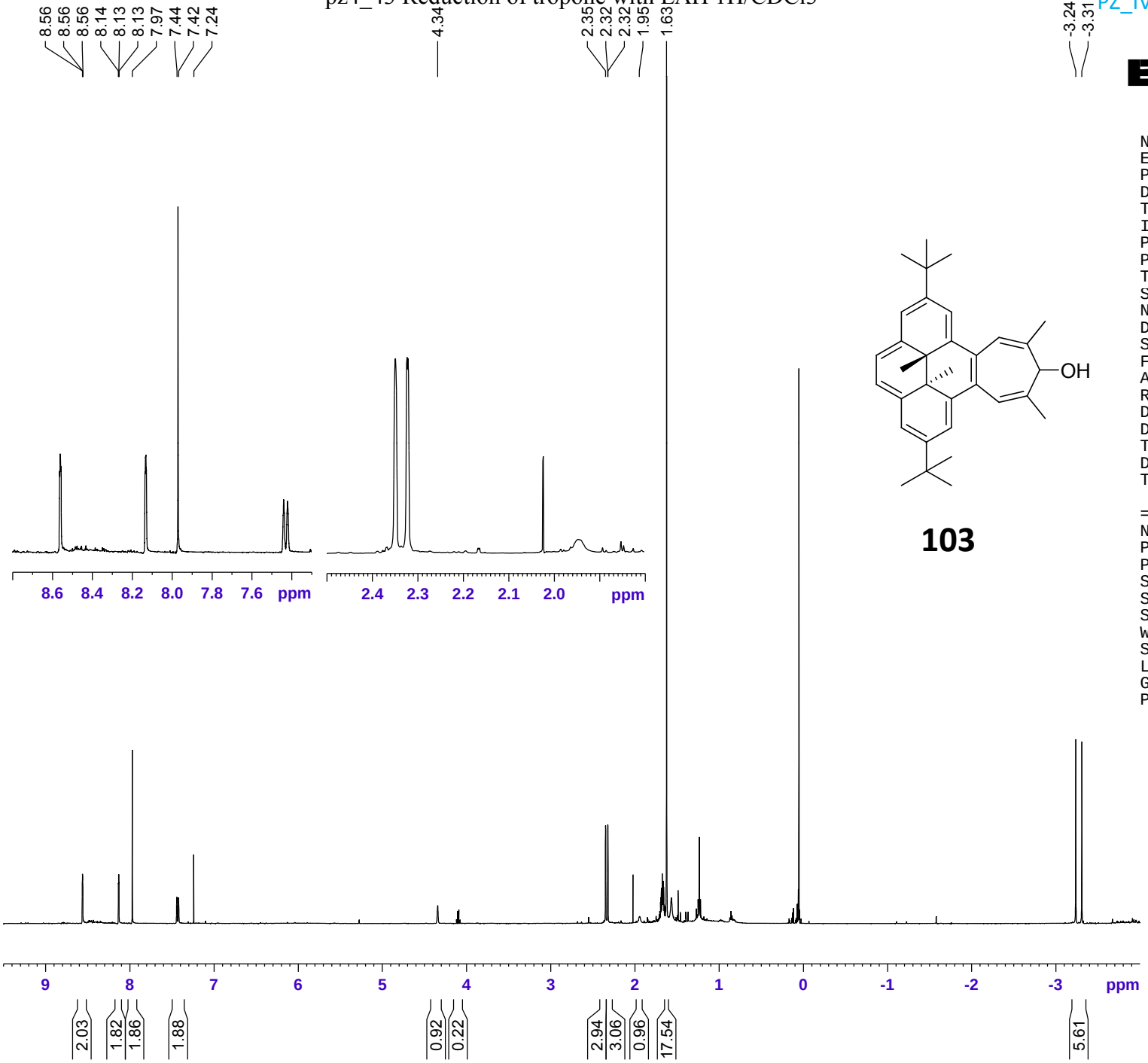




NAME	PZ4_21
EXPNO	7
PROCNO	1
Date_	20090208
Time	20.51
INSTRUM	spect
PROBHD	5 mm PABBO BB-
PULPROG	dept135
TD	65536
SOLVENT	THF
NS	750
DS	4
SWH	30864.197 Hz
FIDRES	0.470950 Hz
AQ	1.0617495 sec
RG	16384
DW	16.200 usec
DE	6.50 usec
TE	297.5 K
CNST2	145.0000000
D1	2.00000000 sec
D2	0.00344828 sec
D12	0.00002000 sec
TD0	1
======== CHANNEL f1 ========	
NUC1	13C
P1	10.00 usec
P2	20.00 usec
PL1	3.00 dB
SFO1	125.7715390 MHz
======== CHANNEL f2 ========	
CPDPRG2	waltz16
NUC2	1H
P3	9.60 usec
P4	19.20 usec
PCPD2	80.00 usec
PL2	-4.00 dB
PL12	14.42 dB
SFO2	500.1325200 MHz
SI	32768
SF	125.7576468 MHz
WDW	EM
SSB	0
LB	0.90 Hz
GB	0
PC	1.40

pz4_43 Reduction of tropone with LAH 1H/CDCl3

PZ_IV_43 CHT ALCOHOL 1H NMR

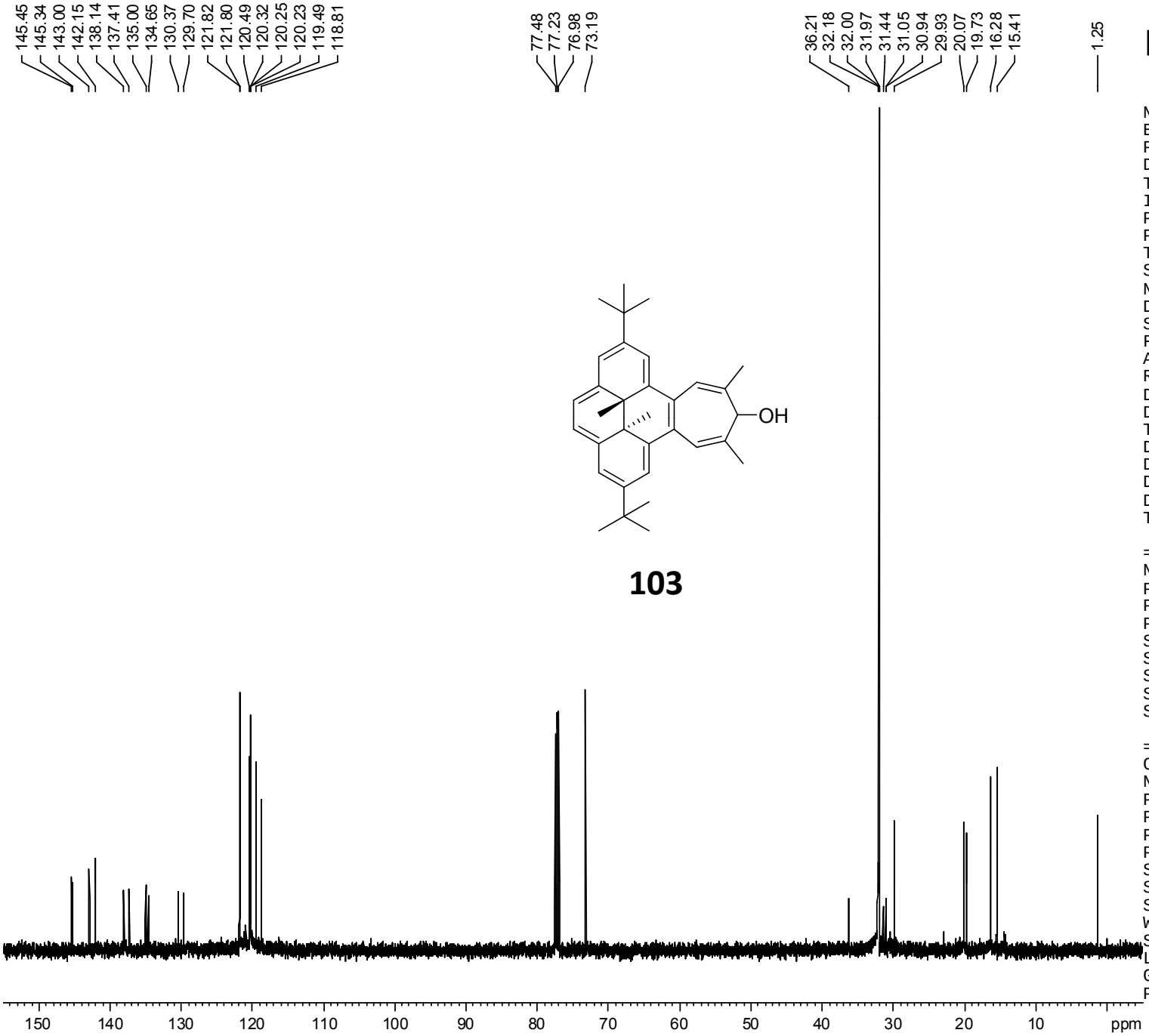


103

NAME	pz4_43
EXPNO	1
PROCNO	1
Date_	20090312
Time	15.36
INSTRUM	spect
PROBHD	5 mm PABBI 1H/
PULPROG	zg30
TD	32768
SOLVENT	CDCl3
NS	16
DS	2
SWH	8012.820 Hz
FIDRES	0.244532 Hz
AQ	2.0448356 sec
RG	71.8
DW	62.400 usec
DE	6.50 usec
TE	297.1 K
D1	1.00000000 sec
TD0	1
======== CHANNEL f1 ========	
NUC1	1H
P1	10.20 usec
PL1	1.00 dB
SFO1	500.1315200 MHz
SI	16384
SF	500.1300234 MHz
WDW	GM
SSB	0
LB	-0.20 Hz
GB	0.5
PC	1.00

Reduction of tropone with LAH 13C/CDCl3

PZ_IV_43 CHT ALCOHOL 13C NMR



103

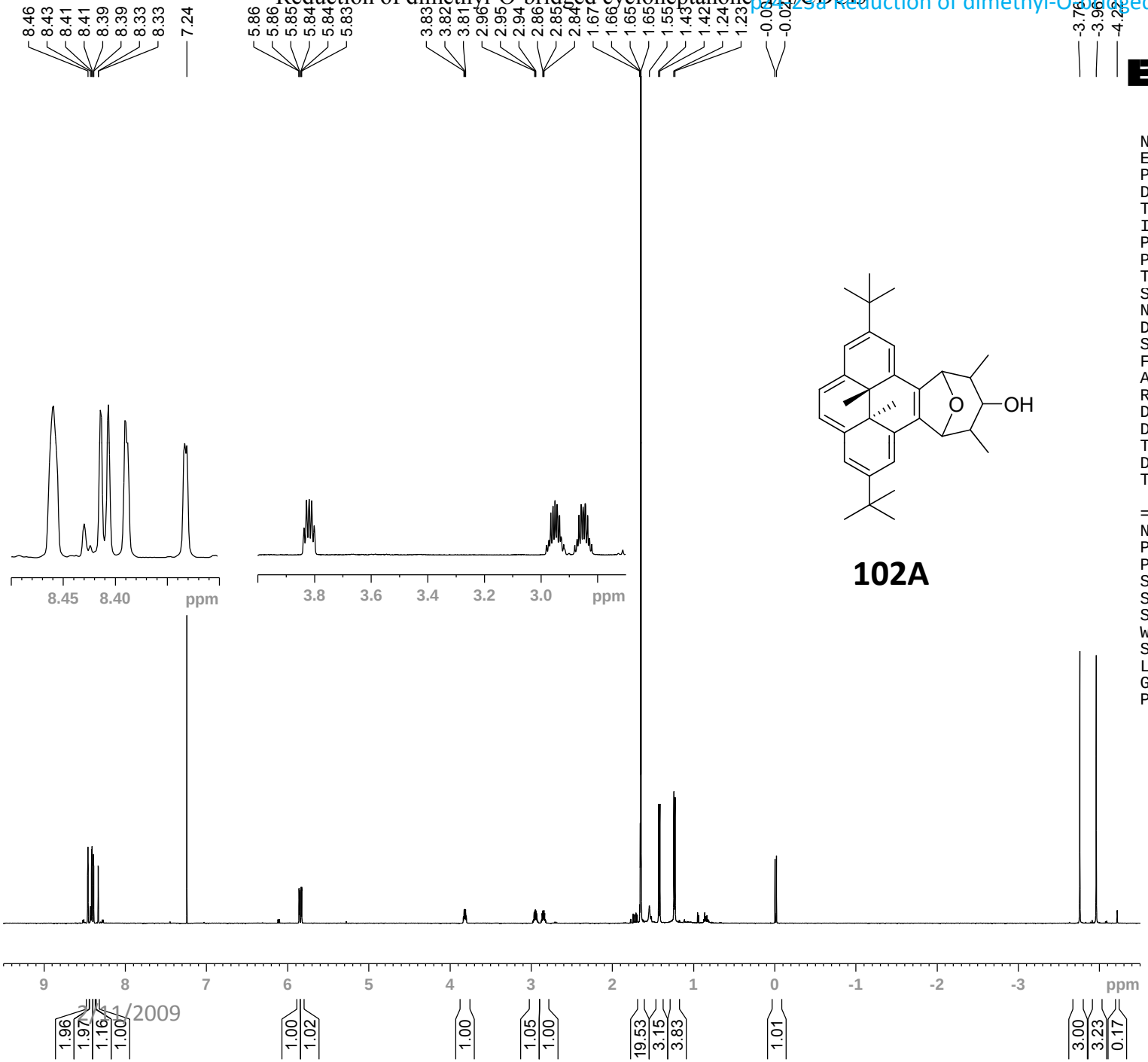
```
NAME                pz4_43
EXPNO                    2
PROCNO                   1
Date_             20090312
Time                 15.44
INSTRUM              spect
PROBHD   5 mm PABBI 1H/
PULPROG  zgpg_echo1.mmod
TD                   65536
SOLVENT              CDCl3
NS                    3486
DS                       4
SWH             30864.197 Hz
FIDRES           0.470950 Hz
AQ               1.0617495 sec
RG                   16384
DW                  16.200 usec
DE                   6.50 usec
TE                  297.5 K
D1              1.00000000 sec
D11             0.03000000 sec
D20             0.00010000 sec
D21             0.00011460 sec
TD0                      1

======== CHANNEL f1 ========
NUC1                   13C
P1                  14.60 usec
P12               2000.00 usec
PL1                 -1.00 dB
SFO1          125.7715390 MHz
SP2                  3.87 dB
SPNAM2       Crp60comp.4
SPOAL2             0.500
SPOFFS2             0.00 Hz

======== CHANNEL f2 ========
CPDPRG2           waltz16
NUC2                   1H
PCPD2               80.00 usec
PL2                  1.00 dB
PL12                19.40 dB
PL13                19.40 dB
SFO2          500.1315200 MHz
SI                   32768
SF            125.7577610 MHz
WDW                    EM
SSB                     0
LB                   0.90 Hz
GB                      0
PC                   1.40
```

Reduction of dimethyl-O-bridged cycloheptanone_1H/CDCl3

pz4_23a Reduction of dimethyl-O-bridged cycloheptanone_1H/CDCl3



102A

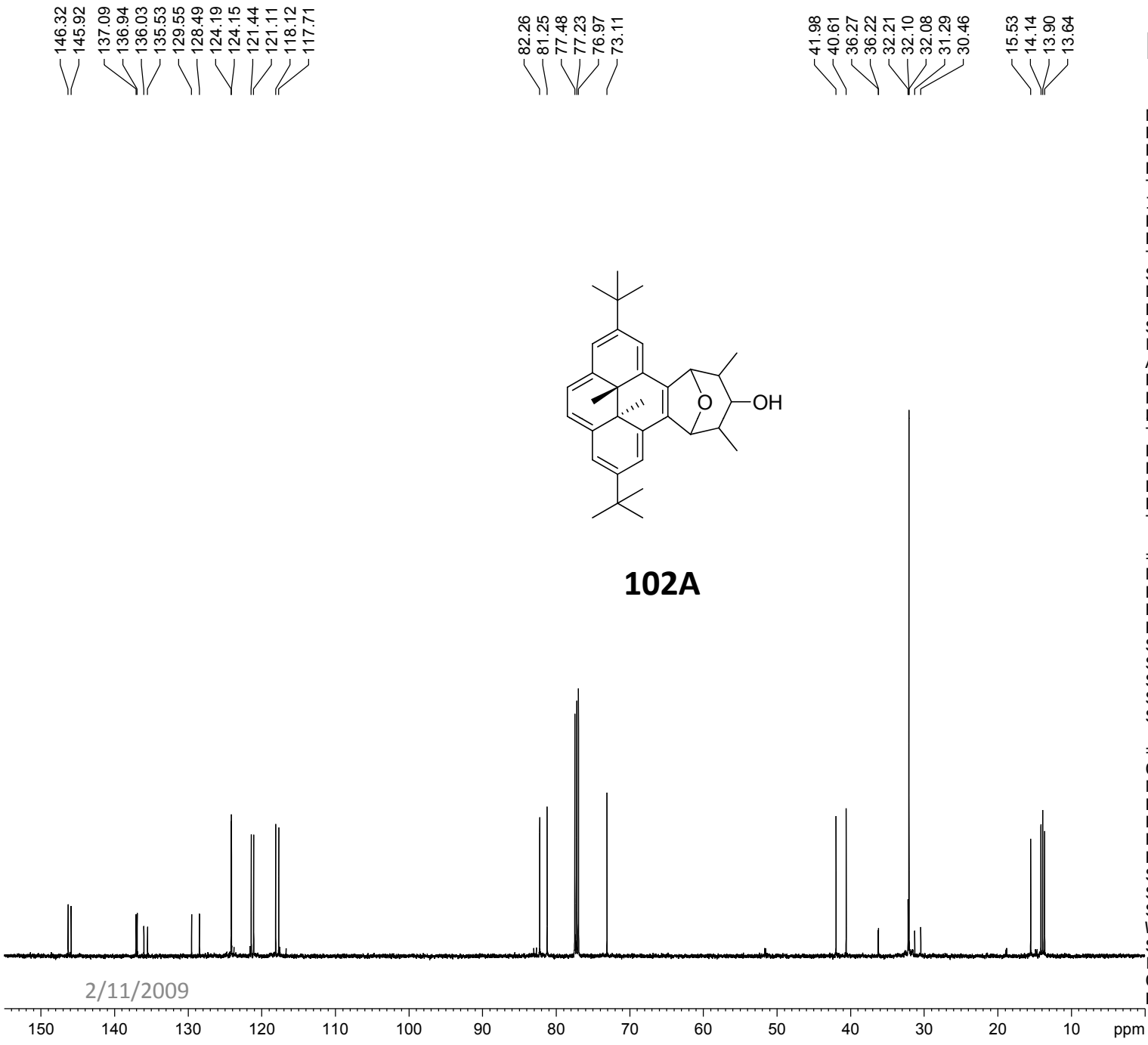
```
NAME                 PZ4_23a
EXPNO                      1
PROCNO                     1
Date_               20090213
Time                   16.35
INSTRUM                spect
PROBHD    5 mm PABBI 1H/
PULPROG                 zg30
TD                     32768
SOLVENT                CDCl3
NS                        16
DS                         2
SWH                 8012.820 Hz
FIDRES              0.244532 Hz
AQ                2.0448356 sec
RG                       128
DW                    62.400 usec
DE                     6.50 usec
TE                    296.4 K
D1                1.00000000 sec
TD0                        1

======== CHANNEL f1 ========
NUC1                      1H
P1                    10.20 usec
PL1                    1.00 dB
SFO1           500.1315200 MHz
SI                     16384
SF             500.1300238 MHz
WDW                       GM
SSB                        0
LB                    -0.20 Hz
GB                       0.5
PC                      1.00
```

2/11/2009

Reduction of dimethyl-O-bridged cycloheptanone_13C/CDCl3

pz4-23a Reduction of dimethyl-O-bridged cycloheptanone_13C/CDCl3



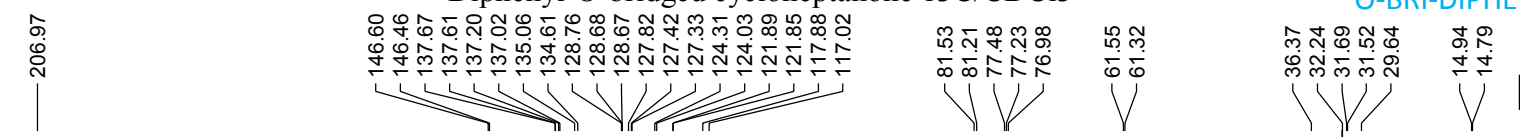

```
NAME                PZ4_23a
EXPNO                    10
PROCNO                    1
Date_              20090214
Time                  16.46
INSTRUM                spect
PROBHD    5 mm PABBI 1H/
PULPROG   zgpg_echo1.mmod
TD                    65536
SOLVENT                CDCl3
NS                    21928
DS                        4
SWH               19531.250 Hz
FIDRES             0.298023 Hz
AQ                 1.6777972 sec
RG                    16384
DW                   25.600 usec
DE                    6.50 usec
TE                   298.0 K
D1                1.00000000 sec
D11               0.03000000 sec
D20               0.00010000 sec
D21               0.00011460 sec
TD0                       1

======== CHANNEL f1 ========
NUC1                    13C
P1                    14.60 usec
P12                 2000.00 usec
PL1                   -1.00 dB
SFO1            125.7675082 MHz
SP2                   3.87 dB
SPNAM2          Crp60comp.4
SPOAL2                0.500
SPOFFS2               0.00 Hz

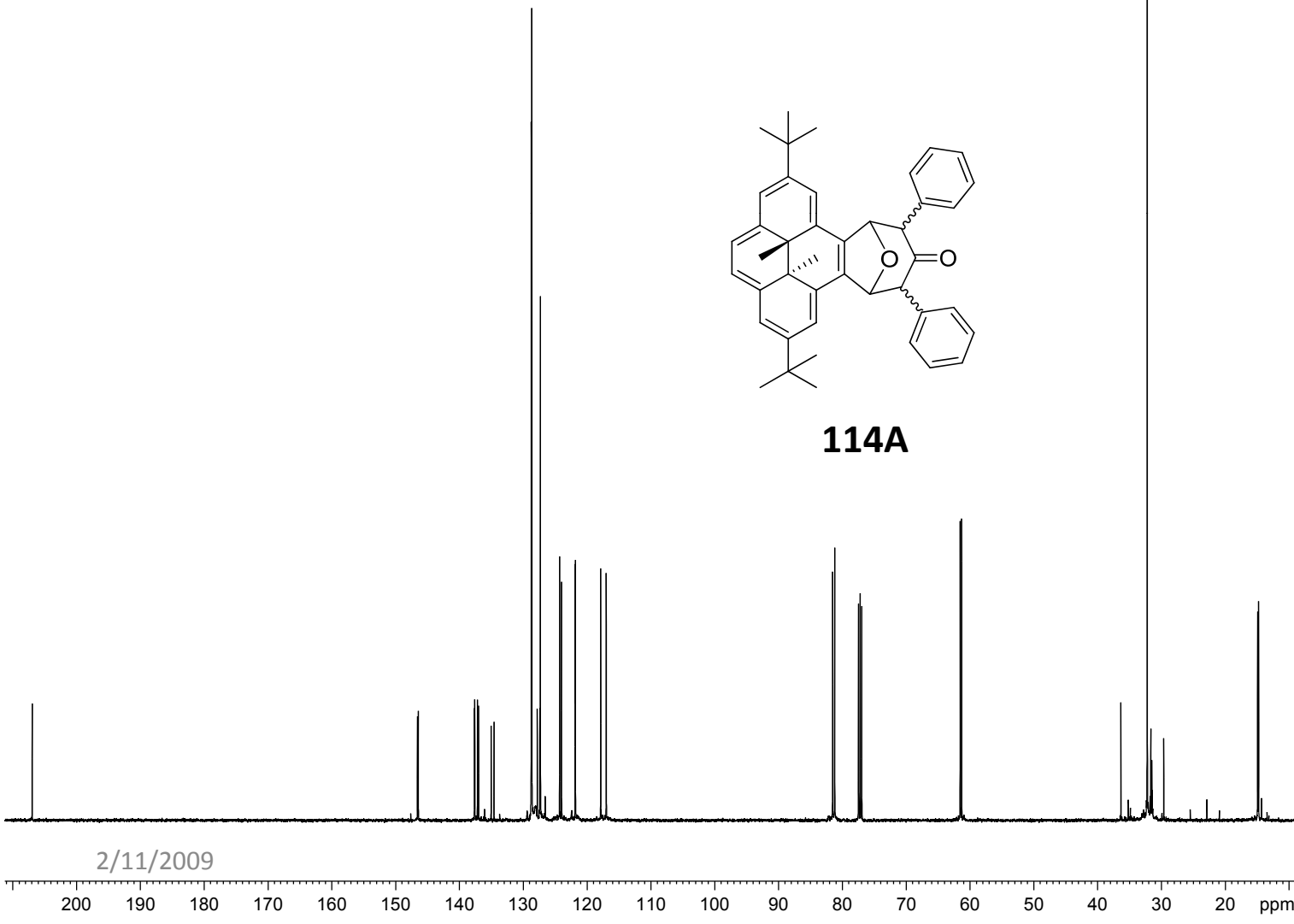
======== CHANNEL f2 ========
CPDPRG2             waltz16
NUC2                    1H
PCPD2                80.00 usec
PL2                   1.00 dB
PL12                 19.40 dB
PL13                 19.40 dB
SFO2            500.1311200 MHz
SI                    32768
SF              125.7577610 MHz
WDW                     EM
SSB                      0
LB                    0.90 Hz
GB                       0
PC                    1.40
```

Diphenyl-O-bridged cycloheptanone 13C/CDCl3

O-BRI-DIPHENYL ONE ISOMER 1 13C NMR



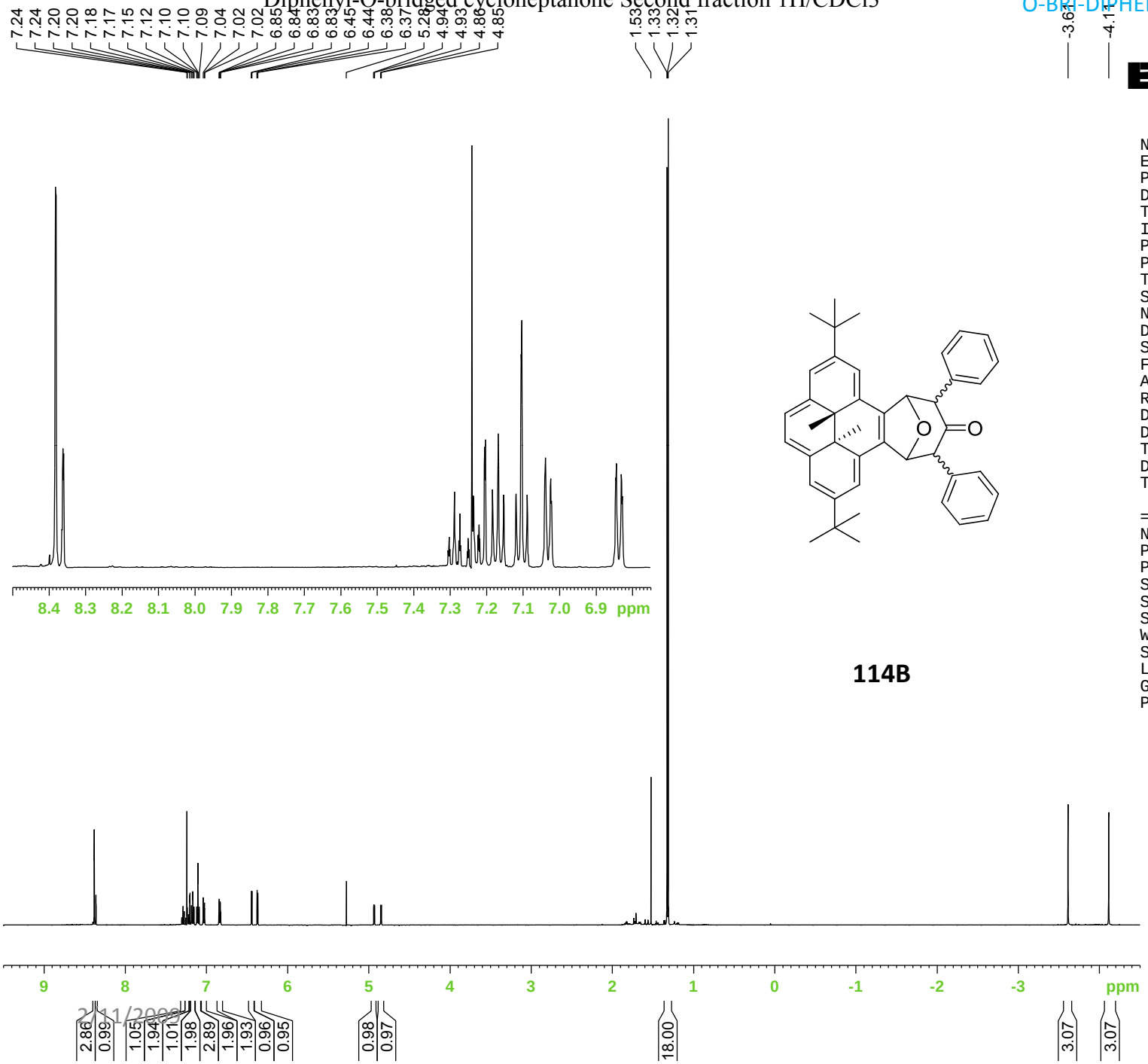
114A



NAME	PZ4_22
EXPNO	9
PROCNO	1
Date_	20090211
Time	11.08
INSTRUM	spect
PROBHD	5 mm PABBI 1H/
PULPROG	zgpg_echo1.mmod
TD	65536
SOLVENT	CDCl3
NS	17450
DS	4
SWH	27777.777 Hz
FIDRES	0.423855 Hz
AQ	1.1797160 sec
RG	16384
DW	18.000 usec
DE	6.50 usec
TE	298.2 K
D1	1.00000000 sec
D11	0.03000000 sec
D20	0.00010000 sec
D21	0.00011460 sec
TD0	1
======== CHANNEL f1 ========	
NUC1	13C
P1	14.60 usec
P12	2000.00 usec
PL1	-1.00 dB
SFO1	125.7716027 MHz
SP2	3.87 dB
SPNAM2	Crp60comp.4
SPOAL2	0.500
SPOFFS2	0.00 Hz
======== CHANNEL f2 ========	
CPDPRG2	waltz16
NUC2	1H
PCPD2	80.00 usec
PL2	1.00 dB
PL12	19.40 dB
PL13	19.40 dB
SFO2	500.1315200 MHz
SI	32768
SF	125.7577643 MHz
WDW	EM
SSB	0
LB	0.90 Hz
GB	0
PC	1.40

Diphenyl-O-bridged cycloheptanone Second fraction 1H/CDCl3

O-BRI-DIPHENYL ONE ISOMER 2 1H NMR



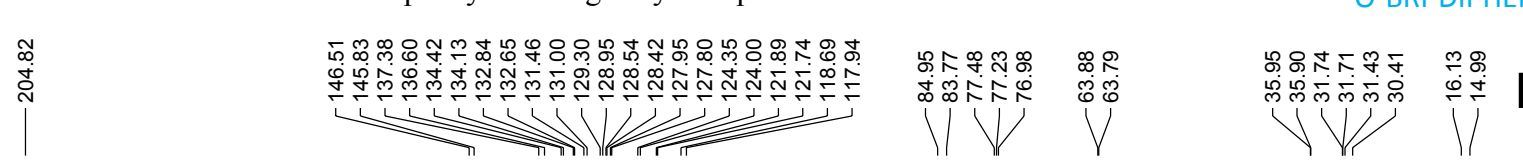
114B

NAME	PZ4_22B
EXPNO	1
PROCNO	1
Date_	20090211
Time	17.46
INSTRUM	spect
PROBHD	5 mm PABBI 1H/
PULPROG	zg30
TD	32768
SOLVENT	CDCl3
NS	16
DS	2
SWH	8012.820 Hz
FIDRES	0.244532 Hz
AQ	2.0448356 sec
RG	90.5
DW	62.400 usec
DE	6.50 usec
TE	297.2 K
D1	1.00000000 sec
TD0	1
======== CHANNEL f1 ========	
NUC1	1H
P1	9.60 usec
PL1	-4.00 dB
SFO1	500.1315200 MHz
SI	16384
SF	500.1300238 MHz
WDW	GM
SSB	0
LB	-0.20 Hz
GB	0.5
PC	1.00

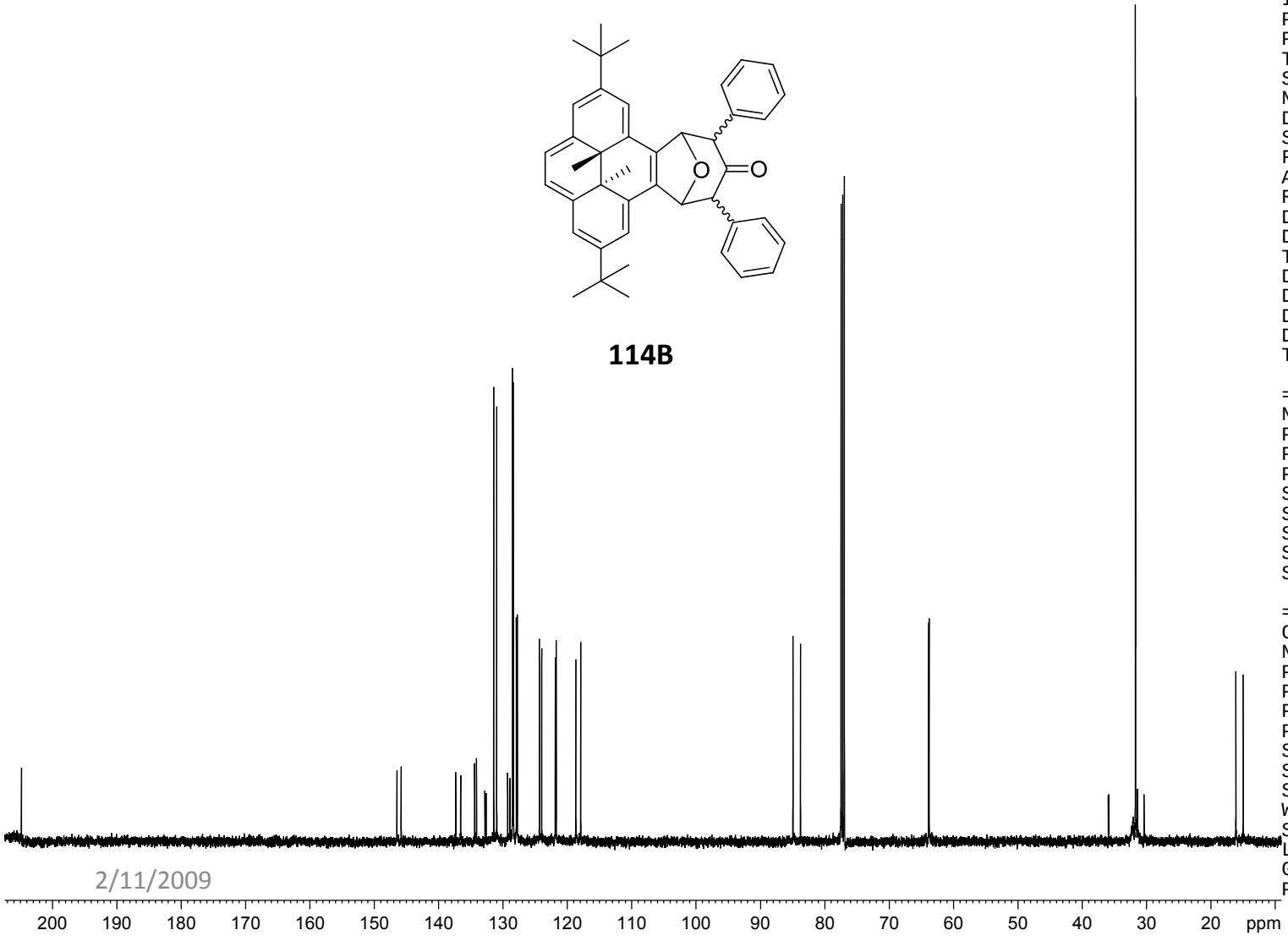
2/11/2009

Diphenyl-O-bridged cycloheptanone 2nd isomer 13C/CDCl3

O-BRI-DIPHENYL ONE ISOMER 2 13C NMR



114B



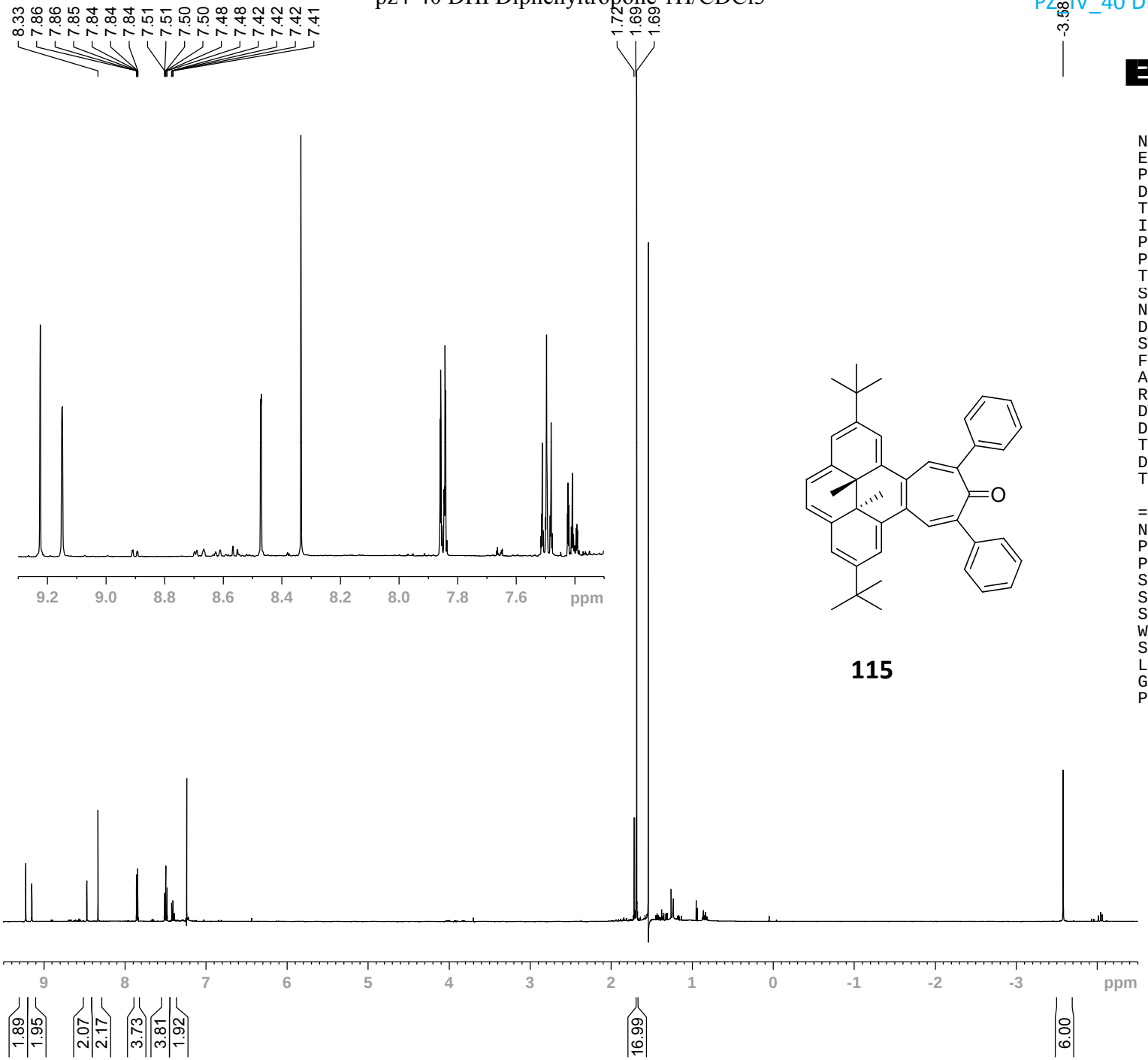

```
NAME                PZ4_22B
EXPNO                    10
PROCNO                    1
Date_              20090212
Time                   8.50
INSTRUM                spect
PROBHD    5 mm PABBI 1H/
PULPROG   zgpg_echo1.mmod
TD                    65536
SOLVENT               CDCl3
NS                    13454
DS                        4
SWH              26455.027 Hz
FIDRES           0.403672 Hz
AQ               1.2386993 sec
RG                    16384
DW                 18.900 usec
DE                  6.50 usec
TE                  297.4 K
D1             1.00000000 sec
D11            0.03000000 sec
D20            0.00010000 sec
D21            0.00011460 sec
TD0                       1

======== CHANNEL f1 ========
NUC1                    13C
P1                  14.60 usec
P12               2000.00 usec
PL1                 -1.00 dB
SFO1          125.7709469 MHz
SP2                  3.87 dB
SPNAM2       Crp60comp.4
SPOAL2             0.500
SPOFFS2             0.00 Hz

======== CHANNEL f2 ========
CPDPRG2           waltz16
NUC2                    1H
PCPD2               80.00 usec
PL2                  1.00 dB
PL12                19.40 dB
PL13                19.40 dB
SFO2          500.1315200 MHz
SI                    32768
SF            125.7577620 MHz
WDW                     EM
SSB                      0
LB                    0.90 Hz
GB                       0
PC                    1.40
```

pz4-40 DHPDiphenyltropone 1H/CDCl3

PZ_IV_40 DIPHENYL TROPONE 1H NMR

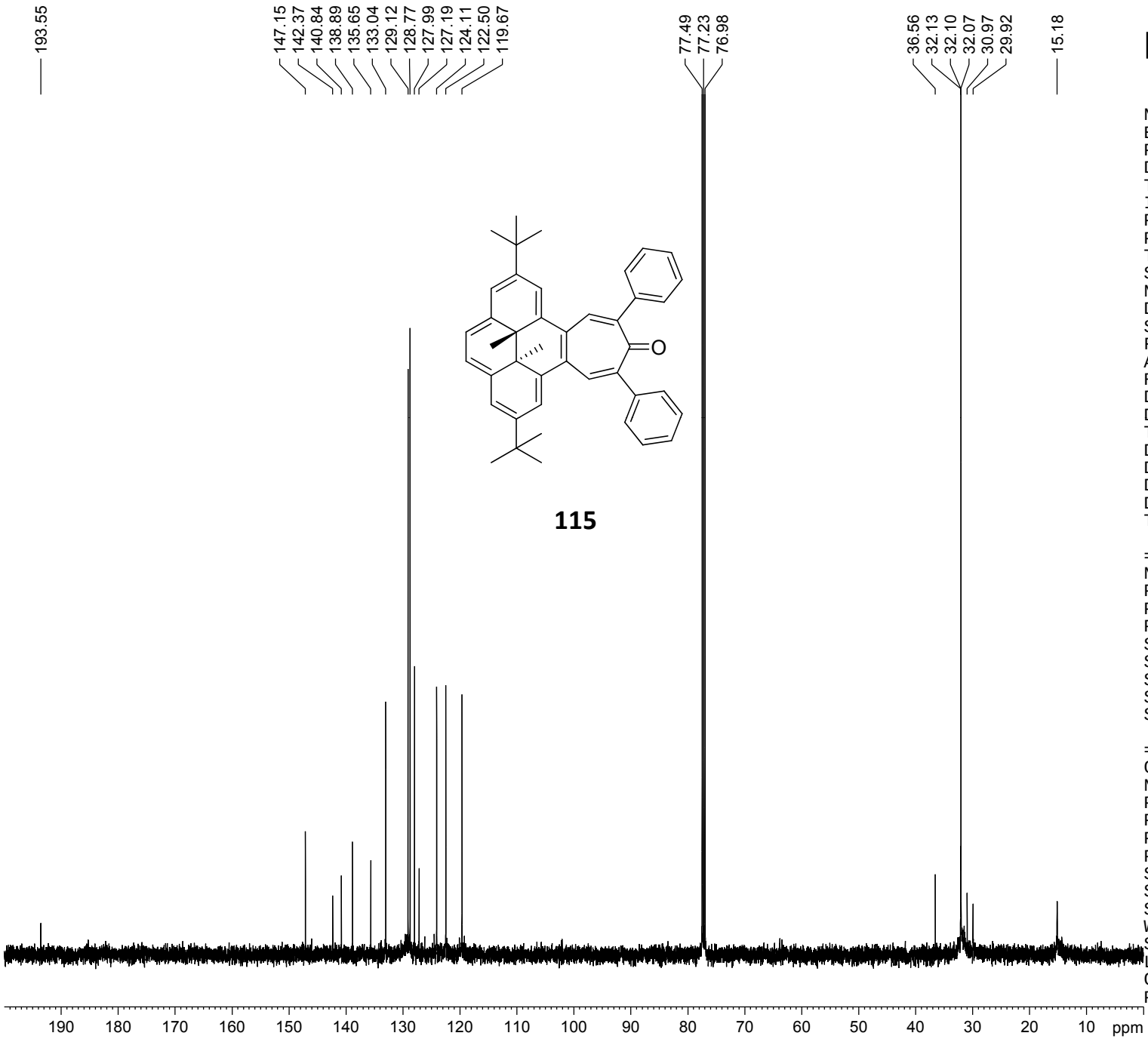


115

NAME	pz4_40
EXPNO	1
PROCNO	1
Date_	20090311
Time	19.20
INSTRUM	spect
PROBHD	5 mm PABBI 1H/
PULPROG	zg30
TD	32768
SOLVENT	CDCl3
NS	16
DS	2
SWH	8012.820 Hz
FIDRES	0.244532 Hz
AQ	2.0448356 sec
RG	128
DW	62.400 usec
DE	6.50 usec
TE	297.1 K
D1	1.00000000 sec
TD0	1
======== CHANNEL f1 ========	
NUC1	1H
P1	9.60 usec
PL1	-4.00 dB
SFO1	500.1315200 MHz
SI	16384
SF	500.1300234 MHz
WDW	GM
SSB	0
LB	-0.20 Hz
GB	0.5
PC	1.00

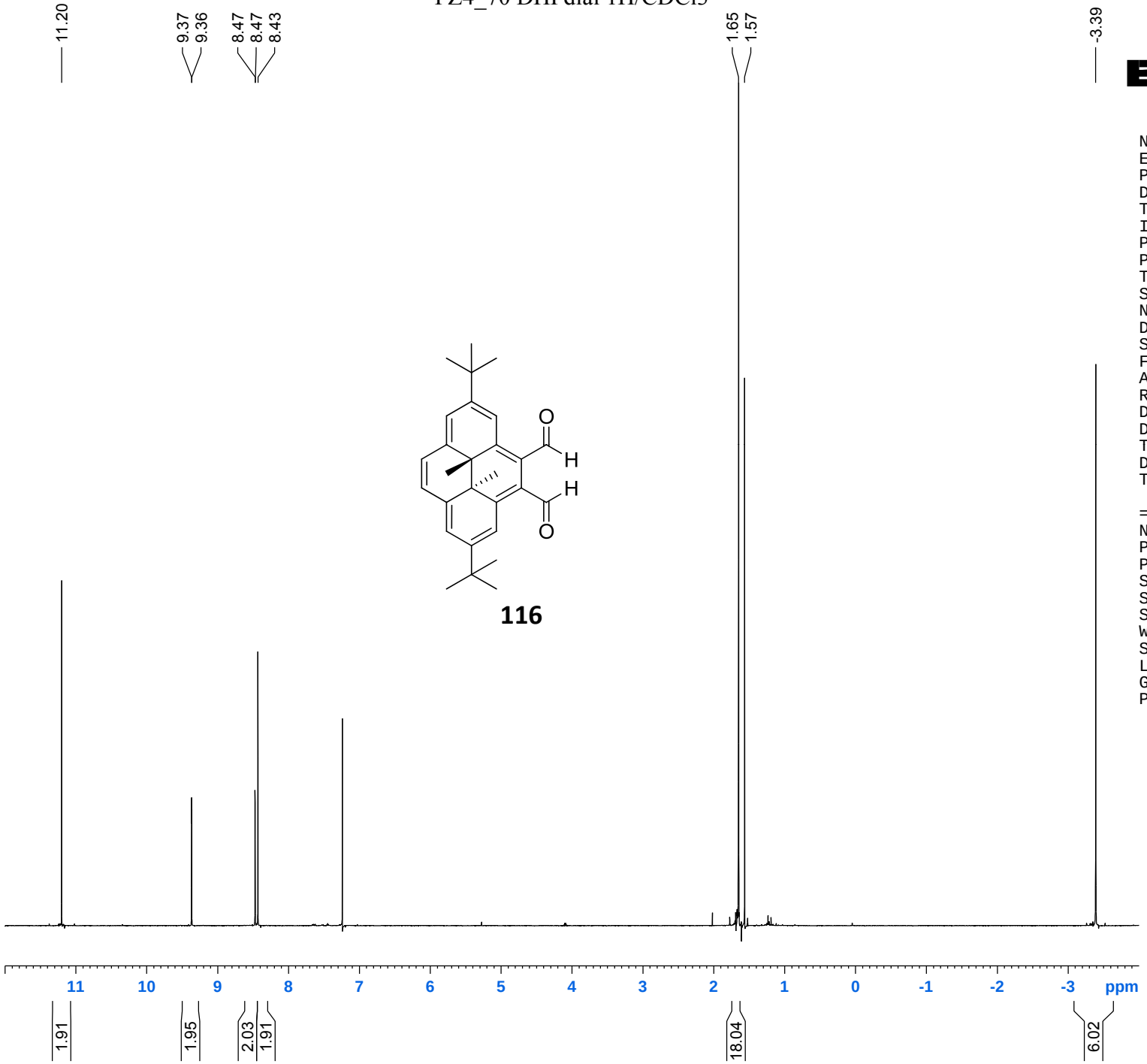
PZ4-40 DHPDiphenyltropone 13C/CDCl3

PZ_IV_40 DIPHENYL TROPONE 13C NMR



NAME	pz4_40
EXPNO	2
PROCNO	1
Date_	20090312
Time	9.18
INSTRUM	spect
PROBHD	5 mm PABBI 1H/
PULPROG	zgpg_echo1.mmod
TD	65536
SOLVENT	CDCl3
NS	9961
DS	4
SWH	30864.197 Hz
FIDRES	0.470950 Hz
AQ	1.0617495 sec
RG	16384
DW	16.200 usec
DE	6.50 usec
TE	297.4 K
D1	1.00000000 sec
D11	0.03000000 sec
D20	0.00010000 sec
D21	0.00011460 sec
TD0	1
======== CHANNEL f1 ========	
NUC1	13C
P1	14.60 usec
P12	2000.00 usec
PL1	-1.00 dB
SFO1	125.7715390 MHz
SP2	3.87 dB
SPNAM2	Crp60comp.4
SPOAL2	0.500
SPOFFS2	0.00 Hz
======== CHANNEL f2 ========	
CPDPRG2	waltz16
NUC2	1H
PCPD2	80.00 usec
PL2	1.00 dB
PL12	19.40 dB
PL13	19.40 dB
SFO2	500.1325200 MHz
SI	32768
SF	125.7577619 MHz
WDW	EM
SSB	0
LB	0.90 Hz
GB	0
PC	1.40

PZ4_70 DHPdial 1H/CDCl3



PZ4_70 DHPdial 1H/CDCl3

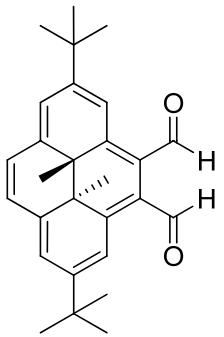
BRUKER

NAME	PZ4_70 dial
EXPNO	1
PROCNO	1
Date_	20090717
Time	17.32
INSTRUM	spect
PROBHD	5 mm PABBI 1H/
PULPROG	zg30
TD	32768
SOLVENT	CDCl3
NS	16
DS	2
SWH	8992.806 Hz
FIDRES	0.274439 Hz
AQ	1.8220063 sec
RG	181
DW	55.600 usec
DE	6.50 usec
TE	296.8 K
D1	1.00000000 sec
TD0	1
======== CHANNEL f1 ========	
NUC1	1H
P1	10.20 usec
PL1	1.00 dB
SFO1	500.1320000 MHz
SI	16384
SF	500.1300238 MHz
WDW	GM
SSB	0
LB	-0.20 Hz
GB	0.5
PC	1.00

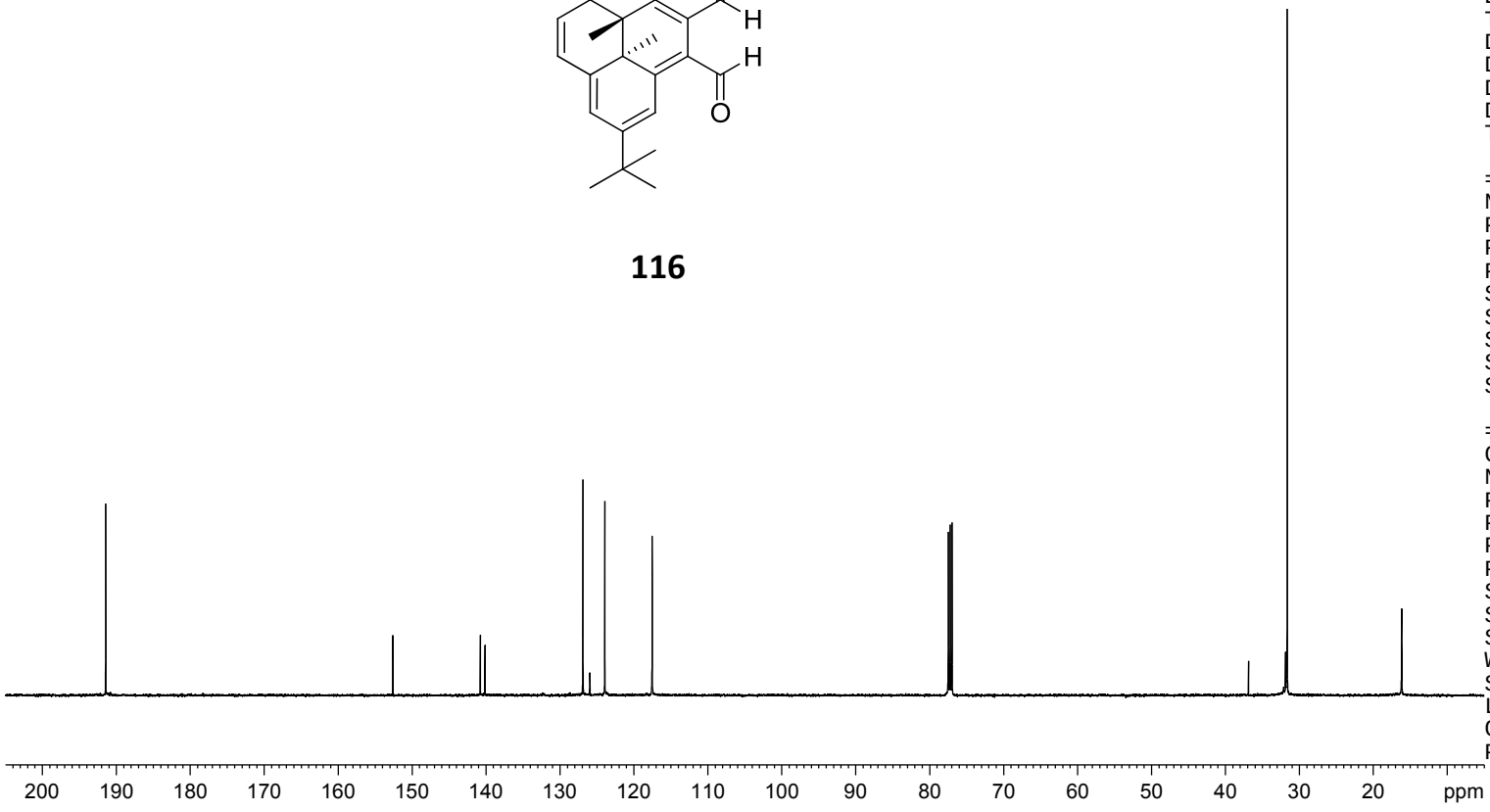
PZ4_70 dial 13C/CDCl3

PZ4_70 DHPdial 13C/CDCl3





116



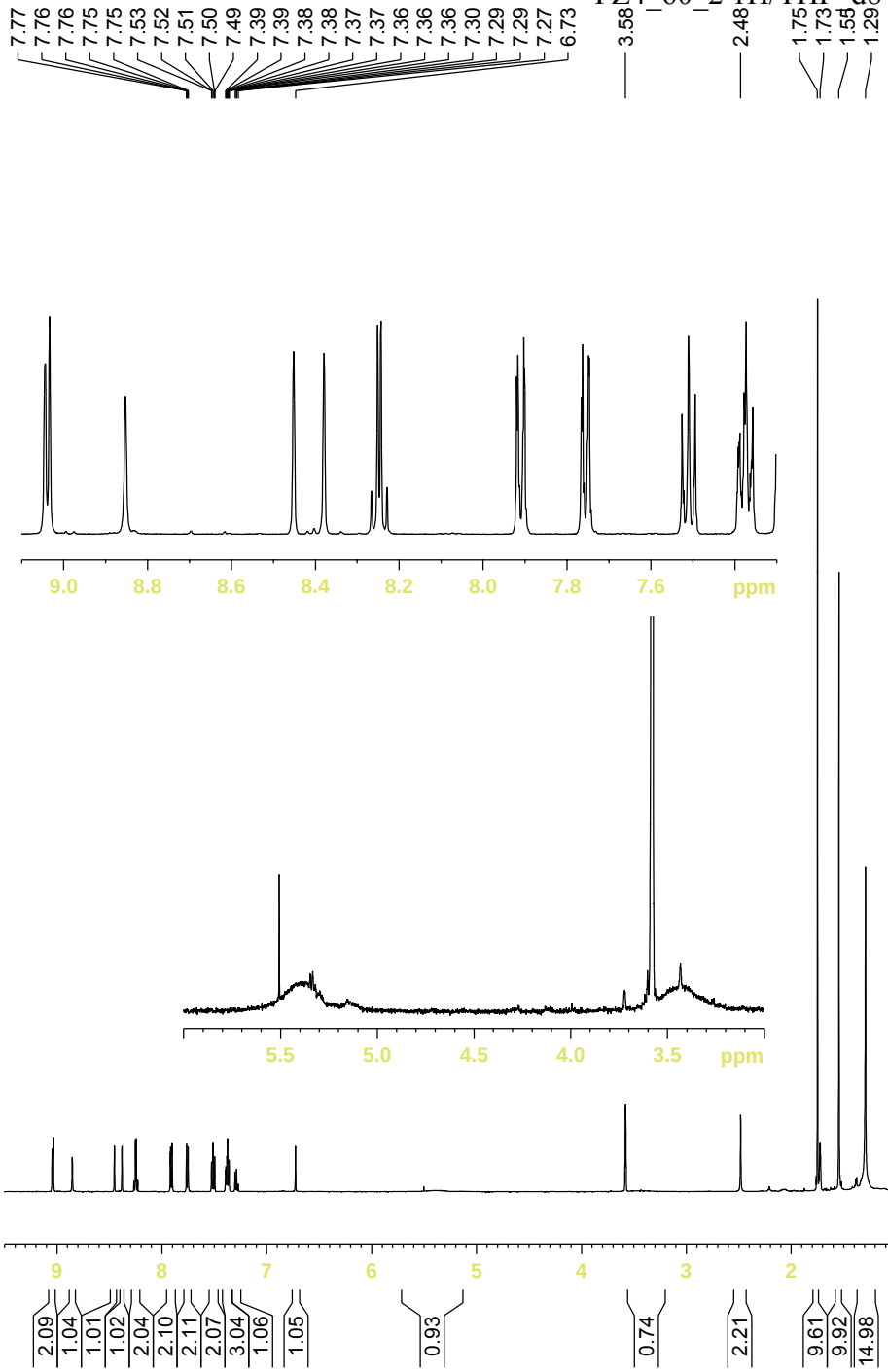

```
NAME          PZ4_70 dial
EXPNO                   2
PROCNO                  1
Date_            20090801
Time                11.23
INSTRUM             spect
PROBHD    5 mm PABBI 1H/
PULPROG   zgpg_echo1.mmod
TD                  65536
SOLVENT             CDCl3
NS                  29241
DS                      4
SWH            30864.197 Hz
FIDRES          0.470950 Hz
AQ              1.0617495 sec
RG                  16384
DW                 16.200 usec
DE                  6.50 usec
TE                 297.8 K
D1              1.00000000 sec
D11             0.03000000 sec
D20             0.00010000 sec
D21             0.00011460 sec
TD0                     1

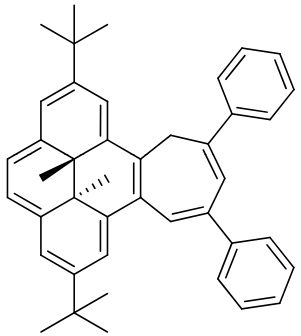
======== CHANNEL f1 ========
NUC1                  13C
P1                 14.60 usec
P12              2000.00 usec
PL1                -1.00 dB
SFO1         125.7715390 MHz
SP2                 3.87 dB
SPNAM2       Crp60comp.4
SPOAL2            0.500
SPOFFS2            0.00 Hz

======== CHANNEL f2 ========
CPDPRG2           waltz16
NUC2                  1H
PCPD2              80.00 usec
PL2                 1.00 dB
PL12               19.40 dB
PL13               19.40 dB
SFO2         500.1325200 MHz
SI                  32768
SF           125.7577628 MHz
WDW                   EM
SSB                    0
LB                  0.90 Hz
GB                     0
PC                  1.40
```

PZ4_60_2 1H/THF_d8

PZ_IV_60_F2 DIPHENYL CHT 1H in THF





117

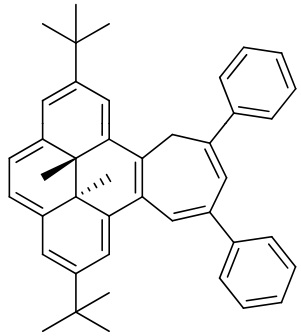
NAME	PZ4_60_2
EXPNO	1
PROCNO	1
Date_	20090618
Time	14.09
INSTRUM	spect
PROBHD	5 mm PABBO BB-
PULPROG	zg30
TD	32768
SOLVENT	THF
NS	16
DS	2
SWH	8012.820 Hz
FIDRES	0.244532 Hz
AQ	2.0448356 sec
RG	114
DW	62.400 usec
DE	6.50 usec
TE	297.9 K
D1	1.00000000 sec
TD0	1
======== CHANNEL f1 ========	
NUC1	1H
P1	9.60 usec
PL1	-4.00 dB
SFO1	500.1315200 MHz
SI	16384
SF	500.1300203 MHz
WDW	GM
SSB	0
LB	-0.20 Hz
GB	0.5
PC	1.00

PZ4_60_2 13C/THF_d8

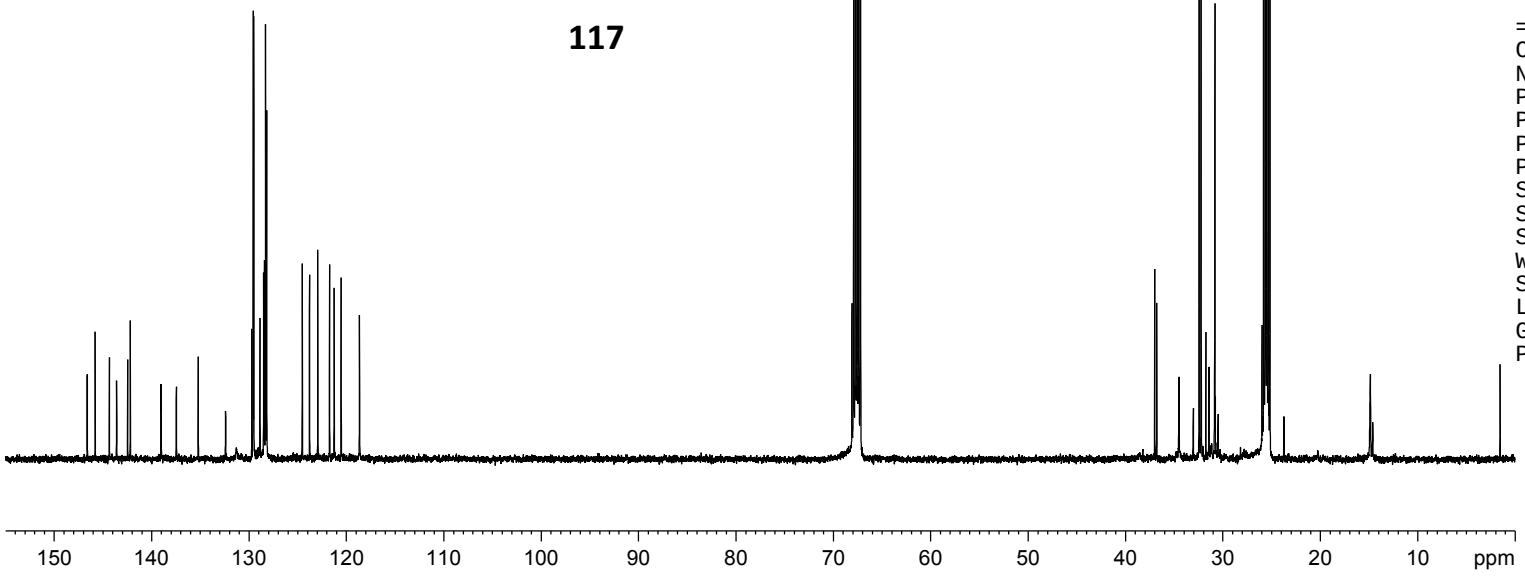
PZ_IV_60_F2 DIPHENYL CHT 13C in THF

142.18 139.05 137.47 135.23 132.42 131.33 129.74 129.59 129.53 128.89 128.52 128.44 128.32 128.21 124.55 123.81 122.97 121.74 121.27 120.55 118.67

37.01 36.81 32.45 32.25 30.82 25.82 25.66 25.50 25.34 25.18 14.85



117



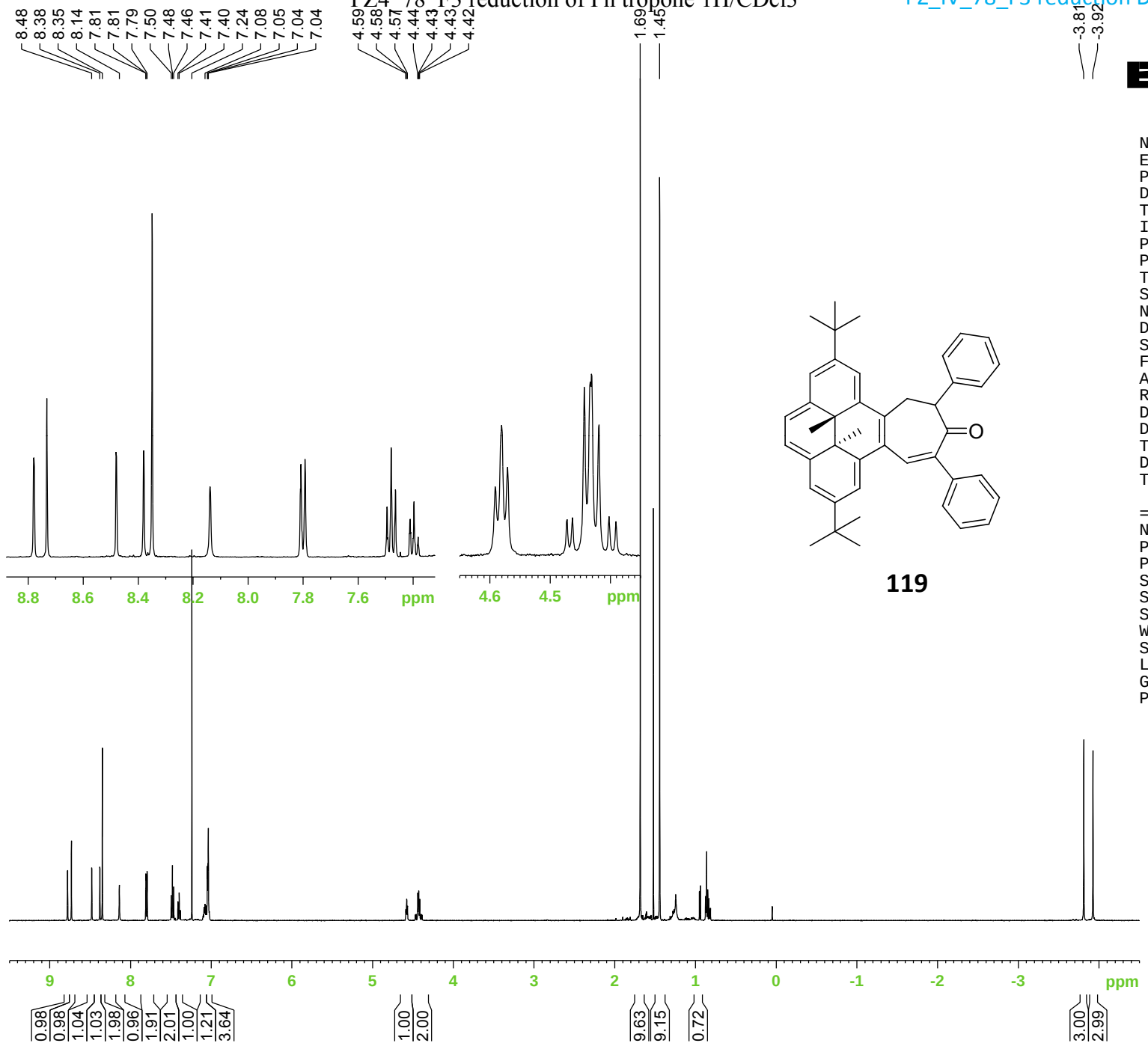

```
NAME              PZ4_60_2
EXPNO                    3
PROCNO                   1
Date_             20090618
Time                 14.25
INSTRUM              spect
PROBHD   5 mm PABBO BB-
PULPROG              zgpg30
TD                    65536
SOLVENT                 THF
NS                     8154
DS                        4
SWH              30864.197 Hz
FIDRES            0.470950 Hz
AQ                1.0617495 sec
RG                  11585.2
DW                  16.200 usec
DE                   6.50 usec
TE                  299.3 K
D1              1.00000000 sec
D11             0.03000000 sec
TD0                       1

======== CHANNEL f1 ========
NUC1                    13C
P1                   10.00 usec
PL1                   3.00 dB
SFO1          125.7715390 MHz

======== CHANNEL f2 ========
CPDPRG2           waltz16
NUC2                    1H
PCPD2                80.00 usec
PL2                  -4.00 dB
PL12                 14.42 dB
PL13                 14.24 dB
SFO2          500.1325200 MHz
SI                   32768
SF            125.7576430 MHz
WDW                     EM
SSB                      0
LB                    0.90 Hz
GB                       0
PC                    1.40
```

PZ4_78_F3 reduction of Ph tropone 1H/CDcl3

PZ_IV_78_F3 reduction DIPHENYL CHD ONE 1H NMR



119

NAME	PZ4_78_F3
EXPNO	1
PROCNO	1
Date_	20090729
Time	20.29
INSTRUM	spect
PROBHD	5 mm PABBI 1H/
PULPROG	zg30
TD	32768
SOLVENT	CDCl3
NS	16
DS	2
SWH	8012.820 Hz
FIDRES	0.244532 Hz
AQ	2.0448356 sec
RG	256
DW	62.400 usec
DE	6.50 usec
TE	297.7 K
D1	1.00000000 sec
TD0	1
======== CHANNEL f1 ========	
NUC1	1H
P1	10.20 usec
PL1	1.00 dB
SFO1	500.1315200 MHz
SI	16384
SF	500.1300238 MHz
WDW	GM
SSB	0
LB	-0.20 Hz
GB	0.5
PC	1.00

PZ4_78_F3 13C/CDcl3

PZ_IV_78_F3 reduction DIPHENYL CHD ONE 13CH NMR

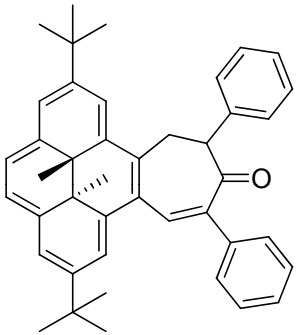
206.91

147.21 145.94 141.66 139.89 138.89 138.86 137.33 136.16 132.87 132.74 129.50 128.89 128.51 128.09 127.71 127.25 127.04 124.37 123.43 122.13 121.49 119.29 116.80

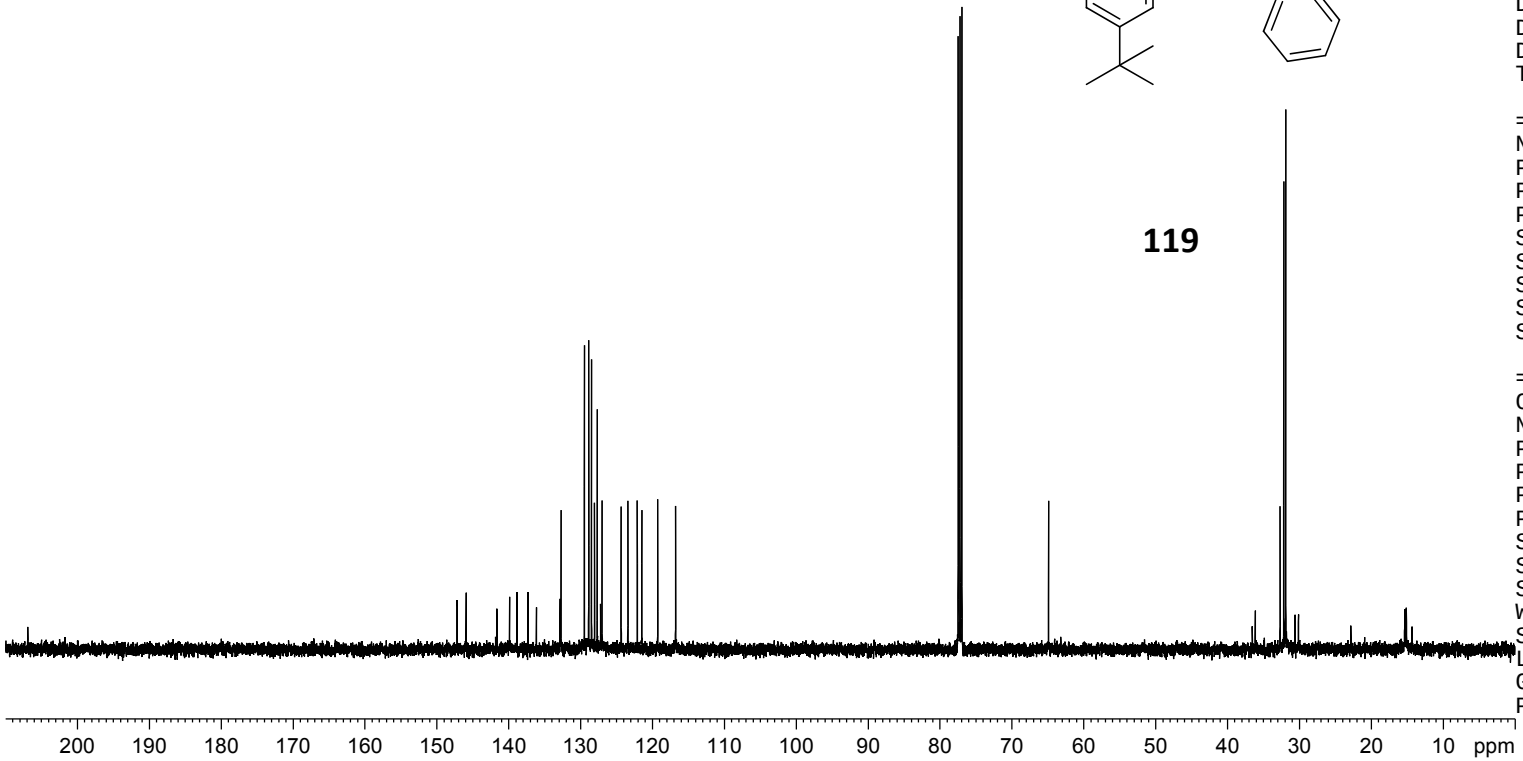
77.49 77.23 76.98

64.92

36.56 36.15 32.70 32.19 31.91 30.62 30.15 22.88 15.36 15.13 14.34



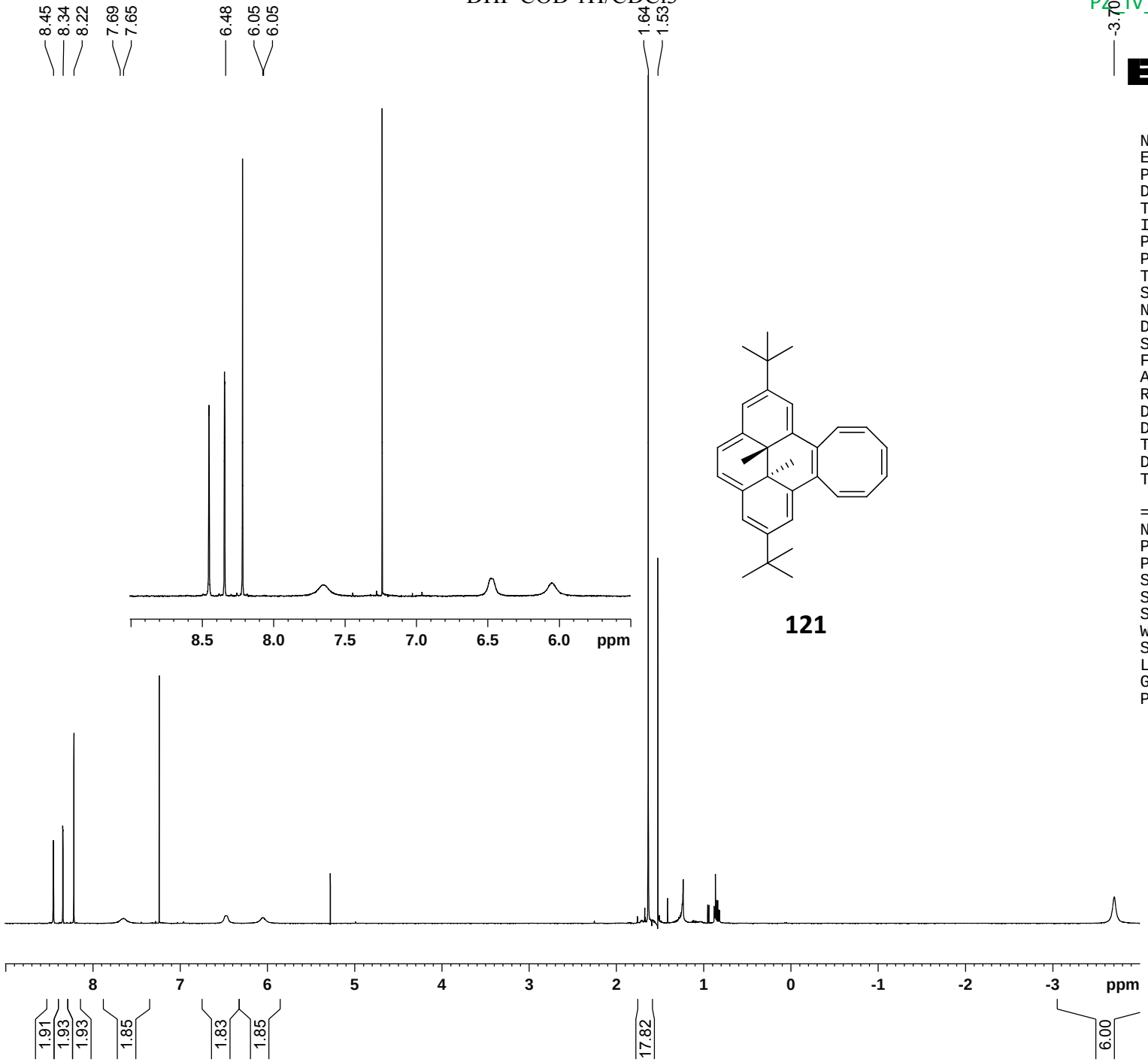
119



NAME	PZ4_78_F3	
EXPNO	3	
PROCNO	1	
Date_	20090730	
Time	5.46	
INSTRUM	spect	
PROBHD	5 mm PABBI 1H/	
PULPROG	zgpg_echo1.mmod	
TD	65536	
SOLVENT	CDCl3	
NS	14200	
DS	4	
SWH	30864.197	Hz
FIDRES	0.470950	Hz
AQ	1.0617495	sec
RG	16384	
DW	16.200	usec
DE	6.50	usec
TE	296.6	K
D1	1.00000000	sec
D11	0.03000000	sec
D20	0.00010000	sec
D21	0.00011460	sec
TD0	1	
======== CHANNEL f1 ========		
NUC1	13C	
P1	14.60	usec
P12	2000.00	usec
PL1	-1.00	dB
SFO1	125.7715390	MHz
SP2	3.87	dB
SPNAM2	Crp60comp.4	
SPOAL2	0.500	
SPOFFS2	0.00	Hz
======== CHANNEL f2 ========		
CPDPRG2	waltz16	
NUC2	1H	
PCPD2	80.00	usec
PL2	1.00	dB
PL12	19.40	dB
PL13	19.40	dB
SFO2	500.1325200	MHz
SI	32768	
SF	125.7577612	MHz
WDW	EM	
SSB	0	
LB	0.90	Hz
GB	0	
PC	1.40	

DHP COD 1H/CDCl3

PZ_IV_12-_F1 DHP COD 1H/CDCl3

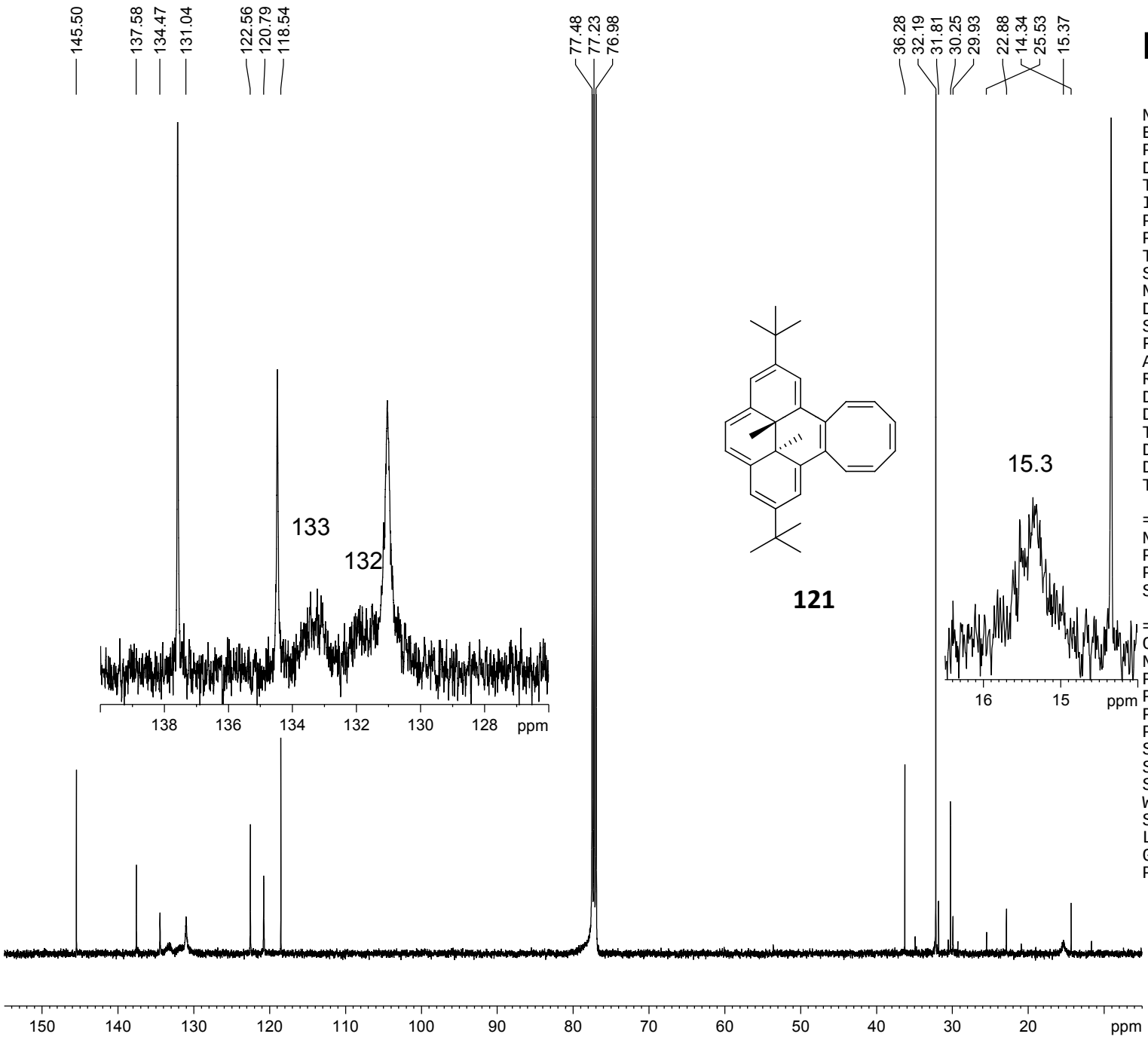


121

NAME	PZ COT
EXPNO	1
PROCNO	1
Date_	20091009
Time	20.58
INSTRUM	spect
PROBHD	5 mm PABBO BB-
PULPROG	zg30
TD	32768
SOLVENT	CDCl3
NS	16
DS	2
SWH	8992.806 Hz
FIDRES	0.274439 Hz
AQ	1.8220063 sec
RG	512
DW	55.600 usec
DE	6.50 usec
TE	297.4 K
D1	1.00000000 sec
TD0	1
======== CHANNEL f1 ========	
NUC1	1H
P1	9.60 usec
PL1	-4.00 dB
SFO1	500.1315000 MHz
SI	16384
SF	500.1300233 MHz
WDW	GM
SSB	0
LB	-0.20 Hz
GB	0.5
PC	1.00

DHP COT 13C/CDCl3

PZ_IV_120_F1 DHP COD 13C/CDCl3

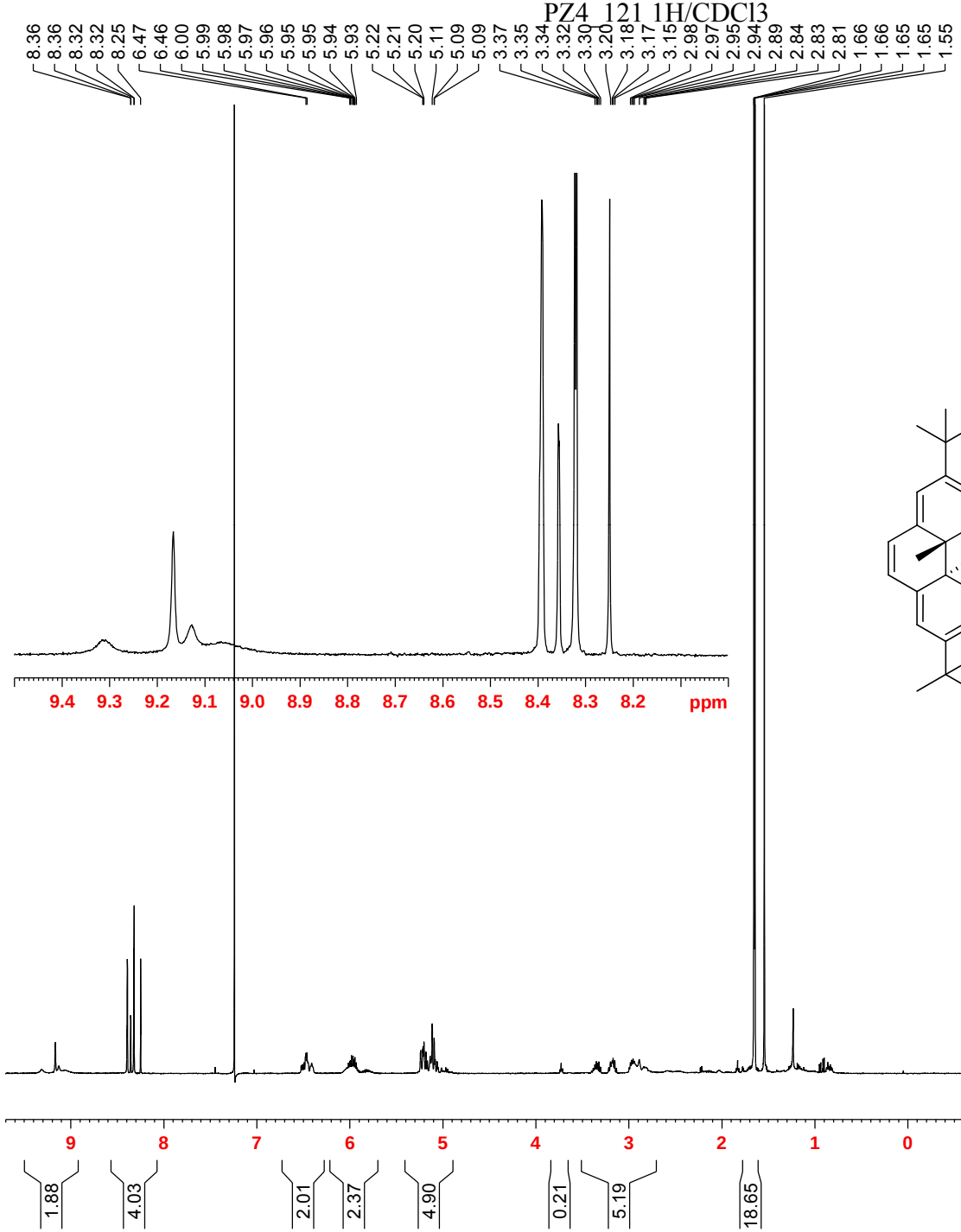


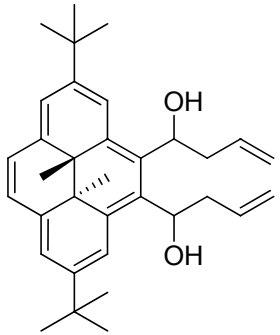
121

NAME	PZ COT
EXPNO	4
PROCNO	1
Date_	20091010
Time	15.05
INSTRUM	spect
PROBHD	5 mm PABBO BB-
PULPROG	zgpg30
TD	65536
SOLVENT	CDCl3
NS	21210
DS	4
SWH	30864.197 Hz
FIDRES	0.470950 Hz
AQ	1.0617495 sec
RG	20642.5
DW	16.200 usec
DE	6.50 usec
TE	298.2 K
D1	1.00000000 sec
D11	0.03000000 sec
TD0	1
======== CHANNEL f1 ========	
NUC1	13C
P1	10.00 usec
PL1	3.00 dB
SFO1	125.7715390 MHz
======== CHANNEL f2 ========	
CPDPRG2	waltz16
NUC2	1H
PCPD2	80.00 usec
PL2	-4.00 dB
PL12	14.42 dB
PL13	60.00 dB
SFO2	500.1315200 MHz
SI	32768
SF	125.7577620 MHz
WDW	EM
SSB	0
LB	0.90 Hz
GB	0
PC	1.40

PZ4_121 1H/CDCl3

PZ4_121 DHPdiol 1H/CDCl3





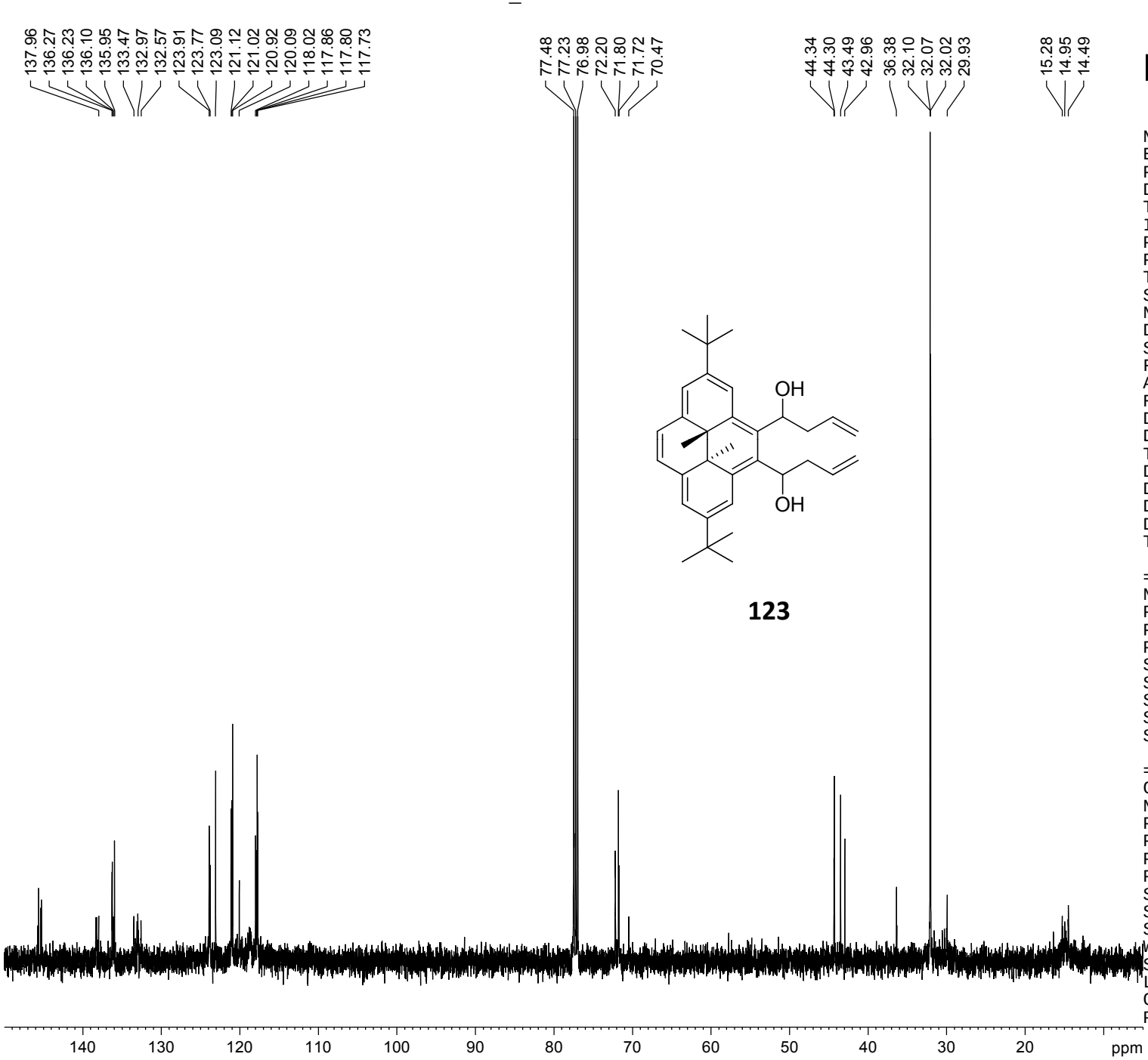
123

```
NAME                PZ4_121
EXPNO                     1
PROCNO                    1
Date_              20091022
Time                  21.33
INSTRUM                spect
PROBHD    5 mm PABBI 1H/
PULPROG                zg30
TD                    32768
SOLVENT               CDCl3
NS                       16
DS                        2
SWH               8012.820 Hz
FIDRES               0.244532 Hz
AQ                2.0448356 sec
RG                      228.1
DW                   62.400 usec
DE                    6.50 usec
TE                    298.1 K
D1              1.00000000 sec
TD0                       1

======== CHANNEL f1 ========
NUC1                     1H
P1                   10.20 usec
PL1                   1.00 dB
SFO1          500.1315200 MHz
SI                    16384
SF            500.1300233 MHz
WDW                     GM
SSB                      0
LB                   -0.20 Hz
GB                      0.5
PC                     1.00
```

PZ4_121 13C/CDCl3

PZ4_121 DHPdiol 13C/CDCl3



123

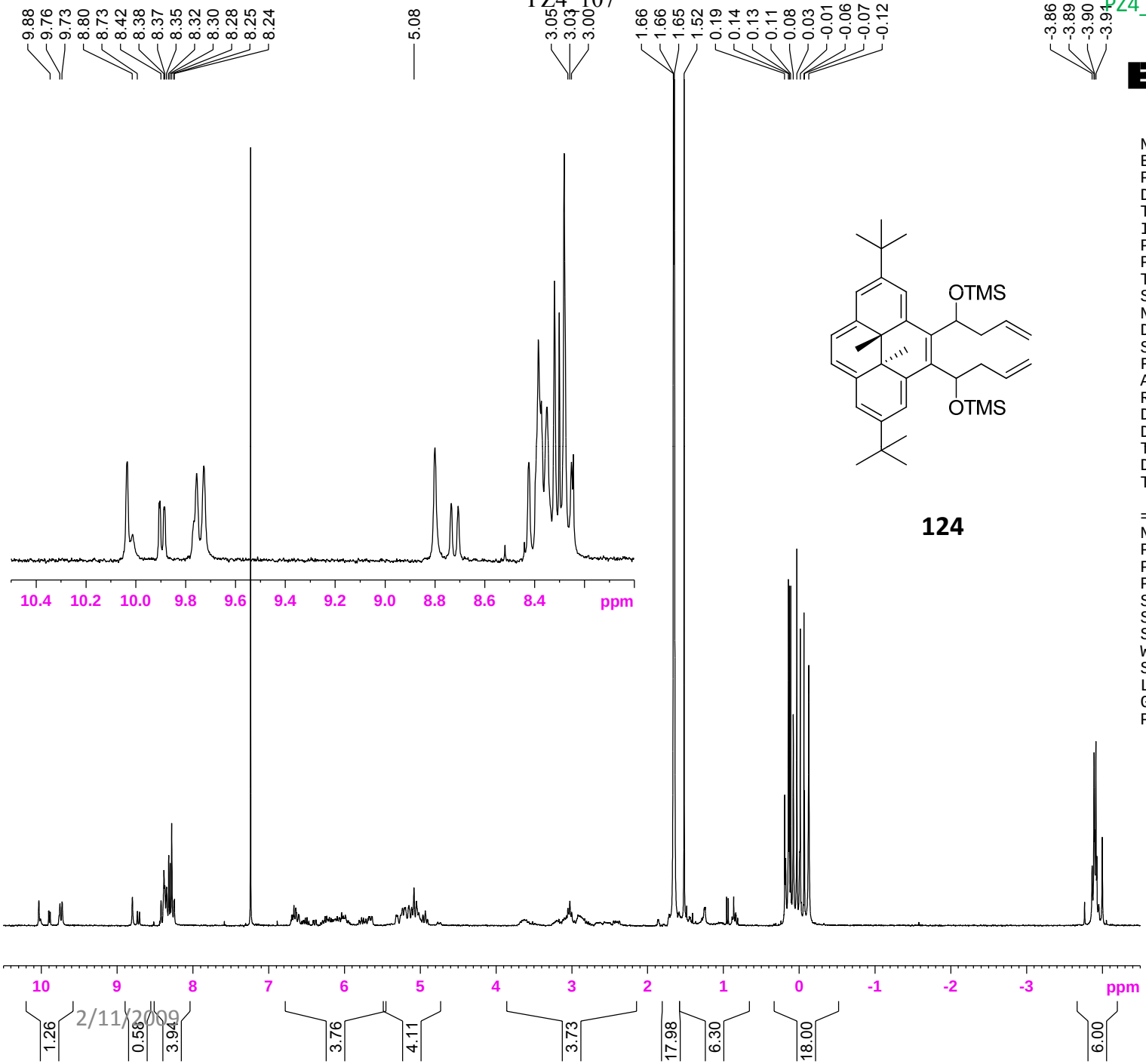
```
NAME                PZ4_121
EXPNO                     4
PROCNO                    1
Date_              20091023
Time                   7.38
INSTRUM                spect
PROBHD    5 mm PABBI 1H/
PULPROG   zgpg_echo1.mmod
TD                    65536
SOLVENT                CDCl3
NS                    15360
DS                        4
SWH               30864.197 Hz
FIDRES             0.470950 Hz
AQ                 1.0617495 sec
RG                    16384
DW                   16.200 usec
DE                    6.50 usec
TE                   298.8 K
D1                1.00000000 sec
D11               0.03000000 sec
D20               0.00010000 sec
D21               0.00011460 sec
TD0                       1

======== CHANNEL f1 ========
NUC1                    13C
P1                    14.60 usec
P12                 2000.00 usec
PL1                   -1.00 dB
SFO1            125.7715390 MHz
SP2                   3.87 dB
SPNAM2          Crp60comp.4
SPOAL2                0.500
SPOFFS2               0.00 Hz

======== CHANNEL f2 ========
CPDPRG2             waltz16
NUC2                    1H
PCPD2                80.00 usec
PL2                   1.00 dB
PL12                 19.40 dB
PL13                 19.40 dB
SFO2            500.1325200 MHz
SI                    32768
SF              125.7577604 MHz
WDW                     EM
SSB                      0
LB                    0.90 Hz
GB                       0
PC                    1.40
```

PZ4_107

PZ4_107 TMS DHPdiol 1H/CDCl3



124

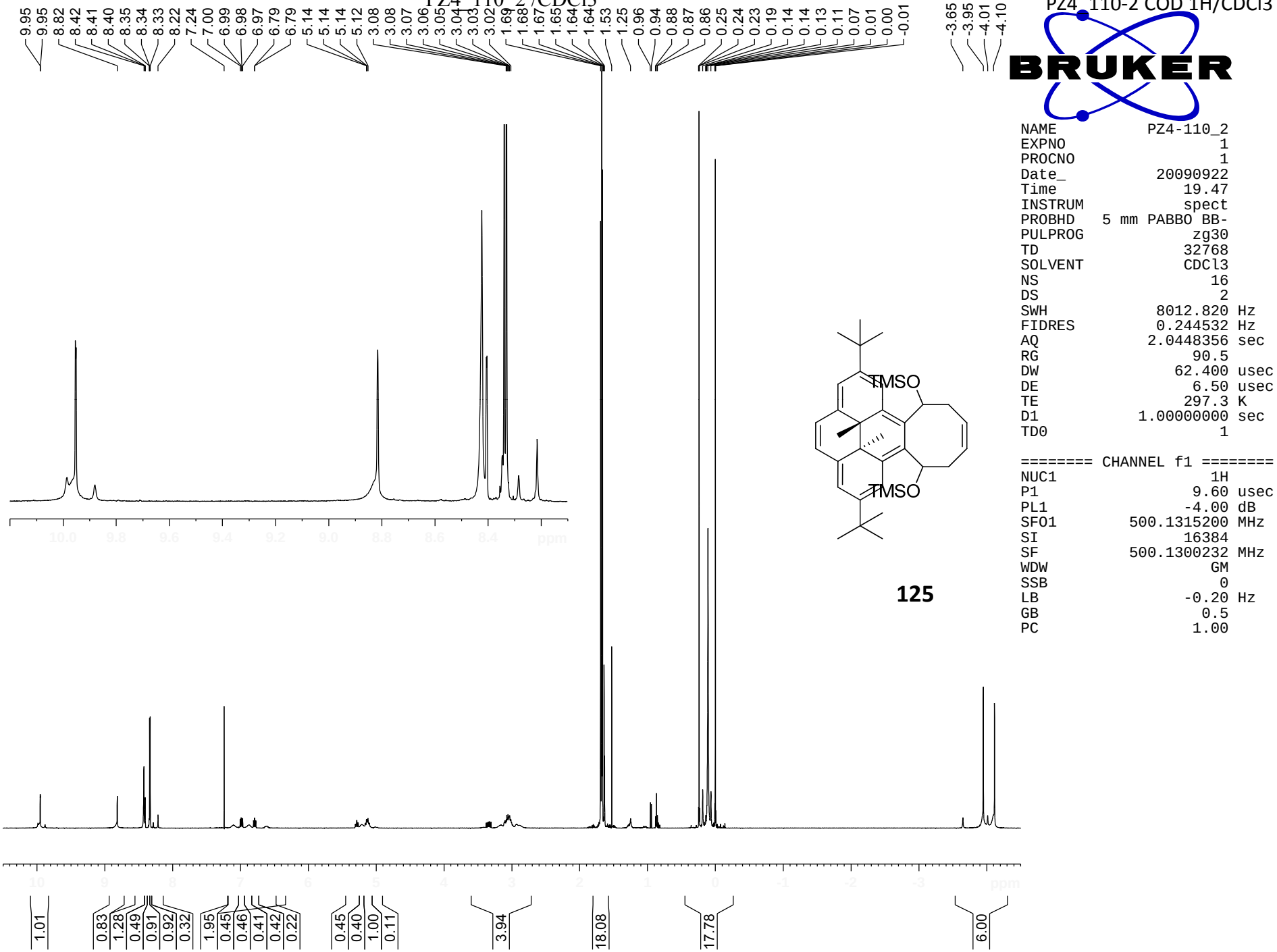
```
NAME                Sep17-2009
EXPNO                       27
PROCNO                       1
Date_                 20090917
Time                     20.52
INSTRUM                  spect
PROBHD    5 mm PABBO BB-
PULPROG                  zg30
TD                      32768
SOLVENT                 CDCl3
NS                         16
DS                          2
SWH                 6009.615 Hz
FIDRES               0.183399 Hz
AQ                   2.7263477 sec
RG                        203
DW                     83.200 usec
DE                      6.50 usec
TE                     300.0 K
D1                  1.00000000 sec
TD0                         1

======== CHANNEL f1 ========
NUC1                       1H
P1                      14.10 usec
PL1                      2.00 dB
PL1W                7.33805561 W
SFO1               300.1312000 MHz
SI                      16384
SF                 300.1300081 MHz
WDW                        EM
SSB                         0
LB                       0.35 Hz
GB                          0
PC                       1.00
```

2/11/2009

PZ4_110_2 /CDCl3

PZ4_110-2 COD 1H/CDCl3

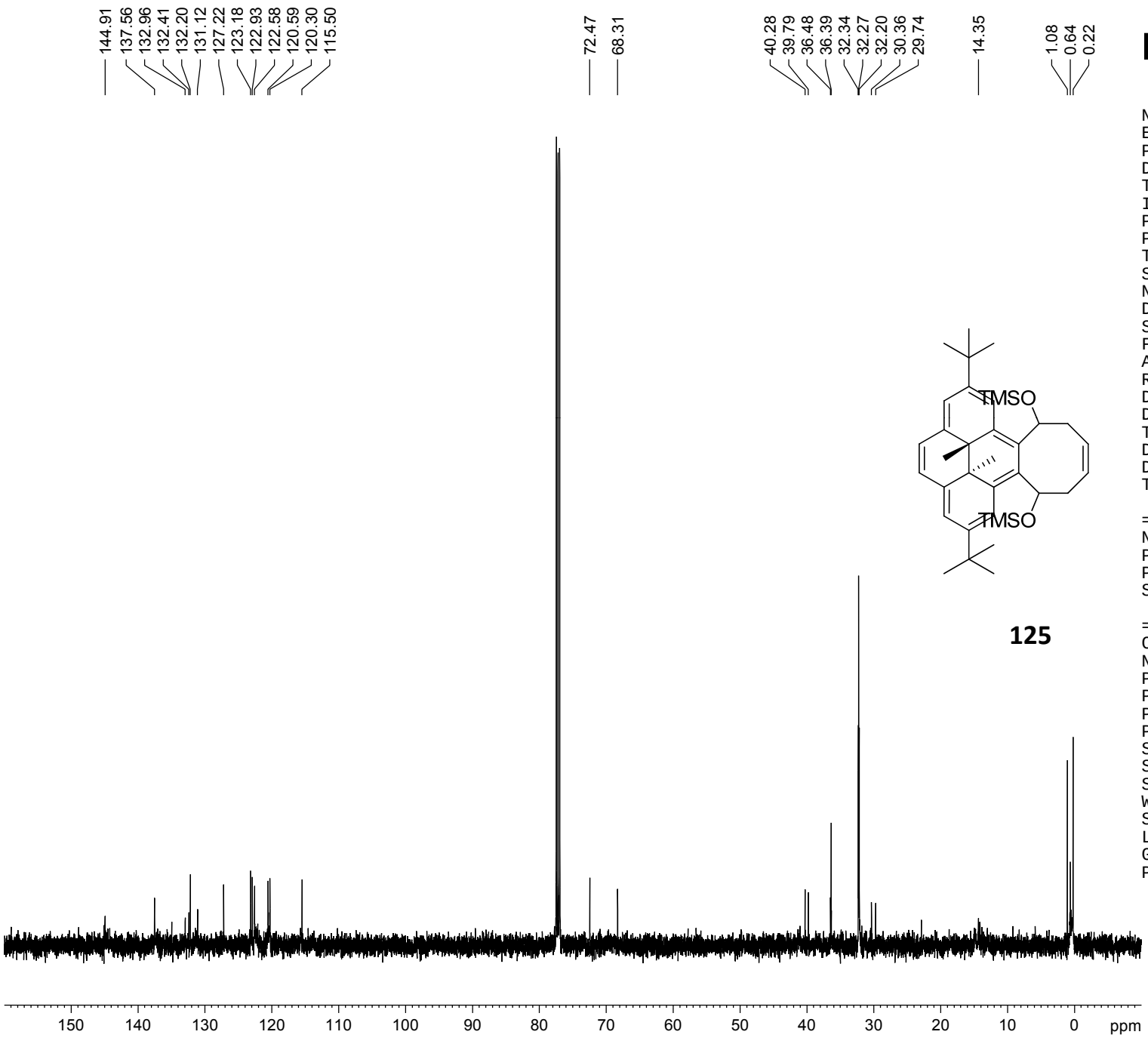


125

NAME	PZ4-110_2
EXPNO	1
PROCNO	1
Date_	20090922
Time	19.47
INSTRUM	spect
PROBHD	5 mm PABBO BB-
PULPROG	zg30
TD	32768
SOLVENT	CDCl3
NS	16
DS	2
SWH	8012.820 Hz
FIDRES	0.244532 Hz
AQ	2.0448356 sec
RG	90.5
DW	62.400 usec
DE	6.50 usec
TE	297.3 K
D1	1.00000000 sec
TD0	1
======== CHANNEL f1 ========	
NUC1	1H
P1	9.60 usec
PL1	-4.00 dB
SFO1	500.1315200 MHz
SI	16384
SF	500.1300232 MHz
WDW	GM
SSB	0
LB	-0.20 Hz
GB	0.5
PC	1.00

PZ4_110_2 13C/CDCl3

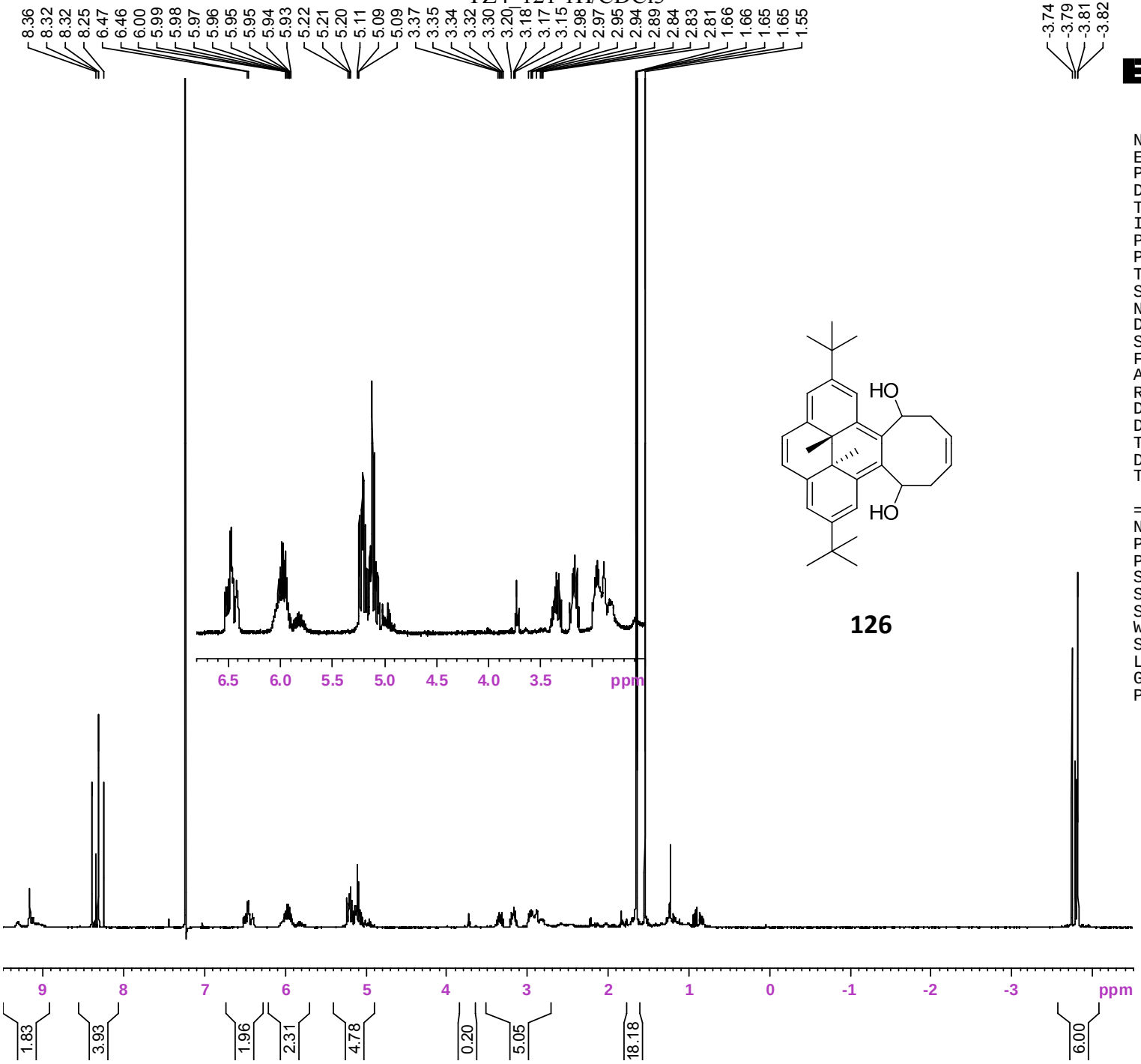
PZ4_110-2 COD 13C/CDCl3



125

NAME	PZ4-110_2
EXPNO	2
PROCNO	1
Date_	20090922
Time	19.54
INSTRUM	spect
PROBHD	5 mm PABBO BB-
PULPROG	zgpg30
TD	65536
SOLVENT	CDCl3
NS	20480
DS	4
SWH	30864.197 Hz
FIDRES	0.470950 Hz
AQ	1.0617495 sec
RG	14596.5
DW	16.200 usec
DE	6.50 usec
TE	298.3 K
D1	1.00000000 sec
D11	0.03000000 sec
TD0	1
======== CHANNEL f1 ========	
NUC1	13C
P1	10.00 usec
PL1	3.00 dB
SFO1	125.7715390 MHz
======== CHANNEL f2 ========	
CPDPRG2	waltz16
NUC2	1H
PCPD2	80.00 usec
PL2	-4.00 dB
PL12	14.42 dB
PL13	14.24 dB
SFO2	500.1325200 MHz
SI	32768
SF	125.7577620 MHz
WDW	EM
SSB	0
LB	0.90 Hz
GB	0
PC	1.40

PZ4_121 1H/CDCl3

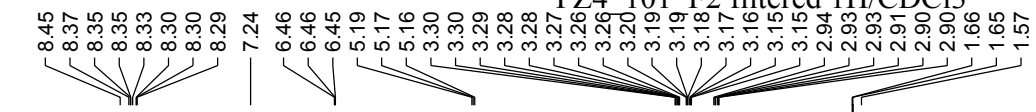


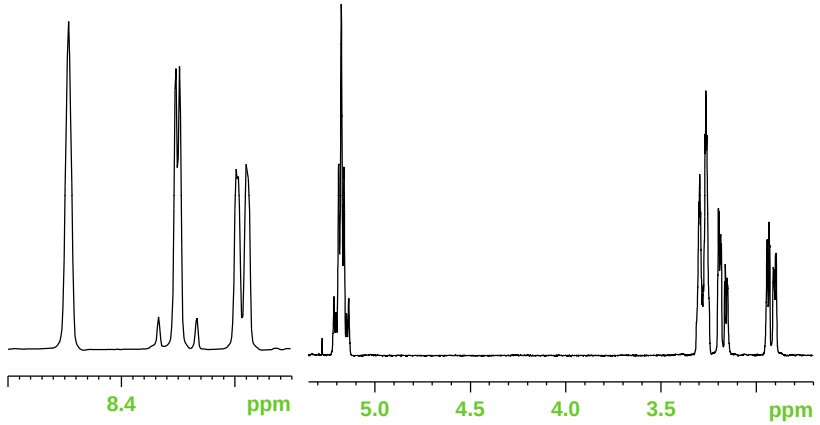
126

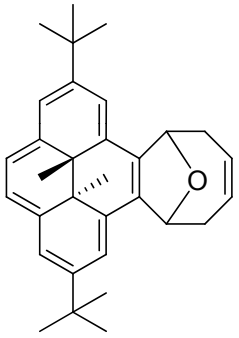
NAME	PZ4_121
EXPNO	1
PROCNO	1
Date_	20091022
Time	21.33
INSTRUM	spect
PROBHD	5 mm PABBI 1H/
PULPROG	zg30
TD	32768
SOLVENT	CDCl3
NS	16
DS	2
SWH	8012.820 Hz
FIDRES	0.244532 Hz
AQ	2.0448356 sec
RG	228.1
DW	62.400 usec
DE	6.50 usec
TE	298.1 K
D1	1.00000000 sec
TD0	1
======== CHANNEL f1 ========	
NUC1	1H
P1	10.20 usec
PL1	1.00 dB
SFO1	500.1315200 MHz
SI	16384
SF	500.1300233 MHz
WDW	GM
SSB	0
LB	-0.20 Hz
GB	0.5
PC	1.00

PZ4_101_F2 filtered 1H/CDCl3

PZ_IV_101_F2 1H/CDCl3

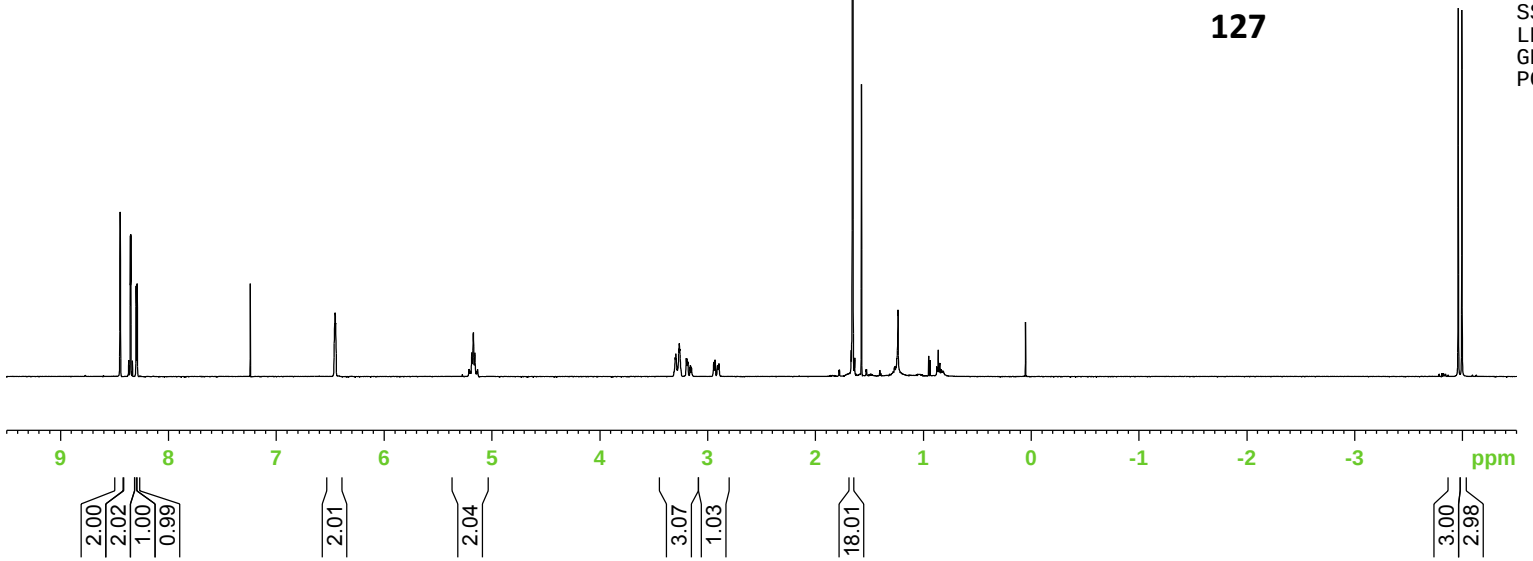






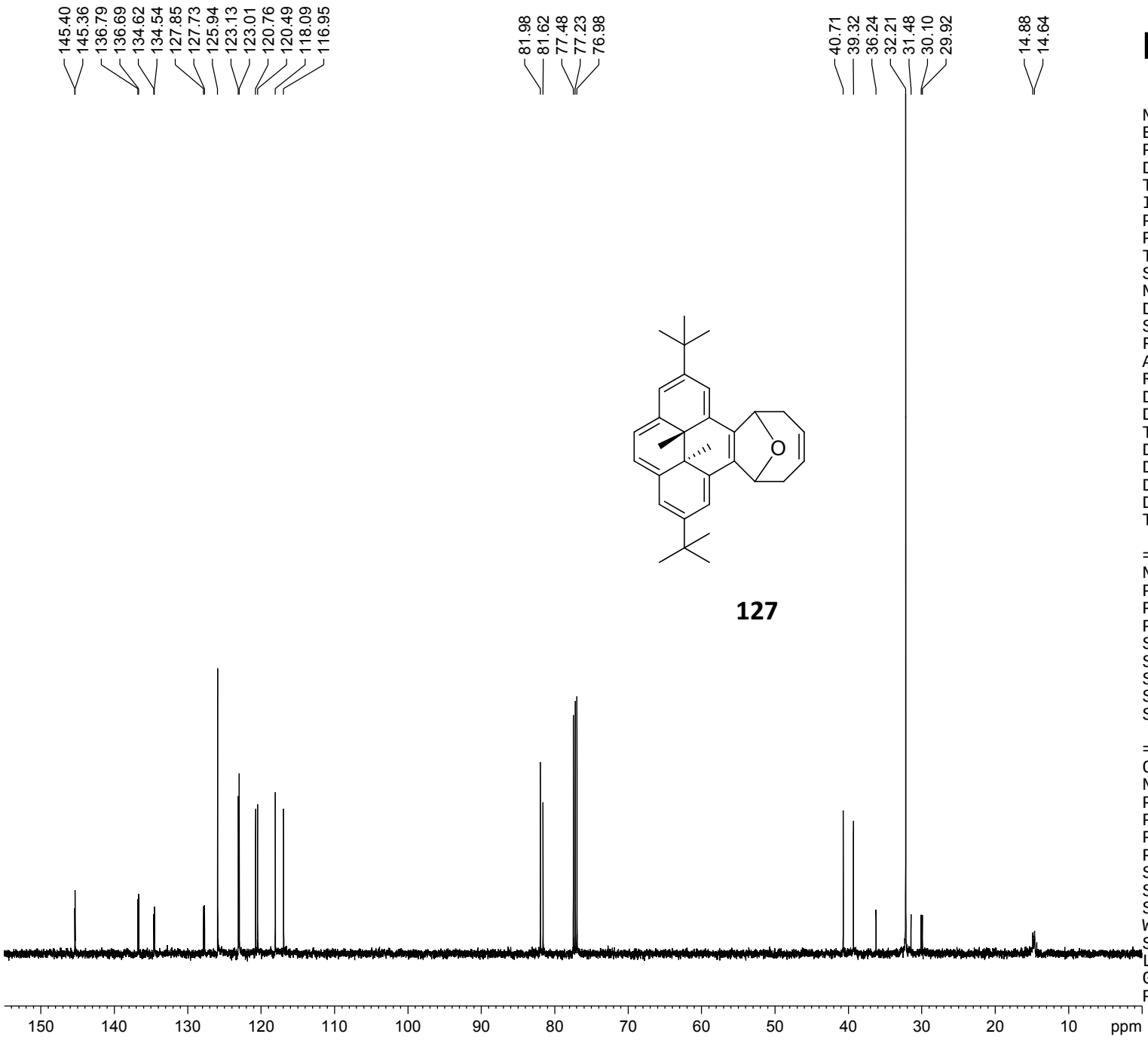
127

NAME	PZ4_101_F2
EXPNO	1
PROCNO	1
Date_	20100824
Time	10.10
INSTRUM	spect
PROBHD	5 mm PABBI 1H/
PULPROG	zg30
TD	32768
SOLVENT	CDCl3
NS	16
DS	2
SWH	8012.820 Hz
FIDRES	0.244532 Hz
AQ	2.0448356 sec
RG	71.8
DW	62.400 usec
DE	6.50 usec
TE	297.1 K
D1	1.00000000 sec
TD0	1
======== CHANNEL f1 ========	
NUC1	1H
P1	10.20 usec
PL1	1.00 dB
SFO1	500.1315200 MHz
SI	16384
SF	500.1300233 MHz
WDW	GM
SSB	0
LB	-0.20 Hz
GB	0.5
PC	1.00



PZ4_101_F2 13C/CDCl3

P_IV_101_F2 13C/CDCl3



127

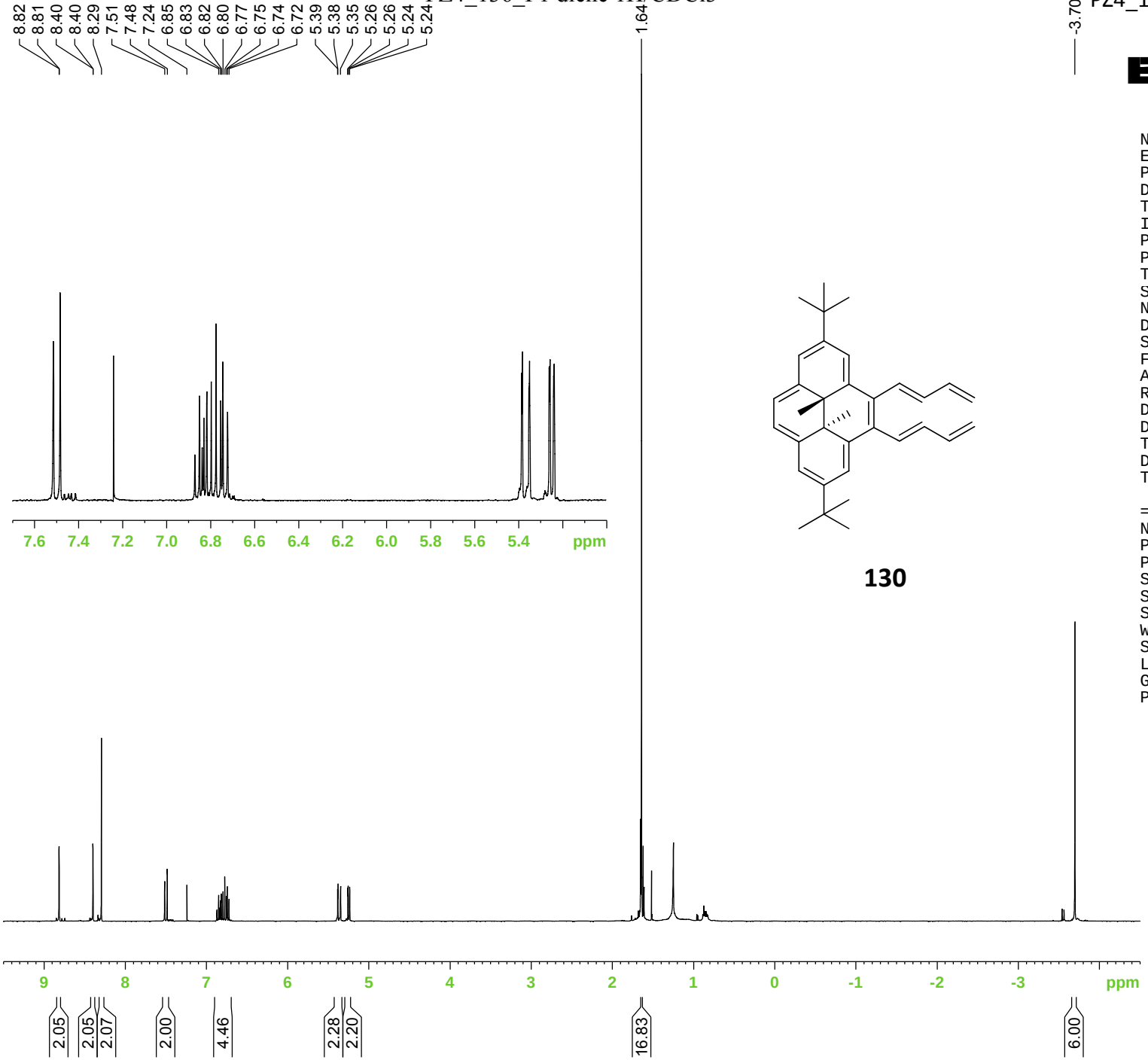
```
NAME            PZ4_101_F2
EXPNO                    2
PROCNO                   1
Date_             20100825
Time                  9.10
INSTRUM              spect
PROBHD    5 mm PABBI 1H/
PULPROG   zgpg_echo1.mmod
TD                   65536
SOLVENT              CDCl3
NS                    2500
DS                       4
SWH             30864.197 Hz
FIDRES           0.470950 Hz
AQ               1.0617495 sec
RG                   16384
DW                  16.200 usec
DE                   6.50 usec
TE                  297.7 K
D1               1.00000000 sec
D11              0.03000000 sec
D20              0.00010000 sec
D21              0.00011460 sec
TD0                      1

======== CHANNEL f1 ========
NUC1                   13C
P1                   14.60 usec
P12                2000.00 usec
PL1                  -1.00 dB
SFO1          125.7715390 MHz
SP2                  3.87 dB
SPNAM2       Crp60comp.4
SPOAL2             0.500
SPOFFS2             0.00 Hz

======== CHANNEL f2 ========
CPDPRG2           waltz16
NUC2                   1H
PCPD2                80.00 usec
PL2                   1.00 dB
PL12                 19.40 dB
PL13                 60.00 dB
SFO2          500.1325200 MHz
SI                   32768
SF            125.7577628 MHz
WDW                    EM
SSB                     0
LB                   0.90 Hz
GB                      0
PC                   1.40
```

PZ4_136_F1 diene 1H/CDCl3

PZ4_136_F1 DHP Diene 1H/CDCl3

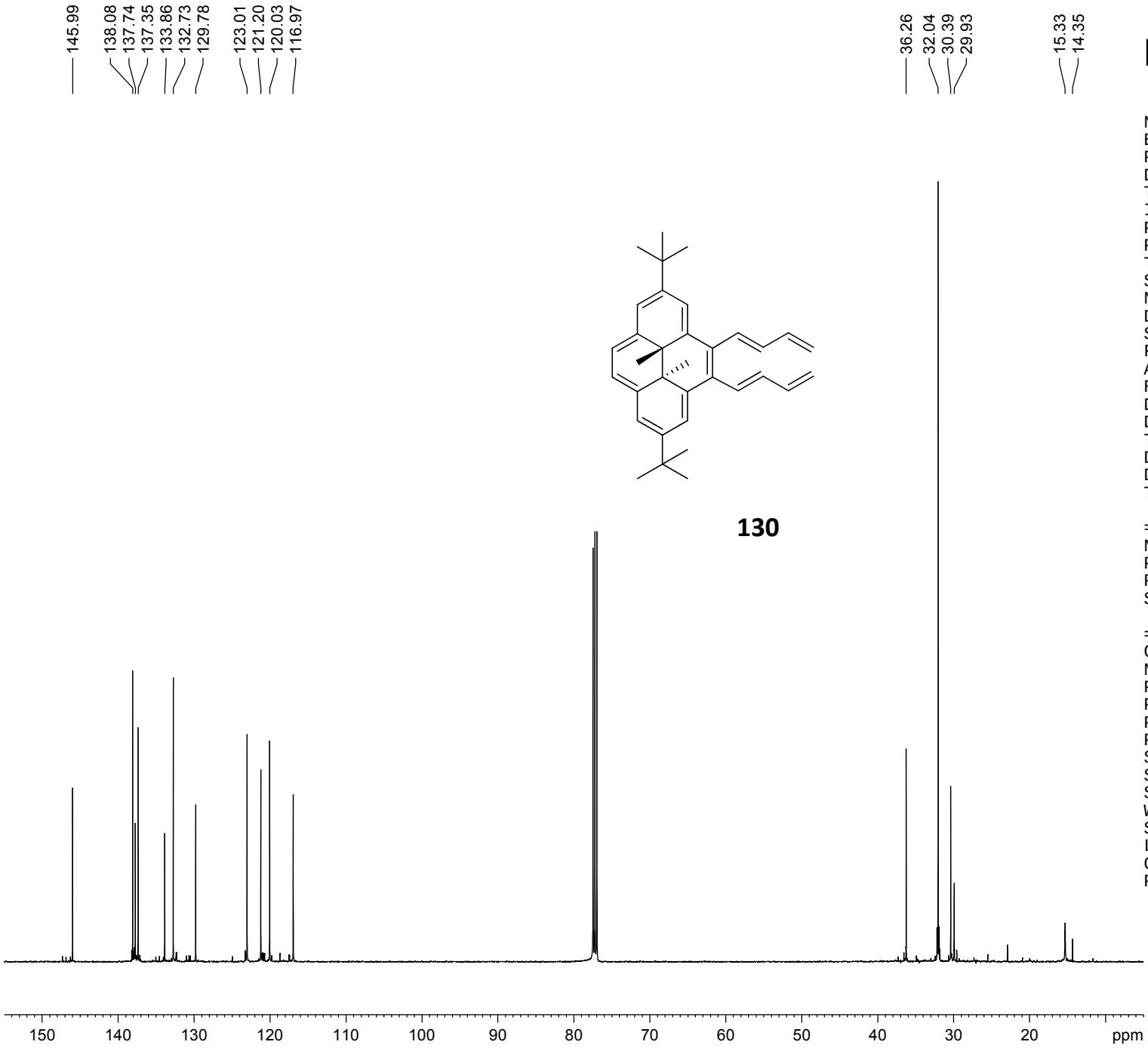


130

NAME	PZ4_136 diene
EXPNO	1
PROCNO	1
Date_	20091128
Time	17.00
INSTRUM	spect
PROBHD	5 mm PABBO BB-
PULPROG	zg30
TD	32768
SOLVENT	CDCl3
NS	16
DS	2
SWH	8012.820 Hz
FIDRES	0.244532 Hz
AQ	2.0448356 sec
RG	71.8
DW	62.400 usec
DE	6.50 usec
TE	298.7 K
D1	1.00000000 sec
TD0	1
======== CHANNEL f1 ========	
NUC1	1H
P1	9.60 usec
PL1	-4.00 dB
SFO1	500.1315200 MHz
SI	16384
SF	500.1300233 MHz
WDW	EM
SSB	0
LB	-0.20 Hz
GB	0
PC	1.00

PZ4_136_F1 Diene 13C/CDCl3

PZ4_136_F1 DHP Diene 13C/CDCl3



130

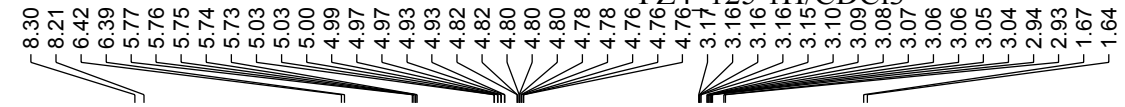
```
NAME          PZ4_136 diene
EXPNO                    2
PROCNO                   1
Date_             20091128
Time                 17.03
INSTRUM              spect
PROBHD   5 mm PABBO BB-
PULPROG             zgpg30
TD                   65536
SOLVENT              CDCl3
NS                   20480
DS                       4
SWH              30864.197 Hz
FIDRES            0.470950 Hz
AQ                1.0617495 sec
RG                  14596.5
DW                  16.200 usec
DE                    6.50 usec
TE                   298.9 K
D1              1.00000000 sec
D11             0.03000000 sec
TD0                      1

======== CHANNEL f1 ========
NUC1                   13C
P1                   10.00 usec
PL1                   3.00 dB
SFO1          125.7715390 MHz

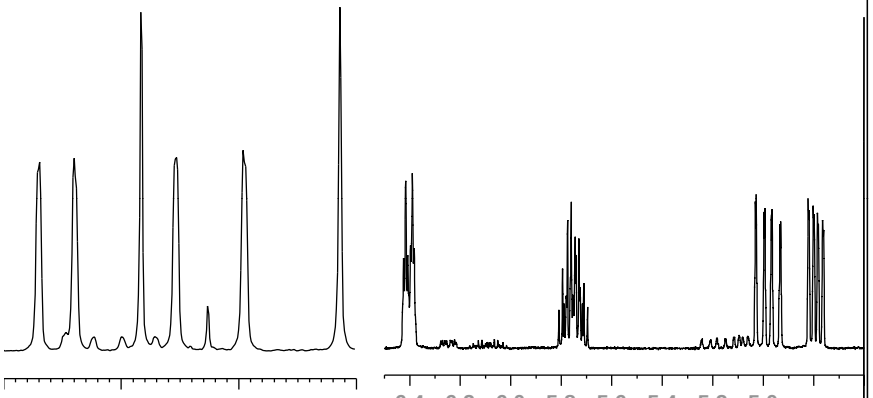
======== CHANNEL f2 ========
CPDPRG2            waltz16
NUC2                   1H
PCPD2                80.00 usec
PL2                  -4.00 dB
PL12                 14.42 dB
PL13                 60.00 dB
SFO2          500.1325200 MHz
SI                   32768
SF            125.7577630 MHz
WDW                    EM
SSB                     0
LB                   0.90 Hz
GB                      0
PC                   1.40
```

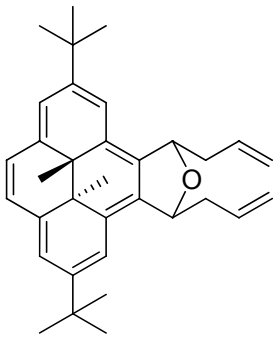
PZ4_125 1H/CDCl3

PZ_HV_125 allylfuranylDHP 1H in CDCl3



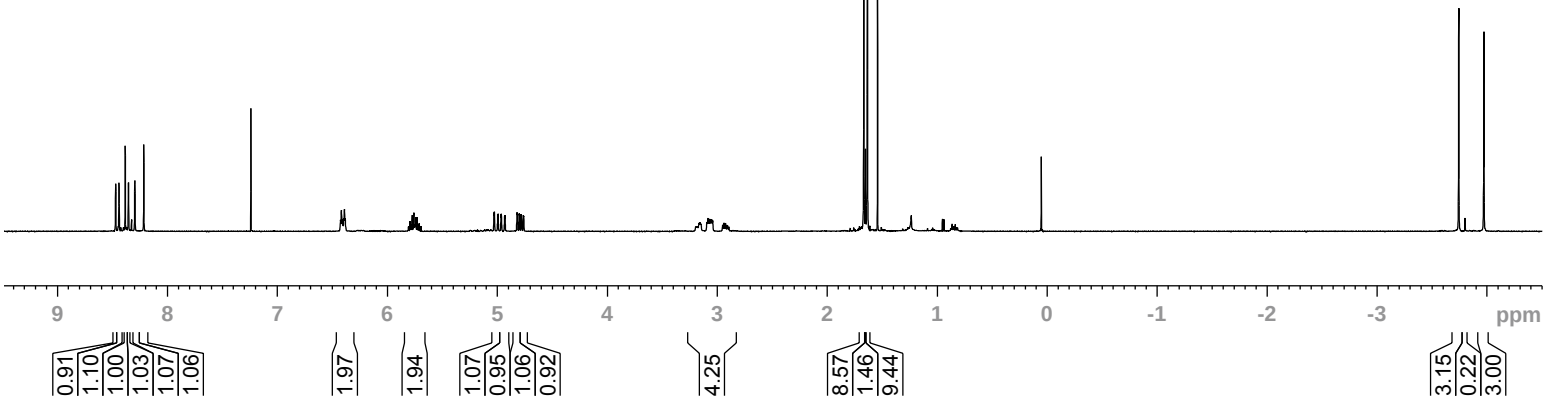






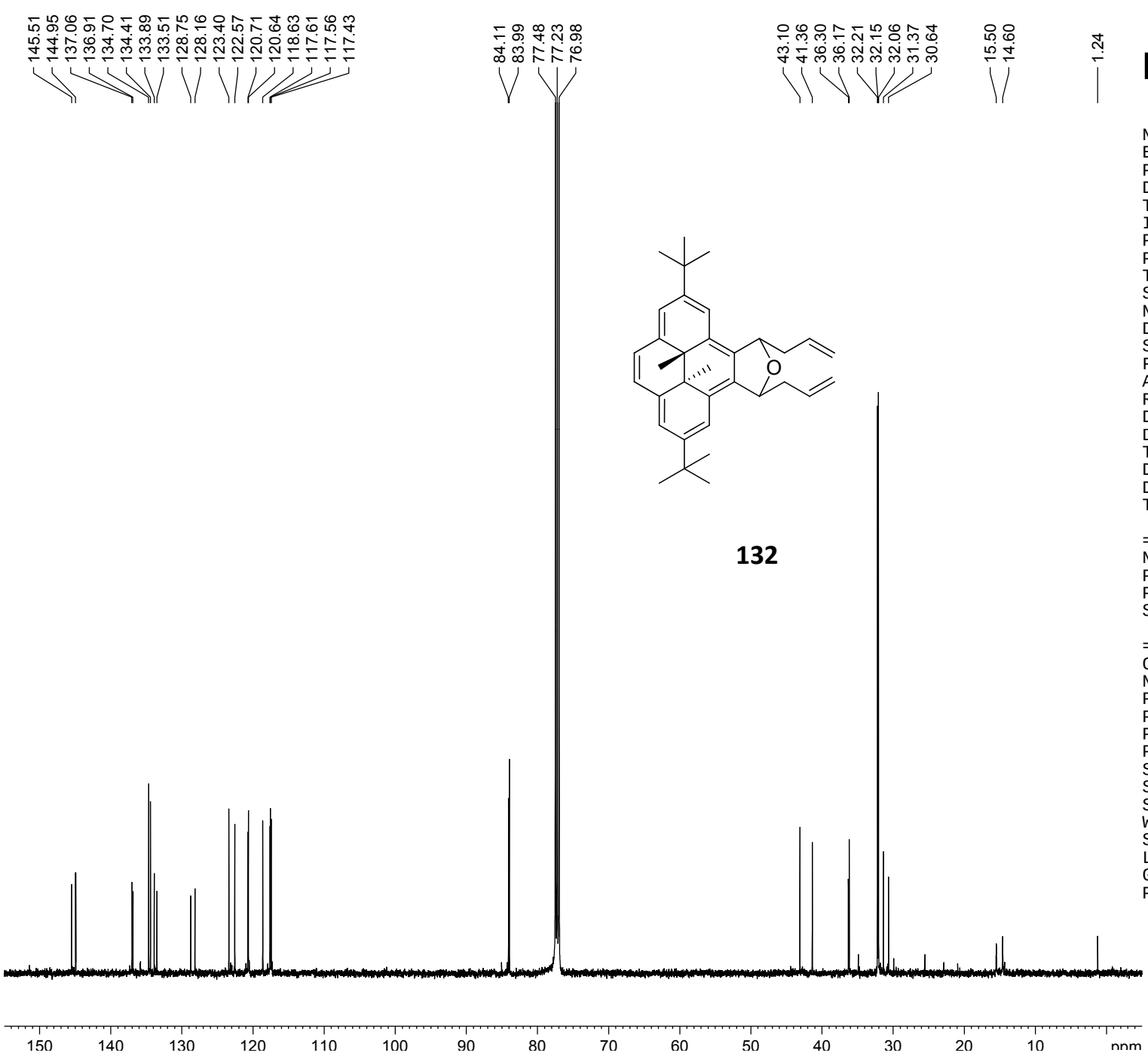
132

NAME	PZ4_125
EXPNO	1
PROCNO	1
Date_	20091026
Time	14.49
INSTRUM	spect
PROBHD	5 mm PABBO BB-
PULPROG	zg30
TD	32768
SOLVENT	CDCl3
NS	16
DS	2
SWH	8012.820 Hz
FIDRES	0.244532 Hz
AQ	2.0448356 sec
RG	256
DW	62.400 usec
DE	6.50 usec
TE	299.0 K
D1	1.00000000 sec
TD0	1
======== CHANNEL f1 ========	
NUC1	1H
P1	9.60 usec
PL1	-4.00 dB
SFO1	500.1315200 MHz
SI	16384
SF	500.1300233 MHz
WDW	GM
SSB	0
LB	-0.20 Hz
GB	0.5
PC	1.00



PZ4_125 13C/CDCl3

PZ_IV_125 allylfuranylDHP 13C in CDCl3



132

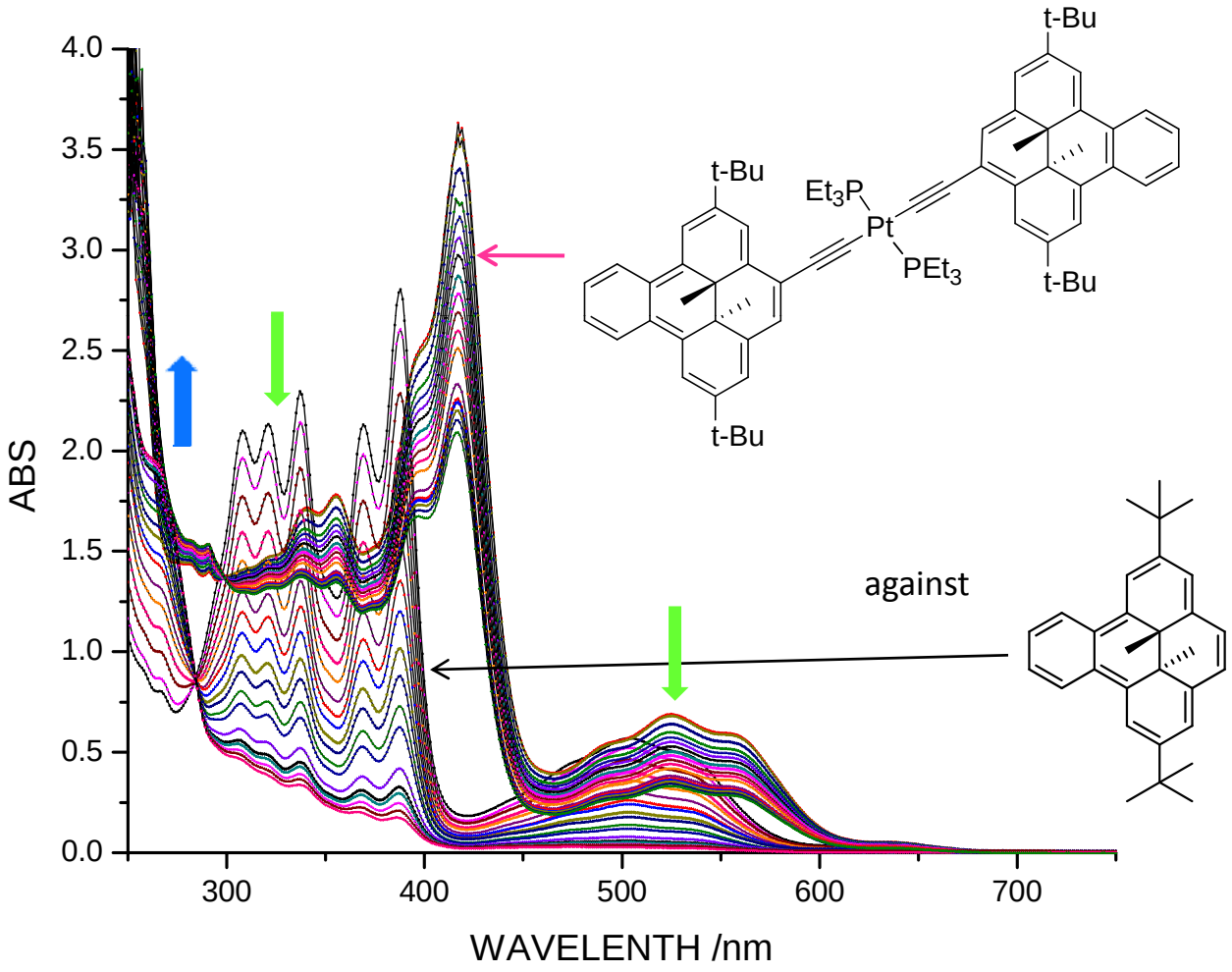
BRUKER

NAME	PZ4_125
EXPNO	4
PROCNO	1
Date_	20091026
Time	14.53
INSTRUM	spect
PROBHD	5 mm PABBO BB-
PULPROG	zgpg30
TD	65536
SOLVENT	CDCl3
NS	9314
DS	4
SWH	30864.197 Hz
FIDRES	0.470950 Hz
AQ	1.0617495 sec
RG	14596.5
DW	16.200 usec
DE	6.50 usec
TE	299.3 K
D1	1.00000000 sec
D11	0.03000000 sec
TD0	1
======== CHANNEL f1 ========	
NUC1	13C
P1	10.00 usec
PL1	3.00 dB
SFO1	125.7715390 MHz
======== CHANNEL f2 ========	
CPDPRG2	waltz16
NUC2	1H
PCPD2	80.00 usec
PL2	-4.00 dB
PL12	14.42 dB
PL13	60.00 dB
SFO2	500.1325200 MHz
SI	32768
SF	125.7577620 MHz
WDW	EM
SSB	0
LB	0.90 Hz
GB	0
PC	1.40

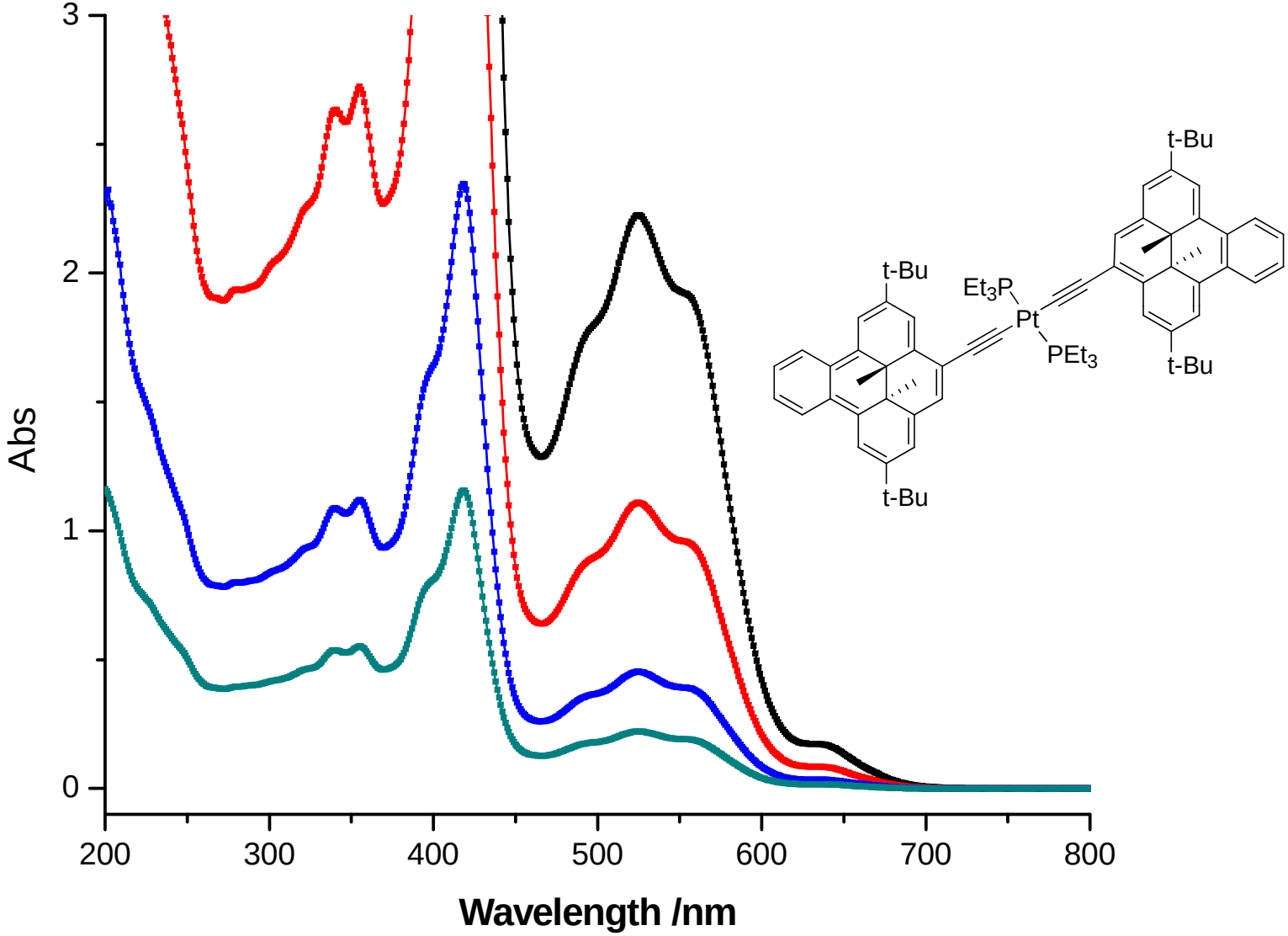
Appendix VII. Selected UV-Vis spectra

(7 pages)

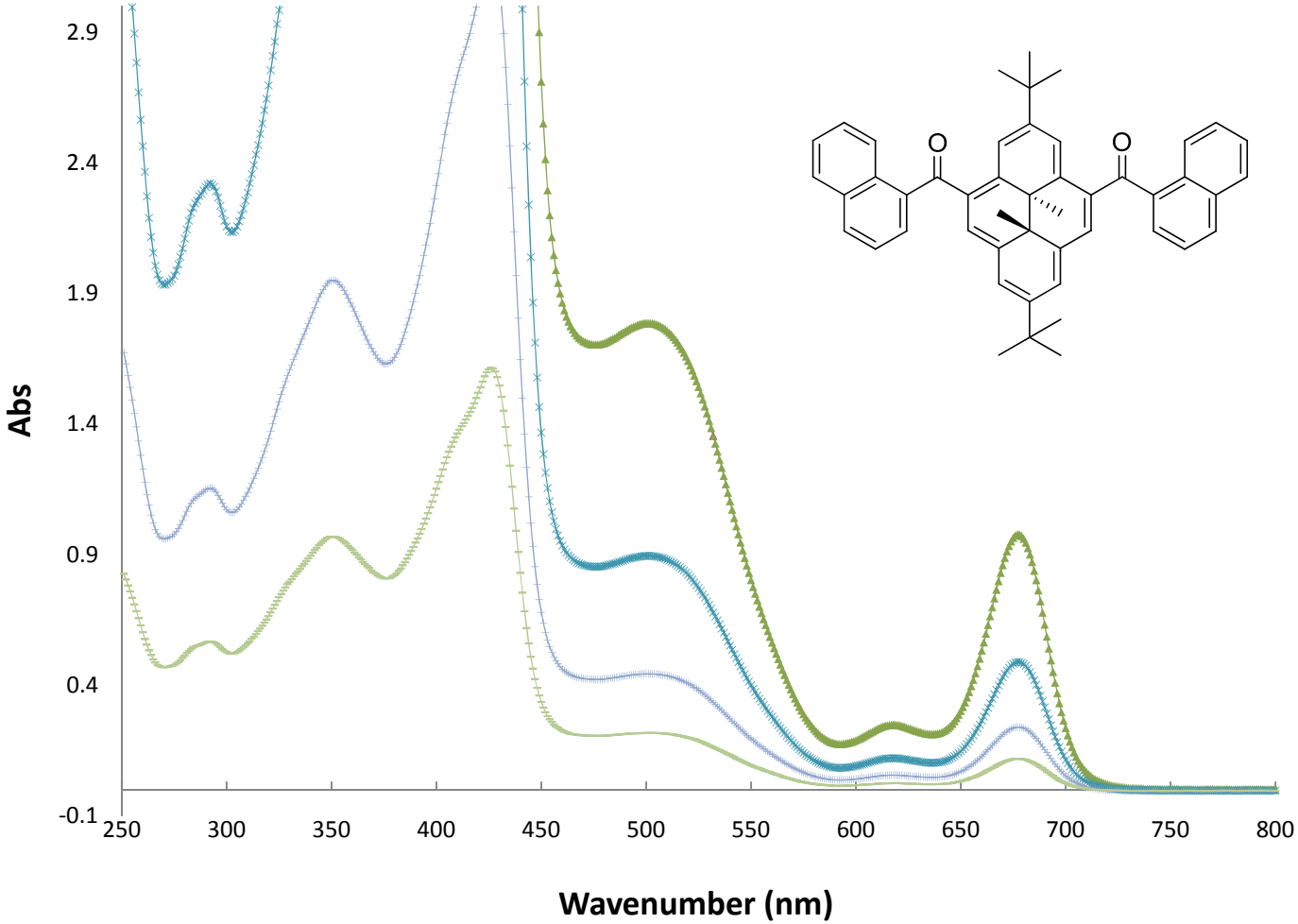
Comparison of the opening rates of complexes **48** with those of BenzoDHP



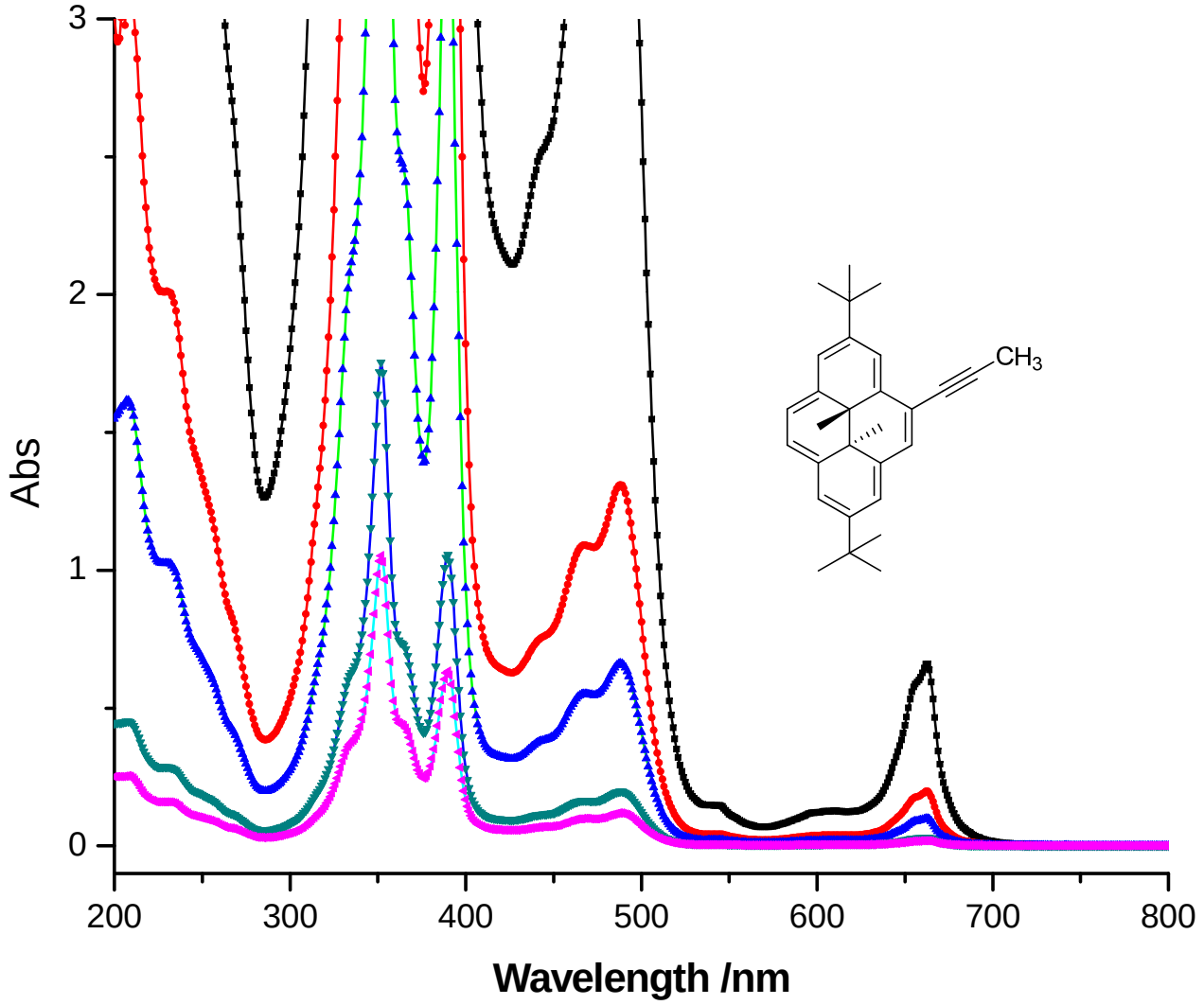
UV-Vis spectrum of **48** in hexanes

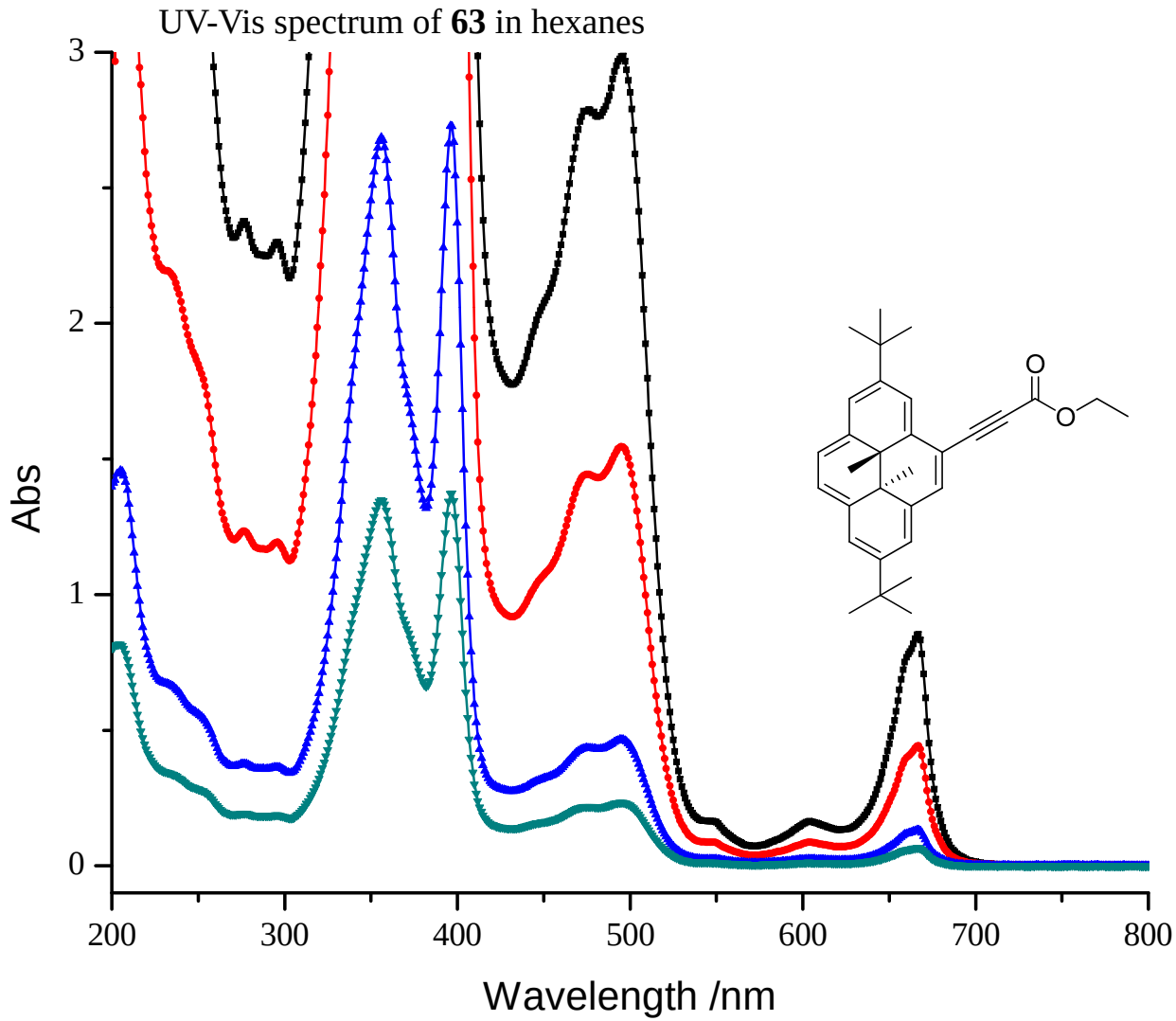


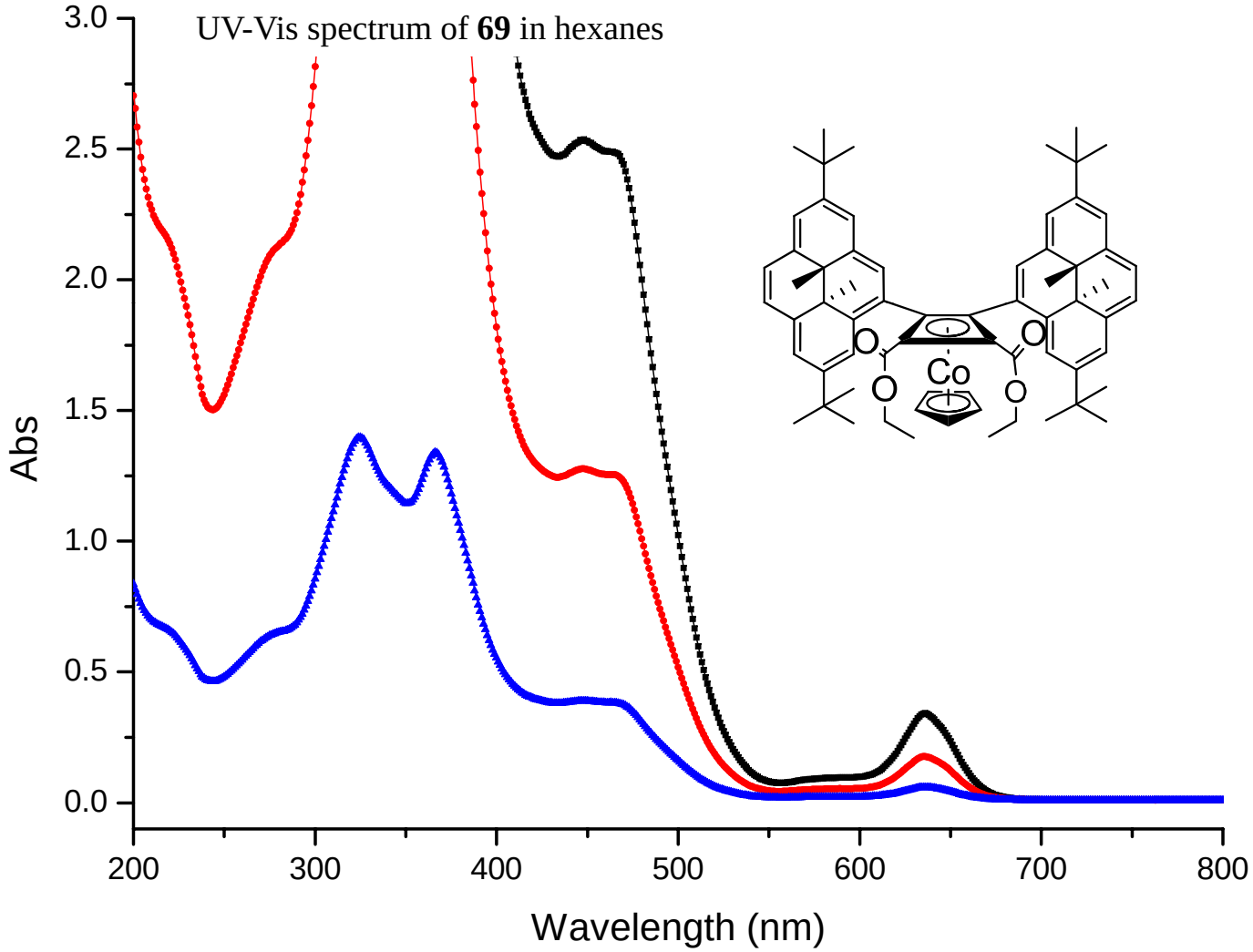
UV-Vis spectrum of **36** in hexanes



UV-Vis spectrum of **23** in hexanes




UV-Vis spectrum of **63** in hexanes
Abs
Wavelength /nm
0
1
2
3
200
300
400
500
600
700
800
O
O


UV-Vis spectrum of 69 in hexanes
Abs
Wavelength (nm)
3.0
2.5
2.0
1.5
1.0
0.5
0.0
200
300
400
500
600
700
800
O
O
O
O
Co

UV-Vis spectrum of **17** in hexanes

